

16th INTERNATIONAL CONFERENCE
**DYNAMICAL SYSTEMS
THEORY AND APPLICATIONS**

ŁÓDŹ, DECEMBER 6-9, 2021

ABSTRACTS



EDITORS

**J. AWREJCEWICZ
M. KAŹMIERCZAK
J. MROZOWSKI
P. OLEJNIK**



**16th Conference
on
DYNAMICAL SYSTEMS
Theory and Applications
DSTA 2021**

ABSTRACTS

EDITORS

J. Awrejcewicz, M. Kaźmierczak, J. Mrozowski, P. Olejnik

Łódź, December 6-9, 2021

POLAND

ORGANIZING COMMITTEE

Lodz University of Technology, Faculty of Mechanical Engineering
Department of Automation, Biomechanics and Mechatronics
1/15 Stefanowski Str., 90-924 Łódź, Poland
Phone: +48 42 631-22-25, Fax: +48 42 631-24-89
<http://abm.p.lodz.pl>

Jan Awrejcewicz — chairman
Jerzy Mrozowski – vice chairman
Paweł Olejnik – vice chairman
Magdalena Jastrzębska — secretary
Olga Jarzyna — secretary
Maksymilian Bednarek
Marek Kaźmierczak
Michał Ludwicki
Krystian Polczyński
Adam Wijata

© Copyright by Politechnika Łódzka
Technical editor and cover design: *Marek Kaźmierczak*
Cover design: *Marek Kaźmierczak*

SCIENTIFIC COMMITTEE

- M. Alves** – Brazil
M. Amabili – Canada
I.V. Andrianov – Germany
J. Awrejcewicz – Chairman, Poland
J.M. Balthazar – Brazil
A. Bartoszewicz – Poland
M. Belhaq – Morocco
B. Birnir – USA
D. Blackmore – USA
T. Burczyński – Poland
V. Danishevs'kyi - Ukraine
F. Dohnal – Switzerland
M. Dosaev - Russia
V.-F. Duma – Romania
O. Gendelman – Israel
O. Gottlieb – Israel
C. Grebogi – UK
P. Hagedorn – Germany
K. (Stevanovic) Hedrih – Serbia
N. Herisanu – Romania
S. Kaczmarczyk – UK
K. Kaliński – Poland
J. Kaplunov – UK
Z. Koruba – Poland
I. Kovacic – Serbia
J. Kozanek – Czech Republic
V.A. Krysko – Russia
L.V. Kurpa – Ukraine
W. Lacarbonara – Italy
C.-H. Lamarque – France
S. Lenci – Italy
R. Lozi - France
A. Luo – USA
E. Macau – Brazil
J.A. Machado – Portugal
N.M.M. Maia – Portugal
Y. Mikhlin – Ukraine
J.E. Mottershead – UK
A. Nabarrete – Brazil
P. Odry– Hungary
G. Olivar Tost – Colombia
V.N. Pilipchuk – USA
C.M.A. Pinto – Portugal
J. Przybylski - Poland
G. Rega – Italy
M.A.F. Sanjuan – Spain
Ch.H. Skiadas – Greece
R. Starosta - Poland
S. Theodossiades – UK
O. Thomas – France
H. True – Denmark
F. Udwardia – USA
A.F. Vakakis – USA
W. Van Horssen – The Netherlands
F. Verhulst – The Netherlands
U. Von Wagner – Germany
J. Warmiński – Poland
H. Yabuno – Japan
K. Zimmermann – Germany

SPONSORS & PATRONAGE



The honorary patronage of DSTA 2021 has been assumed
by the Rector of the Lodz University of Technology,
Prof. Krzysztof Jóźwik



Department of Automation, Biomechanics and Mechatronics

The 16th International Conference
"Dynamical Systems – Theory and Applications – DSTA 2021"
is co-financed by the "Excellent Science"
program of the Polish Ministry of Education and Science



Ministry
of Education
and Science

PREFACE

This is the sixteen time when the conference “Dynamical Systems – Theory and Applications” gathers a numerous group of outstanding scientists and engineers, who deal with widely understood problems of theoretical and applied dynamics.

Organization of the conference would not have been possible without a great effort of the staff of the Department of Automation, Biomechanics and Mechatronics. The patronage over the conference has been taken by the "Excellent Science" program of the Polish Ministry of Education and Science.

It is a great pleasure that our invitation has been accepted by so many people, including good colleagues and friends as well as a large group of researchers and scientists, who decided to participate in the conference for the first time. With proud and satisfaction we welcome **748** authors from **52** countries all over the world. They decided to share the results of their research and many years experiences in the discipline of dynamical systems by submitting many very interesting papers.

This booklet contains a collection of **364** abstracts, which have gained the acceptance of referees and have been qualified for publication in the conference edited books. Included abstracts belong to the following topics:

- asymptotic methods in nonlinear dynamics,
- bifurcation and chaos in dynamical systems,
- control in dynamical systems,
- dynamics in life sciences and bioengineering,
- engineering systems and differential equations,
- experimental/industrial studies,
- mathematical approaches to dynamical systems
- mechatronics,
- non-smooth systems
- optimization problems in applied sciences
- original numerical methods of vibration analysis,
- stability of dynamical systems,
- vibrations of lumped and continuous systems.

Our previous experience shows that an extensive thematic scope comprising dynamical systems stimulates a wide exchange of opinions among researchers dealing with different branches of dynamics. We think that vivid discussions will influence positively the creativity and will result in effective solutions of many problems of dynamical systems in mechanics and physics, both in terms of theory and applications.

Every two years we extend scope and recognition of the conference. This time, we have opened **6** special sessions gathering **86** presentations.

We do hope that DSTA 2021 will contribute to the same extent as all the previous conferences to establishing new and tightening the already existing relations and scientific and technological co-operation between both Polish and foreign institutions.

On behalf of both Scientific and
Organizing Committees

A handwritten signature in blue ink, appearing to read 'Awrejcewicz', is written over a light blue rectangular background.

Chairman

Professor Jan Awrejcewicz

LIST OF ABSTRACTS

KEYNOTE LECTURES

- (OPT337)** BATRA R.C.
Optimization of Sandwich Structures under Blast Loading 39
- (MAT267)** BANERJEE S., ACHARYA A., JEWARE P.
The Dynamical Behavior of a Quantum Impact Oscillator 41
- (VIB135)** CARRERA E., PETROLO M.
Accuracy and Efficiency of Structural Theories for Free Vibration Analyses via Axiomatic/Asymptotic Method and Neural Networks..... 43
- (STA10)** WARMIŃSKI J., MITURA A., ROMEO F., BRUNETTI M.
Nonlinear Dynamics of Multi-Stable Systems..... 45
- (BIF142)** YOUNIS M.I.
Dynamic-Based Micro and Nano Devices and Phenomena..... 47
- (VIB381)** ZHU W.
Dynamics of Continuous Systems: From Time-Varying, Nonlinear, and Flexible Multibody Systems to Phononic Structures 49

SPECIAL SESSION 1

- (EXP151)** BERCIU A.-G., DULF E.H., JURJ D., CZUMBIL L., MICU D.D.
Energy Pulse: Competitive and Accessible Application for Monitoring Electricity Consumption..... 53
- (CON222)** BUNESCU I., BIRS I., DE KEYSER R., MURESAN C.I.
A Novel Toolbox for Automatic Design of Fractional Order PI Controllers Based on Automatic System Identification From Step Response Data..... 55
- (CON379)** GUDE J.J., BRINGAS P.G.
Proposal of a Control Hardware Architecture for Implementation of Fractional-Order Controllers..... 57
- (CON164)** MIHAI M., BIRS I., MURESAN C.I., DULF E., DE KEYSER R.
Comparisons and Experimental Validation of Several Autotuning Methods for Fractional Order Controllers 60
- (CON158)** SANGEORZAN M., DULF E.-H.
Fractional Order Controllers for Twin Rotor Aerodynamical System..... 62

(ENG272) ZAFAR A.A., AWREJCEWICZ J. <i>Influence of Fractional Order Parameter on the Dynamics of Different Vibrating Systems</i>	64
---	----

SPECIAL SESSION 2

(BIF218) AVANÇO R.H., ZANELLA D.A., CANTILLO R.J.A., CUNHA JR A., BALHAZAR J.M., TUSSET A.M. <i>The Influence of the Inductance on the Nonideal Vibrations of a Pendulum Coupled to a DC Motor</i>	69
(ENG70) AVANÇO R.H., ZANELLA D.A., CANTILLO R.J.A., CUNHA JR. A., BALHAZAR J.M., TUSSET A.M. <i>Discussion on the Influence of the Inductance in the Nonlinear Dynamics of DC Motors in Coupled Systems</i>	71
(ENG43) BABADI A.F., BENI Y.T., ŽUR K.K. <i>On the Flexoelectric Effect on Nonlinear Vibration of Three-Layered Functionally Graded Cylindrical Microshells</i>	73
(CON231) BEZERRA J.A., TRENTIN J.F.S., DOS SANTOS D.A. <i>Global Sliding Mode Control for a Fully-Actuated Non-Planar Hexa-Rotor Aerial Vehicle</i>	75
(BIF51) DE OLIVEIRA L.R., BALHAZAR J.M., NABARRETE A., BUENO Á.M., TUSSET A.M., PETROCINO E.A. <i>Some Remarks on Experimental Analysis of a Non-Ideal Conveyor Belt</i>	77
(CON194) GONÇALVES M.A., BALHAZAR J.M., JARZĘBOWSKA E., TUSSET Â.M., RIBEIRO M.A., DAŮM H.H. <i>On a Nonlinear and Non-Ideally Excited Tank</i>	79
(BIF101) GUPTA D., CHANDRAMOULI V.V.M.S. <i>The Existence of Absolutely Continuous Invariant Measures for q-Deformed Unimodal Maps</i>	81
(BIF102) GUPTA D., CHANDRAMOULI V.V.M.S. <i>An Improved q-Deformed Logistic Map and its Implications</i>	82
(STA90) GUTSCHMIDT S., HAYASHI S., LAM N., LENK C. <i>Active MEMS Amplifier for Improved Signal-to-Noise Ratios</i>	83
(CON335) JACKIEWICZ J. <i>Energy Recovery Hybrid System with the Flywheel</i>	85

(CON141) JARZĘBOWSKA E., AUGUSTYNEK K., URBAŚ A. <i>Motion Tracking of a Rigid-Flexible Link Manipulator in a Controller Failure Conditio</i>	87
(VIB147) KACZMARCZYK S. <i>Nonlinear Dynamics and Control of Moving Slender Continua Subject to Periodic Excitations</i>	89
(CON191) KŁAK M., JARZĘBOWSKA E. <i>Guidance and Control System Design for a Free-Flying Space Manipulator Based on a Dynamically Equivalent Manipulator</i>	91
(MAT167) LENCI S. <i>Waves in a Beam Resting on a Bilinear Winkler Foundation</i>	93
(ENG129) MIKHLIN Y.V., LEBEDENKO Y.O. <i>Resonance Regimes in the Non-Ideal System Having the Pendulum as Absorber</i>	95
(VIB8) MOJTABAEI S.M., KACZMARCZYK S. <i>Dynamic Responses of Vertical Transportation Systems in Tall Buildings Under Seismic Excitations</i>	97
(EXP206) PIRES I., AYALA H.V.H., WEBER H.I. <i>Nonlinear System Identification of an Experimental Drill-String Setup</i>	99
(BIF148) RIBEIRO M.A., TUSSET A.M., LENZ W.B., BALTHAZAR J.M., LITAK G. <i>On Non-Linear Dynamics Behaviour of a Fixed Offshore Platform for Energy Harvesting</i>	101
(BIF46) RIBEIRO M.A., TUSSET A.M., LENZ W.B., BALTHAZAR J.M., LITAK G. <i>On Non-Ideal and Fractional Dynamics of a Magneto Piezo Elastic Oscillator with Bouc-Wen Damping to Harvesting Energy</i>	103
(CON331) RICARDO JR. J.A., SANTOS D.A. <i>Super-Twisting Sliding Mode Control for a Formation of Fully-Actuated Multirotor Aerial Vehicles</i>	105
(CON233) TRENTIN J.F.S., DOS SANTOS D.A. <i>Global Sliding Mode Control Design for A 3D Pendulum</i>	107
(BIF103) TUSSET A.M., PIRES D., LENZI G.G., ILIUK I., ROCHA R.T., BALTHAZAR J.M. <i>Piezoelectric Vibration Energy Harvesting from a Portal Frame with a Shape Memory Alloy</i>	109
(CON50) TUSSET A.M., GONÇALVES M., MANUEL C.J.T., BALTHAZAR J.M., LENZI G.G. <i>Passive Vibration Control of a High-Speed Elevator System</i>	111

(MAT37) WESTIN M.F., DA SILVA R.G.A., BALTHAZAR J.M. <i>Some Comments on Nonlinear Aeroelastic Typical Section</i>	<i>113</i>
(CON201) WHIDBORNE J.F., JARZĘBOWSKA E., AGARWAL V., ISHOLA A.A. <i>Manipulator-Aircraft Dynamical System Dedicated for Wind Tunnel Testing</i>	<i>115</i>
(ENG38) ZAPOMĚL J., FERFECKI P., KOZÁNEK J. <i>Reducing Amplitude of Nonlinear Vibration of Rotors Induced by Imbalance Forces and the Disc Collisions Using Magnetically Sensitive Fluids.....</i>	<i>117</i>

SPECIAL SESSION 3

(CON306) ALEKSANDROV A.Yu., TIKHONOV A.A. <i>On the Attitude Stabilization of Artificial Earth Satellite in the Natural Electromagnetic Coordinate System</i>	<i>121</i>
(CON329) ALEKSANDROV A.Yu., TIKHONOV A.A. <i>On the Triaxial Electrodynamical Attitude Stabilization of a Satellite in the Orbital Frame via Control with Distributed Delay</i>	<i>123</i>
(LIF106) ALPATOV I., DOSAEV M., SAMSONOV V., VOROBYEVA E., DUBROV V. <i>An Elastic Rib Modelling.....</i>	<i>125</i>
(CON115) DOSAEV M. <i>Control Algorithm of a Vibrating Robot with a Flywheel and Unbalance with Limited Angular Acceleration</i>	<i>127</i>
(ENG107) DOSAEV M., SAMSONOV V. <i>Sliding of Tabouret with Elastic Legs on a Rough Surface under the Action of a Small Lateral Force.....</i>	<i>129</i>
(ASY22) GARBUZ M., KLIMINA L., SAMSONOV V. <i>Wind Powered Plantigrade Machine Moving Against a Flow.....</i>	<i>131</i>
(MTR35) GOLOVANOV S., KLIMINA L., DOSAEV M., SELYUTSKIY Y. <i>Underwater Capsubot Controlled by Motion of a Single Internal Flywheel</i>	<i>133</i>
(EXP80) HWANG S.-S., LI H.-M., CHEN X.-Y. <i>Study on the Property of Microcellular Injection Molded HDPE/Wheat Straw Composites.....</i>	<i>135</i>
(ASY228) KOSHELEV A., KUGUSHEV E., SHAHOVA T. <i>Dynamics of a Low-Inertia Ball Located Between Two Rotating Planes with Viscous Friction.....</i>	<i>137</i>
(ASY223) KUGUSHEV E., SELEZNEVA M., SHAHOVA T. <i>Periodic Motions in Systems with Viscous Friction.....</i>	<i>139</i>

(OPT42) LIN C.-H., LO J.-H., DOSAEV M., SELYUTSKIY Y. <i>Optimized Spacing Design for Paired Counter-Rotating Savonius Rotors</i>	141
(CON216) RADKOWSKI S., SŁOMCZYNSKI M. <i>Usage of the Nonlinear Method to Control Model of a Half Car Suspension with a Damper Containing MR Fluid</i>	143
(STA32) SELYUTSKIY Y. <i>Dynamics of a 2 DoF Galloping-Based Wind Power Harvester.....</i>	144
(ENG93) SHATSKYI I., PEREPICHKA V. <i>Shock Torsion Wave in an Elastic Rod with Decreasing Function of Viscoplastic External Friction.....</i>	146
(ENG94) SHATSKYI I., MAKOVICHUK M., VASKOVSKIY M. <i>Transversal Straining of Pressurized Pipeline Caused by Vibration of Damaged Foundation.....</i>	147
(OPT30) SMIRNOVA N., MALYKH E., CHERKASOV O. <i>Brachistochrone Problem with Variable Mass</i>	148
(OPT31) SMIRNOVA N., MALYKH E., CHERKASOV O. <i>Zermelo Navigation Problem with State Constraints</i>	150
(MTR83) YEH C.-H., LIN S.-H. <i>Maze Exergame Applied to IoT-Based Tiny Aerobic Equipment.....</i>	152
 <u>SPECIAL SESSION 4</u>	
(STA261) BENEDETTI K.C.B., DA SILVA F.M.A., SOARES R.M., GONÇALVES P.B. <i>Dynamic Integrity of Hyperelastic Spherical Membranes</i>	157
(MAT258) CENEDESE M., AXÃS J., HALLER G. <i>Data-Driven Reduced-Order Nonlinear Models from Spectral Submanifolds</i>	159
(NUM246) HABIB G. <i>A Novel Iterative Procedure for Robustness Assessment</i>	161
(MAT252) LI Z., JUN J., HONG L., KANG J. <i>Global Analysis for Nonlinear Dynamical System Based on Parallel Subdomain Synthesis Method</i>	163
(STA197) NAGY Á.M., PATKÓ D., ZELEI A. <i>Discovery and Online Interactive Representation of the Dimensionless Parameter-Space of the Spring-Loaded Inverted Pendulum Model of Legged Locomotion Using Surface Interpolation</i>	165

(BIF256) SETTIMI V., REGA G.
Global Dynamics of Thermomechanically Coupled Plates..... 167

(BIF33) TAHIRI M., KHAMLICI A., BEZZAZI M.
Track-Bridge Interaction Effect on the Train-Bridge Resonance of Railway Viaducts 169

(BIF11) ZIPPO A., PELLICANO F., IARRICCIO G.
Experiments of Shells with Non-Newtonian Fluid Interaction 171

SPECIAL SESSION 5

(NON154) ABELLA A.F., MORCILLO J.D., ANGULO F.
Control of Bubbling Phenomenon in Bipolar SPWM Inverters..... 175

(NON177) AMADOR J.A., REDONDO J.M., OLIVAR G., ERAZO C.
Effects of the Resources Transfer Between Communities Under a Policy of Responsibility in the Framework of Sustainability..... 177

(MAT145) ANTONIJUAN J., MASSANA I., OLIVAR-TOST G., PRAT J., TRULLOLS E.
Bifurcations in PieceWise-Smooth Systems Associated to Migration 179

(BIF170) AVRUTIN V., BASTIAN F., VON SCHWERIN-BLUME L., ZHUSUBALIYEV Z.T., EL AROUDI A.
Real and Noice-Induced Bubbling: Geometric Approach and Problem of Initial Deviation 181

(NON132) AVRUTIN V., PANCHUK A., SUSHKO I.
Border Collision Bifurcations of Chaotic Attractors 183

(NON138) AVRUTIN V., DAL FORNO A., MERLONE U.
Codimension-2 Bifurcations in a Quantum Decision Making Model 185

(BIF288) ESCOBAR-CALLEJAS C.M., OLIVAR-TOST G.
Zip Bifurcation in PWSC Systems 187

(NON250) ESTEBAN M., FREIRE E., PONCE E., TORRES F.
Piecewise Smooth Systems with a Pseudo-Focus: A Normal Form Approach 189

(NON130) JEFFREY M., AVRUTIN V.
Hidden Dynamics of Maps (And When “Period 2 Implies Chaos”) 191

(BIF251) MORCILLO J.D., MUÑOZ J.-G., OLIVAR-TOST G.
Non-Smooth Dynamics in Ramp-Controlled and Sine-Controlled Buck Converters 192

(NON133) ZHUSUBALIYEV Z.T., AVRUTIN V., BASTIAN F. <i>On Transformations of Closed Invariant Curves in Piecewise-Smooth Maps</i>	194
--	-----

SPECIAL SESSION 6

(ENG279) BURLON A., FAILLA G. <i>On the Dynamics of High-Order Beams with Vibration Absorbers</i>	199
(ENG334) BURLON A., DI PAOLA M., SUCATO V. <i>Non-Stationary Stochastic Dynamics Analysis of Structural Systems Equipped with Fractional Viscoelastic Device</i>	201
(VIB292) CHATZOPOULOS Z., PALERMO A., GUENNEAU S., MARZANI A. <i>Cloaking of Love Waves</i>	203
(CON305) CHILLEMI M., FURTMÜLLER T., ADAM C., PIRROTTA A. <i>Assessing the Effect of Different Configurations of Inerter-Based Devices for Structural Vibration Control</i>	205
(ASY304) DAS R., BAJAJ A.K., GUPTA S. <i>Performance of a Nonlinear Energy Sink Coupled with a Nonlinear Oscillator for Energy Harvesting Applications</i>	207
(CON287) DI MATTEO A., MASNATA C., ADAM C., PIRROTTA A. <i>Tuned Liquid Column Damper Inerter (TLCDI) for Vibration Control of Fixed-Base Structures</i>	209
(CON313) FITZGERALD B., SARKAR S. <i>Inerter-Based Dampers for Vibration Control of Floating Offshore Wind Turbines</i>	211
(VIB348) GHASSEMPOUR M., FAILLA G., ALOTTA G., LAFACE V., RUZZO C., ARENA F. <i>Vibration Mitigation in Offshore Wind Turbines by Tuned Mass Absorbers</i>	213
(VIB289) JANSSEN S., VAN BELLE L., DE MELO FILHO N.G.R., CLAEYS C., DESMET W., DECKERS E. <i>Improving the Noise Insulation Performance of Vibro-Acoustic Metamaterial Panels Through Multi-Resonant Design</i>	214
(CON345) KALDERON M., KALOGERAKOU M., PARADEISIOTIS A., ANTONIADIS I. <i>Locally Resonant Metamaterials Utilizing Dynamic Directional Amplification</i>	216
(EXP275) PARADEISIOTIS A., TSIΟΥMANIS K., ANTONIADIS I. <i>Experimental Prototype of a KDamper Vibration Absorber for Small Vertical Loads Utilizing Compliant Joints</i>	218

(LIF327) PIRROTTA A., EVOLA A., DI MATTEO A., GALVANO A., RUSSO A. <i>Anti-Vibration Knob for the Motorcycle, Customizable on the Basis of the Driver's Ergonomics</i>	220
(VIB293) PU X., PALERMO A., MARZANI A. <i>A 3D Multiple Scattering Formulation to Model Elastic Waves Interacting with Surface Resonators</i>	222
(VIB285) RUSSILLO A.F., FAILLA G. <i>A Dynamic-Stiffness Framework for Locally Resonant Structures</i>	224
(EXP310) SANGIULIANO L., REFF B., PALANDRI J., WOLF-MONHEIM F., PLUYMERS B., DECKERS E., DESMET W., CLAEYS C. <i>Low Frequency Tyre Noise Mitigation in a Vehicle Using Metal 3D Printed Resonant Metamaterials</i>	226
(OPT298) SANTORO R., MAZZEO M., FAILLA G. <i>Interval Frequency Response of Uncertain Locally Resonant Structures</i>	228
(EXP282) ZHOU T.-Y., DING H. <i>Experimental Study of a Tuned Liquid Column Damper with Liquid Turbine</i>	230
 <u>REGULAR SESSION (ID: ASY)</u>	
(ASY273) ABOHAMER M.K., AWREJCEWICZ J., STAROSTA R., AMER T.S., BEK M.A. <i>Modelling and Analysing of a Spring Pendulum Motion in the Presence of Energy Harvesting Devices</i>	235
(ASY143) AKHMETOV R. <i>The Asymptotic Solutions of the Boundary Value Problem of Convective Diffusion Around Drops with Volumetric Nonlinear Chemical Reaction</i>	237
(ASY352) AWREJCEWICZ J., STAROSTA R., SYPNIEWSKA-KAMIŃSKA G. <i>Vibration of the System with Nonlinear Springs Connected in Series</i>	239
(ASY24) DA SILVEIRA ZANIN C., SAVADKOOHI T.A., BAGUET S., DUFOUR R. <i>Energy Exchanges in a Nonlinear Meta-Cell</i>	241
(ASY139) DANIK Y., DMITRIEV M. <i>Algorithm for Suboptimal Feedback Construction Based on Padé Approximation for Nonlinear Control Problems</i>	243
(ASY376) FORTUNATI A., BACIGALUPO A., LEPIDI M., ARENA A., LACARBONARA W. <i>Nonlinear Wave Propagation in One-Dimensional Metamaterials via Hamiltonian Perturbation Scheme</i>	245

(ASY343) IGUMNOVA V.S., LUKIN A.V., POPOV I.A., SHTUKIN L.V. <i>Synchronization of Oscillations of Weakly Coupled Elastic Elements of a Differential Resonant MEMS-Accelerometer in the Mode of a Two-Circuit Self-Oscillator</i>	247
(ASY192) KAPLUNOV J., PRIKAZCHIKOV D.A., PRIKAZCHIKOVA L. <i>Rayleigh-Type Waves in Nonlocal Elasticity</i>	249
(ASY131) MIKHLIN Y.V., SURGANOVA Y.E. <i>Nonlinear Normal Modes and Localization of Vibrations in the Pendulum System Under Magnetic Excitation</i>	250
(ASY346) MOZHGOVA N., LUKIN A., POPOV I. <i>Nonlinear Dynamics of Electrostatic Comb-Drive with Variable Gap</i>	252
(ASY247) PAUL D., JAYAPRAKASH K.R. <i>Nonlinear Oscillations of an Elastica Between Cylindrical Boundaries</i>	254
(ASY182) SALAMON R., SYPNIEWSKA-KAMIŃSKA G., KAMIŃSKI H. <i>Application of Multiple Scales Method to the Problem of Plane Pendulum Motion with Extended Damping Model</i>	256
(ASY249) SYPNIEWSKA-KAMIŃSKA G., AWREJCEWICZ J. <i>Identification of the Model Parameters Based on the Ambiguous Branches of Resonance Response Curves</i>	258
(ASY326) UDALOV P., POPOV I., LUKIN A. <i>Estimation of the Amplitudes of Parametric Oscillations of a Hemispherical Solid-Wave Gyroscope</i>	260
(ASY342) ZAVOROTNEVA E., LUKIN A., POPOV I. <i>Nonlinear Dynamics of Disk-Based MEMS Coriolis Vibrating Gyroscope Under Parametric Excitation of Vibrations</i>	261
(ASY66) ZIMMERMANN K., ZEIDIS I., GAST S., PREM N., ODENBACH S., GOWDA D.K. <i>An Approach to the Modeling and Simulation of Multi-Layered and Multi-Stimulable Material for Application in Soft Robots</i>	265
 REGULAR SESSION (ID: BIF)	
(BIF184) BLACKMORE D. <i>Generalized Neimark-Sacker Bifurcations</i>	269

(BIF176) CAMERON S., ROBERTS S. <i>Governing Equation Construction for Critical Transitions in Langevin Type Neural SDEs</i>	271
(BIF266) CHOLEWA Ł., OPROCHA P. <i>On Dynamics of Lorenz Maps</i>	272
(BIF254) DE LEO R., YORKE J.A. <i>Infinite Towers in the Graph of a Dynamical System</i>	274
(BIF311) ELASKAR S., DEL RÍO E., SCHULZ W. <i>Evaluation of the Reinjection Process in Type V Intermittency</i>	276
(BIF77) EMELIANOVA A.A., NEKORKIN V.I. <i>Emergence of the Third Type of Chaos in a System of Adaptively Coupled Kuramoto Oscillators</i>	278
(BIF2) GAIKO V. <i>Global Dynamics of a Polynomial Mechanical System</i>	279
(BIF363) GLUSHKOV A.V., TSUDIK A.V., DUBROVSKY O.V., MYKHAILOV O.L. <i>Nonlinear Dynamics of Relativistic Backward-Wave Tube: Chaos, Bifurcations and Strange Attractors</i>	281
(BIF205) IARRICCIO G., ZIPPO A., PELLICANO F. <i>Complex Dynamics of Thin Shallow Spherical Caps</i>	283
(BIF198) KUDRA G., WITKOWSKI K., SETH S., POLCZYŃSKI K., AWREJCEWICZ J. <i>Parametric Vibrations of a System of Oscillators Connected with Periodically Variable Stiffness</i>	285
(BIF104) LACERDA J.C., FREITAS C., MACAU E. <i>Multistability in Remote Synchronization Detected via Symbolic Dynamics</i>	287
(BIF195) MAAITA J.-O., PROUSALIS D., VOLOS CH., MELETLIDOU E. <i>The Dynamics of Two Coupled Oscillators with the Same Damping Term</i>	289
(BIF82) MAGNITSKII N. <i>Dynamical Chaos in Hamiltonian Systems with Three Degrees of Freedom</i>	291
(BIF75) MARTSENYUK V., AUGUSTYNEK K., URBAŚ A. <i>On Qualitative Analysis of the Model of Two-Link Manipulator with Time Delays: Stability, Bifurcation and Transition to Chaos</i>	292

(BIF367) MASHKANTSEV A.A., KIR'YANOV S.V., GLUSHKOV A.V., SVINARENKO A.A., BUYADZHI V.V. <i>Nonlinear Dynamics of Semiconductor Lasers and Optical Resonator Systems: Chaos, Bifurcations and Attractors</i>	294
(BIF65) NGUYEN-THAI M.-T., WULFF P., GRÄBNER N., VON WAGNER U. <i>On the Dynamics of a 2-DOF Nonlinear Vibratory System with Bistable Characteristic and Circulatory Forces</i>	296
(BIF109) OGIŃSKA E., GRZELCZYK D., AWREJCEWICZ J. <i>Research of the Dynamics of a Physical Pendulum Forced with an Electromagnetic Field</i>	298
(BIF227) RUCHKIN A., RUCHKIN C. <i>Method of Adaptive Bacterial Foraging Optimization for Detection and Locating Periodic and Multi-Periodic Orbits</i>	300
(BIF91) RUZZICONI L., JABER N., KOSURU L., BELLAREDJ M.L., YOUNIS M.I. <i>Internal Resonance Induced in the Impacting Dynamics in a MEMS Device</i>	302
(BIF34) SKURATIVSKYI S., KUDRA G., WITKOWSKI K., WASILEWSKI G., AWREJCEWICZ J. <i>Nonlinear Dynamics of Forced Oscillator Subjected to a Magnetic Interaction</i>	304
(BIF172) SOSNA P., HADAS Z. <i>Bifurcation Analysis of Nonlinear Piezoelectric Vibration Energy Harvester</i>	306
(BIF79) STOJANOVIC Z., PELIN D. <i>Increase in Current Stresses of the Boost Converter Due to Border Collision Bifurcation</i>	308
(BIF183) TOSYALI E., AYDOGMUS F. <i>Chaos in Thirring Model</i>	310
(BIF377) TSUDIK A.V., DUBROVSKY O.V., TERNOVSKY V.B., BUYADZHI V.V., BILAN I.I. <i>Chaos and Bifurcations in a Nonlinear Dynamics of Chain of the Backward-Wave Tubes: Numerical Analysis</i>	312

REGULAR SESSION (ID: CON)

(CON203) ANANIEVSKI I. <i>Damping of Vibrations of an Elastic Beam by Means of an Active Dynamic Damper in the Presence of Disturbances</i>	317
---	-----

(CON156) ANGULO-GARCÍA D., ANGULO F. <i>Control of Microrgrid Synchronization Based on Feedback Control and Optimization Techniques</i>	319
(CON41) BARTOS M.Á., HABIB G. <i>Hybrid Vibration Absorber for Self-Induced Vibration Mitigation</i>	321
(CON159) CAPEANS R., ALFARO G., SANJUAN M.A.F. <i>Partial Control and Beyond: Forcing Escapes and Controlling Chaotic Transients with the Safety Function</i>	323
(CON128) DĘBOWSKI A., FARYŃSKI J., ŻARDECKI D. <i>Reference Models of the 4WS Vehicle Lateral Dynamics for the Synthesis of Steering Algorithms</i>	324
(CON98) GIDLEWSKI M., JEMIOŁ L., ŻARDECKI D. <i>Modeling and Simulation of the Automated Lane Change Process, Taking Into Account Freeplay and Friction in the Vehicle Steering System</i>	326
(CON105) GIDLEWSKI M., JEMIOŁ L., ŻARDECKI D. <i>Model Based Investigations of an Integrated Control System for Automatic Lane Change in Critical Conditions</i>	328
(CON368) GLUSHKOV A.V., TERNOVSKY V.B., MYKHAILOV O.L., TSUDIK A.V. <i>Optimal Control of Resonance Radiation Processes in Laser Isotopes Separation Systems and Devices</i>	330
(CON160) GRACZYKOWSKI C., FARAJ R. <i>Predictive Control of Semi-Active Fluid-based Dampers Under Impact Excitation</i>	332
(CON166) GREBOGI C. <i>Predicting and Controlling Tipping Points in Networked Systems</i>	334
(CON259) ISMAIL M., CHALHOUB N., PILIPCHUK V. <i>Dynamics and Control of a Two-Ship Ensemble</i>	335
(CON318) KIRROU I., BICHRI A., BELHAQ M. <i>Quasiperiodic Energy Harvesting in a Delayed and Excited Rayleigh-Duffing Harvester Device Near Secondary Resonances</i>	337
(CON85) KOSIARA A., SKURJAT A. <i>Development and Research of a New Type of Vibration Reduction System for Wheel Bucket Loaders</i>	339
(CON59) KULIŃSKI K., PRZYBYLSKI J. <i>Nonlinear Vibrations of a Sandwich Piezo-Beam System under Piezoelectric Actuation</i>	341

(CON61) LATOSIŃSKI P., BARTOSZEWICZ A. <i>Reference Model Trajectory Tracking in Continuous-Time Sliding Mode Control.....</i>	343
(CON244) MAMAEV I.S., KARAVAEV YU.L., SHESTAKOV V.A. <i>Analysis of Non-Slipping Conditions for Omni Wheels Based on Investigations of the Dynamics of a Highly Maneuverable Mobile Robot</i>	345
(CON214) MIROSŁAW M., DEDA J., MIROSŁAW T. <i>The Modelling of Breaking Control of Electric Vehicle.....</i>	347
(CON215) MIROSŁAW M., DEDA J., MIROSŁAW T. <i>The Modelling of Autonomous Control with Hazard of Measurement Noise and Errors.....</i>	349
(CON239) OUNIS H.M., ABDEDDAIM M., OUNIS A. <i>Design Approach for Isolated Buildings in Adequacy with Algerian Regulations and Their Comparison with Several International Codes.....</i>	350
(CON49) PASZKOWIAK W., PELIC M., BARTKOWIAK T. <i>Neural Network Modelling for Steering Control of an Automated Guided Logistic Train</i>	353
(CON330) PAULET-CRAINICEANU F., FLOREA V., LUCA S.G., PASTIA C., ROSCA O.V. <i>Analysis of Practical Application Aspects for an Active Control Strategy to Civil Engineering Structures</i>	355
(CON351) PILIPCHUK V., POLCZYŃSKI K., BEDNAREK M., AWREJCEWICZ J. <i>Energy Flow Control in a System of Coupled Pendulums Using Magnetic Field.....</i>	357
(CON136) PROCHOWSKI L., SZWAJKOWSKI P., ZIUBIŃSKI M. <i>Can the Prognosis of the Results of the Crash be the Basis to Steering the Autonomic Vehicle with the Trailer in the Critical Situation.....</i>	359
(CON210) SCHORR P., EBNET M., ZIMMERMANN K., BÖHM V. <i>Dynamic Modeling of a Rolling Tensegrity Structure with Spatially Curved Members</i>	361
(CON84) SKURJAT A., KOSIARA A. <i>Individual Wheel Braking as a Method for Increasing Velocity of Articulated Vehicles.....</i>	362
(CON13) SOKÓŁ K., PIERZGALSKI M. <i>Vibrations of an Active Rocker – Bogie Suspension Under Motion in Rough Terrain.....</i>	364

(CON325) SONI T., DUTT J.K. <i>Viscoelastic Material Models Based Active Vibration Controllers: An Energy Approach</i>	366
(CON308) VINOD V., BIPIN B. <i>Strategies for Amplitude Control in a Ring of Self-Excited Oscillators</i>	368
(CON54) YE K., JIANG J. <i>Experimental Research on Active Vibration Control of Elastic Plate and Damage Degradation of Actuator</i>	371
(CON237) ZANA R., ZELEI A. <i>Experimental Evaluation of an Underactuated Inverse Dynamics Control Approach based on the Method of Lagrange-Multipliers</i>	373

REGULAR SESSION (ID: ENG)

(ENG120) AMBROŹKIEWICZ B., LITAK G., GEORGIADIS A., SYTA A., MEIER N., GASSNER A. <i>Study on Dynamical Response of Double-Row Self-Aligning Ball Bearing (SABB) Considering Different Radial Internal Clearance (RIC)</i>	377
(ENG224) AMS A. <i>Simulation of Road Surface Profiles by a Stochastic Parametrical Model</i>	378
(ENG374) BAKUNINA E.V., DYKYI O.V., VITAVETSKY A.V. <i>Nonlinear Dynamics of Chaotic Optical Communication Systems: Signal Processing and Cybersecurity</i>	380
(ENG174) BIELSKI W., KOWALCZYK P., WOJNAR R. <i>Two-Temperature Heat Transfer in a Metal and a Longitudinal Elastic Wave Generation</i>	382
(ENG213) BÖHM V., SCHORR P., CHAVEZ J., ZENTNER L. <i>Structural Analyses of Compliant Tensegrity Towers</i>	384
(ENG280) BOUNTIS T., KALOUDIS K., SHENA J., SKOKOS CH., SPITAS CH. <i>Energy Transport in 1-Dimensional Oscillator Arrays with Hysteretic Damping</i>	385
(ENG122) EL HANKARI S., DKIOUAK R., ROKY K. <i>Resonance and Cancellation Phenomena of Simply Supported Partially Clamped Beams: Application to Bridges with Ballasted Track</i>	386
(ENG100) KANDIRAN E., HACINLIYAN A. <i>Continuous Dynamical Systems as Pseudo Random Number Generator</i>	387

(ENG63) KECIK K., MITURA A. <i>Modelling of an Electromechanical Coupling in Magnetic Levitation Energy Harvester</i>	388
(ENG78) KECIK K., MITURA A. <i>Nonlinear Dynamics of a 2DoF Magneto-Mechanical Harvester</i>	390
(ENG271) KŁODA Ł., LENCI S., WARMIŃSKI J., SZMIT Z. <i>Transversal-Transversal Internal Resonances in Planar Timoshenko Beams with an Elastic Support</i>	392
(ENG89) KRÁLIK J. <i>Probabilistic Analysis of NPP Seismic Load Considering the Local Site Effects</i>	394
(ENG361) LOVSKA A., FOMIN O., SZYMANSKI G.M., SKURIKHIN D. <i>Determination of the Loading of an Open Car with Filler in the Center Sill</i>	396
(ENG245) NOSAL P., GANCZARSKI A. <i>Application of the Discrete Element Method to Ductile Materials Subjected to Dynamic Loads</i>	398
(ENG111) POLCZYŃSKI K., BEDNAREK M., AWREJCEWICZ J. <i>Magnetic Oscillator Under Excitation with Controlled Initial Phase</i>	400
(ENG217) RYSAK A., SEDLMAYR M. <i>Application of the Differential Transform Method to the Study of the Duffing System with Fractional Damping and Stiffness</i>	402
(ENG153) SEMENYUK V., MARTSENYUK V., LINGUR V., KAZAKOVA N., PUNCHENKO N., FALAT P., WARWAS K. <i>A Method to Improve the Accuracy of Bridge Cranes Overload Protection Using the Signal Graph</i>	404

REGULAR SESSION (ID: EXP)

(EXP353) ADAMSKI P., OLEJNIK P. <i>Drive-by-Wire of a Converted into Electric Car Syrena 105 Enabling Hardware-In-Loop Tests of Driving</i>	409
(EXP332) ARSLAN K., GUNES R. <i>Evaluation of Stress Wave Propagation in Particle-Reinforced Metal Matrix Composites</i>	411

(EXP117) AUGUSTYNIAK J., PERKOWSKI D.M., ZGŁOBICKA I. <i>Gas Bubble Trajectory in Nanofluid</i>	413
(EXP17) BAJKOWSKI J.M., BAJKOWSKI J. <i>Application of Bulk Granules as a Damping Material for Sports Boards</i>	415
(EXP69) BARSKI M., STAWIARSKI A., ROMANOWICZ P., AUGUSTYN M. <i>Impact of Fiber Orientation Angle on the Phase Velocity of the Fundamental Elastic Wave Modes in Composite Plates of Angle-Ply Configuration</i>	417
(EXP277) BOROWIEC A., SZYNAL D., SZYSZKA Ł. <i>Measurement of Dynamic Parameters of Composite Columns</i>	419
(EXP366) BUYADZHI V.V, IGNATENKO A.V., DUBROVSKAYA Y.V., FLORKO T.A. <i>Damage Dynamics of Engineering Systems Under Varying Operational Conditions: Numerical Analysis and Modelling</i>	421
(EXP295) CHAMBE J.-E., CHARLOTTE M., GOURINAT Y. <i>Vibration Analysis of a Fully- and Partially-Filled Container – Application to Cryogenic Tank Characterization and Dynamic Behaviour</i>	423
(EXP219) DIAS J., MACAU E. <i>A New Index for Topological Vulnerability in Power Transmission Networks</i>	425
(EXP199) DUMA V.-F., HUTIU G., DIMB A.-L., DEMIAN D., BRADU A., PODOLEANU A. <i>Roughness Evaluations for Metallic Parts Using Optical Coherence Tomography (OCT)</i>	427
(EXP309) GIDLEWSKI M., PROCHOWSKI L., JEMIOŁ L., ZIUBIŃSKI M. <i>The Course of the Process of a Motor Car Frontal Impact Against Various Places of the Second Vehicle's Body Side and its Results</i>	428
(EXP338) GIDLEWSKI M., PUSTY T., JEMIOŁ L., KOCHANEK H. <i>Determination of Physical Quantities Describing the Movement of Objects Involved in a Frontal-Side Collision of Vehicles</i>	430
(EXP236) HOUDEK V., KUBÍN Z., SMOLÍK L. <i>Impact Point Localization with the Use of Wavelet Transform</i>	432
(EXP168) JASKOT A., POSIADAŁA B. <i>Modelling of Motion and Experimental Studies of a Four-Wheeled Mobile Robot Considering Slip Occurrence</i>	434
(EXP339) LUTY W., PUSTY T. <i>Analysis of Dynamic Characteristics of Vehicle Steerability in the Context of its Diagnostics and Evaluation of Dynamic Properties</i>	436

(EXP180) MILEWICZ J., NOWAKOWSKI T., SZYMAŃSKI G.M. <i>Determination of Dynamic Parameters of Parts of a Tram Wheel in a Numerical and Experimental Modal Analysis</i>	438
(EXP360) MOKRZAN D., NOWAKOWSKI T., SZYMAŃSKI G.M. <i>The Application of Time-Frequency Methods of Acoustic Signal Processing in the Diagnostics of Tram Drive Components</i>	440
(EXP55) NISHIYAMA N., YAMASHITA K. <i>Simple Suppression Method of Impact Oscillations Between a Pantograph and an Overhead Rigid Conductor Line</i>	442
(EXP268) POSTEK E., SADOWSKI T. <i>Compressive Impact of Sic Foam</i>	444
(EXP296) SHI L., BAI H., KHALIJ L. <i>Uncertainty Evaluation by the Bootstrap for the Staircase Fatigue Limit Test Data</i>	446
(EXP67) STAWIARSKI A., CHWAŁ M., BARSKI M., ROMANOWICZ P. <i>On the Effectiveness of Infrared Thermography in the Detection of the Fatigue Damage Initiation in a Composite Plate with a Hole</i>	448

REGULAR SESSION (ID: LIF)

(LIF349) BEŁDOWSKI P., WEBER P., GADOMSKI A., DOMINO K., PRASAD R. <i>Interaction of Albumin with Chondroitin Sulphate IV and VI, a Molecular Docking Study</i>	453
(LIF262) BIRNIR B. <i>The Probability of Infection, through Aerosol Transmission, by SARSCoV-2 Coronavirus</i>	455
(LIF383) DZYUBAK L., DZYUBAK O., AWREJCEWICZ J. <i>Conditions Regulating Tumor Cell Behaviour in Biological Systems with Memory of States</i>	457
(LIF362) GLUSHKOV A.V., KHETSELIUS O.Y., STEPANENKO S.M., SVINARENKO A.A., IGNATENKO A.V. <i>Chaos in Environmental Radioactivity Dynamics of Some Geosystems: Analyses of the Radon Time Series</i>	459
(LIF23) GRZELCZYK D., JARZYNA O., AWREJCEWICZ J. <i>Design and Simulation of a Lower Limb Exoskeleton with Linear Electric Actuators</i>	461

(LIF336) HEDRIH (STEVANOVIĆ) K., HEDRIH A. <i>Nonlinear Oscillations of a Complex Discrete System of Rigid Rods with Mass Particles on an Elastic Cantilever</i>	463
(LIF276) JAILLET A., RIVIERE P., CARTON X. <i>Influence of Periodic Nutrient Advection on a Simple Ecosystem</i>	465
(LIF230) KIZILOVA N. <i>Nonlinear Dynamics, Stability and Control Strategies: Mathematical Modeling on the Big Data Analyses of Covid-19 in Poland</i>	467
(LIF188) MROZEK A., STRĘK T. <i>Design of Auxetic Damper for Lower Limb Prosthesis</i>	469
(LIF384) PAVLENKO V., SHAMANINA T., CHORI V. <i>Nonlinear Dynamic Model of the Oculo-Motor System Human based on the Volterra Series</i>	471
(LIF137) PROCHOWSKI L., ZIUBIŃSKI M., DZIEWIECKI K., SZWAJKOWSKI P. <i>Impact Energy versus the Hazards for the Occupants During a Front-To-Side Vehicles' Collision</i>	473
(LIF189) RANGARAJAN A.M., KRISHNAN J., SCHUPPERT A. <i>Predicting Future from COVID-19 Time Series Data Using Polynomial Extrapolation</i>	475
(LIF220) SEKHANE D., MANSOUR K. <i>Heart Rate Effects on Intracranial Aneurysm Hemodynamic</i>	478
(LIF124) SEYOUM W., MENGESTIE T., BONET J. <i>Power Bounded and Uniformly Mean Ergodic Composition Operators on Large Class of Fock Spaces</i>	480
(LIF140) VALANI R., HARDING B., STOKES Y. <i>Bifurcations in Inertial Focusing of Particles in Curved Rectangular Ducts</i>	482
(LIF347) WEBER P., BEŁDOWSKI P., GADOMSKI A., DOMINO K., LEDZIŃSKI D. <i>Interaction of Mucin with Glycosaminoglycans in Water Environment</i>	484
(LIF204) ZAJCSUK L., ZELEI A. <i>Correlation of Biomechanic Performace Measures with Acceleration and Deceleration in Human Overground Running</i>	486

REGULAR SESSION (ID: MAT)

(MAT265) ANDRIANOV I.V., AWREJCEWICZ J., STARUSHENKO G.A., KVITKA S.A.
Thermal Waves in Composite Membrane with Circular Inclusions in Hexagonal Lattice Structures 491

(MAT333) ARSLAN K., GUNES R.
Low-Velocity Impact Response of Metal-Ceramic Functionally Graded Plates: a Novel Numerical Modelling Approach..... 493

(MAT150) AUGUSTYNEK K., URBAŚ A., MARTSENYUK V.
Dynamics Analysis of the Spatial Mechanism with Imperfections in the Fifth-Class Kinematic Pairs 495

(MAT200) AWREJCEWICZ J., MAZUR O.
Geometrically Nonlinear Vibrations of Double-Layered Nanoplates..... 497

(MAT121) FENDZI-DONFACK E., TCHEPEMEN N.N., TALA-TEBUE E., KENFACK-JIOTSA A.
On Alphabetical Shaped Soliton for Intrinsic Fractional Coupled Nonlinear Electrical Transmission Lattice Using Sine-Cosine Method 499

(MAT26) FLOSI J., SAVADKOOHI T.A., LAMARQUE C.-H.
Normal Form on Nonlinear Systems and Gröbner Based Exploitation of Resonances..... 501

(MAT301) GOGILAN U., OVEISI A., NESTOROVIĆ T.
Implementation of State Observer-Based Conditioned Reverse Path Method to the Identification of a Nonlinear System..... 503

(MAT356) HAN X., PAGNACCO E.
The Response of Nonlinear Dynamic Systems via Wavelet-Galerkin Method in the Time-Frequency Domain 505

(MAT73) HERISANU N., MARINCA V.
Dynamic Response of Simply-Supported Euler-Bernoulli Beam on Nonlinear Elastic Foundation Under a Moving Load..... 507

(MAT76) HERISANU N., MARINCA V.
Nonlinear Vibration of a Functionally Graded Beam on Winkler-Pasternak Foundation Under a Moving Force..... 509

(MAT380) HUYNH H., KLOEDEN P.E., PÖTZSCHE CH.
Pullback and Forward Dynamics of Nonautonomous Integrodifference Equations: Basic Constructions..... 511

(MAT112) JIMENEZ O.S., PAGNACCO E., DE CURSI E.S., SAMPAIO R. <i>Study of the Stochastic Response of an Offshore Pile to a Combined Morison Force Induced by Current and Turbulence</i>	513
(MAT364) KHETSELIUS O.Y., GLUSHKOV A.V., STEPANENKO S.M., SVINARENK A.A, BUYADZHI V.V. <i>Advanced Complex Plane Field and Differential Equations Approach to Nonlinear Dynamics of the Industrial City's Chaotic Atmospheric Ventilation</i>	514
(MAT163) KILIN A., PIVOVAROVA E. <i>Dynamics of the Chaplygin Sphere on a Moving Plane</i>	516
(MAT371) KIR'YANOV S.V., TERNOVSKY E.V., NOVAK D.A., BILAN I.I. <i>Nonlinear Chaotic Dynamics of Laser Diodes with an Additional Optical Injection: Dynamical and Topological Invariants</i>	518
(MAT235) KIZILOVA N., RYCHAK N. <i>Optimal Strategies for Water Management and Self-Restoration of the Ecosystems: Nonlinear Dynamics, Stability and Controllability</i>	520
(MAT209) LESZCZYŃSKI J. <i>Sensitivity Analysis of Granular Dynamics by the Use of Unique DEM</i>	522
(MAT253) LOZI R., MENACER T., CHEN G., ZAAMOUNE F. <i>Maximal Attractor Range of Multiscroll Chaotic Attractors: Classification of Symmetries in Hidden Bifurcation Routes</i>	524
(MAT294) MINGLIBAYEV M., ZHUMABEK T., PROKOPENYA A. <i>New Non-Stationary Solutions of the Restricted Three-Body Problem</i>	526
(MAT86) MODZELEWSKA R., KRASIŃSKA A., WAWRZASZEK A., GIL A. <i>Scaling Features of Cosmic Rays, Solar, Heliospheric and Geomagnetic Data</i>	528
(MAT152) NAKONECHNYI O., MARTSENYUK V., KŁOSWITKOWSKA A., SHEVCHUK I. <i>On Minimax Parameter Estimation of Nonlinear Dynamic Brown's Model for Enzyme-Substrate Interaction with Distributed Delay</i>	530
(MAT357) NTAOULAS N., DRAKOPOULOS V. <i>Fractal Techniques Associated with Steganography</i>	532
(MAT212) OSIKA M., RADECKI R., ZIAJA-SUJDAK A., STASZEWSKI W.J. <i>An Insight into Amplitude-Depended Modulation Transfer Due to Nonlinear Shear Wave Interaction with Contact Interfaces</i>	535
(MAT211) RADECKI R., ZIAJA-SUJDAK A., OSIKA M., STASZEWSKI W.J. <i>Numerical and Theoretical Investigations of Modulation Transfer Due to Nonlinear Shear Wave Interaction at Frictional Interfaces</i>	537

(MAT123) RDZANEK W. <i>The Effect of a Shaker on the Resonance Frequencies of a Circular Plate</i>	539
(MAT110) REYES P.S., PAGNACCO E., SAMPAIO R. <i>Taking into Account Uncertainties in Non-Linear Dynamical Systems with Nonlinear Energy Sinks (NES)</i>	541
(MAT382) SAKKARAVARTHI K., KANNA T. <i>Controllable Optical Rogue Waves by Modulated Coherent-Incoherent Nonlinearities in Inhomogeneous Fiber</i>	542
(MAT178) STRELBITSKYI V., RAJBA S., PUNCHENKO N., KAZAKOVA N., SZKLARCZYK R., ZIUBINA R. <i>Development of a Mathematical Model for the Functioning of a River Port Discharge Point</i>	544
(MAT27) SZEMELA K., RDZANEK W., WICIAK J., TROJANOWSKI R. <i>Sound Radiation by a Circular Plate Located on a Wall of Rectangular Semi-Infinite Waveguide</i>	546
(MAT297) TRĘBICKA A. <i>Mathematical Modeling and Analysis of Dynamic Changes in the Water Distribution System</i>	547
(MAT144) URBAŚ A., AUGUSTYNEK K., MARTSENYUK V. <i>The Influence of the Load Modeling Methods on Dynamics of a Mobile Crane</i>	549
(MAT243) WAGNER G., SAMPAIO R., LIMA R. <i>Benefits of Observer/Kalman Filter Identification in System Realization with Low Amount of Samples</i>	551
(MAT9) WANG J., VAN HORSSSEN W.T. <i>On Longitudinal Oscillations in a Hoisting Cable with Time-Varying Length Subject to a Nonclassical Boundary Condition</i>	553
(MAT328) WNUK M., ILUK A. <i>Estimation of Resonance Frequencies for Systems with Contact Using Linear Dynamics Methods</i>	555
(MAT291) XIA Z., ISHIKAWA Y., KANEKO S., KUSAKA J. <i>Development of a Cardiovascular Mathematical Model Considering the Thermal Environment</i>	557
(MAT316) YAKUBU G., OLEJNIK P., AWREJCEWICZ J. <i>Mathematical Modelling of an extended Swinging Atwood Machine</i>	559

(MAT4) ZHURAVLOVA Z. <i>Method of Inversion of Laplace Transform in Some Problems of Dynamic Elasticity</i>	561
(MAT312) ZSIROS A., LIGETI Z. <i>Dynamics of an Economic Growth Model with New Stylized Facts</i>	563
(MAT113) ŽARDECKI D. <i>Non-Smooth Models of Wheel-Road Interactions Based on Piecewise-Linear Luz(...) and Tar(...) Projections</i>	565
REGULAR SESSION (ID: MTR)	
(MTR96) BRYKCZYŃSKI M., HARLECKI A. <i>Dynamics Analysis of Hand Wheel Actuator in Steer-By-Wire Electric System of Car</i>	569
(MTR29) DINDORF R., WOŚ P. <i>Study of an Electro-Hydraulic Servo Actuator Flexibly Connected to a Boom Manipulator Mounted on a Jaw Crusher</i>	570
(MTR229) KALIŃSKI K.J., STAWICKA-MORAWSKA N., GALEWSKI M.A., MAZUR M.R. <i>Using the Experiment-Aided Virtual Prototyping Technique to Predict the Best Clamping Stiffness During Milling of Large-Size Details</i>	572
(MTR221) MARTOWICZ A., ZDZIEBKO P., ROEMER J., ŻYWICA G., BAGIŃSKI P. <i>Numerical and Experimental Characterization of the Temperature Profile in a Gas Foil Bearing</i>	574
(MTR97) ODRY Á., KECSKES I., ODRY P. <i>Accuracy Improvement of 3D Position Estimation of Mobile Robots Based on IMU Measurements and NNs</i>	576
(MTR260) ROGALA P., OLEJNIK P., AWREJCEWICZ J. <i>Construction and 3D Model of Stand for Investigating a Non-Ideal Forcing in a Nonlinear Chain Dynamics of Self-Excited Oscillators with Friction</i>	578
(MTR108) SENCEREK J., ZAGRODNY B. <i>Bionic Hand Control Using EMG Signals</i>	580
(MTR173) WOS P., DINDORF R. <i>Hydraulic Levelling Control System Technology of Bricklaying Robot</i>	582

REGULAR SESSION (ID: NON)

(NON119) ANTALI M.
Dynamics of Railway Wheelsets with a Nonsmooth Contact Force Model 587

(NON317) BIBER S.W., CHAMPNEYS A.R., SZALAI R.
Non-Smooth Dynamics of a Bouncing Golf Ball..... 589

(NON64) DĘBOWSKI A., ŻARDECKI D.
Modeling and Simulation of Friction Processes with Applications of Piecewise-Linear Luz(...) and Tar(...) Projections 591

(NON134) KUMAR P., NARAYANAN S.
Nonlinear Dynamics of Dry Friction Oscillator Subjected to Combined Harmonic and Random Excitation..... 593

(NON242) LIMA R., SAMPAIO R.
Analysis of the Dynamics of an Electromechanical System Subjected to Two Orthogonal and Interdependent Dry-Friction Forces..... 595

(NON307) MAHESHWARI S., MURALIDHARAN A., ALI S.F., LITAK G.
A Vibro-Impact Oscillator Based Energy Harvester 597

(NON323) PREMCHAND V.P., BIPIN B., MANI A.K., SAJITH A.S., NARAYANAN M.D.
A New Method to Determine Periodic Solutions in Discontinuous Systems with Application to Mass on Moving Belt 599

REGULAR SESSION (ID: NUM)

(NUM68) AFRAS A., EL GHOULBZOURI A.
Non-linear dynamics analysis of elastically supported beam under moving loads 603

(NUM81) AKAY M.S., SHAW A.D., FRISWELL M.I.
Continuation Analysis of Overhung Rotor Bouncing Cycles with Smooth and Contact Nonlinearities..... 605

(NUM299) BAI H., SHI L., HUANG CH., LEMOSSE D.
A Neural Network Based Surrogate Model for Assessing Vibration Induced Fatigue Damage on Wind Turbine Tower..... 607

(NUM257) BOROWIEC A.
Localization of Changes in Stiffness in Numerical Models of Beams Using Additional Masses 609

(NUM315) DOHNAL F., CHASALEVRIS A. <i>Estimation of Orbits After Blade Loss for a Multi-Disk Rotor</i>	611
(NUM358) EBADI-JAMKHANEH M., AHMADI M., KONTONI D.-P.N. <i>Seismic Response of Adjacent Steel Frames Linked by Friction Dampers.....</i>	613
(NUM359) EBADI-JAMKHANEH M., AHMADI M., KONTONI D.-P.N. <i>Deficient RC Slabs Strengthened with Combined FRP Layer and High-Performance Fiber-Reinforced Cementitious Composite</i>	615
(NUM375) GLUSHKOV A.V., KHETSELIUS O.Y., MANSARLIYSKY V.F., VITAVETSKY A.V. <i>Advanced Computational Modelling Complex Dynamical Systems: the Earth Angular Momentum Balance Nonstationary Model</i>	617
(NUM140) HOLL H.J. <i>Simulation of Non-Linear Coupled Dynamic Systems of First and Second Order Applying A Semi-Analytic Method.....</i>	619
(NUM365) KHETSELIUS O.Y., DUBROVSKY O.V., SERGA I.N., SERGA R.E. <i>Study of Nonlinear Dynamics of Complex Chaotic Systems: Combined Chaos-Geometric and Neural Networks Algorithms</i>	621
(NUM241) RUCHKIN A., RUCHKIN C. <i>A Multi-Agent Computer Program for Automatic Investigation the Behavior of a Nonlinear Dynamic System in Real-Time.....</i>	623
(NUM169) SERFŐZŐ D., PERE B. <i>Numerical Investigation of Dynamic Contact Problems using Finite Element Method.....</i>	625
(NUM146) SHMATKO T., KURPA L., AWREJCEWICZ J. <i>Dynamic Analysis of Functionally Graded Sandwich Shells Resting on Elastic Foundations</i>	627
(NUM303) SHMATKO T. <i>Effect of Porosity on Free Vibration of FG Shallow Shells with Complex Planform.....</i>	629
(NUM3) SIDOROV V.N., BADINA E.S. <i>Nonlocal Damping Model in Finite Element Structural Vibration Analysis</i>	631
(NUM234) SMOLÍK L., RENDL J., BULÍN R. <i>Evaluation of Forces in Dynamically Loaded Journal Bearings Using Feedforward Neural Networks</i>	633
(NUM126) WASZCZUK-MŁYŃSKA A., RADKOWSKI S., MAĆZAK J. <i>Application to of Hilbert Transforms Moments Analysis of Vibration Signals.....</i>	635

REGULAR SESSION (ID: OPT)

(OPT118) BODZIOCH M., FORYŚ U.
Anti-Angiogenic and Chemotherapy Scheduling Optimisation using Mathematical Modelling..... 639

(OPT25) BROCIK R., WAJDA A., SŁOTA D.
Comparison of Selected Artificial Intelligence Algorithms to Deter-Mine the Thermal Conductivity Coefficient of a Porous Material 641

(OPT283) CHEN X., PRUCHNICKI E., DAI H.H.
A New Type of Undimensional Optimized Model for Rod Deduced from Three Dimensional Elasticity 643

(OPT6) CHERKASOV O., MAKIEVA E., MALYKH E.
About the Target-Attacker-Defender Optimal Problem 645

(OPT7) CHERKASOV O., SMIRNOVA N.
Brachistochrone Problem with State Constraints of a Certain Type..... 647

(OPT28) CHMIELOWSKA A., BROCIK R., SŁOTA D.
The Reconstruction of the Heat Transfer Coefficient in the Fractional Stefan Problem..... 649

(OPT74) DUMA V.-F.
Laser Scanners with Rotational Polygon Mirrors: A Multi-Parameter Optomechanical Analysis and Optimization..... 650

(OPT255) FIEBIG W., DMOCHOWSKI A.
Optimization of the Two-Mass Oscillator regarding the Accumulation of Energy at Mechanical Resonance..... 651

(OPT114) FORYŚ U., BODZIOCH M.
Competition Between Populations: Preventing Domination of Resistant Population Using Optimal Control..... 653

(OPT12) GHIBAUDO J., AUCEJO M.
A Unified Bayesian Formulation for the Identification of Force Sources 655

(OPT373) GLUSHKOV A.V., PLISETSKAYA E.K., TERNOVSKY E.V., VITAVETSKY A.V.
Numerical Analysis, Processing and Prediction of a Populations Dynamics of Atomic Systems in a Laser Pulse Field: Quantum Dynamics and Bi-Stability Effects..... 657

(OPT300) HUANG CH., BAI H., SHI L., AOUES Y.
Optimization of Wind Turbine Tower Using Adaptive Algorithm Configuration 659

(OPT87) KLAERNER M., MARBURG S., KROLL L. <i>Optimisation Potentials of Laminated Composites Using Semi-Analytical Vibro-Acoustic Models</i>	661
(OPT155) KURZAWA A., PYKA D., BOCIAN M., JANKOWSKI L., BAJKOWSKI M., JAMROZIAK K. <i>Validation of Numerical Models Describing the Stress-Strain Characteristics in the Strength Tests of Composite Materials on a Metal Matrix Using the Elasto-Optic Method</i>	663
(OPT281) MILLER B., ZIEMIAŃSKI L. <i>Optimisation and State Identification of Composite Shell Using Deep Neural Networks</i>	665
(OPT324) PREMCHAND V.P., BIPIN B., MANI A.K., SAJITH A.S, NARAYANAN M.D. <i>Design of a Vibration Absorber System for Tremor Reduction in Parkinson Patients Using a Cluster Based Algorithm</i>	667
(OPT187) RÓWIENICZ Ł., MALCZYK P. <i>Parameter Identification for a Two-Axis Gimbal System and its Kinematic Calibration</i>	669

REGULAR SESSION (ID: STA)

(STA202) AGÚNDEZ A.G., GARCÍA-VALLEJO D., FREIRE E. <i>Analysis of the Influence of Tyre Cross-Sectional Parameters on the Stability of a Nonlinear Bicycle Model with Elliptical Toroidal Wheels</i>	673
(STA60) BÉDA P.B. <i>On Fractional Viscosity and Material Instability</i>	675
(STA171) BUDAI C. <i>On the Stability of Sampled-Data Systems with Dry Friction</i>	677
(STA62) CEKUS D., KWIATOŃ P. <i>Stability Analysis of Mobile Crane During Load Sway Induced by Wind</i>	680
(STA57) CHINDADA S., SNABL P., PROCHAZKA P., PRASAD CH.S., PESEK L. <i>Numerical Modelling of the Experimental Based High Frequency Subsonic Stall Flutter in Linear Blade Cascade</i>	682
(STA355) DIMOU E., CHASALEVRIS A., DOHNAL F. <i>Parametrically Excited Rotating Shafts on Gas Foil Bearings</i>	683

(STA92) GIESL P., HAFSTEIN S.F. <i>Lyapunov Functions by Interpolating Numerical Quadratures: Proof of Convergence</i>	685
(STA372) GLUSHKOV A.V., KUZNETSOVA A.A., PLISETSKAYA E.K., MYKHAILOV O.L., TERNOVSKY E.V. <i>Nonlinear Dynamics of Atomic Systems in a Free State and in an External Electromagnetic Field: Chaos and Attractors</i>	687
(STA44) GUENKA T.S.D.N., MACHADO M.R. <i>Influence of a Cracked Rod in the Dynamic of a Planar Slider-Crank Mechanism</i>	689
(STA47) HORVÁTH Á., BÉDA P. <i>On the Stability of a Slip Controlled Two-Axle Vehicle with Multiple Time-Delays</i>	691
(STA369) IGNATENKO A.V., TERNOVSKY V.B., SVINARENKO A.A., DUBROVSKAYA Y.V. <i>Nonlinear Dynamics of Molecular Systems in an External Electromagnetic Field: Classical and Quantum Treatment of Chaos and Strange Attractors</i>	693
(STA284) KRAUS Z., KAREV A., HAGEDORN P., DOHNAL F. <i>Enhancing Vibration Mitigation in a Jeffcott Rotor with Active Magnet Bearings Through Parameteric Excitation</i>	695
(STA238) MOLČAN M., FERFECKI P., ZAPOMĚL J. <i>A Computational Study of Vibration Attenuation of the Rotor System with Magnetorheological Squeeze Film Dampers</i>	697
(STA350) MUGHAL H., DOLATABADI N., RAHMANI R. <i>Effect of Gear Mesh Stiffness and Lubricant Nonlinearities on the Dynamic Response of Gear Transmission Systems</i>	698
(STA181) NIKIFOROVA I.V., METRIKIN V.S., IGUMNOV L.A. <i>Dynamics of Impulse Systems with Friction</i>	700
(STA18) PROKOPENYA A. <i>On Stability of Periodic Motion of the Swinging Atwood Machine</i>	702
(STA162) PUZYROV V., AWREJCEWICZ J., LOSYEVA N., SAVCHENKO N., NIKOLAIEVA O. <i>Estimation the Domain of Attraction for a System of Two Coupled Oscillators with Weak Damping</i>	704
(STA161) SELYUTSKIY Y., HOLUB A., LIN CH.-H. <i>Dynamics of a Multiple-Link Aerodynamic Pendulum</i>	706

(STA72) SNABL P., PESEK L., PRASAD CH.S. <i>Time-Variable Normal Contact Force Influence on Dry-Friction Damping of Self-Excited Vibration of Bladed Turbine Wheel</i>	708
(STA39) TOJTOVSKA B., RIBARSKI P. <i>Coupled System of Stochastic Neural Networks with Impulses, Markovian Switching, and Node and Connection Delays</i>	709
(STA185) TOSYALI E., AYDOGMUS F. <i>Dynamical Study of BEC with External Trapping Potential under Noise</i>	711
(STA193) UZNY S., ADAMEK F., KUTROWSKI Ł. <i>Free Vibrations of Two-Stage Hydraulic Cylinder</i>	713
(STA157) WIJATA A., STAŃCZYK B., AWREJCEWICZ J. <i>Anisotropic Friction Sliding Rule Influence on the Mechanical Systems Dynamics</i>	715
 REGULAR SESSION (ID: VIB)	
(VIB52) AFRAS A., EL GHOULBZOURI A. <i>Elastic Bearing Effects on the Dynamic Response of Bridges under High-Speed Moving Load</i>	719
(VIB378) ASTAYKIN D.V., BONDARENKO A.V., DANYLENKO D., DUBROVSKY O.V., TERNOVSKY E.V. <i>Stabilization of Course of Ships and Damping Vibrations Caused by Waves: Nonlinear Differential Equations Model and Optimal Control Theory</i>	721
(VIB269) AWREJCEWICZ J., ANDRIANOV I.I., DISKOVSKY A.A. <i>Higher Order Asymptotic Homogenization for Dynamical Problems</i>	723
(VIB208) BHARAT B., JAYAPRAKASH K.R. <i>Nonlocal Effects on the Dynamics of Carbon Nanotubes</i>	725
(VIB286) BYRTUS M. <i>Non-Synchronous Vibration in a Bistable System Induced by FSI</i>	727
(VIB125) CETIN H., OZTURK B., DUTKIEWICZ M., AYDIN E. <i>Design of an Optimum Tuned Mass Damper for Cantilever Beam Response Reduction</i>	729
(VIB175) DONEVA S., WARMIŃSKI J., MANOACH E. <i>Analytical and Finite Element Models of Nonlinear Dynamic Behaviour of Bi-Material Beam</i>	731

(VIB226) EREMEYEV V.A. <i>On the Surface Anti-Plane Waves in Media with Initial Surface Stresses</i>	733
(VIB186) FREUNDLICH J., SADO D. <i>Analytical Investigation of a Mechanical System Containing a Spherical Pendulum and a Fractional Damper</i>	735
(VIB302) FREUNDLICH J., SADO D. <i>The Effect of Damping on the Energy Transfer in the Spherical Pendulum with Fractional Damping in a Pivot Point</i>	737
(VIB290) HAJJAJ A.Z., ALFOSAIL F., THEODOSSIADES S. <i>Combined Internal Resonances of Slacked Micromachined Resonators</i>	739
(VIB341) INDEITSEV D., LUKIN A., POPOV I., SHTUKIN L. <i>Nonlinear Interaction between Longitudinal and Transverse Vibrations of a Microbeam under Periodic Opto-Thermal Excitation</i>	741
(VIB320) HARSHAN J., PREMCHAND V.P., REMIL G.T. <i>Vibration Isolation in Metamaterial Structures Embedded with Neoprene Resonators</i>	744
(VIB321) HARSHAN J., PREMCHAND V.P., REMIL G.T. <i>Analysing Vibration Attenuation Characteristics of Al 6061 Metamaterial Structures</i>	746
(VIB53) KANDEMIR E.C. <i>Fuzzy Logic Model to Determine Minimum Seismic Separation Gap</i>	748
(VIB196) KHAJIYEVA L., KUDAIBERGENOV A., KUDAIBERGENOV A., UMBETKULOVA A. <i>The Effect of Initial Stress on Nonlinear Lateral Vibrations of Rotating Rods</i>	749
(VIB322) KHAJIYEVA L., KUDAIBERGENOV A., SABIROVA Y. <i>Application of the Lumped-Parameter Method for Modelling Nonlinear Vibrations of Drill Strings with Complicating Factors</i>	751
(VIB225) ŁAGODZIŃSKI J., TKACZ E., KOZANECKI Z. <i>Determination of Global Damping and Stiffness Coefficients of Journal Foil Bearing</i>	753
(VIB278) LIPIŃSKI K. <i>Forced Vibrations in a Dynamic System Equipped with a Mechanism which Trans-Pass Through its Singular Position</i>	754
(VIB48) MACHADO M.R., DUTKIEWICZ M. <i>Broadband Vibration of a Beam under Tensile Load</i>	756

(VIB95) MACHADO M.R., DUTKIEWICZ M. <i>Spectral Analysis of Chimney Vibrations</i>	757
(VIB1) OLEJNIK P., GÓRNIAK VEL GÓRSKI A., CEBULAK M., AWREJCEWICZ J. <i>Influence of a Relatively High Frequency Structure Vibrations on the Dynamics of Real Stick-Slip Motion</i>	759
(VIB232) PLUTA M., TOKARCZYK D. <i>Measurements and Sound Synthesis of a Guitar String Re-Excitation</i>	761
(VIB116) PRZYBYLSKI J. <i>Control of Deformation and Transversal Vibrations of a Clamped Beam by Two Discretely Attached Monolithic Piezoelectric Rods</i>	763
(VIB165) PUZYROV V., AWREJCEWICZ J., LOSYEVA N. <i>Dynamics of Energy Harvesting Mechanical System in the Vicinity of 1:1 Resonance</i>	765
(VIB58) RUSINEK R., ZABLOTNI R. <i>Relaxation Effect in Implanted Human Middle Ear</i>	767
(VIB36) SANTOS J.C., MACHADO M.R., VERNIERES-HASSIMI L., KHALIJ L. <i>Vibration Characterisation of a Tubular Chemical Reactor</i>	769
(VIB264) SARBINOWSKI F., STAROSTA R. <i>Determination of Peak Efficiency of Galloping Energy Harvesters with Various Stiffness Characteristics</i>	771
(VIB207) TANDEL V., JAYAPRAKASH K.R. <i>Piecewise Linear Dynamics of a Cracked Beam with Hysteretic Damping</i>	773
(VIB370) TERNOVSKY E.V., MASHKANTSEV A.A., SVINARENKO A.A., ZAICHKO P.A. <i>A Nonlinear Interaction Dynamics of System of the Coupled Autogenerators: Numerical Analysis of Time Series, Chaos and Bifurcations</i>	775
(VIB240) VISHNU P.N., BHARAT B., JAYAPRAKASH K.R. <i>Dynamics of Rotating Cylindrical Shell Subjected to Pressure Loading</i>	777
(VIB127) WICIAK J., TROJANOWSKI R., LISTEWNIAK K. <i>Numerical Calculations of Target Strength for Large Scale Betssi Models</i>	779
(VIB88) YAMASHITA K., KITAURA K., NISHIYAMA N., YABUNO H. <i>Non-Planar Motions Due to Nonlinear Interactions Between Unstable Oscillatory Modes in a Cantilevered Pipe Conveying Fluid</i>	781

KEYNOTE SPEAKERS

Optimization of Sandwich Structures under Blast Loading

ROMESH C. BATRA

Department of Biomedical Engineering and Mechanics, Virginia Polytechnic Institute and State University,
Blacksburg, VA 24061, USA [ORCID: 0000-0002-7191-2547]

Abstract: Sandwich structures with stiff face sheets and a soft core have high specific energy absorbing characteristics that can be used either as standalone or as bumpers to protect valuable assets. Optimization of materials of the fiber-reinforced face sheets and of the core, their thicknesses, and fiber orientations subject to constraints of given total thickness and areal mass density results in a lightweight blast-resistant design. Challenging issues include characterization of the blast wave produced by detonating a charge, clamping conditions at the edges, failure criteria for different materials, measures of energy dissipated, validation of mathematical models, verification of numerical algorithms, consideration of geometric and material nonlinearities and of uncertainties in values of various parameters, and damage initiation and progression till ultimate failure. We will present team's work completed by using an equivalent single-layer third order shear and normal deformable plate theory, Tsai-Wu failure criteria, honeybee inspired Nest Site Selection Optimization (NESS) algorithm, and the finite element method.

Keywords: Doubly-curved sandwich shell, parameter uncertainties, ANOVA, progressive damage

1. Introduction

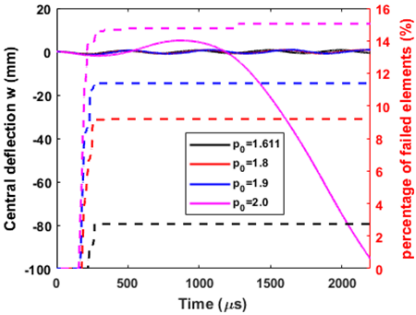
Sandwich structures have wide-ranging applications in civil, aerospace and automotive industries due to their high specific stiffness, strength and tailorability of material properties. Designing them optimally against extreme loads is challenging due to complex interactions among a large number of variables involved. It requires synthesizing results of deformations found using a plate theory, computing stresses from displacements, constitutive relations, and a stress-recovery scheme, identifying when and where a failure initiates first, progressively degrading material properties of a failed material point, and determining when a structure has collapsed. Reviewing the literature on these topics is beyond the scope of the abstract.

We have optimized transparent armor against low velocity impact using genetic algorithms [1], composite laminates with unidirectional fiber-reinforced plies for the first failure load [2] using the NESS, and one and two core sandwich structures exposed to blast loads with fiber-reinforced facesheets and either balsa wood, or honeycomb or foam core [3]. Whereas 3-dimensional (3D) deformations were analyzed in [1], a third-order shear and normal deformable (TSNDT) equivalent single layer (ESL) theory was employed in [2] and [3] with the transverse shear stresses computed using a one-step stress recovery scheme (SRS). In all cases the failure criteria employed 6 components of the stress tensor but delamination between adjacent plies was not considered. The transparent armor was modelled as a thermo-elasto-visco-plastic material and its 3-D finite transient deformations were analyzed using the commercial finite element (FE) software, Lsdyna, with a user defined subroutine for the

constitutive relation. Infinitesimal deformations of the other three structures were analyzed with the in-house developed FE software by using the Tsai-Wu failure initiation criteria and progressively degrading the material elasticities. The FEs in which the material strength had reduced to zero at all of its integration points were deleted from the analysis domain.

	Failure load (MPa)	Failure position
<i>(1) Design j1 (non-uniform & instantaneous)</i>		
transient	1.773	B,C (bottom surf.)
static	1.865	B,C (top surf.)
<i>(2) Design k1 (non-uniform & rise time)</i>		
transient	1.848	B,C (bottom surf.)
static	1.841	B,C (top surf.)
<i>(3) Design l1 (uniform & rise time)</i>		
transient	0.811	B,C (top surf.)
static	0.678	B,C (top surf.)

2. Results and Discussion



Referring the reader to [3] for details, results in the Table illustrate the effect of boundary conditions, inertia forces, and load distribution on the top surface of the plate. The plots in the figure show that at the collapse load the deflection of the centroid of plate’s back surface rapidly increases in time when nearly 13% of the material has reached its ultimate stress.

3. Concluding Remarks

We have successfully developed an algorithm to design lightweight one- and two-core sandwich structures subjected to blast loads, and computed their collapse loads. With an increase in the uncertainty in values of material parameters from 10% to 30%, the median first failure load drops from 6.1 MPa to 5.84 MPa. The validation of the mathematical and numerical models by comparing the computed damage with the experimental one is very challenging because of several failure modes involved that cannot be accurately delineated during tests.

Acknowledgment: The financial support of the work from the Office of Naval Research through grants N000142012876 and N000141812635 with Dr. Y. D. S. Rajapakse as the Program Manager to Virginia Polytechnic Institute and State University is gratefully acknowledged.

References

- [1] G. O. Antoine and R. C. Batra, Optimization of transparent laminates for specific energy dissipation under low velocity impact using genetic Algorithm, *Composite Structures*, 2015, **124**: 29-34.
- [2] U. Taetragool, P. H. Shah, V. A. Halls, J. Q. Zheng, R.C. Batra, Stacking sequence optimization for maximizing the first failure initiation load followed by progressive failure analysis until the ultimate load, *Composite Structures* 2017, **180**:1007-1021
- [3] L. Yuan, R.C. Batra, Optimum first failure load design of one/two-core sandwich plates under blast loads, and their ultimate loads, *Composite Structures* 2019, **224**: Art. No. 111022.
- [4] L. Yuan, U. Taetragool, R. C. Batra, Optimum first failure loads of one- and two-core doubly curved sandwich shells, *AIAA J.* 2020, **58**: 3665-3679

The Dynamical Behavior of a Quantum Impact Oscillator

SOUMITRO BANERJEE^{1*}, ARNAB ACHARYA², PRATIK JEWARE³

1. Department of Physical Sciences, Indian Institute of Science Education & Research, Kolkata, India [0000-0003-3576-0846]
2. Department of Physical Sciences, Indian Institute of Science Education & Research, Kolkata, India [0000-0002-4711-4262]
3. Department of Physical Sciences, Indian Institute of Science Education & Research, Kolkata, India [0000-0003-4807-6293]

* Presenting Author email: soumitro@iiserkol.ac.in

Abstract: It is known that an impact oscillator exhibits complex dynamics and chaos close to the grazing bifurcation. What happens to a similar system in the quantum domain? To explore this question, we simulate the quantum versions of a hard-impacting system and show that such systems would exhibit complex non-chaotic behaviour with a countably infinite number of frequencies.

Keywords: Impact oscillator, quantum mechanics, chaos

1. Introduction

In this work we explore the dynamics of an impact oscillator in the quantum domain. The classical analogue comprises a mass-spring system that can impact a wall placed at a distance. Such a system is known to have square root singularity and exhibits chaos [1,2]. In the quantum version, the potential function is similar to that of a harmonic oscillator, but assumes an infinite value at the position of the wall (Fig.1(a)).

We solve the Schrödinger equation for these systems numerically to obtain the dynamics of the wavefunction. To obtain the visual analogue of the phase space dynamics, we use the Wigner function. The dynamics is finally analysed by obtaining the overlap integral with the initial wavefunction to obtain a real-valued time series. Analysis of the time series shows aperiodic dynamics but without any sensitive dependence on the initial condition.

2. Results and Discussion

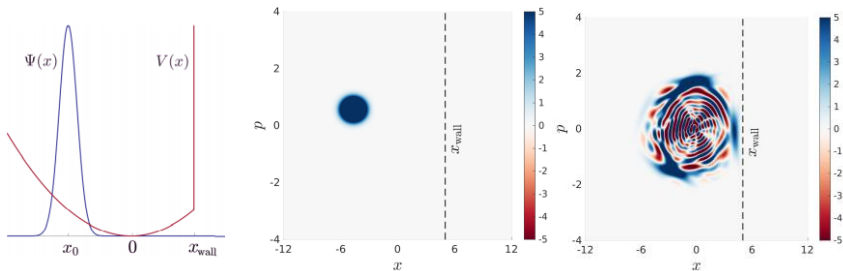


Fig. 1. The potential function and the initial wavefunction (a), and the evolution of the Wigner function when the classical oscillator undergoes grazing: (b) at $t=0$ and (c) at $t=2697$ in natural units.

Fig.1(a) shows the potential function of the system and the initial wavefunction, which is a shifted Gaussian function—the quantum analogue of the mass being released at a stretched position of the spring. In Fig.1(b) and (c) we show the Wigner function in the phase space at two different times under the condition where the classical oscillator would undergo grazing. Note that a quantum system’s wavefunction is spread over a range of the phase space and so the existence of the wall influences the dynamics even when the wall is placed away from the classical impacting condition.

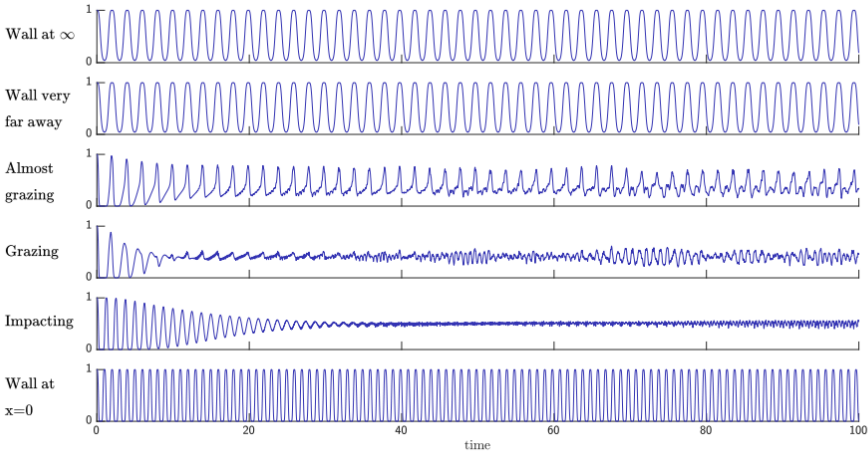


Fig. 2. The time series obtained by computing the overlap integral for different wall positions.

Fig.2 shows that the system exhibits periodic behaviour when the wall is placed far away from the oscillator and when it is placed exactly at the unstretched position of the spring. The system exhibits aperiodic orbits for intermediate positions of the wall. We have analysed these orbits and have found that the Lyapunov exponent is zero, implying no sensitive dependence on the initial condition. The Fourier spectrum reveals an infinite number of discrete frequency components.

3. Concluding Remarks

This work reveals that quantum systems may exhibit a new type of dynamics, where the orbit is aperiodic but the spectrum is neither spread over all frequencies like a chaotic system, nor does it have a finite number of frequency components like quasi-periodic dynamics. It has an infinity of discrete frequency components.

References

- [1] NORDMARK, ARNE B: Non-periodic motion caused by grazing incidence in an impact oscillator. *Journal of Sound and Vibration* 1991, **145**(2): 279-297.
- [2] BERNARDO, M., BUDD, C., CHAMPNEYS, A. R., & KOWALCZYK, P.: *Piecewise-smooth dynamical systems: theory and applications*. Springer Science & Business Media. 2008.

Accuracy and Efficiency of Structural Theories for Free Vibration Analyses via Axiomatic/Asymptotic Method and Neural Networks

ERASMO CARRERA^{1*}, MARCO PETROLO²

1. MUL² Group, Department of Mechanical and Aerospace Engineering, Politecnico di Torino [0000-0002-6911-7763]
2. MUL² Group, Department of Mechanical and Aerospace Engineering, Politecnico di Torino [0000-0002-7843-105X]

* Presenting Author

Abstract: This paper presents novel approaches to investigate the accuracy and computational efficiency of 1D and 2D structural theories. The focus is on free vibration problems in metallic and composite structures. Refined theories are built via the Carrera Unified Formulation (CUF), and the influence of higher-order generalized variables is analysed via the Axiomatic/Asymptotic Approach (AAM). Best theory diagrams (BTD) are built by considering those models minimizing the computational cost and maximizing the accuracy. BTD can estimate the accuracy and efficiency of any structural models, including classical models and refined theories from literature. The construction of BTD can be a cumbersome task as multiple finite element (FE) problems are required. Machine learning through neural networks can significantly reduce such overhead. In other words, surrogate structural models are built using a limited number of FE analyses for training and having as input a structural theory and providing as output the natural frequencies without the need for finite element analyses. Finally, extensions to node-dependent kinematics (NDK) are presented for further optimization of the computational cost.

Keywords: structural dynamics, finite elements, structural theories, neural networks, CUF

1. Introduction

The use of refined structural theories is convenient to extend 1D and 2D theories to problems otherwise requiring 3D models [1, 2]. CUF has emerged as a powerful method to build any-order theories and related finite element matrices [3]. CUF exploits a few formal expressions and index notations to obtain unified governing equations independent of the order of the theory. Via CUF, classical and refined models can be implemented, and any non-classical effect considered, e.g., shear deformability, transverse stretching, and warping. The systematic use of CUF for 1D and 2D models leads to considerable reductions of computational costs estimable in 10-100 times fewer degrees of freedom than 3D FE.

The development of a refined structural theory requires the proper choice of higher-order terms. AAM has been introduced as a tool to select such terms [1]. AAM provides the Best Theory Diagram composed of those models minimizing the computational cost and maximizing the accuracy. BTD can estimate the accuracy and efficiency of any structural models, including classical models and refined theories from literature.

Via CUF, the structural theory can change point-wise, i.e., each node of the FE model can have a different structural model. Such a capability is referred to as NDK and is helpful to use refined models only where needed [4]. The combined use of CUF, AAM, NDK, and Neural Networks (NN) is a

promising approach to build surrogate models that can provide information on the structural theory and finite element discretization for a given problem [5].

2. Results and Discussion

The typical result provided by AAM is shown in Fig. 10, in which the horizontal axis is the error in computing the first ten natural frequencies, and the vertical axis reports the number of nodal degrees of freedom of various theories. The continuous line is composed of those theories with the minimum error for given DOF. Theories from literature are reported as well to evaluate their performances as compared to the best models. As well-known, third-order terms are very significant for this class of problems.

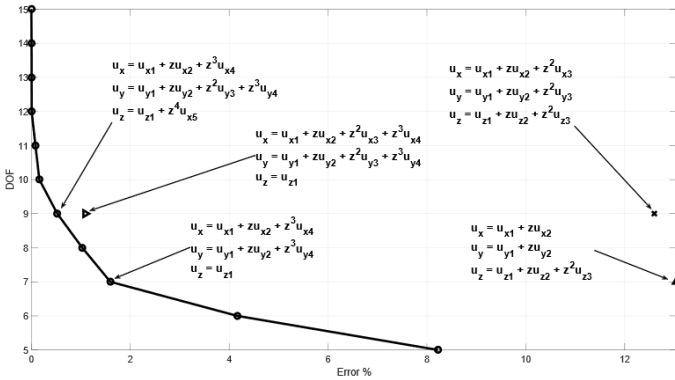


Fig. 1. BTD for first ten mode of a simply-supported shell with 0/90/0 lamination and $a/h = 10$.

3. Concluding Remarks

This paper has presented an overview of refined structural theories for structural dynamics problems. The focus is on methodologies to build and evaluate the role of refined terms and obtain the best theories with superior accuracy and computational efficiency. Furthermore, using machine learning algorithms is promising to obtain indications on how to build refined models and FE discretizations.

References

- [1] PETROLO M, CARRERA E: Methods and guidelines for the choice of shell theories. *Acta Mechanica* 2020, **231**:395-434.
- [2] CARRERA E, ELISHAKOFF I, PETROLO M: Who needs refined structural theories? *Composite Structures* 2021, **264**.
- [3] CARRERA E, CINEFRA M, PETROLO M, ZAPPINO E: *Finite Element Analysis of Structures through Unified Formulation*. John Wiley & Sons, 2014.
- [4] PETROLO M, CARRERA E: Selection of element-wise shell kinematics using neural networks. *Computers & Structures* 2021, **244**.
- [5] PETROLO M, CARRERA E: On the use of neural networks to evaluate performances of shell models for composites. *Advanced Modeling and Simulation in Engineering Sciences* 2020, **7**.

Nonlinear Dynamics of Multi-Stable Systems

JERZY WARMINSKI^{*1}, ANDRZEJ MITURA¹, FRANCESCO ROMEO², MATTEO BRUNETTI³

1. Department of Applied Mechanics, Lublin University of Technology, Lublin, POLAND [0000-0002-9062-1497], [0000-0002-6749-8232]
2. Department of Structural and Geotechnical Engineering, SAPIENZA University of Rome, ITALY [0000-0002-7828-3528]
3. Department of Civil and Industrial Engineering, University of Pisa, ITALY, [0000-0001-8689-6132]

* Presenting Author

Abstract: Nonlinear dynamics of different types of multistable systems is presented in the paper. As an example a multistable shell which exhibits several equilibria in a static configuration and snap-through effect in its dynamic response is investigated. On the basis of the experimental tests, a one degree of freedom model in a form of quintic oscillator is proposed. The local and global dynamics of a bistable oscillator is investigated to detect reversible snap-through effect.

Keywords: nonlinear vibrations, multistable systems, snap-through, control, energy harvesting

1. Multi-Stable Systems

Multi-stability is one of the main features of nonlinear systems. Duffing's oscillator may serve as a classical example where a zone with three different solutions may exist. Moreover, for certain excitation conditions a number of solutions in the Duffing model may increase up to five, as presented in [1]. However, the Duffing type equation has just one equilibrium position, which can be stable or unstable, depending on a shape of a potential function. In a classical Duffing equation the equilibrium is stable and the potential function has just one minimum.

Systems with multi equilibria belong to another group of the multi-stable structures [2]. This type of multi-stability can be created artificially by adding nonlinear external force, for example magnetic force produced by two magnets. The introduced nonlinear force enables to design a potential function which may have two potential wells. Another option is to add axial force to the structure which often may occur naturally due to increased temperature, for example. Then the system operating close to a buckling point has two potential wells, corresponding to two equilibria.

The composite technology offers new possibilities in creating multi-stable structures. The bistability, with associated snap-through mechanisms (a rapid jump from one to another equilibrium) is attractive for a design of efficient energy harvesters [3]. Most of the studies devoted to the dynamics of bistable laminates are characterized by symmetric stable configurations with free boundaries. A special design of a laminate shell with asymmetric configuration has been proposed in [4] where a few equilibria have been detected. The shell designed in [4] is investigated in this paper to detect local (in-well) and global dynamics with the snap-through effect.

2. Shell Model and Results

The studied shell is presented in Fig.2. A number of layers and the layout is designed to get shell multi-stability as presented in [4].



Fig. 2. Multistable shell I-state (a), C-state (b) and function of potential energy with indicated I and C states (c).

In Fig.2 two stable states are presented, I-state (Fig.2a) and C-state (Fig.2b). A corresponding function of potential energy, with two local minima indicated in Fig.2(c), confirm the bistability of the system. On the basis of experiment a reduced shell model is derived in a form of a quintic oscillator which represents dynamics of the shell observed experimentally. The model is used to predict in-well behaviour and the snap-through effect.

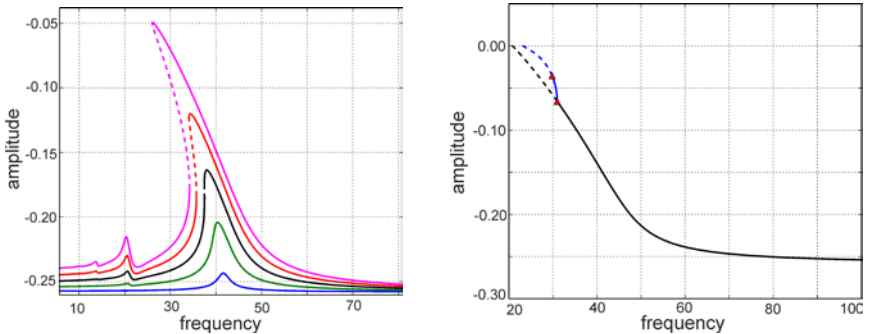


Fig. 2. Resonance curves of a multistable shell structure around I-state, (a) softening effect for selected amplitude of excitation, (b) period doubling indicating possible transition to snap-through effect

The numerical solutions of the elaborated model shows softening effect of the resonance curves for in-well dynamics, as presented in Fig.2(a) for I-state. For large amplitude of excitation the period doubling is observed (Fig.2b) which may lead to the snap-through with chaotic global dynamics.

Acknowledgment: The paper is partially supported from grant PO19MO15 and co-financed by the Polish National Agency for Academic Exchange PPN/BIL/2018/2/00076.

References (10 point, bold)

- [1] EMAM S.A. INMAN D: A Review on Bistable Composite Laminates for Morphing and Energy Harvesting. *Applied Mechanics Reviews*, 2015, **67**(6), 060803, 1-15 .
- [2] WARMINSKI J: Nonlinear dynamics of self-, parametric, and externally excited oscillator with time delay: van der Pol versus Rayleigh models. *Nonlinear Dynamics*. 2020, **99**, 35-56.
- [3] MUKHERJEE A. FRISWELL M.I. ALI S.F. AROCKIARAJAN A: Modeling and design of a class of hybrid bistable symmetric laminates with cantilever boundary configuration. *Composite Structures*, 2020, **239**(6), 112019.
- [4] BRUNETTI M. KLODA L. ROMEO F. WARMINSKI J: T Multistable cantilever shells: Analytical prediction, numerical simulation and experimental validation. *Composites Science and Technology*, 2018, **165**(14), 397-410.

Dynamic-Based Micro and Nano Devices and Phenomena

MOHAMMAD. I. YOUNIS

Physical Sciences and Engineering Division, King Abdullah University of Science and Technology, Thuwal, Saudi Arabia (E-mail: Mohammad.Younis@kaust.edu.sa)

Department of Mechanical Engineering, State University of New York at Binghamton, Binghamton, NY, USA (E-mail: myounis@binghamton.edu).

Abstract: Miniature structures and devices have captured the attention of the scientific community for several decades for their unprecedented attractive features. Along with their distinct practical advantages, micro and nano devices are considered excellent platform to probe and reveal fundamental physical and mechanical phenomena in well-controlled environment [1].

Today, several micro-electro-mechanical systems MEMS devices are being used in our everyday life, ranging from accelerometers and pressure sensors in automobiles, radio-frequency (RF) switches and microphones in cell phones, and inertia sensors in video games. Due to the quest to boost sensitivity, reduce power consumption, and increase integration density, the past two decades have witnessed the emergence of Nano-electro-mechanical systems NEMS. With the increasing demand to embed more intelligence into various applications, MEMS and NEMS continue to play key role on advancing innovation.

Along with their great promise, micro and nano devices have brought new challenges and a wide spectrum of unexplained and less-understandable mechanical behaviors and phenomena. Because these devices employ moveable compliant structures and due to the interaction with short-range forces, many of these challenges are related to their dynamical behavior, which is mostly nonlinear.

The talk will overview some of the recent revealed intriguing phenomena at the micro and nano scale including modes veering, jumps, and internal resonances including three-one, two-one, and one-one [2,3], Figs. 1,2,3. Mode veerings, hybridization of modes, and localization will be also be discussed along with their potential for practical applications. The softening and hardening behaviors and the associated jumps will be shown with examples of proposed devices. The escape-from potential well will also be presented and its potential for realizing smart switches for gas sensing application will be shown. We will also discuss the static and dynamic behavior of actively tunable structures; which can be tuned using electrostatic and or/electrothermal actuation. The talk will end on future directions and perspectives.

Keywords: MEMS, arch, jumps, bifurcations, nonlinearity

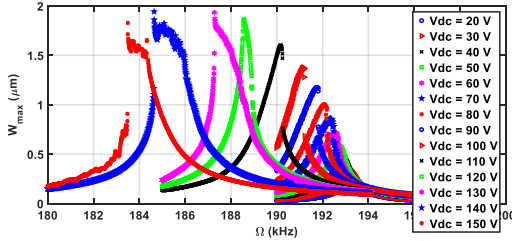


Fig. 1. Experimental data of a clamped-clamped beam actuated by electrostatic forces demonstrating transitions from softening to hardening behaviour.

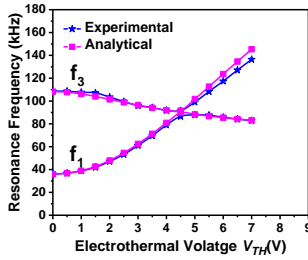


Fig. 2. Mode veering between the first and third modes of a micromachined arch.

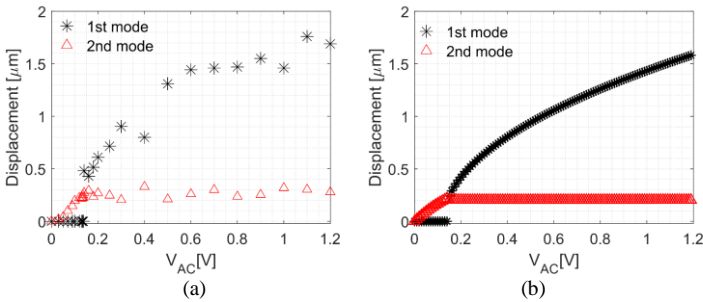


Fig. 3. The saturation phenomenon in a micromachined portal frame: (a) Measurements, (b) Simulations.

Acknowledgment: This research has been supported by KAUST research fund.

References

- [1] Younis M I: *MEMS Linear and Nonlinear Statics and Dynamics*. Springer: New York, 2011.
- [2] Rocha RT Alcheikh N, Khan F, Younis MI: Dynamics Characterization of a U-Shaped Micro-Resonator Portal Frame. *Journal of Microelectromechanical Systems* 2020, **29** (5): 1362-1371.
- [3] Hajjaj A Z, Jaber N, Ilyas S, Alfosail F K, Younis M I: Linear and nonlinear dynamics of micro and nano-resonators: Review of recent advances. *International Journal of Non-Linear Mechanics* 2020, **119**, 103328.

Dynamics of Continuous Systems: From Time-Varying, Nonlinear, and Flexible Multibody Systems to Phononic Structures

WEIDONG ZHU*

Department of Mechanical Engineering, University of Maryland, Baltimore County

* Presenting Author

Abstract: Some interesting results on the dynamics of continuous systems are reviewed. They involve: 1) vibration and stability of translating media with time-varying lengths and/or velocities; 2) nonlinear vibrations of systems with large degrees of freedom and general nonlinearities; 3) new spatial discretization methods for one- and two-dimensional continuous systems; 4) new formulations of flexible multibody dynamics with application to elevator traveling cables; and 5) elastic wave propagation in nonlinear phononic structures. Two types of dynamic stability problems are addressed from the energy viewpoint in the first area: dynamic stability of translating media during extension and retraction, and parametric instabilities in continuous systems with periodically varying lengths and/or velocities. The incremental harmonic balance method is used in the second area to handle periodic responses of high-dimensional models of nonlinear continuous systems and their stability and bifurcations, as well as quasi-periodic responses. New spatial discretization methods in the third area ensures that all boundary conditions of continuous systems are satisfied, and hence uniform convergence of solutions. New nonlinear models of slack cables with bending stiffness and arbitrarily moving ends are developed for moving elevator traveling cables in the fourth area. A minimal number of degrees of freedom are needed to achieve the same accuracy as that of the finite element method. Wave propagation analysis of phononic structures with finite deformations are developed in the fifth area to study influences of nonlinearities on wave propagation characteristics. Some experimental results are presented to validate theoretical predictions.

Keywords: energy methods for finding dynamic stability of continuous systems with variable lengths and velocities, parametric excitation for second-order partial differential equations, nonlinear vibrations of systems with large degrees of freedom and general nonlinearities, new spatial discretization methods for continuous systems, and nonlinear wave propagation.

1. Introduction

All structural systems are continuous systems. While spatial discretization can be used to analyze the dynamics of continuous systems in some cases, spatially discretized, low-dimensional models can lead to misleading results. The goal of this research is to develop new methodologies to analyze the vibration of continuous systems, and to use the new methodologies to solve important industrial problems such as elevator systems. This work integrates vibrations of continuous systems, nonlinear vibrations, flexible multibody dynamics, and nonlinear wave propagation. Continuous system vibrations include time-varying translating media with variable lengths and/or velocities [1-5], and spatial discretization of continuous systems with complicated boundary conditions [6-8]. This deals with mostly time-varying linear systems with small deformations as well as nonlinear systems with intermediate deformations. Extensive nonlinear vibration research focuses on high-dimensional models of

continuous systems with strong and complicated nonlinearities [9-13]. A new flexible multibody dynamics formulation with a minimum number of degrees of freedom is developed for continuous systems with large deformations with application to elevator traveling cables [14-16]. New methodologies for analyzing strongly nonlinear elastic wave propagation are also developed [17-19].

References

- [1] W.D. Zhu, and J. Ni: Energetics and Stability of Translating Media with an Arbitrarily Varying Length. *ASME Journal of Vibration and Acoustics* 2000, **122**:295-304.
- [2] W.D. Zhu, and Y. Chen: Theoretical and Experimental Investigation of Elevator Cable Dynamics and Control. *ASME Journal of Vibration and Acoustics* 2006, **128**:66-78.
- [3] W.D. Zhu, and N.A. Zheng: Exact Response of a Translating String with Arbitrarily Varying Length under General Excitation. *ASME Journal of Applied Mechanics* 2008, **75**(3):031003.
- [4] W.D. Zhu, X.K. Song, and N.A. Zheng: Dynamic Stability of a Translating String with a Sinusoidally Varying Velocity. *ASME Journal of Applied Mechanics* 2011, **78**(6):061021.
- [5] W.D. Zhu, and K. Wu: Dynamic Stability of a Class of Second-order Distributed Structural Systems with Sinusoidally Varying Velocities. *ASME Journal of Applied Mechanics* 2013, **80**:061008.
- [6] W.D. Zhu, and H. Ren: An Accurate Spatial Discretization and Substructure Method with Application to Moving Elevator Cable-Car Systems - Part I: Methodology. *ASME Journal of Vibration and Acoustics* 2013, **135**(5):051036.
- [7] H. Ren, and W.D. Zhu: An Accurate Spatial Discretization and Substructure Method with Application to Moving Elevator Cable-Car Systems - Part II: Application. *ASME Journal of Vibration and Acoustics* 2013, **135**(5):051037.
- [8] K. Wu, and W.D. Zhu: A New Global Spatial Discretization Method for Two-dimensional Continuous Systems with Application to a Rectangular Kirchhoff Plate. *ASME Journal of Vibration and Acoustics* 2018, **140**:011002.
- [9] G.Y. Xu, and W.D. Zhu: Nonlinear and Time-Varying Dynamics of High-Dimensional Models of a Translating Tensioned Beam with a Stationary Load Subsystem. *ASME Journal of Vibration and Acoustics* 2010, **132**(6):0610120.
- [10] J.L. Huang, and W.D. Zhu: Nonlinear Dynamics of High Dimensional Models of a Rotating Vertical Euler-Bernoulli Beam under the Gravity Load. *ASME Journal of Applied Mechanics* 2014, **81**(10):101007.
- [11] X.F. Wang, and W.D. Zhu: A Modified Incremental Harmonic Balance Method based on the Fast Fourier Transform and Broyden's Method. *Nonlinear Dynamics* 2015, **81**(1):981-989.
- [12] X.F. Wang, and W.D. Zhu: A New Spatial and Temporal Incremental Harmonic Balance Method for Obtaining Steady-State Responses of a One-Dimensional Continuous System. *ASME Journal of Applied Mechanics* 2016, **84**:014501.
- [13] J.L. Huang, and W.D. Zhu: An Incremental Harmonic Balance Method with Two Time-Scales for Quasi-Periodic Motion of Nonlinear Systems Whose Spectrum Contains Uniformly Spaced Sideband Frequencies. *Nonlinear Dynamics* 2017, **90**(2):1015-1033.
- [14] W.D. Zhu, H. Ren, and C. Xiao: A Nonlinear Model of a Slack Cable with Bending Stiffness and Moving Ends with Application to Elevator Traveling and Compensation Cables. *ASME Journal of Applied Mechanics* 2011, **78**:041017.
- [15] W. Fan, W.D. Zhu, and H. Ren: A New Singularity-free Formulation of a Three-dimensional Euler-Bernoulli Beam Using Euler Parameters. *ASME Journal of Computational and Nonlinear Dynamics* 2016, **11**(4):041013.
- [16] W. Fan, and W.D. Zhu: Dynamic Analysis of an Elevator Traveling Cable Using a Singularity Formulation. *ASME Journal of Applied Mechanics* 2017, **84**:0440502.
- [17] M. Liu, and W.D. Zhu: Modeling and Analysis of Nonlinear Wave Propagation in One-dimensional Phonic Structures. *ASME Journal of Vibration and Acoustics* 2018, **140**:061010.
- [18] X.F. Wang, W.D. Zhu, and M. Liu: Steady-state Periodic Solutions of the Nonlinear Wave Propagation Problem of a One-dimensional Lattice Using a New Incremental Harmonic Balance Method that Handles Time Delays. *Nonlinear Dynamics* 2020, **100**(2):1457-1467.
- [19] M.T. Song, and W.D. Zhu: Elastic Wave Propagation in Strongly Nonlinear Lattices and Its Active Control. *ASME Journal of Applied Mechanics* 2021, **88**:071003.

-S1-

Advances in fractional order calculus and applications

Energy Pulse: Competitive and Accessible Application for Monitoring Electricity Consumption

ALEXANDRU-GEORGE BERCIU^{1*}, EVA HENRIETTA DULF¹, DACIAN JURJ², LEVENTE CZUMBIL², DAN DORU MICU²

1. Faculty of Automation and Computer Science, Automation Department, Technical University of Cluj-Napoca
2. Faculty of Electrical Engineering, Electrotechnics and Measurements Department, Technical University of Cluj-Napoca

* presenting author; Alexandru.George.Berciu@gmail.com

Abstract: The present work brings to the reader's attention the benefits and facilities of the Energy Pulse application. The application enwraps a complete solution for real-time monitoring of electrical energy consumption of the Faculty of Electrical Engineering buildings, the Swimming Complex from the Technical University of Cluj-Napoca, the Faculty of Building Services Engineering, and from Marasti Student Campus dormitories.

Keywords: electricity consumption, database, software application.

1. Introduction

Given the importance of efficient use of electricity, this paper aims to present a complete IT solution for home and industrial users in terms of monitoring electricity consumption and reducing the cost of the related monthly invoice, to create habits of efficient electrical energy consumption.

Starting from the decentralized data sets that the BEMS UTCN application generates, in this research, the authors aim to develop an integrated solution for monitoring electricity consumption. Following the analysis of consumer data over several years, and the centralization of consumption data in a database, the authors aim to send personalized notifications to the user according to the consumption habits he has. Subsequently, the user will be able to choose from a series of percentages with which he will be able to reduce the cost of his monthly bill, and the Energy Pulse application will automatically disconnect some non-essential consumers, their number being determined according to a control algorithm.

2. Results and Discussion

In order to obtain the best possible results, the authors of this paper aim to develop a new algorithm for forecasting electricity consumption, starting from the results obtained through the algorithm used in [1]. Using the capabilities of the algorithm mentioned above, the authors will add other relevant parameters for electricity consumption, identified from the experiments, in order to increase the efficiency of the prediction: the evolution of temperature and the type of activity in the analyzed day. In this sense, the temperature data provided by the Copernicus program [2] will be used, along with the definition of four categories of day types. To this end, the authors aim to reduce the training time required for a neural network and to facilitate access to information relevant to the end-user.

Moreover, considering the way of saving data in decentralized CSV files by BEMS UTCN application, in order to reduce the execution time, the authors will develop a database containing the centralization of all consumption data saved by the previously mentioned application.

Taking into consideration the reading errors that have been identified in the process [3], [4], the future application will use improved methods for detecting outlier data, which following the standard deviation of the data will update the threshold parameter according to the results obtained previously from the experiments.

In order to validate the future results, the authors will compare them with those of the usual forecasting methods for electricity: MARS, SVR, ARIMA [5].

The final results will be presented to the user both in graphic form and in the form of a notification. In graphical form, the current consumption will be compared with the typical one. The text of the personalized notification will contain information regarding the cost of the monthly invoice and the savings that the user will achieve if he continues to develop the same consumption habit. If the user wants to reduce the cost of the monthly bill, to increase his savings, the Energy Pulse application will allow him to choose a certain percentage of cost reduction. Depending on the user's wishes, the application will automatically disconnect non-essential consumers to obtain the percentage imposed by the user. In order to determine the number of non-essential consumers that must be switched off automatically, a control algorithm will be used, determined after comparison with the performance of the fractional control. Fractional control is a generalization of classical PID control, keeping the meaning of each term but offering performances which cannot be achieved with classical control.

In order to fulfil their objectives proposed in this abstract, the authors will use the facilities offered by the MATLAB development environment, together with those of MATLAB App Designer and MATLAB Web App Server.

3. Concluding Remarks

As a result of the above, this paper aims to draw attention to the facilities that the Energy Pulse application will have. Given its competitors, developed by Efergy [6] and Sense [7], the Energy Pulse application will further integrate the notification of the cost of the monthly bill and can be operated by any smart meter owner, without the need for installing additional devices.

Acknowledgment: The activities carried out will be funded by the HORIZON 2020 research programme, within the project Renewable COGeneration and storage techNologies Integration for energy autonomous buildings, grant ID 815301.

References

- [1] CRETU M, CZUMBIL L, BARGAUAN B, CECLAN A, BERCIU A G, POLYCARPOU A, RIZZO R, MICU D D: Modelling and evaluation of the baseline energy consumption and the key performance indicators in Technical University of Cluj-Napoca buildings within a demand response programme: a case study. *IET Renewable Power Generation* 2020, 14(15):2864-2875.
- [2] COPERNICUS PROGRAMME: Climate variables for cities in Europe from 2008 to 2017. European Centre for Medium-Range Weather Forecasts 2019.
- [3] JURJ D I, MICU D D, CZUMBIL L, BERCIU A G, LANCRAN M, BARAR D: A Analysis of data cleaning techniques for electrical energy consumption of a public building. In: 2020 55th International Universities Power Engineering Conference (UPEC) 2020, Turin.
- [4] JURJ D I, POLYCARPOU A, CZUMBIL L, BERCIU A G, LANCRAN M, BARAR D, MICU D D: Extended analysis of data cleaning for electrical energy consumption data of public buildings. In: 2020 Mediterranean Conference on Power Generation, Transmission, Distribution and Energy Conversion 2020, Online.
- [5] AL-MUSAYLH M S, DEO R C, ADAMOWSKI J F, LI Y: Short-term electricity demand forecasting with MARS, SVR and ARIMA models using aggregated demand data in Queensland, Australia. In: *Advanced Engineering Informatics* 2018, 35:1-16.
- [6] EFERGY: Engage Hub kit. Available: <https://efergy.com/engage>, 2021, Online.
- [7] AMAZON: Sense store. Available: <https://www.amazon.com/stores/Sense/page/35E87DC3-0D4D-4103-A112-4ECDAE9D261C>, 2021, Online.

A Novel Toolbox for Automatic Design of Fractional Order PI Controllers based on Automatic System Identification from Step Response Data

IULIA BUNESCU¹, ISABELA BIRS^{1,2,3}, ROBAIN DE KEYSER^{2,3}, CRISTINA I. MURESAN^{1*}

1. Technical University of Cluj-Napoca, Memorandumului 28, 400114 Cluj-Napoca, Romania
2. DySC research group on Dynamical Systems and Control, Ghent University, Technologiepark 125, B-9052 Ghent, Belgium
3. EEDT group, member of Flanders Make consortium, 9052 Ghent, Belgium

* Presenting Author

Abstract: A novel toolbox for non-experienced users is developed and presented in this paper. The toolbox produces fractional order (FO) controllers to be implemented on various processes. To design the controller, the toolbox requires solely a step response data, experimentally obtained on the process. Based on this data, an automatic system identification algorithm is used that models the process as a second order plus dead-time (SOPDT) transfer function. Then, a FO controller is designed using the previously estimated model parameters and according to performance specifications, such as gain crossover frequency, phase margin and maximization of the gain margin. Several experimental step response data are used and several FO controllers are designed for different processes. The results validate the toolbox.

Keywords: automatic system identification, automatic design of fractional order controllers, experimental results, vertical take-off and landing

1. Introduction

Most of the times accurate modeling implies an increased complexity of the model. However, for a large range of processes simple SOPDT models provide sufficient accuracy and are easily used in the controller design procedure. To determine such a model, the engineer needs knowledge regarding system identification methods. An alternative approach, based on automatic system identification, has been developed and presented in [1]. The approach does not require any system identification expertise. The only process information required from the user is a set of step response data. The current manuscript presents a toolbox that uses an improved version of the algorithm in [1], along with an additional feature for the automatic design of a FO controller. The parameters of this controller are determined by imposing a set of performance specifications and using the model parameters as returned by the automatic system identification algorithm.

The method presented in this paper uses step response data to estimate SOPDT models:

$$G(s) = \frac{K}{(\tau_1 s + 1)(\tau_2 s + 1)} e^{-\tau_d s} \quad (1)$$

where τ_d is the process dead-time, K is the process gain, τ_1 and τ_2 are the time constants. The automatic system identification algorithm is based on step response data, possibly corrupted. Numerical integration and computation of areas in the experimental step response data leads to an efficient and simple estimation of the model parameters. Once the model has been

determined an indirect autotuning method is used to design a fractional order PI (FO-PI) controller:

$$C(s) = k_p \left(1 + \frac{k_i}{s^\lambda} \right) \quad (2)$$

where k_p and k_i are the proportional and integral gains and $\lambda \in (0,2)$ is the fractional order. The analytical equations for computing the k_p and k_i parameters as a function of λ , τ_1 , τ_2 , τ_d and K are determined such that certain gain crossover frequency ω_c and phase margin PM are obtained. The final controller parameters are selected such as the gain margin is maximized.

2. Results and Discussion

To validate the proposed method several experimental step response data are used, including that for a challenging Vertical Take-Off and Landing (VTOL) unit. The experimental unit is described in [2]. A step signal of 6.3V has been supplied to the VTOL unit and the resulting output signal was used to determine an accurate model as in (1). To tune the controller parameters, $\omega_c=0.4\text{rad/s}$ and $\text{PM}=75^\circ$ are imposed. The resulting FO-PI controller was then implemented on the actual unit and the experimental results are provided in Fig. 1. Disturbance rejection tests, as well as robustness tests will be carried out for the final manuscript.

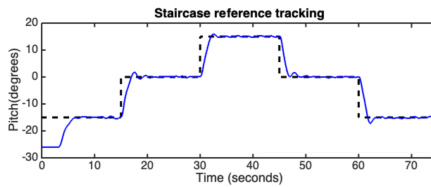


Fig. 1. Experimental results obtained on the VTOL unit using the proposed toolbox

3. Concluding Remarks

In this paper, a first toolbox combining automatic system identification and fractional order controller design is presented. The algorithm behind the SOPDT automatic system identification method is described. Then, the automatic design for a fractional order controller is developed. Several experimental examples, from a wide range of processes are provided to validate the proposed methods and the utility of the toolbox and its user interface.

Acknowledgment: This work was supported by a grant of the Ministry of Research, Innovation and Digitization, CNCS/CCCDI – UEFISCDI, project number PN-III-P1-1.1-TE-2019-0745, within PNCDI III.

References

- [1] DE KEYSER, R., MURESAN, C.I.: Robust Estimation of a SOPDT Model from Highly Corrupted Step Response Data. *European Control Conference 2019*, **1**: 818-823
- [2] MURESAN CI, BIRS IR, DULF EH: Event-Based Implementation of Fractional Order IMC Controllers for Simple FOPDT Processes. *Mathematics 2020*, **8**(8): 1378

Proposal of a control hardware architecture for implementation of fractional-order controllers

JUAN J. GUDE^{1*}, PABLO GARCÍA BRINGAS^{1,2}

1. Faculty of Engineering, University of Deusto. Avda. de las Universidades, 24. 48.007 Bilbao (Spain)
2. D4K Group, University of Deusto. Avda. de las Universidades, 24. 48.007 Bilbao (Spain)

* Presenting Author

Abstract: This paper presents a proposal of a control hardware architecture for the implementation of integer-order (IO) and fractional-order (FO) controllers. In particular, the design and experimental validation of the FO controllers implemented in several control technologies are applied to a temperature laboratory setup in order to demonstrate the effectiveness of the proposed hardware architecture. Some comments relating to industrial practice are offered in this context.

Keywords: fractional-order controllers, control hardware, experimental equipment

1. Introduction

In spite of all the advances in process control over the past several decades, the proportional integral derivative (PID) controller remains to be certainly the most extensive option that can be found on industrial control applications and have become an industrial standard for process control, see [1].

While more powerful control techniques are readily available, the transparency and relative simplicity of the PID control mechanism, the availability of a large number of reliable and cost-effective commercial PID modules, and their widespread acceptance by operators are among the reasons of its success and popularity, see [2].

Over the last decades, the emergence of fractional calculus (FC) has made possible a great deal of academic and industrial effort focused on the transition from classical models and controllers to those described by differential equations of non-integer order. Thus, FO dynamic models and controllers were introduced [3, 4, 5].

The apparent benefit of FC in the field of modelling has been justified from an industrial point of view. However, the adoption of FO-PID controllers in the industry is currently low, even though FO-PID controllers offer clear advantages in comparison with IO-PID controllers. It has been more difficult to convey the advantages of FC on the controller side because of implementation issues [6].

To fill the gap between theoretical FO-PID controllers and their practical implementation in a control hardware device, this paper proposes an architecture that facilitates their real implementation in a real-time target.

In order to test the performance of the proposed hardware architecture, several FO-PID controllers have been implemented in different control technologies and have been applied to a temperature experimental prototype that has recently been designed and developed at the University of Deusto [7].

2. Results and Discussion

Currently, industrial processes are mainly controlled using various control technologies, the most widely used being computer, microprocessor-based, or FPGA-based hardware devices [8].

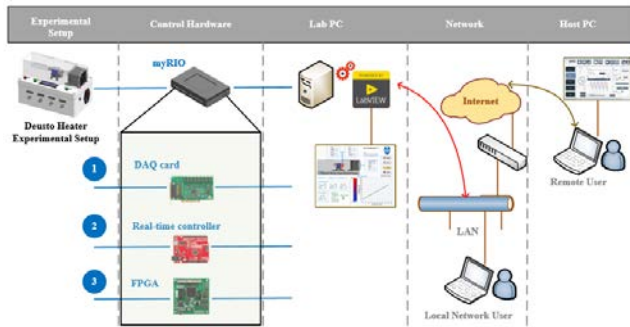


Fig. 1. Scheme of the proposed hardware architecture used to implement control algorithms in the prototype

These technologies are usually included in some Programmable Automation Controllers (PAC). In this paper, a National Instruments® (NI) *myRIO-1900* equipment is used as a control hardware device, although any other microprocessor or control hardware could be easily incorporated. Figure 1 shows the configuration of the control hardware architecture used for controlling temperature in the temperature prototype. The flexibility offered by this control hardware and the configuration of its control architecture allows the following control modes or control technologies:

1. Computer control, using LabVIEW programming language on the Lab PC. In this control mode, the control device is used as a data acquisition (DAQ) card.
2. Control by the NI myRIO real-time controller, where the control algorithm is implemented using LabVIEW RT and the access to input and output (I/O) ports is done through the FPGA interface. The user can interact with the control system from the Local or Host PC.
3. Control by FPGA, where the control algorithms are implemented and LabVIEW FPGA is used for accessing the I/O ports through the FPGA interface. The real-time controller manages the communication between the FPGA and the Local or Host PC.

This paper includes details about the practical implementation of FO-PID controllers with each one of the considered control technologies. In this way, the theoretical methods and developments can be validated experimentally.

3. Concluding Remarks

In this paper, a proposal of control hardware architecture for the implementation of FO-controllers is presented and applied to a laboratory setup in order to validate its performance.

The main advantage that this architecture presents from a control point of view is the flexibility in the control technologies offered to the final user that can be used. Another advantage from the implementation of control algorithms point of view of is that, regardless of the control technology used, the programming language is always the same: LabVIEW.

The way to implement FO-PID algorithms on different real-time targets is described in detail.

It is the opinion of the authors that this type of control hardware prepares engineers in the use of control technologies and low-cost FO controller-embedded system realization that will encourage industrial use of FO controllers.

References

- [1] ÅSTRÖM K., HÄGGLUND T.: *Advanced PID Control*. The Instrumentation, Systems, and Automation Society (ISA), 2006.
- [2] VILANOVA R., VISIOLI A.: *PID Control in the Third Millenium*. Springer-Verlag: London, 2012.
- [3] TEPLJAKOV A.: *Fractional-order Modeling and Control of Dynamic Systems*. Springer: Switzerland, 2017.

- [4] MONJE C.A., CHEN Y., VINAGRE B.M., XUE D., FELIU V.: *Fractional-order systems and Controls*. Springer-Verlag: London, 2010.
- [5] PODLUBNY I.: *Fractional Differential Equations*. Academic: San Diego, 1999.
- [6] TEPLJAKOV A., HOSSEINIA S.H., GONZALEZ E., ALAGOZ B.B., YEROGLU C., PETLENKOV, E.: FOPID controllers and their industrial applications: A survey of recent results. *IFAC-PapersOnLine* 2018, **51**(4):25-30.
- [7] GUDE J.J., GARCÍA BRINGAS, P., CONEJO U.: Development and conceptualization of an experimental equipment for real-time fractional-order modelling and control. Submitted to *Computers & Electrical Engineering*.
- [8] BAI Y., ROTH Z.S.: *Classical and modern controls with microcontrollers*. Springer-Verlag: London, 2018.

Comparisons and Experimental Validation of Several Autotuning Methods for Fractional Order Controllers

MARCIAN MIHAI^{1*}, ISABELA BIRS^{1,2}, CRISTINA I. MURESAN¹, EVA DULF¹,
ROBIN DE KEYSER²

1. Automation Department, Technical University of Cluj-Napoca Romania
 2. Dynamical Systems and Control Research Group, Ghent University, Belgium
- * Presenting Author

Abstract: Accurate process modelling is occasionally difficult. In such situations, autotuning methods enable the design of controllers. Fractional order PIDs have recently emerged as generalization of the standard PIDs, but autotuning methods for these controllers are scarce. In this paper, a new approach is described, based on an extension of the widely-used Ziegler-Nichols method. Comparative tests with two other autotuning methods are performed on a highly non-linear process. The experimental results validate the proposed method.

Keywords: auto-tuning; fractional order; experimental validation; vertical take-off and landing

1. Introduction

The fractional order PID (FO-PID) controller was first introduced by Podlubny [1]. It allows for improved closed loop response and robustness, due to the two supplementary tuning parameters involved, $0 < \lambda, \mu < 1$, the fractional orders of integration and differentiation. The transfer function of the FO-PID controller is described as:

$$G_{FO-PID}(s) = k_p \left(1 + \frac{1}{T_i s^\lambda} + T_d s^\mu \right) \quad (1)$$

where k_p is the proportional gain, while T_i and T_d are the integral and derivative time constants. In this manuscript, we assume $\lambda = \mu$ and $T_i = 4T_d$ [2]. In a large area of applications, including aeronautics, accurate process models are difficult to be obtained. Autotuning methods are preferred in this case, as the popular Ziegler-Nichols approach [2]. The method produces acceptable results in terms of disturbance rejection, but poor results regarding setpoint tracking. Autotuning designs for FO-PID controllers are however scarce. Three autotuning methods for FO-PIDs are compared in this manuscript. One of these is a novel extension of [2]. To obtain the necessary process information, a relay test is used. The process critical frequency and critical gain are obtained in this way.

The proposed method is based on shaping the “direction” of the loop frequency response in a fixed point in the Nyquist plot, corresponding to the critical frequency. It is determined that for a given fractional order of the FO-PID controller, tuning rules similar to the Ziegler-Nichols method can be obtained. The parameters of the FO-PID controller can thus be easily computed, without any complex optimization procedure. For a given fractional order λ , the parameters k_p , T_i and T_d of the Ziegler-Nichols FO method can be computed as indicated in Table 1. Notice that for $\lambda = 1$, the standard parameters of the Ziegler-Nichols method are obtained.

Table 1. FO-PID parameters according to the modified Ziegler-Nichols method

β	k_p	T_i	T_d
0.4	$0.16k_c$	$2.27T_c^{0.4}$	$0.57T_i$
0.6	$0.29k_c$	$1.12T_c^{0.6}$	$0.44T_i$
0.8	$0.42k_c$	$0.71T_c^{0.8}$	$0.33T_i$
1	$0.6k_c$	$0.57T_c^{1.1}$	$0.25T_i$

2. Results and Discussion

The proposed autotuning method is tested on a Vertical Take-Off and Landing (VTOL) system as described in [3]. The designed fractional order controller is implemented on the VTOL unit. The experimental results are given in Fig. 1. For comparative purpose two other FO-PI controllers are implemented. These are designed according to the auto-tuning methods presented in [4] and [5].

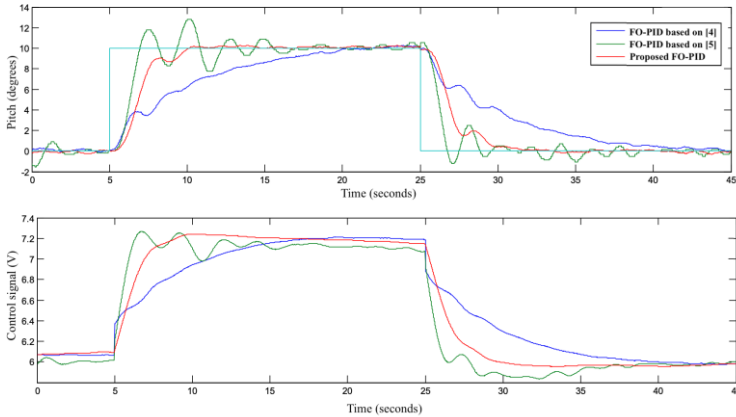


Fig. 1. Experimental closed-loop system response of the VTOL platform with the FO-PID controllers

3. Concluding Remarks

A new auto-tuning method extending the popular ZN approach to fractional order controllers is described in this paper. To validate the method, comparisons with other autotuning methods are performed on a VTOL unit. The experimental results clearly demonstrate that these autotuning methods can be successfully used to control highly nonlinear and poorly damped systems.

Acknowledgment: This work was supported by a grant of the Ministry of Research, Innovation and Digitization, CNCS/CCCDI – UEFISCDI, project number PN-III-P1-1.1-TE-2019-0745, within PNCDI III.

References

- [1] PODLUBNY I: Fractional-order systems and PID-controllers. *IEEE Trans Autom Control* 1999, **44**: 208-214
- [2] ZIEGLER JG, NICHOLS NB: Optimum settings for automatic controllers. *Trans ASME* 1942, **64**: 759–768.
- [3] MURESAN CI, BIRS IR, DULF EH: Event-Based Implementation of Fractional Order IMC Controllers for Simple FOPDT Processes. *Mathematics* 2020, **8**(8): 1378
- [4] DE KEYSER R, MURESAN CI, IONESCU CM: A Novel Auto-tuning Method for Fractional Order PI/PD Controllers. *ISA Transactions* 2016, **62**: 268-275.
- [5] DE KEYSER R, MURESAN CI, IONESCU CM: Autotuning of a Robust Fractional Order PID Controller, *IFAC Papers Online* 2018, **51**: 466-471

Fractional Order Controllers for Twin Rotor Aerodynamical System,

MAGDALENA SANGEORZAN¹, EVA-H. DULF^{2*}

1. Technical University of Cluj-Napoca
2. Technical University of Cluj-Napoca [0000-0002-6540-6525]

* Presenting Author

Abstract: The twin-rotor aerodynamical system (TRAS) is a highly nonlinear system with a cross-coupling effect. Although several controllers are published in the literature, all solutions are with great complexity. The novelty of this work consists in the design of fractional order controllers using two innovative methods. Two controllers are designed for adjusting the rotational speed of the azimuth motor, respectively two controllers for the rotational speed of the pitch motor. The two sets of controllers are implemented and tested on the physical TRAS equipment in the laboratory, yielding results comparable with any complex solution already acknowledged.

Keywords: fractional-order controller; frequency design method; optimum magnitude

1. Introduction

Fractional order controllers ($PI^\lambda D^\mu$) are a generalization of the classical PID controllers with integral and derivative parts replaced by a fractional integral of order λ and a fractional order derivative of order μ . Fractional order controllers perform better for nonlinear systems or for systems with variables that change over time. The fractional order controller uses more degrees of freedom compared to the conventional PID controller and has better robustness and fault rejection properties.

2. Results and Discussion

Two Rotor Aero-dynamical System (TRAS) is an equipment created by INTECO [1]. It is a multi-variable system with two inputs and four outputs. The inputs of the system are the voltages applied on the two DC-motors, while the outputs are the rotational speed of the rotors and the position. The transfer matrix (1) represents the linearized TRAS model identified between the rotational speed of the main, pitch and tail, azimuth motor and the input voltage signals applied on these DC-motors.

$$\begin{pmatrix} \omega_h \\ \omega_v \end{pmatrix} = \begin{pmatrix} \frac{8393}{0.22s+1} & \frac{-28.66}{0.17s+1} \\ \frac{-39.33}{0.75s+1} & \frac{5965}{0.83s+1} \end{pmatrix} \quad (1)$$

The TRAS being a cross-coupled system, decoupling technique is used to control the individual outputs. For the decoupled model, fractional order controllers are designed, based on two generalizations of Kessler's optimum magnitude method [2, 3]. The form of the used fractional order controller is:

$$H_R = K_p + \frac{K_I}{s^\alpha} \quad (2)$$

Given the advantages of the IMC scheme as well as FOPID controllers and taking into account the inevitable presence of delays in a real-life control system, a control scheme is used as in [4], which combines both fractional order controllers and the IMC scheme for phase delay systems. As design performances, the crossover frequency ω_{gc} and the phase margin γ_k of the closed loop system are imposed. The final form of the resulted controllers are presented in equation (3).

$$Q_{fb} = \frac{1}{K\zeta s^n + K T_1 s^{\beta-1}} \left(\psi + \frac{1}{s} + T s^{\alpha-1} + \psi s^\alpha \right) \quad (3)$$

In this way the final control structure is a cascade between a fractional filter and a fractional PID controller. For the implementation of both type of fractional order controllers, the NRTF approximation approach is used, having the advantage of low order [5]. The results are presented in Table 1.

Table 1. Comparison between the two types of designed fractional order controllers

The controller	Steady state error ϵ_{ssp} [rad]	Overshoot σ [%]	Settling time t_s [s]	Control effort [V]
Azimuth controller with [3]: $H_{R,11} = 0.008 + \frac{-1.083 \cdot 10^{-5}}{s-0.0454}$	$\epsilon_{ssp} = 0.0044$	$\sigma = 0$	$t_s = 0.95$	$c_{max} = 2.387$ $c_{min} = 0.00353$
Azimuth controller with [4]: $Q_{fb,11} = \frac{1}{8390 + 0.0774 \cdot s^{0.111}} \left(0.232 + \frac{1}{s} + 0.00263s \right)$	$\epsilon_{ssp} = 0$	$\sigma = 8.8$	$t_s = 0.2$	$c_{max} = 0.0616$ $c_{min} = 0.00358$
Pitch controller with [3]: $H_{R,22} = 0.042 + \frac{-3.546 \cdot 10^{-4}}{s-0.0121}$	$\epsilon_{ssp} = 0.0012$	$\sigma = 0$	$t_s = 0.00935$	$c_{max} = 1.247$ $c_{min} = 0.00501$
Pitch controller with [4]: $Q_{fb,22} = \frac{1}{5930 + 0.0975 \cdot s^{0.0111}} \left(0.837 + \frac{1}{s} + 0.0099s \right)$	$\epsilon_{ssp} = 0$	$\sigma = 4$	$t_s = 0.262$	$c_{max} = 0.5146$ $c_{min} = 0.005055$

3. Conclusion

Fractional order controllers designed by innovative methods are suitable even for cross-coupled nonlinear MIMO systems, because the system becomes much more robust, the performance of the transient mode is realistic. The experimental results prove that these controllers are comparable with complex elements like

References

- [1] <http://www.inteco.com.pl/products/two-rotor-aerodynamical-system/>
- [2] DULF E.H., ŞUŞCĂ M., KOVACS L.: Novel Optimum Magnitude Based Fractional Order Controller Design Method. *IFAC PapersOnline* 2018, 51(4):912-917
- [3] DULF E.H.: Simplified Fractional Order Controller Design Algorithm, *Mathematics* 2019, 7(12), 1166; <https://doi.org/10.3390/math7121166>
- [4] MURESAN C.I., BIRS I.R., DULF E.H.: Event-Based Implementation of Fractional Order IMC Controllers for Simple FOPDT Processes, *Mathematics* 2020, 8(8), 1378; <https://doi.org/10.3390/math8081378>
- [5] DE KEYSER R., MURESAN C.I., IONESCU C.M.: An efficient algorithm for low-order discrete-time implementation of fractional order transfer functions, *ISA Trans.* 2018, 74, 229–238.
- [6] Gu D.W, Petkov P.H, Konstantinov M.M.: Robust Control of a Twin-Rotor Aerodynamic System, In: *Robust Control Design with MATLAB®. Advanced Textbooks in Control and Signal Processing.* Springer, London. 2013, https://doi.org/10.1007/978-1-4471-4682-7_18

Influence of fractional order parameter on the dynamics of different vibrating systems

AZHAR ALI ZAFAR^{1*}, JAN AWREJCEWICZ²

1. Department of Mathematics, Government College University Lahore, Pakistan

2. Department of Automation, Biomechanics and Mechatronics, Lodz University of Technology, Lodz, Poland

* Presenting Author

Abstract: In this work, we will investigate the fractional differential equations associated to different vibration phenomena. More specifically, we will discuss Bagley-Torvik equation, composite fractional relaxation differential equation and the motion of a linear oscillator using fractional derivative operator in the sense of Atangana-Baleanu. In order to be consistent with the physical systems the value of the fractional parameter that characterizes the existence of fractional structures in the system, lies within unit interval. The solutions of the non-integer order differential equation are obtained and expressed in terms of generalized functions depending upon the fractional parameter. The classical cases could be recovered by making the limit of fractional parameter approaches to unity. Moreover, we will analyze and compare the control of the fractional order parameter on the dynamics of the models and useful conclusions are recorded.

Keywords: fractional derivative operator, vibrating systems, linear oscillators

1. Introduction

From the last few decades fractional calculus has been motivating and attracting in a great deal of consideration of researchers, physicists and mathematicians. It is seen that different interdisciplinary problems can likewise be solved with good accuracy by the aid of non integer order derivatives. In viscoelasticity, the introductory implementation of fractional calculus is seem to be done by Bagley and Torvik [1], while Makris et al. [2] approximated the applicable value of non integer order parameter that has good compliance with the experimental and material properties anticipated by non integer order derivative model. In addition, fractional order generalizations of one dimensional viscoelastic models have been found to be of great utility in displaying the response linear regime and they are in agreement with the second law of thermodynamics. So, list of the application of fractional calculus is too long to be included here.

Many physical phenomenon have inherent fractional order characterization, hence, fractional calculus is necessary to explain them. Non integer order derivative provide an excellent instrument for the explanation of memory and hereditary characteristics of various materials and processes. This is the main advantage of fractional calculus in comparison with the classical integer order models, in which such properties are in fact ignored and clearly inadequate to certify suitable correlation with experimental data.

Different investigations are made for the study of fractional oscillator equations, for example Ryabov and Puzenko [3] respectively Naber [4] investigated the fractional oscillator equation in the setting of Riemann-Liouville type and Caputo type fractional derivative operator. Stanislavsky [5] interpreted the fractional oscillator equation as the ensemble of ordinary harmonic oscillators governed by stochastic time arrow. Gaul in [6] discussed the damping description by employing fractional operators and investigated the influence of damping in waves and vibrations. It is important to note that, in the mostly published papers researchers have used Riemann-Liouville or Caputo differential operators with singular kernel. More recently, Atangana and Baleanu [7] have proposed non-singular

kernel based modern definitions of fractional derivative. It possess all advantages of Caputo and Riemann-Liouville operators but have smooth kernels.

With these motivations in mind, our aim is to study the fractional differential equations associated to different vibration phenomena. More specifically, we will discuss Bagley-Torvik equation, composite fractional relaxation differential equation and the motion of a linear oscillator using fractional derivative operator in the sense of Atangana and Baleanu. A thorough investigation is made for different driving force functions and different values of fractional order parameter and useful conclusions will be recorded.

2. Concluding Remarks

From the solutions of the fractional Bagley-Torvik equation, it is noticed that the motion of the plate is the increasing function of the fractional parameters and influence is sensitive to the applied force to the plate. Our results could be used as the exact solutions for the comparison of the new numerical methods for the solution of the Bargley-Torvik equation. From the analysis of the solutions of fractional relaxation oscillator it is observed that for increasing values of fractional order parameter velocity increases. The velocity attains the constant value after its initiation and time to reach this

constant value is smaller for large value of $\frac{\rho_p}{\rho_f}$. From the analysis of the solutions of fractional

damped harmonic oscillator it is observed that the equation of oscillator in the setting of fractional derivative operators without damping term still shows damping features depending upon the fractional order parameter. Fractional oscillators with periodic forcing represents the periodic solutions and time for transients to disappear is proportional to the fractional order parameter. By quasi periodic excitations, the behaviour of the oscillator is quasi periodic but periodicity could be achieved by customizing the fractional derivative operator and its order. For the explanation of memory and hereditary characteristics of oscillator fractional derivative approach is more useful. ABC operators have non-singular kernel, so these operators are more preferable to adopt in the fractional order vibration phenomena.

Acknowledgment: This work has been supported by the Polish National Science Centre under the grant OPUS 14 No. 2017/27/B/ST8/01330.

References

- [1] BAGLEY R L, TORVIK P J: A different approach to the analysis of viscoelastically damped structures. *AIAA Journal*, 1983, **21**(5): 741-748.
- [2] MAKKRIS N, DARGUSH G F, CONSTANTINOUC M C: Dynamic analysis of generalized viscoelastic fluids, *J. Eng. Mech.* 1993, **119** (8): 1663-1679.
- [3] RYABOV Y E, PUZENKO A: Damped oscillations in view of the fractional oscillator equation, *Physical Review* 2002, **B 66**: 184-201.
- [4] NABER M: Linear Fractionally Damped Oscillator, *International Journal of Differential Equations* Volume 2010, Article ID 197020, (Hindawi Publishing Corporation, 2010). doi:10.1155/2010/197020
- [5] STANISLAVSKY A A: Fractional dynamics from the ordinary Langevin equation *Physical Review* 2004, **E 70**: 051103-1051103-6.
- [6] GAUL L: The influence of damping on waves and vibrations, *Mechanical Systems and Signal Processing* 1999, **13**(1): 1–30.
- [7] ATANGANA A, BALEANU D: New fractional derivatives with non-local and non-singular kernel: theory and applications to heat transfer model, *Thermal Sci.* 2016, **20**: 763-769.

-S2-

**Nonlinear behavior,
performance, and control
designs for complex
structures in Civil,
Aeronautical, Aerospace
and Ocean Engineering**

The influence of the inductance on the nonideal vibrations of a pendulum coupled to a DC motor

R.H. AVANÇO^{1*}, D. A. ZANELLA², R. DE JESUS A. CANTILLO³, A. CUNHA JR.⁴
J. M. BALTHAZAR⁵, A. M. TUSSET⁶

¹ Universidade Federal do Maranhão, Balsas, MA, Brazil [0000-0003-2276-0230]

² Universidade Federal do Maranhão, Balsas, MA, Brazil [0000-0001-9613-5900]

³ Universidade Federal do Maranhão, Balsas, MA, Brazil [0000-0001-5052-8389]

⁴ UERJ – Rio de Janeiro State University, RJ, Brazil [0000-0002-8342-0363]

⁵ UNESP: São Paulo State University at Bauru, Bauru, SP, Brazil [0000-0002-6082-4832]

⁶ Universidade Tecnológica Federal do Paraná-Campus Ponta Grossa, Paraná, Brazil, [0000-0003-3144-0407]

* Presenting Author

Abstract: The present analysis focuses on the dynamics of a pendulum vertically vibrated by a DC motor. The pendulum moved on the support by vertical harmonic displacement is extensively studied in the literature because of different types of motion including chaos. When the pendulum is vibrated by a DC motor the system is considered non-ideal and it is common a synchronization in frequency between the pendulum and the motor, where the pendulum exhibits either oscillation or rotation. The analysis in the present text varied the value of the inductance from zero to 1 million times the value of a real motor, but the basins of attraction with rotation and oscillation nearly maintained its features. The influence of the inductance has a major effect while the motor accelerates, which could cause an uncertain during the capture by a coexisting attractor. However, the results demonstrated the influence of inductance in this configuration is minimum.

Keywords: inductance, DC motor, pendulum, non-ideal

1. Introduction

The parametrically excited pendulum is vastly analysed in literature. In this situation, the pendulum may have chaotic motion, rotation, oscillation, periodic mixture of rotation and oscillation and the fixed point, where the pendulum is at rest. Basins of attraction for parametrically excited pendulum with crank-slider mechanism were performed and published in [1]. Recently, non-ideal analyses have been gaining space in literature. The system is called non-ideal when the masses involved interfere on the dynamics of the source of energy. The case simulated for the present paper is a pendulum vertically excited by a DC motor with 250 W using a crank-slider mechanism. The motivation of the present analysis is the conclusion in [2] where the authors consider of high relevance the inductance for the results where a cart is moved by a DC motor. On the other hand, a pendulum horizontally moved by a DC motor with a pendulum had its dynamics studied in [3] neglecting the DC motor inductance.

2. Results and Discussion

The results pointed we do not have changes in the types of motion when the inductance is varied. The types of motion found are oscillations in 2-period represented in green colour in Figs. 1 (a,b,c,d).

In black and red, there are two different rotative 1-period attractors where the red has a positive speed and black a negative speed. The Fig1e represents the mechanism with the pendulum, DC motor and crank-slider. The Eq.(1) represent the electric equation of the motor and the Eq.(2) represent the torque supplied by this DC motor. The Fig.1a demonstrate the basin of attraction when the inductance is neglected in the electric equation. The Fig1(b) presents the basin of attraction with the real value of inductance found in the manufacturer catalogue. This value for inductance is 0.161×10^{-3} Henry from a motor with 250 Watts. In Fig.1c the value for the inductance is 1000 times the value from catalogue and in Fig.1 d, the value is one million times the value from the catalogue.

$$V = L \frac{di}{dt} + Ri + K_E \theta \tag{1}$$

$$M_{motor} = K_T \cdot i \tag{2}$$

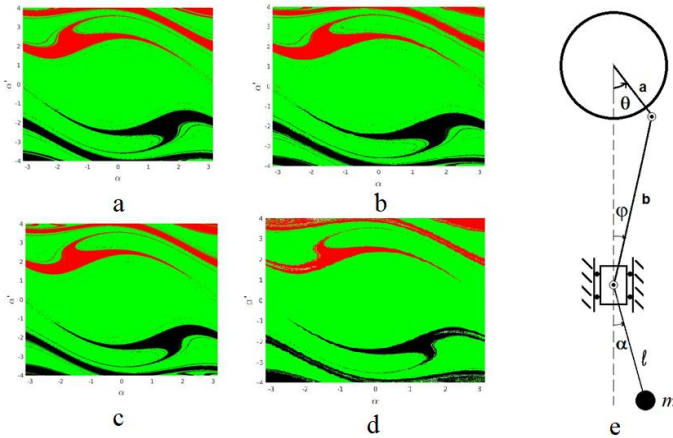


Fig. 1. Basins of attraction. a) No inductance b) Real inductance c)1000 times the inductance d) One million times the inductance e) The figure of the mechanism

3. Concluding Remarks

The results led to conclude that the inductance was not relevant in these mechanism working under the parameters set. The actual idea concerning the inductance is that it is not relevant when the speed of motor does not vary considerable.

References

- [1] AVANÇO RH, NAVARRO RH, ET AL: Statements on nonlinear behavior of a pendulum, excited by crank-shaft-slider mechanism. *Meccanica* 2016, **51**, 1301-1320.
- [2] Lima, R., Sampaio, R., Hagedorn, P. *et al.* Comments on the paper “On nonlinear dynamics behavior of an electro-mechanical pendulum excited by a nonideal motor and a chaos control taking into account parametric errors” published in this journal. *J Braz. Soc. Mech. Sci. Eng.* **41**, 552 (2019)
- [3] Avanço, R.H., Tusset, A.M., Balthazar, J.M., A.Nabarrete, H. A. Navarro . On nonlinear dynamics behavior of an electro-mechanical pendulum excited by a nonideal motor and a chaos control taking into account parametric errors. *J Braz. Soc. Mech. Sci. Eng.* **40**, 23 (2018).

Discussion on the Influence of the Inductance in the Nonlinear Dynamics of DC Motors in Coupled Systems

R.H. AVANÇO^{1*}, D. A. ZANELLA², R. DE JESUS A. CANTILLO³, A. CUNHA JR.⁴
J. M. BALTHAZAR⁵, A. M. TUSSET⁶

¹ Universidade Federal do Maranhão, Balsas, MA, Brazil [0000-0003-2276-0230]

² Universidade Federal do Maranhão, Balsas, MA, Brazil [0000-0001-9613-5900]

³ Universidade Federal do Maranhão, Balsas, MA, Brazil [0000-0001-5052-8389]

⁴ UERJ – Rio de Janeiro State University, RJ, Brazil [0000-0002-8342-0363]

⁵ UNESP: São Paulo State University at Bauru, Bauru, SP, Brazil [0000-0002-6082-4832]

⁶ Universidade Tecnológica Federal do Paraná-Campus Ponta Grossa, Paraná, Brazil, [0000-0003-3144-0407]

* Presenting Author

Abstract: The main goal of this paper is to analyse the influence of the inductance in electromechanical systems. Specifically, a DC motor coupled to a mass horizontally moved by a yoke scotch mechanism. Recent articles claim that the inductance could not be neglected based in electric constant and mechanical constant of the motor. Although many parameters are involved, this analysis intend to demonstrate that the main reason for the relevance of the inductance is the presence of high external load varying in time. The results of torque, electric current and speed of the motor indicates the relevance of the inductance when the mass is high, and the motor has its speed diminished. In conclusion, the inductance will have a greater influence when the motor operates in lower speeds with variable loads. The reason for that is the speed has a minor relevance in the electric equation when the motor is slow, therefore the importance of inductance increases.

Keywords: DC motor, inductance, electromechanical systems, nonideal systems

1. Introduction

The system analysed is a DC motor represented in blue in Fig.1a, coupled to a mass horizontally moved through a scotch yoke. The mass is moved without friction in the wheels or in the pin linked to the DC motor. Note that in [1,2] neglecting the inductance in DC motor causes high differences in the results of the torque and speed, it was studied a problem with varying parameters like the voltage set on DC motor and the distance of the pin to the centre of the motor, while the present paper focus on the mass vibrated because we consider it is the more relevant for the results. Therefore, the present analysis is an expansion in data and in comprehension of the previous study considering the same mechanism with the same parameters. In reference [3] there was a pendulum horizontally excited by a DC motor. In this last, to neglect the inductance was not a problem for the accuracy of results. The reason for that is the size of mass is relatively smaller. All this discussion brings back the idea of the nonideal excitation well discussed in [4].

2. Numerical Results and Discussion

The governing equations of motion are:

$$l\dot{c} + rc + k_e\dot{\alpha} = v \quad (1)$$

$$j_m\ddot{\alpha} + b_m\dot{\alpha} - k_e c = -\tau \quad (2)$$

The term l stand for the inductance, r the resistance, c the electric current, k_e the electric constant, $\dot{\alpha}$ the motor speed, v the voltage set, j_m the moment of inertia of the motor, b_m the damping coefficient, τ is the torque over the motor caused by the mass. The results were found integrating with the Runge-Kutta 4th order and timestep 10^{-6} second, using total time for integration equal to 10 seconds, but only last 10% pointed were plotted. The results in Fig.1b and Fig.1c are the torque of the mass caused on the motor versus the motor speed. The graphics in red represent the model considering the electric inductance on the mechanism. The graphics in blue represent the model which neglects the electric inductance. Comparing the Fig.1(b) and Fig.1(c), it is possible to state that the different models diverge when the masses are high, and the models converge when the mass is small.

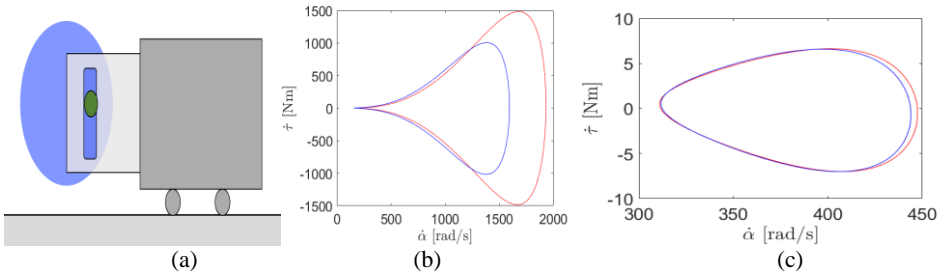


Fig. 1 a) The scotch yoke mechanism with the DC motor and the mass. (Elaborated by the authors) . Results of Torque versus angular speed for b) $m=5\text{kg}$ c) $m=0.05\text{kg}$

3. Concluding Remarks

The current results led to conclude that the inductance may be neglected in some conditions. These conditions include mainly to observe how the angular speed in DC motor evolve during time. When the speed approaches to zero or when it has a high fluctuation, you are probably facing a situation where the inductance cannot be ignored. On the other hand, always to consider the inductance may result in more problems for compute the equations. A stiff equation may require a timestep smaller than the computer offers or just more time consume to complete the calculus. Therefore, ignore the inductance may be useful in some conditions, but in others may change considerably the results.

References

- [1] Lima, R., Sampaio, R., Hagedorn, P. *et al.* Comments on the paper “On nonlinear dynamics behavior of an electro-mechanical pendulum excited by a nonideal motor and a chaos control taking into account parametric errors” published in this journal. *J Braz. Soc. Mech. Sci. Eng.* **41**, 552 (2019)
- [2] LIMA, R., SAMPAIO, R., HAGEDORN, P. One alone makes no coupling. In *Mecanica Computacional Vol xxxvi* . Pags 931-944. Noviembre 2018.
- [3] Avanço, R.H., Tusset, A.M., Balthazar, J.M. , A.Nabarrete, H. A. Navarro . On nonlinear dynamics behavior of an electro-mechanical pendulum excited by a nonideal motor and a chaos control taking into account parametric errors. *J Braz. Soc. Mech. Sci. Eng.* **40**, 23 (2018).
- [4] Cveticanin L., Miodrag Zukovic, Jose Manoel Balthazar. *Dynamics of Mechanical Systems with Non-Ideal Excitation*. ISBN: 978-3-319-54168-6. (2018).

On the flexoelectric effect on nonlinear vibration of three-layered functionally graded cylindrical microshells

ASGHAR FARAMARZI BABADI^{1*}, YAGHOUB TADI BENI^{1,2}, KRZYSZTOF KAMIL ŻUR^{3*,**}

1. Faculty of Engineering, Shahrekord University, Shahrekord, Iran
2. Nanotechnology Research Center, Shahrekord University, Shahrekord, Iran
3. Faculty of Mechanical Engineering, Bialystok University of Technology, Bialystok, Poland

* Presenting Author

**Corresponding Author: k.zur@pb.edu.pl

Abstract: According to past research, the flexoelectricity effect is dependent on the strain gradient noticeable in micro/nanoscales. It can be concluded that flexoelectricity has a considerable effect on the electromechanical behavior of structures in small scale. For the first time, the first-order shear deformation theory (FSDT) and the reformulated flexoelectric theory is used to study nonlinear free vibration of three-layered cylindrical microshell made of a functionally graded piezoelectric (FGP) core and two layers of flexoelectric material. Equations of motion and corresponding boundary conditions are derived from variational Hamilton's principle. Change a volume element due to the elastic deformation is taken into account, so it creates a source of nonlinearity in the derived equations of motion. The nonlinear partial differential equations are numerically solved by perturbation method. Effects of crucial geometric, material and scale parameters on the dynamic response of the flexoelectric structure are comprehensively investigated and discussed.

Keywords: first-order shear deformation theory, reformulated flexoelectric theory, FGM, microshell, nonlinear dynamics

1. Background

Optimized performance of intelligent small structures such as microbeams, microshells, microplates in such cases as measurement equipment, medical equipment, electronic equipment is a fundamental issue in micro- and nanoelectromechanical systems (MEMS/NEMS) [1,2]. Due to the application of MEMS and NEMS in the mechanical, chemistry, and aerospace industries and because of their high performance and high accuracy in adverse environmental conditions, researchers have paid special attention to these systems and tried to determine their electromechanical responses in different environmental conditions. Due to electromechanical properties, mechanical energy (tensile, pressure, bending, and twisting) and electrical energy (voltage, electric field, and electrical polarization) can be converted to each other, and used in the construction of transducers, sensors, actuators, resonators at diverse scales.

Considering the fact that the properties of the functionally graded materials are common in structures at micro scale, therefore, the functionally graded flexoelectric cylindrical microshell is the object of our investigation. By deep investigation of the previous studies, it can be found that modified flexoelectric theory has not been used to study the nonlinear vibration of the flexoelectric cylindrical microshell under electrical loadings [4,5]. Additionally, the effect of functionally graded material on the electromechanical behavior of the flexoelectric microshell under electric forces based on the

modified flexoelectric theory has not been investigated in previous studies. The present study on the behavior of this type of microstructure fills the gaps in the existing literature.

2. FGP microshell

In this study, we consider a three-layer flexoelectric microshell with a total thickness of $h_t = h + 2h_f$, where h_t , h and h_f are the total thickness, core thickness and thickness flexoelectric layers of the structure, respectively. The microshell has a radius equal to R , a length equal to L and a thickness equal to h_t . The upper and bottom layer are assumed to be made of two different flexoelectric materials, and the core is made of functionally graded of two piezoelectric materials. The properties of the microshell core are quite different in the direction of thickness. The schematic of microshell model is presented in Figure 1.

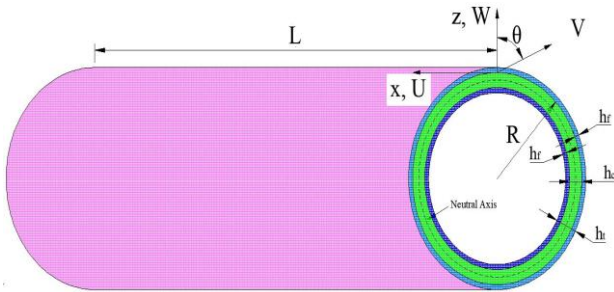


Fig. 1. The geometry and coordinate system of the microshell.

Acknowledgment: Project financing through the program of the Minister of Science and Higher Education of Poland named "Regional Initiative of Excellence" in 2019 - 2022 project number 011 / RID / 2018/19 amount of financing 12,000,000 PLN.

References

- [1] CRAIGHEAD HG: Nano-electromechanical systems. Science 2000, **290**(5496):1532-1535.
- [2] ZHANG J, WANG C, BOWEN C: Piezoelectric effects and electromechanical theories at the nanoscale. Nanoscale 2014, **6**:13314-27.
- [3] LI A, ZHOU S, QIL, CHEN X: A reformulated flexoelectric theory for isotropic dielectrics. Journal of Physics D: Applied Physics 2015, **48**:465502.
- [4] GHOBADI A, GOLESTANIAN H, TADI BENI Y, ŽUR KK: On the size-dependent nonlinear thermo-electromechanical free vibration analysis of functionally graded flexoelectric nano-plate, Communications in Nonlinear Science and Numerical Simulation 2021, **95**:105585.
- [5] GHOBADI A, TADI BENI Y, ŽUR KK: Porosity distribution effect on stress, electric field and nonlinear vibration of functionally graded nanostructures with direct and inverse flexoelectric phenomenon, Composite Structures 2021, **259**:113220.

Global Sliding Mode Control for a Fully-Actuated Non-Planar Hexa-Rotor Aerial Vehicle

JOSÉ AGNELO BEZERRA¹, JOÃO FRANCISCO SILVA TRENTIN^{1*}, DAVI ANTÔNIO DOS SANTOS¹

1. Division of Mechanical Engineering, Aeronautics Institute of Technology (ITA), São José dos Campos, SP, Brazil. [0000-0002-4488-3402],[0000-0002-6726-8699],[0000-0001-5995-3103]. * Presenting Author

Abstract: This paper is concerned with the attitude and position control of a fully-actuated non-planar hexa-rotor aerial vehicle equipped with reversible fixed rotors. A six-degrees-of-freedom force-torque control law is designed using a unit-vector multi-input global sliding mode control. The method is evaluated and demonstrated in a software-in-the-loop simulator, which shows its effectiveness.

Keywords: multicopter aerial vehicle, hexa-rotor, global sliding mode control, dynamics.

1. Introduction

Applications of multicopter aerial vehicles (MAVs) for aerial manipulation, delivery and air taxi are expected in the near future. These tasks require the vehicle to safely manoeuvre in position independently of the attitude, while subject to unknown environmental disturbances (*e.g.* wind) [1]. Therefore, these applications are quite suitable for fully-actuated MAVs, such as the non-planar hexa-rotor aerial vehicle considered in this paper.

To allow a safe flight in the presence of bounded disturbances, we design a sliding mode controller (SMC) suitable for fully-actuated MAVs. The controller provides a six-dimensional command for the resultant force and torque, thus it can control both the vehicle's translational and rotational dynamics. The conventional SMC design consists of two phases: reaching a specified sliding manifold and sliding along this manifold [2]. However, during the reaching phase, robustness is not guaranteed. Therefore, we use the global sliding mode control (GSMC) scheme, which provides robustness from the initial condition until the desired reference [2,3]. This abstract briefly shows the control methodology, which includes the MAV dynamic modelling, the adopted sliding surface, and the proposed GSMC law. Additionally, we present the simulation results of the proposed control compared to a proportional-derivative (PD) feedback linearization control law, considering a non-planar hexa-rotor aerial vehicle.

2. Controller Design and Results

Assume that $\mathbf{x} \triangleq (\mathbf{x}_1, \mathbf{x}_2) \in \mathbb{R}^{12}$ is the vector of state errors, where $\mathbf{x}_1 \in \mathbb{R}^6$ denotes the errors of position and attitude, which is expressed as a Gibbs vector, and $\mathbf{x}_2 \in \mathbb{R}^6$ represents the errors of linear and angular velocities. Moreover, consider the control torque vector $\mathbf{u} \in \mathbb{R}^6$ as a command to the force and torque produced by the MAV, while $\mathbf{d} \in \mathbb{R}^3$ is an unknown force-torque disturbance such that $\|\mathbf{d}\| \leq \rho$, with known $\rho \in \mathbb{R}_+$. Therefore, the complete nonlinear dynamics of the MAV can be modelled as follows

$$\dot{\mathbf{x}}_1 = \mathbf{f}_1(\mathbf{x}), \quad (1)$$

$$\dot{\mathbf{x}}_2 = \mathbf{f}_2(\mathbf{x}) + \mathbf{B}(\mathbf{x})(\mathbf{u} + \mathbf{d}), \quad (2)$$

where $\mathbf{f}_1: \mathbb{R}^{12} \rightarrow \mathbb{R}^6$, $\mathbf{f}_2: \mathbb{R}^{12} \rightarrow \mathbb{R}^6$, $\mathbf{B}: \mathbb{R}^{12} \rightarrow \mathbb{R}^{6 \times 6}$ are given functions. Furthermore, \mathbf{f}_1 and \mathbf{B} are such that $\|(\partial \mathbf{f}_1 / \partial \mathbf{x}_2) \mathbf{B}\| \neq 0, \forall \mathbf{x} \in \mathbb{R}^{12}$. Now, we can define the following time-varying sliding function

$$\mathbf{s}(t, \mathbf{x}) \triangleq \boldsymbol{\sigma}(t) - \mathbf{P}(t)\boldsymbol{\sigma}(\mathbf{0}), \quad (3)$$

where $\sigma(\mathbf{t}) \triangleq \mathbf{C}\mathbf{x}_1 + \mathbf{f}_1 \in \mathbb{R}^6$ with $\mathbf{C} \in \mathbb{R}^{6 \times 6}$ being given a diagonal matrix, and $\mathbf{P}: \mathbb{R}_+ \rightarrow \mathbb{R}^{6 \times 6}$ is a function which satisfies, among other design conditions, $\mathbf{P}(\mathbf{0}) = \mathbf{I}_6$ [3]. Based on (3), consider the set $\mathcal{S} \triangleq \mathbf{x} \in \mathbb{R}^{12}: \mathbf{s}(\mathbf{t}, \mathbf{x}) = \mathbf{0}, \forall \mathbf{t} \geq 0$ as the eventual sliding set. Therefore, to ensure a global sliding mode of system (1)-(2) in \mathcal{S} , we can design the control law [3]

$$\mathbf{u} = - \left(\frac{\partial \mathbf{f}_1}{\partial \mathbf{x}_2} \mathbf{B} \right)^{-1} \left(\left(\mathbf{C} + \frac{\partial \mathbf{f}_1}{\partial \mathbf{x}_1} \right) \mathbf{f}_1 + \frac{\partial \mathbf{f}_1}{\partial \mathbf{x}_2} \mathbf{f}_2 + \dot{\mathbf{P}}(\mathbf{t})\sigma(\mathbf{0}) + \kappa \frac{\mathbf{s}}{\|\mathbf{s}\|} \right), \quad (4)$$

where $\kappa > \|(\partial \mathbf{f}_1 / \partial \mathbf{x}_2) \mathbf{B}\| \rho$ is a design parameter.

Figure 1 shows the controlled position and attitude, as well as the respective commands. The reference trajectory is a step of $(1, 1.5, 2)^T$ for position, combined with a conic motion with frequency of 1/15 Hz and amplitude of 30° for attitude. The disturbances are considered as sinusoidal signals with frequency of 0.1 Hz and amplitudes of 0.02 N and 0.003 Nm for force and torque, respectively. The parameters used for the GSCM are $\kappa = 0.5$, $\mathbf{C} = \mathbf{I}_6$, and $\mathbf{P}(\mathbf{t}) = \exp(-\mathbf{t})\mathbf{I}_6$. For the PD control, $\mathbf{K}_1 = \text{diag}(2, 2, 2, 3, 3, 3)$ is the proportional gain and $\mathbf{K}_2 = 5\mathbf{I}_6$ is the derivative gain. For the position states, we can note that the GSCM does not present overshoot neither oscillation around the commanded value. Furthermore, for the attitude states, the GSCM reaches the reference faster and follows it precisely.

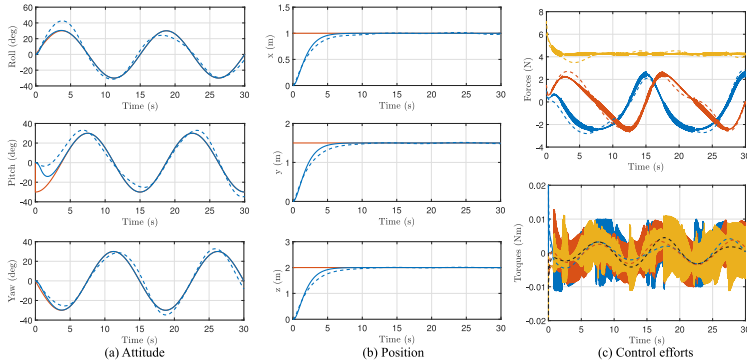


Fig. 1. Numerical results for attitude and position control of a fully-actuated non-planar hexa-rotor aerial vehicle, where for attitude and position - - - PD control, - GSCM, and - the command trajectory. For the GSCM - T_1 , - T_2 , - T_3 the control torques and - F_1 , - F_2 , - F_3 the control forces. For the PD control, - - - T_1 , - - - T_2 , - - - T_3 the control torques and - - - F_1 , - - - F_2 , - - - F_3 the control forces.

3. Concluding Remarks

This paper has presented the design of a global sliding mode control law for a fully-actuated non-planar hexa-rotor and has compared the results with a proportional-derivative feedback linearization control law. We can observe that the GSCM outperforms the PD control, while ensuring robustness against bounded disturbances during all the flight.

Acknowledgment: The authors thank the São Paulo Research Foundation (FAPESP) for the financial support (grants 2019/05334-0 and 2020/12314-3) and CNPq/Brazil (grant 302637/2018-4).

References

- [1] ARIOBERTO L. SILVA, DAVI A. SANTOS: Fast nonsingular terminal sliding mode flight control for multirotor aerial vehicles. *IEEE Transactions on Aerospace and Electronic Systems* 2020, **56**(6):4288-4299.
- [2] YURI SHTESSEL, CHRISTOPHER EDWARDS, LEONID FRIDMAN AND ARIE LEVANT: *Sliding mode control and observation*. Springer: Berlin, 2014.
- [3] A. BARTOSZEWICZ: Time-varying sliding modes for second-order systems. *IEE Proceedings – Control Theory and Applications* 1996, **143**(7):455-462.

Some Remarks On Experimental Analysis Of A Non-Ideal Conveyor Belt.

LEANDRO R. DE OLIVEIRA^{1*}, JOSÉ M. BALTHAZAR², AIRTON NABARRETE³
ÁTILA M. BUENO⁴, ANGELO M. TUSSET⁵, EDUARDO A. PETROCINO⁶

1. São Paulo State University – UNESP, School of Engineering, Bauru, SP, Brazil [0000-0001-5290-9863]
2. São Paulo State University – UNESP, School of Engineering, Bauru, SP, Brazil, [0000-0002-6082-4832]
3. Aeronautics Institute of Technology – ITA, São José dos Campos SP, Brazil [0000-0002-1617-9063]
4. São Paulo State University – UNESP, Institute of Science and Engineering, Sorocaba, SP, Brazil [0000-0002-1113-3330]
5. Federal Technology University of Parana – UTFPR, Academic Department of Mathematics, Ponta Grossa PR, Brazil [0000-0003-1144-0407]
6. São Paulo State University – UNESP, School of Engineering, Bauru, SP, Brazil. [0000-0002-4026-6052]

* Presenting Author

Abstract: The conveyor belt is an important equipment of the preparation system in sugar and alcohol plants. It is responsible for providing the mills with constant feeding of sugar cane mass, avoiding overloads due to excessive feeding. This work aims to develop a small-scale experimental setup of the conveyor belt, which can reproduce its behavior, and thus be able to implement modifications to validate theoretical studies.

Keywords: non-ideal machinery, conveyor belt dynamics, Sommerfeld effect, nonlinear dynamics

1. Introduction

The sugar cane grinding depends on equipment specially designed to receive and prepare the raw material in order to obtain maximum production efficiency. As the last segment of a long equipment's line the conveyor belt depicted in Fig.1(a) is the most important element to keep the feeding constant for the grinding process.

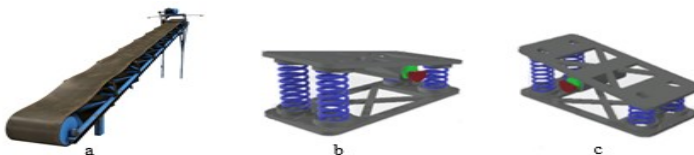


Fig. 1. 3D Model of Conveyor Belt and Apparatus Developed (a: [3]; b, c: Elaborated by the authors).

The experimental setup consists of the lower base connected to the upper base by two pairs of springs of different lengths, as described in Fig.1(b) and Fig.1(c), in order to have the inclination shown in the real equipment. A 9V DC motor was connected on the upper base and its speed control was done by Arduino. The motor speed was measured using an LM393 (optical photosensitive light sensor module) and the Arduino was also responsible data acquisition. Additionally, to acquire the vibration data, the accelerometer of the iPhone 6 cell phone was used, as depicted in Fig.2. Because of the dynamic interaction and energy transfer between the vibration modes of the apparatus when

excited by an unbalanced motor, its torque does not remain constant, which characterizes the motor as non-ideal [1, 2].

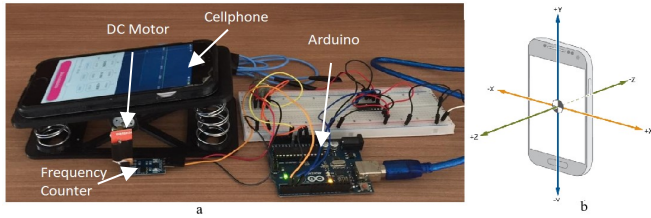


Fig. 2. Equipment's Used in Experience and Accelerometer Coordinates (a: Elaborated by the authors; b: [4]).

2. Results and Discussion

The experimental results showed movements of pitch, roll and bounce, as represented in Fig.3, for which it was observed the Sommerfeld effect [1]. This phenomenon occurs in unbalanced rotating machines supported by flexible structures where power is converted into mechanical vibration instead of increasing the machine rotation speed.

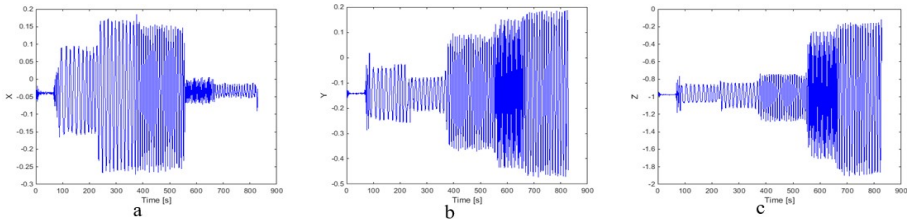


Fig. 3. Time Histories in Physical Coordinates for Conveyor (a) Roll (b) Pitch and (c) Bounce.

3. Concluding Remarks

Experience has shown that on the x-axis, rotation around the longitudinal, the frequency has stagnated although during the experiment the angular velocity continued to increase. There is an increase in the amplitude of vibration in the frequency range of capture near the resonance frequency and then a jump to a higher frequency with lower vibrations. Future results include the exploration of vibration modes and numerical results of mathematical modeling [1, 2].

References

- [1] Balthazar J.M., Tusset, A.M., Brasil, R.M.L.R.F. et al. An overview on the appearance of the Sommerfeld effect and saturation phenomenon in non-ideal vibrating systems (NIS) in macro and MEMS scales. *Nonlinear Dyn* 93, 19–40 (2018).
- [2] Füsün A.G., B.H., Balthazar J.M., Felix J.L.P., Brasil R.M.L.R.F. .On Dynamic Behavior of a Nonideal Torsional Machine Suspension Structure. In: Awrejcewicz J. (eds) *Dynamical Systems: Modelling*. DSTA 2015. Springer Proceedings in Mathematics & Statistics, vol 181. Springer, Cham, (2016).
- [3] Image available in <https://www.turbosquid.com/3D-Models/3d-conveyor-belt-model/827002?referral=3dsecure>. Access in 04-28-2021.
- [4] Image available in <https://physics.stackexchange.com/questions/525519/graph-analysis-of-accelerometer-data>. Access in 04-15-2021.

On a Nonlinear and Non-Ideally Excited Tank

MARIA ALINE GONÇALVES^{1*}, JOSÉ M. BALTHAZAR², ELŻBIETA JARZĘBOWSKA³,
ÂNGELO M. TUSSET⁴, MAURÍCIO A. RIBEIRO⁵, HILSON H. DAÛM⁶

1. São Paulo State University – UNESP, School of Engineering Bauru, SP, Brazil [0000-0001-5231-7390]
2. São Paulo State University – UNESP, School of Engineering Bauru, SP, Brazil [0000-0002-6082-4832]
3. Warsaw University of Technology - WUT, Warsaw, Poland [0000-0003-1407-7546]
4. Federal Technological University of Paraná, Ponta Grossa, PR, Brazil [0000-0003-3144-0407]
5. Federal Technological University of Paraná, Ponta Grossa, PR, Brazil [0000-0001-7314-0723]
6. Federal Technological University of Paraná, Ponta Grossa, PR, Brazil [0000-0003-0771-1035]

* Presenting Author

Abstract: In this work, we revisited and investigated the nonlinear parametric resonance of free surface oscillations of fluid inside a tank excited by a non-ideal power source with limited power supply. Numerical analysis of nonlinear dynamics is presented as phase portrait diagrams, power spectrum and maximum Lyapunov exponents to determine the regions in which the resonant sloshing vibrations have a chaotic or periodic behavior. we also present an Optimal Linear Feedback Control (OLFC) and a State Dependent Riccati Equation (SDRE) Control design that can both reduce to the chaotic movement to a stable condition. The (OLFC) technique is based on Lyapunov stability theory and optimal quadratic linear control (LQR) and has the characteristic of separating nonlinearity from the system and applying feedforward control feedback control. The (SDRE) control method (SDRE) has as main characteristic for calculating the LQR gain the variable state matrix

Keywords: Non-ideal power sources. Parametric resonance. Nonlinear dynamics. Control Design's

1. Introduction

Sloshing inside a tank excited by a non-ideal power source has diverse applications in engineering sciences as in aerospace and nuclear fields. The excitation of the system analyzed by this work is limited by the characteristics of the energy source and its dependency on the vibrating system. We present a model based on [1, 2], composed by a tank of radius R, partially filled with a Newtonian fluid, parametrically excited by an electric motor (Fig. 1(a)). The nonlinear dynamics of system can be represented by equations below:

$$\left. \begin{aligned} \frac{dp_1}{d\tau} &= -\alpha p_1 - (\beta + AE - 2)q_1 + BMp_2; & \frac{dq_1}{d\tau} &= -\alpha p_2 - (\beta + AE - 2)q_1 + BMp_1 & \square \\ \frac{dp_2}{d\tau} &= -\alpha q_1 + (\beta + AE + 2)p_1 + BMq_2; & \frac{dq_2}{d\tau} &= -\alpha q_1 + (\beta + AE + 2)p_2 + BMq_1; & \frac{\beta}{d\tau} &= N_2 - N_1\beta - \mu(p_1q_1 + p_2q_2) \end{aligned} \right\} \quad (1)$$

where, τ : slow time; p_1, q_1, p_2, q_2 : dominant modes amplitudes; α : liquid coefficient of additional viscous damping forces of liquid; β : tuning parameter related to motor frequencies. A and B: constant coefficients dependent on tank diameter and depth of the filled liquid; E and M: energy and angular momentum of fluid vibrations in the fundamental modes. N_1 : constant of linear static performance curve of the motor; N_2 : natural frequency of the fundamental free surface oscillations; μ : natural frequency and physical characteristics of the moto and $E = E_1 + E_2$, $E_n = 12(p_n^2 + q_n^2)$ and $M = p_1q_2 + p_2q_1$.

2. Results and Discussion

The computational numerical method for solution used was the fourth order Runge-Kutta implicit with integration step of $h=0.001$ and time of $t=10^5$ and transient time of 40% of total time. We assume the parameters are $\alpha = 0.8, A = 1.112, B = -1.531, N_2 = -0.25, \mu = 4.5$ and initial conditions to be equal to $p_1(0) = q_1(0) = 1.0, p_2(0) = q_2(0) = 1.0, \beta(0) = 0$, adapted from [1].

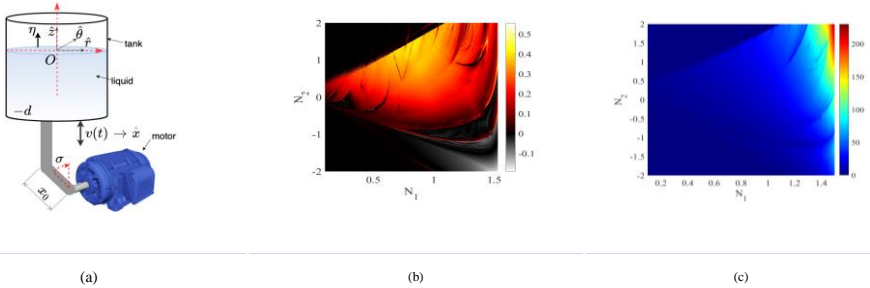


Fig. 1. (a) Schematic diagram of the system composed by a partially filled tank, excited by a motor. (b) Lyapunov exponent λ in range $N_1 \in [0.05, 1.5] \times N_2 \in [-2.0, 2.0]$ (c) Energy total in range $N_1 \in [0.05, 1.5] \times N_2 \in [-2.0, 2.0]$

Fig. 1(b) shows the behavior of maximum Lyapunov exponent (λ) with $N_1 \in [0.05, 1.5] \times N_2 \in [-2.0, 2.0]$. For negative values of λ the system is periodic, for positive values of λ the system is chaotic. Fig. 1(c) illustrates the results for the dimensionless total power [2]. For high values of N_1 and N_2 the rate of change of the total energy is zero. Inside the regions where N_1 and N_2 have intermediate values the total power oscillates around zero but there is no constant period. OLFC and SDRE techniques based on [3] were applied to an orbit was defined with a Fourier Series as $u(i)(t) = a_0 + a_1 \cos(\omega t) + b_1 \sin(\omega t)$ and they have excellent agreement according to Fig 2(a) and (b).

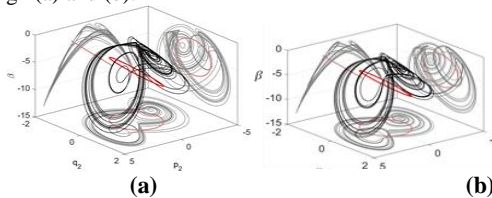


Fig 2 Results using a) OLFC ,b) SRDE

3. Conclusion

This work shows that the OLFC and SDRE strategy applied to the presented mathematical model reduced the chaotic movement of the system to a periodic one. The Fig. 2 illustrates the effectiveness of the control strategy to this interaction fluid-electric motor problem. Future works include sensibility analysis.

References

1. H. A. NAVARRO, J. M. BALTHAZAR, T. S. KRASNOPOL'SKAYA, A. Y. SHVETS, AND F. R. CHAVARETTE, Remarks on parametric surface waves in a nonlinear and non-ideally excited tank, *J. Vib. Acoust. Trans. ASME*, vol. 134, no. 4, pp. 1–6, Aug. 2012. <https://doi.org/10.1115/1.4005844>
2. T. S. KRASNOPOL'SKAYA AND A. Y. SHVETS, Energy Transfer Between Hydrodynamical Systems and Excitation Machines of Limited Power Supply, Proc. ENOC -St. Petersburg, Russia, June 30–July 4, 2008.
3. A. M. TUSSET, BALTHAZAR J. M. ; BASSINELLO, D. ; PONTES B.R. ; FELIX J. L. P. Statements on chaos control designs, including a fractional order dynamical system, applied to a MEMS comb-drive actuator. *Nonlinear Dynamics*, v. 69, p. 1837-1857, 2012. <https://doi.org/10.1007/s11071-012-0390-6>

The Existence of Absolutely Continuous Invariant Measures for q -Deformed Unimodal Maps

DIVYA GUPTA^{1*}, V.V.M.S. CHANDRAMOULI²

1. Department of Mathematics, Indian Institute of Technology Jodhpur, India.
2. Department of Mathematics, Indian Institute of Technology Jodhpur, India.

Abstract: In this paper, we describe the various types of deformation schemes inspired by Heine and Tsallis in reference of q -deformed physical system related to the quantum group structures and the statistical mechanics. We discuss the dynamics of deformed unimodal maps in particular q -Logistic map and q -Gaussian map. Further we show that numerically, there exists a set of the parameter values with positive measure, for which these deformed maps admits absolutely continuous invariant probability measure with respect to the Lebesgue measure.

Keywords: acip, deformed map, deformed Logistic map, deformed Gaussian map.

References

- [1] BALADI V, VIANA M: Strong stochastic stability and rate of mixing for unimodal maps. *Annales scientifiques de l'Ecole normale supérieure* 1996, **29**(4):483-517.
- [2] BANERJEE S, PARTHASARATHY R: A q -deformed logistic map and its implications. *Journal of Physics A: Mathematical and Theoretical* 2011, **44**(4):3-23.
- [3] DE MELO W, VAN STRIEN S: One-dimensional dynamics. *Springer Science & Business Media* 2012.
- [4] JACKSON F H: XI.—on q -functions and a certain difference operator. *Earth and Environmental Science Transactions of the Royal Society of Edinburgh* 1909, **46**(2):253-81.
- [5] JAGANATHAN R, SINHA S: A q -deformed nonlinear map. *Physics Letters A* 2005, **338**(3-5):277-87.
- [6] JAKOBSON M V: Absolutely continuous invariant measures for one-parameter families of one-dimensional maps. *Communications in Mathematical Physics* 1981, **81**(1):39-88.
- [7] KELLER G: Exponents, attractors and Hopf decompositions for interval maps. *Ergodic Theory and Dynamical Systems* 1990, **10**(4):717-44.
- [8] KOZLOVSKY O S: Structural stability in one-dimensional dynamics, 1998.
- [9] NOWICKI T, VAN STRIEN S: Invariant measures exist under a summability condition for unimodal maps. *Inventiones mathematicae* 1991, **105**(1):123-36.
- [10] THUNBERG H: Periodicity versus chaos in one-dimensional dynamics. *SIAM review* 2001, **43**(1):3-0.

An Improved q-Deformed Logistic Map and its Implications

DIVYA GUPTA^{1*}, V.V.M.S. CHANDRAMOULI²

1. Department of Mathematics, Indian Institute of Technology Jodhpur, India.
2. Department of Mathematics, Indian Institute of Technology Jodhpur, India.

Abstract: In this paper we show that the q-deformed Logistic map proposed by Banerjee and Parthasarathy [1] is actually topologically conjugate to the canonical Logistic map and therefore there is no dynamical changes by this q-deformation. We propose a correction on this q-deformed scheme applied on Logistic map and describe the dynamical changes. We illustrate the Parrondo's paradox by assuming chaotic region as the gain. Further, we compute the topological entropy in the parameter plane and show the existence of Li-Yorke chaos. Finally we show that in the neighbourhood of particular parameter value, q-Logistic map has stochastically stable chaos.

Keywords: q-Deformed Logistic map, Heine deformation on nonlinear map, Topological entropy, Stochastically stable chaos.

References

- [1] BANERJEE S, PARTHASARATHY R: A q-deformed logistic map and its implications. *Journal of Physics A: Mathematical and Theoretical* 2011, **44**(4):3-23.
- [2] JAGANATHAN R, SINHA S: A q-deformed nonlinear map. *Physics Letters A* 2005, **338**(3-5):277-87.
- [3] MISIUREWICZ M, SZLENK W: Entropy of piecewise monotone mappings. *Studia Mathematica* 1980, **67**(1):45-63.
- [4] LI T Y, YORKE J A: Period three implies chaos. *In the theory of chaotic attractors* 2004. Springer, New York, NY, 77-84.
- [5] BLANCHARD F, GLASNER E, KOLYADA S, MAASS A: On Li-Yorke pairs. *Journal für die reine und angewandte Mathematik* 2002, **547**:51-68.
- [6] BLOCK L, KEESLING J, LI S, PETERSON K: An improved algorithm for computing topological entropy. *Journal of Statistical Physics* 1989, **55**(5):929-39.
- [7] DE MELO W, VAN STRIEN S: One-dimensional dynamics. *Springer Science & Business Media* 2012.
- [8] THUNBERG H: Periodicity versus chaos in one-dimensional dynamics. *SIAM review* 2001, **43**(1):3-0.
- [9] BALADI V, VIANA M: Strong stochastic stability and rate of mixing for unimodal maps. *Annales scientifiques de l'Ecole normale supérieure* 1996, **29**(4):483-517.

Active MEMS Amplifier for Improved Signal-to-Noise Ratios

STEFANIE GUTSCHMIDT^{1*}, SEIGAN HAYASHI¹, NICHOLAS LAM¹, CLAUDIA LENK²

1. Mechanical Engineering, University of Canterbury, Christchurch, New Zealand

2. Department of Micro- and Nanoelectronic Systems, TU Ilmenau, Germany [0000-0002-3040-1265]

* Presenting Author [0000-0002-1528-809X]

Abstract: The idea of using feedback mechanisms to adaptively amplify signals beyond the linear range is inspired by the human cochlea. The considered active composite MEMS (micro-electromechanical systems) oscillator amplifies input signals distinctively using its passive, active nonlinear, and Hopf dynamics. The amplification level is solely determined by the mechanical properties of the device and the input stimulus strength, making use of the system's complex dynamics. One of the key outcomes of our work is that we can demonstrate amplitude-dependant amplification, which can be likened to the compressive nonlinearity seen in the cochlea. Our comprehensive dynamic and stability analyses are accompanied by experimental validations of new findings, including an evaluation of technological feasibility.

Keywords: active MEMS sensor, signal-to-noise ratio, nonlinear compressive amplification

1. Introduction

The human cochlea is an impressive example of a biological sensor. The cochlea's remarkable dynamic range, highly tuneable sensitivity and nonlinear compressive amplification properties are attributed to its underlying active nature [1, 2]. Theoretical and experimental attempts to create an artificial device include active oscillators with different feedback mechanisms [1], diverse nonlinear systems [1, 3] and operation near bifurcation points such as a Hopf [4]. This novel work explores the dynamics of a self-sensing and self-actuating MEMS oscillator [5] subject to external stimuli and feedback mechanisms (see Fig. 1). Our investigations focus on the amplification properties of the MEMS oscillator operated at selected parameter tuples. Furthermore, selected theoretical findings are validated experimentally and technological feasibility of parameter ranges is discussed.

2. Model

We consider a single MEMS cantilever (Fig. 1) with integrated sensing and actuation capabilities [5]. Based on our previous work [6], the analysis is carried out with a simplified modal representation of the first vibration mode

$$\ddot{q}_w + \delta \dot{q}_w + q_w = \alpha q_\theta + \kappa_{ext}, \quad (1)$$

$$\dot{q}_\theta + \beta q_\theta = \gamma i^2, \quad (2)$$

where q_w and q_θ are the non-dimensionalised mechanical and thermal variables of the system. Parameters α , β , γ , δ are integration constants originating from a modified Ritz discretization [6] and κ_{ext} being the external stimulus.

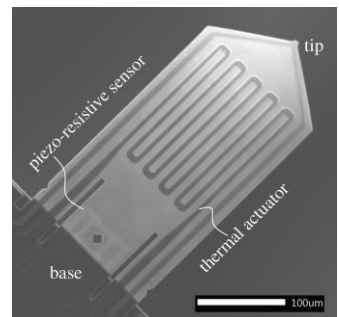


Fig. 1. SEM picture of MEMS sensor. (Taken with JEOL JSTM-IT300)

A feedback mechanism is introduced by means of the thermal actuator as $i = \tanh(i_{DC} + a q_w)$, where i_{DC} is an offset current, which controls control equilibrium states and a is the feedback strength.

3. Results and Discussion

Figure 2 depicts relevant equilibrium states of the system and associated gain properties for a range of feedback values and input strengths. In this brief discussion we highlight the different dynamics of three system configurations. The passive system (black) exhibits a constant gain of 38.42 dB at resonance for any input amplitude and feedback parameter. In contrast, the gain of the active, nonlinear system (blue) is dependent on input amplitude. As a result, the system is capable of demonstrating amplitude-dependant amplification, which can be likened to the compressive nonlinearity seen in the cochlea [2-3]. Certain equilibrium states also feature a Hopf bifurcation (purple), exhibiting another range of gain properties available with this system. Input amplitudes encompassing a parameter range of 10^{-7} to 10^{-3} yield a maximum gain of 76 dB near the Hopf-point at $a = 2.7$ for even a non-optimised system.

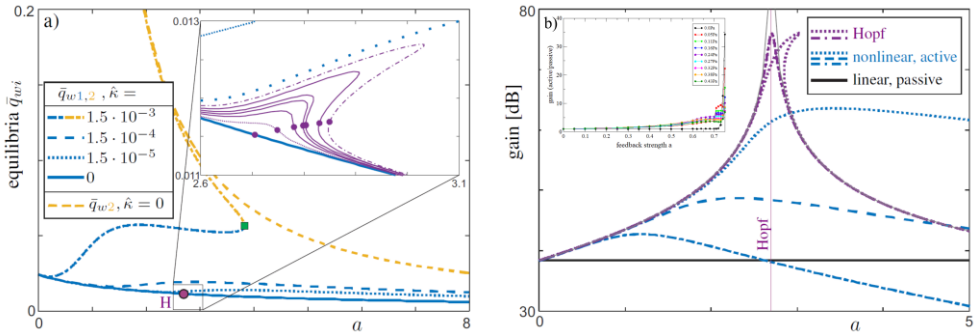


Fig. 2. Simulated behaviour of the MEMS system for different feedback strengths and varying stimuli; a) equilibrium states, b) associated gain properties; insert: initial experimental investigations showing gain at Hopf point.

4. Concluding Remarks

A novel adaptable MEMS sensor with self-sensing/-actuation capabilities has been presented whose complex nonlinear dynamics gives rise to much improved amplification properties. Initial theoretical gain characteristics, which have also been qualitatively validated experimentally (see insert of Fig. 2b), suggest very promising amplification and signal detection properties, even in noisy environments (not directly shown here but observable in Fig. 2b)). A more detailed and satisfying discussion of our new findings in addition to a discussion on the technological feasibility is included in the full paper.

References

- [1] JOYCE B.S., TARAZAGA P.A. (2015) *Smart Mater. Struct.*, **24**, 094004.
- [2] NEELY S. T., RASETSHWANE D.M. (2017) *J. Acoust. Soc. Am.*, **142**(4).
- [3] HUDSPETH A.J. (2008) *Neuron.*, **59**(4): 530-545.
- [4] HUDSPETH A.J., JÜLICHER F., MARTIN P. (2010) *J. Neurophysiol.*, **104**: 1219-1229.
- [5] IVANOV T, GOTSZALK T, GRABIEC P, TOMEROV E, RANGELOW IW (2003) *Microelectron. Eng.*, **67**: 550-556.
- [6] ROESER D., GUTSCHMIDT S., SATTEL T., RANGELOW I.W. (2016). *J. Microelectromech. Syst.*, **25**: 78-90.

Energy recovery hybrid system with the flywheel

JACEK JACKIEWICZ^{1*}

1. Faculty of Mechatronics, Kazimierz Wielki University in Bydgoszcz

* Presenting Author

Abstract: The coupling of drive units of electric and hybrid vehicles with flywheel-based kinetic energy recovery systems is one of the best suitable options to reduce fuel energy usage. And, in consequence, it is also a convenient method to reduce greenhouse gas emissions. The essence of the work will be to design a hybrid traction system cooperating with a flywheel that collects kinetic energy during vehicle braking.

Keywords: electric and hybrid vehicles, flywheel energy storage system, continuously variable transmission

1. Introduction

Electric cars are well known already over one hundred years, but despite this, they are only now beginning to appear on the streets of cities in a noticeable number. Despite the view of many people, an electric car is not a modern idea at all. It cannot be unambiguous to attribute the invention of the electric vehicle to only one originator. In 1828, a Hungarian engineer, physicist, and Benedictine priest, Ányos István Jedlik, created a tiny model of some vehicle powered by the world's first electric motor invented by him. Robert Anderson, the Scottish inventor, created the first-ever prototype of such a vehicle (exactly an electric crude carriage) between 1832 and 1839 (the exact year is uncertain). Non-rechargeable primary power cells powered his electric carriage. However, in 1835 Sibradus Stratingh (Dutch professor of chemistry, as well as an inventor), with Christopher Becker, his assistant, constructed a small-scale cart called the forerunner of the electric car. Their cart used the voltaic pile. Other great inventors built themselves their vehicles powered by electricity. One of them was Thomas Alva Edison. Inventors of electric cars were facing to find as possible both extremely capacious- and durable batteries at those times. By the way, it applies especially to current times as well. Rechargeable batteries of modern electric cars provide them approximate ranges from 100 to over 500 km, depending on their capacities. The maximal car driving range above about 500 km often requires an application of rechargeable batteries with a total capacity of over 100 kWh. For small cars, ranges of 250 km are possible owing to rechargeable batteries of a capacity of 30 kWh at least.

However, the common problem in the electric vehicle implementation on a large scale is that they require a long time to full charge (repeatedly longer than refuelling at a gas station). Compared to internal combustion-powered cars, the most popular electric vehicles are not yet providing such long ranges.

In many electric vehicles, additional cooling and/or heating systems provide advantageous conditions for rechargeable battery packs that guarantee their high efficiency. Such systems also occur in advanced hybrid cars with expanded battery packs. At present, engineers and scientists have coped with many initial technological barriers limiting the application of electric vehicles from 100 years ago. Increasing the driving range of electric cars in a built-up area of cities with frequent start-stops can be performed utilizing kinetic energy recovery systems. However, such systems have a less meaningful effect on fuel efficiency during highway driving. For electric and hybrid vehicles recovering

kinetic energy through regenerative braking seems to be very promising (see [1] & [2]). A flywheel energy storage system is often used. However, the advantage of such energy storage technology in mechanical form is partly lost when this system has electrical or hydraulic type transmission. Such systems with flywheel require the application of low-cost, high-efficiency, continuously variable transmissions. Up to now, no completely satisfactory solution has been found.

2. Results and Discussion

The work aim is to build a modified hybrid kinetic energy recovery system with the flywheel. This system uses an innovative, continuously variable transmission of mechanical energy. An additional benefit resulting from the application of this system will be the improvement of a vehicle's stability by reducing loss of traction (skidding) during braking and acceleration. The torque, M , generated by the flywheel due to the angular momentum change over time will protect against squat, dive, and lift of the vehicle body, as shown in Fig. 1. In other words, this system alters and controls the amount of compression of suspension springs due to acceleration, deceleration, or braking conditions. In Fig. 1, F_{IN} is the inertial force (also called a fictitious force), which appears to act on a vehicle body whose motion is described using a non-inertial frame of reference, such as a decelerating reference frame, in the considering case.

Verification calculations were carried out using the SCILAB development environment to verify the correctness of the design of the vehicle's traction control system.

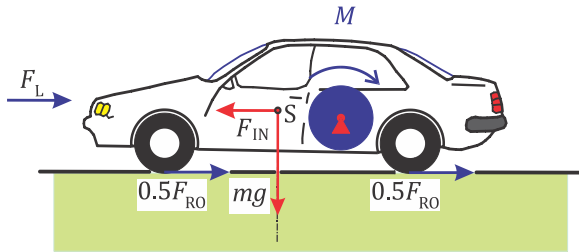


Fig. 1. Forces acting on the vehicle during braking

3. Concluding Remark

This concept of the drive of electric and hybrid vehicles belongs to energy-saving methods. Thus, this method makes the reduction of greenhouse gas emissions possible.

References

- [1] SARDAR, A, DEY RK, MUTTANA SB: A deep drive into kinetic energy recovery system — Part 1. *Auto Tech Rev* 2015, 4(6):20-25, <https://doi.org/10.1365/s40112-015-0927-4>.
- [2] SARDAR, A, DEY RK, MUTTANA SB: A deep drive into kinetic energy recovery system — Part 2. *Auto Tech Rev* 2015, 4(7):20-25, <https://doi.org/10.1365/s40112-015-0942-5>.

Motion tracking of a rigid-flexible link manipulator in a controller failure condition

ELŻBIETA JARZĘBOWSKA^{1*}, KRZYSZTOF AUGUSTYNEK², ANDRZEJ URBAŚ³

1. Warsaw University of Technology, 00-665 Warsaw, Nowowiejska 24, Poland, [0000-0003-1407-7546]
2. University of Bielsko-Biala, 43-309 Bielsko-Biala, Willowa 2, Poland, [0000-0001-8861-4135]
3. University of Bielsko-Biala, 43-309 Bielsko-Biala, Willowa 2, Poland, [0000-0003-0454-6193]

* Presenting Author

Abstract: The paper presents its contribution to tracking control of systems in failure work conditions. The example we examine is a three degrees-of-freedom planar manipulator with rigid and flexible links, for which one of actuators fails during its work. The work task for the manipulator is defined by the programmed constraints. The CoPCoD method is used to derive the reference motion dynamics and the tracking control after one of manipulator failure.

Keywords: manipulator, reference motion dynamics, underactuated systems, tracking control

1. Introduction

Modern mechanical and mechatronic systems like robots, aircraft, satellites and space platforms, underwater vehicles and human servicing systems are designed for delivering work, services, for exploration and military purposes, to mention some of the applications only. Efforts of engineers and researchers aim excellent functionality, durability and reliability of these systems. Also, there are domains where failure is not an option, like space exploration and service delivery or health related devices. The growing demands for reliability lead to the active research in dynamics, nonlinear control theory and optimal control, and others. At the same time, failures are constantly associated with engineering activities. Failures can be costly in work time, equipment or the whole mission, e.g. a space mission, lost. The question thus arises, in all engineering branches, of how to minimize failure costs. From the dynamics and control theory side, an active research dedicated to underactuated systems continues. A fully actuated system, i.e. the one enjoying the number of control inputs equal to the number of degrees of freedom, does its mission as long as the actuators work properly. In case of failure, questions arise of how to minimize risks and danger of damages to the workplace and continue a predefined task up to bringing the system to some rest position, if possible. A system which is not fully actuated refers to as underactuated. An interest in design and control of underactuated systems is driven by two main questions, i.e. can we control underactuated system models (USM) using our current control techniques and whether there are any new control techniques for USM that can solve reliability problems in practice. These questions motivate a lot of current research in USM.

The literature on USM is quite vast, see e.g. [1]. Most of these papers tackle work conditions where there are no other motion limitations and demands, i.e. constraints. The constrained USM dynamics and control are presented in [2,3] for rigid models of underactuated systems. In [4] a dynamics approach to modeling, i.e. the automated computational procedure for constrained dynamics (CoPCoD) is presented. It works for rigid and flexible multibody systems which are fully actuated. Tracking control of USM is still a challenge topic, see e.g. [5-7].

2. Mathematical model of a rigid-flexible link manipulator

A model of three link, three degrees-of-freedom planar manipulator is presented in Fig.1. It is assumed that link 2 can be treated as rigid or flexible. The flexible link is discretised using the Rigid Finite Element Method (RFEM). The motion of the manipulator is forced by means of three driving torques. The aim of the paper is to propose an algorithm for control the manipulator when certain drives stop working due to failure. The algorithm is implemented in three main steps:

- Calculation of reference time courses of joint coordinates for the assumed programmed constraints, in this case the following DAE system is solved:

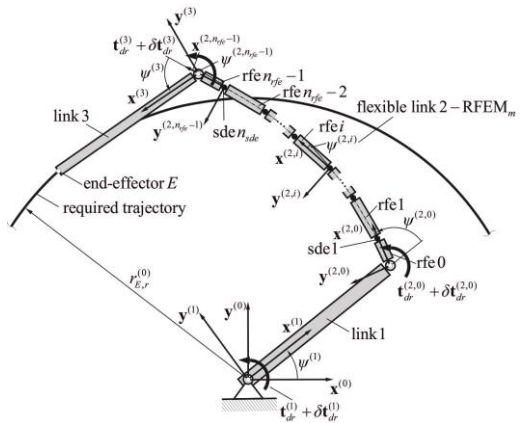


Fig. 1. Model of a rigid-flexible link manipulator

$$\begin{bmatrix} \mathbf{M}_i \Big|_{i \in i_c} + \sum_{j \in i_{fc}} \mathbf{M}_j \frac{\partial \dot{q}_j}{\partial \dot{q}_i} \\ \mathbf{K} \end{bmatrix} \ddot{\mathbf{q}} = \begin{bmatrix} \mathbf{h}_i + \mathbf{Q}_i + \sum_{k=1}^{n_{dof}} \dot{q}_k \frac{\partial \mathbf{Q}_k}{\partial \dot{q}_i} + \sum_{j \in i_{fc}} \left(\mathbf{h}_j + \mathbf{Q}_j + \sum_{k=1}^{n_{dof}} \dot{q}_k \frac{\partial \mathbf{Q}_k}{\partial \dot{q}_j} \right) \frac{\partial \dot{q}_j}{\partial \dot{q}_i} \\ \mathbf{\Gamma} \end{bmatrix}, \quad (1)$$

where all symbols are explained in detail in [4].

- Application of the reference time courses to flexible drives to realize trajectory tracking.
- Compensation of the tracking errors due to the drive failure using the appropriate controller. As a result the analyzed manipulator is transformed from fully actuated to underactuated which is associated with additional numerical challenges.

References

- [1] LIU Y., YU H.: A survey of underactuated mechanical systems. *IET Control Theory & Applications* 2013, 7(7):921–935.
- [2] JARZĘBOWSKA E., SZEWCZYK A.: An Emergency tracking controller design for a manipulator after its actuator failure, *Proc. ASME, IDETC/CIE*, August 2-5, 2015, Boston, MA, USA. <https://doi.org/10.1115/DETC2015-47304>
- [3] JARZĘBOWSKA E.: Tracking control design for underactuated constrained systems. *Robotica* 2006, 24(5):591-593.
- [4] JARZĘBOWSKA E., URBAŚ A., AUGUSTYNEK K.: Analysis of influence of a crane flexible supports, link flexibility, and joint friction on vibration associated with programmed motion execution. *Journal of Vibration Engineering & Technologies* 2020, 8:337–350.
- [5] NERSESOV S.G., ASHRAFIUN H., GHORBANIAN P.: On the stability of sliding mode control for a class of underactuated nonlinear systems. *Proc. of the 2010 American Control Conference*, Baltimore, USA, 3446–3451, 2010.
- [6] ZHONG-PING J.: Controlling Underactuated Mechanical Systems: A Review and Open Problems. in *Lecture Notes in Control and Information Sciences book series* 2010, 407: 77-88.
- [7] HE B., WANG S. A., LIU Y.: Underactuated robotics: A review. *International Journal of Advanced Robotic Systems* 2019, <https://doi.org/10.1177/1729881419862164>.

Nonlinear Dynamics and Control of Moving Slender Continua Subject to Periodic Excitations

STEFAN KACZMARCZYK*

Engineering, Faculty of Arts, Science and Technology, University of Northampton, UK [<https://orcid.org/0000-0002-2762-3131>]

* Presenting Author

Abstract: Tall structures often sway with large amplitude and low frequency due to resonance conditions induced by wind loads and long-period seismic excitations. These sources of excitation affect the performance of vertical transportation systems (VTS) deployed in these structures. The fundamental natural frequencies of tall buildings fall within the frequency range of the wind and seismic excitations and the sway motions form the excitation mechanism which acts upon the VTS. Particularly affected are long moving slender structural components such as the suspension ropes, compensating cables and travelling cables. Complex nonlinear resonance interactions arise in the system when the frequency of the excitation is tuned to the natural frequencies of those elements. The methods to mitigate the effects of dynamic interactions in a high-rise VTS involve the application of passive and active control devices attached at the compensation sheave assembly. In this paper a numerical simulation model is presented to predict and analyse the resonance behaviour of the system equipped with a nonlinear damper-actuator system. The performance and characteristics of this device can then be optimized and adjusted to minimize the effects of adverse dynamic responses of the system.

Keywords: tall structure, slender continua, nonlinear vibration, control

1. Multibody dynamics model

Fig. 1 shows a dynamic model of a high-rise VTS system deployed within a vertical cantilever host structure subject to ground motions $s_r(t)$, $r=1,2$ in the in-plane and out-of-plane directions, respectively [1]. The structure undergoes bending elastic deformations with the in-plane and out-of-plane displacements at the top end ($z = z_0$) denoted as $w_r(t)$, where $r=1,2$, respectively. The equations of motion of the system are formed a system of nonlinear partial differential equations. The dynamic response of the system is defined in terms of lateral displacements of the slender continua elements denoted as $v_i(x_i, t), w_i(x_i, t)$, $i = 1, 2, \dots, 4$, the longitudinal displacements of the discrete masses represented by q_{M1}, q_{M2} and q_{M3} , with the corresponding rotations θ_{M3} .

2. Results and Conclusions

The results presented in the paper demonstrate the resonance behaviour of the system [2,3]. The resonance frequencies of the slender continua can be shifted / changed by the use of different masses of the compensating sheave assembly. The frequencies of the suspension ropes depend on the mass/weight of the car (and the corresponding mass of the counterweight) as well as on the car loading

conditions. The characteristics of the damping -actuator device can be optimised and adjusted to minimize the effects of adverse dynamic responses of the system.

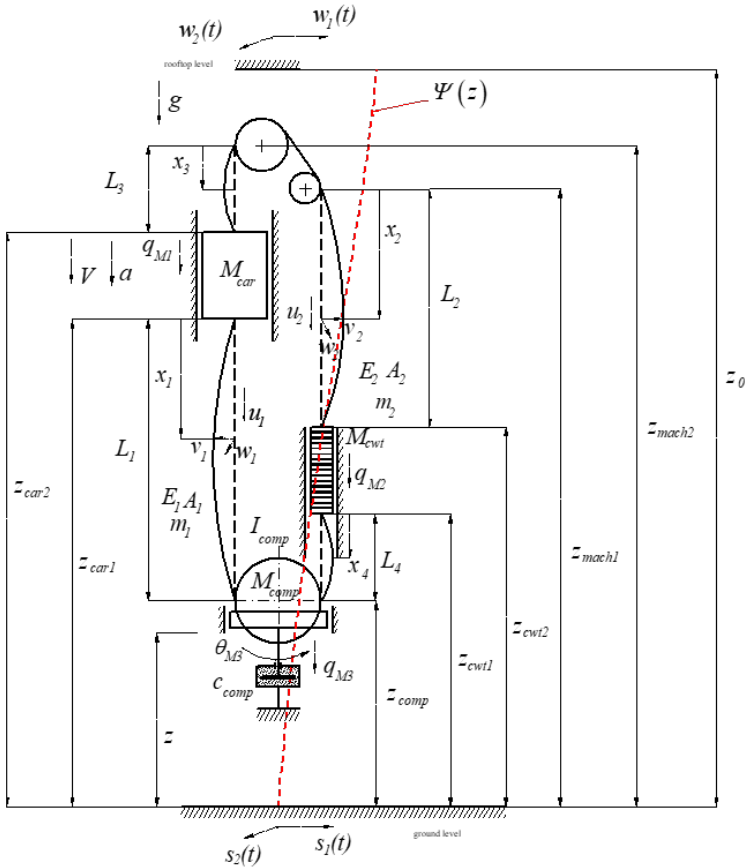


Fig. 1. Dynamic model

References

- [1] SAITO T: Response of high-rise buildings under long period earthquake ground motions. *International Journal of Structural and Civil Engineering Research* 2016, **5**(4):308-314.
- [2] WEBER H, KACZMARCZK S, IWANKIEWICZ R: Nonlinear dynamic response of a cable system with a tuned mass damper to stochastic base excitation via equivalent linearization technique. *Meccanica* 2020, **55**(12):2413-2422.
- [3] KACZMARCZYK S: The Dynamic Interactions and Control of Long Slender Continua and Discrete Inertial Components in Vertical Transportation Systems. In: ABRAMYAN A., ANDRIANOV I, GAIKO V. (EDS) *Nonlinear Dynamics of Discrete and Continuous Systems*. Springer International Publishing, 2021.

Guidance and control system design for a free-flying space manipulator based on a dynamically equivalent manipulator

MARCIN KŁAK^{1*}, ELŻBIETA JARZĘBOWSKA²

1. Warsaw University of Technology, Warsaw, mklak@meil.pw.edu.pl

2. Warsaw University of Technology, Warsaw, elzbieta.jarzebowska@pw.edu.pl [0000-003-1407-7546]

* Presenting Author

Abstract: The paper presents a new approach to guidance and control systems design for a free-flying space manipulator. It takes advantage of a dynamically equivalent manipulator (DEM) model, which is a fixed manipulator representation of a free-floating or a free-flying one and it can be successfully used to handle the guidance problem that is very complex for a non-fixed space manipulator. Also, the free-flying manipulator model includes constraints resulting from linear and angular momentum conservation and its attitude is a function of an actual state and of a path. Since the position of the end effector, joints and base angles are the same in the DEM and in the space manipulator, the fixed representation of a space robot allows for simpler joint and work space transformations and results in simpler path planning and guidance systems design. The novelty is also in the attitude presented in the quaternion description that prevents singularities during computation. The presented design of the guidance and control system allows for effective space manipulators mission design and execution.

Keywords: free-flying manipulator, dynamically equivalent manipulator, quaternion dynamics, control, guidance

1. Introduction

An effective guidance and control design of a space manipulator is challenging and its control can be performed in free-floating or free-flying approaches [1]. The first design allows for control of only the manipulator joints while in the latter the base of the spacecraft is also actuated. A free-floating regime is more power efficient and in case of spacecraft's base actuated with reaction wheels, there is no saturation problem. However, the free-flying approach facilitates use of guidance and control methods developed for a ground-based robotic arms. Stabilized manipulator's base attenuates influence of the arm dynamic coupling on the space robot's attitude but the impact on manipulator's base position still must be considered. Translation of the spacecraft's base could be stabilized by a reaction control system, but it implies some difficulties, e.g. the spacecraft must take additional propellant. Also, a fault of propulsion system can cause a collision. For these reasons, a free-flying control approach is chosen as a baseline for the design. The paper focuses on applying a concept of dynamically equivalent manipulator (DEM) to design an efficient guidance and control system for a free-flying space manipulator. The concept of mapping a free-floating space manipulator into equivalent fixed base manipulator is introduced in [2]. DEM preserves both kinematic and dynamic properties of a space manipulator and allows modeling using classical methods. It is also more suitable for experimental validation of guidance and control algorithms. To map a free-floating space manipulator into a fixed-base robotic one, the base is reproduced by a spherical joint. It can be passive or active responding to free-floating or free-flying space manipulator, respectively. In [3] the quaternion representation

to the DEM approach is introduced. Since DEM maintains the position of manipulator’s end-effector the model can be applied to facilitate the guidance and control design.

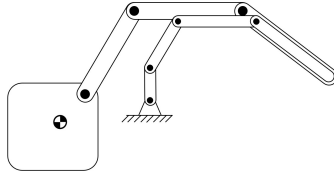


Fig. 1. The space manipulator and its corresponding DEM – end effector’s position is maintained

Mapping the free-flying manipulator to a fixed one allows to efficiently apply guidance and control algorithms developed for ground-based manipulators and mitigate complex dynamic coupling between motion of the robotic arm and translation of the base.

2. Results and Discussion

The use of DEM dynamics in the design allowed for a stable and effective guidance and control system. From the DEM dynamics model of the form

$$\begin{bmatrix} \mathbf{M} & \mathbf{B}^T \\ \mathbf{B} & \mathbf{O} \end{bmatrix} \begin{bmatrix} \dot{\mathbf{x}} \\ \dot{\boldsymbol{\lambda}} \end{bmatrix} = \begin{bmatrix} \mathbf{f} \\ \boldsymbol{\mu} \end{bmatrix} \quad (1)$$

where: \mathbf{M} – mass matrix, \mathbf{B} – matrix of position constraints, $\mathbf{x} = [\mathbf{q} \ \dot{\mathbf{q}}]^T$ – state vector, $\boldsymbol{\lambda}$ – vector of Lagrange multipliers, \mathbf{f} - vector of forces and torques, $\boldsymbol{\mu}$ – term from the extended constraint equations, we can compute the base’s reaction torques which can be further used as a feed forward part of the controller to better stabilize the manipulator’s attitude. The overall guidance and control system structure is presented in fig. 2.

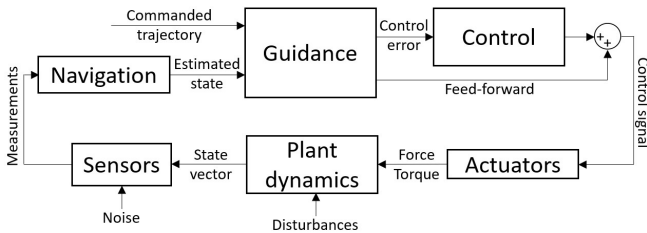


Fig. 2. The overall guidance and control system structure

3. Concluding Remarks

Applying DEM to inverse kinematics as well as to dynamics to calculate the feed-forward controller part allowed to handle efficiently guidance and control designs for free-flying manipulator.

References

- [1] PAPADOPOULOS E: On the dynamics and control of space manipulators. Diss. Massachusetts Institute of Technology, 1990.
- [2] LIANG B, XU Y, BERGERMAN M: Mapping a space manipulator to a dynamically equivalent manipulator. (1998): 1-7.
- [3] JARZĘBOWSKA E, KŁAK M: Quaternion-based spacecraft dynamic modeling and reorientation control using the dynamically equivalent manipulator approach. *Advances in Spacecraft Attitude Control*, 2020

Waves in a beam resting on a bilinear Winkler foundation

STEFANO LENCI^{1*}

1. DICEA, Polytechnic University of Marche, Ancona, Italy [<http://orcid.org/0000-0003-3154-7896>]

* Presenting Author

Abstract: The work addresses the problem of propagation of periodic waves in a beam resting on a bilinear substrate, having different soil stiffness in “compression” and “tension”. The closed form solution is obtained, and some aspects of the complex behaviour are illustrated.

Keywords: wave propagation, bilinear foundation, Euler-Bernoulli beam, phase velocity

1. Introduction

The problem of a beam resting on a bilinear elastic foundation, i.e. a Winkler soil with different stiffnesses in “compression” and in “tension”, has been scarcely studied in the past, despite its practical relevance and despite the fact that it is one of the few nonlinear problems for which an exact mathematical solution can be obtained.

In the static case it has been addressed in [1] and, recently, in [2]. In the more interesting dynamical case, it has been initially studied in [3] where an analytical solution is obtained by means of a perturbation approach. The case of a load moving at a constant velocity have been considered in [4] and [5] by means of a numerical approach. Much more investigated has been the case of a unilateral soil, which is a particular case of a bilinear foundation when one stiffness is set to zero, see [5,6] for an interesting literature survey.

In previous works the problem of a free wave propagation has not been considered, and this constitutes the goal of this work, where periodic waves are studied. This allows us to obtain an analytical solution, and to highlight the complex nature of the response due to its (piecewise) nonlinearity.

2. The problem and main results

The governing equation for the undamped unforced Euler-Bernoulli beam resting on a bilinear Winkler foundation is

$$\rho A \ddot{u} + E J u^{IV} + f(u) u = 0, \quad (1)$$

where u is the transversal displacement, ρA the mass per unit length, EJ the bending stiffness, and

$$f(u) = \hat{h}_1 \text{ if } u < 0; \hat{h}_2 \text{ elsewhere.} \quad (2)$$

Equation (2) underlines the bilinearity of the Winkler foundation, which is the unique source of nonlinearity. The solution is sought after in the travelling wave form $u(x,t)=U(s)$, $s = x - \hat{c}t$, where \hat{c} is the phase velocity, to be determined. Defining the dimensionless parameters (L is the wavelength)

$$c = \hat{c} L (\rho A/EJ)^{1/2}, \quad h_{1,2} = \hat{h}_{1,2} L^4/EJ, \quad \zeta = s/L, \quad (3)$$

we obtain that $U(s)$ satisfies

$$U^{IV} + c^2 U^{II} + f(U) U = 0. \quad (4)$$

Looking for a periodic wave we introduced the following boundary conditions guaranteeing the continuity of the displacements, rotations, bending moments and shear forces:

$$U(0) = U(\alpha) = \Delta U(0) = \Delta U(\alpha) = \Delta U^I(0) = \Delta U^I(\alpha) = \Delta U^{II}(0) = \Delta U^{II}(\alpha) = \Delta U^{III}(0) = \Delta U^{III}(\alpha) = 0. \quad (5)$$

In (5) $\alpha \in [0,1]$ is the parameter that divides the “compression” ($U < 0, \zeta \in [0, \alpha]$) and “tension” ($U > 0, \zeta \in [\alpha, 1]$) parts of the domain.

Equations (4) and (5) constitutes a nonlinear eigenvalue problem, where the unknowns are $c(h_1, h_2)$ and $\alpha(h_1, h_2)$, together with the modal displacement $U(\zeta)$. Note that in the linear case $h_1 = h_2 = h$ the solution is given by $\alpha = 1/2$ and $c_{linear}(h) = 2\pi (1 + h/(2\pi)^4)^{1/2}$. For the bilinear case $h_1 \neq h_2$ the solution is reported in Fig. 1.

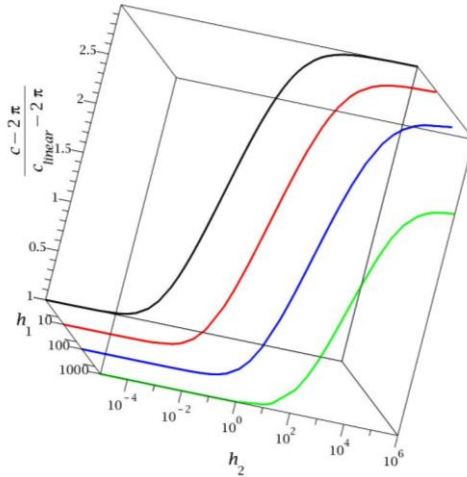


Fig. 1. The solution $c(h_1, h_2)$.

3. Concluding remarks

The propagation of a periodic wave in a bilinear elastic foundation has been considered. The exact close form solution has been obtained thanks to the piecewise linearity of the problem.

Acknowledgment: The author wishes to thank Prof. L. Demeio for fruitful discussions.

References

- [1] TSAI N, WESTMANN R: Beams on tensionless foundation. *ASCE J Engineering Mechanics Division* 1967, **93**(EM5):1-12.
- [2] ZHANG Y, LIU X, WEI Y: Response of an infinite beam on a bilinear elastic foundation: Bridging the gap between the Winkler and tensionless foundation models. *Eur J Mechanics A/Solids* 2018, **71**:394-403.
- [3] FARSHAD M, SHAHINPOOR M: Beams on bilinear elastic foundations. *Int. J. Mechanical Science* 1972, **14**(7):441-445.
- [4] JORGE PC, PINTO DA COSTA A, SIMOES F: Finite element dynamic analysis of infinite beams on a bilinear foundation under a moving load. *J Sound and Vibration* 2015, **23**:328-344.
- [5] FROIO D, RIZZI E, SIMOES F, PINTO DA COSTA A: Dynamics of a beam on a bilinear elastic foundation under harmonic moving load. *Acta Mechanica* 2018, **229**: 4141-4165.
- [6] FROIO D: *Structural dynamics modelization of one-dimensional elements on elastic foundations under fast moving load*. PhD thesis, University of Bergamo, Italy, 2017.

Resonance regimes in the non-ideal system having the pendulum as absorber

YURI V. MIKHLIN^{1*}, YANA O. LEBEDENKO²

1. National Technical University “Kharkiv Polytechnic Institute”, Kharkiv, Ukraine [0000-0002-1780-9346]

2. National Technical University “Kharkiv Polytechnic Institute”, Kharkiv, Ukraine [0000-0002-6152-5973]

* Yuri V. Mikhlin

Abstract: Resonance behavior of the system with a limited power-supply (or non-ideal system) which contains a pendulum as absorber is studied. The system dynamics is described using the multiple scales method. Resonance steady state and frequency responses are constructed. Stability of this stationary regime is studied by the analysis of the state neighborhood. Besides, transient is studied for initial times of the system dynamics.

Keywords: non-ideal system, resonance dynamics, transient

1. Introduction. The principal model

The systems with limited power supply are characterized by interaction of source of energy and elastic sub-system which is under action of the source. Such systems are named also as non-ideal systems. For the non-ideal systems the external applied excitation is a function of coordinates of excited elastic sub-system. The most interesting effect appearing in non-ideal systems is the Sommerfeld effect [1], when in the elastic sub-system it is appeared the stable resonance regime with large amplitudes, and the big part of the vibration energy passes from the energy source to these resonance vibrations. Resonance dynamics of the non-ideal systems was first described by V.Kononenko [2]. Then investigations on the subject were continued in numerous papers. Different aspects of the NIS dynamics are discussed in few books and overviews, in particular, in [3-5].

It is known that nonlinear vibration absorbers permit to reduce essentially amplitudes of resonance elastic vibrations. Here the non-ideal system having the pendulum as absorber (Fig.1) is considered. Such absorber permits to evaluate a decrease of amplitude of resonance vibrations of the elastic sub-system, and to select such parameters of the system when the large amplitude resonance regime is not appearing.

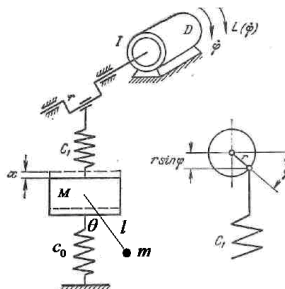


Fig. 1. The model under consideration

2. Results and Discussion

The multiple scales method is used to describe dynamics of the system under consideration with respect to variables x , φ and θ described by the following system:

$$\begin{cases} (M + m)\ddot{x} + (c_0 + c_1)x = c_1 r \sin \varphi - ml(\ddot{\theta} \cos \theta - \dot{\theta}^2 \sin \theta); \\ I\ddot{\varphi} = \varepsilon(a - b\dot{\varphi} + c_1 r(x - r \sin \varphi) \cos \varphi); \\ ml(I\ddot{\theta} + g \sin \theta + \ddot{x} \cos \theta) = 0, \end{cases} \quad (1)$$

where I is the inertia moment of the rotating masses, $L = a - b\dot{\varphi}$ describes the driving moment of the energy source, and the moment of the forces of resistance to the rotation.

. Analysis of modulation equations permits to construct the steady state near the region of the resonance between frequencies of the motor and the elastic sub-system. Choice of the system parameters gives a possibility to decrease essentially amplitudes of the elastic vibrations. Besides, the analysis of the modulation vibrations permits to study a behavior of the system near the resonance regime, and the state stability can be determined. Besides, we can study dynamics of the system at initial times of the dynamical process to analyze an evolution of the system to the steady state.

3. Concluding Remarks

It is shown that the multiple scales method permits to describe the resonance steady state of the system having the pendulum as absorber. A use of the absorber permits to reduce large amplitudes of the system resonance vibrations.

References

- [1] SOMMERFELD A: Beiträge zum dynamischen ausbau der festigkeitslehre. *Phys. Z.* 1902, **3**: 266–286.
- [2] KONONENKO V.O.: *Vibrating Systems with Limited Power*. Supply. Illife Books: London, 1969.
- [3] ALIFOV, A.A., FROLOV, K.V.: *Interaction of Nonlinear Oscillatory Systems with Energy Sources*. Taylor & Francis Inc.: London, 1990.
- [4] ECKERT, M.: The Sommerfeld effect: theory and history of a remarkable resonance phenomenon. *Eur. J. Phys.*, 1996, **17**(5), 285-289.
- [5] BALTHAZAR, J.M. et al.: An overview on the appearance of the Sommerfeld effect and saturation phenomenon in non-ideal vibrating systems (NIS) in macro and mems scales. *Nonl. Dyn.* 2018, **93**(1), 19–40.

Dynamic responses of vertical transportation systems in tall buildings under seismic excitations

SEYED MOHAMMAD MOJTABAEI^{1*}, STEFAN KACZMARCZYK²

1. Faculty of Arts, Science and Technology, University of Northampton, Northampton, UK, NN1 5PH
E-mails: mohammad.mojtabaei@northampton.ac.uk [0000-0002-4876-4857] (Presenting Author)
2. Faculty of Arts, Science and Technology, University of Northampton, Northampton, UK, NN1 5PH
E-mails: stefan.kaczmarczyk@northampton.ac.uk [0000-0002-2762-3131]

Abstract: Tall buildings are susceptible to significant lateral sway in the events of earthquake. Seismic ground motions generally contain low-frequency waves which resonate with the fundamental mode of the buildings. This affects vertical transportation systems, such as lifts, installed in the buildings. Resonance interactions between the building structure and modular vertical transportation installations such as lifts arise then. This can induce the lateral motions of the car/counterweight system, and consequently lead to severe damage in the lift installations. This paper aims to present a detailed Finite Element (FE) model that can predict the dynamic responses of the car/counterweight system installed in tall building structures under seismic excitations. An analytical model is also developed based on the structural dynamics theories, and the results are then compared with those obtained from the FE models. The results of this study can be used to develop design strategies to mitigate the effects of earthquakes on vertical transportation systems.

Keywords: Dynamic responses, seismic ground motions, lift, Finite Element (FE) analysis, tall buildings

1. Introduction

In this paper, a detailed nonlinear FE model using Open System for Earthquake Engineering Simulation (OpenSees) [1] is developed to obtain the dynamic behaviour of a lift car/ counterweight system under earthquake. The El Centro earthquake data are used in the model [2]. An analytical model is also presented to predict the dynamic responses of a cable-mass system which represents a lift suspension rope-car/ counterweight system under seismic conditions. Finally, the seismic responses generated from the analytical model are compared with those obtained from the FE simulations.

2. Results and Discussion

2D models of high-rise buildings made of steel moment-resisting frames are built in OpenSees FE software. The primary members of the steel frame (i.e. beams and columns) are modelled using elastic beam-column elements connected by zeroLength elements which serve as rotational springs to represent the structure's nonlinear behaviour, as shown in Fig.1 (a). The springs follow a bilinear hysteretic response based on the Modified Ibarra Krawinkler Deterioration Model [3]. The reinforcement concrete core is modelled in the mid-span of the frame to take into account the effect of the lift shaft. The mass M is connected to the shaft a spring-viscous damping element of effective coefficient of stiffness k the coefficient of damping c (see Fig.1 (b)). The analytical model is developed using a cable-mass system mounted within a vertical cantilever host structure subject to ground motion $s_0(t)$, as shown in Fig.1 (c) [4]. The mass M is suspended on the cable of length L and is constrained horizontally within the host structure by a spring-viscous damping element.

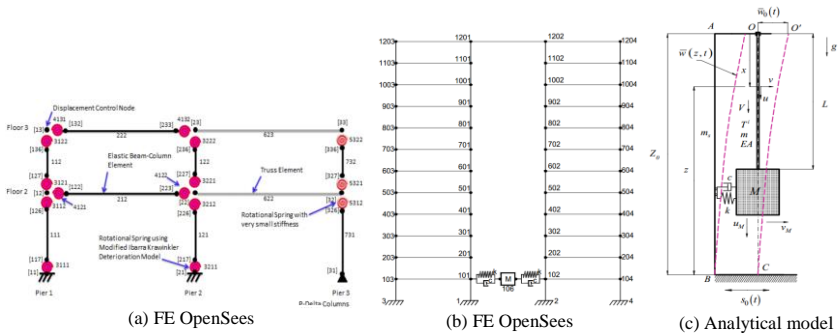


Fig. 1. Modelling of a high-rise building with lift

The maximum seismic responses of the lift car/ counterweight, including lateral displacement ($d_{M,max}$) and acceleration ($a_{M,max}$), obtained from FE and analytical models are listed in Table 1 for 12, 20 and 50 storeys buildings. To investigate the effect of the lift location along with the height of the building, each structure is analysed twice when the mass (M) is located at the bottom and top storeys.

Table 1. Comparison between maximum seismic responses of the lift in the buildings with various number of storeys obtained from FE and analytical models

Number of storeys	Vertical location of the lift	Natural frequency (Hz)	$d_{M,max}$ (m)		$a_{M,max}$ (m/s ²)	
			FE model	Analytical model	FE model	Analytical model
12	1 st storey	1.42	0.009	0.008	1.921	1.988
	12 th storey		0.115	0.105	3.128	3.250
20	1 st storey	1.96	0.014	0.012	3.059	3.288
	20 th storey		0.188	0.162	4.517	4.874
50	1 st storey	2.78	0.032	0.025	8.816	10.570
	50 th storey		0.276	0.204	12.335	15.036
Average error (%)			15%		11%	

3. Concluding Remarks

The following main conclusions can be drawn: (I): The location of the lift along the height of the building can significantly affect the seismic response. The responses at the top floors are 13 times the response at the bottom floors. (II) A good agreement can be achieved between the results of FE and analytical models for the lower storey buildings (e.g. 12 storey) when the frame response either remains in the elastic stage or shows slight plasticity into their beam and column elements. However, a 40% error is observed for the results of higher storey buildings (e.g. 50 storey) when significant plasticity is developed in the main structural elements. This is attributed to the fact that the developed analytical model is unable to take into account the plastic behaviour of the building into calculations.

References

- [1] MCKENNA F, FENVES G L, SCOTT M H, JEREMIC B, Open system for earthquake engineering simulation (OpenSees), Pacific Earthquake Engineering Research Center, University of California, Berkeley (CA), 2000.
- [2] Pacific Earthquake Engineering Research Center (PEER), Strong Ground Motion Databases, El Centro Earthquake.
- [3] IBARRA L F, KRAWINKLER H, Global Collapse of Frame Structures under Seismic Excitations: Pacific Earthquake Engineering Research Center, 2005.
- [4] KACZMARCZYK S, The modelling and prediction of dynamic responses of slender continua deployed in tall structures under long-period seismic excitations. *J. Phys.: Conf. Ser.* 2018, **1048**(012005).

Nonlinear System Identification of an Experimental Drill-String Setup

INGRID PIRES^{1*}, HELON VICENTE HULTMANN AYALA¹, HANS INGO WEBER¹

1. Departamento de Engenharia Mecânica – PUC-Rio

* Presenting Author

Abstract: Torsional vibration is present in most drilling operations and arises from the non-linear bit-rock and string-wall interactions. The stick-slip phenomenon is the most severe stage of torsional oscillations. It results in excessive bit wear and reduces drilling efficiency. Therefore, proper modelling and control of the system dynamics are necessary to optimize drilling procedures. This work aims to identify the physical parameters of an electromechanical system and the model of the friction observed experimentally. The electromechanical system is an experimental setup designed to offer similar dynamic properties as a drill string with a braking device to introduce dry friction in the system, disturbing the rotating motion. For friction identification, this study tests and compares some well-known friction force models considering different friction phenomena. This study intends to be a source for further comprehension of torsional dynamics in slender structures.

Keywords: stick-slip, friction model, system identification

1. Introduction

The stick-slip phenomenon is the most severe stage of the torsional oscillations present in most drilling routines. This type of vibration results in excessive bit wear and reduces drilling efficiency. For these reasons, the comprehension and reduction of stick-slip are of great concern.

Modelling plays an essential role in the simulation, estimation, control, and monitoring of a dynamic process. Practical limitations of first principles motivate the application of system identification, which comprises a set of techniques for building mathematical models on the basis of input and output measurements [1]. In the context of system identification, dynamical systems with friction, and dynamical systems with hysteresis, contributions have been published [2, 3, 4, and 5]. This work aims to identify the physical parameters of a test rig, including the electrical parameters of the DC motor and the mechanical parameters of the rig, and to identify the model of the friction present in the experiments.

2. Experimental Setup

The rig consists of a horizontal apparatus composed of a DC motor, a planetary gearbox with a reduction ratio of 8:1 coupled to the DC motor, two solid discs, and a low-stiffness shaft, that transmits the rotation from the DC-motor to the discs. Figure 1 (right) shows a schematic of the test rig. The discs are free to rotate, and bearings constrain their lateral motion. There are braking devices placed on the discs to induce friction torque in the system. It consists of a pin that passes through the bearing support and meets the disc. The pin and disc dry contact cause friction torque. The friction torque leads the system to experience torsional vibrations and, eventually, stick-slip.

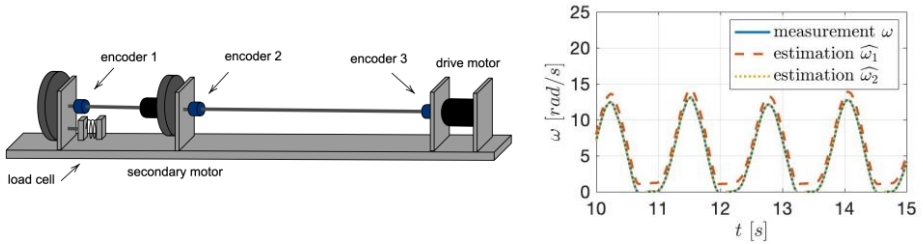


Fig. 1. (right) The schematic of the experimental setup. (left) Comparison between measured and estimated angular velocities of the disc subjected to friction.

3. System Identification

The experimental rig used in this work has a braking device placed on one of the discs to induce friction torque in the system. For friction modelling, this study intends to employ both grey and black-box approaches considering well-known friction models. The graph on the left of Fig. 1 presents some preliminary results of this work. It plots the direct comparison between measured and estimated angular velocities of the disc subjected to friction. In Fig. 1(left), ω is the measured velocity and ω_1 is the estimated velocity simulated with the model proposed in [6]. We used the error between the measurements and the simulation to build an ensemble model. The error is identified adopting a Nonlinear Autoregressive Exogenous (NARX) model. And the estimated velocity simulated with an ensemble model, ω_2 , is plotted in Fig. 1(left).

Experimental results showed the existence of a hysteresis phenomenon in friction [6], which has been already observed in other tribological experiments [7]. As a continuation of [6], this study intends to identify the system friction model that better reproduces the dynamics of the experimental setup. Therefore, it tests and compares some well-known friction force models, identifying their parameters, accounting for the hysteretic aspect of the friction torque. The work also includes the analysis of ensembles of grey and black-box models.

References

- [1] LJUNG L: Perspectives on system identification. *Annual Reviews in Control* 2010, **34**:1-12.
- [2] JANOT A, YOUNG P C, GAUTIER M: Identification and control of electro-mechanical systems using state-dependent parameter estimation. *International Journal of Control* 2017, **90**:643-660.
- [3] Lee C Y, Hwang S H, Nam E, Min B K: Identification of mass and sliding friction parameters of machine tool feed drive using recursive least squares method. *International Journal of Advanced Manufacturing Technology* 2020, **109**:2831-2844.
- [4] ABREU P, TAVARES L A, TEIXEIRA B, AGUIRRE, L A: Identification and nonlinearity compensation of hysteresis using NARX models. *Nonlinear Dynamics* 2020.
- [5] WANG L, GUO J, TAKEWAKI I: Real-time hysteresis identification in structures based on restoring force reconstruction and Kalman filter. *Mechanical Systems and Signal Processing* 2021, **150**.
- [6] PIRES I, CAYRES B, PAMPLONA D C, WEBER H I: Torsional friction-induced vibrations in slender rotating structures. In: Uhl T. (eds) *Advances in Mechanisms and Machine Science. IFToMM WC 2019. Mechanisms and Machine Science*. Springer 2019, **73**.
- [7] LEINE R.; NÜMEIJER H: Dynamics and Bifurcations of Non-Smooth Mechanical Systems. *Lecture notes in applied and computational mechanics*. Springer: Netherlands, 2004, **18**.

ON NON-LINEAR DYNAMICS BEHAVIOUR OF A FIXED OFF-SHORE PLATFORM FOR ENERGY HARVESTING

MAURICIO A. RIBEIRO¹, ANGELO M. TUSSET², WAGNER B. LENZ³, JOSÉ M. BALTHAZAR^{4*}
GREGORZ LITAK⁵

1. Universidade Tecnológica Federal do Paraná-Campus Ponta Grossa, Paraná, Brazil, 0000-0001-7314-0723
 2. Universidade Tecnológica Federal do Paraná-Campus Ponta Grossa, Paraná, Brazil, 0000-0003-3144-0407
 3. Universidade Tecnológica Federal do Paraná-Campus Ponta Grossa, Paraná, Brazil, 0000-0002-1946-4185
 4. UNESP: São Paulo State University at Bauru, Bauru, SP, Brazil, 0000-0002-6082-4832
 5. Lublin University of Technology, Faculty of Mechanical Engineering, Lublin, Poland, 0000-0002-9647-8345
- * Presenting Author

Abstract. In this work we analyze the dynamic behavior of an offshore platform system using piezoelectric material in its structure for a possible energy harvesting. We analyzed the behavior of the average power produced, together with the Maximum Lyapunov Exponent and Bifurcation diagram. Another analysis performed was for a given set of parameters the basins of attraction in which we detected the presence of two attractors for the initial conditions in range of $[-5.5]$, we also analyzed the behavior of the amplitude dynamics (A) of the sea wave applied to the system with parameter (p) related to the damping coefficient of the structure and thus we determine the regions in which the system is chaotic or periodic. With this we calculate the average power for p in $[0,5]$ and for values of $p \rightarrow 5$ there is an increase in the average power of the system with a value of $A = 2.5$.

Keywords: offshore platform, nonlinear dynamics, piezoceramic

1. Introduction

In the last decades, the demand for energy consumption has been growing and several ways to obtain a clean and sustainable energy have been researched. Some examples for obtaining clean and sustainable energy are wind energy, solar energy, etc [1]. However, an energy that is being exploited is obtained by the waves of the sea waves [2]. Thus, we analyzed the behavior of a mathematical model of an oil platform under the action of an external force of the type $F_{ext}(t) = A\sin(\omega_1 t) + B\sin(\omega_2 t)$, where A and B is amplitude of wave sea and ω_1 and ω_2 are the frequencies of wave and applying piezoceramic patches to its structure for possible power generation. The analyzed model is proposed by [2] and described by:

$$\begin{aligned} I\ddot{\varphi} + \mu\dot{\varphi} + c(\varphi + \theta) - p\sin(\varphi + \theta) &= c\theta_0 + F_{ext}(t) + Xv \\ \dot{v} + \lambda v + \kappa\varphi &= 0 \end{aligned} \quad (1)$$

where θ_0 is an initial imperfection (for a perfect model $\theta_0 = 0$); φ , $\dot{\varphi}$ and $\ddot{\varphi}$ represent the perturbed displacement, velocity and acceleration, respectively, I is the generalized inertia, μ is the damping coefficient p is the load parameter and g is the acceleration of gravity. χ is the coupling term of the piezoelectric, κ is the reciprocal temporal constant in electrical circuit, $\lambda \approx 1/RC$ is the reciprocal of the dimensionless time constant of electrical circuit, R is load resistance, C capacitance and v is the dimensionless voltage in load resistor [2, 3]. Figure (1) represents a scheme of platform structure with a piezoelectric material for energy harvesting.

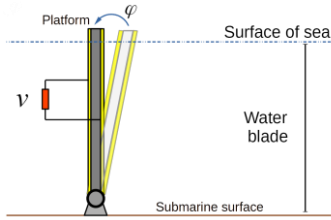


Fig. 1: Scheme of offshore platform structure, adapted to [2].

2. Numerical Results and Discussion

For the numerical analysis of the simplified model, we used the following parameters $\mu=0.1$, $c=0.5$, $\theta=0.95$, $\theta_0=0.009485$, $\chi=0.5$, $\omega_1=2\pi f_1$, $\omega_2=2\pi f_1+0.2$, $f_1=0.2$, $\kappa=0.05$, $B=2.5$ and $\gamma=0.01$. Figure 2. (a) show the basin of attraction for the initial conditions between and with $p = 0.5$, 2 (b) represents the parameter space of the Lyapunov Maximum Exponent for $p \times A$ in $[0, 2.5] \times [0, 5]$ and initial condition $[0, 0, 0]$, 2 (c) show Maximum Lyapunov exponent for $A = 2.5$ and p in $[0, 5]$ and initial condition $[0, 0, 0]$ and 2 (d) the bifurcation diagram for $A = 2.5$ and p in $[0, 5]$ and initial condition $[0, 0, 0]$ and 2 (e) the average power of the systems $P_{avg} = \frac{\lambda}{T} \int_0^T v^2(t) dt$ same initial

condition.

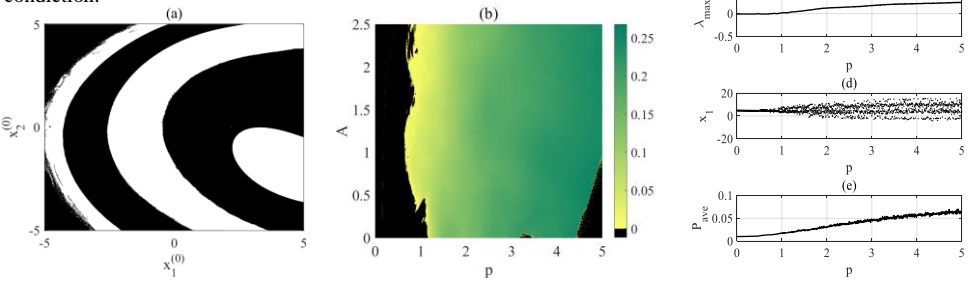


Fig. 2: (a) Basins of attraction of eqs. (1), (b) Maximum Lyapunov Exponent $p \times A$ in $[0, 2.5] \times [0, 5]$, (c) Maximum Lyapunov Exponent for $A=2.5$ and p in $[0, 5]$, (d) Diagram Bifurcation for $A=2.5$ and p in $[0, 5]$ and (e) Average Power for $A=2.5$ and p in $[0, 5]$

3. Concluding Remarks

We analyzed basins of attraction for $p = 0.5$, which revealed the emergence of two attractors. In this way, we establish the initial condition $[0,0,0]$ and analyze the Maximum Lyapunov exponent for parameters A (amplitude of the sea wave) and p (the damping coefficient of the structure) and determine the chaotic and periodic regions. with this we calculate the average power for p at $[0,5]$ and for values of $p \rightarrow 5$ there is an increase in the average power of the system with a value of $A = 2.5$. Future works will be related to erosion of the basis of attractions.

Acknowledgment: The authors acknowledge the support from the Brazilian agency CNPq and the DIALOG 0019/DLG/2019/10, Poland.

References

- [1] W. B. Lenz, A. M. Tuset, M. A., Ribeiro, J.M. Balthazar. Neuro fuzzy control on horizontal axis wind turbine. *Meccanica* 55, 87–101 (2020). <https://doi.org/10.1007/s11012-019-01118-9>
- [2] J. Cassiano, J. M. Balthazar. On chaotic behavior of a fixed offshore structure. *International Journal of Bifurcation and Chaos* 19 (2009). <https://doi.org/10.1142/S0218127409022919>
- [3] A. M. Tuset, J. M. Balthazar, R. T. Rocha, J. L. P. Felix , M. Varanis, M. A. Ribeiro , I. Iliuk, G. Litak. On energy harvesting with time-varying frequency by using magneto piezo elastic oscillators with memory. *NODY-CON2021* 1 (2021).

On non-ideal and fractional dynamics of a magneto piezo elastic oscillator with Bouc-Wen damping to harvesting energy

MAURICIO A. RIBEIRO¹, ANGELO M. TUSSET², WAGNER B. LENZ³, JOSÉ M. BALTHAZAR^{4*}
GREGORZ LITAK⁵

1. Universidade Tecnológica Federal do Paraná-Campus Ponta Grossa, Paraná, Brazil, 0000-0001-7314-0723
2. Universidade Tecnológica Federal do Paraná-Campus Ponta Grossa, Paraná, Brazil, 0000-0003-3144-0407
3. Universidade Tecnológica Federal do Paraná-Campus Ponta Grossa, Paraná, Brazil, 0000-0002-1946-4185
4. UNESP: São Paulo State University at Bauru, Bauru, SP, Brazil, 0000-0002-6082-4832
5. Lublin University of Technology, Lublin, Poland, 0000-0002-9647-8345

* Presenting Author

Abstract: In this work, we explored numerically the fractional dynamics of model with the Riemann-Liouville operator fractional derivative applied to Bouc-Wen's Damping where this damping is related to the hysteresis that constitutes the beam that is coupled to the piezoceramic materials patches. This beam is subject to two magnetic field of the poles in the base and under the action of the external force of a non-ideal motor (RNIS), the external force has two parameters a_0 and b_0 , for $a_0=0$ it is sinusoidal kind force. In this way, we analyzed the behavior of the output power for the fractional system considering parameters of the external force of the non-ideal motor (RNIS) and the parameter of the fractional derivative operator of Riemann-Liouville. Therefore establishing the range in which fractional dynamics is chaotic and periodic and also the behavior of parameter space $a_0 \times q_4$ and $b_0 \times q_4$ establishing the behavior of the system's output power.

Keywords: Fractional Calculus, Bouc-Wen Damping, Energy Harvesting, Non-ideal; Machinery

1. Introduction

In the Design of structures, it is necessary to investigate the relevant dynamics to predict the structural response due to the excitations. But in reality, the excitation sources are non-ideal, they have always limited power, limited inertia and their frequencies varies according to the instantaneous state of oscillating system. Here, we extended earlier works, which constitutes a bar coupled to an electrical system with piezoceramic material inserts when deformed generating electric current. In this paper considering the force applied to the system usable in this work is a non-ideal motor (RNIS) [2], considering the mutual interactions between them. This Mathematical Modeling is considered the Bouc-Wen damping that represents the hysteresis of bar where the piezoceramic material patches are applied. Fig (1) represents the system considered (RNIS) where $F(t) = f_0 \cos(\omega t + a_0 \sin(b_0 \omega t))$, f_0 is amplitude force, ω is natural frequency, a_0 and b_0 is force parameters. If a_0 and b_0 equal to zero we will obtain (the Ideal Excitation) [2], that is no mutual interaction, as considered in [1], using Jacobi-Anger expansion.

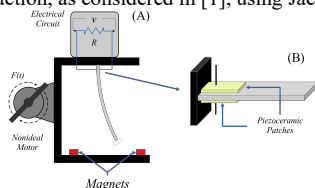


Fig 1: (A) Energy Harvesting model with non-ideal excitation and magnetic poles and (B) is the piezoceramic patches material on beam. Elaborated by the authors.

Therefore, the Riemann-Liouville fractional derivative operator (RL) defined by [2] is used in this paper. Thus, we will obtain the fractional differential equation:

$$D^{\eta} f(t) = x_2$$

$$D^{\eta_2} f(t) = -2\eta x_2 + \frac{x_1}{2}(1 - x_1^2) - \chi x_3 - a_k x_1 - (1 - a) D_k x_4 - f_0 \cos(\omega t) + a_0 \sin(b_0 \omega t) \quad (1)$$

$$D^{\eta_3} f(t) = -\lambda x_3 - \kappa x_2$$

$$D^{\eta_4} f(t) = A x_2 - \beta |x_2| |x_4|^{n-1} - \gamma x_1 |x_4|^n$$

where x is the displacement, v is the dimensionless voltage in load resistor, η is damping coefficient, χ is the coupling term of the piezoelectric, κ is the reciprocal temporal constant in electrical circuit, $\lambda \approx 1/RC$ is the reciprocal of the dimensionless time constant of electrical circuit, R is load resistance, C capacitance.

2. Numerical Results and Discussion

We analyzed the behavior of the nonlinear dynamics of the model described by equations (1). In fig. (2) (a) is $a_0 \in [0,1] \times q_4 \in [0.85,1]$ and fig. (2) (b) is $b_0 \in [0,1] \times q_4 \in [0.85,1]$ showed the behavior of power output, in fig.(2) (c) is the Bifurcation Diagram, taken the initial condition $x_0 = [0.1, 0, 0, 0]$, and the parameters $\eta = 0.01$, $k_l = 0.25$, $\alpha = 1.1$, $n = 4$, $a = 0.25$, $\lambda = 0.01$, $\kappa = 0.5$, $A = 1.0$, $\beta = 0.55$, $\gamma = 0.45$, $f_0 = 0.2$ and $\chi = 0.01$ and fig.(2) (d) is 0-1 Test ($K_{x,t}$) Test 0-1 is observed that values close to 0 the system is periodic and for values close to 1 it has chaotic behavior [3].

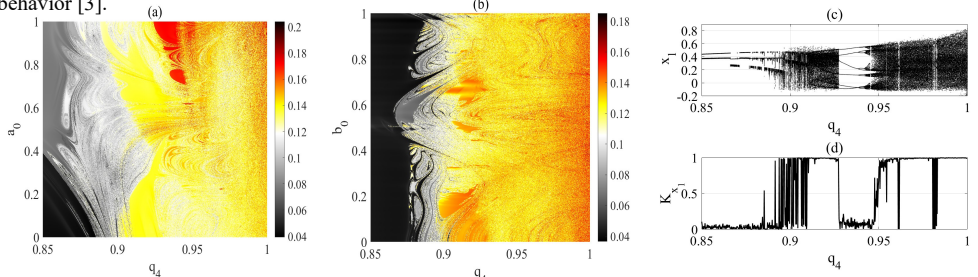


Fig. 2. (a) Average Power ($P_{avg} = \lambda \langle v^2 \rangle$) with $b_0 = 0.5$, (b) Power Average output ($P_{avg} = \lambda \langle v^2 \rangle$) with $a_0 = 0.2$, (c) Bifurcation Diagram with $a_0 = 0.2$, $b_0 = 0.5$ and $q_4 \in [0.85,1]$ (d) 0-1 Test ($K_{x,t}$) with $a_0 = 0.2$, $b_0 = 0.5$ and $q_4 \in [0.85,1]$.

3. Concluding Remarks

It was possible to analyze the behavior of the average output power with RL and the non-ideal motor force parameters, we establish within the range of values of q_4 close to 0.85 the system has minimum power, because the system has a periodic behavior, for values close to $q_4 \rightarrow 1$ the system was chaotic. The Bifurcation diagram and Test 0-1 [3] determined the ranges for periodic behavior for q_4 . So, these analyzes corroborate to understand the behavior of damping with memory effect. Future works, including multiscale entropy analysis.

Acknowledgment: The authors acknowledge the support from the Brazilian agency CNPq and the DIALOG 0019/DLG/2019/10, Poland.

References

- [1] J. L. P. Felix, R. P. Bianchin, A. Almeida, J. M. Balthazar, R. T. Rocha, R. M. Brasil, On energy transfer between vibration modes under frequency-varying excitations for energy harvesting, in: *Applied Mechanics and Materials* **849** (2016) 65–75. DOI:10.4028/www.scientific.net/AMM.849.65
- [2] M. A. Ribeiro, J. M. Balthazar, W. B. Lenz, R. T. Rocha, A. M. Tusset, Numerical Exploratory Analysis of Dynamics and Control of an Atomic Force Microscopy in Tapping Mode with Fractional Order, *Shock and Vibration* **18** (2020). ID 4048307. <https://doi.org/10.1155/2020/4048307>
- [3] Bernardini, D., Litak, G. An overview of 0–1 test for chaos. *J. Braz. Soc. Mech. Sci. Eng.* **38**, 1433–1450 (2016) <https://doi.org/10.1007/s40430-015-0453-y>

Super-Twisting Sliding Mode Control for a Formation of Fully-Actuated Multirotor Aerial Vehicles

JORGE A. RICARDO JR.^{1*}, DAVI A. SANTOS²

1. Aeronautics Institute of Technology [0000-0001-5323-2970]

2. Aeronautics Institute of Technology [0000-0001-5995-3103]

* Presenting Author

Abstract: This work is concerned with the robust attitude and position control of a rigid formation of fully-actuated multirotor aerial vehicles with fixed rotors. A six-degrees-of-freedom force-torque control law is designed for each vehicle using a super-twisting sliding mode controller. The formation position and attitude commands are generated by a S-curve trajectory planner. The method is evaluated for a formation of non-planar fully-actuated hexacopter with fixed rotors and demonstrated using numerical simulations, which shows its effectiveness.

Keywords: multirotor aerial vehicle, super-twisting sliding mode control, nonlinear dynamics.

1. Introduction

Many of the applications for multirotor aerial vehicles (MAVs) seem to benefit from the use of fully-actuated vehicles since they are capable of independently maneuver in position and attitude and perform fast disturbance rejection [1]. On the other hand, the MAV mission area and effectiveness are general limited by its reduced payload capacity and flight autonomy. To overcome or mitigate these problems, it is often more effective to deploy a formation of these vehicles.

In disturbed formation flights, an accurate robust tracking performance of each vehicle is crucial to maintain a desired formation. In this sense, we design a sliding mode control (SMC) strategy for the MAVs. The conventional SMC has two phases: 1) the reaching phase, which is disturbance sensitive and 2) the sliding phase, which is disturbance insensitive. During the sliding phase, chattering appears in real systems due to time discretization and unmodeled dynamics, degrading the designed performance [2]. To diminish chattering, a super-twisting SMC is proposed for each vehicle to reject Lipschitz disturbances. The formation position and attitude reference commands are generated, using a S-curve trajectory planner. In this sense, for limited disturbances, the tracking error of each MAV is bounded in the reaching phase and the formation robustly converges to its desired pose in the sliding phase. This abstract briefly shows the MAVs dynamic modelling, the proposed controller, and the numerical results to demonstrate the effectiveness of the method.

2. Results and Discussion

Consider a formation of n fully-actuated MAVs with fixed rotors. Let $\mathbf{x}^i \triangleq (\mathbf{x}_1^i, \mathbf{x}_2^i) \in \mathbb{R}^{12}$ be the i th MAV vector of state errors, where $\mathbf{x}_1^i \in \mathbb{R}^6$ denotes the position and attitude errors and $\mathbf{x}_2^i \in \mathbb{R}^6$ represents the linear and angular velocities errors. Therefore, the i th MAV nonlinear dynamics is

$$\dot{\mathbf{x}}_1^i = \mathbf{f}_1(\mathbf{x}^i), \quad (1)$$

$$\dot{\mathbf{x}}_2^i = \mathbf{f}_2(\mathbf{x}^i) + \mathbf{B}(\mathbf{x}^i)(\mathbf{u}^i + \mathbf{d}^i), \quad (2)$$

where $f_1: \mathbb{R}^{12} \rightarrow \mathbb{R}^6$, $f_2: \mathbb{R}^{12} \rightarrow \mathbb{R}^6$, $B: \mathbb{R}^{12} \rightarrow \mathbb{R}^{6 \times 6}$ are known functions, $u^i \in \mathbb{R}^6$ is a force-torque control command of the i th MAV, and $d^i \in \mathbb{R}^6$ is an unknown but limited force-torque disturbance with Lipchitz derivative. Moreover f_1 and B are such that $(\partial f_1 / \partial x_2)B$ is non-singular. Now, let us define the i th MAV sliding variable $s^i \triangleq f_1(x^i) + C^i x_1^i \in \mathbb{R}^6$, where $C^i \in \mathbb{R}^{6 \times 6}$ is a design diagonal matrix. Therefore, the following control law guarantees the sliding mode existence ($s^i = 0$):

$$u^i = -\left(\frac{\partial f_1}{\partial x_2} B\right)^{-1} \left(C^i f_1 + \frac{\partial f_1}{\partial x_1} f_1 + \frac{\partial f_1}{\partial x_2} f_2 + K_1^i \Gamma^i \text{sign}(s^i) \right) + w^i, \quad (4)$$

$$\dot{w}^i = -K_2^i \text{sign}(s^i), \quad (5)$$

where $\Gamma^i \triangleq \text{diag} \left((s_1^i)^{0.5}, \dots, (s_6^i)^{0.5} \right)$ and $K_1^i \in \mathbb{R}^{6 \times 6}$ and $K_2^i \in \mathbb{R}^{6 \times 6}$ are diagonal matrices.

The simulation is performed for a delta formation of three non-planar fully-actuated hexacopters with fixed rotors. The formation mission is to displace (2, 10, 4) m from its initial position in 8 s. Figure 1(a) shows the formation path, the MAV size, and the formation shape at specific time instants. Each MAV is subjected to different cosine disturbances with frequency of 0.08 Hz and amplitudes of 1 N for force and 0.2 Nm for torque. Figure 1(b) shows the norm of the relative position between MAV 1 and MAVs 2 and 3, denoted, respectively, by $\tilde{r}^{1/2}$ and $\tilde{r}^{1/3}$. Figure 1(c) shows the position tracking performance of MAV 1.

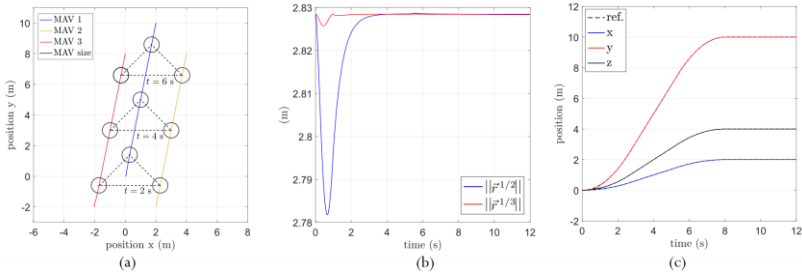


Fig. 1: (a) Formation path, MAV size, and formation shape at time instants 2 s, 4 s, and 6 s. (b) relative distance between MAV 1 and MAVs 2 and 3. (c) position tracking performance of MAV 1.

3. Concluding Remarks

This paper has presented the design of a super-twisting SMC for a formation of fully-actuated MAVs with fixed rotors. A simulation example showed that the proposed super-twisting SMC generates negligible chattering and robustly attains the desired formation pose after a finite time.

Acknowledgment: The authors would like to thank the support of FAPESP/Brazil (2019/05334-0). The first author thanks EMBRAER and ITA for the Academic-Industrial Doctorate Program (DAI). The second author is grateful for the support of CNPq/Brazil (302637/2018-4).

References

- [1] G. JIANG, R. VOYLES, A Nonparallel Hexrotor Uav With Faster Response To Disturbances for Precision Position Keeping, IEEE International Symposium on Safety, Security, and Rescue Robotics 2014, p.1–5.
- [2] J. LEE, V. UTKIN, Chattering Suppression Methods In Sliding Mode Control Systems, Annual Reviews in Control 2007, (31) p.179–188.

Global sliding mode control design for a 3D pendulum

JOÃO FRANCISCO SILVA TRENTIN^{1*}, DAVI ANTÔNIO DOS SANTOS¹

1. Division of Mechanical Engineering, Aeronautics Institute of Technology (ITA), São José dos Campos, SP, Brazil. [0000-0002-6726-8699],[0000-0001-5995-3103]. * Presenting Author

Abstract: The dynamics and control of pendulums attract attention of researchers for a long time. Their mathematical models can approximate many real-world applications besides being very helpful for pedagogical reasons. This paper studies the attitude control of a 3D pendulum using a torque control law based on an unit-vector multi-input global sliding mode control. Numerical simulations are carried out to evaluate the proposed controller and the results are compared to a proportional-derivative feedback linearization control law.

Keywords: nonlinear dynamics, 3D pendulum, global sliding mode control.

1. Introduction

Inverted pendulum-like systems have been deeply studied and until today provide a rich source of non-linear dynamical systems. The 3D pendulum is a rigid body fixed to a pivot, allows three rotational degrees of freedom, and is fully actuated by three control torques [1]. This dynamical system has been used as a benchmark in the past decades for investigating new control techniques, but there are still some open points with respect to robust control. Sliding mode control (SMC) techniques can deal with multi-variable dynamics, nonlinearities, and actuator constraints [2]. It has attractive properties such as insensitivity to bounded uncertainties, disturbances, as well as parasitic dynamics [2]. The present work is concerned with the design of a global sliding mode control (GSMC) law for the 3D pendulum. The GSMC can also be referred to as integral sliding mode control. In this case, the technique designs a sliding manifold that guarantees robustness to bounded uncertainties from the initial condition and there is no reaching phase in such design. Thus, this paper briefly presents the mathematical model of the 3D pendulum, the adopted sliding surface as well as the proposed control law. Numerical results demonstrate the effectiveness of the method.

2. Methodology and Results

The modified Rodrigues parameters (MRPs) are used to describe the attitude of the 3D pendulum to avoid singularities. The MRP $\mathbf{p} \in \mathbb{R}^3$ is defined as $\mathbf{p} \triangleq \tan \frac{\phi}{4} \hat{\mathbf{e}}$, where $\phi \in (-2\pi, 2\pi)$ is the principal angle rotation, $\hat{\mathbf{e}}$ is the principal axis unit vector referring to Euler's principal rotation theorem. The kinematic differential equation of the MRPs is:

$$\dot{\mathbf{p}} = \frac{1}{4} \boldsymbol{\Sigma}(\mathbf{p})\boldsymbol{\omega}, \quad (1)$$

Where $\boldsymbol{\Sigma}(\mathbf{p}) \in \mathbb{R}^{3 \times 3}$ given by $\boldsymbol{\Sigma}(\mathbf{p}) = (\mathbf{1} - \mathbf{p}^T \mathbf{p})\mathbf{I}_3 + 2[\mathbf{p} \times] + 2\mathbf{p}\mathbf{p}^T$ and $\boldsymbol{\omega}$ is the body angular velocity. Based on the angular momentum of the 3D pendulum, it is possible to obtain the following equation of motion:

$$\mathbf{J}\dot{\boldsymbol{\omega}} = -\boldsymbol{\omega} \times \mathbf{J}\boldsymbol{\omega} + \mathbf{t}_g + \mathbf{u} + \mathbf{d}, \quad (2)$$

where $\mathbf{J} \in \mathbb{R}^{3 \times 3}$ is the inertia matrix of the 3D pendulum, $\dot{\boldsymbol{\omega}} \in \mathbb{R}^3$ is the body angular acceleration, $\mathbf{u} \in \mathbb{R}^3$ the control torque vector, and $\mathbf{d} \in \mathbb{R}^3$ represents the unknown disturbances, where $\|\mathbf{d}\| \leq \rho$, with known $\rho \in \mathbb{R}_+$. $\mathbf{t}_g = m\mathbf{g} \mathbf{r}_{cm} \times \mathbf{D} \hat{\mathbf{n}}_3$ provides the external torque caused by gravity, where m is the mass, $\mathbf{r}_{cm} \in \mathbb{R}^3$ the center of mass vector, \mathbf{D} the attitude matrix, and $\hat{\mathbf{n}}_3$ the direction that gravity acts. The complete model of the 3D pendulum can be rewritten in terms of the attitude and dynamics errors

$$\dot{\mathbf{x}}_1 = \mathbf{f}_1(\mathbf{x}), \quad (3)$$

$$\dot{\mathbf{x}}_2 = \mathbf{f}_2(\mathbf{x}) + \mathbf{B}(\mathbf{u} + \mathbf{d}), \quad (4)$$

where $\mathbf{x} \triangleq (\mathbf{x}_1, \mathbf{x}_2) \in \mathbb{R}^6$ is the state errors vector, $\mathbf{x}_1 \in \mathbb{R}^3$ denotes the attitude error in terms of the MRP vector, and $\mathbf{x}_2 \in \mathbb{R}^3$ is the angular velocity error. $\mathbf{f}_1(\mathbf{x})$, $\mathbf{f}_2(\mathbf{x})$, and \mathbf{B} are continuous vector and matrix fields such that $\mathbf{f}_1: \mathbb{R}^6 \rightarrow \mathbb{R}^3$, $\mathbf{f}_2: \mathbb{R}^6 \rightarrow \mathbb{R}^3$, $\mathbf{B}: \mathbb{R}^6 \rightarrow \mathbb{R}^{3 \times 3}$, and $\|(\partial \mathbf{f}_1 / \partial \mathbf{x}_2) \mathbf{B}\| \neq 0, \forall \mathbf{x} \in \mathbb{R}^6$. The control objective is to design a control law \mathbf{u} which makes $\mathbf{x} = \mathbf{0}$ a global exponential stable equilibrium point of (3) and (4). To do so, the following time-varying sliding function can be defined $\mathbf{s}(t, \mathbf{x}) \triangleq \boldsymbol{\sigma}(t) - \mathbf{P}(t)\boldsymbol{\sigma}(\mathbf{0})$, where $\boldsymbol{\sigma}(t) \triangleq \mathbf{C}\mathbf{x}_1 + \mathbf{f}_1 \in \mathbb{R}^3$ with $\mathbf{C} \in \mathbb{R}^{3 \times 3}$ being given a diagonal matrix, and $\mathbf{P}: \mathbb{R}_+ \rightarrow \mathbb{R}^{3 \times 3}$ is a function which satisfies, among other design conditions, $\mathbf{P}(\mathbf{0}) = \mathbf{I}_3$ [3]. Considering the set $\mathcal{S} \triangleq \mathbf{x} \in \mathbb{R}^6: \mathbf{s}(t, \mathbf{x}) = \mathbf{0}, \forall t \geq 0$ the eventual sliding set and to ensure a global sliding mode of (3) and (4) in \mathcal{S} , the following control law is designed [3]

$$\mathbf{u} = - \left(\frac{\partial \mathbf{f}_1}{\partial \mathbf{x}_2} \mathbf{B} \right)^{-1} \left(\left(\mathbf{C} + \frac{\partial \mathbf{f}_1}{\partial \mathbf{x}_1} \right) \mathbf{f}_1 + \frac{\partial \mathbf{f}_1}{\partial \mathbf{x}_2} \mathbf{f}_2 + \dot{\mathbf{P}}(t)\boldsymbol{\sigma}(\mathbf{0}) + \kappa \frac{\mathbf{s}}{\|\mathbf{s}\|} \right), \quad (5)$$

where $\kappa > \|(\partial \mathbf{f}_1 / \partial \mathbf{x}_2) \mathbf{B}\| \rho$ is a design parameter. Figure 1 shows the numerical results for the attitude control of the 3D pendulum presenting the attitude and angular velocity errors as well as the control torques. The goal is to drive the 3D pendulum to the upright (inverted) position and stabilise it there. We can observe that the errors for the GSMC law go to zero faster than the PD control law.

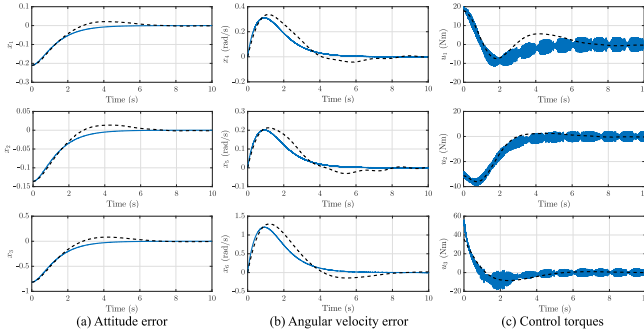


Fig. 1. Results for the control of the 3D pendulum in the upright position, where - - PD control and — GSMC law.

3. Concluding Remarks

This work has presented the design of a global sliding mode control law for the 3D pendulum and compared the results to a PD control law. The GSMC exhibited a better performance taking the 3D pendulum to the upright position faster and presenting no overshoot.

Acknowledgment: The authors thank the São Paulo Research Foundation (FAPESP) for the financial support (grants 2019/05334-0 and 2020/12314-3) and CNPq/Brazil (grant 302637/2018-4).

References

- [1] QIJIA YAO: Robust adaptive finite-time attitude tracking control of a 3d pendulum with external disturbance: Numerical Simulations and hardware experiments. *Nonlinear Dynamics* 2020, **102**(1):223-239.
- [2] YURI SHTESEL, CHRISTOPHER EDWARDS, LEONID FRIDMAN AND ARIE LEVANT: *Sliding mode control and observation*. Springer: Berlin, 2014.
- [3] A. BARTOSZEWICZ: Time-varying sliding modes for second-order systems. *IEEE Proceedings – Control Theory and Applications* 1996, **143**(7):455-462.

Piezoelectric vibration energy harvesting from a portal frame with a shape memory alloy

ANGELO M. TUSSET^{1*}, DIM PIRES², GIANE G. LENZI³, ITAMAR ILIUK⁴, RODRIGO T. ROCHA⁵, JOSE M. BALTHAZAR⁶

1. Federal University of Technology – Paraná (UTFPR) [0000-0003-3144-0407]
2. Federal University of Technology – Paraná (UTFPR) [0000-0002-4254-2081]
3. Federal University of Technology – Paraná (UTFPR) [0000-0003-2065-9622]
4. Federal University of Technology – Paraná (UTFPR) [0000-0001-6904-6240]
5. Federal University of Technology – Paraná (UTFPR) [0000-0001-6770-6380]
6. Federal University of Technology – Paraná (UTFPR) [0000-0002-9796-3609]

Abstract: In the past decades, there has been an accelerated growth in the development of electronic devices. Generally, these devices are low-power consumptions, consequently easy to be powered. Hence, the demand to obtain the needed energy to power up these devices has increased. In this work, the energy harvesting from a simple portal structure accounting for a shape memory alloy (SMA) in its composition material is presented. The portal frame is subjected to an excitation from a non-ideal DC motor with limited supply. The energy harvesting is obtained through a nonlinear piezoelectric material coupled to the structure. The dynamic response of the system is investigated through the variation of the temperature and geometric parameters of the SMA, which are determined by the length and diameter of the alloy. Numerical simulations show the influence of the introduction of the SMA on the dynamics of the system, leading to undesired chaotic behavior to a periodic one. In addition, the energy available for harvesting is computed.

Keywords: Energy harvesting, Nonlinear Dynamics, Shape Memory Alloy, Piezoelectric devices.

1. Introduction

Figure 1 shows an equivalent physical model to represent a portal frame structure with the a piezoelectric material coupled to a column of the structure supporting a DC motor with limited power supply, and unbalanced rotating mass [1].

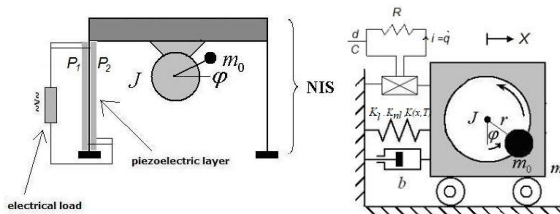


Fig. 1. Schematic of the non-ideal portal frame energy harvester with SMA material

The equations of motion for Fig. 1 can be written as follows:

$$\begin{aligned}
x_1' &= x_2 \\
x_2' &= \frac{1}{1 - \delta_1 \rho_1 \sin(x_3)^2} \left(\begin{array}{l} -\alpha_1 x_2 - k_{sma} (a \Delta T x_1 - b x_1^3 + c x_1^5) + \theta (1 + \Theta |x_1|) x_5 \\ -\beta_1 x_1 - \beta_3 x_1^3 + \delta_1 \sin(x_3) (-\rho_3 x_4 + \rho_2) + \delta_2 \cos(x_3) x_4^2 \end{array} \right) \\
x_3' &= x_4 \\
x_4' &= \frac{1}{1 - \delta_1 \rho_1 \sin(x_3)^2} \left(\begin{array}{l} \rho_1 \sin(x_3) (-\alpha_1 x_2 - k_{sma} (a \Delta T x_1 - b x_1^3 + c x_1^5) - \beta_1 x_1 \\ -\beta_3 x_1^3 + \theta (1 + \Theta |x_1|) x_5 + \delta_2 \cos(x_3) x_4^2) + \rho_2 - \rho_3 x_4 \end{array} \right) \\
x_5' &= \frac{\theta (1 + \Theta |x_1|) x_1}{\rho} - \frac{x_5}{\rho}
\end{aligned} \tag{1}$$

The average power is obtained by: $P_{avg} = \frac{1}{T} \int_0^T P(\tau) d\tau$, with $P = \rho v'^2$.

2. Results and Discussion

Figure 1 shows the numerical results considering the parameters: $a = 0.00156987$, $b = 114.367348$, $c = 7232.49136$, $\alpha_1 = 0.1$, $\beta_1 = -1$, $\beta_3 = 0.2$, $\rho_1 = 0.05$, $\rho_2 = 100$, $\rho_3 = 200$, $\delta_1 = 8.373$, $\theta = 0.20$, $\Theta = 0.60$, $\rho = 1.0$, along with the initial conditions: $x_i(0) = 0$, where $i=1:5$ [1-3].

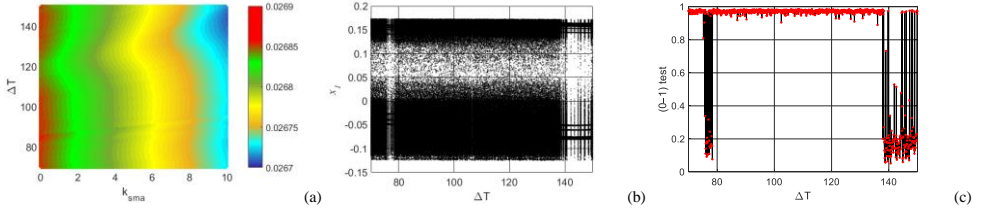


Fig. 1. (a) Average power for $(k_{sma}=[0:10])$ and $\Delta T=[70:150]$, (b, c) Phase diagram and 0-1 test for $a_w(k_{sma}=1)$ and $\Delta T=[70:150]$).

3. Concluding Remarks

The results presented show that the temperature variation of the SMA (ΔT) has little influence on the energy uptake (Fig. 1a), however it has a significant influence on the dynamics of the system (Fig. 1b and 1c). It is also possible to observe that the parameter that represents the dimensions of the SMA (k_{sma}), has a significant influence both in the capture of energy and in the dynamics of the system.

References

- [1] Iliuk, I., Balthazar, J. M., Tusset, A. M., Piqueira, J. R. C., Pontes Jr, B.R., Felix, J. L. P., Bueno, A. M.: *A non-ideal portal frame energy harvester controlled using a pendulum* 2013. The European Physical Journal. Special Topics, **222**: 1575-1586.
- [2] Lima, J. J., Tusset, A. M., Janzen, F. C., Piccirillo, V., Nascimento, C. B., Balthazar, J. M., Brasil, M. R. L. F.: *SDRE applied to position and vibration control of a robot manipulator with a flexible link* 2016. Journal of Theoretical and Applied Mechanics, **54**: 1067-1078.
- [3] Tusset, A. M., Balthazar, J. M., Felix, J. L. P.: *On elimination of chaotic behavior in a non-ideal portal frame structural system, using both passive and active controls* 2013. Journal of Vibration and Control, **19**: 803-813.

Passive vibration control of a high-speed elevator system

ANGELO M. TUSSET^{1*}, MARCOS GONÇALVES², CALEQUELA J. T. MANUEL³, JOSE M. BALTHAZAR⁴, GIANE G. LENZI⁵

1. Federal University of Technology – Paraná (UTFPR) [0000-0003-3144-0407]
2. Federal University of Technology – Paraná (UTFPR) [0000-0003-1544-9356]
3. Federal University of Technology – Paraná (UTFPR) [0000-0002-8819-0667]
4. Federal University of Technology – Paraná (UTFPR) [0000-0002-9796-3609]
5. Federal University of Technology – Paraná (UTFPR) [0000-0003-2065-9622]

Abstract: This paper, the horizontal nonlinear response of a 4 degree-of-freedom vertical transport model excited by rail-guide deformations, and with a nonlinear dynamic vibration absorber (DVA) is numerically investigated. To analyse the vibration levels and comfort of passengers, and the efficiency of using a DVA to reduce cabin vibrations, numerical simulations are performed considering lateral displacement of the cabin, an external disturbance that represents the deformations and misalignment of the rails-guide and the increase in the speed of the elevator, associating the levels of lateral accelerations of the elevator with the levels of comfort felt by passengers in accordance with ISO 2631 and BS 6841. The results of numerical simulations shown that the configuration of the appropriate parameters of the DVA is essential to ensure a better level of comfort to passengers, and that the increase in speed associated with the use of DVA can improve the level of comfort reducing accelerations in the cabin.

Keywords: vertical transport, nonlinear dynamics, dynamic vibration absorber.

1. Introduction

Figure 1 shows an equivalent physical model to represent the horizontal motions of an elevator system, including a nonlinear dynamic vibration absorber (DVA) in cabin.

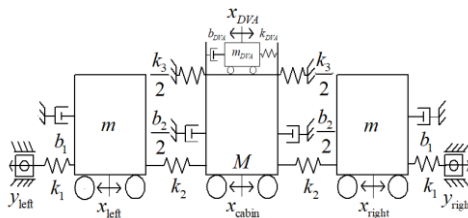


Fig. 1. Motion equivalent model for the horizontal of the elevator

The equations of motion can be obtained considering formula Lagrange and described with differential equations system as follows:

$$\left\{ \begin{array}{l} m\ddot{x}_{left} + b_1\dot{x}_{left} + (k_1 + k_2)x_{left} - k_2x_{cabin} = k_1y_{left} \\ \left(M + m_{DVA} \right) \ddot{x}_{cabin} + b_2\dot{x}_{cabin} + 2k_2cx_{cabin} + k_3x_{cabin}^3 - k_2x_{left} - k_2x_{right} + \\ + b_{DVA}(\dot{x}_{cabin} - \dot{x}_{DVA}) + k_{DVA}(x_{cabin} - x_{DVA})^3 = 0 \\ m_{DVA}x_{DVA} - b_{DVA}(\dot{x}_{cabin} - \dot{x}_{DVA}) - k_{DVA}(x_{cabin} - x_{DVA})^3 = 0 \\ m\ddot{x}_{right} + b_1\dot{x}_{right} + (k_1 + k_2)x_{right} - k_2x_{cabin} = k_1y_{right} \end{array} \right. \quad (1)$$

2. Results and Discussion

Figure 1 shows the compensated acceleration (a_w), and estimated vibration dose value (eVDV), considering the parameters: $M=1120(kg)$, $m=17.5(kg)$; $m_{DVA}=20(kg)$, $k_1=250000(N/m)$; $k_2=19027(N/m)$; $k_3=6.(10^{15})(N/m)$, $b_1=668.21(N.s/m)$; $b_2=2058.2(N.s/m)$; $k_{DVA}=10000(N/m)$, $b_{DVA}=k_{DVA}/2(N.s/m)$, $\omega=31.419(rad/s)$ and $y_{right}=y_{left}=0.Isin(\omega t)$ [1-2].

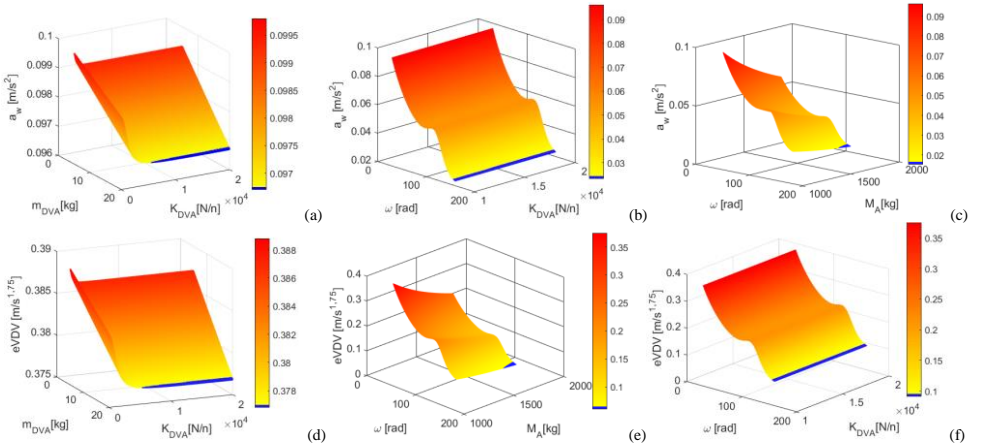


Fig. 1. (a, c) a_w and eVDV for ($m_{DVA}=[5:20]$ and $k_{DVA}=[50:20000]$). (b, d) a_w and eVDV for ($\omega=[30:160]$ and $k_{DVA}=[50:20000]$). (b, d) a_w and eVDV for ($\omega=[30:160]$ and $M=[1120:1720]$).

3. Final Considerations

The results shown that the absorber mass (m_{DVA}) is the most relevant variable in the control, and with its use passenger comfort can be improved in design of the elevator vibration control.

References

- [1] Santo, D. R, Balthazar, J. M, Tusset, A. M., Piccirillo, V., Brasil, R. M. L. R. F., Silveira, M.: *On nonlinear horizontal dynamics and vibrations control for high-speed elevators* 2018. JVC, **24**: 825-838.
- [2] Tusset, A. M.; Santo, D. R., Balthazar, J. M., Piccirillo, V., Santos, L. C. C., Brasil, M. R. L. F.: Active vibration control of an elevator system using magnetorheological damper Actuator. 2017. International Journal of Nonlinear Dynamics and Control, **1**: 114-131.
- [3] A. M.Tusset, V. Piccirillo, J. M. Balthazar, M. R. L. F. Brasil.: *On suppression of chaotic motions of a portal frame structure under non-ideal loading using a magneto-rheological damper* 2015. JTAM: 653-664.

Some Comments on Nonlinear Aeroelastic Typical Section

MICHELLE F. WESTIN^{1*}, ROBERTO G. A. DA SILVA², JOSÉ M. BALTHAZAR³

1. Aeronautics Institute of Technology – ITA, São José dos Campos, SP, Brazil [0000-0001-9333-5835]
2. Aeronautics Institute of Technology – ITA, São José dos Campos, SP, Brazil [0000-0003-0995-9915]
3. São Paulo State University – UNESP, School of Engineering Bauru, SP, Brazil [0000-0002-6082-4832]

* Presenting Author

Abstract: The Aeroelastic typical section, also known as three degrees of freedom Aeroelastic model, is a great way to study nonlinearities in Aeroelastic systems in an isolated way. There is a lack of research using cubic spring commanding the aileron deflection and considering Peters' unsteady loading acting on the model. The model presented here have two linear springs (one commanding the vertical displacement and the other commanding the pitch angle) and one cubic spring for aileron deflection. With the numerical simulated time series, the 0-1 test is performed as well as the Takens' reconstruction and the Lyapunov exponent determination. The 0-1 test result is compared to the Lyapunov exponent, as part of their validation for aeroelastic systems subjected to structural nonlinearities.

Keywords: Aeroelastic system, structural nonlinearity, unsteady aerodynamics

1. Introduction

The typical section with three degrees of freedom, is largely used for various cases in Aeroelasticity, like isolate a specific phenomenon or deal with less and known degrees of freedom. This model, shown in Figure 1, is subjected to unsteady aerodynamic loads, calculated considering Peters' unsteady aerodynamic model [1]. Also, a cubic nonlinear spring is considered in the aileron actuation, which adds the known structural nonlinearity.

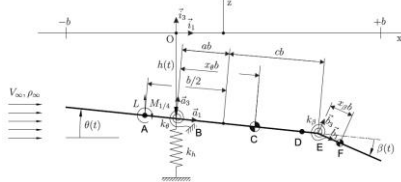


Fig. 1. Three degrees of freedom aeroelastic mathematical model, adapted from [2] by the authors.

The mathematical model in Figure 1 and the unsteady aerodynamic loads are defined in state-space. The unsteady loads consider the inflow as added states, which means that the three degrees of freedom are only the structural states.

2. Results and Discussion

The Aeroelastic system presented in Figure 1 is numerically simulated for various conditions. The time series presented here is only an example of a result and considers an initial vertical displacement of 0 mm, and initial pitch angle (also known as angle of attack) of 2° and an initial aileron deflection of 1°. The airflow speed is also varied, but only one (215m/s) will be shown here for brevity:

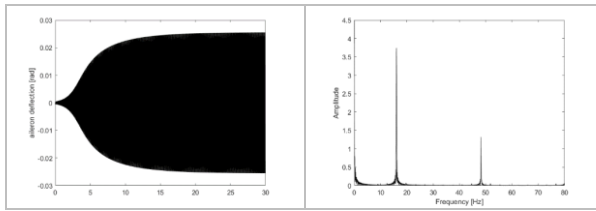


Fig. 2. Time series and FFT.

Figure 2 shows a cubic nonlinearity in FFT and the time series looks a limit-cycle oscillation. The 0-1 test of the time series presented in Figure 2 is:

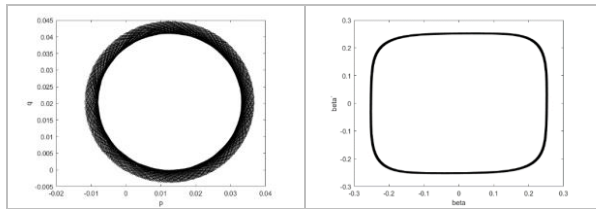


Fig. 3. Shows the 0-1 test result and reconstructed attractor.

The 0-1 test shows a bounded figure, which represents a quasi-periodic system behaviour, since there is mode coupling when dealing with aeroelastic system. The reconstructed attractor also characterizes a limit-cycle. This comparison is also available for a different aeroelastic system in [3].

The Lyapunov exponent compared to 0-1 test also resulted in quasi-periodic system behaviour:

Table 1. Lyapunov exponent x 0-1 test

Lyapunov Exponent	0-1 Test
-8.5884	-0.0216

3. Concluding Remarks

For both 0-1 test and Lyapunov exponent, the Aeroelastic typical section has quasi-periodic behaviour. It is extremely important to highlight that the state-space model also considered three additional states related to the inflow, and their derivatives, totalizing nine states. This system was simulated for three angles of attack, three aileron deflections, eight velocities and two cubic spring parameters and the result presented here is only a representative result. Below 175m/s the aileron deflection amplitude reaches the same value and, by increasing the velocity, the movement amplitude also increases. Lower values of cubic spring parameter resulted in higher amplitudes.

References

- [1] BALVEDI JR., E. A. Linear and Nonlinear Aeroelastic Analyses of a Typical Airfoil Section with Control Surface Freeplay. 2010. 121f. Dissertation (Master in Aeronautical and Mechanical Engineering) – Aeronautical Institute of Technology, São José dos Campos.
- [2] PETERS, D.A.; HSIEH, M.A.; TORRERO, A. A State-Space Airloads Theory for Flexible Airfoils. Presented at the American Helicopter Society 62nd Annual Forum Proceedings, Phoenix, AZ, May 9-11, 2006. Published in August 2007.
- [3] WESTIN, M. F.; BALTHAZAR, J. M. ; DA SILVA, R. G. A . On Comparison Between 0-1 Test for Chaos and Attractor Reconstruction of an Aeroelastic System. Journal of Vibration Engineering & Technologies, v. 2020, p. 1-12, 2020. <https://doi.org/10.1007/s42417-020-00227-0>

Manipulator-aircraft dynamical system dedicated for wind tunnel testing

JAMES F. WHIDBORNE^{1*}, ELŻBIETA JARZĘBOWSKA², VARUL AGARWAL³, A. AFIZ ISHOLA⁴

1. Cranfield University, Cranfield, Bedfordshire MK43 0AL, UK [0000-0002-6310-8946]
2. Warsaw University of Technology, 00-665 Warsaw, Nowowiejska 24, Poland, [0000-0003-1407-7546]
3. Warsaw University of Technology, 00-665 Warsaw, Nowowiejska 24, Poland [0000-0002-7668-0482]
4. Cranfield University, Cranfield, Bedfordshire MK43 0AL, UK [0000-0002-5435-5726]

* Presenting Author

Abstract: This paper describes work focused on the development of a new conceptual design of a directly controlled manipulator placed in the working section of a wind tunnel, with the goal of expanding and diversifying the type of dynamic experiments performed in the tunnel. In this research, our main objective is to develop a model and controllers to simulate a manipulator with an aircraft test model attached to its end. The final model will be fully geometrically qualified to operate in confined spaces and to rigorously evaluate the nonlinear simulation for the determination of stability derivatives with high precision that relates to the *longitudinal flight* and control characteristics of the aircraft. Various simulation tests help to understand how close the calculated values are to reality, which can improve the determination of aircraft control in the *pitch plane*.

Keywords: wind tunnel tests, aircraft flight model, aircraft feedback control

1. Introduction – wind tunnel test challenges

Wind tunnel testing is long established experimental approach for aircraft design and analysis as well as fundamental flight physics and aerodynamics. Most wind tunnel studies involve static models, but dynamic wind tunnel studies are important for both the investigation of non-steady aerodynamics and for flight dynamics, particularly for non-linear flight regimes involving high angles of attack, unsteady aerodynamics, spin and upset recovery. Dynamic wind tunnel testing thus plays an important role in the determination of aerodynamic and flight dynamic parameter identification.

One longstanding ambition of wind tunnel testing has been to ‘fly’ an aircraft inside the wind tunnel [1]. This is clearly an expensive thing to do and is fraught with difficulties which has limited the experience to a few very large facilities and to specific flight regimes such as spin test. However, recent advances in measurement technologies have extended the possibilities and 3 degrees of rotational freedom ‘flight’ is now fairly common [2, for example], with 4 and 5 degrees of freedom (dof) having success in relatively small and low-cost facilities [3, 4]. An extensive review of dynamic wind tunnel testing can be found in [5].

The control of the aircraft in [3] was enacted by the classical elevator, rudder, aileron moving surfaces. However, energy is injected into the dynamic system through the propulsion system, and this affects the dynamics, particularly the longitudinal motion. Whilst the 4-dof rig used in [3] includes the heave motion, the surge motion is constrained, thus limiting the ‘flight’. Mechatronics technologies have also advanced enormously in recent years, so possibilities of mounting the aircraft on a manipulated sting now exist [1, for example]. In this work, the possibilities for full 6-dof flight in a wind tunnel with the ‘propulsion’ enacted by a robotic manipulator are investigated. In order to simplify the problem, 3-dof

longitudinal flight only will be initially considered. Decoupling of longitudinal and lateral motion is a standard assumption in flight dynamics analysis and is valid for many flight regimes. A schematic of the proposed configuration is shown in Figure 1.

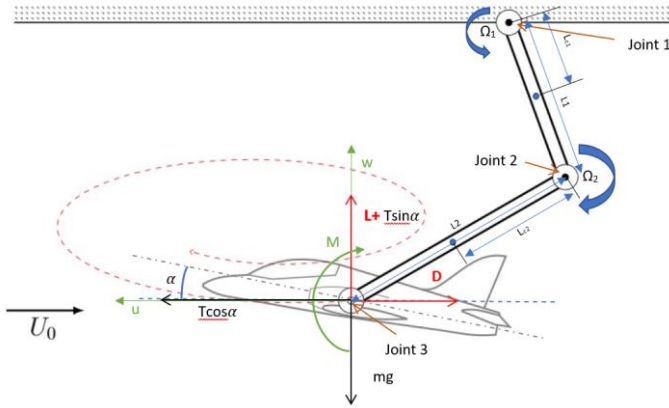


Fig. 1. Schematic diagram of a manipulator with an aircraft test model attached at the end intended for wind tunnel testing. The aircraft can freely rotate or manoeuvre in the x-z plane along the y-axis at joint 3. The pitch of the aircraft can be controlled by the elevator of the test aircraft model, which is assumed to be actuated. The manipulator arm joints, joint 1 and joint 2, are driven by servomotors (the best choice for systems requiring high accuracy) provide control of the aircraft thrust, denoted by T.

2. Results and discussion

The full paper will include the analysis of the system dynamics, including the aerodynamic forces. The 2-R manipulator consists of stiff links connected by mechanical joints and control torques that move the links so that the aircraft model at the end can make its longitudinal flight. The majority of this research is concerned with the design of the feedback loops of the position controllers applied to the joints, which should be properly synchronized to characterize the dynamics of the model being tested in its planar motion. Introducing a reduction in the required power by analyzing different ways to minimize support interference and deflection error correction, which can also lead to a reduction in the reaction transmitted to the tunnel structure.

The research presented here includes modeling the dynamics of a coupled manipulator and aircraft model and controller designs, and various simulations in MATLAB to design the control dynamics with a robust feedback loop.

References

- [1] M. Huang and Z.-W. Wang. Review of wind tunnel based virtual flight testing techniques for evaluation of flight control systems. *Int. J. Aerospace Engineering*, 2015(672423):15 pages, 2015.
- [2] D. D. Ignatyev, M. E. Sidoryuk, K. A. Kolinko, and A. N. Khrabrov. Dynamic rig for validation of control algorithms at high angles of attack. *J. Aircraft*, 54(5):1760–1771, 2017.
- [3] A. Pontillo, S. Yusuf, G. Lopez, D. Rennie, and M. Lone. Investigating pitching moment stall through dynamic wind tunnel test. *Proc. IMechE J. Aero. Eng.*, 232(2):267–279, 2020.
- [4] J. Pattinson, M. H. Lowenberg, and M. G. Goman. Multi-degree-of-freedom wind-tunnel maneuver rig for dynamic simulation and aerodynamic model identification. *J. Aircraft*, 50(2):551–566, 2013.
- [5] D.B. Owens, J.M. Brandon, M.A. Croom, M. Fremaux, G.Heim, and D. Vicroy. Overview of dynamic test techniques for flight dynamics research at NASA LaRC. *25th AIAA Aerodynamic Measurement Technology and Ground Testing Conference*, 2006.

Reducing amplitude of nonlinear vibration of rotors induced by imbalance forces and the disc collisions using magnetically sensitive fluids

JAROSLAV ZAPOMĚL^{1*}, PETR FERFEČKÍ², JAN KOZÁNEK³

1. Institute of Thermomechanics, Department of Dynamics and Vibration
VŠB - Technical University of Ostrava, Department of Applied Mechanics
 2. VŠB - Technical University of Ostrava, Department of Applied Mechanics
VŠB - Technical University of Ostrava, IT4Innovations
 3. Institute of Thermomechanics, Department of Dynamics and Vibration
- * Presenting Author

Abstract: Rotors of rotating machines are often supported by hydrodynamic bearings. The unbalance, ground vibration, assembling inaccuracies, and eccentric position of the rotor journal in the bearing hole may arrive at collisions of the discs with the machine casing. This can be avoided by changing position of the rotor journal in the bearing hole by increasing stiffness of the oil film. This is offered by application of magnetically sensitive fluids. The control of stiffness of the rotor support elements by a magnetic field was examined by computational simulations. The results show that application of a magnetic field makes it possible to prevent impacts and maintain quite running of rotating machines in a certain velocity interval.

Keywords: hydrodynamic bearings, magnetically sensitive lubricant, oil film stiffness control

1. Introduction

Rotors are often supported by hydrodynamic bearings. The design of a number of rotating machines requires very narrow gaps between the discs and the inner wall of the stationary part (e.g. propellers of pumps or fans to minimize leakage of media from the working space). The assembling inaccuracies, imbalance of rotating parts, and eccentric position of the rotor journal in the bearing hole may arrive at collisions between the discs and the rotor casing. Then the hydrodynamic bearings and impacts become the source of highly nonlinear vibration of the rotor and of increase of forces transmitted between the rotating and stationary parts. The change of the rotor journal position in the hydrodynamic bearings gives the possibility how to avoid these undesirable working conditions. This manipulation requires to change the bearing stiffness.

A new approach to control stiffness of hydrodynamic bearings consists in using magnetically sensitive oils. Application of magnetorheological fluids is reported by Wang et al. [1]. The simulation results show that the magnetorheological fluids are applicable for suppressing vibration of rotor systems and for altering their critical speed. The proposal of the bearing and investigation of its response on the change of the current powering the electric coil that is the source of the magnetic flux is reported in [2]. This paper focuses on changing position of the rotor journal in the bearing gap by changing stiffness of the oil film utilizing action of a magnetic field on magnetically sensitive oil with the aim to prevent collisions between the rotor and its casing.

2. Effect of the magnetically controllable bearing on collisions suppression

The investigated rotor consists of a shaft and of one disc. At both its ends it is supported by magnetically controlled hydrodynamic bearings. The rotor rotates at constant angular speed, is loaded

by its weight and is excited by the disc imbalance. The disc is placed in the hole between two parallel vertical walls.

In the computational model the hydrodynamic bearings are represented by force couplings. The pressure distribution in the oil layer is governed by the Reynolds equation, which has been significantly modified to be applicable for lubricants exhibiting the yielding shear stress. The integration of the pressure profile gives components of the hydraulic forces. The Kirchhoff and Hopkinson laws were used to determine distribution of the magnetic field intensity in the bearing gap. The details are reported in [2].

Fig. 1 shows the orbits of the disc centre for two angular speeds of the rotor rotation. If the oil is not affected by a magnetic field, the collisions between the disc and the stationary part take place. Application of the magnetic field shifts the orbits toward the bearing centre, which avoids the impacts. The shape and size of the orbits depend on angular speed of the rotor rotation, application of the magnetic field, and on interaction between the disc and the stationary part.

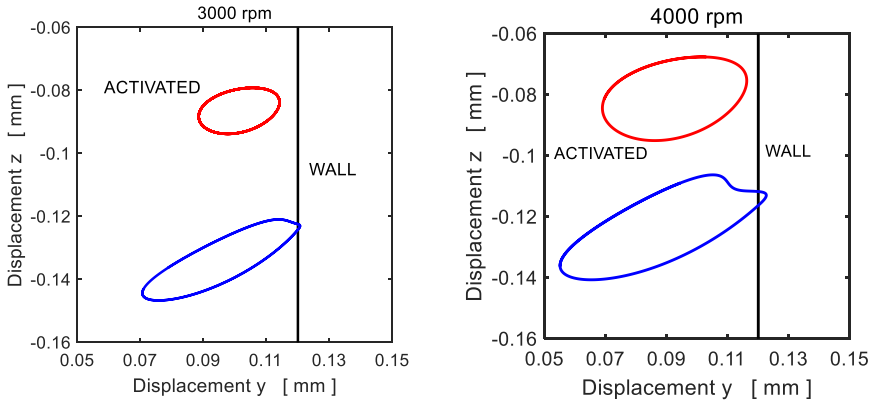


Fig. 1. The disc centre orbit (non-activated and activated bearing)

3. Conclusions

The results of the computational simulations show that (i) if the disc motion is not limited then the vibration bifurcates after exceeding the critical speed and a subharmonic component of large amplitude occurs, (ii) if the disc motion is limited then after exceeding a critical speed the impacts start to take place but increasing angular speed of the rotor rotation does not lead to inducing the subharmonic vibration, and (iii) application of the magnetic field prevents impacts in a certain velocity interval.

Acknowledgment:

The work presented in this paper was supported by the Czech Science Foundation (grant project 19-06666S) and by the Ministry of Education, Youth and Sports (project LQ1602).

References

- [1] WANG X., LI H., LI M., BAI H., MENG G., ZHANG H.: Dynamic characteristics of magnetorheological fluid lubricated journal bearing and its application to rotor vibration control. *Journal of Vibroengineering* 2015, **17**, pp. 1912-1927.
- [2] ZAPOMÉL J., FERFECKI P.: Dynamic characteristics of magnetorheological fluid lubricated journal bearing and its application to rotor vibration control. *Vibroengineering Procedia* 2019, **27**, pp. 133-138.

-S3-

**Mathematical modeling of
nonlinear systems involving
interacting with medium**

On the attitude stabilization of artificial Earth satellite in the natural electromagnetic coordinate system

ALEXANDER YU. ALEKSANDROV¹, ALEXEY A. TIKHONOV^{2*}

1. Saint Petersburg State University, Department of Medical and Biological Systems Control, Saint Petersburg, Russia [ORCID ID: 0000-0001-7186-7996]
2. Saint Petersburg State University, Department of Theoretical and Applied Mechanics, Saint Petersburg, Russia [ORCID ID: 0000-0003-0838-5876]

* Presenting Author

Abstract: A satellite with electrodynamic attitude control system is considered. The satellite possesses an electrostatic charge and an intrinsic magnetic moment. The natural electrodynamic coordinate system associated with the directions of geomagnetic induction vector and Lorentz force vector is introduced and considered as a rotating base coordinate system for satellite attitude stabilization. The problem of the angular stabilization of the satellite in the natural electrodynamic coordinate system is studied. Based on the method of Lyapunov functions, sufficient conditions for the asymptotic stability of the direct equilibrium position of the satellite in the base coordinate system are obtained in the presence of the disturbing effect of the gravitational torque. These conditions make it possible to ensure a rational choice of the parametric control coefficients depending on the parameters of the satellite and its orbit.

Keywords: satellite, electrodynamic attitude control, natural electromagnetic coordinate system, Lyapunov function, asymptotic stability

1. Introduction

An artificial Earth satellite with an electrostatic charge Q and an eigen magnetic moment is considered. In the process of moving through the geomagnetic field with the relative velocity \vec{v} , such a satellite experiences the influence of the Lorentz and magnetic torques [1]. These torques are in the basis of electrodynamic attitude control system [2]. To stabilize the angular position of the satellite, the orbital [3] and König [4] coordinate systems are usually used, which are convenient for practical applications, but not related to the specifics of the forces and torques acting on a charged satellite in the Earth's magnetic field. In this paper, we introduce into consideration a new - natural electrodynamic coordinate system (NECS) associated with the directions typical for a charged satellite: geomagnetic induction \vec{B} and vector $\vec{T} = \vec{v} \times \vec{B}$ associated with the Lorentz force $\vec{F}_L = Q\vec{T}$. The unit vectors along the axes of NECS are introduced as follows:

$$\vec{w} = \frac{\vec{B} \times \vec{T}}{|\vec{B}| |\vec{T}|}, \quad \vec{b} = \frac{\vec{B}}{|\vec{B}|}, \quad \vec{i} = \frac{\vec{T}}{|\vec{T}|}. \quad (1)$$

Such a choice of the basic coordinate system implies that the magnetic control torque is always in plane orthogonal to vector \vec{b} and the Lorentz control torque is in plane orthogonal to vector \vec{i} . This results in simplification of attitude control design.

2. Results and Discussion

It is shown that the NECS is convenient for the implementation of certain modes of scanning the Earth's surface. The purpose of the paper is a rigorous analytical proof of the asymptotic stability of the direct equilibrium position of the satellite in the NECS based on the analysis of nonlinear differential equations of motion [1,5]. The disturbing effect of the gravitational torque acting upon the satellite is taken into account. The corresponding compensating term is involved in control torque alongside with restoring and dissipative terms. The dissipative term is linear with respect to the relative angular velocity of the satellite [6,7]. With the use of the direct Lyapunov method [8] and the development of methods for constructing Lyapunov functions proposed by the authors, sufficient conditions for the asymptotic stability of the satellite program motion are derived. These conditions make it possible to ensure a rational choice of variable coefficients of parametric control depending on the parameters of the satellite and its orbit. Moreover, the possibility of realizing a completely passive version of electrodynamic stabilization in the NECS for an isoinertial satellite has been proved. The results obtained in the paper, are confirmed by computer modelling.

Acknowledgment: This work was supported by the Russian Foundation for Basic Research (grant N 19-01-00146-a).

References

- [1] BELETSKY V.V.: *Motion of an Artificial Satellite about its Center of Mass*. Israel Program for Scientific Translation: Jerusalem, 1966.
- [2] ALEKSANDROV A.Y., TIKHONOV A.A.: Asymptotic stability of a satellite with electrodynamic attitude control in the orbital frame. *Acta Astronautica* 2017 **139**:122-129.
- [3] ALEKSANDROV A.Y., ALEKSANDROVA E.B., TIKHONOV A.A.: Stabilization of a programmed rotation mode for a satellite with electrodynamic attitude control system. *Advances in Space Research* 2018 **62**(1):142-151
- [4] ALEKSANDROV A.Y., ANTIPOV K.A., PLATONOV A.V., TIKHONOV A.A.: Electrodynamic stabilization of artificial earth satellites in the König coordinate system. *Journal of Computer and Systems Sciences International* 2016, **55**(2):296-309.
- [5] LACARBONARA W.: *Nonlinear Structural Mechanics: Theory, Dynamical Phenomena and Modeling*. Springer: 9781441912763, 2013.
- [6] DOSAEV M.: Interaction between internal and external friction in rotation of vane with viscous filling. *Applied Mathematical Modelling* 2019, **68**:21-28.
- [7] AWREJCEWICZ J., OLEJNIK P.: Analysis of Dynamic Systems with Various Friction Laws. *Applied Mechanics Reviews* 2005, **58**(6):389-411.
- [8] AWREJCEWICZ J.: *Ordinary Differential Equations and Mechanical Systems*. Springer: Cham Heidelberg New York Dordrecht London, 2014.

On the triaxial electrodynamic attitude stabilization of a satellite in the orbital frame via control with distributed delay

ALEXANDER YU. ALEKSANDROV¹, ALEXEY A. TIKHONOV^{2*}

1. Saint Petersburg State University, Department of Medical and Biological Systems Control, Saint Petersburg, Russia [ORCID ID: 0000-0001-7186-7996]
2. Saint Petersburg State University, Department of Theoretical and Applied Mechanics, Saint Petersburg, Russia [ORCID ID: 0000-0003-0838-5876]

* Presenting Author

Abstract: The problem of triaxial attitude stabilization of a satellite in the orbital frame is considered. The problem is raised about the possibility of implementing such a system of electrodynamic attitude control by the type of a PID controller, in which the integral component of the control torque contains a distributed delay. A theorem on the asymptotic stability of the stabilized angular position of the satellite is proved. The theorem substantiates the possibility of constructing the indicated control system. The effectiveness of the designed attitude control with a distributed delay is confirmed by computer modelling.

Keywords: satellite, electrodynamic attitude control, PID controller, distributed delay, asymptotic stability

1. Introduction

A satellite with an arbitrary triaxial ellipsoid of inertia in a circular equatorial orbit is considered. The mode of direct equilibrium position in the orbital coordinate system is considered as the programmed mode of the satellite attitude motion. To stabilize the satellite in the programmed motion mode, an electrodynamic attitude control system is used, which generates the Lorentz and magnetic control torques [1]. These two control torques implement the restoring and damping components and also provide compensation [2] of the disturbing gravitational torque [3], that allow stabilizing the satellite in the programmed motion mode.

The novelty of the approach to solving the problem lies in the development of the concept of electrodynamic attitude control by using the restoring torque with a distributed delay [4]. The effectiveness of such type of a PID controller (see [5] and papers cited therein) is investigated.

2. Results and Discussion

A simple and easily verified sufficient conditions for the asymptotic stability of the programmed motion of the satellite has been obtained in a nonlinear formulation with the use of the approach developed in [4, 6] to constructing Lyapunov functions [7]. The obtained conditions impose restrictions on the coefficients at the restoring [1] and dissipative [1, 8] components of control torque and the value of delay. The suggested approach to electrodynamic attitude control design is compared with those considered in the previous publications. It was revealed that the distributed delay (integral term)

- 1) significantly improves the quality of control process and makes it smoother;
- 2) reduces the time of convergence to the program motion.

The first observation implies that the suggested modification of electrodynamic attitude control can be used to avoid undesirable satellite vibrations generated by attitude control system. For this reason, it is suitable for stabilization large-scale space structures. Especially in the cases where dangerous resonance oscillations may occur due to nonlinearity of structure [9]. The second observation implies that the introduction of distributed delay (integral term) makes the electrodynamic attitude control system much more effective compared with earlier known variants.

Thus, the development of the theory of electrodynamic attitude control is given for solving the practically important problem of triaxial attitude stabilization of a satellite in the orbital frame. Numerical modelling confirms the conclusion proved in the theorem.

Acknowledgment: This work was supported by the Russian Foundation for Basic Research (grant N 19-01-00146-a).

References

- [1] ANTIPOV K.A., TIKHONOV A.A.: Parametric control in the problem of spacecraft stabilization in the geomagnetic field. *Automation and Remote Control* 2007 **68**(8):1333-1345.
- [2] TIKHONOV A.A.: On electrodynamic compensation of a torque disturbing satellite orientation. In: PETROSYAN L.A., ZHABKO A.P. (ED.) *2015 International Conference "Stability and Control Processes" in Memory of V.I. Zubov (SCP)*. IEEE: 2015.
- [3] BELETSKY V.V.: *Motion of an Artificial Satellite about its Center of Mass*. Israel Program for Scientific Translation: Jerusalem, 1966.
- [4] ALEKSANDROV A.Y., TIKHONOV A.A.: Stability analysis of mechanical systems with distributed delay via decomposition. *Vestnik Sankt-Peterburgskogo Universiteta, Prikladnaya Matematika, Informatika, Protsessy Upravleniya*. 2021 **17**(1):13-26.
- [5] OLEJNIK P., ADAMSKI P., BATORY D., AWREJCEWICZ J.: Adaptive tracking PID and FOPID speed control of an elastically attached load driven by a DC motor at almost step disturbance of loading torque and parametric excitation. *J. Appl. Sci.* 2021 **11**: 679.
- [6] ALEKSANDROV A.Y., KOSOV A.A.: Stability and stabilization of equilibrium positions of nonlinear nonautonomous mechanical systems. *J. Comput. Syst. Sci. Intern.* 2009 **48**(4):511-520.
- [7] AWREJCEWICZ J.: *Ordinary Differential Equations and Mechanical Systems*. Springer: Cham Heidelberg New York Dordrecht London, 2014.
- [8] DOSAEV M.: Interaction between internal and external friction in rotation of vane with viscous filling. *Applied Mathematical Modelling* 2019, **68**:21-28.
- [9] LACARBONARA W.: *Nonlinear Structural Mechanics: Theory, Dynamical Phenomena and Modeling*. Springer: 9781441912763, 2013.

An Elastic Rib Modelling

ALPATOV IVAN^{1*}, DOSAEV MARAT², SAMSONOV VITALY², EKATERINA VOROBYEVA³,
DUBROV VADIM³

¹ Faculty of Mechanics and Mathematics, Lomonosov Moscow State University, Moscow, Russia

² Institute of Mechanics, Lomonosov Moscow State University, Moscow, Russia

³ Department of Fundamental Medicine, Lomonosov Moscow State University, Moscow, Russia

* Presenting Author; e-mail: alpatov.ivan@list.ru

Abstract: Chest modelling approach to patients with pectus carinatum is presented. A mechanical model of flat rib under load is developed and a method for its parameters identification is proposed.

Keywords: biomechanical modeling, finite-dimensional model, parameter identification

1. Introduction

Keeled chest or pectus carinatum is one of the most widespread chest malformations. There is a way to correct this deformity with a special orthosis. To adjust the orthosis, it is necessary to conduct an experiment, in which the patient is subjected to pressure on the chest in order to find out the pressure of correction (POC), that is, the pressure at which the chest is deformed to normal. However, this experiment can be problematic and undesirable for many reasons. Mathematical modeling of chest deformation under the influence of various loads is a very urgent task. This problem can be solved by finite element methods (FEM) [1, 2], or, for example, by constructing phenomenological models that allow describing the dynamics of the chest and assessing important characteristics of its state. In this paper, a finite-dimensional model of a rib based on processing of CT images is proposed, as well as a 3D FEM model is built for calculation in the Ansys. Bone material is considered to be isotropic and linearly elastic. The coefficient of elasticity of the material is taken from the literature [3]. A technique for identifying the parameters of a finite-dimensional model is proposed.

2. Materials and methods

Due to the structural complexity of the rib cage, we limited ourselves to considering one rib under load. CT scans of a patient with pectus carinatum have been acquired and imported into various medical software. Then a 3D model of the 5th rib segmentation was created. Typical 3D file formats provided by medical software are STL, OBJ, PLY. However, Ansys does not work directly with faceted models such as the STL. We used the commercial medical software DICOM to PRINT (3D Systems, Inc.) to convert the facet model to the smoothed model. This approach allows us to save segmented regions in the IGES file format that can be utilized by Ansys.

To build mechanical model of a rib we made an assumption that the rib is flat, i.e. there is a plane that contains the whole rib. Our mechanical model of the rib consists of five rigid rods connected by linear spiral springs (Fig.1b). Compliance in costovertebral joint is modeled by two linear cylindrical springs that connects the head of the rib with fixed perpendicular planes (we assume that corresponding vertebra is fixed) so that at every moment elastic forces from these springs are directed along corresponding coordinate axes. There is also a linear spiral spring in the head of the rib that

hinder the motion of the rib in costovertebral joint around axis, normal to the plane containing the rib. In initial state all springs in the system are undeformed and A_1 end of first rod coincide with origin O . Displacements x, y of the point A_1 and angles $\varphi_i, i = 1, \dots, 5$ between corresponding rods and Ox axis were chosen as generalized coordinates. The force F with components F_x, F_y is applied to A_6 end of the last rod in the system.

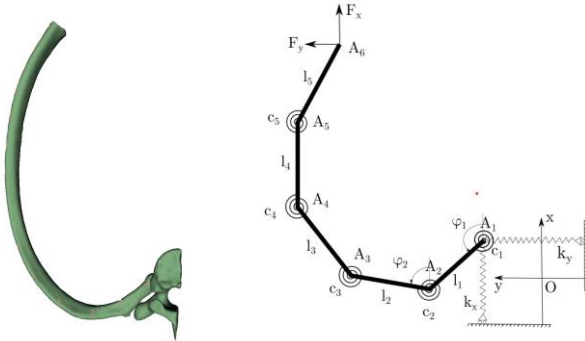


Fig. 1. Undeformed state of the mechanical system. Segmented rib (a), finite-dimensional mechanical model (b)

Lengths of the rods and initial angles between them were measured in open-source 3D Slicer software. The equations of equilibrium for described system were obtained. Numerical solution of these equations, however, depends on values of coefficients of springs' stiffness $k_x, k_y, c_i, i = 1, \dots, 5$. The identification of the coefficients was made with assumption of equality of small displacements of corresponding rods and displacements of non-fixed end of curved beam, which were obtained by Maxwell-Mohr method.

3. Results

Numerical modeling of rib deformation was carried out using the finite-dimensional model and the FEM model built in the Ansys software. The difference in the amount of movement of the end point and several reference points of the rib at a given load does not exceed 10%.

References

- [1] NAGASAO T, MIYAMOTO J, TAMAKI T, et al: Stress distribution on the thorax after the Nuss procedure for pectus excavatum results in different patterns between adult and child patients. *Journal of thoracic and cardiovascular surgery*, 2007 Dec; **134**(6):1502-1507.
- [2] ZHANG G, CHEN X, OHGI J, et al: Biomechanical simulation of thorax deformation using finite element approach. *Biomed Eng Online*, 2016;15:18.
- [3] GRIBOV D.A. Development of a biomechanical model and methodology for planning surgical treatment of pectus excavatum (unpublished), Cand. Eng. Sc. Diss, Bauman Moscow State Technical University, Moscow, 2016. 157 p.

Control algorithm of a vibrating robot with a flywheel and unbalance with limited angular acceleration.

MARAT DOSAEV*

Institute of Mechanics, Lomonosov Moscow State University, Moscow, Russia

Abstract: When developing a robot for moving on the surface of small planets, in addition to low gravity, it is necessary to take into account the influence of an aggressive environment. The design of a vibrating robot, which is an isolated capsule, and moves due to the movement of internal masses and friction of various natures against the planet's surface, is considered. The robot is equipped with one unbalance and one flywheel. The unbalance angular acceleration control algorithm is built on the assumption that the robot can lift off the surface and perform a translational motion. It is shown that if the limitation on the maximum value of the unbalance acceleration is not considered for the selected algorithm, then the average speed of the body can also grow indefinitely. In this case, the standing time of the robot body is reduced, and its horizontal "flight" speed increases. An algorithm for controlling the robot is constructed, taking into account the limits on the angular acceleration of the unbalance and the flywheel.

Keywords: vibration robot; dry friction; mathematical model; control algorithm.

1. Introduction

A vibrating robot (an inertoid) is considered [1]. The robot consists of the body 1, the balanced flywheel 2, and the unbalance (eccentric) 3 (Fig. 1). The plane-parallel motion of the body on a rough surface is considered. The flywheel is driven by the motor around point A . The unbalance is rotated by another motor around point B . The center of mass of the unbalance is located at point C .

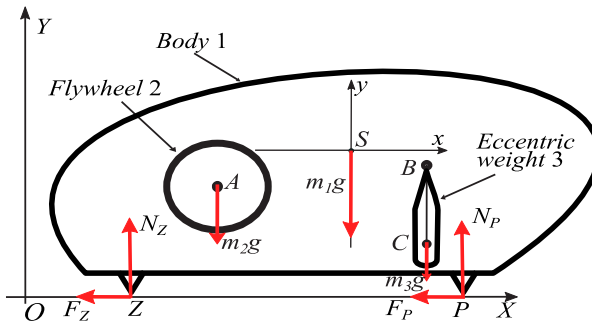


Fig. 1. Vibration robot with the balanced flywheel and the unbalance.

* 119192, Russia, Moscow, Michurinskiy prosp., 1; e-mail: dosayev@imec.msu.ru

The relative position of the centers of the robot body, flywheel and unbalance is arbitrary. We assume that the robot body is equipped with an accelerometer that measures the acceleration of its certain point, and the unbalance motor rotor is equipped with sensors for its angle of rotation and angular velocity, and the flywheel rotor is equipped with an angular velocity sensor. The angular accelerations of rotating structural links are used as control functions.

2. Estimation of the value of the unbalance speed when implementing the control algorithm

An algorithm for controlling the motion of the robot body in the desired direction is proposed. When the algorithm is implemented, with each new revolution of the eccentric, the time of the stages during which the body moves increases. The maximum body speed at each such subsequent stage also increases.

The proposed algorithm provides for sequential relay switching of the unbalance control angular acceleration φ'' . In this case, on the phase plane, the representative point passes from the curve corresponding to the phase of acceleration of the rotating parts and the rest of the robot body (dashed green curve) to another, corresponding to the phase of "flight" and displacement of the robot body (solid red curve) and back. Let us consider the sequence φ_k of angle φ of unbalance rotation, at which the k -th odd switching of the angular acceleration occurs. It is shown that if we do not consider the limitation on the maximum value of acceleration, then the speed of rotation of the unbalance at $k \rightarrow \infty$ grows to infinity.

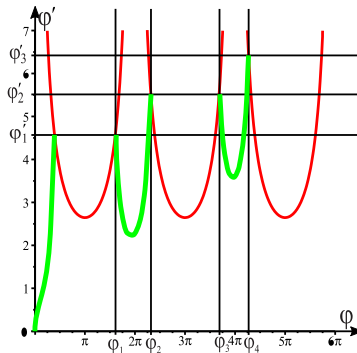


Fig. 2. Switching points on the phase plane.

3. Implementation of the new algorithm

An algorithm for controlling the robot is constructed taking into account the limits on the angular accelerations of the unbalance and flywheel. The impact of these accelerations on the average speed of the robot body is estimated.

References

- [1] DOSAEV M, SAMSONOV V, HWANG SS: Construction of control algorithm in the problem of the planar motion of a friction-powered robot with a flywheel and an eccentric weight. *Applied Mathematical Modelling*. 2021, **89** (2):1517-1527.

Sliding of tabouret with elastic legs on a rough surface under the action of a small lateral force

MARAT DOSAEV*, VITALY SAMSONOV

Institute of Mechanics, Lomonosov Moscow State University, Moscow, Russia

Abstract: The features of the behavior of a dynamically asymmetric body with two elastic supports on a plane with dry friction are discussed. A constant lateral force is applied to the body. The equations of motion are the dynamical system of variable structure. In a position of seemingly obvious vertical equilibrium, the equilibrium conditions are not met. A motion is described, during which one or both supports slide depending on the value of the coefficient of friction. The presence of elasticity in the supports leads to permanent sliding of the body even in the case of a relatively small lateral force.

Keywords: elastic force, dry friction, dynamical system of variable structure.

1. Introduction

When modelling the braking of a vibrating robot on two supports on a rough plane, problems were found with the description of the friction force [1]. Similar problems were encountered in modelling other problems of mechanics [2, 3]. To regularize the description of the interaction of the body with the support, the compliance of the supports is introduced into the model.

2. Description of the mechanical system behavior

Let a heavy body $ABCD$ ($AB = 2a$, $AD = 2b$) of mass m (Fig. 1) perform plane-parallel motion, resting on a horizontal rough plane with two elastic supports AA_1 and BB_1 . When the supports are not stressed, their length $AA_1 = BB_1 = l_0$. The centre of mass G_1 of the body is displaced from its centre G by a distance d along the straight line DC . The springs of the supports act on the body by forces $F_{el1} = -k(l_1 - l_0) - h\dot{l}_1$, $F_{el2} = -k(l_2 - l_0) - h\dot{l}_2$, where k is the stiffness coefficient, h is the damping coefficient of the springs.

The following external forces act on the system: gravity $\mathbf{P} = m\mathbf{g}$ (\mathbf{g} is the acceleration of gravity), normal $\mathbf{N}_1, \mathbf{N}_2$ and tangential $\mathbf{F}_{fr1}, \mathbf{F}_{fr2}$ reactions of the supports, which, in the case of sliding of the supporting legs, are related to each other by the Coulomb law: $F_{fr1} = -\mu \text{signum}(V_{x_{A1}}) |N_1|$, $F_{fr2} = -\mu \text{signum}(V_{x_{B1}}) |N_2|$, as well as the lateral force \mathbf{F}_e applied at the center of mass G_1 . Note that both legs slide if $\mu = 0$.

As generalized coordinates, we choose the coordinates x_{G_1}, y_{G_1} of the center of mass G_1 and the angle φ between the vertical and the direction of the elastic supports. We study the possible types of system behavior. The dynamical system under consideration is the system of variable structure. In

* 119192, Russia, Moscow, Michurinskiy prosp., 1; e-mail: dosayev@imec.msu.ru

general, when both legs slide, the mechanical system has 3 degrees of freedom. The equations of motion in the case of sliding of both legs can be represented as follows:

$$\begin{aligned}
 m\ddot{x}_{G_1} &= F_{fr1} + F_{fr2} + F_e \\
 m\ddot{y}_{G_1} &= -mg + N_1 + N_2 \\
 J\ddot{\varphi} &= N_1((l_1 + b)\sin\varphi + (a + d)\cos\varphi) - N_2(-(l_2 + b)\sin\varphi + (a - d)\cos\varphi) - (F_{fr1} + F_{fr2})(l_0 + b + y_{G_1})
 \end{aligned}$$

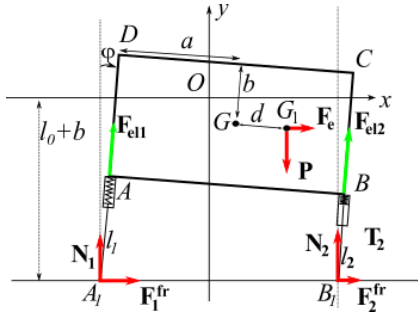


Fig. 1. The body on a rough plane.

During periods of time when one of the supports does not slide, the system has two degrees of freedom. This is equivalent to constraining $x_{A_i} = const$ or $x_{B_i} = const$. In this case, the dynamical system consists of two equations, for example, for generalized coordinates y_{G_1}, φ . In this case, the second support stops only at those moments of time when the angular velocity turns to zero.

A numerical study of the obtained dynamical system of variable structure for various values of the friction coefficient was carried out.

3. Conclusion

It is shown that even the simplest transient motion of the body from a certain state of rest to an equilibrium position is accompanied by slipping of one or both supports, depending on the value of the friction coefficient. With friction equal to the applied lateral force, at which the body on rigid supports would not budge, the centre of mass of the system gains a nonzero velocity.

References

- [1] DOSAEV M, SAMSONOV V, KLIMINA L, LOKSHIN B, HWANG SS, SELUYTSKIY Y: Braking of a solid body supported by two supports on a horizontal rough plane. In: Venture G., Solis J., Takeda Y., Konno A. (eds) ROMANSY 23 - Robot Design, Dynamics and Control. ROMANSY 2020. CISM International Centre for Mechanical Sciences (Courses and Lectures) 2021, 601. https://doi.org/10.1007/978-3-030-58380-4_53
- [2] NEIMARK Y, FUFAYEV N: The Painlevé paradoxes and the dynamics of a brake shoe. *J. Appl. Math. Mech.* 1995, **59** (3):343-352.
- [3] ZHURAVLEV V: The “paradox” of a brake pad. *Dokl. Phys.* 2017, **62**: 271–272. <https://doi.org/10.1134/S1028335817050123>.

Wind powered plantigrade machine moving against a flow

MIKHAIL GARBUZ, LIUBOV KLIMINA*, VITALY SAMSONOV

Institute of Mechanics, Lomonosov Moscow State University, Moscow, Russia

Abstract: Dynamics of the Chebyshev plantigrade machine on a rough horizontal plane is studied. The machine has four legs each of which is represented by a so-called λ -mechanism. A wind turbine is installed on the machine. The turbine transmits energy of the upcoming wind flow into the energy of walking motion of the mechanism. The shaft of the wind turbine is connected with the crank of λ -mechanisms by a reduction gear. The system has no any other drive unit except the wind turbine. The machine aims to move against the wind flow using only the energy of the wind. Aerodynamics of the wind turbine is described using a quasi-steady approach. The mathematical model of the mechanism is constructed in the form of second order dynamical system. Attracting periodic solutions of this system are described which correspond to regimes of self-sustained up-wind motion of the machine. Thus, the possibility of the wind powered walking motion in the up-wind direction is shown.

Keywords: Chebyshev plantigrade machine, wind turbine, self-sustained motion, stability.

1. Introduction

The Chebyshev machine with four λ -mechanism-legs became the first plantigrade machine in the world. Now this machine and its modifications are widely used in design of walking robots [1, 2].

Theo Jansen invented a wind powered walking mechanism based on another kinematic scheme. It is also important for robotic applications [3, 4]. Jansen's wind powered machine is intended for the down-wind motion; some modifications can move in the direction orthogonal to the wind.

Here, we introduce a wind powered walking mechanism designed for the up-wind motion. It is the Chebyshev plantigrade machine supplemented with a wind turbine. Such modification is inspired by Jansen's creations and by wind powered wheeled cars performing the up-wind motion, e.g. [5-7].

2. Description of the mechanical system and the main result

A modification of the Chebyshev plantigrade machine is suggested. Its scheme is represented in Fig. 1. The device is located on a rough horizontal plane and is equipped with a wind turbine. The shaft of the turbine is connected with the crank of the machine by a reduction gear. The machine is located in a steady wind flow and can move along the wind. The up-wind motion is the desired one.

It is supposed that all four shins of the mechanism always keep vertical orientation. Under this assumption, the mechanical system has one degree of freedom. The angle φ of rotation of the crank of λ -mechanisms is chosen as a generalized coordinate. Positive angular speed ω of the crank corresponds to up-wind motion of the machine. Vertical displacements of the body are neglected. Kinetic and potential energy of the system are described by the functions $K(\varphi, \omega)$ and $P(\varphi)$ (which are too cumbersome to present here). Equations of motion of the system are derived using the Lagrange formalism:

* 119192, Russia, Moscow, Michurinskiy prosp., 1; e-mail: klimina@imec.msu.ru

$$\frac{d}{dt} \left(\frac{\partial K(\varphi, \omega)}{\partial \omega} \right) - \frac{\partial K(\varphi, \omega)}{\partial \varphi} + \frac{\partial P(\varphi)}{\partial \varphi} = nT(\varphi, \omega) - f(\varphi)(D(\varphi, \omega) + c(f(\varphi)\omega + V)),$$

$$T(\varphi, \omega) = 0.5\rho S r (f(\varphi)\omega + V)^2 C_T(z), \quad D(\varphi, \omega) = 0.5\rho S (f(\varphi)\omega + V)^2 C_D(z), \quad z = (f(\varphi)\omega + V)^{-1} nr\omega.$$

Here $f(\varphi)\omega$ is the linear speed of the body of the machine, z is the tip speed ratio of the wind turbine, V is the wind speed, ρ is the air density, S and r are the characteristic area and radius of the turbine, n is the gear ratio, c is the coefficient of the drag force acting upon the body of the machine, $C_T(z)$ and $C_D(z)$ are coefficient of aerodynamic torque and drag force acting upon the turbine (they are approximated using experimental data [8], see Fig. 1).

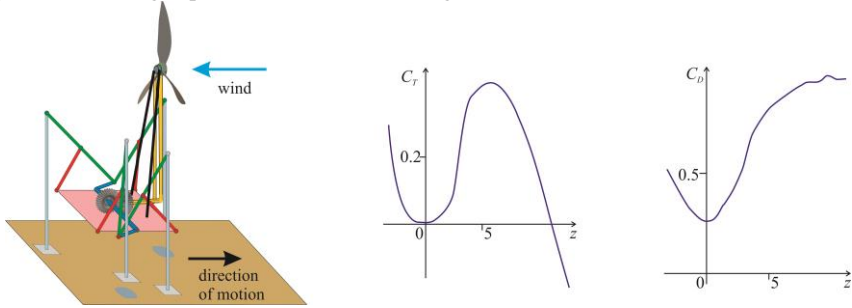


Fig. 1. The scheme of the mechanism. Aerodynamic coefficients.

It was shown numerically that for a wide range of parameters system has an attracting periodic solution with positive ω (reduction coefficient should be larger than a certain limit). Thus, the regime of up-wind walking exists. Parametrical analysis was performed to maximize the speed of the motion. The average speed of the up-wind motion can reach 20% of the wind speed. It is lower than that for a wind powered wheeled cars, but walking motion has advantages in certain areas in applications.

3. Conclusion

The wind powered walking mechanism is suggested that can move up-wind using only the energy of the wind. The average speed of the up-wind motion can be about 20% of the wind speed.

References

- [1] OTTAVIANO E, GRANDE S, CECCARELLI M: A biped walking mechanism for a rickshaw robot. *Mechanics based design of structures and machines* 2010, **38**(2):227-242.
- [2] PAVLOVSKY V: For elaboration of walking machines. *Keldysh Institute Preprints* 2013, **101**:1-32.
- [3] GIESBRECHT D, WU CQ, SEPEHRI N: Design and optimization of an eight-bar legged walking mechanism imitating a kinetic sculpture, "wind beast". *Transactions of the Canadian Society for Mechanical Engineering* 2012, **36**(4):343-355.
- [4] NANSAI S, ELARA MR, IWASE M: Dynamic analysis and modeling of Jansen mechanism. *Procedia Engineering* 2013, **64**:1562-1571.
- [5] BAUER A: Faster than the Wind. In: *First AIAA Symposium on Sailing*. Marina del Rey, California 1969.
- [6] KLIMINA L, DOSAEV M, SELYUTSKIY YU: Asymptotic analysis of the mathematical model of a wind-powered vehicle. *Applied Mathematical Modelling* 2017, **46**:691-697.
- [7] SELYUTSKIY Y, KLIMINA L, MASTEROVA A, HWANG SS, LIN CH: Savonius rotor as a part of complex systems. *Journal of Sound and Vibration* 2019, **442**:1-10.
- [8] ADARAMOLA M, KROGSTAD P: Experimental investigation of wake effects on wind turbine performance. *Renewable Energy* 2011, **36**(8):2078-2086.

Underwater capsobot controlled by motion of a single internal flywheel

SERGEY GOLOVANOV, LIUBOV KLIMINA*, MARAT DOSAEV, YURY SELYUTSKIY

Institute of Mechanics, Lomonosov Moscow State University, Moscow, Russia

Abstract: An underwater capsobot with a single internal flywheel is studied. The robot performs plane-parallel motion. Thus, the system has four degrees of freedom and one control input. The mathematical model is constructed in the form of 5-order dynamical system. For this purpose, quasi-steady model of interaction with the fluid is applied. This model allows not only effective parametrical analysis, but also revealing features of motion associated with presence of lateral component of hydrodynamic force. Control strategy is constructed; parameters of the control law are adjusted. It is shown that the lateral force provides possibility of irreversible motion of the centre of mass in the desired direction. So, it is promising to design underwater capsule robots and control algorithms for them basing on exploitation of lateral force. Results of modelling are verified by experiments with a prototype of the capsobot. Qualitative agreement between model and experiments is confirmed.

Keywords: underwater robot, internal mass motion, quasi-steady model, underactuated system.

1. Introduction

Investigation of capsule water robots is one of the topical problems of the modern science. The detailed review can be found in [1]. Among classical results in this field, there are such works as [2-4]. Among the most recent results, there are e.g. [1, 5-8]. The corresponding mathematical models involve Kirchhoff equations, Navier-Stokes equations, added masses, vortexes and CFD simulation. However, there are only few examples where lateral force is intended for the propulsion e.g. [7, 8].

Plane-parallel motion is, in most cases, organized using two control inputs. Rear examples of plane-parallel motion with a single control input are given in [7, 8]. In [7], the robot has a shape of an airfoil and is controlled via an internal flywheel. Here, we study the scheme of the robot similar to [7], but the mathematical model is totally different, and the control law is essentially modified.

2. Description of the mechanical system and the control law

A rigid capsule with an inner flywheel can perform plane-parallel motion. The capsule has a shape of an airfoil (Fig. 1). A control torque is applied to a flywheel to organize a tacking-kind propulsion of the capsule. Hydrodynamic forces and torque acting on the capsule are described with a quasi-steady model using experimental data for NACA0015 airfoil. Added masses are taken into account. Equation of motion are derived in the form of dynamical system with the following variables: v_x , v_y – components of velocity of the centre of mass of the robot, φ , ω – angle and angular speed of the capsule, w – relative angular speed of the flywheel.

In the desired motion, v_x should be always positive periodic function, v_y , φ , ω and w should be periodic functions with zero mean.

* 119192, Russia, Moscow, Michurinskiy prosp., 1; e-mail: klimina@imec.msu.ru

Two strategies of control were tested: 1) “mixed” control including parametric excitation and feedback: $U = a\sin(bt) + k\varphi + c\omega$, 2) purely feedback control: $U = -a\text{signum}(\omega) + k\varphi + c\omega$. Here U is value of the control torque applied to the flywheel, a, k, c are positive parameters. The second approach to the control is inspired by problems of pumping of oscillations [9].

3. Main results

Numerical integration of the system with varied parameters and initial conditions was performed. It was shown that the both control strategies bring the system to the desired regime. The second strategy (pure feedback) provides faster increasing of the speed v_x and seems to be more energy effective.

Different stages of the desired periodic motion are qualitatively shown in Fig. 1: the velocity \mathbf{V} of the centre of mass and lateral force \mathbf{L} are shown qualitatively (drag force and torque are not depicted).

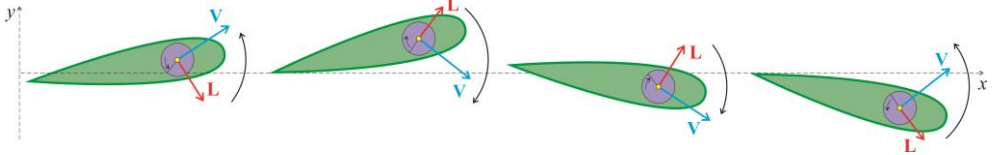


Fig. 1. The role of lateral force in robot propulsion (qualitative scheme; drag force and torque are not shown)

The essential conclusion obtained by means of a quasi-steady model is that the lateral force supports propulsion of the robot along the x axis. Moreover, the model allows parametrical analysis of the system. Parameters were adjusted numerically; and prototype of the capsuobot was constructed and tested. Its motions qualitatively agree with the modelling.

4. Conclusion

The mathematical model of the capsule underwater robot with a single control input is developed in the form of dynamical system. Control laws were constructed that ensure transition of the system to the program motion. In this motion, robot performs irreversible propulsion in the desired direction. The crucial role in supporting of this motion belongs to the lateral hydrodynamic force.

References

- [1] KILIN A, KLENOV A, TENENEV V: Controlling the movement of the body using internal masses in a viscous liquid. *Computer research and modeling* 2018, **10**(4):445-460.
- [2] KOZLOV V, RAMODANOV S: The Motion of a Variable Body in an Ideal Fluid. *Prikl. Mat. Mekh.* 2001, **65**(4):592–601 (in Russian).
- [3] CHERNOUS'KO F: The optimal periodic motions of a two-mass system in a resistant medium. *J. of Applied Mathematics and Mechanics* 2008, **72**(2):116-125.
- [4] CHILDRESS S, SPAGNOLIE S, TOKIEDA T: A bug on a raft: recoil locomotion in a viscous fluid. *J. of fluid mechanics* 2011. **669**:527-556.
- [5] GUO J, BAO Z, FU Q, GUO S: Design and implementation of a novel wireless modular capsule robotic system in pipe. *Medical & Biological Engineering & Computing* 2020, **58**(10):2305-2324.
- [6] KNYAZ'KOV D, FIGURINA T: On the existence, uniqueness, and stability of periodic modes of motion of a locomotion system with a mobile internal mass. *J. of Comp. and Syst. Science Intern.* 2020, **59**(1):129-137.
- [7] POLLARD B, TALLAPRAGADA P: An aquatic robot propelled by an internal rotor. *IEEE/ASME Transactions on Mechatronics* 2016, **22**(2): 931-939.
- [8] KELLY S, HUKKERI R: Mechanics, dynamics, and control of a single-input aquatic vehicle with variable coefficient of lift. *IEEE transactions on robotics* 2006, **22**(6):1254-1264.
- [9] KLIMINA L, FORMALSKII A: Three-Link Mechanism as a Model of a Person on a Swing. *Journal of Computer and Systems Sciences International* 2020, **59**(5):728-744.

Study on the Property of Microcellular Injection Molded HDPE/Wheat Straw Composites

SHYH-SHIN HWANG^{1*}, HAI-MEI LI², XING-YUAN CHEN²

1. Chien-hsin University of Science and Technology, Taiwan
2. School of Materials Science and Engineering, Zhengzhou University, Henan, China

Abstract: This study investigated the effect of wheat straw loading and wheat straw sizes on the property of the microcellular injection molded HDPE/wheat straw composites. Experimental results showed that the tensile strength of foamed materials will be improved with the increase of wheat straw percentage and the decrease of wheat straw size.

Keywords: Wheat straw, HDPE, composites, microcellular injection

1. Introduction

In order to reduce the waste by human being, recycled materials are considered to save energy. Hence, wood plastic composites (WPC) reinforced polymer with natural fiber such as wood, wheat straw and sunflower stalk have become popular due to not only their environmentally friendly and renewable [1], but also there are superior to neat plastics in terms of material costs [2]. In this study, effects of wheat straw loading and wheat straw size on the properties of microcellular injection molded composites are studied. The experimental setup is as shown in Figure 1. Wheat straw loading is from 0, 5, and 10 wt% and wheat straw sizes is from 40-60, 60-80, and >80 mesh.

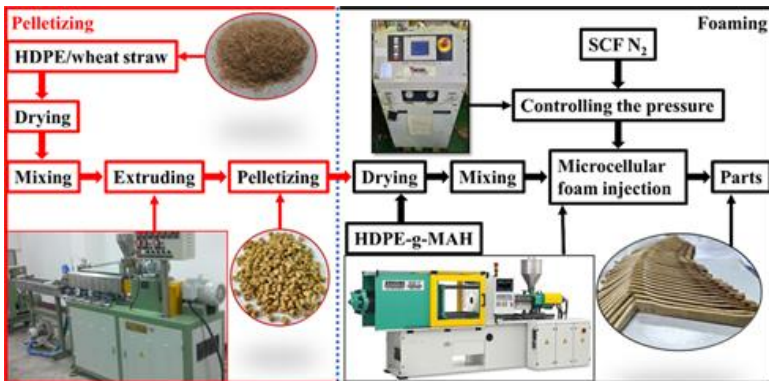


Fig. 1. The flow chart of microcellular injection molding process.

2. Results and Discussion

Figure 2a and 2b show the tensile strength comparisons of different wheat straw loading and straw sizes respectively. The increase of wheat straw content and the decrease of wheat straw size increases the tensile strength. The tensile strength of foamed parts with 0, 5, and 10 wt% wheat straw is 13.86,

14.99, and 15.85 MPa, respectively. The tensile strength of foamed parts for the size of wheat straw 40-60, 60-80, and >80 mesh is 13.86, 14.99, and 15.85 MPa, respectively. The tensile strength of foamed composites with 10 wt% wheat straw increases by 14.36% compared to that of neat PP. The tensile strength of foamed composites with >80 mesh wheat straw increases by 7.40% compared to that with 40-60 mesh wheat straw. As a wood fiber, wheat straw has high strength and rigidity, and the low content of wheat straw can be evenly dispersed in the matrix material grafted with maleic anhydride.

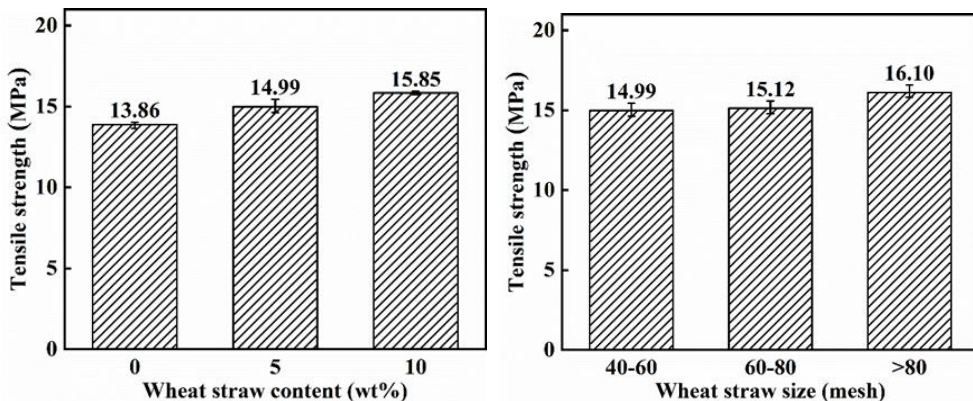


Figure 2 Tensile strength of (a) different wheat straw contents and (b) different wheat straw sizes.

3. Concluding Remarks

In this study, foamed HDPE/wheat straw composites samples were prepared by foaming injection molding and the effects of wheat straw content and wheat straw size on the mechanical properties of the foamed HDPE/wheat straw composites were investigated. It was observed that the increase of wheat straw content and the decrease of wheat straw size results in an increase in tensile strength of foamed HDPE/wheat straw composites.

Acknowledgment: Financial support from MOST 108-2221-E-231-003 is appreciated.

References

- [1] M-Z PAN, C-T MEI, X-B ZHOU, EFFECTS OF RICE STRAW FIBER MORPHOLOGY AND CONTENT ON THE MECHANICAL AND THERMAL PROPERTIES OF RICE STRAW FIBER-HIGH DENSITY POLYETHYLENE COMPOSITES, *J. OF POLYMER SCIENCE*, 2011, **121**(5):2900-2907.
- [2] ZHANG S, RODRIGUE D, RIEDL B. PREPARATION AND MORPHOLOGY OF POLYPROPYLENE/WOOD FLOUR COMPOSITE FOAMS VIA EXTRUSION, *POLYMER COMPOSITES*, 2005, **26**(6):731-738.

Dynamics of a low-inertia ball located between two rotating planes with viscous friction

ALEXANDER KOSHELEV, EUGENE KUGUSHEV, TATIANA SHAHOVA*

Faculty of Mechanics and Mathematics, Lomonosov Moscow State University, Moscow, Russia

Abstract: The problem of the motion of a low-inertia ball between two horizontal uniformly rotating planes with linear viscous friction is considered. The center of mass of the ball coincides with its geometric center, the central inertia tensor of the ball is spherical. Two cases of low inertia of the ball are investigated: in the first case the mass of the ball is constant and concentrated near its center, in the second case the mass of the ball is small. The dynamics of the ball on an arbitrary finite time interval in the limit as the central moment of inertia of the ball tends to zero is studied. In both cases the equations of motion of the ball have the form of the Tikhonov's type equations with a small parameter in the left-hand side. In the first case it is shown that in the limit the center of mass of the ball moves as a material point located between horizontal rotating planes with linear viscous friction. In the second case the dynamics of the ball in the limit coincides with the dynamics of a homogeneous ball moving between two absolutely rough rotating planes.

Keywords: low-inertia ball, viscous friction, small parameter, Tikhonov's theorem.

1. Introduction

Non-ideality of hinges can significantly affects on dynamics of mechanical systems containing hinges. One of the reasons for the violation of the ideality of the hinge is the presence of small alien bodies between the working surfaces of the hinge. The problem of the migration of such alien bodies with relative movements of the working surfaces of the hinge is interesting. In the simplest case the dynamics of a ball constrained by two parallel rotating planes with linear viscous friction is re-searched. The dynamics of a ball along a rotating plane with linear viscous friction was studied in [1].

2. Description of the mechanical system and main result

Suppose a ball of mass m and radius a moves between two horizontal planes. Each plane rotates with the constant angular velocity of value Ω_i around some fixed vertical axis. The force of linear viscous friction $\mathbf{F}_i = -c_i \mathbf{u}_i$ acts on the point of contact of the ball with the plane, where c_i is the coefficient of viscous friction, \mathbf{u}_i is the velocity (i of the contact point relative to the rotating plane ($i = 1, 2$)). The distance between the axes of rotation of the planes is equal to $2l$. The center of mass of the ball coincides with its geometric center, the central inertia tensor of the ball is spherical, the principal central moment of inertia of the ball is equal to I . Let us research the motion of the ball as I tends to zero.

Let us introduce a fixed coordinate system $Oxyz$ so that Oxy is the plane of motion of the ball center, Oz axis is vertical, Oy axis crosses the rotation axes of the planes and the point O is equidistant from these axes. The equations of motion of the ball have the form

* 119991, Russia, Moscow, GSP-1, Leninskie Gory 1, Main Building; e-mail: t.shahova@yandex.ru

$$\frac{d\mathbf{r}}{dt} = \mathbf{v}, \quad m \frac{d\mathbf{v}}{dt} = -\alpha\mathbf{v} + [\mathbf{e}_z, -\beta a\boldsymbol{\omega}_{\parallel} + \gamma\mathbf{r} + \delta\mathbf{l}], \quad I \frac{d\boldsymbol{\omega}_{\parallel}}{dt} = \beta a[\mathbf{e}_z, \mathbf{v}] - \alpha a^2 \boldsymbol{\omega}_{\parallel} + \delta a\mathbf{r} + \gamma a\mathbf{l}, \quad \frac{d\omega_z}{dt} = 0. \quad (1)$$

Here \mathbf{r} , \mathbf{v} are the radius vector and the velocity of the center of mass of the ball, $\boldsymbol{\omega} = \boldsymbol{\omega}_{\parallel} + \omega_z \mathbf{e}_z$ is the angular velocity of the ball, $\mathbf{l} = l\mathbf{e}_y$, $\alpha = c_1 + c_2$, $\beta = c_1 - c_2$, $\gamma = c_1\Omega_1 + c_2\Omega_2$, $\delta = c_1\Omega_1 - c_2\Omega_2$.

Let the mass of the ball be constant and concentrated near its center. Then $I = mr^2$, where $r = \sqrt{\varepsilon}a$ ($0 < \varepsilon \ll 1$) is the radius of inertia of the ball relative to an arbitrary axis passing through the center of mass of the ball. In this case the third group of equations (1) has small parameter ε in the left side. Using Tikhonov's theorem [2] the statement is proved.

Statement 1. Let $\mathbf{r}(t, \varepsilon)$, $\mathbf{v}(t, \varepsilon)$, $\boldsymbol{\omega}(t, \varepsilon)$ be the solution of equations (1) with initial conditions $\mathbf{r}(0) = \mathbf{r}_0$, $\mathbf{v}(0) = \mathbf{v}_0$, $\boldsymbol{\omega}(0) = \boldsymbol{\omega}_0$ on some finite time interval $t \in [0, T]$ for any $\varepsilon \in (0, \varepsilon_0]$. Then as $\varepsilon \rightarrow 0$ the functions $\mathbf{r}(t, \varepsilon)$, $\mathbf{v}(t, \varepsilon)$ converge on the interval $t \in [0, T]$ to the solution $\mathbf{r}^*(t)$, $\mathbf{v}^*(t)$ of

$$\frac{d\mathbf{r}}{dt} = \mathbf{v}, \quad m \frac{d\mathbf{v}}{dt} = \frac{2c_1c_2}{c_1 + c_2} (-2\mathbf{v} + [\mathbf{e}_z, (\Omega_1 + \Omega_2)\mathbf{r} + (\Omega_1 - \Omega_2)\mathbf{l}]) \quad (2)$$

with the initial conditions $\mathbf{r}^*(0) = \mathbf{r}_0$, $\mathbf{v}^*(0) = \mathbf{v}_0$ and the function $\boldsymbol{\omega}(t, \varepsilon)$ converges on the interval $t \in (0, T]$ to the function

$$\boldsymbol{\omega}^*(t) = \frac{1}{(c_1 + c_2)a} ((c_1 - c_2)[\mathbf{e}_z, \mathbf{v}^*(t)] + (c_1\Omega_1 - c_2\Omega_2)\mathbf{r}^*(t) + (c_1\Omega_1 + c_2\Omega_2)\mathbf{l}) + (\boldsymbol{\omega}_0, \mathbf{e}_z)\mathbf{e}_z.$$

Equations (2) have the form of equations of motion of a material point located between two horizontal uniformly rotating planes with linear viscous friction.

Let the mass of the ball be small. Then $I = m\varepsilon M$ ($0 < \varepsilon \ll 1$), M is the characteristic mass. The second and third groups of equations (1) have small parameter ε in the left side.

Statement 2. Let $\mathbf{r}(t, \varepsilon)$, $\mathbf{v}(t, \varepsilon)$, $\boldsymbol{\omega}(t, \varepsilon)$ be the solution of equations (1) with initial conditions $\mathbf{r}(0) = \mathbf{r}_0$, $\mathbf{v}(0) = \mathbf{v}_0$, $\boldsymbol{\omega}(0) = \boldsymbol{\omega}_0$ on some finite time interval $t \in [0, T]$ for any $\varepsilon \in (0, \varepsilon_0]$. Then as $\varepsilon \rightarrow 0$ the function $\mathbf{r}(t, \varepsilon)$ converges on the interval $t \in [0, T]$ to the solution $\mathbf{r}^*(t)$ of the equation

$$\frac{d\mathbf{r}}{dt} = \frac{1}{2} [\mathbf{e}_z, (\Omega_1 + \Omega_2)\mathbf{r} + (\Omega_1 - \Omega_2)\mathbf{l}] \quad \text{with the initial conditions } \mathbf{r}^*(0) = \mathbf{r}_0 \quad \text{and the functions}$$

$\mathbf{v}(t, \varepsilon)$, $\boldsymbol{\omega}(t, \varepsilon)$ converge on the interval $t \in (0, T]$ to the functions

$$\mathbf{v}^*(t) = \frac{1}{2} [\mathbf{e}_z, (\Omega_1 + \Omega_2)\mathbf{r}^*(t) + (\Omega_1 - \Omega_2)\mathbf{l}], \quad \boldsymbol{\omega}^*(t) = \frac{1}{2a} ((\Omega_1 - \Omega_2)\mathbf{r}^*(t) + (\Omega_1 + \Omega_2)\mathbf{l}) + (\boldsymbol{\omega}_0, \mathbf{e}_z)\mathbf{e}_z.$$

In this case the motion of the ball in the limit coincides with the motion of a homogeneous ball located between two absolutely rough rotating planes.

3. Conclusion

The dynamics of a ball moving between two rotating planes with linear viscous friction on some finite time interval in the limit as the central moment of inertia of the ball tends to zero has been researched.

References

- [1] IVANOVA T: The Rolling of a Homogeneous Ball with Slipping on a Horizontal Rotating Plane. *Russian Journal of Nonlinear Dynamics* 2019, **15**(2):171-178.
- [2] TIKHONOV A: Systems of differential equations containing small parameters in the derivatives. *Matematicheskii Sbornik* 1952, **31**(3):575-586.

Periodic motions in systems with viscous friction

EUGENE KUGUSHEV, MARGARITA SELEZNEVA, TATIANA SHAHOVA *

Faculty of Mechanics and Mathematics, Lomonosov Moscow State University, Moscow, Russia

Abstract: An autonomous dissipative system with one degree of freedom in the presence of a small parameter is considered. It is proved that for sufficiently small values of the parameter in such a system there is a unique limit cycle, it is stable, its period smoothly depends on the small parameter. We apply this theory to several certain systems. The problem of motion of a rigid body (tripod or monopod) freely rotating around a fixed vertical axis and leaning on a horizontal plane with isotropic or anisotropic linear viscous friction uniformly rotating around a fixed vertical axis is considered. If the distance between the axes of rotation of the supporting plane and the rigid body is small enough, then the rigid body asymptotically goes into the unique periodic mode of motion. For both models of friction the dependence of the period of the limit cycle on the small distance between the axes of rotation of the plane and the rigid body is explored analytically. An approximate formula connecting this period and the coefficients of friction in the isotropic and anisotropic cases is found. Numerical simulation of the researched systems is carried out and it is shown that the analytically found dependence for the period can be used to determine the parameters of the viscous friction models.

Keywords: dissipative system, small parameter, stable limit cycle, viscous friction.

1. Introduction

An important problem in the research of systems with friction is to develop methods for determining the parameters of the friction model. The analysis of the special modes of motion of systems with friction can give information about the parameters of the friction model. Such an approach in combination with experimental methods is considered in [1]. We also note the paper [2], in this one the coefficients of dry and viscous friction in the pendulum joint are determined by its oscillation amplitude. In this paper systems with viscous friction in which stable limit cycles occur are considered. The period of the limit cycle depends on the parameters of the system, in particular on the coefficients of viscous friction. Such systems are generalized to a wider class of autonomous systems with one degree of freedom and a small parameter, where the function that defines the right-hand side of the equation has some restrictions.

2. Description of the mechanical system and main result

Let us consider a mechanical system with one degree of freedom, the equation of motion of which has the form

$$\ddot{\varphi} = F(\varphi, \dot{\varphi}, \varepsilon), \quad F(\varphi, \omega, 0) = 0, \quad \left. \frac{\partial F}{\partial \dot{\varphi}} \right|_{\dot{\varphi}=\omega, \varepsilon=0} < 0. \quad (1)$$

* 119991, Russia, Moscow, GSP-1, Leninskie Gory 1, Main Building; e-mail: t.shahova@yandex.ru

Here $F(\varphi, \dot{\varphi}, \varepsilon)$ is a smooth (minimum class C^4) function, periodic in the variable φ , ε is small parameter, $\omega > 0$. Using the Taylor series expansion of the function $F(\varphi, \dot{\varphi}, \varepsilon)$ with respect to the variables $\dot{\varphi}$ and ε at the point $\dot{\varphi} = \omega, \varepsilon = 0$, we write equation (1) in the form of the system

$$\dot{\varphi} = z, \quad \dot{z} = -h(\varphi, z)(z - \omega) + \varepsilon f(\varphi, z, \varepsilon). \quad (2)$$

Due to the periodicity in φ the phase space of this system is a cylinder. The function $f(\varphi, z, \varepsilon)$ is bounded in a certain band $[0, 2\pi] \times [\omega - \delta, \omega + \delta]$ ($\delta > 0$) on the phase cylinder and for small ε , and $h(\varphi, z) > c > 0$ in this band. In mechanical systems the term of the form $-h(\varphi, z)z$ occurs in the presence of viscous friction. Using the Brauer's theorem [3] and the Dulac criterion [4, 5], the following statement is proved.

Statement. For sufficiently small ε in the band $[0, 2\pi] \times [\omega - \delta, \omega + \delta]$ on the phase cylinder, where $0 < \delta < \omega$, system (2) has the unique limit cycle, moreover, it is stable and covers the cylinder. The period of this limit cycle is a smooth function of ε .

An example of a mechanical system whose equation of motion has the form (2) is a rigid body (tripod or monopod) that rotates freely around a fixed vertical axis and leans on a uniformly rotating around a fixed vertical axis horizontal plane with isotropic or anisotropic linear viscous friction. In the case of isotropic viscous friction the force $\mathbf{F} = -c\mathbf{v}$ acts on each support point of a rigid body, where c is the coefficient of viscous friction, \mathbf{v} is the speed of the support point relative to the rotating plane. In the case of anisotropic viscous friction the force $\mathbf{F} = -c_1 v^{(1)} \mathbf{e}^{(1)} - c_2 v^{(2)} \mathbf{e}^{(2)}$ acts on each support point, where c_1, c_2 are the coefficients of viscous friction, $\mathbf{e}^{(1)}, \mathbf{e}^{(2)}$ are the unit orthogonal vectors that are fixed relative to the rigid body (the support point of the Chaplygin's skate type) or relative to the rotating plane (there are "furrows" on the plane), $v^{(1)} = \langle \mathbf{v}, \mathbf{e}^{(1)} \rangle, v^{(2)} = \langle \mathbf{v}, \mathbf{e}^{(2)} \rangle$. For sufficiently small distance (small parameter) between the axes of rotation of the supporting plane and the rigid body the system has the unique limit cycle, and this cycle is stable. The dependence of the period of this limit cycle on the distance between the axes of rotation of the plane and the rigid body is sought in the form of a series with respect to small parameter. An approximate formula connecting this period and the coefficients of friction in the isotropic and anisotropic cases is found. Numerical simulation of the researched systems is carried out. It is shown that the analytically found dependence for the period can be used to determine the parameters of the viscous friction models.

3. Conclusion

The existence of the stable limit cycle for the systems with energy inflow and dissipation and small parameter has been proved. The possibility of determining the parameters of the viscous friction model on the dependence of period of the limit cycle on small parameter has been shown.

References

- [1] BORISOV A, KARAVAEV Y, MAMAEV I, ERDAKOVA N, IVANOVA T, TARASOV V: Experimental Investigation of the Motion of a Body with an Axisymmetric Base Sliding on a Rough Plane. *Regular and Chaotic Dynamics* 2015, **20**(5):518-541.
- [2] VASIUKOVA O, KLIMINA L: Modelling of self-oscillations of a controlled pendulum with respect to a friction torque depending on a normal reaction in a joint. *Rus. J. of Nonlinear Dynamics* 2018, **14**(1):33-44.
- [3] ZORICH V: *Mathematical Analysis II*. Springer: Berlin, Heidelberg, 2016.
- [4] ANDRONOV A, WITT A, KHAIKIN S: *Theory of oscillations*. Nauka: Moscow, 1981.
- [5] BAUTIN N, LEONTOVICH E: *Methods and techniques of the qualitative study of dynamical systems on the plane*. Nauka: Moscow, 1990.

Optimized spacing design for paired counter-rotating Savonius rotors

CHING-HUEI LIN^{1*}, JEN-HUNG LO¹, MARAT DOSAEV², AND YURY SELYUTSKIY²

1. Department of Electrical Engineering, Chien Hsin University of Science and Technology, Taoyuan City, Taiwan

2. Institute of Mechanics, Lomonosov Moscow State University, Moscow, Russia

* Presenting Author

Abstract: Two-dimensional CFD models with paired counter-rotating Savonius rotors are applied to investigate how the power coefficient can be promoted. Results show that such configuration can improve the power efficiency up to about 50% in average as the rotor spacing ratio is about 0.6.

Keywords: Paired Savonius rotors, Computation Fluid Dynamics (CFD), Output power curve, spacing of rotors

1. Introduction

Many of large size horizontal axis wind turbines (HAWTs) can obtain the power coefficient up to 0.5. But such kind of HAWTs are not able to be applied to community, factory, hospital, or remote residence. The other type wind turbines, vertical axis wind turbines (VAWTs), may be more suitable for the above regions since they have some advantages such as lower noise, lower maintenance cost.

Some studies [1~4] had adopted methods with counter-rotating arrangement to promote the power coefficient of Darrieus wind turbines, one of VAWTs. In this study, a similar arrangement was applied to Savonius turbines, also one of VAWTs. We construct two-dimensional models of paired counter-rotating Savonius rotors with different spacing lengths. Each rotor is constructed with two semi-circle blades with height 200cm, diameter 50cm and blades overlap 7.5cm. The output power curve of paired rotors with different rotating speed are simulated using computational fluid dynamics (CFD) method for wind speeds with 15m/s, 11m/s and 7m/s.

2. Results and Discussion

Fig. 1 is the power coefficient (C_p) variation with tip speed ratio (TSR) for paired counter-rotating Savonius rotors with wind speed 15m/s. The lowest line is the output of two stand-alone Savonius rotors for comparing. It shows that the TSR of maximum C_p increase to about 1.08 from 0.95 and maximum C_p reaches to 0.31 from 0.21. To check how much enhancement of C_p under different wind speed, we compared the ratio of maximum power of paired rotors with two stand-alone rotors with different spacing length under different wind speeds. The result, shown as Fig. 2, indicates the enhancement effect almost independent on the wind speeds. All three curves also show the enhancement approach to a saturation value about 1.5.

Cases for paired rotors with spacing ratio less than 0.5 may cause two-dimensional model results not inaccurate since the flow may turn to move along two top sides not be enforced to pass through the narrow channel. Further three-dimensional simulations or wind tunnel experiments are needed for such extreme cases study.

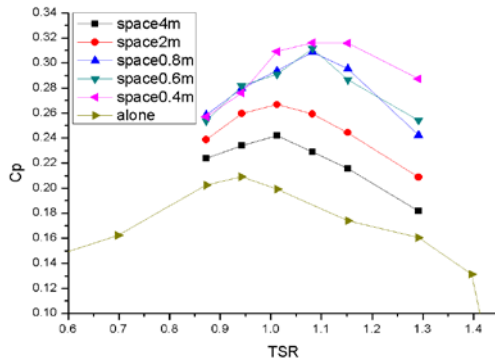


Fig. 1. The power coefficient (C_p) variation with tip speed ratio (TSR) for paired rotors with wind speed 15m/s.

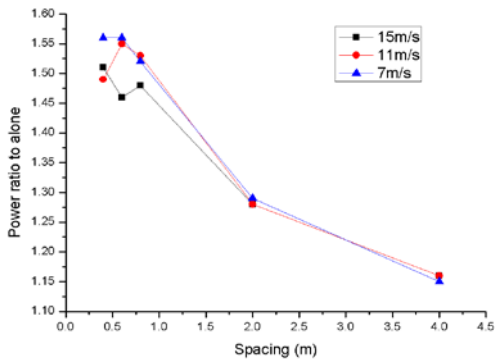


Fig. 2. The ratio of maximum power of paired rotors compared with two stand-alone rotors with different spacing length under different wind speeds.

3. Concluding Remarks

Simulation results show that the smaller spacing of paired rotors and the more output power. It confirmed that the configuration of paired counter-rotating Savonius rotors can improve the power efficiency up to about 50% in average. It also shows that the optimized rotor spacing ratio (a ratio of the spacing to the rotor diameter) is about 0.6.

References

- [1] Simone Giorgetti, Giulio Pellegrinia, and Stefania Zanforlinb, CFD investigation on the aerodynamic interferences between medium-solidity Darrieus Vertical Axis Wind Turbines, *Energy Procedia*, 81, 227 – 239, 2015.
- [2] P. Chaitanya Sai, Richa S. Yadav, R. Nihar Raj and G.R.K. Gupta, Design and Simulation of High Efficiency Counter-Rotating Vertical Axis Wind Turbine Arrays, *International Conference and Utility Exhibition 2014 on Green Energy for Sustainable Development (ICUE 2014)*, Thailand, 19-21 March 2014.
- [3] Jifeng Peng, Effects of Aerodynamic Interactions of Closely-Placed Vertical Axis Wind Turbine Pairs, *Energies*, 11, 2842; doi:10.3390/en1102842, 2018.
- [4] Shalimova Ekaterina, Klimina Liubov, Samsonov Vitaly, and Lin Ching-Huei, Small-scale counter-rotating Darrieus wind turbine, *ENOC 2017*, Budapest, Hungary, June 25 – 30, 2017.

Usage of the nonlinear method to control model of a half car suspension with a damper containing MR fluid,

STANISŁAW RADKOWSKI¹, MACIEJ SŁOMCZYNSKI^{2*}

1. Warsaw University of Technology, Faculty of Automotive and Construction Machinery Engineering, Poland [0000-0003-2083-0514]
 2. Warsaw University of Technology, Faculty of Automotive and Construction Machinery Engineering, Poland
- * Presenting Author

Abstract: The work focuses on the analysis of the suspension system control based on backstepping control method. The backstepping is type non-linear control method based on error control understood as the displacement of the body from the equilibrium position and stability, according to the Lyapunov method especially the second law of Lyapunov theories. Model presents a half of the car's suspension with nonlinear spring and a damper with magnetorheological fluid, by which modify the damping of the suspension - designed in Matlab - Simulink. The main problem is the consideration of the influence of the front axle of the vehicle on the rear axle and the stabilization of the body displacement along with the rotation angle in relation to the CG. In the context of these issues, backstepping control in the MIMO (Many Inputs Many Outputs) strict feedback form is used. Model was tested in various situations which should good describe effectiveness of this solution.

Keywords: Backstepping, Many inputs many outputs, feedback control, Lyapunov's second method for stability

References

- [1] BENAUMEUR, IBARI; LAREDJ, BENCHIKH; AMAR REDA, HANIŃ ELHACHIMI; ZOUBIR, AHMED-FOITH. BACKSTEPPING APPROACH FOR AUTONOMOUS MOBILE ROBOT TRAJECTORY TRACKING. IJEECS 2 3 (2016), PAGES 478-485.
- [2] CHEN, CAI-XUE; XIE, YUN-XIANG; LAN, YONG-HONG (2015): BACKSTEPPING CONTROL OF SPEED SENSORLESS PERMANENT MAGNET SYNCHRONOUS MOTOR BASED ON SLIDE MODEL OBSERVER, INT. J. AUTOM. COMPUT. 12 (2), PAGES 149-155.
- [3] FOSSEN, THOR I.; STRAND, JAN P., TUTORIAL ON NONLINEAR BACKSTEPPING. APPLICATIONS TO SHIP CONTROL., MIC 20 (2), (1999), PAGES 83-135.
- [4] HERBERT G. TANNER; KOSTAS J. KYRIAKOPOULOS, DISCONTINUOUS BACKSTEPPING FOR STABILIZATION OF NONHOLONOMIC MOBILE ROBOTS., IEEE (MAY 2002) PAGES 25-38
- [5] ROGER SKJETNE, THOR I. FOSSEN ON INTEGRAL CONTROL IN BACKSTEPPING: ANALYSIS OF DIFFERENT TECHNIQUES (JUNE 30 - JULY 2, 2004), PAGES 59-67
- [6] [HTTP://WWW.LORDMRSTORE.COM/LORD-MR-PRODUCTS/RD-8040-1-MR-DAMPER-SHORT-STROKE](http://www.lordmrstore.com/lord-mr-products/rd-8040-1-mr-damper-short-stroke).
- [7] MICHAŁ MAKOWSKI, WIESŁAW GRZESKIEWICZ, LECH KNAP, IDENTYFIKACJA PARAMETRÓW STEROWANYCH TŁUMIKÓW MR I PZ., ZESZYTY NAUKOWE INSTYTUTU POJAZDÓW 3(89)/2012. PAGES 33-45
- [8] DEVELOPMENT OF AN EXPERIMENTAL MODEL FOR A MAGNETORHEOLOGICAL DAMPER USING ARTIFICIAL NEURAL NETWORKS (LEVENBERG-MARQUARDT ALGORITHM), RAIZADA, AYUSH ; SINGRU, PRAVIN ; KRISHNAKUMAR, VISHNUVARDHAN ; RAJ, VARUN, ADVANCES IN ACOUSTICS AND VIBRATION, 2016

Dynamics of a 2 DoF galloping-based wind power harvester

YURY SELYUTSKIY^{1*}

1. Lomonosov Moscow State University, Institute of Mechanics [0000-0001-8477-6233]

* Presenting Author

Abstract: Galloping oscillations of bluff bodies are considered as a prospective source of energy for small wind power generating devices. We consider an electromechanical system composed of a rectangular cylinder elastically connected with a magnet that can move in a linear electric generator. The cylinder performs galloping in flow, and the resulting motion of the magnet gives rise to electric current in the circuit. Periodic regimes arising in the system are studied depending on parameters.

Keywords: oscillations, stability, galloping, wind power

1. Introduction

The imperative necessity to reduce the carbon emissions, in order to ensure sustainable development of the society requires active study of different ways of green energy generation. One of such ways, which seems quite applicable for small installations, is extraction of energy from flow induced oscillations, such as fluttering, galloping, etc. Some analysis of dynamics and performance of a galloping-based energy harvester is given in [1].

Energy of oscillations can be converted into electric energy by means of different systems: piezo-elements (which are widely studied in the context of aeroelastic systems, e.g., [2]) or linear generators (e.g., [3]). Here we discuss a 2 degrees of freedom galloping-based system coupled with a linear generator.

2. Results and Discussion

We consider an electromechanical system that comprises a magnet M_1 , a rectangular prism M_2 , and a linear generator G connected to electrical circuit (Fig. 1). The cylinder and the magnet are connected with a spring and can move translationally along a fixed horizontal axis. The system is placed in a steady horizontal airflow. We only take into account the aerodynamic forces acting upon the cylinder and use the quasi-steady approach to describe them.

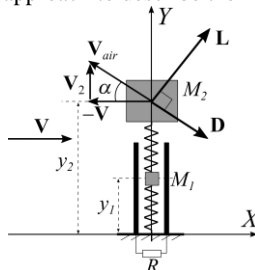


Fig. 1. Scheme of the system

In [4] it was shown that the elastically mounted cylinder (both circular and rectangular) elastically connected with a heavy mass (but without coupling to an electric circuit) performs galloping oscillations under certain conditions. In such situation, the magnet starts moving inside the generator, which induces electric current in the generator coil.

Equations of motion of the system can be represented in the following form:

$$\begin{aligned}
 m_1 \ddot{y}_1 + k_1 y_1 + h_1 \dot{y}_1 + k_2 (y_1 - y_2) + h_2 (\dot{y}_1 - \dot{y}_2) &= F_m \\
 m_2 \ddot{y}_2 + k_2 (y_2 - y_1) + h_2 (\dot{y}_2 - \dot{y}_1) &= L \cos \alpha - D \sin \alpha \\
 L_g \dot{I} &= -RI + E
 \end{aligned}
 \tag{1}$$

Here L , D are lift and drag forces, $k_{1,2}$ and $h_{1,2}$ are stiffness and damping coefficients of springs, E is the EMF (which is proportional to \dot{y}_1), F_m is the force acting upon the magnet from the coil assembly, L_g is the generator inductance, and R is the resistance in the generator circuit.

Evidently, the system has a trivial equilibrium. Analysis of its stability shows that it is unstable if certain conditions on parameters are met. A systematic parametrical analysis of periodic oscillations arising in the system in such case is performed. Characteristics of periodic regimes existing in the system (including the generated power) under different conditions are analysed. Some conclusions about performance of the harvester are drawn.

3. Concluding Remarks

Dynamics of an electromechanical system with two degrees of freedom is considered. Self-sustained oscillations arising in this system due to the galloping effect are studied. The performed simulation shows that this system has a potential for use as a wind power harvester.

References

- [1] DAI HL, ABDELKEFI A, JAVED U, WANG L: Modeling and performance of electromagnetic energy harvesting from galloping oscillations. *Smart Materials and Structures* 2015, **24**(4):045012.
- [2] WANG KF, WANG BL, GAO YJ, ZHOU JY: Nonlinear analysis of piezoelectric wind energy harvesters with different geometrical shapes. *Archives of Applied Mechanics* 2020, **90**:721-736.
- [3] JIN C, KANG HY, KIM MH, BAKTI FP: Performance evaluation of surface riding wave energy converter with linear electric generator. *Ocean Engineering* 2020, **218**:108141.
- [4] SELYUTSKIY Y: Potential forces and alternation of stability character in non-conservative systems. *Applied Mathematical Modelling* 2021, **90**:191-199.

Shock Torsion Wave in an Elastic Rod with Decreasing Function of Viscoplastic External Friction

IVAN SHATSKYI^{1*}, VASYL PEREPICHKA²

1. Department of modelling of damping systems, Ivano-Frankivsk Branch of Pidstryhach-Institute for Applied Problems in Mechanics and Mathematics of NAS of Ukraine, 3, Mykytynetska Str., 76002, Ivano-Frankivsk, Ukraine [0000-0003-0223-038X]
2. Department of modelling of damping systems, Ivano-Frankivsk Branch of Pidstryhach-Institute for Applied Problems in Mechanics and Mathematics of NAS of Ukraine, 3, Mykytynetska Str., 76002, Ivano-Frankivsk, Ukraine [0000-0003-1139-6349]

* Presenting Author

Abstract: The wave problem of propagation and deceleration of shock torsion perturbation in semi-infinite round elastic rod interacting with the medium is investigated using the model of viscoplastic friction with decreasing relation between shear stress and jump of velocity on the lateral surface. After linearization, an exact solution of the initial-boundary problem describing the effect of “negative viscosity” is obtained using the Laplace transforms. A wave pattern of perturbation including the prefront zone of rest, the area of motion and the domain of stationary residual stresses has been built. The three-dimensional diagrams for nonstationary fields of velocity and stresses have been constructed too.

Keywords: elastic rod, torsion wave, viscoplastic friction, negative viscosity

Transversal Straining of Pressurized Pipeline Caused by Vibration of Damaged Foundation

IVAN SHATSKYI^{1*}, MYKOLA MAKOVICHUK², MAKSYM VASKOVSKYI³

1. Department of modelling of damping systems, Ivano-Frankivsk Branch of Pidstryhach-Institute for Applied Problems in Mechanics and Mathematics of NAS of Ukraine, 3, Mykytynetska Str., 76002, Ivano-Frankivsk, Ukraine [0000-0003-0223-038X]
 2. Department of modelling of damping systems, Ivano-Frankivsk Branch of Pidstryhach-Institute for Applied Problems in Mechanics and Mathematics of NAS of Ukraine, 3, Mykytynetska Str., 76002, Ivano-Frankivsk, Ukraine [0000-0003-4202-1953]
 3. SC NSC Naftogaz of Ukraine, 6, Khmelnytskyi Str., 01601, Kyiv, Ukraine
- * Presenting Author

Abstract: A deformation model of buried pipeline under complicated geotechnical conditions of soil slit fracture is developed. The classical theory of rods on an elastic foundation and the membrane theory of shells are used. The influence of the contingency of cyclic discontinuities of transversal displacement in damaged foundation on the stressed state and limit equilibrium of pressurized pipe has been studied in quasi-static and dynamic statement with analytical methods. It is assumed that the frequency of kinematic perturbation does not exceed the cutoff frequency of the system.

Keywords: pipeline, damage foundation, transversal vibration, quasi-static and dynamic stresses

Brachistochrone Problem with Variable Mass,

SMIRNOVA NINA ¹, MALYKH EGOR ², CHERKASOV OLEG ^{3*}

1. Lomonosov Moscow State University, Moscow, Russia [0000-0002-6532-8037]

2. Lomonosov Moscow State University, Moscow, Russia [0000-0002-5081-0584]

3. Lomonosov Moscow State University, Moscow, Russia [0000-0003-1435-1541]

* Presenting Author

Abstract: The motion of a point mass in a vertical plane under the action of gravity forces, viscous friction, support reaction of the curve and the thrust is considered. The slope angle and the thrust are treated as control variables. The amount of the propellant is given. The aim is to maximize the horizontal coordinate of the particle. Time of the process is given. The interrelated Brachistochrone problem is also considered. For the case of frictionless motion, it is shown that optimal thrust control is bang-bang-type, and trajectory consists of two arcs, starting with maximum thrust, and ending with zero thrust. Optimal synthesis in the three dimensional space “mass-velocity-slope angle” is designed. For the case of linear viscous friction the arc with singular thrust includes in the extremal trajectory. It is shown that optimal thrust program consists of either two arcs, maximum thrust at the beginning and zero thrust at the end, or three arcs: maximum thrust at the beginning, then intermediate (singular) thrust and zero thrust at the end. The control logic of the thrust is similar to the Goddard problem. The results of numerical simulation for the case of linear viscous friction illustrating the theoretical conclusions are presented.

Keywords: singular arc, thrust control, brachistochrone problem, viscous friction

1. Introduction

The motion of a material point in a vertical plane in a homogeneous field of gravity and in a homogeneous, resisting medium is considered. The trajectory angle and thrust are considered as control variables. The goal of the control is to maximize the horizontal range for a given time. The amount of fuel is given. Along with the range maximization problem, we can consider a modified brachistochrone problem formulated as follows: find a curve connecting two points in the vertical plane along which a material point in the field of gravity and nonconservative force moves from the initial to the final point in the shortest time.

The classical theory of the calculus of variations and, later, the theory of optimal control were applied to the problem of maximizing the vertical altitude of a rocket with a given amount of fuel. Two special cases, namely, one with a linear dependence of the resistance on the velocity, and the other with a quadratic dependence on the velocity, were considered in [1]. In [2], the optimal flight in the vertical plane for an “intermediate” model of an aircraft was studied. The slope angle was taken as control variable. This model is suitable for studying the optimal motion of special types of aircraft, for which it is possible to change the lifting force without changing the drag force. For various modifications of the brachistochrone problem with viscous friction, the normal component of the reaction force of the curve also allows changing the angle of inclination of the trajectory without changing the resistance force [3]. The Results of numerical simulation for the case of an accelerating force propor-

tional to the velocity were presented in [3]. The Brachistochrone problem in the presence of a constant thrust force and a linear viscous friction force was studied in [4]. In [5], the problem of maximizing the horizontal range with a penalty on fuel consumption was considered, while it was assumed that the change in the amount of fuel does not affect the dynamics of the point movement.

In this paper, the problem of maximizing the range is considered taking into account the influence of the amount of fuel on the dynamics of the point mass.

2. Problem Formulation

Equations of motion are as follows:

$$\begin{cases} \dot{x} = v \cos \theta, \\ \dot{y} = v \sin \theta, \\ \dot{v} = \frac{-kv + cu}{m} - g \sin \theta, \\ \dot{m} = -u; \end{cases} \quad (1)$$

where x, y are horizontal and vertical coordinates of the particle correspondingly, v is the velocity modulus, m is mass of the particle, k is a coefficient of the viscous friction, c is exhaust velocity of the gas flow, g is gravitational acceleration, θ is the slope angle, u is mass change rate, θ and u are considered as control variables. Boundary conditions for the system (1) have the form:

$$x(0) = x_0, y(0) = y_0, v(0) = v_0, m(0) = m_0, m(T) = m_T. \quad (2)$$

T is given process time. The goal function is

$$J = -x(T) \rightarrow \min_{\theta, u} \quad (3)$$

$u \in [0, \bar{u}]$, \bar{u} is a positive constant. The problem (1) - (3) is Mayer optimal control problem.

References

- [1] TSIEN, H. S., EVANS, R. C: Optimum Thrust Programming for a Sounding Rocket, *Journal of American Rocket Society Journal* 1951, 21,(5):99-107.
- [2] MENON, P.K.A., KELLEY, H.J., AND CLIFF, E.M: Optimal Symmetric Flight with an Intermediate Vehicle Model, *J. Guidance* c1985, 8,(3):312-319.
- [3] VRATANAR, B., SAJE, M: On the Analytical Solution of the Brachistochrone Problem in a Non-conservative Field, *Int. J. Non-Linear Mechanics* 1998, 33(3):489-505.
- [4] DRUMMOND, J.E., DOWNES, G.L: The Brachistochrone with Acceleration: A Running Track, *Journal of Optimization Theory and Applications* 1971, 7(6): 444-449.
- [5] CHERKASOV, O., ZARODNYUK, A., SMIRNOVA N: Optimal Thrust Programming along the Brachistochronic Trajectory with Non-Linear Drag, *International Journal of Nonlinear Sciences and Numerical Simulation, Freund Publishing House Ltd.(Israel)*,2019, 20(1):1-6.

Zermelo Navigation Problem with State Constraints

SMIRNOVA NINA¹, MALYKH EGOR², CHERKASOV OLEG^{3*}

1. Lomonosov Moscow State University, Moscow, Russia [0000-0002-6532-8037]

2. Lomonosov Moscow State University, Moscow, Russia [0000-0002-5081-0584]

3. Lomonosov Moscow State University, Moscow, Russia [0000-0003-1435-1541]

* Presenting Author

Abstract: The article uses the example of the Zermelo navigation problem to illustrate a simple way to address state constraints of a certain type. The problem of planning time-minimum trajectory of an autonomous aircraft operating in a steady, homogeneous flow field is considered. The simple particle model of the aircraft is considered. The particle moves in a horizontal plane with a constant modulus velocity relative to the flow of the medium. The angular velocity of rotation of the particle velocity vector is considered as the control variable. The angle between the velocity vector and the horizontal axis is subjected to a phase constraint. The structure of the dynamic system allows to reduce the optimal problem to the problem of a smaller dimension. In reduced problem the state constraints transform to the constraints on the control variables. For the reduced problem, the optimal synthesis is designed. Next, for the original problem, the sequence and the number of the arcs with motion along state constraints are determined. The control law in the initial problem is established.

Keywords: Zermelo navigation problem, state constraints, optimal synthesis

1. Introduction

Solving optimal control problems in the presence of phase constraints is a complex task. The fact that no constructive methods have been developed to solve such problems makes each problem solved valuable. Significant progress can be made if the structure of the optimal trajectory, the number of arcs moving along the constraints, and their sequence are known. In this article, using Zermelo navigation problem [1] as an example, we demonstrate an approach that allows us to construct an optimal synthesis for problems with phase constraints of a certain type. A fairly complete review of the solutions of the Zermelo problem for various types of flows and the rigorous construction of optimal synthesis can be found, for example, in [2]. Of particular interest is the specified problem in the presence of state constraints on the coordinates. In this case, as a rule, the solution could be found using numerical simulation based on the method of penalty functions [3]. The problem is greatly simplified if the structure and sequence of extreme arcs are known. The path-planning problem therefore reduces to identifying the switching points at which straight and trochoidal path segments join to form a feasible path and choosing the true minimum-time solution from the resulting set of candidate extremals [4]. Zermelo problem with state constraints, imposed to the coordinates of the point, considered in [5].

This article describes a simple way to construct an optimal path in the presence of phase constraints of a certain type.

2. Results and Discussion

Equations of motion have a form:

$$\begin{cases} \dot{x} = v \cos \theta + w(y), \\ \dot{y} = v \sin \theta, \\ \dot{\theta} = u. \end{cases} \quad (1)$$

where x, y are horizontal and vertical coordinates of the particle, respectively, v is the velocity of the particle relative to the medium, θ is the heading angle, subjected to state constraints $\theta(t) \in [\theta_1, \theta_2]$, θ_1, θ_2 are constants, $w(y)$ is the drift in the horizontal direction, depending on y , u is a control variable, unbounded piecewise continuous function.

Boundary conditions have a form:

$$x(0) = x_0, y(0) = y_0, \theta(0) \text{ is free}, y(T) = y_T \quad (2)$$

Final time T of the process is given.

The goal function is:

$$J = -x(T) \rightarrow \min_u \quad (3)$$

The problem (1) - (4) is Mayer optimal control problem.

References

- [1] ZERMELO, E.: T Über das Navigationproble bei ruhender oder veränderlicher Windverteilung. *Z. Angew. Math. Mech.* 1931, 11(2):114-124.
- [2] EFSTATHIOS BAKOLAS, PANAGIOTIS TSIOTRAS: Optimal Synthesis of the Zermelo–Markov–Dubins Problem in a Constant Drift Field. *J Optim Theory Appl.* 2013,156:469–492.
- [3] BIN LI, CHAO XU, KOK LAY TEO, JIAN CHU: Time optimal Zermelo’s navigation problem with moving and fixed obstacles. *Applied Mathematics and Computatio* 2013, 224:866-875.
- [4] TECHY, L., WOOLSEY, C. A.: T Minimum-Time Path Planning for Unmanned Aerial Vehicles in Steady Uniform Winds. *Journal of Guidance, Control, 2009, 32(6):1736-1746.*
- [5] CHERTOVSKIH, R., KARAMZIN, D., KHALIL, N.T., PEREIRA, F.L: An indirect numerical method for a time-optimal state-constrained control problem in a steady two-dimensional fluid flow. *Proceedings of IEEE/OES Autonomous Underwater Vehicle Workshop, AUV 2018, Art. No.8729750.*

Maze exergame applied to IoT-based tiny aerobic equipment

CHIEN-HSIEN YEH^{1*}, SHEN-HUNG LIN¹

1. Medical Device Innovation Center, National Cheng Kung University, Taiwan.

* Presenting Author

Abstract: The tiny aerobic equipment is a well-known exercise device. There are some parameters, such as the cycle count, calories consumption, biking distance, et al., displaying on the built-in LCD screen. In general, the rate of equipment utilization is low due to the tedious experience. This study induced a maze exergame in the exercise to enhance the motivation. The exergame was performed in the Android operation system and the maze rotation corresponded to the motion of the tiny aerobic equipment. A Bluetooth module was integrated to transmit the exercise data, such as the rotation speed and the calories consumption. This study used three Hall sensors to detect the rotation direction and speed of the tiny aerobic equipment. And the calories consumption would be estimated using an experimental model of power loss and it is proportional to the rotation speed and the covered area of magnet resistor. The gamification means were applied to this study not only to activate the motivation but also reveal the serious exercise state in entertainment.

Keywords: Aerobic equipment, Bluetooth, Calories consumption, Magnet, Gamification.

1. Introduction

The tiny aerobic equipment looks like a small bike (Fig. 1). It is common in every long-term care center. Most users are the elderly. This kind of exercise device can work on the table and ground which is used to train the upper and lower limb respectively. But the exercise device is tedious so the rate of equipment utilization is usually low.

The gamification applied the game logics and means to our serious activity [1]. To improve the tedious situation when using the tiny aerobic equipment this study developed a maze exergame which is performed in Android operation system. Through the Bluetooth module, Hall sensors, and an embedded system we made an IoT-based equipment. All the exercise data, such as the rotation speed, is transmitted to the platform using Android operation system. Thus the maze rotation can correspond to the motion of the tiny aerobic equipment.

The calories consumption is related to the power output of the equipment. The power is the function of the material characteristics (C), magnet field density (B), rotation speed (ω), and affected conductor area (A). According to Waloyo et al. [2] the torque of the tiny aerobic equipment can be represented as equation (1).

$$T = f(B, C) \cdot R^2 A \omega \quad (1)$$

where R is the distance from the center of cycling plate to the affected conductor area. The torque T would be determined by the rotation speed after the calibration. And furtherly referring to Hill et al. [3], the calories consumption is four times of the power loss.

2. Results and Discussion

This study set up the said sensors and modules in a commercial product (Fig. 1). Ant the exercise data was transmitted to the TV screen, pad, or smartphone by Bluetooth. The maze rotated with the information of the equipment motion. The serious activity was revealed in entertainment.

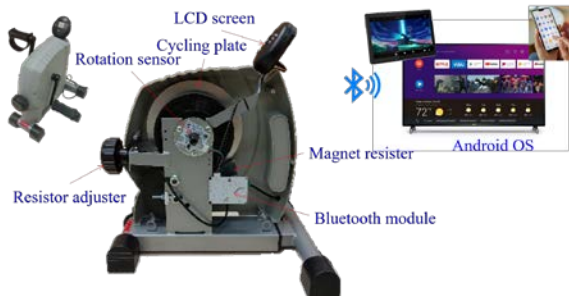


Fig. 1. The tiny aerobic equipment combined the rotation sensor and an embedded module which transmitted the exercise data to a platform using Android operation system, such as the pad or smart phone.



Fig. 2. The mage rotation corresponded to the motion of the tiny aerobic equipment, and the exercise state revealed after playing.

3. Concluding Remarks

This study developed an IoT-based tiny aerobic equipment and associated exergame to improve the tedious experience.

Acknowledgment: This work was financially supported by the Medical Device Innovation Center (MDIC), National Cheng Kung University (NCKU) from the Featured Areas Research Center Program within the framework of the Higher Education Sprout Project by the Ministry of Education in Taiwan.

References

- [1] MATALLAOUI, A., ET AL., HOW EFFECTIVE IS “EXERGAMIFICATION”? A SYSTEMATIC REVIEW ON THE EFFECTIVENESS OF GAMIFICATION FEATURES IN EXERGAMES. *Proceedings of the 50th Hawaii International Conference on System Sciences*, 2017. P. 3316-3325
- [2] WALOYO, H.T., ET AL., A NOVEL APPROACH ON THE UNIPOLAR AXIAL TYPE EDDY CURRENT BRAKE MODEL CONSIDERING THE SKIN EFFECT. *Energies*, 2020. **13**: P. 1561
- [3] HILL, A.V., THE MAXIMUM WORK AND MECHANICAL EFFICIENCY OF HUMAN MUSCLES, AND THEIR MOST ECONOMICAL SPEED. *The Journal of physiology*, 1922. **56**(1-2): P. 19-41.

-S4-

Global problems in nonlinear dynamics

Dynamic Integrity of Hyperelastic Spherical Membranes

KAIO C. B. BENEDETTI^{1,A*}, FREDERICO M. A. DA SILVA^{2,B}, RENATA M. SOARES^{2,C}, PAULO B. GONÇALVES^{1,D}

1. Pontifical Catholic University of Rio de Janeiro, Rio de Janeiro, Brazil [^A0000-0001-6952-9576, ^P0000-0001-8645-3542]
2. Federal University of Goiás, Goiás, Brazil [^B0000-0003-3306-3545, ^C0000-0002-1962-4185]

* Presenting Author

Abstract: There are several applications of thin-walled spherical elastomeric membranes in civil and aerospace engineering, bioengineering and biology. Both geometrical and material nonlinearities play an important role in their static and dynamic behavior. Due to their high nonlinearity they present under pressure load multiplicity of stable solutions, which affect their dynamic integrity due to the competing basins of attraction. Also their response depends on the chosen constitutive law. Here the Ogden model is adopted, due to its generality, and the nonlinear equations of motion are obtained for a preloaded membrane. This work investigates the dynamic integrity of a pressure loaded spherical membrane considering global (GIM) and local (LIM) integrity measures and the integrity factor (IF). For this, initial conditions are sampled in the phase space based on the Monte Carlo method. The numerical results demonstrate the influence of competing solutions on the global dynamic behavior and safety of the structure.

Keywords: spherical membrane, Ogden constitutive model, integrity measures, Monte Carlo method

1. Introduction

Thin-walled spherical elastomeric membranes can undergo large elastic deformations. However, the nonlinear behaviour under high static pressure or large amplitude vibrations depends on the hyperelastic material modelling [1]. Furthermore, multiple solutions can coexist, resulting in competing basins of attraction with varying topologies [1], which can be quantified by different integrity measures [2]. In this work, the numerical procedures proposed in [2] are used to estimate the global (GIM) and local (LIM) integrity measures and the integrity factor (IF) of a pressure loaded spherical membrane.

2. Results and Discussion

A closed homogeneous, isotropic, incompressible and hyperelastic spherical membrane with thickness assumed much smaller than the initial radius is considered. The deformed sphere can be described by the theory of membranes under finite deformations. Only the first vibration mode, consisting of the membrane inflation and deflation (breathing mode), is addressed, allowing a complete static and dynamic description in terms of the radial stretch δ [1]. The equation of motion is extremely dependent on the constitutive model. Considering an Ogden material, due to its generality, it takes the nondimensional form

$$\ddot{\delta}_d + (2\omega_0\zeta + \nu\delta_d^2)\dot{\delta}_d + \sum_{i=1}^n \frac{\mu_i}{\mu_1} [(\delta + \delta_d)^{\alpha_i-1} - (\delta + \delta_d)^{-2\alpha_i-1}] = Q_{sta} (1 + \beta \cos \Omega t) (\delta + \delta_d)^2. \quad (1)$$

where dots represent derivatives with respect to the nondimensional time $\tau = t(4\mu_1/\gamma\alpha^2)^{1/2}$, ω_0 is the natural frequency, Q_{sta} is the static preload, β and Ω are the forcing magnitude and frequency of the radial harmonic excitation, ζ and ν are the linear and nonlinear damping coefficients. In addition, μ_i and α_i are the material parameters of Ogden model with number of terms n . For details regarding the model formulation, refer to Silva et al. [1].

Rich dynamics can be displayed by eq. (1), depending on the parameters' values, as pointed out in [1]. The pressure loaded membrane displays two potential wells. A typical bifurcation diagram as a function of the forcing magnitude β is shown in Fig. 1(a), displaying a stable branch that loses stability through a saddle-node bifurcation, where a dynamic jump to a large amplitude solution can occur. Another saddle-node bifurcation gives rise to a competing solution branch. The integrity measures are reported in Figs. 1(b)-(d), estimated through Monte Carlo algorithms [2] with a total of 10000 initial conditions sampled uniformly. Three solutions are identified, corresponding to the low amplitude oscillations (blue) and large amplitude oscillations (red and orange). The same trait is observed for all measures, with the blue and red basins being progressively eroded. The orange solution only appears after the blue is completely eroded. The error bars of the algorithm are also reported.

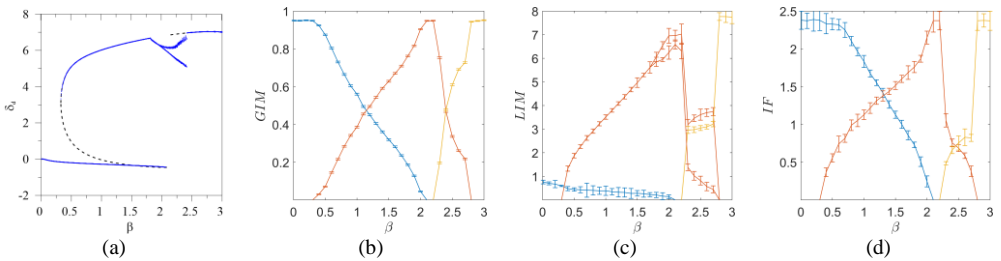


Fig. 1. Integrity analysis of the hyperelastic spherical membrane. Bifurcation diagram (a), GIM (b), LIM (c), IF(d). ($n = 3$, Ogden OSS2 model in [1], $Q_{sta} = 0.15$, $\Omega = 2.1514$, $\omega_0 = 2.1514$ and $\zeta = \nu = 0.01$)

3. Concluding Remarks

In this work the dynamic integrity of a hyperelastic spherical membrane is evaluated via a Monte Carlo approach. This methodology can evaluate with precision the dynamic integrity measures GIM, LIM and IF without the actual basin calculation. The integrity analysis shows that the occurrence of coexisting stable pre- and post-buckling solutions leads to competing basins of attraction. Clarifying their erosion process through the integrity measures enables the engineer to evaluate the system safety in a dynamic environment.

Acknowledgment: Brazilian research agencies CAPES, CNPq, and FAPERJ.

References

- [1] SILVA FMA DA, SOARES RM, PRADO ZJGN DEL, GONÇALVES PB: Intra-well and cross-well chaos in membranes and shells liable to buckling. *Nonlinear Dyn.* 2020, **102** (2) :877–906. <https://doi.org/10.1007/s11071-020-05661-z>
- [2] BENEDETTI KCB, GONÇALVES PB, SILVA FMA: Nonlinear oscillations and bifurcations of a multistable truss and dynamic integrity assessment via a Monte Carlo approach. *Meccanica.* 2020, **55** (12) :2623–2657. <https://doi.org/10.1007/s11012-020-01202-5>

Data-driven reduced-order nonlinear models from spectral submanifolds

MATTIA CENEDESE*, JOAR AXÅS AND GEORGE HALLER

Institute for Mechanical Systems, ETH Zürich, Leonhardstrasse 21, 8092 Zürich, Switzerland

* Presenting Author

Abstract: Data-driven model reduction methods are widespread for linear dynamical systems, while available approaches for nonlinear systems tend to be sensitive to parameter changes and offer limited prediction potential outside the range of data used in their construction. With this contribution, we present an approach that extracts explicit nonlinear models from data capitalizing on the theory of spectral submanifolds. Without specific assumptions on the type of observables or the kind of measurements, our method identifies nonlinear models that uncovers geometric nonlinearities and nonlinear damping in the observed dynamics. Our reduced-order models, which are trained on unforced trajectory data, also show great accuracy in predicting forced-responses of the nonlinear dynamical system. We validate our algorithm in several examples that feature synthetic or experimental data from structural vibrations or fluid dynamics.

Keywords: nonlinear oscillations, normal forms, invariant manifolds, machine learning

1. Introduction

Date-driven modeling is often coupled with dimensionality reduction for generating computationally efficient and possibly interpretable dynamical models. The most common approaches in the literature are Principal Orthogonal Decompositions (POD) followed by Galerkin projections [1] or Dynamic Mode Decomposition (DMD) [2]. While the former requires the knowledge of the full vector field generating the dynamics, the latter is purely data-driven. Yet DMD is only efficient when one uses advantageous observables and the system has a single steady state near which a linear approximation to the dynamics is feasible [3]. Machine learning approaches based on POD are also available [4] but tend to be sensitive and have limited potential for extrapolation and prediction.

We present here an approach based on the theory on spectral submanifolds (or SSMs, for short) which are the unique, smoothest invariant manifolds that act as nonlinear continuations of the modal subspaces of the linearized system [5]. Reducing the dynamics to these SSMs enables us to extract reduced-order models from generic observables, addressing most of the issues we have mentioned for available methods. We illustrate this approach with a numerical example coming from structural dynamics, which shows how our model trained on transient data is capable of extracting information on the system and of predicting forced responses.

2. Results and Discussion

We consider a straight, clamped-clamped Von Kármán beam [6], shown in Fig. 1(a), made of aluminum and has length 1 [m] and thickness 1 [mm]. For the numerical simulations, we use a finite

element model with 16 elements (45 degrees of freedom). We observe trajectories of the beam midpoint that are initialized on the static deflection occurring from loading the midpoint, cf. Fig. 1(a,b). The spectral gap among the linearized system eigenvalue is such that these trajectories rapidly converge on the slowest two-dimensional SSM, on which they decay toward the equilibrium. We feed our algorithm with these scalar signals and seek learn this two-dimensional SSM. After embedding the trajectory in a suitable space, a manifold parametrization is identified, as well as the normal form model for the dynamics. This latter is set to be of $O(7)$ and it has the form

$$\begin{aligned}\dot{\rho} &= -c(\rho)\rho \\ \dot{\theta} &= \omega(\rho)\end{aligned}\tag{1}$$

where c describes the nonlinear damping, while ω is instantaneous frequency of decaying oscillations. The variations of these amplitude-dependent properties are shown in Fig. 1(c,d). We have used one trajectory for training which our reduced-order model can reconstruct with less than 2% relative root mean squared error. Figure 1(e) shows that our model is also able to predict forced responses for several forcing values, when compared to the analytical results obtained from SSMtool [7] and to direct numerical integrations. The external forcing is applied on the FEM model at the midpoint, while the forcing amplitude for the reduced-order model is calibrated on the sweep having the lowest amplitude.

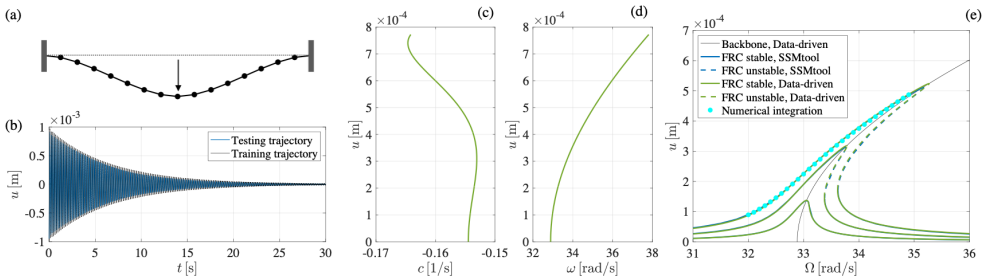


Fig. 1. Plot (a) depicts the Von Kármán beam model, while (b) shows the trajectories of the midpoint. Damping and frequency as function of the amplitude are illustrated in plots (c,d), while plot (e) compares the forced response curves (FRCs) for different forcing levels obtained with the data-driven model, analytical computations and numerical integration.

References

- [1] HOLMES P, LUMLEY JL, BERKOOZ G AND ROWLEY CW: *Turbulence, Coherent Structures, Dynamical Systems and Symmetry*. Cambridge University Press, 2012.
- [2] SCHMID PJ: Dynamic mode decomposition of numerical and experimental data. *J. of Fluid Mech.* 2010, **656**:5–28.
- [3] PAGE J, KERSWELL RR: Koopman mode expansions from simple invariant solutions. *J. of Fluid Mech.* 2019, **879**:1–27.
- [4] BRUNTON SL, PROCTOR JL, KUTZ JN: Discovering governing equations from data by sparse identification of nonlinear dynamical systems. *PNAS* 2016, **113**(15):3932–3937.
- [5] HALLER G, PONSIOEN S: Nonlinear normal modes and spectral submanifolds: existence, uniqueness and use in model reduction. *Nonlinear Dyn.* 2016, **86**(3):1493–1534.
- [6] JAIN S, TISO P, HALLER G: Exact nonlinear model reduction for a von Kármán beam: slow-fast decomposition and spectral submanifolds. *Journal of Sound and Vibration* 2018, **423**:195–211.
- [7] JAIN S, HALLER G: How to compute invariant manifolds and their reduced dynamics in high-dimensional finite-element models? *arXiv:2103.10264*, 2021.

A novel iterative procedure for robustness assessment

GIUSEPPE HABIB

Dept. of Applied Mechanics, Budapest University of Technology and Economics, Budapest, Hungary

Abstract: A new algorithm for estimating the robustness of a dynamical system's equilibrium is presented. Unlike standard approaches, the algorithm does not aim to identify the entire basin of attraction of the solution. Instead, it iteratively estimates the so-called local integrity measure, i.e., the radius of the largest hypersphere entirely included in the basin of attraction of a solution and centred in the solution. The procedure completely overlooks intermingled and fractal regions of the basin of attraction, enabling it to provide a meaningful engineering quantity quickly. The algorithm is tested on various mechanical systems. Despite some limitations, it proved to be a viable alternative to more complex and computationally demanding methods, making it a potentially appealing tool for industrial applications.

Keywords: basin of attraction, global stability, local integrity measure, system integrity

1. Introduction

Local stability is one of the most critical properties of a dynamical state. Engineers heavily exploit this concept. Nevertheless, scientists dealing with dynamical systems are aware that, despite its local stability, a system might diverge from its state if subject to a perturbation sufficient to make it cross the boundary of its basin of attraction (BOA). However, the computation of a system's BOAs is computationally very demanding. A few methods for the identification of BOAs of dynamical systems exist [1]. Analytical methods are generally based on Lyapunov functions. However, they are not a feasible option for the majority of real applications. The cell mapping method is probably the most efficient numerical technique for BOA estimation [2]. Experimental methods are almost inexistent, except for a few exceptions [3].

The objective of this study is to develop an algorithm for the robustness assessment of equilibrium points. The procedure reduces the computational cost for global stability analysis by identifying the local integrity measure (LIM) [1] only, overlooking fractal and intermingled portions of the BOA, which are hard to identify and practically less relevant.

2. Methodology

The algorithm is based on a simple framework. Considering a predefined region of the phase space, initially, the maximal value of the LIM is calculated, being equal to the minimal distance between the equilibrium point of interest and the boundary of the region of the phase space considered. Then, a trajectory of the system in the phase space is computed. If the trajectory does not converge to the desired solution, the LIM is estimated as the minimal distance between the equilibrium point of interest and any point of the non-convergent trajectory. The new estimated value of the LIM (an overestimate of the real LIM value) defines a hypersphere in the phase space denominated hypersphere of convergence, limiting the region of interest. If a simulation converges to the desired solution, then the LIM is not reduced in that iteration. Initial conditions of each simulation are chosen as the farthest point from any other already tracked point within the hypersphere of convergence.

In order to automatically classify the computed trajectories, the phase space is divided into cells. A trajectory is classified as converging or non-converging to the desired solution by analyzing cells in which points of the trajectory lie. To reduce computational time, if a trajectory reaches a cell already tracked by a previous trajectory, the simulation is interrupted; all cells containing points of the trajectory are classified according to the already tracked cell.

3. Results and conclusions

We implemented the algorithm on systems of various dimensions (up to dimension 8); this illustrated that the algorithm could rapidly and efficiently estimate the LIM value in all cases studied. In particular, the first few iterations already provided a relatively accurate estimate of the real LIM value. The majority of the subsequent simulations converged to the equilibrium of interest, except few ones, which improved the initial estimate of the LIM. Figure 1a represents the trend of the LIM estimate for the case of a Duffing-van der Pol oscillator with an attached tuned mass damper. The black line in Fig. 1a follows the described path. Light blue lines represent the LIM trend for other repetitions of the algorithm. All curves have a similar tendency. The system under study presents a stable equilibrium point (red cross in Fig. 1b) coexisting with a stable periodic solution (black line in Fig. 1b) for the considered parameter values. We remark that, in Fig. 1b, tracked points are projected on a section of the phase space, which makes it appear that red dots are within the hypersphere of convergence (green dashed line) while they are not.

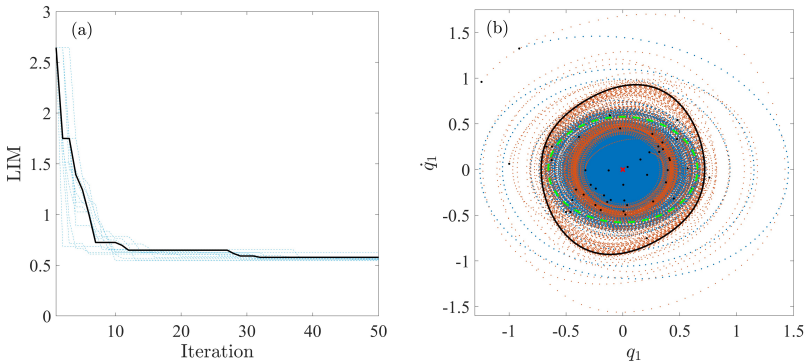


Fig. 1. (a) LIM estimated value; (b) projection of the points tracked during the computation; blue and red points: converging and non-converging points, respectively, dashed green line: section of the hypersphere of convergence.

The obtained results suggest that the proposed algorithm is a viable option for the robustness assessment of an equilibrium point. Future research developments should aim to make the algorithm utilizable for the robustness estimation of other kinds of solutions, such as periodic motions.

Acknowledgment: The Hungarian National Science Foundation financially supported this research under grant number OTKA 134496.

References

- [1] LENCI S, REGA G: *Global Nonlinear Dynamics for Engineering Design and System Safety*, Springer, 2019.
- [2] HSU CS: A theory of cell-to-cell mapping dynamical systems. *J. Appl. Mech.* 1980, **47**(4):931-939.
- [3] VIRGIN LN: *Introduction to Experimental Nonlinear Dynamics: a Case Study in Mechanical Vibration*, Cambridge University Press, 2000.

Global Analysis for Nonlinear Dynamical System Based on Parallel Subdomain Synthesis Method

ZIGANG LI^{1*}, JIANG JUN², LING HONG², JIAQI KANG¹

1. Department of Mechanics, Xi'an University of Science and Technology, Xi'an, China

2. State Key Laboratory for Strength and Vibration, Xi'an Jiaotong University, Xi'an, China

* Presenting Author

Abstract: The generalized cell mapping (GCM) method is an excellent numerical technique to reveal global structures hidden in dynamical responses of system, and the method has shown the powerful performance of global analysis in various model-based system which may be deterministic, stochastic or fuzzy. However, unaffordable memory requirement becomes a bottleneck for the cell mapping method when global analysis is carried out in a chosen domain of the state space with a specific computer in order to depict complex invariant sets with high resolution, and/or in high dimensions. In the work, a subdomain synthesis method with parallel computing based on clustered GPUs Architecture is thus developed to conquer the traditional ticklish problem encountered in global analysis. Several examples from low to high dimensions are illustrated to show the power of the proposed method.

Keywords: global dynamics, cell mapping method, subdomain synthesis, clustered GPUs computing

1. Introduction

Recall that the idea of space discretization has been introduced to GCM method developed originally by Hsu in the 1980s to investigate the global structures of nonlinear dynamical systems such as attractors, boundaries of basin as well as manifolds [1]. The discretization divides a continuous state space \mathbf{R}^N into a set of small and countable hypercubes called *cells*. The probabilities of the system residing in the cells are described by a Markov chain in the cell space as

$$\mathbf{P} \cdot \mathbf{p}(n) = \mathbf{p}(n+1) \quad (1)$$

where $\mathbf{p}(n)$ denotes the probabilistic vector describing the probability of each cell at n th step. $\mathbf{p}(n)$ indicates the probability vector of the response at n -step mappings. \mathbf{P} is a constant matrix with traditional $N_c \times N_c$ size that represents the one-step transition probability of the system.

It is known that the majority of executing time of the GCM is spent on the construction of the \mathbf{P} matrix, which depends predominantly on the number of cells used to discretize on each dimension of the chosen domain in the state space and also on the dimensions of the dynamical system. For a high-dimensional system, therefore, the computational and the storage burden is a great challenge to GCM. In the work, a *subdomain synthesis* method for cell mapping is proposed [2]. By this way, the chosen domain in the state space is divided into smaller subdomains with affordable memory requirements. Then, the cell mapping analysis can be independently carried out on each subdomain, taking advantage of GPUs architecture. The global structure of the system in the complete chosen domain can be finally identified and recovered from the dynamical information revealed in the subdomains.

2. Results and Discussion

One key technique in the proposed subdomain synthesis method is to solve the problem that the loss of invariant sets may occur when the traditional GCM is followed, if the invariant sets are split

into piece due to the domain partition in the state space. Here, the cells in each subdomain is classified as the follows: An *input cell* denotes the cell whose preimage cells are outside the processed subdomain. An *output cell* is the cell whose image cells are outside the processed subdomain. An *intersection cell* is the cell both of whose pre-image and image cells are outside the processed subdomain, as shown in Fig. 1.

In a processed subdomain D_i , suppose that the mapping paths across the partition boundaries from an output cell will surely return back to the processed subdomain through each input cell in finite maps. Then if the output cell is reachable also from the input cell inside the processed subdomain, these reachable cells can be regarded as a self-cycling set, for instance, cells $\{2,5\}$ for the processed subdomain D_1 in Fig. 1. In this paper, the synthesis of these cells, namely $\{2,3,4,5\}$, is called as a *virtual invariant set* in the complete chosen domain. Obviously, the cell set may not be a real strongly connected component of the dynamical system, but contain all possible invariant sets split by the partition boundaries on the chosen domain in the state space. So it is a covering set of the real invariant sets split by the state space partition. Thus, the global structure in the complete chosen domain can be identified and recovered from the virtual invariant sets after all dynamical information revealed in the subdomains are synthesized.

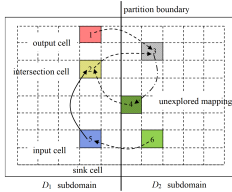


Fig. 1. Schematic representation of subdomain synthesis method

Three examples of application are presented in order to demonstrate the performances of the proposed method. The first example with 2-dimensions is used to validate the basic idea of subdomain synthesis method, and the second one presents 3-dimensional system, devoting to illustrating ability of the method. In the third example, the subdomain synthesis method is applied to a challenging example that is a 12-dimensional rotor system.

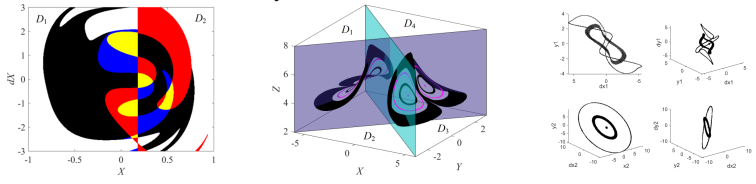


Fig. 2. Global analyses for three examples by the proposed subdomain synthesis method

3. Concluding Remarks

By the proposed method, the memory requirement is usually quite acceptable and much smaller than that of traditional way. The recovery of the global structure from the information of the subdomains takes a relatively little computation. In this way, the proposed method makes it possible to investigate global properties of the high-dimensional and complex systems.

References

- [1] Hsu, C.S.: A generalized theory of cell-to-cell mapping for nonlinear dynamical systems. *Journal of Applied Mechanics*, 1981, 48: 634–642.
- [2] Li Z, Jiang J, et al: A subdomain synthesis method for global analysis of nonlinear dynamical systems based on cell mapping. *Nonlinear Dynamics*, 2019, 95:715–726.

Discovery and Online Interactive Representation of the Dimensionless Parameter-Space of the Spring-Loaded Inverted Pendulum Model of Legged Locomotion Using Surface Interpolation

ÁBEL MIHÁLY NAGY^{1*}, DÓRA PATKÓ², AMBRUS ZELEI³

1. Budapest University of Technology and Economics [0000-0001-9185-5132]
2. Budapest University of Technology and Economics [0000-0001-7594-1882]
3. MTA-BME Research Group on Dynamics of Machines and Vehicles [0000-0002-9983-5483]

* Presenting Author

Abstract: The spring-loaded inverted pendulum (SLIP) is a widely used model of legged locomotion. However, a complete map of the dimensionless parameter regions of stable periodic solutions and the basin of attraction cannot be found in the literature. In this work, the minimum set of independent physical parameters was found using the Buckingham π theorem. The three-dimensional space of two dimensionless physical parameters and the dimensionless total mechanical energy of the conservative system was discovered by means of numerical continuation. The fundament of the stability analysis of the piecewise-smooth system was provided by the numerical calculation of the fundamental solution matrices and the monodromy matrix. The energy conserving and non-energy conserving perturbations were addressed in the stability analysis. An effective iteration procedure based on the Nelder-Mead method is presented which tunes the model parameters in order to imitate the motion characteristics of specific animals and locomotion types such as running, trotting and galloping. The results will be available online in the form of an interactive platform.

Keywords: legged locomotion, spring-loaded inverted pendulum, dimensional analysis, numerical continuation, piecewise-smooth dynamical systems

1. Introduction

The SLIP model [1-4], which combines the flight (F) and the ground (G) phases, interprets the CoM trajectory of a real pedal system. The model consists of a mass m at dimensionless position ξ , η and a spring k with natural length r_0 . The physical parameters are the dimensionless stiffness $\gamma = k r_0 / (mg)$ and the pre-touchdown leg angle β . The mechanical energy is the third independent parameter. We aim to create a database of pre-computed isosurfaces of eigenvalues and basin of attraction.

2. Results, Discussion and Conclusion

Figure 1. shows the behaviour of the SLIP model, which is already intricate for a particular physical parameter set. It is even more challenging to obtain a global picture, such as the assessment of the stable region in Fig 2. Here, the curves represent $|\mu|=1$ for the non-spurious eigenvalue. Isosurfaces defined by $|\mu|=c$ are also generated. Based on the continuation results, we develop an interactive online platform which helps researchers, teachers and students to understand the SLIP model and to choose parameters. The platform provides informative plots regarding the parameter zones, where the stable/unstable solutions exist. Surface interpolation techniques make the real-time rendering and therefore the travelling to different segments of the parameter space possible.

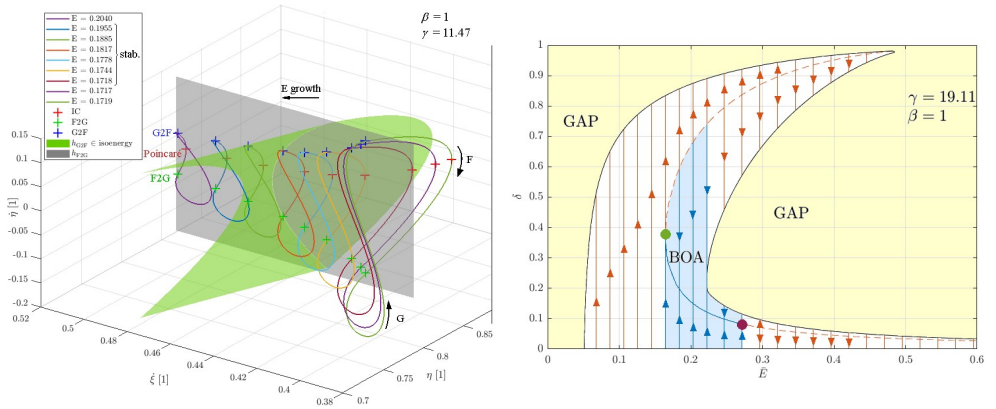


Fig. 1. Stable/unstable periodic solutions on different mechanical energy levels, event- and isoenergy surfaces in the relevant subspace of the state variables (left panel). Stable and unstable periodic solutions shown by blue solid and red dashed curves, respectively; basin of attraction and the gap region, where the Poincaré-return map is not defined, indicated by light blue and pale yellow shading, respectively (right panel).

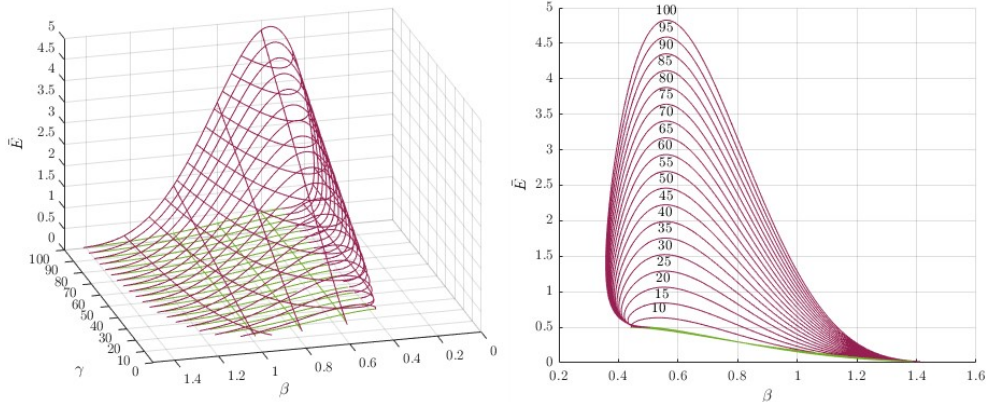


Fig. 2. Enveloping curves of the stable region in the three-dimensional parameter space (left panel). Boundary curves of the stable region for a variety of numerical values of γ (right panel).

Acknowledgment: The research reported in this paper and carried out at BME has been supported by the NRDI Fund (TKP2020 IES, Grant No. BME-IE-BIO and TKP2020 NC, Grant No. BME-NC) based on the charter of bolster issued by the NRDI Office under the auspices of the Ministry for Innovation and Technology and by the Hungarian National Research, Development and Innovation Office (Grant no. NKFI-FK18 128636).

References

- [1] BLICKHAN R: The spring-mass model for running and hopping. *Journal of Biomechanics* 1989, **22**(11/12):1217-1227.
- [2] ANDRADA E, BLICKHAN R, OGIHARA N, RODE C: Low leg compliance permits grounded running at speeds where the inverted pendulum model gets airborne. *Journal of Theoretical Biology* 2020, **494**:110227.
- [3] MASTERS SE, CHALLIS JH: Increasing the Stability of The Spring Loaded Inverted Pendulum Model of Running with a Wobbling Mass. *Journal of Biomechanics* 2021, in press.
- [4] GHIGLIAZZA RM, ALTENDORFER R, HOLMES P, KODITSCHKEK D: A Simply Stabilized Running Model. *SIAM Journal on Applied Dynamical Systems* 2003, **2**(2):187-218.

Global Dynamics of Thermomechanically Coupled Plates

VALERIA SETTIMI^{1*}, GIUSEPPE REGA²

1. Department of Civil and Building Engineering, and Architecture, Polytechnic University of Marche, Ancona, Italy [0000-0002-0555-0883]
2. Department of Structural and Geotechnical Engineering, Sapienza University of Rome, Rome, Italy [0000-0002-7444-0338]

* Presenting Author

Abstract: Thermoelastic analysis of a shear deformable reduced model of laminated plates with von Kármán nonlinearities and cubic temperature along the thickness is presented. Parametric investigation of the response is accomplished by means of bifurcation diagrams, phase portraits and planar cross sections of the four-dimensional basins of attraction, in order to describe the local and global dynamical behavior of the model. Due to the thermomechanical coupling, the slow transient thermal dynamics is proved to be crucial in determining the steady mechanical response, which can be grasped only by proper developing an accurate global dynamics analysis in the multidimensional state space.

Keywords: Composite plates, Reduced order models, Thermomechanical coupling, Local and global dynamics

1. Introduction

Thermomechanical coupling of materials and structures in a nonlinear dynamics environment represents a topic of great interest in fields like aerospace engineering, civil, and mechanical engineering, and in micro-electro-mechanics. To understand the basic, yet involved, effects of coupling on the finite amplitude vibrations of geometrically nonlinear structures, low-order models able to preserve the main features of the underlying continuum formulations turn out to be very important, as they get rid of the complicatedness generally occurring in the analysis and interpretation of nonlinear phenomena when using richer models [1,2]. Moreover, in the context of a global dynamics investigation, low-order models are crucial to perform the nonlinear analyses in a reduced state space, still with the possibility to obtain fundamental insight into thermal-structural interactions [3,4].

2. Results and Discussion

The thermomechanical plate model here used is derived within a unified modelling framework integrating mechanical and thermal aspects which, starting from the three-dimensional physics problem, moves to the two-dimensional and zero-dimensional formulations, as presented in [1]. Assumptions of third-order shear deformability and consistent cubic temperature variation along the thickness are imposed, and, in the absence of internal resonance between the plate transverse modes, a single-mode Galerkin approximation is adopted for the transverse displacement and the two independent bending and membrane temperatures. The choice of a dome-shaped prescribed temperature on the upper and lower surfaces allows to obtain the following three coupled nonlinear ODEs in terms of the deflection of the plate centre W , the membrane temperature T_{Ro} , and the bending temperature T_{R1} (T_{up} and T_{down} are the central values of the dome-shape temperature prescribed on the upper and lower external surfaces, respectively):

$$\begin{aligned} \ddot{W} + a_{12}\dot{W} + a_{13}W + a_{14}W^3 + a_{15}T_{R1} + a_{16}W T_{R0} + a_{17}\cos(\dot{t}) + a_{18}(T_{up} + T_{down})W + a_{19}(T_{up} - T_{down}) &= 0 \\ \dot{T}_{R0} + a_{22}T_{R0} + a_{23}\alpha_1(T_{up} + T_{down}) + a_{24}W\dot{W} + a_{25}e_0 &= 0 \\ \dot{T}_{R1} + a_{32}T_{R1} + a_{33}\dot{W} + a_{34}e_1 + a_{35}\alpha_1(T_{up} - T_{down}) &= 0 \end{aligned}$$

Local and global nonlinear dynamics have been investigated through parametric analysis of the response by means of bifurcation diagrams, phase portraits and planar cross sections of the four-dimensional basins of attraction. The results highlight the non-trivial influence of the slow transient thermal dynamics on the steady outcome of the faster mechanical response, which can be unveiled only via a refined global analysis accomplished in the system actual multidimensional phase space. Indeed, local dynamics intrinsically neglects thermal transient, as continuation analyses are focused on the evolution of stationary responses. Conversely, global dynamics of the coupled system naturally considers both mechanical and thermal transient dynamics, thus representing the most suitable tool to comprehensively describe the response of the thermomechanical plate. When the thermal initial conditions are set to the relevant regime values, the basins of attraction of the coupled model display the same multistable response of the local dynamics analysis, which thus represents only a partial scenario (i.e. a particular section) of the overall four-dimensional plate behaviour.

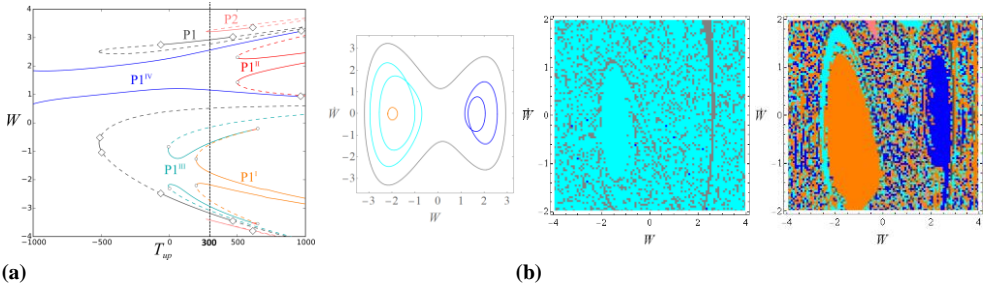


Fig. 1. At $T_{down} = 100$ K: **(a)** Local dynamics: bifurcation diagram and phase portraits of plate multistable periodic solutions; **(b)** Global dynamics: 2D sections of basins of attraction for null and steady state thermal initial conditions ($T_{up} = 300$ K).

3. Concluding Remarks

As a major result, the analyses have proved the ability of the coupled model to capture the actual behaviour of the physical system by correctly catching coupling effects, which turns out to be crucially important for all multiphysics systems, characterized by field variables evolving on different time scales. From a methodological viewpoint, this can be grasped only by complementing the local dynamics analysis with a deep investigation of the global features of the multidimensional response.

References

- [1] SAETTA, E, REGA, G: Third-order thermomechanically coupled laminated plates: 2D nonlinear modelling, minimal reduction and transient/post-buckled dynamics under different thermal excitations. *Composite Structures* 2017, **174**: 420–441.
- [2] SAETTA, E, SETTIMI, V, REGA, G: Minimal thermal modeling of two-way thermomechanically coupled plates for nonlinear dynamics investigation. *Journal of Thermal Stresses* 2020, **43**(3): 345–371.
- [3] SETTIMI, V, SAETTA, E, REGA, G: Nonlinear dynamics of a third-order reduced model of thermomechanically coupled plate under different thermal excitations. *Meccanica* 2020, **55**: 2451–2473.
- [4] REGA, G, SAETTA, E, SETTIMI, V: Modeling and nonlinear dynamics of thermomechanically coupled composite plates. *International Journal of Mechanical Sciences* 2020, **187**: 106106.

Track-bridge interaction effect on the train-bridge resonance of railway viaducts

MOHAMED TAHIRI^{1*}, ABDELLATIF KHAMLI², MOHAMMED BEZZAZI¹

1. Department of Physics, Mechanical and Civil Engineering Laboratory, Faculty of Sciences and Technology, University Abdelmalek Essaadi, Tangier, Morocco
 2. Department STIC, Communication Systems and Detection Laboratory, National School of Applied Sciences, University Abdelmalek Essaadi, Tetouan, Morocco
- * Presenting Author

Abstract:

As demand is increasing on high speed railway lines, proficient and cost-effective design of these vital transportation infrastructures is well expected with ever augmenting traffic speed. The dynamic response of bridges with ballasted track is known to be very dependent on several factors. These may influence largely the response of such composite structures under circulating loads. The interaction occurring in the system is function of the bare bridge track modal properties. But, it is also influenced by the track superstructure including rails, sleepers and ballast. For simply supported (SS) bridges or viaducts which are generally susceptible of experiencing high vibration levels, one of the most demanding requirements for their design is the vertical accelerations and it constitutes one of the Serviceability Limit States for traffic safety prescribed by Eurocode (EC) [1]. Track-bridge interaction influences the dynamic behavior of the structures mentioned above, valuable research has been achieved in this field as indicated from recent literature [2-5]. One of the most successful approaches rendering the essential of ballast-bridge interaction is based on modeling the bridge and the track as two-layer beams connected between them through springs and dampers representing the nonlinear friction behavior occurring at their interface. Experimental evidence has enabled the merit of this approach.

The aim of the work is to analyze the effect of the nonlinear behavior of the ballasted track on the train-bridge resonance of a simply supported single track railway bridge. The studied bridge traversed by moving trains is modeled by two layers beams connected between them through a nonlinear Kelvin-Voight viscoelastic foundation. This approach enabled to account in an efficient way of the ballast effect on the global bridge dynamics under all the high speed load models (HSLM). The obtained results have shown that the dynamics of the system is governed essentially by a Duffing like oscillator where a decreasing in the bridge frequency is observed.

Keywords: Railway bridges, resonance, ballasted track, vertical acceleration.

- [1] CEN. EUROCODE, BASIS OF STRUCTURAL DESIGN, ANNEX A2: APPLICATION FOR BRIDGES. FINAL VERSION, EUROPEAN COMMITTEE FOR STANDARDIZATION, BRUSSELS 2005.
- [2] Rigueiro C, Rebelo C, da Silva L Simoes: Influence of ballast models in the dynamic response of railway viaducts. *Journal of Sound and Vibration* 2010, **329**:3030-3040.
- [3] Biondi B, Muscolino G, Sofi A. A substructure approach for the dynamic analysis of train-track-bridge system. *Computers and Structures* 2005, 2271-2281.
- [4] Fink J, and MahrT. Influence of the ballast superstructure on the dynamics of slender steel railway bridges. Proceedings of NSCC, Oslo, Norway. (2009).
- [5] Battini J-M, Ulker-Kaustell M. A simple finite element to consider the non-linear influence of the ballast vibrations of railway bridges. *Engineering Structures* 2011, **33**:2597-2602.

Experiments of Shells With Non-Newtonian Fluid Interaction

DR. ANTONIO ZIPPO^{1*}, PROF. FRANCESCO PELLICANO², DR. GIOVANNI IARRICCIO³

1. Università di Modena e Reggio Emilia, Dipartimento di Ingegneria “Enzo Ferrari” - Centro Intermech [0000-0001-6206-2619]
2. Università di Modena e Reggio Emilia, Dipartimento di Ingegneria “Enzo Ferrari” - Centro Intermech [0000-0003-2465-6584]
3. Università di Modena e Reggio Emilia, Dipartimento di Ingegneria “Enzo Ferrari” - Centro Intermech [0000-0001-9323-8656]

* Presenting Author

Abstract: In this study the nonlinear vibrations of a fluid-filled circular cylindrical shell under seismic excitation is investigated. A PET thin shell with an aluminum top mass is harmonically excited from the base through an electrodynamic shaker in the neighborhood of the natural frequency of the first axisymmetric mode. The dilatant fluid is composed of a cornstarch-water mixture with 60% cornstarch and 40% water of total weight. The preliminary results show a strong non-linear response due to the coupling between the fluid and structure and the shaker-structure interaction that leads to a very interesting dynamic response of the system. The specimen is a polymeric circular cylindrical shell: an aluminum cylindrical mass is glued on the shell top edge; conversely, the bottom edge of the shell is clamped to a shaking table. The following sensors have been adopted: three triaxial accelerometers placed on the top mass at 120°, a monoaxial accelerometer at the base of the shell, a laser vibrometer to measure the lateral velocity on the mid-height of the shell. The test article has been excited in the axial direction through a harmonic load, with a step-sweep controlled output, the voltage signal sent to the shaker amplifier is closed-loop controlled; to avoid interaction between the control system and the specimen under study, no controls have been used for controlling the shaker base motion. The harmonic forcing load consists of a stepped-sine sweep of frequency band 100-500 Hz with a step of 2.5 Hz. All the tests have been performed with the shell full filled with quiescent fluid. The dynamic scenario is analyzed by means of time histories, spectra, phase portraits and Poincaré maps. The experiments show the onset of complex dynamics: subharmonic and quasiperiodic responses, Chaos.

Keywords: FSI Fluid Structure Interaction, Nonlinear Dynamics, Shells, Chaos, Experimental

1. Introduction

The present paper is the first outcome of the Project *InterFlu* focused on Non-Newtonian fluids and interactions with vibrating structures. Here the goal is to analyze the dynamic scenario of a circular cylindrical shell in presence of interactions with fluids, the study is fully experimental. Our attention was focused on large amplitude of oscillations generated by an highly energetic seismic excitation, having a single tone spectral content, such excitations induces nonlinear vibrations on a fluid-filled cylindrical shell carrying a top mass (upper rigid closer cap), preliminary results of the bifurcation analysis are presented.

2. Results and Discussion

In this section, a short overview of the preliminary results, obtained from the postprocessing of the experimental data, is shown. In addition to the main instability region around the first axisymmetric mode between 235Hz and 300Hz, the bifurcation diagram of the lateral velocity, figure 3a and 3c, shows a second interesting region between 366Hz and 442Hz, where a subharmonic response is predominant, see the spectrum of the lateral velocity in the upward 0.34V case at 400Hz in figure 3i, the branches of the diagram separate and rejoin several times, showing a strong dynamic instability with a period doubling behaviour. This remark is confirmed by the Poincaré maps of the vertical acceleration of the top mass and the radial velocity of the shell: a 4T subharmonic (Figure 3a) move to chaotic states at 250Hz(Figure 3b) confirmed by the time history of the velocity (figure 3c), and in the case of upwards at 0.34 Volt a period-doubling with amplitude modulation at 292.5 Hz: Poincaré maps (figure 3d) and spectrum of lateral velocity normalized respect to the forcing frequency at 292.5Hz (figure 3e) and 400Hz (figure 3f) has been observed in the experimental analysis.

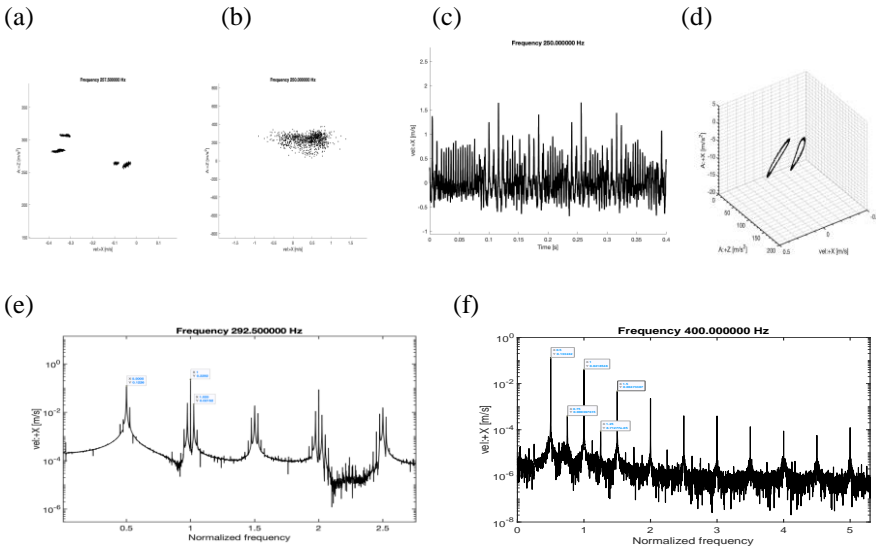


Fig. 1. 4T subharmonic response (a) and chaotic motion: Poincaré maps(b) and time history (c), period-doubling with amplitude modulation: Poincaré maps (d) and spectrum of lateral velocity at 292.5Hz (e),400Hz (f)

Acknowledgment: The authors thank the project FAR2020 Mission Oriented “Fluidi non-Newtoniani e Interazione Fluido Struttura / InterFlu” (tipologia “nodo”) C.U.P. E99C20001160007 for the financial support.

References

- [1] AMABILI, M., PELLICANO, F., PAÏDOUSSIS, M. P., (1998) NONLINEAR VIBRATIONS OF SIMPLY SUPPORTED, CIRCULAR CYLINDRICAL SHELLS, COUPLED TO QUIESCENT FLUID. JOURNAL OF FLUID AND STRUCTURE 12:883-918.
- [2] ZIPPO, A., BARBIERI, M., IARRICCIO, G., PELLICANO, F., NONLINEAR VIBRATIONS OF CIRCULAR CYLINDRICAL SHELLS WITH THERMAL EFFECTS: AN EXPERIMENTAL STUDY (2020) NONLINEAR DYNAMICS, 99 (1), PP. 373-391. DOI: 10.1007/s11071-018-04753-1
- [3] ZIPPO, A., BARBIERI, M., PELLICANO, F., TEMPERATURE GRADIENT EFFECT ON DYNAMIC PROPERTIES OF A POLYMERIC CIRCULAR CYLINDRICAL SHELL (2019) COMPOSITE STRUCTURES, 216, PP. 301-314, DOI: 10.1016/j.compstruct.2019.02.098
- [4] PELLICANO, F., (2011) DYNAMIC INSTABILITY OF CIRCULAR CYLINDRICAL SHELL CARRYING A TOP MASS UNDER BASE EXCITATION: EXPERIMENTS AND THEORY. INTERNATIONAL JOURNAL OF SOLIDS AND STRUCTURES 48:408-427.

-S5-

Piecewise-smooth systems

Control of Bubbling Phenomenon in Bipolar SPWM Inverters

ANDERSON FABIAN ABELLA¹, JOSÉ D. MORCILLO^{2*}, FABIOLA ANGULO³

1. Universidad Nacional de Colombia - Sede Manizales. Facultad de Ingeniería y Arquitectura. Bloque Q, Campus La Nubia. Manizales, 170003 - Colombia. e-mail: aabella@unal.edu.co
2. Universidad de Monterrey. Escuela de Ingeniería y Tecnologías. Monterrey, 66238 - México. e-mail: jose.morcillo@udem.edu.mx [0000-0002-4545-8969]
3. Universidad Nacional de Colombia - Sede Manizales. Facultad de Ingeniería y Arquitectura. Bloque Q, Campus La Nubia. Manizales, 170003 - Colombia. e-mail: fangulog@unal.edu.co [0000-0002-4669-7777]

* Presenting Author

Abstract: Significant growth in the adoption of electric cars and non-conventional energy sources in the electrical grid has led to an increase in the use of power electronic converters, in particular, the power inverter system which is responsible for regulating electrical energy to the user. However, in some cases its performance has been affected by a phenomenon known as bubbling, which consists on a significant distortion of the output waveforms by phase restricted high frequency oscillations. As a consequence, in this paper we propose to vary the frequency of the SPWM to control the bubbling phenomenon reported in the buck-inverter systems [1]-[4]. Our proposed strategy was successfully applied to these inverters with a very relevant advantage, it does not require any physical or structural change to the system configuration, only an appropriate tuning of the ramp frequency signal. This process was performed by using a bifurcation perspective and detecting the frequency values for which the bubbling phenomenon and other nonlinear dynamics of the systems are suppressed.

Keywords: power inverter, bipolar SPWM, bubbling phenomenon.

1. Introduction

Power inverters (DC/AC converter) controlled by different bipolar sinusoidal pulse width modulation (SPWM) strategies have shown high frequency and low amplitude oscillations embedded in the output sinusoidal signals, either in one part or in several parts of these waveforms, and also coexisting with different nonlinear dynamics [1]. This problem has been called bubbling phenomenon, and it increases the total harmonic distortion (TDH) in the output signals (output voltage $V_{out}(t) := V_C$ and output current $I_{out}(t) :=$ current flowing through the load resistance) causing not only a significant distortion to their waveforms, but also a low quality electrical service to the user. Hence, in this paper we present a modification in the control scheme of the system, which consists on changing the switching frequency. This technique was proved in several full-bridge single phase buck-inverter systems with bipolar SPWM [1]-[4]; however, for the sake of brevity, here we only show the results applied to a particular buck-inverter system, which was broadly analyzed in [1].

Fig. 1(a) shows a schematic diagram of the circuit used in this paper. $L=0,1$ H and $C=1$ μ F compose the LC filter, $R_L=100$ Ω and $R=10,6$ Ω are the load and parasitic resistances, respectively. $E_0=8,6$ V, $\beta=1$ is the sensor gain, $V_{ref}(t)=5 \cos(200\pi t)$ is the reference signal and $\alpha=16,59$ is the gain of the proportional control. The bipolar ramp is given by $V_{ramp}(t)=10(t/T_{ramp} - \lfloor t/T_{ramp} \rfloor - 1/2)$, with T_{ramp} being the period of the ramp, and $\lfloor t/T_{ramp} \rfloor$ defines the floor function. S/H is a zero order hold and it is synchronized with $V_{ramp}(t)$. Switches S_1, S_2, S_3 and S_4 are controlled by channels E and D . The dynamical system is

defined by the ordinary differential equations $\dot{x}=Ax \pm Bu$, where $x=[V_C \ I_L]^T$ and $u=1$. A and B are given in Eq. (1). V_C is the voltage across the capacitor and I_L is the current flowing through the inductor. All parameter values as in [1].

$$A = \begin{bmatrix} -1/(CR_L) & 1/C \\ -1/L & -R/L \end{bmatrix}, \quad B = \begin{bmatrix} 1 \\ E_0/L \end{bmatrix} \quad (1)$$

2. Results and Discussion

Previous analysis confirmed that the bubbling phenomenon is influenced by the switching frequency of the system; therefore, our proposed strategy to suppress the undesired bubbling phenomenon consists on changing the frequency of the ramp signal f_{ramp} . The results obtained by varying f_{ramp} in the system are shown in Figs. 1(b) and 1(c). From 10 kHz onwards the bubbling phenomenon ceases, and 1T-periodic orbits are obtained (black dots). For $f_{ramp} < 10$ kHz, the bubbling phenomenon continues appearing and the TDH increases. Considering the f_{ramp} values for which the bubbling does not appear, a frequency $f_{ramp} = 20$ kHz is selected and the behavior of the output temporal signals is shown in Fig. 1(c).

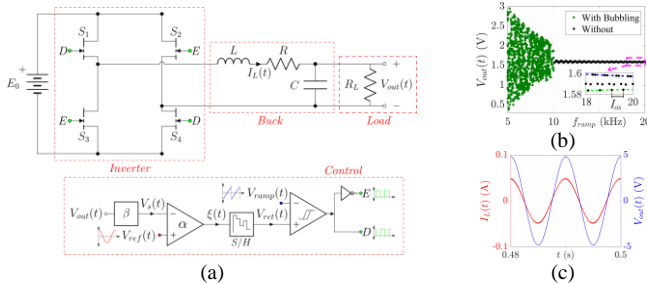


Fig. 1. (a) Single-phase full-bridge buck-inverter with bipolar SPWM. (b) Bifurcation diagram varying the frequency $f_{ramp} \in [5, 20]$ kHz. (c) Temporal output signals with $f_{ramp} = 20$ kHz.

3. Concluding Remark

Our proposed strategy is able to efficiently and effectively find a frequency where nonlinear dynamics and bubbling phenomenon are eliminated for any power inverter system. Here, a very high frequency is not selected ($f_{ramp} = 20$ kHz, Fig. 1(c)), and with this, it is possible to obtain a stable, very well formed and without distortion output signals. Even more, for this particular case for $f_{ramp} > 10$ kHz, the bubbling phenomenon is avoided. On the other hand, our results let us confirm that the bubbling phenomenon is influenced by the switching frequency of the inverter systems.

Acknowledgment: F. Angulo and A.F. Abella thank to Universidad Nacional de Colombia, Manizales, Project 46277 - Vicerrectoría de Investigación.

References

- [1] AVRUTIN V, MORCILLO J.D, ZHUSUBALIYEV Z.T, ANGULO F: Bubbling in a Power Electronic Inverter: Onset, Development and Detection. *Chaos, Solitons and Fractals* 2017, **104**:135–152.
- [2] ZHUSUBALIYEV Z.T, MOSEKILDE E, ANDRIYANOV A.I, SHEIN V.V: Phase Synchronized Quasiperiodicity in Power Electronic Inverter Systems. *Physica D* 2014, **268**:14–24.
- [3] SHANKAR D.P, GOVINDARAJAN U, KARUNAKARAN K: Period-Bubbling and Mode-Locking Instabilities in a Full-Bridge DC-AC Buck Inverter. *IET Power Electronics* 2013, **6**(9):1956–1970.
- [4] LI M, DAI D, MA X, IU H.H.C: Fast-Scale Period-Doubling Bifurcation in Voltage-Mode Controlled Full-Bridge Inverter. *Proceedings - IEEE International Symposium on Circuits and Systems* 2008, 2829–2832.

Effects of the resources transfer between communities under a policy of responsibility in the framework of sustainability

JORGE A. AMADOR^{1*}, JOHAN MANUEL REDONDO², GERARD OLIVAR³, CHRISTIAN ERAZO⁴

1. Instituto de Investigación de Recursos Biológicos Alexander von Humboldt. Bogotá D.C., Colombia. [0000-0002-4296-6271]

2. Universidad Católica de Colombia. Bogotá D.C., Colombia. [0000-0002-9427-1324]

3. Universidad de Aysén, Coyhaique, Chile [0000-0003-1862-4842]

4. Universidad Antonio Nariño. Bogotá D.C., Colombia [0000-0003-4236-362X]

* Presenting Author

Abstract: Transfer resources from a community with abundant resources to one with high consumption but with a clear and strict policy of responsibility in terms of exploitation has been modelled to understand if the dynamics can lead to sustainable development. A system will be said to be sustainable if well-being is a non-negative conservation law. A Filippov system is used to model the interaction between the communities, considering exploitation limits across two switching regions from the high-consumption community, so that the policy from only one of the communities leads to the protection of the resources in both communities. Interpreting well-being as resource tenure in the presence of the population, invariant sets were identified that demonstrate that this policy of responsibility can lead to sustainable development. Finally, if the resilience of the socioecological system is studied through a non-smooth bifurcation analysis, break a sustainability condition does not necessarily mean losing the sustainability.

Keywords: renewable resources transfer, sustainability, Filippov system, non-smooth bifurcations

1. Introduction

The creation of wealth through the division of labour led the territories to specialized production that triggered the need for exchange, giving rise to the supply of the products obtained and the demand for those that the territory lacked. Within the framework of sustainable development, the exchange of resources is of great interest because, for example, a unidirectional exploitation relationship puts the economic situation of the nation supplying raw materials at risk, while the nation that demands them is enriched by granting them added value using science and technology, generating an asymmetry in development that can translate into social instability for the two nations in the relationship. A landscape or territory is said to be sustainable if its definition of well-being is a non-negative conservation law (time symmetry) of the variables that define it [1], which is derived from an interpretation of sustainable development proposed in Our Common Future [2]. In this sense, the emergence of invariant sets in the dynamics of the behaviour of a socio-ecological system such as landscapes and territories show us that sustainability can have different geometries. The purpose of this article is to present the results obtained after modelling the unidirectional exchange between two communities that act under a policy of responsibility, which consists of a clear identification of decision limits regarding the exploitation of their resources through Filippov Systems. The differential system used is a model of the Brander & Taylor type [3], such as the one presented in Equation 1, where there is a conservation policy.

$$\begin{aligned}
\dot{L}_1 &= C_1 \phi_1 \epsilon_1 L_1 S_1 - \sigma_1 L_1 \\
\dot{S}_1 &= \rho_1 S_1 (S_1/T_1 - 1)(1 - S_1/K_1) - \epsilon_1 L_1 S_1 \\
\dot{L}_2 &= \phi_2 \epsilon_2 L_2 S_2 + (1 - C_1) \phi_1 \epsilon_1 L_1 S_1 - \sigma_2 L_2 \\
\dot{S}_2 &= \rho_2 S_2 (S_2/T_2 - 1)(1 - S_2/K_2) - \epsilon_2 L_2 (S_2 - S_{1 \rightarrow 2})
\end{aligned} \tag{1}$$

where L_i y S_i are the population and the resources stock of the i -th community, ϕ_i , ϵ_i , σ_i , ρ_i , T_i and K_i are system parameters, C_1 is a cooperation parameter from community 1 to community 2 and $S_{1 \rightarrow 2}$ is the amount of protected resource. The decision limits are expressed through switching surfaces in the community that uses the resources of the other. For this work, two were used: the emergency region for the protection of own resources and the responsibility region for the protection of the resources of the contributing community.

2. Results and Discussion

Different paths of sustainable development were found, expressed through invariant sets with sliding, as shown in Figure 1, which indicates that responsible exploitation policies from one of the communities can lead to sustainable dynamics between the communities involved. Also is shown that, if the resilience of the socioecological system is studied through a non-smooth bifurcation analysis, break a sustainability condition does not necessarily mean losing the sustainability, but the system can express another sustainability geometry.

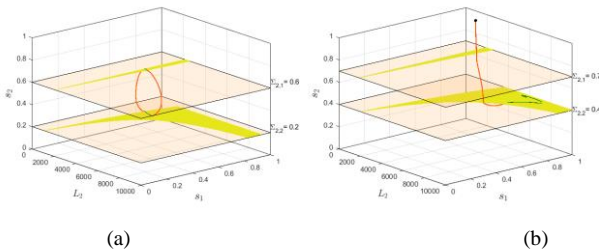


Fig. 1. Different paths of development involving two switching regions. (a) periodic orbit with double sliding, (b) convergence to a pseudo-equilibrium

3. Concluding Remarks

The effect of transferring resources from a community with abundant resources to one with high consumption but with a clear and strict policy of responsibility concerning exploitation can lead to a sustainable dynamic. The result is added to those obtained to affirm that the role of the consumer is preponderant for the generation of well-being, even over those communities with foreign policies but subject to the exchange policy.

References

- [1] REDONDO, J. M., BUSTAMANTE-ZAMUDIO, C., AMADOR-MONCADA, J., & HERNANDEZ-MANRIQUE, O. L.: Landscape sustainability analysis: Methodological approach from dynamical systems. *Journal of Physics: Conference Series* 2019, **1414**(1):012010.
- [2] BRUNDTLAND, G. H., KHALID, M., AGNELLI, S., AL-ATHEL, S., & CHIDZERO, B. J. N. Y.: *Our common future*: New York, 1987.
- [3] BRANDER, J. A., & TAYLOR, M. S.: The simple economics of Easter Island: A Ricardo-Malthus model of renewable resource use. *American economic review* 1998: 119-138.

Bifurcations in PieceWise-Smooth Systems Associated to Migration

JOSEFINA ANTONIJUAN¹, IMMA MASSANA², GERARD OLIVAR-TOST³,
JOANA PRAT⁴, ENRIC TRULLOLS^{5*}

1,2,4,5. Department of Applied Math/SARTI research group, Universitat Politècnica de Catalunya. Catalonia. [0000-0002-7976-1421], [0000-0002-1089-4525], [0000-0001-7628-487X], [0000-0002-0069-3981]

3. Department of Natural Sciences & Technology, Universidad de Aysén, Chile [0000-0003-1862-4842]

* Presenting Author

Abstract: Human migration is a worldwide phenomenon. One of the multiple ways of temporal or periodic migration is tourism. Even though tourism is a relatively new concept in human history, its consequences are noticeable, both on a local and global scale. In general, the introduction of tourism in one country, or community, has not been planned appropriately, or simply not planned at all. Overexploitation of natural resources and inadequate behaviors leads to a conflict between tourists and locals that makes the tourist economy not sustainable. The fall of tourism in 2019-2020 due to a pandemic episode has shown how dependent the economy could be on the tourism industry. In the new start, politicians, social actors, and stakeholders in general, need a tool that gives them the opportunity to plan actions and policies. The modeling of tourist flows could be the tool to face the issue, looking for the balance between natural and socioeconomic resources, the interests and rights of tourists and locals. This paper proposes and analyses a mathematical model of nonlinear differential equations, which allows studying the dynamic interaction between tourists and residents. We use analytical and numerical methods to solve the proposed Filippov piecewise-smooth system. Invariance, equilibrium points, bifurcations, and switching surface have been studied.

Keywords: tourism, migration, bifurcation, PWS systems, non-linearity.

1. Introduction

The Filippov system, which relates tourists (T) to residents (R) in a city, is given by the following piecewise smooth system.

$$\begin{cases} \dot{R} = \alpha_3 R \left(1 - \frac{R}{k - k_1}\right) \left(\frac{R}{k_2} - 1\right) - \alpha_4 RT \\ \dot{T} = \alpha_1 T \left(1 - \frac{T}{k_1}\right) - \alpha_2 R g(R, T). \end{cases}$$

$$g(R, T) = \begin{cases} 1 & \text{si } h(R, T) > 0 \\ 0 & \text{si } h(R, T) < 0 \end{cases} = \begin{cases} 1 & \text{si } T > T_0 \\ 0 & \text{si } T < T_0 \end{cases}$$

where α_1 and α_3 are natural growth factors, α_2 and α_4 are factors related to tourist actions and policies, k 's are asymptotic population limits, and h is the Heaviside function [1,2].

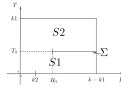


Fig. 1. State space for the Filippov system

Dynamics are defined by different systems of differential equations in regions S1 and S2, being Σ the switching surface (Fig.1). On this surface, the set of crossing points are represented by a dashed curve. In the dashed curve, the projection of the dynamics in the normal surface direction of the two sub-systems are non-zero and have the same sign. The orbits of the Filippov system cross the surface, i.e. the orbit reaching a point x on the surface from S_i , concatenates with the orbit entering S_j ($j \neq i$) from x . The solid curve corresponds to sliding points. The projections of the dynamics on the solid part of the switching surface are non-zero and have different sign. In this case this set is a stable segment. Orbits reaching one of these points, from either region, slide on the surface.

2. Results and Discussion

2.1 Invariance.

Invariance in the state space (R, T) has been analyzed. R and T axes are invariant, and the other lines which determine the rectangle are not crossed by the orbits. This allows us to ensure that for $\alpha 2 > 0$ and $\alpha 4 > 0$ an orbit that begins at an interior point, remains in the rectangle determined by the coordinated axes and the lines $R = k - k1$ and $T = k1$.

2.2 Equilibrium points.

In S1 we have found 3 unstable equilibrium points (named E1, E2 and E3) on the R axis. There are saddle and sources, but none of them corresponds to attractors, which would mean the extinction of the tourists or tourist and resident populations. In S2 we have found an equilibrium point E4 located on the T axis and the equilibrium points resulting from the possible intersection of two curves. The existence from one to five equilibrium points in S2 depends on the T_0 value. The stability of the equilibrium points has been analysed using MatLab. E4 is a stable point. This case would correspond to the disappearance of the residents and the total occupation of the city by the tourists. On the switching surface, sliding points and pseudo-equilibrium points [3] deserves special attention.

3. Concluding Remarks

The relationship between tourist and resident populations has been modeled using a piecewise smooth Filippov system. The equations, for a determined set of parameters, have been solved analytically and numerically (using MatLab). Invariance, equilibrium points, bifurcations, and switching surface have been studied. The obtained results can be associated with situations of stability decrease, increase, or disappearance of tourist and resident populations.

Acknowledgment: Authors acknowledge Department of Applied Maths for their support. MatLab is running under UPC academic license 1113606.

References

- [1] TRULLOLS E., MASSANA I., PRAT J, ANTONIJUAN J, OLIVAR G.: Title of paper. Nonlinear tourist flows in Barcelona. *Perspectives in Dynamical Systems II: Mathematical and Numerical Approaches*. DSTA 2019.
- [2] CHOLO I., MASSANA I., OLIVAR G., PRAT, J., TRULLOLS E.: Bifurcations in a Model of Natural Resources and Human Activity. *World Conference on Natural Resource Modeling*. Barcelona. 2017.
- [3] FILIPPOV AF.: Differential Equations with Discontinuous Righthand Sides. *Springer*. 1988..

Real and Noise-Induced Bubbling: Geometric Approach and Problem of Initial Deviation

VIKTOR AVRUTIN¹, FRANK BASTIAN^{2*}, LASSE VON SCHWERIN-BLUME³,
ZHANYBAI T ZHUSUBALIYEV⁴, ABDELALI EL AROUDI⁵

1. IST, University of Stuttgart, Germany [ID 0000-0001-7931-8844]
2. Department of Applied Mathematics, University College Cork, Ireland and IST, University of Stuttgart, Germany [ID 0000-0003-1910-024X]
3. IST, University of Stuttgart, Germany [ID 0000-0002-4546-8606]
4. Department of Computer Science, Dynamics of Non-Smooth Systems International Scientific Laboratory, Southwest State University, Russia [ID 0000-0001-5534-9902]
5. Departament d'Enginyeria Electronica, University Rovira I Virgili, Tarragona, Spain [ID 0000-0001-9103-7762]

* Presenting Author

Abstract: We explain the mechanisms leading to the bubbling phenomenon, i.e., high-frequency oscillations disrupting the waveform of slowly oscillating signals in a restricted phase interval.

Keywords: Bubbling, Simmering, Power Converters, Inverters

1. Introduction

The term bubbling refers to a phenomenon manifesting itself as high-frequency oscillations that disrupt the waveform of a slowly oscillating signal in a restricted phase interval. Although this phenomenon has been known for more than 20 years and observed (both numerically and experimentally) in all kinds of power electronic converters, no convincing explanation of the mechanism behind its occurrence has been found. It has been reported in many publications it occurs after a smooth bifurcation, such as a pitchfork or Neimark-Sacker, and therefore, it has been widely assumed that bubbling is caused by these bifurcations, although the specific mechanism leading to the onset of bubbling remained unknown. Recently, the onset of bubbling has been observed (both experimentally and numerically, see Fig 1(a) and (b), respectively) in a power electronic inverter that does not exhibit any smooth bifurcations in the relevant parameter domain.

The specific model considered in the presented work describes the behavior of the inverter system mentioned above and is given by a 1D non-autonomous piecewise smooth map (1) $x_{k+1} = f(x_k, k)$ presented in [1]. The signals of the considered inverter correspond to m -cycles of map (1), where the ratio $m=200$ is the ratio between the fast switching frequency and the low reference frequency.

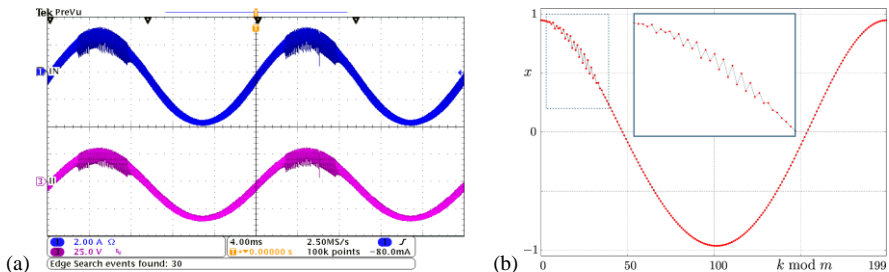


Fig. 1. Bubbling-affected orbits observed (a) experimentally, (b) numerically in discrete time.

2. Results

The first significant result we obtained has been reported in [1]. We have shown that in both cases, (i.e., the onset of bubbling associated with smooth bifurcation, as previously reported, and without as recently discovered) *the mechanism leading to bubbling is of a geometric rather than a topologic nature*. In fact, we identified regions in the state space such that an orbit passing through these regions (non-bubbling intervals) at all phases is not bubbling-affected. If at some phase the point x_k leaves the non-bubbling interval, it exhibits bubbling at this phase.

Furthermore, we discovered a novel phenomenon, called *simmering*, which represents a weaker form of phase-dependent distortion of the signal and manifests itself as bubbling of the first order forward differences (derivative with respect to discrete time). For this phenomenon, similar regions (non-simmering intervals) can be defined. Moreover, the procedure can be generalized for higher-order derivatives, which leads to a sequence of the rank- i non-bubbling intervals in the state space associated with non-bubbling of the i -th derivative. Typically, at each phase, these intervals are nested into each other so that the onset of bubbling of the i -th derivative precedes – in the state space as well as in the parameter space – the onset of bubbling of the $(i-1)$ -th derivative. This demonstrates that *the onset of bubbling is a gradual process*. For example, the onset of simmering precedes the onset of bubbling and can be used, from a practical point of view, as a kind of an early warning system.

The presented geometric approach to bubbling does not explain the reason why an orbit may leave the non-bubbling intervals in a well-defined and clearly restricted phase interval. To understand the reason, note that the behavior of the function $f(x, k)$ can be described by a set of m autonomous functions $f_i(x)$ which – depending on the phase k – may be contractive or expanding. A general property of models for various power converters is that they may have a long phase interval associated with expanding functions only, followed by a phase interval in which all functions are contractive. A *small deviation at the beginning of the expanding phase interval gets amplified by expanding functions, causing the orbit to leave non-bubbling intervals of decreasing ranks*.

We have identified several reasons that cause this initial deviation. In the case that bubbling occurs after a smooth bifurcation, e.g. a pitchfork, the normal form of this bifurcation forces the “new” orbits appearing at the bifurcation to move quickly apart from the “old” orbit which existed before. As a consequence, the “old” (unstable) orbit remains not bubbling-affected, while the “new” solutions successively leave the non-bubbling intervals of decreasing ranks and start to exhibit bubbling. Therefore, the onset of bubbling does not occur immediately at the bifurcation point, as previously assumed, but very soon after. A similar effect may be caused by a persistence border collision, which does not change the stability or the periodicity of the cycles, but may lead to bubbling.

The most unexpected phenomenon we discovered is *noise-induced bubbling*. In this case, the cycles of map (1) are not bubbling-affected, while the signals observed in experiments exhibit well-developed bubbling. Here, the deviation is caused by noise which is omnipresent in physical experiments and gets strongly amplified by expanding functions. Moreover, in numerical simulations, this kind of bubbling occurs as well. Here, the deviation is caused by numerical noise, i.e. the limited precision of floating-point numbers. So, as a curious feature, both physical experiments and numerical simulations might exhibit bubbling while the ideal solution is not bubbling-affected. In this way, map (1) can be used to predict *whether* bubbling occurs and at *which part of the phase domain*, but cannot predict *at which parameter values* unless a suitable noise model is added.

Acknowledgment: The work of V. Avrutin and F. Bastian was supported by the German Research Foundation within the scope of the project “Generic bifurcation structures in piecewise-smooth maps with extremely high number of borders in theory and applications for power converter systems”.

References

- [1] V. AVRUTIN, F. BASTIAN, ZH. T. ZHUSUBALIYEV: A geometric approach to bubbling. *Physica D* 2021,

Border Collision Bifurcations of Chaotic Attractors

VIKTOR AVRUTIN^{1*}, ANASTASIIA PANCHUK², IRYNA SUSHKO³

1. IST, University of Stuttgart, Germany [[ORCID](#) 0000-0001-7931-8844]

2. Institute of Mathematics, NAS of Ukraine, Kyiv, Ukraine [[ORCID](#) 0000-0003-1705-602X]

3. Institute of Mathematics, NAS of Ukraine, Kyiv, Ukraine [[ORCID](#) 0000-0001-5879-0699]

* Presenting Author

Abstract: In 1D piecewise-smooth maps with multiple borders, chaotic attractors may undergo border collision bifurcations, leading to a sudden change in their structure. We describe two types of such border collision bifurcations and explain the mechanisms causing the changes in the geometrical structure of the attractors, in particular in the number of their bands (connected components).

Keywords: piecewise smooth systems, 1D maps, chaotic attractors, border collision bifurcations

1. Introduction

Border collision bifurcations are well-known and represent the main distinguishing feature of piecewise smooth systems [1]. A border collision bifurcation occurs as, under parameter variation an invariant set collides with a border (switching manifold), causing the topological structure of the state space to change. A natural question is, which invariant sets can undergo a border collision bifurcation? For historical reasons, most investigated are border collision bifurcations of fixed points and cycles. As for chaotic attractors, the possibility that they also may undergo a border collision bifurcation has been overlooked for a long time. Indeed, in the most widely investigated class of piecewise smooth 1D maps, namely, in piecewise monotone maps with a single border, a chaotic attractor cannot collide with the border, since if a map belonging to this class has a chaotic attractor, the point of discontinuity is necessarily located inside the attractor [2].

In 1D maps with multiple (at least two) borders, collisions of a chaotic attractor with the borders are possible and may lead to quite interesting bifurcation phenomena, as illustrated in Fig. 1. As one can see, the chaotic attractors are robust in the complete considered parameter range (in the sense of [3], i.e., not interrupted by periodic windows and not affected by coexistence). However, at certain parameter values the geometric structure of the attractor change, additional gaps or bands of the attractors appear. The bifurcation of chaotic attractors known for maps with a single discontinuity (such as merging and expansion bifurcations) are not sufficient to explain the observed structure.

2. Results

In the present work, we investigate bifurcations of chaotic attractors in the piecewise linear map with two discontinuities, defined by

$$x_{n+1} = f(x_n) = \begin{cases} f_{\mathcal{L}}(x_n) = a_{\mathcal{L}}x_n + \mu_{\mathcal{L}} & \text{if } x < -1, \\ f_{\mathcal{M}}(x_n) = a_{\mathcal{M}}x_n + \mu_{\mathcal{M}} & \text{if } -1 < x < 1, \\ f_{\mathcal{R}}(x_n) = a_{\mathcal{R}}x_n + \mu_{\mathcal{R}} & \text{if } x > 1. \end{cases} \quad (1)$$

with $a_{\mathcal{L}}=a_{\mathcal{M}}=a_{\mathcal{R}}=a > 1$. Note that the linearity of the branches of map (1) simplifies the calculations but does not restrict the generality of the analysis, so that the obtained results are applicable to any piecewise monotonous everywhere expanding map with two discontinuities.

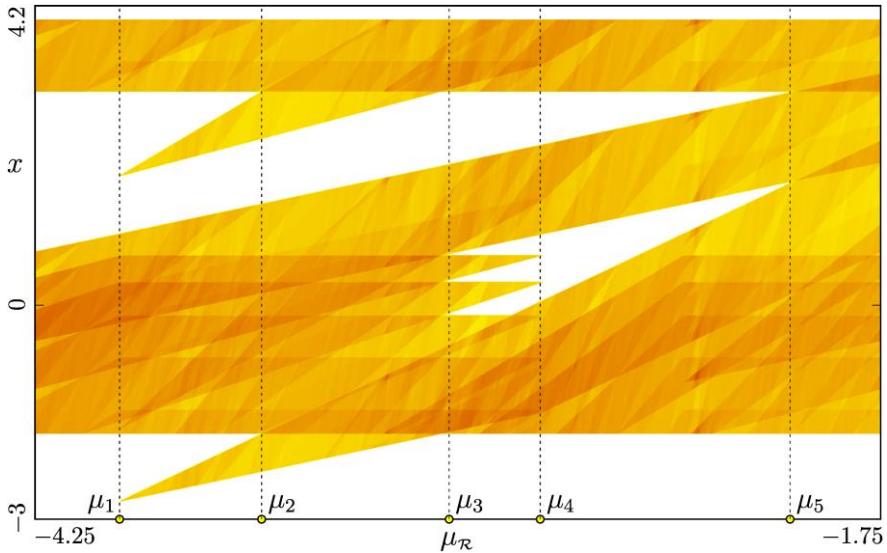


Fig. 1. Bifurcation scenario in map (1) showing exterior (μ_1, μ_4) and interior (μ_2, μ_3, μ_5) border collision bifurcations of chaotic attractors. Parameters: $a=1.25, \mu_L=4.0, \mu_M=4.0$,

So far, we have detected two novel types of bifurcations:

- *Exterior border collision bifurcation of a chaotic attractor:* The bifurcation occurs as a chaotic attractor containing one discontinuity point collides with another discontinuity point. As a result of this bifurcation, a number of additional bands of the attractor appear. A distinguishing feature of this bifurcation is that the size of the additional bands shrinks to zero as the varied parameter approaches the bifurcation value.
- *Interior border collision bifurcation of a chaotic attractor:* The bifurcation occurs as a critical point (an image of a discontinuity) located inside a chaotic attractor and possessing exactly two preimages inside the absorbing interval collides with another critical point and one of its preimages disappears. As a result of this bifurcation, a number of additional gaps in the attractor appear. Here, the size of the additional gaps shrinks to zero as the varied parameter approaches the bifurcation value.

It is worth emphasizing that none of these bifurcations of chaotic attractors are associated with homoclinic bifurcations of repelling cycles. This is a striking difference between these bifurcations and other transformations of chaotic attractors, such as merging, expansion and final bifurcations previously reported [2].

Acknowledgment: The work of V. Avrutin was supported by the German Research Foundation within the scope of the project “Generic bifurcation structures in piecewise-smooth maps with extremely high number of borders in theory and applications for power converter systems”.

References

- [1] M. DI BERNARDO, C. BUDD, A. CHAMPNEYS, P. KOWALCZYK. *Piecewise-smooth dynamical systems: theory and applications*. Springer, 2008.
- [2] V. AVRUTIN, GARDINI, L., SUSHKO, I., TRAMONTANA, F. *Continuous and discontinuous piecewise-smooth one-dimensional maps: invariant sets and bifurcation structures*. World Scientific, 2019

Codimension-2 Bifurcations in a Quantum Decision Making Model

VIKTOR AVRUTIN¹, ARIANNA DAL FORNO^{2*}, UGO MERLONE³

1. IST, University of Stuttgart, Germany [[ORCID](#) 0000-0001-7931-8844]

2. Department of Economics, University of Molise, Campobasso, Italy [[ORCID](#) 0000-0003-0500-3852]

3. Department of Psychology, Center for Logic, Language, and Cognition, University of Torino, Italy [[ORCID](#) 0000-0002-8559-4914]

* Presenting Author

Abstract: We show how a complex bifurcation structure in a 2D parameter space of a piecewise linear discontinuous 2D map modeling the dynamics of a binary choice game using quantum logic can be explained by a few codimension-2 bifurcation points of a type not yet reported in the literature.

Keywords: Border collision bifurcations, Codimension-2 bifurcations, Period adding, Quantum cognition, Binary choices

1. Introduction

Since the influential work of Schelling [1], binary choice games with externalities have become central within social dilemma literature. Previous literature has developed models with agents' behavior mainly based on classical probability. However, recent theoretical and empirical findings have shown how the recurrent contextual effects observed in the psychological literature are better predicted by quantum probability theory [2]. The dynamical population model proposed in [3] introduces quantum cognition in the Schelling model of binary choices (for instance, *left* and *right*) in a minority game. For the sake of simplicity, we assume the population is unitary and variable x is the proportion of population who choose *right*. In order to describe the effect of past choices, the revision protocol of the agents' internal state is given by the context effect rule provided by quantum cognition theory. The phase space $U = [0,1]^2$ is partitioned in four regions:

$$\begin{aligned} U_L &= \{(x_{t-1}, x_t) \in U: x_{t-1} > 1/2, x_t > 1/2\} & U_r &= \{(x_{t-1}, x_t) \in U: x_{t-1} > 1/2, x_t < 1/2\} \\ U_l &= \{(x_{t-1}, x_t) \in U: x_{t-1} < 1/2, x_t > 1/2\} & U_R &= \{(x_{t-1}, x_t) \in U: x_{t-1} < 1/2, x_t < 1/2\} \end{aligned}$$

2. Results

According to the quantum model, the population dynamics $F : U \rightarrow [0,1]$ considers both time periods:

$$F(x_{t-1}, x_t) = \begin{cases} f_L(x_{t-1}, x_t) = (1 - \sin^2 \alpha \cos^2 \beta) x_t & \text{if } (x_{t-1}, x_t) \in U_L \\ f_r(x_{t-1}, x_t) = (1 - \sin^2 \alpha \sin^2 \beta) x_t + \sin^2 \alpha \sin^2 \beta & \text{if } (x_{t-1}, x_t) \in U_r \\ f_l(x_{t-1}, x_t) = (1 - \cos^2 \alpha \sin^2 \beta) x_t & \text{if } (x_{t-1}, x_t) \in U_l \\ f_R(x_{t-1}, x_t) = (1 - \cos^2 \alpha \cos^2 \beta) x_t + \cos^2 \alpha \cos^2 \beta & \text{if } (x_{t-1}, x_t) \in U_R \end{cases}$$

where: $\alpha \in [0, \pi/2]$ defines the unit vector representing the initial decision makers' beliefs about the two choices; $\beta \in [0, \pi/2]$ the vector representing the revised decision makers' beliefs induced by the previous choice. In the following, values $\alpha, \beta = 0$ and $\alpha, \beta = \pi/2$ are referred to as *edges* of the parameter space (although they represent rather symmetry axes than borders). As state variable x_{t-1} appears on the right hand side in the conditions associated with the functions f_l, f_r, f_L, f_R only, the map can also be considered as a piecewise linear bi-valued map with a single border point $x = 1/2$. Functions f_l, f_r, f_L, f_R are contractive and increasing w.r.t. x_t , by construction.

The bifurcation structure in the (α, β) parameter space is illustrated in Fig. 1. It is symmetric w.r.t $\alpha = \pi/4$ and affected by bistability for $\beta < \pi/4$. In the middle of the structure there is a large region asso-

ciated with a 2-cycle O_{lr} and bounded by curves ξ_{lr} and $\xi_{r'l}$ where this cycle undergoes border collision bifurcations (BCBs). The intersection points P_1 and P_2 of these curves with edge $\beta=\pi/2$ represent two organizing centers (two codimension-2 bifurcation points) where two complete period adding structures originate from.

A theory for codimension-2 BCBs in single-valued 1D maps was developed in [4]. In particular, it was shown that at a codimension-2 BCB point –where two different stable cycles collide with the discontinuity from opposite sides– the composite function (defined by the branches of the iterate functions for which the colliding cycles are fixed points) is *continuous*. Then, it was shown that if both involved functions are *contractive* and *locally increasing*, then a complete period adding structure issues from the corresponding codimension-2 BCB point. This theory cannot be directly applied to the points P_1 and P_2 , as the edge $\beta=\pi/2$ does not correspond to a BCB. At $\beta=\pi/2$ however, the map has infinitely many fixed points O_L and O_R as f_l, f_r are identity functions. The case is similar to a degenerate+1 bifurcation, although not identical as the fixed points exist neither before nor after $\beta=\pi/2$. Nevertheless, some significant assumptions of the theorem mentioned above are satisfied: at P_1 the composed function defined by branches f_r and $f_r \circ f_l$ is continuous; both branches are increasing; at least branch $f_r \circ f_l$ is contractive. This suggests that, under the present setting, a theorem similar to the one in [4] can be proven: point P_1 must be the origin of a period adding structure with, for example, the regions of complexity level one being associated with cycles $O_{R(lr)^k}$ and $O_{R^k(lr)}$, in agreement with the numerical results.

The same reasoning can be applied to explain the complex bifurcation structure in the lower part of the parameter space. Several regions issuing from P_1 reach the left edge of the parameter space ($\alpha=0$). Then, the codimension-2 points defined by the intersections of one of their boundaries with this edge (at which functions f_l and f_r are identity functions) are the origins of a further complete period adding structure. The regions issuing from these points overlap both pairwise and with the regions issuing from P_1 , leading to bistability (see Fig. 1(b)).

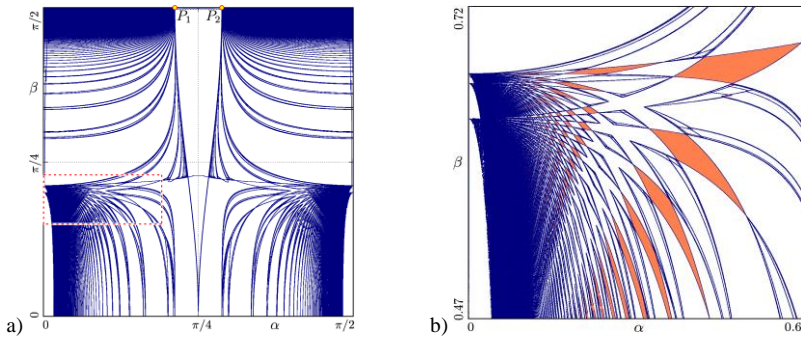


Fig. 1. a) Bifurcation structure in the (α, β) parameter plane. The rectangle in a) is shown magnified in b) where some regions of bistability are highlighted.

Acknowledgment: The work of V. Avrutin was supported by the German Research Foundation.

References

[1] SCHELLING T C. Hockey helmets, concealed weapons, and daylight saving. *J. Conflict Resolution* 1973, **17**:381–428.
 [2] BUSEMEYER J R, BRUZA P D: *Quantum models of cognition and decision*. Cambridge University Press: Cambridge, 2012.
 [3] DAL FORNO A, GRONCHI G, MERLONE U. Binary choices dynamics with quantum decision. *Int. J. Math. Psychology* 2021, **101**:102509.
 [4] GARDINI L, AVRUTIN V, SUSHKO I. Codimension-2 border collision bifurcations in one-dimensional discon-

Zip Bifurcation in PWSC Systems

CARLOS M. ESCOBAR-CALLEJAS¹, GERARD OLIVAR-TOST^{2,*}

1. Universidad Tecnológica de Pereira, Departamento de Matemáticas, Pereira, Colombia. email: ccescobar@utp.edu.co
2. Department of Natural Sciences & Technology, Universidad de Aysén, Coyhaique – Chile. email: gerard.olivar@uaysen.cl [0000-0003-1862-4842]

* Presenting Author

Abstract: This communication extends the concept of zip bifurcation introduced by Miklos Farkas in 1984 in a smooth dynamical system, describing the competition de two predator species for a single regenerating prey species, to a set of PieceWise-Smooth Continuous (PWSC) dynamical systems, that have a continuous set of equilibria, with a discontinuous Jacobian. It also shows a strategy for dynamics classification based on the eigenvalues, for the case which the local two-dimensional invariant manifolds of the system exist. Analysis on the dynamic and asymptotic behavior is obtained through the real and imaginary components of the eigenvalues, associated to the system linearity along its equilibria set. We choose a criterion of geometric classification of bifurcation that preserves information about the stability, topology of the invariant set and the geometry of node and focus on a neighborhood of the isolated hyperbolic equilibrium points. Based on the results obtained in the analysis we show that the zip bifurcation discovered by Farkas is part of a more complex phenomenon. It includes the combination of two geometrical bifurcations caused by simultaneous action of the real and imaginary components of the eigenvalues associated to the system linearity along its equilibria set. The complete bifurcation scenario includes 142 geometric zip bifurcations for the class of PWSC systems studied.

Keywords: Hopf Bifurcation, Zip Bifurcation, k- and r-strategists, PWSC systems.

1. Introduction

In ecology, in studying population dynamics, it is important to know under which ecosystem conditions the coexistence of closely related species is possible or under what circumstances the principle of competitive exclusion acts (as Harden called it in 1940). The previous principle is also known as Gause's principle, in honor of the Russian biologist who observed it in 1932 in the separation of species in experimental crops. Hutchinson and Deevey state that the Gause hypothesis or principle of competitive exclusion is one of the most significant advances in theoretical ecology and one of the foundations of modern ecology. The principle of competitive exclusion is considered as one of the primary mechanisms for the process of natural selection and, therefore, the origin and evolution of species through both intraspecific and interspecific competition.

Specifically, in this work, it is shown that the occurrence of Hopf and zip bifurcations can be extended to a class of Continuous PWS nonlinear systems, which have a continuous set of equilibria. Along the length of the continuous set, the Jacobian matrix of the system is discontinuous and satisfies the Butler-Farkas conditions [1]. We present a strategy for the demonstration of the existence and classification of the so-called PWSC-Zip bifurcation. We base our approach on studying the dynamics of the eigenvalues of the linearization of both vector fields along the set of equilibria. The previous procedure

is done for the case in which the PWSC system preserves each subsystem's local two-dimensional invariant manifolds that cross-intersect the equilibrium segment. When the commutations destroy the local two-dimensional invariant manifolds, it is shown that even the phenomenon of loss of attractiveness is preserved for the equilibrium segment. In this case, the stability of the interior points of the equilibrium segment cannot be determined by linearization.

2. Results and Discussion

Four numerical examples of PWSC models are built up using Mathematica software. The models preserve the two-dimensional local invariant manifolds. Four more examples of PWSC models that maintain only the attractiveness of the equilibrium segment are also created. They represent natural and artificial models of algebraic exponential type and generalize the Gilpin logistic growth model for the prey reproduction rate and the Holling III and Rosenzweig type models for the functional response of the predator. The models were found to satisfy the necessary conditions proposed by Butler and Farkas in each of the subsystems of the PWSC system and the compatibility conditions. As a consequence of the above, the Hsu et al. model is generalized to PWSC systems in the case studied by Wilken [2] and Farkas [3], that is, for the three-dimensional case.

References

- [1] BUTLER, G. J. (1983). Competitive predator-prey systems and coexistence, in population biology. *Lecture Notes in Biomathematics*. 52: 210- 299. Berlin: Springer-Verlag.
- [2] WILKEN, D. R. (1982). Some remarks on a competing predators problem. *SIAM J. appl. Math.* 42: 895-902.
- [3] FARKAS, M. (1984). Zip bifurcation in a competition model. *Nonlinear analysis TMA*, 8: 1295-1309.

Piecewise smooth systems with a pseudo-focus: a normal form approach

MARINA ESTEBAN^{1*}, EMILIO FREIRE², ENRIQUE PONCE³, FRANCISCO TORRES⁴

Common Affiliation: Universidad de Sevilla, Av. de los Descubrimientos s/n. 41092 Sevilla, Spain.

1. [0000-0001-6440-6825] 2. [0000-0001-5852-0699] 3. [0000-0003-0467-5032] 4. [0000-0003-2907-8496]

* Presenting Author

Abstract: The analysis of planar systems with a pseudo-equilibrium point of focus type within its discontinuity line can be more easily done if the classical theory of normal forms is extended for such a case. This methodology allows to remove unessential terms in the expression of the vector field, preserving every point of the discontinuity line and so possible periodic orbits. The approach will be illustrated by considering a rather general family of linear-quadratic planar systems.

Keywords: Discontinuous Systems, Pseudo-Focus, Normal Forms.

1. Introduction

We consider planar piecewise smooth systems with a straight line as the discontinuity manifold. Our main hypothesis is the existence of a pseudo-focus at the origin coming from the collision of an invisible tangency from each side. Our goal is to develop a methodology for the analysis of the dynamics in a neighbourhood of the pseudo-focus, characterizing its stability. In the non-hyperbolic cases, when the pseudo-focus behaves as a weak-focus, we look for the determination of its weakness order, which is associated to the maximum number of limit cycles that can be obtained by perturbation.

The followed approach is based in the obtention of a normal form by making successive near-identity changes of variables and time reparameterizations that must preserve the points of the discontinuity line. The achieved normal form is specially suitable for building the half-return maps, which are the main tools for the analysis.

2. Results and Discussion

Under our hypotheses, we can start from the system

$$\begin{aligned} \dot{x} &= a_{10}^{\pm}x - y + \sum_{p+q \geq 2} a_{pq}^{\pm}x^p y^q \\ \dot{y} &= \pm 1 + b_{10}^{\pm}x + b_{01}^{\pm}y + \sum_{p+q \geq 2} b_{pq}^{\pm}x^p y^q \end{aligned} \quad \text{if } \pm x \geq 0, \quad (1)$$

where the dot represents derivatives with respect to the time variable and such derivatives for the second variable have been normalized in both sides.

Our main result is as follows.

Theorem. For any natural number n , system (1) is, in a neighbourhood of the origin, topologically equivalent to a systems of the form

$$\begin{pmatrix} \dot{x} \\ \dot{y} \end{pmatrix} = \begin{pmatrix} -y + \sum_{k=1}^n \mu_{2k}^{\pm} y^{2k} \\ \pm 1 \end{pmatrix} + \sum_{k \geq 2n} \mathbf{G}_k^{\pm}(\mathbf{x}), \quad (2)$$

where the symbol ‘+’ applies for the right side and the symbol ‘-’ does for the left side, and the final terms \mathbf{G}_k are quasi-homogeneous polynomial vector fields of type (2,1) and degree k , in the terminology of the theory of quasi-homogeneous vector fields.

The coefficients of the even powers in the variable y are obtained in an algorithmic way in terms of the coefficients of system (1). Thanks to the above theorem, it is possible to compute in a straightforward way the coefficients of the half-return maps. We take advantage of the fact that such half-return maps are analytical involutions at the origin. We apply such procedure to a rather general family of linear-quadratic systems emphasizing the maximum number of limit cycles than can bifurcate from the origin.

3. Concluding Remarks

Specific normal forms are proposed for non-smooth systems with a pseudo-focus point, looking for facilitating the computations of the half-return maps, getting also an easy characterization of the order for the pseudo-focus. As a corollary, the maximal number of bifurcating limit cycles from perturbations without introducing sliding sets is obtained.

As a relevant application, we start the study of linear-quadratic systems with a pseudo-focus, which even not completely finished has already given rise to a rich variety of behaviors.

Acknowledgment: Authors are partially supported by the Ministerio de Economía y Competitividad, Spain, in the frame of project PGC2018-096265-B-I00, and by the Consejería de Economía y Conocimiento de la Junta de Andalucía, Spain, under grant P12-FQM-1658.

References

- [1] A. ALGABA, E. FREIRE, E. GAMERO AND C. GARCIA, Quasi-homogeneous normal forms, *Journal of Computational and Applied Mathematics*, 150 (2003), 193–216.
- [2] A.F. FILIPPOV, *Differential equations with discontinuous righthand sides*, Kluwer Academic Publishers Group, Dordrecht, 1988.
- [3] M. HAN AND W. ZHANG, On Hopf bifurcation in non-smooth planar systems, *Journal of Differential Equations*, 248 (2010), 2399–2416
- [4] F. LIANG AND M. HAN, Degenerate Hopf Bifurcations in Nonsmooth Planar Systems, *International Journal of Bifurcations and Chaos*, 22 (2012), 1250057.

Hidden dynamics of maps (and when “period 2 implies chaos”)

MIKE JEFFREY^{1*}, VIKTOR AVRUTIN²

1. Department of Engineering Mathematics, University of Bristol, Ada Lovelace Building, Bristol UK
2. Institute for Systems Theory and Automatic Control, University of Stuttgart, Pfaffenwaldring 9, 70550 Stuttgart, Germany

* Presenting Author

Keywords: nonsmooth, map, discontinuity, hidden dynamics, bifurcation, stability

The term ‘hidden dynamics’ describes behaviour associated with discontinuities in nonsmooth dynamical systems, behaviour this is only evident by careful study of the discontinuity itself. First introduced in continuous time flows in 2013, hidden dynamics was only found in discrete time systems last year in [1]. Hidden periodic orbits have been shown to ‘fill the gaps’ in bifurcations and period adding cascades, so that rather than attractors in nonsmooth maps being able to appear and disappear or change period seemingly arbitrarily, as seemed to be the case until now, they in fact follow familiar bifurcations such as folds and flips well known from continuous systems.

In a discrete time system, a hidden orbit is an infinitely unstable trajectory that involves at least one iterate lying on a point of discontinuity. Hidden orbits can form periodic or chaotic structures much like regular orbits. Like standard unstable orbits, they help organise bifurcation structures and basins of attraction. By accounting for hidden orbits, maps with discontinuities can be shown to obey the rule that ‘period 3 implies chaos’ (or Sharkovskii’s theorem more generally) that until now appeared to require a map to be continuous.

In fact, as we will show here, nonsmooth systems obey a surprising form of this result, namely that ‘period 2 implies chaos’. We will show the conditions under which this implies, and by considering a nonsmooth map to be the singular limit of a continuous map, show how one interprets hidden orbits as unstable structures, and show that if we smooth out a discontinuity, a period 2 orbit perturbs to form orbits of period 3 (and hence all periods in accordance with Sharkovskii’s theorem).

Finally, for the first time, we will show hidden orbits in applied models, taking a model of the homeostatic cycles between sleep-wake transitions, a model of growth and mitosis in yeast cells, and in a toy model of such processes as a 2-dimensional nonsmooth oscillator.

References

- [1] M. Jeffrey and S. Webber. The hidden unstable orbits of maps with gaps. Proc. R. Soc. A, 476(2234):20190473, 2020

Non-smooth Dynamics in Ramp-controlled and Sine-controlled Buck Converters

JOSÉ D. MORCILLO^{1*}, JUAN-GUILLERMO MUÑOZ², GERARD OLIVAR-TOST³

1. Universidad de Monterrey, Escuela de Ingeniería y Tecnologías. Monterrey, 66238 – Mexico. E-mail: jose.morcillo@udem.edu.mx [0000-0002-4545-8969]
2. Instituto Tecnológico Metropolitano. Departamento de Mecatrónica y Electromecánica. Medellín, 050013 – Colombia. E-mail: juanmunozc@itm.edu.co [0000-0001-5496-6503]
3. Department of Natural Sciences & Technology, Universidad de Aysén, Coyhaique – Chile. E-mail: gerard.olivar@uaysen.cl [0000-0003-1862-4842]

* Presenting Author

Abstract: The DC-DC Buck converter is a power converter system that converts high DC voltages to low DC voltages and is widely used in several applications. However, different non-smooth dynamics have been found especially in the ramp-controlled buck converter configuration that lead to undesired behaviors, due to the non-smooth nature of the ramp signal. As a consequence, we propose to change the ramp signal by a sine waveform as a smooth alternative to the non-smoothness of the ramp waveform, and thus try to avoid the non-smooth behaviors of the buck converter system. Nevertheless, we found that non-smooth dynamics remain present in the system even by using a smooth sine waveform instead of a non-smooth ramp waveform. In fact, a new variety of non-smooth bifurcations were found.

Keywords: buck converter, sine-control, ramp-control, non-smooth dynamics, bifurcations.

1. Introduction

DC-DC power converters have become a very relevant research area due to their applicability in a variety of electronic devices. Fig. 1(a) shows the Buck converter system under ramp- and sine-controlled schemes, and its ordinary differential equations are defined as in [2]. A_1 is an amplifier that has gain a , and V_{ref} is the reference voltage; therefore, the control voltage is given by $V_c(t) = a(V_c(t) - V_{ref}(t))$. A_2 is a comparator that generates the control action u , and in this case, in order to compare the sine-control with the ramp-control scheme, the buck converter is studied using a ramp and a sine waveform as T -periodic signals. Hence, u commutes between 1 or 0 when $V_c(t) < V_s(t)$ (or $V_{ramp}(t)$) or $V_c(t) > V_s(t)$ (or $V_{ramp}(t)$) respectively. V_s and V_{ramp} are the periodic sine and ramp waveforms ($T = 400 \mu s$), respectively, and are defined as follows:

$$v_s(t) = V_{LO} + \left(\frac{V_u - V_{LO}}{2} \right) \left(1 + \sin \left(\frac{2\pi t}{T} \right) \right); V_{ramp}(t) = V_{LO} + (V_u - V_{LO}) \frac{t}{T} \quad (1)$$

where V_{LO} and V_u are respectively the lower and upper voltages of the ramp or sine waveforms. The component values used are: $L=20\text{mH}$, $R=22\Omega$, $C=47\mu\text{F}$, $V_{ref}=12\text{V}$, $V_u=8.2\text{V}$, $V_{LO}=3.8\text{V}$, $T=400\mu\text{s}$, $a=8.4$.

2. Results and Discussion

As can be seen in Figs. 1(b)-(c), both smooth and non-smooth bifurcations appear in the ramp-controlled system, as it has been investigated by other authors several years ago [1]-[3]. However, smooth

and non-smooth bifurcations also appear in the sine-controlled system under the same parameter variation (see Figs. 1(d)-(e)). Even though it was changed the non-smooth ramp signal by a smooth sine waveform, non-smooth bifurcations still remain. In fact, note from Fig. 1(e) that a cascade of border collision bifurcations appears, a phenomenon only seen in power inverter systems [4].

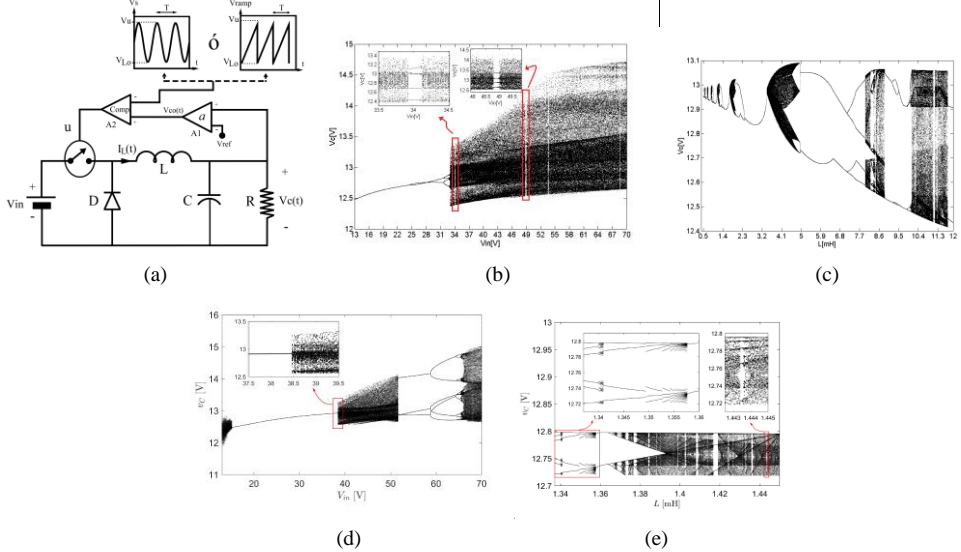


Fig. 1. (a) PWM-controlled DC-DC Buck converter using a sine or a ramp waveform. Bifurcation diagrams of V_c taking (b) V_{in} and (c) L as bifurcation parameters in the ramp-controlled system. Bifurcation diagrams of V_c taking (d) V_{in} and (e) L as bifurcation parameters in the sine-controlled system.

3. Concluding Remark

By changing the T -periodic signal changes radically the system dynamics. Nevertheless, it does not matter if the T -periodic signal is smooth (sine waveform) or non-smooth (ramp-waveform), complex behaviors are still present and non-smooth bifurcations cannot be avoided. In fact, by using a T -periodic sine waveform a cascade of border collision bifurcations was obtained, a phenomenon only seen in power electronic inverters [4]. Even though the T -periodic signal is smooth, tangent bifurcations occurs [3] and non-smooth behaviors appear. This suggests that no matter which type of T -periodic signal is used, non-smooth bifurcations of border collision or tangent type always become evident.

Acknowledgment: José Morcillo wants to acknowledge Universidad de Monterrey for its support to this work.

References

- [1] DEANE, J. H., & HAMILL, D. C. (1990). Analysis, simulation and experimental study of chaos in the buck converter. in *21st annual ieee conference on power electronics specialists* (pp. 491-498). IEEE.
- [2] FOSSAS, E., & OLIVAR, G. (1996). Study of chaos in the buck converter. *IEEE Transactions on Circuits and Systems I: Fundamental Theory and Applications*, **43**(1), 13-25.
- [3] YUAN, G., BANERJEE, S., OTT, E., & YORKE, J. A. (1998). Border-collision bifurcations in the buck converter. *IEEE Transactions on Circuits and Systems I: Fundamental Theory and Applications*, **45**(7), 707-716.
- [4] AVRUTIN, V., MORCILLO, J. D., ZHUSUBALIYEV, Z. T., & ANGULO, F. (2017). Bubbling in a power electronic inverter: Onset, development and detection. *Chaos, Solitons & Fractals*, **104**, 135-152.

On Transformations of Closed Invariant Curves in Piecewise-Smooth Maps

ZHANYBAI T. ZHUSUBALIYEV^{1*}, VIKTOR AVRUTIN², FRANK BASTIAN³

1. Department of Computer Science, Dynamics of Non-Smooth Systems International Scientific Laboratory, Southwest State University, Russia [G0000-0001-5534-9902]
2. Institute for Systems Theory and Automatic Control, University of Stuttgart, Germany [G0000-0001-7931-8844]
3. Institute for Systems Theory and Automatic Control, University of Stuttgart, Germany and Department of Applied Mathematics, University College Cork, Ireland [G0000-0003-1910-024X]

* Presenting Author

Abstract: In this work we discuss a transformation of a smooth closed invariant curve associated with quasiperiodic dynamics into a piecewise smooth one, and its subsequent transitions to chaos. As an intermediate step, the latter transition involves a transformation of a closed invariant curve into a closed-invariant-curve-like chaotic attractor.

Keywords: closed invariant curve, closed invariant curve-like chaotic attractor, piecewise-smooth maps, expansion bifurcation, border collision

1. Introduction

Many problems in engineering and applied science lead us to consider piecewise-smooth maps. Examples of such systems include power-electronic and pulse-modulated control systems mechanical systems with dry friction or impacts, as well as systems involving thresholds, constraints, and decision-making processes in economics and social sciences. In addition to the bifurcations occurring in smooth systems, piecewise smooth systems demonstrate several further bifurcation phenomena, as, e.g., border collision bifurcations. For historical reasons, most deeply studied are bifurcations involving fixed points and cycles, which the corresponding effects for other kinds of invariant sets are still far away from being understood completely.

Closed invariant curves associated with quasiperiodic dynamics is a specific type of dynamic behavior characterized by two or more oscillatory modes with incommensurable frequencies. It is well-known that in smooth maps this type of dynamics appears via a Neimark–Sacker bifurcation, while in piecewise smooth maps it may also appear via a border collision bifurcation [1].

2. Results

In this work, we investigate a piecewise smooth 2D map introduces initially in [2] (see also [3])

$$\begin{pmatrix} x_{k+1} \\ y_{k+1} \end{pmatrix} = F(x_k, y_k), \quad F(x, y) = \begin{cases} F_L(x, y) & \text{if } (x, y) \in \mathcal{I}_L; \\ F_M(x, y) & \text{if } (x, y) \in \mathcal{I}_M; \\ F_R(x, y) & \text{if } (x, y) \in \mathcal{I}_R, \end{cases}$$

where

$$F_L(x, y) = \begin{pmatrix} e^{\lambda_1} x - e^{\lambda_1} + 1 \\ e^{\lambda_2} y - e^{\lambda_2} + 1 \end{pmatrix}; \quad F_M(x, y) = \begin{pmatrix} e^{\lambda_1} x - e^{\lambda_1} + e^{\lambda_1(1-z(x,y))} \\ e^{\lambda_2} y - e^{\lambda_2} + e^{\lambda_2(1-z(x,y))} \end{pmatrix}, \quad z(x, y) = \frac{\alpha\Gamma}{q} \left(x - \frac{\lambda_1}{\lambda_2} y \right)$$

with

$$\mathcal{I}_c = \{(x, y) \mid y < S_-(x)\}, \mathcal{I}_M = \{(x, y) \mid S_-(x) \leq y \leq S_+(x)\}, \mathcal{I}_R = \{(x, y) \mid y > S_+(x)\},$$

$$S_-(x) = \frac{\lambda_2}{\lambda_1} \left(x + \frac{q}{\Gamma} - \frac{q}{\alpha\Gamma} \right), S_+(x) = \frac{\lambda_2}{\lambda_1} \left(x + \frac{q}{\Gamma} \right)$$

and report two specific bifurcation scenarios [3]. Here $\lambda_1 = 0.03125 \cdot T_0$, $\lambda_2 = 0.003125 \cdot T_0$ and $q = 13.7278828553996$, $T_0 = 0.9$ s. The parameters α and Γ are control parameters.

In the first scenario, a smooth closed invariant curve associated with quasiperiodic dynamics appears via a Neimark–Sacker bifurcation and undergoes eventually a border-collision. As the dynamics on the closed invariant curve remains unchanged, this scenario can be seen as a kind of persistence border-collision for closed invariant curves. However, as a result of this transition the closed invariant curve becomes piecewise smooth, containing an infinite number of kink points given by the points at which the closed invariant curve intersects the switching manifold, and by the images of these points.

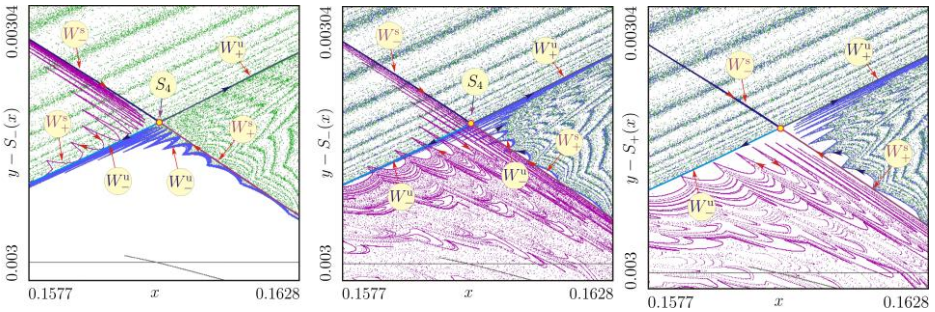


Fig. 1. Homoclinic bifurcation leading to the expansion of a closed-invariant-curve-like chaotic attractor to a large amplitude chaotic attractor. W_{\pm}^s, W_{\pm}^u are the stable and unstable manifolds of a saddle 4-cycle S_4 .

In the second scenario, we consider a transition from an attracting closed invariant curve to a large amplitude chaotic attractor. This transition resembles an expansion bifurcation well-known for chaotic attractors. However, for quasiperiodic attractors no similar bifurcations have been reported so far. In fact, it turns out that the transition takes place in two steps. As a first step, the closed invariant curve undergoes a homoclinic bifurcation and turns into a closed-invariant-curve-like chaotic attractor. Although the overall shape of this attractor very similar to the shape of the previously existing closed invariant curve (which can easily lead to misinterpretations), on a sufficient magnification level the fractal structure of the attractor is recognizable. Eventually, as a second step, the closed-invariant-curve-like chaotic attractor collides with a chaotic repeller and undergoes an expansion bifurcation, leading to the appearance of a large amplitude chaotic attractor.

Acknowledgment: The work of V. Avrutin and F. Bastian was supported by the German Research Foundation within the scope of the project “Generic bifurcation structures in piecewise-smooth maps with extremely high number of borders in theory and applications for power converter systems”.

References

- [1] ZHUSUBALIYEV ZH. T., MOSEKILDE E: Equilibrium-torus bifurcation in nonsmooth systems. *Physica D* 2008, **237**(7):930-936.
- [2] SIMPSON D.J.W: The structure of mode-locking regions of piecewise-linear continuous maps: I. Nearby mode-locking regions and shrinking points. *Nonlinearity* 2017, **30**(1):382-444.
- [3] ZHUSUBALIYEV ZH. T., AVRUTIN V., BASTIAN F: Transformations of closed invariant curves and closed-invariant-curve-like chaotic attractors in piecewise smooth systems. *Int. J. Bifurcation and Chaos* 2021,

-S6-

**New prospects in vibration
mitigation strategies**

On the dynamics of high-order beams with vibration absorbers

ANDREA BURLON^{1*}, GIUSEPPE FAILLA²

1. University of Reggio Calabria, Department of Civil, Energy, Environmental and Materials Engineering, Via Graziella, 89124 Reggio Calabria, Italy [0000-0002-1827-5382]
2. University of Reggio Calabria, Department of Civil, Energy, Environmental and Materials Engineering, Via Graziella, 89124 Reggio Calabria, Italy [0000-0003-4244-231X]

* Presenting Author

Abstract: A novel solution procedure is proposed for a class of high-order boundary value problems governing the dynamic response of beams equipped with vibration absorbers. Using the theory of generalized functions to model the reaction forces of the absorbers, the procedure applies in frequency and time domains. In the frequency domain, the key novelty is the derivation of the exact dynamic Green's functions under harmonic point loads. Further relevant novelties are analytical expressions for the modal response under arbitrary loads, in frequency and time domains. The procedure is general and provides elegant solutions for various engineering problems involving twisted beams, composite beams, coupled bending-torsion beams equipped with different types of absorbers.

Keywords: high-order beam, vibration absorber, generalized functions

1. Introduction

Beam structures equipped with vibration absorbers are generally modelled as one-dimensional continua coupled with point attachments. Typically, this model requires the solution of boundary value problems where the order of the differential equations depends on the beam characteristics, while generalized functions, as Dirac's deltas and/or its formal derivatives, model the reaction forces of the absorbers. In this work, we aim to propose a new and comprehensive mathematical framework providing exact solutions for high-order boundary value problems governing beams with vibration absorbers of relevant engineering interest.

First, we devise a general procedure to construct the exact dynamic Green's functions, which provide the beam frequency response to an arbitrarily placed harmonic point load. This result is based on deriving, in a concise analytical form, the solution of an arbitrary n -th order differential equation under Dirac's deltas and its formal derivatives. The exact dynamic Green's functions are the basis to obtain, by straightforward integration, the frequency response to arbitrarily placed harmonic distributed loads.

Next, orthogonality conditions are derived for the beam modes, which lead to analytical expressions of the modal response under arbitrary loads, in frequency and time domains. For this result, the key concepts are self-adjointness of the beam differential operators and derivation of frequency-dependent stiffness terms expressing the reaction forces of the absorbers. In this context, modes and eigenvalues are derived from a dynamic-stiffness approach, built based on the exact dynamic Green's functions.

The proposed framework encompasses a wide variety of beams, as twisted beams [1], composite beams [2] and coupled bending-torsion beams [3], the equilibrium of which is governed by high-order differential equations of various order, depending on the beam characteristics. Moreover, the frame-

work is appropriate for different types of absorbers, as mass-spring chains or inerter-based absorbers. Viscous damping within the absorbers may be also included.

2. Results and Discussion

We consider the coupled bending-torsion beam shown in Fig. 1, equipped with a tuned mass damper (TMD) at $y=0.5L$. The proposed framework can be used to calculate, e.g., the exact dynamic Green's functions shown in Fig. 2, under a harmonic point load at $y_0=0.275L$. $H(\omega)$ and $\Psi(\omega)$ are the bending deflection and the torsional rotation. The following parameters are considered: $m=7.83 \text{ kgm}^{-1}$, $I_\alpha=0.055 \text{ kgm}$, $GJ=2545 \text{ Nm}^2$, $EI=712194 \text{ Nm}^2$, $x_a=0.051 \text{ m}$, $L=3 \text{ m}$, $M=20 \text{ kg}$, $c=50 \text{ Nsm}^{-1}$, $k=10^6 \text{ Nm}^{-1}$.

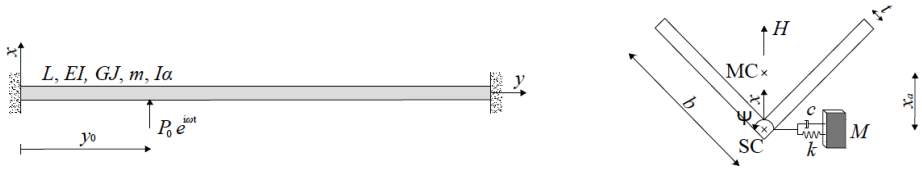


Fig. 1. Beam with V cross section equipped with a TMD and subjected to harmonic point load.

The exact dynamic Green's functions in Fig. 2 are obtained in analytical form, as solution of the sixth-order coupled bending-torsion differential equation of the beam acted upon by a Dirac's delta representing the point load and a Dirac's delta representing the reaction of the TMD.

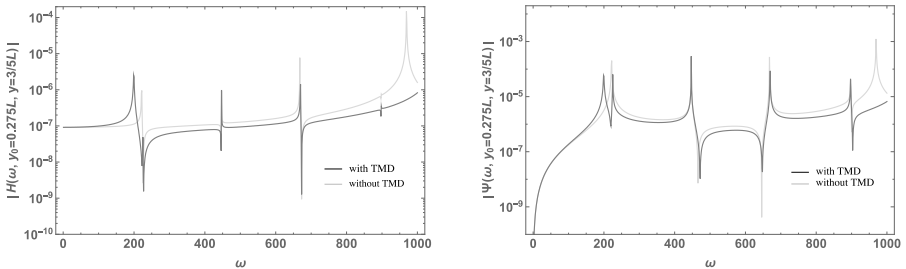


Fig. 2. Dynamic Green's functions for the beam in Fig. 1 computed with and without TMD.

3. Concluding Remarks

We propose a novel solution procedure for high-order boundary value problems of relevant interest in mechanics, involving various types of beams with different types of absorbers. The procedure applies in frequency and time domains, under arbitrary loads.

References

- [1] LEE JW, LEE JY: A transfer matrix method capable of determining the exact solutions of a twisted Bernoulli-Euler beam with multiple edge cracks. *Applied Mathematical Modelling* 2017, **41**:474-493.
- [2] BANERJEE JR, SOBEY AJ: Dynamic stiffness formulation and free vibration analysis of a three-layered sandwich beam. *International Journal of Solids and Structures* 2005, **42**: 2181-2197.
- [3] BANERJEE JR, GUO S, HOWSON WP: Exact dynamic stiffness matrix of a bending-torsion coupled beam including warping. *Computers and Structures* 1996, **59**(4): 613-621.

Non-stationary stochastic dynamics analysis of structural systems equipped with fractional viscoelastic device

ANDREA BURLON^{1*}, MARIO DI PAOLA², VINCENZO SUCATO²

1. DICEAM, University of Reggio Calabria, Reggio Calabria, Italy [0000-0002-1827-5382]
2. Department of Engineering, University of Palermo, Palermo, Italy

Keywords: fractional operators, viscoelastic device, non-stationary white noise

1. Introduction

Viscoelastic materials are commonly used for vibration mitigation. The viscoelastic behaviour is defined by the Creep test, providing the Creep function. Starting from Nutting experiments (1921) [1] the creep function, $C(t)$, is

$$C(t) = t^\beta / E_\beta \Gamma(\beta + 1); \quad 0 \leq \beta \leq 1 \quad (1)$$

where $C(\beta)$, β are found by best fitting procedure and $\Gamma(\cdot)$ is the Gamma function. By using the Boltzmann superposition principle for a power law creep function the fractional constitutive arise. Then, inserting a viscoelastic device into a structural system, a second order derivative, a fractional operator and elastic term appear. In this presentation the stochastic analysis for a non-stationary white noise input is discussed in time domain by using Grünwald-Letnikov integration scheme.

2. Results and Discussion

For a viscoelastic device with a creep function as in eq. (1), the Boltzmann superposition principle gives

$$\varepsilon(t) = \frac{1}{E(\beta)\Gamma(1+\beta)} \int_0^t (t-\tau)^\beta \dot{\sigma}(\tau) d\tau = \frac{1}{E_\beta \Gamma(\beta)} \int_0^t (t-\tau)^{\beta-1} \sigma(\tau) d\tau \quad (2)$$

The last equality in eq. (2) is proportional to the Riemann Liouville fractional integral, ${}_0 I_t^\beta$. The constitutive laws are, for quiescent system ($t \leq 0$)

$$\varepsilon(t) = \frac{1}{E_\beta} ({}_0 I_t^\beta \sigma)(t); \quad \sigma(t) = E_\beta ({}_0 D_t \varepsilon)(t) \quad (3.a,b)$$

where ${}_0^c D_t^\beta$ in eq. (4.b) is the Caputo's fractional derivative. Then, for a structural system equipped with a viscoelastic device we may write:

$$\ddot{X} + 2\zeta_\beta \omega_0 ({}^c D_t^\beta X)(t) + \omega_0^2 x = \Psi^{\frac{1}{2}}(t)W(t); \Psi(t) > 0 \quad (4)$$

where ζ_β is the (anomalous) dissipation factor, ω_0 is the natural frequency, $\Psi(t)$ is a deterministic modulating function and $W(t)$ is characterized by the correlation function $R_w(\tau) = E[W(t)W(t+\tau)] = q\delta(\tau)$, being q the strength of white noise. The operators of derivatives and integrals may be inverted to obtain

$$X + 2\zeta_\beta \omega_0 ({}_0 I_t^{2-\beta} x)(t) + \omega_0^2 ({}_0 I_t^2 x)(t) = {}_0 I_t^2 \left(\Psi^{\frac{1}{2}}(t)W(t) \right) \quad (5)$$

that, by using the Grünwald-Letnikov integration scheme [2] we get

$$\mathbf{A}_n \mathbf{X}_n = \mathbf{B}_n \mathbf{W}_n \quad (6)$$

where $\mathbf{X}_n, \mathbf{W}_n$ are n -vectors whose j -th component are $X(t_j)$ and $W(t_j) =$

$(q\Psi(t_j)/\Delta t)^{1/2} N_j$, respectively. Moreover $t_j - t_{j-1} = \Delta t$; N_j are realizations of standard normal random variables with $E[N_i N_j] = \delta_{ij}$ and

$$\mathbf{A}_n = \mathbf{A}_1 + 2\zeta_\beta \omega_0 \Delta t^{2-\beta} \mathbf{A}_{2-\beta} + \omega_0^2 \Delta t^2 \mathbf{A}_2; \mathbf{B}_n = \mathbf{A}_2 \Delta t^2 \quad (7)$$

being \mathbf{A}_γ ($\gamma=1, 2-\beta, 2$) a lower bound strip matrix [2] whose first column elements are given as $A_{\gamma 1} = 1$, $A_{\gamma 2} = \gamma$, $A_{\gamma ij} = A_{\gamma i, j-1} (1 + \gamma_{j-2}) / (j-1)$ from eq. (5) we get

$$E[\mathbf{X}_n \mathbf{X}_n^T] = \mathbf{A}_n^{-1} \mathbf{B}_n \left[\Psi_n^{\frac{1}{2}} \Psi_n^{\frac{T}{2}} \right] (\mathbf{B}_n^{-T} \mathbf{A}_n^T) \quad (8)$$

From this equation the entire correlation matrix of the response process is easily determined.

3. Concluding Remarks

The stochastic analysis of a structural system with fractional viscoelastic device is presented. The forcing function is modelled as a non-stationary white noise. Integrating the eq. motion by the Grünwald-Letnikov integration scheme returns easily the time dependent statistics of response process at the discretized times t_1, t_2, \dots, t_n .

References

- [1] NUTTING, P. G., *Journal of the Franklin Institute*, Maggio 1921.
- [2] PODLUBNY, I., *Fractional Differential Equations*, Academic Press, San Diego, CA, 1999.

Cloaking of Love Waves

ZINON CHATZOPOULOS^{1*}, ANTONIO PALERMO¹, SEBASTIAN GUENNEAU², ALESSANDRO MARZANI¹

1. Department of Civil, Chemical, Environmental and Materials Engineering - DICAM, University of Bologna, 40136 Bologna, Italy

2. UMI 2004 Abraham de Moivre-CNRS, Imperial College London, London, SW7 2AZ, UK

* Presenting Author

Abstract:

We present the design of an elastic carpet cloak capable of rerouting Love waves around a defect. Love waves are horizontally polarized surface waves that propagate in a soft elastic medium overlaying a stiffer substrate. Their governing equation has the form of the scalar Helmholtz equation. Building upon the invariance of the Helmholtz equation under an arbitrary coordinate transformation, we utilize the principle of transformation elastodynamics to design a surface cloak for Love waves. We evaluate via numerical simulations the validity of our approach by cloaking a triangular-shaped defect that lies within the soft layer. We show that the designed cloak is capable to hide the surface defect by generating near zero scattered field.

Keywords: Love Waves, Cloaking, Transformation Elastodynamics, Metamaterials.

1. Introduction

The prospect of rerouting the propagation of elastic waves around an object and isolate it from unwanted mechanical vibrations have fuelled the research interest towards the realization of elastic cloaking devices. In the past decades, several works proposed theoretical models and experimental realization of cloaking devices for bulk waves, flexural waves in plates or antiplane waves. Cloaking theory can be traced back to [1]. Surprisingly, applications of cloaking for elastic surface waves are scarce. In this work, we explore the possibility of cloaking surface waves of the Love type.

2. Governing Equations

We consider a homogeneous, isotropic elastic layer of thickness h_1 and material properties $(\lambda_1, \mu_1, \rho_1)$ coupled to a semi-infinite medium with properties $(\lambda_2, \mu_2, \rho_2)$ where μ_i and λ_i are the Lamé coefficients and ρ_i the mass densities. The layered medium presents a triangular defect that extends within the thickness of the upper layer (Fig. 1a). We restrict our interest to shear polarized surface waves propagating along the horizontal x -direction and polarized in the y -direction, known as Love waves. In the layer 1, the governing Helmholtz scalar equation reads:

$$\nabla_{(x,z)} \cdot \mu_1 \nabla_{(x,z)} u_y = \rho_1 u_{2,tt} \quad (1)$$

where u_2 is the elastic displacement along y and $u_{2,tt}$ denotes the second order derivative in time of u_2 . Referring to Fig. 1 we introduce a change of coordinates $\{x, z\} \rightarrow \{u, v\}$, to shrink the white region of the triangular defect between $z = 0$ and $z = z_1(x)$ into the region between the curves $z_1(x)$ and $z_2(x)$ (blue region). Following the cloaking strategy in [2], we derive the governing equation in the transformed coordinate system, in a configuration similar to that in [3], as:

$$\nabla_{(u,v)} \cdot \mu'_1 \nabla_{(u,v)} u_y = \rho'_1 u_{2,tt} \quad (2)$$

where $\mu' = \frac{J_{ux} \mu J_{ux}^T}{\det(J_{ux})}$ and $\rho' = \frac{\rho}{\det(J_{ux})}$ are the transformed mechanical properties in the cloaked region (blue region in Fig 1a), and $J_{ux} = \frac{\partial(u,v)}{\partial(x,z)}$ is the Jacobian of the transformation.

Results

We model a triangular pinched cloak in a finite element environment using COMSOL Multiphysics. We performed time harmonic simulations and compared in Fig.1b the surface displacement field ($z=0$) for the (i) by-layer with no triangular defect (Reference), (ii) by-layer with the triangular defect without considering the elastodynamic transformation (Uncloaked), and (iii) the case of the cloaked defect (Cloaked). The results confirm that the out-of-plane displacement field of the cloaked defect configuration finely approximates the one of the pristine elastic media (i.e., no defect).

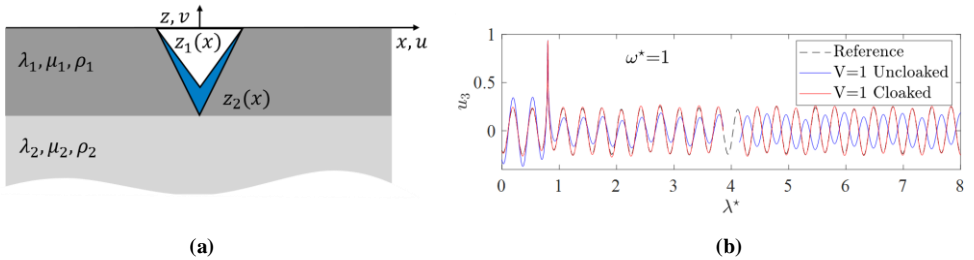


Fig. 1. (a) Schematic of a Carpet-pinned cloak. (b) Reference, Uncloaked and Cloaked displacement field. λ^* is the wavelength at frequency ω^* , normalized with respect to the cut-of frequency of the first Love mode.

3. Concluding Remarks

We provided a brief theoretical account on the cloaking of a surface defect for elastic Love waves. An extension of the present approach to the cloaking of soft and rigid inclusions could pave the way towards the realization of novel isolating devices for out-of-plane surface elastic waves.

Acknowledgment: This project has received funding from the European Union’s Horizon 2020 research and innovation programme under the Marie Skłodowska Curie grant agreement No 813424.

References

- [1] A. Greenleaf, M. Lassas, G. Uhlmann, on nonuniqueness for Calderon’s inverse problem, *Math. Res Lett.* 10 (2003) 685-693.
- [2] J. Li, J.B. Pendry, Hiding under the carpet: a new strategy for cloaking, *Physical review letters* 101 (2008) 203901
- [3] W. J. Parnell, Nonlinear pre-stress for cloaking from antiplane elastic waves, *Proceedings of the Royal Society A: Mathematical, Physical and Engineering Sciences* 468 (2138) (2012) 563-580.

Assessing the effect of different configurations of inerter-based devices for structural vibration control

MIRIAM CHILLEMI^{1*}, THOMAS FURTMÜLLER², CHRISTOPH ADAM³,
ANTONINA PIRROTTA⁴

1. Unit of Applied Mechanics, University of Innsbruck, Technikerstr. 13, 6020 Innsbruck, Austria [00000003-0759-6823]
2. Unit of Applied Mechanics, University of Innsbruck, Technikerstr. 13, 6020 Innsbruck, Austria [0000-0002-5639-3259]
3. Unit of Applied Mechanics, University of Innsbruck, Technikerstr. 13, 6020 Innsbruck, Austria [0000-0001-9408-6439]
4. Department of Engineering, University of Palermo, viale delle Scienze, 90128 Palermo, Italy [0000-0002-8177-0204]

* Presenting Author

Abstract: The use of lightweight materials with enhanced mechanical properties and improved quality of design due to the use of advanced computer methods have led to the trend of designing increasingly slim structures that are more prone to vibrations. To control these structures, the vibrations mitigation effect of well-known passive control systems such as Tuned Mass Dampers (TMDs) and Base Isolation Systems (BISs), can be enhanced by using a mass amplification device called inerter. In this study, the behavior of this device and its influence on the response of vibration-prone systems is investigated by analyzing different configurations in a civil engineering context, finding optimized parameters and assessing the performance of various suspension layouts with the inerter placed at different positions. Indeed, the position of the device can strongly influence the benefits brought in the structural control design. Therefore, a more critical analysis is proposed with respect to previous studies on the use of inerter-based devices for vibration control, with the aim of consistently investigating the exploitation of these innovative systems in practical applications.

Keywords: inerter, passive structural control, vibration absorber

1. Introduction

To achieve the most effective structural control the fabrication of innovative devices capable of reducing and control both horizontal and vertical vibrations is one of the major challenge for researchers and designers in structural engineering. In this regard, inerters are comparatively recent additions to the arsenal of civil engineers and structural control. The inerter is a mechanical device, introduced for the first time by M. Smith [1], that acts as an apparent mass, called inertance, which can be orders of magnitude larger than its physical mass. In general, the device can be considered as a linear mechanical element in which the two terminals develop an internal force proportional to the relative acceleration of its terminals. Specifically, the mass amplification property can allow to enhance the performance of several mass-dependent devices. On this base, to control the acceleration level, several inerter-based suspension layouts can be employed with the inerter placed at different positions. In literature, various configurations have already been proposed. Nevertheless, some works present results could appear not adherent to the reality and not suitable for practical application [2].

2. Results and Discussion

With the aim of investigating the effectiveness of various suspension layouts comprising the inerter, a comparison between the response of a single-degree-of-freedom system (SDOF) coupled with a classical TMD and SDOF systems equipped with different inerter-based devices is shown in Figure 1. As can be seen, the lowest displacement response results from the layout G1, where the inerter is connected between the ground and the TMD mass. A slightly better result, compared to a traditional TMD, is obtained when the inerter is placed between the main mass and the auxiliary mass, which is arranged in series with a dashpot and in parallel with a spring (configuration K1). On the other hand, contrary to the conclusions in [2], the behavior of the proposed configuration, in which the inerter is simply attached between the main and the TMD mass, appears to be even worse than the configuration in which the device is not included (traditional TMD). It can be concluded that, although it is not a normal use for the inerter (in the original mechanical context the inerter has two independently movable terminals), the best performance is obtained in the case where one of the two terminal is grounded. This different behavior could be due to the presence of a negative inertance in the entries not on the diagonal in the mass matrix. These terms, in fact, are not present in the case of a grounded terminal. Thus, the resistance to acceleration can be considered as a mass element of a mass equal to the inertance itself.

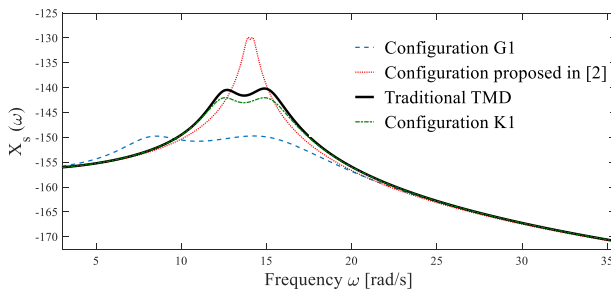


Fig. 1. Displacement response in frequency domain of different configurations

3. Concluding Remarks

This paper demonstrates with a more critical analysis the performance of inerter-based devices for vibration control emphasizing the importance of the inerter location in different suspension layouts. Numerical analysis indicates that to achieve the highest mass amplification effect one of the inerter terminals must be attached to a fixed point.

Acknowledgment: This project has received funding from the European Union’s Horizon 2020 research and innovation programme under the Marie Skłodowska-Curie grant agreement No 847476. The views and opinions expressed herein do not necessarily reflect those of the European Commission.

References

- [1] SMITH M: Synthesis of mechanical networks: the inerter. *IEEE Transaction on Automatic Control* 2002, **47** (10):1648-1662.
- [2] CHEN Q, ZHAO Z, XIA Y, PAN C, LUO H, ZHANG R: Comfort based floor design employing tuned inerter mass system. *Journal of sound and Vibration* 2019, **458**:143-157.

Performance of a nonlinear energy sink coupled with a nonlinear oscillator for energy harvesting applications

RAHUL DAS^{1*}, ANIL K BAJAJ², SAYAN GUPTA^{1,3}

1. Department of Applied Mechanics, Indian Institute of Technology, Madras, India. [am17d201@smail.iitm.ac.in]
 2. School of Mechanical Engineering, Purdue University, Purdue, USA. [bajaj@purdue.edu]
 3. Complex Systems and Dynamics Group, Indian Institute of Technology, Madras, India. [sayan@iitm.ac.in]
- * Presenting Author

Abstract: The challenge in vibration based energy harvesting lies in scavenging the mechanical energy from a vibrating system at a broad range of excitation frequencies. This study focuses on using a nonlinear energy sink to increase the harvesting efficiency in nonlinear oscillators. The system consists of an oscillator with cubic nonlinearity, coupled with an essentially nonlinear cubic oscillator, suitably tuned such that the flow of energy is unidirectional towards the nonlinear attachment. This study investigates analytically, the mechanisms and conditions for unidirectional energy transfer and how the efficiency can be enhanced through proper tuning of the system parameters.

Keywords: Nonlinear energy sink, nonlinear oscillators, targeted energy transfer.

1. Introduction

The idea of simultaneously mitigating vibration and harvesting energy is very effective for various application purposes. A classical vibration based energy-harvesting device consists of a harvesting component typically made of smart materials, attached to a *primary oscillator (PO)* and works efficiently in a narrow band around the natural frequency of the PO. A large body of literature discussed how nonlinearities in the system can increase the operational bandwidth [1-2]. One class of such studies uses the concept of *Nonlinear Energy Sink (NES)*, which is an essentially nonlinear oscillator, attached to a PO. The frequency energy dependency of the system due to its nonlinearity implies the possibility of the system attaining resonance condition at wide frequency bands and is exploited for energy transfer. Most of the energy of a linear PO gets transferred to the NES, in a passive, unidirectional and irreversible manner [3] and is referred to as *Targeted Energy Transfer (TET)*. This energy transfer occurs between the substructures of the system in a passive manner. Due to frequency-energy dependency of NES, TET starts when the instantaneous frequency of NES gets close to the natural frequency of PO, attaining resonating condition. This transferred energy, increases the instantaneous frequency of NES, leading to a mistuning with the frequency of PO. As a result, the transferred energy gets localized in NES, making this entire phenomenon unidirectional. In addition, the system damping ensures that the energy transfer is irreversible.

Unlike existing studies where the PO is usually linear, in this study, the PO is assumed to be an oscillator with cubic nonlinearity, to which NES is attached. The motivation for selecting such a system is to investigate vibration-based energy harvesting from physical systems, which are usually flexible and therefore involve nonlinear effects due to large deformations or fluid-structure interaction effects. To get insights into the physics of TET, an analytical approach is adopted. This involves adopting the method of *complexification-averaging (CX-A)* [4] for studying the system across multiple time scales such that the conditions of 1:1 resonance capture between the PO and NES can be derived. This ena-

bles identifying the optimal TET regime. The system parameters are selected by adopting a tuning methodology [5], which emphasises the optimal TET condition. The modal response of the system at resonance condition are simulated using a harmonic balance based approach, followed by arc-length type continuation process.

2. Results and Discussion

The different TET regimes for the system comprising of a Duffing oscillator attached with a NES is shown in Fig. 1 with respect to the variation of the magnitude of the relative amplitude of the complexified-averaged system, $|u(t)|$ and time. This is a measure of energy transfer as transferred energy is directly related to the relative motion of the substructures. It is observed that there exists three distinct regimes. The initial regime comprises of a segment where energy is transferred due to nonlinear beating phenomenon near $S11^+$ -the in-phase 1:1 resonating manifold. This is followed by an intermediate regime, governed by damping. Finally, there is a transition towards $S11^-$ -the out-of-phase 1:1 resonating manifold, where the energy is completely localized in the NES. More results on finding the dynamics at different regimes will be presented in the work.

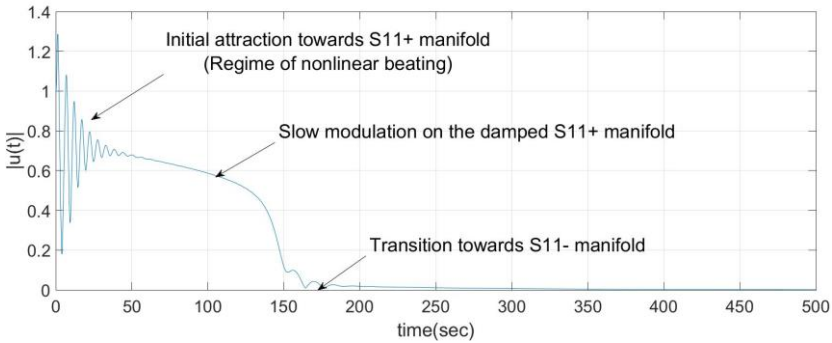


Fig. 1. Different TET regimes on the slow modulation of relative amplitude of complexified-averaged system.

References

- [1] D. D. QUINN, O. V. GENDELMAN, G. KERSCHEN, T. P. SAPSIS, L. A. BERGMAN, A. F. VAKAKIS, EFFICIENCY OF TARGETED ENERGY TRANSFERS IN COUPLED NONLINEAR OSCILLATORS ASSOCIATED WITH 1:1 RESONANCE CAPTURES: PART I, JOURNAL OF SOUND AND VIBRATION 311(3-5) (2008) 1228-1248.
- [2] T. P. SAPSIS, A. F. VAKAKIS, O. V. GENDELMAN, L. A. BERGMAN, G. KERSCHEN, D. D. QUINN, EFFICIENCY OF TARGETED ENERGY TRANSFERS IN COUPLED NONLINEAR OSCILLATORS ASSOCIATED WITH 1:1 RESONANCE CAPTURES: PART II, JOURNAL OF SOUND AND VIBRATION 325(1-2) (2009) 297-320.
- [3] A. F. VAKAKIS, O. V. GENDELMAN, L. A. BERGMAN, D. M. MCFARLAND, G. KERSCHEN, Y. S. LEE, NONLINEAR TARGETED ENERGY TRANSFER IN MECHANICAL AND STRUCTURAL SYSTEMS, VOL. 156, SPRINGER SCIENCE & BUSINESS MEDIA, 2008.
- [4] L. I. MANEVITCH, COMPLEX REPRESENTATION OF DYNAMICS OF COUPLED NONLINEAR OSCILLATORS, IN MATHEMATICAL MODELS OF NONLINEAR EXCITATIONS, TRANSFER, DYNAMICS, AND CONTROL IN CONDENSED SYSTEMS AND OTHER MEDIA, SPRINGER, BOSTON, MA, (1999) 269-300.
- [5] R. VIGUI E, G. KERSCHEN, NONLINEAR VIBRATION ABSORBER COUPLED TO A NONLINEAR PRIMARY SYSTEM: A TUNING METHODOLOGY, JOURNAL OF SOUND AND VIBRATION 326 (3-5) (2009) 780-793.

Tuned Liquid Column Damper Inerter (TLCDI) for vibration control of fixed-base structures

ALBERTO DI MATTEO^{1*}, CHIARA MASNATA¹, CHRISTOPH ADAM²,
ANTONINA PIRROTTA¹

1. Department of Engineering, University of Palermo, viale delle Scienze, 90128 Palermo, Italy
2. Unit of Applied Mechanics, University of Innsbruck, Technikerstr. 13, 6020 Innsbruck, Austria

* Presenting Author

Abstract: In this paper, the use of a novel passive control device defined as Tuned Liquid Column Damper Inerter (TLCDI) is studied to mitigate the seismic response of fixed-base and structures. The TLCDI optimal parameters for pre-design purposes are obtained by means of a statistical linearization technique and an optimization procedure which considers the minimization of the structural displacement variance and a white noise process as base excitation. Closed-form expressions for the optima design parameters are determined under certain reasonable approximations. The validity of the proposed approach is assessed considering also non-white excitation processes as base random input. Further, the performance of the TLCDI-controlled structure is examined using a set of 44 real recorded seismic signals as external input.

Keywords: Tuned Liquid Column Damper, Inerter, Optimal design, Statistical Linearization Technique

1. Introduction

In the field of passive vibration control devices, the Tuned Mass Damper (TMD) and the Tuned Liquid Column Damper (TLCD) are among the most widely systems used for reducing structural vibrations. However, these devices may require large masses to be efficient. Consequently, inerter-based devices have gained increasing interest as lightweight solutions [1]. On this basis, following the same logical flow which led to the development of the Tuned Mass Damper Inerter (TMDI) [2] as a more efficient strategy compared to the classical TMD, the Tuned Liquid Column Damper Inerter (TLCDI) [3] has been recently proposed as a promising passive control device which exploits the synergetic beneficial features of the inerter and the TLCD. TLCDs, being simple U-shape liquid tanks, show some convenient characteristics such as low cost, easy implementation, lack of required maintenance, no need to add mass to the structure using the liquid as water supply. Unlike the classical TLCD, the proposed TLCDI is supposed to be able to translate through a sliding support and it is connected to the structure by a linear spring and a damper and to the ground by an inerter. In this manner, the TLCDI dissipates the structural vibrations by means of a combined action which involves the vertical motion of the liquid and the horizontal motion of the container.

2. Results and Discussion

The optimal design of the TLCDI plays a key role in achieving the best mitigation effect of the structural response. In this regard, in this paper, the TLCDI optimal design parameters are obtained for a classical single-degree-of-freedom (SDOF) fixed-base structure, as the one in Figure 1.

Notably, since the governing equations of the TLCDI are nonlinear, as shown in Eq. (1), in general this process may be rather complex, requiring time consuming numerical optimization procedures. Thus, in this study, approximate optimal TLCDI parameters are evaluated, in closed form, by taking into account a statistical linearization technique and some simplifying hypothesis.

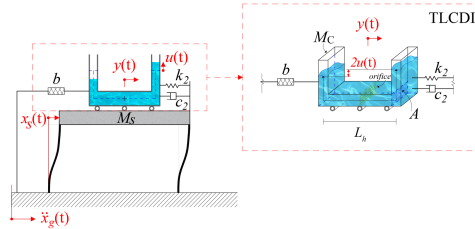


Fig. 1. Analyzed system: fixed-base TLCDI-controlled SDOF structure

$$\begin{cases} M_s \ddot{x}_s(t) + M_s \ddot{x}_s(t) + C_s \dot{x}_s(t) + K_s x_s(t) - c_2 \dot{y}(t) - k_2 y(t) = M_s \ddot{x}_g(t) \\ (\rho AL + M_c + b) \ddot{y}(t) + (\rho AL + M_c + b) \ddot{x}_s(t) + \rho AL_n \ddot{u}(t) + c_2 \dot{y}(t) + k_2 y(t) = -(\rho AL \quad M_c) \ddot{x}_g(t) \\ \rho AL_n \ddot{x}_s(t) + \rho AL_n \ddot{y}(t) + \rho AL \ddot{u}(t) + \frac{\rho A}{2} \xi |\dot{u}(t)| \dot{u}(t) + 2\rho A g u(t) = \rho AL_n \ddot{x}_g(t) \end{cases} \quad (1)$$

Specifically, an optimization procedure based on the minimization of the variance of the structural response is proposed. Notably, by assuming a white noise excitation and neglecting damping effects, pertinent analytical expressions for the optimal TLCDI parameters are provided and optimal design charts are presented as a ready-to-use practical design tool. In order to prove the accuracy of the proposed simplified technique, a comparison with the optimal values obtained through a more computationally demanding numerical procedure on the original system has been performed. Results show a satisfactory agreement in terms of control performance between the proposed analytical approach and the numerical one. However, it is worth noting that the use of analytical expressions provided by the proposed straightforward procedure leads to a significant reduction in computational effort. Therefore, the aforementioned formulation can effectively be regarded as a reliable tool to be employed for the optimal design parameters estimation. In this manner, the control performance of TLCDI for fixed-base structures is discussed for both white noise excitation and also considering a set of 44 real earthquake records. Finally, numerical analyses indicate that coupling the inerter with a TLCDI device significantly reduces the structural responses compared to the uncontrolled structure and to other traditional devices.

References

- [1] SMITH MC: Synthesis of mechanical networks: the inerter. *IEEE Trans Autom Control* 2002, **47**:1648-62.
- [2] DE DOMENICO D, RICCIARDI G: An enhanced base isolation system equipped with optimal tuned mass damper inerter (TMDI). *Earthquake Engineering and Structural Dynamics* 2018, **47**: 1169-1192.
- [3] WANG Q, TIWARI ND, QIAO H, WANG Q: Inerter-based tuned liquid column damper for seismic vibration control of a single-degree-of-freedom structure. *International Journal of Mechanical Sciences* 2020, **184**:1-15.

Inerter-based dampers for vibration control of floating offshore wind turbines

BREIFFNI FITZGERALD^{1*}, SAPTARSHI SARKAR²

1. School of Engineering, Trinity College Dublin, Ireland. [ORCID: 0000-0002-5278-6696]

2. Department of Mechanics and Maritime Sciences, Chalmers University of Technology, Gothenburg, Sweden [ORCID: 0000-0002-2111-2154]

* Presenting Author

Abstract: This paper analyses the performance of tuned mass damper inerters (TMDI) for vibration control of spar-type floating offshore wind turbine towers. The use of an inerter in parallel with the spring and damper of a tuned mass damper (TMD) is a relatively new concept. The ideal inerter has a mass amplification effect on the classical TMD leading to greater vibration control capabilities. In this work we compare an “ideal” TMDI that assumes the use of a mechanical flywheel type inerter, with a “realist” fluid inerter. The fluid inerter is rather simple in design and it comes with very low maintenance. Numerical results demonstrate impressive vibration control capabilities of inerter-based dampers under various stochastic wind-wave loads. It has been shown that the fluid-inerter performs as well as the ideal mechanical inerter. The practical advantages of a fluid-inerter over the standard mechanical inerter makes it an exciting candidate for vibration control in offshore wind turbines.

Keywords: Inerter, Tuned mass damper, stochastic wind-wave loads, wind turbine, floating offshore wind turbine.

1. Introduction

The future of wind energy lies offshore. The cost of offshore wind turbine foundations is about 45% of the wind turbine cost in shallow water depths [1]. The concept of floating offshore wind turbines (FOWTs) was proposed to address the cost issue as turbines are installed in increasingly deeper waters. FOWTs have been realised in recent years in offshore wind farms in Scotland (Hywind) and Portugal (WindFloat). FOWTs present additional challenges to traditional onshore or fixed base offshore turbines. FOWTs are very large flexible structures installed in very harsh environments. These structures are subjected to turbulent aerodynamic and hydrodynamic loads and are constantly rotating. Mitigating the structural vibrations of FOWTs is now a very active area of research since vibrations of the blades and towers of FOWTs will affect the power production [2] and will also affect the reliability of the structures [3]. There have been many different vibration control schemes proposed to reduce vibrations in offshore wind turbines. Passive control via tuned mass dampers has been proposed by researchers and is now standard in the industry for multi-megawatt offshore wind turbines. Some wind turbine vibration control studies have made use of recent developments in damper design due to the emergence of the so-called ‘inerter’. Inerter-based dampers can provide a mass amplification effect which increases the effective mass of the device, thus improving its vibration control performance. Inerter-based dampers have been considered for vibration control of floating offshore wind turbines [4-5], however, all the inerter-based dampers investigated to date in the wind turbine literature have made use of “ideal” mechanical inerters, realised via gearing systems, rack and pinion assemblies, or other mechanical components. In this paper, we propose the use of a

tuned mass damper fluid-inerter (TMDFI) for vibration control of a spar-type floating offshore wind turbine towers. We compare an “ideal” TMDI that assumes the use of a mechanical flywheel type inerter, with a “realist” fluid inerter.

2. Results and Discussion

We have developed a high-fidelity multi-body dynamic model of the FOWT coupled with a TMDFI using Kane's method for numerical investigation in the paper – details to be provided in the full paper. Fig. 1. shows the damper details and a schematic for the installation inside the tower.

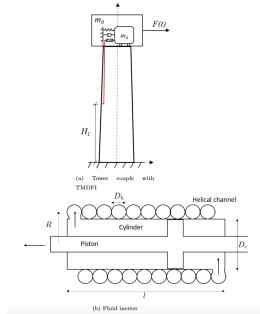


Fig. 1. Schematic of FOWT with TMDFI details

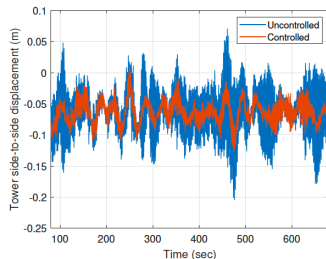


Fig. 2. Load Case 1.1: Tower side-to-side displacement

We have shown that the TMDFI has excellent vibration control performance across a wide envelope of met-ocean conditions and load cases. A typical time-history response is shown in Fig. 2, the vibration control achieved is impressive. The TMDFI performance is as good as the “ideal” TMDI. This is particularly encouraging since the design and maintenance of a fluid inerter is simpler and cheaper than an “ideal” mechanical inerter. Details will be provided in the full paper.

3. Concluding Remarks

The TMDFI offers great potential in vibration mitigation for floating offshore wind turbine towers. This damper performs significantly better than a classical TMD and comparable to an “ideal” mechanical inerter. The extended version of this manuscript will include details on the modelling, design and optimization of the TMDFI. Greater details will also be provided on the environmental loading and the FOWT multi-body dynamic model.

References

- [1] Oh, K. Y., Nam, W., Ryu, M. S., Kim, J. Y., & Epreanu, B. I. (2018). A review of foundations of offshore wind energy converters: Current status and future perspectives. *Renewable and Sustainable Energy Reviews*, 88, 16-36.
- [2] Dueñas-Osorio, L., & Basu, B. (2008). Unavailability of wind turbines due to wind-induced accelerations. *Engineering Structures*, 30(4), 885-893.
- [3] Fitzgerald, B., Sarkar, S., & Staino, A. (2018). Improved reliability of wind turbine towers with active tuned mass dampers (ATMDs). *Journal of Sound and Vibration*, 419, 103-122.
- [4] Ma, R., Bi, K., & Hao, H. (2019). A novel rotational inertia damper for heave motion suppression of semisubmersible platform in the shallow sea. *Structural Control and Health Monitoring*, 26(7), e2368.
- [5] Sarkar, S., & Fitzgerald, B. (2020). Vibration control of spar-type floating offshore wind turbine towers using a tuned mass-damper-inerter. *Structural Control and Health Monitoring*, 27(1), e2471.

Vibration mitigation in offshore wind turbines by tuned mass absorbers

MINA GHASSEMPOUR¹, GIUSEPPE FAILLA¹, GIOACCHINO ALOTTA^{1*}, VALENTINA LAFACE¹, CARLO RUZZO¹, FELICE ARENA¹

1. Department of Civil, Energy, Environmental and Materials Engineering (DICEAM), University of Reggio Calabria, Via Graziella, 89124 Reggio Calabria, Italy

* Presenting Author

Abstract: We investigate the effectiveness of tuned mass absorbers for vibration mitigation in bottom-fixed and floating offshore wind turbines. The starting point of our study is a classical single-degree-of-freedom tuned mass absorber located within the nacelle, targeting the first natural frequency of the system. For this case, fully coupled aero-hydro-servo-elastic simulations, implemented in GH-BLADED [1], will be carried out under various wind-wave states, with the purpose of assessing fatigue behaviour of the support structure. In this context, two different support structures will be considered, a monopile and a tripod, including foundation flexibility. The next step of our study will target floating wind turbines. Innovative concepts of tuned mass absorbers will be proposed for this case, targeting one or multiple frequencies of the response. A preliminary assessment of the proposed concepts will be carried out on simplified numerical models of the system, retaining the essential aerodynamics of the rotor and hydrodynamics of the floating support.

Keywords: offshore wind turbine, tuned mass absorber

[1] BOSSANYI EA: *Bladed for Windows user manual*. Garrad Hassan and Partners: Bristol, 2000.

Improving the noise insulation performance of vibro-acoustic metamaterial panels through multi-resonant design

STEFAN JANSSEN¹, LUCAS VAN BELLE^{1,2,*}, NOÉ GERALDO ROCHA DE MELO FILHO^{1,2},
CLAUS CLAEYS^{1,2}, WIM DESMET^{1,2}, ELKE DECKERS^{1,2}

1. Department of Mechanical Engineering, KU Leuven, Belgium

2. DMMS lab, Flanders Make

* Presenting Author

Abstract: In the search for lightweight solutions with favourable noise and vibration attenuation, locally resonant vibro-acoustic metamaterials have emerged as a promising candidate due to their stop band behaviour. When used in a sound transmission context, vibro-acoustic metamaterial panels allow to greatly improve the acoustic insulation in a targeted frequency range. However, their peak insulation is typically followed by a strong insulation dip, which hampers their broad applicability. In this work, this problem is addressed through the formerly only theoretical concept of dip reduction by optimizing a realizable metamaterial panel with multiple tuned resonators in order to reduce this insulation dip, while preserving peak performance and maintaining similar total mass. The resulting multi-resonant metamaterial design is realized and its improved acoustic insulation performance is experimentally validated.

Keywords: vibro-acoustic metamaterial, noise insulation, dip reduction, multi-resonant design

1. Introduction

Vibro-acoustic metamaterials have shown potential to create targeted frequency ranges of high vibration and noise reduction due to their stop band behaviour, which arises from adding or embedding identically tuned resonant structures on or in a flexible host structure on a sub-wavelength scale [1,2]. A high sound transmission loss (STL) peak can be achieved with vibro-acoustic metamaterial panels around their bending wave stop band frequency range, but it is typically followed by an undesirable, strong STL dip. Although damping in the resonators can improve the STL dip, it also reduces the STL peak performance [3]. A theoretical dip reduction method was recently proposed [4]: using a lumped parameter STL model of a metamaterial partition, incorporating mass-spring systems and the acoustic mass-law, the potential was shown of tuning multiple additional highly damped resonators to the STL dip frequency range in order to suppress the STL dip, while preserving the STL peak. However, only ideal mass-spring resonators were considered, the tuning was performed manually and involved impractically high damping values, and no validation on a realized metamaterial panel was performed.

2. Methodology

To bring dip reduction to reality, in this work, a lumped parameter model is first embedded in an STL optimization routine to tune multiple resonances with realizable damping values. By redistributing the main resonator mass over the additional resonators, the total added mass is maintained. The optimized resonator parameters which minimize the peak difference between STL dip and STL of the bare host panel are next translated to realizable resonators using finite element model-based design optimization [5]. The resulting design is realized and validated using acoustic insertion loss measurements [3].

Corresponding author: lucas.vanbelle@kuleuven.be, Celestijnenlaan 300 – box 2420, B-3001 Heverlee, Belgium

3. Results and Discussion

A conventional metamaterial is considered, composed of a 4 mm thick PMMA (Young's modulus $E=4.85$ GPa, density $\rho=1188$ kg/m³, Poisson ratio $\nu=0.31$, structural damping $\eta=0.05$) host panel with resonators tuned to 600 Hz, with $\eta=0.05$ and adding 50% mass, added with 6x6 cm periodicity. A dip-reduced metamaterial is next designed, considering three additional resonators per periodic cell, with the main resonator tuned to 600 Hz and 70% of the total mass addition, and the additional resonators optimized to reduce the STL dip around 700 Hz (Fig. 1a). The optimized mass-spring resonator properties of both metamaterials are translated to realizable beam-shaped PMMA resonators [3,5], which are laser-cut and glued onto A3-sized PMMA panels (Fig. 1b). Both manufactured panels of approximately the same mass (47% added for conventional, 49% for dip-reduced) are mounted on an acoustic testing cabin to measure the insertion loss (IL) [3]. Comparing the IL difference ΔIL between the metamaterial panels and their bare host panels (Fig. 1c), it is clear that the dip-reduced metamaterial achieves a highly improved STL dip while mainly preserving the targeted STL peak around 600 Hz.



Fig. 1. (a) Predicted STL of conventional and optimized dip-reduced metamaterial panel with its parameters, (b) manufactured conventional (left) and dip-reduced (right) metamaterial panels mounted on the acoustic testing cabin and (c) comparison of the ΔIL of the conventional and dip-reduced metamaterial panel in 1/12 octave bands.

4. Concluding Remarks

In this work, a dip-reduction method for reducing the typical STL dip of metamaterial panels was introduced in an optimization routine and translated into a realizable multi-resonant, dip-reduced metamaterial panel design. Compared to a conventional metamaterial panel, the acoustic insulation of the manufactured dip-reduced metamaterial panel shows an STL dip improvement of 5 dB, while mainly preserving the peak STL performance and maintaining approximately the same total mass.

Acknowledgment: The research of L. Van Belle (fellowship no. 1271621N) is funded by a grant from the Research Foundation - Flanders (FWO). The Research Fund KU Leuven is gratefully acknowledged for their support.

References

- [1] LIU Z ET AL: Locally resonant sonic materials. *Science* 2000, **289**(5485):1734-1736.
- [2] CLAEYS C ET AL: A lightweight vibro-acoustic metamaterial demonstrator: Numerical and experimental investigation. *Mechanical Systems and Signal Processing* 2016, **70**:853-880.
- [3] VAN BELLE L ET AL: The impact of damping on the sound transmission loss of locally resonant metamaterial plates. *Journal of Sound and Vibration* 2019, **461**:114909.
- [4] HALL A ET AL: Multiplying resonances for attenuation in mechanical metamaterials: Part 1—Concepts, initial validation and single layer structures. *Applied Acoustics* 2020, **170**:107513.
- [5] VAN BELLE L ET AL: Fast metamaterial design optimization using reduced order unit cell modelling. *Proceedings of ISMA* 2020, 2487-2501.

Locally resonant metamaterials utilizing Dynamic Directional amplification

MORIS KALDERON^{1*}, MARINA KALOGERAKOU¹, ANDREAS PARADEISIOTIS¹, IOANNIS ANTONIADIS¹

1. National Technical University of Athens, School of Mechanical Engineering, Department of Mechanical Design & Automatic Control, Dynamics & Structures Laboratory, Heroon Polytechniou 9, 15780 Zografou, Athens, Greece [0000-0001-6939-726X], [-], [0000-0002-1593-9892], [-]

* Presenting Author

Abstract: Locally resonant metamaterials (LRM) with unit cells exhibiting local resonance present unique wave propagation properties at wavelengths well below the regime corresponding to bandgap generation based on spatial periodicity. However, they show certain constraints in designing systems with wide bandgaps in the low-frequency range. To face the main practical challenges encountered in such cases, including heavy oscillating masses, a simple dynamic directional amplification (DDA) mechanism is proposed. This amplifier is designed to present the same mass and use the same damping element as a reference two-dimensional (2D) Mass-in-Mass metamaterial. Thus, no increase in the structure mass or the viscous damping is needed. The proposed DDA can be realized by imposing kinematic constraints to the structure's degrees of freedom (DoF), improving inertia and damping on the desired direction of motion. A discrete element lattice model based on mass, stiffness and damping is used to establish dispersion behaviour and frequency response. Depending on the location of the DDA, inner or outer mass, both up-shift and down-shift in the bandgap frequency range and their extent are shown to be possible. The numerical results of an indicative case study show significant improvements and advantages over the reference LRM, such as broader bandgaps and increased damping ratio. Finally, a conceptual design indicates the usage of the concept in potential applications, such as mechanical filters, sound and vibration isolators, and seismic isolators.

Keywords: metamaterial, local resonance, band gap, dynamic directional amplifier; damping

1. Introduction

Acoustic metamaterials (AMs) exhibit unusual dynamic properties not readily realizable in natural or other manmade structural materials from properties of their material constituents alone, owing to their local engineered configurations or “microstructures. Nonetheless, conventional locally resonant AM (LRAM) [1], may require very heavy internal parasitic masses, as well as additional constraints at the amplitudes of the internally oscillating locally resonating structures, which may prohibit their practical implementation [2]. Therefore, aiming for wide low frequency bandgaps based solely on LRAM is a challenge. Here, a simple dynamic directional amplifier [3] is introduced as a means to increase artificially the dynamic mass of the structure. The DDA mechanism is realized without additional masses or complex geometries since the amplification can be achieved by coupling the kinematic DoFs of the mass with a rigid link improving inertia and damping [4] on the desired direction of motion. The objective of this study is to indicate the characteristics of the directional amplification induced bandgaps and provide the theoretical framework.

2. Results and Discussion

Figure 1(a) shows the infinite periodic unit-cell lattice of the LRAM-DDA and figure 1(b) the corresponding conceptual implementation. An indicative example is presented based on the analysis conducted by Dertimanis et. al [5]. The selected parameters are $M_L=1M_{gr}$, $M_R=8M_{gr}$, $k_L=k_R=79kN/m$ and correspond to a seismic isolation application Figure 1(c) illustrates the dispersion curves of the LRMA without (black curves) and with the DDA mechanism, where the latter one increase the normalized bandwidth from $b_w = 1$ to 1.53 ($b_w = f_H - f_L)/f_{av}$).

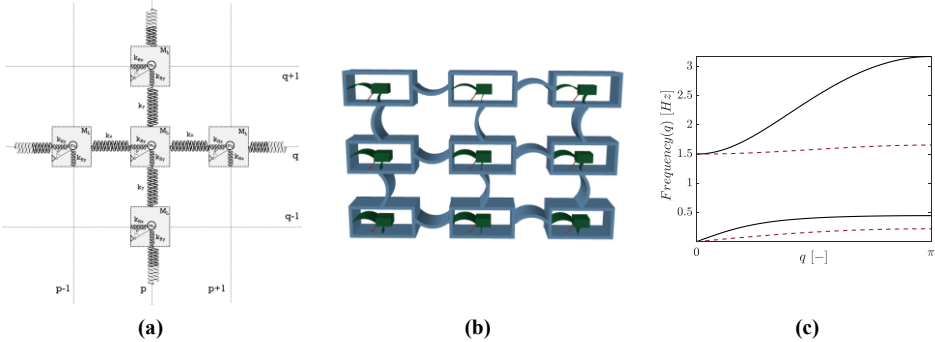


Fig. 1. (a) 2-D Mass-in-Mass lattice with Dynamic Directional Amplifiers (DDA), **(b)** Conceptual design of the proposed Metastructure, **(c)** Dispersion curves: irreducible Brillouin zone. The black curve corresponds to the structure without the DDA and the red curve to the structure with the DDA.

3. Concluding Remarks

The proposed enhanced LRAM shows improved filtering properties in the low frequency regime. The provided indicative implementation of this concept shows promise towards developing low-cost metamaterial designs suitable for acoustic and seismic wave manipulation.

Acknowledgment: This research has been financed by the European Union’s Horizon 2020 research and innovation programme under the Marie Skłodowska-Curie grant, grant number INSPIRE-813424.

References

- [1] HUANG H, SUN C, HUANG G: On the negative effective mass density in acoustic metamaterials. *International Journal of Engineering Science* 2009, **47**(4), 610–617.
- [2] KULKARNI P.P AND MANIMALA J.M: Longitudinal elastic wave propagation characteristics of inertant acoustic metamaterials, *Journal of Applied Physics* 2016, **119**(24): 245101.
- [3] KALDERON M, PARADEISIOTIS A, ANTONIADIS I.A: 2D Dynamic Directional Amplification (DDA) in Phonic Metamaterials. *Materials* 2021, **14**(9):2302.
- [4] HUSSEIN, M.I AND FRAZIER, M.J: An emergent phenomenon in dissipative metamaterials. *Journal of Sound and Vibration* 2013, **332**(20),4767–4774.
- [5] DERTIMANIS V.K, ANTONIADIS I.A, CHATZI E: Feasibility Analysis on the Attenuation of Strong Ground Motions Using Finite Periodic Lattices of Mass-in-Mass Barriers. *Journal of Engineering Mechanics-ASCE* 2016, **142**(2016): 04016060.

Experimental Prototype of a KDamper Vibration Absorber for Small Vertical Loads Utilizing Compliant Joints

ANDREAS PARADEISIOTIS^{1*}, KONSTANTINOS TSIΟΥMANIS¹, IOANNIS ANTONIADIS¹

1. National Technical University of Athens, School of Mechanical Engineering, Department of Mechanical Design & Automatic Control, Dynamics & Structures Laboratory, Heroon Polytechniou 9, 15780 Zografou, Athens, Greece [0000-0001-6939-726X], [-], [-]

* Presenting Author

Abstract: An experimental prototype of a vibration absorption base, designed based on the KDamper concept, is evaluated. The KDamper is a passive vibration absorption and damping concept, based essentially on the optimal combination of appropriate stiffness elements, including a negative stiffness element (NSE). Compared to the traditional Tuned Mass Damper (TMD), it has significantly higher modal damping and achieves greater attenuation in a wider frequency band while utilizing significantly lower additional mass. The inclusion of the NSE facilitates excellent damping properties even at low frequencies without sacrificing the static load bearing capacity of the base as the overall static stiffness of the KDamper is maintained. The design, geared towards machine anti-vibration mounts, concerns a 20 kg seismic mass at frequencies around 3.5 Hz. The NSE is implemented utilizing compliant translational joints to overcome the limitations of conventional helical springs in this context. Finally, transmissibility measurements of the prototype have been performed, which show good agreement with the analytic predictions.

Keywords: KDamper, negative stiffness, vibration control, compliant joints, experimental

1. Introduction

Vibration isolation of systems subjected to periodic excitation with conventional elastic mounting, requires the reduction of the resonant frequency by adjusting its stiffness. At low excitation frequencies, the required stiffness reduction leads to large deflections and/or compromises the structural integrity of the system. Concepts like the Tuned Mass Damper (TMD), quasi-zero stiffness oscillators, inerters etc., have been proposed and implemented to overcome these challenges. The presented design is based on the KDamper concept [1]. A base/mounting mechanism is designed for the absorption of vertical vibrations of machines, is considered in this work. The targeted seismic mass is 20 kg for rotational speeds around 200 RPM.

The KDamper incorporates a negative stiffness element (NSE), the elastic force of which supplements the inertial forces of the added mass. Most significant comparative advantages of the KDamper, especially in the low frequency range, are the superior damping characteristics without the need of heavy additional masses or sacrificing the static loading capacity of the structure by using soft elastic mounting. The NSE of the KDamper can be realized in various ways such as pre-stressed disc springs [2] or helical springs [1] and post-buckled beams [3] among others. However, in cases where high negative stiffness along with large dynamic amplitude of the internal degree of freedom are required, most implementations are proven inadequate, mostly due to high stress development of the structural elements. Configurations of mechanisms utilizing conventional helical compression or extension springs have been investigated, demonstrating drawbacks such as buckling deformation, insufficient

stroke and manufacturing inaccuracies. Here, a configuration consisting in a mechanism with pre-stressed springs is used for the NSE. However, instead of conventional helical springs, appropriate large-displacement compliant joints [4] were utilized to overcome these drawbacks.

The fundamentals of the KDamper and compliant joints design procedure are presented, along with the numerical evaluation including the response of the system in the time and frequency domains. Finally, based on this design, a prototype was built for the conduction of experimental measurements.

2. Results and Discussion

The various manufactured stiffness elements including the compliant joints showed certain deviation relative to the design values which were partly considered during the design process. Nevertheless, the provision for modularity of certain geometrical parameters of the NSE facilitated the required adjustments for optimal operation of the system and furthermore, the testing of two cases for different seismic mass. The transmissibility of the system resulting from the processing of the various cases of experimental measurements, demonstrated very good agreement with the predictions of the numerical models. The comparisons along with relevant signal processing parameters validate the theoretical framework and analytic investigation. Even though at this stage no damping elements were incorporated in the prototype, aside of the structural damping of the various stiffness elements, the excellent damping performance of the KDamper was prevalent at frequencies as low as 2 Hz.

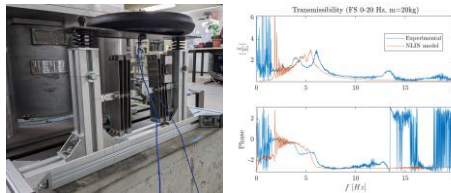


Fig. 1. Experimental prototype of the KDamper base and indicative transmissibility comparisons.

3. Concluding Remarks

An experimental prototype of a KDamper vibration absorption mounting mechanism for small masses and low excitation frequencies was built, utilizing large-displacement compliant joints for the NSE implementation. Conducted experimental measurements compare very well with the analytic predictions and the prototype showcased excellent absorption performance in the intended frequency range.

Acknowledgment: This research has been co-financed by the European Union and Greek national funds through the Operational Program Competitiveness, Entrepreneurship and Innovation, under the call RESEARCH – CREATE – INNOVATE (project code: T1EDK-02827, "Novel Seismic Protection Devices in All Spatial Directions - NOESIS").

References

- [1] ANTONIADIS I.A, KANARACHOS S.A, GRYLLIAS K., SAPOUNTZAKIS I.E: KDamping: A stiffness based vibration absorption concept. *Journal of Vibration and Control* 2016, **24**(3):588-606.
- [2] PARADEISIOTIS A, KALDERON M, ANTONIADIS I.A: Advanced negative stiffness absorber for low-frequency noise insulation of panels. *AIP Advances* 2021, **11**(6):065003.
- [3] HUANG X, LIU X, SUN J, ZHANG Z, HUA H: Vibration isolation characteristics of a non-linear isolator using Euler buckled beam as negative stiffness corrector: A theoretical and experimental study. *Journal of Sound and Vibration* 2014, **333**(4):1132-1148.
- [4] TREASE B.P, MOON Y, KOTA S: Design of Large-Displacement Compliant Joints. *ASME. J. Mech. Des.* 2005, **127**(4):788-798.

Anti-Vibration knob for the Motorcycle, Customizable on the Basis of the Driver's Ergonomics

ANTONINA PIRROTTA^{1*}, ANDREA EVOLA², ALBERTO DI MATTEO¹,
ANTONIO GALVANO³, ANTONIO RUSSO³

1. Department of Engineering, University of Palermo, viale delle Scienze, 90128 Palermo, Italy
2. Skorpion Engineering Divisione Additive Manufacturing, Via Vittime Del Vajont 3/1, 10024 Moncalieri, Italy
3. Department of Surgical, Oncological and Oral Sciences, University of Palermo, via del vespro 90129, zip code 90127, Palermo, Italy.

* Presenting Author

Abstract: Tingling in the hands after hours of driving a motorcycle? Old memory! Anyone, young or adult who has ridden a motorcycle for several kilometers, will remember an unpleasant tingling sensation in the hand. The vibrations induced on humans while riding a motorcycle cause this tingling and other unpleasant sensations. Several more or less serious pathologies are caused by exposure to these vibrations, a very common example is Carpal Tunnel Syndrome. Recent studies on the control of structural vibrations, whose excellent results published in international journals of high impact, have stimulated interest in devolving these methods of analysis also for biomechanical structures, such as those of the bone skeleton of the hand. In particular, by analyzing the vibrations induced on humans while driving a motorcycle, it was decided to design and manufacture knobs with anti-vibration material made according to the anthropometric characteristics of the driver's hand. Experimental investigations assess the efficiency of the anti-vibration knob (Italian Patent Application No. 102021000004691 filed on 01.03.2021), reducing the magnitude of stresses in the most damaging frequency range for the driver.

Keywords: Anti-Vibration, Knob, Biomechanical Structures, International Standards ISO.

1. Introduction

The exposure of the human body to vibration is present in everyday situations and may be a source of discomfort and in some cases may cause health problems. Human exposure to vibrations may be classified into two main classes, in (i) Whole Body Vibrations (WBV) and (ii): Hand-Arm Vibration (HAV). Whole Body Vibrations (WBV) are defined as those vibrations that, as the name suggests, affect the whole body, particularly in a frequency range from 0.5 to 80 Hz. This type of vibration may be present in transportation systems, such as buses, cars, trains, etc. Hand-Arm vibration (HAV) are considered as those vibrations that are transmitted to the hand-arm system, in a frequency range from 6.3 to 1250 Hz. This type of vibrations may be present in hand power-tools like pneumatic hammers and saws or in handlebar of bikes, motorcycles. Specifically, WBV affect the human organism via lower extremities, the pelvis and the back; on the other hand in the case of HAV, disturbances in finger's blood circulation and hand's neurological function injuries may occur.

2. Results and Discussion

The assessment of human exposure to vibration can be performed in accordance with key International Standards ISO (International Organization for Standardization) that for WBV is the ISO 2631 and for HAV is ISO 5349. Moreover, the primary variable used to characterize a vibration measure is the

root mean square (rms) acceleration. This rms acceleration should be weighted in frequency domain, through the use of a weight curve defined in the ISO 2631 and 5349 in such a way to take into account the importance that the vibration at different frequencies may affect human body parts.

Vibrations transmitted to the hand and arm or to the lower-back should be measured in three directions, (x,y,z) according to an orthogonal coordinate system. Since the measurement of vibration should be performed following a system of triaxial coordinates, it will be obtained a value of frequency weighted rms acceleration for each axis, x, y and z, represented by a_{hw_x} , a_{hw_y} and a_{hw_z} in m/s^2 . Following ISO requirements, combining these three values by a vector sum, it will lead to the total weighted vibration acceleration a_{hv} in m/s^2 : $a_{hv} = (a_{hw_x}^2 + a_{hw_y}^2 + a_{hw_z}^2)^{1/2}$. Besides the magnitude of vibration, represented by the total weighted vibration a_{hv} , the assessment of vibration exposure takes into account the daily duration of exposure T , in hours, defined as the amount of time that the hand or lower-back is exposed to the vibrations in one day. Thus, it is defined the daily exposure to vibrations $A(8)$ in m/s^2 , as: $A(8) = a_{hv} (T / T_0)^{1/2}$ where T_0 is referred to eight hours of exposure. The daily exposure to vibration $A(8)$ is interpreted as a total vibration value weighted by the frequency, expressed as an equivalent value for eight hours of exposure.



Fig. 1. Complete Instrumentation

The instrumentation chosen (Fig.1) for data acquisition included the use of the ny-myRio 1900 acquisition card and the triaxial MEMS accelerometers GY-61 ADXL335, suitably wired and protected through 3D printed shells. Through this experimental setup, it was possible to assess the efficiency of the prototype of the anti-vibration knob (Italian Patent Application No. 102021000004691 filed on 01.03.2021). Specifically, recording hand vibrations, induced by driving the motorcycle, in both cases: with the original knob (OK) and with the anti-vibration knob (AK), it was apparent the efficiency of the prototype in reducing vibrations as shown in Fig.2.

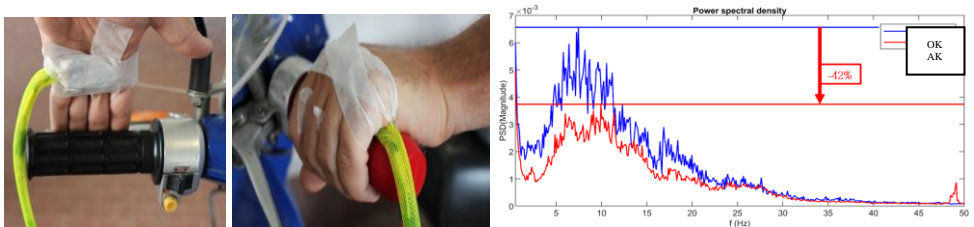


Fig. 2. Original Knob; Anti-Vibration Knob; Power Spectral Density

References

- [1] International Organization for Standardization – ISO. ISO 5349-1. Mechanical vibration: measurement and evaluation of human exposure to hand-transmitted vibration.

A 3D multiple scattering formulation to model elastic waves interacting with surface resonators

XINGBO PU*, ANTONIO PALERMO, ALESSANDRO MARZANI

Department of Civil, Chemical, Environmental and Materials Engineering, University of Bologna, 40136 Bologna, Italy

* Presenting Author: xingbo.pu2@unibo.it

Abstract: We present a closed-form formulation to model the 3D dynamic response of an elastic half-space coupled to a cluster of surface resonators when excited by a harmonic point force. The technique exploits the analytical solution of the canonical Lamb's problem in a multiple scattering methodology to formulate the wavefields generated by the resonators. For an arbitrary number of surface resonators arranged atop an elastic half-space in an arbitrary configuration, the displacement field is obtained in closed-form and validated via finite element simulations in three-dimensional contexts.

Keywords: Elastic metasurfaces, seismic metamaterials, multiple scattering, Rayleigh waves.

1. Introduction

The interaction between waves and surface resonant structures plays an important role in modelling the so-called site-city effect [1] and in designing resonant barriers for ground-borne vibration attenuation [2, 3]. Pivotal for understanding the coupled substrate-resonator response is the possibility of predicting the total wavefield given by both the propagating waves and the scattered fields generated by the resonant structures. Currently, such prediction can be achieved only in finite-size systems by exploiting computationally costly numerical techniques, like finite element (FE), since no closed-form formulations are available for this purpose.

To overcome this limitation, in this work we provide an analytical formulation to predict the wavefield of an elastic half-space coupled to a generic array of vertical surface resonators, as shown in **Fig. 1a**. The methodology exploits the classical Lamb's problem [4] to formulate the incident wavefield and its Green's functions to describe the scattered fields given by the resonators subjected to a base motion.

2. Formulation in brief

According to the multiple scattering technique, the total wavefield can be obtained as:

$$\mathbf{u}(\mathbf{r}) = \mathbf{u}_{inc}(\mathbf{r}) + \sum_{n=1}^N F_n \mathbf{G}(\mathbf{r} - \mathbf{R}_n) \quad (1)$$

In which $\mathbf{u}_{inc}(\mathbf{r})$ is the incident wavefield at position $\mathbf{r} = [x, y, z]$ generated by the harmonic point source acting at $\mathbf{r} = \mathbf{0}$, \mathbf{R}_n denotes the resonator positions, \mathbf{G} is the Green's function, and F_n is the normal stress provided by resonators which can be determined by boundary conditions. Once F_n is obtained, the wavefield can be calculated by substituting it into Eq. (1). The detailed procedure to calculate F_n is provided in [5].

3. Results and Discussion

We consider an elastic half-space coupled with two identical resonators. We set the material properties for the elastic half-space as: $E = 46 \text{ MPa}$, $\nu = 0.25$, $\rho = 1800 \text{ kg/m}^3$, namely Young modulus, Poisson ratio and density, respectively, and the resonators with mass and resonant frequency equal to $m_1 = m_2 = 1000 \text{ kg}$ and $f_{r1} = f_{r2} = 2 \text{ Hz}$, respectively. The resonators are placed at $x_1 = 6 \text{ m}$, $x_2 = 9 \text{ m}$, $y_1 = y_2 = 0$, while a point source $Q = 1 \text{ Pa}$ is located at the origin of the coordinate system. **Fig. 1b** shows the variation of the vertical displacement at the resonators footprint for different frequencies of the input source. The solid and dashed lines denote the analytical results, while dots indicate the results from 3D FE simulations. An excellent agreement between the analytical and the numerical results is found. The drop in the amplitude of the vertical displacement occurs at the resonance frequency of the oscillators as a result of the interaction between the incident and scattered fields.

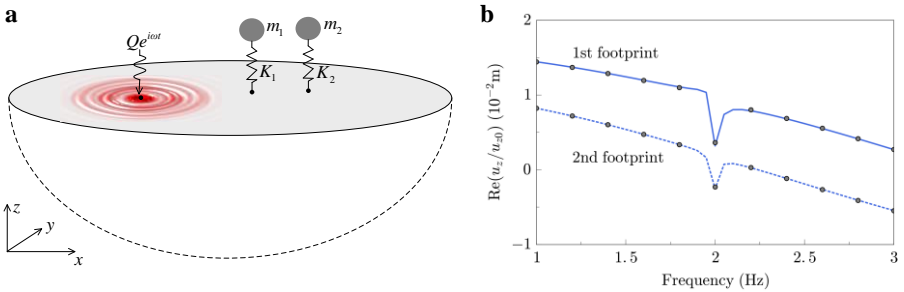


Fig. 1. (a) The schematic of the considered system. (b) The real part of the vertical displacement of resonator footprint vs. frequency. For comparison, we also provide the FE solutions denoted by dots.

4. Concluding Remarks

An analytical formulation to study the interaction of elastic waves with surface resonators is briefly discussed. The formulation makes use of the solution of the canonical Lamb’s problem to calculate the incident field generated by a point source and the scattered field introduced by each resonator motion. The formulation, validated against FE simulations, can handle an arbitrary number of resonators arranged on the surface in a generic configuration.

Acknowledgment: This project has received funding from the European Union’s Horizon 2020 research and innovation programme under the Marie Skłodowska Curie grant agreement No 813424.

References

- [1] M. GHERGU, I. R. IONESCU: Structure-soil-structure coupling in seismic excitation and “city effect”. *International Journal of Engineering Science* 2009, **47**(3):342-354.
- [2] ANTONIO PALERMO, SEBASTIAN KRÖDEL, ALESSANDRO MARZANI, CHIARA DARAIO: Engineered metabarrier as shield from seismic surface waves. *Scientific reports* 2016, **6**(1):1-10.
- [3] XINGBO PU, ANTONIO PALERMO, ZHIBAO CHENG, ZHIFEI SHI, ALESSANDRO MARZANI: Seismic metasurfaces on porous layered media: Surface resonators and fluid-solid interaction effects on the propagation of Rayleigh waves. *International Journal of Engineering Science* 2020, **154**:103347.
- [4] H. LAMB: I. on the propagation of tremors over the surface of an elastic solid. *Philosophical Transactions of the Royal Society of London. Series A, Containing papers of a mathematical or physical character* 1904, **203** (359-371):1-42.
- [5] XINGBO PU, ANTONIO PALERMO, ALESSANDRO MARZANI: Lamb’s problem for a half-space coupled to a generic distribution of oscillators at the surface. *arXiv preprint arXiv:2101.09997*, 2021.

A Dynamic-Stiffness Framework for Locally Resonant Structures

ANDREA FRANCESCO RUSSILLO^{1*}, GIUSEPPE FAILLA²

1. University of Reggio Calabria, Department of Civil, Energy, Environmental and Materials Engineering (DI-CEAM), Via Graziella, 89124 Reggio Calabria, Italy [0000-0002-8451-0141]
2. University of Reggio Calabria, Department of Civil, Energy, Environmental and Materials Engineering (DI-CEAM), Via Graziella, 89124 Reggio Calabria, Italy [0000-0003-4244-231X]

* Presenting Author

Abstract: A comprehensive analytical/numerical framework is presented for locally resonant metamaterial structures, modelled as continuous beams coupled with periodic multi-degree-of-freedom subsystems representing the resonators. An exact reduced-order dynamic-stiffness approach is formulated, where the beam equations are solved exactly upon condensing all the degrees of freedom within the resonators. Solutions to the free-vibration problem are obtained from an exact dynamic-stiffness matrix, whose size is 4×4 for any number of resonators. Solutions to the forced vibration problem under arbitrary loads are obtained by modal superposition, in time and frequency domains, on introducing proper orthogonality conditions for the modes. The framework is suitable for Euler-Bernoulli or Timoshenko beams and typical resonators as mass-spring-dashpot chains, mass-spring-dashpot systems within rigid truss assemblies, inerter-based absorbers. Viscous damping within the resonators can be considered.

Keywords: metamaterial, locally resonant structure, dynamic-stiffness method

1. Introduction

Locally resonant metamaterial structures are an emerging concept in dynamics, with promising applications in many real-life engineering applications. The term “locally resonant structure” refers to a beam or plate coupled with a periodic array of multi-degree-of-freedom resonators where, as a result of the periodic resonance induced by the resonators, elastic waves cannot propagate over stop bands named *band gaps*. For this remarkable property, locally resonant structures attracted a great deal of attention in the last decade, as demonstrated by the outstanding number of works on this topic [1,2].

Here, we focus on locally resonant structures consisting of continuous beams coupled with multi-degree-of-freedom resonators. We promote an exact reduced-order dynamic-stiffness formulation, where the beam equations are solved exactly upon condensing all the resonator degrees of freedom. The formulation delivers an exact dynamic-stiffness matrix of size 4×4 for any number of resonators, from which the solution to the free-vibration problem is obtained. Further, the modal response under arbitrary loads is obtained in a concise analytical form, in time and frequency domains, deriving proper orthogonality conditions for the modes of the beam only. The proposed framework is general, as applies to various beam models (Euler-Bernoulli and Timoshenko) and various resonators, as mass-spring-dashpot chains, mass-spring-dashpot-truss assemblies, inerter-based absorbers.

2. Results and Discussion

We consider the locally resonant Timoshenko beam in Fig. 1a, coupled with 1-degree-of-freedom mass-spring-dashpot resonators. Parameters of beam are $E = 88.5$ MPa, $A = 0.08$ m², $\nu = 0.30$, $\rho = 2700$ kg/m³, $\kappa = 0.85$ (shear correction factor); $k_r = 2 \times 10^5$ N/m, $m_r = 0.2$ kg, $c_r = 0.03$ Ns/m, $a = 0.1$

m and $N = 8$ are taken for the resonators. We calculate complex modes in Table 1 and transmittance of the beam in Fig. 1b by the proposed dynamic-stiffness matrix (DSM) approach (black continuous line), the finite-element method (FEM) in Abaqus (red dashed line); the exact response without resonators (blue continuous line) is included.

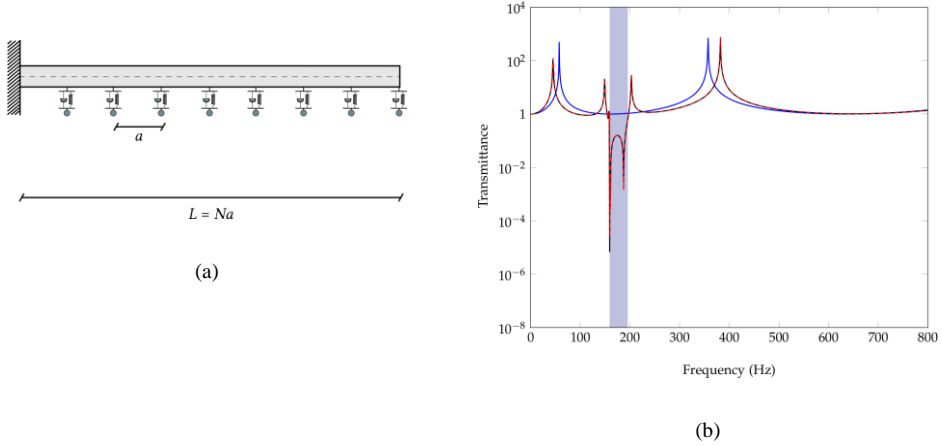


Fig. 1. Locally resonant Timoshenko beam with 1-degree-of-freedom mass-spring-dashpot resonators

Table 1. Complex eigenvalues of the beam in Fig. 1

Mode	Eigenvalue (DSM)	Eigenvalue (FEM)
1	$\pm 283.39 + 0.001$	$\pm 283.39 + 0.001$
2	$\pm 937.19 + 0.056$	$\pm 937.19 + 0.056$
3	$\pm 992.53 + 0.073$	$\pm 992.54 + 0.073$
4	$\pm 998.01 + 0.074$	$\pm 998.01 + 0.074$
5	$\pm 999.22 + 0.075$	$\pm 999.23 + 0.075$
6	$\pm 999.61 + 0.075$	$\pm 999.61 + 0.075$
7	$\pm 999.76 + 0.075$	$\pm 999.76 + 0.075$
8	$\pm 999.82 + 0.075$	$\pm 999.82 + 0.075$
9	$\pm 1274.64 + 0.117$	$\pm 1274.65 + 0.117$
10	$\pm 2401.47 + 0.064$	$\pm 2401.71 + 0.064$

3. Concluding Remarks

We will formulate an exact reduced-order dynamic-stiffness framework for locally resonant metamaterial beams, addressing the free and forced vibration problems.

A relevant aspect of the framework is that it handles various beam models and resonators. Furthermore, we will demonstrate the framework is not applicable to beams only, as generalizations are readily feasible for locally resonant metamaterial Kirchhoff plates.

References

[1] HUSSEIN MI, LEAMY MJ, RUZZENE M: Dynamics of phononic materials and structures: Historical origins, recent progress, and future outlook. *Applied Mechanics Reviews* 2014, **66**(4): 040802.
 [2] LIM T-C: *Mechanics of Metamaterials with Negative Parameters*. Springer Nature: Singapore, 2020.

Low frequency tyre noise mitigation in a vehicle using metal 3D printed resonant metamaterials

LUCA SANGIULIANO^{1,2*}, BJÖRN REFF³, JACOPO PALANDRI³, FRIEDRICH WOLF-MONHEIM³,
BERT PLUYMERS^{1,2}, ELKE DECKERS^{1,2,4}, WIM DESMET^{1,2}, CLAUS CLAEYS^{1,2}

1. DMMS lab, Flanders Make
 2. Division LMSD, Department of Mechanical Engineering, KU Leuven, Heverlee, Belgium
 3. Ford Research & Innovation Center (RIC), Aachen, Germany
 4. Department of Mechanical Engineering Technology, KU Leuven, Diepenbeek, Belgium
- * Presenting Author

Abstract: To comply with stringent environmental and noise standards in the automotive sector, a resonant metamaterial solution is applied to a vehicle to reduce the interior structure-borne noise due to the acoustic tyre resonances around 220Hz. This novel solution consists of metal 3D printed resonant elements applied on the rear wheel arches of a vehicle and replaces the commonly used dynamic damper solution that are typically installed on the suspension or the vehicle body. The objective is to reduce the structural energy propagation into the vehicle body, and in turn the acoustic energy radiated into the vehicle compartment. Numerical and experimental analyses show how 3D printed resonant metamaterials can be a performant lightweight alternative to the common noise and vibration solutions for the automotive sector.

Keywords: resonant metamaterials, structure-borne noise, automotive NVH, metal 3D printing

1. Introduction

The increasingly stringent norms with respect to the energy efficiency of vehicles leads to a strong push to reduce the vehicle's weight, which is often conflicting with noise, vibration and harshness (NVH) requirements. Resonant metamaterials have become an attractive alternative to classical NVH control solutions since they can combine lightweight design and performant NVH behaviour, particularly in targeted low frequency ranges, known as stop bands. These stop bands can be achieved through the addition of resonant elements onto a host structure in a subwavelength scale [1]. Recently, resonant metamaterials for vehicle applications were used in a thermofomed rooftop of a harvester [2], in car floor panels [3], onto the firewall of a car [4] and on the shock tower of an SUV [5]. Extending on the concept of the latter application, in this work, metal 3D printed resonant elements are added onto the rear wheel arches of a hatchback car model to reduce the interior tonal structure-borne noise issue due to the first acoustic tyre resonances around 220Hz. Different from the common dynamic damper solution which can be installed on the suspensions to mitigate this issue, the metamaterial solution is designed to hinder the structural energy from propagating into the vehicle body. For this work, a metamaterial design was made using finite element based structural intensity analyses simulations on the vehicle body. Resonant elements were printed and tested before addition to the rear wheel arches of the vehicle. Finally, the resonant metamaterial performance was verified experimentally in the vehicle using a standard testing procedure at three different speeds, on a road simulating dynamometer, in a semi-anechoic room.

2. Results and Discussion

The considered hatchback car model was mounted with tyres model 205/55 R16. When tested at 40-50-80kph on the dynamometer, the acoustic tyre resonances lead to outspoken peaks in the interior sound pressure level (SPL) between 224Hz to 241Hz. To achieve stop band behaviour in this frequency range and a more effective reduction of the structural energy propagation, each metal 3D printed resonant element was designed to have two bending resonance frequencies at $238\text{Hz}\pm 6.2\text{Hz}$ and $248\text{Hz}\pm 8.8\text{Hz}$, (Fig. 1a). A total of 228 resonant elements (about 0.75kg, similar to that of a classical dynamic damper) are added around the top mounts and the body panels of the rear wheel arches, which are identified as the main energy transfer paths that contribute the most to the interior SPL. The structural intensity analyses (Fig. 1b) show that the resonant metamaterial solution leads to a strong reduction of the energy in the body panels of the rear wheel arches. The test results finally verify the resonant metamaterial potential (Fig. 1c) as confirmed by the ΔSPL , the difference in sound pressure level, between the vehicle without and with the resonant metamaterial, averaged across the frequency band 220-250Hz. The improvement depends on the speed and up to 2dB(A) improvement can be achieved. The SPL improvement in this frequency band is comparable to that achievable by a common dynamic damper solution.

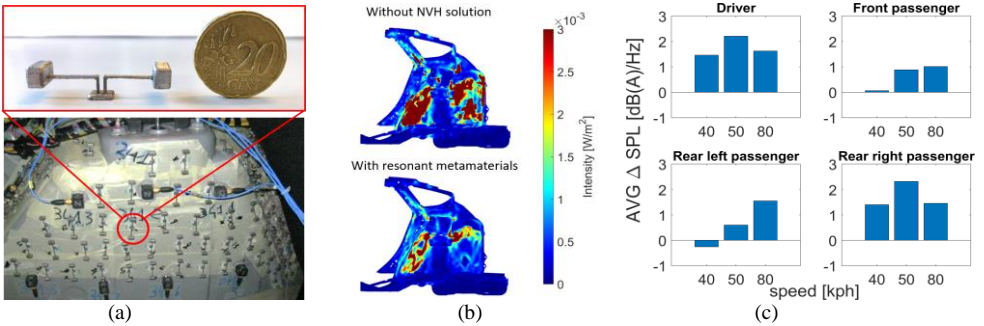


Fig. 1. Picture of the metal 3D printed resonators installed on the rear wheel arch (a). Structural intensity analyses in the rear right wheel arch at 238Hz (b). Measured averaged SPL difference between 220-250Hz of the vehicle without NVH solution and with the resonant metamaterial solution (c). Positive values indicate SPL improvement.

3. Concluding Remarks

A resonant metamaterial solution consisting of metal 3D printed resonant element was applied to the rear wheel arches of a hatchback car model to reduce the structure-borne noise due to the first tyre acoustic resonances. Numerical and experimental analyses demonstrate the potential of this novel solution as a lightweight and performant NVH alternative for the automotive sector.

Acknowledgment: Internal Funds KU Leuven are gratefully acknowledged for their support.

References

- [1] LIU Z ET AL: Locally resonant sonic materials. *Science* 2000, 289(5485):1734-1736.
- [2] MELO ET AL: Realisation of a thermoformed vibro-acoustic metamaterial for increased STL in acoustic resonance driven environments. *Applied acoustics*, 156, 78-82, 2019.
- [3] WU X ET AL: Vibration reduction of a car body based on 2D dual-base locally resonant phononic crystal *Applied acoustics*, 151, 1-9, 2019
- [4] CHANG KJ ET AL: A study on the application of locally resonant acoustic metamaterial for reducing a vehicle's engine noise. *Proceedings of Internoise*, 2019:102-113(12)
- [5] SANGIULIANO L ET AL: Reducing vehicle interior NVH by means of locally resonant metamaterial patches on rear shock towers. *SAE technical paper*, 2019-01-1502, 2019

Interval frequency response of uncertain locally resonant structures

ROBERTA SANTORO¹, MATTEO MAZZEO^{1*}, GIUSEPPE FAILLA²

1. University of Messina, Department of Engineering, Villaggio S. Agata, 98166 Messina, Italy [0000-0002-9245-9702]
2. University of Reggio Calabria, Department of Civil, Energy, Environmental and Materials Engineering (DICEAM), Via Graziella, 89124 Reggio Calabria, Italy [0000-0003-4244-231X]

* Presenting Author

Abstract: The paper aims to evaluate the interval frequency response of uncertain locally resonant structures. Following a non-probabilistic approach, the parameters of the resonators are modelled as uncertain-but-bounded variables defined by lower and upper bounds. The bounds of the frequency response of the locally resonant structure are obtained by a global optimization technique as well as first-order and second-order Taylor approximations, taking full advantage of very simple and explicit expressions ensuring a remarkable reduction of computational effort. Applications on locally resonant beams and plates focus on analysing the frequency response variability due to the uncertainties.

Keywords: locally resonant structures, uncertain-but-bounded parameters, frequency response.

1. Introduction

Structures with periodically attached resonators, generally denoted as locally resonant (LR) structures, are a promising concept for vibration attenuation with several potential applications in mechanical and structural engineering [1,2]. Commonly, LR structures as beams or plates are modelled by elastic continua (using standard beam/plate theories) coupled with discrete mass-spring subsystems modelling the resonators.

In real-life applications, the parameters of the system may be affected by uncertainties due to different sources, e.g. initial manufacturing errors, model inaccuracies and performance of the elements. This variability may lead to significant variability of the response.

The present study investigates how and to which extent the response of LR structures may be affected by uncertainty in the parameters of the resonators. Specifically, within the framework of the interval analysis [3], the parameters of the N resonators of the system, namely stiffness, mass and damping, are described as *uncertain-but-bounded* variables ranging between their lower (LB) and upper (UB) bounds. The interval uncertainty in the parameters of the resonators implies that the LR system frequency response is an interval function as well.

On resorting to a finite element approach in the frequency domain, the innovative point of our study consists in calculating the transfer matrix of the LR structure from the transfer matrix of the host uncontrolled structure as modified by summing an appropriate N -rank matrix, which represents the feedback action of the resonators on the host structure and accounts for the fluctuations of the parameters of the resonators. The proposed calculation is exact and greatly simplifies the evaluation of the interval frequency response function (FRF) of the LR structure. On this basis, we will estimate the bounds of the frequency response of the LR structure by applying a global optimization technique as well as the first-order and second-order Taylor approximations, which provide very simple and explicit expressions with a significant reduction of computational effort.

2. Results and Discussion

Consider the LR Euler cantilever beam under a unit harmonic force at the free end in Fig. 1. $N = 8$ one-degree-of-freedom resonators are attached to the beam at mutual distance a (= cell length).

The beam parameters are: $E = 70$ GPa, $I = 7.85 \times 10^{-9}$ m⁴, $\rho = 0.88$ kgm⁻¹ and $a = 0.02$ m. Fig. 2 shows the bounds of FRF amplitude for the tip deflection of the beam when mass and damping of the resonators are taken as deterministic values, $m_j = 0.01$ kg and $c_j = 0.1$ Nsm⁻¹, while uncertain-but-bounded stiffness k_j^l (for $j = 1, \dots, N$) is assumed to vary in the range [90000, 110000] Nm⁻¹. Using the proposed framework, LBs and UBs are calculated by a global optimization technique. Results of the Monte-Carlo simulation (MCS) are included for validation.

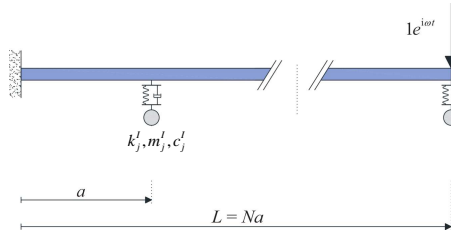


Fig. 1. LR Euler cantilever beam with one-degree-of-freedom resonators

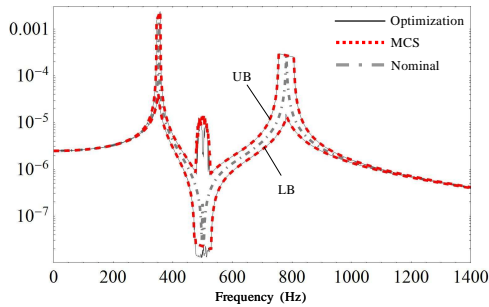


Fig. 2. LB and UB of FRF amplitude for tip deflection of LR beam in Fig. 1 (resonators with uncertain stiffness)

3. Concluding Remarks

We propose a novel computational framework to estimate the effects of uncertainties in the parameters of the resonators on the frequency response of LR structures. The framework is based on an exact expression of the transfer matrix, suitable for any finite element model of LR structures.

References

- [1] XIAO Y, WEN J, YU D, WEN X: Flexural wave propagation in beams with periodically attached vibration absorbers: Band-gap behavior and band formation mechanisms. *Journal of Sound and Vibration* 2013, **332** (4):867-893.
- [2] MIRANDA EJP, NOBREGA ED, FERREIRA AHR, DOS SANTOS JMC: Flexural wave band gaps in a multi-resonator elastic metamaterial plate using Kirchhoff-Love theory. *Mechanical Systems and Signal Processing* 2019, **116**:480-504.
- [3] MOORE RE: *Interval Analysis*. Prentice-Hall: Englewood Cliffs, 1966.

Experimental study of a tuned liquid column damper with liquid turbine

TIAN-YU ZHOU^{1*}, HAO DING²

1. Department of Hydraulic Engineering, Tsinghua University, Beijing, China

2. Department of Hydraulic Engineering, Tsinghua University, Beijing, China [0000-0001-7058-3561]

* Presenting Author

Abstract: Tuned liquid column dampers (TLCDs) are attractive for application in mitigating wind or seismic-induced vibrations of engineering structures. On the basis of the existing TLCDs, this paper designs a novel type of TLCD equipped with liquid turbine that has the potential to simultaneously control vibration and generate power. A Savonius-type turbine is employed in a conventional TLCD. Shaking table tests are performed to examine the control efficiency of the TLCDs with and without liquid turbine. Furthermore, a simple circuit connection is made for the TLCD equipped with the Savonius-type turbine to check its power generation performance. The experimental findings confirm that the proposed TLCD is capable of mitigating the resonant response of structures. More importantly, the light-emitting diode connected to the turbine can be continuously and stably lit. This implies that the turbine successfully generates electricity, which provides a feasible basis for the autonomous semi-active control of TLCDs.

Keywords: TLCD, liquid turbine, shaking table test

1. Introduction

The tuned liquid column damper (TLCD) concept for vibration control of civil engineering structures was proposed by Sakai et al. [1] in 1989. Since its initial development, numerous researchers have investigated the optimization scheme of control solution based on TLCDs through passive, semi-active and active strategies [2]. Meanwhile, TLCDs have successfully achieved the multidirectionality, and the combination of inerters for improving control efficiency [3,4]. Nevertheless, the existing TLCDs are proposed solely for vibration control.

This paper creatively designs the configuration of TLCD equipped with liquid turbine that has the potential to simultaneously control vibration and generate power. The rotating turbine in the oscillating liquid column provides additional liquid damping for the TLCD, also the energy when it is connected to an electric motor. The experimental results reveal that the proposed solution can achieve simultaneous vibration mitigation and power generation, which verifies its feasibility for application in semi-active TLCDs.

2. Results and Discussion

Shaking table tests are performed to examine the control efficiency of the TLCD with Savonius-type turbine. It is found that the TLCD can reduce the vibration of the structure, as shown in Figure 1. It is also found that during the excitation, the light-emitting diode connected to the Savonius-type turbine can be continuously and stably lit, as shown in Figure 2. The results prove that the TLCD with

Savonius-type turbine designed in this paper is capable of mitigating the resonant response of structures, and has the potential to generate electricity during the vibration.

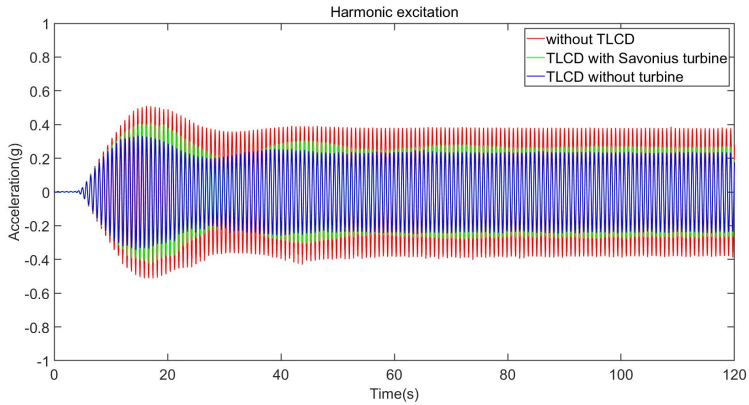


Fig.1. Acceleration of the structure with and without TLCD

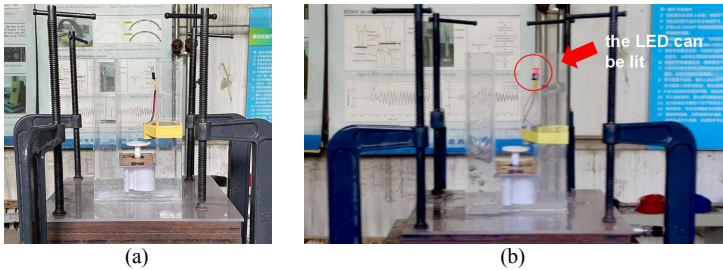


Fig.2. TLCD with Savonius-type turbine before excitation(a) and during excitation(b)

3. Concluding Remarks

This paper proposes the configuration of TLCDs equipped with liquid turbine, which can provide additional liquid damping and generate power. A Savonius-type turbine is used in the shaking table tests. It is demonstrated that the proposed device can be applied to simultaneously suppress vibration and produce electricity.

References

- [1] SAKAI F, TAKAEDA S, TAMAKI T: Tuned liquid column damper-new type device for suppression of building vibration. *Proceedings of the international conference on high-rise buildings*, Nanjing, China, 1989:926-931.
- [2] CHEN Y, DING Y: Passive, Semi-Active, and Active Tuned-Liquid-Column Dampers. *Proceedings of the ASME 2006 Pressure Vessels and Piping/ICPVT-11 Conference. Volume 8: Seismic Engineering*, Vancouver, BC, Canada, 2006:99-106.
- [3] DING H, WANG J, LU L, ET AL: A toroidal tuned liquid column damper for multidirectional ground motion - induced vibration control. *Structural Control and Health Monitoring* 2020, 27(8).
- [4] WANG Q, TIWARI N D, QIAO H, ET AL: Inerter-based tuned liquid column damper for seismic vibration control of a single-degree-of-freedom structure. *International Journal of Mechanical Sciences* 2020, 184:105840.

-ASY-

Asymptotic Methods in Nonlinear Dynamics

Modelling and Analysing of a Spring Pendulum Motion in the Presence of Energy Harvesting Devices

M. K. Abohamer^{1A*}, J. Awrejcewicz^{1B}, R. Starosta², T. S. Amer³, M. A. Bek⁴

1. Lodz University of Technology, Department of Automation, Biomechanics and Mechatronics, Lodz, Poland;
2. Poznan University of Technology, Institute of Applied Mechanics, Poznan, Poland;
3. Tanta University, Faculty of Science, Mathematics Department, Tanta, Egypt;
4. Tanta University, Faculty of Engineering, Department of Physics and Engineering Mathematics, Tanta, Egypt;

^{1A}[[0000-0001-8679-0565](#)], ^{2B}[[0000-0003-0387-921X](#)], ²[[0000-0002-3477-4501](#)], ³[[0000-0002-6293-711X](#)],
⁴[[0000-0002-6052-6181](#)] * Presenting Author

Abstract: Energy harvesting will become more and more essential mechanical vibration applications of many devices. The vibrations can be converted by appropriate devices into electrical energy, which can be used as a power supply instead of ordinary ones. This paper investigates a dynamical system associated with two devices: a piezoelectric device and an electromagnetic one. These devices are connected with a nonlinear damping spring pendulum with 2DOF, in which its supported point moves in a circular path. The equations of motion are obtained using Lagrange's equations of the second kind. The asymptotic solutions of these equations are obtained up to the third approximation utilizing the perturbation approach of multiple scales. The comparison between these solutions and the numerical ones reveals high consistency between them. The steady-state solutions are obtained, and their stabilities are tested. The influences of the excitation amplitudes, the damping coefficients, and the different frequencies on energy harvesting devices outputs are examined and discussed. The work is essential due to its significance in real-life applications. The developed methodology and obtained results can be useful in various applications like power supply of sensors and charging electronic devices.

Keywords: Perturbation methods, Resonance, Stability.

1. Introduction

Energy harvesting (EH) is an essential vital aspect that the research fields work on through the previous few years. It transforms the surrounding energy present in the Earth into electrical power to drive autonomous electronic devices or circuits [1-2]. This energy can be harvested from solar energy, thermal energy, and the most crucial source for harvesting is kinetic energy, especially from vibrational motion [3].

2. Results and Discussion

Two energy harvesting devices, including piezoelectric and electromagnetic, are connected with a pendulum separately 'as two cases' to convert the vibrational motion into electrical. The main governing system of motion is derived using Lagrange's equations, in which the mechanism of the piezoelectric and electromagnetic circuits are used to obtain their corresponding equations as follows

$$\ddot{z} + c_1 \dot{z} + z + 3\alpha \zeta_s^2 z + 3\alpha \zeta_s z^2 + \alpha z^3 - r p^2 (\cos p\tau + \phi \sin p\tau) + \frac{1}{2} W^2 \phi^2 + PM - (1+z)\dot{\phi}^2 = f_1 \cos p_1\tau,$$

$$(1+z)^2 \ddot{\phi} + c_2 \dot{\phi} + W^2 (1+z) (\phi - \frac{\phi^3}{6}) - r p^2 (1+z) (\sin p\tau - \phi \cos p\tau) + 2(1+z)\dot{z}\dot{\phi} = f_2 \cos p_2\tau,$$

$$\dot{v} + \frac{v}{R_p c_p \omega_1} = \frac{l\gamma_1}{c_p} \dot{z}, \quad \dot{q} + \frac{q R_m}{l_m \omega_1} = \frac{l\gamma_2}{l_m} \dot{z}.$$

The asymptotic solutions up the third approximation are obtained utilizing the multiple scale method. External resonance cases between the classified cases of resonance are examined. The numerical results are compared with the approximate ones to reveal the accuracy between them (Fig.1). The modulation equations are obtained to explore the solutions at the steady-state and to examine the stability of the fixed points. The influence of damping coefficients and excitation amplitudes on the output voltage, current, and power are represented graphically (see Fig.2).

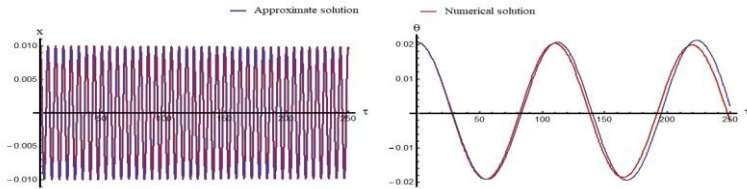


Fig.1: The comparison between the numerical and the approximate solutions.

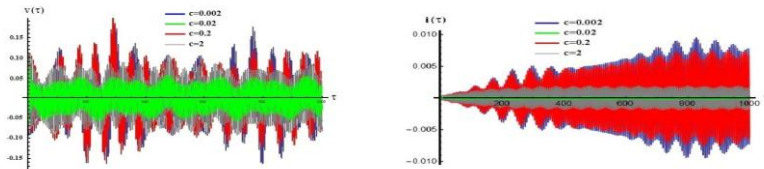


Fig.2: Time histories for the voltage (V) from the piezoelectric device and the current (i) from the electromagnetic device with different values of damping coefficient.

3. Concluding Remarks

A nonlinear damped vibrating spring pendulum system with 2-DOF moving in a circular path with constant angular velocity is investigated which is connected with energy harvesting devices. The governing equations are obtained using Lagrange's equations and solved using the multiple scale method. The time histories of dynamical motion, the responses of the resonance curves, and the solutions at the steady-state cases are plotted to reveal the good impact of the selected values of the model parameters on the motion. A comparison between the numerical and approximate solutions shows high consistency between them. The influence of the damping coefficients and the excitation amplitude on the output voltage, current, and power is examined. Moreover, the response of excitation frequency on the output power of the systems is checked. Electrical energy was generated from the piezoelectric and electromagnetic devices, which were attached to the vibrating system.

References

- [1] Priya S, Inman D: Energy Harvesting Technologies, Springer, 2008.
- [2] Anton S, Sodano H: A review of power harvesting using piezoelectric materials (2003–2006), Smart Materials and Structures 16 (2007)1.
- [3] Harne R. L, and Wang K. W: A review of the recent research on vibration energy harvesting via bistable systems, Smart Mater. Struct. 22 (2013) 023001 (12pp).

The Asymptotic Solutions of the Boundary Value Problem of Convective Diffusion Around Drops with Volumetric Nonlinear Chemical Reaction

Rustyam Akhmetov

Associate Professor: Bashkortostan State Pedagogical University,
Oktyabr'skoy Revolutsii str.3a, Ufa, 450000, Russia

Abstract: We consider a stationary problem of convective diffusion around a droplet, which is streamlined by a liquid flow at low Reynolds numbers, taking into account a nonlinear volumetric chemical reaction. The characteristic feature of the problem is the presence of two dimensionless parameters: a constant of rate of the volumetric chemical reaction k_v , and Peclet number P_e which determine the concentration distribution in the flow. The quantity constant of rate of the volumetric chemical reaction k_v and Peclet number P_e assumed to have a constant value. It is a boundary value problem for a quasilinear partial elliptical equation with a small parameter multiplying in higher derivatives. Small parameter corresponds to large Peclet numbers. The limiting equation, when the small parameter is equal to zero, has singular points of the saddle type. Several boundary layers appear outside the drop. The matching conditions for solutions are formulated at the boundaries between neighboring areas. The principal terms of the asymptotics of the solution are constructed around the drop.

Keywords: asymptotic expansions, convective diffusion, matching method, Peclet number.

1. Introduction

Let us consider stationary diffusion near a spherical droplet of radius a , in a translational flow of a viscous incompressible fluid with a velocity U at infinity at low Reynolds numbers Re , taking into account the bulk chemical reaction. The concentration distribution in dimensionless variables satisfies the boundary value problem (see, for example, [1], Ch. 5, (6.1) - (6.3))

$$\Delta U = Pe(\bar{V}, \nabla) \cdot U + k_v F(U), \quad (1)$$

$$U = 1 \quad \text{at} \quad r = 1, \quad U \rightarrow 0 \quad \text{when} \quad r \rightarrow \infty, \quad (2)$$

where

$$\bar{V} = (V_r, V_\theta, 0), \quad V_r = \frac{1}{r^2} \frac{\partial \psi}{\sin \theta} \frac{\partial \psi}{\partial \theta}, \quad V_\theta = \frac{1}{r \sin \theta} \frac{\partial \psi}{\partial r}, \quad (3)$$

$$\psi(r, \theta) = (r-1) \left(2r - \frac{\lambda}{\lambda+1} \left(1 + \frac{1}{r} \right) \right) \sin^2 \theta / 4, \quad (4)$$

where the Peclet number $P_e = aU / D$, where D is the diffusion coefficient of the substance in the external phase, k_v is the rate constant of the bulk chemical reaction, Δ is the Laplace operator, ∇ is the Hamilton operator. In a spherical coordinate system r, θ with the origin at the center of the drop (the angle θ is measured from the direction of flow at infinity), the velocity field of the liquid outside the spherical drop is determined from the expressions (3) (see [1], Ch. 3), where $\psi(r, \theta)$ is the stream function outside the spherical drop and has the form (4) λ is the ratio of the viscosity of the drop to the viscosity of the environment.

2. Results and Discussion

It is assumed that $F(U)$ is continuous and

$$F: R^l \rightarrow R^l, F(0) = 0, 0 < F'(U), \quad (5)$$

$$F(u) = u + F_2 u^2 + F_3 u^3 + \dots + F_k u^k + O(u^{k+1}), \quad (6)$$

Problems analogous to (1), (2) and a broader class of problems, were considered in [1]. In the absence of chemical reaction (i.e., with $k_v = 0$), problem (1), (2) was analyzed in [1-3] by the method of matched asymptotic expansions [4].

3. Concluding Remarks

It is shown in the work that in the vicinity of the rear critical point the solution of the problem is essentially weakly nonlinear. This affects the nature of mass transfer in the wake of the drop (in the inner boundary).

References

- [1] Levich V.G. Physicochemical Fluid Dynamics. Fizmatgiz. Moscow:1959 [in Russian].
- [2] Sih P.H. and Newman J. Mass Transfer to the Rear of a Sphere in Stokes Flow. Int. J. Heat Mass Transfer. 1967. V. 10. P. 1749-1756
- [3] Gupalo Yu. P., Polyinin A.D., Ryazantsev Yu. S. Mass and Heat Transfer between Reacting Particles and the Flow. Nauka. Moscow: 1985 [in Russian].
- [4] Akhmetov R.G. The asymptotic expansions of the solution for the boundary value problem to a convective diffusion equation with volume chemical reaction near a spherical drop. Communications in Nonlinear Science and Numerical Simulation. V.15 (2011), CNSNS 1577. 2308 – 2312.

Vibration of the system with nonlinear springs connected in series

JAN AWREJCEWICZ¹, ROMAN STAROSTA^{2*}, GRAŻYNA SYPNIEWSKA-KAMIŃSKA²

1. Technical University of Łódź, Department of Automatics and Biomechanics, Łódź, Poland [0000-0003-0387-921X]
 2. Poznań University of Technology, Institute of Applied Mechanics, Poznań, Poland [0000-0002-3477-4501, 0000-0003-0490-2629]
- * Presenting Author

Abstract: Solution of the problem and qualitative analysis of the forced vibration of the spring pendulum containing nonlinear springs connected in series is made in the paper. The method of multiple scales in time domain (MMS) has been employed in order to carry out the analytical computations. The MMS allows one, among others, to predict the resonances which can appear in the systems. The approximate solution of analytical form has been obtained for vibration at main resonance.

Keywords: asymptotic analysis, multiple scales, differential-algebraic system, springs in series

1. Introduction

Elastic elements arranged in various kinds of connections are widely applied in many mechanisms and mechatronic devices [1], [5]. The current analysis concerns a system with massless springs connected in series. The mathematical model of such a system includes differential and algebraic equations. Various kinds of similar problems were investigated by researchers mostly numerically. Asymptotic research of oscillators with two nonlinear springs connected in series is presented in papers [2-4].

2. Mathematical Model

The pendulum with two serially connected springs (Fig. 1), moves in the vertical plane. Z_1 and Z_2 stand for the total elongations of the springs whereas L_{0i} denotes the length of the i th non-stretched spring. The springs nonlinearity is of the cubic type, i.e. $F_i = k_i(Z_i + \Lambda_i Z_i^3)$ for $i = 1, 2$, and the nonlinear contributions to the whole elastic force are assumed to be small. Moreover, there are two purely viscous dampers in the system. The system is loaded by the torque of magnitude $M(t) = M_0 \cos(\Omega_2 t)$ and by the force \mathbf{F} whose magnitude changes also harmonically i.e. $F(t) = F_0 \cos(\Omega_1 t)$.

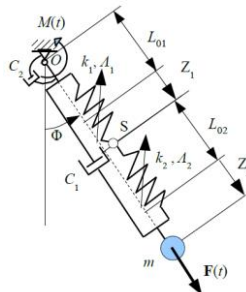


Fig. 1. Forced and damped spring pendulum with two nonlinear springs

Although the system has two degrees of freedom, its state is unambiguously determined by three time functions: the elongations Z_1 and Z_2 and the angle Φ .

Two equations of motion, obtained using the Lagrange formalism, and the equilibrium equation of the joint S govern the dynamic behaviour of the pendulum. They are as follows:

$$m \left(-g \cos(\Phi(t)) - L_0 \dot{\Phi}(t)^2 + \ddot{Z}_2(t) \right) + C_1 \dot{Z}_2(t) + Z_2(t)(k_2 - m \dot{\Phi}(t)^2) - k_2 \Lambda_2 (Z_1(t) - Z_2(t))^3 - k_2 Z_1(t) = F_0 \sin(\Omega_1 t), \quad (1)$$

$$\ddot{\Phi}(t)(m Z_2(t)(2L_0 + Z_2(t)) + L_0^2 m) + C_2 \dot{\Phi}(t) + gm(L_0 + Z_2(t)) \sin(\Phi(t)) + 2m(L_0 + Z_2(t)) \dot{\Phi}(t) \dot{Z}_2(t) = M_0 \sin(\Omega_2 t), \quad (2)$$

$$k_1 Z_1(t)(\Lambda_1 Z_1(t)^2 + 1) = k_2 (Z_2(t) - Z_1(t)) (\Lambda_2 (Z_2(t) - Z_1(t))^2 + 1), \quad (3)$$

where: $L_0 = L_{01} + L_{02}$.

Equations (1) – (3) are supplemented by the initial conditions of the following form

$$Z_2(0) = Z_0, \quad \dot{Z}_2(0) = v_0, \quad \Phi(0) = \Phi_0, \quad \dot{\Phi}(0) = \omega_0, \quad (4)$$

where $Z_0, v_0, \Phi_0, \omega_0$ are known quantities.

The method of multiple scales in time domain with three time variables is applied to solve the considered problem. The method is appropriately modified due to the algebraic-differential character of the equations of motion. The approximate solution allows for the prediction of the resonance conditions. This allowed the equations of motion to be modified appropriately to describe the principal resonance. The solution to the resonant vibration problem has a semi-analytical form because the equations of modulation of the amplitudes and phases are solved numerically.

3. Concluding Remarks

The approximate solution to the governing equations, up to the third order, has been obtained using MMS with three time scales. The forced vibration of the pendulum has been analysed for two cases: far from resonance and in the resonance conditions. The analytical or semi-analytical form of the solution is the main advantage of the applied approach giving the possibility of the qualitative and quantitative study of the pendulum dynamics in a wide spectrum.

Acknowledgment: This paper was financially supported by the grant of the Ministry of Science and Higher Education 0612/SBAD/3567.

References

- [1] ANDRZEJEWSKI R., AWREJCEWICZ J : Nonlinear Dynamics of a Wheeled Vehicle. Springer, Berlin.
- [2] LAI SK, LIM CW: Accurate approximate analytical solutions for nonlinear free vibration of systems with serial linear and nonlinear stiffness. *J. Sound Vib* 2007, **307**:720-736.
- [3] TELLI S, KOPMAZ O: Free vibrations of a mass grounded by linear and nonlinear springs in series. *J. Sound Vib* 2006, **289**: 689-710.
- [4] STAROSTA R, SYPNIEWSKA-KAMINSKA G, AWREJCEWICZ J: Quantifying non-linear dynamics of mass-springs in series oscillators via asymptotic approach. *Mech Syst Signal Pr* 2006, **89**: 149-158
- [5] WANG YJ, CHEN CD, LIN CC, YU JH: A nonlinear suspended energy harvester for a tire pressure monitoring system. *Micromachines* 2015, 6:312-327.

Energy Exchanges in a Nonlinear Meta-Cell

C. DA SILVEIRA ZANIN^{1,2*}, A. TURE SAVADKOOHI¹, S. BAGUET², R. DUFOUR²

1. Univ Lyon, ENTPE, CNRS, LTDS UMR5513, 69518 Vaulx-en-Velin, France

2. Univ Lyon, INSA Lyon, CNRS, LaMCoS, UMR5259, 69621 Villeurbanne, France

* Presenting Author; e-mail: camila.zanin@entpe.fr

Abstract: Vibratory Energy exchanges between particles of a nonlinear meta-cell are studied. The meta-cell is composed of an inner mass with a combined nonlinear restoring forcing term covered by an outer mass. A time multiple scales analysis is carried out in order to find the slow invariant manifold (SIM) and also singular and equilibrium points of the system. A combined nonlinear restoring forcing function of the inner mass makes the behaviour of the SIM different from classical corresponding ones. Finally, quasi-analytical system responses are confronted with numerical ones, obtained by direct integration.

Keywords: meta-cell, nonlinear restoring force, slow invariant manifold, equilibrium/singular points

1. Introduction

In contrast to the classical linear vibration absorber, a nonlinear energy sink (NES) can resonantly interact with the main system for wide frequency ranges [1]. The first studies concerning the NES were based on cubic nonlinearity [2]. Gendelman [3] studied NES with non-polynomial restoring forcing terms, while Lamarque et al [4] investigated systems with piece-wise linear restoring forcing terms. Vibro-impact NES were studied by Gendelman [5] and Gourc et al [6]. In this paper, the response of a single meta-cell with two degrees-of-freedom and a combined nonlinear restoring forcing term is investigated. The organization of the article is as it follows: The analytical methods applied for solving the equations of motion are discussed in Sect. 2. A numerical example is presented in Sect. 3. Finally, the paper is concluded in Sect. 4.

2. Detection of dynamical characteristic of the system

The governing system equations of the 2-dof meta-cell motion have the following expression:

$$\begin{cases} m_1 \ddot{u}_1 + K_1 u_1 + C_1 \dot{u}_1 + F(u_1 - u_2) + C_2 (\dot{u}_1 - \dot{u}_2) = P \sin(\omega t) \\ m_2 \ddot{u}_2 + F(u_2 - u_1) + C_2 (\dot{u}_1 - \dot{u}_2) = 0 \end{cases}, \quad (1)$$

with m_1 and m_2 the outer and inner masses, K_1 and C_1 the linear stiffness and the damping coefficients of the outer mass, C_2 the damping coefficient of the inner mass. Furthermore, $F(\alpha)$ is an odd restoring forcing function of the inner mass. In this study, a combination of a cubic and a non-smooth nonlinearity as $F(\alpha)$ is considered. A nondimensionalized time $\tau = t \sqrt{K/m}$, the coordinates of relative displacement and the centre of mass are introduced to the system variables. After this, the complex variables of Manevitch [7] are applied. A Galerkin method based on truncated Fourier series, via keeping the first harmonics of the system, is employed [8] and a time multiple scales analysis [9] is carried out in order to find the SIM and singular and equilibrium points of the system.

3. Numerical example

The quasi-analytical results for a free system are confronted with those obtained by the direct numerical integration of equations for two different initial conditions. Results are depicted in Fig. 1. The numerical results follow the SIM of the system which possesses two pairs of local extrema (due to the especial nonlinearity of the system) and after one or two bifurcations (depending on the initial conditions), reaches to the rest position.

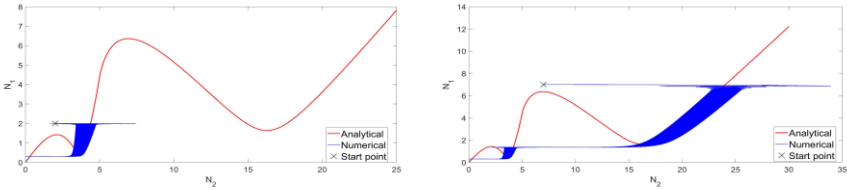


Fig. 1. The SIM and corresponding numerical results for two different initial conditions: $(N_1, N_2) = (2, 2)$ and $(N_1, N_2) = (7, 7)$. N_1 and N_2 stand for amplitudes of the outer and inner masses, respectively.

4. Concluding Remarks

The results presented show that a meta-cell with combined nonlinearity may exhibit a slow invariant manifold which is different from classical systems [3], leading to energy exchanges between particles via several bifurcations.

Acknowledgment: This work was conducted in the framework of the LABEX CELYA (ANR-10-LABX-0060) of the “Université de Lyon” within the program “Investissement d’Avenir” (ANR-11-IDEX-0007) operated by the French National Research Agency (ANR).

References

- [1] VAKAKIS, A.F., GENDELMAN, O.V., BERGMAN, L.A., MCFARLAND, D.M., KERSCHEN, G., LEE, Y.S.: *Nonlinear targeted energy transfer. In: Mechanical and Structural Systems, I&II*. Springer: Berlin, 2009.
- [2] VAKAKIS, A.F.: Inducing passive nonlinear energy sinks in vibrating systems. *Journal of Sound and Vibration* 2001, **123**:324–332.
- [3] GENDELMAN, O.V.: Targeted energy transfer in systems with non-polynomial nonlinearity. *Journal of Sound and Vibration* 2008, **315**:732–745.
- [4] LAMARQUE, C.-H., GENDELMAN, O.V., TURE SAVADKOOHI, A., ETCHEVERRIA, E.: Targeted energy transfer in mechanical systems by means of non-smooth nonlinear energy sink. *Acta mechanica*. 2011, **221**:175-200.
- [5] GENDELMAN, O.V.: Analytic treatment of a system with a vibro-impact nonlinear energy sink. *Journal of Sound and Vibration* 2012, **331**:4599–4608.
- [6] GOURC, E., MICHON, G., SEGUY, S., BERLIOZ, A.: Theoretical and experimental study of an harmonically forced vibro-impact nonlinear energy sink. *J. Vib. Acoust.* 2014, **137**, 031008.
- [7] MANEVITCH, L.I.: The description of localized normal modes in a chain of nonlinear coupled oscillators using complex variables. *Nonlinear Dynamics* 2001, **25**:95–109.
- [8] TURE SAVADKOOHI, A., LAMARQUE, C.-H., WEISS, M., VAURIGAUD, B. ET CHARLEMAGNE, S.: Analysis of the 1 : 1 resonant energy exchanges between coupled oscillators with rheologies. *Nonlinear Dynamics* 2016, **86**:2145–2159.
- [9] NAYFEH, A., MOOK, D.: *Nonlinear Oscillations*. John Wiley and Sons: New York, 1979.

Algorithm for suboptimal feedback construction based on Padé approximation for nonlinear control problems

YULIA DANIK^{1,2}, MIKHAIL DMITRIEV^{1,2*}

1. Federal Research Center Computer Science and Control (FRC CSC RAS), Moscow, Russia [Yu.D.: <https://orcid.org/0000-0001-7836-243X>, M.D.: <https://orcid.org/0000-0002-1184-129X>]
2. Moscow Institute of Physics and Technology (National Research University), Dolgoprudny, Moscow Region, Russia

* Presenting Author

Abstract: On several classes of nonlinear dynamic problems with a parameter the possibility for constructing parametric families of solutions that arise in control theory on the basis of the Padé approximation (PA) is shown using the asymptotic expansions for small and large values of the parameter and finite-dimensional optimization algorithms and also by taking into account the characteristics of the asymptotics on which the PA is based. The possibility for increasing the accuracy of approximations and the enhancement of the interpolation and extrapolation properties of one-point and two-point PAs in comparison with asymptotic approximations is demonstrated.

Keywords: SDRE, finite time interval, parameter, small time step, Padé approximation

1. Asymptotic expansion of the Riccati equation solution on a finite time interval

In the SDRE approach, a large role is played by the differential matrix Riccati equations [1-3] for a finite interval or matrix algebraic Riccati equations with state-dependent coefficients for infinite interval. If the control system contains small or large parameters the synthesis can be constructed using asymptotic expansions by these parameters and the operators based on them (for example, Padé approximations) [4]. For example, consider the following class of nonlinear controlled systems without control constraints

$$\dot{x} = A(x)x + \varepsilon B(x)u, \quad x(0) = x^0, \quad (1)$$

$$x(t) \in X \subset R^n, \quad u \in R^r, \quad t \in [0, T], \quad \varepsilon \in (0, \infty),$$

$$J(u) = \frac{1}{2} x^T(T) F x(T) + \frac{1}{2} \int_0^T (x^T(t) Q(x, \varepsilon) x(t) + u^T(t) R u(t)) dt, \quad (2)$$

where $X \subset R^n$ is a bounded set. In this case the control is chosen in the formally linear feedback form but with state dependent coefficients $u(x) = -\varepsilon R^{-1} B^T(x) P(x, t, \varepsilon) x(t)$, where $P(x, t, \varepsilon)$ is a solution of the modified matrix differential Riccati equation for all $x \in X$ and $\varepsilon \in (0, \infty)$.

$$\begin{aligned} dP/dt = & -P(x, t, \varepsilon) A(x) - A(x)^T P(x, t, \varepsilon) + \varepsilon^2 P(x, t, \varepsilon) B(x) R^{-1} B^T(x) P(x, t, \varepsilon) - \\ & - Q(x, \varepsilon), \quad P(x, t, \varepsilon) \Big|_{t=T} = F, \quad F > 0. \end{aligned} \quad (3)$$

The asymptotic of $P(x, t, \varepsilon)$ in (3) for small ε is constructed as a regular power series $\tilde{P}_2(x, t, \varepsilon) = \tilde{P}_0(x, t) + \varepsilon \tilde{P}_1(x, t) + \varepsilon^2 \tilde{P}_2(x, t)$ [5], and for $\varepsilon \rightarrow \infty$ after the replacement $\varepsilon = \frac{1}{\mu}, \mu \rightarrow 0$ the asymptotic approximation is constructed as a partial sum of the regular and

boundary series by μ [6] $P(x, t, \mu) = \hat{P}_2(x, t, \mu) + \Pi_2 P(x, \tau, \mu), \tau = \frac{t-T}{\mu^2} \leq 0$. Then the two-

point PA [2/2] is constructed in the form

$PA_{[1/2]}(x, t, \tau, \varepsilon) = (M_0(x) + \varepsilon M_1(x) + \varepsilon^2 M_2(x) + IIM_0(x, \tau) + \varepsilon IIM_1(x, \tau) + \varepsilon^2 IIM_2(x, \tau)) \times (E + \varepsilon N_1(x) + \varepsilon^2 N_2(x))^{-1}$. By simultaneously equating the two constructed asymptotic expansions with this representation and then comparing the coefficients with the same powers of the parameter we obtain a system of equations for determining the unknown coefficients of the PA [4].

2. Algorithm and numerical experiments

Using the Pade approximation of the feedback gain matrix as a basic framework all the unknown feedback control elements are approximated by segments of expansions in orthogonal systems, which are selected from the minimum of the functional (2). Experiments show that for the same calculation accuracy the algorithm is more efficient in terms of the calculation time for the construction of parametric families of regulators.

Acknowledgment: Research is supported by the Russian Science Foundation (Project No. 21-11-00202).

References

- [1] ÇİMEN T. Systematic and effective design of nonlinear feedback controllers via the state-dependent riccati equation (sdre) method. *Annual Reviews in control* 2010, **34**(1):32-51.
- [2] HEYDARI A., BALAKRISHNAN S. Approximate closed-form solutions to finite-horizon optimal control of nonlinear systems. *2012 American Control Conference (ACC) 2012*, 2657-2662.
- [3] AFANAS'EV, V. Control of nonlinear plants with state-dependent coefficients. *Autom Remote Control* 2011, **72**:713-726.
- [4] DANIK YU., DMITRIEV M. The construction of stabilizing regulators sets for nonlinear control systems with the help of Padé approximations. In: *Nonlinear Dynamics of Discrete and Continuous Systems*. Springer International, 2021.
- [5] DMITRIEV M, MAKAROV D. Smooth nonlinear controller in a weakly nonlinear control system with state depended coefficients. *Trudy Instituta Sistemnogo Analiza Rossijskoj Akademii Nauk* 2014, **64**(4):53-58.
- [6] VASILIEVA A., BUTUZOV V. *Asymptotic expansions of solutions of singularly perturbed equations*. NAUKA: MOSCOW, 1973.

Nonlinear wave propagation in one-dimensional metamaterials via Hamiltonian perturbation scheme

ALESSANDRO FORTUNATI^{1*}, ANDREA BACIGALUPO², MARCO LEPIDI², ANDREA ARENA¹,
WALTER LACARBONARA¹

1. DISG - Department of Structural and Geotechnical Engineering, Sapienza University of Rome, Italy.
 2. DICCA - Department of Civil, Chemical and Environmental Engineering, University of Genova, Italy.
- * Presenting Author

Abstract: The work investigates the wavefrequencies and waveforms of a periodic waveguide with local vibration absorbers, featuring both weak geometric nonlinearities and nonlinear viscoelastic damping. The approach uses tools borrowed from Hamiltonian perturbation theory, as well as techniques classically employed in the context of nearly-integrable Hamiltonian systems in order to describe the solutions asymptotically. A dedicated analysis is oriented towards the case of weak dissipation, whilst the zero-dissipation limit case is presented for comparison with the literature. The obtained asymptotic expansions for the non-linear frequency spectra and the invariant manifolds of the system are presented. The analysis is carried out either in the non-resonant case or in the 3:1 internal resonance setting, and this is achieved by using an adaptation of the classical tools of resonant normalization techniques developed in the Hamiltonian context. Finally, the asymptotic results are also validated via numerical simulations.

Keywords: Mechanical metamaterials, Nonlinear damping, Cubic nonlinearities, Energy dissipation, Lie series

1. Introduction

Metamaterials with an engineered cellular arrangement of functionalized micromechanisms exhibiting amplitude-dependent dispersion properties are attracting increasing interest in nonlinear dynamics. Moreover, the band structure of microstructured periodic waveguides is of wide interest, especially regarding the amplitude-dependent pass and stop bands of oscillator chains and other periodic structures. Extensive efforts are currently targeted towards designing mechanical cellular metamaterials characterized by large-amplitude band gaps with tunable low-centerfrequency. To this end, intracellular mechanisms of local-global resonance can be realized by highly-flexible and damped oscillators working as propagation inhibitors and energy absorbers.

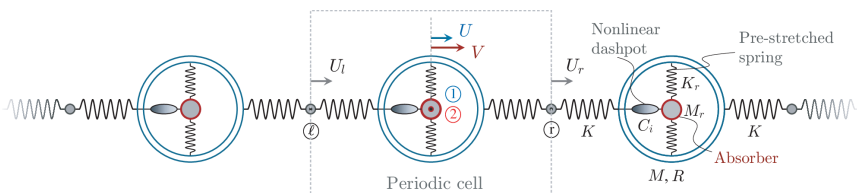


Fig. 1. Cellular metamaterial with embedded locally-resonant vibration absorbers.

2. Results and Discussion

A minimal locally resonant system can be realized as an infinite one-dimensional dissipative chain of rigid rings, embedding oscillators with geometric and material nonlinearities. The introduced nonlinear visco-elastic damping allows a better tunability of the amplitude-dependent damping towards an improved passive control performance (see Fig. 1). Denoting by u and w the displacement of the periodic diatomic cell, and the relative displacement of the resonator, respectively, the free wave propagation is governed by the following coupled system of non-linear dimensionless ODEs

$$(1 + \rho^2)\ddot{u} + \rho^2\ddot{w} + 2u + (1 - \cos \beta)u = 0$$
$$\rho^2\ddot{u} + \rho^2\ddot{w} + \xi_1(1 - \xi_2)\dot{w} + \xi_1\xi_2\xi_3\dot{w}w^2 + 2\mu w + (\eta - \mu)w^3 = 0$$

where β is the wavenumber and the coefficients $\rho^2, \xi_1, \xi_2, \xi_3, \mu, \eta$ are the mechanical parameters. From the methodological viewpoint, the perturbation analysis of the governing equations is carried out in the neighbourhood of a hyperbolic equilibrium for the system after a suitable rescaling [1]. The employed technique relies on the possibility to interpret a given system of ODEs as a Hamiltonian system in a suitably extended phase space. Accordingly, the associated Hamiltonian function can be directly treated by using well established tools of Perturbation Theory for nearly-integrable Hamiltonian systems. Canonical transformations of variables generated through Lie-series operators are employed [2] while the approach here adopted differs from the commonly used perturbation techniques based on the method of multiple scales [3,5]. Under mild non-resonance hypotheses on the eigenvalues of the linearized system, the (first-order) correction to the linear frequencies arise naturally from the normal form construction. A comparison with literature results corresponding to the zero-dissipation limit [4] is discussed, together with the case of weak dissipation in which the construction of invariant manifolds is shown to be feasible. Starting from the study proposed in [1], the case of 3:1 resonance is investigated in this work by proposing an approach which relies on techniques arising from the construction of resonant normal form in the Hamiltonian setting. Either the description of the spectra, or the invariant manifolds construction in the weak dissipation case, require approaches borrowed from the Hamiltonian framework.

Acknowledgments: This research was partially supported by the Italian Ministry of Education, University and Scientist Research under PRIN Grant No. 2017L7X3CS and by the Air Force Office of Scientific Research, Grant N. FA 8655-20-1-7025. The authors acknowledge the financial support from National Group of Mathematical Physics (GNFM-INdAM), from the Compagnia San Paolo, project MINIERA no. I34I20000380007 and from University of Trento, project UNMASKED 2020.

References

- [1] FORTUNATI, A., BACIGALUPO, A., LEPIDI, M., ARENA, A., LACARBONARA, W. Nonlinear wave propagation in locally dissipative metamaterials via Hamiltonian perturbation approach. *Submitted*.
- [2] GIORGILLI, A. Exponential stability of Hamiltonian systems. In *Dynamical systems. Part I, Pubbl. Cent. Ric. Mat. Ennio Giorgi*, pp. 87–198. *Scuola Norm. Sup., Pisa*, (2003).
- [3] GEORGIU, I.T., VAKAKIS, A.F. An invariant manifold approach for studying waves in a one-dimensional array of non-linear oscillators. *International Journal of Non-Linear Mechanics* 1996, **31**(6):871-886.
- [4] LEPIDI, M., BACIGALUPO, A. Wave propagation properties of one-dimensional acoustic metamaterials with nonlinear diatomic microstructure. *Nonlinear Dynamics* 2019, **98**(4):2711–2735.
- [5] LACARBONARA, W., CAMILLACCI, R. Nonlinear normal modes of structural systems via asymptotic approach. *International Journal of Solids and Structures* 2004, **41**(20):5565-5594.

Synchronization of oscillations of weakly coupled elastic elements of a differential resonant MEMS-accelerometer in the mode of a two-circuit self-oscillator

IGUMNOVA V.S.^{1*}, LUKIN A.V.², POPOV I.A.³, SHTUKIN L.V.⁴

1. Peter the Great St. Petersburg Polytechnic University (SPbPU) [0000-0001-7531-0220]
2. Peter the Great St. Petersburg Polytechnic University (SPbPU) [0000-0003-2016-8612]
3. Peter the Great St. Petersburg Polytechnic University (SPbPU) [0000-0003-4425-9172]
4. Peter the Great St. Petersburg Polytechnic University (SPbPU)

* Presenting Author

Abstract: In this paper we investigate the qualitative features of the nonlinear dynamics of a resonant differential MEMS-accelerometer, consisting of two resonators and an inertial mass, which are connected to each other by means of two elastic elements (springs). Excitation and maintenance of resonator oscillations occurs with the help of self-oscillators. When acceleration appears in the system, a longitudinal force of inertia arises in the moving elements, and therefore the natural frequency of one resonator decreases, while the other increases. The acceleration of the object is measured by the difference between the natural frequencies of the resonators, which is determined by tracking the envelope of the beat mode in the output signal of the sensor. In this work the evolution of the amplitude and phase difference in slow variables from the parameters of the initial detuning of the stiffness of the sensitive element (SE) and the magnitude of the axial inertia force is obtained. The transition from a two-frequency mode (beat mode) to a single-frequency mode (synchronization mode) is shown, using analytical methods of nonlinear mechanics, regions in the parameter space corresponding to two-frequency beat modes and phase synchronization are determined, which determines the range of sensor sensitivity to the measured component of the acceleration vector of a moving object.

Keywords: Synchronization, MEMS-accelerometer, self-oscillator, weakly coupled elastic elements

1. Introduction

A model of a MEMS accelerometer is proposed, which consists of two resonators and an inertial mass, which are connected to each other by means of two elastic elements (springs). Excitation and maintenance of resonator oscillations occurs with the help of self-oscillators.

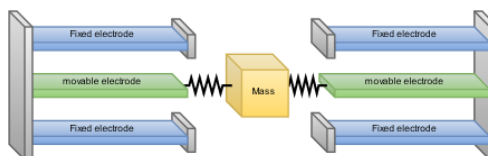


Fig. 1. MEMS accelerometer model

Under the action of portable acceleration, the moving mass is deflected and a longitudinal compressive force appears in the system for one of the resonators and a tensile force for the second resonator, which is a useful signal and allows one to obtain the measured acceleration component with high accuracy.

2. Results and Discussion

Figure 2 shows a bifurcation pattern that demonstrates the transition from dual-frequency mode (limit cycles) to single-frequency mode (synchronization).

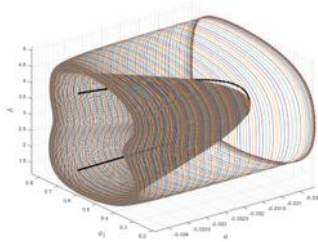


Fig. 2. The two possible modes of operation of the sensor are synchronization (black line) and beating (limit cycles). Where α – is the difference in the frequencies of the first and second resonators, α_1 – is the amplitude of one of the resonators, δ – is the phase difference between the first and second resonators

3. Concluding Remarks

In this paper, we investigate the qualitative features of the nonlinear dynamics of a resonant differential MEMS accelerometer, consisting of two resonators and an inertial mass, which are connected to each other by means of two elastic elements (springs). In this work, the evolution of the amplitude and phase difference in slow variables from the parameters of the initial detuning of the stiffness of the sensitive element (SE) and the magnitude of the axial inertia force is obtained. Shown is the transition from a dual-frequency mode (beat mode) to a single-frequency mode (synchronization mode).

The work was supported by RFBR grant 20-01-00537

References

- [1] S.WIRKUS, R.RAND: THE DYNAMICS OF TWO COUPLED VAN DER POL OSCILLATORS WITH DELAY COUPLING. *Nonlinear Dynamics* 2002, 30:205-221.
- [2] M.KOVALEVA, V.PILIPCHUK, AND L.MANEVITCH: NONCONVENTIONAL SYNCHRONIZATION AND ENERGY LOCALIZATION IN WEAKLY COUPLED AUTOGENERATORS. *PHYSICAL REVIEW E* **94**, 032223 (2016). DOI: [HTTPS://DOI.ORG/10.1103/PHYSREVE.94.032223](https://doi.org/10.1103/PhysRevE.94.032223)
- [3] I.B. SHIROKY, O.V. GENDELMAN: Modal synchronization of coupled bistable van der Pol oscillators. *Chaos, Solitons and Fractals Nonlinear Science, and Nonequilibrium and Complex Phenomena*, 2021.

Rayleigh-type waves in nonlocal elasticity

J. KAPLUNOV¹, D.A. PRIKAZCHIKOV², L. PRIKAZCHIKOVA^{3*}

1. Keele University, UK [ORCID 0000-0001-7505-4546]
2. Keele University, UK [ORCID 0000-0001-7682-3079]
3. Keele University, UK [ORCID 0000-0001-9051-2103]

* Presenting Author

Abstract: Surface waves in nonlocally elastic solids are considered. An asymptotic approach using the ratio of the characteristic internal size to a macroscale wave length as a small parameter, is developed. The results based on differential and integral formulations in nonlocal elasticity are compared. The effect of nonlocal boundary layers localized near free surface is addressed in detail. It is demonstrated that the differential and integral formulations are not equivalent. In addition, the issue of the solvability of the surface wave problem within the framework of integral nonlocal elasticity is raised.

Keywords: nonlocal, integral, differential, Rayleigh wave, boundary layer

Nonlinear normal modes and localization of vibrations in the pendulum system under magnetic excitation

YURI V. MIKHLIN^{1*}, YULIA E. SURHANOVA²

1. National Technical University “Kharkiv Polytechnic Institute”, Kharkiv, Ukraine [0000-0002-1780-9346]

2. National Technical University “Kharkiv Polytechnic Institute”, Kharkiv, Ukraine [0000-0002-6540-3025]

* Yuri V. Mikhlin

Abstract: Dynamics of two coupled pendulums under magnetic excitation is considered. Inertial components of the pendulums are essentially different, and a ratio of masses is chosen as a small parameter. The simulation of the magnetic effect described in [1] is used in the analysis of the dynamics of the system. The small parameter method and the method of multiple scales are used to construct nonlinear normal modes (NNMs) one of them presents localised vibrations in the system. Stability of the NNMs is also studied.

Keywords: pendulum system, magnetic excitation, nonlinear normal modes

1. Introduction. The principal model

The system containing two pendulums under the electromagnetic motor influence is studied in papers [2,3]. Model of one of the pendulums is shown in Fig. 1. Few corresponding mathematical models are constructed, and their validation is discussed after comparison of the numerical simulation and experimental results. Then some aspects of the system dynamics is analyzed. Here we consider a similar system of two pendulums under magnetic force when inertial characteristics of these pendulums are essentially different. In this case a localization of energy on one sub-system is possible. To describe a dynamics of the system the nonlinear normal modes theory is used. Note that an investigation of nonlinear normal modes (NNMs) is an important part of general analysis of many classes of nonlinear dynamical systems. Different theoretical aspects of the NNMs theory and applications of the theory are presented in numerous publications, in particular, in reviews [4,5].

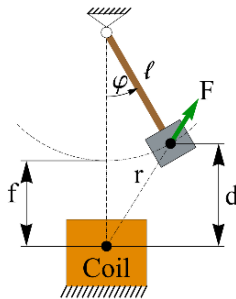


Fig. 1. The pendulum dynamics under magnetic force [2,3]

The analytical approximation of the magnetic force demonstrates a good correspondence with experimental results presented in [2,3] as is shown in Fig.2.

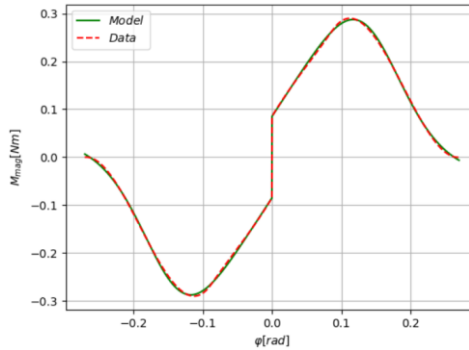


Fig.2. Comparison of the magnetic force analytical approximation with experimental result [2,3].

2. Results and Discussion

The small parameter method in the form by Lindstedt-Poincaré approach is used to describe dynamics of the system under consideration. It is assumed that a mass of one pendulum is essentially smaller than one of the second pendulum. Besides, it is assumed that the magnetic force is smaller than main elastic characteristics of the system. The use of the nonlinear least squares method for constructing the moment of magnetic action makes it possible to construct nonlinear normal modes good accuracy using the small parameters and the multiple scales methods. Two NNMs are obtained. One of them is close to the in-phase motions, and the second one describes vibrations localized at the small mass pendulum. Besides, a stability of these NNMs is studied. It is obtained a region of the system parameters where the localization of vibrations at the small mass pendulum is possible.

3. Concluding Remarks

Two nonlinear normal modes are described in the system with two connected pendulums under magnetic force. It is assumed that inertial characteristics of these pendulums are essentially different. In the case two nonlinear normal modes can be realized in the system. One of them is a mode of in-phase vibrations, and the second one is a mode of localization of the vibration energy on the small mass pendulum.

References

- [1] SIAHMAKOUN A, FRENCH V., PATTERSON J.: Nonlinear dynamics of a sinusoidally driven pendulum in a repulsive magnetic field. *Am J Phys* 1997; **65**: 393–400
- [2] GAJEK, J., AWREJCIEWICZ, J.: Mathematical models and nonlinear dynamics of a linear electromagnetic motor. *Nonlinear Dyn* 2018, **94**:377–396.
- [3] WOJNA, M., WIJATA, A., WASILEWSKI, G., et al.: Numerical and experimental study of a double physical pendulum with magnetic interaction, *J. of Sound and Vibration*, 2018 **430**, 214–230.
- [4] MIKHLIN, Yu.V., AVRAMOV, K.V.: Nonlinear normal modes for vibrating mechanical systems. Review of theoretical developments, *Appl. Mech. Rev.* 2010 **63**: 4–20.
- [5] AVRAMOV, K.V., MIKHLIN, Yu.V.: Review of applications of nonlinear normal modes for vibrating mechanical systems, *Appl. Mech. Rev.* 2013, **65** (2) (20 pages).

Nonlinear dynamics of electrostatic comb-drive with variable gap

MOZHGOVA NADEZHDA^{1*}, LUKIN ALEXEY², POPOV IVAN³

1. Peter the Great St. Petersburg Polytechnic University, Saint-Petersburg, Russia [0000-0002-3901-9484]
2. Peter the Great St. Petersburg Polytechnic University, Saint-Petersburg, Russia [0000-0003-2016-8612]
3. Peter the Great St. Petersburg Polytechnic University, Saint-Petersburg, Russia [0000-0003-4425-9172]

Abstract: This paper is dedicated to investigation of nonlinear dynamics of electrostatic comb-drive with variable gap. Due to the fact, that electrostatic force is in nonlinear dependence on movable electrode displacement, the investigation of the system is provided by approximate asymptotic methods of nonlinear dynamics, in particular multi-scale method and methods of continuation theory. In paper the amplitude-frequency response and amplitude-force response were obtained for various values of parameters of elastic suspension's nonlinear force, DC, and AC constituents of electrostatic force amplitude. The area of parameter's values, in which comb-drive will provide a required amplitude of vibration, is obtained. An influence of second stationary electrode on dynamic of the system is appreciated.

Keywords: MEMS, electrostatic actuation, variable gap, multiple-scale method

1. Introduction

There are many types of microelectromechanical system actuation: electrostatic actuation, piezoelectric actuation, temperature actuation, magnetic actuation and so on. Electrostatic actuation is a most used version because it is easy in implementation and compatible with CMOS circuits. It is based on electrostatic attractive forces on plates with opposite sign electric charges and can be classified on two subtypes – perpendicular and parallel driving relatively to plane of electrodes. An advantage of variable gap actuator in comparison with variable area ones lies in value of created electrostatic force – with changing gap it is bigger. However, the disadvantage of such systems is limitation on displacement of movable electrode – when it will exceed the value equals one third of gap, the pull-in effect would perform, and system would break down.

2. Results and Discussion

A model of an electrostatic drive with a variable gap, consisting of a movable and one fixed electrode with a gap d between them, is considered. To equation of dynamics of an electrostatic drive considering the nonlinearity of an elastic suspension, the multiple-scale method was applied and equations in slow variables were obtained. Figure 1 shows the amplitude-frequency response when variable and constant component of voltage are changed.

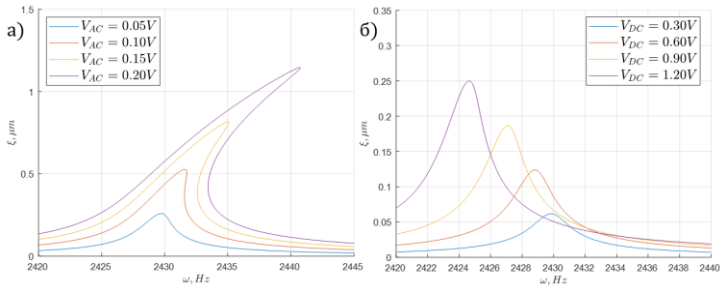


Figure 1. Amplitude-frequency response for different values of voltages

These dependences tilt to the right because the cubic nonlinearity of elastic suspension is included. Also, the resonant frequency become smaller with increasing constant component of voltage. Using the methods of bifurcation theory, the continuation of «limit-point» bifurcation by the parameters of variable and constant component of voltage was carried out and Figure 2 demonstrates meaning of this action.

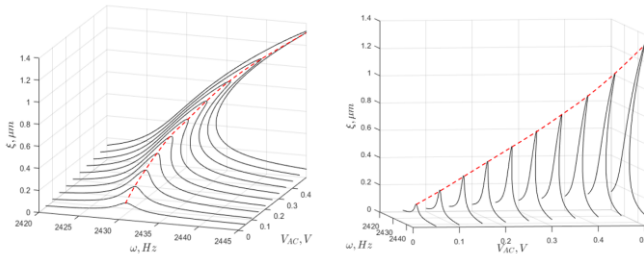


Figure 2. A series of amplitude-frequency responses for different values of voltages

In result the 3D graphs in parameters space were obtained and presented on Figure 3 for case without considering of influence of second stationary electrode is dash line and with considering this factor is solid line.

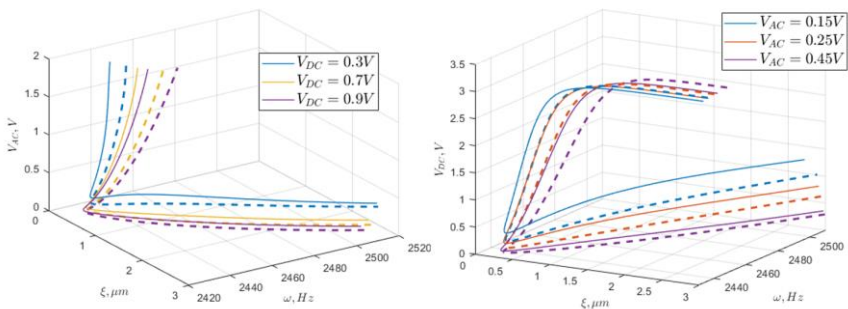


Figure 3. Dependence resonant amplitude and frequency on variable and constant components of voltage. Solid line – with of 2nd fixed electrode, dash line – without

The work was supported by RFBR grant 20-01-00537.

Nonlinear Oscillations of an Elastica Between Cylindrical Boundaries

D. PAUL^{1*}, K. R. JAYAPRAKASH¹

1. Discipline of Mechanical Engineering, Indian Institute of Technology Gandhinagar

* Presenting Author; jp.kalkunte@iitgn.ac.in

Abstract: In this work we consider the free and forced dynamics of a fixed-free elastica in contact with rigid cylindrical boundary. In addition to the geometric nonlinearity due to deformation, the boundaries introduce nonlinearity due to change in effective beam length as it deforms. We consider both unilateral and bilateral constraints and explore the realization of nonlinear normal modes (NNMs) and their forced dynamics in this class of dynamical systems. The current study invokes Galerkin’s method, multi scale analysis and harmonic balancing.

Keywords: Elastica, nonlinear oscillations, Galerkin’s method, perturbation analysis

1. Introduction

It is well known that the time period of oscillations of a simple pendulum is amplitude dependent. Owing to Huygen’s (1656) ingenuity of varying the effective length of string as it wraps/unwraps around (cycloidal) boundary, the oscillations were rendered isochronous. In the late twentieth century, researchers started investigating mechanical elements like flexures as they wrap/unwrap around obstacles to exhibit nonlinear dynamical behaviour. Fung et al. [1] considered Euler-Bernoulli beam with rigid cylindrical boundary on one side and investigated the nonlinearity induced considering no loss of energy during contact. Crespo da Silva et al. [2,3] developed a nonlinear beam model and explored the free and forced nonlinear oscillations and the resonances thereof.

In the current study we consider a nonlinear beam [2,3] and introduce smooth cylindrical boundaries unilaterally and bilaterally to study their effect on its nonlinear dynamics.

2. Mathematical Modelling

Consider a flexure (large slenderness ratio) with the assumptions, (i) inextensible: $(1 + u_s)^2 + v_s^2 = 1$, (ii) no warping/shear deformation: $v_s(1 + u_s)^{-1} = \tan(\theta)$. The planar motion is described by two displacements $u(s, t)$ and $v(s, t)$ as shown in Fig. 1. ‘A’ is the point of loss of contact of the beam with the cylindrical boundary and s at A is $\gamma(t)$. The Lagrange multiplier Λ incorporates the geometric constraint C in domain $0 \leq s \leq \gamma^-$ and since γ^- is varying, the Hamilton’s principle in the general non-contemporaneous form will be used in the following, (where $v_s = \partial v / \partial s, \dots$)

$$\delta \int_{t_1}^{t_2} \left\{ \left(\int_0^{\gamma^-} + \int_{\gamma^+}^l \right) \frac{1}{2} \{ \rho(u_t^2 + v_t^2) - \beta \theta_s^2 + \lambda(1 - (1 + u_s)^2 - v_s^2) \} ds + \left(\int_0^{\gamma^-} \Lambda C ds \right) \right\} dt = 0 \quad (1a)$$

$$C(v, s) = s^2 + v^2 - 2a|v| = 0 \text{ and } |v| = a - \sqrt{a^2 - s^2}; \quad 0 \leq s \leq \gamma^- \quad (1b)$$

$$v(0, t) = v_s(0, t) = v_{ss}(L, t) = v_{sss}(L, t) = 0 \quad (1c)$$

In the absence of the cylindrical boundary, i.e., $\Lambda = 0$, the nondimensional equation of motion considering cubic nonlinear terms is given by

$$w_{\tau\tau} + w_{zzzz} = -(w_z(w_z w_{zz}))_z - \frac{1}{2} (w_z \int_1^z \int_0^z (w_z^2)_{\tau\tau} dz dz)_z \quad (2)$$

Where $w = v/l, z = s/l, \tau = t\sqrt{\beta/\rho l^4}$ and Lagrange multiplier, $\lambda = -w_{zzz}w_z - \int_1^z \int_0^z (w_z^2)_{\tau\tau} dz dz$. Analysis of (2) with BCs (1c) is discussed later. For $\Lambda \neq 0$, additional conditions are imposed:

- a) *Perpendicularity*: A vector $\vec{R} = s\hat{i} + (a - |v|)\hat{j}$ from the centre of the cylindrical boundary to a point s on the neutral axis is perpendicular to the tangent at s , i.e., $\vec{R} \cdot \vec{R}_s = 0; 0 \leq s \leq \gamma^-$
- b) *Continuity*: The displacement and the slope are continuous at $s = \gamma$
- c) *Velocity at $s = \gamma$* : The total time derivative of $v(\gamma(t), t)$ is zero implying, $v_t(\gamma, t) = 0$

3. Results and Discussions

For $\Lambda = 0$, considering Galerkin’s method, we choose $\phi_{(i)}(z)$, the i^{th} (mass) normalized eigenfunction corresponding to a linear beam, as a comparison function. Letting $w(z, \tau) = \phi_{(i)}(z) \eta_{(i)}(\tau)$, the corresponding nonlinear oscillator (disregarding the modal interactions at this stage) is,

$$\ddot{\eta}_{(i)} + \omega^2 \eta_{(i)} + G_1 \eta_{(i)}^3 + G_2 \eta_{(i)} (\eta_{(i)} \ddot{\eta}_{(i)} + \dot{\eta}_{(i)}^2) = 0$$

$$G_1 = \int_0^1 \phi_{(i)} (\phi'_{(i)} (\phi'_{(i)} \phi''_{(i)}))' dz; G_2 = \int_0^1 \phi_{(i)} \left(\phi'_{(i)} \int_1^z \int_0^z \phi_{(i)}^2 dz dz \right)' dz \quad (3)$$

The frequency-amplitude relation (Fig. 2) is derived by harmonic balancing [4]. Interestingly, the first mode shows near isochronous oscillations, whereas the higher modes exhibit amplitude dependence.

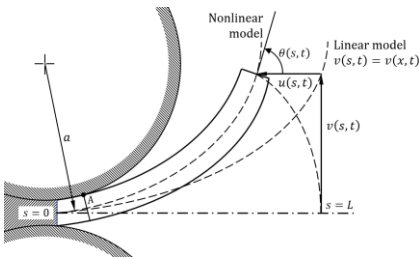


Fig. 1. Kinematics of the nonlinear beam (a is the sum of cylinder radius and half beam thickness)

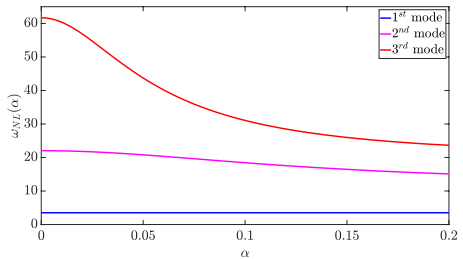


Fig. 2. Amplitude-frequency relation

4. Concluding Remarks

This study considers nonlinear oscillations of a thin elastica oscillating between two rigid cylinders. The amplitude dependent frequency is shown here for few modes in the absence of boundaries. A complete analysis with unilateral and bilateral cylindrical boundaries will be presented in the full version. Additionally, we discuss about the NNMs, their existence and stability in this class of structures. Forced dynamics is studied for a simple point load and the excitation NNMs.

Acknowledgment: DP acknowledges the research assistantship by Ministry of HRD, India.

References

- [1] FUNG R.F., CHEN C.C.: Free and forced vibration of a cantilever beam contacting with a rigid cylindrical foundation. *Journal of Sound and Vibration* 1997, **202**(2):161–185.
- [2] CRESPO DA SILVA M. R. M., GLYNN C. C.: Nonlinear Flexural-Flexural-Torsional Dynamics of Inextensional Beams. I. Equations of Motion. *Journal of Structural Mechanics* 1978, **6**(4):437–448.
- [3] CRESPO DA SILVA M. R. M., GLYNN C. C.: Nonlinear Flexural-Flexural-Torsional Dynamics of Inextensional Beams. II. Forced Motions. *Journal of Structural Mechanics* 1978, **6**(4):449–461.
- [4] NAYFEH A. H., MOOK D. T.: *Nonlinear Oscillations*. Wiley-Interscience: New York, 1979.

Application of multiple scales method to the problem of plane pendulum motion with extended damping model

ROBERT SALAMON^{1*}, GRAŻYNA SYPNIEWSKA-KAMIŃSKA², HENRYK KAMIŃSKI³

1. Institute of Mathematics, Poznan University of Technology, Poznan, Poland [0000-0002-5607-1743]
 2. Institute of Applied Mechanics, Poznan University of Technology, Poznan, Poland [0000-0003-0490-2629]
 3. Institute of Applied Mechanics, Poznan University of Technology, Poznan, Poland [0000-0003-0314-028X]
- * Presenting Author

Abstract: In the paper, the plane motion of a physical pendulum involving the interactions with the surrounding air is considered. These interactions are described employing the model consisting of three components. The linear and quadratic terms are proportional to the magnitude of the velocity and its square, respectively. The last component is proportional to the tangential component of the acceleration. According to the semi-empirical Morison equation, the quadratic term and acceleration dependent component depict the total force exerted on the body i.e. the drag force and inertia force including the concept of mass added. The multiple scales method (MSM) is used to obtain the approximate asymptotic solution to the problem. A slight change in the natural frequency is caused by the inertial component of the total damping force. In turn, the occurrence of the absolute value of velocity in the damping model complicates the solving procedure. The accuracy of solutions obtained using the multiple scales method is compared with the experimental results.

Keywords: damping model, physical pendulum, method of multiple scales

1. Mathematical Model

The plane motion of the physical pendulum of mass m and length L is investigated. The damping force can be presented as the power series of the velocity magnitude [1]:

$$\vec{F}(v) = -(c_0 + c_1 v + c_2 v^2 + \dots) \frac{\vec{v}}{v}, \quad (1)$$

where $\{c_i\}_{i=0}^{\infty}$ are constants. The concept of extending the model with a term depending on the tangential component of the acceleration was inspired by the Morison equation used in hydromechanics. Taking into account only the second and third terms of series (1) and the component related to the added mass, one can obtain the following dimensionless equations of motion

$$\ddot{\varphi}(\tau) + \sin \varphi(\tau) + \alpha_1 \dot{\varphi}(\tau) + \alpha_2 \dot{\varphi}(\tau) |\dot{\varphi}(\tau)| = 0 \quad (2)$$

where

$\tau = \hat{\omega} t$, $\hat{\omega} = \sqrt{\frac{mgL}{6I_0 + 4c_a L^2}}$, I_0 – the mass moment of inertia, c_a – the inertia coefficient, α_1, α_2 – the dimensionless damping coefficients,

The following initial conditions with known quantities φ_0, ω_0 supplement Eq. (2)

$$\varphi(0) = \varphi_0, \quad \dot{\varphi}(0) = \omega_0. \quad (3)$$

2. Asymptotic Solution

The approximate analytical solution to the initial value problem (2)–(3) is obtained using MSM [2]. The system evolution in time is described using n variables of time nature: $\tau_i = \varepsilon^i \tau$, $i = 0, 1, 2, \dots$, where ε is a small parameter. The differential operators of the new variables are redefined according to the chain rule and the solution $\varphi(\tau)$ to the initial value problem (2)–(3) is sought in the form of a power series of the small parameter

$$\varphi(\tau; \varepsilon) = \sum_{k=1}^n \varepsilon^k \phi_k(\tau_0, \tau_1, \tau_2, \dots) + O(\varepsilon^{n+1}), \quad (4)$$

where n denotes the number of time scales. For the initial value problem (2)–(3), at least $n = 3$ should be assumed. Assuming weak damping in the form

$$\alpha_1 = \varepsilon^2 \hat{\alpha}_1, \quad \alpha_2 = \varepsilon \hat{\alpha}_2, \quad (5)$$

and omitting the terms that are accompanied by ε in powers higher than three, one can obtain the set of three differential equations

$$\frac{\partial^2 \phi_1}{\partial \tau_0^2} + \phi_1 = 0, \quad (6)$$

$$\frac{\partial^2 \phi_2}{\partial \tau_0^2} + 2 \frac{\partial^2 \phi_1}{\partial \tau_0 \partial \tau_1} + \phi_2 = 0, \quad (7)$$

$$\frac{1}{6} \phi_1^3 - \phi_3 = \frac{\partial^2 \phi_1}{\partial \tau_1^2} + \hat{\alpha}_1 \frac{\partial \phi_1}{\partial \tau_0} + \hat{\alpha}_2 \frac{\partial \phi_1}{\partial \tau_0} \left| \frac{\partial \phi_1}{\partial \tau_0} \right| + 2 \frac{\partial^2 \phi_1}{\partial \tau_0 \partial \tau_2} + 2 \frac{\partial^2 \phi_2}{\partial \tau_0 \partial \tau_1} + \frac{\partial^2 \phi_3}{\partial \tau_0^2}. \quad (8)$$

3. Concluding Remarks

The equations of the first (6) and second (7) order approximation have been solved many times in the literature [3, 4, 5]. In the equation of the third order approximation (8) there is an absolute value term which significantly complicates the solution of the problem. The damping coefficients for this problem were determined in paper [6]. These results will be used to compare the results obtained by the multiple scale method with the experimental results.

Acknowledgment: This work was supported by the Grant of the Rector of Poznan University of Technology: 0213/SIGR/2154 and by the Grant of the Ministry of Science and Higher Education in Poland SBAD: 0612/SBAD/3576.

References

- [1] LANDAU LD, LIFSHITZ EM: *Mechanics. Course of theoretical physics*. Butterworth-Heinemann, Oxford, 1976.
- [2] AWREJCEWICZ J, KRYSKO VA, *Introduction to asymptotic methods*. Chapman and Hall, Boca Raton, 2006.
- [3] EISSA E, KAMEL M, EL-SAYED AT, *Vibration reduction of multi-parametric excited spring pendulum via a transversally tuned absorber*. *Nonlinear Dyn* 61:109-121, 2010.
- [4] SYPNIEWSKA-KAMIŃSKA G, AWREJCEWICZ J, KAMIŃSKI H, SALAMON R, *Resonance study of spring pendulum based on asymptotic solutions with polynomial approximation in quadratic means*, *Meccanica* 56(4):963-980, 2021.
- [5] LEE WK, PARK HD, *Second-order approximation for chaotic responses of a harmonically excited spring-pendulum system*. *Int J Non Linear Mech* 34:749-757, 1999.
- [6] SALAMON R, KAMIŃSKI H, FRITZKOWSKI P, *Estimation of parameters of various damping models in planar motion of a pendulum*, *Meccanica* 55:1655-1677, 2020.

Identification of the model parameters based on the ambiguous branches of resonance response curves

GRAŻYNA SYPNIEWSKA-KAMIŃSKA^{1*}, JAN AWREJCWICZ²

1. Institute of Applied Mechanics, Poznan University of Technology, Poland [0000-0003-0490-2629]
2. Department of Automation, Biomechanics and Mechatronics, Lodz University of Technology, Poland [0000-0003-0387-921X]

* Presenting Author

Abstract: A concept of the method of determining the parameters describing the damping and the nonlinearity, which can be of physical or geometrical nature, is presented in the paper. The main idea is explained regarding mechanical systems with one degree of freedom, however, the method can be also employed to identification for systems with two DoF provided that the couplings are weak and the resonances do not occur simultaneously. The analysis of stationary resonance states can be reduced only then to the third-degree equation, which is a necessary condition for the applicability of this method. Numerical simulations, which are carried out, confirm the usefulness and accuracy of the method.

Keywords: Duffing's equation, multiple scales method, main resonance, resonance response curves

1. Introduction

Many mechanical systems of one degree of freedom with the nonlinearity of the cubic type and the viscous damping are governed by the Duffing equation of the form [1]

$$\ddot{x}(\tau) + \alpha \dot{x}(\tau) + x(\tau) + \beta x(\tau)^3 = f_0 \cos(p \tau), \quad (1)$$

supplemented with the following initial conditions

$$x(0) = x_0, \quad \dot{x}(0) = v_0, \quad (2)$$

where all quantities are dimensionless, and τ is the time, α, β – parameters to be identified, f_0, p – the amplitude and frequency of the harmonic forcing.

2. Idea of Identification

Employing the method of multiple scales in the time domain [2-3], one can obtain the approximate solution to the problem given by Eqs (1) – (2). An important part of the solving procedure is the problem of determining the amplitudes and phases. The introduction of several variables $\tau_0, \tau_1, \tau_2, \dots$ describing the evolution of the system over time allows one to isolate the problem as an independent one. The changeability of the generalised coordinates with the frequencies of order the mechanical system eigenfrequencies is described using the fast scale τ_0 . The other variables are destined to describe the slow change of the amplitude and phases. In turn, the modulation equations give the possibility to study the periodic stationary vibration at the main resonance. The amplitude of the periodic stationary vibration satisfies the following equation

$$16\alpha a_1^2 + (3\alpha a_1^2 - 8s)^2 a_1^2 - 16f_0^2 = 0, \quad (3)$$

where s is the detuning parameter, i.e. it is assumed that $p = 1 + s$. Regarding Eq. (3) as the equation of the third order with respect to the square of the amplitude a_1 , and analysing the sign of the numerator of its discriminant given by

$$N_{\Delta} = (64s^3 + 144\alpha^2s - 81\beta f_0^2)^2 + 64(3\alpha^2 - 4s^2)^3, \tag{4}$$

one can determine the area Ω on the plane $s - f_0$ the points of which satisfy the inequality $N_{\Delta} < 0$. Each point of the area Ω depicts the parameters of the external force that ensure the existence of three distinct real roots of Eq. (3). The boundaries f_l and f_u of the region Ω , shown in Fig. 1, are defined analytically formulae as follows

$$f_u^2 = \frac{64s^3}{81\beta} + \frac{16s\alpha^2}{9\beta} + \frac{8\sqrt{64s^6 - 144s^4\alpha^2 + 108s^2\alpha^4 - 27\alpha^6}}{81\beta}, \tag{5}$$

$$f_l^2 = \frac{64s^3}{81\beta} + \frac{16s\alpha^2}{9\beta} - \frac{8\sqrt{64s^6 - 144s^4\alpha^2 + 108s^2\alpha^4 - 27\alpha^6}}{81\beta}. \tag{6}$$

By experimentally determining the resonance response curves, one can find the values s_0 and s_e of the frequency of the harmonic force at which the jumps occur, corresponding to the entry or exit from the zone of ambiguous responses. Then, solving the equations (5) – (6) gives the approximate values of the parameters α and β .

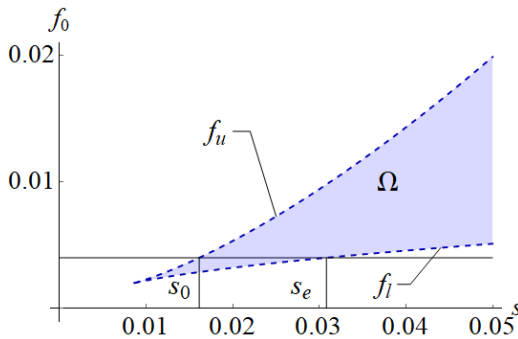


Fig. 1. The region of the ambiguous resonance responses.

The method was initially tested using simulations in which the ambiguous zones of the resonance response curves were determined based on solutions obtained numerically, after confirming that the solutions satisfy the assumptions of the stationary periodic vibration. The results of the tests have been satisfactory, however, it seems advisable to develop methods for estimating the identified parameters based on statistical inference.

Acknowledgment: This work was supported by the Grant of the Ministry of Science and Higher Education in Poland SBAD: 0612/SBAD/3576.

References

[1] NAYFEH A.H, MOOK D.T: *Nonlinear Oscillations*. Wiley&Sons: New York, 1995.
 [2] AWREJCWICZ J, KRYSKO VA, *Introduction to asymptotic methods*. Chapman and Hall: Boca Raton, 2006.
 [3] WEINAN E, *Principles of Multiscale Modeling*. Cambridge University Press: Cambridge, 2011.

Estimation of the amplitudes of parametric oscillations of a hemispherical solid-wave gyroscope

UDALOV PAVEL^{1*}, POPOV IVAN², ALEXEI LUKIN³

1. Peter the Great Saint-Petersburg Polytechnic University, Institute of Applied Mathematics and Mechanics, High School of Mechanics and Control Processes Author [0000-0002-9744-8869]
2. Peter the Great Saint-Petersburg Polytechnic University, Institute of Applied Mathematics and Mechanics, High School of Mechanics and Control Processes Author [0000-0003-4425-9172]
3. Peter the Great Saint-Petersburg Polytechnic University, Institute of Applied Mathematics and Mechanics, High School of Mechanics and Control Processes Author [0000-0003-2016-8612]

* Presenting Author

Abstract: This work presents the parametric oscillations excitation research for hemispherical shell by application a harmonic electrostatic force from drive electrodes. The electrodes structure and its mathematical description were derived. The Hill equations for the hemispherical shell are obtained. The nonlinear equation of vibrations of a hemispherical shell in the regions of increasing vibrations of the Ains-Strett is investigated.

Keywords: Solid-wave gyroscope, parametric oscillations, Ains-Strett diagrams

Nonlinear dynamics of Disk-based MEMS Coriolis Vibrating Gyro- scope under parametric excitation of vibrations

ZAVOROTNEVA EKATERINA^{1*}, ALEXEI LUKIN², POPOV IVAN³

1. Peter the Great Saint-Petersburg Polytechnic University, Institute of Applied Mathematics and Mechanics, High School of Mechanics and Control ProcessesAuthor[0000-0003-3601-3359]
2. Peter the Great Saint-Petersburg Polytechnic University, Institute of Applied Mathematics and Mechanics, High School of Mechanics and Control ProcessesAuthor[0000-0003-2016-8612]
3. Peter the Great Saint-Petersburg Polytechnic University, Institute of Applied Mathematics and Mechanics, High School of Mechanics and Control ProcessesAuthor[0000-0003-4425-9172]

Abstract: This work is devoted to the development of a mathematical model and a qualitative study of the nonlinear dynamics Disk-based MEMS Coriolis Vibrating Gyroscope in the free precession mode of the operating mode of oscillations with parametric excitation of the resonator. Nonlinear equations of the dynamics of a resonator on a movable base are obtained. Using asymptotic methods, the regions of parametric resonance are found, on the basis of which the amplitude-frequency characteristics of the nonlinear system are constructed.

Keywords: keyword 1, keyword 2, keyword 3 (max 5 keywords)

1. Introduction (10 point, bold)

In a gyroscope of this type, a silicon disk is connected to the armature by means of an isotropic elastic suspension, the resonator has a thickness of 40 [μm], the outer and inner radii of the disk are 420 [μm], 210 [μm], respectively, the initial data are taken for a real design from [13]. The system is considered without considering the influence of the stiffness of the elastic suspension. The natural frequency of the operating mode of the resonator is 4.53 [MHz]. The electrode structure, which has capacitive gaps of 270 [nm], consists of 24 electrodes with a circular surface, and due to the symmetry of the working mode of oscillations, it contains 4 independent groups of electrodes located symmetrically relative to the resonator [14]. The purpose of this work is to qualitatively study the dynamics of the resonator with parametric excitation of oscillations considering the geometric and electrostatic nonlinearity of the system. The tasks of the work are: creation and analysis of a compact mathematical model of MTVG, namely, the definition of zones of parametric swing oscillations; construction of resonance curves for a resonator on a fixed base in the region of the main parametric resonance and analysis of their stability.

2. Results and Discussion (10 point, bold)

On the basis of the Hamilton-Ostrogradsky variational principle and the Ritz method, a system of nonlinear differential equations is obtained that describes the dynamics of a disk resonator with an electronic control system, considering the influence of nonlinearity of geometric relationships, the presence of internal friction and the action of electrostatic forces. The equations of motion in dimensionless variables are as follows:

$$\begin{aligned} \ddot{C} + (1 + \sigma_2)C + A_1C(C^2 + S^2) + R\dot{C} + A_2\dot{C} &= (A_3C + A_4C(C^2 + S^2)) \sin((2 + \sigma_1)\tau), \\ \ddot{S} + (1 + \sigma_2)S + A_1S(C^2 + S^2) + R\dot{S} - A_2\dot{S} &= (A_3S + A_4S(C^2 + S^2)) \sin((2 + \sigma_1)\tau), \end{aligned} \quad (1)$$

where σ_2 – dimensionless detuning of the natural frequency of the system caused by the constant component of the electric field, $A_1 - A_4$ – coefficients depending on the selected operating mode of

the resonator, the parameters of the material and components responsible for the electric forces $W_i, \Delta W_i$, introduced in the equation (2), σ_1 – detuning of the excitation frequency from the frequency of the main parametric resonance for an unstressed resonator, R – friction parameter, C, S – modal coordinates normalized over the capacitive gap, τ – dimensionless time.

The voltage V_i on each group of electrodes shown in Figure 1 changes according to a harmonic law and has the form:

$$V_i^2(t) = W_i^2 + \frac{4}{\pi} W_i \Delta W_i \sin((2 + \sigma_1)\tau), \quad j = \overline{1,4}, \quad (2)$$

where $W_i, [B]; \Delta W_i, [B]$ – constant and variable voltage components of the i -th group of electrodes. The asymptotic solution in the first approximation has the form:

$$\begin{aligned} C &= a_1 \cos\left(\left(1 + \frac{1}{2}\sigma_1\right)t + \frac{1}{2}\psi_1\right) + O(\varepsilon), \\ S &= a_2 \cos\left(\left(1 + \frac{1}{2}\sigma_1\right)t + \frac{1}{2}\psi_2\right) + O(\varepsilon), \end{aligned} \quad (3)$$

where $O(\varepsilon)$ – are small expansion terms, $a_1 = a_1(t), a_2 = a_2(t), \psi_1 = \psi_1(t), \psi_2 = \psi_2(t)$ – are slow amplitude-phase variables, which are found from solutions of the following system:

$$\begin{aligned} \dot{a}_1 &= \frac{A_4}{8} a_1 (a_1^2 + a_2^2) \cos \psi_1 - \frac{R}{2} a_1 - \frac{A_2}{2} a_2 \cos\left(\frac{\psi_1}{2} - \frac{\psi_2}{2}\right) + \frac{A_3}{4} a_1 \cos \psi_1 \\ &\quad + \frac{A_1}{8} a_1 a_2^2 \sin(\psi_1 - \psi_2), \\ \dot{a}_2 &= \frac{A_4}{8} a_2 (a_1^2 + a_2^2) \cos \psi_2 - \frac{R}{2} a_2 + \frac{A_2}{2} a_1 \cos\left(\frac{\psi_1}{2} - \frac{\psi_2}{2}\right) + \frac{A_3}{4} a_2 \cos \psi_1 \\ &\quad - \frac{A_1}{8} a_1^2 a_2 \sin(\psi_1 - \psi_2), \\ \dot{\psi}_1 &= 2\sigma_2 - \sigma_1 + \left(\frac{3a_1^2}{4} + \frac{a_2^2}{2}\right) A_1 - \frac{A_3}{2} \sin \psi_1 \left(2 + (2a_1^2 + a_2^2)\right) + \frac{A_2^2}{4} + \frac{a_2}{a_1} A_2 \sin\left(\frac{\psi_1}{2} - \frac{\psi_2}{2}\right) \\ &\quad + \frac{A_4}{4} a_2^2 \sin \psi_2 + \frac{A_1}{4} a_2^2 \cos(\psi_1 - \psi_2), \\ \dot{\psi}_2 &= 2\sigma_2 - \sigma_1 + \left(\frac{3a_2^2}{4} + \frac{a_1^2}{2}\right) A_1 - \frac{A_3}{2} \sin \psi_2 \left(2 + (2a_2^2 + a_1^2)\right) + \frac{A_2^2}{4} + \frac{a_1}{a_2} A_2 \sin\left(\frac{\psi_1}{2} - \frac{\psi_2}{2}\right) \\ &\quad + \frac{A_4}{4} a_1^2 \sin \psi_1 + \frac{A_1}{4} a_1^2 \cos(\psi_1 - \psi_2). \end{aligned} \quad (4)$$

On the basis of the developed mathematical model, the region was investigated and the region of the main parametric resonance was found. The transient curves at various values of the constant voltage are shown in Figure 1. The results obtained allowed us to estimate the starting voltages for a real structure, at a specific value of the deviation of the vibration excitation frequency (σ_1) from the natural frequency of the system ($1 + \sigma_2$). On the basis of the obtained system (4) with the use of numerical methods of the theory of continuation, the amplitude-frequency characteristics of the resonator are constructed when the variable voltage component is varied. Figure 2 shows the dependence of the steady-state oscillation amplitude normalized with respect to the capacitive gap on the frequency detuning σ_1 , the dashed line indicates the unstable branches.

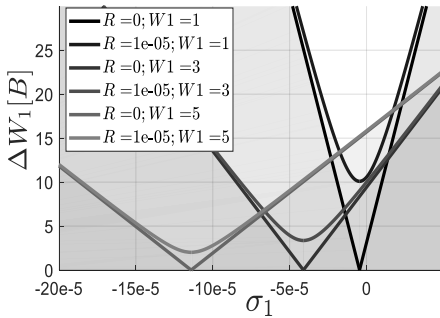


Fig. 1. Transition curves for a parametrically excited resonator, at $\Delta W_1 = \Delta W_2 = \Delta W_3 = \Delta W_4$ и $W_1 = W_2 = W_3 = W_4$.

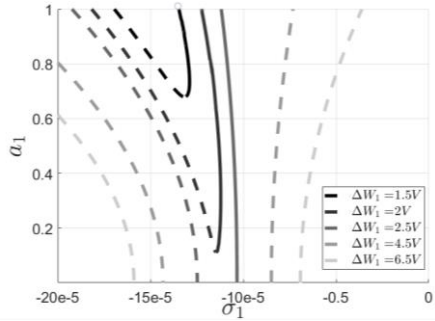


Fig. 2. Amplitude-frequency characteristics for a parametrically excited resonator, constant voltage component $W_1 = W_2 = W_3 = W_4 = 5$ [B], friction parameter $R = 10^{-5}$

3. Conclusion

The paper presents a mathematical model of an CVG with a disk resonator. The nonlinear dynamics of the system is investigated in the region of the main parametric resonance. For specific parameters of the possible design of the CVG, the starting voltages were assessed. Resonance curves of the resonator are constructed, the stability of the found stationary solutions is investigated. The proposed dynamic model of CVG will be used in the future for the parametric analysis of the free precession mode of the operating mode of oscillations of the resonator on a moving base, as well as for the development of algorithms for carrying out calibration tests of the sensor in the presence of material and geometric imperfections, methods of dynamic balancing and algorithms for controlling the oscillations of the sensitive element.

References

- [1] ПЕШЕХОНОВ В. Г. ПЕРСПЕКТИВЫ РАЗВИТИЯ ГИРОСКОПИИ //ГИРОСКОПИЯ И НАВИГАЦИЯ. – 2020. – Т. 28. – №. 2. – С. 3-10.
- [2] ПЕШЕХОНОВ В. Г. СОВРЕМЕННОЕ СОСТОЯНИЕ И ПЕРСПЕКТИВЫ РАЗВИТИЯ ГИРОСКОПИЧЕСКИХ СИСТЕМ //ГИРОСКОПИЯ И НАВИГАЦИЯ. – 2011. – №. 1. – С. 3-16.
- [3] POURKAMALI S., HAO Z., AYAZI F. VHF SINGLE CRYSTAL SILICON CAPACITIVE ELLIPTIC BULK-MODE DISK RESONATORS-PART II: IMPLEMENTATION AND CHARACTERIZATION //JOURNAL OF MICROELECTRO-MECHANICAL SYSTEMS. – 2004. – Т. 13. – №. 6. – С. 1054-1062.
- [4] JOHARI H., AYAZI F. HIGH-FREQUENCY CAPACITIVE DISK GYROSCOPES IN (100) AND (111) SILICON //2007 IEEE 20TH INTERNATIONAL CONFERENCE ON MICRO ELECTRO MECHANICAL SYSTEMS (MEMS). – IEEE, 2007. – С. 47-50
- [5] MIRJALILI R. ET AL. SUBSTRATE-DECOUPLED SILICON DISK RESONATORS HAVING DEGENERATE GYROSCOPIC MODES WITH Q IN EXCESS OF 1-MILLION //2015 TRANSDUCERS-2015 18TH INTERNATIONAL CONFERENCE ON SOLID-STATE SENSORS, ACTUATORS AND MICROSYSTEMS (TRANSDUCERS). – IEEE, 2015. – С. 15-18.
- [6] SERRANO D. E. ET AL. SUBSTRATE-DECOUPLED, BULK-ACOUSTIC WAVE GYROSCOPES: DESIGN AND EVALUATION OF NEXT-GENERATION ENVIRONMENTALLY ROBUST DEVICES //MICROSYSTEMS & NANOENGINEERING. – 2016. – Т. 2. – №. 1. – С. 1-10.

- [7] LYCHEV S. A., MANZHIROV A. V., JOUBERT S. V. CLOSED SOLUTIONS OF BOUNDARY-VALUE PROBLEMS OF COUPLED THERMOELASTICITY //MECHANICS OF SOLIDS. – 2010. – Т. 45. – №. 4. – С. 610-623.
- [8] ДУРУКАН Я., РЫБИНА М. А., ШЕВЕЛЬКО М. М. СОСТОЯНИЕ И ПЕРСПЕКТИВЫ РАЗРАБОТКИ ЧУВСТВИТЕЛЬНЫХ ЭЛЕМЕНТОВ НА ОБЪЕМНЫХ АКУСТИЧЕСКИХ ВОЛНАХ ДЛЯ ДАТЧИКОВ УГЛОВОЙ СКОРОСТИ //Навигация и управление движением. – 2019. – С. 169-171.
- [9] SHARMA J. N., GROVER D., KAUR D. MATHEMATICAL MODELLING AND ANALYSIS OF BULK WAVES IN ROTATING GENERALIZED THERMOELASTIC MEDIA WITH VOIDS //APPLIED MATHEMATICAL MODELLING. – 2011. – Т. 35. – №. 7. – С. 3396-3407.
- [10] JANI S. M. H., KIANI Y. GENERALIZED THERMO-ELECTRO-ELASTICITY OF A PIEZOELECTRIC DISK USING LORD-SHULMAN THEORY //JOURNAL OF THERMAL STRESSES. – 2020. – Т. 43. – №. 4. – С. 473-488.
- [11] YANG Y. ET AL. NONLINEARITY OF DEGENERATELY DOPED BULK-MODE SILICON MEMS RESONATORS //JOURNAL OF MICROELECTROMECHANICAL SYSTEMS. – 2016. – Т. 25. – №. 5. – С. 859-869.
- [12] HU Z., GALLACHER B. J. EFFECTS OF NONLINEARITY ON THE ANGULAR DRIFT ERROR OF AN ELECTROSTATIC MEMS RATE INTEGRATING GYROSCOPE //IEEE SENSORS JOURNAL. – 2019. – Т. 19. – №. 22. – С. 10271-10280.
- [13] SERRANO D. E. ET AL. SUBSTRATE-DECOUPLED, BULK-ACOUSTIC WAVE GYROSCOPES: DESIGN AND EVALUATION OF NEXT-GENERATION ENVIRONMENTALLY ROBUST DEVICES //MICROSYSTEMS & NANOENGINEERING. – 2016. – Т. 2. – №. 1. – С. 1-10.
- [14] JOUBERT S.V., SHATALOV M.Y., SPOELSTRA H. (2017) ON ELECTRONICALLY RESTORING AN IMPERFECT VIBRATORY GYROSCOPE TO AN IDEAL STATE. IN: ALTENBACH H., GOLDSTEIN R., MURASHKIN E. (EDS) MECHANICS FOR MATERIALS AND TECHNOLOGIES. ADVANCED STRUCTURED MATERIALS, VOL. 46. SPRINGER, CHAM

An approach to the modeling and simulation of multi-layered and multi-stimulable material for application in soft robots

KLAUS ZIMMERMANN¹, IGOR ZEIDIS¹, SIMON GAST^{1*}, NINA PREM¹,
STEFAN ODENBACH², DARSHAN KARE GOWDA²

¹Technische Universität Ilmenau, Max-Planck-Ring 12, 98693 Ilmenau, Germany,

²Technische Universität Dresden, George-Bähr-Straße 3, 01069 Dresden, Germany,

* Presenting Author, e-mail: simon.gast@tu-ilmenau.de

Abstract: The behaviour of magnetically stimulable materials is considered. The investigations focus on multi-layered one-dimensional continua where the respective stimulability is based on discrete layers. Vibrations of two-layered elastic Timoshenko's beam are investigated. One of the layers consists of a magneto-sensitive material. Young and shear module in this layer depend on the magnitude of the applied magnetic field those changes periodically in time. A lumped force is applied to the beam. The expressions for the amplitude and phase of the steady-state vibrations of the beam are obtained by the method of averaging. Using the analytical expressions and the measurement data for the amplitude and frequency of the beam vibrations, one can identify the application point of the lumped force. The investigated system can be considered as a model of a tactile sensor for soft robotics.

Keywords: soft robots, sandwich beam, beam vibrations, tactile sensors

1. Introduction

For soft robots the development of compliant smart materials with controllable properties is one of the key problems. Thus, the use of smart materials whose shape and properties can be controlled by external fields is in the focus of research [1], [2]. There are a number of publications that deal with theoretical investigations of multi-layered (sandwich) structures. As a rule, the objects of such investigations are cantilever beams or plates that consist of several layers of different materials, with at least one layer of a smart material [3], [4]. In our study, the vibrations of a two-layered Timoshenko's beam acted upon by a lumped force and a magnetic field are investigated by means of the averaging technique. One of the layers of the beam is non-magnetic, while the material of the other layer is a magneto-sensitive elastomer.

2. Results and Discussion

Vibrations of a two-layered beam of a length L , in which one layer is a magneto-sensitive elastomer, are studied. The beam is acted upon by a lumped force applied at some distance away from the end of the beam. The beam is subjected to a magnetic field that is periodically (harmonically) changing in time (Fig. 1). The dynamics of the vibrations are studied on the basis of Timoshenko's beam model. The vibrations of the beam are governed by the equations

$$\begin{aligned} m_0 \partial_{tt} w - Q(\partial_{xx} w - \partial_x \varphi) &= f - m_0 \partial_{tt} a, \\ \partial_t (J \partial_t \varphi) - P \partial_{xx} \varphi - Q(\partial_x w - \varphi) &= 0. \end{aligned} \quad (1)$$

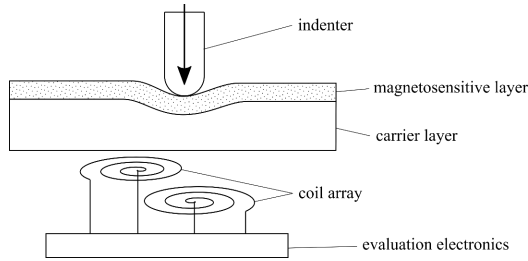


Fig. 1. Concept of a tactile sensor based on a two-layered design

Here, $w(x, t)$ is the transverse deflection of the beam, $\varphi(x, t)$ is the angle of the rotation of the cross section, m_0 is the mass of the beam per unit length, $f(x, t)$ is the external load per unit length, $J(t)$, $P(t)$, $Q(t)$, $a(t)$ are given functions that depend of the elastic constants and densities of the beam materials, as well as on the amplitude and frequency of the periodically changing magnetic field. The boundary conditions are given by

$$w(0, t) = w(L, t) = \partial_x \varphi(0, t) = \partial_x \varphi(L, t) = 0. \quad (2)$$

Assuming that the amplitude is small and neglecting the rotational inertia of the beam cross-section, we found the expressions for the amplitude and phase of the steady-state vibrations. These expressions were obtained by the method of averaging applied to the system of equations of (1) subject to the boundary conditions of (2). Using these expressions, one can identify the application point of the force, if the amplitude is known.

3. Concluding Remarks and Outlook

A model of a tactile sensor that consists of two deformable layers, one of which is magneto-sensitive, is presented. The analytical solution obtained on the basis of the averaged equations demonstrates good agreement with the numerical solution. This model can be used for the development of a tactile sensor, allowing the identification of a force application point on the basis of measured vibration data. The results of the experiments with a sensor prototype that have been performed agree with the conclusions that have been drawn on the basis of the proposed mathematical model. By using additional thermoplastic particles in an elastomer matrix, further controllable effects can be achieved.

Acknowledgement

This research is funded by the Deutsche Forschungsgemeinschaft (DFG) in the framework of the priority programs SPP 2100 (project ZI 540/20-1).

References

- [1] AKHAVAN H, GHADIRI M, ZAJKANI A: A new model for the cantilever MEMS actuator in magnetorheological elastomer cored sandwich form considering the fringing field and Casimir effects. *Mechanical Systems and Signal Processing*, 2019, **121**:551-561.
- [2] GAST S, ZIMMERMANN K: A tactile sensor based on magneto-sensitive elastomer to determine the position of an indentation. *J. of Sensors and Sensor Systems* 2020, **9**:319-326.
- [3] BRUEVICH N G: Vibration behavior of visco-elastically coupled sandwich beams with magnetorheological core and three-phase carbon nanotubes/fiber/polymer composite facesheets subjected to external magnetic field. *J. of Sandwich Structures and Materials* 2019, **21**:2194-2218.
- [4] KOROBKO E, MIKHASEV G, NOVIKOVA Z, ZHURASUKI M: On damping vibrations of three-layered beam containing magnetorheological elastomer. *J. of Int. Mat. Systems and Structures* 2012 **23**:1019-1023.

-BIF-

**BIFURCATIONS AND CHAOS
IN DYNAMICAL SYSTEMS**

Generalized Neimark—Sacker Bifurcations

DENIS BLACKMORE^{1*}

1. Department of Mathematical Sciences, New Jersey Institute of Technology, Newark, NJ 07102-1982, USA
[ORCID #0000-0003-3524-9538]

* Presenting Author

Abstract: We sketch a proof of a new type of bifurcation for discrete dynamical systems in all finite dimensions that generalizes the Neimark—Sacker bifurcation. In addition, we identify an application to discrete predator-prey dynamics.

Keywords: sink, source, bifurcation parameter, homeomorph

1. Introduction

The Neimark—Sacker bifurcation is a rather ubiquitous codimension-1 feature for smooth discrete dynamical systems on smooth surfaces (see [2] – [5]). It can be essentially described as follows: A fixed point spiral sink on a smooth surface changes to a fixed spiral source at the bifurcation value of a single real parameter λ and generates an invariant smooth diffeomorph of the unit circle \mathbb{S}^1 , which encloses the fixed point and expands with increasing λ . We introduced a generalization in [1], which has the following characterization: If a sink fixed point of a smooth discrete dynamical system on a smooth n -dimensional manifold M changes to a source at the bifurcation value of a single real parameter λ , it generates an invariant homeomorph of the unit $(n-1)$ -sphere \mathbb{S}^{n-1} , which encloses the fixed point and expands with increasing λ .

2. Results and Discussion

Our main result is the following:

Theorem

Suppose that

$$f : U \times (-a, a) \rightarrow \mathbb{R}^n, (x, \lambda) \rightarrow f(x, \lambda) := f_\lambda(x), \quad (1)$$

where U is an open set in \mathbb{R}^n containing the origin and $a > 0$, is a smooth map depending on the real parameter λ such that: (i) $f(0, \lambda) = 0$ for all $\lambda \in (-a, a)$; (ii) all eigenvalues of the derivative $f'_\lambda(0)$ are interior or exterior to the unit circle in the complex plane when $\lambda < 0$ or $\lambda > 0$ (so that $\lambda = 0$ is a bifurcation value), respectively; and (iii) $f(U \times (-a, a)) \subset U$.

Then, for $\lambda > 0$ there is an f -invariant homeomorph S_λ of \mathbb{S}^{n-1} enclosing the origin with a diameter that increases with λ .

Proof Sketch. For each small positive value of λ , start with a correspondingly sized $(n-1)$ -sphere $S_0(\lambda)$. It can be shown, with some difficulty, that

$$f_\lambda^m(S_0(\lambda)) \rightarrow S_\lambda$$

as $m \rightarrow \infty$ which is homeomorphic to the $(n-1)$ -sphere and f -invariant. \square

As shown in [1], this theorem has significant applications to discrete dynamical systems models for population dynamics, and is likely be useful for analyzing several other phenomena.

3. Concluding Remarks

Acknowledgment: The author thanks Yogesh Joshi, Michelle Savescu, and Aminur Rahman for numerous useful conversations and assistance.

References

- [1] JOSHI Y, SAVESCU M, SYED M, BLACKMORE D: Interesting features of three-dimensional discrete Lotka—Volterra dynamics.. (*preprint*)
- [2] KUZNETSOV Y.A.: *Elements of Bifurcation Theory*. Springer-Verlag: New York, 1994.
- [3] NEIMARK J: On some cases of periodic motion depending on parameters. *Dokl. Akad Nauk SSSR* **129** (1959), 36-39.
- [4] SACKER R: On invariant surfaces and bifurcations of periodic solutions of ordinary differential equations. *Rep. IMM-NYU* **333** (1964), 1-62.
- [5] WIGGINS S.: *Introduction to Applied Nonlinear Dynamical Systems and Chaos, 2nd ed.*. Springer-Verlag: New York, 2003.

Governing equation construction for critical transitions in Langevin type NeuralSDEs

SCOTT CAMERON^{1,2*}, STEPHEN ROBERTS²

1. InstaDeep Ltd.
 2. Oxford University
- * Presenting Author

Abstract: An appealing property of Langevin stochastic differential equations (SDEs) is their ability to model critical transitions between locally confined states (meta-stable states). Further, the analysis of such transitions is valuable to many scientific and industrial applications, such as the estimation of system failure rates or stock market crashes. Expanding upon recent developments in machine learning for dynamical systems, we propose an analysis methodology for learned SDE models, such as those where the energy function is described by a neural network, in which we construct a meaningful description of the emerging critical transition dynamics.

Our approach starts by identifying the meta-stable states as the basins of attraction in the learned SDE; these are given by level-sets of the potential function. From the heights of the potential barriers separating each pair of basins, we can estimate the mean first passage times between the corresponding meta-stable states. Finally, we approximate the critical transition dynamics in the long-time limit as a discrete Markov jump process between the identified meta-stable states. These dynamics are characterized by a governing equation (the forward Kolmogorov equation) in which the transition rates are calculated from the mean first passage times. Equations of this form can then be solved exactly and meaningful information about the long-term dynamics of the system extracted via expectations.

Keywords: Langevin dynamics, critical transitions, SDE learning

On dynamics of Lorenz maps

ŁUKASZ CHOLEWA¹, PIOTR OPROCHA^{1*}

1. AGH University of Science and Technology, al. Mickiewicza 30, 30-059 Kraków, Poland

* Presenting Author

Abstract: In this talk we will present several dynamical properties of *expanding Lorenz maps*, that is maps f acting on $[0,1]$ satisfying the following three conditions:

- there is a critical point $0 < c < 1$ such that f is continuous and strictly increasing on $[0, c]$ and $(c, 1]$;
- left and right limits of $f(x)$ at c are 1 and 0, respectively;
- f is differentiable for all points not belonging to a finite set F and $f'(x) > 1 + a$ for some $a > 0$ and all x from $[0, 1] \setminus F$;

with special emphasis on piecewise linear case. It was observed many years ago that these maps appear in a natural way as Poincaré maps in geometric models of well-known Lorenz attractor, which was independently observed in works of Guckenheimer [4], Williams [5] and Afraimovich, Bykov and Shil'nikov [6] as a tool for better understanding of chaotic behaviour present in Lorenz model (cf. more recent [7]).

The main dynamical system considered in this talk will be expanding Lorenz maps with constant slope and the structure of their renormalizations. In this model renormalization is again a Lorenz map with constant slope, so in that case renormalization procedure must finish in finite number of steps. In family of all Lorenz maps the renormalization process does not have to end, which may be regarded as infinite "zooming" of the dynamics, so not all Lorenz maps are coming from constant slope model. On the other hand, good understanding of renormalizations can reveal periodic structure of the map, and even in piecewise linear case this structure is highly nontrivial. In the talk we will connect periodic orbits with such properties as transitivity, mixing, renormalizations and proper invariant sets. Starting point of our presentation will be [1] and [2] together with examples from [3] showing several unexpected border cases, where general analysis undertaken in [1,2] failed.

Building on the above-mentioned results, we will highlight problems with relation between completely invariant sets and renormalizations. We will show that while every completely invariant closed subset leads to a renormalisation, there exist renormalizations that cannot be recovered from such a set. Furthermore, it may happen that several renormalizations define the same completely invariant sets. Also, minimal periodic orbit does not always lead to renormalization, or defines a renormalization, but not a minimal one. The talk is based in main part on results in [8].

Keywords: Lorenz map, Lorenz model, renormalization, mixing, periodic orbit

Acknowledgment: P. Oprocha was supported by National Science Centre, Poland (NCN), grant no. 2019/35/B/ST1/02239.

References

- [1] GLENDINNING P.: Topological conjugation of Lorenz maps by β -transformations. *Math. Proc. Cambridge Philos. Soc* 1990, **107**:401-413.
- [2] CUI H, DING Y, Renormalization and conjugacy of piecewise linear Lorenz maps. *Adv. Math* 2015, **271**:235-272.
- [3] OPROCHA P, POTORSKI P, RAITH P, Mixing properties in expanding Lorenz maps, *Adv. Math* 2019, **343**:712-755.
- [4] J. GUCKENHEIMER, A strange, strange attractor, in: J. E. Marsden and M. McCracken (eds.), *The Hopf Bifurcation Theorem and its Applications*, Springer, 1976, pp. 368--381.
- [5] R. F. WILLIAMS, The structure of Lorenz attractors}. *Inst. Hautes Etudes Sci. Publ. Math. No. 50*, (1979), 73-99.
- [6] V. S. AFRAIMOVICH, V. V. BYKOV, L. P. SHIL'NIKOV, On attracting structurally unstable limit sets of Lorenz attractor type. (in Russian) *Trudy Moskov. Mat. Obshch.* **44** (1982), 150-212.
- [7] S. LUZZATTO, I. MELBOURNE, F. PACCAUT, The Lorenz attractor is mixing. *Comm. Math. Phys.* **260**(2) (2005), 393-401.
- [8] Ł. CHOLEWA, P. OPROCHA, Renormalization in Lorenz maps -- completely invariant sets and periodic orbits, arXiv:2104.00110

Infinite Towers in the Graph of a Dynamical System

ROBERTO DE LEO^{1*}, JAMES A. YORKE²

1. Department of Mathematics, Howard University (USA) and INFN, Cagliari (Italy)
 2. Institute for Physical Science and Technology and the Department of Mathematics and Physics, UMD (USA)
- * Presenting Author

Abstract: Chaotic attractors, chaotic saddles and periodic orbits are examples of chain-recurrent sets. Using arbitrary small controls, a trajectory starting from any point in a chain-recurrent set can be steered to any other point in that set. The qualitative behaviour of a dynamical system can be encapsulated in a graph whose nodes are the chain-recurrent sets. There is an edge from node A to node B if, using arbitrary small controls, a trajectory starting from any point of A can be steered to any point of B. We discuss physical systems that have infinitely many disjoint coexisting nodes. Such infinite collections can occur for many carefully chosen parameter values. The logistic map is such a system. To illustrate these very common phenomena, we compare the Lorenz system and the logistic map and we show how extremely similar their bifurcation diagrams are in some parameter ranges. Typically, bifurcation diagrams show how attractors change as a parameter is varied. We call ours “graph bifurcation diagrams” to reflect that not only attractors but also unstable periodic orbits and chaotic saddles are shown.

Keywords: graph of a dynamical system, logistic map, Lorenz system, chain-recurrent sets

1. Introduction

The idea of describing the asymptotics of points in a dynamical system through a graph goes back at least to S. Smale [1] that, in 60s, observed that the flow of the gradient vector field ∇f of a generic function f on a compact manifold M can be encoded into a graph Γ whose nodes are the fixed points of f . Γ has an edge between node A and node B if there is an integral trajectory of ∇f asymptotic to A for $t \rightarrow -\infty$ and to B for $t \rightarrow +\infty$. This idea was generalized by C. Conley [2] in 70s so that it can be applied any kind of continuous or discrete dynamical system. One of his key ideas was replacing the non-wandering set by the larger set of chain-recurrent points. A point x is chain-recurrent if, for any $\varepsilon > 0$, there is an ε -controlled loop based at x , where by ε -controlled trajectory we mean a trajectory where, at every integer time, one is allowed to move the point anywhere within an ε radius from its position. In this talk we present our analytical results on the graphs of the logistic map and our numerical results on the Poincaré map of the Lorenz system. Our results suggest that the graph of the logistic map appears as a subgraph in a large set of dissipative higher-dimensional dynamical systems. In particular, many chaotic processes have a much more complicated structure than theoreticians previously expected.

2. Results and Discussion

In [3] we prove that the graph of the logistic map $I_\mu(x) = \mu x(1-x)$ is a tower, namely there is an edge between each pair of nodes. Since in the graph of a dynamical system there cannot be loops, this means that the nodes of the logistic map can be sorted as N_0, N_1, \dots, N_ρ so that arbitrarily

close to N_k there are points asymptoting to $N_{k'}$ for each $k' > k$. Notice that N_p is always the attracting node and that, for $1 < \mu < 4$, N_0 is the fixed point 0. The number of nodes $p+1$ is infinite when the attractor is a Cantor set (the other two possibilities being a periodic orbit and a (chaotic) cycle of intervals). This happens for an uncountable zero-measure set of parameter values.

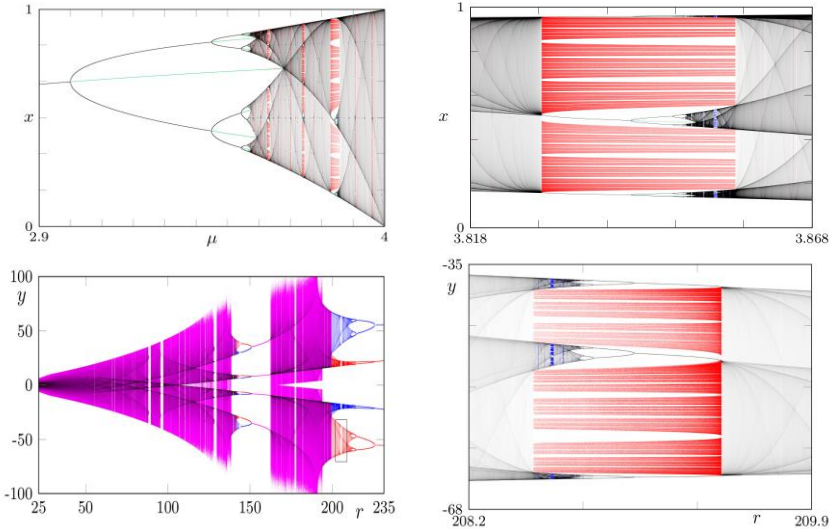


Fig. 1. (Top) Bifurcation diagram of the logistic map. Attractors are painted in shades of gray, repellers in green (periodic orbits), red and blue (Cantor sets). (Bottom) Bifurcation diagram of a Poincaré map of the Lorenz system. The period-3 window shown on the right is the close-up of the one framed in the left picture. Although the systems are completely different, the close-ups of some of their period-3 windows look extremely similar.

Our numerical results, some of which are shown in Fig. 1, suggest that the same graph structure of the logistic map are universal in the sense that they appear in completely unrelated systems such as the celebrated Lorenz system [4].

3. Concluding Remarks

Our numerical investigations suggest that, for some parameter values, even in higher-dimensional dissipative systems infinitely many chain-recurrent sets can arise within a compact set. Notice that this result is “transversal” to the celebrated result of Newhouse that chaotic systems in a compact set can have infinitely many attractors.

Acknowledgment: This material is based upon work supported by the National Science Foundation under Grant No. DMS-1832126.

References

- [1] SMALE S: Differentiable Dynamical Systems. *Bulletin of the AMS* 1967, **73**:747-817.
- [2] CONLEY C: *Isolated invariant sets and the Morse index*. n. 38 AMS, 1972.
- [3] DE LEO R, YORKE J.A.: The graph of the logistic map is a tower. *Discr. and Cont. Dyn. Sys.*, 2021.

Evaluation of the Reinjection Process in Type V Intermittency

SERGIO ELASKAR¹, EZEQUIEL DEL RÍO^{2*}, WALKIRIA SCHULZ³

1. IDIT and Dto. Aeronáutica, FCEfYN, Universidad Nacional de Córdoba and CONICET, Argentina [0000-0002-7250-0392]
 2. Dto. de Física Aplicada, ETSIAE, Universidad Politécnica de Madrid, Spain [0000-0003-3384-9521]
 3. Dto. Aeronáutica, FCEfYN, Universidad Nacional de Córdoba, Argentina [0000-0002-0015-6211]
- * Presenting Author

Abstract: In this paper, a technique to evaluate the reinjection probability density function, and the probability density of the laminar lengths for type V intermittency is implemented. A family of maps with continuous and discontinuous RPD functions is studied. Several tests were performed, where the proposed technique was compared with the M function methodology, the classical theory of intermittency, and with numerical data. The analysis showed that the new technique captures accurately the random values of the numerical data. Therefore, the technique presented here is a useful tool to analytically calculate the statistical variables of type V intermittency.

Keywords: reinjection process, chaotic intermittency, transformation of random variables

1. Introduction

Maps that show intermittency have a local map and a non-linear map that produces the reinjection process. The intermittency type is determined by the local map, and the reinjection mechanism allows the return of the trajectories from the chaotic region to the laminar one. The reinjection probability density function (RPD) is used to quantify the reinjection process, and it expresses the probability of the trajectories to be reinjected in each point of the laminar zone [1]. Hence, the correct evaluation of the RPD function is fundamental to describe the chaotic intermittency phenomenon accurately. Type V intermittency occurs when a stable fixed point loses its stability through a collision with a non-differentiable point forming a channel between the map and the bisector line [2]. In this paper, we use the transformation of random variables to develop a methodology to analytically evaluate the reinjection probability density and the probability density of the laminar lengths (RPDL) for type V intermittency.

2. Model, Results and Discussion

We introduce the following family of maps

$$F(x) = \begin{cases} F_1(x) = \lambda_1 x + \varepsilon & \hat{x} \leq x < 0, \\ F_2(x) = \varepsilon + x + \lambda_2 x^2 & 0 \leq x < x_m, \\ F_3(x) = \hat{x} + \frac{(y_m - \hat{x})(y_m - x)^\gamma}{(y_m - x_m)^\gamma} & x_m \leq x < y_m, \end{cases} \quad (1)$$

where \hat{x} is the lower boundary of reinjection [1]. If we apply the transformation of random variables and we exclude the contributions that do not generate reinjection in the laminar zone [3], the RPD results

$$\phi(x) = \sum_{j \neq l}^n \left| \frac{dF_j^{-1}(x)}{dx} \right| \rho(F_j^{-1}(x)), \quad (2)$$

where l indicates the intervals that do not generate reinjection [3]. If the lower boundary of reinjection verifies $\hat{x} = x_0 - c$, where x_0 is the fixed point and c is the semi-amplitude of the laminar interval, we obtain continuous RPD functions as shown Figure 1 (centre). If the lower boundary of reinjection verifies $\hat{x} < x_0 - c$, type V intermittency shows discontinuous RPDs, which appear by two different processes of reinjection, one produced by $F_3(x)$ and the other by $F_1(x)$ as shown Figure 1 (left and right).

$$\phi(x) = \begin{cases} \phi_I(x) = \phi_1(x) + \phi_3(x) & x < F_1(x_0 - c), \\ \phi_{II}(x) = \phi_3(x) & x \geq F_1(x_0 - c). \end{cases} \quad (3)$$

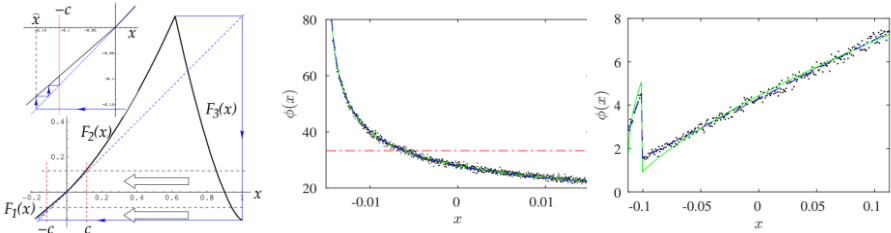


Fig. 1. Left: reinjection process. Centre: continuous RPD, $\gamma = 1.5$, $\varepsilon = 0.0001$, $c = 0.0015$, and the number of reinjected point is $N = 25 \times 10^5$. Right: discontinuous RPD, $\gamma = 0.5$, $\varepsilon = 0.001$, $c = 0.1128$, $N = 15 \times 10^5$ and $\hat{x} = -0.158449931412894$. Blue line: continuity technique. Green line: M function methodology. Red line: classical theory. Black points: numerical data.

3. Concluding Remarks

We presented a new technology to evaluate the statistical properties of type V intermittency, which was obtained from the transformation of random variables. We introduced and applied this technique to calculate continuous and discontinuous RPD and RPD functions. We carried out comparisons of the theoretical results here obtained with those calculated by the M function methodology, the classical theory of intermittency, and numerical data. We have calculated the rate of convergence for all tests, and we have found that the process is convergent with rate of convergence $O(1/N^p)$ within $0.15 < p < 0.5$. Also, we found that the new technique works very accurately for different parameters, either with continuous or discontinuous RPDs. We conclude that the continuity technique has shown to have the ability to evaluate the reinjection probability density function and the probability density of the laminar lengths for type V intermittency.

Acknowledgment: This work was supported by SECyT of Universidad Nacional de Córdoba and Ministerio de Ciencia, Innovación y Universidades of Spain under grand No RTI2018-094409-B-I00.

References

- [1] ELASKAR S, DEL RIO E: *New Advances on Chaotic Intermittency and its Applications*. Springer: New York, 2017.
- [2] BAUER M, HABIP S, HE D, MARTIESSEN W: New type of intermittency in discontinuous maps. *Physical Review Letters* 1992, **68**(11):1625.
- [3] ELASKAR S, DEL RIO E, LORENZÓN D: Calculation of the statistical properties in intermittency using the natural invariant density. *Symmetry* 2021, **13**(6):935.

Emergence of the Third Type of Chaos in a System of Adaptively Coupled Kuramoto Oscillators

ANASTASIIA A. EMELIANOVA*, VLADIMIR I. NEKORKIN

Institute of Applied Physics RAS, 46 Ulyanov Street, 603950 Nizhny Novgorod, Russia
[A. E.: 0000-0002-3418-2602, V. N.: 0000-0002-8345-1557]

* Presenting Author

Abstract: The report is devoted to the phenomenon of mixed dynamics, which is considered the third type of chaos, in a system of adaptively coupled Kuramoto oscillators. Mixed dynamics is characterized by the fundamental inseparability of conservative and dissipative behavior and in this case a chaotic attractor intersects with a chaotic repeller. The system under consideration is the first irreversible system with a new type of chaos. Mixed dynamics is present in the system when there is a small detuning of the natural frequencies of the phase oscillators or when one of the oscillators is forced by a harmonic external force of small amplitude. The properties of a reversible core, the set along which the chaotic attractor and the chaotic repeller intersect, were studied. In the nonautonomous case of mixed dynamics, the question of chaotic forced synchronization of the oscillations was considered. It was shown that mixed dynamics “prevents” forced synchronization of the oscillations. The influence of an external force on the properties of a reversible core formed due to a nonzero detuning of the natural frequencies of the oscillators was considered. The result can be interpreted as the phenomenon of forced synchronization of the reversible core by an external force.

Global Dynamics of a Polynomial Mechanical System

VALERY GAIKO

United Institute of Informatics Problems, National Academy of Sciences of Belarus
[ORCID: 0000-0002-6001-6288]

Abstract: Using a bifurcational geometric approach, we study the global dynamics and solve the problem on the maximum number and distribution of limit cycles in a planar polynomial Euler-Lagrange-Liénard type mechanical system.

Keywords: Euler-Lagrange-Liénard system, bifurcation, field rotation parameter, singular point, limit cycle

1. Introduction

We consider an Euler-Lagrange-Liénard equation

$$\ddot{x} + h(x)\dot{x}^2 + f(x)\dot{x} + g(x) = 0 \quad (1)$$

and the corresponding dynamical system

$$\dot{x} = y, \dot{y} = -g(x) - f(x)y - h(x)y^2. \quad (2)$$

Particular cases of such a system were considered in [1-8]. There are many examples in the natural sciences and technology in which this and related systems are applied. Such systems are often used to model either mechanical or electrical, or biomedical systems, and in the literature, many systems are transformed into Liénard type to aid in the investigations. They can be used, e.g., in certain mechanical systems, where $f(x)$ represents a coefficient of the damping force and $g(x)$ represents the restoring force or stiffness, when modeling wind rock phenomena and surge in jet engines. Such systems can be also used to model resistor-inductor-capacitor circuits with non-linear circuit elements. The Liénard system has been shown to describe the operation of an optoelectronics circuit that uses a resonant tunnelling diode to drive a laser diode to make an optoelectronic voltage controlled oscillator [3].

There are also a number of examples of technical systems which are modelled with quadratic damping: a term in the second-order dynamics model, which is quadratic with respect to the velocity state variable. These examples include bearings, floating off-shore structures, vibration isolation and ship roll damping models. In robotics, quadratic damping appears in feed-forward control and in nonlinear impedance devices, such as variable impedance actuators. Variable impedance actuators are of particular interest for collaborative robotics [9, 10].

We suppose that system (2), where $g(x)$, $h(x)$ and $f(x)$ are arbitrary polynomials, has an anti-saddle (a node or a focus, or a center) at the origin [8].

2. Limit Cycle Bifurcations

Following [1], we study limit cycle bifurcations of (2) by means of canonical systems containing field rotation parameters of (2) [8].

Theorem 1. The Euler-Lagrange-Liénard polynomial system (2) with limit cycles can be reduced to one of the canonical forms:

$$\begin{aligned} \dot{x} &= y, \\ \dot{y} &= -x(1 + a_1x + \dots + a_{2l}x^{2l}) + \\ &+ (\alpha_0 - \beta_1 - \dots - \beta_{2k-1} + \beta_1x + \alpha_2x^2 + \dots + \beta_{2k-1}x^{2k-1} + \alpha_{2k}x^{2k}) + \\ &+ y^2(c_0 + c_1x + \dots + c_{2n}x^{2n}); \end{aligned} \quad (3)$$

$$\begin{aligned} \dot{x} &= y, \\ \dot{y} &= x(x-1)(1 + b_1x + \dots + b_{2l-1}x^{2l-1}) + \\ &+ (\alpha_0 - \beta_1 - \dots - \beta_{2k-1} + \beta_1x + \alpha_2x^2 + \dots + \beta_{2k-1}x^{2k-1} + \alpha_{2k}x^{2k}) + \\ &+ y^2(c_0 + c_1x + \dots + c_{2n}x^{2n}), \end{aligned} \quad (4)$$

where $\alpha_0, \alpha_2, \dots, \alpha_{2k}$ are field rotation parameters, $\beta_1, \beta_3, \dots, \beta_{2k-1}$ are semi-rotation parameters, and system (3) has the only singular point.

By means of the canonical systems (3) and (4), we prove the following theorem [8].

Theorem 2. The Euler-Lagrange-Liénard polynomial system (2) can have at most $k + 1 + 1$ limit cycles, $k + 1$ surrounding the origin and l surrounding one by one the other singularities of (2).

Acknowledgment: This work was supported by the German Academic Exchange Service (DAAD). The author is also very grateful to the Center for Technologies in Robotics and Mechatronics Components of the Innopolis University for hospitality during his stay in January-May 2020.

References

- [1] GAIKO VA: *Global Bifurcation Theory and Hilbert's Sixteenth Problem*. Kluwer: Boston, 2003.
- [2] GAIKO VA: On limit cycles surrounding a singular point. *Differ. Equ. Dyn. Syst.* 2012, **20**:329-337.
- [3] GAIKO VA: The applied geometry of a general Liénard polynomial system. *Appl. Math. Letters* 2012, **25**:2327-2331.
- [4] GAIKO VA: Limit cycle bifurcations of a general Liénard system with polynomial restoring and damping functions. *Int. J. Dyn. Syst. Differ. Equ.* 2012, **4**:242-254.
- [5] GAIKO VA: Limit cycle bifurcations of a special Liénard polynomial system. *Adv. Dyn. Syst. Appl.* 2014, **9**:109-123.
- [6] GAIKO VA: Maximum number and distribution of limit cycles in the general Liénard polynomial system. *Adv. Dyn. Syst. Appl.* 2015, **10**:177-188.
- [7] GAIKO VA: Global bifurcation analysis of the Kukles cubic system *Int. J. Dyn. Syst. Differ. Equ.* 2018, **8**:326-336.
- [8] GAIKO VA, SAVIN SI, KLIMCHIK AS: Global limit cycle bifurcations of a polynomial Euler-Lagrange-Liénard system. *Comput. Res. Model.* 2020, **12**:693-705.
- [9] SAVIN S, KHUSAINOV R, KLIMCHIK A: Control of actuators with linearized variable stiffness. *IFAC-PapersOnLine* 2019, **52**:713-718.
- [10] SHIRIAEV A, ROBERTSSON A, PERRAM J, SANDBERG A: Periodic motion planning for virtually constrained Euler-Lagrange systems. *Systems Control Letters* 2006, **55**:900-907.

Nonlinear Dynamics of Relativistic Backward-Wave Tube: Chaos, Bifurcations and Strange Attractors

ALEXANDER V GLUSHKOV^{1*}, ANDREY V TSUDIK¹, OLEG V DUBROVSKY¹
AND OLEKSII L MYKHAILOV¹

1. Odessa State Environmental University, Mathematics Depr., L'vovskaya str. 15, 65009, Odessa

* Presenting Author

Abstract: The paper is devoted to modelling, analysis, forecasting the dynamics of relativistic backward-wave tube (RBWT) with accounting for relativistic effects (factor γ_0), dissipation factor (factor D) and an effect of presence of the space charge. The temporal dependences of the normalized field amplitudes (power) in a wide range of variation of the governing parameters (electric length of an interaction space, bifurcation parameter, the Pirs parameter and γ_0) are computed and analyzed from the viewpoint of distributed relativistic electron-waved self-vibrational systems. A nonlinear analysis technique (including a multi-fractal approach, the methods of correlation integral, false nearest neighbours, surrogate data, the Lyapunov's exponent's and Kolmogorov entropy algorithms etc) is applied to numerical studying the RBWT chaotic dynamics. There are computed the dynamic and topological invariants in auto-modulation/chaotic regimes. The bifurcation diagrams in the plains of different governing parameters are constructed.

Keywords: relativistic backward-wave tube, chaos, attractors

1. Non-stationary dynamics of relativistic backward-wave tube: Master system of evolutionary equations and nonlinear analysis

At present, a study of regular and chaotic dynamics of nonlinear processes in different classes of devices of so-called relativistic high-frequency or even ultrahigh-frequency microwave electronics is of a great importance (e.g.[1-4]). Despite intensive study of the phenomenon of chaos in the BWT dynamics, now it has been recognized that many features of the self-modulation regimes, primarily chaotic ones, remain unexplored. Moreover, there are no definite answers to the question on the mechanisms of chaos generation, chaotic self-modulation onset. There are absent the quantitative data on the the dynamic and topological invariants of the RBWT dynamics. In this work the results of modelling, analysis, forecasting the RBWT dynamics with accounting for relativistic effects, dissipation factor and an effect of presence of the space charge are presented. The time dependences of the normalized field amplitudes (power) are computed in a wide range of variation of the governing parameters: relativistic factor $\gamma_0 = (1 - \beta_0^2)^{-1/2}$ (where $\beta_0 = v_0 / c$, v_0 is the initial velocity of the electrons), electric length of an interaction space N) and a bifurcation parameter: $L = 2\pi CN / \gamma_0$. Here the Piers parameter C is as follows: $C = \sqrt[3]{I_0 K_0 / (4U)}$, where I_0 is a constant component of the beam current, U is an accelerating voltage, and K_0 is a communication resistance of the deceleration system. The equation in the usual dimensionless form for a phase $\theta(\zeta, \tau, \theta_0)$ of relativistic electron (that flew into the space of interaction with the phase θ_0 and has a coordinate ζ at time τ) and a

complex amplitude $F(\zeta, \tau) = \tilde{E} / (2\beta_0 U C^2)$ ($E(x, t) = \text{Re}[\varepsilon(x, t) \exp[i\omega_0 t - i\beta_0 x]]$) are as follows:

$$\begin{aligned} \partial^2 \theta / \partial \zeta^2 &= -L^2 \gamma_0^3 \left[\left(1 + \frac{1}{2\pi N} \partial \theta / \partial \zeta \right)^2 - \beta_0^2 \right]^{3/2} \text{Re}[F \exp(i\theta)] \\ \partial F / \partial \tau - \partial F / \partial \zeta &= -L \tilde{I}, \quad \tilde{I} = -\frac{1}{\pi} \int_0^{2\pi} e^{-i\theta} d\theta_0 \end{aligned} \quad (1)$$

with corresponding boundary & initial conditions. Further the methods of a chaos theory and a non-linear analysis technique (such as a multi-fractal approach, methods of correlation integral, false nearest neighbours, surrogate data, the Lyapunov's exponent's and Kolmogorov entropy algorithms etc; eg [5]) are applied to numerical analysis of the corresponding time series of the RBWT dynamics.

2. Results and Discussion

As input data, there are used the parameters: energy of electrons - 150keV, starting current of 7A composed impedance connection 0,5Ω , length of interaction space - 0,623m; other parameters are described in [1,4]. The computed temporal dependence of the RBWT power are received for the different injection currents. At current 7A it is set stationary mode that with increasing value of current strength transitioned to the periodic automodulation (I = 30A, on our data, the period of $T_a = 7.3\text{ns}$; experimental value [1]: 8ns), and then when I = 55A it is realized the chaotic auto-modulation mode (Fig 1a). By increasing an current to 75A there is the quasi-periodical auto-modulation (period 13.8 ns) and, finally, when the current value is more than 100A it is realized essentially chaotic regime. Note that reset of the quasi-periodic auto-modulation mode can be explained by an effect of space charge. The obtained results are compared with the similar theoretical estimates (however without the dissipation effect) and experiment data by Ginsburg et al [1]. Further at first the results of computing a set of the dynamical and topological invariants (correlation and embedding dimensions, Lyapunov's exponents, Kaplan-Yorke dimension (d_L), and the Kolmogorov entropy, etc) are listed.

3. Concluding Remarks

The nonlinear analysis technique (including a multi-fractal approach, the methods of correlation integral, false nearest neighbours, surrogate data, the Lyapunov's exponent's algorithm and others) is applied to analysis of numerical parameters of the RBWT chaotic dynamics. The new data on the dynamic and topological invariants of the RBWT dynamics in auto-modulation/chaotic regimes are listed for the first time. The bifurcation diagrams in the planes of different governing parameters are constructed.

References

- [1] GINZBURG N, ZAITSEV N, ILYAKOV E, KULAGIN I, NOVOZHILOVA YU, ROZENTHAL R, SERGEEV A: *Phys. Rev. Lett.* 2002, **89**:108304.
- [2] KUZNETSOV S, TRUBETSKOV D: Chaos and hyperchaos in a backward-wave oscillator *Radiophys. and Quant. Electr.* 2004, **47**:131-138.
- [3] RYSKIN N AND TITOV V: Self-modulation and chaotic regimes of generation in a relativistic backward-wave oscillator with end reflections// *Radiophys. and Quantum Electr.* 2001, **44**:793-802.
- [4] GLUSHKOV A, TSUDIK A, TERNOVSKY V, MYKHAILOV A, BUYADZHI V: Deterministic chaos, bifurcations and strange attractors in nonlinear dynamics of relativistic backward-wave tube. In: AWREJCWICZ J (Ed.) *Perspectives in Dynamical Systems II: Mathematical and Numerical Approaches*. Series: *Springer Proceedings in Mathematics & Statistics*. 2021, **363**:Ch.12
- [5] GLUSHKOV AV: *Methods of a Chaos Theory*. Astroprint: Odessa, 2012.

Complex Dynamics of Thin Shallow Spherical Caps,

G. IARRICCIO¹, A. ZIPPO² AND F. PELLICANO^{1*}

1. Centre InterMech MoRe, Dept. Eng. E. Ferrari, Univ. of Modena and Reggio E. [0000-0001-6206-2619]
2. Centre InterMech MoRe, Dept. Eng. E. Ferrari, Univ. of Modena and Reggio E. [0000-0001-6206-2619]
3. Centre InterMech MoRe, Dept. Eng. E. Ferrari, Univ. of Modena and Reggio E. [0000-0003-2465-6584]

* Presenting Author

Abstract: In the present work, the nonlinear vibrations of shallow spherical caps, under the action of static and fluctuating pressure, are studied. A semi-analytical approach, based on the Novozhilov's nonlinear thin shell theory, is developed; the approach is suitable for treating homogeneous isotropic shells. A meshless method is considered to reduce the partial differential equations (PDEs) to a set of ordinary differential equations (ODEs): the displacement fields are expanded through a mixed series of Legendre polynomials and harmonic functions in the meridional and circumferential directions respectively. The ODEs are obtained by taking advantage from the Lagrange equations and are numerically analysed using continuation and direct integration techniques. The achievements of this study show that nonlinear modal interactions can lead to the activation of non-symmetric vibrational states.

Keywords: spherical cap, nonlinear vibrations, bifurcation analysis

1. Introduction

The present study is focused on the nonlinear vibrations of spherical thin walled caps, which are a kind of structure widely used in engineering: pressure vessels, aerospace and aeronautical components, civil structures like roofs.

In this study a new method is proposed to analyse axisymmetric and asymmetric vibrations of thin walled shallow spherical caps under the action of uniform static and fluctuating pressure; the aim is investigating possible nonlinear modal interactions that can lead to the activation of asymmetric vibrations when the system is excited through a uniform and symmetric pressure field.

The most of previous theoretical studies on this topic were focused on axisymmetric vibrations, see e.g. [1, 2], which neglected the possible onset of non-symmetric vibrations due to the activation of asymmetric modes via nonlinear interactions.

2. Results and Discussion

In order to develop the method, the Novozhilov's thin shell theory is considered [3], such theory allow an accurate kinematical modelling of large thin shell deformations. In order to analyse the nonlinear PDE set arising from the Novozhilov theory a meshless discretization approach (see [4], for details) is considered: the three displacement fields are expanded through a double series, in the azimuthal

direction (Figure 1a) Legendre polynomials are considered and combined in order to respect boundary conditions, in the circumferential direction (Figure 1b) a Fourier series is used due to the periodicity; figures 1a,b show the shell geometry as well as the three displacement fields u, v, w , the azimuthal variable φ and the circumferential variable ϑ .

The main results of this study are summarized in Figure 1c, where the amplitude of the modal coordinate of the axisymmetric mode (1,0), referred to the transversal displacement field w , is represented v.s. the normalized excitation frequency of the fluctuating part of the pressure. One can see that the axisymmetric oscillation loses stability close to the resonance, the instability of axisymmetric vibration gives rise to the onset of asymmetric vibration of the spherical cup, even though the uniform pressure provides axisymmetric excitation

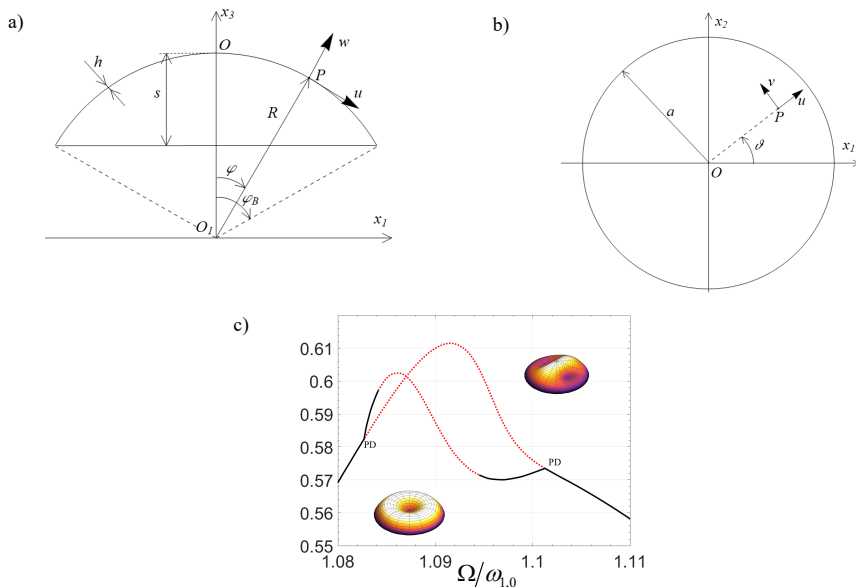


Figure 1: Geometry of the cap, a) lateral view, b) top view. Amplitude frequency diagram c).

Acknowledgments: The authors thank the Region Emilia Romagna for supporting this research through the project “DiaPro4.0” – (PG/2018/632156).

References

- [1] EVENSEN, H. A., AND EVAN-IWANOWSKI, R. M. “DYNAMIC RESPONSE AND STABILITY OF SHALLOW SPHERICAL SHELLS SUBJECT TO TIME-DEPENDENT LOADING,” AIAA JOURNAL, (1967), 5(5):969-976.
- [2] YASUDA, K., AND KUSHIDA, G., “NONLINEAR FORCED OSCILLATIONS OF A SHALLOW SPHERICAL SHELL,” BULL. OF JSME, 1984, 27(232):2233-2240.
- [3] NOVOZHILOV, V.V. FOUNDATIONS OF THE NONLINEAR THEORY OF ELASTICITY, GRAYLOCK PRESS, ROCHESTER, NY, USA (NOW AVAILABLE FROM DOVER, NY, USA), 1953.
- [4] IARRICCIO, G., PELLICANO, F., NONLINEAR DYNAMICS AND STABILITY OF SHALLOW SPHERICAL CAPS UNDER PRESSURE LOADING (2021) J. OF COMP. AND NONLIN. DYNAMICS, 16 (2), DOI: 10.1115/1.4049080

Parametric Vibrations of a System of Oscillators Connected with Periodically Variable Stiffness

GRZEGORZ KUDRA^{1A}, KRZYSZTOF WITKOWSKI^{1B}, SOUMYAJIT SETH^{1C*}, KRYSZTIAN POLCZYŃSKI^{1D}, JAN AWREJCIEWICZ^{1E}

1. Lodz University of Technology, Department of Automation, Biomechanics, and Mechatronics, Łódź, Poland
^A[0000-0003-0209-4664], ^B[0000-0003-1214-0708], ^C[0000-0003-3528-2020], ^D[0000-0002-1177-6109],
^E[0000-0003-0387-921X]

* Presenting Author

Abstract: The work is a part of a larger project concerning investigations of different configurations of connected oscillators with direct and parametric forcing sources. Among others, we present preliminary numerical studies of dynamics of a system composed of two oscillators connected with periodically variable stiffness. Each of the oscillators is connected to the fixed support with the use of a nonlinear magnetic spring. Based on the derived mathematical equations of the parametric system, a bifurcation plot was calculated for different shaft speeds. Bifurcation analysis shows both the ranges of periodic and chaotic motion. As an additional part, we will realize this kind of mechanical system from an electrical point of view, and we shall observe the phenomena experimentally.

Keywords: parametric oscillations, rectangular cross-section shaft, impact, bifurcation

1. Introduction

The dynamics of parametric systems are characterized by the existence of many stable and unstable regions. Examples of such systems where parametric vibrations occur are, for example, shafts with non-circular cross-section or with asymmetrical stiffness in different directions of vibration of such a shaft. A few nonlinear behaviors of these systems have been studied, and the theory is still under process to reach some maturity [1-4]. Our recent work presents a preliminary numerical investigation of a system composed of two oscillators connected with periodically variable stiffness (see Fig. 1a). Each of the oscillators is connected to the fixed support with the use of a nonlinear magnetic spring.

2. Results and Discussion

The system is described by the following differential equations: $m_1\ddot{x}_1 + F_{R1}(\dot{x}_1) + F_{S1}(x_1) + k_c(t)(x_1 - x_2) = 0$ and $m_2\ddot{x}_2 + F_{R2}(\dot{x}_2) + F_{S2}(x_2) + k_c(t)(x_2 - x_1) = 0$, where, $F_{Ri}(\dot{x}_i) = c_i\dot{x}_i + T_i\dot{x}_i(\dot{x}_i^2 + \varepsilon^2)^{-1/2}$ is model of resistance in the bearings and the term $(\dot{x}_i^2 + \varepsilon^2)^{-1/2}$ is smooth approximation of function $\text{sign}(\dot{x}_i)$, $F_{Si}(x_i) = F_M(\delta - x_i) - F_M(x_i + \delta)$ is magnetic spring force, where $F_M(z) = F_{M0}(d_1z + 1)^{-4}$, and $k_c(t) = \frac{k_\xi + k_\eta}{2} + \frac{k_\xi - k_\eta}{2} \cos(2\omega t)$ is the stiffness coupling of the oscillators that varies periodically. We are going to build an experimental rig which is a special configuration of the stand used in the work [5]. For the initial simulation tests, we have assumed the parameter values as: masses of the carts $m_1 = 8.0985$ kg and $m_2 = 6.7838$ kg, linear damping coefficients $c_1 = c_2 = 8$ Ns/m, dry friction forces $T_1 = T_2 = 1.9$ N, parameters of the magnetic spring model $F_{M0} = 360$ N and $d_1 = 50$ m⁻¹, shaft stiffness coefficients $k_\xi = 262.5$ N/m and $k_\eta =$

2916.67 N/m, the distance between the magnets in equilibrium position $\delta = 0.03$ m. Moreover, it is assumed that, $\varepsilon = 0.001$ s/m.

In Fig. 1b, we have shown the numerically obtained bifurcation diagram of the considered system with the angular frequency of parametric forcing ω , playing the role of a control parameter, keeping the rest parameters fixed. There, we can see that there is an interplay between the periodic and chaotic attractors just after the bifurcation point. The periodic attractors with different periodicities are the windows in between chaos.

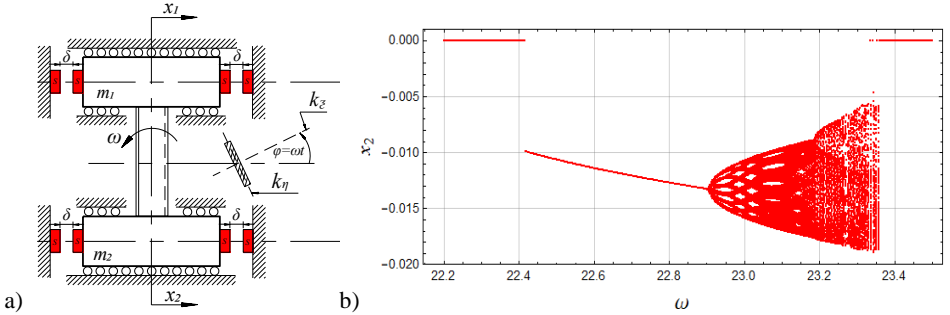


Fig. 1. Scheme of the investigated system (a) and bifurcation diagram (b)

3. Concluding Remarks

The presented investigations are a part of the larger project concerning parametric vibrations of the systems of connected mechanical oscillators with different kinds of excitations. Preliminary studies show that even the dynamics of the system composed of two oscillators connected to the fixed support with the nonlinear magnetic springs and the use of periodically variable linear stiffness exhibit complex bifurcation and chaotic dynamics. The hardening stiffness nonlinearity prevents the system from large oscillations in the vicinity of resonances and, instead of this, leads to complex bifurcation dynamics.

Additionally, we are going to construct the electrical analog of this mechanical system. The motivation is that such experiments are really inexpensive, and it is easy to vary the parameters in an electronic circuit. We shall simplify the equations of motion of the system and implement them in an electronic circuit.

Acknowledgment: This work has been supported by the Polish National Science Centre, Poland under the grant OPUS 18 No. 2019/35/B/ST8/00980.

References

- [1] SAEED, NA.: On vibration behavior and motion bifurcation of a nonlinear asymmetric rotating shaft. *Archive of Applied Mechanics* 2019, 89: 1899–1921.
- [2] SHAHGHOLI, M., KHADEM, SE.: Primary and parametric resonances of asymmetrical rotating shafts with stretching nonlinearity. *Mechanism and Machine Theory* 2012, 51: 131–144.
- [3] HOSSEINI, SAA., KHADEM, SE.: Free vibrations analysis of a rotating shaft with nonlinearities in curvature and inertia. *Mechanism and Machine Theory* 2009, 44: 272–288.
- [4] AWREJCEWICZ, J.: *Ordinary differential equations and mechanical systems*. Springer International Publishing: Cham, 2014.
- [5] WITKOWSKI K., KUDRA G., SKURATIVSKIY S., WASILEWSKI G., AWREJCEWICZ J: Modeling and dynamics analysis of a forced two-degree-of-freedom mechanical oscillator with magnetic springs. *Mechanical Systems and Signal Processing* 2021, **148**:107138.

Multistability in Remote Synchronization Detected via Symbolic Dynamics

JULIANA C. LACERDA¹, CELSO FREITAS¹, ELBERT MACAU^{2*}

1. Associated Laboratory for Computing and Applied Mathematics, National Institute for Space Research - INPE, São José dos Campos, Brazil

2. Institute of Science and Technology, Federal University of Sao Paulo, UNIFESP, Brazil

* Presenting Author

Abstract: In this work, we introduce a new approach, based on symbolic dynamics and complex network formalism, to characterize multistability in the remote synchronization phenomena, where the dynamical system is governed by the Stuart-Landau equation and the topology is star-like. This methodology has already been used to detect periodic windows and chaos in nonlinear systems and we show that it is able to detect the regions where multistability takes place and we compare the results obtained by traditional methods.

Keywords: synchronization, multistability, symbolic dynamics

1. Introduction

Two of the most important phenomena in nonlinear dynamical systems are multistability and remote synchronization. In the first, the system may enter in different states after a transient, due to the coexistence of multiple attractors, which implies that the final state has a strong dependence to the initial conditions, in a way that the synchronous state is reached only by a set of these values [1]. In the latter, dynamical units that are not directly connected enter in a synchronous state [2]. In order to quantify the synchronization of dynamical systems, metrics like the order parameter and the partial synchronization index are used [3].

An alternative approach to study the dynamics of nonlinear systems was proposed [4,5]. With this method, instead of using usual metrics to characterize the system, like Lyapunov exponents and bifurcation diagram, metrics from complex networks like mean degree and betweenness centrality is used. This approach makes use of the time series of the system to generate undirected graphs by utilizing symbolic dynamics and then uses the formalism of complex networks to extract information of these graphs and then characterize the system. It was shown that this method is able to detect periodic windows and chaos in the Logistic and Hénon maps [4].

In this work, we introduce a new way to characterize multistability in the phenomena of remote synchronization making use of symbolic dynamics and complex network formalism. Our approach is not able to differ from a synchronous to a non-synchronous state but it is capable of detecting the region where multistability takes place.

2. Results and Discussion

The system is given by a star topology composed of eleven nodes whose dynamics is modelled by the Stuart-Landau equation [6]. This system was studied by [7] and presented multistability in the synchronization of the peripheral nodes in a certain region of coupling. In this work we make use of

symbolic dynamics (model DCSD in [4]) to turn the time series of the oscillators into a binary series and, after that, into a decimal series. This decimal series is then converted in networks, where each number corresponds to a node and there exists a connection between two nodes in the network only if they are neighbours in the decimal series. Metrics like betweenness centrality, density and mean degree are then calculated. For a fixed value of coupling, twenty distinct time series, and consequently, twenty distinct graphs are generated for each oscillator. Also, this procedure is done for several values of coupling. The mean and standard deviation of these complex network metrics are then calculated and compared to the usual metric used, called partial synchronization index [3], which is frequently used to quantify remote synchronization. By comparing both methods it is able to verify the existence of a multistability region at the same coupling interval.

3. Concluding Remarks

The results show that the methodology applied in this work is capable of detecting the multistability region, although outside this region it can not distinguish from the synchronous to the non-synchronous state.

References

- [1] U. Feudel. Complex dynamics in multistable systems. *International Journal of Bifurcation and Chaos*, 18(06):1607-1626, 2008.
- [2] A. BERGNER, M. FRASCA, G. SCIUTO, A. BUSCARINO, E. NGAMGA, L. FORTUNA, AND J. KURTHS. REMOTE SYNCHRONIZATION IN STAR NETWORKS. *PHYSICAL REVIEW E*, 85(2):026208, 2012.
- [3] J. GOMEZ-GARDENES, Y. MORENO, AND A. ARENAS. PATHS TO SYNCHRONIZATION ON COMPLEX NETWORKS. *PHYSICAL REVIEW LETTERS*, 98(3):034101, 2007.
- [4] V. L. FREITAS, J. C. LACERDA, AND E. E. MACAU. COMPLEX NETWORKS APPROACH FOR DYNAMICAL CHARACTERIZATION OF NONLINEAR SYSTEMS. *INTERNATIONAL JOURNAL OF BIFURCATION AND CHAOS*, 29(13):1950188, 2019.
- [5] X. YU, Z. JIA, AND X. JIAN. LOGISTIC MAPPING-BASED COMPLEX NETWORK MODELING. *APPLIED MATHEMATICS*, 4(11):1558, 2013.
- [6] E. PANTELEY, A. LORIA, AND A. EL ATI. ON THE STABILITY AND ROBUSTNESS OF STUART-LANDAU OSCILLATORS. *IFAC-PAPERSONLINE*, 48(11):645-650, 2015.
- [7] J. LACERDA, C. FREITAS, AND E. MACAU. MULTISTABLE REMOTE SYNCHRONIZATION IN A STAR-LIKE NET-

The Dynamics of Two Coupled Oscillators with the Same Damping Term

MAAITA JAMAL-ODYSSEAS^{1*}, PROUSALIS DIMITRIS², VOLOS CHRISTOS³, AND MELETLIDOU EFTHYMIA⁴

1. Physics Department, Aristotle University of Thessaloniki, Greece [0000-0002-8105-8700]
2. Physics Department, Aristotle University of Thessaloniki, Greece [0000-0002-6200-4707]
3. Physics Department, Aristotle University of Thessaloniki, Greece [0000-0001-8763-7255]
4. Physics Department, Aristotle University of Thessaloniki, Greece

* Presenting Author

Abstract: In this paper we present the dynamic behavior of a system of linear and nonlinear coupled oscillators with the same damping term implemented by a nonlinear electronic circuit. The dynamic behavior is directly related to the damping parameter as well as the other parameters. We observe the alternation between periodic, chaotic and quasi-periodic oscillation.

Keywords: nonlinear oscillator, chaotic behavior, electronic circuits

1. Introduction

Systems of coupled oscillators play an essential role in physics and engineering [1]. In this work, we study a system of linear and nonlinear coupled oscillators with the same damping term. The system is mathematically described by

$$\begin{aligned} \dot{x} &= p_x \\ \dot{p}_x &= -k_1 x^3 - \lambda p_x - \alpha x y \\ \dot{y} &= p_y \\ \dot{p}_y &= -k_2 y - \lambda p_y \end{aligned} \quad (1)$$

k_1 and k_2 are the nonlinear and the linear coefficients, α is a coupling parameter and λ the damping parameter. The system has only one non-hyperbolic equilibrium point $(0,0,0,0)$, so the possible attractors are hidden [2]. The electronic circuit of figure 1 implements the above nonlinear system.

2. Dynamic behavior

Figure 2 presents the bifurcation diagram[3] of the nonlinear variable x related to the damping parameter λ for $k_1 = 1, k_2 = 1, \alpha = 1.5$ and values of the initial conditions $x(0) = 5, p_x(0) = 0.001, y(0) = 1, p_y(0) = 0.001$. The system oscillates in different ways: regularly with variant periods, quasi-periodically, and chaotically related to the damping parameter. The maximal Lyapunov Characteristic Exponent[4] of the system confirms this rich dynamical behavior.

Figure 4 presents the behaviour of the nonlinear variable x related to the coupling parameter α for $k_1 = 1, k_2 = 1, \lambda = 0.2$ and the same initial conditions. For values of $\alpha < 0.2$ the system oscillates periodically and then for $\alpha \geq 0.2$ starts to oscillate chaotically. Also, for $\alpha > 1.2$ there is a change between regular and non regular oscillations.

3. Discussion

The addition of the same damping parameter of the nonlinear oscillator in an undamped oscillator drastically changes the dynamics of the system of the coupled oscillators and leads to a rich dynamical behavior. Both the damping and the coupling parameter play an essential role in the oscillations of the system.

The nonlinear electronic circuit that implements the proposed system allows us to study and experimentally confirm the above results. Also, it opens perspectives for using such oscillators in electronic applications.

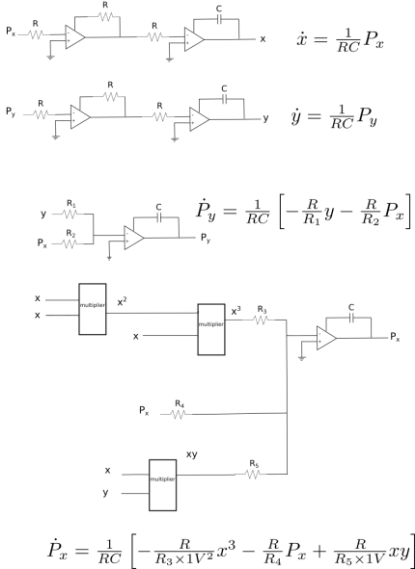


Fig.1: Circuit implementation

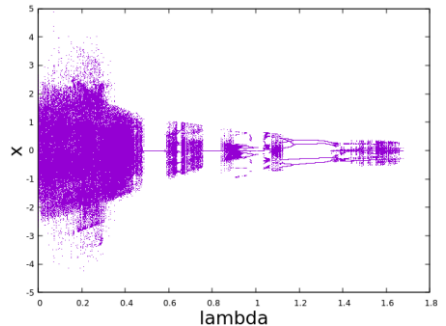


Fig.2: Bifurcation diagram.

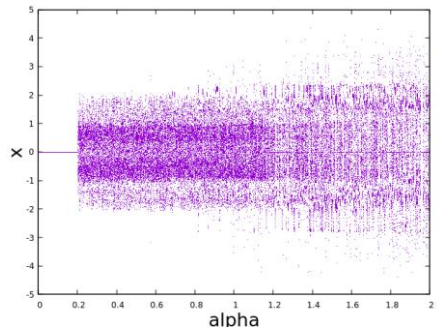


Fig.3: The behaviour of the nonlinear variable related to the coupling parameter.

References

- [1] NAYFEH A.H, MOOK D.T: Nonlinear Oscillations, Wiley 1995.
- [2] LEONOV G. A., KUZNETSOV N.V.: Hidden attractors in dynamical systems. From hidden oscillations in Hilbert–Kolmogorov, Aizerman, and Kalman problems to hidden chaotic attractor in Chua circuits." International Journal of Bifurcation and Chaos 23.01 (2013): 1330002.
- [3] GUCKENHEIMER J., HOLMES P.J.: Nonlinear Oscillations, Dynamical Systems, and Bifurcations of Vector Fields, 1983, Springer- Verlag New York.
- [4] SKOKOS C.: The Lyapunov characteristic exponents and their computation. Dynamics of Small Solar Sys-

Dynamical chaos in Hamiltonian systems with three degrees of freedom

NIKOLAI MAGNITSKII

1. Federal Research Center “Computer Science and Control” of RAS, Lomonosov Moscow State University, Moscow, Russia [0000-0001-6299-7270], E-mail: nikmagn@gmail.com

Abstract: It will be considered a new bifurcation approach to the analysis of solutions of Hamiltonian systems with three degrees of freedom, which implies the construction of an approximating extended two-parameter dissipative system whose stable solutions (attractors) are arbitrarily exact approximations to solutions of the original Hamiltonian system. It will be shown on the basis of numerical experiments for several Hamiltonian systems with three degrees of freedom such as Yang-Mills-Higgs and generalized Mathieu-Magnitskii systems that, in these systems, transition to chaos takes place not through the destruction of two-dimensional or three-dimensional tori of the unperturbed system in accordance with KAM (Kolmogorov-Arnold-Moser) theory, but, conversely, through the generation of complicated two-dimensional and three-dimensional tori around cycles of the extended dissipative system and through an infinite cascades of bifurcations of the generation of new cycles, tori and singular trajectories in accordance with the universal bifurcation FShM (Feigenbaum-Sharkovskii-Magnitskii) theory.

Keywords: keyword 1, keyword 2, keyword 3 (max 5 keywords)

References

- [1] MAGNITSKII N.A. : New approach to the analysis of Hamiltonian and conservative systems. *Differential Equations* 2008, **44**(12): 1618-1627.
- [2] MAGNITSKII N.A. : *Theory of dynamical chaos*. Lenand: Moscow, 2011.
- [3] MAGNITSKII N.A: Universality of Transition to Chaos in All Kinds of Nonlinear Differential Equations. In: AWREJCEWICZ J., HAGEDORN P. *Nonlinearity, Bifurcation and Chaos - Theory and Appl.* InTech: Rijeca, 2012.
- [4] MAGNITSKII N.A. Bifurcation Theory of Dynamical Chaos. In: AL NAIMEE K.A.M. *Chaos Theory*. InTech: Rijeca, 2018.

On Qualitative Analysis of the Model of Two-Link Manipulator with Time Delays: Stability, Bifurcation and Transition to Chaos

VASYL MARTSENYUK^{1*}, KRZYSZTOF AUGUSTYNEK², ANDRZEJ URBAŚ³

1. Department of Computer Science and Automation, University of Bielsko-Biala [0000-0001-5622-1038]
 2. Department of Mechanical Engineering Fundamentals, University of Bielsko-Biala [0000-0001-8861-4135]
 3. Department of Mechanical Engineering Fundamentals, University of Bielsko-Biala [0000-0003-0454-6193]
- * Presenting Author

Abstract: The paper considers the model of a two-link manipulator with constant delays. For the given reference trajectory the model is reduced to the four-order system of ordinary differential equations with two delays, which allows us to apply the methods of qualitative analysis of dynamics' systems. Stability research focuses on local asymptotic stability with the help of analyzing quasipolynomial near equilibrium state. In one special unstable case, the eigenvalues in a clear form are gotten. Nonlinear analysis is based on phase plots and computing some numerical characteristics. Namely, the bifurcation plot which was constructed on the base of the Poincare section has shown the appearance of chaotic behavior as a result of increasing time delays. The analytical results of the work include presenting the model in the form of ordinary differential equations with delays, finding eigenvalues of the characteristic polynomial in some special case. They have been obtained with the help of symbolic computation in the Yacas computer algebra system. Numerical characteristics with the facilities of visualization have been calculated in nonlinearTseries package in R.

Keywords: two-link manipulator, local asymptotic stability, delay, nonlinear analysis, Poincare section, bifurcation plot.

1. Introduction

Recently the model of a two-link manipulator (Fig. 1) attracts more attention from viewpoint of computing facilities of software to get its trajectories [1-3]. On the other hand, its qualitative analysis is of importance. In turn, cumbersome nonlinearities in the right-hand side do not allow us to get clear analytical results, e.g., for stability research. Here we study the delayed model on the basis of the system of nonlinear differential equations with angles θ_1 , θ_2 and velocities

$$z_1 = \frac{d\theta_1}{dt}, z_2 = \frac{d\theta_2}{dt}. \quad (1)$$

Thus, given reference trajectory $(\theta_1^r(t), \theta_2^r(t), z_1^r(t), z_2^r(t))$ we consider the system

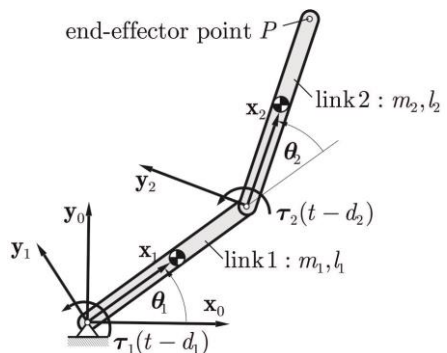


Fig. 1. Model of a two-link manipulator

$$\begin{aligned}\tau_1(t - d_1) &= \left(\frac{m_1 l_1^2}{3} + m_2 l_1^2 + \frac{m_2 l_2^2}{3} + m_2 l_1 l_2 \cos \theta_2\right) \frac{dz_1}{dt} + \left(\frac{m_2 l_2^2}{3} + \frac{m_2 l_1 l_2}{2} \cos \theta_2\right) \frac{dz_2}{dt} - \\ &\frac{m_2 l_1 l_2}{2} \sin \theta_2 z_2^2 - m_2 l_1 l_2 \sin \theta_2 z_1 z_2 + \frac{m_1 g l_1}{2} \cos \theta_1 + \frac{m_2 g l_2}{2} \cos(\theta_1 + \theta_2) + m_2 g l_1 \cos \theta_1, \\ \tau_2(t - d_2) &= \left(\frac{m_2 l_2^2}{3} + \frac{m_2 l_1 l_2}{2} \cos \theta_2\right) \frac{dz_1}{dt} + \frac{m_2 l_2^2}{3} \frac{dz_2}{dt} + \frac{m_2 l_1 l_2}{2} \sin \theta_2 z_1^2 + \frac{m_2 g l_2}{2} \cos(\theta_1 + \theta_2),\end{aligned}\quad (2)$$

where

$$\begin{aligned}\tau_1(t - d_1) &= k_{1,1}^1(\theta_1(t - d_1) - \theta_1^r(t - d_1)) + k_{1,2}^1(z_1(t - d_1) - z_1^r(t - d_1)) + \\ &k_{1,1}^2(\theta_2(t - d_2) - \theta_2^r(t - d_2)) + k_{1,2}^2(z_2(t - d_2) - z_2^r(t - d_2)), \\ \tau_2(t - d_2) &= k_{2,1}^1(\theta_1(t - d_1) - \theta_1^r(t - d_1)) + k_{2,2}^1(z_1(t - d_1) - z_1^r(t - d_1)) \\ &+ k_{2,1}^2(\theta_2(t - d_2) - \theta_2^r(t - d_2)) + k_{2,2}^2(z_2(t - d_2) - z_2^r(t - d_2))\end{aligned}$$

m_1, m_2, l_1, l_2 are masses and lengths of links, g is acceleration of gravity, $k_{i,j}^n$, $i, j, n \in \{1,2\}$ are gains, d_1, d_2 are constant time delays with the respect to the first and second joints respectively. Equations (2) can be presented as nonstationary ordinary differential equations with the delays

$$\begin{aligned}\frac{dz_1}{dt} &= f_1(t, \theta_1(t), \theta_2(t), z_1(t), z_2(t), \theta_1(t - d_1), \theta_2(t - d_2), z_1(t - d_1), z_2(t - d_2)), \\ \frac{dz_2}{dt} &= f_2(t, \theta_1(t), \theta_2(t), z_1(t), z_2(t), \theta_1(t - d_1), \theta_2(t - d_2), z_1(t - d_1), z_2(t - d_2)).\end{aligned}\quad (3)$$

That is (1), (3) combined with the corresponding initial conditions present model to be investigated.

2. Stability Research

In the non-delayed case when investigating local asymptotic stability, we have calculated Jacobian for the system (1), (3) for the neighbourhood of equilibrium state $\mathcal{E}_1^0 = (0,0, \theta_1^0, \theta_2^0)^T$ having the form

$$J = \begin{bmatrix} 0 & 0 & J_{13} & J_{14} \\ 0 & 0 & J_{23} & J_{24} \\ 1 & 0 & 0 & 0 \\ 0 & 1 & 0 & 0 \end{bmatrix}, \quad (5)$$

and corresponding eigenvalues being

$$\lambda_{1,2,3,4} = \pm \sqrt{\frac{1}{2} \left(J_{13} + J_{24} \pm \sqrt{(J_{13} + J_{24})^2 - 4(J_{14}J_{23} - J_{13}J_{24})} \right)},$$

References

- [1] AHMED, S., WANG, H., ASLAM, M. S., GHOU, I., & QAISAR, I. (2019). Robust Adaptive Control of Robotic Manipulator with Input Time-varying Delay. *International Journal of Control, Automation and Systems*. DOI:10.1007/s12555-018-0767-5
- [2] PUSHKAL B., JOSY G.: Two Link Planar Robot Manipulator Mechanism Analysis with MATLAB. *International Journal for Research in Applied Science & Engineering Technology* 2018, **6**(VII):778-788.
- [3] OMID MEHRJOEE, SIYAVASH FATHOLLAHI DEHKORDI & MOHARAM HABIBNEJAD KORAYEM (2019): Dynamic modeling and extended bifurcation analysis of flexible-link manipulator, *Mechanics Based Design of Structures and Machines*, DOI: 10.1080/15397734.2019.1665542

Nonlinear dynamics of semiconductor lasers and optical resonator systems: Chaos, bifurcations and attractors

ALEXANDER A MASHKANTSEV¹, SERGEY V KIR'YANOV¹,
ALEXANDER V GLUSHKOV¹, ANDREY A SVINARENKO¹, VASILY V BUYADZHI^{1*}

1. Odessa State Environmental University, Mathematics Depr., L'vovskaya str. 15, 65009, Odessa

* Presenting Author

Abstract: An advanced chaos-geometric computational approach to analysis, modelling and prediction of the non-linear dynamics of semiconductor laser and optical resonator systems with elements of the deterministic chaos is briefly presented. The approach is based on using the nonlinear analysis and chaos theory techniques such as a wavelet analysis, multi-fractal formalism, mutual information approach, correlation integral analysis, false nearest neighbour algorithm, the Lyapunov's exponents analysis, surrogate data method, prediction models etc. There are listed the advanced numerical data on the topological and dynamical invariants (correlation, embedding, Kaplan-York dimensions, the Lyapunov's exponents, Kolmogorov's entropy etc) of chaotic dynamics for the semiconductor GaAs/GaAlAs laser with a retarded feedback and optical resonator systems.

Keywords: nonlinear dynamics, semiconductor laser and resonator systems

1. Introduction. Universal Chaos-Geometric Approach to Laser and Resonator Systems Dynamics

A quantitative study of the chaos phenomenon features in the quantum electronics systems and devices is of a great interest and importance for many scientific and technical applications [1-3]. Chaotic fluctuations in the laser diodes dynamics deserve much attention because of their potential for unprecedented application of the technologies, secure communication, the construction of chaotic lidars, optical reflectometers, true random number generators etc. It is known that a transition to chaos in dissipative regime of functioning of NMR-maser provides the construction based on a new type of detecting signals with unprecedented sensitivity especially when approaching control parameter to the point of doubling bifurcation. The numerical results of study (data on the topological and dynamic invariants) of chaos generation dynamics in some quantum generator and laser systems with a few controlling parameters have been presented in [1-3].

This paper goes on our work on studying and advancing an effective computational approach to analysis and prediction of the non-linear dynamics of semiconductor laser and optical resonator systems with elements of the deterministic chaos [2-4]. In particular, there are presented the results of analysis, modelling and processing the corresponding chaotic time series of these semiconductor GaAs/GaAlAs laser with a retarded feedback and some optical resonator systems. The computational approach applied includes a combined set of non-linear analysis and chaos theory methods such as an autocorrelation function method, correlation integral approach, average mutual information, surrogate data, false nearest neighbours algorithms, the Lyapunov's exponents (LE) and Kolmogorov entropy analysis, spectral methods and nonlinear prediction (predicted trajectories, neural network etc) algorithms (in versions [2,3,5,6]).

2. Results and Discussion

As illustration in Table 1 our computational data on the Lyapunov's exponents, Kaplan-York attractor dimensions, the Kolmogorov entropy for the corresponding chaotic time series of the semiconductor GaAs/GaAlAs laser with a retarded feedback [(e.g. [1,3]) are listed. In the system an instability is generated by means of the retarded feedback during changing the control parameter such as the feedback strength μ (or in fact an injection current).

Table 1. The Lyapunov's exponents (λ_i), Kaplan-York dimension (d_L), Kolmogorov entropy K_{entr}

Regime	λ_1	λ_2	λ_3	d_L	K_{entr}
Chaos (I)	0.151	0.00001	-0.188	1.8	0.15
Hyperchaos (II)	0.517	0.192	-0.139	7.1	0.71

As the analysis shows there is appeared a multi-stability of different states with the modulation period: $T_n=2\pi/(2n+1)$, $n=0, 1, 2, \dots$. The state $n = 0$ is called as a ground one. With respect to the frequency modulation, other states are called as the 3rd, 5th harmonics and so on. A scenario of chaos generation is in converting initially periodic states into individual chaotic states with increasing the parameter μ through a sequence of the period doubling bifurcations. Further there is appeared a global chaotic attractor after merging an individual chaotic attractors according to a few complicated scenario (e.g. [1,3]. The analogous numerical analysis, modelling, forecasting procedure are realized for some optical resonator systems.

3. Concluding Remarks

There are presented the fundamentals of a chaos-geometric computational approach to analysis, modelling and prediction of the non-linear dynamics of semiconductor laser and optical resonator systems with elements of the deterministic chaos. There are listed the advanced numerical data on the topological and dynamical invariants (correlation, Kaplan-York dimensions, Lyapunov's exponents etc) of chaotic dynamics for the semiconductor laser and optical resonator systems.

References

- [1] FISCHER I, HESS O, ELSABER W AND GOBEL E: High-dimensional chaotic dynamics of an external cavity semiconductor laser. *Phys. Rev. Lett.* 1994, **73**:2188-2191.
- [2] GLUSHKOV AV: *Methods of a Chaos Theory*. Astroprint: Odessa, 2012.
- [3] BUYADZHI V, BELODONOV A, MIRONENKO D, MASHKANTSEV A, KIR'YANOV S, BUYADZHI A GLUSHKOV A: Nonlinear dynamics of external cavity semiconductor laser system with elements of a chaos. In: AWREJCEWICZ J, KAZMIERCZAK M, OLEJNIK P AND MROZOWSKI J (EDS.) *Engineering Dynamics and Life Sciences*. Lodz., 2017:89-96.
- [4] GLUSHKOV A, SVINARENKO A, BUYADZHI V, ZAICHKO P AND TERNOVSKY V: Chaos-geometric attractor and quantum neural networks approach to simulation chaotic evolutionary dynamics during perception process. In: BALICKI J (ED) *Advances in Neural Networks, Fuzzy Systems and Artificial Intelligence, Series: Recent Advances in Computer Engineering*. WSEAS: Gdansk, 2014, **21**:143-150.
- [5] GLUSHKOV A AND KHETSELIUS O: Nonlinear Dynamics of Complex Neurophysiologic Systems within a Quantum-Chaos Geometric Approach. In: GLUSHKOV A, KHETSELIUS O, MARUANI J, BRĀNDAS E (EDS) *Advances in Methods and Applications of Quantum Systems in Chemistry, Physics, and Biology. Series: Progress in Theoretical Chemistry and Physics*. Springer: Cham, 2021, **33**:291-303.
- [6] GLUSHKOV A, BUYADZHI V, KVASIKOVA A, IGNATENKO A, KUZNETSOVA A, PREPELITSA G AND TERNOVSKY V Nonlinear chaotic dynamics of Quantum systems: Molecules in an electromagnetic field and laser systems. In: TADJER A, PAVLOV R, MARUANI J, BRĀNDAS E, DELGADO-BARRIO G (EDS) *Quantum Systems in Physics, Chemistry, and Biology. Series: Progress in Theor. Chem. and Phys.* Springer: Cham, 2017, **30**:169-180.

On the dynamics of a 2-DOF nonlinear vibratory system with bistable characteristic and circulatory forces

MINH-TUAN NGUYEN-THAI^{1*}, PAUL WULFF², NILS GRÄBNER²,
UTZ VON WAGNER²

1. Hanoi University of Science and Technology [ORCID: 0000-0001-8584-8163]

2. Chair of Mechatronics and Machine Dynamics, Technische Universität Berlin

* Presenting Author

Abstract: We consider an autonomous damped 2-DOF mechanical system in which the two DOFs are coupled by a linear spring. A circulatory force is introduced into the system that may result in self-excited vibrations. A nonlinearity is added in the form of a cubic spring so that there are three fixed points, two of them are stable without the circulatory force, i.e., a bistable behaviour. The basins of attraction for different values of the circulatory force are numerically studied to see how the patterns of them change. Using a Poincaré map, the basins of attraction have three dimensions and they are cut with further cross-sections for the ease of visualization. The results are usually complicated maps with non-smooth boundaries, except when the circulatory force uncouples one DOF from the other. Special patterns of the maps are seen when in the nonlinear case a stable limit cycle is about to occur. Even in the case without stable limit cycle, initial conditions within the special range may lead to hundreds of cycles of periodic-like transient motion before asymptotically converge to a stable fixed point. Phase planes and bifurcation diagrams are also used, and multiple coexisting periodic solutions are found. Strong symmetric and asymmetric autonomous bursts are found.

Keywords: basins of attraction, circulatory force, self-excited vibration, transient motion, bursting

1. Introduction

Mechanical systems with circulatory terms show a number of interesting phenomena, e.g., transient growth [1]. In an earlier paper [2], the authors investigated differences in the behaviours of linear 2-DOF systems with and without circulatory matrices having same maximum real parts of eigenvalues. The current presentation is adding the influence of nonlinearities and focusing on the circulatory case. The added nonlinearity is in the form of a cubic spring with a negative linear term which is adjusted according to the circulatory term so that there are two fixed points $(x, z) = (1, 0.1)$ and $(-1, -0.1)$ aside from the unstable trivial solution. Phase planes, basins of attraction and bifurcation diagrams are used to study the global dynamics of the system. Multiple numerical methods, including cell-mapping method, are employed.

2. Results and Discussion

When the circulatory term (characterized by parameter χ) is small enough, solutions are converging to one of the two stable fixed points. The basins of attraction for different values of χ are numerically studied to see how the patterns of them change. The results are maps with non-smooth boundaries, except when the circulatory force uncouples one DOF from the other (Fig. 1a). The cross-sections of the basins of attraction show partially structured as well as fractal pattern (Fig. 1b) when χ increases

to a bifurcation value where the first inter-well limit cycle appears. The basin of attraction of the limit cycle appears and grows within the region of that special pattern (Fig. 1c). Closely before the bifurcation value, the limit cycle does not exist yet, but a periodic-like transient motion lasting for hundreds of cycles is observed.

When χ is high enough, all the fixed points become unstable, and many more periodic solutions appear, both symmetric and asymmetric. The periodic solutions show stronger bursting characteristic when χ is increased. Coexisting stable periodic solutions and period-doubling bifurcations are seen on the bifurcation diagram.

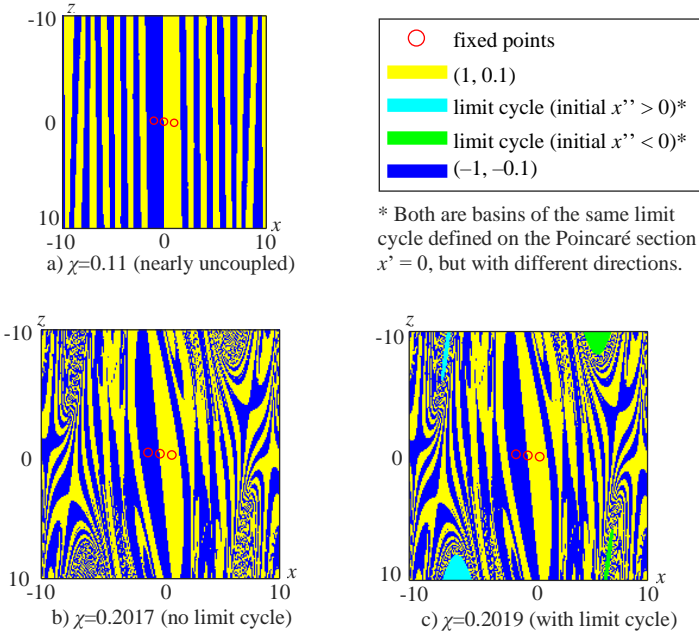


Fig. 1. Basins of attraction

3. Concluding Remarks

The circulatory force strongly affects the system’s behaviour both in the linear case [2] and in the nonlinear case. Special patterns of basins of attraction are seen when in the nonlinear case the first inter-well limit cycle nearly occurs. The considered system also witnesses a long-lasting transient motion, which might not be negligible in practical applications. Many more coexisting stable periodic solutions are found. The solutions are strongly bursting with appropriate parameters.

References

[1] HOFFMANN, N. AND GAUL, L.: Non-conservative beating in sliding friction affected systems: transient amplification of vibrational energy and a technique to determine optimal initial conditions. *Mechanical Systems and Signal Processing*, **18**(3):611-623.

[2] MINH-TUÁN, N.T.; WULFF, P.; GRÄBNER, N.; VON WAGNER, U.: On the influence of external stochastic excitation on linear oscillators with subcritical self-excitation and gyroscopic influence with application to brake squeal. *ZAMM* 2020, **101**(1), <https://doi.org/10.1002/zamm.202000113>.

Research of the dynamics of a physical pendulum forced with an electromagnetic field

EWELINA OGIŃSKA^{1*}, DARIUSZ GRZELCZYK², JAN AWREJCWICZ³

1. Department of Automation, Biomechanics and Mechatronics, Lodz University of Technology, Poland [https://orcid.org/0000-0003-2397-7538]
2. Department of Automation, Biomechanics and Mechatronics, Lodz University of Technology, Poland [https://orcid.org/0000-0002-7638-6582]
3. Department of Automation, Biomechanics and Mechatronics, Lodz University of Technology, Poland [https://orcid.org/0000-0003-0387-921X]

* Presenting Author

Abstract: In this paper, both experimental and numerical results of the dynamics of a pendulum with a neodymium magnet and an aerostatic bearing are presented. The experimental stand includes the pendulum with the neodymium magnet at the end of the rod, whereas four electric coils are placed underneath. The pivot of the pendulum is supported on the aerostatic bearing. As a result, dry friction resistance in the pivot joint can be negligible and it has only a viscous character. The electric current with a given frequency and duty cycle and of a square waveform flows through the coils. Interaction between the neodymium magnet and the electric coils leads to the forced angular motion of the pendulum with the neodymium magnet. Both mathematical and physical models with experimentally confirmed system parameters are derived. The results of the simulation and experiment showed rich dynamics of the system, including various types of regular motion (multi-periodicity) and chaos.

Keywords: nonlinear dynamics, electromagnetic field, physical pendulum, aerostatic bearing

1. Introduction

Non-linear character of the motion and very simple construction make the pendulum an often used object of many investigations of dynamics systems [1, 2, 3]. On the base of the interaction between electric and magnetic fields, for instance an electric motor works, which proves the great popularity of using this dependency nowadays [4, 5, 6, 7]. Physical pendulum driven by electromagnetic field research are willingly extended to create more complex systems and relationships [8, 9]. In this paper, mechanical energy is produced using the above-mentioned interaction in order to force motion of the physical pendulum. The axis of pendulum's rotation coincides with the shaft's axis suspended in the pressured air generated by an aerostatic bearing. This system is coherent, so the pendulum's motion is closely dependent on the force generated by the electromagnetic field, but also on the distance from the coil. The object of studies in this article are the presented dependencies.

2. Results and Discussion

In the presented paper the system of a physical pendulum supported by aerostatic bearing and subjected to an asymmetric repulsive magnetic field was studied. Physical model of the system is shown in Fig. 1. The magnetic field was induced by the four electric coils powered by a rectangular current signal with controlled values of frequency, duty cycle and amplitude. The magnetic field was alternating which directly influenced the dynamics of the pendulum.

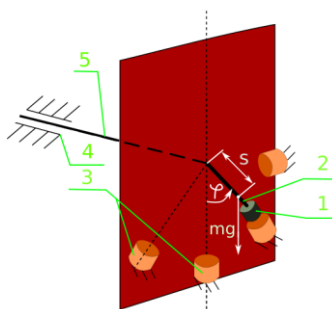


Fig. 1. Physical model of the system: 1 – neodymium magnet, 2 – pendulum, 3 – electric coils, 4 – aerostatic bearing, 5 – shaft.

3. Concluding Remarks

The physical and mathematical models of the considered system were developed. The numerical and experimental time histories plots of periodic motion with good agreement were shown. The bifurcation analysis was presented for increasing and decreasing paths of frequency as a control parameter. A set of phase plots were used to show the evaluation of chaotic motion. The system and experimental stand offer many opportunities for further research.

Acknowledgment: This work has been completed while the first author was the Doctoral Candidate in the Interdisciplinary Doctoral School at the Lodz University of Technology, Poland. This work has been supported by the National Science Centre, Poland, under the grant OPUS 14 No. 2017/27/B/ST8/01330.

References

- [1] KUMAR R., GUPTA S., ALI S.F.: Energy harvesting from chaos in base excited double pendulum. *Mech. Syst. Signal Process* 2019, **124**, 49–64.
- [2] KECIK K., MITURA A.: Energy recovery from a pendulum tuned mass damper with two independent harvesting sources. *Int. J. Mech. Sci.* 2020, **174**.
- [3] PEDERSEN H.B., ANDERSEN J.E.V., NIELSEN T.G., IVERSEN J.J., LYCKEGAARD F., MIKKELSEN F.K.: An experimental system for studying the plane pendulum in physics laboratory teaching. *Eur. J. Phys.* 2020, **41**.
- [4] KRAFTMAKHER Y.: Experiments with a magnetically controlled pendulum. *Eur. J. Phys.* 2007, **28**, 1007–1020.
- [5] BERDAHL J.P., VANDER LUGT K.: Magnetically driven chaotic pendulum. *Am. J. Phys.* 2001, **69**, 1016–1019.
- [6] POLCZYŃSKI K., WIJATA A., WASILEWSKI G., KUDRA G., AWREJCWICZ J.: Modelling and Analysis of Bifurcation Dynamics of Two Coupled Pendulums with a Magnetic Forcing. *IUTAM Symp. Exploit. Non-linear Dyn. Eng. Syst.* 2020, 213–223.
- [7] DONNAGÁIN M.Ó., RASSKAZOV O.: Numerical modelling of an iron pendulum in a magnetic field. *Phys. B Condens. Matter.* 2006, **372**, 37–39.
- [8] WOJNA M., WIJATA A., WASILEWSKI G., AWREJCWICZ J.: Numerical and experimental study of a double physical pendulum with magnetic interaction. *J. Sound Vib.* 2018, **430**, 214–230.
- [9] JIANG W., HAN X., CHEN L., BI Q.: Improving energy harvesting by internal resonance in a spring-pendulum system. *Acta Mech. Sin. Xuebao* 2020, **36**, 618–623.

Method of adaptive bacterial foraging optimization for detection and locating periodic and multi-periodic orbits

ALEXANDER RUCHKIN, CONSTANTIN RUCHKIN*

1. National Technical University of Ukraine "Igor Sikorsky Kyiv Polytechnic Institute", IASA, Address: 37, Prosp. Peremohy, Kyiv, Ukraine, 03056, alex3005r@gmail.com,

* Presenting Author

Abstract: In this paper we consider the problem of detection periodic and multi-periodic solutions of dynamical systems with a special Hamiltonian structure [1]. The detection of periodic solutions of dynamical systems is carried out by means of an analysis of the Poincaré sections of phase space on the plane for the presence of closed trajectories of a special kind on these sections. In most regular cases, the trajectories under investigation represent special geometric shapes - like circles, an ellipse, etc. To solve the problem of recognizing such forms, it is proposed to use the evolutionary method of bacterial search for stochastic global optimization - adaptive bacterial foraging optimization.

Keywords: The dynamical systems, the Hamiltonian systems, the periodic and quasi-periodic orbits the regular behaviour system, the bacterial foraging optimization

1. Introduction

We consider n -dimensional Hamiltonian system. According to the KAM theory, the system with the Hamiltonian is called integrable, if there is a canonical transformation to a new variable angle. The existence of n integrals of motion means are that a $2n$ -dimensional phase space of an integrable Hamiltonian path belongs to the n -dimensional set, which has the topology of the n -dimensional torus. On that torus the system trajectory is presented by the winding. If the ratio of the frequencies along the meridians and parallels rationally, the trajectory is closed. If the frequency ratio is irrational, then the trajectory of a dense way fills the surface n -dimensional torus. In this case, the motion is chaotic. Torus on which the winding «not irrational», frequency ratio does not satisfy become unstable and collapse. Also with the destruction of some torus is born smaller tori, which in the Poincaré section correspond to elliptic fixed points interspersed with hyperbolic fixed points. The process of destruction of some tori and the birth of other smaller breeds continues self-similar distribution of elliptic and hyperbolic fixed points in the Poincaré section. We are interested in automatic detection integrable cases with help numerical researches [1].

2. Results and Discussion

For this we carry out investigations the numerical researches of phase space, which consist of set of not intersected phase trajectories by means of Poincaré's sections. Poincaré's section, which are constructed in the phase space, have dimensionality on unit is less than dimensionality of researched dynamical system. The exceptional interest the dynamical systems of the third and fourth order is represented. Poincaré's sections for such systems will represent certain graphic images on a plane or

in space accordingly. If points of a phase flow are formed a closed curve, then it is possible to speak about the regular behaviour (periodic or multi-periodic) of Hamilton systems. The particular interest is represented by dynamic systems for which there is a possibility of reconstruction and investigation of global Poincare's section. Though creation of section of Poincare of phase space happens approximately by means of integration numerical methods on the fixed interval of time, it appears enough what to understand an overall picture of behaviour of Hamilton system. The received phase portraits of two-dimensional and three-dimensional sections of Poincare of Hamilton systems can be researched by means of automatic pattern recognition techniques.

So, in the integrable cases Poincare section will be of a surface area, which shows a certain type of closed curves: circles, ellipses and other algebraic curves with or without self-intersection. These cases correspond to the regular (periodic or multi-periodic) solution of a nonlinear dynamical system. We use a recently developed swarm intelligence technique, known as the Bacterial Foraging Optimization Algorithm (BFOA) [2] for automatic detecting circle shapes from digital images. We develop an adaptive version of BFOA is then applied to search the entire edge-map for circular shape. Each bacterium here models a trial circle and a fuzzy objective function has been derived over the domain of such trial circles. The better a test shape approximates the actual edge-shape, the lesser becomes the value of this function. Minimization of the objective function with BFOA ultimately leads to the fast and robust extraction of circular shapes from the given image. In the work consider the conditions of applicability of this approach for different geometric forms, which we have classified on the map Poincare. The parameters which the method will give the most optimal result are calculated.

3. Concluding Remarks

In this works for dynamical system [1] with help program Modeler the global spherical Poincaré section are investigated. This section builds a three-dimensional sphere and shows a set of points (point cloud). In regular cases, these sets of points form a three-dimensional «closed curve» with self-crossing or without self-crossing. A particular case of this curve is a circle or ellipse, which lies on the surface of a sphere, with the centre of the circle can pass or not pass through the centre of the sphere.

New program module are develop and integrated to program Modeler. This module are detected and recognised of three-dimensional convex closed analytic curves constructed on the Poisson sphere using the adaptive method of BFOA for all parameters of model.

References

- [1] Ruchkin C. The General Conception of the Intellectual Investigation of the Regular and Chaotic Behavior of the Dynamical System Hamiltonian Structure. In: Awrejcewicz J. (eds) Applied Non-Linear Dynamical Systems. Springer Proceedings in Mathematics & Statistics, vol 93. Springer, Cham, 2014, DOI: 10.1007/978-3-319-08266-0_17
- [2] S. Dasgupta, S. Das, A. Biswas, and A. Abraham, "Automatic circle detection on digital images with an adaptive bacterial foraging algorithm," *Soft Computing*, vol. 14, no. 11, pp. 1151–1164, 2010, DOI: 10.1109/TEVC.2009.2021982

Internal resonance induced in the impacting dynamics in a MEMS device

LAURA RUZZICONI^{1*}, NIZAR JABER², LAKSHMOJI KOSURU³,
MOHAMMED L. BELLAREDJ⁴, MOHAMMAD I. YOUNIS⁴

1. Faculty of Engineering, eCampus University, 22060 Novedrate, Italy
2. King Fahd University of Petroleum and Minerals, Dhahran 31261, Saudi Arabia
3. Physics Department, GITAM University, Telangana State, 502329 Hyderabad, India
4. King Abdullah University of Science and Technology (KAUST), 23955-6900 Thuwal, Saudi Arabia

* Presenting Author

Abstract: This work investigates the dynamics of a microbeam-based MEMS in the neighbourhood of the first natural frequency. The device is intentionally designed to have the capacitor gap larger than the air gap. When the oscillation reaches elevated amplitudes, the microbeam impacts with the substrate. This event causes the lengthening of the resonant branch and the concurrent activation along this range of an internal resonance between the first and the third mode.

Keywords: MEMS, impacting dynamics, internal resonance

1. Introduction

Nonlinear features of MEMS/NEMS are increasingly applied for novel devices to achieve superior performances [1, 2]. Special attention is devoted to the nonlinear interactions among different vibration modes and the related energy transfer [3, 4]. The present work is focused on a MEMS device electrically actuated and investigates the internal resonance induced in the impacting dynamics.

2. Results and Discussion

The MEMS device under investigation is constituted by a clamped-clamped rectangular microbeam electrically actuated by an electrode placed directly underneath it on a substrate. An optical image is reported in Fig. 1(a). For bottom to top, the microbeam is composed of 1.5 μm Silicon Nitride, 50 nm Chrome, and 200 nm Gold. The lower electrode is composed of 50 nm Chrome, and 200 nm Gold. The microbeam has length 400 μm and width 50 μm . The lower electrode spans half of the length of the microbeam. The equivalent capacitor gap is composed of both the air gap plus the contribution due to the Silicon Nitride layer, i.e. is larger than the air gap.

An extensive experimental investigation is conducted, where both forward and backward sweeps are acquired. Both resonant and non-resonant branches are detected, which exhibit hardening bending behaviour. When reaching elevated oscillation amplitudes, the resonant branch impacts with the substrate, after which oscillations continue for a non-negligible range of the driving frequency. Along a part of this interval, the system experiences the activation of the internal resonance with the third mode (second symmetric). An example of the corresponding FFT spectrum extracted from the data experimentally acquired at the internal resonance dynamics is reported in Fig. 1(b), showing the occurrence of both the main first mode peak and the third mode one.

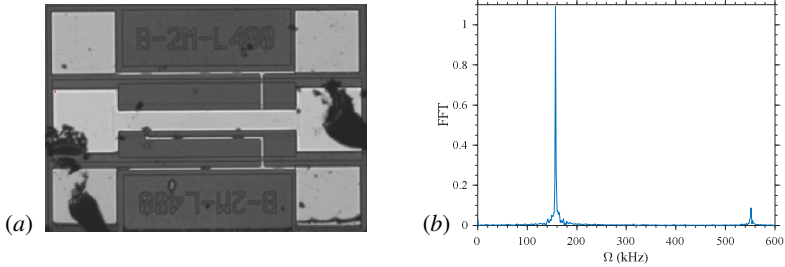


Fig. 1. (a) Optical image of the fabricated MEMS device. (b) FFT spectrum of the device experimental response at the internal resonance in the impacting dynamics.

Constantly referring to the experimental data, numerical simulations are developed. The impact with the substrate is modelled as a nonlinear foundation of springs and dampers. A two degrees of freedom Galerkin reduced-order model is derived accounting for both the first and the third mode dynamics, where the electric force term is integrated numerically. The main aspects induced by the impacts are analysed. The internal resonance activated along this range visibly alters the device response, which occurs for a wide operational range. Close is the correspondence of the theoretical simulations with the experimental data.

3. Concluding Remarks

The impacting dynamics occurring in the experimental data of a MEMS device are analysed. Not only the lengthening of the range of existence of the resonant branch is observed, but also the activation along this interval of an internal resonance is detected. We emphasize the relevance of these results for the design stage.

Acknowledgment: This work has been developed during the visit of Laura Ruzziconi to King Abdullah University of Science and Technology (KAUST), Saudi Arabia; the kind hospitality is gratefully acknowledged. Nizar Jaber acknowledges support of King Fahd University of Petroleum and Minerals. This work is supported through KAUST Funds.

References

- [1] YOUNIS MI: *MEMS Linear and Nonlinear Statics and Dynamics*. Springer: New York, 2011.
- [2] RUZZICONI L, LENCI S, YOUNIS MI: Interpreting and predicting experimental responses of micro- and nano-devices via dynamical integrity. In: LENCI S, REGA G (ED.) *Global Nonlinear Dynamics for Engineering Design and System Safety*, 113-166. Springer: Cham, 2019.
- [3] HAJAJ AZ, JABER N, ILYAS S, ALFOSAIL FK, YOUNIS MI: Linear and nonlinear dynamics of micro and nano-resonators: Review of recent advances. *Int. J. Non-Linear Mech.* 2020, **119**:103328.
- [4] RUZZICONI L, JABER N, KOSURU L, BELLAREDDY ML, YOUNIS MI: Two-to-one internal resonance in the higher-order modes of a MEMS beam: Experimental investigation and theoretical analysis via local stability theory. *Int. J. Non-Linear Mech.* 2021, **129**:103664.

Nonlinear Dynamics of Forced Oscillator Subjected to a Magnetic Interaction

SERGIY SKURATIVSKYI¹, GRZEGORZ KUDRA^{2A*}, KRZYSZTOF WITKOWSKI^{2B}, GRZEGORZ WASILEWSKI^{2C}, JAN AWREJCIEWICZ^{2D}

1. Subbotin Institute of Geophysics NAS of Ukraine, Kyiv, Ukraine [0000-0003-4944-2646]
 2. Lodz University of Technology, Lodz, Poland ^a[0000-0003-0209-4664], ^b[0000-0003-1214-0708] ^c[0000-0002-5549-2976], ^d[0000-0003-0387-921X]
- * Presenting Author

Abstract: It is considered the system composed of a cart moving along a linear rolling bearing with harmonic excitation produced by a stepper motor with an unbalanced disk. The magnetic field is generated by a pair of non-point neodymium magnets, one of which is mounted on the cart, whereas another one is fixed on the guide out of the axis of oscillations. The mathematical model for the cart dynamics is derived where the scaled point dipoles approximation of magnetic interaction is used. The numerical and bifurcation analysis of the model presented is carried out and compared to the experimental results.

Keywords: magnetic pendulum, forced oscillations, bifurcations.

1. Introduction

In contrast to the dynamics of linear system, the behaviour of nonlinear systems are much more diverse and complex [1]. It depends on the peculiarities of system's construction, regimes of its operation, and many other reasons. Therefore, the nonlinear systems are the permanent source of new studies and inventions. This work deals with the relatively simple mechanical model, but the incorporation of nonlinear magnetic interaction leads us to the statement of new problems in the field of nonlinear dynamics. Thus, we continue the studies of the system presented in [2] and we develop the physically motivated description for the magnetic interactions produced by non-point magnets.

2. Results and Discussion

The experimental stand (Fig.1a) we treat consists of trolley moving along a linear rolling bearing with periodic forcing realized by the use of rotating unbalanced disk driven by a stepper motor. The stiffness is composed of linear elasticity generated by linear mechanical spring and nonlinear stiffness produced by a pair of repulsive neodymium magnets of axes perpendicular to the direction of system motion. The position of the system is measured by the use of Hall sensors.

The mathematical description of the physical model (Fig. 1b) of the experimental stand (Fig. 1a) reads as follows :

$$m \ddot{x} + F_R(\dot{x}, x) + F_S(x) = m_0 e \omega^2 \sin \omega t, \quad (1)$$

where $F_R(\dot{x}, x)$ is a resistance force; $F_S(x)$ is a restoring force. When the magnets are absent, the resistance force incorporates the viscous force $c\dot{x}$ and dry friction $T \operatorname{sign} \dot{x}$, whereas $F_S = kx$. Adding the magnets causes the appearance of magnetic repulsive force \vec{F}_M which makes the contribution

to F_S and F_R . To estimate \vec{F}_M , we adopt the point dipoles approximation. According to this approach, the repulsive magnetic force $\vec{F}_M = -\nabla(\vec{n} \cdot \vec{B})$, where $\vec{B} = \frac{F_0}{n^2|\vec{r}|^3}(3(\vec{n} \cdot \hat{r})\hat{r} - \vec{n})$, the magnetic moment $\vec{n} = (0, n)$, $\vec{r} = (x, z)$, $\hat{r} = \vec{r}/|\vec{r}|$. Thus, we get $\vec{F}_M = (F_M^x, F_M^z) = F_0 \left(\frac{3x(4z^2 - x^2)}{(x^2 + z^2)^{7/2}}, \frac{3z(2z^2 - 9x^2)}{(x^2 + z^2)^{7/2}} \right)$. The components of the vector \vec{F}_M provide the horizontal and orthogonal force projections which are incorporated into the restoring and friction forces: $F_S(x) = kx - F_M^x$ and $F_R = c\dot{x} + T \text{sign } \dot{x} + \mu \cdot \text{sign} \dot{x} \cdot F_M^z$. To validate the model (1), the results of experiments [2], carried out at fixed $z = 0.01\text{m}$ and varying frequency ω , are used. It turned out, to describe the cart's dynamic correctly, the expression for the magnetic force should be scaled, i.e. in the equation (1) $\vec{F}_M \rightarrow \alpha \vec{F}_M(x/\beta, z)$, where $\alpha = 2.5$, $\beta = 3$, $\mu = 0.001$, $F_0 = 1.4695 \cdot 10^{-8} \text{ N}\cdot\text{m}^4$, $c = 12.9906 \text{ N}\cdot\text{s/m}$, $k = 929.333 \text{ N/m}$, $T = 1.2267 \text{ N}$, $m_0 e = 0.25152 \text{ kg}\cdot\text{m}$, $m = 6.73766 \text{ kg}$ [2]. The corresponding numerical bifurcation diagram for the equation (1) is presented in Fig.1c, which is in very good agreement with the experimental bifurcation diagram (see [2]). From the diagram it follows that equation (1) possesses the coexisting attractors (color points). These attractors undergo only one period doubling bifurcation at $\omega < 12.54$, whereas at $\omega > 18.91$ their bifurcations are described by the period-doubling cascade. Moreover, the jump phenomenon occurs at $\omega \approx 18.91$.

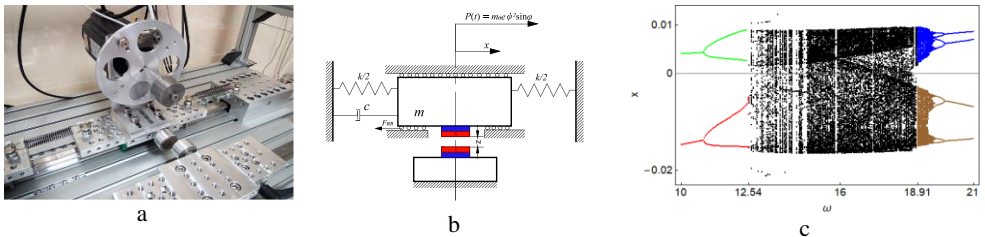


Fig.1. The experimental stand (a) of the oscillator, its physical model (b) and the numerical bifurcation diagram (c) for the equation (1).

3. Concluding Remarks

Thus, the present research deals with the forced oscillator taking into account the influence exerted by field of permanent magnets. To develop the equation of motion for this model, the magnetic interaction is described on the base of the point dipoles approximation. During model validation it is derived the scaled point dipoles approximation describing the experimentally observed regimes in a wide range of frequency interval.

Acknowledgment: This work has been supported by the Polish National Science Centre, Poland under the grant OPUS 14 No. 2017/27/B/ST8/01330.

References

- [1] WITKOWSKI K., KUDRA G., SKURATIVSKIY S., WASILEWSKI G., AWREJCWICZ J: Modeling and dynamics analysis of a forced two-degree-of-freedom mechanical oscillator with magnetic springs. *Mechanical Systems and Signal Processing* 2021, **148**:107138.
- [2] WITKOWSKI K., KUDRA G., WASILEWSKI G., AWREJCWICZ J: Mathematical modelling, numerical and experimental analysis of one-degree-of-freedom oscillator with Duffing-type stiffness Submitted to *International Journal of Non-Linear Mechanics* 2021.

Bifurcation analysis of nonlinear piezoelectric vibration energy harvester

PETR SOSNA^{1*}, ZDENEK HADAS²

1. Faculty of Mechanical Engineering, Brno University of Technology [0000-0001-6187-6151]
2. Faculty of Mechanical Engineering, Brno University of Technology [0000-0002-9097-1550]

* Presenting Author

Abstract: This paper deals with an analysis of nonlinear piezoelectric vibration energy harvesting system, which is capable to generate electrical power from mechanical vibrations. A kinetic energy of vibration is transferred into useful electricity by a strain of piezoelectric layers on an oscillated cantilever. A nonlinear stiffness is created by additional magnets with separation distance. The presented work is concerned with an analysis of this nonlinear magneto-elastic system of piezoelectric vibration energy harvester by use of bifurcation diagrams, where magnet separation distance acts as a control parameter. A response of this energy harvester and harvested power for different separation of magnets are presented.

Keywords: bifurcation diagram, piezoelectric cantilever, magneto-elastic system, bistable, chaotic

1. Introduction

Stiffness nonlinearities are a hot topic in vibration energy harvesting technologies [1]. It could be a promising source of energy for wireless sensors and IoT applications. The presented system is analysed in form of a bimorph cantilever consisting of a fixed-free steel substrate with two piezoelectric patches [2]. The magneto-elastic interaction of two permanent magnets, one is a fixed tip mass and the other one is stationary, provides nonlinearity of the stiffness and a separation of both magnets is analysed.

2. Results and Discussion

Such a nonlinear system can behave in monostable or bistable regimes, depending on the separation gap between the magnets, see Fig. 1. Possible solutions include monostable oscillations, bistable in-well or cross-well oscillations, n-periodic oscillations, or chaotic behaviour.

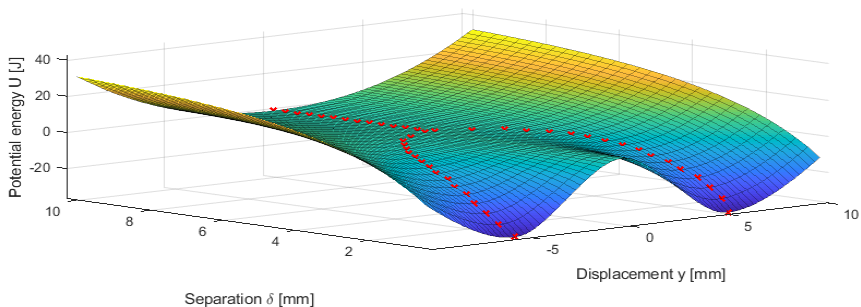


Fig. 1. Potential energy of the nonlinear oscillator as a function of magnet separation.

The complex energy harvesting system is analysed as single-degree-of-freedom system and its behaviour is governed by following coupled differential equations:

$$m\ddot{y}(t) + b\dot{y}(t) + ky(t) + F_{mag}(y(t)) + \theta V(t) = D\dot{z}\sin(\omega t)$$

$$\dot{V}(t) = \frac{1}{C_p} \left(\theta \dot{y}(t) - \frac{V(t)}{R} \right)$$

To study the influence of magnet separation distance on the system’s dynamics the series of bifurcation diagrams were created, see Fig. 2. This bifurcation analysis is accompanied by attractor identification process, that analyses each time evolution based on Poincare points and colour-codes the solutions in said bifurcation diagrams. These diagrams show possible solutions, their periodicity, and generated power as well as a comparison to a linear system with no magnets. Many of these were created for various forcing conditions.

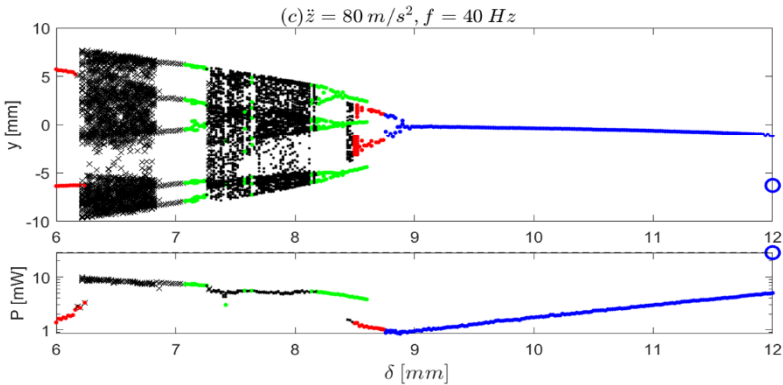


Fig. 2. Bifurcation diagram with magnet separation as a control parameter.

3. Conclusions

The behaviour and harvested power of the nonlinear coupled electromechanical system was analysed via bifurcation diagrams that differ in forcing conditions. The results can be used to find the magnet separation distance that generates the most energy for each pair of forcing conditions.

Acknowledgment:

This presented research and development was supported by the Czech Science Foundation project GA19-17457S „Manufacturing and analysis of flexible piezoelectric layers for smart engineering“.

References

- [1] RUBEŠ O, MACHŮ Z, ŠEVEČEK O, HADAŠ Z: Crack protective layered architecture of lead-free piezoelectric energy harvester in bistable configuration. *Sensors(Switzerland)* 2020, **20**(20):1-18.
- [2] STANTON S.C, MCGEHEE C.C, MANN B.P: Nonlinear dynamics for broadband energy harvesting: Investigation of a bistable piezoelectric inertial generator. *Physica D: Nonlinear Phenomena* 2010, **239**(10):640-653.

Increase in current stresses of the boost converter due to border collision bifurcation

ZELJKO STOJANOVIC^{1*}, DENIS PELIN²

1. Zagreb University of Applied Sciences, Zagreb, Croatia [0000-0002-1535-7665]

2. University of Osijek, Osijek, Croatia [0000-0002-9255-1541]

* Presenting Author

Abstract: Border collision bifurcation in a DC-DC boost converter is under investigation. Mathematical model of the converter is proposed and exact simulation is carried out. The simulation algorithm is based on Runge-Kutta fourth-order method. Bifurcation diagram of the inductor current versus input voltage is simulated. By decrease of the input voltage, the converter undergoes Neimark-Sacker bifurcation and border collision bifurcation. As a consequence of border collision bifurcation the peak value of the inductor current jumps to a considerably higher value. The same phenomena is reproduced experimentally. The inductor currents before and after border collision bifurcation obtained by the simulation and by the measurement qualitatively match. The increase of inductor current may cause the failure or shortening of the service life of the converter switches. By proper change of the converter parameters border collision bifurcation can be avoided. In order to avoid border collision bifurcation the converter load capacitance and feedback proportional gain are adjusted. In both cases the simulation results and the measurement qualitatively match.

Keywords: border collision bifurcation, boost converter, current stresses, Neimark-Sacker bifurcation

1. Introduction

A DC-DC boost converter is a time-varying nonlinear circuit of a second order or a higher. As such, it is prone to various bifurcations [1-4]. Border collision bifurcation [2-4] can be especially undesirable. It can cause large increase of the converter currents and thus lead to converter failure. Thorough researches on this topic has not yet done. In this article simulation and measurement of increase of the converter currents due to border collision bifurcation are presented. Avoidance of bifurcation by changing the converter parameters is also shown.

2. Results and Discussion

A DC-DC boost converter, Fig. 1 is under consideration. Bifurcation diagram of inductor current versus input voltage is shown in Fig.2. At input voltage $E = 12$ V the converter operates in period-one steady-state determined by the PWM-clock frequency. By decrease of input voltage to $E = 11,4$ V the converter undergoes the first Neimark-Sacker bifurcation (NS). By further decrease of input voltage the converter undergoes series of Neimark-Sacker bifurcations [1]. At input voltage $E = 9,4$ V the converter undergoes the first border collision bifurcation (BCB). This lead to the significant increase of inductor current, Fig. 3 and Fig. 4 and consequently increase of switch currents.

¹ Zeljko Stojanovic, Konavoska 2, 10000 Zagreb, Croatia, zeljko.stojanovic@tvz.hr

² Denis Pelin, Kneza Trpimira 2B, 31000 Osijek, Croatia, denis.pelin@ferit.hr

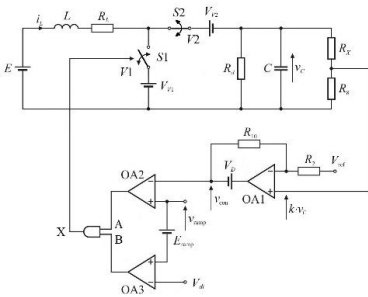


Fig. 1. Schematic circuit diagram of the boost converter

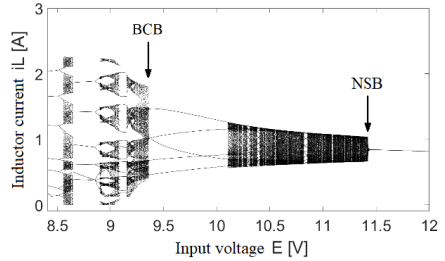


Fig. 2. Bifurcation diagram obtained by decrease of the input voltage

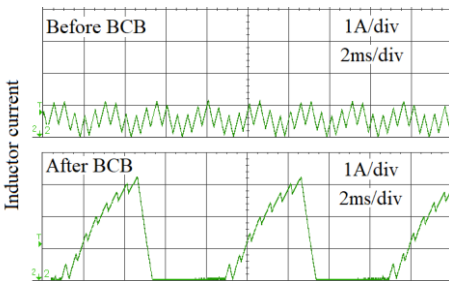


Fig. 3. Inductor current obtained by measurement. Up – Inductor current before the bifurcation. Down – Inductor current after the bifurcation.

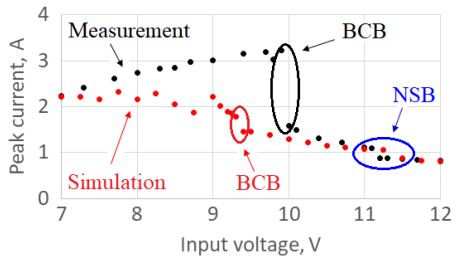


Fig. 4. Peak inductor current versus input voltage obtained by simulation and measurement.

By change of the converter load capacitance and feedback proportional gain an area of period-one steady-state can be broadened and the border collision bifurcation can be avoided.

3. Concluding Remarks

Undesirable large increase of the boost converter current caused by border collision bifurcation is presented. Simulation results corresponds to measurement results. Avoidance of bifurcation by changing the converter parameters is also shown.

References

- [1] EL AROUDI A., BENADERO L., TORIBIO E., OLIVAR G., Hopf bifurcation and chaos from torus breakdown in a PWM voltage-controlled DC-DC boost converter, *IEEE Transactions on Circuits and Systems I: Fundamental Theory and Applications* 1999, **46**(11):1374-1382
- [2] ZHUSUBALIYEV Z. T., MOSEKILDE E., MAITY S., MOHANAN S., BANERJEE S., Border-collision route to quasi-periodicity: Numerical investigation and experimental confirmation, *Chaos* 2006, **16**(2):023122.
- [3] MAITY S., TRIPATHY D., BHATTACHARYA T.K., BANERJEE S., Bifurcation Analysis of PWM-1 Voltage-Mode-Controlled Buck Converter Using the Exact Discrete Model, *IEEE Transactions on Circuits and Systems I: Regular Papers* 2007, **54**(5):1120-1130
- [4] PIKULINS D., TJUKOV S., EIDAKS J. Effects of Control Non-idealities on the Nonlinear Dynamics of Switching DC-DC Converters. In: STAVRINIDES S., OZER M. (ED.) *Chaos and Complex Systems*. Springer: 2020.

Chaos in Thirring Model

EREN TOSYALI^{1*}, FATMA AYDOGMUS²

1. Istanbul Bilgi University, Vocational School of Health Services, [0000-0001-9118-851X]

2. Istanbul University, Faculty of Science, Physics Department [0000-0003-1434-2143]

* Presenting Author

Abstract: Thirring model is a two-dimensional, conformal invariant spinor model that plays an important role as a test model in the Quantum Field Theory. Thirring instantons were found using the method of spontaneously broken conformal symmetry in the Thirring nonlinear spinor field equation. In this study, we investigate the dynamic of Thirring instantons under forcing and damping by constructing Poincare sections. Thirring instantons exhibit regular and chaotic behaviours depending on system parameters.

Keywords: Dynamic, Instanton, Thirring, Chaos.

1. Introduction

Instantons, as a special type of solitons that propagate without losing their shape and speed properties and can maintain their unique properties during any collision, are solutions with zero energy and finite action with space-time expansion [1]. Instantons, which play an important role in theoretical and mathematical physics and correspond to the vacuum state, have space-time expansion. Spinor-type instanton solutions were found by the spontaneously broken conformal symmetry in nonlinear Thirring field equation system [2-3]. Thirring nonlinear differential equation system is given as:

$$2 \frac{dF(u)}{du} + \frac{1}{2} F(u) - \alpha AB(F(u)^2 + G(u)^2)G(u) = 0 \quad (1)$$

$$2 \frac{dG(u)}{du} - \frac{1}{2} G(u) + \alpha AB(F(u)^2 + G(u)^2)F(u) = 0 \quad (2)$$

We present Thirring field equation system with forcing and damping:

$$2 \frac{dF(u)}{du} + \frac{1}{2} F(u) - \beta(F(u)^2 + G(u)^2)G(u) = 0 \quad (3)$$

$$2 \frac{dG(u)}{du} - \frac{1}{2} G(u) + \beta(F(u)^2 + G(u)^2)F(u) - A_T \cos(w_T H(u)) + \gamma G(u) = 0 \quad (4)$$

$$\frac{dH(u)}{du} = 0 \quad (5)$$

2. Results and Discussion

In our previous works, the role of the coupling constant in the evolution of Thirring instantons in phase space has been studied via Heisenberg ansatz [4-5]. Thirring instantons have a Duffing oscillator type characterization without forcing and damping as stated in the Figure 1.

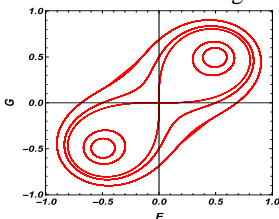


Fig. 1. Duffing oscillator type characterization of Thirring Instantons

In this paper, we investigate the dynamic of nonlinear Thirring instantons by changing the forcing and damping parameters (g , A and ω) to get more information on spinor type Thirring instantons. System parameters for phase space and Poincare sections are taken as $\omega = 0.57$, $\gamma = 0.05$ and initial conditions are $(F(0), G(0) = (0.158, 0.55))$. The differential equations solved with step size 0.1 and length 6000.

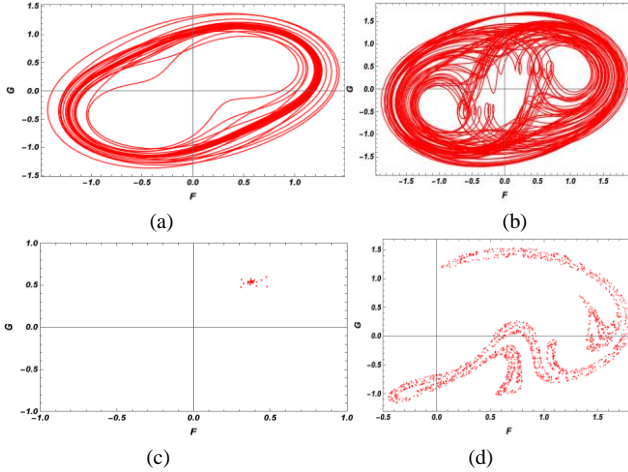


Fig. 2. Phase space diagrams of forced and damped Thirring instantons at $\omega = 0.57$, (a) $A = 0.25$, (b) $A = 1.2$ and Poincare sections (c) $A = 0.25$, (d) $A = 1.2$.

3. Concluding Remarks

The regular and chaotic instanton solutions of forced and damped Thirring model are studied in phase space. The obtained phase space diagrams and the Poincaré sections show that Thirring instantons lost their stability in phase space under forced and damped terms. Forcing and damping terms destroy the regularity and forms a chaotic layer.

Acknowledgment: This work was supported by the Scientific Research Projects Coordination Unit of Istanbul University; Project no: FBA-2018-28954.

References

- [1] DUNAJSKI M., *Solitons, Instantons and Twistors*, Oxford University Press, 2009.
- [2] THIRRING W.E., *A Soluble Relativistic Field Theory*, *Annal Physics*, Vol.3,91-112, 1958.
- [3] AKDENİZ K. G. and SMAİLAGİC A., *Classical Solitons for Fermionic Models*, *II Nuova Cimento*, vol. 51A, No.3, 345-357, 1979.
- [4] AYDOĞMUS F, THE BEHAVIOURS OF SPINOR TYPE INSTANTON ATTRACTORS IN PHASE SPACE, *Istanbul University, Institute of Science*, 2012.
- [5] AYDOĞMUS F, TOSYALI E., COMMON BEHAVIOURS OF SPINOR-TYPE INSTANTONS IN 2D THIRRING AND 4D GURSEY FERMIONIC MODELS, *Advances in High Energy Physics*, 2014.

Chaos and Bifurcations in a Nonlinear Dynamics of Chain of the Backward-Wave Tubes: Numerical Analysis

ANDREY V TSUDIK¹, OLEG V DUBROVSKY^{1*}, VALENTIN B. TERNOVSKY²,
VASILY V BUYADZHI¹ AND IGOR I. BILAN¹

1. Odessa State Environmental University, Mathematics Depr., L'vovskaya str. 15, 65009, Odessa

2. National University "Odessa Maritime Academy", Didrikhson str. 8, 65001, Odessa

* Presenting Author

Abstract: The paper is devoted to studying dynamical characteristics of non-linear processes in the chain of non-relativistic and relativistic backward-wave tubes (BWT) and modeling parameters for the corresponding chaotic time series, which are the solutions of the BWT integral-differential dynamical equations. The computational chaos-geometric approach includes a combined set of non-linear analysis and chaos theory methods such as an autocorrelation function method, correlation integral approach, average mutual information, surrogate data, false nearest neighbours algorithms, the Lyapunov's exponents and Kolmogorov entropy analysis, spectral methods and nonlinear prediction (predicted trajectories, neural network etc) algorithms. There are computed the dynamic and topological invariants in auto-modulation/chaotic regimes. The bifurcation diagrams in the planes of different governing parameters are constructed.

Keywords: chain of backward-wave tubes, chaos, bifurcations, attractors

1. Introduction.

It is well known that the back-ward tube (BWT) is an electronic device for generating electromagnetic vibrations in the super high frequencies range. The intensive theoretical studies (e.g. [1-3]) have been performed for were of dynamics of a non-relativistic BWT, in particular, phase portraits, statistical quantifiers for a weak chaos arising via period-doubling cascade of self-modulation and the same characteristics of two non-relativistic backward-wave tubes. The differential equations of non-stationary nonlinear theory for the O-type BWT without account of the spatial charge, relativistic effects, energy losses etc have been solved. It has been shown that the finite-dimension strange attractor is responsible for chaotic regimes in the BWT.

In our paper the advanced results of studying dynamical characteristics of non-linear processes in the chain of non-relativistic and relativistic BWTs are presented. It has been performed a detailed analysis and modeling the parameters of the corresponding chaotic time series for the characteristic amplitudes, which are the solutions of the BWT integral-differential dynamical equations. The computational chaos-geometric approach includes a combined set of non-linear analysis and chaos theory methods such as an autocorrelation function method, correlation integral approach, average mutual information, surrogate data, false nearest neighbours algorithms, the Lyapunov's exponents and Kolmogorov entropy analysis, spectral methods and nonlinear prediction (predicted trajectories, neural network etc) algorithms (in versions [3-5]). A dynamics of the chain of two backward-wave tubes is in details considered. There are computed the dynamic and topological invariants in auto-modulation/chaotic regimes.

2. Dynamics of backward-wave tubes chain: Results and Discussion

A chain of two relativistic BWTs can be described by the standard master system of evolutionary differential equation as follows:

$$\begin{aligned} \partial^2 \theta_{1,2} / \partial \xi^2 &= -(1 + \nu \partial \theta / \partial \xi)^{3/2} \operatorname{Re} \left\{ \frac{1}{2} L_{1,2} [\delta(\xi) + \delta(\xi - L) F_{1,2} e^{i\theta_{1,2}}] \right\}, \\ \partial F_{1,2} / \partial \tau - \partial F_{1,2} / \partial \xi &= - \left[\frac{1}{\pi} \int_0^{2\pi} e^{-i\theta_{1,2}} d\theta_0 \right] \frac{1}{2} L_{1,2} [\delta(\xi) + \delta(\xi - L_{1,2})]. \end{aligned} \tag{1}$$

where $\theta_{1,2}$ are the phases of electron relative to the wave, θ_0 - the initial phase, $F_{1,2}$ are the dimensionless slowly varying amplitudes of fields $\{ E(x, t) = \operatorname{Re}[E(x, t) \exp(i\omega_0 t - i\beta_0 x)] \}$, $\xi = \beta_0 Cx$ and τ are the dimensionless coordinate and time, respectively; parameter $L = \beta_0 l C = 2\pi CN$ is the dimensionless length of the interaction space, l is a length of the system, N is a number of slow waves, covering over the length of system, $C = \sqrt[3]{I_0 K_0 / (4U)}$ is the known Pierce parameter, I_0 is a current of beam, U is an accelerated voltage, K_0 is a resistance of link of the slowing system, ν is the known relativistic parameter, C - modified gain parameter. The first equation in the system (1) represent equation of motion of electrons in the field of the electromagnetic wave and the second equation is the non-stationary equations of excitation of a decelerating structure by a current of the slowly varying amplitude. The subscripts indicate the item number of the chain. The dynamics of the partial generator depends on a single bifurcation parameter $L = 2\pi CN$. Two different modes of operation are considered. In the first case it is supposed that the BWTs are operating in regime of the periodical automodulation. The values of the L parameter are: $L_1 = 4.05$, $L_2 = 4.55$. In the first case one deals with the Feigenbaum type scenario. In the second case there is the transition “chaos-order” through intermittency that is confirmed by the corresponding chaos-geometric numerical analysis data.

3. Concluding Remarks

Study of the dynamic characteristics of non-linear processes in the chain of non-relativistic and relativistic BWTs is performed and modeling the dynamic characteristics for the corresponding chaotic time series is carried out. The new data on the dynamic and topological invariants of the BWT chain dynamics in auto-modulation/chaotic regimes are obtained. The bifurcation diagrams in the planes of different governing parameters are constructed.

References

- [1] KUZNETSOV S, TRUBETSKOV D: Chaos and hyperchaos in a backward-wave oscillator *Radiophys. and Quant. Electr.* 2004, **47**:131-138.
- [2] RYSKIN N AND TITOV V: The transition to the development of chaos in a chain of two unidirectionally-coupled backward-wave tubes. *Journ. Techn. Phys.* 2003, **73**:90-94.
- [3] TERNOVSKY V, GLUSHKOV A, TERNOVSKY E AND TSUDIK A: Dynamics of non-linear processes in a backward-wave tubes chain: Chaos and strange attractors. In: AWREJCWICZ J, KAZMIERCZAK M AND OLEJNIK P (Eds.) *Applicable Solutions in Non-Linear Dynamical Systems*. Lodz, 2019:491-498.
- [4] GLUSHKOV AV: *Methods of a Chaos Theory*. Astroprint: Odessa, 2012.
- [5] GLUSHKOV A, TSUDIK A, TERNOVSKY V, MYKHAILOV A, BUYADZHI V: Deterministic chaos, bifurcations and strange attractors in nonlinear dynamics of relativistic backward-wave tube. In: AWREJCWICZ J (Ed.) *Perspectives in Dynamical Systems II: Mathematical and Numerical Approaches*. Series: *Springer Proceedings in Mathematics & Statistics*. 2021, **363**:Ch.12.

-CON-

**CONTROL IN DYNAMICAL
SYSTEMS**

Damping of Vibrations of an Elastic Beam by Means of an Active Dynamic Damper in the Presence of Disturbances

IGOR ANANIEVSKI

Laboratory of Control of Mechanical Systems
Ishlinsky Institute for Problems in Mechanics RAS, Moscow, Russia
Prospekt Vernadskogo, 101-1, Moscow 119526 Russia [ORCID 0000-0003-3907-5715]
anan@ipmnet.ru

Abstract: We consider the problem of dampening the load, attached at the end of the elastic beam, by means of an active dynamical damper with a mass moving along the guide. The system is controlled by the force of the interaction between the damper and the load. A bounded feedback control is proposed which brings the system to a prescribed equilibrium state in a finite time even in the presence of disturbances, for example, the forces of dry friction.

Keywords: linear mechanical system, control synthesis, disturbances, stabilization in a finite time

1. Introduction

We consider the problem of damping oscillations of a load attached to the end of an elastic beam, using an active a dynamic damper with a translationally moving mass. The control variable is the force of interaction between the damper and the load. Systems of this type are used, for example, in a spacecraft, where the platform P (Fig. 1) with measuring devices is placed, using a long rod 1, at a considerable distance from the body of the spacecraft SC. To damp the lateral oscillations of the rod a controlled damper located on the platform itself, can be used. The damper consists of a guide 2 perpendicular to the axis of the rod, and a movable mass 3 driven along the guide by an electric motor.

Since the damper guide is limited in size and due to the restricted possibilities of the drive, it is natural to imposed constraints on the displacement of the mass relative to the platform and on the control force. In [1], a feedforward control is constructed which meets such constraints and drives the system to a prescribed state in a finite time. The Kalman approach is used for designing the control as a linear combination of the basis solutions of the uncontrolled system.

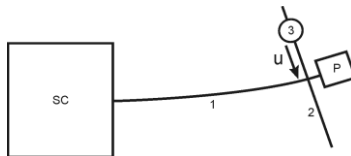


Fig. 1.

In the present paper, keeping the constraints mentioned, we assume also that a friction force with unknown and variable parameters acts between the mass and the guide, preventing accurate positioning of the platform. The presence of the friction force as an unknown disturbance makes us construct a feedback (not feedforward) control.

2. Control problem and control algorithm

Under certain simplifying assumptions, in dimensionless variables the equations of motion can be written in the form

$$\dot{z} = \begin{pmatrix} 0 & 1 & 0 & 0 \\ -1 & 0 & 0 & 0 \\ 0 & -2 & 0 & 0 \\ 0 & 0 & -3 & 0 \end{pmatrix} z + \begin{pmatrix} 1 \\ 0 \\ 0 \\ 0 \end{pmatrix} (u + v). \tag{1}$$

The following constraints are imposed on the control force u , the disturbance v , and the phase variables z :

$$|u| \leq U, \quad |v| \leq \rho U, \quad U > 0, \quad 0 \leq \rho < 1, \quad |p^T z| \leq 1 \tag{2}$$

(the constant vector p depends on mass-inertial and technical characteristics of the system).

The problem is to construct a feedback control $u(z)$ that satisfies constraints (2) and brings system (1) to the coordinate origin for sufficiently small ρ .

The approach used is based on [2]. We introduce the matrix

$$Q = \begin{pmatrix} 20 & -180 & 420 & -280 \\ -180 & 2220 & -5880 & 4200 \\ 420 & -5880 & 16800 & -12600 \\ -280 & 4200 & -12600 & 9800 \end{pmatrix}$$

and define the function $T(z)$ by the equation

$$(Q\delta(T)z, \delta(T)z) = U^2/5,$$

where $\delta(T) = \text{diag}\{T^{-1}, T^{-2}, T^{-3}, T^{-4}\}$. The control function

$$u(z) = -\frac{10}{T(z)} z_1 + \frac{90}{T^2(z)} z_2 - \frac{210}{T^3(z)} z_3 + \frac{140}{T^4(z)} z_4 - z_2$$

solves the above problem.

3. Concluding Remark

The proposed approach can be used to control the dynamics of various technical objects, in particular, precise positioning systems.

Acknowledgment: The study was supported by the Government program (contract AAAA-A20-120011690138-6) and by RFBR (Grant 21-51-12004).

References

- [1] CHERNOUSKO F.L., ANANIEVSKI I.M., RESHMIN S.A.: *Control of Nonlinear Dynamical Systems. Methods and Applications*. Springer: Berlin, 2008.
- [2] OVSEEVICH A: A local feedback control bringing a linear system to equilibrium. *J. Optim. Theory Appl.* 2015, **165**, 532–544.

Control of Micogrid Synchronization Based on Feedback Control and Optimzation Techniques

DAVID ANGULO-GARCÍA^{1*}, FABIOLA ANGULO²

1. Universidad de Cartagena. Instituto de Matemáticas Aplicadas. Grupo de Modelado Computacional Dinámica y Complejidad de Sistemas. Cartagena de Indias, Bolívar - Colombia. [0000-0003-2231-9904]
2. Universidad Nacional de Colombia - Sede Manizales. Facultad de Ingeniería y Arquitectura. Manizales, Caldas - Colombia. [0000-0002-4669-7777]

* Presenting Author; dangulog@unicartagena.edu.co

Abstract: In this paper, we propose a secondary feedback control of a droop-controlled smart grid, modelled via the first order Kuramoto model. We show that we can improve the transient evolution of the system by applying a harmonic secondary control on each oscillator which only makes use of the error between the node's state and the desired equilibrium state. We show in a 2 dimensional coupled oscillator model that, while the effect of this control action is to move the spectrum of the eigenvalues, the topology of the system imposes restrictions over the admissible eigenvalues that need to be preserved in the controlled system. To overcome this, we find the set of gains that fulfills the restriction over one eigenvalue while allowing to move the second one to a desired value, achieving improved transient dynamics in terms of settling times.

Keywords: Synchronization, Kuramoto oscillators, microgrids, feedback control

1. Introduction

A droop-controlled smart grid can be represented as a First Order Kuramoto model [1,2]

$$\dot{\theta}_i(t) = \omega_i + K \sum_j^N A_{ij} \sin(\theta_j(t) - \theta_i(t)) \quad (1)$$

Power sharing conditions require $\sum_i \omega_i = 0$. This guarantees that synchronization is reduced to the study of stability of the equilibrium θ^* . An approximation of the equilibrium point as: $\theta^* = \frac{L^+ \omega}{K}$. In this equation, L is the Laplacian matrix and L^+ denotes the Moore-Penrose pseudoinverse. Linearizing Eq. (1) around the equilibrium leads to the Jacobian matrix:

$$J_{ij} = \begin{cases} -K \sum_{j \neq i} A_{ij} \cos(\theta_j^* - \theta_i^*) & \text{if } i = j \\ KA_{ij} \cos(\theta_j^* - \theta_i^*) & \text{otherwise} \end{cases} \quad (2)$$

Following [3], a secondary feedback control can be applied in the following form:

$$\dot{\theta}_i(t) = \omega_i + K \sum_j^N A_{ij} \sin(\theta_j(t) - \theta_i(t)) + F_i \sin(\theta_i^* - \theta_i).$$

Here, F_i acts as the gain of the controller for the i -th oscillator and modifies the diagonal entries of the Jacobian matrix, as $J_{ii} = -K \sum_{j \neq i} A_{ij} \cos(\theta_j^* - \theta_i^*) - F_i$. We propose the application of this type of feedback control, to modify the dynamics of the phase oscillator model, by placing the eigenvalues of the

system according to a desired design criteria, taking into account that one eigenvalue must remain on the origin, in order to preserve the rotational degeneracy of phase oscillator. With these ideas in mind, the solutions of the gains in terms of the desired controlled eigenvalue $\lambda_2^{(c)}$ are:

$$F_{1,2} = -\frac{1}{2} \left(\lambda_2^{(c)} + \lambda_2^{(u)} \pm \sqrt{-\lambda_2^{(c)} - \lambda_2^{(u)}} \right) \tag{3}$$

In the above equation the superscripts (c) and (u) stand for controlled or uncontrolled eigenvalues. Recall that, due to the restrictions $\lambda_1^{(c)}$ is strictly equal to zero.

2. Results and discussion

Figure 1(a) shows the solutions of F_i as a function of the desired eigenvalue $\lambda_2^{(c)}$. It is important to notice that $F_1 = F_2 = 0$ corresponds to the uncontrolled system, therefore the controlled eigenvalue is always smaller than the uncontrolled one. Fig 1(b) shows the improved dynamics of the controlled system (red) compared with the uncontrolled one (black). This can be seen with the smaller settling time of the order parameter, quantifying the degree of synchronization between the oscillators (top panel). It is also possible to observe that the system reaches the same steady value as the uncontrolled case as expected, since the control does not vary θ^* .

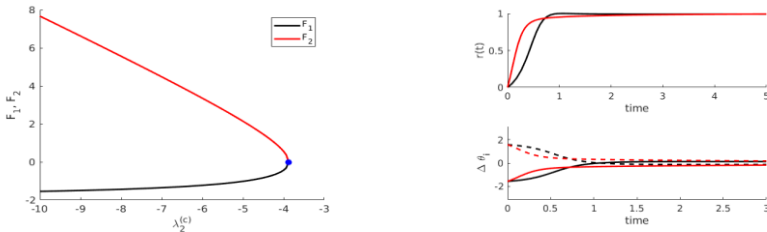


Fig. 1. Left: Gains as a function of the desired eigenvalue given by Eq. (3) for the two oscillator system. For this graphic, $\omega_1 = 1/2$, $\omega_2 = -1/2$, and $K = 2$. **Right:** Dynamics of the controlled system (red) compared with the uncontrolled system (black). **Top:** the order parameter is depicted. **Bottom:** The error between the values of the phases and its steady value.

3. Concluding Remarks

The secondary control loop was successful to improve the performance of the controlled system. The transient response showed a faster dynamics than the uncontrolled one and we obtained an analytical expression to calculate the feedback gains. We propose to extend the algorithm to higher order systems which requires the implementation of optimization routines subject to restrictions. This will be the topic of the extended version of this manuscript.

Acknowledgments: D. Angulo-García thanks Vicerrectoría de Investigaciones, Project 004-2019, Fabiola Angulo thanks to Universidad Nacional de Colombia, Manizales, Project 46277 - Vicerrectoría de Investigación.

References

- [1] ACEBRON J.A, BONILLA L.L, PEREZ C.J, RITORT F, SPIGLER R. The Kuramoto model: A simple paradigm for synchronization phenomena. *Rev. Mod. Phys* 2005, **77**(1):137
- [2] SKARDAL P.S, ARENAS A. Control of coupled oscillators networks with application to microgrid technologies. *Science Advances* 2015, **1**(7):E1500339.
- [3] SIMPSON-PORCO J.W, DÖRFLER F. AND BULLO F. Synchronization and power sharing for droop-controlled inverters in islanded microgrids. *Automatica* 2013, **49**(9):2603-2611

Hybrid vibration absorber for self-induced vibration mitigation

MARCELL ÁKOS BARTOS^{*1}, GIUSEPPE HABIB

Dept. of Applied Mechanics, Budapest University of Technology and Economics, Budapest, Hungary

* Presenting Author

Abstract: Various active and passive methods for vibration mitigation exist, each presenting its own advantages and drawbacks. The objective of this study is to compare the performance of a hybrid active-passive dynamic vibration absorber and of a purely passive one, with respect to their ability in suppressing self-excited oscillations. The host system considered is a simple linear oscillator with a negative damping, while the actuator of the hybrid absorber generates a force proportional to the acceleration of the system's lumped masses. The presence of a time delay in the feedback loop is also considered. Results illustrate that the two systems have practically identical performance.

Keywords: vibration absorber, time-delayed system, self-induced vibrations

1. Introduction

Self-induced vibrations (SIVs) are vibrations generated by the system's inherent instability, and not by an external forcing. Real life examples of this phenomenon are the friction-induced vibrations, shimmy, and the regenerative chatter [1]. SIVs are generally detrimental in the engineering practice; therefore, several methods for their suppression were developed, encompassing active and passive vibration mitigation tools.

In this study, a hybrid vibration absorber (HVA) [2] is implemented for SIV suppression. The HVA is composed of an active and a passive part. The passive part is essentially a dynamic vibration absorber (DVA), i.e. a secondary mass-spring-damper system attached to the host system. The active part, which consists of an actuator connecting the primary system and the DVA, is controlled through a feedback loop, reading in input the acceleration of the system. The cases of time delay and no time delay in the feedback loop are considered. The main advantage of HVAs compared to DVAs is that they are capable of attenuating vibrations occurring at different frequencies [2]. Our research focuses on investigating the HVA's ability to improve the system's stability, in comparison with a simple, passive, uncontrolled DVA.

2. Methods

The host system considered in this study consists of a linear single degree-of-freedom oscillator possessing a negative damping, which models the system's instability. A HVA is attached to it through a spring, a damper, and an actuator, as illustrated in Fig. 1. After partially nondimensionalizing the equations of motion by transitioning to dimensionless time and introducing further dimensionless parameters, we carried out the stability analysis. For the case without time delay, the Routh-Hurwitz criterion was adopted. Further analytical proof is presented in the paper regarding the evolution of the stable region as the parameter used to represent the unstable feature of the system (ψ)

¹ 1111 Budapest, Műegyetem rkp. 5., Hungary. Email: bartos.marcell24@gmail.com

approaches its critical value (ψ_{cr}), above which the passive DVA is unable to stabilize the system, as it is discussed in [3].

The stability boundaries corresponding to the delayed acceleration feedback control have been determined by implementing the D-subdivision method. In order to decide which regions correspond to a stable behaviour, numerical methods have been applied. We used numerical tools to investigate the HVA's effect on the rate by which, in stable conditions, oscillations decay. The results were validated through numerical simulations.

3. Results

The stability analyses have shown that the stable region shrinks and eventually disappears as ψ approaches ψ_{cr} , regardless of the presence of time delay (Fig. 2). On the other hand, we have found that it is possible to choose the control law parameters so that the implementation of a HVA results in faster settling.

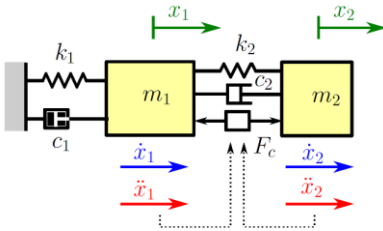


Fig. 1. The mechanical model

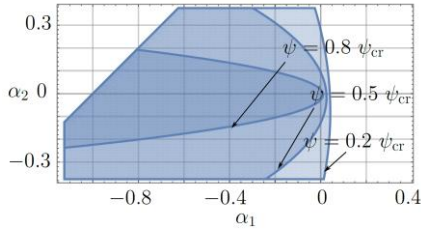


Fig. 2. Evolution of the stable region (without delay)

4. Concluding Remarks

A comparison of the performance of a passive DVA and of a HVA illustrated that the additional active controller, present in the HVA, does not improve stability properties of the system. The introduction of time delay in the feedback loop, often used for enhancing the effectiveness of acceleration based active controllers [4], was also ineffective with respect to improving the system's stability. On the other hand, the HVA, if correctly tuned, provides a faster convergence than a passive DVA.

Acknowledgement: This research was financially supported by the Hungarian National Science Foundation under grant number OTKA 134496.

References

- [1] STÉPÁN G.: Modelling nonlinear regenerative effects in metal cutting. *Philosophical Transactions of the Royal Society of London A* 2001, **359**(1781):739–757.
- [2] COLLETTE C., CHESNÉ C.: Robust hybrid mass damper. *Journal of Sound and Vibration* 2016, **375**:19 – 27, 2016. Springer: Berlin, 1988.
- [3] HU J.L., HABIB G.: Friction-induced vibration suppression via the tuned mass damper: Optimal tuning strategy. *Lubricants* 2020, **8**:100.
- [4] VYHLÍDAL T., OLGAC N., KUCERA V.: Delayed resonator with acceleration feedback – Complete stability analysis by spectral methods and vibration absorber design. *Journal of Sound and Vibration* 2014, **333**(25):6781–6795.

Partial Control and Beyond: Forcing Escapes and Controlling Chaotic Transients with the Safety Function

RUBEN CAPEANS¹, GASPAR ALFARO², MIGUEL AF SANJUAN^{3*}

1. Nonlinear Dynamics, Chaos and Complex Systems Group, Departamento de Física, Universidad Rey Juan Carlos, Tulipán s/n, 28933 Móstoles, Madrid, Spain [0000-0001-8029-0658]
2. Nonlinear Dynamics, Chaos and Complex Systems Group, Departamento de Física, Universidad Rey Juan Carlos, Tulipán s/n, 28933 Móstoles, Madrid, Spain
3. Nonlinear Dynamics, Chaos and Complex Systems Group, Departamento de Física, Universidad Rey Juan Carlos, Tulipán s/n, 28933 Móstoles, Madrid, Spain [0000-0003-3515-0837]

* Presenting Author

Abstract: A new control algorithm based on the partial control method has been developed. The general situation we are considering is an orbit starting in a certain phase space region Q having a chaotic transient behavior affected by noise, so that the orbit will definitely escape from Q in an unpredictable number of iterations. Thus, the goal of the algorithm is to control in a predictable manner when to escape. While partial control has been used as a way to avoid escapes, here we want to adapt it to force the escape in a controlled manner. We have introduced new tools such as escape functions and escape sets that once computed makes the control of the orbit straightforward. The partial control method aims to avoid the escape of orbits from a phase space region Q where the transient chaotic dynamics takes place. The technique is based on finding a special subset of Q called the safe set. The chaotic orbit can be sustained in the safe set with a minimum amount of control. We have developed a control strategy to gradually lead any chaotic orbit in Q to the safe set by using the safety function. With the technique proposed here, the safe set can be converted into a global attractor of Q .

Keywords: partial control, transient chaos, safety function, controlling transient chaos

References

- [1] SABUCO J, SANJUAN MAF, YORKE JA: Dynamics of Partial Control. *Chaos* 2012, **22**:047507.
- [2] CAPEANS R, SABUCO J, SANJUAN MAF: A new approach of the partial control method in chaotic systems.. *Nonlinear Dynamics* 2019, **98**:873-887.
- [3] ALFARO G, CAPEANS R, SANJUAN MAF: Forcing the escape: Partial control of escaping orbits from a transient chaotic region. *Nonlinear Dynamics* 2021, **104**:1603-1612.
- [4] CAPEANS R, SANJUAN MAF: Beyond partial control: Controlling chaotic transients with the safety function. <https://arxiv.org/abs/2105.0335>

Reference models of the 4WS vehicle lateral dynamics for the synthesis of steering algorithms.

DĘBOWSKI ANDRZEJ¹, FARYŃSKI JAKUB², ŻARDECKI DARIUSZ^{3*}.

1. Military University of Technology (WAT) [ORCID 0000-0003-1446-4415]

2. Military University of Technology (WAT) [ORCID 0000-0001-6515-0921]

3. Military University of Technology (WAT) [ORCID 0000-0002-3934-2150]

* Presenting Author

Abstract: The presented paper describes selected reference models describing the kinematics and dynamics of four-wheel steering (4WS) vehicle motion in a plane of the road. These models are based on well known “bicycle model” (two second order linear differential equations) supplemented by non-linear equations of trigonometric transformation of variables from local to global coordinate system. After linearization and Laplace transformation, these models acquire the forms of transfer functions. which, as shown in computational examples presented in the paper, greatly facilitates the analysis of vehicle motion, as well as the synthesis of control algorithms. Especially, transmittance form of the reference models facilitate sensitivity analysis of vehicle lateral dynamics and steering system algorithms, because their parameters are analytical functions of “mechanical” parameters. For synthesis of steering system algorithms which should be adequately effective for on-line computations, the transfer functions can be reduced in several ways. One of them is discussed in the paper.

Keywords: 4WS cars, reference models, control algorithms

1. Introduction

Four-wheel steering (4WS) is one of the distinguishing features of passenger cars equipped with advanced mechatronic systems supporting the driver [2], [3], [4]. In such systems, there are digital controllers coupled by-wire with actuators of steering mechanisms of the front and rear wheels, which allows not only to shape the waveforms controlling the steering of the wheels on-line according to the actions of the driver and the reaction of the driven vehicle, but also to modify the steering when the driver's actions are at risk of an accident. Active steering of the wheels in 4WS vehicles requires appropriate algorithms, the basis of which are reference models describing the movement of the driven vehicle [1], [5], [6]. The role of the reference models is twofold. On the one hand, they are to be an element of the control algorithm, so they must meet the time requirements of on-line calculations, on the other hand, they are to be the basis for the proper design of regulators correcting control signals. Such a situation occurs in the case of the 4WS car control algorithm performing the lane change maneuver. The aim of the article is to present the reference models of 4WS vehicle used in the design of a controller of the lane change process.

2. Results and Discussion

According to a general concept of car control when changing lanes where the controller contains a reference signals' generator (reference waveforms of control and response signals) and a system of regulators correcting the control signals (responsible for shifting the vehicle to a new track and its angular stabilization). The algorithm for generating reference signals and the algorithms of the regula-

tors are based on the reference models of the 4WS car's motion dynamics. These models are derived from the "bicycle model" (which express linear and angular velocities in the local coordinate system related to the moving vehicle) supplemented by the transforming equations (which transform wave-forms from the local system to the global system related to the road). It well known from driver practice that steering signal should have a form of short "bang-bang"-type signal for realization of lane change processes. In such case the maximal angle of vehicle deviation is small, so the linearization of the model is possible. Then the linearized model of the 4WS vehicle dynamics, can be presented as "the black box" form with four transfer functions expressing actions of two input signals (angles of front and rear vehicle wheels) on two output signals (linear and angular dislocation of the vehicle body) - fig.1.

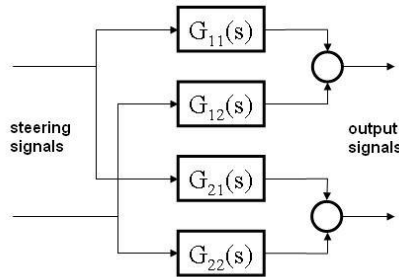


Fig. 1. Idea o transmittance type reference models

The reference models in transfer function forms enable sophisticated analysis of 4WS vehicle lateral dynamics and control processes in time as well as in frequency domain. Note, that transfer functions parameters (gains, time constants, characteristic frequencies, etc), are associated with mechanical parameters (vehicle speed, mass, yaw moment of inertia, wheels cornering stiffness, etc.) by analytical formulae. For synthesis of steering system algorithms, the transfer functions can be reduced in several ways including these analytical dependencies. For example, thanks to omitting "subtle" dynamic components in transfer functions one obtains analytical formulae (important for on-line calculations) describing reference "bag-bang" steering signals (magnitude and time period).

3. Concluding Remarks

The method of synthesis control system algorithms for 4WS vehicles on the base of elaborate reference models seems to be an attractive proposition for engineer s working on autonomous cars.

References

- [1] AKITA T., SATOH K.: Development of 4WS control algorithms for an SUV, *JSAE Review*, 2003, **24**, 441-448.
- [2] FIJALKOWSKI B. T.: *Automotive Mechatronics: Operational and Practical Issues. Vol II*, .Springer 2011, 73-116.
- [3] HEROLD P. WALLBRECHER M.: All-Wheel Steering , chapter 17 in *Steering Handbook* Ed. HARRER M, PFEFFER P., Springer 2017, 493-512.
- [4] ONO E., HATTORI Y., MURAGISHI Y., KOIBUCHI K.: Vehicle dynamics integrated control for four-wheel-distributed steering and four-wheel-distributed traction/braking \systems. *Vehicle System Dynamics*, 2006, **44**(2), 139-151.
- [5] POSTALCIOGLU S.: Improvement of Four Wheel Steering System. *Journal of the Institute of Science and Technology*, 2019, **9**(4), 1876-1886.
- [6] SIAHKAIROUDI V.N., NARAGHI M.: Model Reference Tracking Control a 4WS Vehicle Using Single and Dual Steering Strategies, *SAE Paper 2002-01-1590*, 2002, 1-11.

Modeling and simulation of the automated lane change process, taking into account freeplay and friction in the vehicle steering system.

MIROSLAW GIDLEWSKI¹, LESZEK JEMIOŁ², DARIUSZ ŻARDECKI^{3*}

1. Military University of Technology, (WAT); Łukasiewicz Research Network – Automotive Industry Institute [ORCID 0000-0001-5775-184X]
 2. University of Technology and Humanities in Radom [ORCID 0000-0001-8898-4937]
 3. Military University of Technology (WAT), [ORCID 0000-0002-3934-2150]
- * Presenting Author

Abstract: The paper reports rather unique research on the influence of freeplay and friction in the car steering mechanism on automatically controlled process of lane change. The developed controller algorithm was based on very simplified (and thus effective in on-line calculations) reference models of the car dynamics, obviously without taking into account the nonlinearities of its steering system. Extensive simulation investigations of the developed controller algorithm carried out in a very wide range of changes in road and operational conditions, with regard to two-axle medium-duty truck, confirmed its advantages. The research presented in this article concerns the unpublished area of analyzes concerning the sensitivity of the lane change controller to freeplay and friction occurring in the steering mechanism of a controlled car. Some results of the simulation tests turned out to be surprising. The piecewise-linear luz(...) and tar (...) projections used in these studies to describe the freeplay and friction effects facilitated modeling and simulation calculations.

Keywords: automatic lane change, steering system, freeplay, friction, modeling and simulation

1. Introduction

The influence of (backlash, clearance) and friction (viscous and dry friction with stiction) on system control is discussed in a number of publications, see reviews papers [1, 5]. But these works do not relate directly to the automotive issue. Due to the real-time signal processing requirements, the controllers of embedded mechatronic systems are based on relatively simple models describing the dynamics of the controlled car. Therefore, when designing controllers, non-smooth nonlinearities, such as freeplay and friction, which are difficult to calculate, are ignored, which means that in fact the control algorithms created relate only to “new” vehicles. Therefore, it is reasonable to ask about the sensitivity of the designed control algorithms to the appearance of freeplay and friction in the steering mechanisms. Such analyzes are extremely rarely reported in available scientific publications and refer to classic steering systems rather than active systems equipped with controllers, eg. [4, 6]

In previous papers, eg [2, 3], the authors presented design and research works on a steering system controller that automates the process of changing lane by a car when an obstacle suddenly appears. The developed controller algorithm has been extensively tested by simulation in relation to a truck (treated as MBS object, but always without freeplay and friction in its steering mechanism), in a wide range of changes in road and operation conditions. The maneuver to bypass the obstacle in the vast majority of attempts was successful without the need to change the previously adopted assumptions and the determined values of the controller parameters, even in the presence of signals’ disturbances. The time has come to extend the scope of research to include the sensitivity of the controller to the occurrence of freeplay and friction in the vehicle steering mechanism.

2. Results and Discussion

This article presents the latest research on the sensitivity analysis of the lane change controller, this time due to the steering gear freeplay and the steering king-pins friction that have been ignored in the design. In connection with the above, the previously used model of the dynamics of a truck, has been supplemented with a fairly detailed model (MBS-type, with non-smooth characteristics, and variable-structure differential equations) of its steering mechanism operation, taking into account freeplay (in steering gear) and friction (in king-pins). In modeling the freeplay and friction nonlinearities, the piecewise-linear $\text{luz}(\dots)$ and $\text{tar}(\dots)$ projections have been used (Fig.1) [7]. They simplify the synthesis of the model, as well as its functioning in the simulation program.

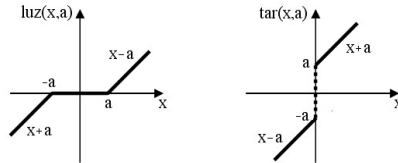


Fig. 1. Geometric interpretations of the $\text{luz}(\dots)$ and $\text{tar}(\dots)$ projections

Due to the expansion of the object model, peculiar phenomena related to the stick-slip operation occurred in the waveforms describing the lane change process. The presence of freeplay and friction in steering system, worsened the effect of lane change control when certain values of these factors are exceeded. The sensitivity of the system to the presence of freeplay and friction increases with the deterioration of road and operational conditions (slippery road, unloaded vehicle, high speed).

3. Concluding Remarks

The simulation studies taking into account the freeplay and friction in the steering system are very important for design the lane change process controller. Such studies should be continued to cover also issues related to electric signal disruptions.

References

- [1] ARMSTRONG-HELOUVRY B., DUPONT P., CANUDAS DE WIT C.: A Survey of Models, Analysis Tools and Compensation Methods for the Control of Machines with Friction. *Automatica*: 1994, **30** (7), 1083-1138
- [2] GIDLEWSKI, M.; ŻARDECKI, D.: Linearization of the lateral dynamics reference model for the motion control of vehicles. *Mechanics Research Communications*, 2017, **82** (Jun), 49-54.
- [3] GIDLEWSKI M., JEMIOŁ L., ŻARDECKI D.: Sensitivity investigations of the automated lane-change manoeuvre – selected issues. *Proceedings of the Institution of Mechanical Engineers, Part I: Journal of Systems and Control Engineering*. 2019, **233** (4), 360-369.
- [4] LOZIA Z., ŻARDECKI D.: Vehicle Dynamics Simulation with Inclusion of Freeplay and Dry Friction in Steering System. (*SAE Technical Paper 2002-01-0619*). *SAE 2002 Transactions Journal of Passenger Car – Mechanical Systems: 2002, Section 6 – Vol.111, 2002*. (Also published in *Special Publication SP-1654 “Steering and Suspension Technology Symposium 2002” - SAE’2002 World Congress*).
- [5] NORDIN M, GUTMAN P.O.: *Controlling mechanical systems with backlash - a survey*. *Automatica*: 2002, **38** (10), 1633-1649
- [6] WIĘCKOWSKI D., ŻARDECKI D.: Influence of freeplay and friction in steering system on double lane change manoeuvre – modeling and simulation studies. *Journal of KONES Powertrain and Transport*, 2011, **18** (2), 483-492.
- [7] ŻARDECKI D.: Piecewise Linear $\text{luz}(\dots)$ and $\text{tar}(\dots)$ Projections. Part 1 - Theoretical Background. Part 2 - Application in Modeling of Dynamic Systems with Freeplay and Friction. *Journal of Theoretical and Applied Mechanics*, 2006, **44** (1), 163-202.

Model based investigations of an integrated control system for automatic lane change in critical conditions.

MIROSLAW GIDLEWSKI ¹, LESZEK JEMIOŁ ², DARIUSZ ŻARDECKI ^{3*},

1. Military University of Technology, (WAT); Łukasiewicz Research Network – Automotive Industry Institute [ORCID 0000-0001-5775-184X]
 2. University of Technology and Humanities in Radom [ORCID 0000-0001-8898-4937]
 3. Military University of Technology (WAT), [ORCID 0000-0002-3934-2150]
- * Presenting Author

Abstract: The article presents the concept of an automatic, integrated control system for a two-axle truck activated at the time of a critical road situation, consisting in the need to bypass a suddenly appearing obstacle. In earlier works, the authors used only the controller coupled to the steering system for sudden lane changes. Currently, the operation of the steering system controller has been integrated with the ESC (Electronic Stability Control) system, which causes temporary braking of selected wheels of the vehicle to stabilize its movements. Simulation tests of the functioning of the integrated control system during sudden lane change were carried out for an unladen and fully loaded vehicle driven with a high speed on a wet road - in conditions close to critical. The test results were compared with the results obtained during this maneuver only with the use of the steering system controller. They show undoubted advantages of such integration of both systems.

Keywords: automatic lane change, critical conditions, integrated control system

1. Introduction

The dynamic development of controllers, actuators, sensors, monitoring devices, networks and telecommunications technologies favor the emergence of more and more effective systems supporting the driver's actions related to driving a vehicle. In recent years, a significant effort has been placed on the development of assistance systems that are activated automatically when a critical road situation occurs and replace the driver in the selection and implementation of an effective or at least the most beneficial defensive maneuver. Advanced research on such systems is carried out in many research centers, eg [1,2] and in the near future they will be used in mass-produced cars.

In previous publications, eg. [3,4], the authors presented design and research works on a steering system controller that automates the lane change process of a car when an obstacle suddenly appears. This controller generates a "bang-bang" reference steering signal and then corrects it through two regulators that minimize the deviations between the reference and actual waveforms describing the vehicle movement. The developed control algorithm was based on simplified (and therefore effective in on-line calculations) reference models. Simulation tests of the sensitivity of the developed controller were carried out in a wide range of changes in road and operating conditions, in relation to a "difficult" object such as a truck. The maneuver of avoiding the obstacle in the vast majority of attempts was successful without the need to change the previously adopted assumptions and the established values of the controller parameters. However, in a few cases of steering an unladen car at high speed and on a slippery surface, the directional stability was lost.

There is a statement in the professional literature, eg [5] that the steering system provides good driving properties only when the lateral acceleration is low, the vehicle drift angle is low, and the tire

sideslip characteristics are linear. However, in emergency situations, accompanied by high lateral acceleration (such as occur during sudden lane changes), the characteristics of the tires become non-linear and the desired effect of controlling the car's movement cannot be achieved by steering the steering wheel alone. In this case, the additional inclusion of the braking system in the vehicle motion control may prove very beneficial. In connection with the above, research was undertaken on the integration of the developed steering system controller with the ESC (Electronic Stability Control) system, which causes temporary braking of selected vehicle wheels when destabilization threatens.

The article will present the concept of an integrated control system, models as well as analytical and simulation tests.

2. Results and Discussion

The integrated assistant system consists of an active steering system that triggers the given steering angles of the front wheels and the electronic control of the track (ESC), which causes temporary braking of selected vehicle wheels.

The two systems that make up the assistant system use as a reference model a flat, single-track "bicycle model" of a car known from numerous publications, but modified by performing simple transformations to express the vehicle's motion in a global system and by linearization of the equations of motion. The assistant system initiates a sudden lane change maneuver, initially carried out only by appropriate steering of the front wheels, so that the car is shifted to the adjacent lane in the shortest possible time and on the shortest possible road. In practice, the implementation of such a maneuver requires very fast turning of the steering wheel from one side to the other ("bang-bang" steering). The ESC system is superior to the steering system controller and when the vehicle approaches the limit of adhesion, it brakes the appropriate wheels, increasing the radius of the path and reducing the speed of the car, which additionally secures the vehicle's stable movement.

The integration of these systems allows for simultaneous control of these subsystems and enables the mutual exchange of information from individual sensors and actuators. Coordination, on the other hand, ensures the harmonious functioning of the systems and the synchronization of partial activities of individual systems, enabling the correct implementation of the main goal, i.e. a sudden lane change.

3. Concluding Remarks

The use of an integrated system controlling the sudden lane change maneuver effectively eliminated the loss of directional stability of an unloaded car on a slippery road.

References

- [1] Hayashi R. et.al: Autonomous collision avoidance system by combined control of steering and braking using geometrically optimized vehicular trajectory. *Vehicle System Dynamics*, 2012, **50** (Supplement), 151-168.
- [2] Jiménez F.: Autonomous collision avoidance system based on accurate knowledge of the vehicle surroundings. *IET Intelligent Transport Systems*, 2015, **9** (1), 105-117.
- [3] Gidlewski, M.; Żardecki, D.: Linearization of the lateral dynamics reference model for the motion control of vehicles. *Mechanics Research Communications*. 2017, **82**, 49-54.
- [4] Gidlewski M., Jemioł L., Żardecki D.: Sensitivity investigations of the automated lane-change manoeuvre – selected issues. *Proceedings of the Institution of Mechanical Engineers, Part I: Journal of Systems and Control Engineering.*, 2019, **233** (4), 360-369.
- [5] Doumiati M., Sename O., Dugard L., Martinez-Molina J.-J., Gaspar Szabo, Integrated vehicle dynamics control via coordination of active front steering and rear braking, *European Journal of Control*, 2013, **19** (2), 121-143.

Optimal Control of Resonance Radiation Processes in Laser Isotopes Separation Systems and Devices

ALEXANDER V GLUSHKOV¹, VALENTIN B. TERNOVSKY^{2*},
OLEKSII L MYKHAILOV¹ AND ANDREY V TSUDIK¹,

1. Odessa State Environmental University, Mathematics Dept., L'vovskaya str. 15, 65009, Odessa

2. National University "Odessa Maritime Academy", Didrikhson str. 8, 65001, Odessa

* Presenting Author

Abstract: The paper is devoted to presentation of an effective numerical approach to construction of an optimal laser photoionization (LPI) isotope separation scheme (technology). The construction of the LPI optimal models requires quantum numerical modelling of the corresponding radiation processes (due to collisions, or ionization by a pulsed electric field etc) in complex atomic systems. The optimal laser action model and density matrices formalism are used for numeric computing the optimal LPI scheme parameters. One of the possible LPI optimization model entails a search for an optimal shape of a laser resonant pulse in order to obtain maximum number of ionized particles in the LPI scheme with ionization at the final stage by a pulsed electric field. The solution of the optimal control problem gives the condition for the existence of optimal laser exposure in the form of a single pulse and its optimal shape.

Keywords: optimal control, laser isotopes separation scheme

1. Introduction. Optimal Control Task for Resonance Radiation Processes

A multi-staged LPI isotope separation method comprises a selective laser pulse excitation of the isotope atoms into the excited and further Rydberg states (first and middle stages) and their ionization in the final stage [1-3]. The criteria to be considered on pursuing optimality and efficiency of multi-staged LPI scheme include the minimum required energy densities of laser pulses, a maximum yield of ionization and its selectivity. A construction of optimal isotope separation LPI models requires numerical modelling of the corresponding radiation processes in atomic ensemble. One of the possible models for LPI optimization entails the search for a laser pulse optimal shape in order to obtain maximum number of ionized particles in the LPI scheme with ionization at the final stage [1,2]. If the quantity R is an atomic ionization rate, x_2 is the normalized population of the excited states of the atom and $\bar{\tau}$ is the duration of radiation pulse, then the corresponding performance criterion is reduced to the minimization of the functional (J), which determines the number of ionized atoms:

$$J = - \int_0^{\bar{\tau}} R(\tau) x_2 d\tau \rightarrow \min; \quad (1)$$

A simple ionization model can be represented by a system of standard Bloch's-like equations with the following initial conditions [3]:

$$dx_1/d\tau = x_2 - \bar{u}(x_1 - x_2), x_1(0) = 1; \quad (2)$$

$$dx_2/d\tau = -[R(\tau) + 1]x_2 + \bar{u}(x_1 - x_2), x_2(0) = 0; \quad (3)$$

$$dx_3/d\tau = \tilde{u}, x_3(0) = 0, x_3(\tau_f) = E_f; \quad (4)$$

where $0 \leq \tau \leq \tau_f, \tilde{u}(\tau) \geq 0$; x_1 is the normalized population of the ground state of an atom; $\tilde{u} = u/\gamma$ is a dimensionless rate of induced emission and absorption processes of the resonant radiation; γ is the probability of spontaneous decay per unit time; $\tau = t\gamma$ is a dimensionless time; $R=R'/\gamma$ is a dimensionless ionization rate from excited state; $u(t)=\sigma_{12}I_1(t)/\hbar\omega_{21}$ is the rate of induced transitions ($1 \rightarrow 2$ transition); ω_{21} is a radiation frequency; σ_{12} is the absorption cross section; $R'(t) = \sigma_{ph}I_2(t)/\hbar\omega_{ph}$ is the photoionization rate; ω_{ph} is a radiation frequency for photoionization; σ_{ph} is a photoionization cross section; I_1, I_2 are the intensities of laser pulses for excitation from the ground state and ionization from the excited one; E_f, τ_f are an energy and duration of pulse.

2. Results and Discussion

The solution of the optimal control problem gives the condition for the existence of optimal laser exposure in the form of a single pulse as follows:

$$p = \exp(-2E_f)\{1 + 2/R_0 + \exp[-(R_0 + 1)\tau_f]\} / (1 + 2/R_0)\{1 - \exp[-(R_0 + 1)\tau_f]\}, p \geq 1 \quad (6)$$

where the parameter p has an expression similar to the analogous parameter in the Krasnov-Shaparev-Shkedov scheme [2]. The optimal resonant laser pulse is given by:

$$\tilde{u}(\tau) = \begin{pmatrix} E_1 \delta(\tau) + \tilde{u}'(\tau), \tau \in [0, \tau_1] | p < 1 \\ 0, \dots, \dots, \tau \in [\tau_1, \tau_f] | p < 1 \\ E_f \delta(\tau), \dots, \dots, \tau \in [0, \tau_f] | p \geq 1 \end{pmatrix} \quad (7)$$

where $\delta(\tau)$ is the Dirac delta-function, $E_l (E_l < E_f)$ is the amplitude of the δ -pulse; τ_m is the time parameter, which is matched numerically ($\tau_m < \tau_f$); R_0 is the ionization rate from the ground state of atom. More mathematical and physical details of the model can be found in [2-4].

3. Concluding Remarks

An effective numerical approach to construction of an optimal laser photoionization LPI isotope separation scheme for radioactive elements is presented. It is numerically solved a LPI optimization problem, connected with a search for an optimal shape of a laser pulse of resonant radiation in order to obtain maximum number of ionized particles in the LPI scheme.

References (10 point, bold)

- [1] LETOKHOV V: *Nonlinear Selective Photoprocesses in atoms and molecules*. Nauka: Moscow, 1983.
- [2] GLUSHKOV A.V., PREPELITSA G.P., SVINARENKO A ET AL: New laser photoionization isotope separation scheme with autoionization sorting of highly excited atoms for highly radioactive isotopes and products of atomic energetics. *Sensors Electr and Microsyst. Techn.* 2011, **8**(2):81-86.
- [3] GLUSHKOV A: Multiphoton spectroscopy of atoms and nuclei in a laser field: Relativistic energy approach and radiation atomic lines moments method. *Adv.Quant Chem.* (Elsevier) 2019, **78**:253-285
- [4] KRASNOV I, SHAPAREV N, SHKEDOV I: Optimal control of resonance radiation processes. *Opt. Comm.* 1980, 34(2), 181-184.

Predictive Control of Semi-active Fluid-based Dampers Under Impact Excitation

CEZARY GRACZYKOWSKI^{1*}, RAMI FARAJ²

1. Institute of Fundamental Technological Research, Polish Academy of Sciences [0000-0001-6917-148X]
2. Institute of Fundamental Technological Research, Polish Academy of Sciences [0000-0001-7604-0090]

Abstract: The contribution presents recent progress in development of the control systems for semi-active fluid-based dampers equipped with fast-operating valves. The attention is focused on the case when the damper is subjected to impact of mass moving with initial velocity and additional excitation force acting during the process. The objective of the corresponding control problem is to find the change of valve opening which provides absorption of the entire impact energy with minimal value of generated reaction force. The contribution presents two different approaches to solution of the challenging control problem with unknown excitations and disturbance forces, which are based on the concept of Model Predictive Control.

Keywords: fluid-based dampers, semi-active dampers, Hybrid Prediction Control, Identification-based Predictive Control

1. Introduction

Semi-active fluid-based dampers consist of two chambers filled with hydraulic or pneumatic fluid and connected by the orifice, which is equipped with fast-operating valve controlling the actual rate of fluid flow. The most often used types of fluid-based shock-absorbers are semi-active dampers with fast electromagnetic or piezoelectric valves. These devices can be used in both vibration suppression problems and impact mitigation problems. Although many control strategies have been successfully developed for protection against vibration, the problem of optimal impact absorption has not gained sufficient attention of researchers and has not been completely solved so far.

2. Results and discussion

In the considered impact absorption problem the damper is subjected to the impact of a rigid object of mass M moving with initial velocity v_0 and external force $F_{\text{ext}}(t)$, as shown in Fig. 1a. The objective of the control problem is to find the change of valve opening in time $A_v(t)$, which provides absorption and dissipation of the entire impact energy with minimal value of total discrepancy between force generated by the absorber F_{abs} and its theoretical optimal value $F_{\text{abs}}^{\text{opt}}$, see Fig. 1b (black and red lines, respectively).

The direct mathematical formulation of the impact mitigation problem, which has been studied in detail by the authors reads:

$$\text{Minimize: } \int_0^T (F_{\text{abs}}(A_v(t), t) - F_{\text{abs}}^{\text{opt}})^2 dt \quad (1a)$$

$$\text{With respect to: } A_v(t) \geq 0 \quad (1b)$$

$$\text{Subject to: } \int_d \vec{F}_{\text{abs}} d\vec{s} = E_{\text{imp}}^0 + E_{\text{imp}}^{\text{ext}} = \frac{1}{2}Mv_0^2 + \int_d \vec{F}_{\text{ext}} d\vec{s} \quad (1c)$$

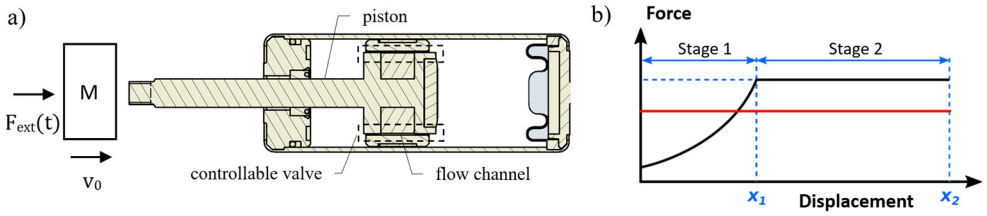


Fig. 1. a) The problem considered: damper subjected to the impact excitation, b) force-displacement characteristics: red – theoretical optimal force, black – schematic optimal change of force obtained using pneumatic damper

The solution of the above control problem is straightforward (and for pneumatic damper assumes form shown in Fig. 1b) only in a special case when no limitations on valve operation are considered, impact excitation is a priori known and theoretical value of optimal force can be directly calculated. In the opposite situation, the impact mitigation problem requires reformulation and application of advanced methods of control theory.

In particular, when external excitation is not a priori known the problem has to be reformulated into its kinematic version, the so called *state-dependent path-tracking*, based on minimization of the actual and currently optimal value of deceleration, which is continuously updated during the process:

$$\text{Minimize: } \int_0^T \left[\ddot{u}(A_v(t), t) + \frac{\dot{u}(t)^2}{2(d-u(t))} \right]^2 dt \quad (2a)$$

$$\text{With respect to: } A_v(t) \text{ such that } A_v(t) \in \langle A_v^{\min}, A_v^{\max} \rangle \text{ and } \frac{dA_v(t)}{dt} \leq v_v^{\max} \quad (2b)$$

$$\text{Subject to: condition of entire energy absorption (1c)} \quad (2c)$$

In such a case, the efficient approach is application of the Model Predictive Control, which assumes repetitive solution of the control problems defined at finite time horizon Δt of arbitrary length:

$$\text{Minimize: } \int_{t_i}^{t_i+\Delta t} \left[\ddot{u}(A_v(t), t) + \frac{\dot{u}(t_i)^2}{2(d-u(t_i))} \right]^2 dt \quad (3)$$

The approximate solution can be based on the proposed by the authors methods including Hybrid Prediction Control (HPC) [1] and Identification-based Predictive Control (IPC) [2]. The HPC provides efficient impact mitigation using system kinematics measurements, prediction of valve operation mode and prediction of required change of valve opening. In turn, the IPC additionally utilizes repetitive identification of selected system parameters in order to improve system performance at each control step.

3. Final remarks

Within this contribution the impact mitigation problem has been reformulated into kinematic version and two dedicated control methods (HPC, IPC) have been proposed. Both methods are proved to provide efficient mitigation of dynamic response of the system subjected to unknown impact excitation.

Acknowledgment: The financial support of the National Science Centre, Poland, granted under agreement DEC-2018/31/D/ST8/03178, is gratefully acknowledged. RF is supported by the Foundation for Polish Science (FNP) under the START scholarship.

References

- [1] FARAJ R., GRACZYKOWSKI C. Hybrid prediction control for self-adaptive fluid-based shock-absorbers. *Journal of Sound and Vibration* 2019, **449**: 427-446
- [2] GRACZYKOWSKI C., FARAJ R., Identification-based Predictive Control of semi-active shock-absorbers for adaptive dynamic excitation mitigation, *Meccanica* 2020, **12**: 2571-2597

Predicting and controlling tipping points in networked systems

CELSO GREBOGI^{1*}

1. Institute for Complex Systems and Mathematical Biology, King's College, University of Aberdeen, Aberdeen AB24 3UE, UK [ORCID 0000-0002-9811-4617]

* Presenting Author

Abstract: A variety of complex dynamical systems, ranging from ecosystems and the climate to economic, social, and infrastructure systems, can exhibit a tipping point at which an abrupt transition to a catastrophic state occurs. To understand the dynamical properties of the system near a tipping point, to predict the tendency for the system to drift toward it, to issue early warnings, and finally to apply control to reverse or slow down the trend, are outstanding and extremely challenging problems. We consider empirical mutualistic networks of pollinators and plants from the real world and investigate the issues of control, recovery, and early warning indicators. In particular, when considering bipartite networks, both exhibit a tipping point as a parameter characterising the population decay changes continuously, at which the system collapses suddenly to zero abundance for all the species. We articulate two control strategies: (a) maintaining the abundance of a single influential pollinator and (b) eliminating the factors contributing to the decay of the pollinator. In both cases, we find that control can turn the sudden collapse into a more gradual process in the sense that extinction of the species occurs sequentially with variation of the parameter, indicating that control can effectively delay the occurrence of global extinction. We then investigate population revival as the bifurcation parameter varies in the opposite direction away from the tipping point. Without control, there is a hysteresis loop which indicates that, in order to revive the species abundance to the original level, the parameter needs to be further away from the tipping point, i.e., the environment needs to be fitter than before the collapse. However, with control the hysteresis behaviour diminishes, suggesting the positive role of control in facilitating species revival. To develop effective control strategies to prevent the system from drifting towards a tipping point is an unsolved problem at the present, and we hope our work can shed light on the challenging and significant problem of understanding and controlling tipping point dynamics in nonlinear and complex systems. Based on compressive sensing, I will also present an efficient approach to reconstructing complex networks from small amounts of data.

Keywords: networked systems, control, early warning indicators

References

- [1] WANG W.-X., LAI Y.-C., GREBOGI C: Data based identification and prediction of nonlinear and complex dynamical systems. *Physics Reports* 2010, **644**:1-76.
- [2] HUANG Z.-G., SEAGER T.P., LIN W., GREBOGI C., HASTINGS, A., LAI Y.-C.: Predicting tipping points in Mutualistic Networks through dimension reduction. *PNAS (Proc. Nat. Acad. Sci.)* 2018, **115**: E639-E647.

Dynamics and control of a two-ship ensemble

MOHAMAD ISMAIL^{1*}, NABIL CHALHOUB², VALERY PILIPCHUK³

1. Wayne State University, Detroit, MI, USA [\[0000-0003-3884-5220\]](tel:0000-0003-3884-5220)
2. Wayne State University, Detroit, MI, USA [\[0000-0002-0605-0098\]](tel:0000-0002-0605-0098)
3. Wayne State University, Detroit, MI, USA [\[0000-0001-7051-3539\]](tel:0000-0001-7051-3539)

* Presenting Author

Abstract: The current study represents a fundamental step toward automating the towing mission of disabled vessels. It deals with the control of transient planar dynamics for a two-ship ensemble connected by a massless cable. This is a multibody structure whose components are coupled by non-holonomic inequality constraints. The control strategy is designed by exploiting the essential temporal scale difference between relative tugboat-ship dynamics induced by the constraints and the relatively slow motion of the mass center of the two-ship ensemble. The proposed control strategy reduces the controller's susceptibility to sharp variations in the towline tension. The results demonstrate the viability of the controller and illustrate its robustness to environmental disturbances.

Keywords: multibody system, autonomous towing, interconnected vessels control

1. Introduction

Emergency towing vessels (ETVs) and harbour tugs are relied on to rescue wrecked or disabled ships in bad weather on the open seas by towing them to a safe location [1,2]. This challenging problem involves the dynamics and control of an under-actuated multi-body system subjected to non-holonomic inequality constraints. The control variables in the two-ship ensemble are restricted to the propeller thrust and angular displacement of the leading ship. The control actions are transmitted to the disabled ship through the cable force. A schematic of the physical system is depicted in Fig. 1.

2. Model of the Two-Ship Ensemble and Controller Design

An ensemble of two ships connected by a massless towline with one vessel being totally disabled has been considered in this study. Three-degree of freedom models were developed for the tugboat and the towed ship to describe their motions in the horizontal plane. The effects of unilateral, non-holonomic, inequality constraints, induced by the limits on the distance between the points on the marine vessels where the cable extremities are attached, are represented by a specific potential energy function having a shallow potential well when the cable is not taut. However, this function tends to increase exponentially as the cable is stretched beyond its original length, which emulates the strain energy stored in a cable under tension. The equations of motion of the two-ship ensemble were derived by using the Lagrange principle. The external forces and moments applied on both ships are induced by drag and wave excitations along with the control force and moment on the tugboat. Empirical formulations were incorporated to account for the effects of wave excitations, wind and sea current drag forces and moments. The control scheme is designed by exploiting the essential temporal scale difference between the relative tugboat-ship dynamics induced by the constraints and the relatively slow motion of the mass center of the two-ship ensemble. It is designed to maintain a

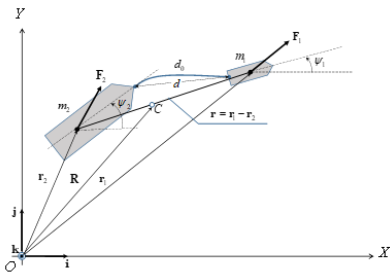


Fig. 1. A disabled ship towed by an ASV through an ideal flexible cable.

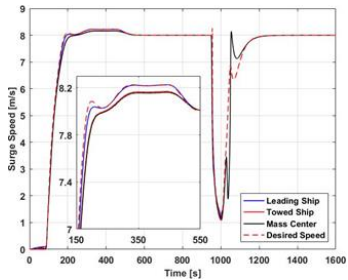


Fig. 2. Surge speeds in the presence of both wave excitations and sea current disturbances.

prescribed heading angle and surge speed for the mass center of the two-ship ensemble. The rationale is to reduce the controller's susceptibility to sharp variations in the towline tension force. Note that the dynamics of the leading ship are directly and adversely impacted by large spikes in the cable tension normally occurring during transient periods. The challenge in designing the controller stems from the fact that the disabled ship becomes uncontrollable whenever the cable cease to be taut. The controller of the tug has to simultaneously perform a tracking task while preserving the controllability of the system by ensuring that the cable is always taut. This has to be done without producing large impulsive tension force in the cable that could result in the ships moving towards each other with the possibility of a collision. Thus, the propeller thrust control signal of the leading ship is defined as $P_1(t) = P_1^c(t)[1 - w(t)] + P_1^T(t)w(t)$ where P_1^c is responsible for keeping the cable taut, P_1^T is the trajectory tracking control signal and w is a weighting factor ensuring a smooth transition between P_1^c and P_1^T . The PID control scheme was implemented in the design of both propeller controller and heading controller of the leading ship. Note that the desired surge speed and heading angle of the leading ship were computed to yield the desired surge speed and heading angle of the mass center of the two-ship ensemble.

3. Results and Discussion

Figure 2 demonstrate the viability of the proposed controller and illustrates its disturbance rejection characteristic to wave excitations and sea current disturbances. The latter varied in magnitudes and applied at different times on the leading and disabled vessels. The disturbance on the leading ship led to a zero tension in the towline causing the controller to lose its controllability over the disabled ship. Also, the two vessels exhibited out-of-phase heading angles during this phase of the maneuver. However, within a short period of time, the controller regained its controllability over the disabled ship, stabilized the cable length and forced the two-ship ensemble to once again behave almost like a single rigid body. The disturbance on the disabled ship had an opposite effect on the towline. It served to drastically increase the cable tension that enhanced the capability of the two-ship ensemble to preserve its behavior almost like a single rigid body under severe transient conditions.

References

- [1] UK House of Commons Transport Committee, 2011, *The Coastguard, Emergency Towing Vessels and the Maritime Incident Response Group*, The Stationery Office by Order of The House, 6th Report of Session 2010 – 12, HC 948.
- [2] Shigunov V., Schellin T., "Tow Forces for Emergency Towing of Containerships," *Transactions of the ASME* 2015, **137**: 051101-1 – 051101-8.

Quasiperiodic Energy Harvesting in a Delayed and Excited Rayleigh-Duffing Harvester Device Near Secondary Resonances

ILHAM KIRROU^{1*}, AMINE BICHRI², MOHAMED BELHAQ³

¹ENSA Agadir, University Ibn Zohr, Morocco

²FST Errachidia, University Moulay Ismael, Morocco

³Faculty of Sciences Ain Chock, University Hassan II of Casablanca, Morocco

Abstract. This paper studies quasiperiodic vibration-based energy harvesting in a delayed and excited Rayleigh-Duffing oscillator coupled to piezoelectric harvester device. Analytical investigation is performed using the multiple scales method to obtain approximation of periodic and quasiperiodic amplitude responses as well as the corresponding power output near secondary resonances of order 3. The influence of different parameters of the harvester on the amplitude of solutions and powers is examined. Results show that for moderate values of the amplitude of the external forcing, time delay can substantially improve quasiperiodic vibration-based energy harvesting in the vicinity of a secondary resonance.

Introduction

We consider a harvester device consisting in a delayed and excited Rayleigh-Duffing oscillator coupled to an electrical circuit through a piezoelectric device. The corresponding equation of motion for the harvester is given in the non-dimensional form by

$$\ddot{\eta}(t) + \omega_0^2 \eta(t) - \alpha \left(1 - \dot{\eta}(t)^2\right) \dot{\eta}(t) + \gamma \eta(t)^3 - \theta v(t) = F \cos(\omega t) + D_p \eta(t - \tau) + D_v \dot{\eta}(t - \tau)$$

$$\dot{v}(t) + \beta v(t) + \kappa \dot{\eta}(t) = 0$$

where $\eta(t)$ is the relative displacement of the rigid mass m , $v(t)$ is the voltage across the load resistance, α is the mechanical damping ratio, θ is the piezoelectric coupling term in the mechanical attachment, κ is the piezoelectric coupling term in the electrical circuit, β is the reciprocal of the time constant of electrical circuit, F and ω are, respectively, the amplitude and the frequency of the external excitation, τ is the time delay, while D_p , D_v are, respectively, the position, the velocity feedback gains. Investigation of quasiperiodic vibration-based energy harvesting for this harvester device has been carried out near the principal resonance in [1]. The purpose here is to study quasiperiodic vibration-based energy harvesting performance near the secondary resonances of order 3. Analytical investigation is performed using perturbation methods [2, 3].

References

- [1] Bichri, A., Kirrou, I., Belhaq, M., Energy harvesting from quasiperiodic vibrations in a delayed Rayleigh-Duffing harvester device, Journal of Vibration Testing and System Dynamics 1(1) (2017) 75-93.

- [2] Nayfeh, A.H., Mook, D.T., Nonlinear Oscillations. Wiley, New York (1979).
- [3] Belhaq, M., Houssni, M., Quasi-periodic oscillations, chaos and suppression of chaos in nonlinear oscillator driven by parametric and external excitations, Nonlinear Dyn., 18, (1999) 1-24.

Development and research of a new type of vibration reduction system for wheel bucket loaders

ANDRZEJ KOSIARA¹, ALEKSANDER SKURJAT^{2*}

1. Wrocław University of Science and Technology [0000-0001-6870-5961]
2. Wrocław University of Science and Technology [0000-0002-3780-1691]

* Presenting Author

Abstract: While driving, various industrial off-road vehicles with booms experience intense vibrations. These vibrations significantly reduce the comfort of their operation and efficiency. Due to the specificity of the operation of these machines, it is usually impossible to apply the vibration reduction measures developed for other types of vehicles. In turn, the developed and implemented vibration reduction methods for these particular machines are insufficient. The article analyses the possibility of using a new type of vibration reduction system in the mentioned machines. The proposed system is an active system, while other systems used so far in practice are passive systems. The very idea of using active vibration reduction systems has already been considered in the technical literature, but to this day it has not been unequivocally assessed. Depending on the control algorithms used, the researchers obtained significantly different final results. The paper describes the results of a synthesis of the control system made by the author based on the analytical model of a wheel bucket loader. The author's analytical model of the loader used in the calculations takes into account three degrees of freedom of the real machine. The effectiveness of the developed vibration reduction system was verified using a more complex simulation model built in MSC Adams. The performance of the developed vibration reduction system was compared with that of a typical passive vibration reduction system.

Keywords: active vibration reduction system, bucket loader, industrial off-road vehicle

1. Introduction

A large part of industrial vehicles with a boom with a working tool, e.g., in the form of a bucket, cannot be equipped with the traditional suspension of road wheels. Such suspension would unacceptably reduce, inter alia, the tipping stability of this type of mobile machinery. As a result, excitations from the road are able to stimulate the vehicle with vibrations of low frequency and high amplitude. Due to the fact that the energy stored in the form of vibrations is not dissipated, the vibrations can persist for a relatively long time. This results in a reduction of the operator's work comfort and efficiency. To minimize this effect while driving, the lower chambers of the boom's hydraulic cylinders are connected to the hydraulic accumulators. As a result, a flexible support of the boom is obtained and an increase in the intensity of damping of the excited vibrations of the vehicle. Unfortunately, the reduction of vibrations obtained this way is insufficient. That is why new and better solutions are sought. One of the ideas currently being researched is to force micromovements with the boom actuators while driving. Several solutions of this type have been submitted for patent protection. However, the results of research conducted by independent research units so far give contradictory results as to the effectiveness of such an approach. Therefore, the author decided to develop a control algorithm and test the vibration reduction system based on it.

2. Results and Discussion

To synthesize the controller for the active vibration reduction system, a mathematical model of a vehicle with a boom was built. The model was based on an actual bucket loader. The physical model of the vehicle, which is the basis for the construction of the mathematical model, is presented in Figure 1. In deriving the equations of motion, the formalism of the 2nd type Lagrange equations was used.

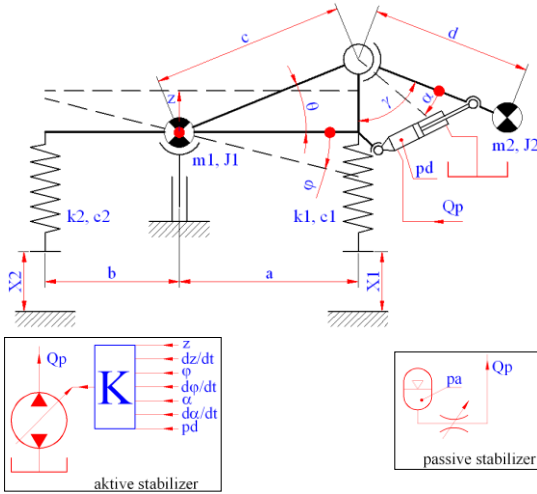


Fig. 1. Physical model of a bucket loader with a passive and active vibration reduction system (vibration stabilizer)

For the synthesis of the controller, the mathematical model was linearized. The linearized form of the model was written in the form of state equations. The model in this form was used to synthesize the LQR (Linear-quadratic regulator) regulator. While determining the parameters of the LQR controller, various parameters of the weight matrices in the cost equation were experimented with. To verify the effectiveness of the developed vibration reduction system with the LQR controller, a simulation model was built in the MSC Adams system (see Figure 2). Then the virtual bucket loader was driven over a road with stochastic unevenness with a passive and the other time with an active vibration reduction system. The test runs made it possible to compare both solutions.

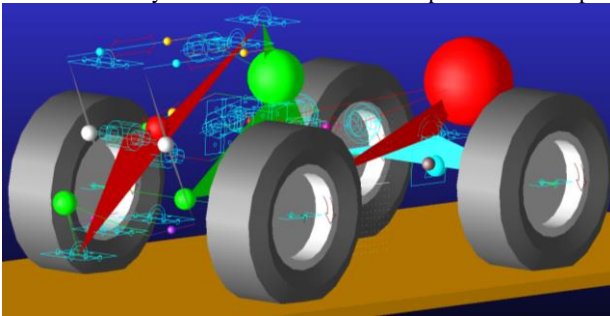


Fig. 2. A simulation model of a bucket loader built in the MSC Adams system to test the performance of the developed vibration reduction system

3. Concluding Remarks

The article proposes a synthesis method for the LQR controller for an active vibration reduction system of a bucket loader. The performance of the proposed vibration reduction system was compared with that of the passive system commonly used in modern bucket loaders.

Nonlinear vibrations of a sandwich piezo-beam system under piezoelectric actuation

KRZYSZTOF KULIŃSKI^{1*}, JACEK PRZYBYLSKI²

1. Department of Civil Engineering, Faculty of Civil Engineering, Częstochowa University of Technology, Częstochowa, Poland, [ORCID: 0000-0001-9850-9144]
2. Division of Mechanics and Machine Design Fundamentals, Faculty of Mechanical Engineering and Computer Science, Częstochowa University of Technology, Częstochowa, Poland

Abstract: In this paper the problem of nonlinear vibrations of an actuated sandwich slender piezo-system is discussed. The considered system is composed of a host beam with piezoelectric patches bonded to its top and bottom surface, respectively. The host beam ends are supported to prevent longitudinal displacements. By introduction a constant and uniform electric field to each piezo element, an axial compressive or tensile piezoelectric force is induced. Once opposing directions of the electric field vector for both piezo patches, one of the piezo element is compressed, whereas the second one is under tension, what results in the system's bending. The main objective of performed studies is to analyse how different ways of piezoelectric actuation affect the system deflection, which, as a result, modifies its natural nonlinear frequency. The priority parameters are the beam and piezo elements thicknesses, the level of piezoelectric forces actuation, the pattern of forces induction. The problem is formulated on the basis of Hamilton's principle and solved with the use of a perturbation method. During the first sequence of performed calculations, the geometry of the system modified by the electric field is considered. After determination of the structure configuration, the dynamic system response is examined to find its characteristic features. It is proved that the system deflection and its nonlinear frequency depends strongly on the way of the piezoelectric forces induction. Moreover, it is shown that both the static and dynamic responses are very sensitive to any changes in physical or geometrical properties of the structure.

Keywords: piezoelectric actuation, piezoelectric bending, sandwich beam, nonlinear vibrations

1. Introduction

In recent years, smart structures solutions are strongly sought and deeply investigated by many researchers due to its properties giving the possibility of actively or passively enhance system performance. Piezoceramic rods, plates, patches, rings etc. are one of these smart elements, where under applied stress one generates voltage on its surface (direct piezoelectric effect) or under applied constant electric field a shape deformation may be observed (reverse piezoelectric effect). In engineering applications, the main goal is to enhance system prebuckling capacity and/or move the natural frequencies of elastic structures far enough from a possible excitation band. Enhancement of buckling capacity via the piezoelectric actuation in a simply supported beam with the possibility of one of the supports to move in the longitudinal direction in comparison to the beam with both ends preventing longitudinal displacements was discussed by de Faria [1]. It is proved that in the beam with both ends preventing longitudinal displacement the stress stiffening effect achieved via piezoelectric actuation allow to counteract the beam instability. Static and dynamic response control in Euler-Bernoulli beam with different end supports and a pair of perfectly bonded piezoelectric patches is discussed in [2]. It

is demonstrated that the lower the overall stiffness of the system, the higher the influence of the residual force is observed on both critical load and transversal vibration frequency. Zenz and Hummer [3] investigated critical load, tip displacements and natural vibrations in a cantilever beam subjected to the conservative compressive force, where on top and bottom surface of host beam were attached piezo patches. By introducing into the piezo elements different voltage values, system was forced to bend. It is shown forced bending influence the load-frequency relationship. In this paper the idea of using actuating bending moment is adopted for the shape and vibrations control of a simply supported beam with both ends preventing longitudinal displacements, shown in Fig. 1.

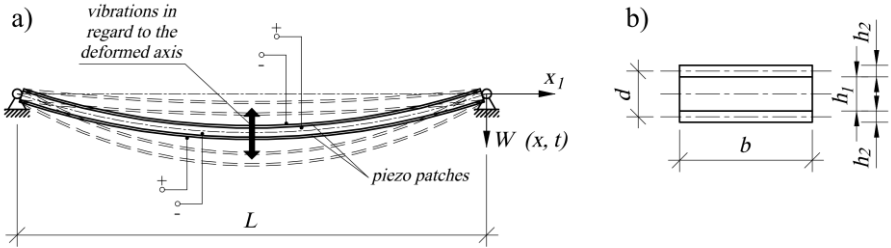


Fig. 1. Vibrations of a deformed simply supported beam via piezoelectric bending actuator (a), cross-section (b)

2. Problem statement

The main aim of this work is to investigate how different ways of piezoelectric actuation affect system deflection, which in result modifies its natural nonlinear frequency. Knowing that in slender structures the axial and bending stiffness as well as mass has a crucial influence on system dynamic response, the priority parameters are beam and piezo elements dimensions, their mechanical and electro-mechanical properties. Moreover, the level of piezoelectric forces actuation and forces induction patterns are taken under investigation.

The stated problem is formulated on the basis of Hamilton’s principle and solved with the use of perturbation method. The slenderness of the system allows to classify the problem into Euler-Bernoulli beam theory. In the first sequence of numerical calculations the system geometry affected via piezoelectric actuation is investigated. Having determined static structure configuration, the dynamic response is analysed.

It is demonstrated, that the use of different piezoelectric actuation patterns has a strong influence on system deflection and its nonlinear frequency. Moreover, it is proved that for the analysed system configuration even a small change in physical or geometrical properties may lead to quantitatively and qualitatively different static and dynamic results.

References

- [1] FARIA A.R.: On buckling enhancement of laminated beams with piezoelectric actuators via stress stiffening. *Composite Structures* 2004, **65**:187-192.
- [2] PRZYBYLSKI J., KULIŃSKI K.: Piezoelectric effect on transversal vibrations and buckling of a beam with varying cross section. *Mechanics Research Communications* 2017, **87**:43-48.
- [3] ZENZ G., HUMER A.: Stability enhancement of beam-type structures by piezoelectric transducers: theoretical, numerical and experimental investigations. *Acta Mechanica* 2015, **226**:3961-3976.

Reference model trajectory tracking in continuous-time sliding mode control

PAWEŁ LATOSIŃSKI^{1*}, ANDRZEJ BARTOSZEWICZ²

1. Institute of Automatic Control, Lodz University of Technology, B. Stefanowskiego 18/22, 90-924 Łódź [ORCID: 0000-0001-5580-352X]
2. Institute of Automatic Control, Lodz University of Technology, Stefanowskiego 18/22, 90-924 Łódź [ORCID: 0000-0002-1271-8488]

* Presenting Author

Abstract: Controller design for a continuous-time system subject to nonlinear disturbance is a complex task with many challenges. One must ensure that the effects of disturbance on system dynamics are properly compensated, while at the same time keeping state and input constraints in mind. Disturbance rejection by itself is easily achieved using sliding mode controllers (SMC). However, such controllers give no insight into the dynamics of individual state variables, which may be subject to physical constraints. In this paper we propose a solution, which allows one to benefit from the disturbance rejection property of SMC and at the same time obtain better insight into system dynamics. The proposed approach involves a reference model obtained from a canonical form of the controlled system. A sliding mode control strategy is applied to the plant with the aim of driving its state alongside that of the model. Then, since model dynamics are inherently simpler, one can modify them to impose specific constraints on the motion of the system. It is demonstrated that, when the proposed SMC strategy is applied, individual states of the original plant always exactly follow those of the model, regardless of uncertainties.

Keywords: robust control, sliding mode control, trajectory tracking, continuous-time systems

1. Introduction

Continuous-time sliding modes are an excellent tool for controlling system subject to nonlinear uncertainties, as they are able to reject the effect of matched disturbance on the system entirely [1]. However, since sliding mode controllers are based on the virtual system output referred to as a sliding variable, they do not typically provide any direct way of controlling the magnitude of individual system states. This is a concern, since in many practical applications, these states may need to follow strict physical constraints. Motivated by this problem, in our paper we propose a trajectory tracking sliding mode control scheme which imposes strict bounds on individual system states, and at the same time ensures the valuable disturbance rejection property that sliding mode controllers are known for.

In particular, in our research we explore sliding mode control of continuous-time dynamical systems transformed to the following canonical form

$$\dot{\mathbf{x}}(t) = \mathbf{A}\mathbf{x}(t) + \mathbf{b}u(t) + \mathbf{d}(t), \quad (1)$$

where state matrix \mathbf{A} , input distribution vector \mathbf{b} and disturbance \mathbf{d} are expressed as

$$A = \begin{bmatrix} 0 & 0 & 1 & \cdots & 0 \\ 0 & 0 & 0 & & 0 \\ \vdots & & & \ddots & \vdots \\ 0 & 0 & 0 & & 1 \\ -a_0 & -a_1 & -a_2 & \cdots & -a_{n-1} \end{bmatrix}, \quad \mathbf{b} = \begin{bmatrix} 0 \\ 0 \\ \vdots \\ 0 \\ 1 \end{bmatrix}, \quad \mathbf{d}(t) = \begin{bmatrix} 0 \\ 0 \\ \vdots \\ 0 \\ f(t) \end{bmatrix} \quad (2)$$

for a certain nonlinear function $f(t)$ and constants a_0, \dots, a_{n-1} . The objective of this paper is to design a reference model of system (1) which will ensure desirable state dynamics in the absence of disturbance. Then, a trajectory tracking control scheme will be applied to the original plant with the aim of driving its state towards that of the model, thus satisfying state constraints imposed on the system.

2. Results and Discussion

The approach proposed in our paper uses a disturbance-free reference model of plant (1), in which feedback gains a_0, \dots, a_{n-1} are omitted. In other words, the model is essentially an n -th order integrator, which is inherently easy to control. In particular, we use linear state-feedback control with feedback gains selected to ensure that all states of the model stay within specific bounds. Then, a sliding mode control strategy is applied to the plant in order to drive its states alongside those of the model.

It is demonstrated that the proposed continuous-time sliding mode control scheme with a reference model ensures that the specified state trajectories are always followed exactly. This is achieved even in the presence of nonlinear uncertainties, which means that physical constraints placed on the system can be satisfied even in difficult conditions. Similar model reference schemes have been proposed in the past [2], but in this work we explicitly prove that exact trajectory tracking can be achieved in an uncertain continuous-time system.

It is known that perfect disturbance rejection in sliding mode control is only possible in a purely continuous-time system. When the digital implementation of the control scheme is considered, one observes the undesirable chattering phenomenon, i.e. high frequency oscillations around the target state [3]. This phenomenon is also present when our approach is applied to the plant. However, it can be demonstrated that, if proper disturbance compensation based on past data is applied, the magnitude of these oscillations can be reduced to a negligible level [4]. Thus, it can be concluded that for all practical purposes, our approach ensures full disturbance rejection and ensures boundedness of all system states.

References

- [1] SHTESSEL Y, EDWARDS C, FRIDMAN L, LEVANT A: *Sliding Mode Control and Observation*. Springer: New York, 2014.
- [2] BARTOSZEWICZ A, ADAMIAK K: Reference trajectory based discrete time sliding mode control strategy. *International Journal of Applied Mathematics and Computer Science*. **29**(3): 87-97.
- [3] UTKIN V, LEE H: Chattering problem in sliding mode control systems. *International Workshop on Variable Structure Systems (VSS'06)*: 346-350, 2006.
- [4] BARTOLINI G, PISANO A, USAI E: Digital sliding mode control with $O(T^3)$ accuracy. In: *Advances in Variable Structure Systems*. World Scientific Publishing, 2000.

Analysis of non-slipping conditions for Omni wheels based on investigations of the dynamics of a highly maneuverable mobile robot

I. S. MAMAEV^{1*}, YU. L. KARAVAEV², V. A. SHESTAKOV³

1. Kalashnikov Izhevsk State Technical University/ Department of Mechatronic Systems, Izhevsk, Russia; Udmurt State University/ Ural Mathematical Center, Izhevsk, Russia [0000-0003-3916-9367]
2. Kalashnikov Izhevsk State Technical University/ Department of Mechatronic Systems, Izhevsk, Russia; Chuvash State University, Cheboksary, Russia [0000-0002-6679-1293]
3. Kalashnikov Izhevsk State Technical University/ Department of Mechatronic Systems, Izhevsk, Russia [0000-0002-1007-8261]

Abstract: The paper presents the investigations of the dynamics of Omni wheels considered as part of a mobile platform. The equations of motion are presented in the form of Lagrange equations of the second kind with undetermined multipliers. The investigation of the dynamics is based on the analysis of reaction forces, acting on wheels from the side of the support surface. The analysis of the dependences of reaction forces is carried out for different motion parameters: velocities, accelerations, and trajectory curvature.

Keywords: omnidirectional mobile robot, nonholonomic model, slipping, simulation.

1. Introduction

Mobile robots with omniwheels have a distinctive feature – the ability to implement omnidirectional motion. Control tasks for a mobile robot with omniwheels were previously considered in [1] – [4]. However, for mobile robots with omniwheels the control actions can be determined if the non-slipping conditions for wheels are satisfied. This work is devoted to the investigation of the dynamics of wheels for various motion parameters: velocities, accelerations, and trajectory curvature.

2. Mathematical model

Let's consider the robot's motion in a horizontal plane (see Fig. 1a). Details on the design, kinematic and dynamic models of the mobile platform with omniwheels can be found in [1, 2]. In other works [5, 6] the dynamics of mobile robots with omniwheels is considered only for limited sets of trajectory segments.



Fig. 1. a) The scheme of a mobile platform with omniwheels and b) curvilinear trajectory of motion

To determine the possibility of implementing motion along a trajectory with different motion parameters consider the dynamics of an individual wheel as part of a mobile platform. The equations of motion of an individual wheel consider in the form of Lagrange equations of the second kind with undetermined multipliers relative to the coordinate system associated with the mobile robot (see Fig. 1a):

$$m_i \dot{v}_i + m_i \omega \mathbf{J} \mathbf{v}_i = \frac{\lambda_i}{(\alpha_i, p_i) h_i} \alpha_i + \mu_i, \quad (1)$$

$$I \dot{\omega} = -(\mu_i, \mathbf{J} \gamma_i). \quad (2)$$

Solving the system (1)-(2) relative to undetermined multipliers λ_i , taking into account the radius of curvature of the trajectory, we obtain:

$$F_i = \frac{(\alpha_i, p_i)}{(\alpha_i, \mathbf{J} \gamma_i)} \left((I + m_i \gamma_i^2) \ddot{\theta} + m_i (\mathbf{Q} \tau, \mathbf{J} \gamma_i) \ddot{s} + m_i (\mathbf{Q} n, \mathbf{J} \gamma_i) \frac{\dot{s}^2}{R} + 2 m_i (\mathbf{Q} \tau, \gamma_i) \dot{\theta} \dot{s} \right), \quad (3)$$

where $F_i = (\lambda_i / h_i)$ - the module of the reaction force, acting on the i th wheel from the side of the support surface, \dot{s} - the module of linear velocity, $\dot{\theta}$ - angular velocity of the mobile robot.

The resulting expression (3) describes a combination of several cases of mobile robot's motion. These cases require separate consideration:

1. Non-stationary motion along a straight line with a constant orientation.
2. Non-stationary rotation.
3. Stationary motion along a straight line with constant linear and angular velocities.
4. Stationary motion along a curvilinear trajectory with a constant orientation.

3. Conclusion

In this work, the influence of velocities, accelerations and trajectory curvature was determined based on investigations of the dynamics and numerical modeling.

Acknowledgment: The work was carried out within the framework of the state assignment of the Ministry of Education and Science of Russia FZZN-2020-0011.

References

- [1] Borisov A. V., Kilin A. A., Mamaev I. S., Dynamics and Control of an Omniwheel Vehicle, Regular and Chaotic Dynamics, 2015, vol. 20, no. 2, pp. 153-172.
- [2] Kilin A. A., Bobykin A. D. Control of a Vehicle with Omniwheels on a Plane // Russian Journal of Nonlinear Dynamics, 2014, vol. 10, no. 4, pp. 473-481.
- [3] Kilin A., Bozek P., Karavaev Y., Klekovkin A., Shestakov V. Experimental investigations of a highly maneuverable mobile omniwheel robot // International Journal of Advanced Robotic Systems, 2017, vol. 14, no. 6, pp. 1-9.
- [4] Shestakov V. A., Mamaev I. S., Karavaev Yu. L. Controlled motion of a highly maneuverable mobile robot along curvilinear trajectories // 2020 International Conference Nonlinearity, Information and Robotics (NIR), 2020, pp.1-4, doi: 10.1109/NIR50484.2020.9290159.
- [5] Hendzel Z., Rykala L. Modelling of dynamics of a wheeled mobile robot with mecanum wheels with the use of lagrange equations of the second kind // Int. J. of Applied Mechanics and Engineering, 2017, vol. 22, no. 1, pp. 81-89.
- [6] Abdelrahman M., Zeidis I., Bondarev O., Adamov B., Becker F., Zimmermann K. A description of the dynamics of a four-wheel mecanum mobile system as a basis for a platform concept for special purpose vehicles for disabled persons // 58th Ilmenau Scientific Colloquium, 2014, pp 1 – 10.

The modelling of breaking control of electric vehicle

MARCIN MIROSLAW^{1*}, JAKUB DEDA², TOMASZ MIROSLAW²

1. Warsaw University of Technology, Faculty of Power and Aeronautical Engineering, Institute of Aeronautics and Applied Mechanics
2. Warsaw University of Technology, Faculty of Automotive and Construction Machinery Engineering, Institute of Vehicles and Construction Machinery Engineering

* Presenting Author

Abstract: In this paper the problem electric vehicle braking is presented with its model. For year many systems have been developed and introduced as the standard to conventional vehicle with any kind of ICE. Currently the electrical vehicle safety system follow it adding the function of energy recuperation, but electric motors give more various opportunities and function. The braking with energy recuperation makes the: hybrid or battery EV more ecological in urban use. But some problems appear during emergency braking in any kind of vehicle. In the paper the overview of most popular electric vehicle propelling systems is presented with their physical and mathematical models. Classical scenarios of emergency braking with various control algorithms for DC and AC motors is simulated and discussed. The thesis about the self-adjustment of braking force by DC or asynchronous electric motor shortage (dynamic braking) is set and verified. In the simulation the phenomena of: batteries recharging current limitation, tire slip and wheel blocking have been taken account and modelled.

Keywords: Emergency braking, electric vehicle propelling systems, complex electric vehicle model, EV emergency braking

1. Introduction

The vehicle braking is extremely important for safety of vehicle occupant and others on the road. The ICE vehicle can break with motors movement resistance or brakes. Contemporary modern ICE vehicle control of braking process to avoid the wheel blocking with the board-computers. The standardized ABS systems are responsible for safety during braking by controlling the wheel rotation speed and releasing the braking force when one wheel is blocked. If all wheels are blocked system can not react. Blocked wheels are sliding on the road and aren't able to control the vehicle movement direction. Other problem is the value of propelling and braking force which depends on slip s defined as [1,2,3,4,5]:

The typical characteristic of friction coefficient $\mu(s)$ to the slip is presented in figure 1. [1, -6].

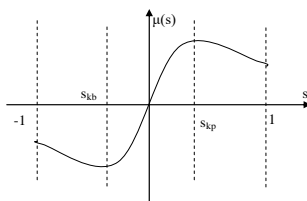


Fig. 1. The typical characteristic of friction coefficient to the slip

The most effective braking is when the slip is S_k . It is not easy to be reached for ICE driven vehicle. If we use the electric motors, we can control it braking with motor. In EV we can use various strategy of electric motor braking. In the paper the usage of dynamic braking as self-force adjustable system is discussed and modeled.

2. Results and Discussion

For simulation of dynamic process series of model has been developed. As the first approach the one wheel model (fig.2) was built with battery Control Device CD, Motor M and wheel to road interaction.

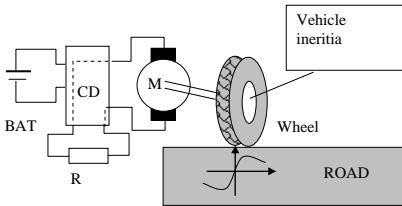


Fig. 2. The Electric vehicle driving system model with: BAT – battery, CD – transistor switch control device, R- resistor; M Permanent magnet DC motor

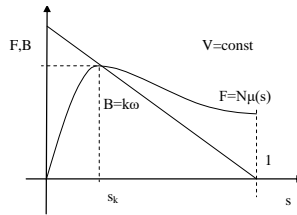


Fig. 3. The relation of motor dynamic braking and tire braking force slip characteristic

The concept of emergency dynamic braking base on assumption of self -optimization of braking force as the interaction of braking characteristics for tire and motor (fig.3)

For verification the full 3D model of electric vehicle was built in 4 versions [8,9,10]: One axle on motor drive; 2 axle two motor drive, one axle two motor (wheel with motor) drive. As the result of simulation for dynamic braking and dynamic braking controlled with transitory and energy recuperation with resistance control is presented in fig. 4

3. Concluding Remarks

Application of dynamic braking simplifies the control of maximum braking force seems to be promising of many advantages like less harmful for batteries energy recuperation, mitigation of brakes pads wears etc.

Such a solution is self-adjustable and fault tolerant in wider range than other braking strategies.

The combination of dynamic control with energy recuperation improves the battery recharging efficiency and safety.

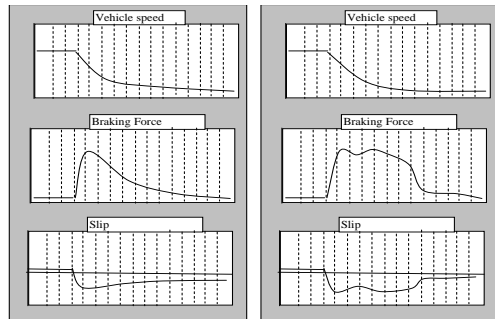


Fig. 4. Result of simulation. with constant shortage resistance a) with controlled shortage resistance and energy recuperation

References

- [1] B. GORIACZKIN, THEORY OF WHEEL, (1937).
- [2] M. BEKKER, : INTRODUCTION TO TERRAIN-VEHICLE SYSTEMS. (1969).
- [3] A. GREČENKO, AGRARTECHNISCHE KOLLOQUIUM, 69, 4 (1989)
- [4] D. KUTZBACH, GRUNDLADEN LANDTECHNIK 32, 2 (1982).
- [5] H.PACEJKA, TIRE AND VEHICLE DYNAMICS, (2006).
- [6] G. ERDOGAN, VEHICLE SYSTEM DYNAMICS IJVM 51, 5 (2013)
- [7] M. SCHREIBER, D. KUTZBACH, TERRAMECHANICS, 44, 6 (2007)
- [8] T. MIROSLAW, Z. ŻEBROWSKI, THEORETICAL AND EXPERIMENTAL ANALYSIS, SPRINGER PROCEEDINGS IN MATHEMATICS & STATISTICS, PP. 261-278 (2016)
- [9] T. MIROSLAW, Z. ŻEBROWSKI, PRZEGLĄD MECHANICZNY 6`13, PP. 37-41 (2013).
- [10] T. MIROSLAW, ZAMM 101, 2 (2021)

The Modelling of Autonomous Control with Hazard of Measurement Noise and Errors

MARCIN MIROSLAW^{1*}, JAKUB DEDA², TOMASZ MIROSLAW²

1. Warsaw University of Technology, Faculty of Power and Aeronautical Engineering, Institute of Aeronautics and Applied Mechanics
2. Warsaw University of Technology, Faculty of Automotive and Construction Machinery Engineering, Institute of Vehicles and Construction Machinery Engineering

* Presenting Author

Abstract: Autonomous vehicles are introduced to everyday life. Currently they are mainly on test tracks, but very soon they will be on our roads. The risk of vehicle mistake is currently discussed, and it mitigate the grow of public road application. Although the sensors for autonomous vehicles and algorithms make great progress, the risk of mistake and non-responsibility for that is still great problem. Especially when some error synergy appears and the system have to recognise mistake. The article discusses the typical design and sensors used for vehicle autonomy. The methodology of simulation of control system and sensors, with randomly modified scenarios of situation changing or sensor's fault is proposed. The model of control system with self-learning by experience is presented.

Keywords: Risk of autonomation, vehicle situation awareness sensors, machine learning, risk evaluation,

Design Approach for Isolated Buildings in Adequacy with Algerian Regulations and Their Comparison with Several International Codes

OUNIS HADJ MOHAMED^{1*}, ABDEDDAIM MAHDI², OUNIS ABDELHAFID³

1. Department of civil engineering, University Mostepha Benboulaïd, Batna2 Algeria

2. Faculty of Science and technology, University Mohamed Khider Biskra, Algeria

3. Department of civil engineering, University Mohamed Khider Biskra, Algeria

* Presenting Author

Abstract: In recent decades, base Isolation represented a new approach and a very promising alternative, allowing the protection of structures against strong earthquakes and winds. Therefore, several codes around the world have introduced chapters relating to the base isolation technique. It is essential to put forward a new methodology design relating to isolated buildings in the Algerian earthquake regulations. The aims of this research suggest a new design approach for LRB type isolators (Lead Rubber Bearing), based on the equivalent static method, and it employs an iterative process that determines the isolator's displacement design depending on the mechanical and geometric characteristics of the building. Thus, to confirm the proposed model validity, a vast parametric study was undertaken using an isolated building with the same geometric and mechanical characteristics, as well as, the same soil conditions used in different regulations in the world such as Japanese, Chinese, Taiwanese, Italian, IBC 2000 and Algerian. The results obtained from this new design approach show a very good agreement with the various international codes envisaged.

Keywords: Base isolation, Lead Rubber Bearing, Algerian seismic code, Hysteresis behaviour

1. Introduction

Following the devastating earthquakes affecting several countries in the world, such as the Northridge in 1994 in the USA, Hyogoken-Nanbu in 1995 in Japan, Chi-Chi in 1999 in Taiwan, Wenchuan in 2008 in China, and the L'Aquila earthquake 2009 Italy, the base isolation technology has been extensively deployed in these countries with high seismicity. During this period, seismic codes have been revised and improved to introduce requirements for buildings seismic design with base isolation [9].

At the national level and following the recent earthquake events in Algeria, considerable damages and heavy casualties were recorded; this is due to the shortcomings of the design practices and even the inadequacy of controlling buildings seismic response.

The equivalent linear method analysis, based primarily on one DOF system, is used in several international anti-seismic regulations. However, the restrictive assumptions and conditions for applying this method involve certain limitations.

Following the normative code development in the world, a new review is important for improving the current Algerian regulations by introducing the vibration control techniques to mitigate significantly the excess of energy developed by earthquakes. Therefore, the introduction of a chapter on the vibration control technique in the Algerian seismic code becomes essential.

2. Equivalent linear analysis in accordance with the Algerian seismic regulations

2.1. Process of the proposed method

The convergence process of the equivalent linear analysis method is summarized as follows:

1. It is assumed an initial displacement of the isolation system D_D ,
2. The effective stiffness and the effective damping (ξ) of the isolation system were calculated,

$$K_e = \frac{Q_d}{D_d} + K_2 \quad \xi = \frac{2Q_d}{\pi K_e D_d} \left[1 - \frac{Q_d}{(\beta - 1)D_d K_2} \right] \quad \beta = 13$$

3. The equivalent period of the isolation system was computed as follows: $T_e = 2\pi \sqrt{\frac{M}{K_e}}$

4. The reduction factor and the spectral acceleration: $\eta = \sqrt{\frac{7}{(2 + \xi)}}$ $S_a(T_e)$

5. A new design displacement was acquired: $D_d = \frac{F_{ek}}{K_e}$

6. Steps 1 to 5 are repeated until convergence of the design displacement.

2.2 Analytical model and assumptions

The model used in this analysis is a ten-stories building in reinforced concrete with a rectangular plan of $15 \times 20 \text{ m}^2$ composed of four bays in the longitudinal direction and three bays in the transverse direction with a length of 5 m each. The beams are of section $30 \times 45 \text{ cm}^2$, the columns are of section $50 \times 50 \text{ cm}^2$ and the story height is 3 m with solid 20 cm thick slabs [21].

The bilinear behavior of the LRB isolation system, making it possible to successively determine the geometric and mechanical characteristics of the different types of isolators considered in this study.

3. Results

This investigation allowed us to obtain the following results:

- The design displacement of the LRB isolator obtained by the American code IBC2000, estimated at 22.41 cm, is very close to the value found by the proposed approach for the Algerian earthquake code, estimated at 28.46 cm.
- The base shear force evaluated by the novel approach for the Algerian seismic code concurs with the nonlinear analysis method according to the IBC2000 code for near source seismic excitations, with more than 90% similar results.

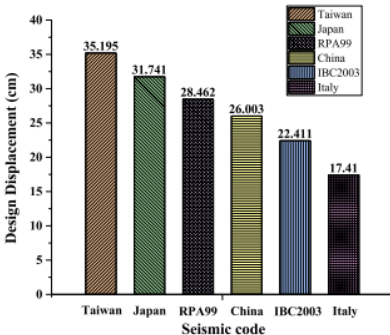


Fig. 6 Design displacement between different codes

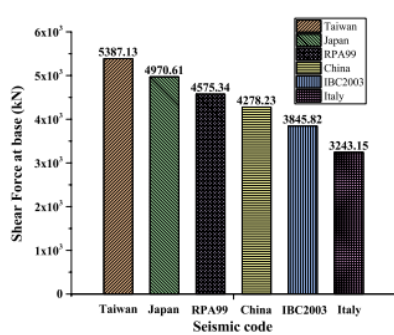


Fig. 7 Shear base between different codes

4. Conclusion

The new approach gives very good results according to various regulations cited in literature. The response in design displacement and shear force at the base obtained by the proposed method represents an average value considering the various regulations.

A comparative analysis of the proposed approach, based mainly on the equivalent linear method, with the nonlinear history analysis shows good agreement for seismic excitations at near field.

5. References

- [1] KANAMORI H: QUANTIFICATION OF EARTHQUAKES. NATURE (1978),**271**(5644): 411
- [2] TAKEWAKI I: *BUILDING CONTROL WITH PASSIVE DAMPERS OPTIMAL PERFORMANCE-BASED DESIGN FOR EARTHQUAKES*. JOHN WILEY & SONS, 2011.
- [3] KELLY J. M: ASEISMIC BASE ISOLATION: REVIEW AND BIBLIOGRAPHY. SOIL DYNAMICS AND EARTHQUAKE ENGINEERING 1986, **5**(4): 202-216.
- [4] CAMERON, W I., GREEN R. A. DAMPING CORRECTION FACTORS FOR HORIZONTAL GROUND-MOTION RESPONSE SPECTRA. BULLETIN OF THE SEISMOLOGICAL SOCIETY OF AMERICA, 2007,**97**(3), 934–960.
- [5] DJEDOU N, OUNIS A., MAHDI A. AND S. ZAHRAI M. SEMI-ACTIVE FUZZY CONTROL OF TUNED MASS DAMPER TO REDUCE BASE-ISOLATED BUILDING RESPONSE UNDER HARMONIC EXCITATION. JORDAN JOURNAL OF CIVIL ENGINEERING 2018, **12**(3).
- [6] BHANDARI M., BHARTI S., SHRIMALI M. AND DATTA T. PERFORMANCE OF BASE-ISOLATED BUILDING FRAME FOR EXTREME EARTHQUAKES. RECENT ADVANCES IN STRUCTURAL ENGINEERING 2019, VOLUME 1, SPRINGER: 1025-1036.
- [7] OUNIS, H. M. AND OUNIS A. PARAMETERS INFLUENCING THE RESPONSE OF A BASE-ISOLATED BUILDING. SLOVAK JOURNAL OF CIVIL ENGINEERING 2013, **21**(3): 31-42.
- [8] FENG D., MIYAMA T., LIU W., YANG Q. AND CHAN T.-C. (). "A NEW DESIGN PROCEDURE FOR SEISMICALLY ISOLATED BUILDINGS BASED ON SEISMIC ISOLATION CODES WORLDWIDE." PROCEEDINGS OF 15WCEE 2012.
- [9] MEVADA, S. V. AND JANGID R. SEISMIC RESPONSE OF TORSIONALLY COUPLED SYSTEM WITH SEMI-ACTIVE VARIABLE DAMPERS." JOURNAL OF EARTHQUAKE ENGINEERING 2012, **16**(7): 1043-1054

Neural network modelling for steering control of an automated guided logistic train

WOJCIECH PASZKOWIAK^{1*}, MARCIN PELIC², TOMASZ BARTKOWIAK³

1. Poznan University of Technology, Poland [ORCID: 0000-0003-2571-6737]

2. Poznan University of Technology, Poland [ORCID: 0000-0002-5076-8128]

3. Poznan University of Technology, Poland [ORCID: 0000-0002-4715-6358]

* Presenting Author

Abstract: The logistic train is a modern intralogistics transport system that consists of a tractor and towed trailers. It bases on the concept of a milk-runner which collects or supplies a defined number of delivery points with a precise amount of material at a given point of time on a pre-planned route. It is also difficult to achieve the same trajectory for a manually operated train for multiple train runs. The problem complicates if there are multiple towed trailers or dynamic drive on slippery ground are present. One solution to this problem is to replace the driver with an automated steering system. This paper presents a dynamic model of a logistic train, based on the Lagrange formalism, which is controlled by artificial neural networks. The artificial neural network algorithm provides the most appropriate tractor steering input parameters for a given transportation area. The result of integration of the dynamic model developed in Mathematica and the neural network modelled in Python is presented in a graphic form. The modelled algorithm ensures a collision-free ride of the train.

Keywords: logistic train, vehicle, neural network, dynamic model

1. Introduction

Intensive development of intralogistics is the reason for seeking new solutions for improving material flow in manufacturing systems. An example of such a solution is a logistics train. This is an applied means of transport across all sectors of production supply, especially in the intralogistics [1]. A logistic train is usually called a milk-runner, which concept is derived from the method of delivering or receiving supplies in the dairy industry. The idea is to regularly visit assigned locations by one supplier in a single run [2]. Milk run system minimizes the total distance travelled, as a single vehicle is used instead of many, especially in case of repeatable flow of materials between the same locations.

The discussed train consists of a tractor and a certain number of trailers also called logistics trolleys. The tractor usually has an Ackermann steering system. Rear wheels are fixed and front wheels are castor wheels. There exist three different steering kinematics for trailer and the most advanced is double Ackermann system [3]. For this steering system, a number of degrees of freedom is higher than for others assuming the same number of trolleys. Paszkowiak and Bartkowiak, presented a brief comparison of dynamics of a logistic train with different steering systems [3, 4].

A simple trajectory control for logistic train was applied using a PD controller. This was done for the kinematic model of logistic train with a double Ackermann steering system. This was first attempt to control the automated logistic train. Dynamic model of logistic train was not considered yet with a control system, especially with artificial neural network.

2. Results and Discussion

In our work is used the dynamic model of a logistic train developed by Paszkowiak and Bartkowiak. The main equations of this system are based on Lagrange formalism [3]. The developed control system is based on iterative model of a logistic train. Exemplary drive of a train in a given corridor as shown in Fig. 1. Sensors are placed on the tractor and each trailer.



Fig. 1. Train transport corridor and visualization of the distance between sensors and obstacles

Algorithm of the artificial neural network generates input data (torques applied to wheels) for the tractor. Simulation time is very short to ensure real-time of response to the environment. The distance to obstacles from each unit is determined based on new position of the logistic train obtained by simulation. The distance travelled by the tractor and information about collision are also obtained. These data are sent to the neural network model, which choose new input data for the tractor. Again, the data is used to run the simulation. This process is repeated until a collision occurs (Fig. 2).

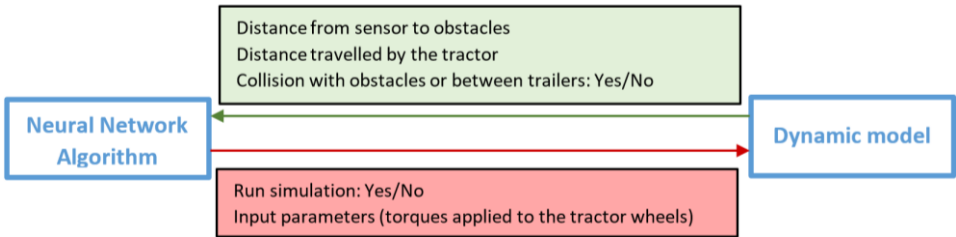


Fig. 2. The iterative process – connection between the Neural Network Algorithm and the dynamic model

3. Concluding Remarks

Modern control system based on the Neural Network Algorithm has been developed. The artificial neural network algorithm provides the most appropriate tractor steering input parameters for a given transportation area. The modelled algorithm ensures a collision-free ride of the train.

References

- [1] LIEB C, PRINZ T, GUNTNER W, FOTTNER J: Modeling and Simulation of Generic Handling Operations in In-Plant Milk-Run Systems. . *8th International Conference on Industrial Technology and Management (ICITM)* 2019.
- [2] KLUSKA K, PAWLEWSKI P: The use of simulation in the design of Milk-Run intralogistics systems. *IFAC-PapersOnLine* 2018, **51**(11):1428-1433.
- [3] PASZKOWIAK W, BARTKOWIAK T: Dynamic Model Of A Logistic Train With Different Steering Systems And Tire Models. *Latin American Journal of Solids and Structures* 2021, **18**(1):e339.
- [4] PASZKOWIAK W, BARTKOWIAK T, PELIC M: Kinematic Model of a Logistic Train with a Double Ackermann Steering System. *International Journal of Simulation Modelling* 2021, **20**(2):243-254.

Analysis of practical application aspects for an active control strategy to Civil Engineering structures

FIDELIU PAULET-CRAINICEANU^{1*}, VITALIE FLOREA², SEPTIMIU GEORGE LUCA³,
CRISTIAN PASTIA⁴, OCTAVIAN VICTOR ROSCA⁵

1. “Gheorghe Asachi” Technical University of Iasi, Romania [0000-0003-2337-4702]
2. “Gheorghe Asachi” Technical University of Iasi, Romania [0000-0002-8060-639X]
3. “Gheorghe Asachi” Technical University of Iasi, Romania [0000-0002-9022-2795]
4. “Gheorghe Asachi” Technical University of Iasi, Romania [0000-0002-6603-1294]
5. “Gheorghe Asachi” Technical University of Iasi, Romania

* Presenting Author

Abstract: Last years have brought the use of information technology in all domains. For Civil Engineering, the Smart City concept, involving the new technologies, is pointing to (among other aspects) the community safety. In this line, a structural active control strategy based on full states LQR optimal control has been relatively recent improved, numerically tested and verified. In order to apply this newer strategy, practical aspects are in the views of the present work: reduced order controller, observer introduction, time delay effects and their consequences on the effectiveness of the control strategy. The numerical simulations are performed on a multi-storey building loaded by strong earthquakes’ recorded accelerations. Using in-house software under Matlab, the seismic response of the structures is simulated and evaluated after introduction of Active Tuned Mass dampers. Time and frequency domain responses are obtained. The viability of the improved strategy involving application of practical considerations is determined and discussed.

Keywords: active control, seismic response, Active Tuned Mass dampers, reduced order controller

1. Introduction

Requirements of already continuous technological revolution, are pointing toward security of urban communities. Civil Engineering plays a major and, in many cases, critical role in assuring the safety of structures’ inhabitants or users. Strong earthquakes and strong winds are between the most stressing loads acting buildings and bridges. Therefore, any technological methods for obtaining a better behaviour to these loads is needed. Passive and active structural control are using devices, as Tuned Mass Dampers (TMDs) and Active Mass Dampers (AMDs), as possible solutions.

Optimal active structural control, in the form of Linear Quadratic Regulator (LQR), have been studied in [1] using a full state strategy. The weighting matrices Q and R had been proposed (based on an energy approach) in a simple manner to just one variable, r , as shown in Equation (1) and where \mathbf{K}_s and \mathbf{M}_s are the structure’s stiffness and mass matrices.

$$\mathbf{Q} = \begin{bmatrix} \mathbf{K}_s & 0 \\ 0 & \mathbf{M}_s \end{bmatrix} = \begin{bmatrix} \mathbf{Q}_1 & 0 \\ 0 & \mathbf{Q}_2 \end{bmatrix}, \mathbf{R} = \text{diag} \{ r_1 \quad \dots \quad r_m \} = \mathbf{R} = r\mathbf{I} \quad (1)$$

The methodology in [1] had been relatively recent improved in [2]. It was mathematically shown that the $2n$ -dimensional Riccati Equation (2)

$$\mathbf{P}\mathbf{A} - \mathbf{P}\mathbf{B}\mathbf{L}_1\mathbf{R}^{-1}\mathbf{L}_1'\mathbf{B}'\mathbf{P} + \mathbf{A}'\mathbf{P} + \mathbf{Q} = \mathbf{0} \quad (2)$$

can be reduced to two one n-dimensional Riccati equations, (3) and (4).

$$\mathbf{P}_{12}\mathbf{A}_{21} - \mathbf{P}_{12}\mathbf{B}_2\mathbf{R}^{-1}\mathbf{B}'_2\mathbf{P}_{21} + \mathbf{A}'_{21}\mathbf{P}_{21} + \mathbf{Q}_1 = \mathbf{0} \quad (3)$$

$$\mathbf{P}_{21} + \mathbf{P}_{22}\mathbf{A}_{22} - \mathbf{P}_{22}\mathbf{B}_2\mathbf{R}^{-1}\mathbf{B}'_2\mathbf{P}_{22} + \mathbf{P}_{12} + \mathbf{A}'_{22}\mathbf{P}_{22} + \mathbf{Q}_2 = \mathbf{0} \quad (4)$$

Equation (3) is a symmetric Riccati equation while the Equation (4) is a non-symmetric one.

2. The methodology and applications

In reference [3], the proposed improved methodology was numerically tested and verified. Typical time response and spectral seismic response are shown in Figure 1 (left and center).

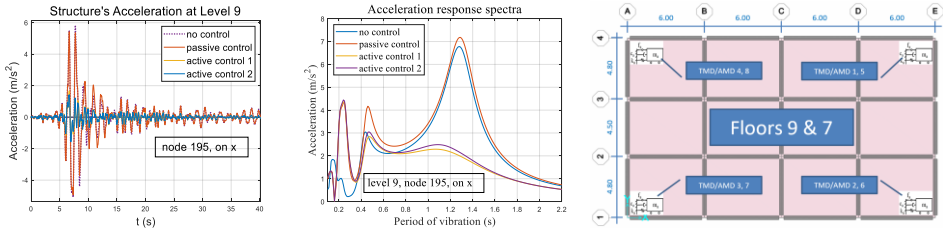


Fig. 1. Left and center: typical time and spectral seismic response; right: plan of TMDs/AMDs locations

The numerical simulations are performed on a multi-storey building loaded by strong earthquakes' recorded accelerations. In Figure 1 (right side), the plan of TMDs/AMDs typical locations on building is presented.

The initial methodology in [1] was used also in [4] for use with reduced order controller, observer and time delay effects. Their consequences on the effectiveness of the control strategy were evaluated. For the present study, the goal is to adapt the improved methodology in [3] for the same practical aspects of implementations.

3. Concluding remarks

Improvements had been made to an optimal active control strategy based on obtaining gain matrix calculations on two half size-dimensional Riccati equations. Results of implementing this new technique are shown. In addition, the extended paper is presenting the details and conclusions of simulations' results when practical aspects (as reduced order controller, observer introduction, time delay) are also implemented.

References

- [1] PAULET-CRAINICANU F: Seismic response control of long cable-stayed bridges. *Proc. the 2nd World Conf. on Structural Control*, Vol. 2, 959-964. John Wiley & Sons: Chichester, 1999.
- [2] PAULET-CRAINICANU F, LUCA S-G, PASTIA C, FLOREA V: Improved strategy for optimal control of Civil Engineering structures. *15th Int. Conf. on Computational Civil Engineering*, IOP Conference Series: Materials Science and Engineering, Vol. 586, 1, 1-6 (online). IOP Science: Bristol, 2019.
- [3] PAULET-CRAINICANU F, FLOREA V, PASTIA C, LUCA S G, ROSCA O V: Performance analysis for an improved strategy in optimal control of Civil Engineering structures. *16th Int. Conf. on Computational Civil Engineering*, IOP Science: Bristol, 2021 (in print).
- [4] BAKULE L, PAULET-CRAINICANU F, RODELLAR J, ROSSELL J M: Overlapping Reliable Control for a Cable-Stayed Bridge Benchmark. *IEEE Trans. C.S.T.* 2005, **13**, 4, 663-669.
- [5] THE MATHWORKS INC: *Matlab R2021a*, www.mathworks.com. 2021.

Energy flow control in a system of coupled pendulums using magnetic field

Valery Pilipchuk^{1a}, Krystian Polczyński^{2b}, Maksymilian Bednarek^{2c*}, Jan Awrejcewicz^{2d}

1. Department of Mechanical Engineering Wayne State University 5050 Anthony Wayne Drive, Detroit, Michigan 48202, U.S.A. ^a pilipchuk@wayne.edu [0000-0001-7051-3539]
2. Department of Automation, Biomechanics and Mechatronics Lodz University of Technology 90-924 Lodz, 1/15 Stefanowskiego Str., A22, Poland ^bkrystian.polczynski@dokt.p.lodz.pl [0000-0002-1177-6109], ^cmaksymilian.bednarek@dokt.p.lodz.pl [0000-0002-7669-119X], ^djan.awrejcewicz@p.lodz.pl [0000-0003-0387-921X]

* Presenting Author

Abstract: In the presented work, we proposed a methodology of controlling the resonance energy exchange in mechanical systems by creating appropriate electromagnetic fields around the system's structural subcomponents. It has been shown theoretically and confirmed experimentally that properly guided magnetic fields can effectively change mechanical potentials in such a way that the energy flow between the oscillators takes the desired direction. In particular, a model of two weakly coupled pendulums subjected to an electromagnetic load using a specific set of descriptive functions was considered. The developed control strategies are based on the observation that, in the case of antiphase oscillation, the energy is moving from the pendulum, which is in the repelling magnetic field, to the oscillator not subjected to magnetic field. The advantage of the suggested control strategy is that the temporal rate of inputs is dictated by the speed of beating, which is relatively slow compared to the carrying oscillations.

Keywords: Resonance energy exchange, magnetic pendulums, beating control, feedback loop

1. Introduction

Passive control of the energy flow between a recipient and a donor has been considered in both physics and engineering based on different physical principles [1-4]. In the presented work, we suggest to actively guide the direction of energy flow by generating appropriate magnetic fields around the interacting mechanical oscillators. In the present illustrating example, two pendulums are weakly coupled with torsion spring (see Fig. 1). One of the pendulums is endowed with a magnet which is placed above an electric coil. A specific electric current in a form of $i(t) = 0.001 + 0.1 \sin^2(\pi t / 10.31)$ was chosen to enhance passive transition of energy from one pendulum 1 to pendulum 2. System is described by equations (1) and (2).

$$\frac{d\phi_j}{dt} = v_j, \quad \frac{dv_j}{dt} = -\Omega^2 \phi_j - f_j; \quad j=1,2, \quad (1)$$

$$f_1 = 2\Omega \left[\zeta_1 \operatorname{sgn} \dot{\phi}_1 + \nu(\dot{\phi}_1 - \dot{\phi}_2) \right] + \Omega^2 \left[\beta(\phi_1 - \phi_2) - \frac{1}{6} \phi_1^3 \right] - \frac{i_1(t)}{J} \frac{dU_{\text{mag}}(\phi_1)}{d\phi_1}, \quad f_2 = 2\Omega \left[\zeta_2 \operatorname{sgn} \dot{\phi}_2 + \nu(\dot{\phi}_2 - \dot{\phi}_1) \right] + \Omega^2 \left[\beta(\phi_2 - \phi_1) - \frac{1}{6} \phi_2^3 \right] \quad (2)$$

2. Results and Discussion

The sample results of direct simulations and comparison with experimental data are illustrated in Fig 2. The solution of numerical integration of eqs. (1)-(2) are represented by Fig. 2b. At this point, we make preliminary remarks on some effects already observed from simulations. In particular, fragments (c), (d) of Fig. 2 show the response quite different compared to the response of a free system (b) under zero input currents. It is confirmed that in the case of free vibration, the total energy is gradually dissipating while its very small portion keeps moving from one pendulum to another in beat wise manner. In contrast, the gradually increasing currents eventually break the symmetry in such a way that the energy is almost completely transferred from the pendulum 1 with positive input current to the pendulum 2. The effect becomes most explicit in case of two magnets combining both attracting and repelling properties.

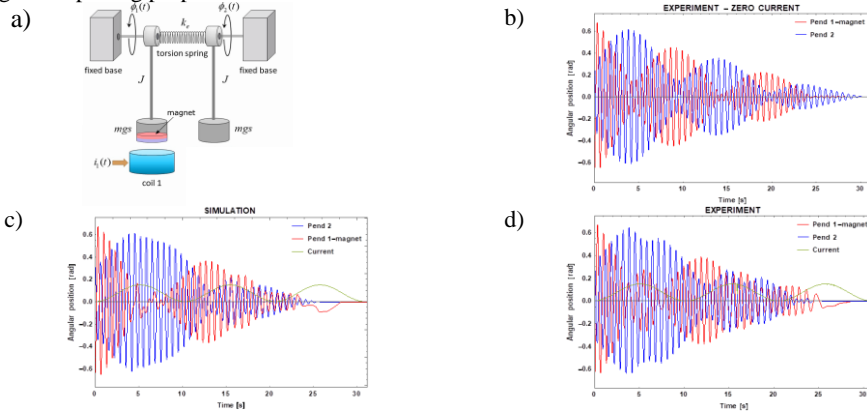


Fig. 2. Model (a), sample free motion (b), and the response to input current (c-d).

3. Concluding Remarks

Open-loop control strategy is suggested in this paper for guiding the energy flow between two interacting oscillators by means of magnetic fields. Control strategy is based on the observation that, in the case of antiphase oscillation, the energy is moving from the oscillator, which is in the repelling magnetic field, to the oscillator not subjected to magnetic field.

Acknowledgment: The construction of the experimental setup presented in the work was supported by the Polish National Science Centre under the grant OPUS 14 No. 2017/27/B/ST8/01330.

References

- [1] AUBRY, S., KOPIDAKIS, G., MORGANTE, A. M., & TSIRONIS, G. P. (2001). ANALYTIC CONDITIONS FOR TARGETED ENERGY TRANSFER BETWEEN NONLINEAR OSCILLATORS OR DISCRETE BREATHERS. *PHYSICA B: CONDENSED MATTER*, 296(1–3), 222–236.
- [2] VAKAKIS, A. F., GENDELMAN, O. V., BERGMAN, L. A., MCFARLAND, D. M., KERSCHEN, G., & LEE, Y. S. (2008). *NONLINEAR TARGETED ENERGY TRANSFER IN MECHANICAL AND STRUCTURAL SYSTEMS I. SOLID MECHANICS AND ITS APPLICATIONS (1ST ED., VOL. 156)*. SPRINGER.
- [3] LI, T., GOURC, E., SEGUY, S., BERLIOZ, A. Dynamics of two vibro-impact nonlinear energy sinks in parallel under periodic and transient excitations. *International Journal of Non-Linear Mechanics*, 2017, **90**, 100–110.
- [4] TURE SAVADKOOHI, A., LAMARQUE, C. H., DIMITRIJEVIC, Z. Vibratory energy exchange between a linear and a nonsmooth system in the presence of the gravity. *Nonlinear Dynamics*, 2012, **70**(2), 1473–1483.

Can the prognosis of the results of the crash be the basis to steering the autonomic vehicle with the trailer in the critical situation?

LEON PROCHOWSKI¹, PATRYK SZWAJKOWSKI^{2*}, MATEUSZ ZIUBIŃSKI³

1. Military University of Technology (WAT), Institute of Vehicles and Transportation, ul. gen. Sylwestra Kaliskiego 2, 00-908 Warsaw, Poland; Łukasiewicz Research Network – Automotive Industry Institute (Łukasiewicz-PIMOT), ul. Jagiellońska 55, 03-301 Warsaw, Poland, leon.prochowski@wat.edu.pl [0000-0003-2093-1585]
2. Łukasiewicz Research Network – Automotive Industry Institute (Łukasiewicz-PIMOT), Electromobility Department, ul. Jagiellońska 55, 03-301 Warsaw, Poland, patryk.szwajkowski@pimot.lukasiewicz.gov.pl [0000-0003-4832-826X]
3. Military University of Technology (WAT), Institute of Vehicles and Transportation, ul. gen. Sylwestra Kaliskiego 2, 00-908 Warsaw, Poland, mateusz.ziubinski@wat.edu.pl [0000-0003-4955-2095]

* Presenting Author

Abstract: The autonomous vehicles move to follow up a pre-planned trajectory, which is generated by the trajectory planning model of the control system. The same situation is observed during obstacle avoidance maneuvers. Autonomous vehicle (A) (without occupants onboard) with a cargo trailer (CT unit) movement has been considered in this paper. During the CT unit motion at high speed on a road intersection, the car (driven by the driver, D) entered the lane of the CT unit and thus to become an obstacle. It was affirmed that in some cases of considered road critical situation, there is a lack of the safe obstacle' avoidance maneuvers. In such cases, planning of the CT unit trajectory is also necessary. Among all of the trajectories, some of them consider the possibility of the collision (impact). The aim of this study is to show the possibility of movement trajectory selection, based on assessments to risk associated with possible vehicle D occupants injury. The basis for this selection are the results of the numerical modelling of the vehicles' collision effects. The research carried out have shown the relations between the selected driving trajectory and possible consequences of the vehicles' collision. Set of these relations from the model research, can be stored in the autonomous vehicle controller memory and be used by for selection the movement trajectory in an obstacle avoidance maneuver. This would help to plan the trajectory to reduce injuries risk of the vehicle D occupants to lowest possible level in investigated critical road situation.

Keywords: autonomous vehicle with cargo trailer, road accidents, occupants injuries.

1. Introduction

The autonomous vehicles move to follow up a ongoing planned and generated movement trajectory. The same situation is observed during obstacle avoidance maneuvers. Autonomous vehicle (A) (without occupants onboard) with a cargo trailer (CT unit) movement has been considered in this paper. During the CT unit motion at high speed on a road intersection, the car (driven by the driver, D) entered the lane of the CT unit and thus to become an obstacle blocking one of the road lane along a driving trajectory in relation to the car A. The method of selecting a defensive maneuver by the system controller in a critical situations has been considered.

The result of the research presented in [1] was to determine the method of generating the planned driving trajectory to safely avoid the obstacle. The results of these research provide grounds for a statement that several possibilities of the considered road critical situation lack a safe driving trajectory. How to proceed in such a situation? One way is to select a trajectory taking into account a collision (impact) with the least severe consequences (the strategy of the lesser evil).

The aim of this study is to show the possibility of movement trajectory selection, based on assessments to risk associated with possible vehicle D occupants injury (the strategy of the lesser evil). In autonomous vehicle (A) there are no people. The basis for this selection of the driving strategy in analyzed critical situation are the results of the numerical modelling of the vehicles' collision effects. This paper is an extension of [1].

2. Research methods

The research carried out (example in fig. 1) have shown the relations between the selected CT set driving trajectory and possible consequences of the vehicles' collision. Set of these relations from the model research, can be stored in the autonomous vehicle controller memory and be used by for selection the movement trajectory in an obstacle avoidance maneuver.

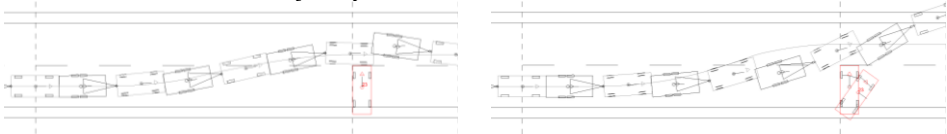


Fig. 1. Road traffic situation, depending on the selection of driving trajectory

In this study, short-term vehicles collision proces is analyzed (various variants of road collisions) in order to determine the risk indicators for occupants (research results example in fig. 2). The 10 degree of freedom (DOF) model of CT set was developed. The vehicle D has 6 DOF and occupant/driver dummy (Hybrid III) has 19 DOF.

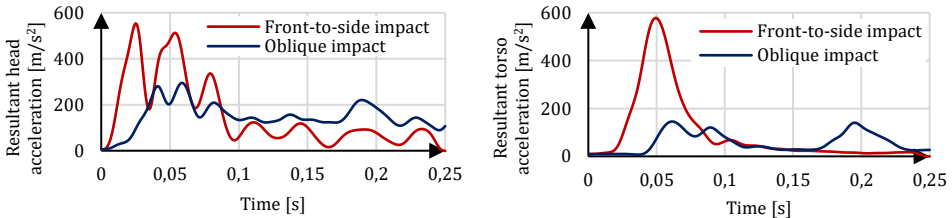


Fig. 2. The course of the vehicle D occupant head acceleration (left figure) and torso (right figure) during a front-to-side and oblique impact

During assessment of the injury risk was used so-called risk curves in the AIS scale (Abbreviated Injury Scale). The total risk of injury (P_{Joint}) for a side impacts in percent is calculating:

$$P_{Joint} = 1 - (1 - P_{head}) \times (1 - P_{chest}) \times (1 - P_{abdomen}) \times (1 - P_{pelvis}) \times 100\%$$

where: $P_{head} = f(HIC)$; $P_{chest} = f(\text{chest displacement})$; $P_{abdomen} = f(\text{the resultant force acting on the abdomen})$; $P_{pelvis} = f(\text{force acting on the pelvis})$.

Mentioned above risk indicators are determined for the set of collision variants in the range of driving speeds 40-90 km/h for the CT set and the impact angle 0-90 deg of the vehicle D. This has made it possible to further planning of the trajectories, which would decrease injuries risk indicators of the vehicle D occupants to lowest possible level in investigated critical road situation.

References

[1] Prochowski L., Ziubiński M., Szwajkowski P., Pusty T., Gidlewski M., *Experimental and simulation examination of the impact of the control model on the motion of a motorcar with a trailer in a critical situation*. Conference Paper. Proceedings of 15th International Conference Dynamical Systems - Theory and Applications DSTA 2019, Lodz, December 2-5, 2019.

Dynamic modeling of a rolling tensegrity structure with spatially curved members

P. SCHORR^{1,2*}, M. EBNET², K. ZIMMERMANN¹, V. BÖHM²

1. Technische Universität Ilmenau, Max-Planck-Ring 12, 98693 Ilmenau, Germany

2. Ostbayerische Technische Hochschule Regensburg, Galgenbergstr. 30, 93053 Regensburg, Germany

* Presenting Author

Abstract: Tensegrity Structures were recently accessed in the field of engineering due to their advantageous properties like shock resistance and shape changeability. Especially, in (soft) robotics, the application of those structures is a promising approach. Various types of locomotion can be realized using tensegrity structures. Here, a rolling locomotion system based on a tensegrity structure with precurved members is presented. The rolling locomotion is initialized by varying the center of mass due to shifting an internal mass. Furthermore, a proper shape change is applied to steer on a horizontal plane. The locomotion system is modeled as a multibody system and the corresponding non-holonomic dynamics are derived. Simulations considering the locomotion behavior are performed for various actuation strategies and mechanical parameters. Based on these results a reliable actuation strategy to maneuver in two dimensions by pure rolling is derived. Furthermore, recommendations regarding the constructive development of a real prototype based on a tensegrity structure are given.

Keywords: Compliant tensegrity structure, non-holonomic constraints, dynamics

Individual wheel braking as a method for increasing velocity of articulated vehicles

ALEKSANDER SKURJAT^{1*}, ANDRZEJ KOSIARA²

1. Wrocław University of Science and Technology, Department of Mechanical Engineering, Department of Off-Road Machine and Vehicle Engineering, Wybrzeże Wyspiańskiego 27, 50-370, Wrocław, [0000-0002-3780-1691]
 2. Wrocław University of Science and Technology, Department of Mechanical Engineering, Department of Off-Road Machine and Vehicle Engineering, Wybrzeże Wyspiańskiego 27, 50-370, Wrocław, [0000-0001-6870-5961]
- * Presenting Author

Abstract: Increasing higher and higher velocities of articulated wheeled vehicles requires finding a new methods for stabilizing oscillations in articulated joint. It allows to achieve more in-line path of a vehicle. In the paper, a method for individual wheel braking is proposed and tested in computer simulations. Control algorithm allows for braking from 1 up to 3 wheels for increasing damping and reducing oscillations amplitude in articulation joint. A method for calculating braking torque is presented. Author proposed and compared signals obtained from vehicle angular acceleration and angle in the articulated joint to engage or disengage braking of wheel(s). Several methods are presented in the paper, allowing for faster damping of oscillations and reduction of amplitudes through the use of a brake system. The tests were carried out for 2 different simulation models (different vehicles). Several methods are presented - variants of the system operation. Simulations shows that proposed control algorithms allows to increase damping and decrease oscillation amplitude.

Keywords: articulated vehicle, braking system, control system, snaking, lateral stability, vehicles path

1. Introduction

The rapid development of the automotive industry has contributed to an increase in the number of vehicles reaching higher and higher speeds and moving on public roads. For this reason, safety while driving has become an extremely important factor when designing new earth-working machines and vehicles moving on the streets. Most systems improving safety can be seen in passenger car designs. These include active braking, acceleration slip control, power steering, steering traction control and many others. It should be noted that such systems are not used in earth-working machines and the location of the tool, e.g. an excavator bucket or loader in the event of a pedestrian collision can be extremely dangerous. Increasing the speed of earth-working vehicles is desirable because it brings great economic benefits. One of the phenomena that prevent these machines from moving at speeds in excess of 50 km/h is the phenomenon of snaking. This phenomena can be considered as a spontaneous undesirable by driver vehicle path change [1, 2, 3]. A method for reducing snaking phenomenon is not well designed for articulated vehicles. When vehicles with articulated steering are in motion,

oscillation between the front and rear frames is often generated due to the low stiffness of the hydraulic system. Low damping value and forcing from the ground make the oscillations persist for a long time. Several methods are presented in the paper, allowing for faster damping of oscillations and reduction of amplitudes through the use of a brake system. The tests were carried out for 2 different simulation models (different vehicles). Several methods are presented - variants of the system operation.

2. Results and Discussion

Results obtained from simulations for different braking control signal and braking mode are presented in Fig. 1.

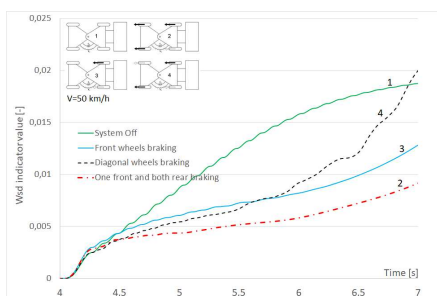


Fig. 1. W_{sd} indicator value and vehicle trajectory for different braking control system. Velocity $V=50$ km/h

The systems eliminate the phenomenon of snaking by braking at least one wheel contribute to a significant increase in motion stability. It is a solution that can be easily applied to almost all wheeled vehicles. It can be seen that the further development of the steering system should include increasing the energy efficiency of its operation. For this purpose, an algorithm should be developed that, based on control signals, will in a short time automatically select the method and number of braked wheels. An important issue is also the economy of the applied system and the determination of the typical braking time of the wheels on a given typical road. The increase in fuel consumption and wear when this system is used should be considered.

References

- [1] Aleksander R. Skurjat, Tests of influence of geometry and elasticity of hoses of hydraulic articulated steering system on its stiffness. W: Engineering Mechanics 2018 : 24th international conference : extended abstracts, May 14-17, 2018, Svratka, Czech Republic / ed. Cyril Fischer and Jiří Náprstek. Prague : Institute of Theoretical and Applied Mechanics of the Czech Academy of Sciences, cop. 2018. s. 769-772.
- [2] Piotr Dudziński, Aleksander R. Skurjat, Research on the influence of geometric parameters on the phenomenon of snaking of articulated vehicles. Zeszyty Naukowe - Wyższa Szkoła Oficerska Wojsk Lądowych im. gen. T. Kościuszki. 2017, t
- [3] Piotr Dudziński, Aleksander R. Skurjat, Directional dynamics problems of an articulated frame steer wheeled vehicles. Journal of KONES. 2012, vol. 19, nr 1, s. 89-98.

Vibrations of an active rocker – bogie suspension under motion in rough terrain

KRZYSZTOF SOKÓŁ¹, MACIEJ PIERZGALSKI^{2*}

1. Institute of Mechanic and Machine Design Foundations, Czestochowa University of Technology, Czestochowa, Poland, sokol@imipkm.pcz.pl [0000-0002-8661-1763]

2. Institute of Mechanic and Machine Design Foundations, Czestochowa University of Technology, Czestochowa, Poland, pierzgalski@imipkm.pcz.pl [0000-0002-1300-4911]

* Presenting Author

Abstract: Mobile platforms are used in many aspects of our everyday life, mostly by military, rescue teams, miners or scientists. In most of them installed suspension units have constant dimensions what limits area of operating range. Presented in this paper active rocker – bogie suspension can change length of each suspension section in order to self – level base platform what will lead to increase in stability by means of control of location of centre of gravity and application area by change in space required during work and transportation. The main scope of this study is to investigate and influence of different length of suspension members on vibration frequency as well as vibration modes. On the basis of the results one will find optimum solutions for creating a prototype.

Keywords: frequency analysis, suspension, rover, mobile platform, rocker - boogie

1. Introduction

Mobile platforms often use six or more wheels or even track drive sets [1]. Due to fact that their frames contain manipulators, radars, scanners and other fragile items one requires great stability during operations in rough and uneven terrain. This gives great challenge to the engineers during the design and test phases. In construction available on the market one can find ones that use multi-link suspension system [2] which has simple design and does not immobilize platform at failure of one suspension unit. Another type of used suspension is rocker – bogie type [3] which can be found in Opportunity and Curiosity rovers. This construction is characterized by the fact that left and right side wheels are connected by a differential bar which ensures ground contact for all wheels. Moreover rocker – bogie suspension does not have springs and it ensures overcome an obstacle equal to the length of the wheelbase. Simplified version of rocker – bogie suspension is boogie type [4] which has two swingarms on each side instead of combined one and does not have differential bar. Regardless to installed suspension system, stability in rough terrain is limited by the location of the center of gravity. In the active rocker – boogie suspension [5] studied in this paper one can control its location what greatly increases platform terrain application area. The main scope of performed studies is to check an influence of different length of suspension members on vibration modes and vibration frequency of the mobile platform. In future, one will also consider different material types such as Aluminum 6060 T66, Steel S235 or Titanium grade 1. The obtained results will allow finding the best material for prototype production.

2. Model presentation and results of numerical simulations

In figure 1 one presents investigated mobile platform, which can change wheelbase what results in control of location of centre of gravity. The markings are as follows: 1,2 – suspension arms; 3,4,5 – wheels with electric motors; 6 – main frame; 7 – differential bar; 8 – electric motors for suspension control.

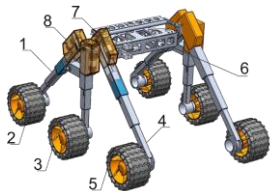


Fig. 1. Investigated suspension system

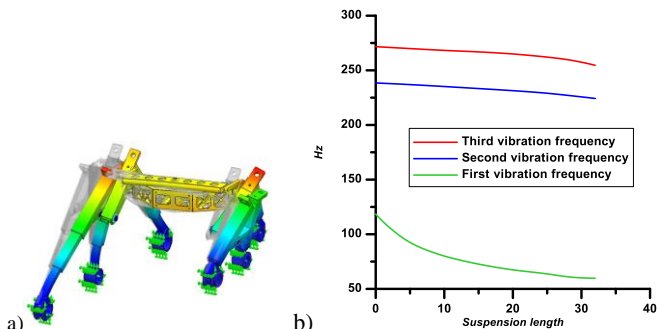


Fig. 2. a) 1st vibration mode- AI. 6060, b) change in vibration frequency

Figure 2a shows a sample of results from vibration mode investigations while figure 2b describes the change in vibration frequency magnitude at different suspension length. The frequency studies were done at different length of one side (the change in length was equal to all three wheels on one side) while the other remained fully extended. This simulates a motion of a platform on terrain with different elevation in relation to the longitudinal axis of symmetry. In the presented case the change in suspension length has the greatest influence on first vibration frequency which is being reduced significantly between min. and max. positions. The second and third vibration frequencies are much less vulnerable to change in suspension length and their reduction is more linear in relation to the first one.

3. Conclusions

As presented in section 2 the behaviour of the investigated mobile platform is very complex in relation to different lengths of suspension members. Detailed studies on vibration frequency – suspension length and vibration modes must be done before prototype production.

References

- [1] MOSKVIN L, LAVRENOV R, MAGID E, SVININ M: Modelling a crawler robot using wheels as pseudo-tracks: model complexity vs performance. *IEEE 7th International Conference on Industrial Engineering and Applications* 2020:1-5.
- [2] ȚOȚU V, ALEXANDRU C: Multi-criteria kinematic optimization of a front multi-link suspension mechanism using DOE screening and regression model. *Applied Mechanics and Materials* 2013,**332**:351-356.
- [3] BABU B, DHAYANIDHI N, DHAMOTHARAN S: Design and fabrication of rocker bogie mechanism geosurvey rover. *International Journal of Scientific Development and Research* 2018,**3**(8):154-159.
- [4] PTAK P, PIERZGALSKI M, CEKUS D, SOKÓŁ K: Modeling and stress analysis of a frame with a suspension of a mars rover. *Procedia Engineering* 2017,**177**:175-181.
- [5] SOKÓŁ K, PIERZGALSKI M: An influence of the material properties on the endurance of the self-adjustable rocker-bogie suspension. *Archives of Metallurgy and Materials* 2021,**66**(2):543-548.

Viscoelastic Material Models Based Active Vibration Controllers:

An Energy Approach

TUKESH SONI^{1*}, J. K. DUTT²

1. UIET, Panjab University, Chandigarh, India 160014

2. Mechanical Engineering, IIT Delhi, Hauz Khas, New Delhi, 110016 India

* Presenting Author

Abstract: Viscoelastic polymers have been employed for passive vibration mitigation in structures and rotating machines, however, its mechanical properties change with time. Taking inspiration from this passive technique of vibration reduction, this paper presents the fundamentals of designing control laws based on the constitutive relationship of a viscoelastic material for an active vibration control scheme. To this end, energy absorbed by the material model for a viscoelastic material model is formulated and compared for different models. The control law based on these material models will be designed based on maximization of energy absorbed by the material model in order to effectively mitigate vibrations from the system. The control laws based on the viscoelastic material models are shown to perform better as compared to conventional control laws. This analysis paves way for designing control laws based on the viscoelastic material models.

Keywords: active vibration control, viscoelastic material model, passive vibration

1. Introduction

In this paper a new approach to build control laws based on viscoelastic material models is presented. Viscoelastic material are known to improve stability and vibration characteristics when used in rotating machinery support [1], [2]. In recent literature, some control laws have been designed by taking inspiration from the viscoelastic material model ([3] [4],[5], [6]), however, an energy analysis-based design of such control laws, which forms the basis, has not been presented. This work therefore provides a theoretical framework behind the design of control laws based on energy absorbed by the viscoelastic material models.

2. Results and Discussion

Fig. 1(a) shows a schematic of a single degree of freedom discrete system mounted on a 2-element support (a stiffness and a damper) and acted upon by a harmonic force. Energy dissipated in one cycle in steady state is found using the following relation, $E_2 = \int_0^{2\pi/\omega} c\dot{x}^2 dt$. For Three element model (Fig. 1(b), two stiffness and one damper), the governing equation is, $m\ddot{x} + c(\dot{x} - \dot{y}) + kx = F\cos(\omega t)$. Now, energy dissipated in one cycle at steady state can be found using the following relation, $E_3 = \int_0^{2\pi/\omega} c(\dot{x} - \dot{y})\dot{x} dt$. Evaluating the integral, one finds E_3 . Similarly, the energy dissipated by the four element model (figure 1(c)) can be evaluated. The Non-Dimensional Energy absorption Ratio for three element model to two element model (NDER₃₂) and four element model to three element model (NDER₄₃) is shown in **Fig. 2**, where ξ is the damping ratio and λ is the stiffness ratio equal to $\frac{k_3}{k}, \frac{k_4}{k}$, for

three element model and four element model respectively. The values of the ratios > 1 promise efficacy of higher element model over conventional 2-element model.

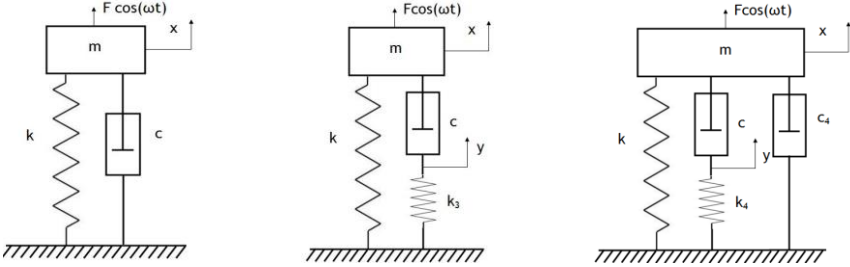


Fig. 1: (a) Two element model (b) Three element model (c) Four element model

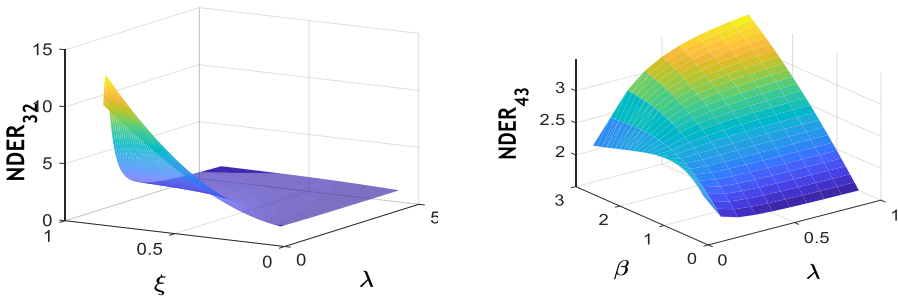


Fig. 2: Non dimensional energy ratio between (a) three element model and two element model (b) four element model and three element model

3. Concluding Remarks

This paper proposes novel approach in building control laws for active vibration control by taking inspiration from passive viscoelastic material properties. Energy absorbed by the viscoelastic material model is considered as a criterion for designing control laws. Properly designed higher element models promise very efficient energy dissipation and ensure better stability and vibration control over conventional controllers.

References

- [1] J. K. Dutt and B. C. Nakra, “Stability of Rotor Systems with Visco-elastic Supports,” *J. Sound Vib.*, vol. 153, pp. 89–93, 1992.
- [2] J. K. Dutt and B. C. Nakra, “Vibration Response Reduction of a Rotor Shaft System Using Viscoelastic Polymeric Supports,” *ASME Journal Vib. Acoust.*, vol. 115, 1993.
- [3] T. Soni, J. K. Dutt, and A. S. Das, “Parametric Stability Analysis of Active Magnetic Bearing Supported Rotor System With a Novel Control Law Subject to Periodic Base Motion,” *IEEE Trans. Ind. Electron.*, vol. 67, no. 2, pp. 1160–1170, Feb. 2020, doi: 10.1109/TIE.2019.2898604.
- [4] T. Soni, A. S. Das, and J. K. Dutt, “Active vibration control of ship mounted flexible rotor-shaft-bearing system during seakeeping,” *J. Sound Vib.*, vol. 467, p. 115046, Feb. 2020, doi: 10.1016/j.jsv.2019.115046.
- [5] T. Soni, J. K. Dutt, and A. S. Das, “Magnetic Bearings for Marine Rotor Systems—Effect of Standard Ship Maneuver,” *IEEE Trans. Ind. Electron.*, vol. 68, no. 2, pp. 1055–1064, Feb. 2021.
- [6] T. Soni, J. K. Dutt, and A. S. Das, “Dynamic behavior and stability of energy efficient electro-magnetic suspension of rotors involving time delay,” *Energy*, vol. 231, p. 120906, Sep. 2021, doi: 10.1016/j.energy.2021.120906.

Strategies for Amplitude Control in a Ring of Self-Excited Oscillators

VINOD V^{1*}, BIPIN BALARAM²

1. Department of Mechanical Engineering, Mar Baselios College of Engineering and Technology, APJ Abdul Kalam Technological University, TVPM 695015, INDIA. [ORCID: 0000-0003-3897-3388]
2. Department of Mechanical Engineering, Amrita School of Engineering, Amrita Vishwa Vidyapeetham, Coimbatore, 641 112, INDIA [ORCID: 0000-0002-6577-3149]

*Presenting Author

Abstract: This paper presents different methods for amplitude control in a ring network of van der Pol oscillators. The slow flow equations for amplitude and phase difference are derived by the method of averaging. These slow flow equations are used to show that configuration symmetry of the network can be utilised to cause amplitude death. It is further shown that stable manifold associated with the equilibrium point at the origin can be used for control. Apart from these system characteristics, this paper also shows that a first order active control connected to any one of the oscillators can cause amplitude death in the whole network. The synchronising property of the ring network causes the propagation of control to all the oscillators for strong enough coupling. Frequency control to bring about synchronised dynamics and amplitude control to effect amplitude death are analysed in this work.

Keywords: Ring network, Synchronization, Amplitude death, Active control.

1. Introduction

Different methods like linear feedback and time-delay feedback have been proposed recently for control of coupled self-excited systems [1]. There have also been efforts to apply active control in forced van der Pol systems and to study its stability [2]. This work analyses different control strategies in a van der Pol ring network.

2. Van der Pol oscillators in a ring – Slow flow dynamics

N van der Pol oscillators connected in a ring network with linear dissipative coupling between nearest neighbours can be represented by [3]:

$$\ddot{x}_i + \varepsilon(x_i^2 - 1)\dot{x}_i + \omega_i^2 x_i = \sigma(\dot{x}_{i-1} - 2\dot{x}_i + \dot{x}_{i+1}) \quad (1)$$

Here, ε is the nonlinearity, σ is the coupling strength and ω_i is the linear natural frequency of each oscillator. The slow flow equations of Eq. (1) using the method of averaging [4] are in Eq. (2) and (3) where A_i is the amplitude and θ_i represents the phase difference.

$$\dot{A}_i = \frac{\varepsilon A_i}{2} - \frac{\varepsilon A_i^3}{8} + \frac{\sigma}{2} (A_{i-1} \cos \theta_{i-1} - 2A_i + A_{i+1} \cos \theta_i) \quad (2)$$

$$\dot{\theta}_i = (\omega_{i+1} - \omega_i) + \frac{\sigma}{2} \left\{ \frac{A_{i-1}}{A_i} \sin \theta_{i-1} - \frac{A_i^2 + A_{i+1}^2}{A_i A_{i+1}} \sin \theta_i + \frac{A_{i+2}}{A_{i+1}} \sin \theta_{i+1} \right\} \quad (3)$$

Email for correspondence: vinodv@mbcet.ac.in

Address for correspondence: Associate Professor, Department of Mechanical Engineering, MBCET, Nalanchira, TVPM, Kerala, INDIA, 695015.

3. Results and Discussion

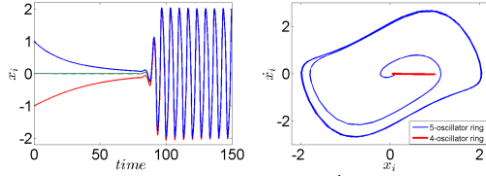


Fig. 1. (a) Frequency synchronization due to the presence of a 5th oscillator. (b) Limit cycle oscillation in a 5-oscillator ring changes to amplitude death in a 4-oscillator ring.

Configuration Symmetry: We extend the studies on influence of configuration symmetry on the dynamics of large ring networks [5] for framing control strategies. Two rings of $N = 5$ and $N = 4$ are considered with oscillator parameters as $\epsilon_i = 1$, $\sigma_i = 0.1$, $\omega_i = 1$. The slow flow equations (Eq. (2), (3)) are numerically integrated by Runge-Kutta method. For the 4-oscillator ring, fixed point at the origin has a stable manifold given by $S = \{(a,0), (-a,0), (a,0), (-a,0) \dots\}$, a being any real positive number. This stable manifold does not exist in a 5-oscillator ring, as shown in Fig. 1(a). This amplitude control through frequency synchronization is destroyed by the removal of an oscillator which makes the ring symmetric. Under the same set of oscillator parameters, we observe the annihilation of amplitude across the entire network (Fig. 1(b)) in a 4-number ring.

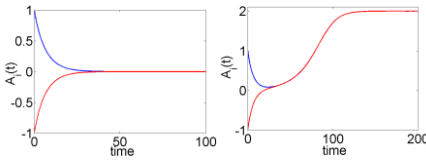


Fig. 2. Evolution of amplitude in a symmetrical ring. (a) Amplitude annihilation (b) Amplitude preservation

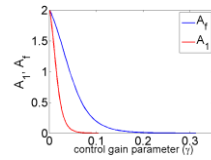


Fig. 3. Spread of amplitude death across the ring by active control.

Perturbation in stable manifolds: In even number rings, the symmetry in the network aids the annihilation of amplitude. Beginning the dynamics on stable manifold given by $S = \{(a,0), (-a,0), (a,0), (-a,0) \dots\}$ leads to amplitude death as shown in Fig. 2(a). Any slight perturbation ($a + \Delta a$) leads to restoration of the amplitude and achievement of synchronisation as given in Fig. 2(b).

Influence of an active control: Amplitude control in the whole network can also be realised by connecting a first order active control to any one oscillator in the ring. The synchronisation property of the network helps in the spread of amplitude control in one oscillator to the entire network. Fig. 3 shows amplitude death in first oscillator (which is connected with active control) and the oscillator farthest from it.

4. Concluding Remarks

This paper investigated three methods for amplitude annihilation or restoration in a ring of limit cycle oscillators. Whereas the first two methods utilised inherent properties of the system, the third method utilises an external control mechanism. But the propagation of the control throughout the network happens due to its synchronising property.

Acknowledgment: We greatly acknowledge the contributions of Prof. Narayanan M.D., National Institute of Technology, Calicut, INDIA and Prof. Mihir Sen, University of Notre Dame, USA.

References

- [1] PER SEBASTIAN SKARDAL, ALEX ARENAS: On controlling networks of limit-cycle oscillators. *Chaos* 2016, **26**:094812.
- [2] B R NANA NBENDJO, R YAMAPI: Active control of extended Van der Pol equation. *Communications in Nonlinear science and Numerical simulation* 2007, 12:1550-1559.
- [3] MIGUEL A. BARRON, MIHIR SEN: Synchronization of four coupled van der Pol oscillators. *Nonlinear Dynamics* 2009, 56 (**4**):357-367.
- [4] VINOD V, BIPINBALARAM, NARAYANAN M.D., MIHIR SEN: Effect of oscillator and initial condition differences in the dynamics of a ring of dissipative coupled van der Pol oscillators, *Journal of Mechanical Science and Technology* 2015, 29 (**5**):1931-1939.
- [5] VINOD V, BIPINBALARAM, NARAYANAN M.D., MIHIR SEN: Effect of configuration symmetry on synchronization in a Van der Pol ring with nonlocal interactions, *Nonlinear Dynamics* 2017, 89 (**3**):2103-2114.

Email for correspondence: vinodv@mbcet.ac.in

Address for correspondence: Associate Professor, Department of Mechanical Engineering, MBCET, Nalanchira, TVPM, Kerala, INDIA, 695015.

Experimental Research on Active Vibration Control of Elastic Plate and Damage Degradation of Actuator

KE YE ¹, JINHUI JIANG ^{2*}

1. State Key Laboratory of Mechanics and Control of Mechanical Structures, Nanjing University of Aeronautics and Astronautics, Nanjing, 210016, China
 2. State Key Laboratory of Mechanics and Control of Mechanical Structures, Nanjing University of Aeronautics and Astronautics, Nanjing, 210016, China
- * JINHUI JIANG

Abstract: Achieving more effective real-time vibration control of structures has been an ongoing exploration in the field of vibration engineering, and the actuator is an extremely important part of vibration active control research. In this paper, we propose a simplified iterative learning control algorithm using the real-time response of the controlled system as the control input, and build a vibration active control experimental system based on NI CompactRIO and LabVIEW platform. In the experiment, the control efficiency of the negative velocity feedback method and the iterative learning control method are compared with the elastic airfoil plate as the object. The verification results show that the vibration suppression efficiency of the latter can be improved by more than 62% compared with that of the former. At the same time, the experiments simulate the damage degradation process during the actuator life cycle, and we obtain that the decay of the actuator performance will be greatly accelerated when the damage degradation of the actuator is assumed to be linear and the damage rate is more than half. In addition, the vibration active control experimental system can obtain better vibration suppression performance at high frequency excitation under the same setup.

Keywords: Elastic airfoil, Vibration active control, Iterative learning control, LabVIEW

1. Introduction

One of the popular topics in ACSR research is the active control of vibration of laminated piezoelectric smart structures, which focuses on: numerical simulation of smart structures, numerical solution of dynamics problems and their experimental validation, design of controllers and their optimization, and optimization of piezoelectric sensor/actuator positions.

Yang et al.^[1] proposed an optimal iterative learning control (ILC) for a linear discrete-time system to optimize cumulative quadratic linear indicators in the iterative domain and proved its stability, convergence, robustness, and optimality. Bai et al.^[2] combined P-type iterative learning (IL) control, fuzzy logic control and artificial bee colony (ABC) algorithm to design a novel optimal fuzzy IL controller for active vibration control of piezoelectric smart structures.

There is still room for exploring the efficiency and convenience of real-time vibration control of piezoelectric intelligent structures in engineering applications. In this study, a simplified iterative learning control algorithm using only the real-time response of the controlled system as the control input is proposed, and the experimental platform and software are designed for the experiments, taking the elastic airfoil plate as the experimental object. And then, the experimental results are com-

pared and analyzed to verify the advantages of the scheme. Finally, the influence of the performance decay on the control effect during the actuator damage degradation is experimentally investigated, and the data sets are compared and summarized.

2. Results and Discussion

The conventional negative velocity feedback control method is used as a comparison to verify the effectiveness of this vibration active control system and the iterative learning control law. In view of the fact that many papers have achieved excellent vibration suppression by various methods, this paper does not seek to maximize the vibration suppression effect, and the method comparison shows that the iterative learning control scheme used in this paper can improve the vibration reduction efficiency by more than 62% compared to the conventional negative velocity feedback scheme.

Table 1. Experimental real-time amplitude

Conditions	Before control	Feedback control	Iterative learning control
Response amplitude(g)			
First order frequency	1.920	1.691	1.312
Second order frequency	0.879	0.679	0.369

Table 2. Experimental real-time amplitude

Output Voltage	5V	4V	3V	2V	1V
Response amplitude(g)					
First order frequency	1.312	1.383	1.467	1.686	1.839
Second order frequency	0.369	0.432	0.527	0.675	0.772

When the damage to the piezoelectric sheet is relatively minor, the overall effect of vibration suppression is only slightly reduced, while in the case of larger damage to the piezoelectric sheet (the linear damage rate of the actuator is more than half, i.e., the output control voltage at the software side is reduced by more than half of the original voltage), the performance of the piezoelectric sheet decays significantly faster. At the same time, in the case of the same damage to the actuator, the control system has a better active vibration suppression performance to a certain extent when the high frequency excitation.

3. Concluding Remarks

Acknowledgment: The authors would like to acknowledge the support provided by the National Natural Science Foundation of China, No. 51775270.

References

- [1] SHENGYUE YANG, ZHIHUA QU, XIAOPING FAN et al.: Novel iterative learning controls for linear discrete-time systems based on a performance index over iterations. *Automatica* 2008, **44**(5): 1366-1372.
- [2] BAI LIANG, YUNWEN FENG, NING LI et al.: Optimal fuzzy iterative learning control based on artificial bee colony for vibration control of piezoelectric smart structures. *Journal of Vibroengineering* 2019, p.111-132.

Experimental Evaluation of an Underactuated Inverse Dynamics Control Approach based on the Method of Lagrange-Multipliers

ROLAND ZANA^{1*}, AMBRUS ZELEI²

1. Budapest University of Technology and Economics [0000-0003-1081-2742]
2. MTA-BME Research Group on Dynamics of Machines and Vehicles [0000-0002-9983-5483]

* Presenting Author

Abstract: Underactuated dynamical systems possess higher number of degrees of freedoms than independent control inputs. Surprisingly, numerous controlled dynamical systems have this property, such as flying and underwater robots, flexible and lightweight manipulators, pedal locomotors, cable tethered and crane systems. The tracking control of underactuated robots are more challenging than the fully-actuated systems, because of the intricate relation of the input and output and the stability problems emerging from the zero-dynamics. Several control approaches have appeared in the literature. However, their performance is usually presented on a specific device best-fit to the actual control algorithm. Our goal is to carry out a series of benchmark test, with which the performance of the different algorithms are compared and ranked objectively. In this work, the method of Lagrange-multipliers is employed in an inverse dynamics control algorithm. The testbed is an underactuated 12DoF ceiling based hanging robot. The position and orientation accuracy were assessed: the absolute position error was below 25mm and the orientation error was below 2.5 degrees.

Keywords: underactuated dynamical systems, crane-like systems, inverse dynamics control

1. Introduction

The Acroboter [1] is a crane-like indoor domestic robot prototype (mechanical model in Fig. 1. left). From mechanical point of view, it is a spatial double pendulum, where the climbing unit, the cable connector and the swinging unit is connected with the one main and three secondary cables. The 12DoF robot is equipped with winches and fan actuators, which sums up to 7 independent control inputs. Indeed, the system is under actuated. The Acroboter is a good experimental tool for testing underactuated control algorithms [2, 3]. An inverse dynamics controller was tested experimentally, which is based on servo-constraints [3] and on the Method of Lagrange-Multipliers. The control input \mathbf{u} is obtained by using the following formula with mass matrix \mathbf{M} , geometric constraint Jacobian Φ_q , servo-constraint σ and servo-constraint Jacobian \mathbf{G}_q :

$$\begin{bmatrix} \mathbf{M} & \Phi_q^T & -\mathbf{H} \\ \Phi_q & \mathbf{0} & \mathbf{0} \\ \mathbf{G}_q & \mathbf{0} & \mathbf{0} \end{bmatrix} \begin{bmatrix} \ddot{\mathbf{q}} \\ \lambda \\ \mathbf{u} \end{bmatrix} = \begin{bmatrix} -\mathbf{C} \\ -\dot{\Phi}_q \dot{\mathbf{q}} \\ -\dot{\mathbf{G}}_q \dot{\mathbf{q}} - \dot{\mathbf{c}} - \mathbf{K}_d(\mathbf{G}_q \dot{\mathbf{q}} + \mathbf{c}) - \mathbf{K}_p \sigma \end{bmatrix} \quad (1)$$

2. Results and Conclusion

In contrast to a linear feedback controller, the MLM method takes into consideration the dynamics of the entire mechanical system. This results in good trajectory tracking properties as it is shown in

Fig. 1. right. Figure 2. shows the position errors in x , y and z directions, the absolute position errors and the error of the orientation about the vertical axis. In future work several alternative control algorithms will be benchmarked on the same testbed in the same circumstances.

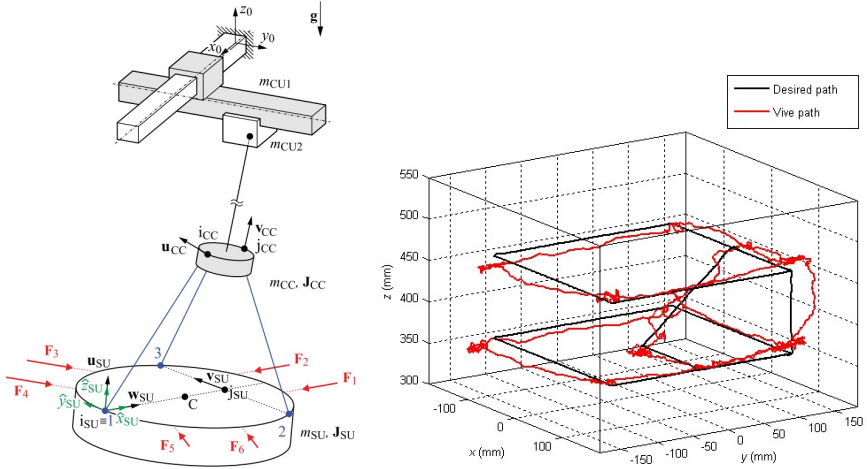


Fig. 1. This is the figure caption (Times New Roman 8 pt.)

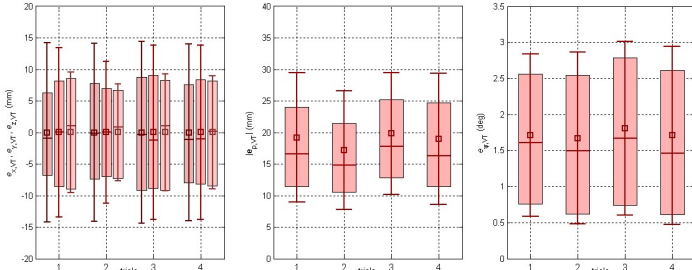


Fig. 2. This is the figure caption (Times New Roman 8 pt.)

Acknowledgment: The research reported in this paper and carried out at BME has been supported by the NRDI Fund (TKP2020 IES, Grant No. BME-IE-BIO and TKP2020 NC, Grant No. BME-NC) based on the charter of bolster issued by the NRDI Office under the auspices of the Ministry for Innovation and Technology and by the Hungarian National Research, Development and Innovation Office (Grant no. NKFI-FK18 128636).

References

[1] ZANA RR, ZELEI A: Feedback motion control of a spatial double pendulum manipulator relying on swept laser based pose estimation. *International Journal of Optomechatronics* 2021, **15**(1):32-60.

[2] SPONG WM: Partial Feedback Linearization of Underactuated Mechanical Systems. In: *Proc. of IEEE/RSJ International Conference on Intelligent Robots and Systems (IROS'94)*. Munich, Germany, 1994.

[3] OTTO S, SEIFRIED R: Real-time trajectory control of an overhead crane using servo-constraints. *Multibody System Dynamics* 2017, **42**(1):1-17.

-ENG-

**ENGINEERING SYSTEMS
AND
DIFFERENTIAL EQUATIONS**

Study on Dynamical Response of Double-Row Self-Aligning Ball Bearing (SABB) Considering Different Radial Internal Clearance (RIC)

BARTŁOMIEJ AMBROŹKIEWICZ^{1,2*}, GRZEGORZ LITAK^{1*},
ANTHIMOS GEORGIADIS², ARKADIUSZ SYTA³, NICOLAS MEIER²,
ALEXANDER GASSNER²

1. Lublin University of Technology, Faculty of Mechanical Engineering, Department of Automation, Nadbystrzycka 36, 20-618, Lublin, Poland, B.A. [0000-0002-8288-2020], G.L. [0000-0002-9647-8345]
2. Leuphana University of Lüneburg, Institute of Product and Process Innovation (PPI), Universitätsallee 1, 21335 Lüneburg, Germany
3. Lublin University of Technology, Faculty of Mechanical Engineering, Department of Computerization and Robotization, Nadbystrzycka 36, 20-618, Lublin, Poland, [0000-0002-3846-835X]

* Presenting Author

Abstract: Ball bearings are widely used in variety of rotary mechanisms expecting their maintenance-free operation. One of the main factors influencing bearing life is radial internal clearance (RIC), which can be simply described as relative movement of ball and raceway perpendicular to the bearing axis. Mentioned parameter has a significant impact on dynamic response of applied ball bearing in the system and brings strong nonlinear effects. In the paper nonlinear 3 degrees of freedom (3-DOF) model of double-row self-aligning ball bearing is established. Mentioned type of bearing is very important from operation point of view, because it is used in applications, where strong misalignments are expected coming from assembly of shaft deflection. That is why third z-axis, in shaft's axis is considered. Model input data are based on characteristics of bearing 2309SK. Results of bearing dynamic response are studied for different values of radial internal clearance, one from each different clearance class. For quantitative and qualitative analysis of nonlinear time series a few statistical indicators and FFT are applied, providing information on bearing's behavior regarding RIC's value. Moreover simulation was performed with different rotational velocities of inner ring. Results can be used in the validation process with acceleration response coming from the real bearing node.

Keywords: rolling-element bearing, radial internal clearance, nonlinear dynamics

Acknowledgment: The research was funded in the framework of the project Lublin University of Technology – Mechanics – International Study at Lublin University of Technology, funded by the European Social Found (project code: POWR.03.02.00-00-1017/16-00).

References

- [1] AMBROŹKIEWICZ B., LITAK G., GEORGIADIS A., MEIER N., GASSNER A.: Analysis of Dynamic Response of a Two Degrees of Freedom (2-DOF) Ball Bearing Nonlinear Model, *Applied Sciences* 2021, **11**(787).
- [2] AMBROŹKIEWICZ B., SYTA A., MEIER N., LITAK G., GEORGIADIS A.: Radial Internal Clearance Analysis in Ball Bearings, *Eksplotacja i niezawodność – Maintenance and Reliability* 2021, **23**(1):42-54.

Simulation of Road Surface Profiles by a Stochastic Parametrical Model

Alfons Ams

Institute of Mechanics and Fluidynamics
Technical University of Freiberg, Germany

Abstract: Road irregularities have an important influence on the dynamic behavior of vehicles. Knowledge of their characteristics and magnitude is essential for the design of the vehicle. The problem of interest is the simulation of road surface profiles because modern test facilities and computer simulations of vehicle dynamics needs driving excitations. An import issue is the power spectral densities and the approximation by analytical formulas. In the paper a stochastic parametrical nonlinear model of first order with bounded amplitudes will be discussed. Some analytical and numerical results will be shown.

Keywords: road surface profiles, stochastic parametrical model, simulation

1. Road Surface Profiles

The road surface profiles are defined by ISO8608 Mechanical vibration – Road surface profiles – Reporting of measured data [1]. Figure 1 shows an example of a measured road.

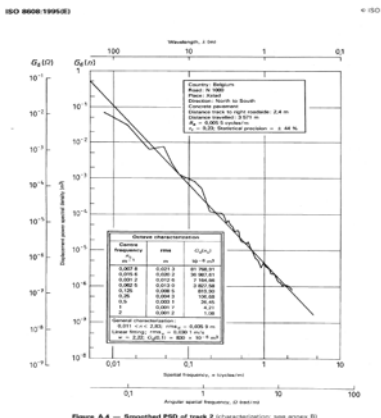


Fig. 1. Measured – road surface profile [1]

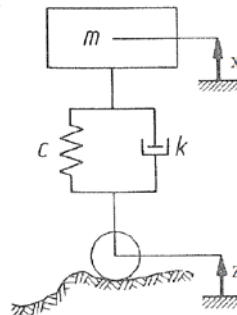


Fig. 2. A quarter car (1 DOF) with road surface profile Z_t

2. Stochastic Parametrical Model

The stochastic parametrical nonlinear model of first order

$$\dot{Z}_t = \left(\frac{1}{2} \sigma^2 - \omega_0 \right) Z_t + \sqrt{Z_0^2 - Z_t^2} \sigma \dot{W}_t$$

with σ intensity of white noise, Z_0 the maximum amplitude, ω_0 the corner frequency and W_t the Wiener process with the mean value $E\{dW_t\} = 0$ and the variance $E\{dW_t^2\} = dt$. The stochastic differential equation (Ito) is

$$dZ_t = -\omega_0 Z_t dt + \sqrt{Z_0^2 - Z_t^2} \sigma dW_t \quad |Z_t| \leq Z_0$$

The Fokker Planck equation of the probability density function is

$$\frac{\partial p}{\partial t} - \omega_0 \frac{\partial}{\partial z} [zp] - \frac{\sigma^2}{2} \frac{\partial^2}{\partial z^2} [(Z_0^2 - z^2)p] = 0$$

The stationary solution of the density function can be calculated to

$$p(z) = C (Z_0^2 - z^2)^{-1+\omega_0/\sigma^2} \quad \sigma^2 < \omega_0$$

The constant C fulfilled the normalization condition $\int_{-Z_0}^{+Z_0} p(z) dz = 1$. The auto correlation function of the stationary process Z_t is

$$R_z(\tau) = \sigma_z^2 e^{-\omega_0|\tau|}$$

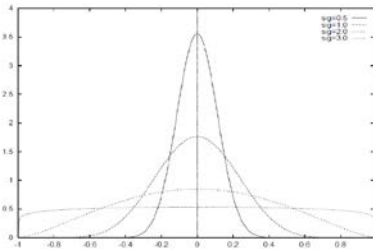


Fig. 3. Stationary density distributions $p(z)$ with $\omega_0 = 10$, $Z_0 = 1$ and different σ

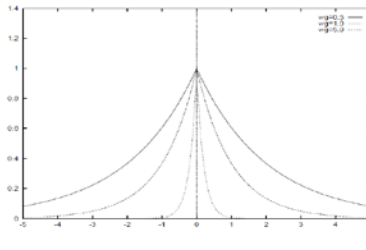


Fig. 4. Auto correlation function $R_z(\tau)$ with $\sigma_z = 1$ and different ω_0

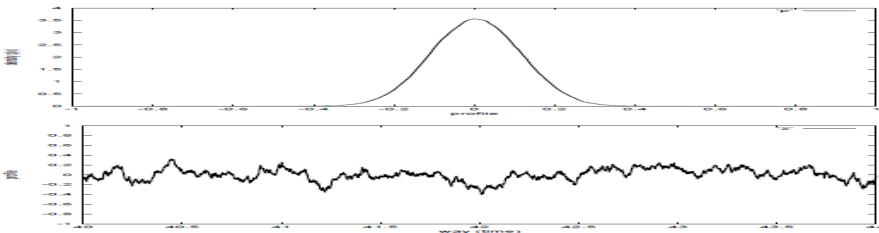


Fig. 5. Numerical realization of the stationary process Z_t with the parameters $\omega_0 = 10$, $Z_0 = 1$, $\sigma = 0.5$ and $N = 10^6$ time steps

References

- [1] ISO 8608:1995(E), Mechanical vibration - Road surface profiles - Reporting of measured data.
- [2] Wedig W.: Dynamics of Cars Driving on Stochastic Roads, In: Spanos P., Deodatis G. (Eds), CSM-4., Rotterdam, Millpress, p. 647 - 654, 2003.
- [3] Doods C. J., Robson J. D.: The Description of Road Surface Roughness, Journal Sound and Vibration, 31, p. 175 - 183, 1973.
- [4] Arnold L.: *Stochastic Differential Equations*. New York, Wiley, 1974

Nonlinear Dynamics of Chaotic Optical Communication Systems: Signal Processing and Cybersecurity

ELENA V BAKUNINA¹, OLEG V. DYKYI¹ AND ARTEM V. VITAVETSKY^{1*}

1. National University "Odessa Law Academy", 28, Rishel'evskaya str., Odessa, 65012
 2. Odessa State Environmental University, Mathematics Depr., L'vovskaya str. 15, 65009, Odessa
- * Presenting Author

Abstract: A chaos–geometric approach to investigation of complex chaotic dynamical systems is applied to an analysis, modeling and processing the time series of emission intensities of chaotic transmitter/receiver systems (two unidirectionally coupled semiconductor laser systems in the all-optical scheme) suited for encoding at rates of GBit/s. The problem of a signal processing is directly connected with the corresponding cybersecurity in some chaotic optical communication systems. The estimated values for the dynamic and topologic invariants such as the correlation and Kaplan-York dimensions, Lyapunov indicators, Kolmogorov entropy etc for investigated chaotic signal time series of two unidirectionally coupled semiconductor laser systems are obtained. For the first time it is constructed a numerical prediction model for the corresponding chaotic signal time series. The obtained data on the chaotic dynamical parameters can be utilized for indirect estimate of a privacy in the communication as the higher the complexity of the carrier the more difficult is to decode a message without the appropriate receiver.

Keywords: chaotic optical communication systems, nonlinear dynamics, invariants

1. Introduction. Nonlinear Dynamics of Chaotic Optical Communication Systems

At present time there are carried out the intensive investigations in the field of signal processing and cybersecurity in different optical chaos communication systems that is provided by a great importance and interest due to its technical applications [1,2]. One should note that a message could be encoded and decoded within a high dimensional chaotic carrier in devices with using coupled single-mode semiconductor lasers subjected to coherent optical feedback or injection, or fiber ring lasers. The important feature of such scheme is connected with successful possibility to synchronize two spatially separated chaotic semiconductor lasers to each other. The authors [1] have presented a review of the main characteristics for emitter/receiver devices concentrating on two kind of chaotic systems: a semiconductor laser subject to a delayed all-optical feedback and a semiconductor lasers subject to a delayed non-linear electro-optical feedback. It has been shown: i) there is generated a direct-chaotic carrier in dynamics of both systems; ii). availability of chaotic regime in system is sufficient to provide a privacy in the communication as the higher the complexity of the chaotic carrier the more difficult is to decode the message without the appropriate receiver [1].

In this paper an effective chaos –geometric approach [2-5] is applied to analysis, modeling and processing the time series of emission intensities of chaotic transmitter/receiver systems (two unidirectionally coupled semiconductor laser systems in the all-optical scheme) suited for encoding at rates of GBit/s. There are listed the estimated values for the dynamic and topologic invariants such as the correlation and Kaplan-York dimensions, Lyapunov indicators, Kolmogorov entropy etc for investigated chaotic signal time series.

2. Results and Discussion

Using a chaos geometric approach in versions [2-5] there are obtained the numerical data of analysis and modeling time series of emission intensities of chaotic transmitter/receiver systems (two coupled semiconductor laser systems in the all-optical scheme). The concrete step is an analysis of the corresponding time series with 8×10^3 points and $\Delta t = 0.0125$ ns. The corrective algorithms have been used in order to reconstruct the missing time series terms. There is an important chaos emergency parameter such as the Gottwald-Melbourne $E_{gm} \leq 1$.

The calculation allows to get the following values of the main topologic and dynamic invariants, namely, the time lag $v=8$, the embedding dimension $D_E=5$, the correlation dimension $D_C=3.2$, the Kaplan-York dimension: $D_L=2.3$, the positive and negative Lyapunov indicators $\delta_1=0.233$, $\delta_2=0.003$, $\delta_3=-0.004, \dots$, the Kolmogorov entropy: $E_K=0.236$.

The performed calculation allows to pay attention at a few important dynamic features in the system. Firstly, availability of two positive Lyapunov indicators is an evidence of a chaos availability in the temporal dynamics and existence of the respective strange attractor in a phase space. It is important to underline that the Kaplan-York dimension is very close to the correlation dimension, but indeed is smaller than the embedding dimension. The latter confirms the correctness of the choice of the latter.

It is important to underline that a changing the governed parameters in a system will result in changing the main dynamic and topologic parameters and can be performed in regime of the numerical experiment. As the problem of a signal processing in investigated chaotic optical communication system is directly connected with the corresponding cybernetic security, it is obvious that the obtained data on the chaotic dynamic parameters and carrier can be utilized for indirect estimate of a privacy in the communication as the higher the complexity of the carrier the more difficult is to decode a message without the appropriate receiver [2].

3. Concluding Remarks

In order to conclude, a chaos-geometric approach (in versions [2-5]) has been applied to investigation of complex chaotic optical communication dynamical systems with the aim of modeling and processing data of the time series for emission intensities of chaotic transmitter/receiver systems. The values of some dynamic and topologic invariants such as the correlation and Kaplan-York dimensions, Lyapunov indicators, Kolmogorov entropy etc are obtained. These data on the chaotic dynamical parameters can be utilized for indirect estimate of a privacy in the communication.

References

- [1] MIRASSO C, FISCHER I, PEIL M AND LARGER L: Optoelectronic Devices For Optical Chaos Communications. *Proc. Spie* 5248, *Semiconductor Optoelectronic Devices For Lightwave Communication*, 2003.
- [2] BAKUNINA E AND DYKYI O: Signal processing and cybersecurity in some chaotic optical communication systems. *Photoelectronics*. 2020, 29:45-51.
- [3] GLUSHKOV AV: *Methods of a Chaos Theory*. Astroprint: Odessa, 2012
- [4] GLUSHKOV A, SVINARENKO A, BUYADZHI V, ZAICHKO P AND TERNOVSKY V: Chaos-geometric attractor and quantum neural networks approach to simulation chaotic evolutionary dynamics during perception process. In: BALICKI J (ED) *Advances in Neural Networks, Fuzzy Systems and Artificial Intelligence, Series: Recent Advances in Computer Engineering*. WSEAS: Gdansk, 2014, 21:143-150.
- [5] GLUSHKOV A, IGNATENKO A, KUZNETSOVA A, BUYADZHI A, MAKAROVA A AND TERNOVSKY E: Nonlinear dynamics of atomic and molecular systems in an electromagnetic field: Deterministic chaos and strange attractors. In: AWREJCIEWICZ J (Ed.) *Perspectives in Dynamical Systems II: Mathematical and Numerical Approaches*. Series: *Springer Proceedings in Mathematics & Statistics*. 2021, 363:Ch.11.

Two-Temperature Heat Transfer in a Metal and a Longitudinal Elastic Wave Generation

W. BIELSKI¹, P. KOWALCZYK², R. WOJNAR^{3*}

1. Institute of Geophysics, Polish Academy of Sciences, Księcia Janusza 64, 01-452 Warszawa, Poland
2. Institute of Applied Mathematics and Mechanics, Faculty of Mathematics, Informatics, and Mechanics, University of Warsaw, Banacha 2, 02-097 Warszawa, Poland
3. Institute of Fundamental Technological Research PAS, ul. Pawińskiego 5B; 02-106 Warszawa, Poland [0000-0001-5927-3087]

* Presenting Author

Abstract: A new version of the classic Danilowskaya's problem is presented. To describe the formation of a longitudinal elastic wave in the metal by a laser beam, we use a two-temperature theory of heating such a metal. In this theory of thermoelasticity, there are two temperatures simultaneously, the temperature of the electron gas T_e and the temperature of the ionic lattice T_i , and both are functions of position and time. The energy transferred by electrons to the lattice per unit volume of the crystal per unit time is proportional to the difference $T_e - T_i$. We give the equations of energy conservation and entropy production, whose thermodynamic consistency is verified. The equations of the problem are quasi-linear, since the specific heat of the electron gas in the considered temperature range depends on the temperature (degenerate electron gas). The one-dimensional process of transmitting thermal energy to the crystal lattice and the formation of mechanical wave is analyzed by the numerical method and illustrated in the pictures for various exemplary cases.

Keywords: electron gas, photon-electron interaction, energy balance, entropy growth

1. Introduction

In Danilowskaya problem the surface of an elastic half-space is suddenly heated, and due to the thermoelastic effect a longitudinal elastic wave is created, [1]. In our case we use a pulse laser beam to heat the metal crystal half-space surface. The energy transfer of the laser beam to the ionic lattice of the metal occurs in two stages. First, the electron gas is heated and this one, in turn, transfers part of the acquired energy to the crystal lattice. In this second stage it follows a thermal deformation of the crystal lattice, what means formation of a longitudinal thermoelastic wave. Emerging of equilibrium between electrons and the lattice in crystals, in particular in metals, is realized by relaxation processes. During the relaxation processes crystal must be looked upon as a two-temperature system. Estimates based on the electrical conductivity of metals give values of α of the order $10^{10} \text{J}/(\text{cm}^3 \text{ s K})$. The relaxation time for the phonon temperature is of the order of 10^{-10} s . For laser pulses of shorter duration, the violation of equilibrium between the electrons and the lattice becomes important. After estimating the contribution of individual components, [2-4], we arrive to the system of equations for temperatures T_e and T_i , and displacement u

$$c_e(T_e) \frac{\partial T_e}{\partial t} = \chi \frac{\partial^2 T_e}{\partial x^2} - \alpha (T_e - T_i) + r(x, t)$$

$$c_a(T_i) \frac{\partial T_i}{\partial t} = \alpha (T_e - T_i)$$

$$\frac{\partial^2 u}{\partial t^2} = c_i^2 \frac{\partial^2 u}{\partial x^2} - \frac{\gamma}{\rho} \frac{\partial T_i}{\partial x}$$

The coefficients in this equation are constants or given functions. The problem given by this system is nonlinear and requires numerical solution.

2. Results and Discussion

The exemplary results of calculation for some values of parameters are presented in the following figures:

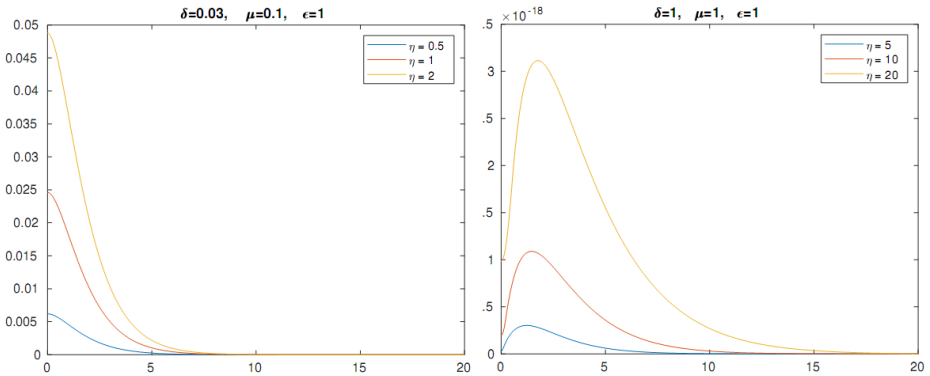


Fig. 1. The ionic lattice temperature (left) and the displacement (right) propagations

3. Concluding Remarks

The two-temperature non-equilibrium system in metal was considered, and two temperatures and displacement fields are found. Moreover, it is shown that for a rectangular in time laser pulse, the temperature and stress are continuous function of time t , while their time derivatives suffer jumps on the t -axis.

References

- [1] DANILOVSKAYA V I, Thermal stresses in elastic semi-space due to a sudden heating of its boundary, *Prik. Mat. Mekh.* 1950, **14** (3) 316-318.
- [2] ANISIMOV S I, KAPELIOVICH B L, PERELMAN T L, Electron emission from metal surfaces exposed to ultrashort laser pulses, *Sov. Phys. JETP* 1974, **39**, 375-377.
- [3] PETROV Yu V, MIGDAL K P, INOGAMOV N A, ZHAKHOVSKY V V, Two-temperature equation of state for aluminum and gold with electrons excited by an ultrashort laser pulse, *Applied Physics B* 2015, **119** (3) 401-411.
- [4] LINDSAY L, KATRE A, CEPULLOTT A and MINGO N, Perspective on ab initio phonon thermal transport, *J. Appl. Phys.* 2019, **126**, 050902.

Structural analyses of compliant tensegrity towers

V. BÖHM¹, P. SCHORR^{1,2*}, J. CHAVEZ¹, L. ZENTNER²

1. Ostbayerische Technische Hochschule Regensburg, Galgenbergstr. 30, 93053 Regensburg, Germany

2. Technische Universität Ilmenau, Max-Planck-Ring 12, 98693 Ilmenau, Germany

* Presenting Author

Abstract: Tensegrity Structures were originally established in the fields of architecture and modern arts. Due to their structural assembly, those prestressed structures are filigree and enable an immense weight-to-load ratio. These features allow the development of large sculptures or buildings, e.g. Needle Tower. However, due to their advantageous properties, tensegrity structures are also suitable for applications in engineering. In this work, various pattern principles to realize such chain-like tensegrity-based systems by cascading modular substructures are presented. In order to evaluate the structural dynamics, the equations of motion are derived. The equilibrium configurations and the corresponding stiffness properties are evaluated. In particular, the deformation capability, as well as the physical limits due to external loads and dead weight, are considered. Subsequently, modal analyses of the linearized systems are performed. The vibration modes and the corresponding eigenfrequencies of tensegrity towers with various topologies are compared. Based on these results constructive guidelines regarding the development of chain-like cascaded tensegrity structures are defined.

Keywords: Compliant tensegrity structure, non-linear dynamics, modal analysis

Energy Transport in 1-Dimensional Oscillator Arrays With Hysteretic Damping

TASSOS BOUNTIS^{1*}, KONSTANTINOS KALOUDIS², JONIALD SHENA³, CHARALAMPOS SKOKOS⁴, CHRISTOS SPITAS²

1. Department of Mathematics, University of Patras, Patras, Greece [0000-0002-8103-8152]
 2. Department of Mechanical and Aerospace Engineering, Nazarbayev University, Nur-Sultan, Kazakhstan
 3. National University of Science and Technology "MISiS", Moscow, Russia
 4. Department of Mathematics and Applied Mathematics, University of Cape Town, South Africa
- * Presenting Author

Abstract: Energy transport in 1-dimensional oscillator arrays has been extensively studied to date in the conservative case, as well as under weak viscous damping. In particular, when driven at one end by a sinusoidal force, such arrays are known to exhibit the phenomenon of *supratransmission*, or sudden energy surge, above a critical driving amplitude. In this paper, we examine such arrays in the presence of *hysteretic damping*, which occurs when energy loss per cycle is independent of the deformation frequency, and include nonlinear stiffness forces that are important for many materials at relatively high energies. We employ Reid's model of local hysteretic damping and Spitas' model of nearest neighbor dependent hysteretic damping and compare their supratransmission and wave packet spreading properties in the deterministic as well as stochastic case. The results have important quantitative differences, which should be helpful when comparing the merits of the two models in specific engineering applications.

Keywords: Oscillator arrays, hysteretic damping, supratransmission, energy transport

Resonance and cancellation phenomena of simply supported partially clamped beams: application to bridges with ballasted track.

S. EL hankari*, R. Dkiouak, K. Roky

Faculty of Science and Techniques at Tangier, Department of Physics, Box 416, 90 000 Tangier, Morocco

Abstract: Since the development of new railway lines of high speed; the dynamic response of bridges constitutes a subject interest of researchers and engineers; several Scientifics have investigated the resonance phenomena in railway bridges; resonance phenomena occur as the excitation frequency coincide with the proper frequency of the bridge. In this work the dynamic behavior of beams leaning on identical rotational springs subjected to the circulation of moving loads at constant speeds is investigated. The free vibration response of the beam when traversed by a single load is obtained analytically and the conditions for maximum response and cancellation in free vibration are derived and interpreted. Then the response of the simply supported partially clamped (SSPC) beam under series of equidistant loads is addressed focusing in the possibility of exciting resonance situations of the former for particular traveling velocities. Equating the conditions for resonance of a particular beam with that of maximum free response and cancellation under a single load, ratios of the bridge length and train characteristic distances leading to resonances of remarkable amplitudes or, contrarily, cancelled resonances are obtained. The possibility to predict both situations could be of especial interest in the set up of dynamic tests in experimental campaigns performed on High-Speed railway bridges.

Keywords: resonance, cancellation, high railway bridge, partially clamped beam

References

- [1] L. FRYBA. A rough assessment of railway bridges for high speed trains. *Engineering Structures* Vol .23 (2001) PP.548-556.
- [2] P. MUSEROS, E. MOLINER, M.D. MARTINEZ-RODRIGO. Free vibrations of simply-supported beam bridges under moving loads: Maximum resonance, cancellation and resonant vertical acceleration. *Journal of Sound and Vibration* 332 (2013) 326–345
- [3] MARIA D. MARTINEZ-RODRIGO, A. DOMENECH, P. MUSEROS. Maximum resonance and cancellation phenomena in elastically-supported beams and its application to railway bridges under High-Speed traffic 2010.
- [4] Y.B. YANG, C.L. LIN, J.D. YAU, D.W. CHANG, Mechanism of resonance and cancellation for train-induced vibrations on bridges with elastic bearings, *Journal of Sound and Vibration*, Vol. 269, Elsevier (2004), pp. 345-360
- [5] M.D. MARTINEZ-RODRIGO, J. LAVADO, P. MUSEROS, Dynamic performance of existing high-speed railway bridges under resonant conditions retrofitted with fluid viscous dampers, *Engineering Structures*, Vol. 32, Elsevier (2010), pp. 808-828.

Continuous Dynamical Systems as Pseudo Random Number Generator

ENGİN KANDIRAN^{1*}, AVADIS HACINLIYAN²

1. Yeditepe University, School of Applied Sciences, Software Development Department, Ataşehir, Turkey
[ORCID: 0000-0002-6171-1346]
2. Yeditepe University, Faculty of Arts and Science, Department of Physics, Ataşehir, Turkey
[ORCID:0000-0002-4667-9659]

* Presenting Author

Abstract: Random number generators are very crucial for both security applications and numerical simulations. There are two main categories of random numbers: those generated by Pseudo Random Generators (PRNGs) and True Random Number Generators (TRNGs). Chaotic systems have been recently used as a random number generator especially in cryptography and data encryption. Researchers prefer to use chaotic dynamical systems as PRNG due to their non-periodic behavior and usability as fast random number generators. The important characteristic of chaotic systems is their sensitive dependence on initial conditions which implies that in integrating equations of motion of such a system, the effect of even an infinitesimal change in the initial conditions will increase exponentially over time and will easily collapse the accuracy of the prediction. In this study, we have proposed a pseudo random number generator (PRNG) based on well-known two chaotic dynamical systems: Rössler system and Duffing oscillator. We test our PSRNGs using statistical test suite NIST and we have shown that both systems pass the test and they are feasible for cryptographic usage. Finally, as an application we use our PRNGs in image encryption and present the performance of them in encryption.

Keywords: pseudo random number generators, image encryption, chaos

Modelling of an Electromechanical Coupling in Magnetic Levitation Energy Harvester

KRZYSZTOF KECIK^{1*}, ANDRZEJ MITURA²

1. Department of Applied Mechanics, Lublin University of Technology, Poland [0000-0001-8293-6977]

2. Department of Applied Mechanics, Lublin University of Technology, Poland [0000-0002-6749-8232]

* Presenting Author

Abstract: This paper concerns the research of electromagnetic energy harvesting consisting of a moving magnet in a specially designed coil consisting of four modules. The electromechanical coupling is modelled by different configurations of the coil. The voltage induced from the interaction between the coil modules differs from the case of a classic single coil. First, the electromechanical coupling models are validated by a free fall test. Then, performances of the harvester are simulated and tested. The obtained results show that the proper configuration of each coil module allows modifying the shape of the electromechanical coupling and the increase of energy harvesting efficiency.

Keywords: electromechanical coupling, energy harvesting, magnetic levitation, multi-segments coil

1. Introduction

Vibration energy harvesters have been expected to be a promising way to solve the energy supply problem for small sensors and MEMS devices. The vibration harvester can convert mechanical energy into electrical energy and has gained much attention in recent years because of the rapid development of systems with low power consumption. The electromagnetic harvester generates electrical power through Faraday's law of induction and induced electromotive force [1]. This force is produced in the coil when it cuts through the magnetic field generated by the moving magnets.

The power density of electromagnetic harvesters can vary depending on the size and coupling (called electromechanical) between the mechanical and electrical components. Therefore, the amount of electricity depends upon the strength of the magnetic field, the velocity of the relative motion between the magnet and coil, and the number of turns of the coil. These harvesters are usually designed for micro and macro scales and the operating frequency range can vary from a few hertz to a couple of hundred hertz.

Electromechanical coupling is defined as the ability to convert mechanical energy into electrical energy. It is mainly studied using the analytical approach and assumed as the constant value due to the small magnet's oscillations leading to the fixed electrical damping [2]. However, as shown in [3] the electromechanical coupling is a strongly nonlinear function. For this, the electromechanical coupling coefficient can be modelled as a function of the magnet position of the coil at any instant.

A promising solution for low-frequency energy harvesting is the development of magnetic levitation systems. This paper presents an analysis of a prototype magnetic levitation harvester with a specially designed coil that consists of four independent coil segments. This is to control the profile of magnetic field variation in the region of the coil movement. Finally, an increase in energy recovery effectiveness is expected.

2. Results and Discussion

Fig. 1(a) shows the design of a vibration-based energy harvester consisting of a single moving permanent cylindrical magnet placing it in a repelling configuration between two stationary ring magnets in a tube. On the tube, a specially designed solenoid coil consisting of four connected in series coil segments is wrapped. Each of the modules can be activated separately or together.

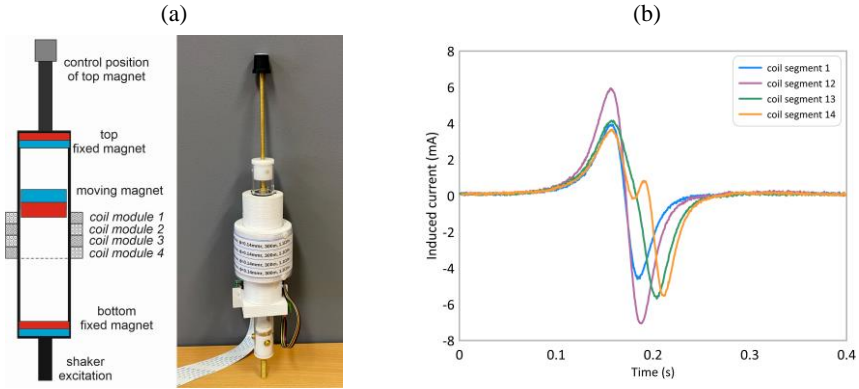


Fig. 1. Scheme and photo of the electromagnetic harvester with modular coil (a) and induced current across versus time for the free fall test and different configuration of coils (b).

Fig. 1(b) shows the result of a free fall test. A simple way to do this is to drop a magnet through a coil. A magnet was released from an initial distance of 0.06m for different combinations of active coil modules. The measured voltage has been obtained from the module combinations: 1, 1:2, 1:3 and 1:4. As we can see, the voltage induced from the interaction between the magnet and coils differs significantly from the case of a single active coil.

3. Concluding Remarks

The obtained results show that the proper configuration of the coil allows to modify of the induced current as well as the electromechanical coupling function. This electromechanical coupling function can be moving, expanded and significantly modified. Interestingly, for some configurations additional peaks close to the coil centre are observed.

Acknowledgment:

The research was financed in the framework of the project: *Theoretical–experimental analysis possibility of electromechanical couplings shaping in energy harvesting systems*”, no. DEC-2019/35/B/ST/01068, funded by the National Science Centre, Poland.

References

- [1] KECIK K, MITURA A: Theoretical and experimental investigations of a pseudo-magnetic levitation system for energy harvesting. *Sensors* 2020, **20**(6):1623.
- [2] SARAIVA CM, RAMIREZ JM, GATTI CG: A hybrid numerical-analytical approach for modeling levitation based vibration energy harvesters. *Sensors and Actuators A: Physical – Journal* 2017, **257**:20-29.
- [3] KECIK K, MITURA A, LENCIS S, WARMINSKI J: Energy harvesting from a magnetic levitation system. *International Journal of Non-Linear Mechanics* 2017, 94:200-206.

Nonlinear Dynamics of a 2DOF Magneto-Mechanical Harvester

KRZYSZTOF KECIK^{1*}, ANDRZEJ MITURA²

1. Department of Applied Mechanics, Lublin University of Technology, Poland [0000-0001-8293-6977]

2. Department of Applied Mechanics, Lublin University of Technology, Poland [0000-0002-6749-8232]

* Presenting Author

Abstract: The nonlinear dynamics of a two-degree-of-freedom (2DOF) magneto-mechanical harvester based on magnetic levitation is modelled and investigated. The equations of motions have been derived while taking into account the magnetic nonlinearity. The experimental relationship of magnetic forces versus the distance between the magnets was determined. Based on these dependencies a strongly nonlinear model of a system with two degrees of freedom was proposed. Finally, the obtained results allowed the determination of nonlinear effects in the investigated system.

Keywords: energy harvesting, magnetic suspension, nonlinearity,

1. Introduction

Magnetic levitation systems have practical importance in many engineering systems. In our previous research, the investigations of a system with one degree of freedom for energy harvesting were presented. Inspiring by [1,2] where the model with one movable magnet between two fixed magnets and inside the coil was presented. Properties of this model were determined from analytical analysis and they were experimentally verified. The obtained results confirmed the existence of nonlinear effects such as bifurcations, amplitude jumps, multistability. Whereas, in the article [3], the interaction between mechanical and electrical was analysed. The obtained results show that the nonlinear resonance and recovered energy can be controlled by the simple configuration of the magnet coil position.

The presented research is a continuation of our previous works. An extension of magnetic levitation for a multi-degree of freedom vibration harvester is proposed. The new concept composed of two levitating magnets is proposed. An additional magnet is introduced to investigate the possibility of increasing the level of energy recovery.

2. Results and Discussion

Fig. 1(a) shows a photo and scheme of the prototype 2DOF harvester. The two identical cylindrical magnets denote A_1 and A_2 are mounted in the tube and experience magnetic levitation. All magnets are placed vertically and have the same magnet orientation (repulsion). Outside the tube, two identical coils are connected. When the harvester is subjected to external excitation, the moving magnets oscillate around their equilibrium state, and the current is induced in both electrical circuits.

The restoring forces were determined from the experiment tests. Top Fig. 1(b) shows the nonlinear relation between the magnets moving magnet A_1 and the fixed magnets B_1 - B_2 . Because the moving magnets are identical, the same characteristic is obtained for the second moving magnet A_2 . As we can see this characteristic is strongly nonlinear and similar to the Duffing model. The restoring force between the two moving magnets at the bottom of Fig. 1(b) is shown. This relation is also strongly nonlinear.

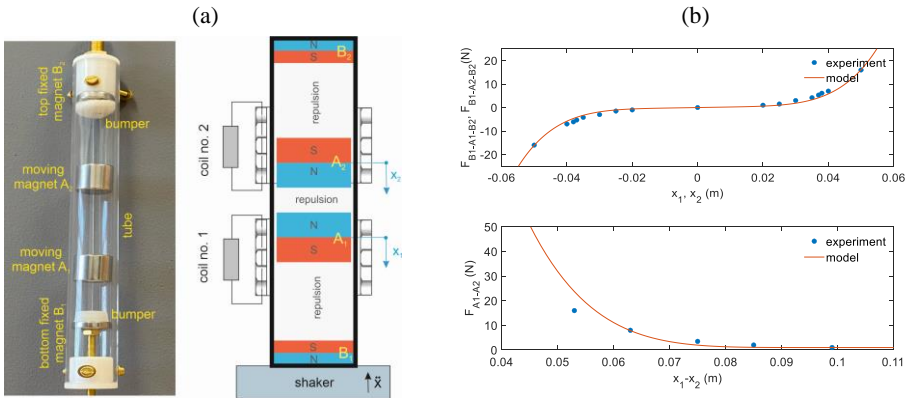


Fig. 1. Photo and scheme of 2DOF magnetic levitation harvester (a) and exemplary induced current during the moving magnet with constant velocity (b).

The experimental measured repulsion force-displacement relations were approximated by the polynomial functions using a least-squares regression method. Polynomial fit is often used due to its simplicity and easy numerical application. The analytical models for magnetic interaction were developed and integrated into the equations of motion directly to simulate the dynamic behaviour of energy harvester configurations.

Acknowledgment:

The research was financed in the framework of the project: *Theoretical-experimental analysis possibility of electromechanical couplings shaping in energy harvesting systems*”, no. DEC-2019/35/B/ST8/01068, funded by the National Science Centre, Poland.

References

- [1] KECIK K, MITURA A: Theoretical and experimental investigations of a pseudo-magnetic levitation system for energy harvesting. *Sensors* 2020, **20**(6):1623.
- [2] KECIK K, MITURA A, LENCI S, WARMINSKI J: Energy harvesting from a magnetic levitation system. *International Journal of Non-Linear Mechanics* 2017, 94:200-206.
- [3] KECIK K., KOWALCZUK M: Effect of nonlinear electromechanical coupling in magnetic levitation energy harvester. *Energies* 2021, 14:2715.

Transversal-transversal internal resonances in planar Timoshenko beams with an elastic support

LUKASZ KLODA^{1*}, STEFANO LENCI², JERZY WARMINSKI¹, ZOFIA SZMIT¹

1. Department of Applied Mechanics, Lublin University of Technology, ul. Nadbystrzycka 36, 20-618, Lublin, Poland [0000-0001-7029-5885, 0000-0002-9062-1497, 0000-0003-1964-3885]
2. Department of Civil and Buildings Engineering, and Architecture, Polytechnic University of Marche, via Breccia Bianche, 60131, Ancona, Italy [0000-0003-3154-7896]

Abstract: The goal of the present work is to explore flexural-flexural internal resonance in an analytical model of Timoshenko beams with whatever axial boundary constraint. First, a set of partial differential equations is treated by multiple time scales method, and next selected results are compared with finite element simulations. Two way coupling between longitudinal and transverse deformations, stability analysis, detached solutions and transfer of energy are studied in depth.

Keywords: nonlinear beam, modal interactions, multiple time scales method, internal resonance

1. Introduction

We study the nonlinear dynamics of a planar, initially straight, extensible Timoshenko beam subjected to the hinged-simply supported boundary conditions and an axial elastic spring k_s at one end, see Fig. 1. Nonlinearities arise from the beam geometry as well as axial, transversal and rotary inertia of the beam, while a linear elastic behavior is assumed in the model [1]. Coupled free and forced-damped nonlinear oscillations of the primary and higher order resonances in the absence internal resonance condition have been studied by the multiple time scales method, considering quadratic and cubic nonlinearities, in [2,3]. The axial-transversal modal interaction between large amplitude flexural oscillations which in 2:1 internal resonance with the longitudinal displacement has been observed in [4].

In the present work the dynamic behavior of the beam with different modal interaction between two successive flexural modes is analyzed by using numerical and analytical approaches. The frequency of the second mode is approximately three times that of the first mode and hence a 3:1 internal resonance can be activated [4,5]. The influence of the longitudinal spring stiffness on the nonlinear system response is investigated and stability is checked by the Jacoby method.



Fig. 1. The beam-spring system

2. Results and concluding remarks

The natural frequencies of the first and second modes are independent of the axial spring stiffness k_s . Despite this fact, the fundamental resonance can be varied from softening to hardening in term of passive control. In addition, the natural frequency in the longitudinal direction trigs the secondary resonance born, which can lead to detached solution path (isolas) as well, see Fig.2. The k_s increment demonstrates secondary resonance reduction, which translates into blocking the longitudinal displacement of the beam tip (hinged-hinged beam).

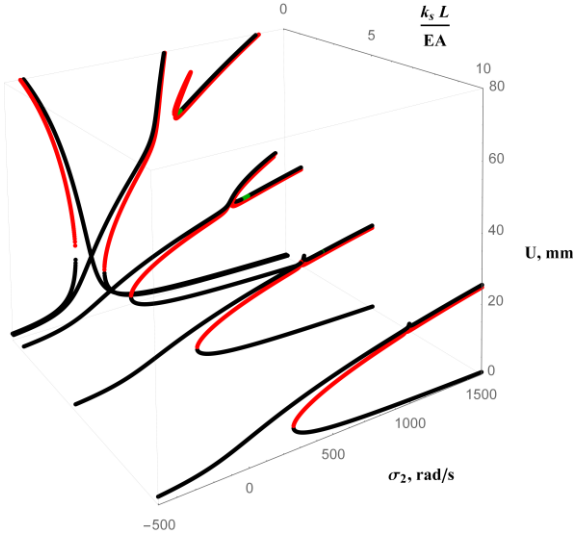


Fig. 2. Frequency response curves of the beam-spring system for $Z=1/4L$ and dimensionless stiffness coefficients $k_s L/EA$ equal 0, 0.1, 1, 5 and 10 (back to front). Jacoby stability analysis: stable (black), unstable saddle-type (red) and unstable source type (green) solutions.

In the future, extension of present work to experimental validation by the kinematical excitation on slip table is planned. The analytical and numerical model will be improved to consider the additional tip mass and moment of inertia at the ends.

Acknowledgment: The work is financially supported by grant 2019/33/N/ST8/02661 from the National Science Centre, Poland.

References

- [1] LENCI S, REGA G: Axial-transversal coupling in the free nonlinear vibrations of Timoshenko beams with arbitrary slenderness and axial boundary conditions. *Proceedings of the Royal Society A: Mathematical, Physical and Engineering Sciences* 2016, **472**:20160057.
- [2] KLODA L, LENCI S, WARMINSKI J: Nonlinear dynamics of a planar beam-spring system: analytical and numerical approaches. *Nonlinear Dynamics* 2018, **94**:1721-1738.
- [3] LENCI S, CLEMENTI F, KLODA L, WARMINSKI J, REGA G: Longitudinal-transversal internal resonances in Timoshenko beams with an axial elastic boundary condition. *Nonlinear Dynamics* 2021, **103**:3489-3513.
- [4] CHIN C M, NAYFEH A H: Three-to-one internal resonances in hinged-clamped beams. *Nonlinear Dynamics* 1997, **12**:129-154.
- [5] KLODA L, LENCI S, WARMINSKI J, SZMIT Z: Flexural-flexural internal resonances 3:1 in initially straight, extensible Timoshenko beams with an axial spring. In press 2021.

PROBABILISTIC ANALYSIS OF NPP SEISMIC LOAD CONSIDERING THE LOCAL SITE EFFECTS

JURAJ KRÁLIK¹

1. Faculty of Civil Engineering, STU Bratislava, Radlinského 11, 810 05 Bratislava, SK
[ORCID 0000-0002-3706-6041]

Abstract: The paper presents the methodology of the seismic load modification considering the local site effects in accordance with IAEA recommendation in large-scale project “Stress Tests of NPP” [3]. The earthquake level is defined with seismological parameters of a given site and response spectrum at the free terrain level as the peak ground acceleration (PGA) corresponded to 84.1% probability of no-exceedance in 10^4 years. The previous probabilistic seismic hazard analysis (PSHA) of the NPP Bohunice site were defined for the homogenous rigid soil [7]. The 3D synthetic ground motion accelerograms $a_x(t)$, $a_y(t)$ and $a_z(t)$, compatible with a design response spectrum were generated in software COMPACEL [4-6]. The influences of the layered subsoil and level of bedrock is investigated in this paper. Two methodology was used. Firstly, the simplified model of homogenous viscoelastic layered subsoil based on continuous solution of wave-equations and Fast Fourier Transform (FFT) algorithm in software SHAKESI [5]. Secondly, 3D nonlinear model based on SFEM in software ANSYS was used to determine the design acceleration spectrum at reactor building foundation level. The probability solution was based on RSM approximation method.

Keywords: Seismic, SSI, Nuclear Power Plants, FEM, ANSYS

1. Introduction

After the accident of nuclear power plant (NPP) in Fukushima the IAEA in Vienna adopted a large-scale project "Stress Tests of NPP" [3], which defines new requirements for the verification of the safety and reliability of NPP. The methodology for calculating local design spectra is based on the following assumptions [1, 3]:

- PGA values for RLE seismicity were determined for the free field assuming the rigidity of the bed of the corresponding to the rock subsoil (for $v_s > 1100\text{m/s}$).
- The response spectrum acceleration for SL-2 [3] were defined based on a probabilistic analysis of the site effects.
- Synthetic 3D accelerograms compatible with response spectra were generated in accordance with the requirements [3].

Based on these input data, the calculation of local design spectra, considering the real geological composition at the location of the SVP object, is carried out in the following steps:

- Calculation of the synthetic accelerograms on the base at level -100m from the free level in accordance with IAEA [3] standards.
- Calculation of the local synthetic accelerograms and the design response spectra at level of foundation from the excitation synthetic accelerations using the program SHAKESI for original and modified geological conditions.

- Calculation of the smoothed design spectra at foundation level than the median values and the statistical envelope for 84.5% probability of failure is based on previous analyses for characteristic excitation frequencies.

Table 1. Comparison of the global and local response spectrum on original subsoil.

Acceleration response spectrum for 5% damping [m/s ²]				
Horizontal accelerations				
Frequency [Hz]	Base level		Free field level	
	RLE	Local	RLE	Local
0.5	0.025	0.059	0.050	0.087
2	0.173	0.159	0.364	1.082
5	0.319	0.293	0.837	1.285
10	0.229	0.240	0.780	0.782
33	0.140	0.136	0.367	0.574

Table 2. Comparison of the global and local response spectrum on original subsoil.

Acceleration response spectrum for 5% damping [m/s ²]				
Vertical accelerations				
Frequency [Hz]	Base level		Free field level	
	RLE	Local	RLE	Local
0.5	0.015	0.043	0.050	0.086
2	0.085	0.061	0.364	1.048
5	0.199	0.167	0.837	0.815
10	0.215	0.242	0.780	0.599
33	0.103	0.096	0.367	0.531

3. Concluding Remarks

This paper presents that the consideration of the local site effects based on the experimental investigation of the subsoil properties is very important from the point of view of the safety and reliability NPP structures [3, 5].

Acknowledgment: The project was realized with the financial support of the Slovak Grant National Agency VEGA 1/0453/20.

References (10 point, bold)

- [1] ASCE 4-98: *Seismic Analysis of Safety Related Nuclear Structures*, ASCE Standard, New York, 1999.
- [2] CLOUGH R.W, PENZIEN J: *Dynamics of Structures*, Mc Graw-Hill, Inc. 1993
- [3] IAEA: *Specific Safety Guide No. SSG-9, Seismic Hazards in Site Evaluation for Nuclear Installations*. IAEA, Vienna, 2010.
- [4] KRÁLIK J, ŠIMONOVIC M: Earthquake response analysis of nuclear power plant buildings with soil-structural interaction. In: *Mathematics and Computers in Simulation 50. IMACS/Elsevier Science B.V.* 1999.
- [5] KRÁLIK J: *Safety and Reliability of Nuclear Power Buildings in Slovakia. Earthquake-Impact-Explosion*, STU Bratislava 2009.
- [6] KRÁLIK J: *Safety and Reliability of NPP in Slovakia Within IAEA Project "Stress Tests"*, pp. 21-36 In: Monograph, Ed. I. Major & M. Major, Częstochowa 2015.
- [7] LABÁK P, MOCZO P: *Determination of the Review Level Earthquake Characteristics for the Bohunice Nuclear Power Plant Site*, Geophysical Institute SAV Bratislava, 1998.

Determination of the Loading of an Open Car with Filler in the Center Sill

ALYONA LOVSKA^{1*}, OLEKSIJ FOMIN², GRZEGORZ M. SZYMANSKI³, DMYTRO SKURIKHIN⁴

1. Ukrainian State University of Railway Transport, Department of Wagon Engineering and Product Quality, Kharkiv, Ukraine [0000-0002-8604-1764]
2. State University of Infrastructure and Technologies, Department of Cars and Carriage Facilities, Kyiv, Ukraine [0000-0003-2387-9946]
3. Poznan University of Technology, Institute of Transport, Poznan, Poland [0000-0002-2784-9149]
4. Ukrainian State University of Railway Transport, Department of Wagon Engineering and Product Quality, Kharkiv, Ukraine [0000-0002-3746-5157]

* Presenting Author; E-mail: alyonaLovskaya.vagons@gmail.com

Abstract: The dynamic loading in the bearing structure of an open car can be decreased with the application of fillers in the center sill. The research included the mathematic modelling of the dynamic loading of an open car. The calculation was made for elastic, viscous, and elastic-viscous fillers. The results of the calculation demonstrated that the application of viscous or elastic-viscous fillers is the most optimal technological solution in terms of decreasing the dynamic loading of an open car. The article presents the results of the computer modelling of the dynamic loading on the bearing structure of an open car. The authors determined the numerical values and the acceleration fields for the open car frame. The dynamic loading models of a car were verified with an F-test. It was found that the hypothesis on adequacy was not rejected. The research also included the strength calculation for the bearing structure of an open car. The maximum equivalent stresses were in the interaction zone between the center sill and the body bolster beam; they were 298.5 MPa, i.e. 9% lower than the stresses in the frame without filler. The research can be used by those who are concerned about designing the innovative structures of freight cars and improving their operational efficiency.

Keywords: transport mechanics, open car, bearing structure, dynamic loading, dynamic modelling, acceleration of the structure.

1. Introduction

Railway transportation plays an important role in the transport complex of many countries. And improvements in the rolling stock, modernization of existing structures, and a decrease of the coefficient of material capacity are the factors which can guarantee the maintenance of the leading position for any big rail operator in Eurasia. Therefore, the introduction of modern rolling stock with improved technical and economic characteristics is an urgent and promising task.

2. Results and Discussion

The dynamic loading on the bearing structure of an open car during operational loading modes can be decreased with some improvements in the frame, which is the main bearing element of the body. It implies the use of a box-section center sill formed with two profiles instead of the standard center sill (fig. 1, a). This solution can decrease the frame mass by about 4% in comparison to that in the stand-

ard structure. Here, it is possible to use filler in the center sill (fig. 1, b). The material of elastic or elastic-viscous characteristics can be used as the filler.

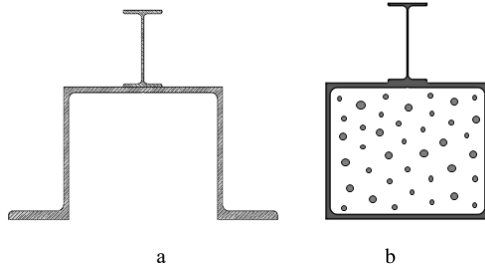


Fig. 1. Section of the center sill with filler a – standard; b – with filler

The loading of the improved bearing structure of an open car was determined with the computer modelling. It was found that the most efficient way is the application of viscous filler. The maximum accelerations to the bearing structure of an open car was 36.8 m/s^2 . This value was 4% lower than that obtained for the bearing structure without filler. The acceleration fields in an open car frame were determined with the computer modelling of the dynamic loading. The calculation was made with the finite element method in SolidWorks Simulation [1, 2]. The dynamic loading models were verified with an F-test [3]. It is found that the hypothesis on adequacy was not rejected. Besides, the research was made for the basic strength characteristics of the open car frame. The maximum equivalent stresses were in the interaction zone between the center sill and the body bolster beam; they were 298.5 MPa, i.e. 9% lower than the stresses in the frame without filler. The maximum displacements were in the middle part of the frame; they were 7.6 mm that was 11% lower than the displacements in the frame without filler.

3. Concluding Remarks

The results of the research can be used by those who are concerned about decreasing the damage in the bearing structure of an open car in operation, reducing the maintenance costs, collecting the data on the designing of the innovative structures of the rolling stock with enhanced operation characteristics.

Acknowledgment: The presented results have been co-financed from the subsidies appropriated by the Ministry of Education and Science - 0416 / SBAD / 0001 and 0416 / SBAD / 000. The authors also gratefully acknowledge supporting from specific research “Innovative principles for creating resource-saving structures of railroad cars based on the refined dynamic loads and functionally adaptive flash-concepts” by the Ministry of Education and Science of Ukraine 2020.

References

- [1] HARAHA S. S., SHARMA S. C., HARSHA S. P.: Structural dynamic analysis of freight railway wagon using finite element method. *Procedia Materials Science* 2014, 6:1891–1898.
- [2] CHEN CHAO, HAN MEI, HAN YANHUI: Study of Railway Freight Vehicle Body’s Dynamic Model Based on Goods Loading Technical Standards. *Procedia Engineering* 2012, 29: 3572–3577.
- [3] FOMIN O., LOVSKA A.: Improvements in passenger car body for higher stability of train ferry. *Engineering Science and Technology an International Journal* 2020, 23, 6: 1455–1465.

Application of the discrete element method to ductile materials subjected to dynamic loads

PRZEMYSŁAW NOSAL^{1*}, ARTUR GANCZARSKI²

1. AGH University of Science and Technology [0000-0001-9751-0071]

2. Cracow University of Technology [0000-0001-7482-3227]

* Presenting Author

Abstract: Dynamic loads accompanying metal forming processes are demanding with regard to numerical simulation. During the deformation process there comes to an interaction between several physical phenomena, where deformation and temperature are the dominant fields. The use of the finite element method in the case of large deformations is problematic and is associated with the fulfillment of the conditional requirements, which will allow to obtain convergence of calculations. One way to overcome these limitations is to use the discrete element method. In this work the possibility to use this method for dynamic analysis was presented. The mathematical model used in simulation takes into account coupling the mechanical field with the thermal field. Due to the large deformation of the material in the presented work, considerable attention was paid to plasticity and the evaluation of flow function used.

Keywords: discrete element method, dynamic load, thermo-plasticity.

1. Introduction

The work of Cundall and Strack [1] is considered the beginning of the formulation of the discrete element method. In its original form it was dedicated to granular materials. In subsequent stages, this method was adapted to other types of materials, mainly used in geomechanics. Currently using this method it is possible to simulate the evolution of the microstructure in materials or to analyze the crack propagation [2-4]. Another advantage of this method is the simplicity of the equations that describe the interactions between the elements. These equations are based on Newton's dynamic laws, thanks to which we can determine the position of the particle in successive time steps

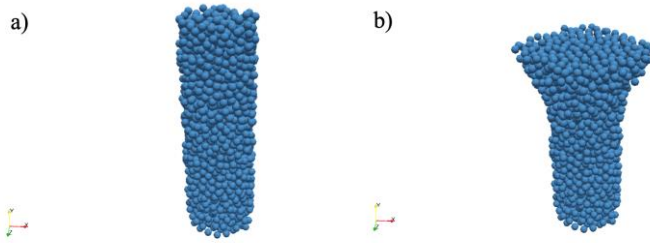
$$m_i \frac{dv_i}{dt} = F_{ij} \quad (1)$$

$$I_i \frac{d\omega_i}{dt} = \sum_j M_{ij} \quad (2)$$

By applying the method of discrete elements to the analysis of solid material, we are forced to replace the material continuum with a set of particles for which the set of mathematical equations has been supplemented with appropriate constitutive models. In the general concept, the material model has isotropic properties, but some modifications to the equations also allow the introduction of anisotropy [2].

2. Numerical modelling and discussion

The constitutive equations that determine the strength of the interaction of particles with each other are assigned to a point located on the contact plane. In this work, the existence of a plane stress state was assumed at the point where the only stresses are σ_x and τ_{xy} . This assumption simplifies the formulation of the flow function and increase the computation time of the algorithm related to the estimation of the plastic deformation. For computational reasons, phenomena related to phase changes of the material were omitted in the paper. Therefore, the energy dissipated during the process is com-



pletely converted into thermal energy.

Fig. 1. Test of deformation in dynamic compression of aluminum sample. Initial geometry a) and deformed sample b).

The dynamic load, which may be related to the metal forming process, leads to intensive plastic deformation of the material in the area where the force is applied (Fig. 1.). This effect is counteracted as the speed of the punch is reduced. It was also noted that the number of particles used for volume discretization influenced the results. This is also confirmed by the works of other authors [3-4].

3. Concluding remarks

The analyzed case allows for the formulation of the following conclusions. The use of the discrete element method enables simulation of the metal forming process taking into account large deformations and the accompanying dissipation of energy in the form of thermal energy, under the basic formulation of constitutive equations. The use of the presented method of volume discretization affects the obtained results. It is necessary to carry out further work to eliminate this problem.

References

1. CUNDALL P.A., STRACK O.D.L.: A discrete numerical model for granular assemblies. *Geotechnique* 1979, **29**:47-65.
2. TRUSZKOWSKA A., YU Q., GREANEY P.A., EVANS T.M., KRUZIC J.J.: A discrete element method representation of an anisotropic elastic continuum. *Journal of the Mechanics and Physics of Solids* 2018, **121**:363-386.
3. NGUYEN V.D.X., KIET TIEU A., ANDRÉ D., SU L., ZHU H.: Discrete element method using cohesive plastic beam for modeling elasto-plastic deformation of ductile materials. *Computational Particle Mechanics* 2020, <https://doi.org/10.1007/s40571-020-00343-4>.
4. O'SULLIVAN C.: *PARTICULATE DISCRETE ELEMENT MODELLING*. Spon Press: London, 2011.

Magnetic oscillator under excitation with controlled initial phase

KRYSTIAN POLCZYŃSKI^{1*}, MAKSYMILIAN BEDNAREK², JAN AWREJCWICZ³

1. Lodz University of Technology, Department of Automation, Biomechanics, and Mechatronics, Łódź, Poland [0000-0002-1177-6109]
2. Lodz University of Technology, Department of Automation, Biomechanics, and Mechatronics, Łódź, Poland [0000-0002-7669-119X]
3. Lodz University of Technology, Department of Automation, Biomechanics, and Mechatronics, Łódź, Poland [0000-0003-0387-921X]

* Presenting Author

Abstract: The work contains the results of numerical simulations of the dynamics of a magnetic pendulum system subjected to excitation with a varying initial phase. A magnetic pendulum consists of a magnet fixed to the end of its arm and an electric coil below it. The initial phase of the excitation is presented as a linear function of the dynamic variable of the system, which is the angular position of the pendulum. The obtained basins of attraction indicate the occurrence of multi-periodic solutions in the system depending on the changes in the parameters of this system. The periodicities of the observed solutions are quantified mostly by odd numbers.

Keywords: pendulum, magnetic field, basins of attraction, controlled excitation, nonlinear dynamics

1. Introduction

Magnetic oscillators and their dynamics have been a frequently undertaken research topic in recent years, which is confirmed by the following works [1–3]. The dynamics of such systems is highly nonlinear, which generates surprising behaviour of the system. Following the example of work [4], we decided to check how the dynamics of the magnetic pendulum is influenced by the dependence of the exciting torque on the dynamic variable – angular position. The general equation of motion of the considered system is presented in the following dimensionless form

$$\theta'' + \beta\theta' + \alpha\theta + \gamma \sin\left(\frac{1}{\gamma}\theta\right) + \left[\delta + \zeta \exp\left(\nu(\theta')^2\right)\right] \tanh(\sigma\theta') = A_0 \exp(-\theta^2) \sin(\Omega\tau + \phi_0), \quad (1)$$

where: θ is the dimensionless angular position of the pendulum, ϕ_0 represents an initial phase, and rest of the coefficient, i.e., β , α , γ , δ , σ , A_0 are constant values. The values of these parameters were determined on the constructed experimental setup and are as follows: $\alpha = 0.323$, $\beta = 0.036$, $\gamma = 7.468$, $\delta = 0.068$, $\zeta = 0.135$, $\nu = -1.029$, $\sigma = 5.549$, $A_0 = 402.569$. We studied the case where the initial phase was a linear function $\phi_0(\theta) = p\theta$, where p is a slope coefficient. Figure 1 shows the numerically obtained basins of attraction calculated for the studied system for a different value of A_0 and p parameters, and constant values of Ω . The initial conditions used in the calculation of the periodicity of the solution were the same for all parameter configurations and were $\theta = 0.001$, $\theta' = 0$.

2. Results and Discussion

The basins of attraction indicate the existence of a range of different multi-periodic solutions. The overwhelming majority of solutions are period-14 or chaotic. Solutions with smaller periodicity create areas of an elliptical shape.

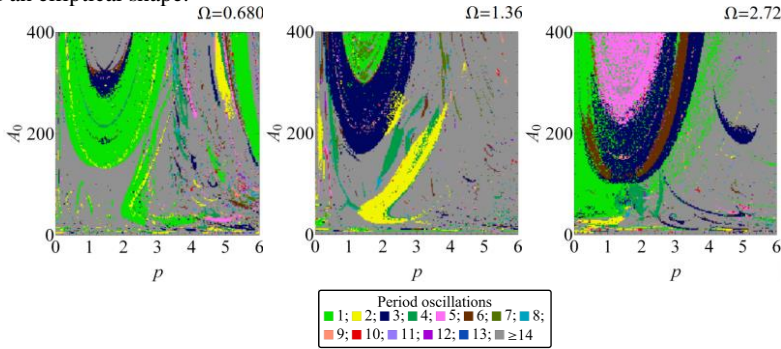


Fig. 1. Basins of attraction computed for system (1) in terms of different values of A_0 and p parameters for three cases of Ω .

It is worth noting that most of these solutions are odd periodicity, i.e., period-1, period-3, period-5. It is also important that for higher values of the p parameter, obtaining a solution with a periodicity of less than 14 significantly decreases.

3. Concluding Remarks

The presented magnetic pendulum is an example of a highly nonlinear mechatronic system whose dynamics are rich with regard to both periodic and chaotic solutions. The linear dependence of the initial phase of the excitation on the dynamic variable (angular position) yields significant changes in the solutions.

Analysis of the basins of attraction shows that for certain ranges of parameter p (slope of the linear function describing initial phase) the variety of solutions increases, however exceeding a certain threshold value ($p \approx 4$) causes the diversity of periodicity to disappear.

References

- [1] WIJATA A, POLCZYŃSKI K, AWREJCEWICZ J: Theoretical and numerical analysis of regular one-side oscillations in a single pendulum system driven by a magnetic field. *Mech. Syst. Signal Process.* 2021, **150**, 107229.
- [2] POLCZYŃSKI K, SKURATIVSKYI S, BEDNAREK M, AWREJCEWICZ J. Nonlinear oscillations of coupled pendulums subjected to an external magnetic stimulus. *Mech. Syst. Signal Process.* 2021, **154**, 107560.
- [3] LUO Y, FAN W, FEN C, WANG S, WANG Y. Subharmonic frequency response in a magnetic pendulum. *Am. J. Phys.* 2020, **88**, 115.
- [4] KRYLOSOVA D. A, SELEZNEV E. P, STANKEVICH N. V. Dynamics of non-autonomous oscillator with a controlled phase and frequency of external forcing. *Chaos, Solitons and Fractals.* 2020, **134**, 109716.

Application of the Differential Transform Method to the Study of the Duffing System with Fractional Damping and Stiffness

ANDRZEJ RYSAK^{1*}, MARTYNA SEDLMAYR²

1. Faculty of Mechanical Engineering, Lublin University of Technology
Nadbystrzycka 36, 20-618 Lublin, Poland [0000-0001-9631-9785]
 2. Division of Applied Sciences, Faculty of Aviation, Polish Air Force University, Dywizjonu 303, 08-521 Dęblin, Poland
- * Presenting Author

Abstract: Non-linear differential equations with fractional derivatives provide a satisfactory description of many real dynamical systems and life phenomena. In this study, a relatively new method for solving the fractional differential equations, i.e. the differential transform method (DTM), is applied to test the Duffing system with fractional stiffness and damping.

Keywords: Duffing system, fractional equations, differential transform method

1. Introduction

The DTM was proposed by Zhou [1] to solve both linear and non-linear problems in electrical circuits. The differential transform of a function $f(x)$ is defined in a similar way to the Taylor series expansion:

$$F(k) = \frac{1}{k!} \left. \frac{d^k f(x)}{dx^k} \right|_{x=0} \quad (1)$$

and the inverse transform is defined as

$$f(x) = \sum_{k=0}^{\infty} F(k)x^k. \quad (2)$$

The method was extended to solve fractional differential equations by Arikoglu and Ozkol [2], with the inverse transform described by the equation

$$f(x) = \sum_{k=0}^{\infty} F(k)(x - x_0)^{k\alpha}, \quad (3)$$

where α is the order of fraction. Despite the fact that DTM derives from the Taylor series expansion, it does not require that the derivative be evaluated symbolically. Instead, relative derivatives are calculated iteratively. Differential transforms of the various expressions are given with proofs in a number of studies (for example [3]). Due to the method's simple iterative scheme, solving fractional differential equations by DTM is numerically fast and gives very accurate solutions.

2. Results and Discussion

In this study, we analyse the Duffing oscillator system with additional damping and stiffness factors that depend on previous states of the system and can, therefore, be described by fractional derivatives. In preliminary tests, the method was approved by comparing the Duffing System solutions obtained using DTM and Runge-Kutta 4 algorithms. An example of typical results is presented in Fig. 1.

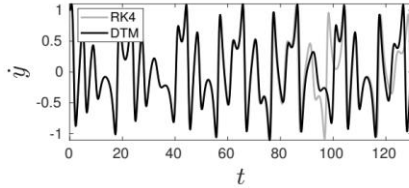


Fig. 1. Solutions of the integer Duffing system, obtained using DTM and RK4 methods.

The calculations assumed an integration step of $h=0.01$ s (DTM) and $h=0.001$ s (RK4). Both solutions change in time identically (by eye) for about 80 seconds. A comparison of the DTM and ode45 Matlab function (RK method with a variable time step) shows that it is possible to obtain the convergence of both solutions for hundreds of seconds provided that the integration step in the ode45 function is appropriately limited.

The analysis starts with the following equation:

$$\ddot{x} = -b\dot{x} - b_p D^{\beta_p} \dot{x} - b_m D^{\beta_m} \dot{x} + k_p D^{\alpha_p} x + kx - cx^3 + f_0 \sin(\omega t), \quad (4)$$

where b_p , b_m , an k_p are the coefficients of the fractional factors with the fractional orders of β_p , β_m , and α_p , respectively. These coefficients define the fractional forces that disturb the Duffing system, whereas the fractional orders determine the influence of the history of the system on the fractional terms. This paper presents the results of the fractional system simulations performed for different values of the coefficients and orders of fractional factors.

3. Concluding Remarks

In each simulation, the average kinetic and potential energies of the system are calculated for the selected time period. As a result, it is easier to distinguish vibration modes in the comparison diagrams and thus assess the influence of fractional factors on the vibration energy accumulated in the system. The results of this study can be useful for designing energy harvesting or dissipation systems using fractional two-well oscillators.

Acknowledgment: The research was financed in the framework of the project Lublin University of Technology-Regional Excellence Initiative, funded by the Polish Ministry of Science and Higher Education (contract no. 030/RID/2018/19).

References

- [1] ZHOU JK: Differential Transformation and Its Application for Electrical Circuits. *Huazhong University Press*, Wuhan, 1986 (in Chinese).
- [2] ARIKOGLU A, OZKOL I: Solution of fractional differential equations by using differential transform method. *Chaos, Solitons & Fractals* 2007, **34**:1473-1481.
- [3] ODIBAT Z, MOMANI S, ERTURK VS: Generalized differential transform method: Application to differential equations of fractional order. *Applied Mathematics and Computation* 2008, **197**:467-477.

A method to improve the accuracy of bridge cranes overload protection using the signal graph

VOLODYMYR SEMENYUK¹, VASYL MARTSENYUK^{2*}, VALERIY LINGUR¹, NADIYA KAZAKOVA³, NATALIIA PUNCHENKO³, PAWEŁ FALAT², KORNEŁ WARWAS²

1. Odessa National Polytechnic University, Ukraine [0000-0002-7240-2848]
2. University of Bielsko-Biala, Poland [0000-0001-5622-1038, 0000-0002-3593-9750, 0000-0003-2577-550X]
3. Odessa State Environmental University, Ukraine [0000-0003-3968-4094, 0000-0003-1382-4490]

* Presenting Author

Abstract: Often during the bridge cranes operation, there occur the crane major components' breakdowns, due to overload. Therefore, to prevent these breakdowns, overhead cranes are equipped with safety devices to protect the mechanism from the overload. The system of bridge cranes protection against overload should expediently provide the crane securing against peak overloads as well as systematic overloads, another necessary requirement being to ensure such protection high accuracy, assessed using the accuracy coefficient. To determine the overhead crane overload protection accuracy coefficient, the "crane - limiter - load" system movement is presented in the form of a signal graph. Transfer functions' dependencies are found by determining the dynamic loads applied to on the hoisting ropes. A method has been developed to improve the accuracy of bridge cranes protection from systematic and peak overloads by the means of a quasi-zero stiffness load limiter designed. It is proposed to use in this load limiter design a roller transmission mechanism that allows to achieve the load limiter's quasi-zero stiffness.

Keywords: overload protection accuracy factor, systematic and peak overloads, transfer functions, quasi-zero stiffness, roller transmission mechanism

1. Introduction

In Figure 1 there is shown the signal graph of the overhead crane's lifting mechanism illustrating the change in force $S(t)$ at the hoisting ropes stepwise in accordance with the stages of "crane - limiter - load" system movement. In this figure, $W_1(t), W_2(t), W_3(t), W_4(t), W_5(t)$ are the transfer functions for each of these stages.

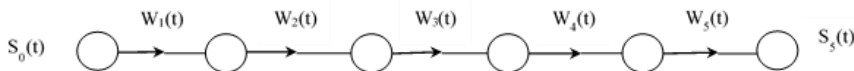


Fig 1. Overhead crane's lifting mechanism signal graph

Now having examined the "crane - limiter - load" system movement corresponding stages, we find the transfer functions' dependences determining the dynamic loads acting on the hoisting ropes, we consider the variance with load limiter installing in a hook suspension.

The calculated dynamic schemes of an overhead crane bearing a load limiter installed in a hook suspension, the pre-detachment and post-detachment movement stages, are shown in Fig. 2 and Fig. 3 respectively.

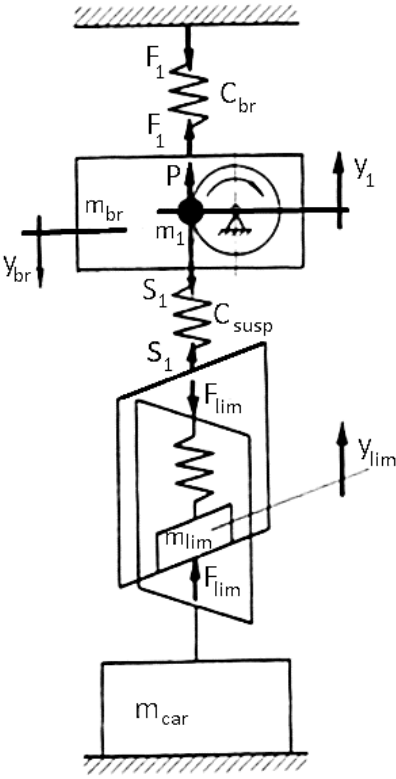


Fig. 2. Calculated dynamic scheme of an overhead crane bearing a load limiter installed in a hook suspension, pre-detachment movement stage

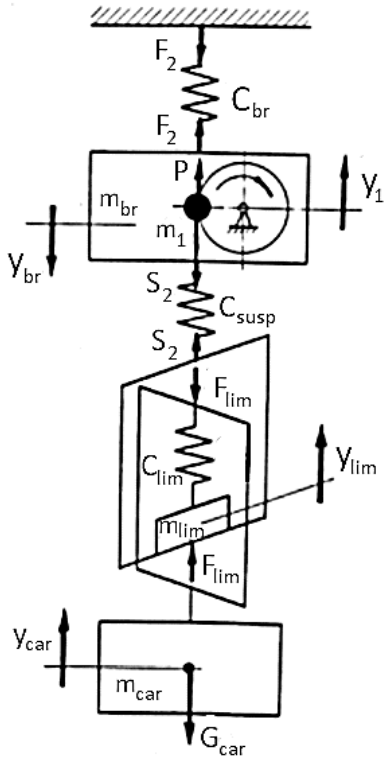


Fig. 3. Calculated dynamic scheme of an overhead crane bearing a load limiter installed in a hook suspension, post-detachment movement stage

2 Conclusions

Dividing the “crane – limiter – load” system movement process into characteristic stages and this process representation in the form of a signal graph allows us to determine ways to improve the accuracy of bridge cranes protection from overload.

An increase in the load limiter stiffness leads to a decrease in the accuracy of bridge cranes protection. The authors elaborated a method to improve the accuracy of bridge cranes protecting against systematic and peak overloads by creating a quasi-zero stiffness load limiter.

There was proposed to use in the new limiter design a roller gear mechanism, allowing to provide quasi-zero stiffness of the load limiter due to the variable gear ratio.

-EXP-

**EXPERIMENTAL/
INDUSTRIAL STUDIES**

Drive-by-wire of a converted into electric car Syrena 105 enabling Hardware-In-Loop tests of driving

PAWEŁ ADAMSKI^{1*}, PAWEŁ OLEJNIK¹

1. Department of Automation, Biomechanics and Mechatronics, Lodz University of Technology, 1/15 Stefanowski Str., 90-924 Lodz, Poland [PO ORCID: 0000-0002-3310-0951]

* Presenting Author

Abstract: In this work, replacing an electronic throttle pedal and a driver in an electric car converted into electric by a hardware-in-loop workbench is described, highlighting the advantage of drive-by-wire feature that appeared after conversion. Drive-by-wire facilitates replacing a driver by Hardware-In-Loop (HIL) workbench, as instead of simulating a mechanical pedal depression by a servomechanism, electric signals can be transmitted directly from the workbench. Thanks to one-pedal-driving feature of the motor controller used in the car, there is a possibility of performing a variety of road tests replacing only the electronic throttle pedal. Hardware interventions in the car are described and sample HIL test results are presented.

Keywords: driving cycles, HIL driving, PID, conversion

1. Introduction

Despite the best knowledge of a car under consideration and best conversion design, to acquire the full performance of a converted car, there is a need of performing driving tests without any human error – specifically HIL drive tests. Car conversions into electric imply some changes among which exchanging mechanical throttle pedal by electronic one, which is commonly called drive-by-wire [1] and substantially facilitates any automation or HIL testing. The car under consideration is Syrena 105 family car produced in Poland in 1979, and converted into the electric vehicle.

2. Results and Discussion

Some basic parameters that can be set in the controller used in the car are: Creep torque – torque generated when stationary vehicle is ready to drive (imitation of ICE car with hydrokinetic clutch automated gearbox), Neutral torque, that stands for regenerative braking in case of releasing the throttle pedal when cruising (imitation of engine braking caused by friction of compression).

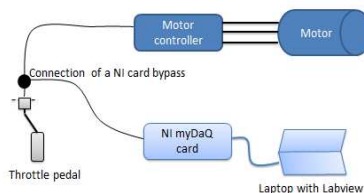


Fig. 1. Open-loop control HIL schematics

Setting the last one to big values enables achieving a car that is possible of one-pedal-driving, as throttle pedal can be used for accelerating from stationary, adjusting actual speed, and also for deceleration until stationary.

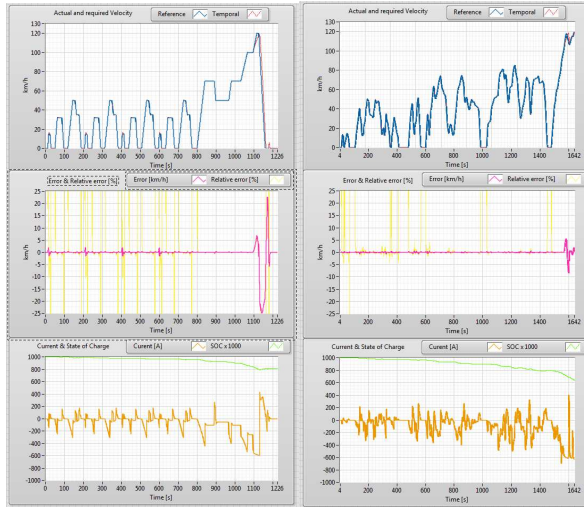


Fig. 2. Time histories of two state variables of a virtual vehicle model's drive cycles

To realise it, a mathematical model of the electric car was programmed in LabVIEW environment, and a numerical PID controller was used in the program to adjust the throttle pedal's signal in such a way, to minimise an error between the reference speed profile of a standardised driving cycle and the actual vehicle speed calculated from measurement of motor speed in a feedback loop.

Tests were carried out both in open (see Fig. 1) and closed-loop control, with HIL and fully virtually. Results of cycling a virtual car model over WLTP and NEDC drive cycles (Fig. 2) show error between reference and actual car velocity, along with battery current and State-Of-Charge (SOC) given as a percentage and multiplied by 10.

3. Concluding Remarks

It is possible to drive a converted into electric car with a one-pedal-driving. It is relatively easy technical task to substitute an electronic throttle pedal by a signal from an acquisition card attached to a laptop. It is possible to run standardised driving cycles in a HIL test procedure with a converted into electric vehicle using simple acquisition cards.

Acknowledgment: The authors would like to acknowledge Prof. Damian Batory for support in sharing the best possible research environment and Dr Marian Jerzy Korczyński for on-going support in each e-mobility topic.

References

- [1] STANTON N, MARSDEN P.: Drive-by-wire systems: Some reflections on the trend to automate the driver role. *Proceedings of the Institution of Mechanical Engineers, Part D: Journal of Automobile Engineering*, 1997, 211(4):267-276.

Evaluation of stress wave propagation in particle-reinforced metal matrix composites

KEMAL ARSLAN^{1,2,*}, RECEP GUNES³

1. Graduate School of Natural and Applied Sciences, Erciyes University, Turkey [0000-0002-2162-3923]
2. Department of Mechanical Engineering, Adana Alparslan Turkes Science and Technology University, Turkey [0000-0002-2162-3923]
3. Department of Mechanical Engineering, Erciyes University, Turkey [0000-0001-8902-0339]

* Presenting Author

Abstract: This study presents an experimental evaluation of stress wave propagation induced by high strain-rate compression in particle-reinforced MMCs (Metal Matrix Composites) with different ceramic volume fractions. Composite specimens that are produced by powder metallurgy technique are utilized in the experiments. The high strain-rate compression tests are carried out using a SHPB (Split-Hopkinson Pressure Bar) setup at various strain-rates to evaluate the stress wave propagation in the composite specimens. Additionally, a quasi-static compression test for each specimen is conducted using a universal testing machine to understand the strain-rate sensitivity of the composites. The quasi-static and dynamic compression test results are examined in terms of stress-strain response and strain-rate sensitivity of the composite specimens, and the effect of ceramic volume fraction is also investigated. The compressive yield strength of the composites is found to be strain-rate sensitive, and it increases with increasing strain-rate and increasing ceramic volume fraction.

Keywords: metal matrix composites, particle reinforcement, stress wave propagation, dynamic compression

1. Introduction

Metal matrix composites (MMCs) draw a great attention in engineering applications with their desirable properties over monolithic metal alloys such as higher specific strength and stiffness, higher wear, fatigue, creep, and corrosion resistance and over polymer matrix composites such as higher strength, stiffness, service temperature, electrical and thermal conductivity, radiation resistance, and minor or no moisture absorption [1]. Therefore, MMCs have been employed in several engineering fields such as automotive, aerospace, and military industries. Especially, utilizing lightweight matrix material such as an aluminium alloy makes these composites a strong candidate for these industries due to high strength to weight ratio. In these application fields, they can be exposed to impulsive loadings during their service life. Thus, it is important to understand the dynamic mechanical response of MMCs for design of structural components.

In the literature, the high strain-rate compression behaviour of MMCs is studied for various matrix and reinforcement materials and different volume fractions of reinforcement, generally low or intermediate fractions [2-5]. In this study, the dynamic compressive behaviour of a ceramic particle-reinforced MMC with an aluminium alloy matrix is investigated for both low and high ceramic volume fractions at various strain-rates. The effects of strain-rate and ceramic volume fraction are discussed on the compressive behaviour of the composites. Different ceramic fractions are considered to understand the effect of ceramic content on the plastic deformation capability of the composites.

References

- [1] CHAWLA N, CHAWLA KK: *Metal Matrix Composites*. Springer-Verlag: New York, 2013.
- [2] LEE WS, SUE WC, LIN CF: The effects of temperature and strain rate on the properties of carbon-fiber-reinforced 7075 aluminum alloy metal-matrix composite. *Composites Science and Technology* 2000, **60**(10):1975-1983.
- [3] ZHANG H, RAMESH KT, CHIN ESC: High strain rate response of aluminum 6092/B₄C composites. *Materials Science and Engineering: A* 2004, **384**(1-2):26-34.
- [4] TAN ZH, PANG BJ, QIN DT, SHI JY, GAI BZ: The compressive properties of 2024Al matrix composites reinforced with high content SiC particles at various strain rates. *Materials Science and Engineering: A* 2008, **489**(1-2):302-309.
- [5] LIU J, HUANG X, ZHAO K, ZHU Z, ZHU X, AN L: Effect of reinforcement particle size on quasistatic and dynamic mechanical properties of Al-Al₂O₃ composites. *Journal of Alloys and Compounds* 2019, **797**:1367-1371.

Gas bubble trajectory in nanofluid

JAKUB AUGUSTYNIAK^{1*}, DARIUSZ M. PERKOWSKI^{2*}, IZABELA ZGŁOBICKA³

1. Faculty of Mechanical Engineering, Białystok University of Technology [0000-0003-4881-1841]
2. Faculty of Mechanical Engineering, Białystok University of Technology [0000-0001-5114-7174]
3. Faculty of Mechanical Engineering, Białystok University of Technology [0000-0002-4432-9196]

* Presenting Author

Abstract: Nanoliquids are gaining in popularity in a relatively short period of time in various industrial applications. This work concerns an attempt to control the two-phase flow process due to the addition of nanofluid to the well-known phenomenon of gas bubble movement in liquid. The analysis of the obtained results based on the registration of individual bubble will be mainly based on a non-linear analysis, which is the multifractal analysis.

Keywords: trajectory, nanofluid, multifractal, image analysis

1. Introduction

The growing industry demand for optimization, accuracy and pollution reduction is driving the re-examination of fundamental process problems. One of the main such issues concerns two-phase flows, and in particular the free movement of gas bubbles in a liquid. Over the past decades, countless experimental studies have been carried out, the results of which have allowed us to understand the observed phenomenon to a large extent. Nevertheless, there is still a lot of room to improve both the understanding of the phenomenon itself and its optimization. This paper deals with the analysis of the trajectory of gas bubbles in water with the addition of silica nanopowder. The influence of nanofluid addition to distilled water is investigated in terms of the movement of individual gas bubbles and their repeatability, as well as the process of periodic detachment from the nozzle front.

2. Results and Discussion

The tests were carried out in a glass tank filled with distilled water, to which a solution of distilled water with silica nanopowder at a concentration of 0.5%, 0.8% and 1.0% was then added. The scheme of the setup is shown in Fig. 1 In the conducted experiment, the air flow rate, the diameter of the nozzle generating bubbles and the height of the liquid column in the tank will be controlled.

The nano liquid was prepared in distilled water into which diatom powder was introduced. The solution was then broken into smaller particles using an ultrasonic cleaner. The liquid prepared in this way was added to a tank filled with distilled water at a temperature of about 21 degrees Celsius . The result of the obtained liquid is shown in Fig. 2. It is worth mentioning that it is an SEM photo of a liquid sample that was put on the table and allowed to evaporate freely.

Then, using the image processing algorithm [1], it becomes possible to create three-dimensional trajectories of the movement of individual gas bubbles. Each trajectory will be subjected to non-linear data analysis [2,3], as a result of which a graph will be obtained showing the spectrum of singularities with information on the two-phase flow process itself, the movement of a single bubble and the long-term memory phenomenon of the entire system.

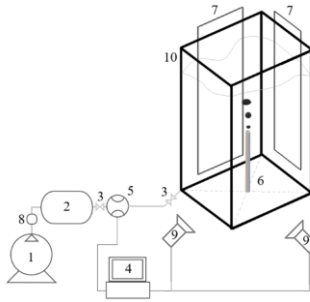


Fig. 1. Experimental setup: 1 - compressor, 2 - air tank, 3 - ball valves, 4 - computer, 5 - mass flow meter, 6 - brass nozzle, 7 - led panels, 8 - proportional valve, 9 – double camera system, 10 – glass tank.

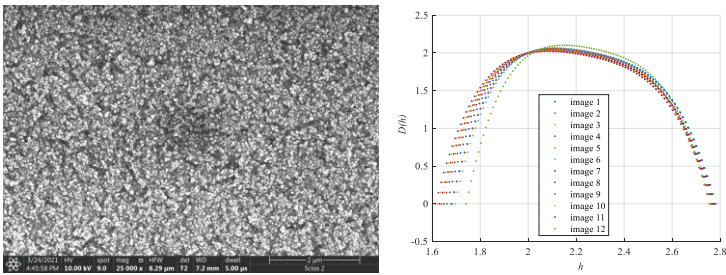


Fig. 2. SEM image of the prepared nanofluid sample and exemplary multifractal spectra.

3. Concluding Remarks

As a result of the research, singularity spectra will be obtained, which will provide information on the three characteristic points, the width of the multifractal spectrum and the placement in the singularity domain. Thanks to such an analysis, it will be possible to draw conclusions about the two-phase flow process itself and the quality of the obtained nanofluid.

Acknowledgment: This work has been accomplished under the research project No. 2018/29/N/ST8/01672 financed by the Poland National Science Center by Jakub Augustyniak. This work has been accomplished under the research project WZ/WM-IIM/3/2020 financed by the Białystok University of Technology by Dariusz M. Perkowski.

References

- [1] AUGUSTYNIAK J., PERKOWSKI D. M.: Compound analysis of gas bubble trajectories with help of multifractal algorithm. *Experimental Thermal and Fluid Science* 2021, vol. 124, s.1-18.
- [2] AUGUSTYNIAK J., PERKOWSKI D. M., MOSDORF R. P.: Measurement of multifractal character of bubble paths using image analysis. *International Communications in Heat and Mass Transfer* 2020, vol. 117, s.1-10.
- [3] GOLDBERGER A, AMARAL L, GLASS L, HAUSDORFF J, IVANOV PC, MARK R, MIETUS JE, MOODY GB, PENG CK, STANLEY HE. PhysioBank, PhysioToolkit, and PhysioNet: Components of a new research resource for complex physiological signals. *Circulation* [Online]. 101 (23), pp. e215–e220.

Application of bulk granules as a damping material for sports boards

JACEK M. BAJKOWSKI^{1*}, JERZY BAJKOWSKI²

1. Faculty of Production Engineering, Warsaw University of Technology, Narbutta 85, 02-524 Warsaw, Poland
[<https://orcid.org/0000-0002-4829-0479>]
 2. Polish Air Force University, Dywizjonu 303 35, 08-521 Dęblin, Poland
- * Presenting Author

Abstract: Sport boards like snowboard decks or skis undergo continuous deformation caused by manoeuvres performed on irregular surface of snow, which leads to rapid vibrations during dynamic ride. A container partially filled with bulk granules was attached to the top layer of different boards to suppress lateral or torsional vibrations by dissipating energy through non-conservative interactions among colliding granules. The system is generally a layered cantilever beam, subjected to various dynamic loads. The performance of such dynamic systems was verified experimentally on a custom designed laboratory stand and on-snow. An empirical mode decomposition and Hilbert transform were used to track the damping performance. Vibration amplitude was proven to be reduced more effectively in laboratory and on-snow, when granules fill the container, than when the boards were damped intrinsically.

Keywords: granular material, vibration, damping, bending, experiment

1. Introduction

During dynamic gliding, snowboard decks or skis experience random vibrations caused by continuous deformations from the irregularities of the snow surface. An important challenge is to provide a certain amount of damping, without adding too much weight or bending stiffness, ensuring that the sport experience is not compromised.

The dominating approach to mitigate these vibrations is to introduce damping layers to the inner structure. A rather rare approach uses external damping elements attached to the deck. The presented solution explores the possibility of using bulk granular material to attenuate these unwanted vibrations. Movement of the loose granules causes dissipation of energy through non-conservative interactions.

A container was attached to the upper surface of the ski and snowboard tip, and filled with different number of spherical granules. The transient response was expected to be nonlinear, with granular damping varying over amplitude. A Hilbert transform (HT) analysis, based on the approach developed by Feldman, as well as Huang et al. [1, 2] was performed.

In the laboratory, ski and snowboard were fixed to a massive support and secured between the toe and the heel piece of the binding with a clamp, while the shovel remained free. Laser sensors were used to record displacement at the selected point of the excited board.

During on-snow pilot study performed in one of the ski resorts, a container with granules was fixed to one ski, while the other one was only damped intrinsically. Skis were instrumented with wireless accelerometers with integrated data recorder. The experimental stand used in laboratory, the photo taken during on-snow tests and exemplary results from field tests are presented in **Fig. 1**.

2. Results and Discussion

It takes some time for granules to reach peak damping, since in the initial phase of motion, granules are resting on the bottom of the container and need at least one full swing of the ski or snowboard to start impacting the lid. During laboratory tests, in cases of higher initial deflection, a larger degree of damping is observed during the first stage of motion. The intrinsic damping ratio for skis reaches 0.1 for amplitudes from 40-20 mm, while granular damping is up to 2.5 times higher, reaching almost 0.25 for selected number of granules.

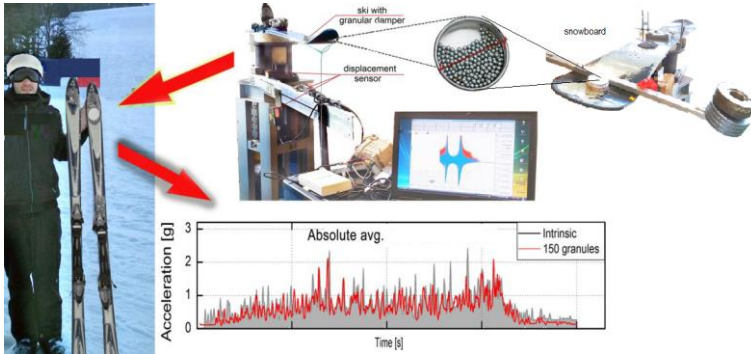


Fig. 1. Graphical abstract of the research: experimental stand, on-snow tests and field recorded results for damping of the ski with 150 granules.

When field-tests are concerned the granular damper device is most efficient when absorbing large oscillations of the shovel on moguls, hardpacked or icy snow. Although the recorded acceleration history seems similar for both skis, the granular damper reduces peak amplitudes quickly after excitation. The calculated average amplitude of all peaks above 1 g was 2.42 g for intrinsic damping and 2.2 g for granular damping. An average value of acceleration reveals that vibrations of a ski with granular damper are usually below values obtained for intrinsic damping. Granular damping remain effective usually in short periods, reducing acceleration peaks.

3. Concluding Remarks

The experimental and field test results showed, that it is possible to modify the damping of full-size sport boards with loose granular material. The solution is passive, but the efficacy can be adjusted by changing the fill ratio of the container. The damping ratio depends on the amplitude, since transient vibrations can be divided into stages corresponding to different granular damping capacities. Vibratory energy is dissipated within granules especially well during the first cycles of the motion. With a small weight penalty, granular damping can be up to 2.5 times higher than intrinsic damping.

References

- [1] FELDMAN M.: Non-linear system vibration analysis using Hilbert transform-I. Free vibration analysis method 'FREEVIB', *Mech. Syst. Signal Process* 1994, **8**(2):119–127.
- [2] HUANG E., ZHENG S., LONG S.R., ET. AL.: The empirical mode decomposition and the Hilbert spectrum for nonlinear and non-stationary time series analysis 1998, **454**:903–995.

Impact of Fiber Orientation Angle on the Phase Velocity of the Fundamental Elastic Wave Modes in Composite Plates of Angle-Ply Configuration

MAREK BARSKI^{1*}, ADAM STAWIARSKI², PAWEŁ ROMANOWICZ³, MARCIN AUGUSTYN⁴

1. Chair of Machine Design and Composite Structures; Cracow University of Technology [0000-0002-2247-5846]
2. Chair of Machine Design and Composite Structures; Cracow University of Technology [0000-0002-5700-4841]
3. Chair of Machine Design and Composite Structures; Cracow University of Technology [0000-0001-7475-1577]
4. Chair of Machine Design and Composite Structures; Cracow University of Technology [0000-0002-8023-9198]

* Presenting Author

Abstract: The present work is mainly devoted to the problem of the determination of the dispersion curves for the elastic waves, which propagate in the composite plates of angle-ply configuration. The plates are made of carbon fibers and epoxy resin. The dispersion curves are determined with the use of the stiffness matrix method. The specially dedicated software DisperseWin has been developed in C++. Next, the obtained values of phase and group velocity and corresponding values of the frequency are verified with the use of standard FE simulations. The elastic wave modes (symmetric and shear horizontal) are identified by applying the envelope method based on the Hilbert transform. It is observed that in the case of a simple box-shaped model of the piezoelectric elements (actuators) placed on the up and bottom surface of the plate and excited by the same signal, the symmetric and shear horizontal elastic wave modes are generated at the same time. In the case of some composite configurations, these modes are overlapped each other, and it is not possible to distinguish between them. Thus the special method of exciting the shear horizontal wave mode is proposed. A very good correlation between the values of group velocities obtained from the analytical calculation (dispersion curves) and the numerical simulation is observed.

Keywords: composite plates, fundamental elastic waves, dispersion curves, FE simulation.

1. Introduction

One of the very promising possibilities is the analysis of the phenomenon of the propagation of the elastic wave through the interrogated composite structure [1–3]. What more, this kind of damage detection system can be also implemented in the online mode and it can operate without the need of stopping the exploitation of the analyzed structure. These kinds of systems are known as structural health monitoring (SHM). However, the phenomenon of elastic wave propagation in composite structures possesses a very complex character. In the general case, the elastic wave consists of three different fundamental wave modes (symmetric S, anti-symmetric A, and shear horizontal SH) as is shown. Moreover, each mentioned fundamental wave mode together with increasing frequency possesses also higher modes. Some of these modes are very sensitive on the dispersion and some of them are almost not dispersive. These facts significantly complicates the proper interpretation of the registered dynam-

ic response of the analyzed structure in order to detect the potential damage. Therefore, the very important part of the designing of the SHM systems, especially in the case of composite structures, is determining of the dispersion properties of the elastic waves.

2. Results and discussion

In the present work, the dispersion curves are determined for the laminate made of carbon fiber/epoxy resin (fibers T300, matrix N5208). The mechanical properties of the layers are as follows: $E_1 = 181$ GPa, $E_2 = 10.3$ GPa, $G_{12} = 7.17$ GPa, $\nu_{12} = 0.28$, and density $\rho = 1.6$ g/cm³. The laminate consists of 8 layers of identical thickness, where $t_i = 0.25$ mm. It is assumed that the studied laminate is of the angle-ply configuration, namely $[\pm\theta]_4$, where θ denotes the angle between the fibers in a particular layer and the X direction of the global coordinate system. In Figure 1 is presented the sets of dispersion curves, which are generated for the laminates where the fiber orientation angle is equal to $\theta = 0^\circ$. The assumed range of frequency is 0.05 MHz $< f < 1$ MHz and corresponding range of phase velocity is 0.2 km/s $< c < 12$ km/s.

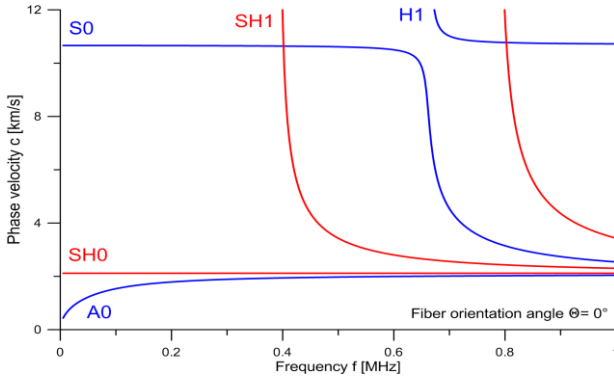


Fig. 1. Dispersion curves obtained for the carbon laminate of configuration $[\pm 0^\circ]_4$

The following values of θ are studied, namely: $\theta=0^\circ, 5^\circ, 15^\circ, \dots, 90^\circ$. The stiffness matrix method is applied. It should be stressed here that this method occurred to be a very effective approach even in the case of composite materials with strongly anisotropic mechanical properties. To the contrary of the other matrix methods, this method is unconditionally numerically stable. The impact of the laminate configuration (in other words, the fiber orientation angle θ) can be summarized as follows:

- the phase c and group velocity c_g of the fundamental symmetric elastic wave mode S_0 monotonically decreasing;
- quite different behavior can be observed in the case of the fundamental shear horizontal mode SH_0 . The clear maximum is found for the $\theta \approx 45^\circ$. Moreover, for the $55^\circ < \theta < 75^\circ$ the phase velocity c as well as group velocity c_g of the fundamental symmetric mode S_0 is much lower in comparison with the fundamental shear horizontal mode SH_0 ;
- the phase c and group velocity c_g of the fundamental anti-symmetric wave mode A_0 decreases slightly together with increasing of the fiber orientation angle θ ;
- the first higher elastic wave modes are observed for the frequency $f \approx 400$ [kHz].

References

- [1] SU Z, YE L, LU Y: Guided Lamb waves for identification of damage in composite structures. *Journal of Sound and Vibration* 2006, **295**:753-780.
- [2] GIURGIUTIU V: *Structural Health Monitoring with Piezoelectric Wafer Active Sensors*. Elsevier, 2008.

Measurement of Dynamic Parameters of Composite Columns

ARTUR BOROWIEC^{1*}, DANIEL SZYNAL², ŁUKASZ SZYSZKA³

1. Rzeszów University of Technology [0000-0002-9475-3251]

2. Rzeszów University of Technology [0000-0002-7020-2367]

3. Rzeszów University of Technology [0000-0001-5017-7611]

* Presenting Author

Abstract: The paper presents the results of measurements of dynamic parameters of composite lighting columns in the laboratory. The subject of the research were two types of composite poles 9.0 m high. The poles were made of GFRP (Glass Fiber Reinforced Polymer) or G/BFRP (Glass/Basalt Fiber Reinforced Polymer) composites.

Keywords: modal analysis, composites, lighting columns

1. Introduction

Nowadays, the use of composite materials is more and more common in all types of industries. Starting from the aviation industry, through shipbuilding, automotive industry, and ending with civil engineering [1]. Designing and applying composites as an element of construction requires verification of their mechanical properties. From the point of view of resistance to dynamic loads (vibrations, shocks), it is important to determine their real dynamic parameters (resonance frequencies, damping, vibration modes). Most often, experimental modal analysis [2] is used for the estimation of modal models. This knowledge can be used to validate their numerical models.

2. Results

The tested poles were designed and manufactured by Alumast S.A. The experimental tests of the poles were carried out at the Faculty Research Laboratory of Structures. Three columns were tested for each type, six columns in total. The composite part of round columns was with variable stiffness along the height. The research was carried out using the modal analysis system with impulse and kinematic excitation. The analysis was performed for the frequency band 0.5-160.0 Hz. The following were used for the measurements:

- multi-channel recorders Scadas-LMS,
- acceleration sensors,
- modal hammer PCB 086D20 (soft tip),
- shaker TIRA TV59389,
- software LMS TEST.LAB v.16A.

For the excitations of the tested elements were used modal hammer and white noise. The response to the excitations was recorded in the 0.5-204.0 Hz band with a resolution of 0.05 Hz. The arrangement of measurement accelerometers (P1-P7) on the tested elements and the place of impulse excitations (PHx, PHy) are shown in Fig. 1. The reference (Ref) and control (Pk) accelerometers were used to control the shaker excitation.

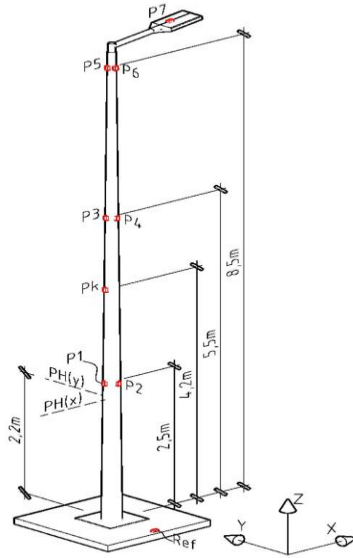


Fig. 1. Distribution of acquisition points on the tested elements

During the tests, 16 vibration modes were identified in the range up to 120 Hz. Their resonant frequency values and damping coefficients were determined. The Table 1. shows the eight resonance frequencies of the tested composite elements. Lower frequencies were measured for columns made of G/BFRP composite.

Table 1. Comparison of measurement results

	f_1 [Hz]	f_2 [Hz]	f_3 [Hz]	f_4 [Hz]	f_5 [Hz]	f_6 [Hz]	f_7 [Hz]	f_8 [Hz]
GFRP	1.15	1.17	3.75	4.33	8.75	9.67	22.45	23.38
G/BFRP	1.00	1.04	3.38	4.04	7.62	7.82	18.13	19.32

3. Concluding Remarks

The measurement of dynamic parameters allowed to establish modal models of the tested elements. The obtained measurement results were used to build numerical models for analyses taking into account wind and seismic loads.

References

- [1] HOLLOWAY L.C, HEAD P.R: *Advanced Polymer Composites and Polymers in the Civil Infrastructure*, Elsevier, 2001
- [2] EWINS D.J: *Modal Testing: Theory, Practice and Application*. Wiley, 1988.

Damage Dynamics of Engineering Systems Under Varying Operational Conditions: Numerical Analysis and Modelling

VASILY V BUYADZHI¹, ANNA V IGNATENKO¹, YULIYA V. DUBROVSKAYA¹ AND
TAT'YANA A. FLORKO¹

1. Odessa State Environmental University, Mathematics Depr., L'vovskaya str. 15, 65009, Odessa

* Presenting Author

Abstract: The paper is devoted to development and application of an effective computational approach to analysis, modelling and prediction of a chaotic behaviour of dynamic properties of vibrating structures. There are listed data of analysis, modelling, processing chaotic time series, which represent the structural dynamic properties of engineering structures. The computational approach includes a combined set of non-linear analysis and chaos theory methods such as an autocorrelation function and correlation integral approach, average mutual information, surrogate data, false nearest neighbours algorithms, the Lyapunov's exponents (LE), Kolmogorov entropy analysis, spectral methods, prediction (predicted trajectories, neural network etc) algorithms (in versions [1-4]). The results of numerical studying the topological & dynamical invariants of the time series for the experimental cantilever beam [5] (forcing and environmental conditions are imitated by the damaged structure, the variable temperature and availability of the pink-noise force) are listed. Application of the approach to monitoring the health (security) of a nuclear reactor vessel is presented.

Keywords: numerical modelling, engineering structures, time series, chaos

1. Introduction. Universal Chaos-Geometric Approach to Dynamics of Geosystems

An analysis, identification and further prediction of the presence of damages (cracks), which above a certain level may present a serious threat to their performance of the technical structures, remains challenging problem in their monitoring engineering structures. The correct treatment requires extensive use of measurement and advanced mathematical and computational tools of processing. Usually change of structural properties due to operational and other effects (temperature, moisture, pressure etc) allows to detect an existence, location and size of damages. Changing these conditions may cause significant changes in their properties and result in the damage detection algorithms to false decisions. The standard way is using so called structural health monitoring methods that allow early identification and localization of damages (e.g. [1]). Usually change of dynamic properties due to environmental, operational and other effects allows to determine the existence, location and size of damages.

This paper goes on our work on studying and advancing an effective computational approach to analysis and prediction of a chaotic behaviour of dynamic properties of the vibrating structures. There are listed the results of analysis, modelling and processing the corresponding chaotic time series, which represent the structural dynamic properties of the engineering structures. The computational approach applied includes a combined set of non-linear analysis and chaos theory methods such as an autocorrelation function method, correlation integral approach, average mutual information, surrogate

data, false nearest neighbours algorithms, LE and Kolmogorov entropy analysis, spectral methods and prediction (predicted trajectories, neural network etc) algorithms (e.g. [1-4]).

2. Results and Discussion

As illustration, there are listed data of the complete numerical investigation of a chaotic elements in time series for the simulated 3DOF system and an experimental cantilever beam. The corresponding cantilever beam time domain response series data are taken from [5], where there are listed the detailed data of experimental studying a cantilever beam excited by white and pink noise forces. As example, in Table 1 the results of computational reconstruction of the attractors (the correlation dimension (d_2), embedding dimension (d_E), the first two LE (λ_1, λ_2), the Kaplan-Yorke dimension (d_L), as well as the Kolmogorov entropy (K_{entr}), and average limit of predictability (Pr_{max}) are listed.

Table 1. The correlation dimension (d_2), embedding dimension (d_E), first two LE (λ_1, λ_2), Kaplan-Yorke dimension (d_L), and the Kolmogorov entropy, average limit of predictability (Pr_{max} , hours)

d_2	d_E	λ_1	λ_2	d_L	K_{entr}	Pr_{max}
5.45	6	0.0197	0.0061	3,98	0.026	39

These data are related to a case of the damaged structure, the variable temperature and availability of the pink-noise force. System is generally considered to exhibit chaotic elements. The dimension of an attractor is defined as embedding dimension, in which the number of false nearest neighbouring points is less than 3%. The presence of 2 positive λ_i suggests the conclusion above regarding presence of a chaos. The non-linear methods [2-4] are used for the temporal evolution prediction. Even though the simple procedure is used to construct the non-linear model, the results are quite satisfactory.

3. Concluding Remarks

An universal chaos-geometric approach is applied to analysis, modelling and forecasting a chaotic behaviour of dynamic properties of the engineering structures. The advanced numerical data on the topological and dynamical invariants of the time series for the experimental cantilever beam [4] (the forcing and environmental conditions are imitated by the damaged structure, the variable temperature and availability of the pink-noise force) are listed. The presented chaos-geometric approach in combination with the blind source separation methods has been proposed as a powerful signal processing method capable of monitoring health of large class of engineering structures, in particular, nuclear reactor vessel safety.

References

- [1] GLUSHKOV AV: *Methods of a Chaos Theory*. Astroprint: Odessa, 2012.
- [2] GLUSHKOV A, BUYADZHI V, MASHKANTSEV V, LAVRENKO A: Deterministic chaos in a damage dynamics of the engineering structures under varying environmental and operational conditions. In: AWREJCEWICZ J, KAZMIERCZAK M, OLEJNIK P AND MROZOWSKI J (EDS.) *Theoretical Approaches in Non-Linear Dynamical Systems*. Łódź, 2019:155-162.
- [3] KHETSELIUS O: Forecasting evolutionary dynamics of chaotic systems using advanced non-linear prediction method. In: AWREJCEWICZ J, KAZMIERCZAK M, OLEJNIK P AND MROZOWSKI J (EDS.) *Dynamical Systems Applications*. Politechniki Łódzkiej: Łódź, 2013, **T2**:145-152.
- [4] GLUSHKOV A AND KHETSELIUS O: Nonlinear Dynamics of Complex Neurophysiologic Systems within a Quantum-Chaos Geometric Approach. In: GLUSHKOV A, KHETSELIUS O, MARUANI J, BRĀNDAS E (EDS) *Advances in Methods and Applications of Quantum Systems in Chemistry, Physics, and Biology. Series: Progress in Theoretical Chemistry and Physics*. Springer: Cham, 2021, **33**:291-303.
- [5] TJIRKALLIS A AND KYPRIANOU A: Damage detection under varying environmental and operational conditions using wavelet transform modulus maxima decay lines similarity. *Mech. Syst. Signal Process.* 2016, **66-67**:282-297.

Vibration analysis of a fully- and partially-filled container – Application to cryogenic tank characterization and dynamic behavior

JEAN-EMMANUEL CHAMBE^{1*}, MIGUEL CHARLOTTE¹, YVES GOURINAT¹

1. Université de Toulouse, Institut Clément Ader, UMR CNRS 5312,
INSA/UPS/ISAE-SUPAERO/IMT Mines Albi, 3 rue Caroline Aigle, 31400 Toulouse, France.

* Presenting Author

Keywords: Structural dynamics, Dynamic testing, Vibration analysis, Filled tank, Granular materials.

Abstract:

1. Introduction

The discussed work focuses on the experimental set-up, acquisition and subsequent structural modal analysis of a suspended representative cryogenic tank, submitted to vibrating stimulations, with the aim of characterizing its dynamic behavior to help ease the certification process of actual tanks used in aerospace applications. The objective of the research is to obtain a modal behavior similar in term of mode shapes and natural frequencies to the behavior of a tank filled with Liquid Hydrogen.

The main postulate -and innovative approach – in this work is to consider Granular Materials as a substitute to cryogenic fluids or compressed gases, namely Liquid Hydrogen (Fig. 1).

Most of the related studies are using water as a surrogate material for fuel or gas tank testing [1-5]. None were found to focus and use Granular Material as a substitute to achieve the same goal, except from Chiambaretto et al. [6] and Nguyen et al. [7,8]. The goal of the present study, directly following these preliminary works, is to explore further possibilities in terms of material substitution and system fixations, as well as filling rate influence and change of excitation modes.

2. Results and Discussion

Experimental set-up: In the current set-up, the cylindrical tank is vertically suspended and isolated, whereas it was vertically standing on its base on the previous work, directly in contact and bounded to the shaking equipment. Investigations are carried out on empty, then fully, and partially filled tanks subjected to vibration, using an impact hammer then a vibrating shaker as testing device. The natural frequency reflecting the dynamic behavior of the system for each vibration mode is measured for the different configurations. Frequency Response Functions are used to represent modal deformations.

Preliminary results: Previous works [6-8] were conducted using only one Granular Material type. Results showed the evolution of each flexural mode as a function of the applied pre-stress. In the current testing, prominent frequencies for the modal deformed shapes are occurring as follow, 55 Hz, 75/80 Hz, 555 Hz, 1035 Hz, 1333 Hz, 1520 Hz, and 2045 Hz on an empty suspended aluminum tank, with the associated shapes of flexion, flexion-torsion, ovalization, trefoil, quadrifoil, then combined and lobed modes, respectively. Observations and analysis from preliminary trials on filled tank tend to display the same deformed shapes as on empty tank, in the same order of occurrence, but at lower frequencies. First results tend to show that materials with lower mass density should be preferred in order to better reach the flexural modes, highlighting the surrogate materials density as paramount.

e-mail for correspondence: jean-emmanuel.chambe@isae-superaero.fr

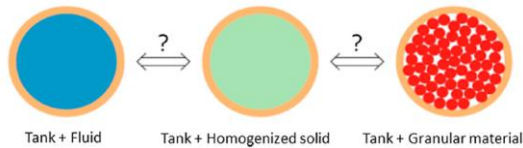


Fig. 1. Theorized equivalence between fluid-filled beam and grains-filled beam using a homogeneous fluid for granular material. (Chiambaretto et al.)[6]

Conclusions: The objective of the current experimental work is to analyze the modal behavior of a tank filled with Granular Materials, and after validating its equivalence with regular fluids, achieve comparisons based on influence of Granular Material types as well as filling rate in vibration analysis. Preliminary results tend to validate the hypothesis of material substitution. The first few modal deformed shapes are correctly observed. The main parameter of influence seems to be the density.

3. Concluding Remarks

The presented work is dealing with the vibration analysis and dynamic characterization behavior of a modelled cryogenic tank system, which is an important thematic in energy propulsion and aerospace engineering. The major objective is to highlight then evaluate the influence of the different parameters, namely Granular Material types, filling rates, excitation mode, and boundary conditions. Results will help validate the new methodology and comfort the hypothesis of material substitution.

Acknowledgment: The authors would like to thank DynaS+ Toulouse and A.T.E.C.A. Montauban.

References

- [1] [AMABILI 1995] AMABILI, M., DALPIAZ, G. Breathing Vibrations of a Horizontal Circular Cylindrical Tank Shell, Partially Filled With Liquid, *Journal of Vibration and Acoustics*, Volume 117, Issue 2, April 1995, Pages 187-191, ISSN 1048-9002, DOI 10.1115/1.2873885.
- [2] [AMABILI 1995] AMABILI, M. Free Vibration of a Fluid-Filled Circular Cylindrical Shell with Lumped Masses Attached, Using the Receptance Method, *Shock and Vibration*, Volume 3, No 3, 1996, Pages 159-167, ISSN 1070-9622, DOI 10.3233/SAV-1996-3302.
- [3] [AMABILI 2001] AMABILI, M., PAGNANELLI, F., PELLEGRINI, M. Experimental modal analysis of a water-filled circular cylindrical tank, *WIT Transactions on the Built Environment*, Volume 56, 2001, Page 267-276, ISSN 1743-3509, DOI 10.2495/FSI010241.
- [4] [AMABILI 2003] AMABILI, M. Theory and experiments for large-amplitude vibrations of empty and fluid-filled circular cylindrical shells with imperfections, *Journal of Sound and Vibration*, Volume 262, Issue 4, 2003, Pages 921-975, ISSN 0022-460X, DOI 10.1016/S0022-460X(02)01051-9.
- [5] [BADRAN 2012] BADRAN, O., GAIATH, M.S., AL-SOLIHAT, A. The Vibration of Partially Filled Cylindrical Tank Subjected to Variable Acceleration, *Engineering*, Volume 4, No 9, September 2012, Pages 540-547, ISSN 1947-3931, DOI 10.4236/eng.2012.49069.
- [6] [CHIAMBARETTO 2016] CHIAMBARETTO, P.-L., CHARLOTTE, M., MORLIER, J., VILLEDIEU, P., GOURINAT, Y. Surrogate granular materials for modal test of fluid filled tanks, In: *Proceedings of the 34th International Modal Analysis Conference (IMAC)*, A Conference and Exposition on Structural Dynamics, 25-28 January 2016, Orlando, FL, United States, DOI 10.1007/978-3-319-29910-5_14.
- [7] [NGUYEN 2018] NGUYEN, S.-K., CHIAMBARETTO, P.-L., CHARLOTTE, M., VILLEDIEU, P., MORLIER, J., GOURINAT, Y. Towards an analytical formulation for fluid structure tank vibration analysis: Modal equivalency using granular materials, *Engineering Structures*, Volume 177, 2018, Pages 345-356, ISSN 0141-0296, DOI 10.1016/j.engstruct.2018.09.077.
- [8] NGUYEN, S.-K., CHIAMBARETTO, P.-L., CHARLOTTE, M., MICHON, G., MORLIER, J., GOURINAT, Y. Experimental testing of pre-stressed granular assemblies as a surrogate material for the dynamic analysis of launcher cryogenic tanks, *Engineering Structures*, Volume 197, 2019, 109433, ISSN 0141-0296, DOI 10.1016/j.engstruct.2019.109433.

A new index for topological vulnerability in power transmission networks

JUSSARA DIAS^{*}, ELBERT MACAU

1. Associated Laboratory for Computing and Applied Mathematics, National Institute for Space Research, INPE.
2. Institute of Science and Technology, Federal University of São Paulo.

Abstract: Large interconnected systems that provide critical infrastructures, such as power transmission networks, can be affected by occasional or random failures. The vulnerability of such structures can be analyzed taking into account the electrical properties of the network, its topology, and the environment where it is located. This work aim to introduce indexes that allows to classify how vulnerable a network is in regard to the topology of the transmission networks. As so, taking an energy transmission network, it can be represented by a complex network and its topology can be studied by means of centrality measures. This work identifies centrality measures that can be used for identify power network vulnerability, such as the centrality of the generator tree, the intermediation of the current flow, the dimension of the disconnected components. These measures reflect the reality of the functioning of these networks, as they consider their connections and the distribution of energy in the network. Based on these measures, we propose a new index to assess vulnerability, composing the characteristics of measures previously studied in the literature. This new index comprises measures of centrality that can be used for the vulnerability analyse of transmission networks.

Keywords: Vulnerability index, complex network, effective resistance, power grid.

1. Introduction

Power grid vulnerability analysis from topology perspective holds a bright prospect of providing system operators a fast with easy to interpret information on critical operating point in a disturbed network [1]. Transmission networks can be represented by a complex networks due to the high amount of connections between their components. These components can be represented by generators and substations (consumers) and their connections are made by transmission lines.

A simulation of cascading faults in the network can be performed by removing the edges of the network. These edges are selected from indexes that measure their importance in the network. Each index selects and removes a border for a different purpose, and the efficiency of the network can be reduced for all applied indices. The idea for the new index proposed in this work is to use centrality measures that can be used in the context of energy transmission networks.

2. Results and Discussion

Betweenness centrality [3] measures the importance of a vertex/edge due to its participation in the shortest paths between vertices. For energy networks, information does not use the shortest path, but all of them. Therefore, we use a variation of this intermediation measure, the betweenness current flow [4].

Another way to identify important edges is through the spanning tree centrality measure [5] and number of disconnected components. We created a new index composing these three measures in a single index using a geometric mean between them. The Fig. 1 shows the result of this new measure in comparison with the metrics, in this example the metrics were simulated in the iee118 network [6]. Efficiency[7] was used to measure the drop in network performance when the edges were removed. Effective resistance [8] was used to calculate efficiency.

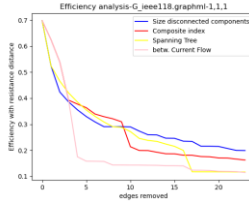


Fig. 1. This figure represents the simulation of attacks on the iee118 network and the drop in efficiency by the three measures of centrality and the index composed of them.

3. Concluding Remarks

A new vulnerability index is presented, based on measures of centrality that can be applied in situations where flow analysis through several paths is important. In this way, it is possible to identify other edges, which even with a secondary importance influence the efficiency of the network in the face of events that can interrupt the distribution of energy, such as severe weather events.

Acknowledgment: The authors would like to thank Conselho Nacional de Desenvolvimento Científico e Tecnológico - CNPq for the financial support, including grant 307714/2018-7. This research is also supported by grants 2015/50122 and 2018/03211-6 of São Paulo Research Foundation (FAPESP).

References

- [1] KIM, Charles J.; OBAH, Obinna B. Vulnerability assessment of power grid using graph topological indices. *International Journal of Emerging Electric Power Systems*, v. 8, n. 6, 2007.
- [2] V. S. S. Vos, Methods for determining the effective resistance, Ph.D. thesis, Masters thesis, 20 December, 2016.
- [3] D. Vukicevic, R.Skrekovski, A. Tepeh, Relative edge betweenness centrality, *Ars Mathematica Contemporanea* 12, 2016.
- [4] E. Bozzo, M. Franceschet, Resistance distance, closeness, and betweenness, *Social Networks* 35 (3), 2013.
- [5] A. S. M. Teixeira, Complex networks analysis from an edge perspective, Ph.D. thesis, INSTITUTO SUPERIOR TÉCNICO, 2019.
- [6] WANG, Xiangrong et al. A network approach for power grid robustness against cascading failures. In: 2015 7th international workshop on reliable networks design and modeling (RNDM). IEEE, 2015.
- [7] GUAN, Xuezhong et al. Power grids vulnerability analysis based on combination of degree and betweenness. In: The 26th Chinese Control and Decision Conference (2014 CCDC). IEEE, 2014
- [8] KLEIN, Douglas J.; RANDIĆ, Milan. Resistance distance. *Journal of mathematical chemistry*, v. 12, n. 1, p. 81-95, 1993.

Roughness evaluations for metallic parts using optical coherence tomography (OCT)

VIRGIL-FLORIN DUMA^{1,2*}, GHEORGHE HUTIU¹, ALEXANDRU-LUCIAN DIMB²,
DORIN DEMIAN¹, ADRIAN BRADU³, ADRIAN PODOLEANU³

1. 3OM Optomechatronics Group, Aurel Vlaicu University of Arad, 77 Revolutiei Ave., 310130 Arad, Romania [<http://orcid.org/0000-0001-5558-4777>]
 2. Doctoral School, Polytechnic University of Timisoara, 1 Mihai Viteazu Ave., 300222 Timisoara, Romania
 3. School of Physical Sciences, University of Kent, Canterbury, United Kingdom, CT2 7NR
- * Presenting Author

Abstract: Roughness parameters are essential to characterize the quality of mechanical parts. Their most common evaluation method uses mechanical profilometers. The aim of this work is to use a non-contact method, Optical Coherence Tomography (OCT) [1,2], to assess roughness of different metallic materials processed with several types of methods, including milling and turning. An in-house developed swept source (SS), Master-Slave (MS) enhanced OCT system is employed [3]. Using the interferometry capabilities of OCT, a (large) number of profiles can be determined in milliseconds on the metallic surface. A processing algorithm of the retrieved data is developed. The obtained roughness parameters are compared with those provided by profilometers. Advantages of drawbacks of each method are discussed. This work comes in the context of previous researches where we demonstrated that OCT can replace the gold standard of Scanning Electron Microscopy (SEM) in evaluating the different types of fractures of metallic materials [4,5]. Thus, while OCT is most useful because of its cross-sectional capability of non-reflective materials, optical profilometry of metallic parts can become a valuable tool in Non-Destructive Testing (NDT) of mechanical systems.

Keywords: roughness, metallic surfaces, optical coherence tomography (OCT), low coherence interferometry, signal processing, mechanical profilometer, measuring systems.

Acknowledgment: This research is supported by the Romanian Ministry of Research, Innovation and Digitization, through CNCS/CCCDI–UEFISCDI project PN-III-P2-2.1-PED-2020-4423, within PNCDI III (<http://3om-group-optomechatronics.ro/>).

References

- [1] HUANG D, SWANSON EA, LIN CP, SCHUMAN JS, STINSON WG, CHANG W, HEE MR, FLOTTE T, GREGORY K, PULIAFITO CA, FUJIMOTO JG: Optical coherence tomography. *Science* 1991, **254**:1178-1181.
- [2] DREXLER W, LIU M, KUMAR A, KAMALI T, UNTERHUBER A, LEITGEB RA: Optical coherence tomography today: speed, contrast, and multimodality. *J. Biomed. Opt.* 2014, **19**:071412.
- [3] PODOLEANU A, BRADU A: Master–slave interferometry for parallel spectral domain interferometry sensing and versatile 3D optical coherence tomography. *Opt. Express* 2013, **21**:19324–19338.
- [4] HUTIU G, DUMA V-F, DEMIAN D, BRADU A, PODOLEANU AG: Surface imaging of metallic material fractures using optical coherence tomography. *Appl. Opt.* 2014, **53**(26):5912-5916.
- [5] HUTIU G, DUMA V-F, DEMIAN D, BRADU A, PODOLEANU AG: Assessment of Ductile, Brittle, and Fatigue Fractures of Metals Using Optical Coherence Tomography. *Metals* 2018, **8**:117.

The course of the process of a motor car frontal impact against various places of the second vehicle's body side and its results

MIROSLAW GIDLEWSKI¹, LEON PROCHOWSKI², LESZEK JEMIOŁ³, MATEUSZ ZIUBIŃSKI^{4*}

1. Military University of Technology (WAT), Institute of Vehicles and Transportation, ul. gen. Sylwestra Kaliskiego 2, 00-908 Warsaw, Poland; Łukasiewicz Research Network – Automotive Industry Institute (Łukasiewicz-PIMOT), ul. Jagiellońska 55, 03-301 Warsaw, Poland, miroslaw.gidlewski@wat.edu.pl [ORCID 0000-0001-5775-184X]
2. Military University of Technology (WAT), Institute of Vehicles and Transportation, ul. gen. Sylwestra Kaliskiego 2, 00-908 Warsaw, Poland; Łukasiewicz Research Network – Automotive Industry Institute (Łukasiewicz-PIMOT), ul. Jagiellońska 55, 03-301 Warsaw, Poland, leon.prochowski@wat.edu.pl [0000-0003-2093-1585]
3. University of Technology and Humanities in Radom, ul. Malczewskiego 29, 26-600 Radom, Poland [ORCID 0000-0001-8898-4937]
4. Military University of Technology (WAT), Institute of Vehicles and Transportation, ul. gen. Sylwestra Kaliskiego 2, 00-908 Warsaw, Poland, mateusz.ziubinski@wat.edu.pl [0000-0003-4955-2095]

* Presenting Author

Abstract: The aim of the study is to determine the influence of the impact place on the side of passenger car body on the course of the front-to-side vehicles' collision process. The study combines experimental research and mathematical modelling. In experimental research six crash tests taking into account different mutual positions of the vehicles at initial collision time were carried out. In mathematical modeling a simple collision model (2D) and the results of experimental tests have been used. This allowed to determine the courses of important quantities for the road accidents reconstruction. They were, among others forces of interaction between vehicles, displacements and vehicle velocities, characteristics of deformation of the front and side of the vehicle's body, components of energy lost during a collision. The results are shown in the 0-0.2 s time interval. After this time the cars separate and continue to move based on their kinetic energy of translational and rotary motion.

Keywords: road traffic safety, front-to-side vehicles' collision, road accidents reconstruction

1. Introduction

Front-to-side vehicles' collisions are a very common type of road accident. In 2020, they accounted for 31.5% of all road accidents in Poland. They often have a complicated and unpredictable course. Changes in vehicle motion parameters during and after a collision depend on many factors that have been poorly defined so far. The reconstruction of this type of accidents is very difficult and requires the use of the experimental studies results [1, 2]. In order to improve the road accidents reconstruction methods, six crash tests were carried out at the Łukasiewicz Research Network – Automotive Industry Institute (Łukasiewicz-PIMOT) with the use of 12 passenger cars of the same manufacturer and model. In each test, car A hit in the left side of car B head-on. The velocity of car A immediately before the collision was approx. 50 km / h and was twice as high as the car B velocity. In subsequent crash tests, the relative initial positions of cars A and B were changed (Fig. 1). The presented work summarizes the results of the crash tests carried out. Considerations introducing the analysis of the front-to-side vehicles' collision process have already been presented by the authors in previous works [3,4,5].

2. Results and Discussion

A planar model of the dynamics of the vehicles' collision was developed. Using the developed model and the accelerations and angular velocities of the cars measured during the crash tests, the courses of important quantities for the road accidents reconstruction were determined. They were, among others forces of interaction between vehicles, displacements and vehicle ve-locities (translational and rotating), characteristics of deformation of the front and side of the vehicle's body, components of energy lost during a collision. Figure 1 shows the deformation characteristics of the front of car A and of the side of car B obtained in six crash tests as the example result of the calculations.

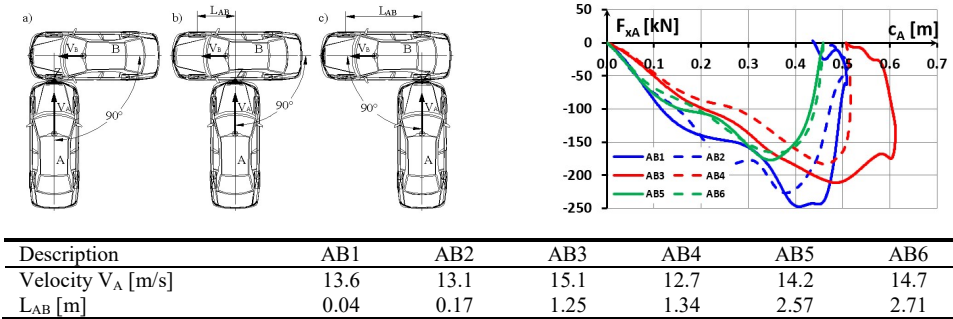


Fig. 1. Relative positions of cars A and B during the crash tests and combined deformation of the front of car A and the side of car B

3. Concluding Remarks

Considering the results of the experimental and mathematical modeling results together, it was possible to describe the course of the front-to-side vehicles' collision depending on the impact place of the vehicle's body side. The place of an impact by a vehicle on the another car's body side significantly influences the course and consequences of the collision. It determines the values of parameters that have a significant impact on the vehicles movement trajectories after a collision and their final positions after an accident. The obtained results can be used to improve the methods of reconstruction of this type of road accidents.

References

- [1] BRACH, R. M., BRACH, R. M.: Vehicle accident analysis and reconstruction methods. SAE International (2005).
- [2] GERMANE G.,MUNSON T., HENRY K.: Side impact motor vehicle structural characteristics from crash tests. SAE Technical Paper No 2003-01-0495.
- [3] GIDLEWSKI M., PROCHOWSKI L., JEMIOŁ L., ŻARDECKI D.: The process of energy dissipation during a front-to-side collision of passenger cars. Proceedings of 14th DSTA2017 Conference. „Engineering Dynamics and Life Sciences” - praca zbiorowa pod redakcją J. Awrejcewicz, M. Kaźmierczak, J. Mrozowski, P. Olejnik. ISBN 978-83-935312-4-0.
- [4] GIDLEWSKI M., PROCHOWSKI L., JEMIOŁ L., ŻARDECKI D.: The process of front-to-side collision of motor vehicles in terms of energy balance. Nonlinear dynamics. Vol. 97 No.3.
- [5] GIDLEWSKI M., PROCHOWSKI L., WACH W.: Determining the position and state of post-impact motion of a motor vehicle struck on its side at a road intersection, based on experimental. Transport. Vol. 33/2019. Issue 3.

Determination of physical quantities describing the movement of objects involved in a frontal-side collision of vehicles

MIROSLAW GIDLEWSKI¹, TOMASZ PUSTY^{2*}, LESZEK JEMIOŁ³, HANNA KOCHANEK⁴

1. Military University of Technology, (WAT); Łukasiewicz Research Network – Automotive Industry Institute [ORCID 0000-0001-5775-184X]
2. Łukasiewicz Research Network—Automotive Industry Institute (Łukasiewicz-PIMOT), Jagiellońska 55 Street, 03-301 Warsaw, Poland [ORCID 0000-0003-1324-5384]
3. University of Technology and Humanities in Radom, Malczewski Street 29, 26-600 Radom, Poland, e-mail: leszek.jemiol@uthrad.pl [0000-0001-8898-4937]
4. University of Technology and Humanities in Radom, Malczewski Street 29, 26-600 Radom, Poland, e-mail: hankoch@uthrad.pl [0000-0002-6628-8479]

* Presenting Author

Abstract: The paper compares the displacement and speed courses of cars, motorbikes and motorcyclists during a road accident obtained with the use of two measurement methods. In the first method, the course of the impact recorded by a fast camera recording 1000 frames per second was used ("frame by frame" film analysis). In the second method, the courses of accelerations and angular velocities of the objects were used (numerical integration of the recorded courses). The measurements were carried out during crash tests involving a frontal-side collision of two cars or a motorcycle with a car. The results are shown in the time interval 0-0.5s. During this period, the following phases of the experiment are observed: vehicle collision and the process of their deformation, the separation of vehicles, the start of independent movement of both vehicles after the collision. The measurement results obtained with the use of both methods are burdened with errors resulting, among others, from limited data sampling frequency, offset errors, calibration errors and sensor noise, duration of the analyzed waveforms. The use of two of the above-mentioned measurement methods simultaneously allows to minimize measurement errors

Keywords: crash tests, frame-by-frame film analysis, numerical integration of acceleration and angular velocity

1. Introduction

Obtaining physical quantities describing the movement of vehicles and people is of interest to many entities researching: passive safety systems [1, 2], active e.g. during the modeling of autonomous lane change algorithms [3, 4], compliance of technological solutions with the applicable standard documents, e.g. LDWS (Lane Departure Warning System) or experts analyzing the records of UDS (Unfall Daten Speicher) or ADR (Accident Data Recorder) black boxes [5]. The obtained data is subject to uncertainty due to the limited frequency of data sampling, errors of offset, calibration and noise of sensors, duration of

measurements. Therefore, it seems advisable to conduct research focused on determining the uncertainty range of the obtained results of certain physical quantities describing the motion parameters with various methods. The paper compares the course of displacement and velocity of objects during the collision and immediately after the collision, determined on the basis of post-frame analysis of films and numerical integration of acceleration and angular velocity waveforms recorded during several frontal-lateral collisions of vehicles carried out in the Łukasiewicz Research Network - The Automotive Industry Institute in Warsaw.

2. Results and Discussion

Three front-side car crash tests in motion and one motorcycle-car crash test were analyzed. Fig. 1 shows as an example the test results from a crash test of a motorcycle with a passenger car.

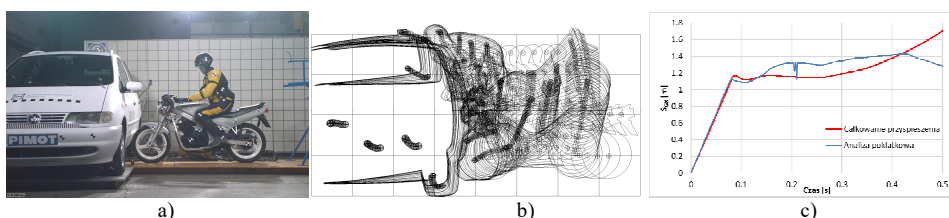


Fig. 1. Frontal-side collision of a motorcycle with a car a) location of the motorcycle and car at the time of first contact, b) frame-by-frame analysis of the collision course, c) comparison of the horizontal displacement of the rider's head determined by two methods.

3. Concluding Remarks

Research has shown that both of the measurement methods used give comparable results. However, errors in the calibration of the acceleration and angular velocity sensors must be minimized. This can be achieved by simultaneously analyzing the results obtained from two measurement methods.

References

- [1] BURACZEWSKI P, JACKOWSKI J: Porównanie metod określania parametrów ruchu pojazdu podczas zderzenia z przeszkodą. XXXI Seminarium Kół Naukowych Wydziału Mechanicznego.
- [2] DĄBROWSKI F, GIDLEWSKI M: Front and Side Crash of Cars in Motion – comparative analysis of experimental and modelling test results. Zeszyty Naukowe Instytutu Pojazdów Politechniki Warszawskiej nr 4/2015.
- [3] PROCHOWSKI L, ZIUBIŃSKI M, SZWAJKOWSKI P, GIDLEWSKI M, PUSTY T, STAŃCZYK TL: Impact of Control System Model Parameters on the Obstacle Avoidance by an Autonomous Car-Trailer Unit: Research Results. *Energies* 2021, Vol 14(10).
- [4] DZIEWIECKI M, GIDLEWSKI M: Limitations of Use of an Inertial Positioning System in a Truck During a Maneuver of Avoiding a Suddenly Appearing Obstacle. ESV Conference Paper Number 15-0341. 24th ESV International Technical Conference on the Enhanced Safety of Vehicles. Goteborg, Szwecja 2015, available on the Internet www.nhtsa.gov/ESV.
- [5] GUZEK M, LOZIA Z: Possible Errors occurring during Accident Reconstruction based on Car "Black Box" Records. 2002 World SAE Congress and Exposition. Detroit, Michigan USA. March 2002. SAE TP 2002-01-0549

Impact point localization with the use of wavelet transform

VÁCLAV HOUDEK^{1*}, ZDENĚK KUBÍN², LUBOŠ SMOLÍK¹

1. VZÚ Plzeň (Research and Testing Institute Pilsen), Czech Republic, houdek@vzuplzen.cz
2. VZÚ Plzeň, Czech Republic, kubin@vzuplzen.cz [0000-0001-8054-5948]
3. VZÚ Plzeň, Czech Republic, smolik@vzuplzen.cz [0000-0001-5280-5001]

* Presenting Author

Abstract: This paper provides an experimental method to localise a point of impact in three-dimensional structures. The impact induces vibration anomalies such as shockwaves in various devices or structures. Concurrent measurement of vibration waveforms in several measuring points allows determining the times of arrival of the shockwave. However, the path between the impact and the measuring point depends on the geometry of the structure. Therefore, ordinary triangulation methods cannot be used because apparent wave speeds differ across the measuring points. This paper proposes a set of nonlinear equations with unknown wave speeds and the location of the impact, which are solved using constrained optimisation. The results of this method depend on initial conditions and optimisation parameters, so their influence is also analysed and discussed.

Keywords: impact point, signal processing, wavelet transformation, localization,

1. Introduction

In terms of signal processing, the impact is an unsteady signal. If the measurement is performed in situ, this signal is also corrupted with noise resulting from machine operation, electrical noise, mechanical noise or noise from other machines. This implies that the impact (like Dirac impulse) and its transient response can be challenging to observe in the time domain. In this case, transformation to the time-frequency domain using the short-time Fourier transform (STFT) is beneficial. On the other hand, the Heisenberg theory does not allow for short time windows and high-frequency resolution. Therefore, the STFT is inevitably inaccurate in the precise localisation of short transients.

The wavelet transform offers the solution. The method described in [1,2] based on the Gabor wavelet is utilised for the fast wavelet calculation. It is necessary to tune the Gabor wavelet input

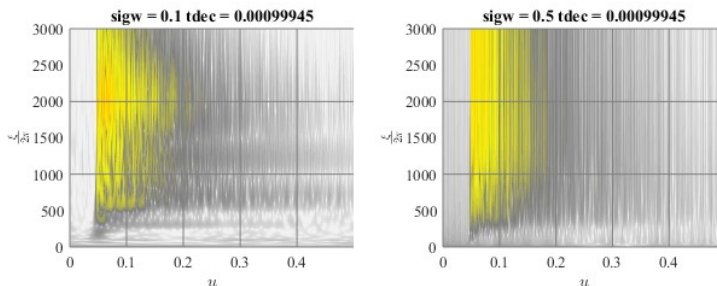


Fig. 1. Tuning of the Gabor wavelet to obtain best results in term of the time of arrival estimation

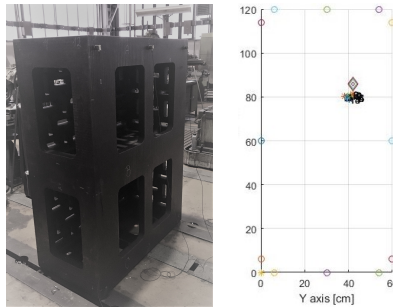


Fig. 2. (left) Test sample and (right) exact (\diamond) and computed ($*$) positions of the impact point

parameters and select the best frequency for the subsequent processing. Fig. 1 shows how the parameter σ_w change the wavelet results. Here, the most suitable wavelet parameters for time of arrival (TOA) estimation are $f = 3000$ Hz and $\sigma_w = 1$. TOA is then estimated at several scales using an approach based on optimal data partitioning according to their variance [3].

2. Results and Discussion

For example, we demonstrate the localisation of hammer-induced impacts in a hollow cube, see Fig. 2 left. Similar structures are utilised as housings of many industrial machines, including gearboxes and clutches. In these machines, impacts occur when the machine is damaged, e.g. when a crack develops in a tooth.

Five trial impact points were chosen arbitrarily, and a controlled test with an impact hammer was performed. The induced vibrations were measured at 36 points using two moving triaxial accelerometers and one stationary (reference) triaxial accelerometer.

The system of nonlinear equations was constructed using the obtained TOAs. The main advantage of the system are the variable velocities of the shockwave; this advantage compensates for the unknown shockwave path through the structure and structure geometry. However, velocities and impact point coordinates are bounded to fulfil fair values when solving the equation system.

The proposed method proceeded with the collected data; its localisation accuracy varies from 3 to 25 cm (Fig. 2 right), depending on the chosen location of the impact point and the number of sensors.

3. Concluding Remarks

The wavelet transform has been proposed to acquire the time of arrival of waves, which result from impacts. Next, a special system of equations has been constructed to estimate the location of these impacts. The proposed method produces consistent results with reasonable accuracy.

Acknowledgment: This work was supported by institutional support for long-term conceptual development of research institutions provided by the Ministry of Industry and Trade of the Czech Republic.

References

- [1] CARASSALE L., MARRÈ-BRUNENGGI M., PATRONE S.: Wavelet-based identification of rotor blades in passage-through-resonance tests. *Mechanical Systems and Signal Processing* 2018, **98**, 124-138.
- [2] CARASSALE L., MARRÈ-BRUNENGGI M., PATRONE S.: Estimation of damping for turbine blades in non-stationary working conditions. In: ASME Turbo Expo 2015: Turbine Technical Conference and Exposition. ASME: New York, 2015.
- [3] KILLICK R., FEARNHEAD P. AND ECKLEY I.A.: Optimal detection of changepoints with a linear computational cost. *Journal of the American Statistical Association* 2012, **107**(500): 1590-1598.

Modelling of Motion and Experimental Studies of a Four-Wheeled Mobile Robot Considering Slip Occurrence

ANNA JASKOT^{1*}, BOGDAN POSIADAŁA²

1. Czestochowa University of Technology, Faculty of Civil Engineering, anna.jaskot@pcz.pl [ORCID: 0000-0002-5478-0685]
2. Czestochowa University of Technology, Faculty of Mechanical Engineering and Computer Science, bogdan.p@imipkm.pcz.pl [0000-0002-3127-6136]

* Presenting Author

Abstract: The results of the simulation and experimental investigations of motion of the four-wheeled mobile platform are presented in the paper. The simulation results have been based on the description of the dynamics of wheeled mobile platforms. The description of the platform dynamics is presented in the paper. The initial problem of the platform motion has been solved using the Runge-Kutta integration method of fourth order. The relationship between active and passive forces accompanying the platform motion have been taken into account in the dynamic model of the motion of the system. The dynamics model has been verified by experimental tests using the LEO Rover robot. On the basis of the dynamics model, simulations of motion have been carried out in order to obtain the system response to the given forcings. The proposed model of motion dynamics has been verified by examining the real motion of the robot. Experimental studies of the robot's test runs along a rectilinear and curvilinear trajectory have been presented. The obtained motion parameters in the form of trajectory, velocities and accelerations have been compared with the results of experimental tests, and the results of this comparison have been included in the paper.

Keywords: motion dynamics; wheel slippage; wheeled mobile platforms, friction.

1. Introduction

The model of the dynamics of motion of a four-wheeled mobile platform has been presented in the work. Mobile platforms find a number of applications to support human work or to replace it in places inaccessible to him. The design of the platform results from the intended purpose of its work. Hence, there are many technical solutions that, for example, perform the tasks of inspecting the inner part of the pipes [1], help in the movement of people, where in the work [2] a special trolley equipped with a collision-free system for tracking pedestrians has been described. Moreover, robot solutions are being developed to facilitate visiting museums and libraries. More and more often, mobile platforms are equipped with a set of independent steering wheels, which makes it possible to drive them in multiple directions and to implement complex translational and rotational trajectories. Therefore, it is necessary to study the movement of wheeled mobile robots, which in essence focus on the study of kinematics and dynamics of motion. The problem of simple kinematics has been described, among others in [3]. Investigation of the kinematics and inverse dynamics of a three-wheeled mobile robot with two steerable wheels and one self-adjusting one, using virtual work methods have been included in [4], however, the impact of slippage has been neglected. In modelling the kinematics and dynamics of motion of wheeled mobile platforms, the plane motion model is most often adopted. This is due to

the purpose and nature of the work of mobile platforms. Therefore, considerations about the relationship between a drive wheel and the road surface are very important. In modelling the kinematics and dynamics of motion, the problem should not be simplified to the assumption of pure wheel rolling, as this may indicate that the longitudinal and/or transverse slip in the wheel-ground contact does not occur, i.e. it is equal to zero.

The aim of this work was to propose a model of the dynamics of movement, with the use of which it will be possible to map the trajectory of the movement of a four-wheeled mobile platform not only taking into account the influence of friction forces, but also under the influence of exceeding the value of developed friction, which in turn will lead to skid of the drive wheels [5]. The results of such an analysis have been partially presented in [6]. Based on the results of the motion simulation and experimental tests, the results of test runs along a straight-line and curvilinear trajectories have been presented.

2. Results and Discussion

On the basis of the proposed description of the dynamics of motion of the wheeled mobile platform, the simulation tests of the movement of such an object with the use of various configurations of inputs implemented through an appropriately controlled wheel drive and taking into account the conditions of cooperation between the wheels and the ground have been carried out through appropriate models of such cooperation. The adopted model of the mobile platform has been built so that the description of the movement reflects the kinematic properties of the platform, as well as the control possibilities occurring during its operation. The verification of the robot's motion dynamics model was based on demonstrating compliance in the nature and values of the waveforms of the motion parameters obtained by experimental and analytical methods. The obtained results confirm the adopted assumptions and show compliance in both character and values.

3. Concluding Remarks

A computational model has been proposed, including an algorithm for solving the formulated problem of the initial movement of a four-wheeled mobile platform. On the basis of the developed calculation programs, simulation tests of the four-wheeled platform have been carried out, as a result of which the waveforms of the platform motion parameters have been obtained in relation to selected configurations of construction parameters and wheel drive configurations, including their slippage. On the basis of the proposed model of the dynamics of motion, it is possible to analyse various cases of motion, including the slip of road wheels. It is also possible to study the forces and reactions occurring during the movement.

References

- [1] GIERGIEL J., KURC K.: Mechatronics of the inspective robot. *Mechanics and Mechanical Engineering* 2006, **10**:56-73.
- [2] ABDELGABAR Y.E., LEE J.H., OKAMOTO S.: Motion control of a three active wheeled mobile robot and collision-free human following navigation in outdoor environment. *Proceedings of the International MultiConference of Engineers and Computer Scientists* 2016, **I**:4.
- [3] STANIA M., STETTER R., POSIADAŁA B.: Modelowanie kinematyki mobilnego robota transportowego. *Zeszyty Naukowe Instytutu Pojazdów* 2021, **4**(85):73-84.
- [4] STAICU S.: Dynamics equations of a mobile robot provided with caster wheel. *Nonlinear Dynamics* 2009, **58**:237-248.
- [5] JASKOT A., POSIADAŁA B., ŚPIEWAK S.: Dynamics Modelling of the Four-Wheeled Mobile Platform, *Mechanics Research Communications* 2017, **83**:58-64.
- [6] JASKOT A.: Modelowanie i analiza ruchu platform mobilnych z uwzględnieniem poślizgu. *Ph.D. dissertation*, Czestochowa University of Technology, Czestochowa, 2021.

Analysis of dynamic characteristics of vehicle steerability in the context of its diagnostics and evaluation of dynamic properties

WITOLD LUTY¹, TOMASZ PUSTY^{2*}

1. Łukasiewicz Research Network—Automotive Industry Institute (Łukasiewicz-PIMOT), Jagiellońska 55 Street, 03-301 Warsaw, Poland [ORCID 0000-0002-8133-113X]
2. Łukasiewicz Research Network—Automotive Industry Institute (Łukasiewicz-PIMOT), Jagiellońska 55 Street, 03-301 Warsaw, Poland [ORCID 0000-0003-1324-5384]

* Presenting Author

Abstract:

Tests were carried out, which included the determination of the dynamic driving characteristics for the purpose of assessing the dynamic properties and technical condition of the vehicle. The dynamic properties were analyzed for the vehicle in running order and with an additional load. The introduced changes to selected vehicle features caused clear changes in the value of transmittance and the phase shift angle of the measured physical quantities characterizing the lateral dynamics of the vehicle in relation to the excitation in the form of dynamic turning of the steered wheels with a frequency of approx. 0.75 Hz. The preliminary tests used showed a clear influence of changes made to the vehicle on its behavior as observed on the basis of the measured physical quantities. This shows that the method of dynamic steering of steered wheels in the broadest possible frequency range can be used in the process of assessing the properties of a vehicle or its technical condition in the context of turning dynamics and safety in curvilinear motion. **Keywords:** dynamic steering characteristics, frequency characteristics, sinusoidal excitation by turning the wheels

1. Introduction

The basic methods of testing the vehicle's steerability characteristics are the tests described in the normative documents, they are well described in the work [1]. These include, among others: tests of the vehicle response to a step excitation with the linear process of increasing the angle of rotation of the steering wheel (ISO 7401: 2011); tests of vehicle response to steady motion in a circle according to ISO 4138. An extended method of testing the driving characteristics is the test of random or sinusoidal rotation of the steering wheel [2, 3]. The description of determining the dynamic characteristics is described in [5]. The sinusoidal input test method gives a chance to draw conclusions about the dynamic properties of the vehicle, which may be particularly useful during the research of car prototypes. One should also look for new methods of assessing the properties of dynamic prototypes in terms of active safety of vehicles, but also as a method of assessing their technical condition.

2. Results and Discussion

The response of the vehicle to the dynamic impulse to turn by the steered wheels was determined on the basis of the determined: transmittance of the steering angle input by the steered wheels δ_K and the response of the lateral acceleration A_{cy} and the phase shift. The excitation frequency was 0.75 Hz. Fig. 1 shows excerpts of the results of calculations of the transmittance module and the phase angle in the variants of technical condition changes (Base=base version, Belka=Base+additional load, Luz=Base+backlash in the steering gear).

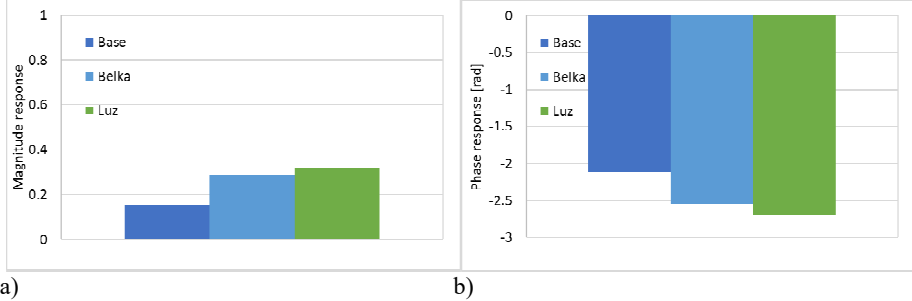


Fig. 1. Results of experimental tests - vehicle response to the dynamic forcing to turn by steered wheels; a) steering angle input transmittance module δ_K and A_{cy} , b) phase shift

The test results showed that even at the steady frequency of steering of the steered wheels, changes in the state of the vehicle cause clearly recognizable changes in the transmittance module and the phase shift of the response to the excitation.

3. Concluding Remarks

Based on the results of experimental tests, changes in the dynamic properties of the vehicle were confirmed based on the increase in transmittance and the phase shift angle. This means that the method is sensitive to the change of the vehicle's features, including e.g. the design feature, which is the mass / moment of inertia, as well as the operational feature resulting e.g. from the technical condition of the vehicle, i.e. the play in the steering linkage. The analyzed method is promising in terms of the assessment of the vehicle's properties and its technical condition, but it requires extension and testing in a wide range of changes in the frequency of forcing a turn with steered wheels, which will be the subject of further works.

References

- [1] Lozia Z., Guzek M., Metody badań stateczności i kierowności pojazdów samochodowych, analiza metod przydatnych podczas badań pojazdów o nietypowych parametrach, Prace Naukowe Politechniki Warszawskiej, z 34, Transport 1995.
- [2] Walczak S., Charakterystyki amplitudowo-częstotliwościowe samochodu osobowego, Zeszyty Naukowe Politechniki Świętokrzyskiej. Mechanika, 2004, z. 79
- [3] Mancosu F., Savi C., Vehicle sensitivity to tyre characteristics both in open and closed loop manoeuvres, Presented at the 2000 Adams Conference - Rome, November 15th-16th
- [4] Borkowski W., Konopka S., Prochowski L., Dynamika maszyn roboczych, Wydawnictwo WNT, 1997
- [5] Bendat J. S., Piersol A. G., Random Data. Analysis and Measurement Procedures. Second edition, A Wiley-Interscience Publication, New York, Chichester, Brisbane, Toronto, Singapore 1986

Determination of dynamic parameters of parts of a tram wheel in a numerical and experimental modal analysis

JULIA MILEWICZ^{1*}, TOMASZ NOWAKOWSKI², GRZEGORZ M. SZYMAŃSKI³

1. Poznan University of Technology, Institute of Transport, Poland [ORCID: 0000-0002-7360-0790]

2. Poznan University of Technology, Institute of Transport, Poland [ORCID: 0000-0001-5415-7052]

3. Poznan University of Technology, Institute of Transport, Poland [ORCID: 0000-0002-2784-9149]

* Presenting Author

Abstract: During the investigations, the authors performed a numerical model of a system composed of a rim and an inner disc of a wheel fitted in a Konstal 105Na tram followed by a frequency analysis in Solidworks aiming at determining the frequencies and the form of natural vibration. The simulation results were compared with the results of the experiment utilizing an impact modal hammer and piezoelectric transducers. When analyzing the measurements, the authors applied FRF and CMIF. This allowed the obtainment of frequency characteristics of the vibroacoustic response to the impact, the visualization of the form of natural vibration and the determination of the dynamic parameters of the actual object. Similarities and potential sources of differences between the numerical and the experimental results were identified.

Keywords: modal analysis, rail vehicle, natural vibration

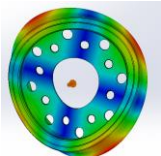
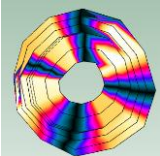
1. Introduction

The determination of modal parameters frequently takes place in the analysis of vehicle dynamics and in the diagnostics of the vehicle components. The analysis of the properties of a solid, its mass, rigidity and mutual interactions with the environment allows determining the conditions of resonance and the impact of the formed or propagating damage [1]. In this paper, the authors performed an analysis of the similarities between the modal characteristics of a numerical model of parts of a tram wheel and the experimental results. A simulation-based determination of frequency and form of natural vibration of a wheel of a rail vehicle has been described in [2], however, the conditions and the impact of the vehicle dynamics on the generated vibration were presented when the vehicle was stationary under gravitational loads only.

2. Results and Discussion

Based on the detailed results, 13 natural vibration frequencies were selected in the range 0-3000 Hz. The selection was made based on: FRF and CMIF characteristics, correlation matrix between the modes and similarity of forms obtained in the numerical analysis (Solidworks) and the experiment. Out of 13 modes, only one experimental result did not have its numerical counterpart, which most likely resulted from a small groove in the rim material in the vicinity of one of the transducers. In the outstanding cases, the experimental and numerical values varied by 244.6 Hz maximum and 0.5 Hz minimum. Table 1 presents the comparison of the frequencies and natural vibration forms obtained numerically and experimentally.

Table 1 Comparison of a selected frequency and form of natural vibration determined numerically and experimentally

Natural vibration frequency (simulation)	Form of natural vibration (simulation)	Natural vibration frequency (experiment)	Form of natural vibration (experiment)
524,1		524,6	

The authors have observed that for the same (or very close) frequency, some modes assume similar forms only turned by a certain angle against the axis of the wheel, the value of which depends on the form of the mode. This is the case for both the low frequency vibration related to the object inertia and for the more non-uniform forms. The determined natural vibration frequencies were characterized by a low damping coefficient (except the first two modes) and a varied percentage of form complexity.

During the experiment, the most difficult was the extraction of the modes having displacements towards the longitudinal axis of the wheel and having revolutions around it. The closest to the numerical analysis were forms characterized by the symmetrical displacement of the rim.

The reasons for the differences between the experimental and simulation results were divided into those resulting from the mere measurement methodology, the quality of its performance and the numerical limitations.

3. Concluding Remarks

Upon detailed analysis of the results of the experiment, 12 forms of natural vibration were selected that are also reflected in the simulation and one form that may potentially be correlated with the structure of the rim. The modes differed among one another with their damping coefficient and complexity.

The experimental results, upon appropriate selection in the post-process, can be deemed more reliable than the theoretical ones, determined numerically due to the fact that a greater number of external factors was taken into account, high sensitivity of the measurement equipment and a better calculation accuracy of the BK Connect software. The frequency analysis carried out in Solidworks helped planning the experiment, including the selection of the frequency ranges and the initial illustration of the expected measurement results, yet, its application cannot not always stand in place of the actual object examination, due to, *inter alia*, simulation-related limitations of the software.

Acknowledgments: The presented results have been co-financed from the subsidies appropriated by the Ministry of Science and Higher Education - 0416/SBAD/0003.

References

- [1] HARAK S.S, SHARMA S.C, HARSHA S.P: Structural Dynamic Analysis of Freight Railway Wagon Using Finite Elements Method. *Procedia Mater Science* 2014, **6**:1891-1898. <https://doi.org/10.1016/j.mspro.2014.07.221>
- [2] SOWINSKI B: Analysis of high frequency vibration of tram monobloc wheel. *Archives of Transport*: 2016, **39**(3):65-75. DOI: 10.5604/08669546.1225450

The application of time-frequency methods of acoustic signal processing in the diagnostics of tram drive components

DANIEL MOKRZAN^{1*}, TOMASZ NOWAKOWSKI², GRZEGORZ M. SZYMAŃSKI³

1. Poznan University of Technology, Institute of Transport, Poland [ORCID: 0000-0001-8274-7009]

2. Poznan University of Technology, Institute of Transport, Poland [ORCID: 0000-0001-5415-7052]

3. Poznan University of Technology, Institute of Transport, Poland [ORCID: 0000-0002-2784-9149]

* Presenting Author

Abstract: The paper presents the course of investigations and an analysis of the possibilities of application of time-frequency methods of acoustic signal processing in the assessment of the technical condition of tram drive components. A pass-by acoustic pressure emission experiment was performed on a Solaris Tramino S105p. An analysis of the recorded signal was carried out using Short-Time Fourier Transform (STFT) and Continuous Wavelet Transform (CWT). It was confirmed that the potential damage of a drivetrain is characterized by the formation of high amplitude frequency components that do not occur in fully operative systems. The highest number of these components occurs in the frequency band of 0-3.2 kHz. The authors also observed that, owing to its signal window scaling functionality, CWT is a more efficient tool in time-frequency signal interpretations compared to STFT.

Keywords: vibroacoustic diagnostics, time-frequency methods, STFT, CWT

1. Introduction

In maintenance of machinery, including rail vehicles, one of the most efficient and economical methods of diagnostics of the technical condition of an object is the analysis based on the processing of vibroacoustic signals, i.e. the time realizations of wavelet phenomena, representing mechanical and acoustic vibration as accompanying processes. The variability of signals in time in a wide band of frequencies constitutes a vast source of information that is sensitive to any variations in the system, which also includes damage [1].

In the presented work, the authors used STFT in equation 1 and CWT described by equation 2 for the time-frequency decomposition of the acoustic signal recorded by the measurement matrix during a pass-by test of a Solaris Tramino S105p rail vehicle [2].

$$STFT[x_w(t, \tau)] = \int_{-\infty}^{\infty} w(t, \tau)x(t) \cdot e^{-i2\pi ft} dt \quad (1)$$

where $x(t)$ – representation of the input signal under analysis in the time domain, τ – position of the floating window in the time domain, $x_w(t, \tau) = w(t-\tau)x(t)$ – separated segment of data under analysis.

$$CWT_{\Psi}(a, b) = \frac{1}{\sqrt{a}} \int_{-\infty}^{+\infty} x(t) \cdot \Psi^* \left(\frac{t-b}{a} \right) dt \quad (2)$$

where $\Psi(t-\tau)$ – base wavelet (mother function), $x(t)$ – continuous signal in the time domain, a – scale parameter, b – displacement parameter (position), Ψ^* – function conjugate $\Psi(t-\tau)$.

2. Results and Discussion

The comparison of the STFT spectrograms obtained for the signal originating in a pass-by of an operative as well as damaged vehicle has been presented in Fig. 1. A damaged part of the drivetrain located in the third bogie of tram 554 is characterized by the formation of high-amplitude frequency components in the band 0-3.2 kHz that do not occur in the characteristics of a bogie of a fully operative vehicle. The CWT scalogram presented in Fig. 2, due to its different method of signal window formation, differs from the spectrogram of vehicle 554 and differently presents the high-amplitude components.

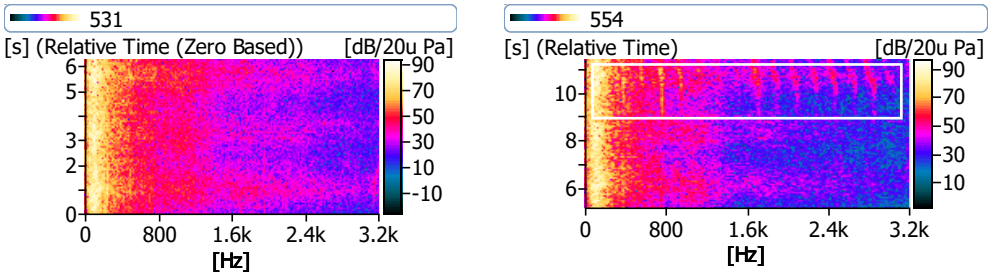


Fig. 1. The comparison of spectrograms for an undamaged vehicle (left) and a vehicle with third bogie's drivetrain damaged (right) with high-amplitude frequency components marked

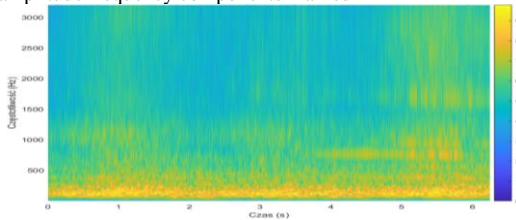


Fig. 2. CWT Scalogram of vehicle 554 – Morse wavelet of densified scaling applied

3. Concluding Remarks

During the investigations, the authors have confirmed that damage of tram drive components can be identified through the measurement of the acoustic signal and its decomposition using STFT and CWT. The modification of the parameters of both transforms may have impact on the obtained results and their interpretation. CWT allows the obtainment of a more accurate time-frequency representations owing to the use of scaled windows, contrary to the constant resolution windows characteristic of STFT.

Acknowledgments: The presented results have been co-financed from the subsidies appropriated by the Ministry of Science and Higher Education - 0416/SBAD/0003.

References

- [1] Randall RB. *Vibration-based Condition Monitoring*. Chichester, UK: John Wiley & Sons, Ltd; 2011. <https://doi.org/10.1002/9780470977668>.
- [2] Zhu Q, Wang Y, Shen G. Research and comparison of time-frequency techniques for nonstationary signals. *Journal of Computers* 2012;7:954–958. <https://doi.org/10.4304/jcp.7.4.954-958>.

Simple suppression method of impact oscillations between a pantograph and an overhead rigid conductor line

NAOTO NISHIYAMA^{1*}, KIYOTAKA YAMASHITA²

1. Department of Mechanical Engineering, Fukui University of Technology, Japan [https://orcid.org/0000-0003-4956-9858]
2. Department of Mechanical Engineering, Fukui University of Technology, Japan [https://orcid.org/0000-0002-2176-0485]

* Presenting Author

Abstract: The railway current collection system consists of a pantograph and a conductor line. In some cases, the pantograph separates from the conductor line. This phenomenon is called a contact loss. The system can be modeled as impact oscillations between a spring-supported mass and an oscillating plate. In the previous study, we investigated the effect of an additional mass spring system on the impact oscillations. When the frequency of excitation is near the second mode natural frequency, the impact oscillations are strongly restricted. In this paper, we propose the simple method to restrict the impact oscillations. In this method, an additional mass is replaced by the flexible beam. We theoretically and experimentally investigate the effects of additional beam on the restriction of the contact loss. It is theoretically clarified that the impact oscillations are strongly restricted when the frequency of excitation is near the second mode natural frequency. We conducted the experiments to verify the theoretical predictions. The experimental results show qualitatively good agreement with the theoretical ones.

Keywords: Impact Oscillation, Vibration Suppression, Railway system

1. Introduction

The railway current collection system consists of a pantograph and a conductor line. In some cases, the pantograph separates from the conductor line. This phenomenon is called a contact loss. The system can be modeled as impact oscillations between a spring-supported mass and an oscillating point. The frequency of excitation is equivalent to V/λ , where V and λ are a train speed and a main wave length of the wear. In the previous study, we investigated the effect of an additional mass spring system on the impact oscillations[1]. When the frequency of excitation is near the second mode natural frequency, the impact oscillations are strongly restricted. In this paper, we propose the simple method to restrict the impact oscillations. In this method, an additional mass is replaced by the flexible beam. We theoretically and experimentally investigate the effects of additional beam on the restriction of the contact loss. It is theoretically clarified that the impact oscillations are strongly restricted when the frequency of excitation is near the second mode natural frequency. We conducted the experiments to verify the theoretical predictions. The experimental results show qualitatively good agreement with the theoretical ones.

2. Results and Discussion

Figure 1 shows the analytical model of an impact oscillation between a spring-supported mass m_1 and a sinusoidal oscillating point. Spring constant is k . A mass is placed at the middle of the attached flexible beam (overall length l , flexural rigidity EI , mass per unit length ρ). Let $y = \delta \sin \omega t + d$ and v be the displacement of an oscillating point and a beam, where δ , ω , t and d are the amplitude of the

sinusoidal wear, time t , the frequency of excitation and static push up distance, respectively. e represents a coefficient of restitution between a sinusoidal point and a spring-supported mass. We discretized the governing equations considering first and second mode and derived the equations which govern the velocity the relation at the impacts. We numerically investigate the impact oscillations between a mass and an oscillating point. When ω is near the second mode natural frequency, impact oscillations are strongly restricted. The numerical value of second mode natural frequency can be easily adjusted up or down by varying the flexural rigidity EI and the overall length l . Next, we conducted the experiments to verify the theoretical predictions. We use the aluminium block as a main mass $m_1 = 367\text{g}$. The first and second mode natural frequencies are 6.3Hz and 14.0Hz, respectively. Figure 2 (a) shows the times histories of y and $v(0)$ at $\omega/2\pi = 13.5\text{Hz}$. A mass collides two or three times during a period of y . When $\omega/2\pi$ is near the second mode natural frequency, the impact oscillations disappear. Figure 2(b) shows the restriction of the impact oscillations. The experimental results show qualitatively good agreement with the theoretical ones.

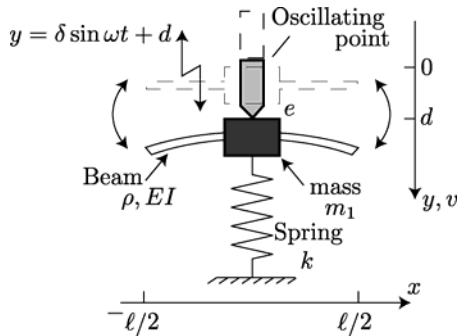


Fig. 1. Analytical model

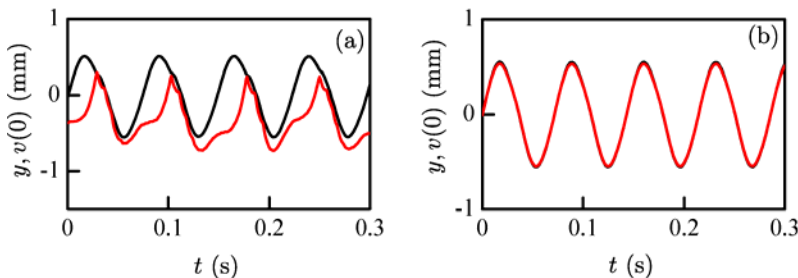


Fig. 2. Time histories of y and $v(0)$ in Experiments. (a): $\omega/2\pi = 13.5\text{Hz}$, (b) $\omega/2\pi = 14.0\text{Hz}$. Black and red lines indicate y and $v(0)$, respectively.

3. Concluding Remarks

In this paper, we propose the simple method to restrict the impact oscillations between a pantograph and an overhead rigid conductor line. The flexural beam is attached at the mass in order to have excited states with infinite degrees of freedom. We numerically calculated the discretized equations which is obtained by two mode expansions. When the excitation frequency is near the second mode natural frequency, the impact oscillations can be strongly restricted. The experiments are conducted to verify the theoretical predictions. The observation in experiments show good agreement with the theory.

Acknowledgment: The authors would like to thank Professor H.Yabuno for the useful discussions.

References

- [1] NISIYAMA, N, YAMASHITA K: Effect of the coupled oscillatory system on impact oscillations between a pantograph and a rigid conductor line. *Transactions of JSME* (in Japanese) 2020, **86**(881):1-13.

Compressive impact of SiC foam

ELIGIUSZ POSTEK*, TOMASZ SADOWSKI²,

1. Institute of Fundamental Technological Research PAN [0000-0002-5757-8757]

2. Lublin University of Technology [0000-0001-9212-8340]

* Presenting Author

Abstract: The silicon carbide (SiC) can be used for its foam production. It is used for infiltrated composites fabrication. In this paper, a problem of an impact of a steel plate travelling with high velocity hitting a silicon carbide sample (SCF) is considered. The presentation concerns the modes of failure and degradation.

Keywords: SiC, silicon carbide foam, impact, compression, peridynamics

1. Introductory statement

The SCF material stands for the skeleton of the infiltrated metal/SCF composites. Therefore, a study is undertaken to elaborate numerical modelling of the SCF under impact conditions.

2. Problem statement

In peridynamics, the model is dependent on peridynamics states [1]. The deformation of the body is shown in Fig. 1(a). The bond definition, the reference state and the deformation state are defined in Eq. (1). The scalar state definition and decomposition into the spherical and deviatoric parts is given in Eq. (2). The force state is given in Eq. (2) as well, where k is the bulk modulus, $x=|\xi|$ is the scalar state, θ is the dilatation, m is the weighted volume, $\alpha=15\mu/m$ depends on the shear modulus μ .

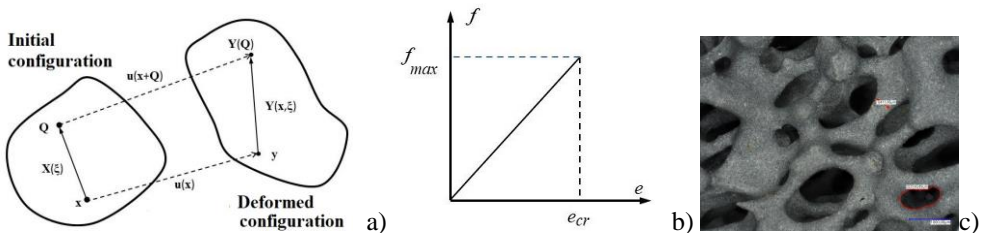


Fig. 1. Deformation of the peridynamic body (a), constitutive law (b), SCF sample under consideration.

$$\xi = \mathbf{Q} - \mathbf{x}, \quad \mathbf{Y}(\mathbf{x}, \xi) = \mathbf{y}(\mathbf{Q}) - \mathbf{y}(\mathbf{x}), \quad \mathbf{U}(\mathbf{x}, \xi) = \mathbf{u}(\mathbf{Q}) - \mathbf{u}(\mathbf{x}) \quad (1)$$

$$e(\mathbf{Y}) = |\mathbf{Y}| - |\mathbf{X}|, \quad e = e^i + e^d, \quad t(\mathbf{Y}) = (3k\theta/m)\omega x + \alpha\omega e^d, \quad (2)$$

A particular case of the state model is the bond based model shown in Eq. 2 (left). The force in a bond is proportional to the constant $c=18h/\pi/h^4$, where h is the radius of the horizon, namely, the sphere in which the integration is done.

$$f = ce\zeta(\mathbf{x}, t, \xi), \quad e_{cr} = \sqrt{5G_{ci}/(9kh)}, \quad d(x, t) = 1 - \int_{\Omega} \zeta(x, t, \xi) d\Omega / \int_{\Omega} d\Omega \quad (3)$$

The critical stretch is given in Eq. (3) in the middle, Fig. 2(b), where the G_{ci} is the fracture energy corresponding with the crack mode I. The damage variable d is equal to 0 for the pristine material and 0 for the damaged.

3. Demonstrative example

An example of dynamic compression is shown in Fig. 2. The physical image of the SCF is shown in Fig. 1(c). The SCF sample of the dimensions 34.7 mm height, 8.9 mm thick and 18.6 wide is dynamically compressed by a steel piston with the velocities of 40 m/s and 385 m/s. The time of the process is 3.06E-05 s. The material properties of the SiC: Young's modulus 430.0 GPa, Poisson's ratio 0.37, mass density 3200 kg/m³, fracture toughness 4.1 MPa.m^{1/2}. The base and the piston are made of steel with Young's modulus 210 MPa, Poisson's ration 0.3 and mass density 7800 kg/m³.

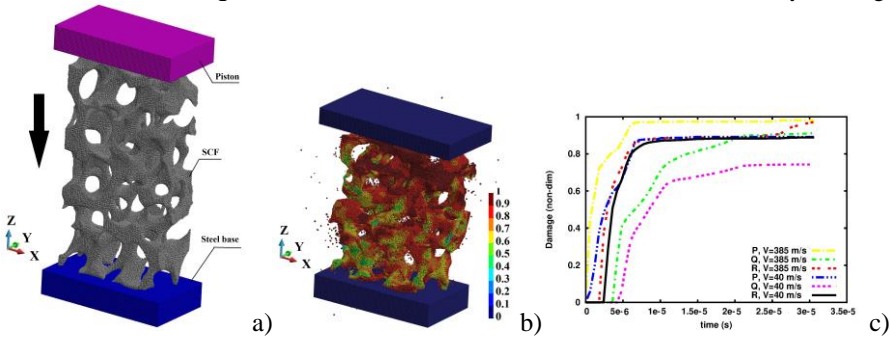


Fig. 2. Scheme of the structure (a), deformed configuration (b), damage-time dependence for 385 m/s and 40 m/s piston velocity at points P, Q, R.

The scheme is shown in Fig. 2(a). The deformed structure under the piston velocity 385 m/s is given in Fig. 2(b). The structure exhibits fragmentation and self-contact between the branches of the pores. In Fig. 2(c), the damage dependence on time at the selected points is presented for the two velocities of the piston. The points P, Q and R are placed close to base, in one-third of the height of the SCF and close to the piston, respectively. Damage appears earlier and is higher in the case of higher piston velocity than in the case of the lower one.

3. Concluding Remarks

An outline of the numerical modelling with peridynamics is presented. In the Author's opinion, it is a promising tool to evaluate the behaviour of the considered materials even though it requires up-to-date high-performance computers (HPC) to obtain the results in a reasonable time.

Acknowledgment: This work was funded by the National Science Centre (Poland) under project No UMO-2019/33/B/ST8. The calculations were done using PL-GRID national computational resources at the Interdisciplinary Centre for Mathematical and Computational Modeling, University of Warsaw, Poland.

References

[1] SILLING SA, EPTON M, XU J, ASKARI E, : Peridynamics states and constitutive modelling. *J. Elasticity* 2007, **88**:151-184.

Uncertainty evaluation by the bootstrap for the staircase fatigue limit test data

LUJIE SHI^{1*}, HAO BAI^{1†}, LEILA KHALIJ¹

1. Laboratory of Mechanic of Normandy (LMN), INSA Rouen Normandy, 76000 Rouen, France [0000-0001-7849-7019]

* Presenting Author

† Corresponding Author: hao.bai@insa-rouen.fr

Abstract: The uncertainty analysis is carried out to evaluate the staircase test for determining the fatigue limit of a material. Using the bootstrap method on the staircase data to obtain the scatter of mean and standard deviation of the distribution for the fatigue limit. Combined with the results of a bending fatigue test, the evaluation process and results of the uncertainty of the staircase data under several strain levels are given. The outcomes of uncertainty based on the experimental application prove the feasibility of the bootstrap methods for staircase data.

Keywords: fatigue limit, staircase method, uncertainty, bootstrap, resampling

1. Introduction

The fatigue test of metallic materials is a commonly used way to evaluate the mechanical properties and the reliability of materials. Staircase test method [1] is widely practiced to determine the fatigue limit of material. Though the staircase test provides a precise value of fatigue limit, it is hard to measure the uncertainty from test results due to the test benches, sensors and specimens. To investigate this problem, an increasing number of recent researches on post-processing [2] and uncertainty evaluation [3][4] of the staircase method can be observed in literature. In this paper, a new methodology is proposed to assess the uncertainty on fatigue limit involved in the staircase test.

2. Results and Discussion

By convention, no more than 30 specimens [4] are loaded in real staircase experimental test. Bootstrap method provides an efficient way to reproduce more samples from small-size dataset. It utilizes multiple random draws from experimental test results to make statistical inferences about the primary population. To examine the uncertainty in experiment, we propose:

Step 1: Representing the dataset from staircase method by $X = [x_1, x_2, \dots, x_n]$, and dividing them to different part according to different strain (or stress) level j , $X^j = [x_1^j, x_2^j, \dots, x_m^j]$, that is $X^1 \cup X^2 \cup X^j = X$;

Step 2: Start sampling with random stress level j from the test data. If the sampled specimen is failure, the next sample is selected from specimens in lower stress level $j-1$; otherwise, the next sample selected from specimens in upper stress level $j+1$;

Step 3: Repeating the step 2 until all collected specimens can accurately represents the true distribution of fatigue limit, which should be more than 50 [1] as one group data; each group is still can be seen as a virtual staircase test data, donated as $\bar{X}_1 = [\bar{x}_1, \bar{x}_1, \dots, \bar{x}_M]$;

Step 4: Repeating step 2 and step 3, to sample enough groups data, $[\bar{X}_1, \bar{X}_2, \dots, \bar{X}_N]$, to estimate the uncertainty;

Step 5: Fitting the distribution of each group data and obtain mean and standard deviation, and then fitting the distribution of all means and standard deviations as uncertainty estimation.

To validate the proposed method, an experimental fatigue limit test is performed on low carbon steel DC01 resulting in a dataset of 36 specimens. A close looped strain-control on electrodynamic system is carried out with a maintain of the excitation until $1e6$ cycles. The staircase result is post-processed by the Kernel Density Estimation (KDE) that reveals the mean and standard deviation of fatigue limit are $1366.88 \mu\text{m}/\text{m}$ and $24.36 \mu\text{m}/\text{m}$, respectively. To apply the bootstrap method, 30 groups are drawn from the dataset each contains 50 samples. The related mean and standard deviation distributions are depicted in Fig. 1.

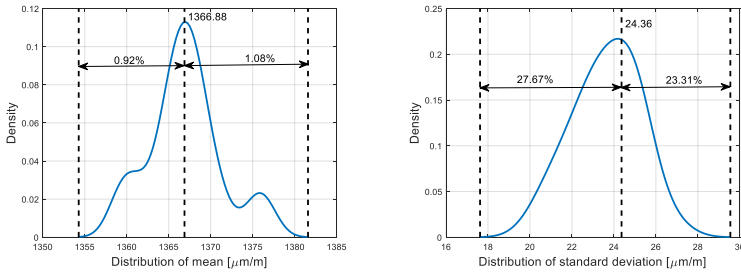


Fig. 1. Distributions of mean and standard deviation

From the results in Fig. 1, small interval in the mean value of fatigue limit is observed, while huge interval takes place in standard deviation. The staircase test offers a good estimation of median value but with higher uncertainty to standard deviation estimation.

3. Concluding Remarks

Evaluation on statistical uncertainty in the staircase test for fatigue limit based on bootstrap methods is presented. To avoid repetition of the staircase tests, a sampling with replacement procedure for staircase data is used to quantify the uncertainties of the mean and standard deviation of the fatigue limit obtained from one staircase test. The results show that the standard deviation of fatigue limit is more dispersive with more than 20%, leading to conclude that it should be conservative to use staircase results in fatigue design.

Acknowledgment: This study is supported by the European Regional Development Fund (ERDF) and the Regional Council of Normandie through the AMED project, as well as the China Scholarship Council (CSC).

References

- [1] DIXON W J, MOOD A M: A method for obtaining and analysing sensitivity data. *Journal of the American Statistical Association*, 1948, **43**(241):109-125.
- [2] MÜLLER C, WÄCHTER M, ET AL: Accuracy of fatigue limits estimated by the staircase method using different evaluation techniques. *International Journal of Fatigue*, 2017, **100**:296-307.
- [3] ROUÉ V, DOUDARD C, ET AL: Simulation-based investigation of the reuse of unbroken specimens in a staircase procedure: Accuracy of the determination of fatigue properties. *International Journal of Fatigue*, 2020, **131**:105288.
- [4] WALLIN K: Statistical uncertainty in the fatigue threshold staircase test method. *International Journal of Fatigue*, 2011, **33**(3):354-362.

On the effectiveness of infrared thermography in the detection of the fatigue damage initiation in a composite plate with a hole

ADAM STAWIARSKI¹, MAŁGORZATA CHWAŁ², MAREK BARSKI^{3*}, PAWEŁ ROMANOWICZ⁴

1. Chair of Machine Design and Composite Structures; Cracow University of Technology [0000-0002-5700-4841]
2. Chair of Machine Design and Composite Structures; Cracow University of Technology [0000-0001-6626-607X]
3. Chair of Machine Design and Composite Structures; Cracow University of Technology [0000-0002-2247-5846]
4. Chair of Machine Design and Composite Structures; Cracow University of Technology [0000-0001-7475-1577]

* Presenting Author; Corresponding author: adam.stawiarski@pk.edu.pl

Abstract: The necessity of monitoring the state of the structures is increasingly important especially in the composite structures because of the difficult estimation of the fatigue life. The number of non-destructive measurement and monitoring methods grows allowing for in details observation of the fatigue behaviour of the composite structures. In this study, the effectiveness and accuracy of the infrared thermography have been studied in the fatigue damage tests of the composite plate with a hole. The effectiveness of the early damage detection method associated with appropriate measured data analysis was analysed. The digital image correlation system has been also used to observe the fatigue behaviour of the analysed structure. Experimental tests have been preceded by the numerical finite element analysis of the composite structure to determine the expected damage initiation area. The practical aspects of the considered measurement technique were discussed in the context of the permanent structural health monitoring and utilization in the real SHM systems.

Keywords: fatigue damage, SHM system, infrared thermography, wave propagation

1. Introduction

The difficulties in the accurate prediction of the failure form and service life cause that composite structures are often designed with the use of the high value of the safety factors. The growing importance of the non-destructive testing methods and structural health monitoring systems is the consequence of the dynamic technological progress and optimization of the composite production processes [1-4]. The improvement of the accuracy of the damage detection is still of interest to researchers. However, quite often the accuracy improvement is associated with sophisticated techniques of data analysis, algorithms, or advanced procedures that quite often cause effectiveness decrease. In this paper, the effectiveness of the non-destructive passive infrared thermography was taken into account in the early damage detection under fatigue loading conditions. The fatigue of the GFRP composite plate with the hole was carried out with the use of visual non-destructive monitoring systems. The digital image correlation system coupled with infrared thermography monitoring allows for accurate determination of the fatigue damage evolution of the analysed structure.

2. Results and Discussion

Composite plates with a circular hole in the middle made of GFRP laminates were considered. The fatigue tests were carried out with the utilization of the passive infrared thermography system monitoring the temperature distribution during the fatigue tests. The digital image correlation system was responsible for the visual, online determination of the displacement, and strain distribution. The temperature distribution, maximal temperature value and temperature histogram observed during the test were taken into account as straightforward markers of the fatigue damage initiation (Fig. 1). The temperature difference was also calculated to determine the relation between fatigue test parameters and the energy release intensity.

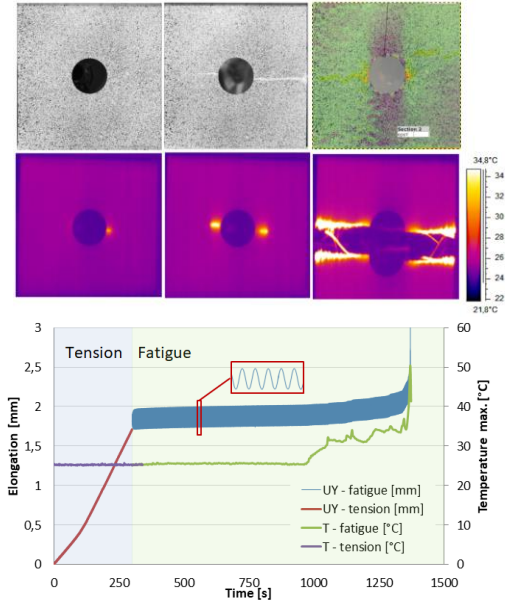


Fig. 1. The fatigue test results of the composite plate with hole registered by the infrared thermography and the digital image correlation systems.

The efficiency of the infrared thermography depends on the inspection parameters. In the cases of dynamic evolution of the damage, the accurate indication of the damage initiation depends on the infrared camera frame rate and sensitivity of the system. Nevertheless, the permanent monitoring of the structure by the infrared thermography system allows for detection of the failure form initiation before significant reduction of the strength capacity which may lead to catastrophic consequences.

References

- [1] STAWIARSKI A, BARSKI M, PAJĄK P: Fatigue crack detection and identification by the elastic wave propagation method *Mechanical Systems and Signal Processing* 2017, **89**:119-130.
- [2] STAWIARSKI A: The non-destructive evaluation of the GFRP composite plate with an elliptical hole under fatigue loading conditions *Mechanical Systems and Signal Processing* 2018, **112**:31-43.
- [3] STAWIARSKI A, MUC A: On transducers localization in damage detection by wave propagation method *Sensors* 2019, **19**:1937.
- [4] STAWIARSKI A, MUC A, BARSKI M: Experimental and numerical studies of laminated plates with delamina-

-LIF-

**DYNAMICS IN LIFE SCIENCES
AND BIOENGINEERING**

Interaction of albumin with chondroitin sulphate IV and VI, a molecular docking study

PIOTR BELDOWSKI^{1A*}, PIOTR WEBER², ADAM GADOMSKI^{1B},
KRZYSZTOF DOMINO^{3A}, ROHIT PRASAD^{3B}

1. Institute of Mathematics and Physics, UTP University of Science and Technology, Bydgoszcz, Poland ^A[0000-0002-7505-6063] ^B[0000-0002-8201-1736]
2. Gdańsk University of Technology, Faculty of Applied Physics and Mathematics, Institute of Physics and Computer Science, Department of Atomic, Molecular and Optical Physics, Gdańsk, Poland [0000-0002-9405-5461]
3. Institute of Theoretical and Applied Informatics, Polish Academy of Sciences, Poland ^A[0000-0001-7386-5441]

* Presenting Author

Abstract: This work presents a study of the mechanism of physical interaction of albumin with chondroitin sulfate IV and albumin with chondroitin sulfate VI in a water environment. We use the molecular docking method. That gives information about supramolecular complexes, which statistical tools can study.

Keywords: albumin, chondroitin sulphate IV and chondroitin sulphate VI, molecular docking method

1. Introduction

We study the interaction between albumin and chondroitin sulfate IV and VI in an aqueous environment. Albumin is the most abundant component of synovial fluid. Interaction with other compounds of synovial fluid determines the appearance of a synergistic effect, the low friction between articulating cartilage surfaces [1]. Chondroitin sulfate IV and chondroitin sulfate VI are organic chemical compounds from the group of glycosaminoglycans, which are also an essential component of cartilage tissue.

Despite many theories and dynamical models that describe articulating cartilage lubrication phenomenon, there is still little information about the nanoscopic function of components of the synovial fluid under physiological conditions at the nanometer level [2]. This work is a step towards analysis processes between the components of the synovial fluid at the nanoscopic level under physiological conditions and is an extension of our previous study [3].

2. Results and Discussion

We perform a molecular docking procedure, a molecular modeling method that allows us to find the location (and conformation) of a ligand at the receptor-binding site. We perform numerical simulations by means of YASARA docking method VINA. The information from simulations enables the evaluation of the free energy of binding (free enthalpy) and the calculation of the chemical affinity. In the Fig.1 we present graphical result of the docking of chondroitin sulphate IV (CS-4) to the albumin and the docking of chondroitin sulphate VI (CS-6) to the albumin.

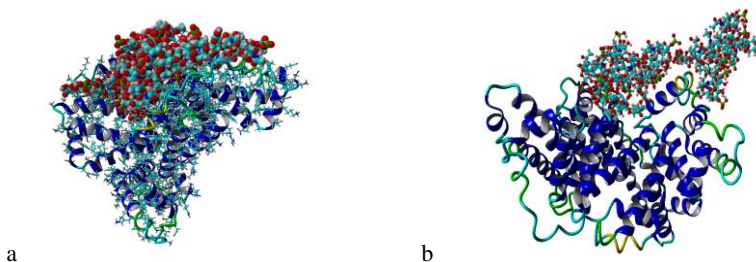


Fig. 1. The panel a presents albumin and chondroitin sulphate IV as a results of docking algorithm and in the panel b presents a albumin and chondroitin sulphate VI.

Complex no	Affinity [kcal/mol]	
	CS-4	CS-6
1	4,432	2,643
2	4,429	2,5885
3	4,247	2,677
4	4,0435	2,5897
5	3,929	2,618
6	3,916	2,587
7	3,912	2,5295
8	3,886	2,571
9	3,878	2,5194
10	3,834	2,437

Fig. 2. Result of molecular docking, of albumin - CS complexes.

3. Concluding Remarks

Our results imply that binding chondroitin sulfate 4 has the highest affinity to albumin. As the ratio between CS4:CS6 changes with age in synovial fluid, this may result in frictional properties of lubricin. The current consensus among scientists studying the subject is that efficient lubrication results from synergy between SF components.

References

- [1] PAWLAK Z, *Articular Cartilage: Lamellar - Repulsive Lubrication of Natural Joints*. ,2018.
- [2] GADOMSKI A, BELDOWSKI P, RUBI J M, URBANIAK W, AUGÉ II W K, SANTAMARIA-HOLEK I, PAWLAK Z: Some conceptual thoughts toward nanoscale oriented friction in a model of articular cartilage. *Mathematical Biosciences* 2013, **244**, 188–200.
- [3] BELDOWSKI P, WEBER P, DEDINAITE A, CLAESSEON P, GADOMSKI A: Physical crosslinking of hyaluronic acid in the presence of phospholipids in an aqueous nano-environment. *Soft Matter* 2018, **14**, 8997-9004.

The Probability of Infection, through Aerosol Transmission, by SARS-CoV-2 Coronavirus

Björn Birnir^{1*}

1. Department of Mathematics and the Center for Complex, Nonlinear and Data Science
University of California Santa Barbara, CA 93106

Abstract: The spread of the exhaled cloud of aerosols carrying the SARS-CoV-2 Coronavirus is computed using the Lagrangian theory of passive scalars.

Keywords: Lagrangian turbulence, passive scalars, SARS-CoV-2 Coronavirus, aerosols.

1. Introduction

It is now generally accepted that infections by the SARS-CoV-2 Coronavirus beyond the social distance of 2 meters or 6 feet, are primarily caused by aerosol transmission. It has also been shown that the virus can live for several hours and the flow of air plays a larger role in transmitting the virus than social distancing of 2 meters.

The details of how the virus-laden aerosols are carried around by airflow are complicated. This is because the airflow is very turbulent and thus hard to simulate. This makes the application of computational fluid dynamics (CFD) hard, since in order to compute the concentration of the aerosols, one must perform many simulations and take their average, a labour intensive and time-consuming process.

There is another mathematical theory, which can be applied more easily to compute the distribution of the virus-laden aerosols in turbulent airflow. This is the so-called Lagrangian theory of passive scalars [1],[2].

This theory explains how particles that are too small and light to disturb the flow are distributed in the fluid. It was developed by theoretical physicists 50 year ago and has been used successfully to compute the distributions of many different types of particles that are carried around by the air-flow, without disturbing the airflow itself [3].

2. Results and Discussion

We employ the theory of passive scalars in Lagrangian flow to compute the infection rate for infectious diseases. The theory of passive scalars allows one to do two things. First, given how many aerosols a person is emitting during a time period, we can compute the aerosol concentration in the cloud of air that is emanating from them. This is the air mixed with their exhaled air, by the ambient airflow. The concentration will vary depending on whether the person is at rest, doing heavy exercise or singing. Secondly, if the ventilation is deficient in the space where the person is located, we can compute what part of that space gets contaminated, and the concentration of the aerosol in that part of the space. This frequently depends on the airflow, and in many spaces the air is not well-mixed in the whole space.

If the ventilation is better, however, the air in the whole space is well mixed and then it is easier to compute the concentration of aerosols. We provide and explain a program that does this. This program has been used to configure safe work-spaces at the University of California, Santa Barbara. We

will explain how that is done using two study rooms for the students in the UC Santa Barbara Library as an example. The program computes how many students can safely work in these spaces, given their volume and ventilation, and how long a time they can safely spend in them.

We give an example [4] below, by using the program to plot the number of people that can safely be inside a restaurant versus the ventilation in the restaurant, measured in air exchanges per hour (ACH), in the restaurant. ACH measures how often the air in the restaurant is completely replaced by fresh or filtered air in one hour. We need to know the size (volume) of the restaurant and the how large a percentage of the population has been vaccinated. Let us assume that the restaurant has the volume 125 cubic meters (or roughly 4,400 cubic feet). This is restaurant, with the height of the ceiling 2.5 meters, could contain 50 guests under normal conditions.

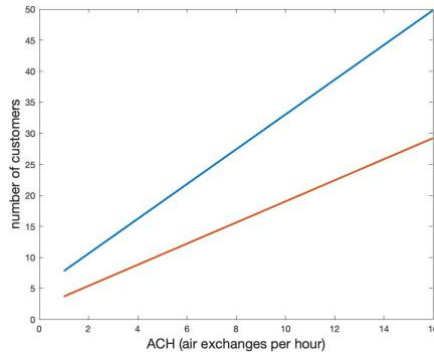


Fig. 1. The figure shows the number of customers that can safely be in a restaurant, that can have 50 customers under normal conditions. The number of customers is on the vertical axis and the ventilation, measured in ACH, on the horizontal axis. The blue line shows the number of customers when 70% of the population has been vaccinated, the red line when 50% of the population has been vaccinated. Safe means that the probability of infecting 2 customers in two hours is 10% or less. The probability of one person being infected is high, if that person is sitting next to or directly across the infected person in the exhaled aerosol cloud. But the probability that two or more people are infected can be effectively controlled by the ventilation.

3. Concluding Remarks

The spread of the aerosols carrying the SARS-CoV-2 Coronavirus can be effectively controlled by ventilation. The probability of infection is minimized, using the Lagrangian theory of passive scalars.

Acknowledgment: The author wants so to thank Luiza Angheluta for useful discussions.

References

- [1] Birnir, B., (2020). The Build-Up of Aerosols Carrying the SARS-CoV-2 Coronavirus, in Poorly Ventilated, Confined Spaces [online] Available at: <https://www.medrxiv.org/content/10.1101/2020.08.11.20173195v2>
- [2] Birnir, B. (2020). Ventilation and the SARS-CoV-2 Coronavirus, *Analysis of outbreaks in a restaurant and on a bus in China, and at a Call Center in South Korea*. [online] Available at: <https://www.medrxiv.org/content/10.1101/2020.09.11.20192997v2>
- [3] Warhaft, Z., (2000). Passive Scalars in Turbulent Flows. *Annual Review of Fluid Mechanics*, 32(1), pp.203-240.
- [4] Birnir, B., (2001). SARS-CoV-2 coronavirus: How it spreads in confined spaces. To appear in *Research Features*, June 2021.

Conditions Regulating Tumor Cell Behaviour in Biological Systems with Memory of States

LARYSA DZYUBAK^{1*}, OLEKSANDR DZYUBAK², JAN AWREJCEWICZ³

1. National Technical University "Kharkiv Polytechnic Institute", Department of Applied Mathematics, Kharkiv, Ukraine [0000-0001-5530-830X]
2. Ascension All Saints Cancer Center, Racine, WI, US [0000-0002-0717-1887]
3. Łódź University of Technology, Department of Automation, Biomechanics and Mechatronics, Łódź, Poland [0000-0003-0387-921X]

* Presenting Author

Abstract: For biological systems with memory of states there were found conditions which regulate tumor cell behaviour. These conditions depend on parameters of the multi-parametric space. Based on the Masing–Bouc–Wen’s framework, the state memory in the biological system was simulated by means of supplemental state variables (internal variables). The additional state variables were introduced into the generalized non-linear multi-scale diffusion cancer invasion model and the chaotic cancer attractors were found. To quantify chaotic cancer attractors, the technique based on the wandering trajectories analysis was applied.

Keywords: biological system with memory of states, tumor growth, carcinogenesis, chaotic attractors, response delay

1. Introduction

This work is the continuation of the studies presented in our earlier publications [1, 2] in which the conditions controlling cancer invasion were defined depending on parameters of the multi-parametric space as well as the influence of the initial state of a biological system on carcinogenesis.

The biological systems with memory of states do not react instantly to external perturbations. Such systems have a response delay. In this study, the memory of states was simulated by means of additional state variables (internal variables) using Masing–Bouc–Wen’s framework [3–4]. Applications to different types of hysteresis loops confirmed that models with internal variables are appropriate to simulate hysteresis from very different fields.

2. Mathematical Model and Simulation Results

In the model studied in this work, the tumor development is governed by the inhomogeneous dissipative set of differential equations:

$$\dot{n} = 0, \quad (1)$$

$$\dot{f} = \alpha\eta(m - f) + h_f z_f, \quad (2)$$

$$\dot{z}_f = \left[A_f - (\gamma_f + \beta_f \operatorname{sgn}(\dot{f}) \operatorname{sgn}(z_f)) \right] |z_f|^{n_f} \dot{f}, \quad (3)$$

$$\dot{m} = \beta_k n + f(\gamma - c) - m + h_m z_m, \quad (4)$$

$$\dot{z}_m = \left[A_m - (\gamma_m + \beta_m \operatorname{sgn}(\dot{m}) \operatorname{sgn}(z_m)) \right] |z_m|^{n_m} \dot{m}, \quad (5)$$

$$\dot{c} = \nu f m - \omega n - \delta \phi c + h_c z_c, \quad (6)$$

$$\dot{z}_c = \left[A_c - (\gamma_c + \beta_c \operatorname{sgn}(\dot{c}) \operatorname{sgn}(z_c)) |z_c|^{n_c} \right] \dot{c}. \quad (7)$$

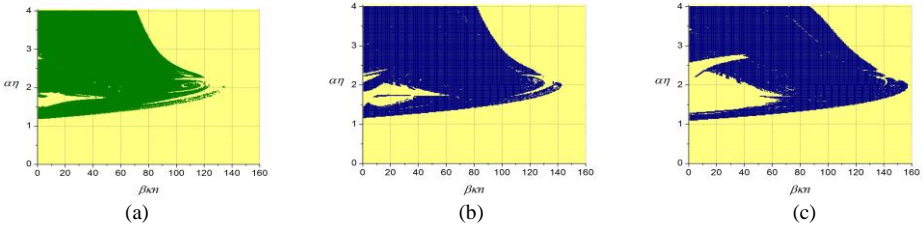


Fig. 1. Conditions leading to cancer invasion in the biological systems with memory of states (1)-(7) in control parameter plane $(\beta kn, \alpha \eta)$ –tumor cell volume vs glucose level: (a) $h_f=h_m=h_c=0$; (b) $h_f=0.5, h_m=0.4, h_c=0.3$; (c) $h_f=h_m=h_c=0.9$

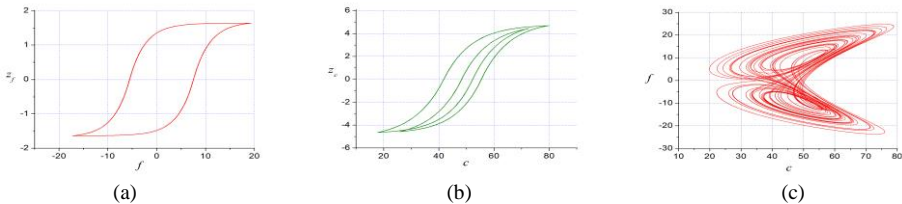


Fig. 2. Responses delay of the biological systems with memory of states (1)-(7) with $h_f=0.5, h_m=0.4, h_c=0.3$: (a), (b) hysteresis loops at $\beta kn=3.0, \alpha \eta=1.75$ (a chemical clock); (c) a chaotic attractor in MM, MDE and oxygen concentrations phase space projected to phase plane (c, f) at $\beta kn=3.0, \alpha \eta=4.0$

The meaning of variables is as follows: n – tumor cell density; f – matrix–metalloproteinases (MM) concentration; m – matrix-degradative enzymes (MDE) concentration; c – oxygen concentration; z_f, z_m, z_c present the hysteretic part of the system considered. On the other hand, the fitting parameters are defined as follows: α – tumor cell volume; β – glucose level; γ – number of tumor cells; δ – diffusion saturation level; η and κ are coefficients describing a growth and decay of MM and MDE concentration, respectively; v, ω, φ govern growth and decay of the oxygen concentration. The parameters $(A_f, \beta_f, n_f), (A_m, \beta_m, n_m), (A_c, \beta_c, n_c) \in R^+$ and $\gamma_f, \gamma_m, \gamma_c \in R$ govern the shape of the hysteresis loops. The parameters h_f, h_m, h_c characterise a hysteresis contribution to the system considered.

3. Concluding Remarks

Analysis of the results obtained demonstrates a significant influence of the state memory on the evolution of conditions leading to cancer invasion in biological systems depending on components of the multi-parametric space ‘number of tumor cells – tumor cell volume – glucose level – diffusion saturation level’.

References

- [1] DZYUBAK L, DZYUBAK O, AWREJCEWICZ J: Controlling and stabilizing unpredictable behaviour of metabolic reactions and carcinogenesis in biological systems. *Journal of Nonlinear Dynamics* 2019, **97**:1853–1866.
- [2] DZYUBAK L, DZYUBAK O, AWREJCEWICZ J: Multi-parametric evolution of conditions leading to cancer invasion in biological systems. *Applied Mathematical Modelling* 2021, **90**:46-60.
- [3] AWREJCEWICZ J, DZYUBAK L: Hysteresis modelling and chaos prediction in one- and two-dof hysteretic models. *Archive of Applied Mechanics* 2007, **77**:261-279.
- [4] AWREJCEWICZ J, DZYUBAK L, LAMARQUE C-H: Modelling of hysteresis using Masing–Bouc–Wen’s framework and search of conditions for the chaotic responses. *Communications in Nonlinear Science and Numerical Simulation* 2008, **13**:939-958.

Chaos in Environmental Radioactivity Dynamics of Some Geosystems: Analyses of the Radon Time Series

ALEXANDER V GLUSHKOV^{1*}, OLGA Y KHETSELIUS¹, SERGIY M STEPANENKO¹,
ANDREY A SVINARENKO¹, AND ANNA V IGNATENKO¹

1. Odessa State Environmental University, Mathematics Dept., L'vovskaya str. 15, 65009, Odessa

* Presenting Author

Abstract: The paper is devoted to development and application of an effective universal complex chaos-geometric approach to studying of a deterministic chaos, the strange attractors in dynamics of the environmental radioactivity systems. In particular, the atmospheric radon ²²²Rn concentration temporal dynamics is studied and computed. The analysis methods include advanced versions of the correlation integral, fractal analysis, algorithms of average mutual information, false nearest neighbors, Lyapunov exponents, surrogate data, predicted trajectories algorithms, spectral methods etc. to solve problems of modeling the atmospheric ²²²Rn time series. The topological and dynamical invariants for the ²²²Rn concentration time series for some regions of the USA are computed and analysed.

Keywords: deterministic chaos, attractors, dynamics of geosystems, radon time series

1. Introduction. Universal Chaos-Geometric Approach to Dynamics of Geosystems

A study of the phenomenon of stochasticity or chaos in different dynamical systems is provided by a great importance for a whole number of applications, including a necessity of understanding chaotic features in different geophysical (hydrometeorological, environmental etc) systems. New field of investigations of the similar systems has been provided by a great progress in a development of a chaos and dynamical systems theory methods [1-5]. In our previous papers [2,4,5] we have given a review of new methods and algorithms to analysis of different systems of environmental and Earth sciences. In this paper the fundamentals of an universal complex chaos-geometric approach to Des of the deterministic chaos, strange attractors in dynamics of the environmental radioactivity systems are presented. In particular, the atmospheric radon ²²²Rn concentration temporal dynamics for some US regions is studied and computed. As many blocks of the used approach have been developed earlier and need only to be reformulated regarding the problem studied in this paper, here we are limited only by the key moments following to Refs. [2,4,5]. In our problem the approach includes a realization of the following blocks: I. Analytical and numerical study of of convective transport in a general circulation model; II. Analysis and processing of a number of basic dynamic characteristics of the system, including application of general criteria for the existence of chaos in dynamics (e.g. the known Gottwald- Melbourne test, use of Fourier expansions, spectral methods); III. Reconstruction and determination of the phase space of the system (choice of time lag using the methods of autocorrelation function, average mutual information, application of the methods of correlation integral and nearest neighboring points, fractal geometry); IV. Chaos-cybernetic study of chaos in dynamics and construction of the prediction models: a) determination of chaos parameters, incl. topological, dynamic invariants (such as the Lyapunov's exponents, Kolmogorov entropy etc); b) forecasting temporal evolution of chaotic systems using novel prediction models [2]

2. Results and Discussion

The time series of the atmospheric Rn concentrations extending for a least one year are available from five sites in the Unites States (Environmental Measurement. Lab., USA Dept. of Energy). The record of the radon concentrations at the Chester cite is by far the most extensive. Measurements had been made round-the-clock 10 m above ground in a open field and data from July 1977 to November 1983 are available as continuous time series of 0.5-3 hour average concentrations (Harlee, 1978,1979; Fisenne, 1980-1985) (see details in [5,6]). Table 1 shows the results of computing a set of the dynamical and topological invariants, namely: correlation dimension (d_2), embedding dimension (d_E), first two Lyapunov's exponents, (λ_1, λ_2) , Kaplan-Yorke dimension (d_L), and the Kolmogorov entropy, average limit of predictability (Pr_{max} , hours) for the studied ^{222}Rn time series.

Table 1. The correlation dimension (d_2), embedding dimension (d_E), first two Lyapunov's exponents, (λ_1, λ_2) , Kaplan-Yorke dimension (d_L), and the Kolmogorov entropy, average limit of predictability (Pr_{max} , hours) for the 1978 ^{222}Rn time series at the Chester site

d_2	d_E	λ_1	λ_2	K_{ent}	d_L	Pr_{max}
6,03	7	0,0194	0,0086	0,028	5,88	35

Analysis of the data shows that the Kaplan-Yorke dimensions (which are also the attractor dimensions) are smaller than the dimensions obtained by the algorithm of false nearest neighbours. It is very important to pay the attention on the presence of the two (from six) positive (chaos exists!) Lyapunov's exponents λ_i . One could conclude that the system broadens in the line of two axes and converges along four axes that in the six-dimensional space. Other values of the Lyapunov's exponents λ_i are negative.

3. Concluding Remarks

An universal chaos-geometric approach is applied to analysis, modelling and prediction of the atmospheric radon ^{222}Rn concentration time series with using the data of surface observations of the Environmental Measurements Laboratory (USA Dept. of Energy) for some sites in the United States (Chester site). The topological and dynamical invariants for the ^{222}Rn concentration time series are computed and analysed

References

- [1] ABARBANEL H, BROWN R, SIDOROWICH J AND TSIMRING L: The analysis of observed chaotic data in physical systems. *Rev. Mod. Phys.* 1993, **65**:1331-1392.
- [2] GLUSHKOV AV: *Methods of a Chaos Theory*. Astroprint: Odessa, 2012.
- [3] KENNEL M, BROWN R, AND ABARBANEL H: Determining embedding dimension for phase-space reconstruction using a geometrical construction. *Phys. Rev. A* 1992, **45**:3403-3411.
- [4] KHETSELIUS O: Forecasting evolutionary dynamics of chaotic systems using advanced non-linear prediction method. In: AWREJCEWICZ J, KAZMIERCZAK M, OLEJNIK P AND MROZOWSKI J (EDS.) *Dynamical Systems Applications*. Politechniki Łódzkiej: Łódź, 2013, **T2**:145-152..
- [5] GLUSHKOV AV, DUBROVSKAYA YV, BUYADZHI VV AND TERNOVSKY EV: Chaos and strange attractors in environmental radioactivity dynamics of some geosystems: Atmospheric radon ^{222}Rn . In: AWREJCEWICZ J, KAZMIERCZAK M AND MROZOWSKI J (EDS.) *Mathematical and Numerical Aspects of Dynamical Systems Analysis*. ARSA Publishing: Łódź, 2017, **2**:205-214.
- [6] JACOB D AND PRATHER M: Radon-222 as a test of convective transport in a general circulation model. *Tellus*. 1990, **42b**:118-134.

Design and simulation of a lower limb exoskeleton with linear electric actuators

DARIUSZ GRZELCZYK¹, OLGA JARZYNA^{2*}, JAN AWREJCEWICZ³

1. Lodz University of Technology, Department of Automation, Biomechanics and Mechatronics, Lodz, Poland [0000-0002-7638-6582]

2. Lodz University of Technology, Department of Automation, Biomechanics and Mechatronics, Lodz, Poland [0000-0001-5883-9958]

Lodz University of Technology, Department of Automation, Biomechanics and Mechatronics, Lodz, Poland [0000-0003-0387-921X]

* Presenting Author

Abstract: In the present study, we proposed and investigated a relatively simple and inexpensive construction of a lower limb exoskeleton driven by linear electric actuators and controlled by an Arduino microcontroller board. Moreover, to study crucial kinematic and dynamic parameters of the proposed device, we developed a general, three-dimensional simulation model of the exoskeleton in Mathematica software. To control individual joints of the investigated exoskeleton, we employed time histories of human joint angles in normal gait, recorded with the use of a motion capture system. As a result, we developed a novel human gait generator, which can be used to produce rhythmic movements in hip, knee and ankle joints of both limbs. Finally, the developed control approach was verified with the use of the constructed prototype of the exoskeleton.

Keywords: human lower limbs, exoskeleton, human movement

1. Introduction

Locomotor dysfunctions are common especially in highly developed societies, and the number of people suffering from such a kind of impairment is expected to grow in the future [1]. Although conventional physiotherapy helps restore mobility, it is labour-intensive and leads to occupational conditions among therapists. To overcome these drawbacks, lower limb rehabilitation can be performed with the aid of robots such as lower limb exoskeletons (LLEs). Information about developments and challenges in the field of LLEs can be found in review paper [2].

2. Results

We proposed and investigated a simple and economical lower limb exoskeleton aimed at rehabilitation. The device is driven by linear electric actuators. To realize the control algorithm, a popular Arduino microcontroller board is employed. Joints of the exoskeleton are driven according to time histories of human joint angles during normal gait recorded with a motion capture system [3,4].

A CAD model of the proposed LLE, created in Inventor Professional 2019, is presented in Fig. 1. Mechanical design consists of the main static pelvic frame, back part providing support for the upper body, and two limbs, each equipped with three linear actuators. A limb consists of three main segments actuated by active hip, knee and ankle joints. By changing the lengths of particular segments, it is possible to adapt the construction to people of different heights. Each active joint consists of a linear actuator with DC motor, gear ratio and screw-nut system.

To study the proposed LLE, we developed a 3D simulation model of the exoskeleton (see Fig. 1). The simulation model is fully parametric, therefore arbitrary values of all parameters determining the kinematic model of the exoskeleton can be applied to numerical study. As a result, the implemented simulation model can be used to visualize the mechanical design and verify the correctness of simulated results, namely the spatial positions of its elements. In a further study, it can help understand key parameters of virtual experiments of the prototype made of aluminium profiles.

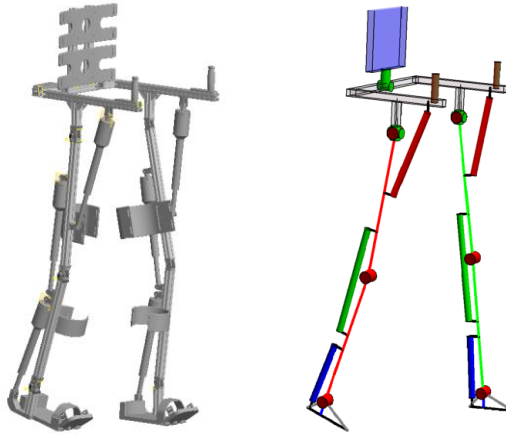


Fig. 1. CAD model of the designed LLE driven by linear actuators with DC motors, gear ratios, screw-nut systems and potentiometers (on the left), and a general, 3D full parametric simulation model of the LLE (on the right)

3. Discussion and conclusions

Both in the proposed design and the developed simulation model, we considered the biocompatibility aspects of the simulated device. As a result, in a further study, the developed simulation model can be successfully employed for more advanced and more accurate virtual studies of a walking process and determination of the most important kinematic and dynamic gait parameters. To verify the proposed control technique, a prototype of the LLE was constructed. The carried out experimental investigations gave promising results regarding control of the device in practical applications. To conclude, we showed that it is possible to develop relatively inexpensive and efficient LLE with a simple control system. The obtained results may contribute to a better access to LLE-assisted rehabilitation in the future and reduce the workload of physiotherapists eventually.

References

- [1] BACH J.P., DEUSCHL G., DOBLHAMMER G., ZIEGLER U., DODEL R.: Projected numbers of people with movement disorders in the years 2030 and 2050. *Movement Disorders*, 2011, **26**(12):2286-2290.
- [2] CHEN B., MA H., QIN L.-Y., GAO F., CHAN K.-M., ET AL.: Recent developments and challenges of lower extremity exoskeletons. *Journal of Orthopaedic Translation*, 2016, **5**, 26-37.
- [3] GRZELCZYK D., SZYMANOWSKA O., AWREJCEWICZ J.: Gait pattern generator for control of a lower limb exoskeleton. *Vibrations in Physical Systems*, 2018, **29**, 2018007.
- [4] JARZYNA O., GRZELCZYK D., STAŃCZYK B., AWREJCEWICZ J.: Generation of a gait pattern for a lower limb rehabilitation exoskeleton, *Mechanics Based Design of Structures and Machines*, 2020, DOI: 10.1080/15397734.2020.1858868

Nonlinear oscillations of a complex discrete system of rigid rods with mass particles on an elastic cantilever

KATICA (STEVANOVIĆ) HEDRIH^{1,2}, ANDJELKA HEDRIH^{1*}

1. Department of mechanics, Mathematical Institute of Serbian Academy of Sciences and Arts (MI SANU) Belgrade, Serbia [ORCID: 0000-0001-7598-900X]

2. Faculty of Mechanical Engineering, University of Niš, Serbia [ORCID: 0000-0002-2930-5946]

* Presenting Author

Abstract: We analyzed forced oscillations of a complex cantilever. The non-linearity of the system is introduced by a spring with nonlinear properties that oscillates in a vertical plane. The description and approximations of the system are given. The system oscillates in two orthogonal planes - horizontal and vertical with four degrees of freedom in each plane. In the horizontal plane, the system oscillates with eigen frequencies of free linear oscillations; in the vertical plane with forced nonlinear oscillations. For describing oscillatory behavior of this complex system under an external single-frequency force, influence coefficients of deflection of cantilever were used. Oscillatory behavior of this complex system in vertical plane can be described by subsystems of nonlinear differential equations that are solved using a newly introduced, generalized method of variation of constants and the method of averaging, as well as the Krilov-Bogolyubov-Mitropolski asymptotic method of nonlinear mechanics of approximation. The presented generalized methods of constants variation, together with the averaging method, opens the possibility of studying the forced nonlinear oscillations, under the influence of external forces with different frequencies, each in the corresponding resonant range frequency interval.

Keywords: nonlinear dynamics, complex cantilever, influence coefficients of deflection, averaging method, method of constant variations

1. Introduction

Complex vertical oscillations [1] and non-linear equations of motion of L-shaped beam structures [2] were studied by other authors. We modified the previously proposed elastic cantilever model with symmetric attached rigid rods with mass particles [3] introducing nonlinearity in the form of a spring with nonlinear properties that oscillates in the vertical plane. Fig.1.

2. Model and methods

The influence coefficients of cantilever deflection are determined and introduced in nonlinear differential equations for describing forced oscillations of a discrete complex system in the vertical plane. The system of 4 nonlinear differential equations described forced nonlinear oscillations in the vertical plane. The equation describing the oscillations in the vertical plane in dynamical configuration 1 is:

$$y_i = \alpha_{i1} \left[F_{01y} \sin \Omega_y t + \left(-c y_1 - c_N y_1^3 \right) \right] + \alpha_{i2} (-2m_2 \ddot{y}_2) + \alpha_{i3} (-2m_3 \ddot{y}_3) + \alpha_{i4} (-m_4 \ddot{y}_4) + \delta_{i2} (-2m_2 \ddot{y}_2 \ell_2 \cos \beta_2) + \delta_{i3} (-2m_3 \ddot{y}_3 \ell_3 \cos \beta_3); \quad i = 1, 2, 3, 4 \quad (1)$$

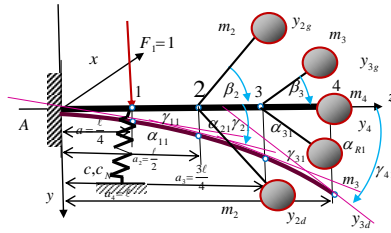


Fig. 1. Oscillations of a complex oscillatory model in the vertical plane.

The system of nonlinear differential equations is solved using a newly introduced, generalized method of variation of constants and the Krilov-Bogolyubov-Mitropolyski asymptotic method of nonlinear mechanics. The Krilov-Bogolyubov-Mitropolyski method was used for non-stationary regime when the frequency of the external force is in the resonant frequency range of one of the eigen frequencies of free oscillations of the linearized system. In this case, frequency changes with the different speed. In the method of variation of constants, the assumption is that the frequency of the external force in nonlinear system, is approximately equal to one of own eigen circular frequency [4].

3. Results and Discussion

In the case where Krilov-Bogolyubov-Mitropolyski method was used, frequency changes with the different speed. By obtained system of nonlinear differential equations along four phases and four amplitudes in the first asymptotic approximation, it is possible to obtain numerical/graphical solutions for amplitude-frequency curves of small forced nonlinear oscillations.

3. Concluding Remarks

The paper contains a generalization of the method of variation constants in combination with averaging method for obtaining a system of ordinary nonlinear differential equations of first order along corresponding number of amplitudes and phases in first approximations describing non-linear modes of the complex discrete system. This system is simpler than a system of governing differential equations along amplitudes and phases of generalized coordinates, and permits qualitative analysis of the non linear phenomena in the systems with nonlinear dynamics, specifically stability and instability of the amplitudes and phases of nonlinear modes in the first approximation.

Acknowledgment: Parts of this research were supported by the Ministry of Education, Sciences and Technology of Republic of Serbia trough Mathematical Institute of Serbian Academy of Sciences and Arts (MI SANU), Belgrade, Serbia.

References

- [1] GEORGIADIS F, WARMINSKI J, CARTMELL P.M: Towards Linear Modal Analysis for an L-Shaped Beam: Equations of Motion. *Mechanics Research Communications* 2013, **47**:50-60.
- [2] ŁYGAS K, WOLSZCZAK P, LITAK G, STACZEK P: Complex response of an oscillating vertical cantilever with clearance. *Meccanica* 2019, **54**:1689–1702.
- [3] HEDRIH A, JOVANOVIĆ Dj, (STEVANOVIĆ) HEDRIH K. Theoretical modeling of forced oscillations of herbaceous plant. *XXV ICTAM*, 23-28 August 2020+1, Milano, Italy.
- [4] STEVANOVIĆ K: Two-frequency non stationary forced vibrations of a beam, *Marhematical Physics*, Kiev, 1972, **12**:127-140. (in Russian).

Influence of Periodic Nutrient Advection on a Simple Ecosystem

ANNA JAILLET¹, PASCAL RIVIERE², XAVIER CARTON^{1*}

1. LOPS/IUEM/UBO
 2. LEMAR/IUEM/UBO
- * Presenting Author

Abstract: In this paper, we study the time evolution of a simple NPZ system, with periodic physical forcing. We address the effect of this forcing on the limit cycle of the ecosystem dynamics.

Keywords: ecosystem modeling, NPZ, periodic forcing

1. Introduction

Ecosystem dynamics have often been studied in applied mathematics, with several formulations starting from the simple Lotka-Volterra predator-prey system, up to complex oceanic biogeochemical systems. Most studies determined the time evolution of the individual elements of the ecosystem, determined the existence of steady states or of limit cycles and their stability. Fewer papers were concerned by the interaction of the physical evolution of the environment with the ecosystem internal dynamics [1,2]. Our study is concerned with a NPZ (nutrient-phytoplankton-zooplankton) ecosystem controlled by a nutrient flux, which can be varied according to the physical inflow into the system. Our aim is first to study the stability of the ecosystem, the fixed points, their stability and the limit cycles without physical influence. Then we introduce a small-amplitude, periodic modulation of the nutrients on a period equal to that of the limit cycle or half this value to trigger harmonic or subharmonic resonance. The equations for the system are

$$dN / dt = D(t)(N_0(t) - N) - f(N), \quad (1)$$

$$dP / dt = \alpha f(N)P - D_1 P - g(P)Z \quad (2)$$

$$dZ / dt = \beta g(P)Z - D_2 Z. \quad (3)$$

The model is composed of three ordinary differential equations which represent the evolution the concentration of respectively nutrient available in the system, Phytoplankton and Zooplankton according to time. The model used for our study also neglects the remineralization of phytoplankton and zooplankton into dissolved organic matter via decomposition. The parameters of the model and the initial conditions of all variables are positive. To simplify the model further, the function $f(N)$ is continuous and follows a Michaelis-Menten form

$$f(N) = \mu_{max} N / (K + N) = bN / (a + N) \quad (4)$$

$$g(P) = cP / (1 + dP) = c'P / (d' + P). \quad (5)$$

The parameters and structure of the equations are similar to those of [3,4,5,6]. The equations were solved numerically with a 4th order Runge-Kutta scheme.

2. Results and Discussion

For fixed D and N_0 , steady states with only N or only N and P have been calculated; their stability has been found; this is obtained by solving a second degree equation which yields the region for instability in parameter space. When N , P and Z are all present, a limit cycle can be obtained when taking large values of N_0 . From this limit cycle, we can compute the period of oscillation and force either D on the half period to obtain sub-harmonic resonance or N_0 on the full biological period to obtain harmonic resonance.

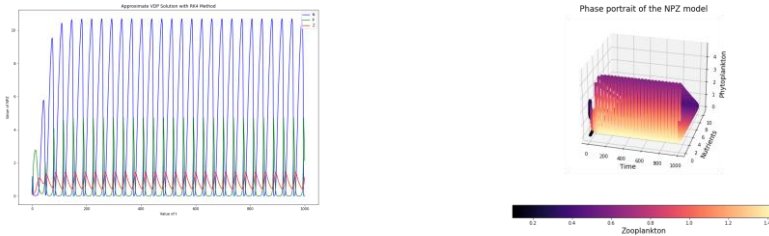


Fig. 1. (left) time oscillation of N, P, Z in the limit cycle; (right) phase portrait of N, P, Z in the limit cycle

3. Concluding Remarks

The time variability of the physical inflow of nutrients is essential to ecosystems in particular in the case of resonance between the physical and biological timescales.

References

- [1] GUSEVA K, FEUDEL U: THE EFFECT OF INTERMITTENT UPWELLING EVENTS ON PLANKTON BLOOMS. [arXiv.org > q-bio > arXiv:1905.02064](https://arxiv.org/abs/1905.02064)
- [2] CHAKRABORTY S, FEUDEL U, 2014: HARMFUL ALGAL BLOOMS: COMBINING EXCITABILITY AND COMPETITION. *Theor Ecol*, **7**, 221-237.
- [3] PERRUCHE C, RIVIERE P, PONDAVEN P, CARTON X, 2010: PHYTOPLANKTON COMPETITION AND COEXISTENCE: INTRINSIC ECOSYSTEM DYNAMICS AND IMPACT OF VERTICAL MIXING. *J. MAR. SYST.*, **81**, 99-111.
- [4] ZHANG T, WANG W, 2012: HOPF BIFURCATION AND BISTABILITY OF A NUTRIENT-PHYTOPLANKTON-ZOOPLANKTON MODE. *APPLIED MATHEMATICAL MODELLING* **36**, 6225-6235
- [5] CHAKRABORTY S, CHATTOPADYAYH J., 2008: NUTRIENT-PHYTOPLANKTON-ZOOPLANKTON DYNAMICS IN THE PRESENCE OF ADDITIONAL FOOD SOURCE - A MATHEMATICAL STUDY. *JOURNAL OF BIOLOGICAL SYSTEMS*, **16**, 4, 547-564.
- [6] MOROZOV AY, NEZLIN NP, PETROVSKII V, 2005: INVASION OF A TOP PREDATOR INTO AN EPIPELAGIC ECOSYSTEM CAN BRING A PARADOXICAL TOP-DOWN TROPHIC CONTROL, *BIOLOGICAL INVASIONS*, **7**, 5845-861.

Nonlinear Dynamics, Stability and Control Strategies: Mathematical Modeling on the Big Data Analyses of Covid-19 in Poland

NATALYA KIZILOVA*

Warsaw University of Technology, Institute of Aeronautics and Applied Mechanics [0000-0001-9981-7616]

Abstract: Detailed numerical data on covid-19 epidemic have been collected since February 2020, and now >200 countries and regions are presented in online databases. A brief review of the data analyses and mathematical modelling for different countries is given. The time series on three ‘waves’ of pandemic in 16 provinces of Poland are analyzed. Statistical regularities, self- and cross-correlations, common and different features in the regions are revealed. Spectral analysis of oscillating components and phase curves demonstrated non-linear quasi-regular and chaotic dynamics. Based on the comparative analyses of the 7-day averaged curves, the non-linear SEIDQRV model with time delay was estimated as the most proper mathematical model. Material parameters of the model for each ‘wave’ and region have been used for stability analysis and controllability of the pandemic. The \mathfrak{R} -factor (reproduction number) for each region/wave have been obtained as the stability criterion for the systems of equations of the SIR, SIRS, SEIR, SEIRS, SEIDQR models with and without time delay. Sensitivity of the models to different control functions (social restrictions, lockdown measures, availability/quality of medical treatment, vaccination level) revealed different sets of the most influencing parameters in different provinces and waves. The results are compared for similar data for Poland and other European countries. It is shown; the nonlinear dynamics and best control strategies differ at the level of the country and its regions that needs more complex local governmental measures against further development of epidemic.

Keywords: covid-19 pandemic, data analyses, nonlinear dynamics, mathematical modelling, stability and control

1. Introduction

Rapid development of the covid-19 pandemic produced Big Data with high volume, velocity and variety that in combination with geographic, climatic, meteorological, social, economic data¹ give a rich source for statistical analysis and mathematical modelling [1-3]. It is a unique field of research with >60,000 papers published and indexed in ScienceDirect, ~138,000 – in PubMedCentral, >3800000 – in Google Scholar on different aspects of the pandemic development and outcomes. In this study the very first results on the detailed data analysis for Poland, its 16 provinces and neighbour European countries is presented. The most popular mathematical models of covid-19 pandemic are analyzed based on the data for each province and each of the three ‘waves’ of the epidemic.

2. Results and Discussion

The online databases are continuously updated by the data on new/cumulative cases, deaths, recoveries, vaccinations, and other information related to the epidemic over the world¹. The diagrams

¹ <https://ourworldindata.org/>, <https://www.worldometers.info/>

on new daily cases $N_{nd}(t)$ in Poland confirms the current decay of the 3-rd ‘wave’ (Fig.1a) while similar distributions for 3 selected provinces reveal different dynamics and time delay (Fig.1b). Dynamics of the 3 ‘waves’ in the provinces distinct (Fig.1b) and demonstrate significant differences and time delay with averaged data on the country (Fig. 1a). Similar conclusions can be derived by comparison to the data treatment for USA, Canada, Australia, different European and Asian countries [3].

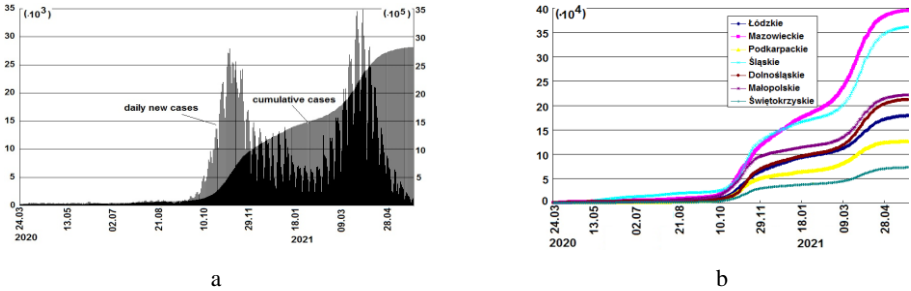


Fig. 1. New daily and cumulative cases in Poland (a), cumulative cases in 7 provinces (b)

The most popular SEIDQR mathematical model is based on the ODEs for the numbers of susceptible (S), exposed (E), infected (I), diagnosed (D), quarantined (Q), and Recovered (R) individuals. In this study a generalization of the model for vaccinated (V) people is proposed in the form

$$\frac{d}{dt} X_j(t) = f_{j1}(X_j)X_1(t - \tau_1) + f_{j2}(X_j)X_2(t - \tau_2) + \dots + f_{jn}(X_j)X_n(t - \tau_n), \quad (1)$$

where $X_j = \{S, E, I, D, Q, R, V\}$, $f_{jn}(X_j)$ are known non-linear functions [1-3].

Simplified SIR, SIRS, SEIR, SEIRS models can be obtained from (1) by elimination of some variables and simplification the functions $f_{jn}(X_j)$. The steady state solution $\{S^0, E^0, I^0, D^0, Q^0, R^0, V^0\}$ for each of the models can be computed from (1) at $dX_j / dt = 0$. Then stability of the dynamical system (1) can be estimated as the conditions $Re(\lambda) < 0$ for the solutions $X_j(t) = X_j^0 + X_j^* e^{\lambda t}$. The Lyapunov exponent $Re(\lambda)$ is considered as an informative parameter $\Re(\lambda)$ (reproduction number) for the dynamical instability of the epidemic. This critical value is important for the stability, control and prognosis local and global dynamics of the pandemic.

3. Concluding Remarks

Statistical analysis of the covid-19 Big Data for Poland, its provinces and other countries revealed non-linear quasi-regular and chaotic dynamics. The reliable estimations of the pandemic development and measures for its decay can be obtained from the proposed generalized model with time delay.

References

- [1] Sharma S, Volpert V, Banerjee M: Extended SEIQR type model for COVID-19 epidemic and data analysis. *Mathematical Biosciences and Engineering* 2020, 17(6):7562–7604.
- [2] Machado T, Ma J: Nonlinear dynamics of COVID-19 pandemic: modeling, control, and future perspectives. *Nonlinear Dynamics* 2020, 101:1525–1526.
- [3] Radulescu A, Williams C, Cavanagh K: Management strategies in a SEIR-type model of COVID 19 community spread. *Nature* 2020, 10:21256.

Design of Auxetic Damper for Lower Limb Prosthesis

AGATA MROZEK^{1*}, TOMASZ STREK¹

1. Poznan University of Technology, Faculty of Mechanical Engineering, Institute of Applied Mechanics, Jana-Pawła II 24, 60-965 Poznan [A.M.: orcid.org/0000-0002-6684-7066, T.S.: orcid.org/0000-0002-2411-8236]

* Presenting Author; agata.mrozek@doctorate.put.poznan.pl

Abstract: Performing everyday activities can be a challenge for amputees. The usage of inappropriate prosthetic devices may cause patients to be unable to provide the foot stable ground contact. This can result in a loss of stability. Due to this fact, dampers are added to the prosthetic appliances to assist amputees' walking locomotion. They have a significant impact on the transfer of vertical ground reaction force to the lower limb joints. To increase the effectiveness of the dampers, the use of auxetic materials in their construction has been proposed. These materials, with a negative value of Poisson's ratio, could be characterized by some enhanced mechanical properties like higher vibration or energy absorption. In this study, different auxetic cells were compared in terms of damping properties. The aim of this research was to propose new application of auxetic materials in lower limb prosthetics. First, the geometry of the damper was proposed. The auxetic damper model was numerically tested for various gaits phases. The parametric study was conducted to determine optimal shape and geometrical characteristics of the auxetic structure for this purpose.

Keywords: auxetics, dampers, prosthesis, negative Poisson's ratio

1. Introduction

The phenomenon of damping is an important aspect to consider during designing lower limb prostheses. The application of inappropriate prosthetic devices may cause patients to be unable to provide the foot stable ground contact which can result in a loss of stability [1]. In prostheses, which structure does not have adequate damping properties, additional dampers should be included [2].

Materials, which possess a negative Poisson's ratio are called auxetic metamaterials [3]. This property results in unintuitive behavior — when auxetics are stretched in one direction, their structures undergo expansion in the transverse direction. During compression, the auxetic materials contract [3,4]. These materials are characterized by unique properties such as high energy absorption or indentation resistance [4]. In the study described in [5], the energy absorption capacities of auxetic re-entrant cells and non-auxetic honeycomb structures were compared. The re-entrant structure provides more advantageous damping properties. The study [6] demonstrates that auxetics structures could provide low relative density and outstanding damping properties synergistically. In this study, the unique properties of auxetic structures were used in dedicated dampers for lower limb prostheses.

2. Models and methods

In the study, a damper model was created using auxetic structures. The construction was numerically tested for different gait phases. Auxetic structures, made from materials with positive Poisson's ratio, achieve unique properties like negative Poisson's ratio via cell geometry. Two auxetic struc-

tures were investigated in the study (Fig. 1). The influence of individual geometrical features of the structures on the obtained damping properties was also investigated.

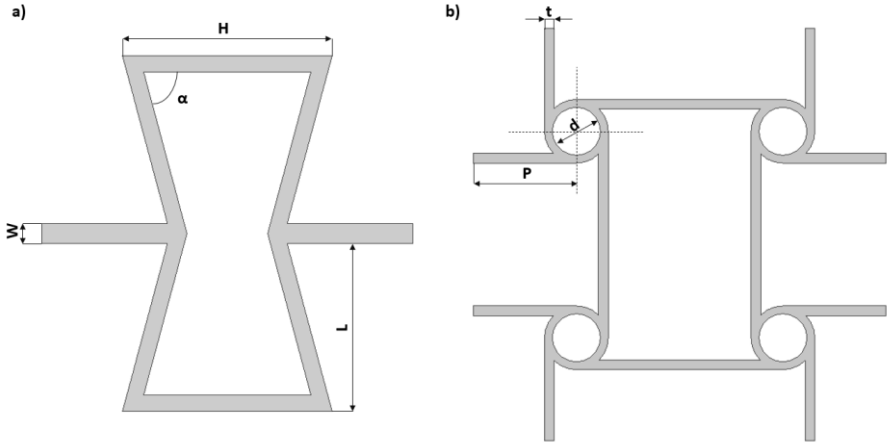


Fig. 1. Geometrical parameters of auxetic structures a) re-entrant unit cell, b) anti-tetra chiral unit cell

Acknowledgment: The work was supported by the grant 0612/SBAD/3576 funded by the Ministry of Science and Higher Education, Poland.

References

- [1] NASERI A, MOHAMMADI MOGHADDAM M, GHARINI M, AHMAD SHARBAFI M: A novel adjustable damper design for a hybrid passive ankle prosthesis. *Actuators* 2020, **9**:74.
- [2] AL-RIFAJE H, SUMELKA W: The Development of New Shock Absorbing Uniaxial Graded Auxetic Damper (UGAD). *Materials* 2019, **12**:2573.
- [3] LIM T-C: *Auxetic Materials and Structures*. Springer: Singapore, 2015.
- [4] NAJAFI M, AHMADI H, LIAGHAT G: Experimental investigation on energy absorption of auxetics structures. *Materials Today: Proceedings* 2021, **34**(1):350-355.
- [5] QI C, REMENNIKOV A, PEI L-Z, YANG S, YU Z-H, NGO T: Impact and close-in blast response of auxetic honeycomb-cored sandwich panels: Experimental tests and numerical simulations. *Composite Structures* 2017, **180**:161-178.
- [6] CHEN Y, WANG X, MA L: Damping mechanisms of CFRP three-dimensional double-arrow-head auxetic metamaterials. *Polymer Testing* 2020, **81**:106189.

Nonlinear Dynamic Model of the Oculo-Motor System Human based on the Volterra Series

VITALIY PAVLENKO¹, TETYANA SHAMANINA², VLADYSLAV CHORI^{3*}

1. Odessa National Polytechnic University [0000-0002-5655-4171]

2. Odessa National Polytechnic University [0000-0002-3857-1867]

3. Odessa National Polytechnic University [0000-0001-7823-8383]

* Presenting Author

Abstract: The biometric identification method is proposed based on the Volterra model and eye tracking data in dynamics. The instrumental computational and software tools for constructing a nonparametric nonlinear dynamic model (Volterra model) of the human oculo-motor system (OMS) were developed on the basis of data from experimental "input-output" studies using innovative eye tracking technology. The obtained multidimensional transient functions are used to build a biometric identification system for individuals.

Keywords: oculo-motor system, eye tracking, identification, nonlinear dynamic model, Volterra series

1. Introduction

Since the importance of nonlinearities in understanding the complex mechanisms of physiological functions becomes more relevant, the demand for effective and practical modelling methodologies that address the problem of nonlinear dynamics in the life sciences becomes more and more urgent [1], [2]. As a basic model for the study, a universal nonlinear dynamic model based on the Volterra integro-power series, which represents the input-output relationship of the studied physiological system, was chosen [3]. The goal is to develop computational methods and software tools for constructing a nonparametric dynamical model of the human OMS, taking into account its inertial and nonlinear properties, based on data from experimental input-output studies using test visual stimulus and innovative eye tracking technology; implementation of the obtained information models into the diagnostics practice of states' cognitive processes.

2. Results and Discussion

The study uses the identification approximation method based on the selection of the n -th partial component in the OMS response by constructing linear combinations of responses to test signals with different amplitudes [4].

Let the test signals $a_1x[m], a_2x[m], \dots, a_Nx[m]$ (N is approximation model order, a_1, a_2, \dots, a_N are different real numbers satisfying the term $|a_j| \leq 1$ for $\forall j=1, 2, \dots, N$; $x[m]$ is an arbitrary function) are successively given to the system input. Then the linear combination of the OMS responses with the coefficients c_j stands at the n -th partial component $\hat{y}_n[m]$ of the OMS response to the input signal $x[m]$.

In this case, a methodical error arises when choosing of the n -th partial component due to the partial components of the OMS response of higher orders $n > N$:

$$\hat{y}_n[m] = \hat{h}_n[m, \dots, m] = c_1^{(n)} y_{a_1}[m] + c_2^{(n)} y_{a_2}[m] + \dots + c_N^{(n)} y_{a_N}[m], \quad n = 1, 2, \dots, N, \quad (1)$$

where $y_{a_j}[m] = y(a_j\theta[m])$ – OMS response to a test signal with an amplitude a_j ; $\theta[m]$ is a unit function (Heaviside step function); $h_n[m, \dots, m]$ is a diagonal section of the discrete transition function of the n -th order

$$h_n[m, \dots, m] = \sum_{k_1, \dots, k_n=0}^m w_n[m - k_1, \dots, m - k_n] \tag{2}$$

in these parts $w_n[k_1, \dots, k_n]$ is a Volterra kernels of the n -th order; m is a discrete time variable.

To identify the OMS in the form of multidimensional transient functions according to eye tracking data, program Signal Manager was created to generate test visual stimuli on the computer monitor screen [5]. In the studies of each respondent, three experiments were sequentially carried out for the three amplitudes a_1, a_2, a_3 ($N=3$) of the test signals in the horizontal direction. Experimental studies of OMS were conducted using high-tech equipment – eye tracker TOBII PRO TX300 (300 Hz) [6].

The variability (deviation) of the transient functions average values of different orders n ($n=1,2,\dots,N$) of OMS models for $N=1,2,3$ of two individuals – the respondent #1 $\hat{h}_{1n}^{(N)}[m]$ and the respondent #2 $\hat{h}_{2n}^{(N)}[m]$ is quantified using indicators: σ_{nN} is maximum deviation, ε_{nN} is standard deviation. Indicators of transient functions deviations of different orders of n models of respondents #1 and #2 OMS for $N = 1, 2, 3$ are given in Table 1.

Table 1. The multidimensional transient functions deviation indicators

N	ε_1	σ_1	ε_2	σ_2	ε_3	σ_3
1	0.025	0.056	-	-	-	-
2	0.066	0.118	0.489	0.264	-	-
3	0.158	0.22	0.83	0.808	1.182	0.66

3. Concluding Remarks

Experimental studies of OMS were carried out for two individuals. Based on the data obtained using the eye tracker, the transition functions of the first, second and third orders of the OMS were determined. There is a significant difference between the diagonal sections of the two individuals' second and third order transition functions. Thus, they can be used to form a space of informative features and build statistical classifiers of the personality using machine learning.

References

- [1] LOHR D, GRIFFITH H, KOMOGORTSEV O: Eye Know You: Metric Learning for End-to-end Biometric Authentication Using Eye Movements from a Longitudinal Dataset. CoRR abs/2104.10489 (2021)
- [2] FRIEDMAN L, STERN H, PRICE L, KOMOGORTSEV: Why Temporal Persistence of Biometric Features, as Assessed by the Intra-class Correlation Coefficient, Is So Valuable for Classification Performance. *Sensors*, 2020, **4555**, 20(16)
- [3] DOYLE F., PEARSON R., OGUNNAIKE B.: *Identification and control using Volterra models*. Springer: Germany, 2002.
- [4] PAVLENKO V, PAVLENKO S, SPERANSKY V: Identification of Systems using Volterra Model in Time and Frequency Domain. In: HAASZ V and MADANI K (ED.) *Advanced Data Acquisition and Intelligent Data Processing*. River Publishers, 2014: 233-270
- [5] PAVLENKO V, SALATA D, DOMBROVSKYI M, MAKSYMENKO Y: Estimation of the multidimensional transient functions oculo-motor system of human. *Mathematical Methods and Computational Techniques in Science and Engineering: AIP Conf. Proc. MMCTSE*, UK, Cambridge, 2017, **1872**. Melville, New York, 2017: 110-117
- [6] PAVLENKO V, MILOSZ M, DZIENKOWSKI M: Identification of the oculo-motor system based on the Volterra model using eye tracking technology: 4th Int. Conf. on Applied Physics, Simulation and Computing (APSAC 2020) 23-25 May, Rome, Italy. *Journal of Physics: Conference Series*, 2020, **1603**, IOP Publishing: 1-8

Impact energy versus the hazards for the occupants during a front-to-side vehicles' collision

LEON PROCHOWSKI, MATEUSZ ZIUBIŃSKI^{2*}, KRZYSZTOF DZIEWIECKI³,
PATRYK SZWAJKOWSKI⁴

1. Military University of Technology (WAT), Institute of Vehicles and Transportation, ul. gen. Sylwestra Kaliskiego 2, 00-908 Warsaw, Poland; Łukasiewicz Research Network – Automotive Industry Institute (Łukasiewicz-PIMOT), ul. Jagiellońska 55, 03-301 Warsaw, Poland, leon.prochowski@wat.edu.pl [0000-0003-2093-1585]
2. Military University of Technology (WAT), Institute of Vehicles and Transportation, ul. gen. Sylwestra Kaliskiego 2, 00-908 Warsaw, Poland, mateusz.ziubinski@wat.edu.pl [0000-0003-4955-2095]
3. University of Technology and Humanities in Radom, ul. Malczewskiego 29, 26-600 Radom, Poland, krzysztof.dziewiecki@uthrad.pl [0000-0003-4734-6378]
4. Łukasiewicz Research Network – Automotive Industry Institute (Łukasiewicz-PIMOT), Electromobility Department, ul. Jagiellońska 55, 03-301 Warsaw, Poland, patryk.szwajkowski@pimot.lukasiewicz.gov.pl [0000-0003-4832-826X]

* Presenting Author

Abstract: The deformation process of the side part of the vehicle body in the culminating phase of the front-to-side vehicles' collision is considered. This is the basis for modeling the risk development process for occupants during a road accident. The danger and injuries to the occupants arise as a result of short-term dynamic loads in the culminating phase of vehicles deformation process. As a measure of these hazards, biodynamic indicators calculated from the course of acceleration and the forces acting on the occupant were adopted. During the collision, the occupant is being hit by the deforming structure of the vehicle body frequently. This phenomena significantly increases the risk of injury as a consequence of a road accident. The aim of the work is to analyse the influence of the impact energy on the occupants load in the struck vehicle during front-to-side collision. The results of inertial interactions and the vehicle body structure deformation forces were considered. The realization of the aim of the work was based on numerical research with usage of the developed front-to-side vehicles' collision model. The partial model of the interaction of the dummy with the vehicle body structure was taken into account. The performed numerical research allowed for the analysis of the relationship between the energy of a vehicle lateral impact and the dynamic loads to which the occupant is subjected.

Keywords: vehicles' collision, vehicle body deformation model, occupants injuries and safety

1. Introduction

The issue of the front-to-side vehicles' collision is being considered. In the culminating phase of the collision, hazards and injuries to the occupants arise as a result of short-term dynamic loads. The analysis of the emergence of these dynamic loads and their effects requires prior knowledge of many other processes, including the kinematics of vehicles in the collision phase and the velocity of the vehicle bodies deformation in the collision contact area. The authors of the study undertook considerations in this respect, f.e. in [1] and [2]. Particular attention was paid to model validation. Based on numerical studies, the kinematics of the side part of the vehicle body deformation process in the front-to-side vehicles' collision was determined. Dynamic deformation of the lateral part of the vehicle body is the main component of the hazard occurring process. A frequent phenomenon accompanying this deformation is the impact of the occupant by the deforming structure of vehicle body (Fig. 1).

The aim of the study is to analyze the influence of the lateral vehicle impact energy on the occupant's load. This influence is assessed, among others, by on the basis of biomechanical indicators, which are the basis for an inference about the risk of human injury as a result of a road accident.



Fig. 1. Occupant's impact by side structure of the vehicle body deforming during the front-to-side cars crash test; frames every 0.02 s from the beginning of the collision contact [3]

2. Research methods and results

The numerical research were carried out with the usage of the developed model of the front-to-side vehicles' collision. The model was presented in [1] and in [2]. The interaction of the dummy with the deforming structure of vehicle body was included. The model of dynamic interaction between dummy and the vehicle is shown in Figure 2.

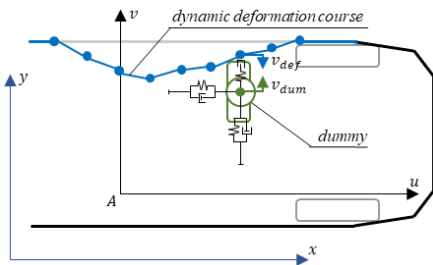


Fig. 2. Model of the interaction between the vehicle and the dummy

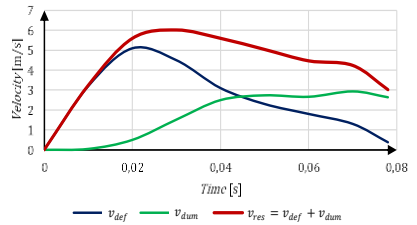


Fig. 3. Research results as velocity courses: the vehicle body deformation in the occupant's seat area v_{def} , the dummy v_{dum} and the dummy's impact in the deforming structure of the vehicle body v_{res}

Figure 3 shows an example of the numerical research results as the course of the vehicle body deformation velocity and the velocity of the dummy's movement towards the deforming structure of the vehicle body. This reveals the resultant velocity at which the dummy strikes by the vehicle body. In the event of the vehicle lateral impact with a velocity of approx. 13 m/s, the dummy collides with the deforming vehicle body structure with a velocity of approx. 6 m/s. On this basis, the occupant impact energy in relation to the initial velocity of the front-to-side vehicles' collision was concluded and the occupant risk of injury was predicted.

References

- [1] Prochowski L., Gidlewski M., Ziubinski M., Dziewiecki K., (2019) *The kinematics analysis of the body deformation process during frontal and lateral collision according to the FMVSS 214 procedure and classical test.* Conference Paper. Abstracts, 15th Conference Dynamical Systems Theory and Applications, DSTA 2019, Lodz, 2019.
- [2] Prochowski, L., Gidlewski, M., Ziubiński, M. et al. *Kinematics of the motorcar body side deformation process during front-to-side vehicle collision and the emergence of a hazard to car occupants.* Meccanica 56, 901–922 (2021). <https://doi.org/10.1007/s11012-020-01274-3>
- [3] National Highway Traffic Safety Administration. Vehicle Crash Test Database, www.nhtsa.gov/research-data/databases-and-software

Predicting Future from COVID-19 Time Series Data Using Polynomial Extrapolation

AJAY MANDYAM RANGARAJAN^{1*}, JEYASHREE KRISHNAN², ANDREAS SCHUPPERT³

1. AICES Graduate School, RWTH Aachen University, Aachen, Germany [0000-0002-1209-7909]
- 2, 3. Joint Research Center for Computational Biomedicine (JRC-Combine), RWTH Aachen University, Aachen, Germany [0000-0003-3355-0415], [0000-0003-3783-6605]

* Presenting Author

Abstract:

We propose a method to analyze small data coming out of the pandemic, particularly at region level. Standard data-driven approaches may be insufficient to predict the immediate future on small data. Here we propose a reliable numerical method based on polynomial projection and extrapolation that can estimate the true number of cases everyday based on the past data for very small times series datasets. The proposed method relies on smoothing out small-scale variations using moving averages, followed by cubic spline interpolation to move from discrete to continuous representation of the data followed by polynomial projection and extrapolation for prediction. The key to this numerical extrapolation relies on chunking the time series into train, benchmark and predict slices wherein different polynomial orders are allowed to train, the best fit is picked during benchmark. This method operates on fewer than 100 data points to train, fit and predict the immediate future with a dynamic moving window method that boosts the robustness of the prediction. This method is in principle, applicable for learning on any other (small) time series data.

Keywords: Polynomial Projection, Vandermonde Matrix, Chebyshev Nodes, Time Series Extrapolation, Small Data

1. Introduction

The ongoing Coronavirus (SARS-Cov-2) pandemic is now a global crisis that has already caused more than 3.3 million deaths worldwide (as of 20th May 2021), with health implications to tens of millions of people and economic fallout around the world. There has been a spike in research related to the virus and in particular, in the areas of modeling epidemic spreading and prevention. Apart from the well-established epidemic models, deep learning based methods and graph based machine learning methods have been commonly used to develop heuristics to stop epidemic or to identify patient zero [4][5][6][7]. However, much of the data coming out of the pandemic including daily new cases or deaths, particularly at region level, are not sufficient to use these approaches to predict the immediate future. It can be expected that future predictions on time series data with few data points is challenging. In this work, we propose a reliable numerical method that can estimate the true number of cases everyday based on the past data. We illustrate the method using the data obtained from the Robert Koch Institute (RKI) for incidences reported in the Aachen area, Germany [3].

2. Results and Discussion

Given cumulative COVID data for cases vs days we can construct cubic splines between each day. Such a spline reconstruction ensures continuity in the function and first and second derivatives [1]. We approximate the function by a polynomial of order k for which we require a set of $k+1$ points, where the value of the polynomial is *exactly* the same as the function. Substituting the set of points

into polynomial equation on can construct the *Vandermonde matrix*. This system could be ill-conditioned for high n and one could also encounter the issue of Runge’s phenomenon if one uses equidistributed datapoint to alleviate this we use the *Chebyshev nodes* to compute the points [2]. Now the given dataset can now be split into train (Fig. 1(B)), benchmark (Fig. 1(C)) and test (Fig. 1(F)) chunks. The benchmark is used to find the best fit polynomial order n^* in an L2 sense. As we can see from Fig. 1(C), each of the polynomial order predicts differently and allowed to show the future trajectories. Based on the relative error computed from this benchmark set, the top three best predicting polynomial orders were identified. With this, we do a two-day window moving prediction and estimate the number of cases expected in Aachen, Germany in the next week to be 2109 as can be seen in Fig. 1(E) (true number of cases being 1675). With this reliable prediction, we make unknown prediction for the near future (Fig 1. (F)). An implementation of this method is available to be published open source.

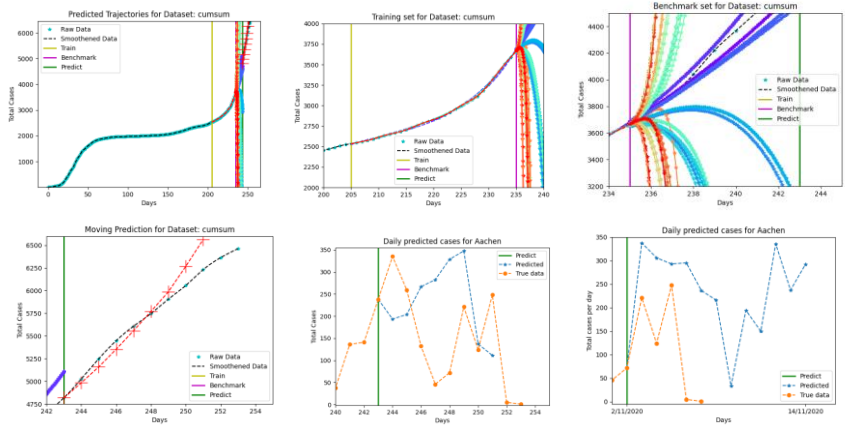


Fig. 1. Predicting Future from COVID-19 RKI Time Series Data for Aachen, Germany using Polynomial Extrapolation, period in days. Curves of different colors indicate predictions from different polynomial order, $n \in [3, 20]$: Top Left Subfigure (A) shows the complete time series window including training chunk, benchmark chunk and predict chunk. Top center subfigure (B) shows the training chunk period [205, 235]. Top right subfigure (C) shows the benchmark chunk where the best polynomial order is identified with true data as reference. Bottom left subfigure (D) shows the predict chunk [243, 251] where prediction happens two days at a time. Bottom center subfigure (E) compares the predicted test over a 8 day time interval (2109 cases) to true number of cases over the 8 days (1675 cases). Bottom right subfigure (F) shows the unknown future prediction for the next 12 days

3. Concluding Remarks

We have proposed a method here that promises reliable prediction of future from small time series data such as that of COVID-19 infection statistics obtained locally. The method operates on fewer than 100 data points to train, fit and predict the immediate future. A dynamic moving window method is used at small time steps to make robust predictions. This method is in principle, applicable for learning on any other time series data.

Acknowledgment: The authors would like to thank Pejman Farhadi for the support in handling the RKI data.

References

1. R. H. Bartels, J. C. Beatty, and B. A. Barsky. An Introduction to Splines for Use in Computer Graphics and Geometric Modeling. Morgan Kaufmann Series in Computer Graphics and Geometric Modeling. Elsevier Science, 1995.
2. John P. Boyd and Fei Xu. Divergence (Runge Phenomenon) for Least-Squares Polynomial Approximation on an Equispaced Grid and Mock-Chebyshev Subset Interpolation. In Applied Math. Comput. 210. 1 (2009)
3. Robert Koch Institute (RKI) COVID-19 Pandemic Database, https://www.rki.de/EN/Home/homepage_node.html
4. Gihan Chanaka Jayatilaka et al. Use of Artificial Intelligence on Spatio-Temporal Data to Generate Insights During COVID-19 Pandemic: A Review. MedRXiv (2020)
5. Eli A. Meirom et al. How to Stop Epidemics: Controlling Graph Dynamics with Reinforcement Learning and Graph Neural Networks (2020)
6. Chintan Shah et al. Finding Patient Zero: Learning Contagion Source with Graph Neural Networks. arXiv:2006.11913 (2020)
7. Afshin Shoeibi et al. Automated Detection and Forecasting of COVID-19 using Deep Learning Techniques: A Review. arXiv: 2007.10785v3 (2020)

Heart rate effects on intracranial aneurysm hemodynamic.

DJALAL SEKHANE^{1,3}, KARIM MANSOUR^{2,3}

1. Faculty of technology, electrical engineering department, University 20 august 1955 Skikda [https://orcid.org/0000-0002-4458-9713]
2. Faculty of medicine Constantine, university Constantine 3- chalet des pins, Constantine.
3. Laboratory of Electronic Materials Study for Medical Applications – Brothers Mentouri University – Constantine 1- Algeria.

Abstract: The hemodynamic is a biomechanical factor influencing the development of different forms of vascular diseases, especially intracranial aneurysms, in where hemodynamic factors influence strongly their genesis, growth, and rupture. The purpose of this study is to assess the influence of the Heart rate (HR) variation on different hemodynamic parameters inside intra-aneurysmal circulation, using computational fluid dynamics combined with patient-specific MRI images. By the variation of the HR, we observed disturbance of the overall hemodynamic parameters assessed on the geometry. The increase of the HR allowed observing de disturbance of the association between flow and pressure inside the aneurysmal sac. The intra-aneurysmal flow is highly influenced by the feeding inlet frequency, which may cause growth or in the extreme case, the rupture of the aneurysm.

Keywords: Intracranial aneurysms, Hemodynamics, flow, pressure.

1. Introduction.

Intracranial aneurysms (IA) are abnormal bulging or a focal dilatation located on cerebral arteries, frequently found in the bifurcations of the circle of Willis (CoW). The exact mechanism of the IA prevalence is still unknown; however, the physical cause can be described as a decrease of the middle muscular resistance of the artery involving a structural defect and localized weakness of the vessel wall. It is known that hemodynamic influences the development of different forms of vascular diseases [1], especially (IAs), where the hemodynamic environment influences strongly their genesis, growth, and rupture [2]. Therefore, knowledge of hemodynamic factors becomes very important. This work aims to investigate the effect of the heart rate (HR) on hemodynamics parameters inside IA. We focused on two parameters, which are: inlet-intra-aneurysmal delay and pressure-flow shift.

To study the HR effect on the hemodynamic factors cited above we have performed Time Of Flight (TOF) Magnetic Resonance Angiography (MRA) with GE HDxt system (General Electric Healthcare). The 3D patient-specific aneurysm model is obtained by gathering the MRA images and truncated using the software 3DSlicer (www.slicer.org). Fig. 1 represents a patient-specific aneurysm of 52 years female located in the internal carotid artery (ICA). Inside the obtained geometry, the blood flow behaviour can be described by unsteady Navier-Stokes equations for an incompressible fluid. We performed 27 simulations using rescaled volumetric flow rate (inlet) and pressure (outlet). Further, three pulses were used to ensure results stability.

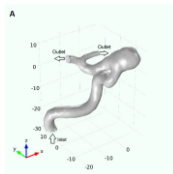


Fig. 1. Patient specific ICA aneurysm.

2. Results and Discussion

Varying the HR, we observed a delay between the intra-aneurysmal flow and the inlet flow rate (IFD). This delay can be quantified using the following formula: $IFD=(T_{PS}-T_{MIF})/CD$.

Where T_{PS} and T_{MIF} are the temporal positions respectively of the systolic peak and the maximum intra-aneurysmal flow. CD is the cycle duration.

By the variation of the HR, the IFD varies between 2.87 and 4.21% with a mean delay of $(3.56\pm 0.42)\%$ (fig 2.a). Furthermore, the IFD increases linearly with the HR according the following equation:

$$IFD=0.049.HR-0.28 /r^2=0.86$$

In addition, we observed a shift between the flow and the pressure in the intra-aneurysmal is noted. The pressure-flow shift (PFS) can be calculated by :

$$FPS=(T_{Mip}-T_{MIF})/CD.$$

Where T_{Mip} is the instant of the maximum of the pressure inside the aneurysmal dome.

By varying the HR, the PFS varies from 0.98 to 3.25% with a mean shift of $(1.71\pm 0.55)\%$. Furthermore, it presents a linear increasing with the HR (fig 2.b). These variations are given by the following equation:

$$PFS=0.048.HR-2.13 /r^2=0.81$$

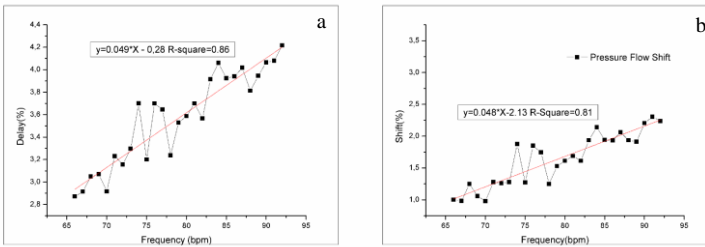


Fig. 2. a) delay between Inlet and the intra-aneurysmal flows. b) intra-aneurysmal pressure flow shift

Inside normal arteries, the relation between the pressure and the flow waves, taking into account the reflected pressure waves, is opposite [3]. The presence of an aneurysm can affect the hemodynamic factors inside the vessel. A. Sorteberg et al. [4] have found a pressure-flow shift in the aneurysmal dome by varying the HR. However, this can cause an alteration of the pressure inside the vessel and creates a new pressure of stability [5,6]. Our results, obtained by the HR variation, show that pressure value disturbance is a sign of a loss of the pressure-flow equilibrium, causing fluctuations of pressure inside the aneurysmal dome and the feeding vessels. In addition, the numerical simulations of blood flow inside the aneurysm allowed the quantification of the pressure-flow shift and revealed its linear dependence on the feeding frequency. The flow structure inside the IA not only depends on the size and the shape of the aneurysmal dome but also on how the aneurysm is feed [6]. Therefore, increasing inlet frequency may cause unfavorable blood circulation inside the aneurysm. The increase of the blood stagnation disturbs the flow inside the aneurysm and affects the different hemodynamic factors inside the aneurysmal dome and the parent arteries.

[1] Westerhof N, Stergiopulos N, Noble MI. Snapshots of hemodynamics: an aid for clinical research and graduate education: Springer Science & Business Media; 2010.

[2] Tanoue T, Tateshima S, Villablanca J, Viñuela F, Tanishita K. Wall shear stress distribution inside growing cerebral aneurysm. American Journal of Neuroradiology. 2011;32(9):1732-7.

[3] Salvi P. Pulse waves. How vascular hemodynamics affects Blood pressure. 2012.

[4] Sorteberg A, Sorteberg W, Aagaard BD, Rappe A, Strother CM. Hemodynamic versus hydrodynamic effects of Guglielmi detachable coils on intra-aneurysmal pressure and flow at varying pulse rate and systemic pressure. American Journal of Neuroradiology. 2004;25(6):1049-57.

[5] Austin GM, Schievink W, Williams R. Controlled pressure-volume factors in the enlargement of intracranial aneurysms. Neurosurgery. 1989;24(5):722-30.

[6] Harders AG. Intra-aneurysmal Flow Pattern. Neurosurgical Applications of Transcranial Doppler Sonography: Springer; 1986. p. 72-7.

Power Bounded and Uniformly Mean Ergodic Composition Operators on Large Class of Fock Spaces

WERKAFERAHU SEYOU^{*1}, TESFA MENGESTIE², AND JOSÉ BONET³

1. Mathematics Department, Kotebe Metropolitan University
E-mail address: Werkaferahus@gmail.com. [<https://orcid.org/0000-0002-6035-9440>]
2. Mathematics Section, Western Norway University of Applied Sciences, Klin-genbergvegen 8, N-5414 Stord, Norway. E-mail address: Tesfa.Mengestie@hvl.no.
3. Universitario de Matematica Pura y Aplicada, Universitat Polit_tecnica de Valencia, Spain
E-mail address: jbonet@mat.upv.es

* Presenting Author

Abstract: For a given holomorphic mapping ψ and f on a complex plane \mathbb{C} , composition operator induced by ψ is defined by $C_\psi f = f \circ \psi$. Composition operator C_ψ acting on Fock spaces $F_\phi^p, 1 \leq p < \infty$ generated by weights ϕ satisfying $\limsup_{|z| \rightarrow \infty} \phi(z) = \infty$ is bounded if and only if $\psi(z) = az + b, |a| \leq 1$ and $b = 0$ whenever $|a| = 1$. We have shown that every bounded composition operator acting on the Fock spaces $F_\phi^p, 1 \leq p < \infty$ is power bounded. Mean ergodic and uniformly mean ergodic composition operators on the spaces are also characterized.

Keywords: Composition operators, Fock spaces, power bounded operator, mean ergodic operator, uniformly mean ergodic operator.

1. Introduction

Given an entire function on the complex plane \mathbb{C} , the composition operator induced by ψ is defined by $C_\psi f = f \circ \psi$ for each entire function f . The study of composition operators acting between spaces of analytic functions defined on the disc or on the complex plane has quite a long and rich history. Many properties of composition operators on spaces of entire functions have been also investigated. In the frame of Fock spaces, Carswell, MacCluer and Schuster [1], Guo and Izuchi [2], and first two authors [4, 3] characterized bounded and compact composition operators on the Fock spaces

$F_\phi^p, 1 \leq p < \infty$. They showed that only the class of linear $\psi(z) = az + b, |a| \leq 1$ and $b = 0$ whenever $|a| = 1$ induces bounded composition operators, when $\limsup_{|z| \rightarrow \infty} \phi(z) = \infty$. Compactness of the composition operator was described by the strict requirement $|a| < 1$.

We recall some definitions. Let $\phi: [0, \infty) \rightarrow [0, \infty)$ be a twice continuously differentiable function.

We extend ϕ to the whole complex plane by setting $\phi(z) = \phi(|z|)$.

The generalized Fock spaces F_φ^p , $1 \leq p < \infty$ associated with φ are the spaces consisting of all entire functions f such that

$$\|f\|_{(\varphi,p)} = \left(\int_C |f(z)|^p e^{-p\varphi(z)} dA(z) \right)^{1/p} < \infty,$$

Where dA denotes the usual Lebesgue area measure on the space of complex plane C .

Let X be a Banach space, and T a bounded operator acting on X . We denote the n -th ergodic mean T_n by

$$T_n := \sum_{m=1}^n T^m.$$

T is said to be power bounded if $\sup_{n \in \mathbb{N}} \|T^n\| < \infty$. We say that T is mean ergodic if there exists a

bounded operator P on X such that for every f in X ,

$$\lim_{n \rightarrow \infty} \|T_n f - P f\| = 0,$$

and uniformly mean ergodic if the above point-wise convergence is uniform.

In this paper we have characterized some dynamical properties of composition operators: power bounded, mean ergodic, and uniformly mean ergodic composition operators on Fock spaces when

$$\limsup_{|z| \rightarrow \infty} \varphi(z) = \infty.$$

2. Results

We state the main result of our paper as follows.

Theorem 2.1. Let C_ψ be a bounded composition operator on Fock space F_φ^p , $1 \leq p < \infty$ with $\limsup_{|z| \rightarrow \infty} \varphi(z) = \infty$. Then

- (1) C_ψ is power bounded.
- (2) If $\psi(z) = az + b$: $|a| < 1$, then C_ψ is uniformly mean ergodic.
- (3) If $\psi(z) = az + b$: $|a| = 1$ and a is a root of the unity, then C_ψ is uniformly mean ergodic.
- (4) If $\psi(z) = az + b$: $|a| = 1$ and a is not a root of the unity, then C_ψ is mean ergodic but not uniformly mean ergodic.

References

[1] B. J. Carswell, B. D. MacCluer, A. Schuster, Composition operators on the Fock space. Acta Sci. Math. (Szeged), 69, 871{887 (2003).

[2] K. Guo, K. Izuchi, composition operators on Fock type space, Acta Sci. Math. (Szeged), 74, 807{828 (2008).

[3] T. Mengestie, W. Seyoum, Spectral Properties of Composition Operators on Fock-Type Spaces, Quaestiones Math. <https://doi.org/10.2989/16073606.2019.1692092> (2019)

[4] T. Mengestie, W. Seyoum, Topological and dynamical properties of composition operators, Complex Analysis and Operator Theory <https://doi.org/10.1007/s11785-019-00961-8> (2020)

[5] W. Seyoum, T. Mengestie, J. Bonet, Mean ergodic composition operators on generalized Fock space, RACSAM, <http://doi.org/10.1007/s13398-019-00738-w> (2019)

Bifurcations in inertial focusing of particles in curved rectangular ducts

RAHIL VALANI^{1*}, BRENDAN HARDING², YVONNE STOKES¹

1. School of Mathematical Sciences, University of Adelaide, South Australia, Australia

2. School of Mathematics and Statistics, Victoria University of Wellington, New Zealand

* Presenting Author

Abstract: Motion of particles suspended in a fluid flow is governed by hydrodynamic forces acting on the particle from the surrounding flow. In particular, the inertial lift force may cause particles to deviate from the streamlines of the background fluid flow. This was first demonstrated in the classical experiment of Segré & Silberberg [1] where particles suspended in flow through a straight pipe with a circular cross-section were observed to migrate to an annular region approximately 0.6 times the radius of the pipe. The phenomenon of inertial migration has found many applications in medical and industrial settings such as isolation of circulating tumour cells, separation of particles and cells, bacteria separation, cell cycle synchronization and identification of small-scale pollutants in environmental samples [2,3].

Harding et al. [4] developed a general asymptotic model for forces that govern the motion of a spherical particle suspended in a fluid flow through a curved duct and used it to investigate the inertial migration of a neutrally buoyant spherical particle suspended in flow through curved ducts with square, rectangular and trapezoidal cross-section. They identified stable and unstable equilibrium points in the cross-section of the duct which vary with the cross-section geometry, the bend radius of the duct and particle size. Moreover, they showed that for low flow rates, the lateral focusing position of particles approximately collapses with respect to a dimensionless variable κ that is dependent on particle radius, duct height and duct bend radius.

In this talk, I will present the results of our detailed investigation of the various bifurcations that take place in a curved rectangular duct as a function of the bend radius, particle size and the aspect ratio of the rectangular cross-section. We have used the asymptotic model of Harding et al. [4] as well as a reduced order model for small particles to investigate the dynamics and bifurcations of particles. The reduced order model is a system of nonlinear coupled ODEs with a single parameter κ . This simplified model allows us to analytically investigate the stability and bifurcations. Using this reduced order model, we have been able to analytically solve for the equilibrium points and its linear stability for the limiting cases of very large and very small bend radius of the curved duct. Exploration of numerical solution of the reduced model as a function of κ results in rich dynamical behaviour and a large variety of bifurcations. For relatively large bend radius, we observe the existence of several fixed points. These include stable nodes, unstable nodes and saddle points. As the bend radius is progressively decreased, several bifurcations take place for these fixed points such as saddle-node, pitchfork and Hopf bifurcations. At relatively small bend radius, either a stable spiral or an unstable spiral with a limit cycle remains along with one saddle point. Implications of these results for particle separation will also be discussed.

Keywords: Inertial microfluidics, Inertial migration, Inertial lift, Bifurcations, particle/fluid flow

Acknowledgment: This research is supported under an Australian Research Council's Discovery Project funding scheme - DP200100834.

References

- [1] SEGRE G, SILBERGERG A: Radial particle displacements in Poiseuille flow of suspensions. *Nature* 1961, **189**:209-210.
- [2] ZHANG J, YAN S, YUAN D, ALICI G, NGUYEN N, WARKIANI M, LI W: Fundamentals and applications of inertial microfluidics: a review. *Lab Chip* 2016, **16**:10-34.
- [3] MARTEL J, TONER M: Inertial focusing in microfluidics. *Annual Review of Biomedical Engineering* 2014, **16**:371-396.
- [4] HARDING B, STOKES Y, BERTOZZI A: Effect of inertial lift on a spherical particle suspended in flow through a curved duct. *Journal of Fluid Mechanics* 2019, **875**:1-43.

Interaction of Mucin with Glycosaminoglycans in Water Environment

PIOTR WEBER^{1*}, PIOTR BELDOWSKI^{2A}, ADAM GADOMSKI^{2B}, KRZYSZTOF DOMINO³,
DAMIAN LEDZIŃSKI⁴.

1. Gdańsk University of Technology, Faculty of Applied Physics and Mathematics, Institute of Physics and Computer Science, Department of Atomic, Molecular and Optical Physics, Gdańsk, Poland [0000-0002-9405-5461]
2. Institute of Mathematics and Physics, UTP University of Science and Technology, Bydgoszcz, Poland ^A[0000-0002-7505-6063], ^B[0000-0002-8201-1736]
3. Institute of Theoretical and Applied Informatics, Polish Academy of Sciences, Poland [0000-0001-7386-5441]
4. Faculty of Telecommunications, Computer Science and Technology, UTP University of Science and Technology, Bydgoszcz, Poland [0000-0003-0796-4390]

* Presenting Author

Abstract: We present a study of the interaction between mucin and several glycosaminoglycans. These molecules are a compound of extracellular matrix in the articular cartilage and play a significant role in the lubrication phenomenon. We use molecular docking numerical experiments that allow to describe the interaction between one mucin molecule and one selected glycosaminoglycan molecule. As a result, we obtain binding energy, hydrogen bonds, and hydrophobic contacts between two molecules. For one pair of molecules we can generate several values of one above-mentioned property and use a statistical methods to compare this property between pairs.

Keywords: glycosaminoglycans, mucin, biolubrication, molecular docking method

1. Introduction

The joint organ surfaces are covered by articular cartilage (AC) and separated by a thin layer of synovial fluid (SF). The SF of the joints organ functions as a biological lubricant. It provides low-friction and low-wear properties to articulating cartilage surfaces. This property is due to the synergistic interaction between high molecular weight molecules in an aqueous solution which build SF and extracellular matrix of AC. These components are secreted by cells: chondrocytes in the AC and synoviocytes in the synovium. One of the components of the extracellular articular cartilage matrix is complexes of mucin with glycosaminoglycans (GAGs). GAGs are linear polysaccharides, which are highly polar and water-soluble. Mucin is a heavily glycosylated protein, which can form gels. In Fig.1, we present some GAGs.

Many theories and dynamical models are contributing to the lubrication phenomenon in AC due to SF. But there are not many studies that conclusively describe the nanoscopic function of components of SF and extracellular articular cartilage matrix [1]. This work, like our previous works [2], is a step towards analysis biolubrication processes at the nanoscopic level under physiological conditions.

2. Results and Discussion

Our calculation suggest that that there are some significant differences between chemical affinity in the pair of molecules: mucin and one GAG – Fig.1. In Fig. 2 graphical visualisation of interaction.

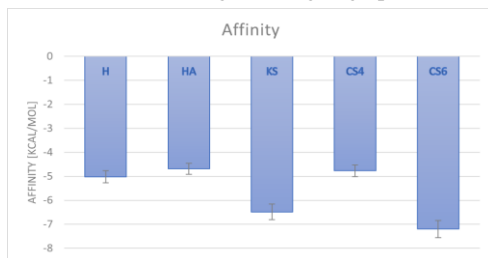


Fig. 1. Affinity between mucin and selected GAGs. Hyaluronic acid (HA), chondroitin sulfate-4 (CS4), chondroitin sulfate-6 (CS6), keratan sulphate (KS) and heparin (H).

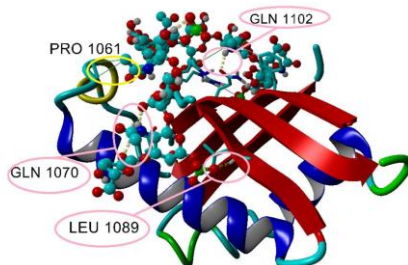


Fig. 2. Visualization of interactions between one selected GAG and mucin: a) hydrogen bonds (yellow dotted lines); b) hydrophobic contacts (green lines).

3. Concluding Remarks

Our results imply that binding between GAGs and mucin is more robust than those present in the synovial fluid (SF), i.e., all but heparin. SF is a natural lubricant that contributes to an extremely low friction coefficient. Main finding: chondroitin sulfate 6 has the highest affinity to mucin. As the ratio between CS4:CS6 changes with age in synovial fluid, this may result in frictional properties of lubricin. Namely, different hydration of the complex and hydration repulsion may not be as efficient. The current consensus among scientists studying the subject is that efficient lubrication results from synergy between SF components.

References

- [1] GADOMSKI A, BELDOWSKI P, RUBI J M, URBANIAK W, AUGÉ II W K, SANTAMARIA-HOLEK I, PAWLAK Z: Some conceptual thoughts toward nanoscale oriented friction in a model of articular cartilage. *Mathematical Biosciences* 2013, **244**, 188–200.
- [2] BELDOWSKI P, WEBER P, DEDINAITE A, CLAEISSON P, GADOMSKI A: Physical crosslinking of hyaluronic acid in the presence of phospholipids in an aqueous nano-environment. *Soft Matter* 2018, **14**, 8997-9004.

Correlation of Biomechanic Performace Measures with Acceleration and Deceleration in Human Overground Running

LILIÁNA ZAJCSUK^{1*}, AMBRUS ZELEI²

1. Budapest University of Technology and Economics [0000-0003-3198-0526]

2. MTA-BME Research Group on Dynamics of Machines and Vehicles [0000-0002-9983-5483]

* Presenting Author

Abstract: Biomechanics of human running has been researched by many scientists over the last decades. However, there are still open questions, especially about the role and operation of the central nervous system. Obviously, a certain optimization process, which employs a combination of possibly time variant cost functions, makes adaptation possible to the changing conditions. Our long-term goal is the understanding of these processes based on experimental evidences. Narrowing down this mighty problem, we focus on the exploration of the changes in kinematics, related to well-defined cost functions, such as energy dissipation, energy conservation or energy accumulation. These cost functions are in analogy with deceleration, constant speed locomotion and acceleration. Hence, we collected measurement data of eight athletes with five different tasks: 1) slow, 2) moderate, 3) high speed running, 4) acceleration and 5) deceleration. We identified the biomechanics performance measures from the literature that are in statistically proven correlation with the cost functions. Wilcoxon signed-rank test indicated the most significant difference in the relative and absolute angles, total force, angular velocity and distance between the centre of pressure and centre of mass in case of different cost functions.

Keywords: human running, biomechanics, acceleration, deceleration, gait optimization

1. Introduction

Scientific papers exuberate in measurement data related to acceleration in the stance phase [1, 2]. However, the literature lacks of analyses for deceleration, and particularly for the airborne phase. Thus, we collected new data related to varying speed locomotion. Eight non-professional athletes were observed while they were performing five different tasks. The kinematics was recorded by OptiTrack optical motion capture system, and we used Moticon Science Insoles to assess the foot pressure distribution. Metrics characterizing the locomotion were calculated from the raw data, including the joint/segmental angles, centre of pressure position and ground reaction force components.

2. Results and Discussion

The metrics $m_i(t)$, such as segmental angles and force data were stored as time functions. The scalar measures at phase-transitions and extremes were extracted: $m_i(t_{IC})$ at initial contact, $m_i(t_{TO})$ at toe off, $\max(m_i(t))$ and $\min(m_i(t))$. The average and the confidence interval (significance level $p=0.95$) were calculated to visualize the data. The most used visualization techniques are collected in Fig. 1. Wilcoxon signed-rank test was used to identify the metrics, based on which the cost-functions could be identified. According to the Wilcoxon signed-rank test, there is a significant difference in case of

the relative and absolute segment angles, total force, angular velocity of the foot and distance between the centre of pressure and centre of mass.

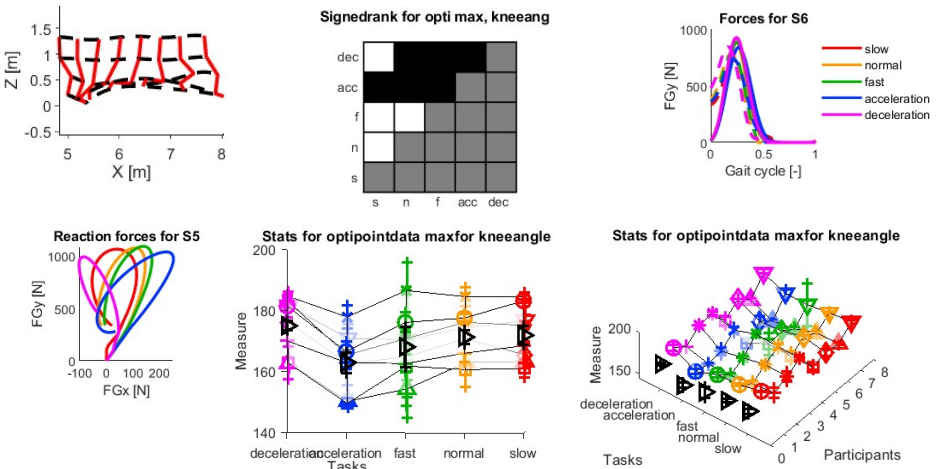


Fig. 1. Tools for data comparison and statistics: stroboscopic visualization of the motion (top left panel); matrix plot of the signed-rank test, where black / white tiles indicate significant difference / not proven difference for each scalar measure (top middle panel); measured and inverse dynamics calculated vertical ground reaction force (solid and dashed lines on the top right panel respectively); path of the ground-reaction force vector [1] (bottom left panel); confidence intervals for each task in case of each scalar measure (bottom middle panel); confidence intervals for each task and each subject in case of each scalar measure (bottom right panel).

3. Concluding Remarks

Metrics, which are already introduced in the literature, were used to observe quantitative changes between different cost functions in case of different velocities, acceleration or deceleration. These results allow us to create predictive models of human gait and kinematics reproduction. Functional role and movement strategy of each joint would be identified [2, 3] and included into the models in future work.

Acknowledgment: The research reported in this paper and carried out at BME has been supported by the NRDI Fund (TKP2020 IES, Grant No. BME-IE-BIO and TKP2020 NC, Grant No. BME-NC) based on the charter of bolster issued by the NRDI Office under the auspices of the Ministry for Innovation and Technology and by the Hungarian National Research, Development and Innovation Office (Grant no. NKFI-FK18 128636).

References

- [1] VAN CAEKENBERGHE I, SEGERS V, AERTS P, WILLEMS P, DE CLERCQ D: Joint kinematics and kinetics of overground accelerated running versus running on an accelerated treadmill. *Journal of The Royal Society Interface* 2013, **10**(84): 20130222.
- [2] FARRIS DJ, RAITERI BJ: Modulation of leg joint function to produce emulated acceleration during walking and running in humans. *Royal Society Open Science* 2017, **4**(3): 160901.
- [3] JIN L, HAHN ME: Modulation of lower extremity joint stiffness, work and power at different walking and running speeds. *Human Movement Science* 2018, **58**: 1-9.

-MAT-

**MATHEMATICAL
APPROACHES
TO DYNAMICAL SYSTEMS**

Thermal waves in composite membrane with circular inclusions in hexagonal lattice structures

I.V. ANDRIANOV^{1*}, J. AWREJCWICZ¹, G.A. STARUSHENKO^{3A}, S.A. KVITKA^{3B}

1. Chair and Institute of General Mechanics, RWTH Aachen University, Eilfschornsteinstraße 18, D-52062 Aachen, Germany [0000-0002-2762-8565]
 2. Lodz University of Technology, Department of Automation, Biomechanics and Mechatronics, Lodz, Poland [0000-0003-0387-921X]
 3. Dnipropetrovs'k Regional Institute of State Management of National Academy of State Management at the President of Ukraine, Dnipro, Ukraine A[0000-0003-4331-4723], B[0000-0003-3786-9589]
- * Presenting Author

Abstract: Non-stationary heat conduction in the fibre composite materials is studied. 2D composite media consists of matrix with circular inclusions in hexagonal lattice structures. The perfect contact between different materials is assumed on the boundary of the fibres. The local temperature field in the unit cell is modeled by the heat equation. Time variable excludes from the original boundary value problem using of Laplace transform. Asymptotic homogenization method allows to reduce original problem for multiply-connected domain to the sequence of boundary value problems in simply-connected domains. Composite material is supposed densely-packed with a high-contrast. In this case, the local boundary value problem includes a small parameter equal to the ratio of the distance between the inclusions to the characteristic cell size. Using of additional small parameter and thin layer asymptotics allows to solve local problem analytically. Closed form expression for effective heat conductivity is obtained.

Keywords: Unsteady heat conduction, fibre composite, effective conductivity, Laplace transform, homogenization approach.

1. Introduction

Problem of non-stationary heat transfer in composite media have attracted the attention of researches due to the wide occurrence of the media in engineering applications. As a rule, we are talking about determining the effective characteristics of the considered inhomogeneous material. For this purpose phenomenological and experimental approaches, mixture theory, self-consistent approximation are used. It is natural to use the asymptotic homogenization method (AHM) to solve the described problem. Allaire and Habibi [1] used AHM to the heat conduction problem in a periodically perforated domain with a nonlinear and nonlocal boundary condition modeling radiative heat transfer in the perforations. In 2D case cell problem is solved numerically. AHM with FEM in many cases allow one to obtain numerically effective characteristics and local fields [2], and construct boundary layer correctors [3]. The analytical solution of the problem on a cell requires the use of additional small parameters. Small parameters typical of low-contrast composites or composites with small volume fraction of inclusions are widely used [4,5]. In our work, an analytical solution for densely-packed high-contrast composite is obtained with a help of thin layer asymptotics [6].

2. Results and Discussion

We consider the problem of nonstationary heat transfer in a composite with periodically distributed inclusions of a circular cross section which are placed in regular hexagonal cells (Fig. 1). We take Newton's law of cooling for matrix and inclusions, $T^\pm = T_c^\pm(x, y)\exp(-\gamma t)$.

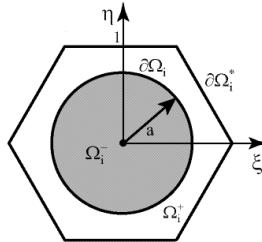


Fig. 1. Structure of the composite cell.

The original eigenvalue problem can be formulated in the following way

$$\begin{aligned}
 k_+ \left(\frac{\partial^2 T_c^+}{\partial x^2} + \frac{\partial^2 T_c^+}{\partial y^2} \right) &= -c_+ \rho_+ \gamma T_c^+ \quad \text{in } \Omega_i^+, & k_- \left(\frac{\partial^2 T_c^-}{\partial x^2} + \frac{\partial^2 T_c^-}{\partial y^2} \right) &= -c_- \rho_- \gamma T_c^- \quad \text{in } \Omega_i^-, \\
 T_c^+ &= T_c^-, & k_+ \frac{\partial T_c^+}{\partial \mathbf{n}} &= k_- \frac{\partial T_c^-}{\partial \mathbf{n}} \quad \text{at } \partial \Omega_i, & T_c^\pm &= 0 \quad \text{at } \partial \Omega.
 \end{aligned}
 \tag{1}$$

Using the AHM and thin layer asymptotics [6] for the analytical solution of the cell problem, we obtain the homogenized boundary value problem in the following form:

$$q \left(\frac{\partial^2 T_{c0}}{\partial x^2} + \frac{\partial^2 T_{c0}}{\partial y^2} \right) + \tilde{q} \gamma_0 T_{c0} = 0 \quad \text{in } \Omega^*, \quad T_{c0} = 0 \quad \text{at } \partial \Omega,
 \tag{2}$$

where $\frac{c_\pm \rho_\pm}{k_\pm} = \varpi_\pm$, $\tilde{q} = \frac{\varpi_+ |\Omega_i^+| + \varpi_- |\Omega_i^-|}{|\Omega_i^*|}$.

3. Concluding Remarks

The obtained solution of a regularly periodic problem has extreme properties with respect to random composites. Thus, it can be used to assess the behavior of real composite materials. Note that the solution at the initial moment of time is rapidly changing not only in spatial variables, but also in time. Description of this state requires additional research.

References

- [1] ALLAIRE G, HABIBI Z: Homogenization of a conductive, convective, and radiative heat transfer problem in a heterogeneous domain. *SIAM Journal on Mathematical Analysis* 2013, **45**(3):1136-1178.
- [2] WASEEM A, HEUZE T, STAINIER L, GEERS MGD, V. G. KOUZNETSOVA VG: Model reduction in computational homogenization for transient heat conduction. *Computational Mechanics* 2020, **65**:249-266.
- [3] LEFIK M, SCHREFLER BA: Modelling of nonstationary heat conduction problems in micro-periodic composites using homogenisation theory with corrective terms. *Archives of Mechanics* 2000, **52**(2):203-223.
- [4] MITYUSHEV V, OBNOVOSOV YU, PESETSKAYA E, ROGOSIN S: Analytical methods for heat conduction in composites. *Mathematical Modelling and Analysis* 2008, **13**(1):67-78.
- [5] RYLKO N. Calculation of the effective thermal conductivity of fiber composites in non-stationary case. *Composites* 2005, **5**(4):96-100 (in Polish).
- [6] TAYLER AB: *Mathematical Models in Applied Mechanics*. Oxford: Clarendon Press, 2001.

Low-velocity impact response of metal-ceramic functionally graded plates: A novel numerical modelling approach

KEMAL ARSLAN^{1,2,*}, RECEP GUNES³

1. Graduate School of Natural and Applied Sciences, Erciyes University, Turkey [0000-0002-2162-3923]
2. Department of Mechanical Engineering, Adana Alparslan Turkes Science and Technology University, Turkey [0000-0002-2162-3923]
3. Department of Mechanical Engineering, Erciyes University, Turkey [0000-0001-8902-0339]

* Presenting Author

Abstract: This study presents a numerical modelling procedure for the low-velocity impact response of metal-ceramic FGM (Functionally Graded Materials) plates. Numerical modelling is performed using the explicit finite element code, LS-DYNA[®]. The actual mechanical response of the FGM plates is considered to develop a realistic numerical model, and the actual plasticity behaviour of the FGM plates is described using an elastoplastic material model, MAT_PIECEWISE_LINEAR_PLASTICITY. The numerical results are evaluated in terms of contact force and kinetic energy histories of the plates. To represent the accuracy and success of the developed numerical model, it is compared to the low-velocity impact test results and an existing elastoplastic model from the literature that is widely used to describe the elastoplastic behaviour of FGM structures, TTO (Tamura-Tomota-Ozawa) model. It is stated from the results that the present numerical model shows a good agreement with the experimental results, and the TTO model exhibits a stiffer response overestimating the contact force and underestimating the contact duration.

Keywords: functionally graded materials, low-velocity impact, numerical modelling, finite element method

1. Introduction

Functionally graded materials (FGMs) are a special class of composite materials with a continuous material composition change throughout the volume with respect to spatial coordinates that is obtained by a gradual variation of the volume fractions of constituents. FGM structures generally consist of metal and ceramic materials, and the material properties vary through the thickness direction. By combination of metal and ceramic constituents in a single volume and varying their combined properties continuously, they provide additional special features over conventional composite materials such as good thermal resistance and toughness which are very important in extreme loading conditions. FGMs are used in some critical fields such as aerospace, nuclear, automotive, and defence industries where dynamic effects are highly important. Therefore, it is important to determine the dynamic mechanical behaviour of FGMs subjected to impulsive loadings and to develop an accurate numerical model for saving experimental costs and predicting plasticity, damage, and fracture phenomena of FGMs for engineering design. However, numerical modelling of FGMs, especially for nonlinear impact problems, has some difficulties by reason of complexity of their structure.

In the literature, studies on the low-velocity impact response of FGMs are generally performed using only numerical or analytical approaches [1-2]. However, there is a lack of knowledge about combined experimental and numerical investigations on the low-velocity impact behaviour of FGMs. Therefore,

a realistic numerical model that considers the actual mechanical response and plasticity of the FGM plates are developed in this study. A comparative evaluation between the present numerical model, experiment, and an existing elastoplastic model, TTO (Tamura-Tomota-Ozawa) model [3] is performed for the low-velocity impact response of the FGM plates. For this purpose, different stress to strain transfer ratios in the TTO model are considered from the literature [4-5]. It is indicated that the present numerical model shows a good agreement and gives more accurate results than the TTO model.

References

- [1] APETRE NA, SANKAR BV, AMBUR DR: Low-velocity impact response of sandwich beams with functionally graded core. *International Journal of Solids and Structures* 2006, **43**(9):2479-2496.
- [2] MAO YQ, FU YM, CHEN CP, LI YL: Nonlinear dynamic response for functionally graded shallow spherical shell under low velocity impact in thermal environment. *Applied Mathematical Modelling* 2011, **35**(6):2887-2900.
- [3] TAMURA I, TOMOTA Y, OZAWA M: Strength and ductility of Fe-Ni-C alloys composed of austenite and martensite with various strength. *Proceedings of the 3rd International Conference on Strength of Metals and Alloys* Cambridge, 1973, pp. 611-615.
- [4] GUNES R, AYDIN M, APALAK MK, REDDY JN: Experimental and numerical investigations of low velocity impact on functionally graded circular plates. *Composites Part B: Engineering* 2014, **59**:21-32.
- [5] BHATTACHARYYA M, KAPURIA S, KUMAR AN: On the stress to strain transfer ratio and elastic deflection behavior for Al/SiC functionally graded material. *Mechanics of Advanced Materials and Structures* 2007, **14**(4):295-302.

Dynamics analysis of the spatial mechanism with imperfections in the fifth-class kinematic pairs

KRZYSZTOF AUGUSTYNEK^{1*}, ANDRZEJ URBAŚ², VASYL MARTSENYUK³

1. University of Bielsko-Biala, 43-309 Bielsko-Biala, Willowa 2, Poland, [0000-0001-8861-4135]
2. University of Bielsko-Biala, 43-309 Bielsko-Biala, Willowa 2, Poland, [0000-0003-0454-6193]
3. University of Bielsko-Biala, 43-309 Bielsko-Biala, Willowa 2, Poland, [0000-0001-5622-1038]

* Presenting Author

Abstract: The paper presents the mathematical model of the spatial mechanism with imperfect revolute and prismatic joints. Imperfections are taken into account in the form of clearance and friction in joints. Contribution to the paper includes new models of the revolute and prismatic joints formulated for the system which the kinematics is modeled using joint coordinates and homogeneous transformations. Different approaches to modeling clearance in joints, in the cut-joint and other joints of the mechanisms, will be presented in the paper. Thanks to the use of joint coordinates for joints that are not cut-joints, displacements resulting from the clearance in a joint can be taken directly from the generalized coordinate vector without the need for additional calculations. Numerical simulations allow us to analyze an interaction between links' flexibility and imperfections due to clearance and friction in the joints.

Keywords: spatial mechanism, clearance, friction, link's flexibility

1. Introduction

Different imperfections and nonlinearities in joints of mechanisms have a significant impact on their dynamics. They can cause additional vibrations, joint wear, significant reduction of accuracy and energy efficiency. Additional impact forces due to clearance can damage mechanical parts. In the literature, it can be found many papers dealing with modeling of the clearance in joints for mechanisms whose movement is described by absolute coordinates [1, 2]. Contribution to the paper includes new models of the revolute and prismatic joints formulated for RPSUP mechanism which the kinematics is modeled using joint coordinates and homogeneous transformations (Fig. 1). The presented models are a continuation of the work, the results of which are shown in [3]. In the paper, the clearance is analyzed not only in the cut-joint but also in other joints. It is assumed that the clearance exists at cut-joint C and slider (2,1). The dynamics equations of motion are derived using the Lagrange equations of the second kind [4]. The normal contact force is modeled using the Nikravesh-Lankarani hypothesis [5]. Friction in joints is modeled by means of the LuGre friction model [6]. It is assumed that the coupler can be flexible and the Rigid Finite Element Method is used to model effects due to the link's flexibility [4].

2. Mathematical model of a RPSUP spatial mechanism

The cut-joint technique is applied to divide the closed-loop chain into two open-loop kinematic chains. The generalized coordinate vector is composed of the following components

$$\mathbf{q} = \left[\psi^{(1,1)} \quad x^{(1,2)} \quad \psi^{(1,3,0)} \quad \theta^{(1,3,0)} \quad \varphi^{(1,3,0)} \quad \mathbf{q}_f^{(1,3)^T} \quad ; \quad z^{(2,1)} \quad \mathbf{q}_c^{(2,1)^T} \quad \psi^{(2,2)} \right]^T \quad (1)$$

where: $\mathbf{q}_f^{(1,3)}$ - vector containing the generalized coordinates of the rigid finite elements,

$\mathbf{q}_c^{(2,1)} = \left[x^{(2,1)} \quad y^{(2,1)} \quad \psi^{(2,1)} \quad \theta^{(2,1)} \quad \varphi^{(2,1)} \right]^T$ - vector containing displacements of slider (2,1) due to the clearance in joint. It can be noted that displacements resulting from the clearance in a joint can be taken directly from the generalized coordinate vector without the need for additional calculations.

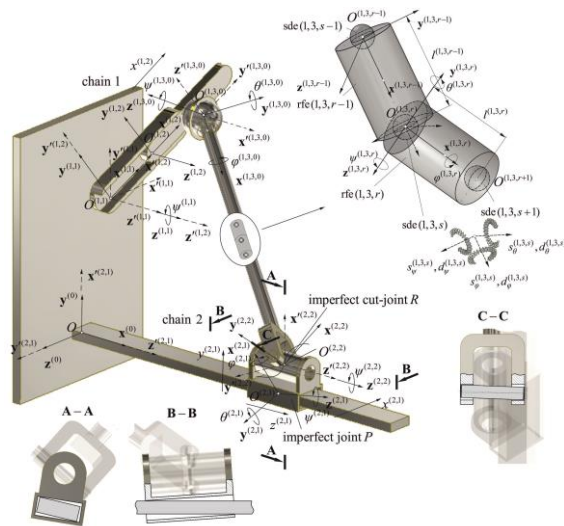


Fig. 1. Model of a rigid-flexible link spatial mechanism

Finally, dynamics equations of motion together with the state equations formulated for the LuGre friction model form a set of ordinary differential equations in the following form [3]

$$\dot{\mathbf{z}} = \mathbf{L}\mathbf{G}(t, \dot{\mathbf{q}}, \mathbf{z}) \quad (2.1)$$

$$\mathbf{M}\ddot{\mathbf{q}} = \mathbf{Q} - \mathbf{h} - \mathbf{g} + \mathbf{f}_c - \mathbf{f}_{flex} - \mathbf{f}_{fric} \quad (2.2)$$

where: \mathbf{M} - mass matrix, \mathbf{Q} - vector of the Coriolis, gyroscopic and centrifugal forces, \mathbf{g} - vector of gravity forces, \mathbf{f}_c , \mathbf{f}_{fric} , \mathbf{f}_{flex} - vectors of forces resulting from clearance and friction in joints and coupler's flexibility, \mathbf{z} - vector of state variables, $\mathbf{L}\mathbf{G}(t, \dot{\mathbf{q}}, \mathbf{z})$ - functions of right-hand sides of the LuGre friction model. In numerical simulations interactions between the clearance in joints and coupler's flexibility will be analyzed.

References

- [1] TIAN, Q., FLORES, P., LANKARANI, H.M.: A comprehensive survey of the analytical, numerical and experimental methodologies for dynamics of multibody mechanical systems with clearance or imperfect joints. *Mech. Mach. Theory* 2017, **116**: 123–144.
- [2] LIU, C., TIAN, Q., HU, H.: Dynamics and control a spatial rigid-flexible multibody system with multiple cylindrical clearance joints. *Mech. Mach. Theor.*, 2012, **52**: 106–129.
- [3] AUGUSTYNEK, K., URBAŚ, A.: Analysis of the Influence of the Links' Flexibility and Clearance Effects on the Dynamics of the RUSP Linkage. In: KECSKEMÉTHY A., GEU FLORES F. (EDS) *Multibody Dynamics 2019. ECCOMAS 2019. Computational Methods in Applied Sciences*, vol 53. Springer, Cham, 2020: 104–111.
- [4] WITTBRODT, E., SZCZOTKA, M., MACZYŃSKI, A., WOJCIECH, S.: *Rigid Finite Element Method in Analysis of Dynamics of Offshore Structures*. Ocean Engineering & Oceanography. Springer: Heidelberg, 2013.
- [5] LANKARANI, H.M., NIKRAVESH, P.E.: A contact force model with hysteresis damping for impact analysis of multibody systems. *J. Mech. Des.* 1990, **112**: 369–376.
- [6] ÅSTRÖM, K.J., CANUDAS-DE-WITT, C.: Revisiting the LuGre model. *IEEE Control Syst. Mag. Inst. Electr. Electron. Mag.* 2008, **28**(6): 101–114.

Geometrically nonlinear vibrations of double-layered nanoplates

JAN AWREJCEWICZ¹, OLGA MAZUR^{2*}

1. Lodz University of Technology, Department of Automation, Biomechanics and Mechatronics
2. National Technical University "KhPT", Department of Applied Mathematics

* Presenting Author

Abstract: The geometrically nonlinear vibrations of simply supported double-layered graphene sheet systems are considered in the presented manuscript. The interaction between layers is taken into account due to van der Waals forces. The investigation is based on the nonlocal elasticity theory, Kirchhoff plate theory and von Kármán theory. The governing equations are used in mixed form by introducing the stress Airy function. The analytical presentation of the nonlinear frequency ratio for in-phase vibration and anti-phase vibration modes is presented. It is shown that the nonlocal parameter included in the compatibility equation can significantly change the vibrating characteristics.

Keywords: double-layered nanoplate system, the nonlocal elasticity theory, Kármán plate theory, Bubnov-Galerkin method.

1. Introduction

The modern industry is developing rapidly in the field of nanotechnology. This fact leads to the need for new studies of the nanostructures (nanobeams, nanoplates, nanoshells) using in the design of sensors, resonators, nanoelectromechanical systems (NEMS), nanooptomechanical structures, energy storage systems, DNA detectors, drug delivery. An important role is played by graphene objects, the study of which is the focus of our work. We employed the nonlocal elasticity theory, which is based on the fact that the stress at a given point is a function of strains at all other points of structure, to study double-layered nanoplate system.

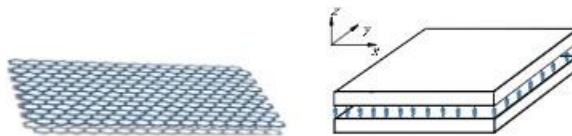


Fig. 1. Diagram of double-layered graphene sheet system

According to nonlocal theory the constitutive relation for the nonlocal stress tensor at a point x in an integral form is presented as follows

$$\sigma = \int_V K(|X' - X|, \tau) \sigma'(X') dX' \quad (1)$$

where σ, σ' are nonlocal and local stress tensors, $K(|X' - X|, \tau)$ is the nonlocal modulus, $\tau = e_0 \alpha / l$, α is the internal characteristic length, e_0 stands for a constant appreciate to material, whereas l is external characteristics length. Interaction between two layers regards the action of van der Waals force (vdW). This interaction is often modeled as the Winkler foundation. We assume that both nanoplates have the same mechanical properties.

2. Formulation of the problem

The governing equations for each layer are taken as:

$$D\Delta^2 w_1 = (1 - \mu \nabla^2)L(w_1, F_1) - c(w_1 - w_2) - \rho h \frac{\partial^2 w_1}{\partial t^2}, \quad (2)$$

$$(1 - \mu \nabla^2) \frac{1}{E} \Delta^2 F_1 = -\frac{h}{2} L(w_1, w_1),$$

$$D\Delta^2 w_2 = (1 - \mu \nabla^2)L(w_2, F_2) - c(w_2 - w_1) - \rho h \frac{\partial^2 w_2}{\partial t^2}, \quad (3)$$

$$(1 - \mu \nabla^2) \frac{1}{E} \Delta^2 F_2 = -\frac{h}{2} L(w_2, w_2),$$

where μ stands for the nonlocal parameter and ∇^2 is the Laplacian operator, E is Young's modulus, ν is Poisson's ratio, D is flexural nanoplate rigidity, ρ is density of the plate, h is thickness, whereas $L(w, F)$, $L(w, w)$ are differential operators determined in [1] and c stands for interaction coefficient [2]. Note that we propose using the nonlocal compatibility equation for DLGs, where the nonlocal parameter is introduced based on the nonlocal constitutive relation. System of the governing equations is supplemented with the simply supported boundary conditions.

We present the deflections $w_i(x, y, t)$, $i = 1, 2$ of each nanoplate as

$$w_i(x, y, t) = y_i(t)W(x, y), i = 1, 2,$$

where $W(x, y)$ is shape function and $y_i(t)$ is generalized coordinate for i -th layer. Further application of the Bubnov-Galerkin approach gives the system of the coupled second order ordinary differential equations which discussed for in-phase vibration (IPV) mode and anti-phase vibration (APV) mode.

3. Concluding Remarks

The nonlinear vibrations of double-layered graphene sheet systems are studied. The governing equations of the problem are based on the nonlocal elasticity theory, Kirchhoff hypothesis, the von Kármán equations and presented in the mixed form with Airy function. Two graphene sheets are bonded by van der Waals force. The investigation of the influence of the nonlocal parameter in the compatibility equation is performed. It is concluded that the nonlocal parameter in the compatibility equation can significantly change the results and should be taken into account in order to achieve reliable results.

Acknowledgment: This work has been supported by the Polish National Science Centre under the grant OPUS 14 No. 2017/27/B/ST8/01330.

References

- [1] VOLMIR, A.S., *Nonlinear Dynamics of Plates and Shells*, Moscow, Nauka, 1972.
- [2] HE X. Q., KITIPORNCHAL, S., LIEW, K. M., Resonance analysis of multi-layered graphene sheets used as nanoscale resonators., *Nanotechnology* 16 (10), 2005.

On alphabetical shaped soliton for intrinsic fractional coupled nonlinear electrical transmission lattice using sine-cosine method,

FENDZI-DONFACK EMMANUEL^{1,2,*}, TCHEPEMEN NKOUESSI NATHAN¹, TALA-TEBUE ERIC³, KENFACK-JIOTSA AURELIEN².

1. *Pure Physics Laboratory, Group of Nonlinear Physics and Complex Systems, Department of Physics, Faculty of Sciences, University of Douala, P.O. Box 24157, Douala, Cameroon.*
2. *Nonlinear Physics and Complex Systems Group, Department of Physics, The Higher Teacher's Training College, University of Yaounde I, P.O. Box 47 Yaoundé, Cameroon.*
3. *Laboratoire d'Automatique et d'Informatique Appliqué (LAIA), IUT-FV of Bandjoun, The University of Dschang, BP 134, Bandjoun, Cameroon.*

* Presenting Author [ORCID: 0000-0001-8635-1159].

Abstract: We investigate the effect of fractional order on alphabetical shaped solitons solutions for intrinsic fractional (2+1)-D coupled nonlinear electrical transmission lattice using sine-cosine method in addition to higher order of dispersion.

Keywords: Fractional complex transform, sine-cosine method and fractional alphabetical shaped solitons.

1. Introduction (10 point, bold)

In recent years, investigating on solitary waves called solitons has been of great interest [1]. More recently, researchers pay attention on fractional calculus and prove that it is a useful tool to model faithfully nonlinear complex physical phenomena (NCPP) [2-4]. In fact, introducing fractional derivative operators in NPDEs modelling nonlinear complex systems (NCS) such as nonlinear electrical transmission lines or lattice (NETLs) is fascinating for some aims like involve the memory effect. So, obtain exact solutions of fractional nonlinear partial differential equations (FNPDEs) is utmost important as well as derive ones of the NPDEs [2-5]. In this study, we consider the Curie's empirical law [6] governing the current flowing through a fractional nonlinear capacitor such as through the skin effect, this empirical law is also applied to the inductor. This fractional derivatives Ohm's laws lead us for a (2+1)-D NETL [7] to get an intrinsic fractional discrete NPDE (FDNPDE) of the voltage wave. We derive by using the semi-discrete approximation with higher order of dispersion in addition to fractional complex transform a nonlinear evolution equation (NEE) solved by the sine-cosine method [8].

2. Results and Discussion (10 point, bold)

By using the Kirchhoff's laws in addition of Curie's empirical laws, we get:

$$\frac{d^{2\delta} C_0 (V_{n,m} - aV_{n,m}^2 + bV_{n,m}^3)}{dt^{2\delta}} = \frac{1}{L_1} (V_{n+1,m} - V_{n-1,m} + 2V_{n,m}) + \frac{1}{L_2} (V_{n,m+1} - V_{n,m-1} + 2V_{n,m}), 0 < \delta \leq 1. \quad (1)$$

By introducing the semi-discrete approximation with higher order of dispersion in addition to the fractional complex transform (FCT)

$$V_{n,m}(t) = V(t, x, y) = A \cos^p(\xi), \quad \xi = k_1 x + k_2 y + \frac{ct^\delta}{\Gamma(1+\delta)}, \quad k_1 = k_2 = k \quad (2)$$

with A, p, k and c the unknown parameter. We obtain a NEE such as the solutions are established through the sine-cosine method. Some findings depicted below show singular bright solitary wave (SBSW) such as, due to the fractional order (FO), we attain M-shaped solitons and explore more amplified solutions like bright solitary wave (BSW) depending on physical parameters and FO.

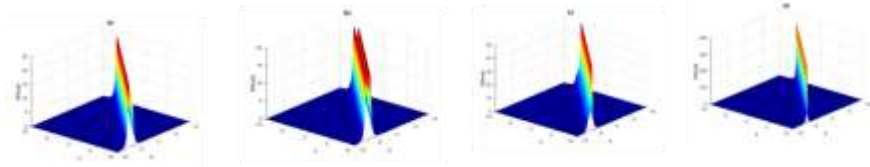


Fig. 1. These graphs display $|V(x, y)|$ with $U_0=3, l_1=1, W_0=4, l_2=1, a=0.21, b=-0.0197, t=1: (a) \delta=1, (b) \delta=0.975, (c) \delta=0.875, (d) \delta=0.75$.

3. Concluding Remarks (10 point, bold)

We have investigated the effect of fractional order on alphabetical shaped solitons solutions for an intrinsic fractional (2+1)-D coupled nonlinear electrical transmission lattice by using sine-cosine method in addition to fractional complex transform.

Acknowledgment: The authors acknowledge all the anonymous peer-reviewers and participants for their pertinent remarks and helpful discussions.

References (10 point, bold)

- [1] HIROTA R, SUZUKI K. THEORETICAL AND EXPERIMENTAL STUDIES OF LATTICE SOLITONS IN NONLINEAR-LUMPED NETWORKS. PROCEEDINGS OF THE IEEE 1973;61(10):1483–91.
- [2] DONFACK EF, NGUENANG JP, NANA L. ON THE TRAVELING WAVES IN NONLINEAR ELECTRICAL TRANSMISSION LINES WITH INTRINSIC FRACTIONAL-ORDER USING DISCRETE TANH METHOD. CHAOS, SOLITONS AND FRACTALS 2020;131:109486.
- [3] FENDZI-DONFACK E, NGUENANG JP, NANA L. FRACTIONAL ANALYSIS FOR NONLINEAR ELECTRICAL TRANSMISSION LINE AND NONLINEAR SCHRÖDINGER EQUATIONS WITH INCOMPLETE SUB-EQUATION. THE EUROPEAN PHYSICAL JOURNAL PLUS 2018;133(2):1–11.
- [4] FENDZI-DONFACK, E., NGUENANG, J.P., NANA, L. ON THE SOLITON SOLUTIONS FOR AN INTRINSIC FRACTIONAL DISCRETE NONLINEAR ELECTRICAL TRANSMISSION LINE, NONLINEAR DYN., 2021, 104(1):691-704.
- [5] AYDIN O, SAMANCI B, OZOGUZ S, CHARACTERIZATION AND MEASUREMENT OF CABLE LOSSES USING FRACTIONAL-ORDER CIRCUIT MODEL, BALKAN J. ELECTR. COMPUTING 2018; 6(4): 266.
- [6] WESTERLUND S, EKSTAM L, CAPACITOR THEORY, IEEE TRANS. DIELECTRIC INSUL. 1994; 1(5): 826-839.
- [7] TALA-TEBUE E, TSOBGNI-FOZAP D.C, KENFACK-JIOTSA A, KOFANE T.C., ENVELOPE PERIODIC SOLUTIONS FOR A DISCRETE NETWORK WITH THE JACOBI ELLIPTIC FUNCTIONS AND THE ALTERNATIVE (G'/G)-EXPANSION METHOD INCLUDING THE GENERALIZED RICCATI EQUATION, EUR. PHYS. J. PLUS, 2014; 129(6), 136.
- [8] YONGAN X, SHENGQIANG T, SINE-COSINE METHOD FOR NEW COUPLED ZK SYSTEM, APPLIED MATHEMATICAL SCIENCES 2011; 5(22): 1065-1072.

Normal Form on Nonlinear Systems and Gröbner Based Exploitation of Resonances

J. FLOSI¹*, A. TURE SAVADKOOHI¹, C.-H. LAMARQUE¹

1. Univ Lyon, ENTPE, LTDS UMR 5513, 3 Rue Maurice Audin, 69518 Vaulx-en-Velin Cedex

* Presenting Author; *jean.flosi@entpe.fr*

Abstract: The Normal Form application is introduced on dynamical systems with diagonal and Jordan block matrices. Spectrum rearrangement allows to exhibit resonant terms associated with periodic behaviours of the system. Resonance equations are forming Gröbner generators and associated Gröbner bases allow to linearize equations depending on amplitude-frequency conditions.

Keywords: Normal Form, Gröbner bases, nonlinear, spectrum

1. Introduction

This work focuses on the study of general nonlinear dynamics systems using the Normal Form perturbation method [1,2] as long as the amplitude of the response is relatively limited [3]. The Gröbner bases are then used to solve algebraic equations of normal coordinates. After spectrum optimisation, nonlinear terms can be classified between non-resonant and resonant terms providing new physical equations. Gröbner bases firstly presented by Buchberger [4] are generalising the polynomial division of a polynomial by other multivariable polynomial. Normal Form compatibility equations are used to generate the ideals and then to reduce governing Normal coordinates equations by the generalised Euclidian division. In optimal cases, linear solutions $X = M(\Omega).U$ are obtained, supposing that potentially nonlinear generators equations are verified. Except the spectrum definition, this process can be automatized [6,7].

2. Results and Discussion

2.1. General case

Let us consider following general dynamical system:

$$\dot{X} = A.X + F(X) \quad (1)$$

where $F(X) = F_2(X) + \dots + F_n(X)$ are vectors of polynomial nonlinearities. Let's assume that $A = P^{-1}.D.P$, with $D = D_0 + D_1(\epsilon)$ a diagonal matrix, $\mathcal{O}(D_1(\epsilon)) \geq 1$. Normal coordinates $Y = P^{-1}.X = U + \phi_2(U) + \dots + \phi_n(U)$ allow to introduce normal transformation $\phi = \phi_2 + \dots + \phi_n$ and resonant terms $R = R_2 + \dots + R_n$. The system takes the new form

$$\begin{cases} \dot{Y} = D_0.Y + D_1.Y + P^{-1}.F(P.Y) \\ \hat{D}_1 = 0, & \mathcal{O}(D_1.Y) = 2, & \mathcal{O}(P^{-1}.F(P.Y)) \geq 3 \end{cases} \quad (2)$$

The Normal Form resolution is done degree per degree and leads to the expression of X as a function of U and to compatibility equations:

$$\begin{cases} X = P^{-1}.Y = P^{-1}.(U + \phi_2(U) + \dots + \phi_n(U)) \\ \dot{U} - D_0.U - R_2 - \dots - R_n = 0 \end{cases} \quad (3)$$

Compatibility equations are providing amplitude-frequency conditions in order to assure periodic behaviours. Euclidian division by the Gröbner bases elements is applied to $X(U)$. Gröbner generators are defined by these equations as $G_k = 0$ and allow to decompose $X = M_1(\Omega).U + M_2(U).U$, where $M_2(U)$ is a simplified expression derived from normal transform and Gröbner bases.

2.2. An example: a two Degrees of Freedom (DoF)

To illustrate this process, we apply it to a two DoF cubic nonlinear system where $D = D_0$. Normal form equations are

$$\begin{cases} \text{deg}_1: DU = DU \\ \text{deg}_2: \partial\phi_2 DU - D\phi_2(U) = H_2 - R_2 \\ \text{deg}_3: \partial\phi_3 DU - D\phi_3(U) = H_3 - R_3 \\ G_k = i\Omega u_k - \lambda_k u_k - R_{2k} - R_{3k} \end{cases} \quad (4)$$

where H_k gathers k-order nonlinear terms. We obtain the final normal expressions

$$\begin{cases} X = M_1(\Omega).U + M_2(U).U \\ G_1, \dots, G_4 = 0 \end{cases} \quad (5)$$

For this system, M_1 could be associated to linear homogenous solution if we obtain $M_2 = 0$. All nonlinearities remain in the variety of G_1, \dots, G_4 . In this two DoF case, $M_2(U)$ terms are either $u_1 u_4$ or $u_2 u_3$ terms. According to compatibility equations, the variety and accepted amplitudes impose that either $u_1 = 0$ or $u_3 = 0$. In both cases, $M_2 = 0$ and a linear expression is finally obtained.

3. Concluding Remarks

The solution of the system cannot be expressed linearly in Normal coordinates in general, unless uncoupling issuing from the analysis of the frequency compatibility condition due to the amplitude equations. Nevertheless, a perspective work could be that Gröbner bases should be also used in order to define new normal coordinates and introduce less pairing, especially when D is a Jordan matrix [5].

Acknowledgment: The authors would like to thank the following organizations for supporting this research: (i) The “Ministère de la transition écologique et solidaire” and (ii) LABEX CELYA (ANR-10-LABX-0060) of the “Université de Lyon” within the program “Investissement d’Avenir” (ANR-11-IDEX- 0007) operated by the French National Research Agency (ANR).

References

- [1] H. POINCARÉ: Les Méthodes Nouvelles de la Mécanique Céleste. Gauthier-Villars: Paris, 1889.
- [2] A.; H. NAYFEH: *Method of Normal Forms*. Wiley: New York, 1993.
- [3] C.-H. LAMARQUE, C. TOUZÉ: An upper bound for validity limits of asymptotic analytical approaches based on normal form theory. *Nonlinear Dynamics*, 2012, **70**(3):1931-1949.
- [4] B. BUCHBERGER: B. Buchberger’s PhD thesis 1965: An algorithm for finding the basis elements of the residue class ring of a zero dimensional polynomial ideal. *Journal of Symbolic Computation*, 2006, **41**(3):475-511.
- [5] J. MURDOCK: *Normal Forms and Unfoldings for Local Dynamical Systems*. Springer: New York, 2003.
- [6] P. YU: Computation of normal forms via a perturbation technique. *International Journal of Bifurcation and Chaos*, 1998, **8**(12):2279-2319.
- [7] A. GROLET, F. THOUVEREZ: Computing multiple periodic solutions of nonlinear vibration problems using the harmonic balance method and Groebner bases. *Mechanical Systems and Signal Processing*, 2015, **52**(3):529-547.

Implementation of State Observer-Based Conditioned Reverse Path Method to the Identification of a Nonlinear System

UMAARAN GOGILAN^{1*}, ATTA OVEISI², TAMARA NESTOROVIĆ³

1. Mechanics of Adaptive Systems, Institute of Computational Engineering, Ruhr University Bochum, Germany
2. Mechanics of Adaptive Systems, Institute of Computational Engineering, Ruhr University Bochum, Germany [ORCID: 0000-0002-6507-9448]
3. Mechanics of Adaptive Systems, Institute of Computational Engineering, Ruhr University Bochum, Germany [ORCID: 0000-0003-0316-2171]

* Presenting Author

Abstract: The conditioned reverse path (CRP) method is a method for the frequency response estimation nonlinear systems to extract the properties of an underlying linear model (ULM). This method recalculates the nonlinearity coefficients by using spectral techniques and recovers the frequency response function (FRF) of the ULM [1]. However, applying the CRP method is challenging if the system states are not accessible for measurement. For this reason, a state estimation process is integrated with the CRP method resulting into observer-based conditioned reverse path (OBCRP) method. The state estimation process based on the Kalman filter technique is employed in this work to reconstruct the system states. Applying spectral techniques with the CRP/OBCRP method, the resulting nonlinear spectra consist of real and imaginary parts. Since imaginary parts have no physical meaning, the nonlinear coefficients based only on the real parts of the spectra are thus distorted. To minimize the distortion of nonlinear coefficients the OBCRP method is extended by a novel weighting scheme. In the present study, this method is exemplarily applied in a simulation. The OBCRP method successfully recovered the FRF of the ULM and accurately parameterized the nonlinearities of the system.

Keywords: nonlinear system identification, Kalman filter, reverse path method

1. Introduction

Analysis of dynamic structures may be performed in frequency domain using the frequency response estimation as a basis. With growing requirements on dynamical systems analysis, influences of the nonlinearity should be taken into account. The CRP method parameterizes the nonlinearities of the system and recovers the FRF of the nonlinear model. However, the application of this method requires the measurement of all states at the same time. In large-scale structures, the frequency range of operation may encompass several hundreds of states, so that the measurement of all system states may become impossible due to the deficiency of appropriate sensors. The state estimation based on the Kalman filter technique provides the access to all required system states resulting in turn into reduction of the required number of sensors. This combination of the CRP method and the system states estimation is referred to as the observer-based conditioned reverse path method (OBCRP). By using the CRP method, some information of the nonlinear spectra is lost due to the presence of imaginary parts, and the resulting nonlinear coefficients are distorted. A novel frequency-dependent weighting scheme is applied to the nonlinear coefficients, which leads to better extraction of the FRF of the nonlinear system.

2. Results and Discussion

The performance of the OBCRP method is investigated in the simulation of a nonlinear mass-spring-damper system with five degrees of freedom, shown in Fig. 1. The parameters for mass, stiffness and damping are given, and the observability and controllability conditions are fulfilled. The system possesses nonlinear stiffnesses depicted as spring elements with an arrow. Mass m_1 is excited by an external multisine force f_1 . At the two masses m_1 and m_5 , the velocity and acceleration measurements are carried out, while the state estimation process of the OBCRP method is applied to estimate the displacements x_2 , x_3 and x_4 .

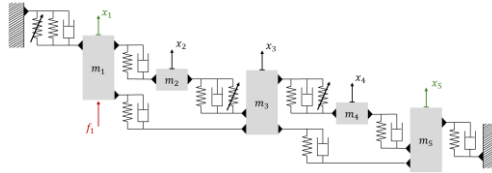


Fig. 1. Mass-spring-damper system with five degrees of freedom

Based on the estimated states, the frequency-dependent spectra for the estimation of the nonlinear coefficients are calculated by the application of the OBCRP method. To present the estimation quality of the proposed novel weighting scheme, the estimation errors of the weighted and unweighted nonlinear coefficients are compared in Table 1. Finally, the FRF between f_1 and x_1 obtained by the OBCRP method is compared to the FRF based on the classical H_1 method, as shown in Fig. 2. The FRF based on the OBCRP method is significantly less distorted, and the conditioned spectral analysis of the OBCRP method recovers the ULM correctly.

Table 1. Estimation error of the weighted and unweighted nonlinear coefficients

Coefficients	True value	Estimation error (%)	
		Unweighted	Weighted
α_1	-500kN/m ³	23.38	4.02
α_2	100kN/m ³	48.1	13.58
β_1	3 MN/m ³	22.32	1.09
β_2	-0,2 MN/m ³	407.22	0.79
γ_1	4 MN/m ³	18.72	27.4

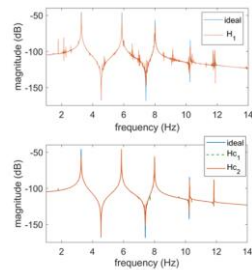


Fig. 2. Unconditioned and conditioned FRFs

3. Concluding Remarks

The OBCRP method has been successfully applied to a nonlinear lumped-mass model problem in a simulation. Based on the state estimation and input design, the nonlinear coefficients are calculated using the spectral estimation techniques of the OBCRP method. To reduce the distortion due to imaginary parts, the nonlinear coefficients are subjected to a novel weighting scheme. The FRF of the ULM is then successfully recovered by the OBCRP method. It furthermore accurately parameterizes the nonlinearities within the model. Validation of the method on an experimental setup is in prospect.

References

- [1] RICHARDS C. M., SINGH R.: Identification of multi-degree-freedom non-linear systems under random excitations by the ‘Reverse Path’ spectral method. *J. Sound Vib.*1989, pp. 673–708.

The response of nonlinear dynamic systems via Wavelet-Galerkin method in the time-frequency domain

XIAOJING HAN^{1*}, EMMANUEL PAGNACCO¹

1. Laboratory of Mechanics of Normandy (LMN), INSA Rouen Normandy, Rouen 76000, France [0000-0003-0252-7060]

* Presenting Author

Abstract: The periodic generalized harmonic wavelet (PGHW) method is used to analyze the response of nonlinear dynamic systems with seismic excitation. This excitation is a non-stationary stochastic process with non-uniform modulation. The nonlinear term of the system is a typical cubic nonlinear term. First, the theoretical background of PGHW is briefly introduced, and the relationship between the power spectral density (PSD) of the stochastic process and the corresponding wavelet coefficients is given. Then, a set of algebraic equations for solving the wavelet coefficients can be obtained by using the Wavelet-Galerkin method. The Quasi-Newton method is used to solve these equations. It is more efficient than the Newton method because it does not require the calculation of complex Jacobian matrices. Then, the displacement and estimated power spectral density (EPSD) of the response can be obtained by using the wavelet coefficients. In the numerical example, the ode45 and Monte Carlo methods are used to verify the correctness of the results.

Keywords: nonlinear dynamic system, stochastic process, wavelet method, Quasi-Newton method, frequency domain

1. Introduction

The wavelet analysis is first proposed in 1980s [1]. Based on wavelet theory, harmonic wavelet (HW) [2], generalized harmonic wavelet (GHW) [3], periodic generalized harmonic wavelet (PGHW) [4] are proposed. The PGHW is a good method to deal with the vibration signals with limited duration in the engineering field. The main composition of Fourier transform is sinusoids of different frequencies, and the main composition of wavelet transform is wavelets of different scales and positions.

2. Results and Discussion

The Wavelet-Galerkin method is used to deal with the dynamic equation of the nonlinear system. Then, a set of algebraic equations for solving the wavelet coefficients can be obtained. The Quasi-Newton method is used to solve these equations. It approximates the Jacobian matrix by using the difference quotient, DFP and BFGS algorithms which simplifies the calculation process. Then, the displacement of response $x(t)$ can be obtained and shown in Fig. 1.

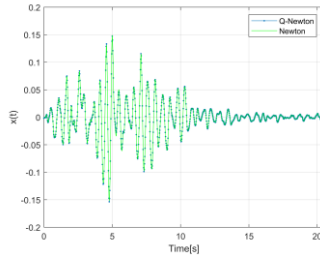


Fig. 1. The displacement of $x(t)$

From Fig. 1 we can see that the results by using Newton and Quasi-Newton methods are consistent. But the total time required for the Newton method is 327s, for the Quasi-Newton method 67s. Thus, the Quasi-Newton method is five times faster than the Newton method.

For the stochastic excitations (Nsample=200), the surface and contour of the response EPSD can be obtained and shown in Fig. 2. They all show the consistency of the results.

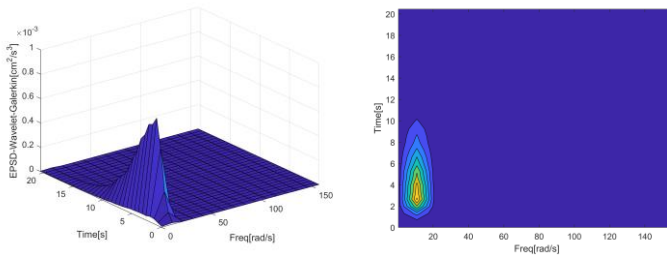


Fig. 2. The surface and contour of the response EPSD

3. Concluding Remarks

The displacement and EPSD of the responses can be obtained by using the PGHW. The Quasi-Newton method is used to solve those algebraic equations, which is more efficient than the Newton method.

References

- [1] A. Grossmann and J. Morlet. Decomposition of hardy functions into square integrable wavelets of constant shape. *Siam Journal on Mathematical Analysis*, 1984, 15(4):723–736.
- [2] David E Newland. Harmonic wavelet analysis. *Proceedings of the Royal Society of London. Series A: Mathematical and Physical Sciences*, 443(1917):203–225, 1993.
- [3] David E Newland. Harmonic and musical wavelets. *Proceedings of the Royal Society of London. Series A: Mathematical and Physical Sciences*, 444(1922):605–620, 1994.
- [4] Kong F, Li S, Zhou W. Wavelet-Galerkin approach for power spectrum determination of nonlinear oscillators[J]. *Mechanical Systems and Signal Processing*, 2014, 48(1-2): 300-324.

Dynamic Response of Simply-Supported Euler-Bernoulli Beam on Non-linear Elastic Foundation Under a Moving load

NICOLAE HERISANU^{1*}, VASILE MARINCA²

1. University Politehnica Timisoara, Romania
2. University Politehnica Timisoara, Romania

* Presenting Author

Abstract: The dynamic response of a Euler-Bernoulli beam with uniform cross-section resting on a nonlinear elastic foundation under a moving load is obtained by means of the Optimal Auxiliary Functions Method (OAFM). The Galerkin method is applied to discretize the nonlinear partial differential governing equation of the forced vibration and then the OAFM is employed to investigate the nonlinear behavior. This new approach provides a simple but rigorous technique to control the convergence of the solutions, which proved to be very efficient in this kind of problems.

Keywords: moving load, nonlinear vibration, Euler-Bernoulli beam, OAFM

1. Introduction

The problems related to moving loads on nonlinear foundations are very common for mechanical structures such as railway equipment, vehicle-bridge interaction, pipelines transversally supported, power transmissions. Many studies can be found on this domain. Mustafa et al. [1] studied the vibration of an axially moving beam traveling axially on a curved frictionless foundation with nonlinear elastic characteristics. The effects of a speed-dependent tension and a tension dependent speed with the inhomogeneous boundary conditions arising from Kelvin viscoelastic constitutive relations are taken into account by Tang and Ma [2]. The traveling wave modes are investigated for axially moving string and beam by Lu et al. [3]. Ri et al. [4] proposed a forced vibration model of composite beams under the action of periodic excitation force considering geometric nonlinearity. In this paper, the dynamic response of simply-supported Euler-Bernoulli beam on nonlinear elastic foundation under a moving load is investigated by means of a new approach, using the Optimal Auxiliary Functions Method (OAFM) [5].

2. Results and Discussion

A simply supported beam-type structure of length L , moment of inertia I , cross-sectional area A and modulus of elasticity E resting on nonlinear Winkler foundation is considered. Using Hamilton's principle and considering Euler-Bernoulli beam theory, the differential governing equation is derived as

$$\rho A \frac{d^2 \bar{W}(\bar{x}, \bar{t})}{d\bar{t}^2} + \frac{d^2}{d\bar{x}^2} \left[\frac{EI W''(\bar{x}, \bar{t})}{\sqrt{1 - W'^2(\bar{x}, \bar{t})}} \right] + P W''(\bar{x}, \bar{t}) + \bar{K}_1 W(\bar{x}, \bar{t}) + \bar{K}_3 W^3(\bar{x}, \bar{t}) - \bar{K}_2 W''(\bar{x}, \bar{t}) = \bar{F}_0 \delta(\bar{x} - \bar{v}\bar{t}) \quad (1)$$

Assuming a three-mode approach one obtains

$$\bar{W}(\bar{x}, \bar{t}) = \sum_{i=1}^3 q_i(\bar{t}) X_i(\bar{x}), \quad X_i(\bar{x}) \quad (1)$$

and applying the Galerkin method we have

$$\int_0^L [\rho A \bar{W}'' + EI(\bar{W}^{(IV)}) + \frac{1}{2} \bar{W}^{(IV)} \bar{W}'^2 + 3\bar{W}' \bar{W}'' \bar{W}''' + \bar{W}''^3] + (P - K_2) \bar{W}'' + K_1 \bar{W} + K_3 \bar{W}^3 - F_0 \delta(x - vt)] X_i(\bar{x}) d\bar{x} = 0, \quad i = 1, 2, 3 \quad (1)$$

After introducing some dimensionless parameters, one obtains the nondimensional nonlinear differential equation

$$\ddot{q}_1 + (\pi^4 r^2 + K_1 - \pi^2 K_2) q_1 + \frac{1}{4} (5\pi^6 r^2 + 3K_3) q_1^3 + (K_3 - \pi^6 r^2) q_1 q_2^2 + \frac{1}{8} (171\pi^6 r^2 - 3K_3) q_1^2 q_3 + \frac{1}{4} (27\pi^6 r^2 + 6K_3) q_1 q_3^2 + 246\pi^6 r^2 q_2^2 q_3 = F_0 \sqrt{2} \sin \pi vt \quad (1)$$

Following the same procedure, similar nonlinear equations are obtained for q_2 and q_3 .

The initial conditions for the vibration of the considered simply supported Euler-Bernoulli beam based on the triple-mode assumption are

$$q_1(0) = A_1, \quad q_2(0) = A_2, \quad q_3(0) = A_3, \quad \dot{q}_1(0) = \dot{q}_2(0) = \dot{q}_3(0) = 0 \quad (1)$$

At this stage, the Optimal Auxiliary Function Method is applied to obtain analytical approximate solution of the form

$$\bar{q}_1 = q_{10} + q_{12}; \quad \bar{q}_2 = q_{20} + q_{22}; \quad \bar{q}_3 = q_{30} + q_{23} \quad (1)$$

where the initial approximations and the first-order approximations can be determined from the specific linear equations according to OHAM procedure, while the natural frequencies of every mode of vibration are determined by avoiding secular terms. Every term of the first-order approximation contains a set of so-called convergence-control parameters, whose values are optimally determined by rigorous procedure.

3. Concluding Remarks

The Optimal Auxiliary Functions Method was applied to comprehensively investigate the nonlinear behaviour of a simply-supported Euler-Bernoulli beam on nonlinear elastic foundation under a moving load. The capabilities of OAFM were successfully tested on a very complex problem, which does not have exact solutions and it is very difficult to be solved by traditional methods. Highly accurate explicit analytical solutions are obtained by the proposed technique, which proves its applicability in investigating systems of strongly nonlinear differential equations in the absence of small parameters.

References

- [1] MUSTAFA A.M., HAWA M.A., HARDT D.E.: Vibration of an axially moving beam supported by slightly curved elastic foundation. *J. Vibr. Control* 2017, **24**(17):4000-4009.
- [2] TANG Y.Q., MA Z.G.: Nonlinear vibration of axially moving beam with internal resonance, speed dependent tension and tension-dependent speed. *Nonlin. Dyn.* 2019, **98**:2475-2490.
- [3] LU L., YANG X.D., ZHANG W., LAI S.K.: On traveling wave modes of axially moving string and beam. *Shock & Vibration* 2019, ID 9496180
- [4] RI K., HAN P., KAN I., KIM V., CHA H.: Nonlinear forced vibration analysis of composite beam combined with DQFEM and IHB. *AIP Advances* 2020, **10**:085112.
- [5] MARINCA V., HERISANU N., MARINCA B.: *Optimal Auxiliary Functions Method for Nonlinear Dynamical Systems*. Springer, Berlin, 2021.

Nonlinear Vibration of a Functionally Graded Beam on Winkler-Pasternak Foundation Under a Moving Force

NICOLAE HERISANU^{1*}, VASILE MARINCA²

1. University Politehnica Timisoara, Romania

2. University Politehnica Timisoara, Romania

* Presenting Author

Abstract: In this work we investigate the nonlinear thermomechanical vibrations of a functionally graded beam on Winkler-Pasternak elastic foundation. Using von Karman geometric nonlinearity, we obtain a forced nonlinear differential equation with quadratic and cubic nonlinear terms. The accuracy of the analytical results obtained by means of the Optimal Auxiliary Functions Method is proved by numerical simulations developed in order to validate the proposed procedure.

Keywords: Nonlinear vibration, functionally graded beam, Winkler-Pasternak foundation

1. Introduction

Functionally graded materials (FGM) have a wide range of applications in various fields of engineering like automotive, semiconductor industry, manufacturing industry, aerospace or defence industry. Many researchers have investigated different aspects of FGM. Nguyen and Bui [1] formulated a higher-order beam element for dynamic analysis of FGM Timoshenko beams. Soncco et al [2] utilized higher-order nodal-spectral interpolation functions to approximate the field variables minimizing the locking problem. Finite element model based on third order efficient lager-wire theory for smart FGM beam has been presented by Yasin et al [3].

In this paper we apply the Optimal Auxiliary Functions Method (OAFM) [4] to investigate dynamic behaviour of a functionally graded beam (FGB) on a Winkler-Pasternak foundation subjected to a moving force.

2. Results and Discussion

The functionally graded beam under investigation in this study is presented in figure 1.

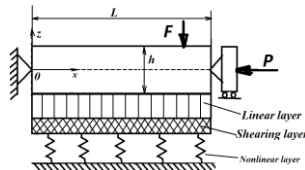


Fig. 1. Schematic of the FGB with nonlinear foundation

The functionally graded beam having the length L , the width b and the thickness h is resting on an elastic foundation of Winkler-Pasternak type and is subject to an axial force P and an axially moving force F . The mechanical properties of FGB can be varied as a power function

$$E(z) = (E_2 - E_1) \left(\frac{z + 0.5h}{h} \right)^k + E_1, \quad \rho(z) = (\rho_2 - \rho_1) \left(\frac{z + 0.5h}{h} \right)^k + \rho_1 \quad (1)$$

$$v(z) = (v_2 - v_1) \left(\frac{z + 0.5h}{h} \right)^k + v_1$$

where subscript 1 and 2 denote the top and bottom surface. Based on Euler-Bernoulli theory, we have

$$\bar{u}(x, z, t) = u(x, t) + z \frac{\partial W}{\partial x} \quad \bar{W}(x, z, t) = W(x, t) \quad (2)$$

Taking into consideration the curvature of the beam, the axial coupling and bending stiffness, the resultant force and thermal momentum, the axial force, as well as the reaction of the elastic Winkler-Pasternak foundation, the governing nonlinear thermomechanical vibration equation of FGM is

$$I\bar{W}'' + \left(D_{11} - \frac{B_{11}^2}{A_{11}L} \right) \bar{W}^{(IV)} - \bar{W}'' \left[\frac{A_{11}}{2L} \int_0^L \bar{W}^{\prime 2} dx + \frac{B_{11}}{L} (\bar{W}'(L, t) - \bar{W}'(0, t)) + N_{T\bar{x}} - P \right] = F_{\bar{W}} \quad (3)$$

where the dot and the prime denote derivative with respect to time and with respect to the variable x , respectively. After introducing dimensionless parameters and using Galerkin method, we have

$$W(x, t) = \sum_{i=1}^N X_n(x) T_n(t) \quad (4)$$

Further, after simple manipulations one obtains

$$\begin{aligned} \ddot{T}_n + \sum_{i=1}^3 a_{ij} T_j + \sum_{i=1}^3 b_{ij} T_j^3 + \sum_{i \neq j=1}^3 C_{nij} T_i T_j^2 + d_n T_1 T_2 T_3 + \sum_{i=1}^3 e_{ni} T_i^2 + \sum_{i \neq j=1}^3 f_{nij} T_i T_j = \\ = F [\cosh p_n vt - \cos p_n vt - \frac{\cosh p_n - \cos p_n}{\sinh p_n - \sin p_n} (\sinh p_n vt - \sin p_n vt)] \end{aligned} \quad (5)$$

with the corresponding initial conditions

$$T_1(0) = A, \quad T_2(0) = B, \quad T_3(0) = C, \quad \dot{T}_1(0) = \dot{T}_2(0) = \dot{T}_3(0) = 0 \quad (6)$$

At this stage, the Optimal Auxiliary Functions Method (OAFM) is employed to obtain explicit analytical solutions to (5)-(6), which are in excellent agreement with the numerical integration results.

3. Concluding Remarks

The nonlinear behaviour of the considered functionally graded beam on Winkler-Pasternak foundation was comprehensively investigated by means of an efficient analytical technique, namely the Optimal Auxiliary Functions Method which proved to be very effective and accurate in solving this kind of problems.

References

- [1] HGUEN D.K., BUI V.T.: Dynamic analysis of functionally graded Timoshenko beams in thermal environment using a higher-order hierarchical element. *Math. Problems in Eng* 2017, ID 7025750.
- [2] SONCCO K, JORGE X., ARCINIEGA R: Post buckling analysis of a functionally graded beam. *Mater. Sci. Eng.* 2019, **473**:12028.
- [3] YASIN M.Y., BEG M.S., PRAKASH B.: Static shape control of smart functionally graded beams using an efficient finite element model. *AIP Conf. Proceed.* 2020, **2273**:050059.
- [4] MARINCA V, HERISANU N, MARINCA B: *Optimal Auxiliary Functions Method for Nonlinear Dynamical Systems*. Springer: Berlin, 2021.

Pullback and forward dynamics of nonautonomous integrodifference equations: Basic constructions

HUY HUYNH^{1*}, PETER E. KLOEDEN², CHRISTIAN PÖTZSCHE¹

1. Institut für Mathematik, Universität Klagenfurt, 9020 Klagenfurt, Austria [ORCID: 0000-0002-7364-5702]
2. Mathematisches Institut, Universität Tübingen, 72076 Tübingen, Germany [ORCID: 0000-0001-9505-2257]

* Presenting Author

Abstract: In theoretical ecology, models describing the spatial dispersal and the temporal evolution of species having non-overlapping generations are often based on integrodifference equations. For various such applications the environment has an aperiodic influence on the models leading to nonautonomous integrodifference equations. In order to capture their long-term behaviour comprehensively, both pullback and forward attractors, as well as forward limit sets are constructed for general infinite-dimensional nonautonomous dynamical systems in discrete time. While the theory of pullback attractors, but not their application to integrodifference equations, is meanwhile well-established, the present novel approach is needed in order to understand their future behaviour.

Keywords: pullback attractor, forward attractor, forward limit set, nonautonomous difference equation, integrodifference equation

1. Introduction

Integrodifference equations (IDEs) occur as temporal discretisations of integrodifferential equations or as time-1-maps of evolutionary differential equations. We are interested in their iterates from a dynamical systems perspective, especially the long term behaviour of recursions based on a fixed nonlinear integral operator. In applications, the iterates for instance represent the spatial distribution of interacting species over a habitat.

2. Results and Discussion

One of the central questions in this paper is the existence and structure of an attractor. These invariant and compact sets attract bounded subsets of an ambient state space and fully capture the asymptotics of an autonomous dynamical system [4]. Extending this situation, the first main part of this paper is devoted to general nonautonomous difference equations in complete metric spaces. In particular, only a combination of several attractor notions yields the full picture:

- *Pullback attractors* [2, 5, 8, 10] are compact, invariant nonautonomous sets which attract all bounded sets from the past. As fixed target problem, they are based on previous information, at a fixed time from increasingly earlier initial times. Consisting of bounded entire solutions to a nonautonomous system [10], a pullback attractor can be seen as an extension of the global attractor to nonautonomous problems and apparently captures the essential dynamics to a certain point. However, pullback attractors reflect the past rather than the future of systems [7].
- *Forward attractors* [8] are also compact and invariant nonautonomous sets. This concept depends on information from the future and given a fixed initial time, the actual time increases beyond all bounds. Forward attractors are not unique, independent of pullback attractors, but

often do not exist. Nevertheless, we will describe forward attractors using a pullback construction, even though this has the disadvantage that information on the system over the entire time axis of integers is required.

- *Forward limit sets* is also a concept related to the information from the future. They correctly describe the asymptotic behaviour of all forward solutions to a nonautonomous difference equation [6]. These limit sets have forward attraction properties, but different from pullback and forward attractors, they are not invariant and constitute a single compact set, rather than a nonautonomous set. Nonetheless, asymptotic forms of positive and negative invariance do hold.

The initial construction of forward attractors and forward limit sets in [6] requires a locally compact state space, but recent continuous-time results in [3], which extend these to infinite-dimensional dynamical systems, will be transferred here.

For the second purpose, the above abstract setting allows concrete applications to a particularly interesting class of infinite-dimensional dynamical systems in discrete time, namely IDEs. We provide sufficient criteria for the existence of the above-mentioned notions of various IDEs. In particular, we illustrate the above theoretical results by studying pullback attractors and forward limit sets.

More complicated equations and the behaviour of attractors under spatial discretisation will be tackled in future papers.

Acknowledgment: The work of Huy Huynh has been supported by the Austrian Science Fund (FWF) under grant number P 30874-N35.

References

- [1] ATKINSON K.E: A survey of numerical methods for solving nonlinear integral equations. *J. Integr. Equ. Appl.* 1992, **4**(1):15-46.
- [2] CARVALHO A.N, LANGA J.A, ROBINSON J.C: *Attractors for Infinite-dimensional Non-autonomous Dynamical Systems*. Applied Mathematical Sciences 182. Springer: Berlin, 2012.
- [3] CUI H, KLOEDEN P.E, YANG M: Forward omega limit sets of nonautonomous dynamical systems. *Discrete Contin. Dyn. Syst. Ser. B* 2019, **13**:1103-1114.
- [4] HALE J.K: *Asymptotic Behaviour of Dissipative Systems*. Mathematical Surveys and Monographs 25. AMS: Providence, 1988.
- [5] KLOEDEN P.E: Pullback attractors in nonautonomous difference equations. *J. Differ. Equa. Appl.* 2000, **6**(1):33-52.
- [6] KLOEDEN P.E, LORENZ T: Construction of nonautonomous forward attractors. *Proc. Am. Math. Soc.* 2016, **144**(1):259-268.
- [7] KLOEDEN P.E, PÖTZSCHE C, RASMUSSEN M: Limitations of pullback attractors for processes. *J. Differ. Equ. Appl.* 2012, **18**(4):693-701.
- [8] KLOEDEN P.E, RASMUSSEN M: *Nonautonomous Dynamical Systems*. Mathematical Surveys and Monographs 176. AMS: Providence, 2011.
- [9] KOT M, SCHAFER W.M: Discrete-time growth-dispersal models. *Math. Biosci.* 1986, **80**:109-136.
- [10] PÖTZSCHE C: *Geometric Theory of Discrete Nonautonomous Dynamical Systems*. Lecture Notes in Mathematics, Vol. 2002. Springer: Berlin, 2010.

Study of the stochastic response of an offshore pile to a combined Morison force induced by current and turbulence

OSCAR SANCHEZ JIMENEZ^{1*}, EMMANUEL PAGNACCO², EDUARDO SOUZA DE CURSI³,
RUBENS SAMPAIO⁴

1. LMN, INSA de Rouen-Normandie
2. LMN, INSA de Rouen-Normandie
3. LMN, INSA de Rouen-Normandie
4. PUC-Rio, Mechanical Eng. Dept

* Presenting Author

Abstract: A set of relationships is derived allowing the characterization of the stochastic response of an offshore pile subject to the combined Morison force arising from a gaussian unidirectional stationary velocity flow and its acceleration. This equation contains a nonlinear term on the velocity and a linear term on the acceleration. The input stochastic processes, that is, the velocity and acceleration arise from a turbulent marine medium with current.

The set of relationships are established using polynomial transformations of the stochastic processes in the Morison equation and represent a link between the known statistical moments and power spectral density of the velocity and acceleration process and those of the response. The expressions allow the consideration of bending moment and shear force as responses in a straightforward fashion.

The information provided by these relationships is then applied to further study the characteristics of the response. The statistical moments are used to obtain the maximum entropy estimation of the probability density function of the response. Some connections between the asymmetry of the response and the statistical properties of the inputs can be established, with the main advantage of not requiring the time-consuming Monte-Carlo approach. The present analysis is restricted to up to the fourth moment but can be easily expanded.

Finally, the transformations of the covariance function allow the calculation of the power spectral density of the response. This information is used to estimate the extreme value distribution of the response by means of the theory of translated Gaussian processes.

Keywords: non-gaussian process, extreme value distribution, random field, maximum entropy distribution, translated gaussian process

Advanced Complex Plane Field and Differential Equations Approach to Nonlinear Dynamics of the Industrial City's Chaotic Atmospheric Ventilation

OLGA Y KHETSELIUS^{1*}, ALEXANDER V GLUSHKOV¹, SERGIY M STEPANENKO¹,
ANDREY A SVINARENKO¹ AND VASILY V BUYADZHI¹

1. Odessa State Environmental University, Mathematics Depr., L'vovskaya str. 15, 65009, Odessa

* Presenting Author

Abstract: The paper is devoted to development of an advanced mathematical approach to analysis, modelling and forecasting a chaotic dynamics of industrial city's atmospheric ventilation on the basis of complex geophysical plane field and differential equations methods. New advanced version of the Arakawa-Schubert convection model and modified hydrodynamical prediction models are presented. The methods of a plane complex field and spectral expansion algorithms are applied to calculate the air circulation for the cloud layer arrays, penetrating into the territory of the industrial city. The results of the PC simulation experiments for an chaotic air ventilation and a chaotic heat transfer in atmosphere of industrial city, including the data of modelling ventilation (meso-circulation) parameters over Gdansk (Poland) region are presented.

Keywords: nonlinear dynamics, atmospheric ventilation, complex field, differential equations

1. Introduction. Nonlinear Dynamics of Atmospheric Ventilation

Investigation of regular and chaotic energy-, heat-, mass-transfer in continuous mediums and systems is very actual and complex problems of the modern physics of dynamical systems, computational hydrodynamics etc. At present time one could remind about different simplified models that allow to estimate a structure of chaotic air ventilation in an atmosphere. However, these approaches are based on the classical laws of molecular diffusion, as well as the known regression relations models (e.g. [1]) with known disadvantages. More sophisticated approaches such as different versions of the Lagrangian particle dispersion models etc provide significantly more accurate results, however, such approaches require very complicated simulation [2]. Here a novel approach to analysis, modelling and forecasting a chaotic dynamics of industrial city's atmospheric ventilation is presented. Sketch for air ventilation between a city and its periphery in a presence of atmosphere convection is in Fig 1.

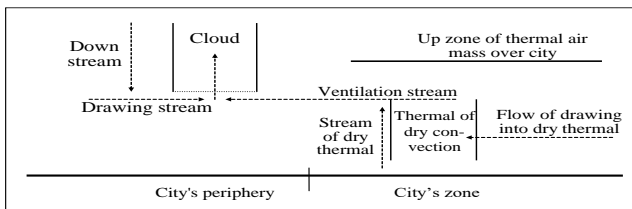


Fig. 1. Sketch for air ventilation between a city and its periphery in a presence of atmosphere clouds convection

2. Model of Nonlinear Dynamics, Results and Discussion

The Arakawa-Schubert model includes the budget equations for mass, moist static energy, total water content plus the equations of motion [1,2]. In the case of air ventilation emergence, mass balance equation in the convective thermals is as follows [13]:

$$m_B(\lambda) = F(\lambda) + \beta \int_0^{\lambda_{\max}} m_B(\lambda') K(\lambda, \lambda') d\lambda' \quad (1)$$

Here λ is a velocity of involvement, $m_B(\lambda)$ is an air mass flux, $K(\lambda, \lambda')$ is the integral equation kernel, which determines the dynamical interaction between the neighbours clouds; β is parameter which determines disbalance of cloud work due to the return of part of the cloud energy to the organization of a wind field in their vicinity. The solution of Eq. (1) is determined by a resolvent method [1,2]:

$$m_B(\lambda) = F(\lambda) + \beta \int_0^{\lambda_{\max}} F(s) \Gamma(\lambda, s; \beta) ds, \quad \Gamma(\lambda, s; \beta) = \sum_{i=1}^{\infty} \beta^{i-1} \cdot K_i(\lambda, s) \quad (2)$$

The key idea [2] is to determine the resolvent as an expansion to the Laurent series in a complex plane ζ . Its centre coincides with the centre of the city's "heating" island and the internal cycle with the city's periphery. The external cycle can be moved beyond limits of the urban recreation zone. The Laurent representation for resolvent is provided by the standard expansion:

$$\Gamma = \sum_{n=-\infty}^{\infty} c_n (\zeta - a)^n, \quad c_n = \frac{1}{2\pi i} \oint_{|\zeta|=1} \frac{\Gamma(\zeta) d\zeta}{(\zeta - a)^{n+1}} = \frac{1}{2\pi i} \int_0^{2\pi} \Gamma(e^{it}) e^{-int} dt, \quad (3)$$

where a is center of the series convergence. The method for calculating a turbulence spectra inside the urban zone should be based on the standard tensor equations of turbulent tensions (e.g. [1,11]). The velocity components, say, v_x, v_y , of an air flux over the city area are computed in an approximation of "shallow water". The necessary solution for $v_x - iv_y$ component for the city's heat island has a form of expansion into series on the Bessel functions. From the other side, the velocity of an air flux over city's periphery in a case of convective instability can be found by method of a plane complex field theory in a full analogy with the known Karman vortices chain model [1]. The results of modeling and forecasting [3] the air ventilation parameters for different synoptic situations in the Gdansk (Poland) region are presented. The detailed data about a current function and a velocity potential are listed.

3. Concluding Remarks

To conclude, a new approach to modelling an air ventilation and turbulence in the urban area is developed. The computational data on air ventilation for the typical situations in the Gdansk (Poland) region are presented. New version of the Arakawa-Schubert convection model and modified hydrodynamical prediction models are developed. The methods of a plane complex field and spectral expansion algorithms are applied to calculate the atmospheric circulation parameters.

References

- [1] KHETSELIUS O, GLUSHKOV A, STEPANENKO S, SVINARENKO A, BUYADZHI V: Nonlinear dynamics of the industrial city's atmospheric ventilation: New differential equations model and chaos. In: AWREJCWICZ J (Ed.) *Perspectives in Dynamical Systems III: Control and Stability*. Series: *Springer Proceedings in Mathematics & Statistics*. 2021, **364**:Ch.16
- [2] GLUSHKOV A, KHETSELIUS O, AGAYAR E, BUYADZHI V, ROMANOVA A, MANSARLIYSKY V: Modelling dynamics of atmosphere ventilation and industrial city's air pollution analysis: New approach. *IOP Conf. Series: Earth and Env. Sci.* 2017, 92:012014.
- [3] KHETSELIUS O: Forecasting evolutionary dynamics of chaotic systems using advanced non-linear prediction method. In: AWREJCWICZ J, KAZMIERCZAK M, OLEJNIK P AND MROZOWSKI J (EDS.) *Dynamical Systems Applications*. Politechniki Łódzkiej: Łódź, 2013, **T2**:145-152.

Dynamics of the Chaplygin sphere on a moving plane

ALEXANDER KILIN¹, ELENA PIVOVAROVA^{2*}

1. Ural Mathematical Center, Udmurt State University, Izhevsk, Russia [0000-0003-1358-5960]

2. Ural Mathematical Center, Udmurt State University, Izhevsk, Russia [0000-0001-7779-7183]

* Presenting Author

Abstract: This paper addresses the problem of a dynamically asymmetric balanced sphere rolling on a plane performing horizontal periodic oscillations. It is shown that, in the absence of gyrostatic momentum, the system admits additional integrals of motion. It is shown that the system under consideration has no steady-state solutions which exist in the unperturbed problem (in the absence of the plane's oscillations). The rolling of the sphere along a straight line can occur only in the direction of the plane's oscillations. In this case, the angular velocity vector of the sphere lies in the horizontal plane and is perpendicular to the direction of the plane's oscillations. Special attention is given to the problem of the controlled motion of the sphere by means of the variable gyrostatic momentum. Algorithms for controlling the motion of the sphere are constructed to make it rotate about the vertical and to make it move in a straight line with constant velocity relative to the moving and absolute coordinate systems.

Keywords: Chaplygin sphere, vibrating plane, nonholonomic constraint, permanent rotations, control

1. Introduction

The problem of the rolling of a dynamically asymmetric balanced sphere (the Chaplygin sphere) is one of the classical problems of nonholonomic mechanics, which was first posed and investigated in the work of S.A. Chaplygin [1]. Chaplygin obtained equations of motion of the sphere and integrated them by quadratures. Later, further inquiry into this problem was carried out in [2-4], in particular, a bifurcation analysis was performed, the trajectories of the sphere in absolute space were classified etc. This paper deals with the dynamics and control of the Chaplygin sphere moving on a plane performing periodic horizontal oscillations. The problems of controlling the motion of spherical bodies with internal propulsion devices (spherical robots) are of much current interest due to the development of robotics. In particular, in [5,6], proofs are given of the complete controllability of the system by means of three rotors, and control torques are presented for cases of motion along various trajectories, including the case where the motion occurs with friction. In [7], the dynamics and control of a spherical robot using two internal rotors is investigated. The dynamics of rigid bodies on a vibrating plane is another developing direction of research. For example, the dynamics of a wobblestone on a vibrating plane with friction is investigated in [8]. Among publications on the dynamics of spherical bodies we mention [9], where the dynamics of the sphere on the surface of complex form performing vibrations is modeled. Ref. [10] investigates the stability and addresses the problems of stabilizing the spin of the sphere with an axisymmetric pendulum rolling on a plane performing vertical vibration.

2. Results and Discussion

This paper considers the rolling of a dynamically asymmetric balanced sphere of mass m and radius ρ on a horizontal plane. It is assumed that the motion of the sphere occurs without slipping and

that the supporting plane performs horizontal periodic oscillations with velocity $\dot{\xi}(t)$. The oscillations of the plane are directed along a fixed vector α . We also assume that the sphere has gyrostatic placed inside it, which do not change the position of the center of mass of the sphere, but generate gyrostatic momentum k , which can be used to control the motion of the sphere.

The equations of motion of the Chaplygin sphere on the vibrating plane have the form

$$\begin{aligned}\tilde{\mathbf{I}}\dot{\omega} + \mathbf{k} &= (\mathbf{I}\omega + \mathbf{k}) \times \omega + m\rho\dot{\xi}(t)\beta, \\ \dot{\alpha} &= \alpha \times \omega, \quad \dot{\beta} = \beta \times \omega, \quad \dot{\gamma} = \gamma \times \omega, \\ \dot{x}_c &= \rho(\omega, \beta) - \dot{\xi}(t), \quad \dot{y}_c = -\rho(\omega, \alpha).\end{aligned}$$

where $\tilde{\mathbf{I}}\omega = \mathbf{I}\omega + m\rho^2\gamma \times (\omega \times \gamma)$, $\mathbf{I} = \text{diag}(i_1, i_2, i_3)$ is the central tensor of inertia of the sphere, ω is its angular velocity, x_c, y_c are the coordinates of the point of contact, and α, β, γ are the projections of the unit vectors of the fixed coordinate system onto the axes of the moving coordinate system attached to the sphere.

In this paper we show that, in the case of a sphere moving on a plane performing horizontal oscillations, free rolling motion in a straight line is possible only in the direction of oscillations, and the angular velocity of rotation of the sphere is horizontal and perpendicular to the direction of the plane's oscillations.

In this paper we also address the problem of controlling the motion of the sphere on a moving plane. In particular, we consider a number of problems of stabilizing the motion of the sphere by means of gyrostatic momentum k both relative to the oscillating plane and relative to the absolute coordinate system. We have obtained algorithms enabling vertical rotation and uniform motion of the sphere along a straight line relative to the moving and absolute coordinate systems. The study of these problems is motivated by the practical interest in the stabilization of the motion of a spherical robot on a moving plane (for example, inside a moving vehicle).

Acknowledgment: This work was supported by the Ministry of Science and Higher Education of Russia (FEWS-2020-0009) and the grant of the Russian Science Foundation (20-71-00053).

References

- [1] CHAPLYGIN SA: On a sphere rolling on a horizontal plane. *Mathematical Collection of the Moscow Mathematical Society* 1903, **24**:139-168.
- [2] KILIN AA: The dynamics of Chaplygin ball: the qualitative and computer analysis. *Regular and Chaotic Dynamics* 2001, **6**(3):291-306.
- [3] DUISTERMAAT JJ: Chaplygin's sphere. *arXiv:math/0409019* 2004, 101 pp.
- [4] BORISOV AV, KILIN AA, MAMAEV IS: The problem of drift and recurrence for the rolling Chaplygin ball. *Regular and Chaotic Dynamics* 2013, **18**(6):832-859.
- [5] BORISOV AV, KILIN AA, MAMAEV IS: How to control the Chaplygin ball using rotors. II. *Regular and Chaotic Dynamics* 2013, **18**(1-2):144-158.
- [6] BORISOV AV, KILIN AA, MAMAEV IS: How to control Chaplygin's sphere using rotors. *Regular and Chaotic Dynamics* 2012, **17**(3-4):258-272.
- [7] SVININ M, MORINAGA A, YAMAMOTO M: On the dynamic model and motion planning for a spherical rolling robot actuated by orthogonal internal rotors. *Regular and Chaotic Dynamics* 2013, **18**(1):126-143.
- [8] AWREJCEWICZ J, KUDRA G: Mathematical modelling and simulation of the bifurcational wobblestone dynamics. *Discontinuity, Nonlinearity, and Complexity* 2014, **3**(2)123-132.
- [9] UDWADIA FE, DI MASSA G: Sphere rolling on a moving surface: Application of the fundamental equation of constrained motion. *Simulation Modelling Practice and Theory* 2011, **19**(4)1118-1138.
- [10] KILIN AA, PIVOVAROVA EN: Stability and stabilization of steady rotations of a spherical robot on a vibrating base. *Regular and Chaotic Dynamics* 2020, **25**(6):729-752.

Nonlinear Chaotic Dynamics of Laser Diodes with an Additional Optical Injection: Dynamical and Topological Invariants

SERGEY V KIR'YANOV¹, EUGENY V TERNOVSKY^{1*}, DMITRY A NOVAK¹
AND IGOR I BILAN¹

1. Odessa State Environmental University, Mathematics Dept., L'vovskaya str. 15, 65009, Odessa

* Presenting Author

Abstract: Nonlinear chaotic dynamics of the chaotic laser diodes with an additional optical injection is computed within rate equations model, based on the a set of rate equations for the slave laser electric complex amplitude and carrier density. To calculate the system dynamics in a chaotic regime the known chaos theory and non-linear analysis methods such as a correlation integral algorithm, the Lyapunov's exponents and Kolmogorov entropy analysis are used. There are listed the data of computing dynamical and topological invariants such as the correlation, embedding and Kaplan-Yorke dimensions, Lyapunov's exponents, Kolmogorov entropy etc. New data on topological and dynamical invariants are computed and firstly presented. It has been developed an effective temporal evolutionary dynamics prediction model.

Keywords: chaotic dynamics, laser diodes, dynamical and topological invariants

1. Introduction. Nonlinear Dynamics of Chaotic Laser Diodes

The elements of chaotic dynamics in different laser systems and devices, including semiconductor lasers, laser diodes, resonators etc are of a great importance and interest because of their potential applications in laser physics and quantum electronics, optical secure communications and cryptography, and many others. At the same time, the laser's relaxation oscillation limits the bandwidth of chaotic light emitted from a laser diode and similar devices with single optical injection or feedback. This circumstance as well as a general interest to new theoretical dynamics phenomena make necessary the further studying and improvement the main features of the optical chaos communications. In Ref. [1] the authors experimentally and numerically demonstrate the route to band width enhanced chaos in a chaotic laser diode with an additional optical injection; they used the own unique experimental setup, which includes a distributed feedback (DFB) laser with a 4 m fiber ring feedback cavity (the slave laser) and the other solitary DFB laser as an injection laser (the master laser) to enlarge the bandwidth of the chaotic laser (see detailed description in Ref. [1]). The concrete technological characteristics are as follows: slave laser is biased at 28.0 mA (1.27 times threshold), and its wavelength is stabilized at 1553.8 nm with 0.3 nm linewidth (at -20 dB) and a 35 dB side mode suppression ratio; respectively, the laser's output power is 0.7 mW, and the relaxation frequency and modulation bandwidth were about 2 GHz and 5 GHz. The original set of the chaotic states before optical injection is obtained with -6.1 dB optical feedback (the feedback injection strength with a scale of the solitary slave laser's power). In this paper it has been presented the detailed numerical analysis, modelling and forecasting nonlinear dynamics of the chaotic laser diode with an additional optical injection and characteristic dynamical and topological invariants are computed.

2. Results and Discussion

The dynamics of the system can be described by a set of rate equations for the slave laser electric complex amplitude F and carrier density n , correspondingly and is represented as follows:

$$\frac{dF}{dt} = \frac{1+i\beta}{2} \left\{ \frac{g(n-n_0)}{1+\delta|F|^2} - \tau_p^{-1} \right\} F + \frac{k_f}{\tau_l} F(t-\tau) \cdot \exp[-i2\pi\eta\tau] + \frac{k_i}{\tau_l} F_j \exp[i\Delta\eta t], \quad (1)$$

$$\frac{dn}{dt} = \frac{i}{qV} - \frac{n}{\tau_N} - \frac{g(n-n_0)}{1+\delta|F|^2} |F|^2 + G(n) \quad (2)$$

where k_f and k_i denote the feedback and injection strength, the amplitude of injection laser $|F_j|$ is equal to that of the solitary slave laser, and $\Delta\eta = \eta_j - \eta_s$ is the detuning between the injection and the slave lasers. The feedback delay $\tau = 20\text{ns}$ is chosen according to [1]. As the input data for the solving the rate equations system the numerical values of the parameters have been used as: transparency carrier density $n_0 = 0.455 \times 10^6 \text{ m}^{-3}$, threshold current $i_{\text{thr}} = 22 \text{ mA}$, differential gain $g = 1.414 \times 10^{-3} \mu\text{m}^3 \text{ ns}^{-1}$, the carrier lifetime $\tau_N = 2.5 \text{ ns}$, photon lifetime $\tau_p = 1.17 \text{ ps}$, round-trip time in laser intracavity $\tau_l = 7.38 \text{ ps}$, the linewidth enhancement factor $\beta = 5.0$, gain saturation parameter $\delta = 5 \times 10^{-3} \mu\text{m}^3$ and active layer volume $V = 324 \text{ m}^3$; the simulated slave laser is biased at $1.7i_{\text{thr}}$ with 5.2 GHz modulation bandwidth. Under $k_j = 0$, growth of the parameter k_f results in a period-doubling bifurcation route to chaos, followed by a reversed route out of chaos. A chaos is realized in the region $\sim 0.04 - 0.16$ of k_f and bandwidths are $\sim 4.0 - 6.2 \text{ GHz}$. The rate equations system is numerically solved and the corresponding time series for amplitude and density are obtained. Computational processing allows to receive the following values of the correlation dimension d_2 , the Kaplan-York attractor dimension (d_L), the Lyapunov's exponents (λ_i), Kolmogorov entropy (K_{entr}), the Gottwald-Melbourne parameter (look Table 1).

Tab. 1. Correlation dimension d_2 , Lyapunov's exponents ($\lambda_i, i=1,2$), Kaplan-York attractor dimension (d_L), Kolmogorov entropy (K_{entr}), Gottwald-Melbourne parameter K_{GW}

d_2	λ_1	λ_2	d_L	K_{entr}	K_{GW}
2.94	0.358	0.096	2.80	0.454	0.94

3. Concluding Remarks

To conclude, it is presented the numerical analysis, modelling and forecasting nonlinear dynamics of the chaotic laser diode with an additional optical injection. There are listed the advanced numerical data on the topological and dynamical invariants (correlation, Kaplan-York dimensions, Lyapunov's exponents etc) of chaotic dynamics for the semiconductor laser and optical resonator systems.

References

- [1] WANG A-B, WANG Y-C, WANG J-F: Route to broadband chaos in a chaotic laser diode subject to optical injection. *Optics Lett.* 2009, 34(8):1144-1146.
- [2] GLUSHKOV AV: *Methods of a Chaos Theory*. Astroprint: Odessa, 2012
- [3] BUYADZHI V, BELODONOV A, MIRONENKO D, MASHKANTSEV A, KIR'YANOV S, BUYADZHI A, GLUSHKOV A: Nonlinear dynamics of external cavity semiconductor laser system with elements of a chaos. In: AWREJCEWICZ J, KAZMIERCZAK M, OLEJNIK P AND MROZOWSKI J (EDS.) *Engineering Dynamics and Life Sciences*. Lodz., 2017:89-96.
- [4] GLUSHKOV A, SVINARENKO A, BUYADZHI V, ZAICHKO P AND TERNOVSKY V: Chaos-geometric attractor and quantum neural networks approach to simulation chaotic evolutionary dynamics during perception process. In: BALICKI J (ED) *Advances in Neural Networks, Fuzzy Systems and Artificial Intelligence, Series: Recent Advances in Computer Engineering*. WSEAS: Gdansk, 2014, 21:143-150.

Optimal Strategies for Water Management and Self-Restoration of the Ecosystems: Nonlinear Dynamics, Stability and Controllability

NATALYA KIZILOVA^{1*}, NATALYA RYCHAK²

¹Warsaw University of Technology, Institute of Aeronautics and Applied Mechanics [0000-0001-9981-7616]

²V.N. Karazin Kharkov National University, Institute of Ecology [0000-0003-1620-3059]

Abstract: Water management strategies for water quality and availability at different population/weather/economic scenarios are considered. Different compartmental model of the water transfer between the atmosphere, surface waters, soils, groundwater to the consumer have been studied on the data available for several regions of the Ukraine. It is shown; different models predict similar non-linear dynamics with possible bifurcations between the probable trajectories depending on the population growth/death/migration rates, meteorological conditions at the global climate changes, and economic development of the region. Stability and controllability of the systems on a set of the control functions is studied. The multiscale sample entropy (MSE) approach has been used for estimation of the irregularity and stochasticity of different scenario curves. It is shown, the MSE value measured on the available experimental data can be a good predictor of the best control strategy for water management when the behaviour of the dynamical system correspond to the self-restoration processes proper to a closed ecosystem.

Keywords: ecosystems, data analyses, nonlinear dynamics, mathematical modelling, stability and controllability

1. Introduction

Drinking water quality of and availability, as well as the self-restoration abilities of ecosystems especially at the urban areas are important and difficult problems especially at the conditions of global climate change [1]. Recently the system dynamics approaches have become the most promising for quantitative estimations of possible future scenarios at given sets of model parameters proper to different ecosystems [2, 3]. The water dynamics in such systems can demonstrate chaotic dynamics [4]. In this study the scenarios with deterministic/chaotic dynamics, bifurcations, stability and controllability of the ecosystem dynamics are considered for the water management on urban territories with given distribution of the pollution sites, soils, ground and surface waters, etc.

2. Results and Discussion

An ecological system can be studied on the compartmental models with different contents of water, mineral/organic components and pollutions (Fig.1a). Such models are based on the equations of balance between the water sources and its use in manufacture, agriculture, domestic area of given relatively closed areas. The domestic water sector, as the main consumer of water, is expanding due to population growth, which in turn is a function of several variables, including birth rate (b), death rate (d), and migration rate (m) that could also be functions of time. The balance equation is [1-4]

$$N'(t) = (b+m-d)N(t), \quad (1)$$

where $N(t)$ is the population; time t is determined in months or years; $(\cdot)'$ is the time derivative; b, m and d are birth, migration and death rate coefficients for the region studied.

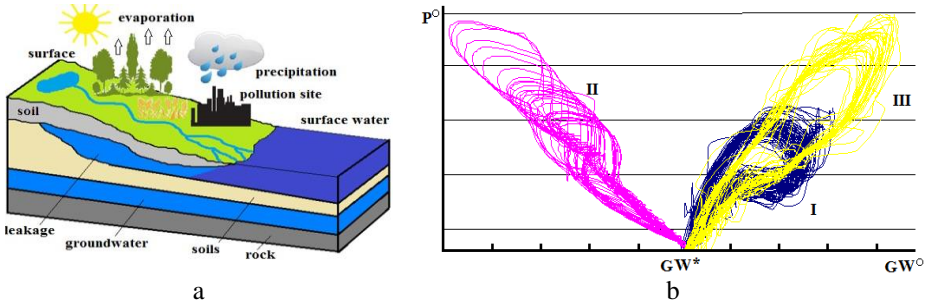


Fig. 1. Compartments of the ecological system (a) and dynamical curves $GW(P)$ (b)

The water available $W(t)$ is determined by the balance between water sources and sinks

$$W' t = k_1 SW t + k_2 GW t + k_3 CW t - k_4 U t - k_5 LW t, \quad (2)$$

where SW and $GW(t)$ are the surface and ground water, CW is controlled water saved due water economy, UW is the general used water (in industry, agriculture, domestic, etc.), LW is the lost water.

The coefficients $k_{1-5}(t)$ are known from statistical reports

Other equations are hydrologic water balance in the region, efficient changes in the groundwater potential and precipitation dynamics [1-4]

$$\sum Q_{in} t - \sum Q_{out} t = -Q_{pw} t + Q_{uw} t + Q_{sw} t + Q_r t - Q_{vp} t - Q_{pl} t, \quad (3)$$

where Q_{pw} , Q_{uw} , Q_{sw} , Q_r , Q_{vp} , Q_{pl} are percolated water, ground, surface, returned, evaporated and absorbed waters that calculated on table data with specific coefficients.

A set of trajectories of the dynamical system (1)-(3) with additional equations computed on data for Kharkov region with different future scenarios is presented in Fig.1b. It is shown, different levels of non-dimensional precipitation (P°) could result in the same level of the groundwater (GW°) and, thus, in the amount of drinking water available. Non-linear dynamics, bifurcations and control have been studied based on the multiscale sample entropy (MSE) approach.

3. Concluding Remarks

Based on the systems dynamics approach modeling the nonlinear dynamics with possible chaotic behaviour in water management and drinking water availability at different scenarios in the population, climate and economic development of a region is shown. The multiscale sample entropy value is proven to be a good predictor of the optimal strategy for water management when the behaviour of the dynamical system correspond to the self-restoration processes proper to a closed ecosystem.

References

- [1] Bjornstad O: Nonlinearity and chaos in ecological dynamics revisited. *PNAS* 2015, 112(20):6252-6253.
- [2] Burkett V, Wilcox D, Stottlemeyer R: Nonlinear dynamics in ecosystem response to climatic change: Case studies and policy implications. *Ecological Complexity* 2005, 2:357-394.
- [3] Oddi F, Miguez F, Ghermandi L: A nonlinear mixed - effects modeling approach for ecological data: Using temporal dynamics of vegetation moisture as an example. *Ecology and Evolution* 2019, 9(18):10225-10240.
- [4] Pahl-Wostl C: *The Dynamic Nature of Ecosystems: Chaos and Order Entwined*. Wiley, 1995.

Sensitivity analysis of granular dynamics by the use of unique DEM

JACEK LESZCZYŃSKI¹*

1. AGH University of Science and Technology, Faculty of Energy and Fuels, Department of Thermal and Fluid Flow Machines, Mickiewicz 30, 30-059 Krakow, Poland [https://orcid.org/0000-0001-7512-994X]

* Presenting Author

Abstract: In this study we focus on particle imperfections and simplification of processes and phenomena to their direct and/or indirect influence on the dynamics of granular matter. This has significant meaning where one may use the Discrete Element Method (DEM) for large scale computations as well as for tiny particles, i.e. particles having ultrafine dimensions. Particularly, we assess how particle size distribution (PSD), frictional forms of particle-particle collisions and Van der Waals and liquid cohesive forces, shape the particle motions. We show how neglect of above features influence on computations of particle positions and particle linear and angular velocities over time.

Keywords: granular dynamics, DEM, fractional repulsive force, particle frictions, particle cohesions

1. Introduction

Discrete Element Method (DEM) [3] is one of most popular approach that model the dynamics of granular matter and/or granular flows. Every particle is distinguished as an individual object, where its motion and linear and angular velocities versus time are registered. In this approach particle-particle and particle-wall interactions play the dominant role and many simplifications given in the modelling process could not reflect the real dynamics of particle motions. This improper dynamics is highly visible in particles having very low dimensions – called fine or ultrafine particles, and for high particle concentrations in space where multiparticle collisions occur. In this study we show how simplifications in the mathematical modelling have strong influence on the dynamics particle motions, i.e. drastic changes of particle trajectories and particle velocities.

2. Results and Discussion

We assume population of particles where n indicates the total number of particles which one takes into account in computer simulations. Individual motion of centre-mass of particle “ k ” is described by the following system of ordinary differential equations:

$$\begin{cases} m_{p_k} \ddot{\mathbf{x}}_{p_k} = \sum_l \mathbf{F}_{p_l} \\ \mathcal{I}_{p_k} \dot{\boldsymbol{\omega}}_{p_k} = \sum_l \mathbf{M}_{p_l} \end{cases} \quad (1)$$

for particles moving individually, i.e. without particle-particle or particle-wall collisions and

$$\begin{cases} m_{p_k} \ddot{\mathbf{x}}_{p_k} = \sum_{j(k), j(k) \neq k} (\mathbf{P}_{j(k)}^{rep} + \mathbf{P}_{j(k)}^{att}) + \sum_l \mathbf{F}_{p_l} \\ \mathcal{I}_{p_k} \dot{\boldsymbol{\omega}}_{p_k} = \sum_{j(k), j(k) \neq k} (\mathbf{M}_{j(k)}^{rep} + \mathbf{M}_{j(k)}^{att}) + \sum_l \mathbf{M}_{p_l} \end{cases} \quad (2)$$

taking into account particle-particle or/and particle-wall collisions. Symbolic meaning for above expressions one can find in [1,2].

Let us show the first case, where variations of initial PSDs are taken into account. Fig. 1 shows the dynamics of emptying of a container filled by dry-pea particles.

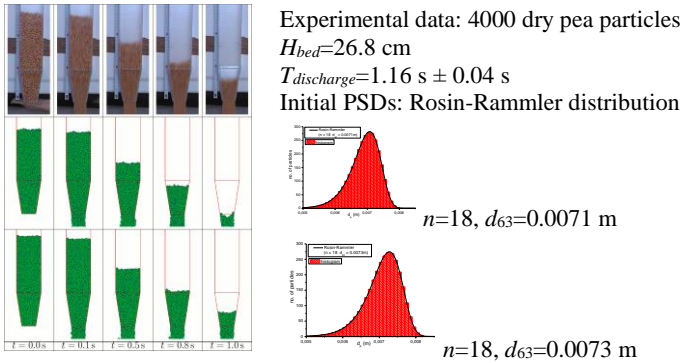


Fig. 1. Initial PSD and its influence on the discharge dynamics of pea particles from a container

Note that small variations in d_{63} delays outflow of particles, i.e. prolongs the discharge time. Fig.2 shows another scenario, i.e. the particle positions for friction and frictionless particle collisions.

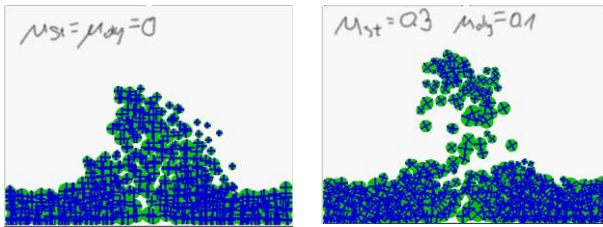


Fig. 2. The dynamics/screenshot of 500 ultrafine particles for $t=1$ s: left figure – friction-less particle collisions; right figure – static/dynamic particle frictions

Note that neglecting particle frictions one observes different particle motions.

3. Concluding Remarks

In this study we highlighted some particular aspects of DEM taking into account sensitivity analysis of variations in initial PSDs as well as friction/frictionless particle collisions having direct influence on the particle dynamics. Reflecting the real scenarios one should take into account preliminary assessment of processes and phenomena influencing to the dynamics of granular matter.

Acknowledgment: The work was carried out as part of a research subvention under contact no. 16.16.210.476 supported by the Polish Ministry of Science and Higher Education.

References

- [1] LESZCZYNSKI J.S.: Using the fractional interaction law to model the impact dynamics of multiparticle collisions in arbitrary form. *Physical Review E* 2004, **70**: 051315-1-15.
- [2] LESZCZYNSKI J.S., BLASZCZYK T.: Modelling the transition between stable and unstable operation while emptying a silo. *Granular Matter* 2011, **13**(4): 429–438.
- [3] LUDING S.: Introduction to discrete element methods. *European Journal of Environmental and Civil Engineering* 2011, **12**(7-8): 785-826.

Maximal attractor range of multiscroll chaotic attractors: classification of symmetries in hidden bifurcation routes

RENE LOZI^{1*}, TIDJANI MENACER², GUANRONG CHEN³, FAIZA ZAAMOUNE⁴

1. Université Côte d'Azur, CNRS, LJAD, Nice Cedex, France [ID 0000-0003-0451-4255]
2. University Mohamed Khider, Biskra, Algeria [ID 0000-0001-5305-3235]
3. City University of Hong Kong, Hong Kong SAR, China [ID 0000-0003-1381-7418]
4. University Mohamed Khider, Biskra, Algeria

Abstract: Multiscroll chaotic attractors of a 3D autonomous Chua-like system with saturated function series are considered. The method used to reveal hidden bifurcation routes (HBR) depending upon two parameters p and q is similar to the method recently introduced for classical Chua multiscroll attractors. However, the HBR of the saturated function series system are characterized by the maximal range extension (MARE) of their attractors and the appearance order of the scrolls which presents interesting symmetries with respect to both parameters. The approximate value of MAREs depending upon both parameters are given. They are linked to the size of the scrolls. This allows to obtain the coding of the HBR without any numerical computation.

Keywords: Hidden bifurcation, Multiscroll chaotic attractor, Saturated function series, Symmetry.

1. Introduction

Several methods have been proposed in the last three decades to generate multiscroll chaotic attractors due to their promising applications in various real-world technologies, like piecewise linear functions and nonlinear modulating functions. In electronic circuits, step, hysteresis, and saturated circuits have been built for generating multidirectional multiscroll chaotic attractors. For all the multiscrolls already known, the number of scrolls (or spirals) is a fixed integer, which depends on one or more discrete parameters. Although the majority of such multiscroll generations are known for many years, it is only recently that they are studied under the scope of bifurcation theory. Menacer et al. [1] changed the paradigm of discrete parameters by introducing hidden bifurcations, generating multiscrolls in a family of systems possessing a continuous bifurcation parameter. Then, all the classical theories of dynamical systems and their powerful tools can be used for studying the multiscrolls. In this article, the focus is on the study of the symmetries of hidden bifurcation routes in the multiscroll chaotic attractors generated by saturated function series [2].

2. Results and Discussion

The following example of multiscroll chaotic attractor (1-2) is considered:

$$\begin{cases} \dot{x} = y \\ \dot{y} = z \\ \dot{z} = -ax - by - cz + d_1 f(x, k, h, p, q) \end{cases} \quad (1)$$

with parameter values $a = b = c = d_1 = 0.7$. The number n of scrolls (also denominated spirals in [1]) satisfies $n = p + q + 2$.

$$f(x, k, h, p, q) = \begin{cases} y_{1,k} & \text{if } x > qh + 1 \\ y_{2,k,i} & \text{if } |x - ih| \leq 1, \quad i \in [-p, q] \\ y_{3,k,i} & \text{if } l_{1,i} \leq x \leq l_{2,i}, \quad i \in [-p, q - 1] \\ y_{4,k} & \text{if } x < -ph - 1 \end{cases} \quad (2)$$

Using the method defined in [1], bifurcation routes versus a continuous parameter ε in which the number of spirals is increasing are revealed (Fig. 1). The maximal attractor range extension (MARE p,q) is the size of the x -projection of the considered attractor defined by parameter values p and q , when $\varepsilon=1$ and $t \rightarrow +\infty$. It is shown that MARE $p,q = [-20 \times (p+1), 20 \times (q+1)]$, and bifurcation routes can be coded using a basic cell ($[0, 20]^{(\varepsilon)} / L$) or ($[-20, 0]^{(\varepsilon)} / R$) and some symmetry rules.

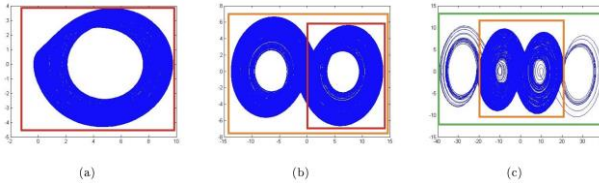


Fig. 1. The increasing number of spirals of system (1-2) modified following [1] according to increasing ε values, when $p = 2$ and $q = 3$, $k = 10$ and $h = 20$. (a): The first scroll between lies between 0 and 20 for $\varepsilon = 0.42$, (b): The second scroll on the left for $\varepsilon = 0.6$, (c): The third and the fourth scrolls: two left-right symmetrical for $\varepsilon = 0.95$. The horizontal axis is the x -axis, the vertical axis is the y -axis.

$p \backslash q$	0	1	2	3
0		[-40,20]/ B/L	[-60,20]/ B/L/L	[-80,20]/ B/L/L/L
1	[-20,40]/ B/R	[-40,40]/ B/2Sym	[-60,40]/ B/2Sym/L	[-80,40]/ B/2Sym/L/L
2	[-20,60]/ B/R/R	[-40,60]/ B/2Sym/R	[-60,60]/ B/2Sym/2Sym	[-80,60]/ B/2Sym/2Sym/L
3	[-20,80]/ B/R/R/R	[-40,80]/ B/2Sym/R/R	[-60,80]/ B/2Sym/2Sym/R	[-80,80]/ B/2Sym ³

Fig. 2. Symmetries of the hidden bifurcation routes : HBR p,q and MARE p,q , numerically computed (black) and inferred from symmetry rules (red).

3. Concluding Remarks

Hidden bifurcation routes in multiscroll chaotic attractors generated by saturated function series have been explored. These routes have interesting symmetries with respect to the two parameters allowing to obtain their coding using the new introduced tool (MARE p,q) without any numerical computation.

References

- [1] MENACER T, LOZI R, CHUA O: Hidden bifurcations in the multiscroll Chua attractor. *Int. J. Bifur. Chaos* 2016, **16**(4):1630039
- [2] LU J H, CHEN G, YU H, LEUNG H: Design and analysis of multiscroll chaotic attractors from saturated function series paper. *IEEE Trans. Circ. Syst.-I.* 2004, **51**(12):2476-2490

New Non-Stationary Solutions of the Restricted Three-Body Problem

MUKHTAR MINGLIBAYEV¹, TOREBEK ZHUMABEK²,
ALEXANDER PROKOPENYA^{3*}

¹ Al-Farabi Kazakh National University, department of mechanics [orcid 0000-0002-8724-2648]

² Al-Farabi Kazakh National University, department of mechanics [orcid 0000-0001-6865-8309]

³ Warsaw University of Life Sciences - SGGW [orcid 0000-0001-9760-5185]

* Presenting Author

Abstract: The classical restricted three-body problem is investigated analytically on basis of the concept of forces center. In the introduced special non-inertial central reference frame, we obtained new differential equations of the classical restricted three-body problem. An invariant of the forces center have been established in this reference frame. The problem is divided into two subproblems – the triangular and the collinear restricted three-body problems. New analytical exact particular non-stationary solutions of these two subproblems are found out.

Keywords: restricted three-body problem, libration points, non-inertial central reference frame, exact particular non-stationary solutions.

1. Introduction

The motion of small natural or artificial celestial body in the gravitational field of two primary bodies is well described by the mathematical model that is known as the restricted three-body problem [1-3]. Due to absence of a general solution in finite form, much aspects of the problem are studied by various qualitative and numerical methods. Search for new exact particular analytical solutions is actual except for those which are already known. In the present paper the classical restricted three-body is investigated analytically with application of a new concept based on a notion of the forces center [3].

2. Results and Discussion

We derived the differential equations of motion in the restricted three-body problem in a new special non-inertial central reference frame with the origin located at the forces center [4]. Masses of primary bodies are different. Based on properties of the new special non-inertial central reference frame, an invariant of the forces center in the restricted three-body problem is found out in analytical form. In the introduced special non-inertial central reference frame, the restricted three-body problem is divided into two different subproblems on the level of differential equations of motion [4,5]. The first one is the triangular restricted three-body problem when three bodies form triangle during all the time of their motion. The second one is the collinear restricted three-body problem when three bodies lie on the same straight line during all the time of their motion. A possibility of such separation of investigation in special non-inertial reference frame is provided by the invariant of the forces center obtained in this reference frame.

We obtained new exact analytical particular non-stationary planar solutions of differential equations of motion in the *triangular circular restricted three-body problem* in the form of isosceles triangle with variable height in the special non-inertial central reference frame [5]. The corresponding stationary solutions are well-known as the Lagrange triangular libration points. Note that obtained solutions coincide with the corresponding formulas in the particular case of the symmetrical problem of two fixed

centers [2]. We also obtained the differential equations of motion of the triangular restricted three-body problem in the rotating special non-inertial central reference frame in the pulsating variables and the obtained solutions of the triangular problem are analyzed.

There have been derived differential equations of the collinear restricted three-body problem in the rotating non-inertial central reference frame in pulsating variables [6]. We obtained three new differential equations of motion in the collinear restricted three-body problem, in three areas of possible location of the massless body, stationary solution of which corresponds to three well-known Euler libration points. We established new exact non-stationary particular analytical solutions of obtained three new differential equations of motion of the *circular collinear restricted three-body problem*.

3. Concluding Remarks

There have been obtained new exact particular analytical solutions of the planar circular restricted three-body problem. These results generalize the well-known two stationary Lagrange solutions and three stationary Euler solutions onto new areas in form of non-stationary solutions.

References

- [1] Szebehely V.: Theory of orbits: The Restricted Problem of Three-Bodies. Academic Press: New York, 1967.
- [2] Duboshin G.N.: Celestial Mechanics. Analytical and Qualitative Methods. 2nd ed. Moscow: Nauka, 1978.
- [3] Wintner A.: The Analytical Foundations of Celestial Mechanics. Dover Publications, 2014.
- [4] Minglibayev M.Zh., Zhumabek T.M., Mayemerova G.M.: Investigation of the restricted three-body problem in special non-inertial central reference frame. *Bulletin of the Karaganda University*, «Mathematics» series 2017, No. 3(87): 95-109.
- [5] Minglibayev M.Zh., Zhumabek T.M.: New exact particular analytical solutions of the triangular restricted three-body problem. *Bulletin of the Karaganda University, Mathematics series* 2020. No. 1(97): 111-121. <http://doi.org/10.31489/2020M1/111-121>
- [6] Minglibayev M.Zh., Zhumabek T.M.: On the restricted three-body problem. *News of NAS RK. Physico-mathematical series* 2021, 336 (2): 138-144. <http://doi.org/10.32014/2021.2518-1726.33>

Scaling features of cosmic rays, solar, heliospheric and geomagnetic data

RENATA MODZELEWSKA^{1*}, AGATA KRASIŃSKA², ANNA WAWRZASZEK², AGNIESZKA GIL^{1,2}

1. Institute of Mathematics, Faculty of Exact and Natural Sciences, Siedlce University, Poland
[R. Modzelewska ORCID: 0000-0002-9669-7716]

2. Space Research Centre, Polish Academy of Sciences, Bartycka Str.18A, 00-716 Warsaw, Poland

* Presenting Author

Abstract

Hurst exponent states one of the time series descriptors, allowing for the quantitative consideration of the state of the randomness, persistence or anti-persistence mode. This parameter has been used, in various types of real dynamical systems e.g., in financial analyses, solar physics or astrophysical processes. In our work we apply Hurst exponent to the revealing of the scaling features of cosmic ray intensity and anisotropy measurements over the solar cycle 24 (years 2007-2019). More precisely, using two different approaches: structure function and detrended fluctuation analysis methods we perform systematic calculation of Hurst exponent for selected physical parameters. Additionally solar, heliospheric and geomagnetic data are considered. Conducted analysis allows to identify periods with randomness and to obtain more complete picture of cosmic rays transport in the heliosphere and Earth magnetosphere throughout the solar cycle.

Keywords: scaling properties of time series, Hurst exponent, structure function, detrended fluctuation analysis

Introduction

The concept of Hurst exponent has its origins in hydrology (Hurst, 1951), and from that time it has been increasingly used in other disciplines: in finances (e.g., Di Matteo, 2007), in bio-medical time series (e.g., Ihlen, 2012), or space weather studies (e.g., Takalo and Timonen, 1998; Wanliss, 2004; De Michelis et al., 2021; Alberti et al., 2021), as well as in solar activity predictions (e.g., Singh and Bhargawa, 2017). Moreover, using Hurst exponent (e.g., Ruzmaikin et al., 1994), revealed the stochastic character of the solar activity time profile. The Hurst exponent properties were used in the analysis of compound diffusion properties, i.e., when the particles are closely connected to the magnetic field lines and the perpendicular transport origins in the random walk (Kota and Jokipii, 2000).

There are several techniques for the determination of H exponent from experimental data. In this paper, we use two approaches for establishing the Hurst exponent: the structure function and detrended fluctuation analysis methods.

Here we apply the scaling techniques to analyze the Hurst exponents of the daily cosmic ray count rates data from neutron monitor stations around the world, amplitude and phase of the diurnal (24-hours) variation of cosmic rays intensity, solar, heliospheric and geomagnetic data.

Results

The Hurst exponent is evolving with the 11-year solar activity cycle with significant variability for different cosmic ray parameters, as well as solar, heliospheric and geomagnetic data. Time series of the cosmic ray diurnal amplitude and phase evolve from the more persistent structure in and near the solar minimum to the more random character in and near the solar maximum. It is seen a transition from a weakly correlated structure near the solar minimum to uncorrelated near the solar maximum of solar cycle of heliospheric dynamics represented by cosmic ray diurnal variation. It is in agreement with the general configuration of the heliosphere, being more regular-structured near the solar minimum with the established heliospheric magnetic field and more turbulent near the solar maximum.

References

1. Hurst, H.E.: 1951, Long-term storage capacity of reservoirs. *T. Am. Soc. Civ. Eng.* 116, 770
2. Di Matteo, T.: 2007, Multi-scaling in finance. *Quantitative Finance* 7(1), 21
3. Ihlen, E.A.F.: 2012, Introduction to multifractal detrended fluctuation analysis in Matlab. *Frontiers in Physiology* 3(141), 1
4. Takalo, J. and Timonen, J.: 1998, On the relation of the AE and PC indices. *Journal of Geophysical Research* 103(A12) 29393
5. De Michelis, P., Consolini, G., Tozzi, R., Pignalberi, A., Pezzopane, M., Coco, et al.: 2021, Ionospheric Turbulence and the Equatorial Plasma Density Irregularities: Scaling Features and RODI. *Remote Sens.* 13(4), 759
6. Alberti, T. Consolini, G., De Michelis, P.: 2021, Complexity measures of geomagnetic indices in the last two solar cycle. *Journal of Atmospheric and Solar-Terrestrial Physics* 217, 105583
7. Singh, A.K., and Bhargawa, A.: 2017, An early prediction of 25th solar cycle using Hurst exponent. *Astrophys Space Sci.* 362, 199
8. Ruzmaikin, A., Feynman, J., Robinson, P.: 1994, Long-term persistence of solar activity. *Solar Physics* 149, 395
9. Oliver, R., Ballester, J.L.: 1996, Rescaled range analysis of the asymmetry of solar activity. *Solar Physics* 169, 215
10. Kóta, J. and Jokipii, J. R.: 2000, Velocity Correlation and the Spatial Diffusion Coefficients of Cosmic Rays: Compound Diffusion. *Astrophys. J.* 531, 1067

On minimax parameter estimation of nonlinear dynamic Brown's model for enzyme-substrate interaction with distributed delay

OLEKSANDR NAKONECHNYI¹, VASYL MARTSENYUK^{2*}, ALEKSANDRA KŁOS-WITKOWSKA², IULIA SHEVCHUK¹

1. Faculty of Computer Science and Cybernetics, Taras Shevchenko National University of Kyiv, Kyiv, Ukraine [0000-0002-87053070, 0000-0003-3572-4968]
2. Faculty of Mechanical Engineering and Computer Science, University of Bielsko-Biala, Bielsko-Biala, Poland [0000-0001-5622-1038, 0000-0003-2319-5974]

* Presenting Author

Abstract: The work offers Brown's model for enzyme-substrate interaction with distributed delay. The method of minimax parameter estimation is developed. The guaranteed mean-square a posteriori error is presented in terms of minimal eigenvalue of the linear operator. An example of experimental data on electrochemical biosensor design is considered.

Keywords: delayed differential equations, parameter estimation, minimax, enzyme-substrate interaction, Brown's model, Michaelis-Menten model

1. Introduction

In this paper, we offer the algorithm for finding minimax parameter estimation of Brown's model. In [1] such a minimax method was followed for finding parameter estimation of nonstationary differential equations. Similar approaches were used for the building of prediction estimations of the Gompertzian model's dynamics by Nakonechnyi O. et al [2], [3], recurrent neural networks [4], differential equations in Hilbert space [5]. We consider the Brown's model

$$\begin{cases} \dot{n}_S(t) = -k_d n_E(t) n_S(t), \\ \dot{n}_E(t) = -k_d n_E(t) n_S(t) + k_d \int_{-\tau_{\min}}^0 f(\tau) n_E(t+\tau) n_S(t+\tau) d\tau, \quad t \in (0, \bar{T}), \\ \dot{n}_P(t) = k_d \int_{-\tau_{\min}}^0 f(\tau) n_E(t+\tau) n_S(t+\tau) d\tau, \end{cases} \quad (1)$$

with initial conditions $n_S(t) = n_S^0, n_E(t) = n_E^0, n_P(t) = 0, \quad t \in [-\tau_{\min}, 0]$.

Here k_d is unknown value; $f(\tau), \tau \in [-\tau_{\min}, 0]$ is unknown function and this function is a quadratically integrable function; $\tau_{\min} > 0$ and $f(s) = 0, s < -\tau_{\min}$.

Consider that there are numbers k_0, q_1 and functions $q_2(\tau)$ and $f_0(\tau), \tau \in [-\tau_{\min}, 0]$ such that the unknown parameters k_d and $f(\tau), \tau \in [-\tau_{\min}, 0]$ belong to the set

$$G_1 = \left\{ k_d, f : |k_d - k_0| \leq q_1^2, \int_{-\tau_{\min}}^0 q_2(\tau) (f(\tau) - f_0(\tau))^2 d\tau \leq 1 \right\} \quad (2)$$

Suppose that $y_k, k = \overline{1, N}$ are the known observations of the function $n_P(t), t \in (0, \bar{T})$ with the certain k_d and $f(\tau), \tau \in [-\tau_{\min}, 0]$, namely, $y_k = n_P(t_k) + \eta_k, t_k \in (0, \bar{T}), k = \overline{1, N}$.

Here η_k , $k = \overline{1, N}$ are unknown observation errors and $\sum_{k=1}^N \eta_k^2 \sigma_k^2 \leq \gamma_N^2$, where σ_k , $k = \overline{1, N}$ and γ_N are known values. Denote $I(k_d, f) = \sum_{k=1}^N \sigma_k^2 (y_k - n_p(t_k))^2$.

Definition 1. The a posteriori set is $G_y = \left\{ (k_d, f) : I(k_d, f) \leq \gamma_N^2 \right\} \cap G_1$.

Definition 2. The value \hat{k}_d and the function $\hat{f}(\tau)$, $\tau \in [-\tau_{\min}, 0]$ are a posteriori estimations of k_d and $f(\tau)$, $\tau \in [-\tau_{\min}, 0]$ if the following condition is fulfilled: $(\hat{k}_d, \hat{f}) \in \text{Arg} \min_{(k_d, f) \in G_1} I(k_d, f)$.

Definition 3. The guaranteed mean-square a posteriori error δ of the estimations \hat{k}_d and $\hat{f}(\tau)$, $\tau \in [-\tau_{\min}, 0]$ is called the special value $\delta = \sup_{(k_d, f) \in G_y} \left(\left| k_d - \hat{k}_d \right|^2 + \int_{-\tau_{\min}}^0 (f(\tau) - \hat{f}(\tau))^2 d\tau \right)^{1/2}$.

Theorem 1. We assume that exist value β_N^2 and the positive-definite quadratically integrable function γ_N^2 , $\tau, s \in [-\tau_{\min}, 0]$ such that satisfying $G_y \subset \overline{G}_y$, where $\overline{G}_y = \left\{ (k_d, f) : \bar{I}(k_d, f) \leq 1 \right\}$,

$$\bar{I}(k_d, f) = \beta_N^2 (k_d - \hat{k}_d)^2 + \int_{-\tau_{\min}}^0 \int_{-\tau_{\min}}^0 K_N(\tau, s) (f(\tau) - \hat{f}(\tau)) (f(s) - \hat{f}(s)) d\tau ds.$$

Then the following condition for the guaranteed mean-square a posteriori error is satisfied

$$\delta \leq \left(\beta_N^2 + \lambda_{\min}(K_N) \right)^{\frac{1}{2}}. \quad (3)$$

Here $\lambda_{\min}(K_N)$ is the smallest eigenvalue of the operator $(K_N f)(\tau) = \int_{-\tau_{\min}}^0 K_N(\tau, s) f(s) ds, \tau \in [-\tau_{\min}, 0]$.

References

- [1] Nakonechnyi O. G. Shevchuk Iu. M. Chikrii V. K. Estimating Nonstationary Parameters of Differential Equations Under Uncertainty. *Cybernetics and Systems Analysis* 2018, **54**(4):610-623. doi.org/10.1007/s10559-018-0062-8
- [2] Nakonechnyi O. Zinko P. Shevchuk Iu. Guaranteed predictive estimation of solutions of system of differential equations with the Gompertzian dynamics. *Mathematical modeling and computing* 2019, **6**(1):92-100. doi.org/10.23939/mmc2019.01.092
- [3] Nakonechnyi O. Zinko P. Zinko T. Shevchuk Iu. Guaranteed Prediction Estimates of Solving Systems of Differential Equations with Gompertz Dynamics under Observations at Discrete Time Instants. *Journal of Automation and Information Sciences* 2019, **51** (5):38-53. doi.org/10.1615/JAutomatInfScien.v51.i5.40"
- [4] Nakonechnyi O. Martsenyuk V. Sverstiuk A. On Application of Kertesz Method for Exponential Estimation of Neural Network Model with Discrete Delays. Engineer of the XXI Century. *Mechanisms and Machine Science* 2020, **70**: 165-176. doi.org/10.1007/978-3-030-13321-4_14
- [5] Nakonechnyi O. Martsenyuk V. On the reduction of the identification of the parameters of a differential equation in a Hilbert space to a boundary value problem. *Miskolc Mathematical Notes* 2019, **20** (1):425-440. doi.org/10.18514/MMN.2019.2816

Fractal Techniques Associated with Steganography

NIKOLAOS NTAOULAS¹, VASILEIOS DRAKOPOULOS^{2*}

1. Department of Computer Science and Biomedical Informatics, University of Thessaly, 2–4 Papasiopoulou St., Lamia, Greece [0000-0002-7016-9974]
2. Department of Computer Science and Biomedical Informatics, University of Thessaly, 2–4 Papasiopoulou St., Lamia, Greece [0000-0002-6478-3943]

Abstract: Exploiting the properties of chaotic systems and fractals is a field of great interest and attracted a lot of attention in the last decades as far as steganography and cryptography are concerned. Their dynamic and sensitive properties lead to numerous applications and research gradually increasing through the years. The exploration of the field and the proposed applications is the main purpose of this work, through an effort to classify the main directions and techniques. The wide spread of networking and vast amount of data circulating everyday through internet reveal opportunities and dangers as far as security is concerned. The opportunity arising for steganography is obvious allowing to select various channels to transmit information hidden in a variety of multimedia files. The most frequently used files for steganography are images as there are billions transmitted every day and as they efficiently provide the properties required for hiding information. The main goals of the field, presenting the role fractals and chaos theory play, is robustness, tamper resistance, hiding capacity and perceptual transparency.

Keywords: Fractals, Steganography, Chaos, Information Hiding

1. Introduction

Privacy and Security is of high concern in general and of great importance in Information Systems. Cryptography and Steganography are the vital and fundamental methods in securing information in multiple ways (confidentiality, integrity, authentication, non-repudiation). Since the 5th century B.C. that Herodotus firstly annotates the use of wax tablets as a mean to conceal hidden messages many efforts has taken place to hide information in seemingly innocuous “vessels”. Nowadays, the wide spread of networking and vast amount of data circulating everyday through internet reveal opportunities and dangers as far as security is concerned. The opportunity arising for steganography is obvious allowing to select various channels to transmit information hidden in a variety of multimedia files. While classical cryptography is about concealing the content of messages, steganography is about concealing their existence (Anderson & Petitcolas, 1998). In digital era the hidden message is embedded in some data, normally a multimedia file which is referred to as cover and the result is referred to as stego-file. A secret key referred to as stego-key is employed for the embedding and the corresponding extraction process. Employing a cryptosystem before embedding has become familiar in steganography to enhance security. The main purpose of this work is to point out the techniques that are used in order to exploit fractals and chaos, the robustness and efficiency that is appeared as well as the security issues that arise and how these are handled.

2. Fractal techniques - Applications

The techniques used more in fractal-based steganography vastly rely on the generation of cover images. In (Zhang, Hu, Wang, & Zhang, 2011) the authors use the Julia sets to create images based on the Escape Time Algorithm. (Thamizhchelvy & Geetha, 2014) use SHA-256 hash function for the text to be hidden before embedding in a fractal image produced with a stego-key as the initial state of the IFS (Iterated Function System) provided by a Fibonacci series initialized by a PRNG (Pseudo-Random Number Generator). Some techniques involve fractal-based compression as well. In (Davern & Scott, 1996), fractal-based image compression techniques identify parts of the image that are most suited for data hiding. (Chang, Chiang, & Hsiao, 2005) employ fractal-based compression to a hidden image and embed it using a PRNG for the DCT (Discrete Cosine Transform) embedding.

Chaotic maps are extensively used in cryptography exploiting their properties. Chaotic maps are found either as a method to encrypt data before embedding or, and mostly, as a source for randomizing the embedding process. In (Enayatifar, Mahmoudi, & Mirzaei, 2009) two logistic maps randomize the selection of the modified pixels in rows and columns, respectively. (Yu, Lifang and Zhao, Yao and Ni, Rongrong and Li, 2010) use the Adaptive LSB (Least Significant Bit) method shuffling the hidden data bits by a logistic map which parameters are produced by a GA (Genetic Algorithm) with PSNR (Peak signal-to-noise ratio) as the fitness function. (Singh & Siddiqui, 2012) proposed a DCT method, embedding in the middle band coefficients, using two sequences deriving from a logistic map to embed a logo image. In (Mishra, Ranjan Routray, & Kumar, 2012) the method uses modified Arnolds cat map to scramble the hidden image and employs LSB method achieving the best result for embedding data in one Bit Plane. (Parah, Ahad, Sheikh, & Bhat, 2017) scale up medical images to produce a cover for watermark and ERP (Electronic Patient Record) which are encrypted using a logistic map and an irritative exclusive-or implementation providing results for robustness of a method embedding in the second least significant bit of the produced cover image. (Gambhir & Mandal, 2020) experiment with the efficiency of multicore processing for an LSB method using logistic map for the encryption of data before and after embedding.

3. Results – Discussion

The most familiar methods take place in the spatial domain altering, substituting or matching the LSB providing highest capacity (up to 4 LSBs can be used in each pixel's color representation). Adaptive methods in the specific domain take advantages of the edge regions or in general Regions of Interest (ROI) which provide less perceivable stego-images. Other methods proposed are in the Transform domain, like DCT, DWT (Discrete Wavelet Transform) and so on, which offer higher robustness. PSNR is the main tool to measure the disruption of a cover image. The noise added to the cover image directly affects its capacity as more information adds more noise. The capacity in most of the cases is evaluated. Moreover, there are methods generating the cover image from scratch, a familiar technique in fractal-based steganography in which the receiver's keys include the process of the image generation. Thus, there is no need for obtaining the cover image, a technique also known as blind steganography. There is an obvious trade-off between capacity and robustness as well as the level of imperceptibility, making capacity and less perceivability valuable for steganography and robustness valuable for watermarking and fingerprinting. The lack of robust information about key space and the keys characteristics is a general problem. As proven, chaotic maps are extensively researched in steganography providing mainly the randomness needed either for encryption of the secret message or the selection of the pixels and coefficients corresponding to the spatial and the transform domain methods. Logistic map is the most studied map useful in producing random sequences and Arnold's cat map is proposed secondly as a way to diffuse the pixels of a secret image taking advantage of the irritation which leads back to the initial image. Recently, research is enriched with more details of their experiments, entropy of colours, homogeneity, contrast etc. added up to the

well-known PSNR value as a metric for comparing the cover image with the stego-image. Spatial domain methods are much more prone to attacks, but they trade off the higher capacity they provide in comparison to the transform domain methods.

References

- Anderson, R. J., & Petitcolas, F. A. P. (1998). On the limits of steganography. *IEEE Journal on Selected Areas in Communications*, 16(4), 474–481. <https://doi.org/10.1109/49.668971>
- Chang, C. C., Chiang, C. L., & Hsiao, J. Y. (2005). A DCT-domain system for hiding fractal compressed images. *Proceedings - International Conference on Advanced Information Networking and Applications, AINA*, 2, 83–86. <https://doi.org/10.1109/AINA.2005.17>
- Davern, P., & Scott, M. (1996). Fractal based image steganography. *Lecture Notes in Computer Science (Including Subseries Lecture Notes in Artificial Intelligence and Lecture Notes in Bioinformatics)*, 1174, 279–294. https://doi.org/10.1007/3-540-61996-8_47
- Enayatifar, R., Mahmoudi, F., & Mirzaei, K. (2009). Using the chaotic map in image steganography. *Proceedings - 2009 International Conference on Information Management and Engineering, ICIME 2009*, 491–495. <https://doi.org/10.1109/ICIME.2009.155>
- Gambhir, G., & Mandal, J. K. (2020). Multicore implementation and performance analysis of a chaos based LSB steganography technique. *Microsystem Technologies*. <https://doi.org/10.1007/s00542-020-04762-4>
- Mishra, M., Ranjan Routray, A., & Kumar, S. (2012). High Security Image Steganography with Modified Arnold's Cat Map. *International Journal of Computer Applications*, 37(9), 16–20. <https://doi.org/10.5120/4636-6685>
- Parah, S. A., Ahad, F., Sheikh, J. A., & Bhat, G. M. (2017). Hiding clinical information in medical images: A new high capacity and reversible data hiding technique. *Journal of Biomedical Informatics*, 66, 214–230. <https://doi.org/10.1016/j.jbi.2017.01.006>
- Singh, S., & Siddiqui, T. J. (2012). A Security Enhanced Robust Steganography Algorithm for Data Hiding. *International Journal of Computer Science Issues*, 9(3), 131–139. Retrieved from www.IJCSI.org
- Thamizhchelvy, K., & Geetha, G. (2014). Data hiding technique with fractal image generation method using chaos theory and watermarking. *Indian Journal of Science and Technology*, 7(9), 1271–1278.
- Yu, Lifang and Zhao, Yao and Ni, Rongrong and Li, T. (2010). Improved Adaptive LSB Steganography Based on Chaos and Genetic Algorithm. *EURASIP Journal on Advances in Signal Processing*, 2010, 1–6. <https://doi.org/10.1155/2010>
- Zhang, H., Hu, J., Wang, G., & Zhang, Y. (2011). A steganography scheme based on fractal images. *Proceedings - 2nd International Conference on Networking and Distributed Computing, ICNDC 2011*, 28–31. <https://doi.org/10.1109/ICNDC.2011.13>

An insight into amplitude-depended modulation transfer due to nonlinear shear wave interaction with contact interfaces

MARIUSZ OSIKA^{1*}, RAFAŁ RADECKI², ALEKSANDRA ZIAJA-SUJDAK³,
WIESŁAW J. STASZEWSKI⁴

1. Department of Robotics and Mechatronics, AGH University of Science and Technology, al. Mickiewicza 30, 30-059 Krakow, POLAND [0000-0002-7999-4305]
2. Department of Robotics and Mechatronics, AGH University of Science and Technology, al. Mickiewicza 30, 30-059 Krakow, POLAND [0000-0003-0987-7661]
3. Department of Robotics and Mechatronics, AGH University of Science and Technology, al. Mickiewicza 30, 30-059 Krakow, POLAND [0000-0002-2101-3009]
4. Department of Robotics and Mechatronics, AGH University of Science and Technology, al. Mickiewicza 30, 30-059 Krakow, POLAND [0000-0003-3071-7427]

* Presenting Author

Abstract: This paper discusses the influence of the excitation amplitude on the transferred side-bands due to interaction between propagating shear waves and contact interfaces. Two cases of contact model are scrutinized using numerical tool based on Local Interaction Simulation Approach (LISA), namely the frictional contact and piecewise elasticity change. It is shown for the first case that comparable values of amplitudes of the modulated pumping wave and the probing wave leads to the modulations transfer phenomenon. However, in the latter case, it is necessary for the amplitude of the modulated pumping wave to be larger than the one of the probing wave to observe a transfer of modulation. This work lays the foundation for further analysis, which will help to distinguish the input condition for monitoring the state of the structures using methods based on the shear wave modulation transfer.

Keywords: Nonlinear Shear Wave, Friction, Piecewise Elasticity, LISA, L-G

1. Introduction

The structural evaluation techniques based on the nonlinear features of the propagating ultrasonic waves have recently received a lot of academic attention. It is known, that nonlinear sources can impact the propagating ultrasonic wave, generating high-order harmonics, side-bands (cross-modulation), frequency shift or modulation transfer. The physical mechanism of these phenomena are different, and appropriate models need to be established to facilitate in-depth understanding of the experimentally observed dependences, e.g. between the wave amplitude and the modulation transfer intensity.

In this paper, a particular case of the modulation transfer phenomenon for shear horizontal (SH) waves is analysed using the Local Interaction Simulation Approach (LISA) framework. Two crack surfaces contact models are considered, the Coulomb friction model and the nonclassical piecewise elastic model [1]. For the latter, a piecewise stress-strain relation with stiffness reduction is assumed. A parametric study is conducted to check the influence of the excitation amplitude on the modulation transfer, due to nonlinear interaction of the shear waves and contact interfaces.

2. Results and Discussion

The results from two numerical models based are presented in Fig. 1. The top and bottom one corresponds to the implemented Coulomb friction model and a local piecewise elastic nonlinearity model, respectively. To observe the modulation transfer, the pumping and probing waves are excited simul-

taneously by a displacement uniformly distributed over the thickness of the plate. For both numerical cases, the pumping wave is a high frequency amplitude modulated acoustic wave with the carrier frequency $f_1 = 490$ kHz and the modulation frequency $f_m = 21$ kHz [2]. The probing wave is a mono-harmonic wave with the frequency $f_2 = 85$ kHz. A parametric study was performed to investigate the influence of the amplitude ratio on the manifested modulation transfer. The results presented in Fig.1 correspond to the displacement excitation amplitudes of the pumping and probing waves both equal to $1 \mu\text{m}$ for Coulomb friction model; and respectively $1 \mu\text{m}$ and $0.2 \mu\text{m}$ for the piecewise elastic crack model.

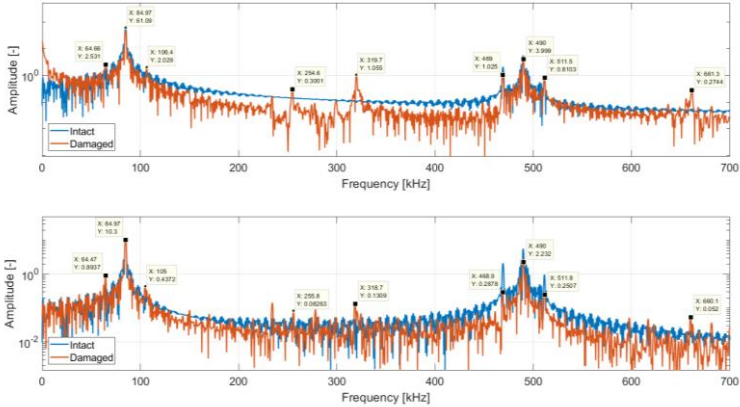


Fig. 1. Numerical results obtained from SH-LISA in frequency domain for intact and damaged structures for Coulomb friction model (top) and nonclassical local elastic nonlinearity (bottom).

Regardless of the chosen excitation amplitudes, for both models of the crack, in the frequency spectrum of results, it is possible to identify the modulation transfer sidebands ($f_2 \pm f_m$), the odd higher harmonics $(2n+1) f_1$ and $(2n+1) f_2$, and the mixed terms responsible for the generation of sidebands around the frequency $f_1 \pm 2 f_2$. Also, for the classical friction model, the modulation transfer is always present. In contrast, for the assumed piecewise elastic model of the crack, the amplitude of the excited pumping wave had to be chosen as at least five times greater than the probing wave to observe a significant modulation transfer.

3. Concluding Remarks

In this work, the impact of the crack models and amplitude of the excitation on the frequency characteristics of guided SH waves is investigated. The simulation results show that the modulation transfer from the high frequency pumping wave to the probing wave can be observed for both implemented crack models. However, the intensity of this phenomenon is amplitude dependent and requires further research.

Acknowledgment: The work presented in this paper was performed within the scope of the research project UMO-2018/30/Q/ST8/00571 financed by the Polish National Science Centre.

References

- [1] KLEPKA A., *ET AL.*: Experimental investigation of hysteretic stiffness related effects in contact-type nonlinearity. *Non. Dyn.* 2019, **95**:1513-1528.
- [2] CARCIONE A., *ET AL.*: Modulated high frequency excitation approach to nonlinear ultrasonic NDT. *J. Sound Vib.* 2019, **446**: 238-248.

Numerical and theoretical investigations of modulation transfer due to nonlinear shear wave interaction at frictional interfaces

RAFAL RADECKI¹, ALEKSANDRA ZIAJA-SUJDAK², MARIUSZ OSIKA³,
WIESLAW J. STASZEWSKI⁴

1. Department of Robotics and Mechatronics, AGH University of Science and Technology, al. Mickiewicza 30, 30-059 Krakow, POLAND [0000-0003-0987-7661]
2. Department of Robotics and Mechatronics, AGH University of Science and Technology, al. Mickiewicza 30, 30-059 Krakow, POLAND [0000-0002-2101-3009]
3. Department of Robotics and Mechatronics, AGH University of Science and Technology, al. Mickiewicza 30, 30-059 Krakow, POLAND [0000-0002-7999-4305]
4. Department of Robotics and Mechatronics, AGH University of Science and Technology, al. Mickiewicza 30, 30-059 Krakow, POLAND [0000-0003-3071-7427]

* Presenting Author

Abstract: Presented paper investigates the modulation transfer observed for the propagating shear wave due to the interaction with the nonlinear frictional contact interfaces. The analytical results based on the Harmonic Balance expansion, are compared with a numerical approach based on the Local Interaction Simulation Approach (LISA). In the scrutinized case, two source shear wave excitations are considered. First referred as probing wave is a single frequency sine wave, and a second referred as pumping wave is a single frequency sine wave modulated by a sine wave of one-order lower frequency. The excited wave interacts with the nonlinear frictional interfaces, causing a modulation transfer. Interestingly, despite the symmetric characteristic of considered local source of nonlinearity, the transfer of all orders of sidebands is observed.

Keywords: Nonlinear Shear wave, Friction, Modulation, LISA, Harmonic Balance

1. Introduction

The maintenance of engineering structures requires reliable methods for detection and assessment of structural damages and material degradation. Various methods based on elastic waves propagation in solids were proposed and implemented to detect fatigue cracks, delamination, debonding etc. Recently, nonlinear ultrasonic-based methods are of a particular interest, as they offer remarkable sensitivity to broad class of damage related phenomena, at early stages. Incipient defects can be investigated by virtue of classical nonlinear effects such as higher harmonic generation, or non-classical effects e.g. hysteresis, slow dynamics, stress-strain hysteresis, or modulation phenomenon. In particular, the modulation phenomenon draws our attention. First, due to the fact that its is not particular investigated for the shear wave propagation in the structure, and second, the possibility to observe the existence of the nonlinear phenomenon in the close proximity of the excited frequency in a form of side-bands. In this work, a particular case of modulation transfer phenomenon is investigated using a numerical tool based on LISA [1], and a theoretical approach based on Harmonic Balance method (HBM) [2].

In the presented study, propagation of the Shear Horizontal (SH) waves in a linear medium with a local nonlinearity is considered. As a source of the nonlinear phenomenon, the shear stick-slip movement of fatigue crack surfaces is assumed. The faces of the crack interact mechanically by the friction force, which results from the contact between asperities under a normal force. This is imple-

mented in the numerical model as Coulomb friction formulation of crack surfaces behaviour. To facilitate the comparison of LISA and HBM, the crack is modelled as a through-thickness crack localized in the middle of the plate length. In order to observe the modulation transfer, pumping and probing waves are excited simultaneously in the structure by a displacement uniformly distributed over the thickness of the plate.

2. Results and Discussion

The results from two modelling approaches are presented in Fig 1. The pumping wave is a high frequency amplitude modulated acoustic wave with $f_1 = 490$ kHz and $f_m = 21$ kHz and the probing wave is monoharmonic acoustic wave with $f_2 = 85$ kHz.

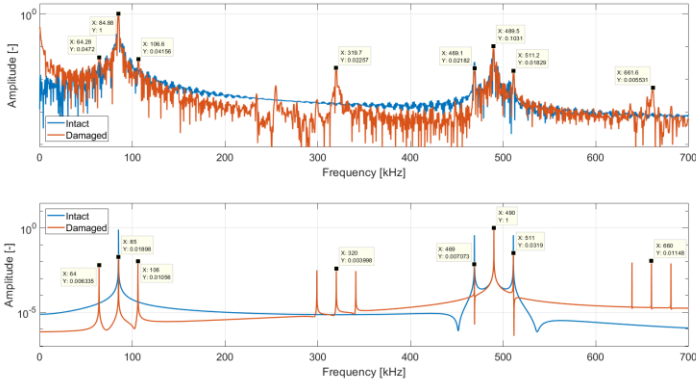


Fig. 1. Numerical results obtained from SH-LISA (top) and HB (bottom) in frequency domain for intact and damaged structures.

In the results of both models, it is possible to distinguish the following terms: the modulation transfer sidebands ($f_2 \pm f_m$), the odd higher harmonics $-(2n+1)f_1$ and $(2n+1)f_2$ – and the mixed terms responsible for the generation of sidebands around the frequency $f_1 \pm 2f_2$.

3. Concluding Remarks

The results clearly indicate that the modulation transfer from the high frequency pumping wave to the probing wave is invariant/insensitive to the type of nonlinearity in the examined structure. Because Coulomb friction is a symmetric type of nonlinearity, in the higher-harmonic generation analysis only odd harmonics are expected. Similarly, in the cross-modulation– f_2 signal modulating f_1 – only even side-bands should appear. These phenomena are observed for the investigated models. In contrast, the f_m modulation components have transferred in all orders, both for LISA and HBM models. This gives a new insight on the conditions of modulation transfer, which depends on the type of source of nonlinearity.

Acknowledgment: The work presented in this paper was performed within the scope of the research project UMO-2018/30/Q/ST8/00571 financed by the Polish National Science Centre.

References

- [1] OSIKA M., *ET AL.*: Modelling of the shear horizontal waves high-order harmonics generation using local interaction simulation approach. *EWSHM: special collection of 2020 papers*, 2020, **1**:200-209.
- [2] RADECKI R., *ET AL.*: Prediction of higher-order harmonics generation due to contact stiffness hysteresis using Harmonic Balance: theory and experimental validation. *Non. Dyn.* 2021, **103**(1): 541–556.

The effect of a shaker on the resonance frequencies of a circular plate

WOJCIECH RDZANEK¹

University of Rzeszow, Rzeszow, Poland, 0000-0003-4328-5563

Abstract: This study presents the analysis of the effect of the concentrated mass on the resonance frequencies of a vibrating thin circular plate. The eigenfunction expansion has been used to express the transverse displacement of the plate. The appropriate number of modes is determined approximately to achieve physically correct results. Then highly accurate results are obtained numerically. The mean square vibration velocity used to determine the resonance frequencies of the plate. The introducing of the concentrated mass is justified by modelling the added mass of the moving component of the exciter.

Keywords: added mass, exciter, circular plate, resonance frequencies, modal expansion

1. Introduction

An accurate determination of the resonance frequencies of vibrating structures is of the utmost importance in diagnostics and design both in mechanical engineering and physical systems. So far, a number of studies dealt with such problems. Some examples are the results proposed by Ostachowicz et al. [1] who used a diagnostic method for localization of concentrated masses on a vibrating plate. They used the method of analysing the shifts in the resonance frequencies. Further, Cho et al. [2] examined dynamic responses of stiffened panels with added masses and openings. Wrona et al. [3] applied the added masses for shaping the dynamic responses of rectangular planar panels.

One of the methods of examining the frequency responses of structures is using the electromagnetic exciters. The investigated structure is then excited within the desired frequency range and the normal vibration velocity is measured in selected points on the structure. The exciter needs to have sufficient force over the analyzed frequency interval. Usually the mass of the moving component of the excited is significant compared to mass of the structure. In such cases the effect of the added mass of the exciter on the resonance frequencies of the structures should not be neglected. This paper focuses on this problem. The examined structures is a thin circular plate. The plate is free at its circumferences and mounted at its centre to the excited. This selection motivated by the simplicity of the structure and numerical analysis. The modal expansion of the plates vibrations is used along with the in-vacuo eigenfrequencies of the plate. Applying this expansion requires to carefully determine all the necessary modes of the plate to achieve physically correct results. Therefore the nondimensionalized added mass incrementals are determined to estimate roughly the resonance frequencies. Then some more modes will be taken for calculations to achieve desired numerical accuracy. The proper and accurate determination of the resonance frequencies of structures is an important practical problem. Therefore some sample results are presented herein.

2. Results and Discussion

The equation of motion of the excited plate can be presented as follows (e.g. Rao [4] Eq. (14.200) or Ostachowicz et al.)

$$D\nabla^4 W - \rho h \omega^2 W - m_c \omega^2 \delta(\vec{r} - \vec{r}') W = P, \quad (1)$$

where W is the transverse displacement of the plate, D is the plate's stiffness, ∇^4 is the biharmonic operator, ρ is the plate's density, h is its thickness, ω is the angular frequency, m_c is the concentrated mass of the moving component of the exciter, δ is the Dirac delta, \vec{r} is the radius vector on the plate, \vec{r}' is the radius vector of the concentrated mass, and P is the external excitation. In this particular study the external excitation is the point excitation at the same point as the concentrated mass of the exciter.

3. Concluding Remarks

The method of modal expansion can be successfully applied for analysis of dynamic responses of a vibrating circular plate given that the following requirements are satisfied. The resonance frequencies are initially predicted using the approximated calculations for a single dominant mode. Then the appropriate number of modes can be determined to obtain physically correct results. Further, the accurate values of resonance frequencies can be determined by finding local maximums of the mean vibration velocity on the plate. As the main disadvantage of the point excitation is that it can point to a nodal line, the dynamic responses of the physical system should be averaged over a number of different excitation points.

Acknowledgment: The research presented in this paper was partially supported under The Centre for Innovation and Transfer of Natural Sciences and Engineering Knowledge Project at The University of Rzeszow in Poland.

References

- [1] OSTACHOWICZ W, KRAWCZUK M, CARTMELL M: The location of a concentrated mass on rectangular plates from measurements of natural vibrations, *Computers & Structures* 2002, **80**(16–17): 1419-1428.
- [2] Cho DS, Kim BH, Kim J-H, Choi TM, Vladimir N: Free vibration analysis of stiffened panels with lumped mass and stiffness attachments, *Ocean Engineering* 2016, **124**:84-93.
- [3] Wrona S, Pawelczyk M, Qiu X: Shaping the acoustic radiation of a vibrating plate, *Journal of Sound and Vibration* 2020, **476**:115285.
- [4] Rao S: *Vibrations of Continuous Systems*, Wiley, New Jersey, 2007.

Taking into account uncertainties in non-linear dynamical systems with nonlinear energy sinks (NES)

PATRICIA SANTANA REYES^{1*}, EMMANUEL PAGNACCO², RUBENS SAMPAIO³

- 1*. Institut National des Sciences Appliquées (INSA)
2. Institut National des Sciences Appliquées (INSA)
3. Pontifical Catholic University of Rio de Janeiro (PUC-Rio)

Abstract:

We will study the dynamics of a linear principal system, which is weakly coupled to a nonlinear attachment. This nonlinearity of the accessory allows it to resonate with any of the linearized modes of the principal system, allowing us to have a passive and irreversible energy transfer from the principal system to the NES.

An interesting feature of linear systems with essentially nonlinear attachments is the possibility of resonance capture cascades, meaning that nonlinear attachments can be designed to resonate and extract energy from an a priori specified set of modes of a nonlinear structure. As a result, even when the forcing conditions are simple as periodic, the system response can be quasi-periodic.

The objective of this study is to study the absorption of energy when uncertainties are considered in the coupling parameters between the principal system and the NES. Hence, we will propose and compare the accuracy and efficiency of different uncertainty quantification strategies based on Polynomial Chaos and Proper Orthogonal Decomposition. While it is well known -and prove- that the use of Polynomial Chaos has severe shortcomings for dynamical systems, we will demonstrate that new proposals allow to obtain accurate results with good efficiency, even in the non-linear and particularly difficult context of NES.

Keywords: dynamical system, nonlinear energy sink, uncertainty propagation, polynomial chaos, proper orthogonal decomposition.

Controllable Optical Rogue Waves by Modulated Coherent-Incoherent Nonlinearities in Inhomogeneous Fiber

K. SAKKARAVARTHI^{1*}, T. KANNA²

¹ Asia-Pacific Center for Theoretical Physics (APCTP), Pohang - 37673, Korea [0000-0002-1864-474X]

² Nonlinear Waves Research Lab, PG & Research Department of Physics, Bishop Heber College (Autonomous), Tiruchirappalli - 620017, Tamil Nadu, India [0000-0003-4543-1501]

* Presenting Author Email: ksakkaravarthi@gmail.com

Abstract: The system under consideration is a coherently coupled nonlinear Schrödinger equation consisting of temporally varying coherent and incoherent nonlinearities. We investigate the impact of nonlinearity modulation in the dynamics of doubly-localized optical rogue waves appearing in Kerr-type nonlinear optical media. We explore the possibility of controlling bright-dark and bright-bright rogue waves possessing different localized structures by adopting the constructed rogue wave solution and similarity transformation through appropriately choosing the modulated nonlinearities by elliptic functions. We demonstrate our arguments by choosing two types of nonlinearities that can expose the existence of single and multi-peak (with double or multi-dip) symmetric/asymmetric rogue waves appearing on the periodic background and tunnelling through a barrier/well with modulations in their profiles.

Keywords: Rogue wave, Inhomogeneous optical media, Coherently coupled NLS equation

1. Introduction

The dynamics of localized nonlinear waves and their existence/interaction with other waves are attracting considerable in the past few decades. With the help of computational tools, it becomes relatively possible to investigate any theoretical model of either multicomponent or multi-dimensional nature possessing various categories of nonlinear waves. Much attention is being paid to localized waves such as solitons, breathers, and rogue waves, and so on. Considering the above intention and experimental observation, we aim to investigate the nature and evolution of rogue waves under a nonlinearity-managed optical fiber system. For this purpose, we consider the following two-component coherently coupled nonlinear Schrödinger equations describing the beam propagation in an optical fiber [1-3]:

$$\begin{aligned}iQ_{1T} + Q_{1XX} + \gamma(T)(|Q_1|^2 + 2|Q_2|^2)Q_1 - \gamma(T)Q_2^2Q_1^* - V(X, T)Q_1 &= 0, \\iQ_{2T} + Q_{2XX} + \gamma(T)(2|Q_1|^2 + |Q_2|^2)Q_2 - \gamma(T)Q_1^2Q_2^* - V(X, T)Q_2 &= 0,\end{aligned}$$

where X and T are the normalized distance and retarded time, while $V(X, T)$ denotes a graded refractive index profile. Further, the model consists of a constant second-order dispersion along with temporally varying incoherently-coupled (self-and cross-phase modulations) and coherently-coupled type four-wave mixing nonlinearities. There exist a considerable number of works providing a detailed study on solitons, breathers, and rogue waves of Eq. (1) and similar versions, for which one can refer to [4-6] and references therein.

2. Results and Discussion

We identify a similarity transformation that can relate Eq. (1) with varying coefficients to that of a constant-coefficient coupled NLS equation along with a condition as Riccati equation and the form of

modulated spatial and temporal parameters [7,8]. Using the known rogue wave [9], we construct an explicit form of rogue wave solution with temporally varying nonlinearity. The solution admits symmetric bright type doubly-localized rogue waves in both components as a simple case. Further, the rogue waves support bright, grey, and dark type asymmetric profiles having single or double peaks and two or multiple dips in amplitude, that can be altered by tuning the four arbitrary complex parameters apart from six real similarity constants used to manipulating them to appear on different background and undergo deformation/modulation of structure. To understand, we have demonstrated grey-bright and bright-dark rogue waves and their nonlinearity-controlled behaviour in Fig. 1. Here we can note that the rogue waves appear on the periodic background for $\gamma(t)=h_1+h_2 \sin(h_3 t+h_4)$ and tunnel through a localized barrier when $\gamma(t)=h_1+h_2 \operatorname{sech}^2(h_3 t+h_4)$ with modulations in their profiles.

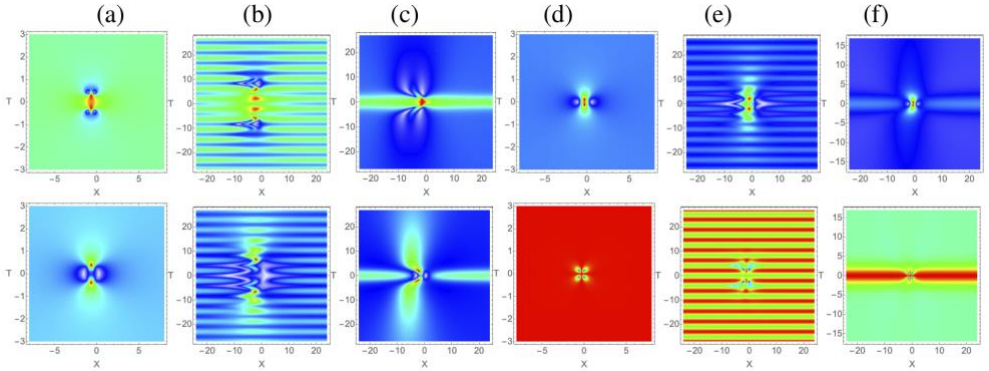


Fig. 1 (a) Grey-bright and (d) bright-dark rogue waves with constant nonlinearity. (b & e) Modulated rogue waves on periodic type for $\gamma(t)=I+0.5 \sin(0.75 t+0.25)$. (c & f) Manipulated rogue waves due to a localized barrier backgrounds for $\gamma(t)=I+1.5 \operatorname{sech}^2(0.75 t+0.25)$. Top panel: Q_1 and bottom panel: Q_2

3. Conclusions

Nonlinear waves (especially rogue waves) admitting different localized structures can be manipulated by appropriately choosing the temporally-varying nonlinearity in inhomogeneous optical fiber system.

Acknowledgment: KS was supported by Asia Pacific Center for Theoretical Physics (APCTP) as a Postdoctoral Researcher through Young Scientist Training program.

References

- [1] KIVSHAR YS, AGRAWAL GP: Optical Solitons: From Fibers to Photonic Crystals, Academic Press, San Diego (2003).
- [2] PARK QH, SHIN HJ: Phys. Rev. E **59** (1999) 2373.
- [3] CENTURION M, PORTER MA, KEVREKIDIS PG, PSALTIS D: Phys. Rev. Lett. **97** (2006) 033903.
- [4] KANNA T, VIJAYAJAYANTHI M, LAKSHMANAN M: J. Phys. A: Math. Theor. **43** (2010) 434018.
- [5] KANNA T, SAKKARAVARTHI K: J. Phys. A: Math. Theor. **44** (2011) 285211.
- [6] SAKKARAVARTHI K, KANNA T: J. Math. Phys. **54** (2013) 013701.
- [7] SAKKARAVARTHI K, BABU MAREESWARAN R, KANNA T: Phys. Scr. **95** (2020) 095202.
- [8] BABU MAREESWARAN R, SAKKARAVARTHI K, KANNA T: J. Phys. A: Math. Theor. **53** (2020) 415701.
- [9] LI Z-D, HUO C-Z, LI Q-Y: Chin. Phys. B **27** (2018) 040505.

Development of a mathematical model for the functioning of a river port discharge point

VIKTOR STRELBITSKYI¹, STANISLAW RAJBA³, NATALIJA PUNCHENKO²,

NADIJA KAZAKOVA², RAFAL SZKLARCZYK³, RUSLANA ZIUBINA³

1. Odessa National Maritime University [ORCID]
2. Odessa State Environmental University [ORCID]
3. University of Bielsko-Biala

* Presenting Author

Abstract: The current stage in the development of transportation in river ports is characterized by an increase in requirements for the timing of cargo delivery, quality of transportation, reduction of costs for transport and storage operations. In the transportation system, transport hubs are the central link, since cargo delivery begins and ends in them, processes of transshipment of cargo from one mode of transport to another take place. Should be noted that transshipment operations at the port are among the most time-consuming and difficult work on river and sea transport, the implementation of which is impossible without the use of modern information technologies and automated systems. Since the use of such systems can reduce the time and increase the quality of cargo handling. A mathematical model of a discharge point at the port is explicated, which describes the process of its functioning, is a state graph for a transport node. To calculate the probabilities of all possible states of this system, a system of algebraic equations is used. This allows to simplify the calculation of the possibility of transition from one state to another, which are determined by the state of trucks, since the solution of the resulting system of linear algebraic equations is not difficult and can be implemented in any mathematical program package. The waiting and maintenance times of trucks A and B are determined, with calculated by the ratio of the probabilities of the system states, quantitative values can be considered as justification for deciding on determining the efficiency of the transport system.

Keywords: graph, states, transshipment point, freight autocar, transport system

1. Introduction

The transport industry is one of the basic elements of the state economy, which operates an extensive railway network, a developed network of roads, seaports and river terminals, airports and a wide network of air connections, cargo customs terminals. Transport is one of the basic elements of the state economy.

Therefore, meeting the needs of the citizens regarding the provision of necessary transport services and business development is prioritized.

2. Results

Tables Transshipment of cargo is a complex technological process, which depends on the following factors: uneven receipt of vehicles and goods, failure of loading and unloading mechanisms and points, interchangeable level of operational reliability, intra-terminal movement of goods, etc.

The incoming flow of actions is formed by machines that arrive at the transshipment point at random times. According to the survey, it was revealed that the cargo point is a queuing system (waiting line), the functioning of which is a random process with discrete states and continuous time. In addition, the analysis of statistical data showed that this process is Markov [8-10].

When developing a model, the following restrictions are used:

- 1) 1 point is considered, which is served by 2 trucks (machine A and machine B) with an equal priority of unloading among machines ($A = B$);
- 2) the conditions of the transport system are determined by the conditions of trucks A and B, which may be in the following states: 0 – absence of the machine at the unloading point; 1 – unloading the machine at the point; 2 – waiting for the machine for maintenance;
- 3) when developing a system state graph, due to the low probability of events, we exclude the simultaneous arrival and instant arrival of machine B after unloading machine A;
- 4) the model is stochastic and the states of the vertices of the graph are independent of each other.

If all possible transitions of the system from state to state according to the operating conditions of the unloading point are described graphically, we obtain a model of the point in the form of an oriented state graph, which describes the "behaviour" of the transport system.

$$\begin{cases} P_0 + P_1 + P_2 + P_3 + P_4 = 1 \\ -(\lambda_{10} + \lambda_{13}) \cdot P_1 + \lambda_{01} \cdot P_0 + \lambda_{41} \cdot P_4 = 0 \\ -(\lambda_{20} + \lambda_{24}) \cdot P_2 + \lambda_{02} \cdot P_0 + \lambda_{32} \cdot P_3 = 0 \\ -\lambda_{32} \cdot P_3 + \lambda_{13} \cdot P_1 = 0 \\ -\lambda_{41} \cdot P_4 + \lambda_{24} \cdot P_2 = 0 \end{cases} \quad (1)$$

The resulting system of equations (1) forms the basis of the created mathematical model of a discharge point in the port. The numerical values of λ_i of the system for equations can be determined experimentally or according to the standards [1–3]. The waiting and maintenance times of trucks A and B are determined, respectively, by the ratio of the probabilities of the states of the system P_4/P_1 and P_3/P_2 , the expectation is not more than a given number in % of their service time. The developed graph-model of transshipment processes will allow to describe the functioning of the port transshipment point and effectively draw up routes for vehicles.

The proposed methodology for assessing the risks of vehicle downtime. The proposed approach is universal, since it does not depend on the type of cargo and machine. This model, after some refinement, can be used when servicing an item with many machines. The practical significance of the work lies in the application of its results to create new and improve existing processes for the transport of goods by road in the port, to evaluate the effectiveness of their work, to justify the cost of transportation of goods. The results can be used to justify production decisions.

3. Concluding

The approaches to the development of a mathematical model of a transport unit in the form of a graph-model considered in the article allow to solve the problem of the efficiency of cargo transshipment in a transport unit.

References

- [1] 1. KIA, M.; SHAYAN, E.; GHOTB, F. THE IMPORTANCE OF INFORMATION TECHNOLOGY IN PORT TERMINAL OPERATIONS. INT. J. PHYS. DISTRIBUT. LOGIST. MANAG. (2000).
- [2] 2. STEPANOV A. L., TUARSHEVA O. A. TECHNOLOGY AND ORGANIZATION OF THE RELOADING PROCESS. SPB.: PUBLISHING HOUSE GMA THEM. ADM. S. O. MAKAROVA (2004).
- [3] 3. VETRENKO L. D., ANAN'INA V. Z., STEPANETS A. V. ORGANIZATION AND TECHNOLOGY OF CARGO HANDLING PROCESSES IN THE SEAPORTS: TEXTBOOK FOR UNIVERSITIES. MOSCOW, TRANSPORT PUBL., (1989).

Sound radiation by a circular plate located on a wall of rectangular semi-infinite waveguide

KRZYSZTOF SZEMELA^{1*}, WOJCIECH RDZANEK², JERZY WICIAK³, ROMAN TROJANOWSKI⁴

1. College of Natural Sciences, Institute of Physics, University of Rzeszów, Prof. S. Pigonia 1, Podkarpackie 35-310, Rzeszów, Poland, email: alpha@ur.edu.pl [0000-0002-6946-8694]
2. College of Natural Sciences, Institute of Physics, University of Rzeszów, Prof. S. Pigonia 1, Podkarpackie 35-310, Rzeszów Poland [0000-0003-4328-5563]
3. Department of Mechanics and Vibroacoustics, Faculty of Mechanical Engineering and Robotics, AGH University of Science and Technology, Al. Mickiewicza 30, 30-059 Kraków, Poland [0000-0002-3932-6513]
4. Department of Mechanics and Vibroacoustics, Faculty of Mechanical Engineering and Robotics, AGH University of Science and Technology, Al. Mickiewicza 30, 30-059 Kraków, Poland [0000-0003-3785-2576]

* Presenting Author

Abstract:

An acoustic field inside a rectangular waveguide with one outlet closed by a transverse baffle was theoretically investigated. The sound source is a clamped circular plate located on a longitudinal waveguide's wall at the boundary of two regions. The first region is the waveguide's interior and the second one is the half-space bounded by a perfectly rigid infinite baffle. The waveguide walls were considered as perfectly rigid. It was assumed that acoustic waves propagate in the air. The equation describing forced non-axisymmetric vibrations of the plate was solved. The influence of fluid on both plate's surfaces was included. The linear viscoelastic Kelvin-Voigt plate model was employed. The Helmholtz equation was solved to find acoustic field. The sound pressure into the half-space was expressed with the use of the Fourier series and the Hankel transform. To describe sound propagation inside the waveguide, the region was divided into two sub-regions and the continuity conditions were used. The coefficients describing the interaction between the surface of the sound source and the fluid inside the waveguide were calculated based on the series containing the Bessel functions. The obtained solution was used to illustrate and analyze the acoustic field and to formulate some conclusions.

Mathematical modeling and analysis of dynamic changes in the water distribution system

AGNIESZKA TRĘBICKA¹

1. Department of Technology and Systems of Environmental Engineering, Białystok, University of Technology, Białystok, Poland, [orcid.org/0000-0002-0400-0396]

Abstract: The aim of the article is to present the analysis of dynamic changes in the water distribution system through the mathematical modeling process. An attempt was made to recreate the actual operating conditions of the Juchnowiec water supply network on the basis of a numerical model. The calculations gave a picture of the functioning of the water distribution system and showed the possibility of working with the modeling computer program EPA-NET, which allows periodic hydraulic simulations and insight into the preservation of water quality in a pressure pipeline network. In the process of creating the model, the results of field tests were used, which allowed to adjust the values and their parameters to real conditions. Pressure measurements were the basic part of these tests. The obtained data allowed for the calibration of the models made.

Keywords: calibration, computer simulation, distribution systems, water supply network, water works.

1. Introduction

Managing the water distribution system is an extremely complicated and complex task. A number of highly specialized industry companies are appointed to handle the tasks related to this project. Keeping up with the constantly changing standards results in considerable expenditure on development, and the consequences of wrong decisions force the network managers to search for tools for quick and effective planning. A good development strategy for a company means optimally used inputs[2]. The ability to model and predict the operation of the network is a valuable facility which, until recently, required a lot of resources and human resources. The possibility of immediate observation of the results makes it easier to visualize the situation without having to be guided by intuition [5]. The benefits of using mathematical modeling are invaluable, and taking into account the dynamics of the model through the time factor is irreplaceable.

2. Results and Discussion

The model of water supply networks was made using the Epanet program [3]. In the first phase of model construction, a raster map was used. After processing the map of the water supply network, a file was created that served as the basis for the computer model. It contains the basic elements of the water supply - the main sections with marked diameters. The ordinates of these elements in the field were also introduced into the model [4]. In the process of creating the model, the results of field tests were used, which allowed to adjust the values and their parameters to real conditions. Pressure measurements were the basic part of these tests.

The obtained data allowed for the calibration of the models made [1]. The water distribution model mapped in the computer program consists of nodes and connections). Connections are represented by

pipes (Rys.1). The nodes are joints and reservoirs. The losses in the water flowing in the pipe due to friction against the walls were calculated using the Darcy-Weisbach formula [5]. In order to calculate the water consumption in individual nodes, a database of readings from water meters in the format of a spreadsheet was used, in which data on the average daily water consumption was compiled. Average daily consumption for individual water meters was calculated, and then - as a result of grouping by address - determination of the average daily consumption in a given network node [6].

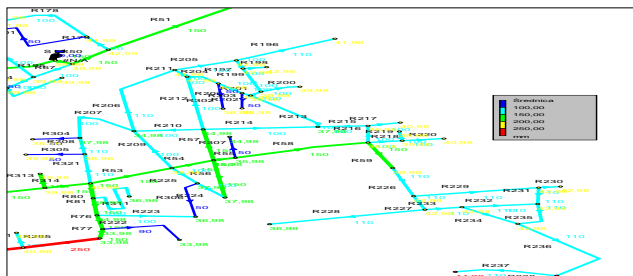


Fig. 1. Model of the water network of the city of Juchnowiec commune taking into account the ordinates

3. Concluding Remarks

As a result of the model tests carried out in the field of the dynamics of the water supply network, the results were obtained which influenced the quality of the better functioning of the system. Building a model that reflects real conditions, through correct mapping, has brought invaluable benefits in the form of reliable results. Tests have shown that the water flow velocity in the water pipes is lower than the recommended 0,5 m/s. Places where water stagnation were found due to low water consumption were identified. The simulations of the adopted concepts became an indication to improve the working conditions of the tested water distribution system.

Acknowledgment: The research was accomplished at Białystok University of Technology, as part of the grant WZ/WBIIS/2/2019 financed from subsidies of Polish Ministry of Science and Higher Education.

References

- [1] ABE, N., PETER, B.C. (2010). Epanet Calibrator – An integrated computational tool to calibrate hydraulic models. Integrating Water Systems. Boxall & Maksimovic (eds).
- [2] ALEGRE, H., COVAS, D., COELHO, S. T., ALMEIDA, M. C., CARDOSO, M. A. (2012). An integrated approach for infrastructure asset management of urban water systems. Water Asset Management International, 8, 10–14.
- [3] ROSSMAN, L.A. (2000). EPANET 2 Users Manual. EPA United States Environmental Protection Agency, Cincinnati.
- [4] TRĘBICKA, A. (2018). Efficiency End Optimum Decisions in the Modelling Process of Water Distribution, Journal of Ecological Engineering, Vol. 19, 6, 254-258.
- [5] TRĘBICKA, A. (2018). Dynamic model of the water distribution system as an analysis tool in the management of the Łapy water supply network. Economic and Environment, No. 3, 118-126.
- [6] ZHENG, F.; SIMPSON, A.; ZECCHIN, A. (2015). Improving the efficiency of multi-objective evolutionary algorithms through decomposition: An application to water distribution network design. Environ. Model. Softw., 69, 240–252.

The Influence of the Load Modeling Methods on Dynamics of a Mobile Crane

ANDRZEJ URBAŚ^{1*}, KRZYSZTOF AUGUSTYNEK², VASYL MARTSENYUK³

1. University of Bielsko-Biala, 43-309 Bielsko-Biala, Willowa 2, Poland, [0000-0003-0454-6193]

2. University of Bielsko-Biala, 43-309 Bielsko-Biala, Willowa 2, Poland, [0000-0001-8861-4135]

3. University of Bielsko-Biala, 43-309 Bielsko-Biala, Willowa 2, Poland, [0000-0001-5622-1038]

* Presenting Author

Abstract: A mathematical model for the dynamics analysis of a mobile crane is presented in the paper. The proposed model of a mobile crane is in the form of a tree structure of a kinematic chain with closed-loop subchains. The carried load is treated in the two cases, as a lumped mass and a rigid body. The formulated model takes also into account the flexibility of supports, tires, rope(s), and drives. Dry friction in joints is also considered. The formalism of joint coordinates and homogeneous transformation matrices are used to describe the kinematics of the crane. The equations of motion are derived using the Lagrange equations of the second kind. These equations are supplemented by the Lagrange multipliers and constraint equations formulated for each cut-joint.

Keywords: mobile crane, dynamics, flexibility, friction, load modeling

1. Introduction

The proposed mathematical model of a mobile crane is presented in Fig.1. In this model, a main structure of the crane is modeled in the form of open-loop kinematic chain mounted on the body of a vehicle. The hydraulic cylinders are modeled in the form of closed-loop subchains. The load is modeled in the form a lumped mass with three degrees of freedom [1,2] and a rigid body six three degrees of freedom [3,4]. The formulated model takes into account the flexibility of supports, tires, rope(s), and drives.

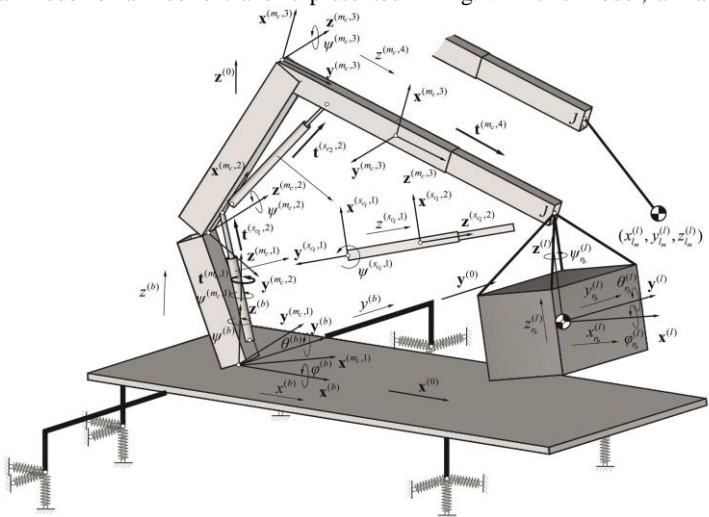


Fig. 1. Model of a mobile crane

The LuGre friction model is used to take into account dry friction in joints. The formalism of joint coordinates and homogeneous transformation matrices, based on the Denavit-Hartenberg notation, are used to describe the kinematics of the crane. Equations of motion are derived using the Lagrange equations of the second kind. These equations are supplemented by the Lagrange multipliers and constraints equations formulated for joints in which closed-loop kinematic chains are divided using the cut-joint technique.

Vector of the generalized coordinates is defined as follows

$$\mathbf{q} = \left[\mathbf{q}^{(b)T} \quad \mathbf{q}^{(m_c)T} \quad \mathbf{q}^{(s_{q_1})T} \quad \mathbf{q}^{(s_{q_2})T} \quad \mathbf{q}^{(l)T} \right]^T, \quad (1)$$

where: $\mathbf{q}^{(b)} = \left[x^{(b)} \quad y^{(b)} \quad z^{(b)} \quad \psi^{(b)} \quad \theta^{(b)} \quad \varphi^{(b)} \right]^T$, $\mathbf{q}^{(m_c)} = \left[\psi^{(m_c,1)} \quad \psi^{(m_c,2)} \quad \psi^{(m_c,3)} \quad z^{(m_c,4)} \right]^T$,

$$\mathbf{q}^{(s_{q_1})} = \left[\psi^{(s_{q_1,1})} \quad z^{(s_{q_1,2})} \right]^T, \quad \mathbf{q}^{(s_{q_2})} = \left[\psi^{(s_{q_2,1})} \quad z^{(s_{q_2,2})} \right]^T,$$

$$\mathbf{q}^{(l)} = \begin{cases} \left[x_m^{(l)} \quad y_m^{(l)} \quad z_m^{(l)} \right]^T & \text{if lumped mass,} \\ \left[x_{r_b}^{(l)} \quad y_{r_b}^{(l)} \quad z_{r_b}^{(l)} \quad \psi_{r_b}^{(l)} \quad \theta_{r_b}^{(l)} \quad \varphi_{r_b}^{(l)} \right]^T & \text{if rigid body.} \end{cases}$$

The state equations for the LuGre friction model (formulated for each joint with friction) together with the dynamics' equations of motion can be written in the following general form

$$\dot{\mathbf{z}}^{(\alpha)} \Big|_{\alpha \in \{m_c, (s_{q_1}), (s_{q_2})\}} = \mathbf{LuGre}(t, \dot{\mathbf{q}}^{(\alpha)}, \mathbf{z}^{(\alpha)}), \quad (2.1)$$

$$\begin{bmatrix} \mathbf{M}(\mathbf{q}) & -\mathbf{C}(\mathbf{q}, \dot{\mathbf{q}})^T \\ \mathbf{C}(\mathbf{q}, \dot{\mathbf{q}}) & \mathbf{0} \end{bmatrix} \begin{bmatrix} \ddot{\mathbf{q}} \\ \mathbf{f}_j \end{bmatrix} = \begin{bmatrix} \mathbf{e}(\mathbf{q}, \dot{\mathbf{q}}) - \mathbf{s}(\mathbf{q}, \dot{\mathbf{q}}) - \mathbf{d}(t, \mathbf{q}, \dot{\mathbf{q}}) - \mathbf{f}(t, \mathbf{q}, \dot{\mathbf{q}}) \\ \mathbf{c}(\mathbf{q}, \dot{\mathbf{q}}) \end{bmatrix}, \quad (2.2)$$

where: $\mathbf{z}^{(\alpha)}$ is the vector of bristles' deflections, $\mathbf{M}(\mathbf{q})$ is the mass matrix, $\mathbf{C}(\mathbf{q}, \dot{\mathbf{q}})$ is the constraints' matrix, \mathbf{f}_j is the vector of the reaction forces in the cut-joints, $\mathbf{e}(\mathbf{q}, \dot{\mathbf{q}})$ is the vector of the Coriolis, gyroscopic and centrifugal forces, $\mathbf{s}(\mathbf{q}, \dot{\mathbf{q}})$ is the vector of the spring and damping forces formulated for the supports and rope(s), $\mathbf{d}(t, \mathbf{q}, \dot{\mathbf{q}})$ is the vector of the driving forces and torques, $\mathbf{f}(t, \mathbf{q}, \dot{\mathbf{q}})$ is the vector of the friction forces and torques, $\mathbf{c}(\mathbf{q}, \dot{\mathbf{q}})$ is the vector of the right side of constraints' equations.

References

- [1] URBAŚ A., AUGUSTYNEK K.: Modelling of the dynamics of grab cranes with a complex kinematic structure, taking into account the links' flexibility and advanced friction models. Proceedings of the 13th World Congress on Computational Mechanics (WCCM XIII) and 2nd Pan American Congress on Computational Mechanics (PANACM II), New York, USA, 2018
- [2] URBAŚ A., AUGUSTYNEK K.: Mathematical model of a crane with taking into account friction phenomena in actuators. Multibody Dynamics 2019: Proceedings of the 9th Eccomas Thematic Conference on Multibody Dynamics. Springer International Publishing 2020, 299-306
- [3] KACALAK W., BUDNIAK Z., MAJEWSKI M: Stability assessment as a criterion of stabilization of the movement trajectory of mobile crane working elements. *International Journal of Applied Mechanics and Engineering* 2018, **23**(1):65-77.
- [4] CEKUS D., KWIATOŃ P.: Effect of the rope system deformation on the working cycle of the mobile crane during interaction of wind pressure. *Mechanism and Machine Theory* 2020, **153**:104011.

Benefits of Observer/Kalman Filter Identification in System Realization with Low Amount of Samples

GUSTAVO WAGNER^{1*}, RUBENS SAMPAIO², ROBERTA LIMA³

1. PUC-Rio / Mechanical Engineering Department, Rio de Janeiro, Brazil
2. PUC-Rio / Mechanical Engineering Department, Rio de Janeiro, Brazil [ORCID 0000-0002-3533-3054]
3. PUC-Rio / Mechanical Engineering Department, Rio de Janeiro, Brazil [ORCID 0000-0002-2697-0019]

* Presenting Author

Abstract: Impulse responses are function that characterize linear systems uniquely. They can be used to predict the responses of a system once the applied excitation is known. With the input and output signals of vibration tests, the impulse responses of mechanical systems can be estimated using different methods. Once those functions have been correctly estimated, the modal parameters can be identified using time-domain methods, as for example, the eigensystem realization algorithm (ERA). Problems can arise when the acquired data consist in only a few noisy samples. This paper analyses the benefits of the Observer/Kalman filter identification (OKID) to estimate the impulse responses and how it interferes in the identification of modal parameters. Experimental data of a uniform beam is used to exemplify the benefits of OKID in the modal identification using the ERA.

Keywords: Impulse response estimation, System realization, Experimental modal analysis, Observer/Kalman filter identification

1. Introduction

Impulse responses are functions that characterize linear systems since they relate input (excitation) signals with the output signals (responses). For linear time-invariant systems, the output signals can be seen as a sum of convolutions between the inputs and the impulse response functions (IRF). Using modal analysis, it is possible to decompose the IRF in terms of modal parameters (natural frequencies, damping factors and mode shapes). Hence, an estimation of this function becomes the main source of information about a structure in time-domain modal identification methods.

A proper system identification only occurs when reliable data is used. Modal parameters can only be accurately identified (in time-domain methods) if the impulse responses have been correctly estimated. Good experimental procedures and dedicated data processing are two main concerns when estimating the impulse responses. For the latter, the quality of the estimation usually depends on the number of samples recorded and in the signal-to-noise ratio of the measurements. When only a few noisy samples are recorded, the estimation process becomes challenging. The goal of this paper is to analyse the influence of the impulse response estimation in the identification of modal parameters, especially for tests with a low number of noisy samples.

2. Methods

Two impulse response estimators are compared in this paper: the inverse Fourier transform of the H_1 estimator and the Observer/Kalman filter identification (OKID). The H_1 estimator is a popular frequency response function (FRF) estimator that can be used to estimate the impulse responses using

the inverse Fourier transform. It is an indirect method since it requires first the estimation in the frequency domain [1]. Differently, the OKID is a direct time-domain method that uses an observer to deal with noise and computational costs. Under certain noise assumption, the added observer can be related to the Kalman filter gain. The OKID method was first introduced in the literature by Phan et al. [2]. To evaluate the influence of the impulse response estimation in the identification of modal parameters, the eigensystem realization algorithm (ERA) is used here. This time-domain identification method is part of a larger group, known as realization algorithms, which are based on the minimum realization theory. The formal application of this theory in modal identification was first introduced by Juang and Pappa [3].

3. Results and Conclusions

A simple Experimental Modal Analysis (EMA) of a free-free uniform beam was conducted to demonstrate the quality of the IRF estimation. Since it is easier to visualize this function in the frequency domain, Fig. 1 shows the respective transformed estimations (FRF). When only a few noisy samples were used and only one data block was used in the H_1 estimator. Therefore, the noise was not averaged out and it is still present in the estimation. This led to a poor identification since a few modes were not identified. With the same number of samples, the estimation using the OKID led to a much better and smooth estimation. All modal parameters were correctly identified. By incising the number of samples and using more data blocks in the H_1 estimation, the noise was partially removed, and the identification was improved. Nevertheless, the estimation with OKID is still superior.

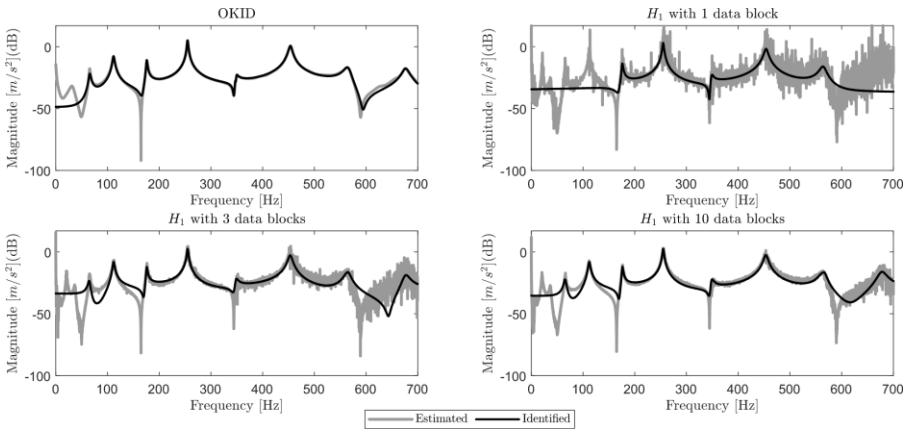


Fig. 1. FRF estimated using OKID and H_1 method. Modal synthesis after identification with ERA.

Acknowledgment: The authors gratefully thank the CNPq and the FAPERJ for the financial support.

References

1. BRANDT A: *Noise and Vibration Analysis: Signal Analysis and Experimental Procedures*. John Wiley & Sons: United Kingdom, 2011
2. PHAN H, HORTA LG, JUANG JN, LONGMAN RW: Linear System Identification Via an Asymptotically Stable Observer. *NASA Technical Paper* 1992, **3164**.
3. JUANG JN, PAPPAS RS: An eigensystem realization algorithm for modal parameter identification and model reduction. *Journal of Guidance, Control, and Dynamics* 1985, **8**:620-627.

On Longitudinal Oscillations in a Hoisting Cable with Time-varying Length subject to a Nonclassical Boundary Condition

JING WANG^{1,2*}, Wim T. van Horssen²

1. School of Mathematics and Statistics, Beijing Institute of Technology, Beijing, 100081, PR China.

2. Department of Mathematical Physics, Delft Institute of Applied Mathematics, Delft University of Technology, Mekelweg 4, Delft, 2628CD, Netherlands.

* Presenting Author

Abstract: In this work, a model of a flexible hoisting system is presented. By applying Hamilton's principle, an initial-boundary value problem for a wave equation is derived on a time-varying spatial interval with a small harmonic boundary disturbance at one end and a moving nonclassical boundary at the other end. Due to the small harmonic disturbance at one end, large resonance behavior of the system may occur. By applying an adapted version of the method of separation of variables, averaging and singular perturbation techniques, and a three time-scales perturbation method, resonances in the system are detected and accurate, analytical approximations of the solutions of the problem are constructed. It will turn out that small order ε excitations can lead to order $\sqrt{\varepsilon}$ responses. Finally, numerical simulations are presented, which are in full agreement with the obtained analytical results.

Keywords: interior layer analysis, multiple-timescales perturbation method, resonance manifold.

1. Introduction

In elevator cables, large axial oscillations can occur when a cage subject to disturbances is lifted up and down. An example of these oscillations can be founded in the mining cables, which are used to transport the cargos in a cage between the working platform and the ground. External disturbances exerted on the cage, such as airflow, can induce large vibrations and damage to the performance of the system can be caused. In order to prevent failures, it is important to understand the nature of the longitudinal vibrations of a cable with time-varying length and involving various boundary conditions. There is a lot of research on these types of problems. Gaiko and van Horssen in [1] discussed resonances and vibrations in an elevator cable system due to boundary sway. Wang et al. in [2] established a coupled dynamic modelling of the flexible guiding hoisting system and computed the response by using numerical simulations.

In this paper, a hoisting system consists of a drum, a head sheave, a driving motor, a hoisting moving conveyance and a hoisting rope with time-varying length. The upper end of the hoisting rope is fixed on the drum driven by a driving motor, which leads to the fundamental excitation. And the flexible hoisting rope lets the hoisting conveyance run up and down (Fig.1).

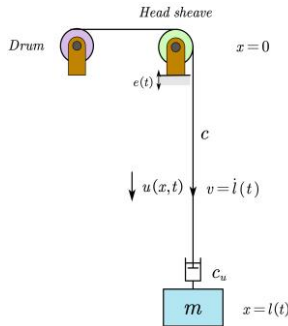


Fig. 1. The longitudinal vibrating string with time-varying length.

2. Formulation of the problem

By using Hamilton's principle, the system to describe the longitudinal vibration of a moving string as shown in Fig. 1 can be derived, and is given by:

$$\begin{cases} \rho(u_{tt} + 2vu_{xt} + v^2u_{xx} + au_x + a) - EAu_{xx} + c(u_t + vu_x) = 0, & 0 \leq x \leq l(t), t > 0, \\ [m(u_{tt} + 2vu_{xt} + v^2u_{xx} + au_x + a) + EAu_x + c_u(u_t + vu_x)]|_{x=l(t)} = 0, & t > 0, \\ u(0, t) = e(t), & t > 0, \\ u(x, 0) = u_0(x), \quad u_t(x, 0) = u_1(x), & 0 \leq x \leq l(t), \end{cases} \quad (1.1)$$

where $u(x, t)$ is the longitudinal displacement, $l(t) = f(\varepsilon t)$ is the length of the hoisting rope, v and a are the longitudinal velocity and acceleration of the hoisting rope, respectively, ρ is the linear density of the hoisting rope, m is the mass of the hoisting conveyance, EA is the longitudinal stiffness, c is the viscous damping coefficient of the hoisting rope, c_u is the viscous damping coefficient in the hoisting conveyance, and $e(t) = \varepsilon \sin(kt)$ is the longitudinal fundamental excitation along the axis of the hoisting rope.

3. Methods

Firstly, since $l(t)$ changes slowly in time, by introducing an adapted version of the method of separation of variables, the original partial differential equation can be transformed into linear ordinary differential equations with slowly varying (prescribed) frequencies. Next, the slow variation leads to a singular perturbation problem. By applying an interior layer analysis in the averaging procedure a resonance manifold is found. By using a three time-scales perturbation method, resonances in the problem are detected and accurate, analytical approximations of the solutions of the problem are constructed. It will turn out that small order ε excitations can lead to order $\sqrt{\varepsilon}$ responses.

References

- [1] N. V. GAIKO, W. T. VAN HORSSSEN: Resonances and vibrations in an elevator cable system due to boundary sway. *Journal of Sound and Vibration* 2018, **424**:272-292.
- [2] N. WANG, G. CAO, L. YAN, L. WANG: Modelling and passive control of flexible guiding hoisting system with time-varying length. *Mathematical and Computer Modelling of Dynamical Systems* 2020, **26**(1):31-54.

Estimation of resonance frequencies for systems with contact using linear dynamics methods

MACIEJ WNUK^{1*}, ARTUR ILUK¹

1. Wrocław University of Science and Technology, Department of Machine Design and Research

* Presenting Author

Abstract: In the paper the method based on linear analysis was presented to estimate resonance frequency of systems with contact. Methods that are taking into account contact during vibrations nowadays are in time domain, for general purpose problems, or base on nonlinear solutions for specific problem. Both of them have high demand on solving resources. General method that is easy for application and cost effective with acceptable accuracy might be a helpful tool for quick prediction or for complicated models assessment. Equation that allows the prediction bases on two modal analysis with different constraints configurations is presented in the paper. The method was tested in a numerical way by nonlinear vibration simulations in time domain and in an experimental way for flat CFRP specimens with several contact lengths and additional masses attached to the moving end of the specimens. Additionally the estimation method was verified for ESEO satellite antenna as complex geometry. Detail description of preparing and validating the method is described in the paper as well as results and further possibilities of the research.

Keywords: vibrations, contact, resonance frequency estimation

1. Introduction

Vibrations assessment for systems where contact appears is not clear and easy for engineers and researchers. There is possibility to analyse such a systems in time domain, but these numerical simulations are very expensive in terms of resources. Application of the time domain methods is limited for simple cases only, because of the problem complexity. For specific geometries there were presented methods in frequency domain, like *Multi-Harmonic Balance Method* combined with *Alternating Frequency Time* [1]. Other alternatives are system DOF reduction, that was described in [2] and energy conserving schemes described in [3].

During nonlinear dynamic simulations of vibrating CFRP flat beam, it was observed, that frequency response in specimen resonance is built out of two different frequencies across “half-cycles”. The half-cycle with closed contact was characterized by higher resonance frequency and the half-cycle with open contact was characterized with lower resonance frequency. The idea appeared to verify these frequencies of both half-cycles according to the model and look for equation that connects both resonance frequencies values with the resonance frequency of the specimen.

Nonlinear dynamics was used for the research on the specimen with several variables. Basing on the results, equation that combines resonance frequencies of both half-cycles was created. The equation allows to estimate resonance frequency of the system with contact, basing on two modal analysis - closed and open contact variant of boundary conditions. Validation was performed in both numerical and experimental way for different geometries, contact length and mass of the system.

2. Results and Discussion

The equation that was created has form of:

$$f_i = \frac{1}{\left(\frac{1}{2 \cdot f_0}\right) + \left(\frac{1}{2 \cdot \left(f e - \left(\frac{f e}{f_0}\right)^2\right)}\right)} \quad (1)$$

where f stands for resonance frequency and indexes $i, 0, e$ are responding to – specimen, with open contact, with closed contact. An example of convergence of input data and calculated values is shown in figure 1.

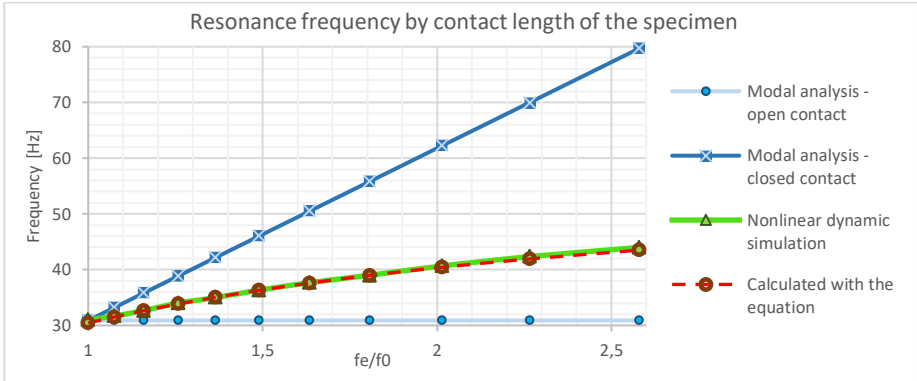


Fig. 1. Convergence of calculated resonance frequencies and obtained with nonlinear dynamic simulation

The numerical validation was done for 8 different shapes of the specimen. Experimental tests were done for 45 different cases, with 3 repeats for each. For all of the tests maximum registered error between estimated value and obtained by nonlinear dynamics or measured with barometer was 3,91%.

3. Concluding Remarks

The presented method of resonance frequency estimation based on modal analysis showed good correlation with real values of resonance frequency for studied specimens. The approach allows analysis of resonance frequency of systems with contact with usage of linear simulations, what makes it applicable for very big models. Further work should be done in verification of the method for more complex geometries, where modal shape is not obvious for open and closed contact variant.

References

- [1] ANNA HERZOG, MALTE KRACK: Comparison of two widely-used frequency-time domain contact models for the vibration simulation of shrouded turbine blades. *Proceedings of ASME Turbo Expo 2014: Turbine Technical Conference and Exposition GT2014*.
- [2] E. P. PETROV: *A high-accuracy model reduction for analysis of nonlinear vibrations in structures with contact interfaces*. Journal Engineering for Gas Turbines and Power. 2011.
- [3] VASILEIOS CHATZIOANNOU, MAARTEN VAN WALSTIJN: Energy conserving schemes for the simulation of musical instrument contact dynamics. *Journal of Sound and Vibration*, 2014.

Development of a Cardiovascular Mathematical Model Considering the Thermal Environment

Z. XIA^{1*}, Y. ISHIKAWA², S. KANEKO³, J. KUSAKA⁴

1. 1st Master Student in Waseda University, Department of Modern Mechanical Engineering
2. 2nd Master Student in Waseda University, Department of Environment Energy
3. Professor in Waseda University, Center for Science and Engineering
4. Professor in Waseda University, Department of Modern Mechanical Engineering

* Presenting Author

Abstract: Recently, traffic accidents caused by the drowsy driving are frequently featured by medias. One of the evaluation indexes of drowsy level is a RR interval variation which is deemed as an indicator that reflect the effects of autonomic nervous activity. However, physical meaning and mechanism how a RR interval variation is connected to the autonomic nervous activity is not yet well understood.

The purpose of this research is to propose a mathematical model to construct a coupling model based on the thermoregulation model and the cardiovascular model. In this model, the effect of the cabin temperature on the circulatory system is mainly reflected by the change of peripheral resistance.

Keywords: RR interval, Thermoregulation model, Cardiovascular model, Circulatory system, Drowsy driving countermeasure

1. Introduction

Among the cause of traffic accidents, fatigue driving including drowsy driving accounts for the top reason for traffic accidents. Therefore, fatigue driving countermeasures, especially drowsy driving countermeasures are highly required to reduce the cases of total traffic accidents. In the field of medical research, it is well known that the drowsy level can be evaluated by a RR interval variation which is an index extracted from the waveform of blood pressure time history. Recently, the relation between this drowsy level and the effect of the cabin thermal environment on circulatory system attracts attention.

This research is aimed at constructing a coupling mathematical model used to estimate the blood pressure and a RR interval variation considering the cabin thermal environment based on the thermoregulation model and the cardiovascular model. In this research, 『Gagge model』^{〔2〕〔3〕} is used as the thermoregulation model capable of simulating the skin temperature and core temperature in terms of room temperature considering the effect of metabolic, blood flow, sweating and respiration. In addition, 『Kotani model』^{〔4〕} is used as the cardiovascular model which can simulate the blood pressure and a RR interval variation taking the central nerves activity, the autonomic nerves activity, respiration activity and peripheral resistance into consideration.

In the current model, the effect of the cabin temperature on the circulatory system is mainly reflected by the change of peripheral resistance.

2. Results and Discussion

We consider the coupling model with the information flow explaining the effect of the thermal environment on cardiovascular system as shown in Fig.1

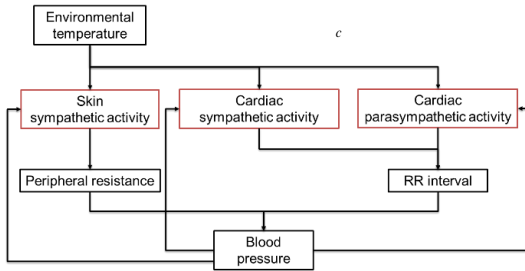


Fig. 1 Information flow of the effect of thermal environment on cardiovascular system.

The simulation results of systolic blood pressure and RR interval at room temperature of 22°C, 26°C and 30°C using the coupling mathematical model are shown in Fig.2 and Fig.3 respectively.

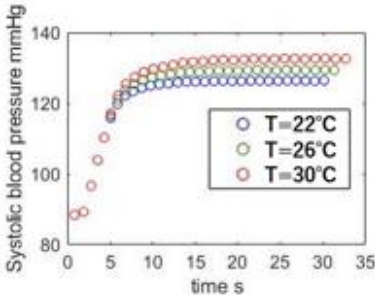


Fig. 2 Comparison of systolic blood pressure at room temperature of (22°C ,26°C, 30°C)

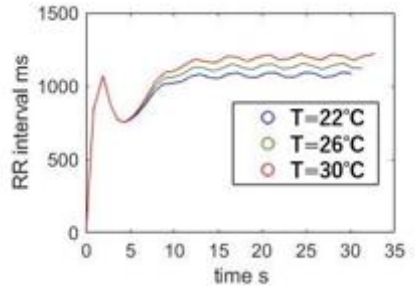


Fig. 3 Comparison of RR interval at room temperature of (22°C, 26°C, 30°C)

3. Concluding Remarks

This mathematical model succeeded in simulating the blood pressure and RR interval influenced by the change of diameter of vessels, especially the peripheral resistance caused by the fluctuation of room temperature. In the future, the accuracy of the model will be evaluated with experimental data of more subjects. The effect of other parameters such as illuminance, CO₂ concentration, etc. can be added to the current model to optimize its versatility.

References

- [1] S. Sakagami, and S. Kaneko, "A method of sleepiness estimation", JSME Dynamics and Design Conference 2015, Vol.222(2015), pp.1-12.
- [2] E. H. Wissler, "A mathematical model of the human thermal system", The bulletin of mathematical biophysics, Vol. 26, 1964, pp. 147-166.
- [3] Y. Nishi, and A. P. Gagge, "Moisture Permeation of Clothing – A Factor Governing Thermal Equilibrium and Comfort", ASHRAE TRANSACTIONS, Vol. 76, 1970.
- [4] K. Kotani, K. Takamatsu, Y. Ashkenazy, H. E. Stanley, and Y. Yamamoto, "Model for cardiorespiratory synchronization in humans", Physical review E, vol. 65, No. 051923, 2002.

Mathematical Modelling of an extended Swinging Atwood Machine

GODIYA YAKUBU^{1*} PAWEŁ OLEJNIK¹, JAN AWREJCWICZ¹

1. Department of Automation, Biomechanics and Mechatronics, Lodz University of Technology, 1/15 Stefanowski Str., 90-924 Lodz, Poland [G.Y. ORCID: 0000-0001-8295-7890, P.O. ORCID: 0000-0002-3310-0951, J.A. ORCID: 0000-0003-0387-921X]

* Presenting Author

Abstract: An extended model for a variable-length pendulum’s mechanical application is being derived from the Swinging Atwood Machine (SAM). An electrical component consisting of an electromagnet and armature coil is attached on the link connected to the counterweight mass on the left-hand side of the modified SAM to provide an excitation force for the system when an electric current is induced. The extended SAM presents a novel SAM concept being derived from a variable-length double pendulum with a suspension between the two pendulums. The equations of motion are simulated to see the trajectory of the two pendulums. The results of original numerical simulations show some compact regions of attraction at some regimes. Therefore, the extended SAM’s nonlinear dynamics presented in the current work can be thoroughly studied, and more modifications can be achieved. The new technique can reduce residual vibrations through damping when the desired level of the crane is reached. It can also be used in simple mechatronic and robotic systems.

Keywords: variable-length pendulum, swinging Atwood machine, suspension, vibration, damping

1. Introduction

Mathematical concepts gives the ability to transfer knowledge from one setting to another, which will significantly be enhanced and easy modifications and application for the real-time implementation of engineering projects.

The variable-length pendulum is a physical concept associated with parametric oscillations governed by certain forms of differential equations and functional principles [1]. A parametric oscillator can be treated as a harmonic oscillator whose physical features change over time [2]. The presented mathematical model is derived from the SAM illustrated in [2].

2. System description

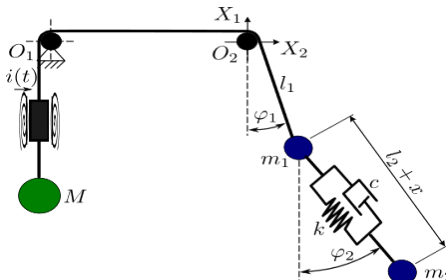


Fig. 1. Schematic diagram of the proposed modification of the SAM model

Figure 1 shows the modified SAM. A suspension system with a stiffness k and a damper c placed between the two pendulums with masses m_1 and m_2 . Point O_1 is fixed, while O_2 is movable and can oscillate in the plane (X_1, X_2) , which allow the variation of the length l_1 and the double pendulum couplings. An electrical component consisting of an electromagnet and armature coil is attached on the link connected to the counterweight mass on the left-hand side of the modified SAM to provide an excitation force for the system when an electric current is induced.

3. Results and Discussion

Kinetic Energy:

$$T = \frac{1}{2}M(\dot{l}_1^2 + \dot{x}^2) + \frac{1}{2}m_1(\dot{l}_1^2 + l_1^2\dot{\phi}_1^2) + \frac{1}{2}m_2(\dot{x}^2 + (l_2 + x)^2\dot{\phi}_2^2) \tag{1}$$

Potential Energy:

$$U = \frac{1}{2}kx^2 + Mg(l_1 + (l_2 + x)) - m_1gl_1\cos\phi_1 - m_2g(l_1\cos\phi_1 + (l_2 + x)\cos\phi_2) \tag{2}$$

With the Lagrange equation, $L = T - U$, we find four degrees of freedom (l_1, x, ϕ_1 , and ϕ_2). The following equations are obtained:

$$(M + m_1)\ddot{l}_1 + gM - v_0\cos(\omega t) - g(m_1 + m_2)\cos\phi(t) - m_1l_1\dot{\phi}_1^2 \tag{3}$$

where, v_0 – voltage in the armature winding, ω – excitation frequency.

$$(M + m_2)\ddot{x} + m_2(l_2 + x)\dot{\phi}_2^2 + c_1\dot{x} + kx - g(M - m_2\cos\phi_2) = 0 \tag{4}$$

$$m_1l_1^2\ddot{\phi}_1 + 2m_1\dot{l}_1\dot{\phi}_1 + l_1(g(m_1 + m_2)\sin\phi_1) = 0 \tag{5}$$

$$m_2(l_2 + x)^2\ddot{\phi}_2 + 2m_2(l_2 + x)\dot{x}\dot{\phi}_2 + c_2\dot{\phi}_2 + gm_2\sin\phi_2(l_2 + x) = 0 \tag{6}$$

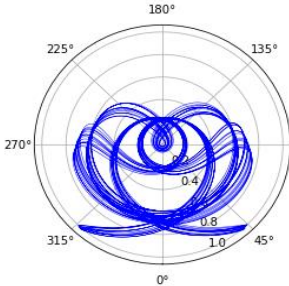


Fig. 2. An orbit of the Modified SAM (ϕ_1, l_1)

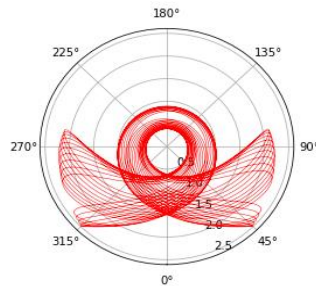


Fig. 3. An orbit of the Modified SAM ($\phi_2, (l_2 + x)$)

4. Concluding Remarks

The presented results show the nonsingular orbit under swinging, with no physical contact between the swinging assemble and the fixed points. Interestingly, in some regimes, compact regions of attraction as can be seen in Figure 2 and 3 appear in the system. Therefore, the nonlinear dynamics of the presented modified SAM can be thoroughly studied, and more modification can be achieved.

Acknowledgment: This research was funded by Narodowe Centrum Nauki grant number 2019/35/B/ST8/00980 (NCN Poland).

References

- [1] L. HATVANI, "On the parametrically excited pendulum equation with a step function coefficient," *International Journal of Nonlinear Mechanics*, vol. 77, pp. 172–182, 2015.
- [2] Wikipedia contributors. Swinging Atwood's machine. Wikipedia, The Free Encyclopedia. August 27, 2020, https://en.wikipedia.org/w/index.php?title=Swinging_Atwood%27s_machine&oldid=975234521

Method of inversion of Laplace transform in some problems of dynamic elasticity

ZINAIDA ZHURAVLOVA^{1*}

1. Odessa I.I. Mechnikov National University [0000-0002-3271-8864]

* Presenting Author

Abstract: the approach for analytical inversion of Laplace transform is proposed for some widely used in dynamic elasticity theory problems cases. The theorems are formulated and proved in the general form, and the proves for the series converges are done for two important cases, which frequently arise in applications.

Keywords: Laplace transform, analytical inversion, series

1. Introduction

Laplace transform is widely used in many applications. It is worth noting dynamic problems of elasticity, such as Lamb problem, problem for elastic semi-strip etc. The most difficult part is in inversion of Laplace transform [1]. As it is known, numerical inversion of Laplace transform is not correct problem, so the search for new formulae for analytical inversion of Laplace transform is extremely relevant. In this work, the new approach for the analytical inversion of Laplace transform of the form that is widely used in many problems is proposed.

2. Results and Discussion

The following transform is considered

$$1 / \left(c_0 + \sum_{i=1}^N c_i e^{-w_i(s)} \right) \quad (1)$$

Here $w_i(s), i = \overline{1, N}$ are continuous functions, $w_i(s) > 0, i = \overline{1, N}, \operatorname{Re} s > 0, c_i, i = \overline{1, N}$ and $c_0 \neq 0$ are real constants or functions that do not depend on $s, N \geq 1$ is natural number.

In the case when $w_i(s) = n_i w(s), n_i \in \mathbb{N}, i = \overline{1, N}$ the theorem 1 can be used.

Theorem 1. If $L^{-1} [e^{-kw(s)}]$ exists for each $k = 0, 1, 2, \dots$ and the series $\sum_{k=0}^{\infty} \frac{f^{(k)}(0)}{k!} L^{-1} [e^{-kw(s)}]$ converges, than the following formula takes place

$$L^{-1} \left[1 / \left(c_0 + \sum_{i=1}^N c_i e^{-n_i w(s)} \right) \right] = \sum_{k=0}^{\infty} \frac{f^{(k)}(0)}{k!} L^{-1} [e^{-kw(s)}] \quad (2)$$

Here $f(z) = 1 / \left(c_0 + \sum_{k=1}^N c_k z^{n_k} \right)$.

In the most general case when $w_i(s) = \sum_{j=1}^m n_{ij} w_{q_j}(s), n_{ij} \in \mathbb{N}, i = \overline{1, N}, j = \overline{1, m}$ for some fixed numbers $1 \leq q_j \leq N, j = \overline{1, m}$ the theorem 2 can be used.

Theorem 2. If $L^{-1} \left[e^{-k_j w_{q_j}(s)} \right], j = \overline{1, m}$ exists for each $k_j = 0, 1, 2, \dots$ and the series $\sum_{k_1, \dots, k_m=0}^{\infty} \frac{1}{k_1! \dots k_m!} \frac{\partial^{k_1 + \dots + k_m} f(0, \dots, 0)}{\partial z_1^{k_1} \dots \partial z_m^{k_m}} L^{-1} \left[e^{-k_1 w_{q_1}(s)} \right] * \dots * L^{-1} \left[e^{-k_m w_{q_m}(s)} \right]$ converges, than the following formula takes place

$$L^{-1} \left[1 / \left(c_0 + \sum_{i=1}^N c_i e^{-\sum_{j=1}^m n_{ij} w_{q_j}(s)} \right) \right] = \sum_{k_1, \dots, k_m=0}^{\infty} \frac{1}{k_1! \dots k_m!} \frac{\partial^{k_1 + \dots + k_m} f(0, \dots, 0)}{\partial z_1^{k_1} \dots \partial z_m^{k_m}} L^{-1} \left[e^{-k_1 w_{q_1}(s)} \right] * \dots * L^{-1} \left[e^{-k_m w_{q_m}(s)} \right] \quad (3)$$

Here $f(z_1, \dots, z_m) = 1 / \left(c_0 + \sum_{k=1}^N c_k \prod_{j=1}^m z_j^{n_{kj}} \right)$.

The most difficulty in using of these two theorems is in the proving that the series in right-hand sides in (2) and (3) converges. Such proves were done for two most frequent cases of the functions $w(s)$ and $w_i(s), i = \overline{1, N}$:

- $w(s) = As$ or $w(s) = b\sqrt{s^2 + a^2}$;
- $w_i(s) = s \sum_{j=1}^m n_{ij} A_{q_j}, i = \overline{1, N}$ or $w_i(s) = \sum_{j=1}^m n_{ij} b_j \sqrt{s^2 + a_j^2}, i = \overline{1, N}$.

Here $A, b, A_{q_j}, b_j > 0, a, a_j, j = \overline{1, m}$ are some real constants or functions that do not depend on $s, q_j, j = \overline{1, m}$ are natural numbers.

3. Concluding Remarks

The new method that allows to derive analytical inversion of Laplace transform for some cases is proposed. The theorems are formulated and proved in general form, and two frequently used cases are considered, for which the series convergence were proved. These formulae can be used in many applied problems, such as dynamic elasticity problem for a semi-strip.

References

[1] DOETSCH G: *Introduction to the Theory and Application of the Laplace Transformation*. Springer-Verlag: New York, 1974

Dynamics of an Economic Growth Model with New Stylized Facts

ADAM ZSIROS^{1*}, ZSOMBOR LIGETI^{1,2}

1. Budapest University of Technology and Economics, Faculty of Economic and Social Sciences, Department of Economics, Budapest, Hungary
2. Email: ligeti.zsombor@gtk.bme.hu

* Presenting Author

Abstract: The last two decades' social and economic events have proven the importance of feedback mechanisms for determining the income dynamics of countries of the world. The first feedback mechanism is the neglected endogenous population: the inverse relationship between income and population growth. The second feedback mechanism is – partly as a consequence of the previous one – aging society: the simultaneous reduction of labour force and increasing economic cost of the dependency ratio, additionally, the lower technological adaptability of the aging society to new technological innovations. The third feedback mechanism is the rising functional income inequality: the increasing relative income share of the rich. The consequence of these mechanisms is a qualitatively new national and global income path in the 21st century compared to that of the 20th century. The results of these feedback mechanism question not only the stability of social and economic performance but the sustainability of these systems, as well.

Keywords: economic growth, new stylized facts, endogenous population, functional income inequality, aging society

1. Introduction

United Nations Sustainable Development Goals (SDGs) summarize the most important environmental, social, economic, and global challenges. In the 20th century the – investment based – technological change driven economic growth was thought to be the solution for them. As the 2019 Nobel laureates in Economics, Abhijit Banerjee and Esther Duflo describe, however, one of the biggest illusions of the last 40 years – that the savings of the rich stimulate economic growth more than the savings of the poor – has been refuted [1]. This illusion-led-policy has caused increasing inequality, environmental degradation and unsustainable social and economic institutions. What did go wrong?

A standard economic growth model (the Solow model) consists of a Cobb-Douglas type production function and the standard capital-accumulation feedback loop. Macroeconomic income is the function of production factors: technological change $A(t)$, capital $K(t)$, and labour $L(t)$:

$$Y(t) = A(t) \cdot [K(t)]^\alpha \cdot [L(t)]^{1-\alpha}, \quad 0 \leq \alpha \leq 1. \quad (1)$$

The dynamics of per capita capital

$$k(t) = \frac{K(t)}{L(t)}, \quad (2)$$

and thus per capita income

$$y(t) = \frac{Y(t)}{L(t)} = A(t) \cdot [k(t)]^\alpha, \quad (3)$$

are given by capital accumulation – investment – and a set of constants (saving rate s , population growth rate n , capital depreciation rate δ and technological growth rate g):

$$\dot{k} = sy(t) - (n + \delta + g)k. \tag{4}$$

The mechanism of developed countries’ enrichment was characterised by stylized facts of the 20th century [2] which were enlarged and revisited at the beginning of the 21st century [3]. By the second decade of the 21st century, the long run results of – so far neglected – interactions of social and economic factors have been proven. The two Nassim Taleb-type Grey Swan events (the financial crisis of 2007–2009 and the present COVID-19 pandemic), the increasing income inequality elaborated by Thomas Piketty [4] and the rapidly aging societies of rich countries are revealed new stylized facts for the analysis of economics growth. We can conclude, what was wrong with the former models: they neglected important feedback mechanisms.

2. Results and Discussion

We present three new stylized facts published in the recent literature, that are essential to be considered for a better description of developed economies. These empirical facts can be determined with feedback mechanisms which are supported by econometric analysis. Thus, we integrate the following three terms into the standard growth model:

1. *Aging population*: dependency ratio $D(t)$ is increasing tendentiously in developed countries.
2. *Endogenous population*: the growth of the population is inversely proportional to the income per capita ($g_N(y), dg_N/dy < 0$).
3. *Time-varying functional income distribution*: the share of labour and capital in total output tends to vary over time. The presumed determining factor of the changes is income ($\alpha(y(t))$)

Considering these new stylized facts, we had run simulations. The qualitative changes of the expected income values compared to the original Solow model (red line) can be seen in Figure 1: recent changes in society (new stylized facts) imply qualitative changes in GDP per capita predestination of the Solow model. Maintaining the current growth requires the replanning of current economic policies.

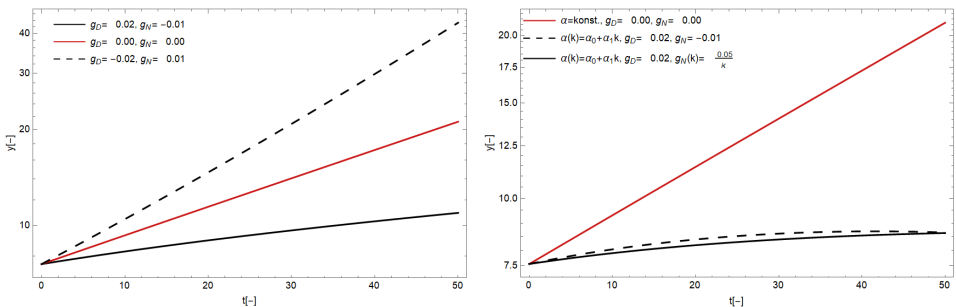


Fig. 1. Forecasted time path scenarios of GDP per capita considering the new stylized facts.

References

- [1] BANERJEE, A. V., DUFLO, E.: *Good Economics for Hard Times. Better Answers to Our Biggest Problems.* Penguin Random House UK, 2019.
- [2] KALDOR, N. (1957): A MODEL OF ECONOMIC GROWTH. *THE ECONOMIC JOURNAL* 67(268): 591–624.
- [3] JONES, C. I., ROMER, P. M. (2010): THE NEW KALDOR FACTS: IDEAS, INSTITUTIONS, POPULATION, AND HUMAN CAPITAL. *AMERICAN ECONOMIC JOURNAL: MACROECONOMICS* 2(1): 224–245.
- [4] PIKETTY, T.: *Capital in the Twenty-First Century.* Harvard University Press, 2014.

Non-smooth models of wheel-road interactions based on piecewise-linear $\text{luz}(\dots)$ and $\text{tar}(\dots)$ projections

ŻARDECKI DARIUSZ*

Military University of Technology (WAT) [ORCID 0000-0002-3934-2150]

* Presenting Author

Abstract: Vehicle modeling is often practiced on the concept of partial models created independently to describe the dynamics of longitudinal movements (related to drive and braking processes), the dynamics of lateral movements (related to the vehicle handling processes), the dynamics of vertical movements (related to the effects of road unevenness and suspension work). The paper presents a set of three innovative non-smooth dynamical models describing the interaction of the pneumatic wheel with the road in terms of the longitudinal, lateral and vertical dynamics of the vehicle motion. They are based on simple two-mass substitute physical model. The presented mathematical models use piecewise-linear $\text{luz}(\dots)$ and $\text{tar}(\dots)$ projections. Thanks to these projections and their mathematical apparatus, the developed models are useful for simpler description and analysis of strong nonlinear non-smooth processes, including the most difficult ones related to wheel locking, wheel sudden slipping, or wheel detachment from the road surface.

Keywords: Tire wheel - road interactions, dynamics, mathematical modeling, projections.

1. Introduction

Mathematical modeling of tire wheel - road interactions is still the subject of scientific research, despite the fact that in the literature on Vehicle System Dynamics there are mathematical models (physical based and experimental, static and dynamic) with an established reputation (e.g. Dugoff model, "Magic Formula" model, "LuGre" model, etc.) [2]. These models were designed to describe the wheel-road interactions in normal states (without sudden changes accompanying full skid or wheel detachment from the uneven road), and usually they have been parts of complex models expressing vehicle "smooth dynamics" (in standard situations). Note, that in many cases the vehicle dynamics is analyzed by partial models created independently for longitudinal movements (drive and braking processes), for lateral movements (handling processes) and for vertical movements (effects of road unevenness and suspension work) and therefore the models of tire wheel - road interactions have the same character of partial description. Despite a number of simplifying assumptions such models have rather sophisticated forms and require many parameters.

2. Results and Discussion

The paper presents a set of three dynamical models describing the tire wheel - road interactions in terms of longitudinal, lateral and vertical dynamics of the vehicle motion. These new models are intended to describe non-smooth effects (sudden changes accompanying full skid or wheel detachment from the uneven road).

The substitute physical model of a tire wheel (Fig.1) adopted in the study is a cylinder (wheel rim) with an applied ring (tire) treated as rigid body rolling elements. Both elements can be twisted relative to each other (in the plane of the wheel and transversely) according to linear torsion models, and they can also shift relative to each other (non-linear model, used in the description of drift). The

rigid cylinder represents the inner part of the wheel that is acted upon by driving torque (from differential driven wheels), braking torque (from brake) and rolling resistance torque (from the bearings). The ring represents the outer part of the wheel along with the tire tread. For description of vertical dynamics, it can be assumed that the ring is an elastic structure (rheological properties of the Kelvin-Voight type). The outer side of the ring is a friction system with a road surface, with anisotropic properties specified for longitudinal, transverse and torsional movements. The road tire contact is treated pointwise without entering into the description of the force distribution in the actual contact area. The modeling of wheel dynamics did not take into account the geometry of wheel position in king-pin mechanism (it is "hidden" in parameters and disclosed in the description of the stabilization moments).

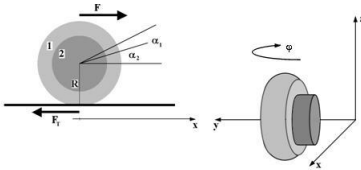


Fig.1. Idea of substitute physical model of a rubber wheel

For description of friction effects the classic Coulomb theory is applied. So the models have to have variable-structure forms expressing kinetic and static friction. Due to the presence of two connected elements in the wheel model, there is no fear that static indeterminacy problems appear.

The models are built with using special piecewise-linear luz(...) and tar(...) projections (Fig.2) and their original mathematical apparatus [3]. Note, that luz(...) and tar(...) can be applied also for the friction characteristics expressing Stribeck effect, for characteristics with non-symmetry, etc.. The forms of models are “compact” and clear for analytical interpretation. Thanks to these, the developed tire wheel models are very useful for description and analysis of strong nonlinear non-smooth processes, including the most difficult ones related to wheel locking, sudden slipping, or wheel detachment from the road surface. An application of the method for suspension analysis shown in [1].

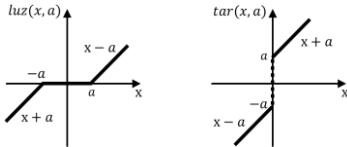


Fig.2. Geometric interpretations of the luz(...) and tar(...) projections

3. Concluding Remarks

The luz(...) and tar(...) projections seem to be very efficient for modeling non-smooth wheel-road interactions and mechanical systems which are engaged in control of the car. Aggregations of partial models enables simplified describing of wheel-road dynamic interactions in 2D and 3D space.

References

[1] DEBOWSKI A, ŻARDECKI D.: Non-smooth models and simulation studies of the suspension system dynamics basing on piecewise linear luz(...) and tar(...) projections. *Applied Mathematical Modeling*. 2021, **94**, 619-634.
 [2] KHLEGHIAN S., EMAMI A., TAHERI S.: Survey on tire-road friction estimation. *Friction*, 2017, **5** (2), 123-146.
 [3] ŻARDECKI D.: Piecewise Linear luz(...) and tar(...) Projections. Part 1 – Theoretical Background, Part 2 – Application in Modeling of Dynamic Systems with Freeplay and Friction. *Journal of Theoretical and Applied Mechanics*, 2006, **44** (1), 163-202.

-MTR-

MECHATRONICS

Dynamics Analysis of Hand Wheel Actuator in Steer-By-Wire Electric System of Car

MAREK BRYKCYŃSKI^{1*}, ANDRZEJ HARLECKI²

1. University of Bielsko-Biala, Faculty of Mechanical Engineering and Computer Science
[0000-0002-9691-0062]

2. University of Bielsko-Biala, Faculty of Mechanical Engineering and Computer Science
[0000-0001-6230-6900]

* Presenting Author

Abstract: Mechanically coupled electric power steering systems of cars are expected to be replaced by steer-by-wire electrical systems. In general, steer-by-wire system is composed of two sub-systems: road wheel actuator and hand wheel actuator. Road wheel actuator is responsible to set wheels at correct angle and in consequence to steer the vehicle in correct direction. Hand wheel actuator reads the driver's commands (senses the external torque exerted by driver), provides the road feedback to the driver and sends commands to the road wheel actuator. Lack of mechanical coupling between steer-by-wire system components enforces employment of additional safety measures. In the paper dynamics of hand wheel actuator in steer-by-wire electric system of car is analysed. An existing model of a conventional electric power system is used to determine characteristic of the torque exerted at the steering wheel. This is followed by the creation of a hand wheel actuator model in order to examine and compare its characteristics with the reference model.

Study of an electro-hydraulic servo actuator flexibly connected to a boom manipulator mounted on a jaw crusher

RYSZARD DINDORF¹, PIOTR WOŚ^{2*}

1. Kielce University of Technology [0000-0002-2242-3288]
 2. Kielce University of Technology [0000-0003-3107-366X]
- * Presenting Author

Abstract: The study deals with the electro-hydraulic servo actuator (EHSA) for position control of the boom manipulator mounted on the jaw crusher. The manipulator is used to move a hydraulic rock hammer. The SHD is rigidly connected to the main boom and flexibly connected to the inner boom via a spring damping device (SDD). The nonlinear dynamic model of a dynamic system with 2 degrees of freedom (DoF) has been presented. In the Simscape Fluid simulation tests, the dynamic responses of the dynamic system to cyclical excitations generated by the rock breaker were analysed. Based on the dynamic responses, the dynamic properties of EHSA rigidly and flexibly connected to the load mass excited by a constant force or a cyclic force generated by a rock breaker were compared. The EHSA dynamic system based on the Hammerstein model using the third-order polynomial function for the nonlinear static subsystem and the ARX model for the dynamic linear subsystem was identified.

Keywords: electro-hydraulic servo actuator, crusher manipulator, flexible connection

1. Introduction

The mechanical vibrations from the rock breaker to the crusher manipulator and the hydraulic system components are transmitted. This contributes significantly to trouble with the operation and maintenance of hydraulic components and systems. The designer of the crusher manipulator and the hydraulic system should foresee operational problems related to long-term mechanical vibrations. However, the most common practice is simple design solutions that provide short-term operational benefits.

2. Results and Discussion

The use of EHSA has been considered, in which the cylinder is rigidly mounted to the main boom and the piston rod is flexibly connected via an SDD to the inner boom of a hydraulic crusher manipulator. The simulation results to select the SDD and the vibration exciter on the test stand were used. A spring with viscous damping devices enables effective damping of vibrations at high dynamic loads, such as a hydraulic rock breaker. The EHSA used consists of a differential hydraulic actuator, a 4/3 proportional directional control valve with electrical position feedback, and integrated control electronics (ICE) so-called On-Board electronics (OBE). The purpose of the simulation tests is to assess the dynamic properties of an EHSA rigidly and flexibly connected to a load mass excited by a cyclic force. The step response of an EHSA rigidly and flexibly connected to a load mass at constant force or cyclic force generated by the rock breaker was compared. The experimental test aims to select such a control system for the EHSA flexibly connected to the mass of the load, which will ensure the accurate extension of the internal telescopic boom at the cyclic excitation force (impact force).

Fig. 1 shows the model of a jaw crusher with a rock conveyor and a mounted boom manipulator.

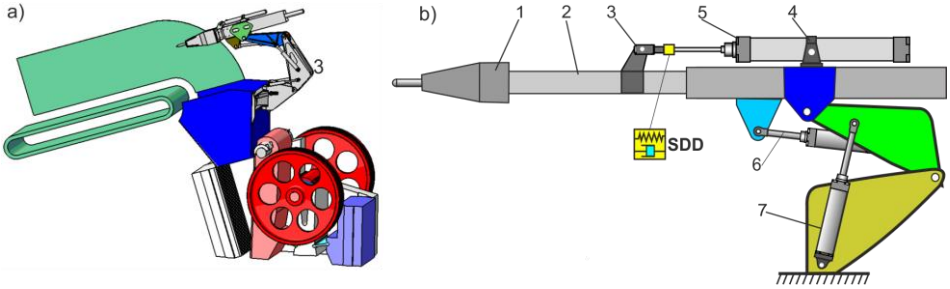


Fig. 1. The boom manipulator mounted on a jaw crusher a) model of a jaw crusher, b) model of a boom manipulator: 1 – hydraulic rock breaker, 2 – telescopic boom, 3 – clevis bracket, 4 – center trunnion, 5 – inner boom cylinder, 6 – rotation cylinder, 7 – lifting cylinder, SDD – spring damping device

Fig. 2 compares the step response of an EHSA rigidly and flexibly connected to a payload mass at constant force or cyclic force generated by the rock breaker.

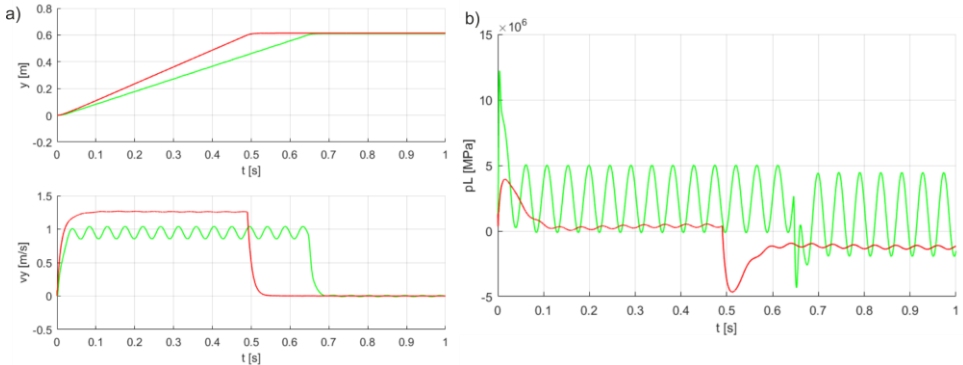


Fig. 2. Comparison of dynamic responses of the displacement $y(t)$, the speed $v_y(t)$ (a), and load pressure $p_L(t)$ (b) of an EHSA rigidly (green line) and flexibly (red line) connected to a payload mass $m_L = 250\text{kg}$, for $y_{set} = 0.6\text{m}$ and excitation force $F(t)$ at frequency $f_e = 21.8\text{Hz}$

The comparison of the EHSA step response shows a difference in the SHD dynamic properties for a rigid and flexible connection with a load mass at constant force or cyclic force, generated by the rock breaker.

3. Concluding Remarks

The paper analyses the difficult and complex problem of EHSA control flexibly connected to the load mass excited by the cyclic force generated by a rock breaker mounted on the boom of a jaw crusher manipulator. The EHSA control system on the test stand has been verified. This test stand will be used to carry out research projects of EHSA-SDD systems for constructors of hydraulic manipulators of crushers, users of jaw crushers, and producers of aggregates for the cement industry. Simulation and experimental studies of the EHSA-SDD system are of great importance in the design and operation of heavy hydraulic manipulators with large moving masses and mechanical structures susceptible to elastic deformation. These manipulators are used in construction mining machines.

Using the Experiment-Aided Virtual Prototyping technique to predict the best clamping stiffness during milling of large-size details

KRZYSZTOF J. KALIŃSKI¹, NATALIA STAWICKA-MORAWSKA^{2*},
MAREK A. GALEWSKI³, MICHAŁ R. MAZUR⁴

1. Gdańsk University of Technology, Department of Mechanics and Mechatronics, Gdańsk, Poland [0000-0003-1658-4605]
2. Gdańsk University of Technology, Department of Mechanics and Mechatronics, Gdańsk, Poland [0000-0002-6565-1977]
3. Gdańsk University of Technology, Department of Mechanics and Mechatronics, Gdańsk, Poland [0000-0003-3703-4012]
4. Gdańsk University of Technology, Department of Mechanics and Mechatronics, Gdańsk, Poland [0000-0003-1405-909X]

* Presenting Author

Abstract: During machining of large-size details, the main cause of the problems are relative vibrations "tool-workpiece" [1], which lead to deterioration of the quality of machined surfaces and increased tool wear [2, 3]. The article presents considerations on the reduction of vibrations during milling with the use of an innovative method of adjusting the best stiffness for mounting large-size details. Contrary to another author's approach, concerning the minimization of the work of cutting forces in the direction of the layer width [4], the method in question is based on a selected mechatronic design technique, i.e. Experiment-Aided Virtual Prototyping (E-AVP) [5]. As an example of the effectiveness of the proposed vibration reduction method, the results of simulation of the face milling process in industrial conditions of selected surfaces of a large-size object are illustrated.

Keywords: clamping stiffness, face milling, vibration suppression, mechatronic design techniques

1. Introduction – description of the method

The proposed method has been modified and its application consists in:

- a one-time assessment of the compliance of the modal model parameters of the workpiece itself with the real object. Based on the results of the model parameters identification using the ERA (Eigenvalue Realization Algorithm) method, it was found that the parameters obtained from the experiment and the model using the Finite Element Method (FEM) were correctly defined;
- repetitive change in the values of the stiffness coefficients of supports that fasten the workpiece. The static characteristics of the supports, enabling the desired values of these coefficients to be set, were determined experimentally during research on the Zwick Roell testing machine;
- a one-time selection of parameter values describing the dynamic properties of the cutting process, based on the experience resulting from previous observations of analogous machining processes;
- conducting a cycle of repetitive simulations for the above-accepted reliable process data. On the basis of the obtained results, the values of the dominant "peaks" in the amplitude spectra and the values of the Root Mean Square (RMS) of the displacements in the time domain are assessed. The minimum values of these quantities indicate the best configuration of the adopted workpiece mounting stiffness coefficients from the point of view of minimizing the level of "tool-workpiece" vibrations.

Acknowledgment: The research was supported by the Polish National Centre for Research and Development, project number TANGO1/266350/NCBR/2015, on “*Application of chosen mechatronic solutions to surveillance of the large-size workpieces cutting process on multi axial machining centers*”. Experimental investigations on the MIKROMAT 20V portal milling center were performed thanks to cooperation with the PHS HYDROTOR Inc. in Tuchola, Poland.

References

- [1] QUINTANA G., CIURANA J.: *Chatter in machining processes: A review*, International Journal of Machine Tools and Manufacture 51 (5), pp. 363 – 376, 2011.
- [2] AJAYAN M., NISHAD P. N.: *Vibration control of 3D gantry crane with precise positioning in two dimensions*. IEEE Emerging Research Areas: Magnetics, Machines and Drives (AICERA/iCMMD), Annual International Conference on 24–26 July 2014, pp. 1–5, 2014.
- [3] NOUARI M., LIST G., GIROT F.: *Wear mechanisms in dry machining of aluminium alloys*, International Journal of Mechanical Production Systems Engineering, pp. 22-29, Avril, 2003.
- [4] KALIŃSKI K.J., GALEWSKI M., MAZUR M., DZIEWANOWSKI L., MORAWSKA N.: *A method of choosing an optimal clamp torque for fastening a flexible workpiece mainly for a face milling process*, Gdansk University of Technology, International Patent Application EP18460012 (European Patent Office) 2018, Patent No EP3530403 2020.
- [5] KALIŃSKI K.J., GALEWSKI M., MAZUR M., MORAWSKA N.: *Minimization of vibrations during milling of flexible structures using mechatronic design techniques*, The 20th International Carpathian Control Conference (ICCC), 2019, pp. 1-6, DOI: 10.1109/CarpathianCC.2019.8765681.

Numerical and experimental characterization of the temperature profile in a gas foil bearing

ADAM MARTOWICZ^{1*}, PAWEŁ ZDZIEBKO¹, JAKUB ROEMER^{1,2},
GRZEGORZ ŻYWICA³, PAWEŁ BAGIŃSKI³

1. AGH University of Science and Technology, Department of Robotics and Mechatronics, al. Mickiewicza 30, 30-059 Krakow, Poland: AM [0000-0001-9630-0355], PZ [0000-0001-5296-1485], JR [0000-0002-7481-028X]
 2. OsloMet - Oslo Metropolitan University, Postboks 4, St. Olavs Plass, 0130 Oslo, Norway
 3. Institute of Fluid Flow Machinery, Polish Academy of Sciences, Department of Turbine Dynamics and Diagnostics, Fiszerza 14, 80-231 Gdańsk, Poland: GZ [0000-0002-6848-5732], PB [0000-0003-3753-7525]
- * Presenting Author; email: adam.martowicz@agh.edu.pl

Abstract: In the paper, the authors present the outcomes from the investigation on the thermal properties of a gas foil bearing. At the current stage of the conducted research a test stand has been constructed and experimentally tested. The temperature field on the bearing's top foil has been considered as the object of the study. This physical quantity becomes important for maintaining the nominal working configuration in the bearing. In reference, numerical simulations have been also performed employing finite element method. The conducted virtual tests are crucial as enabling for cost-effective, convenient and reliable inference on the bearing's operational properties. In the paper the measurement instrumentation employed for temperature identification as well as a specialized sensing top foil are described. The work is concluded with the pointed directions for the planned future developments regarding more comprehensive characterization of the gas foil bearings' properties.

Keywords: gas foil bearing, temperature profile, thermocouple, numerical simulation, experimental identification

1. Introduction

Rotating machineries require bearing systems since they assure desired load capacities and rotational degree of freedom. Durability of the machineries depends on the condition of the bearings [1]. Hence, various algorithms developed for the assessment of their properties have been proposed. However, the specificity of a technical solution being considered requires dedicated methods to be used for the bearing characterization. In the current paper, the results of the investigation on the properties of a gas foil bearing (GFB) are reported. GFBs are fluid film bearings consisting of a set of thin foils mounted between the rotating shaft and solid bushing. They are especially dedicated to support lightly-loaded but high-speed rotors [2]. GFBs exhibit a unique capability since a gaseous medium directly taken from the surroundings is used for lubricating. It is however worth noting that stable operation of a GFB strictly depends on the thermally induced mechanical behaviour of the thin foils. In the worst case scenario, the required clearance between the shaft's journal and the top foil may be suddenly lost due to unexpected thermal behaviour [3]. Excessive thermal elongations of the bearing's components may lead to its break and machinery failure. Being motivated by the above presented challenges for the GFBs development, the authors of the current work constructed a prototype installation equipped with the specialised sensing top foil dedicated for temperature identification, as shown in Fig. 1.

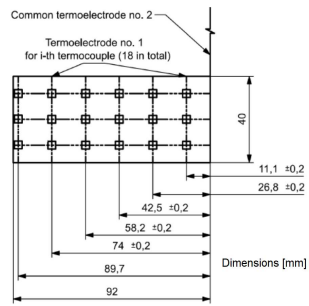
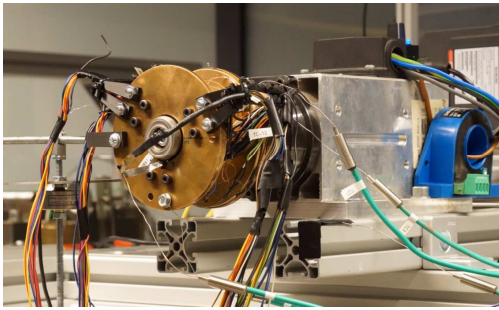


Fig. 1. GFB with integrated thermocouples: prototype (left), thermocouples locations (right).

2. Results and Discussion

Fig. 2 presents the temperature profiles identified in both experimental and numerical tests. The integrated sensors show uneven temperature profile for the top foil which corresponds to the investigations reported in the literature [4].

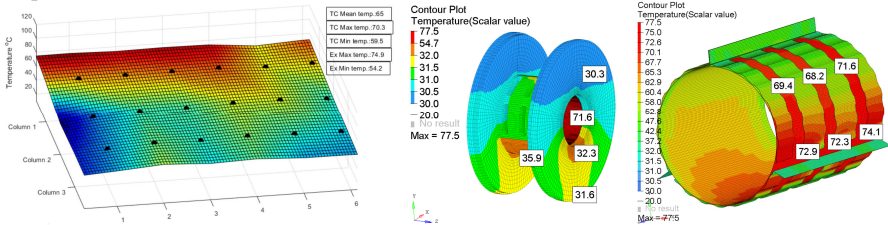


Fig. 2. Temperature identified for: top foil during experiment (left), simulations (centre and right).

3. Concluding Remarks

The paper presents the proof of concept for the method of temperature characterization for a GFB. The proposed approach makes use of a dedicated specialised sensing foil with integrated thermocouples. As of the future work, the authors plan to improve the developed numerical model via validation procedure. The authors' ongoing work is focused on the enhancement of the set up with integrated strain gauges. The final goal is to characterize the thermomechanical coupling in a GFB.

Acknowledgment: This research was funded by the National Science Center, Poland, within the project grant number 2017/27/B/ST8/01822.

References

- [1] AMBROŹKIEWICZ B, SYTA A, MEIER N, LITAK G, GEORGIADIS A: Radial internal clearance analysis in ball bearings. *Eksplotacja i Niezawodność - Maintenance and Reliability* 2021, **23**(1):42–54.
- [2] MARTOWICZ A, ROEMER J, LUBIENIECKI M, ŻYWICA G, BAGIŃSKI P: Experimental and numerical study on the thermal control strategy for a gas foil bearing enhanced with thermoelectric modules. *Mechanical Systems and Signal Processing* 2020, **138**, NO. 106581.
- [3] ŻYWICA G, BAGIŃSKI P, KICIŃSKI J: Selected operational problems of high-speed rotors supported by gas foil bearings. *Technische Mechanik* 2017, **37**(2–5):339–346.
- [4] SIM K, KIM TH: Thermohydrodynamic analysis of bump-type gas foil bearings using bump thermal contact and inlet flow mixing models. *Tribology International* 2012, **48**:137–148.

Accuracy improvement of 3D position estimation of mobile robots based on IMU measurements and NNs

ÁKOS ODRY^{1*}, ISTVAN KECSKES^{2*}, PETER ODRY²

1. Faculty of Engineering, University of Szeged, Szeged, Hungary [0000-0002-9554-9586]

2. Institute of Informatics, University of Dunaujváros, Dunaujváros, Hungary

* Presenting Authors

Abstract: This paper proposes a novel approach of fusing inertial measurement unit (IMU) data and neural network (NN) models with the aim to provide IMU-based position/velocity estimation results with enhanced accuracy for mobile robots. First, a comprehensive database of random dynamic motions is generated based on low-cost quadcopter motions, where both raw IMU measurements and ground truth data of system states are recorded. This process is performed with a six degrees of freedom (6-DOF) test environment, which alters both the position and orientation (6D pose) of an IMU model and simultaneously builds the database. Then, a cascade forward NN is developed and trained to estimate the true acceleration of the dynamical system. Different input combinations of IMU measurements are evaluated in the training of the NN, moreover extended Kalman- (EKF) and gradient descent (GRD) orientation filters are also incorporated in the training process to further enhance the effectiveness of the NN model. It is shown that the NN-based external acceleration estimate significantly enhances the rotation matrix-based acceleration vector calculation accuracy, therefore it enables the obtainment of reliable velocity and position results in shorter time windows.

Keywords: pose estimation, inertial measurement unit, neural network, Kalman filter, gradient filter

1. Introduction

The 3D position estimation based on the double integration of acceleration signals is a challenging problem since the uncertainty of the IMU sensor measurements is significant due to both the noisy environment and limitations of the employed measurement system [1]-[3]. This paper investigates the sufficiently accurate IMU-based acceleration determination performance, which can be used to obtain reliable velocity and position estimates for shorter time windows. For this purpose, the true acceleration is estimated with a trained cascade forward NN from solely the IMU sensor readings.

2. Results and Discussion

The first part of Table 1 is the reference-baseline group, which shows the baseline method estimations without the application of NN. In the evaluated cases the orientation was estimated with EKF or GRD based on the raw IMU measurements. The second part is the applicable NN group, which represents the feasible solutions that can be applied in pose estimation problems of mobile robots. The third part is the reference NN group, which employs the ground truth instead of the estimated orientation, i.e., these results highlight the theoretical maximum performance in case of perfect orientation estimation. The achieved performances are shown with correlation measures between the true and estimated accelerations, where various NN models have been evaluated.

Table 1. The performance comparison of NN models on different input channels

Group	Estimated Acceleration		NN correlation with true acceleration			
	Model Channels	Inputs	X	Y	Z	All
Reference - baseline	Sensor acceleration (Acc)	3	0.42	0.20	0.89	0.264
	GRD on Acc+Gyr+Mag	9	0.18	0.35	0.78	0.491
	EKF on Acc+Gyr+Mag	9	0.55	0.48	0.93	0.725
Applicable NN with estimated angles (Ekf or Grd)	NN on Acc	3	0.65	0.40	0.94	0.674
	NN on Acc+Gyr	6	0.69	0.68	0.95	0.758
	NN on Acc+Ekf	6	0.75	0.71	0.96	0.783
	NN on Acc+Grd	6	0.68	0.54	0.95	0.721
	NN on Acc+Gyr+Ekf	9	0.77	0.77	0.96	0.808
	NN on Acc+Gyr+Grd	9	0.71	0.73	0.96	0.772
	NN on Acc+Mag	6	0.78	0.71	0.96	0.803
	NN on Acc+Gyr+Mag	9	0.80	0.78	0.97	0.830
	NN on Acc+Gyr+Mag+Ekf	12	0.82	0.80	0.97	0.836
Reference NN with truth angles (Ang)	NN on Acc+Ang	6	0.98	0.98	0.97	0.957
	NN on Acc+Gyr+Ang	9	0.993	0.993	0.9767	0.9643
	NN on Acc+Gyr+Mag+Ang	12	0.993	0.993	0.9768	0.9642

It is found that EKF gives the highest correlation results from the baseline groups ($r=0.725$). The best reference NN becomes the Acc+Gyr+Ang combination ($r=0.965$), however the version with an additional magnetometer is very similar. The best applicable NN is the Acc+Gyr+Mag+Grd combination ($r=0.848$), which is halfway between the baseline and theoretical perfect solution. The results prove that the most important factor is the accuracy of the estimated orientation for the NN-based acceleration estimation. NN, as a supervised method, is a powerful model for both aggregating the available measurements and estimating the external accelerations of mobile robots. Fig. 1 depicts an example of the estimated position and velocity values. This outcome was obtained by simple double integration of the obtained acceleration. NN-based accelerations yield reliable data for 10 seconds.

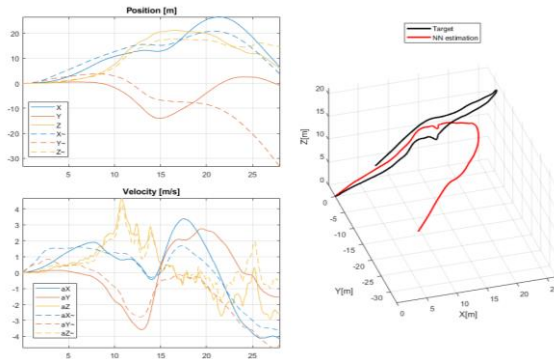


Fig. 1. Position and velocity estimation results based on the estimated acceleration by the best NN model.

References

- [1] KECSKES I, ODRY Á, TADIC V, ODRY P: Simultaneous calibration of a hexapod robot and an IMU sensor model based on raw measurements. *IEEE Sensors Journal* 2021, DOI: 10.1109/JSEN.2021.3074272.
- [2] ODRY Á: An Open-Source Test Environment for Effective Development of MARG-Based Algorithms. *Sensors* 2021, **21**(4):1183.
- [3] KECSKES I, ODRY Á, ODRY P: Uncertainties in the movement and measurement of a hexapod robot. In: AWREJCWICZ J (ED.) *Perspectives in Dynamical Systems I: Mechatronics and Life Sciences*. Springer: Berlin, 2021.

Construction and 3D model of stand for investigating a non-ideal forcing in a nonlinear chain dynamics of self-excited oscillators with friction

PATRYK ROGALA^{1*}, PAWEŁ OLEJNIK¹, JAN AWREJCWICZ¹

1. Department of Automation, Biomechanics and Mechatronics, Lodz University of Technology, 1/15 Stefanowski Str., 90-924 Lodz, Poland [P.R. ORCID: 0000-0002-9417-9480, P.O. ORCID: 0000-0002-3310-0951, J.A. ORCID: 0000-0003-0387-921X]

* Presenting Author

Abstract: The research involves application and research on a non-ideal forcing to modelling and identification of vibrating systems with friction. It is still an innovative approach in the numerical analysis of vibrations of mechatronic machines and devices. This will allow to make a much real numerical modelling and more efficient identification of nonlinear dynamic phenomena observed in vibrating systems with friction, and thus, a better modelling of such phenomena in computer programs. To obtain the goal, initial 3D model of the mechanical stand was made in the CAD software. Based on the 3D model, real stand will be built, and experiments will be held to obtain data that will be necessary to ensure correctness of the mathematical model, which also will be studied and developed.

Keywords: friction, dynamics, oscillators, non-ideal power source, CAD software

1. Introduction

In order to obtain experimental data, that would be compared to a results from a mathematical model, real stand needs to be built. Main idea was to make it as much modular and universal as it is possible. Such a conception will allow to make even dozens of different experiments using only one machine, by doing only few changes in the construction. Because of using two different linear actuators, comparison of how they can affect the stick-slip motion of the investigating bodies will be able to observe. It was discovered that when the rotor speed of the motor was close to resonance, an increment of the input power produced only a very slight increase of the rotor speed, while the oscillation amplitude increased considerably. It is one of the aspects of investigating the non-ideal forcing and it is also known as Sommerfeld effect [1], that may be observed during the experiments with proper parameters. Also, stage of complicity of the mathematical model of the system including non-deal energy source coupled with additional element, sometimes can give much different results [2], so different ways of approach will be investigated to give as much similar results as it is possible in comparison to obtained experimental data.

2. Results and Discussion

Prepared 3D model of the stand consists of few key components. First one is a base (1), to which aluminium strut profiles will be used. They give a lot of possibilities to make the stand universal and modular, because of additional elements that give a chance to connect them mount additional components in various ways and. Next components are linear actuators. One of them is lead screw (2) and the second is belt driven (3), but they could be easily changed into another one if necessary for some additional experiments. On top of the carriage of the actuators are placed handles for treadmills (4),

on which investigated bodies (5) are placed. They have one degree of freedom because of the guide roller (6). More than one body can be placed on each treadmill to make a chain of oscillators, between which springs (7) can be placed. First step will be to investigate the behaviour of the system with DC motors with low vibrations they generate and can transfer to the construction, but also investigation with stepper motors (8) will be able to do to check if the vibrations affect the friction coefficient between bodies and the treadmills. To make measurements, high speed camera will be used with proper postprocessing.

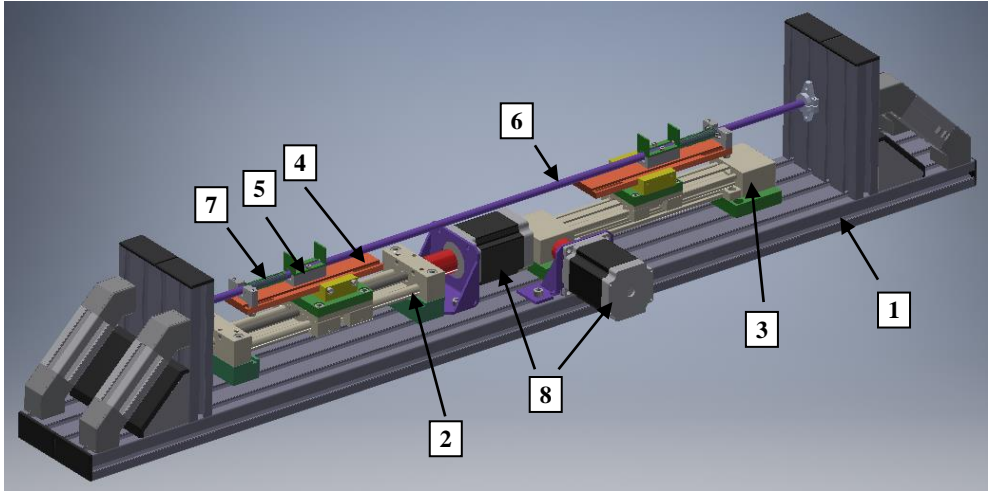


Fig. 1. 3D CAD model of the stand.

3. Concluding Remarks

3D model of the stand was made. Current construction will provide possibility of carrying out various experiments concerning non-deal forcing and chain dynamics of self-excited oscillators with friction. Different degrees of freedom system, caused by number of investigated bodies, will be able to create with various stiffness of the springs, such as many materials of the bodies and treadmills. Creating 3D model is an iterative task, therefore still some improvements are applying.

Acknowledgment: This research was funded by Narodowe Centrum Nauki grant number 2019/35/ B/ST8/00980 (NCN Poland).

References

- [1] GONZÁLEZ-CARBAJAL, JAVIER; DOMÍNGUEZ, JAIME. NON-LINEAR VIBRATING SYSTEMS EXCITED BY A NONIDEAL ENERGY SOURCE WITH A LARGE SLOPE CHARACTERISTIC. MECHANICAL SYSTEMS AND SIGNAL PROCESSING, 2017, 96: 366-384.
- [2] SGHAIER, EMNA, ET AL. COUPLED BENDING TORSIONAL VIBRATIONS OF NON-IDEAL ENERGY SOURCE ROTORS UNDER NON-STATIONARY OPERATING CONDITIONS. INTERNATIONAL JOURNAL OF MECHANICAL SCIENCES, 2019, 163: 105155.

Bionic hand control using EMG signals

Jędrzej Sencerek¹, Bartłomiej Zagrodny²

Faculty of Electrical, Electronic, Computer and Control Engineering, Lodz University of Technology,
Stefanowskiego 1/15, 90-537 Lodz, Poland¹,

Department of Automation, Biomechanics and Mechatronics, Lodz University of
Technology, Stefanowskiego 1/15, 90-537 Lodz, Poland²,

208830@edu.p.lodz.pl¹

bartlomiej.zagrodny@p.lodz.pl²

Abstract: Abstract. 3D printed prototype a human hand which is controlled by sEMG signal was created to simulate two types of fingers motions. The first one includes fingers flexion/extension and the second one is focused on opposing the thumb. These two types of motions are executed by one pair of biological muscles, by the meaning of sEMG signals. The recruiting electrodes are attached to both biceps brachii. One of them is responsible for fingers flexion/thumb abduction, and the other is for fingers extension/thumb adduction. The simultaneous contraction of both muscles causes a change in the mode of movement (fingers - thumb). Control is based on the Arduino microcontroller extended by two EMG Olimex shields and two servos. The main idea behind this project was to create an easy and cheap alternative to commercial prosthetic solutions.

Keywords: electromyography, bionic hand, 3D print, prosthetics

1. Introduction

The issue of upper limb amputation in Poland may seem to be a rare problem (in 2016, it was less than 1% of the population on the national scale [1], [2]). However, patients affected by this problem require specialized care, from the need of surgery and create a prosthesis, through social services, to the help of a psychologist. This is a very complex problem, where a functional prosthesis will help a lot. This project of myoelectric hand prosthesis is devoted to transradial amputation or wrist disarticulation. The aim of the prototype will be to simulate the movement of the fingers. Various solutions can be observed among commercial products. For example, the company Glaze Prosthetics specializes in printing cosmetic artificial limb, BeBionic or iLimb create myoelectric ones, and an important representative of mechanical ones is e-Nable - the open-source project, enabling volunteers to print their own prosthesis.

2. Results and Discussion

The prosthesis model was designed in CAD environment and printed on a 3D printer. The construction of presented artificial hand limits the range of the motion in joints between phalanges. The entire system consists of printed model, servos, Arduino UNO extended by EMG Olimex shield with electrodes that reads the signals from both biceps brachii muscles of the arms. The whole set is presented in Figure 1.

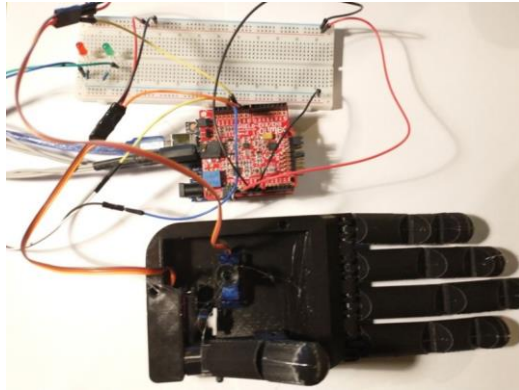


Fig.1. General view of the model with Arduino microcontroller and servos.

The prosthesis performs two types of fingers movement:

I mode - flexion and extension

II mode - abduction and adduction of the thumb

To switch the mode of motion the simultaneous contraction of the both muscles is needed. The estimations shown that the torque generated by servo to move fingers is approximately equal to 2.3% of torque of the weakest finger in the human body [3]. Despite this fact, the servo allows to move the prosthesis in full range of motion for demonstration purposes.

3. Concluding Remarks

The project uses an electromyographic signal to control two servos that drives the hand model. Despite its simple design, it has a full range of motion and the chosen solution allows for an easy control.

References

- [1] The number of limb amputations comes from the IT system of the National Health Fund.: <https://zdrowedane.nfz.gov.pl/course/view.php?id=5> (access: 11.11.2020).
- [2] Szałtys D. and Rogalińska D.: Atlas Demograficzny Polski. GUS: Warszawa, 2017.
- [3] Gedliczka A.: Atlas Miar Człowieka. CIOP: Warszawa, 2001.

Hydraulic levelling control system technology of bricklaying robot

PIOTR WOS^{1*}, RYSZARD DINDORF²

1. Kielce University of Technology [0000-0003-3107-366X]

2. Kielce University of Technology [0000-0002-2242-3288]

* Presenting Author

Abstract: The article presents a hydraulic control system for the auto-levelling of a mobile bricklaying robot platform. To stabilize the position of the robotic bricklaying system, four extendable hydraulic supporting legs were used. For the correct operation of the robot, its horizontal position is important. To control the self-levelling process, the system uses a two-axis tilt sensor and proportional directional control valves. After the target practical test, the results show that this method is a simple and reliable adjustment and perfectly realizes the precise and fast levelling of the hydraulic platform of the bricklaying robot. It can also be used for other multi-point automatic levelling systems.

Keywords: self-levelling system, bricklaying robot, hydraulic control

1. Introduction

Masonry works are one of the very early human craftsmanship. However, this discipline has not achieved a high degree of automation. Several attempts were made to develop mobile construction works, the most advanced of which were the projects [1], [2], [3]. During capturing and laying bricks, the robot should avoid collisions with obstacles. For such a dynamic area as a construction site, obstacles detection requires active motion planning techniques based on real-time sensory data. In addition, the bricklaying machine must be "aware" of the progress of wall evolution.

2. Dynamic model

Mobile Hydraulic Module (MHM) is a support platform for further development of devices used in cooperating construction works, such as: construction manipulator, material warehouse or lifting platform. Both of these tasks are significantly influenced by the dynamic behaviour of the mobile module itself and the mechanisms mounted on it. Fig. 1 shows the model of the Mobile Hydraulic Module (MHM).

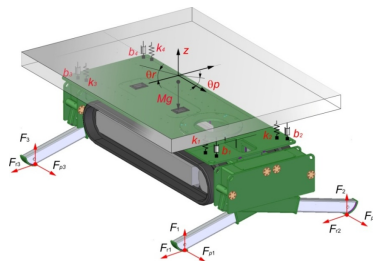


Fig. 1. Mobile Hydraulic Module (MHM)

3. Levelling

To obtain the relationship between the slope and displacement angles of hydraulic cylinders, it was assumed that the angle θ_p (pitch) is measured from the X axis and the angle θ_r (roll) from the Y axis in the direction of the Z axis. The purpose of levelling is to set the surface of the robot platform so that these angles are zero. The determined coordinate system is shown in Fig. 2.

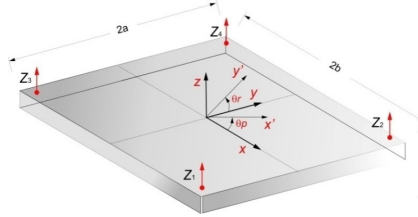


Fig.2. The coordinate system for the mobile hydraulic module

For this coordinate system, we can write rotation matrices:

$$R_x(\theta_r) = \begin{bmatrix} 1 & 0 & 0 \\ 0 & \cos\theta_r & \sin\theta_r \\ 0 & -\sin\theta_r & \cos\theta_r \end{bmatrix}, R_y(\theta_p) = \begin{bmatrix} \cos\theta_p & 0 & \sin\theta_p \\ 0 & 1 & 0 \\ -\sin\theta_p & 0 & \cos\theta_p \end{bmatrix} \quad (1)$$

In fact, during the levelling process, the deviation in the platform level is small. With this assumption, we can determine the following relationships: $\cos\theta_r = \cos\theta_p = 1$ and $\sin\theta_r = \theta_r$, $\sin\theta_p = \theta_p$.

3. Concluding Remarks

A technical solution was presented to the lifting and levelling system of the mobile hydraulic module (MHM) unit, where electro-hydraulic control and drive systems were used. A model of platform MHM dynamics was presented along with a model of hydraulic drives. A control system diagram was developed. Simulation tests were carried out to test the accepted scheme of the bricklaying robot. The presented MHM control system uses feedback from platform bracket position errors, synchronization errors and tilt angles.

Acknowledgment: This research was financially supported by The National Centre for Research and Development in Poland (Grant No. POIR.04.01.02-00-0045/18-00).

References

- [1] AGUIR, MATEUS L., KAMRAN BEHDINAN, Design, Prototyping, and Programming of a Bricklaying Robot, *Journal of Student Science and Technology*, **8** (3), 2015.
- [2] ANDRES J., BOCK T., AND GEBHART F., First results of the development of the masonry robot system ROCCO in *Proceedings of the 11th International Symposium on Automation and Robotics in Construction*, Brighton, p. 87–93, 1994.
- [3] ARDINY H., WITWICKI S., AND MONDADA F., Are Autonomous Mobile Robots Able to Take Over Construction? A Review, *Int. J. Robot*, **4** (3), p. 10–21, 2015.

-NON-

NON-SMOOTH SYSTEMS

Dynamics of Railway Wheelsets with a Nonsmooth Contact Force Model

MATE ANTALI

Department of Applied Mechanics, Budapest University of Technology and Economics, Budapest, Hungary

Abstract: The dynamics of a railway wheelset is investigated, focusing on the effect of the contact force models. For large values of creep velocities, the Coulomb model can be used as an asymptotic approximation of wheel-rail contact forces. Then, we get a nonsmooth dynamical system with codimension–2 discontinuities. At the discontinuity of the phase space, the so-called limit directions can be found, which correspond to the possible transitions between slipping and rolling. By this analysis, the nonsmooth model can complement the usual linear creep force model from the opposite approach, and we can explore more details about the qualitative behaviour of the wheelset.

Keywords: railway wheelset, Coulomb friction, nonsmooth dynamics

1. Introduction

Consider a wheelset of a vehicle running with a constant speed v . In the literature (see, e.g. [1] and [2]), the oscillating motion of the wheelset is often described by the lateral displacement y and the yaw angle ψ (see Fig. 1). Then, the so-called creep velocities u_x and u_y can be defined from the linearised kinematics,

$$u_x = -u_x^+ = u_x^- = b\dot{\psi} + \frac{vh}{r} \cdot y, \quad u_y = u_y^+ = u_y^- = \dot{y} - v\psi, \quad (1)$$

where the conicity h of the wheelset is assumed to be small.

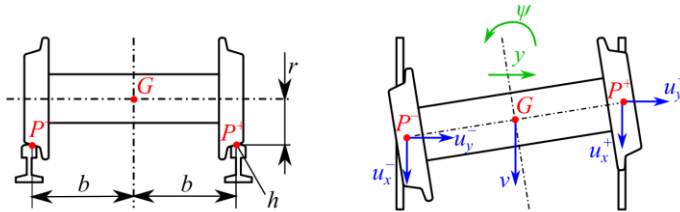


Fig. 1. Front view (left panel) and top view (right panel) of the mechanical model.

Assume that the centre point G of the wheelset is rigidly connected to the vehicle in the longitudinal direction, while the lateral and yaw motions are supported by linear springs. Then, the equations of motion of this two–degree–of–freedom model become

$$m\ddot{y} + k_y y = 2F_{\text{lat}}(u_x, u_y), \quad J\ddot{\psi} + k_\psi \psi = 2bF_{\text{long}}(u_x, u_y), \quad (2)$$

where m, J are the mass and mass moment of inertia of the wheelset; k_y, k_ψ are resultant stiffnesses with respect to the lateral and yaw directions; and $F_{\text{lat}}, F_{\text{long}}$ denote the components of the tangential (creep) forces at the contact points P^+ and P^- .

2. Nonsmooth contact model as a limit case of saturation

The empirical models of creep forces F_{lat} and F_{long} shows the tendency of *sigmoid* functions containing a nearly linear region at the origin with a slope reciprocal to the vehicle speed v , and the saturating region of the creep forces for large creep velocities (see Fig. 2). By including these two effects, we can consider the *nonlinear creep model* in the form

$$F_{\text{long}}(u_x, u_y) = \frac{-Cu_x}{\sqrt{u_x^2 + u_y^2 + C^2v^2/c_x^2}}, \quad F_{\text{lat}}(u_x, u_y) = \frac{-Cu_y}{\sqrt{u_x^2 + u_y^2 + C^2v^2/c_y^2}}, \quad (3)$$

where c_x, c_y are the linear creep coefficients and C is the saturation value of the creep forces.

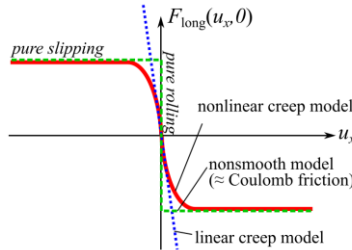


Fig. 2. The nonlinear creep characteristics (continuous line) and its approximate models.

In the limit case of *small creep velocities* in the sense $C^2v^2(u_x^2 + u_y^2) \ll \min(c_x, c_y)^2$, the model (3) tends to the classical linear creep model $F_{\text{long}}(u_x, u_y) = -c_x/v \cdot u_x$ and $F_{\text{lat}}(u_x, u_y) = -c_y/v \cdot u_y$, which can be used for stability analysis as a leading-order approximation.

In the limit case of *large creep velocities* in the sense $C^2v^2(u_x^2 + u_y^2) \gg \max(c_x, c_y)^2$, the nonlinear creep model (3) becomes

$$F_{\text{long}}(u_x, u_y) = -Cu_x / \sqrt{u_x^2 + u_y^2}, \quad F_{\text{lat}}(u_x, u_y) = -Cu_y / \sqrt{u_x^2 + u_y^2}. \quad (4)$$

The model (4) has the form of the Coulomb friction model, and it is *discontinuous* at $u_x = u_y = 0$. Now, we investigate the nonsmooth contact model (4) as an asymptotic approximation of the creep force curve to explore the qualitative behaviour of the wheelset at the saturation of the creep force curve. For that, we apply the recently developed methods of codimension-2 discontinuities [3], and determine the possible directions of trajectories at slipping-rolling transitions. A similar method was earlier applied to the vibrations of towed wheels of road vehicles [4].

A further research direction is to insert the possibility of creep associated with the rotation of the wheelset about its symmetry axis. Then, the condition $u_x^+ = u_x^-$ is not valid any more, and we get a nonsmooth vector field with discontinuities at the surfaces $u_x^+ = u_y = 0$ and $u_x^- = u_y = 0$. In this case, a careful analysis is required at the intersection of these discontinuities in the of the vector field.

References

- [1] SZABO ZS, LORANT G: Parametric excitation of a single railway wheelset. *Vehicle System Dynamics*, 2000, **33**(1):49–55.
- [2] MEIJAARD J. P: The motion of a railway wheelset on a track or on a roller rig. *Procedia IUTAM*, 2016, **19**: 274–281.
- [3] ANTALI M, STEPAN G: Sliding and crossing dynamics in extended Filippov systems. *Journal of Applied Dynamical Systems*, 2018, **17**(1):823–858.

Non-Smooth Dynamics of a Bouncing Golf Ball

STANISLAW W. BIBER^{1*}, ALAN R. CHAMPNEYS², ROBERT SZALAI³

1. Department of Engineering Mathematics, University of Bristol, Bristol, UK [0000-0001-5157-2904]
2. Department of Engineering Mathematics, University of Bristol, Bristol, UK [0000-0001-7772-3686]
3. Department of Engineering Mathematics, University of Bristol, Bristol, UK [0000-0002-3602-2397]

* Presenting Author

Abstract: We present a problem regarding the mathematical modelling of a bouncing golf ball. Experimental data shows a significantly different behaviour of the ball during the bounce depending on whether it slips throughout the whole time is in contact with a bouncing surface or if it enters rolling (grips the surface) at any stage of the bounce. We present a simple piecewise-smooth linear model of the compliant ground based on Kelvin-Voigt mechanism and analyse its dynamics. Assuming Coulomb friction between the ball and the ground a discontinuity arises in the equations of motions and thus one evaluates the dynamics of the mechanism treating it as a Filippov system. We recognise numerous behaviours that can arise from such model which agree with the commonly known outcomes in the game of golf.

Keywords: piecewise-smooth dynamics, Coulomb friction, Filippov systems

1. Introduction

The bounce of a ball in sports such as tennis, cricket or football has been studied extensively with many experimental data available to support the analysis. The common denominator for these models is an impact of a compliant ball off a rigid ground. A bounce of a golf ball is a very different problem, where the analysis focuses on the impact of a rigid body off a compliant surface. Previous studies have either focused heavily on obtaining and interpreting specific data [1] or presented models for the bounce but with little experimental validation [3] leaving a large gap between scientific models and data. In this project we aim at developing the fundamental understanding behind the science of the golf ball bounce by presenting an appropriate model for the behaviour of a compliant golf turf which we will aim to support by experimental validation.

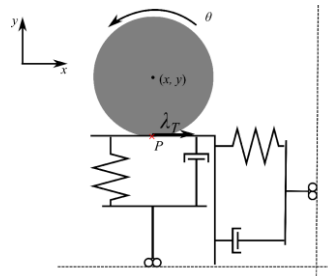


Fig. 1. Illustration of the compliant ground model

In this project we aim at developing the fundamental understanding behind the science of the golf ball bounce by presenting an appropriate model for the behaviour of a compliant golf turf which we will aim to support by experimental validation.

We consider a setting in which a rigid sphere of unit radius impacts a compliant surface based on Kelvin-Voigt mechanism – see Fig. 1. for the illustration of the mechanism. Denoting the centre of mass of the ball with (x, y) and its spin with ω the equations of motion are

$$\ddot{x} + \frac{2d_x}{\varepsilon_x} \dot{x} + \frac{1}{\varepsilon_x} x = \lambda_T, \quad \ddot{y} + \frac{2d_y}{\varepsilon_y} \dot{y} + \frac{1}{\varepsilon_y} y = -g, \quad \dot{\omega} = \frac{5}{2} \lambda_T, \quad (1)$$

where λ_T is the tangential force governed by the Coulomb friction law. We introduce the vector of state variables $\mathbf{p} = [\mathbf{x}, \dot{\mathbf{x}}, \mathbf{y}, \dot{\mathbf{y}}, \boldsymbol{\omega}]^T$, and thus the equations of motion are rewritten as

$$\dot{\mathbf{p}} = \begin{cases} \mathbf{F}_1 \mathbf{p} + \mathbf{g} & \text{if } \mathbf{H}(\mathbf{p}) > \mathbf{0}, \\ \mathbf{F}_R \mathbf{p} + \mathbf{g} & \text{if } \mathbf{H}(\mathbf{p}) = \mathbf{0}, \\ \mathbf{F}_2 \mathbf{p} + \mathbf{g} & \text{if } \mathbf{H}(\mathbf{p}) < \mathbf{0}, \end{cases} \quad (2)$$

where $\mathbf{F}_1, \mathbf{F}_R, \mathbf{F}_2 \in \mathbb{R}^{5 \times 5}$, $\mathbf{g} = [\mathbf{0}, \mathbf{0}, \mathbf{0}, -\mathbf{g}, \mathbf{0}]^T$ and $\mathbf{H}(\mathbf{p}) = \dot{\mathbf{x}} + \boldsymbol{\omega}$. This gives us three discontinuous, piecewise-smooth differential equations, where the switching condition is the velocity of the point of contact of the ball. Situations where $\mathbf{H}(\mathbf{p}) > \mathbf{0}$ and $\mathbf{H}(\mathbf{p}) < \mathbf{0}$ correspond to slipping with positive and negative tangential velocities at the point of contact respectively, whereas the ball is rolling when $\mathbf{H}(\mathbf{p}) = \mathbf{0}$.

Such system with a discontinuous first derivative is known as a *Filippov system*. In the analysis of this system we focus on the possible dynamics of the ball after it enters rolling, with a particular focus on whether the ball can enter slip again.

2. Results and Discussion

For a golf turf we select $\epsilon_y \ll \epsilon_x$, which means that the ground is a significantly more compliant in the normal direction than it is in the horizontal one. Alternative choices will lead to unphysical results, a particular example of which is $\epsilon_x \approx \epsilon_y$, in which both directions behave similarly and thus the lift off trajectories follow the inbound ones. In the physical setting the ball will enter the bounce slipping and may either change the direction from positive to negative slip without entering rolling, may slip throughout the impact or will enter rolling at some point. If the ball enters rolling it may then enter slipping again, but *only with a negative tangential velocity* of the contact point. It is also possible for the ball to remain rolling for the remaining part of impact, in which case an appropriate modelling framework, such as Utkin equivalent control law, must be applied to understand how the ball can remain on the boundary between the rolling surface and the negative slip region [2].

3. Concluding Remarks

The model of a compliant ground we propose presents a number of relevant behaviours that can be observed in the game of golf. Experimental campaign carried out in a controlled environment showed these to be applicable, however the data set is soon to be expanded by data from regular golf turf.

A problem that remains is the one of fitting parameters to the data. This proves to be difficult due to the discontinuities in the model which depend on the parameters themselves. We are in process of developing a structured approach which will see the use methods from finite element analysis and linear complementarity problems.

Acknowledgments: This work is partially funded and developed in cooperation with R&A Rules Ltd. We also acknowledge further funding from the UKRI EPSRC.

References

- [1] CROSS R: Backward bounce of a spinning ball. *European Journal of Physics* 2018, **39**(4):045007.
- [2] DI BERNARDO M, BUDD C.J., CHAMPNEYS A.R., KOWALCZYK P: *Piecewise-smooth Dynamical Systems. Theory and Applications*. Springer: London, 2008.
- [3] PENNER A.R.: The run of a golf ball. *Canadian Journal of Physics* 2002, **80**(8):931-940.

Modeling and simulation of friction processes with applications of piecewise-linear luz(...) and tar(...) projections

DĘBOWSKI ANDRZEJ¹, ŻARDECKI DARIUSZ^{2*}

1. Military University of Technology (WAT) [ORCID 0000-0003-1446-4415]
2. Military University of Technology (WAT) [ORCID 0000-0002-3934-2150]

* Presenting Author

Abstract: Modeling and simulation of systems with friction is still one of the most sophisticated problems of mechanics science, even it concerns “macroscopic” descriptions of friction actions in discrete MBS-type systems (Multi-Body Systems). Due to dry friction, such systems must function as systems with a variable structure resulting from stick-slip processes. The application of the Gauss principle enables to “circumvent” the problems of indeterminate forces of static friction in the states of total stiction. The use of luz(...) and tar(...) projections facilitates the synthesis of models in possibly compact forms. The article presents a “library” of ready-to-use mathematical models of several important elementary structures of MBS systems with friction that can be used in modeling of more complex mechanical systems. The created non-smooth models have no entangled forms, and are easy to use in computer programs with standard numerical procedures. The developed method can be used in the analysis of stick-slip phenomena in complex mechanical structures even in cases of static friction forces undetermined distribution. The article presents representative examples of the application of the method.

Keywords: systems with friction, stick-slip, modeling, simulation, projections.

1. Introduction

Two main categories of friction problems are noticed [3]: The first one concerns “microscopic” friction models and is representative for the tribology and contact theory. The second one concerns “macroscopic” descriptions of friction actions (stick-slip phenomena) in discrete systems and is representative for the MBS theory. Even though the macroscopic descriptions of the systems with friction based on Coulomb friction laws have a simplified character, a synthesis and analysis of such MBS models is usually very sophisticated [1]. Note, that even in 1D or 2D structures we can find peculiar problems (static friction force indeterminacy, Painleve paradoxes, etc.). In complex 3D MBS-type systems such problems are even more complicated. Modeling of discrete mechanical systems with friction must be supported by the mathematical theory relating to non-smooth dynamic systems, variable structure differential equations and inclusions [2]. Therefore in many cases simulation methods use iterative algorithms or heuristic procedures.

2. Results and Discussion

Meanwhile, as shown in the authorial works [4], [5], [6] a number of difficult problems of modeling friction systems can be resolved in a strict manner with using luz(...) and tar(...) piecewise linear projections (fig.1) and their mathematical apparatus.

Several friction systems discussed in that works have the variable structure analytical form of model (without algebraic constraints), ready to use in simulation programs with standard numerical procedures. Note that among these systems are the systems (for example two-mass system with three friction actions) with the problem of static friction indeterminacy resolved. Resolution of static friction

indeterminacy and synthesis of variable structure differential equations of motions has been here possible thank to application of the Gauss rule (minimization of acceleration energy in total stiction).

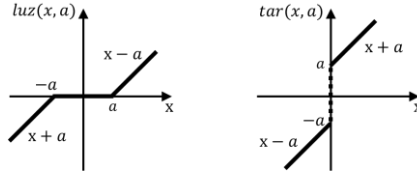


Fig. 1. Geometric interpretations of the luz(...) and tar(...) projections

The method of modeling and simulation friction processes with application luz(...) and tar(...) projections will be shown on the model of the system being activated on a special test stand. This stand is intended for very sophisticated experiments. It will be an instrument for verification elaborated models of elementary systems acting with friction in different mechanical configurations (fig.2).

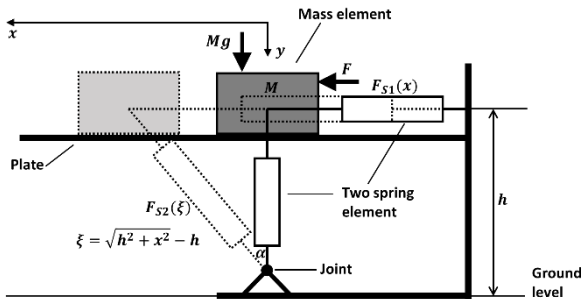


Fig. 2. Example configuration of the stand for testing friction processes

3. Concluding Remarks

The piecewise linear description basing on the luz(...) and tar(...) projections can be applied also for the friction characteristics expressing Stribeck effect, for characteristics with non-symmetry, etc.. Although the stick-slip models have been derived here for simplest friction characteristics, their final forms can be easy adapted to the other more complicate characteristics.

The luz(...) and tar(...) projections seem to be very efficient for modeling non-smooth mechanical systems.

References

- [1] AWREJCWICZ J., LAMMARQUE C.H.: Bifurcation and Chaos in Nonsmooth Mechanical Systems. World Scientific Publ. Co. Singapore, 2003.
- [2] BROGLIATTO B., DAM A.A.T., PAOLI L., GENOT F., ABADIE M.: Numerical simulation of finite dimensional multibody nonsmooth mechanical systems. *Applied Mechanical Review*: 2002, **55**(2), 107-150.
- [3] IBRAHIM R.A.: Friction-induced vibration, chatter, squeal, and chaos. Part I: Mechanics of contact and friction. Part II: Dynamics and modeling. *Applied Mechanical Review*: 1994, **47**(7), 207-253.
- [4] ŻARDECKI D.: Piecewise Linear luz(...) and tar(...) Projections. Part I – Theoretical Background, *Journal of Theoretical and Applied Mechanics*, 2006, **44** (1), 163-184.
- [5] ŻARDECKI D.: Piecewise Linear Modeling of Friction and Stick-Slip Phenomenon in Discrete Dynamic Systems, *Journal of Theoretical and Applied Mechanics*, 2006, **44** (2), 255-277.
- [6] ŻARDECKI D.: Static Friction Indeterminacy Problems and Stick-Slip Phenomenon Modeling in Discrete Dynamic Systems, *Journal of Theoretical and Applied Mechanics*, 2007, **45** (2), 289-310.

Nonlinear Dynamics of Dry Friction Oscillator Subjected to Combined Harmonic and Random Excitation.

Pankaj Kumar^{1*}, S Narayanan²

1: Dynamic Analysis Group, Bharat Heavy Electricals Limited, Nagpur, 440001, India

2: Mechanical Engineering, Indian Institute of Information Technology Design and Manufacturing, Kancheepuram, 600121, India. (Formerly, IIT Madras, 600036, India)

* Presenting author: pankajit1@yahoo.co.in

Abstract: A nonlinear dry friction oscillator to combined harmonic and stochastic excitation is considered. The discontinuous oscillator is modelled as a Filippov system. The oscillator exhibits discontinuity induced bifurcations (DIB) such as adding sliding bifurcations under harmonic excitation. The influence of noise on DIB is investigated by numerically integrating the equation of motion by an adaptive variable time stepping method (ATSM) combined with a bisection approach to accurately determine the discontinuity point. A Brownian tree approach is used for the solution to follow the correct Brownian path.

Keywords: Filippov model, Brownian tree, Discontinuity induced bifurcations

1. Introduction

Fig.1 shows a single degree of freedom nonlinear oscillator consisting of a mass, linear Spring, linear dashpot, nonlinear spring and nonlinear damper on a belt with dry friction moving with velocity V subjected to harmonic excitation and additive white noise. The equation of motion is given by[1]

$$\ddot{X} + \gamma_1 \dot{X} + \gamma_2 X^3 + \alpha g(\dot{X} - V) + \beta g(\dot{X} - V)^3 + \mu g \operatorname{sgn}(\dot{X} - V) = f_0 \cos \omega t + \sigma W(t)$$

where $\gamma_1 = k_1/m$, $\gamma_2 = k_2/m$, $\alpha = c_1/mg$, $\beta = c_2/mg$ and $f_0 = F_0/m$ and $W(t)$ is the white noise with intensity σ .

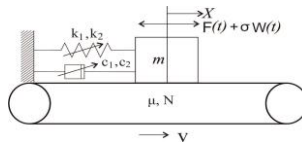


Fig. 1 Schematic diagram of dry friction oscillator with a moving belt.

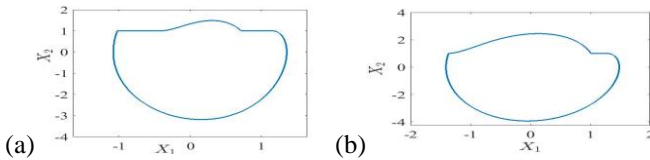


Fig. 2 phase space plot for $\sigma = 0$ (a) $\omega = 1.95$ (b) $\omega = 2.44$.

Santhosh *et al*[1] analysed the oscillator by modelling it as a Filippov system in which the dynamics in the smooth regions are described by two smooth vector fields F1 and F2 and in the discontinuous region by a convex combination of F1 and F2. It is seen that there is relative motion between mass and belt in the sticking phase, which was not observed when the sgn function was approximated by arc tangent function. This is indicative of adding sliding bifurcation which belongs to a class of DIBs. Figs 2(a) and 2(b) show respectively the phase plane diagrams for $\omega = 1.95$ and $\omega = 2.44$ obtained by using the Filippov model and event space numerical integration method. These are also verified by the ATSM, The other parameters adopted are $f_0 = 10m / s^2, \gamma_1 = 10s^{-2}, \alpha = 0.05s / m, \beta = \gamma_2 = 0, V = 1m / s, \mu = 0.6$.

2. Results and Discussion

The system is now investigated with the same set of parameters with noise included and using the Filippov convex combination model. The equation of motion was integrated using the ATSM [2] in combination with bisection method to determine accurately the discontinuity point. A Brownian tree approach is adopted so that the solution follows the correct Brownian path at each integration time step. It is observed that by proper tuning of the noise intensity the sliding region in the sticking phase can be altered. The phase planes for $\sigma = 0.25$ and $\sigma = 0.75$ are shown in Figs 3 (a) and (b) respectively for $\omega = 1.95$ which show chaos like behaviour modifying the motion in the sticking phase.

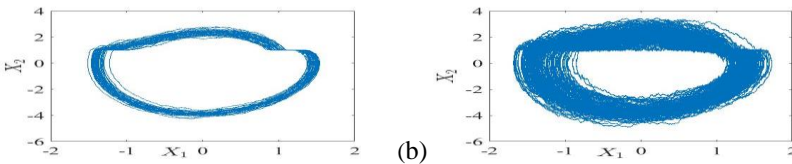


Fig. 3. phase space plot using ATSP for (a) $\sigma = 0.25$ (b) $\sigma = 0.75$.

3. Concluding Remarks

The dynamics of a dry friction nonlinear oscillator subjected to combined harmonic excitation and white noise is investigated by using Filippov model. The inclusion of noise alters the motion in the sticking phase considerably. The dynamics is further investigated by solution of corresponding Fokker-Planck equation and computing the largest Lyapunov exponent which are indicative of P and D bifurcations. These will be reported in the full paper.

References

- [1] Santhosh, B., Padmanabhan, C., Narayanan, S.: Discontinuity Induced Bifurcations in Nonlinear Systems. *Procedia IUTAM* 19, 219 – 227 (2016) .
- [2] Kumar, P., Narayanan, S.: Chaos and bifurcation analysis of stochastically excited discontinuous nonlinear oscillators. *Nonlinear Dynamics* 102, 927–950 (2020).

Analysis of the dynamics of an electromechanical system subjected to two orthogonal and interdependent dry-friction forces

ROBERTA LIMA^{1*}, RUBENS SAMPAIO²

1. Mechanical Engineering Department, PUC-Rio, Rio de Janeiro, Brazil [ORCID 0000-0002-2697-0019]

2. Mechanical Engineering Department, PUC-Rio, Rio de Janeiro, Brazil [ORCID 0000-0002-3533-3054]

* Presenting Author

Abstract: This work analyzes an electromechanical system with dry-friction forces. The system is composed of two coupled subsystems, a mechanical and an electromagnetic (a DC motor). The mechanical subsystem is subject to two dry-friction forces, modeled as Coulomb friction. Due to these two dry-friction forces, the resulting motion of the mechanical subsystem can be characterized by two qualitatively different and alternate modes, the stick- and slip-modes, with a non-smooth transition between them. The dry-friction forces acting on the mechanical subsystem are orthogonal and interdependent. In this paper, we construct the initial value problem that governs the system dynamics and we define the necessary conditions for the occurrence of the stick- and slip-modes. Numerical simulations are performed and the system response is analyzed for different combinations of mechanical and electromagnetic parameter values. One of the objectives is to quantify the stick-duration.

Keywords: electromechanical systems, dry-friction, stick-slip oscillations, stick-duration

1. Introduction

The presence of dry-friction in mechanical systems may induce stick-slip oscillations, a type of non-smooth dynamics [1,2]. When stick-slip occurs, the system response is characterized by two qualitatively different modes, the stick- and slip-modes [3-5]. The occurrence of stick-slip oscillations in mechanical systems is usually related to the existence of a force that saturates, i.e., a force whose magnitude is bounded, that is, the norm of the force is bounded, in certain conditions. The end of a stick-mode is related to the saturation of this force.

In this paper, we analyze stick-slip oscillations in a system with two orthogonal and interdependent dry-friction forces. Besides that, the system analysed is composed of two subsystems that interact, a mechanical and an electromagnetic (DC motor). Traditionally, stick-slip is analysed as the interplay of a friction force and an elastic one. In our case, there is no elastic force, it is substituted by a force generated by the motor. Then, we analyze stick-slip as the interplay of three forces: two dry-friction forces and one electromagnetic force (generated by the motor). The coupling between the two subsystems means mutual influence, i.e., the dynamics of the mechanical subsystem influences and is influenced by the dynamics of the electromagnetic subsystem [6-9]. Consequently, the dry-friction forces present in the mechanical subsystem affect and is affected by the interaction. Furthermore, the stick-slip oscillations affect and are affected by the electromechanical coupling. This paper is a continuation of our previous work [10] in which we analyze a simpler electromechanical system than the studied here. In [10] the electromechanical system was

subjected to just one dry-friction force. The presence of two orthogonal and interdependent dry-friction forces turns the system dynamics richer.

2. Results and Discussion

The system analyzed is a simple electromechanical system. It has just one mechanical and one electromagnetic degree of freedom. Due to the dry-friction forces, the system mode at each instant (stick or slip) depends on the state of the whole system, i.e., depends on mechanical and electromagnetic variables. Besides, during the stick mode, the motor rules the system dynamics. This is described by an initial value problem involving the current in the electric circuit of the motor. We consider that the construction of the dynamics (the initial value problem) that governs the dynamics of an electromechanical system with stick-slip is the major contribution of our work. Another contribution is the definition of the necessary conditions for the occurrence of the stick- and slip-modes. Depending on the values of the electromagnetic and mechanical parameter variables, the system response can be composed by: only slip mode (stick does not happen); sequence of alternate slip and stick modes (stick-slip oscillations); a slip followed by only a stick; only stick mode (the stick lasts forever). Numerical simulations are performed and it is shown the stick- and slip-modes parts in the response of the mechanical and electromagnetic subsystems.

3. Concluding Remarks

We analyze stick-slip oscillations without an elastic force (the most usual configuration in the literature). Instead of the elastic force, one has the force generated by a DC motor. Besides, we analyze stick-slip in a system subjected to two orthogonal and interdependent dry-friction forces. After the construction and analysis of the system dynamics, we quantify the stick-duration, one of the variables of great interest in systems with stick-slip dynamics.

Acknowledgment: The authors acknowledge the support given by FAPERJ, CNPq and CAPES.

References

- [1] LIMA, R., SAMPAIO, R.: Stick-mode duration of a dry-friction oscillator with an uncertain model. *J. Sound Vib.* 2015, **353**:259-271.
- [2] LIMA, R., SAMPAIO, R.: Two parametric excited nonlinear systems due to electromechanical coupling. *Journal of the Brazilian Society of Mechanical Sciences and Engineering* 2016, **38**:931-943.
- [3] AWREJCWICZ, J., OLEJNIK, P.: Occurrence of stick-slip phenomenon. *J. Theor. Appl. Mech.* 2007, **175**(1):33-40.
- [4] THOMSEN, J., FIDLIN, A.: Analytical approximations for stick-slip vibration amplitudes. *Int. J. Non Linear Mech.* 2003, **38**:389-403.
- [5] GALVANETTO, U., BISHOP, S.: Dynamics of a simple damped oscillator under going stick-slip vibrations. *Meccanica* 1999, **34**:337-347.
- [6] LIMA, R., SAMPAIO, R.: Construction of a statistical model for the dynamics of a base-driven stick-slip oscillator. *Mech. Syst. Signal Process* 2017, **91**:157-166.
- [7] LIMA, R., SAMPAIO, R.: Parametric analysis of the statistical model of the stick-slip process. *J. Sound Vib.* 2017, **397**:141-151.
- [8] LIMA, R., SAMPAIO, R., HAGEDORN, P.: One alone makes no coupling. *Mec. Comput.* 2018 **36**(20):931-944.
- [9] LIMA, R., SAMPAIO, R., HAGEDORN, P., DEÜ, J-F.: Lima, R., Sampaio, R., Hagedorn, P., Deü, J.: Comments on the paper “on nonlinear dynamics behavior of an electromechanical pendulum excited by a nonideal motor and a chaos control taking into account parametric errors” published in this journal. *Journal of the Brazilian Society of Mechanical Sciences and Engineering* 2019 **41**:552.
- [10] LIMA, R., SAMPAIO, R.: Stick–slip oscillations in a multiphysics system. *Nonlinear Dyn.* 2020, **100**:2215-2224.

A vibro-impact oscillator based energy harvester

SHUBHANSHU MAHESHWARI¹, ARAVINDAN MURALIDHARAN¹, SHAIKH FARUQUE ALI¹,
GRZEGORZ LITAK^{2*}

1. Department of Applied Mechanics, Indian Institute of Technology Madras, India
2. Department of Applied Mechanics, Lublin University of Technology, Poland

* Presenting Author

Abstract A piezoelectric energy harvesting system based on vibro-impact is investigated in the present study. The harvesting configuration comprises a primary unimorph beam which undergoes impact with two other unimorph beams on its either side. The governing equations of the piecewise-smooth linear dynamical system are developed using Hamilton's principle of least action. The dynamics and harvesting performance of the system under study are characterized through numerical simulations. The effect of parameters such as the clearance between the harvesters, frequency and amplitude of excitation on the magnitude of power and bandwidth are discussed in this study.

Keywords: vibro-impact, unimorph, energy harvesting, piezoelectric

1. Introduction

Wireless sensor systems are highly desirable in areas such as structural health monitoring as they reduce the maintenance requirements and this can only be accomplished by using batteries and/or harvested energy. Several works in the literature demonstrate that the power density obtained through piezoelectric vibration energy harvesters are comparable to thermoelectric generators and lithium-ion batteries. The common configuration of piezoelectric cantilever with a tip mass works well for harmonic excitation and exploits the linear resonance of the system [1]. Vibro-impacts are known to be a source of high kinetic energy. Recently, few of the works on energy harvesting have briefly outlined the importance of vibro-impacts in improving the power output [2]. Along these lines, a new harvesting system undergoing vibro-impacts is studied in this paper for its role in harnessing sizeable magnitude of power.

2. Harvester model and solution

The configuration of the system is inspired from the work done by Krishna and Padmanabhan [3] on investigation of second mode response of impacting cantilever beam and is shown in Fig. 1(a). The system includes a primary cantilevered unimorph in the middle separated from the secondary cantilevered unimorphs by a clearance. The mathematical model of the system is derived based on Euler Bernoulli's assumptions. Euler-Lagrange method is used to develop the governing electromechanical equations of the system. Since there is a time dependent contact between the unimorphs during vibro-impacts, the system is idealised as piecewise-smooth linear oscillators. The primary unimorph is given a harmonic base excitation, which is then transferred to the secondary unimorphs due to vibro-impacts. The governing equations the system are given by,

$$M\ddot{x} + C\dot{x} + Kx - \theta v = F$$

$$C_p \dot{v} + \frac{v}{R_l} + (\theta)^T \dot{x} = 0 \quad (1)$$

where M is the mass matrix, C is the damping matrix, K is the stiffness matrix, θ is coupling coefficient vector, x is the displacement vector, F is the vector of forces due to base displacement and v is the voltage vector. The stiffness matrix includes the terms accounted for both the stiffness of the system as well as the contact stiffness arising during impacts. The solutions of the governing equations are obtained through numerical simulations.

3. Results and Discussion

The natural frequencies of the primary (10.42 Hz) and secondary beams (14.75 Hz) are kept to be constant for all the studies carried out in this work. The effect of two different types of impacts namely the soft and hard impacts (classified depending upon the magnitude of contact stiffness relative to the stiffness of beams) for a given amplitude of excitation (2 mm) and clearance (1.2 mm) on the total power output are captured in the frequency responses shown in Fig 1(b). The magnitude of power harvested during hard impacts is observed to be significantly higher than during soft impacts. Hard impacts are also observed to enable the harvester to operate over a broader bandwidth as opposed to soft impacts. Time series analysis conducted in the study also showed that hard impacts predominantly involve chaotic responses than the soft impacts the effect of which on the magnitude of power averaged over time has been discussed in this work. Parametric studies are also conducted to study the influence of bifurcations arising due to the variation of amplitudes of excitation and clearance on the total output power.

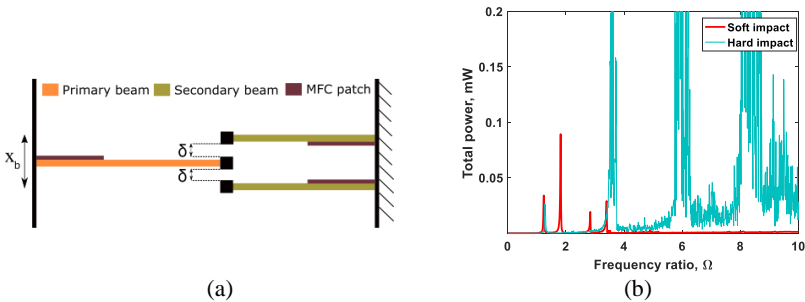


Fig. 1. (a) Schematic representation of the harvesting system (a) Frequency response of total power during soft and hard impacts

4. Concluding Remarks

The present study explores the possibility of exploiting vibro-impacts for improving the power output of a piezoelectric energy harvesting system. Results presented in the study show that vibro-impacts positively influence the magnitude and bandwidth of the harvested power for a given set of system parameters. The operating parametric regimes for enhanced energy harvesting are also identified from the bifurcation plots presented in the study.

References

- [1] FRISWELL M I, ALI S F, BILGEN O, ADHIKARI S, LEES A W, AND LITAK G: Non-linear piezoelectric vibration energy harvesting from a vertical cantilever beam with tip mass. *J. Intell. Mater. Syst. Struct.* 2012 **23**(13):1505–1521.
- [2] AFSHARFARD A: Application of nonlinear magnetic vibro-impact vibration suppressor and energy harvester. *Mech. Syst. Signal Process.* 2018 **98**:371–381.
- [3] KRISHNA I R P and PADMANABHAN C: Experimental and numerical investigation of impacting cantilever beams: Second mode resonance. *Int. J. Mech. Sci.* 2015 **92**:187–193.

A new method to determine periodic solutions in discontinuous systems with application to mass on moving belt

PREMCHAND V P^{1*}, BIPIN BALARAM, AJITH K MANI, SAJITH A S, M D NARAYANAN,

1. Department of Mechanical Engineering, Mar Baselios College of Engineering and Technology Trivandrum, India 695015 [ORCID: 0000-0002-0060-0634]
 2. Department of Mechanical Engineering, Amrita School of Engineering, Amrita Vishwa Vidyapeetham, Coimbatore, 641 112, India [ORCID: 0000-0002-6577-3149]
 3. Department of Mechanical Engineering, Saint Gits college of Engineering Kottayam , 686532 India
 4. Department of Civil Engineering, National Institute of Technology Calicut 673601, India
 5. Department of Mechanical Engineering, National Institute of Technology Calicut, 673601, India
- * Presenting Author (email - premchand.vp@mbcet.ac.in)

Abstract: Dry friction is one of the most complex nonlinear phenomena occurring in general machine dynamics. This work deals with the analysis of mass in motion on a moving belt which is undergoes stick slip oscillations due to dry friction between the contact surfaces. The mass attached to a spring damper system and placed on a conveyor belt with a specified velocity is subjected to a periodic excitation. This work generalises a Cluster Based Algorithm (CBA) developed by the authors for design optimisation of nonlinear systems to multi-harmonic excitations. The focus of the work is in the evaluation of parameters of spring and viscous damper in order to obtain a pure slipping condition when the mass is subjected to single and multi-frequency excitations. A cluster based analysis technique based on force and energy balance is used here for parameter evaluation and for finding the parameter regimes which yield pure-slip dynamics.

Keywords: Dry friction, Pure slip, Parameter estimation, Cluster analysis

1. Introduction

Frictional forces arising from sliding relative motion between surfaces are a well-known form of energy dissipation. The initial work dealing with modelling of friction in mechanical systems was done by Den Hartog [1] and well-studied by many authors [2-4]. In this section, a Cluster Based Algorithm as discussed in [5] is implemented in design of mass on moving belt systems subjected to multi-harmonic excitation with friction induced vibrations, to arrive at periodic solutions of pure slip type. The system parameters are the sliding mass (m), Damping coefficient (c), spring stiffness (k) and the friction force (f_r). The system is schematically shown in Fig. 1 and modelled as Eq(1).

$$m\ddot{x} + c\dot{x} + kx + fr\text{sign}(\dot{x} - v_b) = F(t) \quad (1)$$

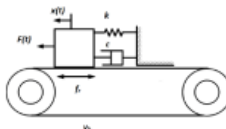


Fig. 1

In this work we consider two excitations (i) $F(t)=F \cos \omega t$, (ii) $F(t)=F_1 \cos \omega_1 t + F_2 \cos \omega_2 t$ and arrive at system parameters (k and c) to arrive at periodic solutions using the cluster based algorithm.

2. Results and Discussion

It is seen that the parameter sets yielding pure slip periodic solutions will converge to a cluster for single harmonic as well as multi-harmonic excitations. Any parametric point from the cluster will yield to a periodic pure slip orbit as evident from the phase plane plots, which are plotted using the design parameter values obtained from the cluster.

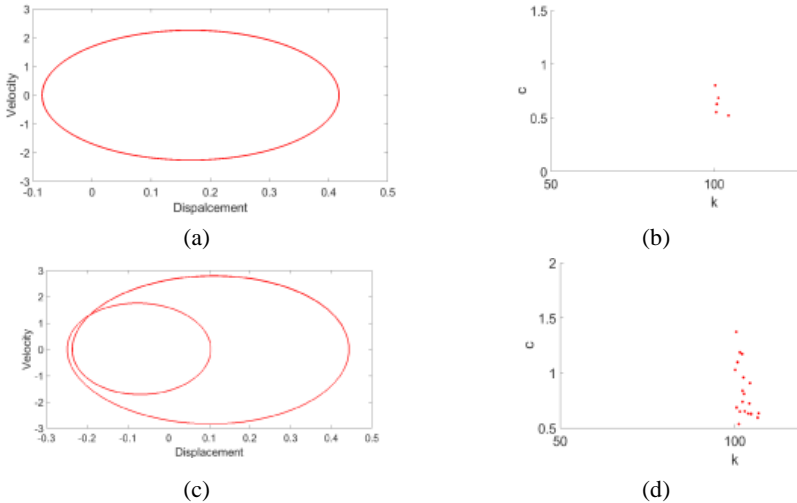


Fig. 2 (a) Phase plane plot for single frequency excitation (b) Optimal parameter cluster for single frequency excitation (c) Phase plane plot for multi-frequency excitation (d) Optimal parameter cluster for multi-frequency excitation

3. Concluding Remarks

In this work the cluster based algorithm is applied to mass on moving belt systems subjected to single and multi-harmonic excitation to arrive at design parameters (k, c) yielding pure-slip periodic response. It is seen that the algorithm can be applied to evaluate design parameters of nonlinear systems subjected to multi-harmonic excitation as well.

References

- [1] JP Den Hartog. Lxxiii. Forced vibrations with combined viscous and coulomb damping. *The London, Edinburgh, and Dublin Philosophical Magazine and Journal of Science*, 9(59):801-817, 1930.
- [2] MS Hundal. Response of a base excited system with coulomb and viscous friction. *Journal of Sound and Vibration*, 64(3):371-378, 1979.
- [3] U Andreaus and P Casini. Dynamics of friction oscillators excited by a moving base and/or driving force. *Journal of Sound and Vibration*, 245(4):685-699, 2001.
- [4] Jin-Wei Liang and Brian F Feeny. Balancing energy to estimate damping parameters in forced oscillators. *Journal of Sound and Vibration*, 295(3-5): 988-998, 2006.
- [5] Premchand V. P., M. D. Narayanan, Sajith A.S. A New Cluster-Based Harmonic Balance Aided Optimization Procedure With Application to Nonlinear Vibration Absorbers". *ASME Journal of Computational and Non-linear Dynamics*, 14(7), 2019.

-NUM-

**ORIGINAL NUMERICAL
METHODS OF VIBRATION
ANALYSIS**

Non-linear dynamics analysis of elastically supported beam under moving loads

Afras Abderrachid ^{1*}, El Ghoulbzouri Abdelouafi ²

1. Afras Abderrachid, Modelization, optimization and dynamics of civil engineering structures unit, National School of Applied Sciences Al Hoceima, university Abdelmalek Essaadi, Morocco.
2. El Ghoulbzouri Abdelouafi, Modelization, optimization and dynamics of civil engineering structures unit, National School of Applied Sciences Al Hoceima, university Abdelmalek Essaadi, Morocco.

*
Presenting Author

Abstract: In engineering practice we often come across the analysis of beams under moving loads, the beam design is largely and commonly used in modeling bridges, piles columns, railway track, and so on. Moreover, the design of beams based on elastic analysis is extremely likely to be conservative due to the unaccounted of geometric or material nonlinearities. As the common beam model which is highly used is the Euler-Bernoulli model, Bishop and Drucker [1] becoming the early study of the geometric nonlinearity in the E-B model, where an analytical solution was derived. Numerical schemes were also proposed to dealing with the problem can be viewed [2-4].

Especially in the field of dynamics of railway Bridge, as the beam deflections become larger, the generated geometric nonlinearities result in consequences that are not detected in linear systems. Concerning the corresponding nonlinear problem, very few papers have been published on this topic. In this paper the dynamic response of an elastically supported E-B beam constant cross-section undergoing moderate large deflections, traversed by moving loads is analyzed, the effects of the load speed, elastic stiffness on the dynamic response of the studied system is also investigated.

Keywords: nonlinearity, dynamic response, moving load, support elastic, resonance, bridge.

References

- [1] Bishop K, Drucker D. Large deflection cantilever beams, *Q. Appl Math*, 3 (1945) 272-275.
- [2] Chucheepsakul S, Buncharoen, Huang T. Elastica of simple variable-arc length beam subjected to end moment, *Jour Eng Mecha* 121 (1995) 767-772.
- [3] Chucheepsakul S, Buncharoen, Wang C.M. Large deflection of beam under moment gradient, *Jour Eng Mecha* 120 (1994) 1848-1864.
- [4] Malekzadeh P, Karami G. Large amplitude flexural vibration analysis of tapered plates with edges elastically restrained against rotation using DQM, *Engin Struct* 30 (2008) 2850-2858.

Continuation analysis of overhung rotor bouncing cycles with smooth and contact nonlinearities

MEHMET SELIM AKAY*, ALEXANDER D. SHAW, MICHAEL I. FRISWELL

Swansea University/College of Engineering, Swansea, United Kingdom

* Presenting Author;

Abstract:

The “brute force” time simulation approach for understanding the wide range of nonlinear phenomena linked to rotating machinery is inefficient because of the requirement for the transients to die out for every case, the need to examine multiple initial conditions, and the inability to trace unstable responses. With rotor-to-stator contact in the definition of the model, the accurate location of the contact places yet more computational load on the time simulations. Instead, a more standardised approach is used here by employing numerical continuation. Smooth nonlinearities such as cubic stiffness can give similar patterns of bouncing cycles to those seen with discontinuous stiffness rotor-stator contact models. Therefore, a 2-dof overhung rotor with cubic stiffness nonlinearity replacing the snubber contact is investigated in the rotating frame, which is used as a base to find the response of a smooth-contact definition using a hyperbolic tangent function. This work not only provides more insight into such responses, but also demonstrates numerical continuation as a potential tool to explore the nonlinear rotating system’s response in a more structured way.

Keywords: Rotor-stator contact, nonlinearity, internal resonance, numerical continuation

1. Introduction

Understanding the sustained intermittent rotor-to-stator contact response in rotating machinery is important as it might be dangerous in operating conditions. Zilli et al. [1] interpreted the internal resonance on a 2-dof overhung rotor with phasors. Shaw et al. [2] defined this relation as an internal resonance condition and generalised the idea to multi-dof models. Some authors modelled the contact with an impact definition [3]. An ongoing study has revealed the similarity of bouncing cycles between cubic and discontinuous stiffness models [4]. In the present study of the nonlinear overhung rotor shown in the left of Fig. 1, the rotor-stator contact interaction is initially replaced by an isotropic cubic stiffness. Once the solution branches are known, a homotopy to a hyperbolic tangent function approximating a contact nonlinearity is applied, to explore the characteristics of the system with contact and gain new insights.

2. Models and methods

Equation (1) shows the nondimensionalised nonlinear equations of motion of the 2-dof overhung rotor in rotating coordinate frame (Fig. 1).

$$U'' + (-\hat{\Omega}J(\hat{f}_p - 2) + 2\zeta)U' + (\hat{\Omega}^2(\hat{f}_p - 1) + 1 + 2\zeta\hat{\Omega}J)U + \kappa f_{snub} + (\kappa - 1)f_{cubic} = \hat{m}\hat{\epsilon}\hat{\Omega}^2 \begin{Bmatrix} 1 \\ 0 \end{Bmatrix}, \quad J = \begin{bmatrix} 0 & -1 \\ 1 & 0 \end{bmatrix} \quad (1)$$

where, U is the position vector in the rotating frame, ζ is damping ratio, $f_{snub} = 0.5 \tanh(K(\hat{r} - 1) + 1)\beta(\hat{r} - 1)$ and $f_{cubic} = \gamma\hat{r}^2U$ are the smooth contact and cubic stiffness restoring forces, respectively; K is the steepness of the tanh function, β is the measure of snubber-ring stiffness, and γ is the measure of cubic stiffness.

3. Results and Discussion

A converged 2:1 and 3:1 internal resonance response from the cubic stiffness simulations is used as a starting point for the numerical continuation scheme, which yields an entire solution branch. An orbit on this branch is used to start continuation of the homotopy parameter switching to the contact definition. The results are shown in the right of Fig. 1. The smooth-contact case shows period doubling, which would in a “brute force” analysis, cause difficulty in obtaining the whole branch. Period doubling bifurcations can be seen on the smooth-contact model, towards lower amplitudes. Note that the lowest amplitude level for the 3:1 cubic branch (bold green) is below the contact level; after the nonlinearity switch (thin green), the lowest point moves upward above the contact level. Although close to contact amplitude the response is mostly unstable, in the small region between nondimensional rotor speeds of 4.4 – 5.0, the unstable periodic orbits of 3:1 might push the transitional responses to the 2:1 stable periodic orbits.

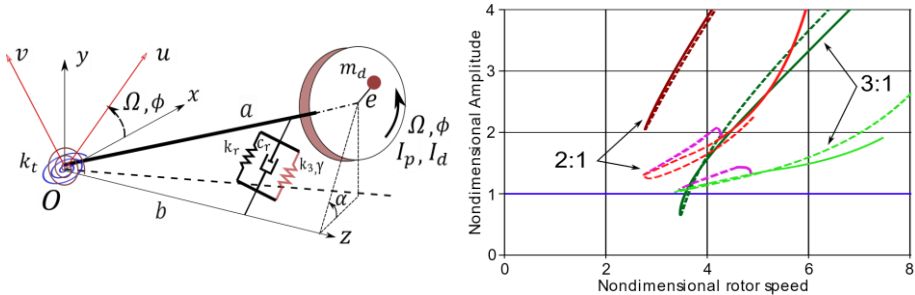


Fig. 1. Left: Schematic representation of the cubic stiffness model. Right: Bifurcation diagram with the cubic (bold lines) and with tanh nonlinearity (thin lines). Purple branches show period doubling response. Dashed lines show unstable responses. Blue line shows the contact amplitude.

This method enables one to start from an easier nonlinearity and explore the response in a more complex one without the expensive of brute force simulations, which does not guarantee even to find all stable solution responses, while completely diverging from the unstable periodic orbits.

Acknowledgment: This research was funded by the Ministry of National Education of the Republic of Turkey.

References

- [1] ZILLI A, WILLIAMS RJ, EWINS DJ: Nonlinear Dynamics of a Simplified Model of an Overhung Rotor Subjected to Intermittent Annular Rubs. *J Eng Gas Turbines Power* 2015, **137**(6):1-10.
- [2] SHAW AD, CHAMPNEYS AR, FRISWELL MI: Asynchronous partial contact motion due to internal resonance in multiple degree-of-freedom rotordynamics. *Proc R Soc A Math Phys Eng Sci* 2016, **472**(2192).
- [3] MORA K, CHAMPNEYS AR, SHAW AD, FRISWELL MI: Explanation of the onset of bouncing cycles in isotropic rotor dynamics. *Proc R Soc A Math Phys Eng Sci* 2020, **476**(2237).
- [4] AKAY MS, SHAW AD, FRISWELL MI: Continuation analysis of a nonlinear rotor system, *Nonlinear Dyn.*, Under review.

A neural network based surrogate model for assessing vibration induced fatigue damage on wind turbine tower

HAO BAI^{1*}, LUJIE SHI^{1†}, CHANGWU HUANG², DIDIER LEMOSSE¹

1. Laboratory of Mechanics of Normandy (LMN), INSA Rouen Normandy, Rouen 76000, France [0000-0003-3546-8802]
2. Department of Computer Science and Engineering, Southern University of Science and Technology, Shenzhen 518055, China [0000-0003-3685-2822]

* Presenting Author

† Corresponding Author: Lujie Shi, lujie.shi@insa-rouen.fr

Abstract: The vibration-induced fatigue damage is a critical issue for both the structural safety and the producibility of the wind turbine. However, the conventional fatigue assessment based on computational mechanics is usually time-consuming. To overcome this drawback, a surrogate model based on the deep neural network is proposed in this work. The numerical results validate both the effectiveness and the accuracy of the proposed model.

Keywords: Fatigue damage, Residual neural network, Wind turbine tower, Numerical method

1. Introduction

The random nature of the wind actions could cause unexpected fatigue damage and thus reduce the wind turbine's operating lifetime. With the increasing size of wind turbine towers, the fatigue damage induced by the vibrations and cyclic loads becomes more and more crucial. Therefore, a reliable mechanical design is essential for high-rise wind turbines to ensure their operating lifetime. To assess the fatigue damage on wind turbine towers, a probabilistic framework was newly proposed [1]. The concept is based on a combination of deterministic fatigue analysis and probabilistic approach. Therefore, a large number of numerical simulations is required to prepare a dataset for fatigue estimation which is a heavily time-consuming task. To overcome this drawback, we propose a surrogate model for the proposed framework using a deep neural network in this paper.

The model is based on residual multilayer perceptrons (ResMLP) [2] that the skip connections are introduced to an ordinary neural network. The proposed surrogate model is compared to the direct numerical solutions for NREL 5MW reference wind turbine [3] using the simulation tool FAST [4].

2. Results and Discussion

Firstly, the trained model is used to predict the fatigue response of the reference wind turbine under wind conditions with turbulence. The neural network was trained by using the fatigue damage calculated for mean wind speed from [3.0 m/s, 4.0 m/s, ..., 25.0 m/s]. The test set was to predict the fatigue damage in the same wind condition except that the mean wind speeds are drawn from [3.5 m/s, 4.5 m/s, ..., 24.5 m/s]. These cases of mean wind speed have never appeared in the training dataset nor the validation dataset. Likewise, the number of simulations per mean wind speed is also fixed to 10 000 runs which implies a total of 220 000 numerical simulations in FAST codes. The 10-min cumulative fatigue damages acquired in these numerical simulations are compared to those ob-

tained from the trained neural network. To keep this paper to be brief, only the comparison near cut-in speed (i.e., 3.0 m/s) and cut-out speed (i.e., 25.0 m/s) are graphed in Fig. 1.

The correlation between the predicted damages and the simulated damages proves that the predicted values are mostly conformed to the simulated values of the fatigue damage. Among 10 000 points at each mean wind speed, only tens of points are away from the linearly correlated line (red line).

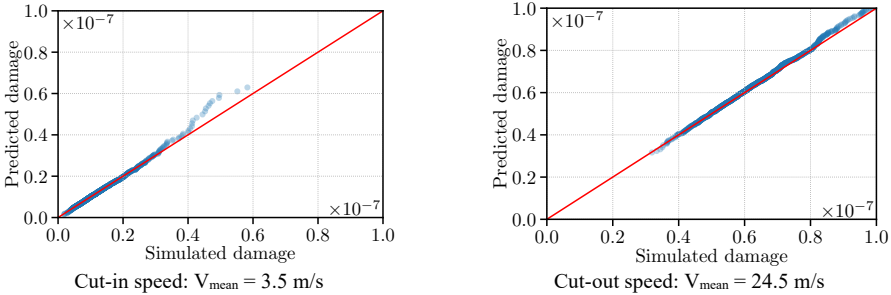


Fig. 1. Comparison between the predicted values and the simulated values for 10-min cumulative fatigue damage at (a) cut-in speed and (b) cut-out speed

The good accuracy of the trained residual neural network in predicting 10-min cumulative fatigue damage for untested mean wind speeds encourages the author to use it in predicting the fatigue response of the wind turbine tower under stochastic mean wind speeds.

3. Concluding Remarks

In this paper, a surrogate model using a deep neural network with residual learning is developed for assessing the fatigue damage induced by the vibrations. The model implements a 13-hidden-layers neural network with 300 perceptrons on each layer to predict the 10-min cumulative fatigue damage of the NREL 5MW reference wind turbine under wind with turbulence. The reference wind turbine is assumed to generate electrical power normally during a fixed simulated time of 10 minutes.

A sample including 23 000 observations for the training dataset and 5750 observations for the validation dataset is used to train the ResMLP. The accuracy of the predictions from the trained model is assessed by comparing with the numerical results computed directly from FAST simulator. It is demonstrated that the surrogate models can accurately and economically predict the distribution of 10-min cumulative fatigue damage for any mean wind speed in the operating range, i.e., between cut-in speed and cut-out speed. This advantage opens the opportunity to implement the proposed probabilistic framework for fatigue assessment in the wind energy industry in which a quick-response design process is usually required.

References

- [1] BAI H, LEMOSSE D, AOUES Y, CHERFILS JM, HUANG C: A probabilistic approach for long-term fatigue analysis of onshore wind turbine tower. *14th World Congress on Computational Mechanics*, 2020.
- [2] HE K, ZHANG X, REN S, SUN J: Deep residual learning for image recognition. *Proceedings of the IEEE conference on computer vision and pattern recognition*, 2015;:770-778.
- [3] JONKMAN J, BUTTERFIELD S, MUSIAL W, SCOTT G: Definition of a 5-MW Reference Wind Turbine for Offshore System Development. *National Renewable Energy Laboratory (NREL)*, 2009.
- [4] JONKMAN J, JR. BUHL M: FAST User's Guide. *National Renewable Energy Laboratory (NREL)*, 2005.

Localization of Changes in Stiffness in Numerical Models of Beams Using Additional Masses

ARTUR BOROWIEC^{1*}

1. Rzeszów University of Technology, Rzeszów, Poland [0000-0002-9475-3251]

* Presenting Author

Abstract: The paper presents the possibilities of developing a damage localization method that is not based on a reference model. The work presents examples of stiffness changes localization in numerical models of beam based on changes in natural frequency in combination with the Laplacian differential operator. The changes were caused by two additional masses moving on the nodes of the cantilever beam model.

Keywords: damage localization, eigenfrequencies, Laplacian differential operator

1. Introduction

Damage detection using modal analysis has been developed in civil engineering since the 1970s. Most modal diagnostics is based on changes in the natural frequency or the mode of natural vibrations. Most of the methods are based on a reference model for which the values of the dynamic parameters of an undamaged structure are known. In the work [1], for the location of the damage, a comparison of vibration curves with the use of a differential operator was used. Currently, methods without a reference model are also used [2]. In the article [3] was taking into account an additional parameter (mass, support), which made it possible to locate damage by analysing changes in the natural frequency with respect to its position.

The paper proposes the use of the Laplacian differential operator to evaluate the change in dynamic parameters caused by two masses in order to determine the position of stiffness changes in the beam model.

2. Results and Discussion

The numerical model of the considered cantilever beam (Fig.1) was built in the Matlab environment with FEM libraries from the Calfem package.

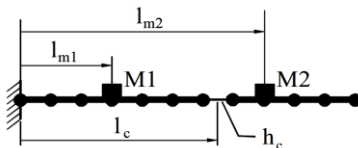


Fig. 1. Numerical model.

The simple model was constructed of 24 elements and contained of 25 nodes. During the analyzes, the eigenfrequencies ω_i were calculated for the selected locations of stiffness changes (l_c) and for the selected range of stiffness changes (h_c) with the masses (M_1, M_2) added at the nodes (l_{m1}, l_{m2}).

The obtained results include changes in the eigenfrequencies ω_i performed using discrete Laplacian approximation:

$$L(\omega_{l_{m1}, l_{m2}}) = \frac{\omega_{l_{m1}+1, l_{m2}} - 2\omega_{l_{m1}, l_{m2}} + \omega_{l_{m1}-1, l_{m2}}}{d_{l_{m1}}^2} + \frac{\omega_{l_{m1}, l_{m2}+1} - 2\omega_{l_{m1}, l_{m2}} + \omega_{l_{m1}, l_{m2}-1}}{d_{l_{m2}}^2} \quad (1)$$

The results on Fig. 2a shows changes in second eigenfrequency ω_2 with stiffness reduction (40%) of the 14th element. The most significant changes of $L(\omega_2)$ were observed near location of stiffness changes (Fig. 2b).

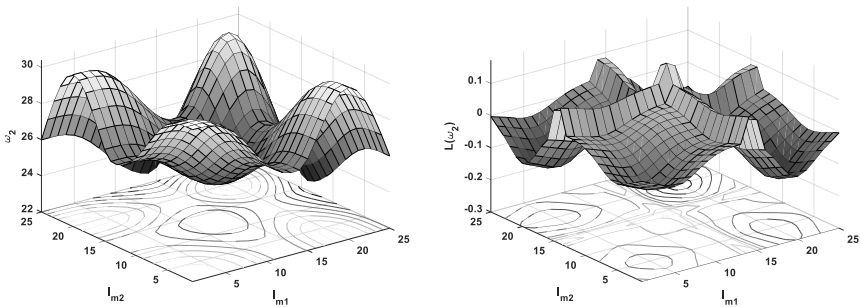


Fig. 2. Localization of change in stiffness in the 14th element: a) ω_2 ; b) $L(\omega_2)$.

3. Concluding Remarks

The main advantage of the presented approach is the possibility of stiffness changes localization without a reference model using two addition masses. The use of Laplacian operator improved the ability to identify the position of changes in stiffness.

References

- [1] PANDEY A, BISWAS M, SAMMAN M: Damage detection from changes in curvature mode shapes. *Journal of Sound and Vibration* 1991, **145**:321-332.
- [2] ZHONG S, OYADJI O, DING K: Response-only method for damage detection of beam-like structures using high accuracy frequencies with auxiliary mass spatial probing, *Journal of Sound and Vibration* 2008, **311**(3-5):1075-1099.
- [3] DEMS K, MRÓZ Z: Identification of damage in beam and plate structures using parameter-dependent frequency changes, *Engineering Computations* 2001, **18**(1/2):96-120.

Estimation of orbits after blade loss for a multi-disk rotor

FADI DOHNAL^{1*}, ATHANASIOS CHASALEVRIS²

1. Division for Mechatronics Lienz, UMIT - Private University for Health Sciences, Medical Informatics and Technology, Austria [0000-0002-9289-4069]

2. School of Mechanical Engineering, National Technical University of Athens, Greece [0000-0002-6891-439X]

* Presenting Author

Abstract: A flexible rotor supported by fluid-film bearings is investigated in the case of light, intermediate and heavy blade loss. In this first study, the rotor is supported by circular fluid-film bearings. The resulting rotor orbits at the bearing locations are determined for different levels of blade loss unbalance and support flexibility. This is a critical scenario for industrial rotors and usually leads to convergence problems for high unbalance forces at which the rotor approaches or even hits the bearing housing. Strategies for improving convergence as well as reducing calculation time are explored for this demanding numerical solution. The industrial rotor dynamics tool MADYN/NOLIN is chosen for modelling the fluid-film dynamics and unbalance response in case of small unbalance forces. Add-on code is developed for enabling convergence for large unbalance forces. The results are benchmarked against investigations in literature. The impact of a heavy blade loss is outlined and the resulting bearing orbits are evaluated.

Keywords: rotor dynamics, nonlinear dynamics, flexible rotor, fluid-film bearing

1. Introduction

Blade loss in a rotor is a severe condition that causes a sudden change in unbalance, which results in general to an increase of the dynamic load. An industrial rotor and its support structure need to be designed for a safe run-down in case of blade loss. For large values of unbalance, the dynamic forces are no longer negligible compared to the static load [1-3]. At this extreme condition, the linearized bearing characteristics are no longer valid and the nonlinear behaviour of the fluid-film and the bearing support become dominant.

2. Results and Discussion

We investigate the rotor deflection at the bearing locations for the simple multi-disk rotor as visualised in Fig. 1. This rotor is physically available in the lab and fully instrumented and allows for an experimental verification at a later stage. In our study, we develop a calculation procedure for achieving the numerical convergence for intermediate and heavy dynamic loads. Typical orbits for a light and intermediate dynamic load are shown in Fig. 2. These results are based on the simplified short bearing theory

$$\begin{aligned}
 F_t &= \frac{\eta_{oil} B^3 \Omega}{D \psi^2} \left[\frac{\pi}{2} \left(1 - \frac{2\dot{\gamma}}{\Omega} \right) \frac{\varepsilon}{(1 - \varepsilon^2)^{3/2}} + \frac{\dot{\varepsilon}}{\Omega} \frac{4\varepsilon}{(1 - \varepsilon^2)^2} \right] \\
 F_r &= -\frac{\eta_{oil} B^3 \Omega}{D \psi^2} \left[\left(1 - \frac{2\dot{\gamma}}{\Omega} \right) \frac{2\varepsilon^2}{(1 - \varepsilon^2)^2} + \pi \frac{\dot{\varepsilon}}{\Omega} \frac{1 + 2\varepsilon^2}{(1 - \varepsilon^2)^{5/2}} \right]
 \end{aligned} \tag{1}$$

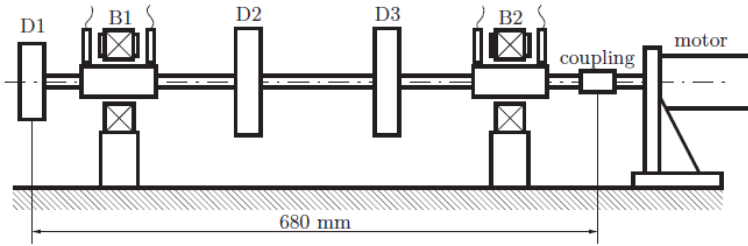


Fig. 1. Flexible, multi-disk rotor supported by two bearings.

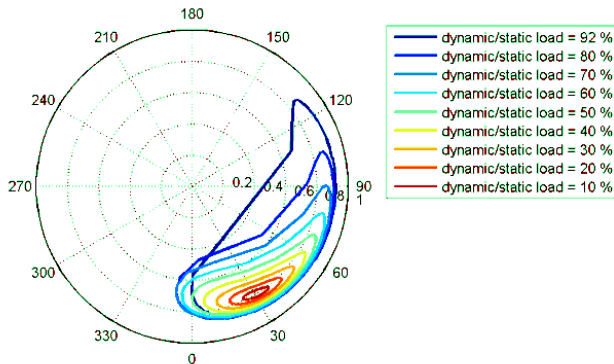


Fig. 2. Rotor orbits of a point mass in a short circular fluid-film bearing for light and intermediate unbalance.

This simplified estimation is benchmarked against a full nonlinear rotordynamic calculation using MADYN/NOLIN with improved convergence.

References

- [1] THIERY F, GANTASALA S, AIDANPÄÄ J-O, Numerical evaluation of multilobe bearings using the spectral method, *Advances in Mechanical Engineering* 2017, **9**:1–10
- [2] MONMOUSSEAU P, FILLON M, FRÈNE J, Transient Thermoelastohydrodynamic Study of Tilting-Pad Journal Bearings Under Dynamic Loading, *J. Eng. Gas Turbines Power* 1998, **120**(2):405-409
- [3] WANG N, LIU C, JIANG D, Prediction of transient vibration response of dual-rotor-blade-casing system with blade off, *Proceedings of the Institution of Mechanical Engineers, Part G: Journal of Aerospace Engineering* 2019, **233**(14): 5164–5176

Seismic response of adjacent steel frames linked by friction dampers

MEHDI EBADI-JAMKHANEH^{1*}, MASOUD AHMADI², DENISE-PENELOPE N. KONTONI^{3,4*}

1. Assistant Professor, Department of Civil Engineering, School of Engineering, Damghan University, Damghan, Iran. E-mail: m.ebadi@du.ac.ir [<https://orcid.org/0000-0001-9914-8280>]
2. Assistant Professor, Department of Civil Engineering, School of Engineering, Ayatollah Boroujerdi University, Boroujerd, Iran. E-mail: masoud.ahmadi@abru.ac.ir [<https://orcid.org/0000-0002-3694-0518>]
3. Associate Professor, Department of Civil Engineering, School of Engineering, University of the Peloponnese, GR-26334 Patras, Greece. E-mail: kontoni@uop.gr [<https://orcid.org/0000-0003-4844-1094>]
4. School of Science and Technology, Hellenic Open University, GR-26335 Patras, Greece. E-mail: kontoni.denise@ac.eap.gr [<https://orcid.org/0000-0003-4844-1094>]

* Presenting Author

Abstract: The simplest way for the elimination of earthquake-induced pounding that occurs between two adjacent structures is to have a proper gap between the two structures. However, this method is not applicable in all cases, and we should search for methods that can reduce the pounding effects. Linking the two adjacent structures with different elements like friction dampers (FDs) is one of the applicable strategies that can be studied. A friction damper (FD) absorbs energy by friction, and the slip force is the most important factor in these dampers. In this study, the effect of pounding on adjacent frames with different heights and also the effect of considering friction dampers with optimum slip force that are distributed uniformly in the stories, have been discussed. It is concluded that the pounding results in decreasing the responses of the low-rise frame and in increasing the responses of the high-rise frame. It is revealed that linking dampers does not reduce pounding effects in all cases, and their performance in reducing or increasing the responses of the frames belongs to the characteristics of the adjacent frames and the acceleration time history.

Keywords: impact, friction damper, damage index, non-linear dynamic analysis, adjacent frames

1. Introduction

An earthquake has always endangered human life and property as one of the most dangerous natural disasters. By observing the past seismic events, it can be known that one of the phenomena caused by earthquakes and which intensifies the damage is the impact phenomenon. Impact refers to the collision of two structures that have different dynamic properties and therefore vibrate non-simultaneously. Lack of sufficient gap between the two structures is another condition that is necessary to create a collision. This phenomenon has been observed in recent decades with the increase in the value of urban lands and cost of buildings, and in several earthquakes has caused various damages, including the destruction of walls, failure of collided columns, and complete collapse of buildings. Researchers have always been looking for a way to eliminate or reduce the damage caused by this phenomenon. The simplest way to eliminate impact is to create enough gap between the two structures so that they do not collide with each other due to non-phase vibration. But this method is not always applicable and is also an uneconomical method. Therefore, a solution must be provided to reduce the effects of this phenomenon. Among these, methods such as filling the space between two structures with shock-absorbing materials or connecting two buildings with high-strength beams in the form of two pin ends were proposed [1]. Another method proposed by the researchers is to use

dampers between two structures that are subjected to impact [2]. Since a few research has been done on how friction dampers affect impact responses in adjacent tall and short buildings under an earthquake, more research is needed. In this study, the effects of friction dampers (FDs) on the seismic behavior of steel buildings are investigated.

2. Results and Discussion

In this study, the pounding effect on two adjacent 9-story and 12-story frames is investigated under the Landers earthquake (component ABY090 seismic record). The displacement of the floors in the case of the gap distance is zero, sometimes increased and sometimes decreased compared to the single case, with a maximum change of 4%, which is not a considerable value. In the distance of 72 mm and 144 mm, the response due to impact is severely reduced by 45%. A 31% reduction in displacement at a distance of 288 mm indicates that the effect of the impact has decreased with increasing the distance between two frames. By connecting the two frames per each floor level with friction dampers at a distance of 72 mm, an increase in displacement can be seen compared to the case where there is no damper between the two frames, which in the maximum case increases by 24%. At a distance of 144 mm, the displacement of the floors with the dampers sometimes decreased and sometimes increased, which can be reduced by 38.9% and increased by 25%. Placing the dampers at a distance of 288 mm causes the displacement to be significantly reduced under the seismic record with a maximum value of 47%. At a distance of 144 mm, in most cases, there was an increase in response, which averaged 8.2%. By increasing the distance to 288 mm, the damage index decreases by an average of 0.4%.

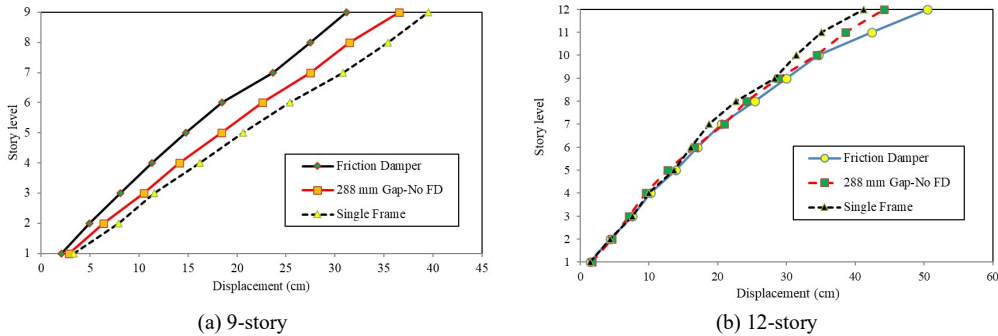


Fig. 1. Distribution of floor lateral displacements with and without friction dampers under the Landers earthquake in (a) 9-story and (b) 12-story frames

3. Concluding Remarks

By increasing the distance between the two frames, the friction dampers are able to absorb more energy by being able to displace more and have a better performance at reducing the responses. When the distance between the two frames is zero, the responses are always close to the single state, and a little change is observed in them. By examining the effect of impact, it was concluded that the impact between buildings with a different number of floors reduces all responses in the shorter building and increases them in the taller building.

References

- [1] AHMADI M, EBADI-JAMKHANEH M: Numerical Investigation of Energy Dissipation Device to Improve Seismic Response of Existing Steel Buildings with Soft-First-Story. *International Journal of Steel Structures* 2021, **21**(2): 691-702.
- [2] PATEL CC, JANGID RS: Dynamic response of adjacent structures connected by friction damper. *Earthquakes and Structures* 2011, **2**(2): 149-69.

Deficient RC slabs strengthened with combined FRP layer and high-performance fiber-reinforced cementitious composite

MEHDI EBADI-JAMKHANEH^{1*}, MASOUD AHMADI², DENISE-PENELOPE N. KONTONI^{3,4*}

1. Assistant Professor, Department of Civil Engineering, School of Engineering, Damghan University, Damghan, Iran. E-mail: m.ebadi@du.ac.ir [<https://orcid.org/0000-0001-9914-8280>]
2. Assistant Professor, Department of Civil Engineering, School of Engineering, Ayatollah Boroujerdi University, Boroujerd, Iran. E-mail: masoud.ahmadi@abru.ac.ir [<https://orcid.org/0000-0002-3694-0518>]
3. Associate Professor, Department of Civil Engineering, School of Engineering, University of the Peloponnese, GR-26334 Patras, Greece. E-mail: kontoni@uop.gr [<https://orcid.org/0000-0003-4844-1094>]
4. School of Science and Technology, Hellenic Open University, GR-26335 Patras, Greece. E-mail: kontoni.denise@ac.eap.gr [<https://orcid.org/0000-0003-4844-1094>]

* Presenting Author

Abstract: Today, strengthening of concrete structures in order to withstand excessive loads and increase the ductility of the structure, etc., using high-performance fiber-reinforced cementitious composite (HPFRCC) and fiber-reinforced polymer composite (FRP) is very common. In this study, a reinforced concrete (RC) slab under vertical load with different strengthening methods is investigated using the finite element method (FEM). If the quality of the slab is poor and 60% of the concrete strength is lower than the standard design status, the flexural stiffness of the slab is reduced by 75%, and the need for reinforcement is felt. By changing the width of the FRP layer with a strip arrangement from 50 to 100 cm and changing the thickness from 2 to 7 mm per slab with a width of 4 m, the maximum stiffness and bearing capacity are experienced with an increase of 23% and 10%. Also, by changing the width of the FRP layers in the checkered arrangement from 50 to 100 cm and changing the thickness from 2 to 7 mm, the maximum hardness and bearing capacity are experienced with an increase of 22% and 25%. It can be concluded that the use of the checkered arrangement is more effective in increasing the bearing capacity.

Keywords: concrete slab, strengthening method, FRP layer, HPFRCC, crack

1. Introduction

At present, various methods are used to repair and strengthen the members and connection of reinforced concrete (RC) structures. The new fiber reinforced polymer (FRP) material, in addition to being resistant to corrosive environments and having a tensile stiffness equal to or even higher than steel, is lightweight and easy to apply. For this reason, strengthening RC members with FRP sheets is an important issue. In recent years, the use of FRP sheets in the strengthening of the existing structures has received much attention, and therefore scientific studies on this issue seem necessary. Also, the weakness of concrete in the tensile zone and its replacement with HPFRCC concrete can eliminate the tensile weakness of concrete. Despite the fact that this method can be very effective in various fields such as repair and reinforcement of concrete members, but the study and finite element analysis on the strengthening of RC slabs compared to other concrete members is less investigated. One of the applications of FRP is to place the layers on the replacement part of ordinary concrete with HPFRCC concrete to strengthen the flexibility of concrete slabs in long openings. In these cases, if the initial

design of the member is unsuitable, its stiffness and flexural strength can be increased by using FRP sheets. Therefore, in this study, the effect of FRP sheets located on HPFRCC concrete on the flexural strength of reinforced concrete slabs is investigated. For this purpose, the deficient RC slab of a bridge with two reduced levels of compressive strength of concrete is strengthened with the use of carbon fiber reinforced polymer (CFRP) sheets, and the validity of numerical studies is checked using the available test results.

2. Results and Discussion

Loading is done in the case of a slab with a span of 4 m according to the passage of the 700 kN tank and a slab with a span of 5 m according to the loading pattern of the train. The compressive strength of concrete in the initial state is 30 MPa. Initially, a 4 m concrete slab is placed under the tank load by reducing the compressive strength by 30% (the compressive strength of concrete, in this case, is equal to 21 MPa), and then with a further drop, the compressive strength of 30 MPa is decreased to 12 MPa to evaluate the behaviour of the system and simulate the state of damage or weakness in the concrete mix at the time of construction. Based on the result, it is determined that with a 30% decrease in concrete strength, the flexural stiffness of the slab by 89%, and with a 60% decrease in concrete strength, the initial flexural stiffness of the model is only 9% compared to the damaged model. By reducing the strength by 30% of the initial strength of concrete, tensile cracks were not observed in the model despite the displacement of 5 mm. However, with a further reduction of the resistance from 21 to 12 MPa, it was observed that the system underwent nonlinear behaviour, and tensile cracks were observed in the edges of the slab and the lower surface of the slab. If three layers of CFRP are used as a strip next to each other with a distance of half the width of each layer and different thicknesses, it is observed that by increasing the width from 50 to 100 cm in a fixed thickness (2 mm), the flexural stiffness increases by only 5%. By changing the thickness from 2 to 7 mm by keeping the width of the CFRP constant, it is observed that the bending stiffness is increased by 15% and the bearing capacity is increased by up to 8%. By changing the width from 50 to 100 cm and changing the thickness from 2 to 7 mm, the maximum stiffness and bearing capacity are experienced with an increase of 23% and 10%, respectively. In the case of using three layers of CFRP layers in a checkered pattern next to each other with a distance of half the width of each CFRP layer and different thicknesses, it is observed that by increasing the width from 50 to 100 cm in constant thickness (2 mm), bending stiffness increases by only 4% and bearing capacity increases by more than strip model (8%). By changing the thickness from 2 to 7 mm by keeping the width of the CFRP constant, it is observed that the bending stiffness has increased by 17% and the bearing capacity has increased by 21%. By changing the width from 50 to 100 cm and changing the thickness from 2 to 7 mm, the maximum hardness and bearing capacity are experienced with an increase of 22% and 25%. It can be concluded that the use of the checkered pattern is more effective in increasing the bearing capacity.

3. Concluding Remarks

Based on the results, it is determined that with a 30% decrease in concrete strength, the flexural stiffness of the slab decreased by 89%, and with a 60% decrease in concrete strength, the initial flexural stiffness of the specimen is only 9% compared to the damaged specimen. By reducing the strength by 30% of the initial strength of concrete, tensile cracks were not observed in the model in the displacement of 5 mm.

References

- [1] KODUR VK, BISBY LA, GREEN MF: Preliminary Guidance for the Design of FRP-strengthened Concrete Members Exposed to Fire. *Journal of Fire Protection Engineering* 2007, **17**(1):5-26.
- [2] NASER MZ, HAWILEH RA, ABDALLA J: Modeling Strategies of Finite Element Simulation of Reinforced Concrete Beams Strengthened with FRP: A Review. *Journal of Composites Science* 2021, **5**(1):19.

Advanced Computational Modelling Complex Dynamical Systems: The Earth Angular Momentum Balance Nonstationary Model

ALEXANDER V GLUSHKOV¹, OLGA Y KHETSELIUS¹, VALERY F. MANSARLIYSKY¹,
ARTEM V. VITAVETSKY^{1*}

1. Odessa State Environmental University, Mathematics Depr., L'vovskaya str. 15, 65009, Odessa

* Presenting Author

Abstract: The paper presents the elements of new mathematical formalism to computational modelling complex dynamical systems, in particular, such as planetary balance of angular momentum of the Earth. The approach provides a correct treatment of global mechanisms in the balance of the angular momentum of the Earth, macroturbulent atmospheric low-frequency processes, including processes of heat-mass transfer at spatial and temporal macro scales, teleconnection effects etc. The methods of a plane complex geophysical field and spectral expansion algorithms are applied to describe the circulation processes. The detailed description of the computational algorithm with accounting for the macro turbulent, circulation low-frequency processes is presented. The results of the PC simulation experiments on calculating a balance of planetary angular momentum (including an atmospheric part) are presented for a whole Pacific ocean region.

Keywords: nonlinear dynamics, planetary balance of angular momentum, numerical modelling

1. Introduction. Nonlinear Dynamics of Atmospheric Ventilation

The mathematical modelling nonlinear chaotic (macroturbulent) large scaled low-frequency processes in different complex dynamical system attracts a great interest because of a principal importance of such studies. From the other side, as a rule, such modeling encounters colossal computational difficulties, and sometimes the only way out is to find optimal mathematical approaches and to create effective computing algorithms for analyzing and modeling of complex dynamical systems. One of the most complex problem in theory of planetary dynamical systems is modelling planetary balance of angular momentum of the Earth as well as large scaled macroturbulent atmospheric processes. In our work starting from the key positions of a dynamical systems theory and nonlinear computational hydrodynamics the fundamentals of a new mathematical formalism to computational modelling complex dynamical systems, in particular, balance of angular momentum of the Earth are presented.

2. Model, Results and Discussion

An advanced non-stationary angular momentum balance equation can be written as follows [1,2]:

$$\begin{aligned} \frac{\partial}{\partial t} \int \rho M dV &= \int_{\varphi_1}^{\varphi_2} \int_0^H \int_0^{2\pi} \rho v M d\varphi dz d\lambda + \int_0^H \int_0^{2\pi} \int_{\varphi_1}^{\varphi_2} (p_E^i - p_W^i) a \cos \varphi dz d\varphi d\lambda + \\ &+ \int_{\varphi_1}^{\varphi_2} \int_0^{2\pi} \int_0^H \tau_0 a \cos \varphi d\varphi d\lambda 2\pi, \end{aligned} \quad (1)$$

where $M = \Omega a^2 \cos \varphi + u a \cos \varphi$ - angular momentum; Ω - the angular velocity of rotation of the Earth; a - radius of the Earth; φ - Latitude ($\varphi_1 - \varphi_2$ - separated latitudinal belt between the Arctic and polar fronts); λ - longitude; u, v - zonal and meridional components of the wind speed; ρ - air density; V - the entire volume of the atmosphere in this latitude belt from sea level to the average height of the elevated troposphere waveguide - H ; $p_E^i - p_W^i$ - the pressure difference between the eastern and western slopes of the i -th mountains; z - height above sea level; τ_0 - the shear stress on the surface. From the point of view of physics, the cycle of balance of angular momentum in the contact zones with the hydrosphere and lithosphere becomes a singularity. This singularity can be detected through the occurrence of zones of fronts and soliton-type front. Then the kernel of equation (1) can be defined in the density functional ensemble of complex velocity potential [1,3]

$$w = \overline{v_\infty} z + \frac{1}{2\pi} \sum_{k=1}^n q_k \ln(z - a_k) + \frac{1}{2\pi} \sum_{k=1}^p \frac{M_k e^{\alpha_k i}}{z - c_k} - \frac{i}{2\pi} \sum_{k=1}^m \Gamma_k \ln(z - b_k) \quad (2)$$

and the complex velocity, respectively, will be

$$v = \frac{dw}{dz} = \overline{v_\infty} + \frac{1}{2\pi} \sum_{k=1}^n \frac{q_k}{z - a_k} - \frac{1}{2\pi} \sum_{k=1}^p \frac{M_k e^{\alpha_k i}}{(z - c_k)^2} - \frac{i}{2\pi} \sum_{k=1}^m \Gamma_k / (z - b_k), \quad (3)$$

where w - complex potential; v_∞ - complex velocity general circulation background (mainly zonal circulation); b_k - coordinates of vortex sources in the area of singularity; c_k - coordinates of the dipoles in the area of singularity; a_k - coordinates of the vortex points in areas of singularity; M_k - values of momenta of these dipoles; α_k - orientation of the axes of the dipoles; Γ_k, q_k - values of circulation in the vortex sources and vortex points, respectively. Besides, it is necessary to have an effective method for modelling macroturbulent atmospheric processes [3-5]. It is used an advanced version of the standard tensor equations of turbulent tensions. As usually, it is convenient to partition velocity $\mathbf{u}(v_x, v_y, w) = (U, V, W)$, pressure p , temperature θ into equilibrium and departures from equilibrium values (for example: $p = p_0 + p'$ etc). The total system includes equations for the Reynolds tensions, moments of connection of the velocity pulsations with entropy ones and the corresponding closure equations. The technique of using Reynolds tension tensors of the second rank is well known (for example, in the form of an analytical representation). The results of calculating the balance of angular momentum, atmospheric circulation in link with continuity of atmospheric circulation forms are presented for a whole region of Pacific ocean. The numerical data for the a current function and a complex velocity potential are listed.

References

- [1] GLUSHKOV A., KHETSELIUS O., AMBROSOV S., BUNYAKOVA YU., MANSARLIYSKY V., The use of microsystems technology "Geomath" to modeling the balance of the angular momentum of the Earth, atmospheric processes and parameters of radio waveguides. *Sensor Electr. and Microsyst. Techn.* 2013, **10**(1):22-28.
- [2] GLUSHKOV A, KHETSELIUS O, SVINARENKO A, BUYADZHI V: *Methods of computational mathematics and mathematical physics*. P.1. TES: Odessa, 2015
- [3] KHETSELIUS O, GLUSHKOV A, STEPANENKO S, SVINARENKO A, BUYADZHI V: Nonlinear dynamics of the industrial city's atmospheric ventilation: New differential equations model and chaos. In: AWREJCWICZ J (Ed.) *Perspectives in Dynamical Systems III: Control and Stability*. Series: *Springer Proceedings in Mathematics & Statistics*. 2021, **364**:Ch.16
- [4] RUSOV V, GLUSHKOV A, VASCHENKO V ETAL: Galactic cosmic rays – clouds effect and bifurcation model of Earth global climate. Part 1. *Theory. J. of Atmos. and Solar-Terrestrial Phys.* 2010, **72**:498-508.
- [5] KHETSELIUS O: Forecasting evolutionary dynamics of chaotic systems using advanced non-linear prediction method. In: AWREJCWICZ J, KAZMIERCZAK M, OLEJNIK P AND MROZOWSKI J (EDS.) *Dynamical Systems Applications*. Politechniki Łódzkiej: Łódź, 2013, **T2**:145-152.

Simulation of non-linear coupled dynamic systems of first and second order applying a semi-analytic method

HELMUT J. HOLL^{1*}

1. Institute of Technical Mechanics, Johannes Kepler University, Linz, Austria

Abstract: Mechanical models for non-linear dynamic systems are defined by differential equations of second order where also first order differential equations are present frequently. Differential equations of first order are present if some degrees of freedom have no corresponding mass, if the stiffness parameters vanish in a part of the equations or if a controller is implemented in the system. For linear systems of first and second order various numerical procedures for solving the differential equations are available. A semi-analytical method is presented which is exact for the linear dynamic and decoupled systems of first and second order. A modal transformation of the partitioned system equations is necessary for each part. After a discretization in the time-domain the relevant equations for a suitable and effective time-integration algorithm are defined taking the non-linearity into account. The resulting procedure is derived and it turns out that the formulation is analogous to a BEM-formulation in time as Green's functions are used. The method is extended to the coupled non-linear differential equations of first and second order and is applied to a system with two degrees of freedom.

Keywords: first and second order systems, time-integration, non-linear dynamics

1. Introduction to dynamic systems of first and second order

The differential equations of motion for non-linear dynamic system are given in the form

$$\mathbf{M}\ddot{\mathbf{X}} + \mathbf{D}\dot{\mathbf{X}} + \mathbf{K}\mathbf{X} + \mathbf{F}_N = \mathbf{F}(t). \quad (1)$$

The non-linear equations of motion with the mass matrix \mathbf{M} , the damping matrix \mathbf{D} , the stiffness matrix \mathbf{K} , the vector of non-linear reaction force \mathbf{F}_N , the vector of excitation force $\mathbf{F}(t)$ and the vector of degrees of freedom $\mathbf{X}(t)$ with n components. For mechatronic system the equations for dynamic systems frequently include first and second order differential equations. Examples for such systems are the temperature in a body with heat exchange, the balance of mass with inflow and outflow and control of dynamic systems. For such systems the solution is computed frequently after a transformation into a system of differential equations of first order. For linear systems of first and second order a variety of solutions is presented in [1] and [2] and various numerical procedures for solving the differential equations in [3] and [4]. Due to the high effort of this method specially for Finite Element models a semi-analytic method is presented. The equations of motion can be partitioned and with the assumptions that $\mathbf{M}_{12} = \mathbf{0}_{12}$, $\mathbf{M}_{21} = \mathbf{0}_{21}$, $\mathbf{M}_{22} = \mathbf{0}_{22}$ after additional manipulations it follows

$$\begin{aligned} \begin{bmatrix} \mathbf{M}_{11} & \mathbf{0}_{12} \\ \mathbf{0}_{21} & \mathbf{0}_{22} \end{bmatrix} \begin{Bmatrix} \ddot{\mathbf{X}}_1 \\ \ddot{\mathbf{X}}_2 \end{Bmatrix} + \begin{bmatrix} \mathbf{D}_{11} & \mathbf{0}_{12} \\ \mathbf{0}_{21} & \mathbf{D}_{22} \end{bmatrix} \begin{Bmatrix} \dot{\mathbf{X}}_1 \\ \dot{\mathbf{X}}_2 \end{Bmatrix} + \begin{bmatrix} \mathbf{K}_{11} & \mathbf{0}_{12} \\ \mathbf{0}_{21} & \mathbf{K}_{22} \end{bmatrix} \begin{Bmatrix} \mathbf{X}_1 \\ \mathbf{X}_2 \end{Bmatrix} = \begin{Bmatrix} \mathbf{F}_1 \\ \mathbf{F}_2 \end{Bmatrix} - \begin{Bmatrix} \mathbf{F}_{N1} \\ \mathbf{F}_{N2} \end{Bmatrix} \\ - \begin{bmatrix} \mathbf{0}_{11} & \mathbf{D}_{12} \\ \mathbf{D}_{21} & \mathbf{0}_{22} \end{bmatrix} \begin{Bmatrix} \dot{\mathbf{X}}_1 \\ \dot{\mathbf{X}}_2 \end{Bmatrix} - \begin{bmatrix} \mathbf{0}_{11} & \mathbf{K}_{12} \\ \mathbf{K}_{21} & \mathbf{0}_{22} \end{bmatrix} \begin{Bmatrix} \mathbf{X}_1 \\ \mathbf{X}_2 \end{Bmatrix} \quad (2) \end{aligned}$$

For the first part of a differential equation of second order a modal analysis and transformation is performed to get diagonal matrices of the first partition. For the second part of a differential equation of first order an eigenvalue computation is done and decoupled equations follow after the corresponding transformation. The coupling forces of this modified equations are considered in the convolution integral. With a linear interpolation of the generalized coordinates an implicit procedure results. The non-linear force within the time step are assumed to be a linear function of time. After a reformulation to an incremental and iterative Newton-Raphson-procedure results. The formulation of the derived procedure is analogous to the BEM-formulation in time, described in [5] for a system of second order, where the formulation of the system of first order and the coupling of the sub-systems is considered.

2. Results and Discussion

The computation is demonstrated for a dynamic system with two degrees of freedom. In this special case the eigenvalue analysis is very simple and the results can be studied for different parameters represented in three different models. The non-linearity of the springs for the mechanical model of Fig. 1a are given by $F_{c1} = c_1(q_1 - q_2) + c_3(q_1 - q_2)^3$ and $F_{c2} = c_2q_2 + c_3q_2^3$. The parameters for the *linear Model 1* are $m_1 = m_2 = 1$ kg, $d_1 = d_2 = 0.1$ Ns/m, $c_1 = c_2 = 1$ N/m, $c_3 = c_4 = 0$ N/m³ and $F_1 = F_2 = 1$ N. The *non-linear Model 2* differs from Model 1 by $c_3 = c_4 = 0.5$ N/m³ and the *non-linear Model 3* differs from Model 2 by the mass $m_2 = 0$ kg. In Fig. 1b and 1c the computed solution is shown for the three models. A comparison to conventional time integration algorithms shows a better performance of the present method. Analogous to the analysis of the semi-analytic time-integration method for variable mass non-symmetric and non-linear systems in [4] the present method is analyzed with respect to the numerical behavior. The numerical behavior of the algorithm is analyzed for a defined non-linearity and additionally the stability and accuracy of the algorithm are studied. The resulting algorithm shows a high efficiency when compared with well-known numerical methods.

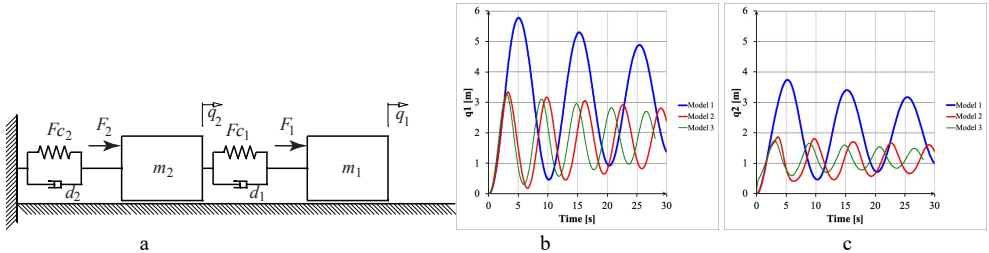


Fig. 1. Mechanical Model and solution of the mechanical system with homogeneous initial conditions

Acknowledgment: Support of the author by the COMET K2-Center is gratefully acknowledged.

References

- [1] ANGELES J: *Dynamic Response of Linear Mechanical Systems*. Springer, 2011.
- [2] CAMPBELL SL, HABERMAN R: *Introduction to Differential Equations with Dynamical Systems*. Princeton University Press, 2008.
- [3] HAIRER E, NORSTETT SP, WANNER G: *Solving Ordinary Differential Equations I: Nonstiff Problems*. 2nd ed. Springer, 1993.
- [4] HAIRER E, WANNER G: *Solving Ordinary Differential Equations II: Stiff and Differential-Algebraic Problems*. 2nd ed. Springer, 2002.
- [5] HOLL HJ: Analysis of Variable Mass Rotordynamic Systems with Semi-Analytic Time-Integration. In: CAV-ALCA KL, WEBER HI (ED.) *IFToMM Rotordynamics: Mechanisms and Machine Science* 62(3):412-425, 2018.

Study of Nonlinear Dynamics of Complex Chaotic Systems: Combined Chaos-Geometric and Neural Networks Algorithms

OLGA Y KHETSELIUS^{1*}, OLEG V DUBROVSKY¹, INGA N SERGA AND
ROSTISLAV E SERGA¹

1. Odessa State Environmental University, Mathematics Depr., L'vovskaya str. 15, 65009, Odessa

* Presenting Author

Abstract: An advanced numerical approach to modelling nonlinear processes of chaotic systems is presented and based on the combined chaos theory methods, including generalized concept of compact geometric attractors (CGA), and a neural networks (NNW) simulation algorithm. The use of the fundamental data on a phase space evolution of the nonlinear process in time and the neural networks computational simulation can be considered as one of the novel approaches in the construction of global nonlinear prediction models for evolutionary dynamics of the complex chaotic systems. The approach provides an accurate description of the structure of the corresponding strange attractors for significantly chaotic dynamical systems. As the illustrative examples, the approach is applied to analysis, modelling, and construction of prediction model for a few chaotic dynamical systems (geophysical and quantum electronics, laser systems). The corresponding topological and dynamical invariants for the dynamic time series are computed and analysed.

Keywords: complex chaotic system, dynamics, attractors, neural networks

1. Introduction. Universal Chaos-Geometric Approach to Complex System Dynamics

Multiple physical, chemical, biological, technical, and other systems (devices) demonstrate the typical complex chaotic behaviour. In many important applications a typical dynamic of these systems is the world of strong nonlinearity and chaos. In principle, the most conventional direct approach to dynamics treating problem consists in building an explanatory model using an initial data and parameterizing sources and interactions between process properties. Unfortunately, such that kind of approach is realized with difficulties, and its outcomes are insufficiently correct. In this paper we go on our work on development of a novel, effective approach to modelling nonlinear processes in the significantly chaotic systems. This approach should be based on the combined using of a generalized CGA concept, chaos theory methods and NNW algorithms. Combined using information on the phase space evolution of the nonlinear process in time and the NNW simulation techniques can be considered as one of the fundamentally new approaches in the construction of global nonlinear models. Moreover it is waited that such an approach could provide the most effective and accurate description of the structure of the corresponding strange attractors for significantly chaotic dynamic systems.

Figure 1 presents the flowchart of our combined chaos-geometric and NNW computational approach to nonlinear analysis and prediction of dynamics of a complex system (e.g. [1-5]). As usually one should consider some scalar measurements $s(n) = s(t_0 + n\Delta t) = s(n)$, where t_0 is the start time, Δt is the time step, and n is the number of the measurements. The principal tasks are to reconstruct phase space using as well as possible information contained in $s(n)$ as well as to build the corresponding prediction model and define how predictable is a nonlinear dynamic of the studied system. The new element is using the NNW algorithm in forecasting nonlinear dynamics of chaotic systems [4].

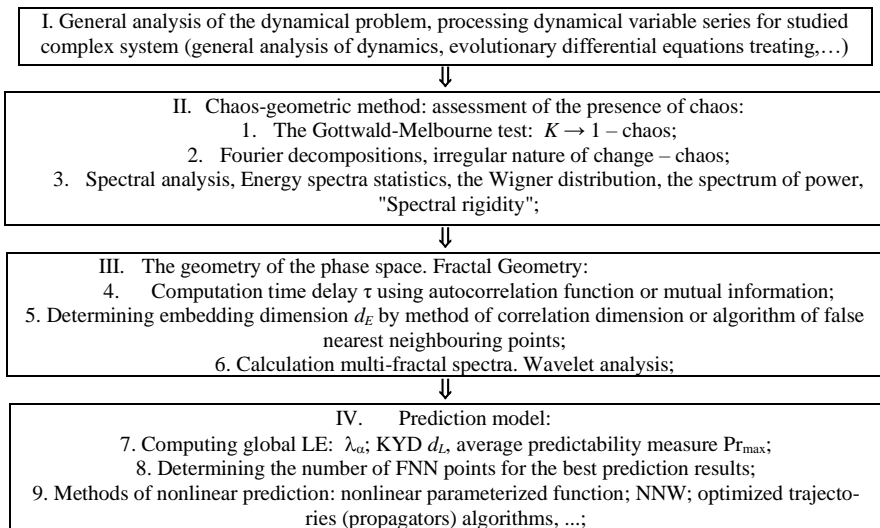


Figure 1. Flowchart of the combined chaos-geometric approach and NNW to nonlinear analysis and prediction of chaotic dynamics of the complex systems (structures, devices)

2. Results and Concluding Remarks

The approach presented is tested by means of numerical analysis, modelling and forecasting nonlinear temporal dynamics for a number of different in nature dynamic systems (quantum electronics systems: semiconductor GaAs/GaAlAs laser device with delayed feedback; atmospheric and hydrologic systems with chemical pollutants). The key topological and dynamical invariants (embedding and correlation dimensions, the Lyapunov's exponents, Kaplan-Yorke dimension, Kolmogorov entropy, average limit of predictability etc) for the corresponding time series are computed and analysed. To conclude, an advanced numerical approach to modelling nonlinear processes of chaotic systems is presented and based on the combined chaos theory methods, CGA concept and NNW simulation algorithms. It is shown that low-dimensional chaos exists in the time series under investigation and quite sufficient predictability is obtained in the forecasting a temporal dynamic of studied systems. The approach can be considered as an effective computational tool for analysis and processing the data of chaotic quantum and laser systems and quantum devices (sensors).

References

- [1] GLUSHKOV AV: *Methods of a Chaos Theory*. Astroprint: Odessa, 2012.
- [2] KHETSELIUS O: Forecasting evolutionary dynamics of chaotic systems using advanced non-linear prediction method. In: AWREJCEWICZ J, KAZMIERCZAK M, OLEJNIK P AND MROZOWSKI J (EDS.) *Dynamical Systems Applications*. Politechniki Łódzkiej: Łódź, 2013, **T2**:145-152.
- [3] KHETSELIUS OY, SVINARENKO AA, IGNATENKO AV, BUYADZHI AA: New generalized chaos-geometric and neural networks approach to nonlinear modeling of complex chaotic dynamical systems. In: AWREJCEWICZ J, KAZMIERCZAK M AND OLEJNIK P (EDS.) In: *Applicable Solutions in Non-Linear Dynamical Systems*. Łódź, 2019:267-276.
- [4] PACKARD N, CRUTCHFIELD J, FARMER J AND SHAW R: Geometry from a time series. *Phys Rev Lett*. 1988, **45**:712–716.
- [5] ABARBANEL H, BROWN R, SIDOROWICH J AND TSIMRING L: The analysis of observed chaotic data in physical systems. *Rev. Mod. Phys* 1993, **65**:1331-1392.

A multi-agent computer program for automatic investigation the behavior of a nonlinear dynamic system in real-time

ALEXANDER RUCHKIN, CONSTANTIN RUCHKIN*

1. National Technical University of Ukraine "Igor Sikorsky Kyiv Polytechnic Institute", IASA, Address: 37, Prosp. Peremohy, Kyiv, Ukraine, 03056, alex3005r@gmail.com,

* Presenting Author

Abstract: In continuation of construction of the general concept of automatic investigation of dynamic systems [1], the general scheme and computer system of the analysis of behaviour of nonlinear dynamic system in real-time are developed. The computer system of multi-agents are implementing functions of an interface with user, an processing of data, a scheduling and a control of calculation, a control of time and special functions of recognition. The specification of the multi-agent system, its agents and database, the structure, functions and operation of the system are presented and are discussed.

Keywords: The dynamical systems, the periodic and quasi-periodic orbits, the regular behaviour system, multi-agent computer system

1. Introduction

The task of building a multi-agent system (MAS) for automation research and detection of the behaviour of dynamic systems is a modern and difficult task. It is necessary to investigate and predict the behaviour of a nonlinear autonomous multi-parametric dynamic system based on graphical information, which is obtained in real time. The difficulty of solving this problem is that, it is poorly formalized and can be attributed to the problems of artificial intelligence. For example, conducting separate studies of Poincaré sections is not enough to solve the initial problem. Also for the construction of Poincaré sections, an unfixed time is required to calculate the cross-sections. Short time - does not allow you to build adequate cross-sections, long time - allows you to accumulate errors. The problem is complicated by the fact that the dynamic system is very parametric. Depending on the parameters, it may have opposite properties: be well predicted or not. To solve these problems, it is proposed to use multi-agent-oriented technology and develop an appropriate multi-agent system for predicting the behaviour of a nonlinear dynamic system in real-time [2].

As is known, in modern research of artificial intelligence systems, agent-oriented technologies are increasingly used. These technologies can be considered as a new paradigm for the analysis, design, development and implementation of complex software systems in the intellectual direction. In agent-oriented technologies, agents are complex computer programs that can act autonomously to solve tasks according to the chosen behaviour strategy. However, more and more tasks require the use of several different strategies, as well as several agents. In multi-agent systems, agents must interact cooperatively with each other and produce more adequate cooperative solutions. Multi-agent intelligent systems have more significant advantages over classical artificial intelligence systems and are able to solve more complex problems, such as search, recognition and prediction.

2. Results and Discussion

So, the aim of this work is to develop a multi-agent system based on the use of the method of distributed artificial intelligence and designed to predict the behaviour of a nonlinear dynamic system in real-time. For this, we have done the following: describe the general scheme of solving the problem; design system agents, describe their roles and functions; develop the structure of the system database; describe the general architecture and technical aspects of the implementation of the developed multi-agent system.

The multi-agent system had the following requirements: autonomy; operation in real-time; recognition of different types of trajectories on graphical representations of the model under study; regulation of the calculation time of each individual trajectory; determination of starting points for calculating trajectories; optimization of the recognition process by adjusting the number of components of the system involved in it; minimization of recognition errors by using many autonomous recognizers; maintaining a database that contains a description of the detected trajectories of the dynamic system.

The developed scheme of the multi-agent intelligent system is implemented as part of the application software. This software solution is used to increase the efficiency and automation of certain activities related to the study of models of dynamic systems.

The obtained program has the following advantages: full automation of the process of finding trajectories; high efficiency of trajectory recognition due to the use of many recognizers of statistical data accumulated during the study; availability of self-regulation mechanisms to minimize the error in calculating trajectories and optimize the consumption of system resources.

References

- [1] Ruchkin C. The General Conception of the Intellectual Investigation of the Regular and Chaotic Behaviour of the Dynamical System Hamiltonian Structure. In: Awrejcewicz J. (eds) Applied Non-Linear Dynamical Systems. Springer Proceedings in Mathematics & Statistics, vol 93. Springer, Cham, 2014, DOI: 10.1007/978-3-319-08266-0_17
- [2] K.A. Ruchkin Analysis and design development of a multi-agent system for predicting behavior nonlinear dynamic system in real time / K.A. Ruchkin // Bionics of Intellect. - 2013. -P.125-129.

Numerical Investigation of Dynamic Contact Problems using Finite Element Method

DÁNIEL SERFŐZŐ^{1*}, BALÁZS PERE²

1. Széchenyi István University, Department of Applied Mechanics Győr, Hungary
[ORCID: 0000-0003-3515-0650]

2. Széchenyi István University, Department of Applied Mechanics Győr, Hungary
[ORCID: 0000-0002-1161-4206]

* Presenting Author; serfozo.daniel@ga.sze.hu

Keywords: numerical method, contact, impact, oscillation, wave propagation

1. Introduction

There is a great interest towards the examination of dynamic contact and impact problems [1] due to their widespread applicability. The proper solution of these kinds of problems can be especially momentous in such fields like cogwheel drives and cutting metalwork. Contact and impact problems are hard to handle as a substantial nonlinearity occurs in the displacement field. The main problem is that due to the spatial discretization a spurious high frequency oscillation emerges in the resulting functions, which can easily cause divergence in the contact algorithm. Thus, in our study we focused on the best possible elimination of these oscillations by which the choice of the proper numerical method has a great importance.

2. Results and Discussion

When assessing the developed method, a simple one-dimensional problem is reviewed (see Fig. 1) which contains an elastic rod moving towards a rigid wall with a constant v_0 velocity. In the literature, this 1D example is regarded as a standard test problem in which the exact solution have not been accurately reproduced yet using numerical methods. It emerges in many recent publications such as in the paper by Kim [2] showing that it is still actual to deal with this problem.

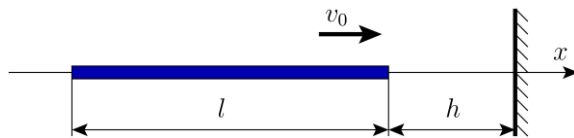


Fig. 1. The mechanical model of the examined 1D problem

After the spatial discretization using the finite element method [3], the equation of motion can be written in the form of

$$\mathbf{M}\ddot{\mathbf{u}} + \mathbf{C}\dot{\mathbf{u}} + \mathbf{K}\mathbf{u} + \mathbf{G}^T\lambda = \mathbf{f} \quad (1)$$

where \mathbf{M} is the mass matrix, \mathbf{C} is the damping matrix, \mathbf{K} is the stiffness matrix, \mathbf{G} is the contact constraint matrix, \mathbf{f} is the load vector, \mathbf{u} is the nodal displacement vector and λ denotes the contact pressure. In the solution of the contact problem, the Lagrange multiplier technique was applied using the method published by Carpenter et al. [4]. The time integration of equation (1) was performed

applying our newly developed forward increment method. In order to obtain the effectiveness of the proposed method, other solutions are also considered using well-known time integration methods like the backward Euler method, the Newmark method [5] and the HHT- α method [6] (see Fig. 2). Further details will be provided in the presentation.

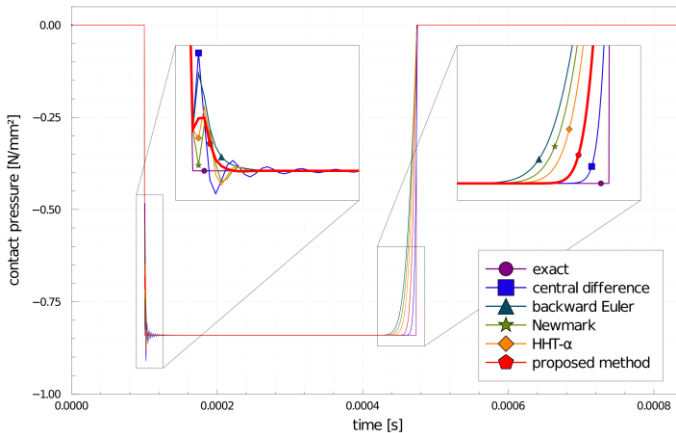


Fig. 2. Time evolution of contact pressure

3. Concluding Remarks

Compared to other widely used methods, our novel approach yields a significantly better solution for the examined model. The considered 1D contact problem is very simplistic, but the phenomena observed here have similar characteristics in higher dimension cases. Thereby, the proposed method must be applicable for more complex problems.

Acknowledgments

The presentation and the research was funded by the project "HU-MATHS-IN – Intensification of the activities of the Hungarian Service Network of Mathematics for Industry and Innovations" (grant number EFOP-3.6.2.-16-2017-00015).

References

- [1] WRIGGERS, Peter. Computational Mechanics, John Wiley Sons Ltd, 2002.
- [2] KIM, Wooram. A new family of two-stage explicit time integration methods with dissipation control capability for structural dynamics. *Engineering Structures*, 2019, 195: 358-372.
- [3] BATHE, Klaus-Jürgen. Finite element procedures. Klaus-Jurgen Bathe, 2006.
- [4] CARPENTER, Nicholas J.; TAYLOR, Robert L.; KATONA, Michael G. Lagrange constraints for transient finite element surface contact. *International journal for numerical methods in engineering*, 1991, 32.1: 103-128.
- [5] NEWMARK, Nathan M. A method of computation for structural dynamics. *Journal of the engineering mechanics division*, 1959, 85.3: 67-94.
- [6] HILBER, Hans M.; HUGHES, Thomas JR; TAYLOR, Robert L. Improved numerical dissipation for time integration algorithms in structural dynamics. *Earthquake Engineering & Structural Dynamics*, 1977, 5.3: 283-292.

Dynamic analysis of functionally graded sandwich shells resting on elastic foundations

SHMATKO TETYANA^{1*}, KURPA LIDIYA², AWREJCEWICZ JAN³

1. Department of Higher Mathematics, National Technical University "KhPI", Kharkov, Ukraine [ORCID 0000-0003-3386-8343].
2. Department of Applied Mathematics, National Technical University "KhPI", Kharkov, Ukraine [ORCID 0000-0001-8380-1521].
3. Department of Automation, Biomechanics and Mechatronics, Lodz University of Technology, Lodz, Poland [ORCID 0000-0003-0387-921X]

*Presenting author (ktv_ua@yahoo.com)

Abstract: Free vibrations of sandwich shallow shells resting on elastic foundations are investigated. It is assumed that shell consists of three layers of the different thickness. Different schemes of arrangement of layers are considered. Namely, the core is made of ceramics or metals, and the upper and lower layers are made of FGM. The volume fractions of metal and ceramic are described by the power law. Shear deformation shell theory of the first (FSDT) that includes interaction with elastic foundations is applied. To study shells with an arbitrary plan form the R-functions theory combined with the variational Ritz method are used. Validation of the proposed method and developed software has been examined on test problems for FG shell with rectangular plan form. New results for shallow shells with complex plan form were obtained. Effects of the power law index, boundary conditions, thickness of core and face sheet layers, elastic foundations on fundamental frequencies are studied in this work.

Keywords: FGM shell, R-functions, Ritz's method, elastic foundation.

1. Introduction

Functionally graded materials (FGM) are one of advanced inhomogeneous composite materials. Usually they are fabricated from a mixture of metal and ceramics. This combination of material constituents makes the design lighter, provide heat resistant and strength of a construction very well [1, 2]. Among the different types of functionally graded (FG) structures FG sandwich structures resting on elastic foundation have shown its advantages in mechanical strength, thermal high-gradient insulation, and lightweight demands. By literature review we conclude that numerical of studies devoted to FG sandwich shallow shells resting on elastic foundation is very limited. As for shells with a complex plan shape, the authors are not aware of such works. In this paper functionally graded sandwich shallow shells supported by elastic foundations are considered by application RFM [3, 4] approach.

2. Formulation of the problem

We will consider the sandwich shallow shells with FGM face –sheets and ceramic core (model A) or metal core (model B). Denote the total thickness of the shells by h , thickness of face–sheet by h_f and thickness of core (central layers) by h_c (Fig. 1, Fig. 2).

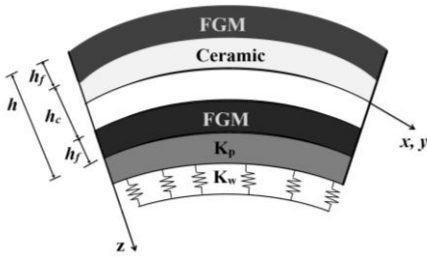


Fig. 1. (Model A)

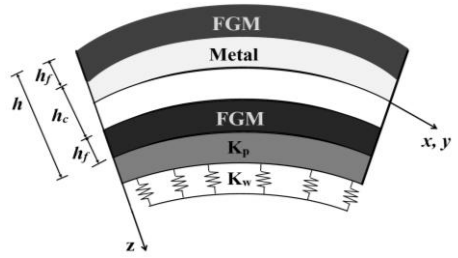


Fig. 2. (Model B)

The effective material properties: elastic modulus E , Poisson's ratio ν , and the density ρ of the FGM are defined by the following relations

$$E = (E_c - E_m)V_c + E_m, \quad \nu = (\nu_c - \nu_m)V_c + \nu E_m, \quad \rho = (\rho_c - \rho_m)V_c + \rho_m. \quad (1)$$

Indexes c and m correspond to characteristics of ceramics and metal relatively. Fraction of ceramic V_c and metal phases V_m are related by formula $V_c + V_m = 1$. For considered problems the corresponding expressions V_c are:

$$\begin{array}{l} \text{Model A} \\ \left\{ \begin{array}{l} V_c = \left(\frac{h + 2z}{h - h_c} \right)^p, \quad z \in \left[-\frac{h}{2}, -\frac{h_c}{2} \right], \\ V_c = 1, \quad z \in \left[-\frac{h_c}{2}, \frac{h_c}{2} \right], \\ V_c = \left(\frac{h - 2z}{h - h_c} \right)^p, \quad z \in \left[\frac{h_c}{2}, \frac{h}{2} \right] \end{array} \right. \\ \text{Model B} \\ \left\{ \begin{array}{l} V_c = \left(\frac{h_c + 2z}{h_c - h} \right)^p, \quad z \in \left[-\frac{h}{2}, -\frac{h_c}{2} \right], \\ V_c = 0, \quad z \in \left[-\frac{h_c}{2}, \frac{h_c}{2} \right], \\ V_c = \left(\frac{h_c + 2z}{h + h_c} \right)^p, \quad z \in \left[\frac{h_c}{2}, \frac{h}{2} \right] \end{array} \right. \end{array} \quad (2)$$

In formula (2) index p denotes the volume fraction exponent (gradient index). Influence of the foundation is taken into account through relation $p_0 = K_w w - K_p \nabla^2 w$. Where K_w, K_p are the Winkler and Pasternak parameters relatively for elastic foundation.

Mathematical statement of the problem is carried out within the first and higher order shear deformation theory of shallow shells: FSDT and HSDT. To solve this problem we apply variational Ritz's method combined with the R-functions theory (RFM method) [3]. In order to illustrate the possibilities of the proposed approach we have considered the shallow shells with cutout of the complex form. Influence of the different parameters on fundamental frequencies are studied in this work.

References

- [1] HUI-SHEN, HAI WANG: Nonlinear vibration of shear deformable FGM cylindrical panels resting on elastic foundations in thermal environments. *J.Composites, Part B* 2014, **60**, 167-177.
- [2] FARID M., ZAHEDINEJAD P., MALEKZADEN P. Three dimensional temperature dependent free vibration analysis of functionally graded material cylindrical panels resting on two parameter elastic foundation using a hybrid semianalytic, differential quadrature method. *Mater.DES* 2010; **31**:2-13.
- [3] RVACHEV V.L. The R-functions theory and its applications. Kiev: Nauk.Dumka (in Russian), 1982.

Effect of porosity on free vibration of FG shallow shells with complex planform

SHMATKO TETYANA

Department of Higher Mathematics, National Technical University "KhPI", Kharkov, Ukraine [ORCID 0000-0003-3386-8343].

*Presenting author (ktv_ua@yahoo.com)

Abstract: This paper presents application of the R-functions method for investigation of free vibrations of shallow shells with an arbitrary planform. It is assumed that shell is fabricated of functionally graded materials with porosities. Two types of porosity is considered: evenly and unevenly distributed porosities. The volume fractions of metal and ceramic are described by the power law. The first order shear deformation theory is applied to describe mathematical formulation of the problem. Solution of the problem is carried out by the variational Ritz method and the R-functions theory. Very good agreement with available results is shown for FG shell with rectangular planform. Detailed numerical study for shallow shell with complex planform is fulfilled to show effectiveness of the proposed approach. In particular, effects of porosity coefficient, the power law index, boundary conditions on fundamental frequencies are examined.

Keywords: Porous, shallow shell, arbitrary planform, FGM, variational method, R-functions.

1. Introduction

As known functionally graded materials (FGM) are widely used in the various field industry: aerospace, nuclear, biomedical engineering and other ones. Usually FGMs have been fabricated from a mixture of metal and ceramics by sintering. During this process micro-porosities or voids can occur in the materials. Therefore, recently many scientists [1, 2, 3] have paid a great attention to investigation of static and dynamic behavior of porous FG plates and shell. From author review it follows that number of studies devoted to porous FG shallow shells with complex plan form is limited enough.

The present paper focuses on the free vibration analysis of FG shallow shells with complex planform for evenly and unevenly porosity distribution. This problem can be solved by application of the R-functions theory and variational Ritz method [4].

2. Formulation of the problem

Thin shallow shell of an arbitrary planform and constant thickness h made of FGM is considered. It is assumed that porosities appear during the sintering process of metal and ceramics. Suppose that the volume fraction of metal V_m and ceramics phases V_c change by power law distribution

$$V_m = \left(\frac{z}{h} + \frac{1}{2} \right)^p, \quad V_m + V_c = 1. \quad (1)$$

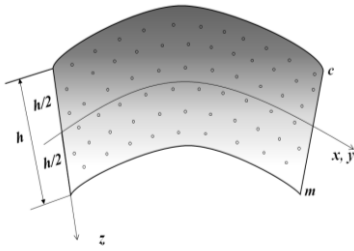


Fig. 1a. Evenly distribution of porosity

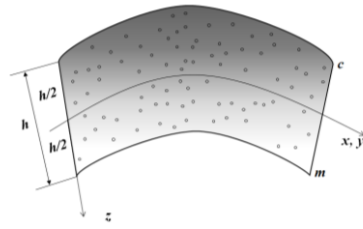


Fig. 1b. Unevenly distribution of porosity

In formula (1) index p denotes the volume fraction exponent (gradient index).

We study evenly (Fig.1a) and unevenly (Fig.1b) distributions of porosities in material. The effective material properties: elastic modulus E , Poisson's, and density ρ of FGMs (general designations as P) are defined for evenly distribution of porosities by the following relations [1]:

$$P(z) = (P_m - P_c)V_m + P_c - \frac{1}{2}\alpha(P_m + P_c). \quad (2)$$

For unevenly distribution of porosities the expression (1) takes the form

$$P(z) = (P_m - P_c)V_m + P_c - \frac{1}{2}\alpha\left(1 - 2\frac{|z|}{h}\right)(P_m + P_c). \quad (3)$$

Indexes c and m correspond to characteristics of ceramics and metal relatively, and α characterizes volume fraction of porosities. Values P_m, P_c depend on temperature of the environment [2].

Mathematical statement of the problem is carried out within the first order shear deformation theory of shallow shells (FSDT). The variational Ritz method is applied to solving given problem. The validation of the proposed approach and created software is confirmed by comparison of the obtained results with known. A good agreement allowed to investigate the shells with complex planform.

References

- [1] MIH CHIEN TRINH, SEUG-EOCK KIM: A three variable refined shear deformation theory for porous functionally graded doubly curved shell analysis. *J.Aerospace Science and technology* 2019, **94**, 105356: 11-15.
- [2] MERDACI SLIMANE, HADJ MOSTEFA ADDA, and other: Effects of even pores distribution of functionally graded plate porous rectangular and square. *Procedia Structural Integrity* 2020, **26**: 35-45.
- [3] J.ZHAO, F.XIE, A.WANG, C.SHUAI, J.TANG, Q.WANG: Vibration behavior of the functionally graded porous (FGP) doubly –curved panels and shells of revolution by using a semi-analytical method. *Composites Part B: Engineering* 2019, **157**: 219-238.
- [4] RVACHEV V.L: *The R-functions theory and its applications*. Kiev: Nauk.Dumka (in Russian), 1982.

Nonlocal damping model in finite element structural vibration analysis

VLADIMIR N. SIDOROV^{1,2}, ELENA S. BADINA^{1,2*}

1. Russian University of Transport (RUT (MIIT))

2. Moscow State University of Civil Engineering

* Presenting Author

Abstract: The paper is devoted to development of an uncomplicated, flexible and controllable damping model for structurally complex materials such as composites and nanomaterials. The model is applicable for the computer dynamic analysis of composite structures. The Newmark method modification, which is used for the finite element dynamic structural analysis, is considered. This modification allows one to consider both external and internal damping when studying the dynamic response of a structure. For internal damping simulation in an implicit Newmark scheme the matrix FE nonlocal in time model is used. This model is further called “damping with memory”. The model is controlled by its key parameters. Damping with memory model is calibrated on the data of composite beam dynamic analysis. The characteristics of beam material were determined experimentally. In this paper the numerical simulation results obtained in Simulia Abaqus software are used as the base for nonlocal model calibration. In the numerical simulation the reasonably detailed 3D FE beam model is used. The composite material of the beam is considered as orthotropic. The results of 1D modelling of beam vibrations considering damping with memory coincide with those via the 3D FE modelling with sufficient accuracy.

Keywords: structural dynamics, nonlocal damping, computer simulation, composite materials

1. Introduction

The problem of damping process simulation for structural elements made of composite materials is significantly complicated. Generally, detailed 3D finite element models are used to simulate numerically the dynamic behaviour of composite structures. In cases when such approach is inefficient, the models that are flexible and controllable are needed, such as fractional hereditary models [1,2] or nonlocal damping models [3-6]. The present paper is devoted to the damping model nonlocal in time.

2. Results and Discussion

Within the nonlocal in time model, damping of a structure at current time t is assumed to be dependent not only on instant value of motion velocity at this point $\dot{v}(t)$, but also on the values of motion velocity in the previous time history. The more the gap between the two time points, the lower influence that one of them has on the other. Such damping model is further called “damping with memory”.

Since the finite element method is the dominant method of engineering calculations, the damping with memory is integrated to its algorithm.

In the algorithm of the finite element analysis, the equilibrium equation of a structure deformed in motion is represented in the matrix form [7, 8]:

$$M \cdot \ddot{\vec{V}}(t) + D_{int} \cdot \dot{\vec{V}}(t) + D_{ext} \cdot \dot{\vec{V}}(t) + K \cdot \vec{V}(t) = \vec{F}(t). \quad (1)$$

Here $\bar{v}(t)$ is the displacement vector, K is the stiffness matrix of the finite element model, D_{int} and D_{ext} are the matrices of internal and external damping, respectively, M is the mass matrix, and $\bar{F}(t)$ is the load vector. As well as matrices M and K , matrices D_{int} and D_{ext} are derived according to the stationary requirement of the full energy of moving deformable structure change.

The Newmark implicit scheme is used for the numerical integration of the equation, and it is more stable than the method of central differences. To modify the Newmark scheme for the damping with memory model, the part which is responsible for the internal damping is supplemented with the discrete analogue of the integral of normalized kernel function, that describes the diminishing of the influence of the time points on one another.

After modified Newmark method application, equation (1) transforms to

$$M \cdot \left[\frac{2}{\Delta t^2} (\bar{v}_{i+1} - \bar{v}_i - \dot{\bar{v}}_i \Delta t) - \ddot{\bar{v}}_i \right] + D_{int} \cdot \sum_{j=0}^i \bar{G}(i, j) \dot{\bar{v}}_j + D_{ext} \frac{1}{\Delta t} (\bar{v}_{i+1} - \bar{v}_i) + K \cdot \bar{v}_{i+1} = \bar{F}_{i+1}(t). \quad (2)$$

The key parameters of the model were determined on the base of 3D composite [9,10] beam vibration numerical simulation data. The root mean square error for calibrated nonlocal model is four times less than that for the classical Kelvin-Voight damping model.

3. Concluding Remarks

In comparison to classic local models, the model presented in this paper allows one to manage the main characteristics of the simulated vibration process in more reliable and flexible way. Increased flexibility makes it possible to use one-dimensional models of beam elements in the dynamic analysis of structures which are made of modern composite materials with orthotropic properties.

Acknowledgment: This research is supported by the Russian Science Foundation, Project # 21-19-00634

References

- [1] ROSSIKHIN YU A, SHITIKOVA M V: Application of fractional calculus for dynamic problems of solid mechanics. *Novel Trends and Recent Results Applied Mechanics Reviews* 2010, Vol. 63 / 010801: 1–52
- [2] DI PAOLA M, PINNOLA F P, ZINGALES M: A discrete mechanical model of fractional hereditary. *Mechanica* 2013, 48(7): 1573-1586
- [3] BANKS H T, INMAN D J: On damping Mechanisms in Beams. *Journal of Applied Mechanics* 1991, 58(3): 716–723
- [4] LEI Y, FRISWELL M I, ADHIKARI S: A Galerkin method for distributed systems with non-local damping. *International Journal of Solids and Structures* 2006, V 43: 3381–3400
- [5] POTAPOV V D: On the stability of rods under stochastic loading considering nonlocal damping. *Problems of Machinery and Reliability* 2012, 25–31
- [6] SHEPITKO E S, SIDOROV V N: Defining of nonlocal damping model parameters based on composite beam dynamic behaviour numerical simulation results *IOP Conf. Series: Materials Science and Engineering* 2019
- [7] SIDOROV V N, BADINA E S: Computer simulation of structural vibration damping taking into account its nonlocal properties. *International Journal for Computational Civil and Structural Engineering* 2020, V. 16, I.4L: 84-89
- [8] BATHE K-J, WILSON E L: *Numerical Methods in Finite Element Analysis*. New Jersey, Prentice-Hall, 1976
- [9] LANDHERR J C: *Dynamic analysis of a FRP deployable box beam*. Master of Applied Science Thesis. Kingston: Queen's University, 2008
- [10] XIE A: *Development of an FRP Deployable Bridge*. Master of Applied Science Thesis, Department of Civil Engineering, Royal Military College of Canada, 2007

Evaluation of forces in dynamically loaded journal bearings using feed-forward neural networks

LUBOŠ SMOLÍK^{1*}, JAN RENDL², RADEK BULÍN³

1. NTIS – New Technologies for the Information Society, University of West Bohemia [0000-0001-5280-5001]
 2. NTIS – New Technologies for the Information Society, University of West Bohemia [0000-0003-3904-7976]
 2. NTIS – New Technologies for the Information Society, University of West Bohemia [0000-0002-3429-2975]
- * Presenting Author

Abstract: This paper explores the usage of artificial neural networks to evaluate forces acting in dynamically loaded finite-length journal bearings. This practice can significantly accelerate transient simulations of systems that employ such bearings without compromising their non-linear properties. The proposed method utilizes a feedforward neural network, which uses a precomputed database of nondimensional forces for training. This database is supplemented with corresponding relative displacements and velocities of a rotating journal to a stationary bearing shell. The trained network can evaluate the acting forces from the relative displacement and velocities and can be directly implemented to various computational models.

Keywords: feedforward neural networks, submodeling, hydrodynamic lubrication

1. Introduction

Hydrodynamic (HD) forces acting in a dynamically loaded finite-length journal bearing cannot be evaluated analytically. This fact hinders the efficiency of simulation of dynamics in many rotating and flexible multi-body systems because the numerical computation of the HD forces is relatively time-consuming. Some techniques can reduce the computational time at the cost of accuracy. These include database methods based on interpolation of precomputed forces [1], various approximative analytical solutions, and best-fit methods [2].

2. Summary of the Proposed Method

The proposed method vaguely resembles the method introduced in [3]. First, the configuration space of the bearing (CS), i.e., all possible positions and velocities, is generated. Then, nondimensional hydrodynamic forces $\bar{F}^{(i)}$ are numerically computed in a finite number of equidistant interior points of the CS. These nondimensional forces are further transformed using the relation

$$\bar{F}_{ANN}^{(i)} = \text{sgn}(\bar{F}^{(i)}) \cdot \log_{10}(|\bar{F}^{(i)}| + 1), \quad (1)$$

which helps to maintain the same relative accuracy across scales, see Fig. 1a. The database of the transformed forces, together with the CS, serves as a training dataset for feedforward neural networks with a structure shown in Fig. 1b. Hidden layers consist of neurons with a sigmoid transfer function

$$x_{\text{out}} = b_1 + w_1 \cdot \tanh(b_2 + w_2 \cdot x_{\text{in}}), \quad (2)$$

which ensures that the relation between input x_{in} and output x_{out} is smooth.

The networks are trained in a parallel pool using Bayesian regularisation.

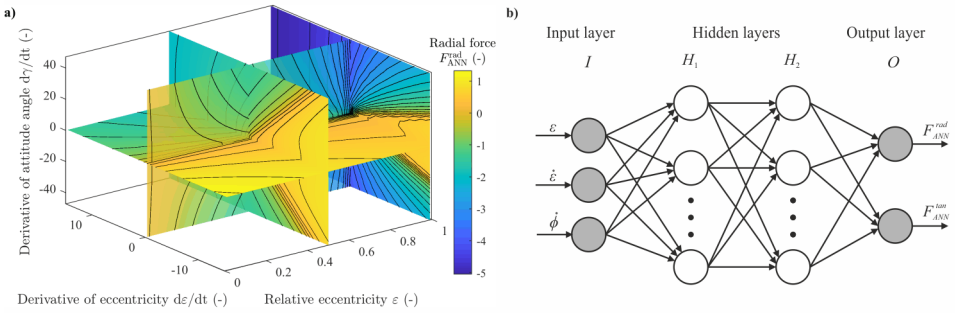


Fig. 1. (a) Transformed dimensionless radial force acting in the journal bearing with length-to-diameter ratio 0.625 and (b) scheme of a feedforward neural network with two hidden layers.

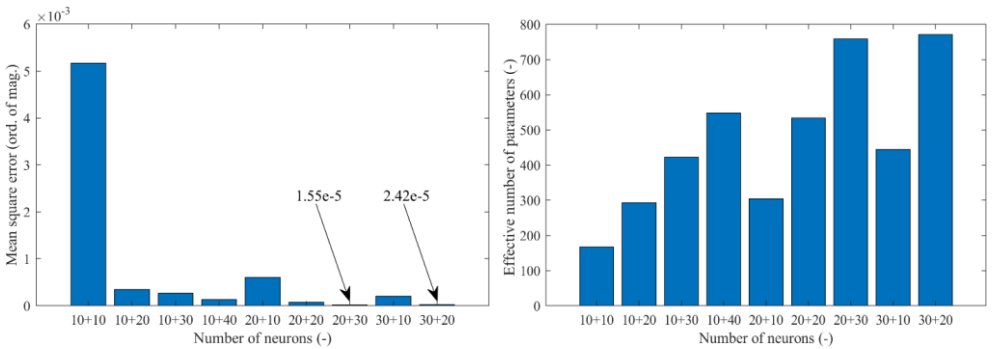


Fig. 2. Mean square errors and effective number of parameters of some trained two-layer networks.

3. Results and concluding remarks

Some results of the training with 132 651 configuration points and 27 000 random validation points are shown in Fig. 2. The networks with as low as 40 neurons have the same accuracy as the regression method introduced in [2]. The higher number of neurons secure even more accurate estimates of the HD forces. Interestingly, the composition of the hidden layers significantly influences the accuracy.

Acknowledgment: This work was supported by project SGS-2019-009 and by European Regional Development Fund-Project No. CZ. 02.1.01/0.0/0.0/17 048/0007267. Verification would not be possible without the AVL Excite software which is available in the framework of the University Partnership Program of AVL List GmbH.

References (10 point, bold)

- [1] CHASALEVRIS A., LOUIS J.-CH.: Evaluation of transient response of turbochargers and turbines using database method for the nonlinear forces of journal bearings. *Lubricants* 2019, **7**(9): 78.
- [2] BASTANI Y., DE QUEIROZ M.: A new analytic approximation for the hydrodynamic forces in finite-length journal bearings. *Journal of Tribology* 2010, **132**(1): 014502.
- [3] CHOI H.-S., AN J., HAN S., KIM J.-G., JUNG J.-Y., CHOI J., ORZECZOWSKI G., MIKKOLA A., CHOI J.-H.: Data-driven simulation for general-purpose multibody dynamics using deep neural networks. *Multibody System Dynamics* 2021, **51**(4): 419-454.

Application to of Hilbert transforms moments analysis of vibration signals

ALEKSANDRA WASZCZUK-MŁYŃSKA^{1*}, STANISŁAW RADKOWSKI², JĘDRZEJ MAĆZAK³

1. Warsaw University of Technology, Faculty of Automotive and Construction Machinery Engineering, Narbutta St. 84, 02-524 Warsaw, Poland [0000-0001-7587-9097]
2. Warsaw University of Technology, Faculty of Automotive and Construction Machinery Engineering, Narbutta St. 84, 02-524 Warsaw, Poland [0000-0003-2083-0514]
3. Warsaw University of Technology, Faculty of Automotive and Construction Machinery Engineering, Narbutta St. 84, 02-524 Warsaw, Poland [0000-0002-5460-5588]

* Presenting Author

Abstract: Each element has its own natural vibration frequencies, which are of great importance for the operation of the device, , it is important for the comfort of work, e.g. noise, for the safety of the machine or operators. Detection of disturbances and damage occurring and developing in a dynamic system in many cases, it uses the effect of modulating carrier frequencies as a phenomenon of generating information about degradation process occurring in the system. Particular importance is attached to the detection of qualitative changes, including the detection of disturbances in the assumed cycle of the production process [1], [2]. In this work, the authors present a method that uses the generalized Hilbert transform [3], [4] that have been processed as a result of monitoring the operation of a flash furnace and are aimed at determining the conditions leading to a non-stationary course of the process .

Keywords: Generalised Hilbert transform, fractional Hilbert transform, spectral moments

References

- [1] RADKOWSKI S.: Vibro-acoustic diagnostics of low-energy stage of failures evolution, *Proceedings of the Institution of Mechanical Engineers, Part G: Journal of Aerospace Engineering* 2009, t. 223, nr 5.; 589–597.
- [2] MAĆZAK J.: Local meshing plane analysis as a source of information about the gear quality, *Mechanical Systems and Signal Processing* 2013, t. 38, nr 1, ss. 154–164.
- [3] LUO Y., AL-DOSSARY S., MARHOON M., ALFARAJ I M.: Generalized Hilbert transform and its applications in geophysics, *Leading Edge (Tulsa, OK)2003*, t. 22, nr 3, ss. 198–202.
- [4] SARKAR S., MUKHERJEE K., RAY I A.: Symbolic analysis of time series signals using generalized hilbert transform, *Proceedings of the American Control Conference*, 2009, ss. 5422–5427.

-OPT-

**OPTIMIZATION PROBLEMS
IN APPLIED SCIENCES**

Anti-Angiogenic and Chemotherapy Scheduling Optimisation using Mathematical Modelling

MARIUSZ BODZIOCH^{1*}, URSZULA FORYS²

1. Faculty of Mathematics and Computer Science, University of Warmia and Mazury in Olsztyn, Poland [ORCID: 0000-0002-1991-5062]

2. Faculty of Mathematics, Informatics and Mechanics, University of Warsaw, Poland [ORCID: 0000-0002-6198-3667]

* Presenting Author

Abstract: One of the main obstacles in chemotherapy planning is acquired drug resistance. It causes that even though the initial response to a drug may show promising results, re-administration of the drug may have no effect. Based on the Hahnfeldt et al. model, we formulate a new model of tumour growth under angiogenic signalling that is adapted to heterogeneous tumours and accounts for the Norton-Simon hypothesis. Using mathematical modelling and applying optimal control framework we show that lower doses of chemotherapy may be beneficial for patients by reducing resistance. Our analysis offers insights into the effects of combined anti-angiogenic agent and chemotherapy. By numerical simulations we show the longest survival time is achieved for intermediate doses. It supports the concept of metronomic therapy.

Keywords: tumour growth, resistance, chemotherapy, anti-angiogenic treatment, optimal control

1. Introduction

The most frequently used therapy strategy in cancer treatment is chemotherapy. However, chemotherapy is not selective and affects not only tumour cells but also healthy cells. Genetic instability of tumour cells, coupled with high proliferation rates may lead to acquired drug resistance (ADR), which is one of the biggest obstacles in chemotherapy scheduling. Using mathematical modelling we would like to make insights into the hypothesis: delaying the onset of drug resistance by appropriate chemotherapy scheduling may maintain tumour size at low level and prolong patient survival time.

In 1999 Hahnfeldt et al. proposed a model of tumour growth under angiogenic signalling assuming that the tumour population is homogeneous. In order to model ADR, we propose an extension of the Hahnfeldt et al. model, which takes into account heterogeneity of tumour cells in the context of resistance. In [1] we proposed another version of such model accounting for log-kill hypothesis.

Minimizing tumour volume together with some constraints on the drug dosage is the standard therapeutic goal. However, it does not ensure that tumour does not switch to the resistant phenotype. Such tumours do not respond properly to treatment, which may result in therapy failure. In [2] we formulated a new objective functional that penalizes drug resistance and presented mathematical analysis of the relevant optimal control problem. Optimization of chemotherapy scheduling using a three-dimensional model with varying carrying capacity can be found in [3]. Here our aim is to find optimal chemotherapy scheduling when a small constant supply of anti-angiogenic agent is applied during the therapy. We assume that the tumour population is divided into two sub-populations: sensitive and resistant to chemotherapy. We include constant flow between compartments caused by mutations and assume that sensitive cells are killed by the drug according to the Norton-Simon hypothesis, i.e. the rate of cancer cell death in response to treatment is proportional to the tumour growth rate.

2. Results and Discussion

Under the above assumptions, we consider the following system of differential equations

$$\begin{aligned} \frac{dN_1}{dt} &= -(\lambda_1 - \beta_1 u(t))N_1 \ln \frac{N_1 + N_2}{K} - \tau_1 N_2 + \tau_2 N_2, \\ \frac{dN_2}{dt} &= -\lambda_2 N_2 \ln \frac{N_1 + N_2}{K} + \tau_1 N_2 - \tau_2 N_2, \\ \frac{dK}{dt} &= -\mu K + b(N_1 + N_2) - d(N_1 + N_2)^{2/3} - \beta K u(t) - \gamma K v(t), \end{aligned} \quad (1)$$

where N_1 and N_2 denote sizes of sensitive and resistant sub-populations, K is the carrying capacity related to the size of the vasculature, λ_1 and λ_2 are proliferation rates, τ_1 and τ_2 are mutation rates, μ is natural death rate of endothelial cells, b is vascular growth rate stimulated by cancer cells, d is vascular inhibition rate by cancer cells, β_1 is sensitivity rate of sensitive cells to the chemotherapy agent, β and γ are sensitivity rates of the vasculature to the chemotherapy and anti-angiogenic agent, respectively, while $u(t)$ and $v(t)$ are concentration of chemotherapy and anti-angiogenic agent, respectively.

We formulate the optimal control problem for System (1) as follows: find a measurable function $u: [0, T] \rightarrow [0, 1]$ for a given fixed terminal time T , which minimizes the functional

$$J(u) = \omega_1 N_1(T) + \omega_2 N_2(T) + \int_0^T \eta_1 N_1(t) + \eta_2 N_2(t) + \frac{\xi}{2} \left(1 + \tanh \left(\frac{N_2(t) - N_1(t)}{\epsilon} \right) \right) + \theta u(t) dt.$$

Here, ω_i , η_i and ξ are non-negative weights, while ϵ is positive parameter. Terms involving ω_i and η_i penalize the size of the whole cell population at the end and during therapy, respectively, while the term $\theta u(t)$ minimizes side-effects. We include the term $\frac{\xi}{2} \left(1 + \tanh \left(\frac{N_2(t) - N_1(t)}{\epsilon} \right) \right)$ in order to penalize time period during which the tumour is resistant (i.e. consists of more resistant than sensitive cells).

We consider two therapeutic protocols. First one is a long-time horizon protocol, where our aim is to prolong the patient survival time the most. We show that the longest survival time occurs for intermediate chemotherapy doses. The second protocol consists of two 14-day therapy windows. We show that the optimal therapy scheduling is consisted of two short MTD protocols at the beginning and at the end of therapy and a singular dosage in between. To solve the optimal control problem we choose the numerical approach ‘‘First Discretize then Optimize’’. To examine how the solution depends on the model parameters, we perform a sensitivity analysis with respect to those parameters.

3. Concluding Remarks

We consider a mathematical model of tumour growth that encompass heterogeneity of cell population and incorporates for the Norton-Simon hypothesis. Using optimal control theory, we obtain numerically optimal combined chemotherapy and anti-angiogenic protocols. As optimal dosages are time-varying, they may not be practically realizable. We provide a tool that can be used to design piecewise-constant intermediate or average-optimal dose protocols and precisely indicate switching points. Derivation of such suboptimal protocols without theoretical analysis would be extremely difficult.

References

- [1] BAJGER P, BODZIOCH M, FORYŚ U: Role of cell competition in acquired chemotherapy resistance. In: *Proc. of the 16th Conference on Computational and Mathematical Methods in Science and Engineering*, 1 (2016).
- [2] BAJGER P, BODZIOCH M, FORYŚ U: Singularity of controls in a simple model of acquired chemotherapy resistance. *Discr. Cont. Dyn. Syst., Ser. B* 2019, **24**:2039-2052.
- [3] BAJGER P, BODZIOCH M, FORYŚ U: Numerical optimisation of chemotherapy dosage under antiangiogenic treatment in the presence of drug resistance. *Math. Meth. Appl. Sci.* 2020, **43**(18): 10671-10689.

Comparison of selected artificial intelligence algorithms to determine the thermal conductivity coefficient of a porous material

RAFAL BROCIEK^{1*}, AGATA WAJDA², DAMIAN SŁOTA¹

1. Department of Mathematics Applications and Methods for Artificial Intelligence, Faculty of Applied Mathematics, Silesian University of Technology, 44-100 Gliwice, Poland, [R.B.: orcid.org/0000-0002-7255-6951, D.S.: orcid.org/0000-0002-9265-5711]
2. Department of Technologies and Installations for Waste Management, Faculty of Energy and Environmental Engineering, Silesian University of Technology, 44-100 Gliwice, Poland [orcid.org/0000-0002-1667-3328],

* Presenting Author

Abstract: The paper considers the inverse problem of determining the thermal conductivity coefficient of a porous material. The two-dimensional anomalous diffusion equation with Riemann-Liouville fractional derivative is adopted as the model of the direct problem. Presented model (equations and initial-boundary conditions) can be used to describe anomalous diffusion, for example the heat conductivity in porous materials. To solve the direct problem, the finite differences method supplemented by the scheme based on the alternating direction implicit method (ADIM) is used. The input data for the inverse problem are temperature measurements at selected points in the area. Using the input data and the solution of the direct problem, a functional describing the error of the approximate solution is built. Two artificial intelligence algorithms, the ant colony optimization (ACO) and artificial bee colony (ABC), are used to minimize this functional. In the presented numerical example, these algorithms are compared in terms of accuracy, stability and speed of operation.

Keywords: inverse problem, fractional derivative, parameter identification, anomalous diffusion, optimization, artificial intelligence

1. Introduction

The article is divided into three main parts. The first part presents the model and formulates the inverse problem. In this case, the inverse problem consists in selection the thermal conductivity coefficient in such a way that the model output matches the input data for the output problem (values of the state function at selected points in the domain). The second part presents the methods of solving the direct and inverse problems. To solve the direct problem, the differential scheme with alternating direction implicit method was used and the inverse problem is reduced to the search for the minima of the objective function (using swarming algorithms). The last part is devoted to examples and discussion of the results.

In the paper we consider the following model, which is a differential equation with a fractional derivative:

$$c\rho \frac{\partial u(x, y, t)}{\partial t} = \frac{\partial}{\partial x} \left(\lambda_{x1}(x, y) \frac{\partial^\alpha u(x, y, t)}{\partial x^\alpha} - \lambda_{x2}(x, y) \frac{\partial^\alpha u(x, y, t)}{\partial (-x)^\alpha} \right) + \frac{\partial}{\partial y} \left(\lambda_{y1}(x, y) \frac{\partial^\beta u(x, y, t)}{\partial y^\beta} - \lambda_{y2}(x, y) \frac{\partial^\beta u(x, y, t)}{\partial (-y)^\beta} \right) + f(x, y, t), \quad (1)$$

where $(x, y, t) \in \Omega \times [0, T]$, $\lambda_{x1}, \lambda_{x2}, \lambda_{y1}, \lambda_{y2} > 0$, and $\alpha, \beta \in (0, 1)$ are orders of fractional derivatives. To the Equation (1) the initial-boundary conditions are added:

$$u(x, y, t)|_{\partial\Omega} = 0, \quad t \in (0, T]$$

$$u(x, y, t)|_{t=0} = \varphi(x, y), \quad (x, y) \in \Omega$$

Derivatives in the Equation (1) were defined as Riemann-Liouville fractional derivatives:

$$\frac{\partial^\alpha u(x, y, t)}{\partial x^\alpha} = \frac{1}{\Gamma(1-\alpha)} \frac{\partial}{\partial x} \int_0^x (x-s)^{-\alpha} u(s, y, t) ds,$$

$$\frac{\partial^\alpha u(x, y, t)}{\partial (-x)^\alpha} = \frac{-1}{\Gamma(1-\alpha)} \frac{\partial}{\partial x} \int_x^{L_x} (s-x)^{-\alpha} u(s, y, t) ds.$$

REFERENCES

1. Brociek R., Wajda A., Słota D.: *Inverse problem for a two-dimensional anomalous diffusion equation with a fractional derivative of the Riemann-Liouville type*, Energies 14, 2021, 1—14.
2. Brociek R., Chmielowska A., Słota D.: *Comparison of the probabilistic ant colony optimization algorithm and some iteration method in application for solving the inverse problem on model with the Caputo type fractional derivative*, Entropy 22, 2020, 1—12.

A New Type of Undimensional Optimized Model for Rod Deduced from Three Dimensional Elasticity

XIAOYI CHEN^{1*}, ERICK PRUCHNICKI², HUI HUI DAI³

1. Division of Science and Technology, BNU-HKBU United International College, Zhuhai, China [0000-0003-1044-7829]^[sc]

2. Université de Lille, Villeneuve d'Ascq, France [0000-0003-3807-4585]^[sc]

3. Department of Mathematics and Department of Materials Science and Engineering, City University of Hong Kong, Kowloon, Hong Kong [0000-0003-1352-2281]

* Presenting Author: X.Chen, BNU-HKBU, Zhuhai, China, xiaoyichen@uic.edu.cn

Abstract: This paper develops a dynamic elastic linear curved rod theory consistent with three-dimensional Hamilton's principle under general loadings with a second-order error. An asymptotic reduction method is introduced to construct a curved rod theory for a general anisotropic linearized elastic material. For the sake of simplicity, the cross section is assumed to be circular. The starting point is Taylor expansions about the mean-line in curvilinear coordinates, and the goal is to eliminate the two spatial variables in the cross section in a pointwise manner in order to obtain a closed system for the displacement coefficients. We achieve this by using a Fourier series for the lateral traction condition together with the use of polar coordinates in the cross section and by considering exact tridimensional equilibrium equation. We get a closed differential system of ten vector unknowns, and after a reduction process we obtain a differential system of the vector of the mean line displacement and twist angle. Six boundary conditions at each edge are obtained from the edge term in the tridimensional virtual work principle, and a unidimensional virtual work principle is also deduced from the weak forms of the rod equations.

Keywords: curved rod theory, reduction method, anisotropic linearized elasticity, rod variational formulation, Fourier series

1. Introduction

Rods are very important engineering structures. For straight or curved rods, the dimension of the cross section is much smaller than the third one, its length. Due to this relative smallness, one may model the behaviours of these thin structures by one-dimensional rod theory through certain dimensional reduction processes. The most popular approach is to introduce some kinematic assumptions which leads to classical rod theories, such as Euler-Bernoulli rod theory, Timoshenko rod theory and well known Reddy's third-order rod theory. *In this work we propose a new optimised approach.* For plate and shell, a novel method of dimension reduction, deduced from tridimensional equilibrium equation and boundary condition on the upper and lower faces of the plate or the shell, is introduced in [1], [2], [3], [4]. This approach was used in [5] to obtain a plane-stress rod model for a linearized isotropic elastic material with pointwise error estimates. In this way [6] obtains a unidimensional model for a rod with rectangular cross section. Obtention of a rod theory is more complicated than plate or shell ones. For rod with circular cross section, we present a one dimensional model as already done in a previous work for straight rod [7] and curved rod [8]. In this paper we extend the work [8] to dynamical curved rod.

2. Results

By using the 3-D Hamilton's principle and the differential system, we can derive the dynamic linear curved elastic rod theory which is consistent with the 3-D weak formulation (as it is made for plate in [2] and shell in [3]). We can easily obtain this model by replacement in [8], the vector coefficients of the asymptotic expansion of the body force

$$\mathbf{f}^{(k, n-k)} \text{ by } \mathbf{f}^{(k, n-k)} - \rho \ddot{\mathbf{u}}^{(k, n-k)} \quad \text{for } n = 0, 5 \text{ and } k = 0, n. \quad (1)$$

in which ρ is the mass density of the rod material and $\ddot{\mathbf{u}}^{(k, n-k)}$ is the second time derivative of the coefficient of asymptotic expansion of the displacement field (see equation (24) in [8]).

By considering remark (1), we obtain the differential system of equations (59)-(62) in [8] (with the use of recursive relations (39) and (54)). The Neumann type boundary conditions are given by (73)-(76) in [8] and the Dirichlet one by (77) in [8]. So we obtain the weak variational formulation (78) in [8] which provides a framework for implementing finite-element schemes.

3. Conclusion and discussion

The main purpose of this work is to provide a new asymptotic reduction method for constructing a consistent curved rod dynamic theory for linearized anisotropic elastic material. The starting point of our derivation is a Taylor–Young expansion of the displacement field. Then we consider the corresponding expansion of the deformation gradient and the stress tensor and make some development which are needed for the success of our procedure. More precisely we summarize the main idea. To write lateral boundary condition we use polar coordinates in cross section together with Fourier series expansion. This leads to seven equations with fifteen unknown coefficients of the displacement field. Equilibrium equations give supplementary relations between stress coefficients and we show that it is possible to obtain a closed system of ten equations with ten unknowns. The linear dependence with respect to three second order displacement coefficients is used to eliminate them. Elaborated calculations furnish bending and torsion terms and also lead to asymptotically-consistent closed three vector equations with three unknowns. Then we formulate the unidimensional rod virtual work principle. Now, we have a working paper for the case of linear elastic rod with double symmetric cross section and it would be applicable to other rod problems: geometric and/or material nonlinearity/incompressible material, multilayered rod.

Acknowledgments: Hui Hui Dai acknowledges the support by a GRF grant (Project No.: CityU 11303718) from the Research Grants Council of the Government of HKSAR, P.R. China and Xiaoyi Chen acknowledges a grant (Project No.: 11702027) from National Natural Science Foundation of China.

References

- [1] DAI H.H., SONG Z. On a consistent finite-strain plate theory based on three-dimensional energy principle. *Proc R Soc London, Ser A* 2014 470 (2171) doi.10.1098/rspa.2014.0494.
- [2] SONG Z, DAI, H.H. On a consistent dynamic finite-strain plate theory and its linearization. *J Elast* 2016, 125(2):149–183.
- [3] YU X, Fu Y, DAI H.H., A refined dynamic finite-strain shell theory for incompressible hyperelastic materials: equations and two-dimensional shell virtual work principle. *Proc. R. Soc. A* 476: 20200031.
- [4] WANG F.F, STEIGMANN D.J, DAI H.H. On a uniformly-valid asymptotic plate theory. *Int J Non Linear Mech* 2019, 112:117–125.
- [5] CHEN X, SONG Z, DAI H.H. Pointwise error estimate for a consistent beam theory. *Anal Appl* 2018, 16(01):103–132.
- [6] PRUCHNICKI E. Contribution to beam theory based on 3-D energy principle. *Math Mech Solids* 2018, 23 (5):775–786.
- [7] CHEN X, DAI H.H, PRUCHNICKI E. On a consistent rod theory for a linearized anisotropic elastic material: I. Asymptotic reduction method. *Math Mech Solids* 2021, 26(2) : 217–229.
- [8] PRUCHNICKI E, CHEN X, DAI H.H. New refined model for curved linear anisotropic rods with circular cross section. *Applications in Engineering Science* 2021, 6 doi.org/10.1016/j.apples.2021.100046.

About the Target-Attacker-Defender Optimal Problem,

CHERKASOV OLEG^{1*}, MAKIEVA ELINA², MALYKH EGOR³

1. Lomonosov Moscow State University, Moscow, Russia [0000-0003-1435-1541]
2. Lomonosov Moscow State University, Moscow, Russia [0000-0002-0134-3350]
3. Lomonosov Moscow State University, Moscow, Russia [0000-0002-5081-0584]

* Presenting Author

Abstract: The Target-Attacker-Defender problem is considered. Assumed that all participants move in a horizontal plane with velocities of constant modulus. The Attacker uses the pure chase method to pursue the Target. The Defender launched from the Target's wingman and the role of Defender is to minimize the distance to the Attacker when the Attacker approaches the Target at a given distance. The Defender's strategy is also a method of pure pursuit. The angular velocity of rotation of the Target velocity vector considered as a control. The structure of the dynamic system allows to reduce it to a system of less dimension. In the reduced system, the angle between velocity vector and line-of-sight Target-Attacker is considered as a new control variable. Pontryagin maximum principle procedure allows to reduce the optimal control problem a boundary-value problem (BVP) for a system of nonlinear differential equations of the fourth order. The system of the BVP consists from the initial variables and does not includes co-state variables. For solving the BVP, the shooting method is applied. The results of solving the BVP for various values of parameters demonstrated.

Keywords: Target-Attacker-Defender problem, Pure pursuit, Optimal control

1. Introduction

Traditionally, two approaches are used to investigate the Target-Attacker pursuit-evasion problem. The first one is based on the application of methods of the theory of differential games. The second approach assumes that the strategy of the pursuer is known and fixed, and the task is to build an optimal strategy for the evader [1]. One of the advantages of the second approach is the ability to use more realistic models of the dynamics of participants. In the pursuit-evasion problems for three objects, the Target-Attacker-Defender (TAD), in the differential game, both independent actions of all participants and cooperation between the target and the defender are possible [2]. TAD problem with three participants is also investigated in the case when the strategy of one of them is fixed [3]. In this paper, we consider the case when the strategy of both the Attacker and the Defender is fixed. As a prescribed strategy, the method of pure pursuit is adopted, in which the velocity vector of the pursuer is directed exactly along the line of sight of the pursuer-target. In this formulation, the trajectories of the other participants are determined by Target motion. Therefore, the problem is to find the optimal strategy of the Target. The goal function is the distance between the Defender and the Attacker, when the distance between the Attacker and the Target becomes equal to a given value. Thus, the duration of the process is free. It is assumed that all objects move in a horizontal plane with velocities of constant modulus.

2. Problem Formulation

Equations of motion are as follows:

$$\begin{cases} \dot{\varphi} = -\frac{\sin \varphi}{R} + u, \\ \dot{\theta} = -\frac{a}{R} \sin \varphi + \frac{1}{r} \sin \theta, \\ \dot{R} = a \cos \varphi - 1, \\ \dot{r} = -b - \cos \theta. \end{cases} \quad (1)$$

where φ is the angle between LOS Target-Attacker and the velocity vector of Target, θ is the angle between the velocity vector of Attacker and Defender, R – normalized distance between Attacker and Target, r – normalized distance between Defender and Attacker, u is the control variable, a is the ratio of Target velocity modulus to Attacker velocity modulus, b is the ratio of Defender velocity modulus to Attacker velocity modulus.

Boundary conditions are as follows:

$$\theta(0) = \theta_0, R(0) = R_0, r(0) = r_0, \varphi(0) \text{ is free}, R(T) = R_T \quad (2)$$

The goal function is:

$$J = r(T) \rightarrow \min_u \quad (3)$$

where T is free.

The problem (1) - (3) is Mayer optimal control problem.

References

- [1] BEN-ASHER, J.Z., CLIFF, E.M: Optimal evasion against proportionally guided pursuer. *Journal of Guidance, Control and Dynamics*. 1989, **12**(4):598-600.
- [2] TURETSKY, V., GLIZER V.,Y: Open-loop solution of a defender–attacker–target game: penalty function approach. *Journal of Control and Decision*. 2018 **6**(1):1-25.
- [3] GARCIA E., CASBEER D.W., KHANH PHAM D., PACHTER, M: Cooperative aircraft defense from an attacking missile. *Proceedings of the IEEE Conference on Decision and Control*. 2015:2926-2931.

Brachistochrone Problem with State Constraints of a Certain Type,

CHERKASOV OLEG¹, SMIRNOVA NINA^{2*}

1. Lomonosov Moscow State University, Moscow, Russia [0000-0003-1435-1541]

2. Lomonosov Moscow State University, Moscow, Russia [0000-0002-6532-8037]

* Presenting Author

Abstract: The problem of maximizing the horizontal coordinate of a point mass moving in a vertical plane under the action of gravity forces, viscous friction, support reaction of the curve and thrust is considered, as well as the interrelated Brachistochrone problem. Two cases are addressed. The first is when the thrust applied is constant. The second is when the penalty for the control expenditures is included in the goal function. Assumed that inequality-type constraints are imposed on the slope angle of the trajectory. The system of equation belongs to a certain type that allows reduce the optimal control problem with state constraints to the optimal problem with control constraints. The maximum Principle procedure is applied, and the qualitative analysis of the boundary-value problem is presented. As a result, the sequence and the number of the arcs with motion along the phase constraints are determined and the synthesis of the optimal control is designed. The results of numerical simulation for the case of quadratic resistance are presented to illustrate the theoretical conclusions. It is shown that optimal trajectory of the Brachistochrone problem with viscous friction contains no more than one section of motion along the lower constraint and no more than two sections of motion along the upper one. For the frictionless Brachistochrone the extremal trajectory reaches for each constraint no more than once.

Keywords: brachistochrone problem, state constraints, viscous friction, qualitative analysis

1. Introduction

The presence of state constraints significantly complicates the study of optimal control problems. An effective solution can be designed if the structure of the optimal trajectory, the number of arcs with motion along the constraints and their sequence are determined. In this paper, the approach that allows one to construct an optimal synthesis for state constraints of a certain type is demonstrated using Brachistochrone problems with thrust.

Consider the motion of a material point in a vertical plane in a homogeneous field of gravity forces and in a homogeneous resisting medium. The problem is to determine the shape of the trajectory that maximizes the horizontal coordinate of a point when it is transferred from a given initial state to a given height in a fixed time interval. Along with the problem of maximizing the range, the minimum-time problem is considered: the problem of choosing the shape of the trajectory connecting two given points of the vertical plane, the travel time along which will be minimal.

The minimum-time problem in the considered formulation is called the Brachistochrone problem [1]. The frictionless brachistochrone with state constraints in the form of a linear function imposed on the coordinates of a point was considered in [2-3]. In [2], an analytical solution is proposed under the assumption that the solution contains single arc with motion along the state constraint. In [3] the Brachistochrone problem serves as an example of the efficiency of numerical methods for solving

problems with state constraints. In [4], the problem of optimal maneuver over the lunar surface is reduced to the Brachistochrone problem with a constraint on the trajectory inclination angle.

The purpose of this article is the qualitative analysis of the range maximization problem in a given time in the presence of viscous resistance, thrust and state constraints on the trajectory inclination angle. As a result of this analysis, it is possible to construct an optimal synthesis, to determine the number and sequence of the arcs with motion along the state constraints.

2. Problem Formulation

Equations of motion in dimensional variables are as follows:

$$\begin{cases} \dot{x} = v \cos \theta, \\ \dot{y} = v \sin \theta, \\ \dot{v} = -v - \sin \theta + p. \end{cases} \quad (1)$$

Here x, y are horizontal distance and vertical altitude, respectively, v is the module of the velocity, p is the thrust, subjected to inequality $-\bar{p} \leq p \leq \bar{p}$, where \bar{p} is a positive constant, θ is the slope angle. θ and p are considered as control variables.

Boundary conditions have the form:

$$x(0) = x_0, y(0) = y_0, v(0) = v_0, y(T) = y_T \quad (2)$$

where T is final time (is considered as given). The cost function has the following form

$$J = -x(T) + \int_0^T p^2 dt \rightarrow \min \quad (3)$$

State constraints are as follows:

$$\theta(t) \in [\theta_1, \theta_2] \quad (4)$$

where θ_1, θ_2 are constants. The problem (1) - (4) is Mayer optimal control problem.

References

- [1] HERMAN H. GOLDSTINE: *A history of the calculus of variations from the 17 th through the 19 th century, Studies in the History of Mathematics and Physical Sciences, Vol. 5*, Springer-Verlag, New York-Heidelberg-Berlin, 1980.
- [2] A.E. BRYSON, Y.C.HO: *Applied Optimal Control*, Blaisdell Publishing Company, Waltham, Massachusetts, 1969..
- [3] B. C. FABIEN: Numerical Solution of Constrained Optimal Control Problems with Parameters, *Applied Math. and Computation* 1996,80:43-62.
- [4] R.K. CHENG, D. A. CONRAD: Optimum translation and the brachistochrone, *American Institute of Aeronautics and Astronautics (AIAA), Aerospace Sciences Meeting*, 1964, 49 DOI:10.2514/6.1964-49.

The reconstruction of the heat transfer coefficient in the fractional Stefan problem

AGATA CHMIELOWSKA^{1*}, RAFAŁ BROCIEK², DAMIAN SŁOTA³

1. Department of Mathematics Applications and Methods for Artificial Intelligence, Faculty of Applied Mathematics, Silesian University of Technology, 44-100 Gliwice, Poland, [orcid.org/0000-0003-2268-5023]
2. Department of Mathematics Applications and Methods for Artificial Intelligence, Faculty of Applied Mathematics, Silesian University of Technology, 44-100 Gliwice, Poland, [orcid.org/0000-0002-7255-6951]
3. Department of Mathematics Applications and Methods for Artificial Intelligence, Faculty of Applied Mathematics, Silesian University of Technology, 44-100 Gliwice, Poland [orcid.org/0000-0002-9265-5711]

* Presenting Author

Abstract: The paper presents the algorithm for solving the inverse fractional Stefan problem. The considered inverse problem consists in determining the heat transfer coefficient on one of the boundaries of the considered region. The additional information necessary for solving the inverse problem is the set of temperature values in selected points of the region. The fractional derivative with respect to time used in the considered Stefan problem is of the Caputo type. The direct problem was solved by using the alternating phase truncation method adapted to the model with the fractional derivative. Using the given temperature values and the values computed by solving the direct problem for the chosen value of the heat transfer coefficient the functional representing the error of the approximate solution was constructed. The sought solution of the considered inverse problem was the argument for which the functional gained its minimum. The functional was minimized by the use of the ant colony algorithm. It is the probabilistic artificial intelligence algorithm inspired by the behaviour of the ants swarm. The paper contains an example illustrating the accuracy and the stability of the presented algorithm.

Keywords: optimization, artificial intelligence, inverse problem, fractional derivative, solidification

Laser scanners with rotational polygon mirrors: A multi-parameter optomechanical analysis and optimization

VIRGIL-FLORIN DUMA^{1,2}

1. 3OM Optomechatronics Group, Aurel Vlaicu University of Arad, 77 Revolutiei Ave., 310130 Arad, Romania [<http://orcid.org/0000-0001-5558-4777>]
2. Doctoral School, Polytechnic University of Timisoara, 1 Mihai Viteazu Ave., 300222 Timisoara, Romania

Abstract: We analyse laser scanning heads with rotational polygonal mirrors (PMs) [1]. A comparison to the most common galvanometer scanners (GSs) is performed from the point of view of their non-linear scanning functions and variable scanning speeds [2-4]. The novel theory we developed for PM scanners is used [5]. A multi-parameter analysis of PMs is carried out, considering all their constructive and functional parameters, including the PM apothem, their number of facets, the eccentricity of the incident laser beam on the PM, the distance from this beam to the objective lens, and the rotational speed. The impact of these parameters on the non-linearity of the scanning function is studied, for applications that range from industrial measurements to high-end imaging systems [6,7]. Solutions are explored to decrease this non-linearity, including by employing supplemental mirrors. A Finite Element Analysis (FEA) of polygons is performed, and conclusions are drawn on their maximum rotational speed from the condition to preserve their structural integrity; this analysis considers both material characteristics and all PM and assembly dimensions. An optimized designing scheme that incorporates both optical and mechanical aspects concludes the study.

Keywords: laser scanners, optomechanics, mechatronics, polygon mirror, galvanometer scanners, scanning function, multi-parameter analysis, Finite Element Analysis (FEA), optimization.

Acknowledgment: This research is supported by the Romanian Ministry of Research, Innovation and Digitization through CNCS/CCCDI–UEFISCDI project PN-III-P4-ID-PCE-2020-2600, within PNCDI III (<http://3om-group-optomechatronics.ro/>).

References

- [1] MARSHALL, GF, STUTZ GE, Eds.: *Handbook of optical and laser scanning*, 2nd ed.; CRC Press: London, 2011.
- [2] MONTAGU J: Scanners: Galvanometric and Resonant. In HOFFMAN C, DRIGGERS R (Eds.) *Encyclopedia of Optical and Photonic Engineering*, 2nd ed. CRC Press: 2015.
- [3] DUMA V-F, TANKAM P, HUANG J, WON JJ, ROLLAND JP: Optimization of galvanometer scanning for Optical Coherence Tomography. *Appl. Opt.* 2015, **54**:5495-5507.
- [4] DUMA V-F: Laser scanners with oscillatory elements: Design and optimization of 1D and 2D scanning functions. *Applied Mathematical Modelling* 2019, **67**(3):456-476.
- [5] DUMA V-F: Polygonal mirror laser scanning heads: Characteristic functions. *Proc. of the Romanian Academy Series A* 2017, **18**(1):25-33.
- [6] OH WY, YUN SH, TEARNEY GJ, BOUMA BE: 115 kHz tuning repetition rate ultrahigh-speed wavelength-swept semiconductor laser. *Opt. Letters* 2005, **30**:3159-3161.
- [7] MU X, ZHOU G, YU H, et al. Compact MEMS-driven pyramidal polygon reflector for circumferential scanned endoscopic imaging probe. *Opt. Express* 2012, **20**:6325-6339.

Optimization of the Two-Mass Oscillator regarding the Accumulation of Energy at Mechanical Resonance

WIESŁAW FIEBIG¹, ADAM DMOCHOWSKI^{2*}

1. Wrocław University of Science and Technology [0000-0001-5847-9200]

2. PHS Dmochowski, Wrocław

Abstract: *In the considered two-mass oscillator, the excitation force is acting on one mass (small mass) and the reception of the energy occurs on the second mass (bigger mass). The two-mass oscillator will be optimized regarding the maximal energy accumulation of the second mass. The values of the stiffness of particular connecting spring elements, mass values, and amplitude of excitation force will be used as parameters of the optimization process. The continuously delivered energy to the oscillator will be compared with the energy impulses received from the second mass.*

Keywords: Mechanical resonance, vibration, energy accumulation , oscillator

1. Introduction

In this article, the task of optimizing the parameters for a dual mass oscillator was undertaken. In the example considered (Fig. 1), the masses are connected by means of 3 springs. The harmonic forcing $F = F_0 \sin \omega t$ acts on the smaller mass m_1 , which vibrates with amplitude A_1 . The second mass vibrates freely with amplitude A_2 .

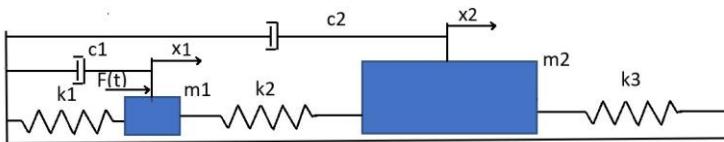


Fig. 1. The schematic view of the investigated two-mass oscillator

Based on known relationships, the amplitudes of A_1 and A_2 vibrations of both masses during resonance can be determined. From the point of view of a certain application, it becomes important to optimize the oscillator parameters such as the stiffness coefficients k_1 , k_2 and k_3 from the point of view of maximizing the amplitude of vibrations A_2 at the assumed masses m_1 and m_2 and at the given amplitude of the exciting force. This type of topic has not been discussed so far.

2. Results and Discussion

For optimization purposes Strength Pareto Evolutionary Algorithm was used. As multi-criteria and pareto algorithm, SPEA satisfied need of both minimalization of A_1 amplitude and maximalization of A_2 , and possibility of choice of realizable solution (not only optimal one). Using mathematical

formulas for A1 and A2 amplitude, algorithm is searching for close to optimal solutions and presenting them in form of pareto front.

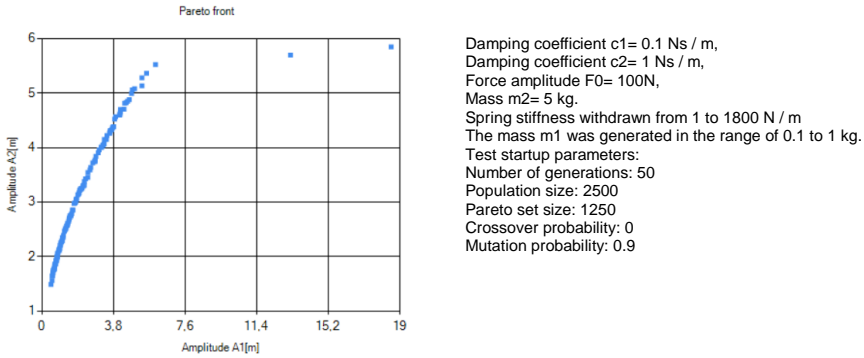


Fig. 2 Exemplary pareto front graph

Algorithm is working with fixed values of c_1 and c_2 damping and the amplitude of the external force F_0 , while stiffnesses k_1, k_2, k_3 and masses m_1 and m_2 are changeable. Except minimalization and maximalization of goal functions solutions are also limited by natural frequency of system.

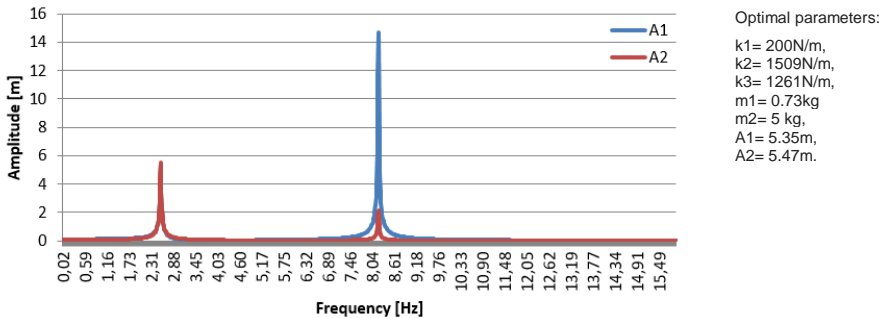


Fig. 3 Exemplary amplitude dependency on frequency graph

The results of optimization have been confirmed experimentally.

3. Concluding Remarks

Based on the optimization, the configuration of the stiffness coefficients of individual spring elements at which the maximum amplitude A_2 of the mass m_2 occurs. The influence of the masses m_1 and m_2 as well as the damping coefficients c_1 and c_2 on the maximization of the objective function was also determined.

References

- [1] FIEBIG W., WRÓBEL, J: Simulation of Energy flow at mechanical resonance, *22th International Congress on Sound and Vibration*, 12-16 July, Florence, 2015
- [2] HORN J., NAFPLIOTIS, N: DAVID E. GOLDBERG, D.E: A Niche Pareto Genetic Algorithm for Multiobjective Optimization, *IEEE 1994*, Volume 1, pp. 82-87..

Competition Between Populations: Preventing Domination of Resistant Population Using Optimal Control

URSZULA FORYŚ^{1*}, MARIUSZ BODZIOCH²

1. Faculty of Mathematics, Informatics and Mechanics, University of Warsaw, Poland [ORCID: 0000-0002-6198-3667]
2. Faculty of Mathematics and Computer Science, University of Warmia and Mazury in Olsztyn, Poland [ORCID: 0000-0002-1991-5062]

* Presenting Author

Abstract: We present an optimal control problem related to the task of controlling a growth of two competing sub-populations in the context of chemical control. One of the considered sub-populations is sensitive to the chemical and the other is resistant. We use a non-standard objective functional to prevent domination of the resistant sub-population. We show that optimal control can consist of: (1) full dose, (2) no dose, (3) singular arc. We numerically check that small doses of chemicals applied according to singular control are optimal in the main part of time interval we consider.

Keywords: competition model, resistant population, optimal control problem

1. Introduction

In the real world, there is often a situation where the use of chemicals produces resistance. This is the case with bacterial populations becoming drug resistant, tumour cell populations no longer responding to chemotherapy, or pest insect populations in various habitats that become resistant to pesticides used. Over the years, the same mistake has been made in trying to use maximum doses of drugs or pesticides to wipe out the “bad” population we are fighting. However, it often did not bring the expected results. In general, when using chemicals, it is expected that the entire population will be subdivided into sub-populations with varying levels of sensitivity, from full sensitivity to full resistance. It is therefore inevitable that there appears a competition between these sub-populations. We consider two sub-populations, for simplicity and due to the fact that analysing models with more sub-populations we have got the results very similar to those for the simplified case. We expect that without external interference in the system the sensitive sub-population outcompetes the resistant one. However, with prolonged usage of chemicals, the resistant sub-population wins the competition.

In our previous works related to the chemotherapy of tumours, we used optimal control trying to reconcile the two goals: minimizing the overall population size and maintaining the dominance of the sensitive sub-population over the resistant one. Preliminary results can be found in [1], while the analysis of the relevant optimal control problem is presented in [2] for the model of competing cellular sub-populations and in [3] for the three-dimensional model with varying carrying capacity.

Here we would like to study in more details the same problem for a minimal model describing competing sub-populations. In general, for short-time optimization we expect that mutation terms included into the models considered in [2,3] are less important than competition between sub-populations. Therefore, in the following we present the results of optimization for such model.

* Correspondence: Banacha 2, 02-097 Warsaw, Poland; email: urszula@mimuw.edu.pl

2. Results and Discussion

We consider the following non-dimensional competition model with an external interference

$$\frac{dn_1}{dt} = \gamma_1 n_1 (1 - n_1 - n_1 n_2) - n_1 u(t), \quad \frac{dn_2}{dt} = \gamma_2 n_2 (1 - n_2 - b_2 n_1),$$

where n_1 and n_2 are non-dimensional sizes of sub-populations, sensitive and resistant, respectively, γ_i is a growth rate, b_i is a competition coefficient, while $u(t)$ reflects the control (dose of chemicals). Because of the general properties of the competition model we assume $b_1 < 1 < b_2$.

The dynamics of this system is studied in the optimal control problem in which we minimize

$$J(u) = \omega(n_1(T) + n_2(T)) + \int_0^T M(n_1(t), n_2(t), u(t)) dt,$$

where the first term reflects the overall population size at the end of control action and M accounts for both overall population size during the control and penalization of the population to become resistant (we call the population resistant whenever $n_2 > n_1$), as well as the cost of external interference, that is

$$M(n_1, n_2, u) = \eta(n_1 + n_2) + \xi G\left(\frac{n_2 - n_1}{\epsilon}\right) + \theta u,$$

with positive coefficients. Note that as G we use the function \tanh for numerical purposes, while in mathematical analysis it is enough to assume that this function has the same properties as \tanh .

In the analysis of the presented control problem we use the Pontryagin Minimum Principle, formulate the adjoint system and appropriate Hamiltonian. We prove that singular control is of order 1 and satisfies the Legendre-Clebsch condition of optimality only for $n_1 > n_2$. In this case we are able to express the singular control as a function of state variables. Although we know the structure of singular control, we are not able to prove that it is optimal. Hence, we complete our theoretical analysis with numerical analysis performed, as before [2,3] in the context of tumours chemotherapy. In numerical analysis we look for 15-day treatment protocol optimal in the context described above. It occurs that numerically optimal scenario consists of two (at the beginning and the end of the therapy) short periods of maximal tolerated dose (MTD) treatment, while in between small doses of the drug (around 10% of MTD) are applied, in which singular arc is followed. This again confirms our previous findings that in general it is not good to apply MTD and smaller doses could lead to better final results.

3. Concluding Remarks

Our analytical results are obtained with reference to a general control problem and can be applied to various populations. However, in numerical simulations we focus on the response of the heterogeneous tumour to the therapy. We consider the tumour consisting of sensitive and resistant cells and find optimal control for drug-resistant tumour growth that penalizes the resistant population. The model suggests that it is desirable to leave a certain number of sensitive cells to limit the growth of resistant ones by cell competition, which is provided by singular (intermediate) chemotherapy dose.

References

- [1] BAJGER P, BODZIOCH M, FORYŚ U: Role of cell competition in acquired chemotherapy resistance. In: *Proc. of the 16th Conference on Computational and Mathematical Methods in Science and Engineering*, 1 (2016).
- [2] BAJGER P, BODZIOCH M, FORYŚ U: Singularity of controls in a simple model of acquired chemotherapy resistance. *Discr. Cont. Dyn. Syst., Ser. B* 2019, **24**:2039-2052.
- [3] BAJGER P, BODZIOCH M, FORYŚ U: Numerical optimisation of chemotherapy dosage under antiangiogenic treatment in the presence of drug resistance. *Math. Meth. Appl. Sci.* 2020, **43**(18): 10671-10689.

A Unified Bayesian Formulation for the Identification of Force Sources

J. GHIBAUDO^{1*}, M. AUCEJO¹

1. Structural Mechanics and Coupled Systems Laboratory, Conservatoire National des Arts et Métiers, 2 Rue Conté, 75003 Paris, France, julian.ghibaudo@lecnam.net, mathieu.aucejo@lecnam.net

* Presenting Author

Abstract:

Structures undergo some mechanical impacts during their life phase, which may create high vibration levels that induce damage and failure of the system itself. However, the mechanical characteristics of the shock are often not well known and inverse methods are generally used to estimate these complex sources. Among all the existing methods, Kalman filtering provides a lightweight and elegant solution to solve force reconstruction problems in time domain. In the literature, several Kalman-like filters have been proposed. We demonstrate in this contribution that all these formulations can be unified by expressing them from a Bayesian perspective.

Keywords: Inverse problem, Force reconstruction, Kalman Filter, Structural dynamics.

1. Introduction

Kalman-like filtering is an attractive way of solving joint input-state estimation problems in the time domain. Over the last 20 years, various Kalman-based techniques have been proposed. From an algorithmic standpoint, each method exhibits some clear differences. From a theoretical perspective, however, it can be shown that all these methods can be derived from a unique Bayesian formulation of the problem.

2. Results and Discussion

The space-state representation of problem that is intended to solve, is given by:

$$\begin{cases} \mathbf{x}_{k+1} = \mathbf{A} \mathbf{x}_k + \mathbf{B} \mathbf{u}_k + \mathbf{w}_k \\ \mathbf{y}_k = \mathbf{C} \mathbf{x}_k + \mathbf{D} \mathbf{u}_k + \mathbf{v}_k \end{cases} \quad (1)$$

where \mathbf{x}_k , \mathbf{u}_k and \mathbf{y}_k are the state, input and output vectors at sample k , while \mathbf{A} , \mathbf{B} , \mathbf{C} and \mathbf{D} are the system matrices. Here, \mathbf{w}_k (resp. \mathbf{v}_k) denotes the Gaussian process noise (resp. measurement noise) with zero mean and covariance matrix \mathbf{Q}_k^x (resp. \mathbf{R}_k).

From a Bayesian perspective, \mathbf{x}_k and \mathbf{y}_k are considered as random variables defined such that $\mathbf{x}_k \sim p(\mathbf{x}_k | \mathbf{x}_{k-1}, \mathbf{u}_{k-1})$ and $\mathbf{y}_k \sim p(\mathbf{y}_k | \mathbf{x}_k, \mathbf{u}_k)$. In the context of joint input-state estimation problems, additional assumptions must be made on the input vector \mathbf{u}_k .

A first idea consists in including in the state-space representation (1) the fictive state equation $\mathbf{u}_{k+1} = \mathbf{u}_k + \mathbf{w}_k^u$ (\mathbf{w}_k^u is a Gaussian noise with zero mean and covariance matrix \mathbf{Q}_k^u) to define an augmented state vector and performing the input-state estimation from a standard Kalman filter. This approach, known as AKF (for Augmented Kalman Filter), provides accurate estimates of the mean of the state and input vectors, but with large uncertainties on these estimated quantities [1]. Another option consists in making an assumption on the input vector \mathbf{u}_k predicted from all the data measured until the previous time step $k - 1$, namely $\mathbf{y}_{1:k-1}$. A careful analysis of the existing literature shows that the state-of-art

Kalman-like filters are all based on the assumption that \mathbf{u}_k given $\mathbf{y}_{1:k-1}$ follows a Gaussian distribution with mean \mathbf{m}_k and covariance matrix \mathbf{P}_k , that is:

$$p(\mathbf{u}_k | \mathbf{y}_{1:k-1}) = N(\mathbf{u}_k | \mathbf{m}_k, \mathbf{P}_k) \tag{2}$$

For instance, Sedehi considers $\mathbf{m}_k = \mathbf{0}$ and $\mathbf{P}_k = \mathbf{P}_{k-1}^u$, corresponding to the covariance matrix of the excitation estimated at $k - 1$ [2], whereas Gillijns and de Moor (GDM) considers an excitation uniformly distributed over the structure (equivalent to a Gaussian distribution with zero mean and infinite covariance matrix) [3]. Finally, the Dual Kalman Filter (DKF) is composed of two classic Kalman filters running sequentially: prediction/estimation of the input vector followed by prediction/estimation of the state vector [4]. In this case, the authors consider $\mathbf{m}_k = \mathbf{u}_{k-1}$ and $\mathbf{P}_k = \mathbf{Q}_{k-1}^u + \mathbf{P}_{k-1}^u$.

All the previously estimation methods allow properly identifying both the location and the time history of the excitation, as shown in figure 1, presenting the estimation of a hammer impact exerted on a simply supported beam from a set of acceleration measurements.

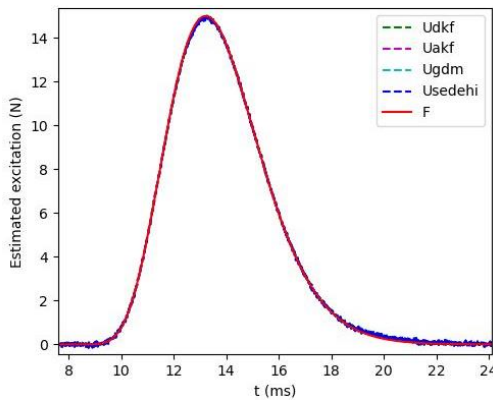


Fig. 1. Force identification for AKF, DKF, GDM and Sedehi methods.

3. Concluding Remarks

In this contribution, the Bayesian paradigm has been adopted to derive a unified vision of the state-of-the-art joint input-state estimation methods, classically used in structural mechanics. This unified Bayesian formulation points out the main differences between these identification strategies, which allows to explore some new assumptions and consequently propose original methods.

- [1] E. LOURENS : An augmented Kalman filter for force identification in structural dynamics, *Mechanical Systems and Signal Processing* 27 (2012) 446–460
- [2] O. SEDEHI, C. PAPADIMITRIOU ET AL. : Sequential Bayesian estimation of state and input in dynamical systems using output-only measurements, *Mechanical Systems and Signal Processing* 131 (2019) 659–688
- [3] S. GILLIJNS, B. DE MOOR : Unbiased minimum-variance input and state estimation for linear discrete-time systems with direct feedthrough, *Automatica* 43 (2007) 934 – 937
- [4] S. AZAM, ET AL. : A dual Kalman filter approach for state estimation via output-only acceleration measurements, *Mechanical Systems and Signal Processing* (2015)

Numerical Analysis, Processing and Prediction of a Populations Dynamics of Atomic Systems in a Laser Pulse Field: Quantum dynamics and Bi-stability Effects

ALEXANDER V GLUSHKOV¹, EVGENIYA K PLISETSKAYA^{1*},
EUGENY V TERNOVSKY¹ AND ARTEM V. VITAVETSKY¹

1. Odessa State Environmental University, Mathematics Depr., L'vovskaya str. 15, 65009, Odessa

* Presenting Author

Abstract: The paper is devoted to presentation of an effective approach to numerical analysis, modelling and forecasting a populations dynamics of atomic ensembles in a field of laser pulse of different shape and quantitative studying the dynamical bi-stability (optical hysteresis) effects. The results of computing kinetics of resonant levels for atoms in the laser pulse of different shape (sinusoidal, rectangular, etc) on the basis of the modified Bloch equations are presented. Cited equations describe an interaction between two-level atoms ensemble and resonant radiation with an account of the atomic dipole-dipole interaction. It has been found for a case of $ch^{-1}t$ laser pulse a strengthened possibility of manifestation of the internal optical bi-stability effect in the temporal dynamics of populations for the atomic resonant levels under adiabatic slow changing the acting field intensity.

Keywords: processing and prediction, atomic dynamics, laser puls, bistability

1. Introduction. Dynamics of atomic Systems in a Laser Field and Bi-stability

Present paper has for an object (i) to simulate numerically a temporal dynamics of populations' differences at the resonant levels of atoms in a large-density medium in a nonrectangular form laser pulse and (ii) to determine possibilities that features of the effect of internal optical bistability at the adiabatically slow modification of effective filed intensity appear in the sought dynamics. It is known that the dipole-dipole interaction of atoms in dense resonant mediums causes the internal optical bistability at the adiabatically slow modification of radiation intensity [1-4]. The modified Bloch equations, which describes the interaction of resonance radiation with the ensemble of two-layer atoms subject to dipole-dipole interaction of atoms, are as:

$$\frac{dn}{d\tau} = \frac{i2\mu T_1}{\hbar} (E^* P - P^* E) + (1-n) \quad (1)$$

$$\frac{dP}{d\tau} = \frac{i2\mu T_1 n}{\hbar} - p T_1 \frac{1-i(\delta+bn)}{T_2},$$

where $n = N_1 - N_2$ are the populations' differences at the resonant levels, P is the amplitude of atom's resonance polarization, E is the amplitude of effective field, $b = 4\pi\mu^2 N_0 T_2 / 2\hbar$ is the constant of dipole-dipole interaction, T_1 is the longitudinal relaxation time, $\delta = T_2(\omega - \omega_{21})$ is the offset of the frequency ω of effective field from the frequency of resonance transition ω_{21} , N_0 is the density of resonance atoms, μ is the dipole moment of transition, $\tau = t/T_1$.

2. Results and Discussion

There are obtained the results on atomic dynamics for different shapes of laser pulse, including the following one:

$$E(\tau) = |E_0|^2 ch^{-1} \frac{\pi T_1}{T_2}. \quad (2)$$

In the numerical experiment τ varies within $0 \leq \tau \leq T_p/T_1$ and T_p is equal to $10T_1$. On the assumption of $b > 4$ and $b > |\delta|$ with $\delta < 0$ (the long-wavelength offset of incident light frequency is less than Lorenz frequency $\omega_L = b/T_2$) and if the intensity of light field has certain value ($I_0 = 4|E_0|^2 \mu^2 T_1 T_2 / h^2$) then there are three positive stationary states n_i (two from them with maximal and minimal value of n are at that stable). A fundamental aspect lies in the advanced possibility that features of the effect of internal optical bistability at the adiabatically slow modification of effective field intensity for pulse of $ch^{-1}t$ form, in contrast to the pulses of rectangular form, appear in the temporal dynamics of populations' differences at the resonant levels of atoms. Figure 1 shows the results of our numerical modeling the temporal dynamics of populations' differences at the resonant levels of atoms for the nonrectangular form pulse (2). More mathematical and physical details of the model can be found in [1-3].

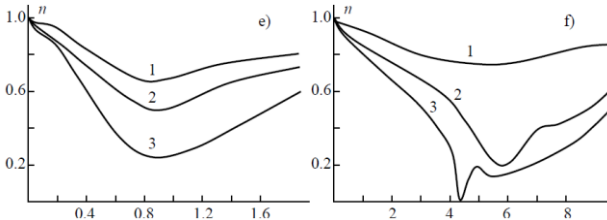


Fig.1 - Results of modeling temporal dynamics of populations' differences $n(\tau)$ at resonant levels of atoms for pulse (2) with $\delta = 2$, $T_1 = 5T_2$; $b = 0$ (e); $b = 6.28$ (f); $I_0 = 2$ (1), 5 (2), and 10 (3)

3. Concluding Remarks

The increase of field intensity above certain value $I_0 = 2.5$ for selected parameters (shown in Fig. 1) leads to the abrupt increase of populations' differences. This fact represents the Z-shaped pattern of dependence $n(I)$ observed in the stationary mode. For rectangular-shaped pulse, the dependence $n(\tau)$ tends to stationary state with magnitude defined by zero values of right-hand terms in the set (1) [4]. For the sinusoidally-shaped pulse, the slow rise of intensity is typical, and the explicit hysteresis pattern for the dependence of populations' differences from the field intensity is obtained.

References

- [1] LETOKHOV V: *Nonlinear Selective Photoprocesses in atoms and molecules*. Nauka: Moscow, 1983.
- [2] GLUSHKOV A: Multiphoton spectroscopy of atoms and nuclei in a laser field: Relativistic energy approach and radiation atomic lines moments method. *Adv. Quant Chem.* (Elsevier) 2019, **78**:253-285
- [3] GLUSHKOV A, LOBODA A, KHOKHLOV V, PREPELITSA G: Numerical modelling a populations differences dynamics of the resonant levels of atoms in a nonrectangular form laser pulse: Optical bistability effect. *Laser and Fiber-Optical Networks Modeling*, LFNM 2006:428-430.
- [4] AFANAS'EV A AND VOITIKOVA M: Effect of the local field on transient processes in a dense ensemble of two-level atoms. *Opt. Spectr.* 2001, 90:799-802.

Optimization of wind turbine tower using adaptive algorithm configuration

CHANGWU HUANG¹, HAO BAI^{2*†}, LUJIE SHI², YOUNES AOUES²

1. Department of Computer Science and Engineering, Southern University of Science and Technology, Shenzhen 518055, China [0000-0003-3685-2822]
2. Laboratory of Mechanics of Normandy (LMN), INSA Rouen Normandy, Rouen 76000, France [0000-0003-3546-8802]

* Presenting Author

† Corresponding Author: Hao Bai, hao.bai@insa-rouen.fr

Abstract: This paper aims to solve the black-box optimization problem by using an optimization algorithm with adaptive hyperparameter tuning. The method is applied to a real-world optimization problem in the wind industry to validate its effectiveness. The results reveal that the proposed method is much effective than the other genetic algorithms in solving optimization problems in applied science.

Keywords: Black-box optimization, Wind turbine tower, Differential evolution, Adaptive parameter control

1. Introduction

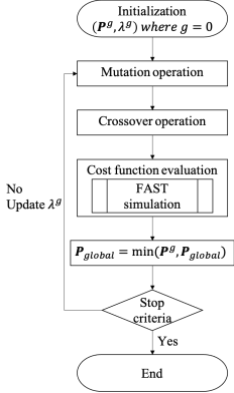
Black-box optimization has always been a tough problem in engineering since it superposes a time-consuming procedure (such as computational mechanics, computational fluid dynamics, etc.) on an optimization loop. To tackle this problem, some researchers propose to replace the numerical models with surrogate models to reduce the demand in time and physic materials. However, these techniques remain an approximate solution comparing to that calculated directly by the numerical models. Another approach is to develop adaptive optimization algorithms which adjust their hyperparameters dynamically during the searching procedure and reduce consequently the need for trial-and-error.

In this paper, an adaptive optimization algorithm with automatic parameter control is proposed based on differential evolution (DE) algorithm. The algorithm is applied to solve a real-world optimization problem in the wind industry and compared to other genetic algorithms in terms of solution quality and optimization effectiveness.

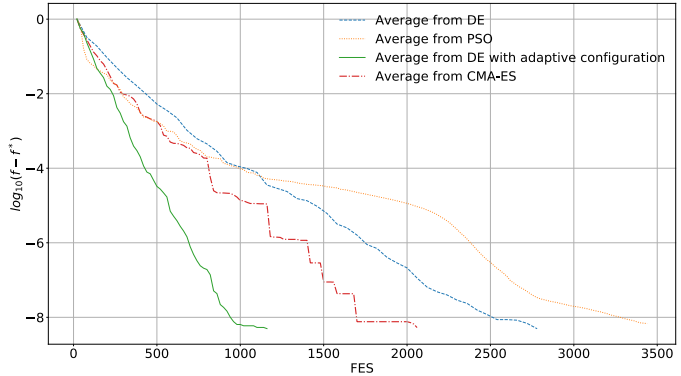
2. Results and Discussion

The objective of the optimization is to minimize the tower mass with respect to the probability of fatigue failure. The initial design is borrowed from [1] where a 140 m reinforced concrete tower is involved to support a 3 MW wind turbine. The dynamic analysis is carried out by using a numerical simulation tool FAST [2]. As a population-based algorithm, the proposed optimization algorithm initiates the initial population \mathbf{P}^0 by Latin Hypercube Sampling method in the design space then updates the optimal solution $\mathbf{P}_{\text{global}}$ at each generation \mathbf{g} . The relative error between 2 consecutive generations is calculated. When the error falls below 10^{-8} , the optimization is considered as converted.

The initial configuration for optimization algorithm λ^0 is selected randomly in a single run. It will be updated periodically when the stop criteria are not met. The hyperparameters from mutation operation and crossover operation are tuned in the way to explore the search space in early generations and to exploit the optimal solution in later generations.



(a) Workflow of the adaptive optimization



(b) Optimization performance of the proposed method compared to other algorithms (DE, PSO and CMA-ES) for 25 random runs

Fig. 1. Workflow and results comparison

The overall workflow of the proposed algorithm is illustrated in Fig. 1(a). Fig. 1(b) compares the proposed method with some other population-based optimization algorithms, i.e., DE [3], PSO [4], and CMA-ES [5]. The optimization performance is evaluated by repeating each algorithm 25 times with a random initial population and initial hyperparameters.

It is clear that the slope of the proposed method (green line) is larger than the others which indicates that the proposed DE with adaptive configuration converges more quickly to reach the global optimum. In 25 runs, the averages cost function evaluations (FES) for the proposed method is around 1 000 while the others require more than 1 500 evaluations to reach the same quality of the solution. On the other hand, for a given number of FES, the proposed method offers always the best quality of the solution among all algorithms.

3. Concluding Remarks

In this paper, a population-based adaptive optimization algorithm is proposed to address the black-box optimization problem. The proposed method is used to solve a real-world optimization problem involving numerical modelling. The time consumption in terms of function evaluation is much reduced by comparing to other genetic algorithms. Further investigations on the adaptability of the proposed method for other time-consuming tasks should take place.

References

- [1] BAI H, CHERFILS JM, AOUES Y, LEMOSSE D: Optimization of a tall wind turbine tower. *Congrès Français de Mécanique* 2017.
- [2] JONKMAN J, JR, BUHL M: FAST User's Guide. *National Renewable Energy Laboratory (NREL)*, 2005.
- [3] PRICE KV: Differential evolution. In: *Handbook of optimization*. Springer: Berlin, 2013.
- [4] MARINI F, WALCZAK B: Particle swarm optimization (PSO). A tutorial. *Chemometrics and Intelligent Laboratory Systems* 2015, **149**:153-165.
- [5] HANSEN N: The CMA Evolution Strategy: A Tutorial. *arXiv preprint arXiv:1604.00772* 2016.

Optimisation potentials of laminated composites using semi-analytical vibro-acoustic models

MATTHIAS KLAERNER^{1*}, STEFFEN MARBURG², LOTHAR KROLL¹

1. Chemnitz University of Technology, Institute for Lightweight Structures, 09107 Chemnitz, Germany

2. Technical University of Munich, Chair of Vibroacoustics of Vehicles and Machines, 85748 Garching, Germany

* Presenting Author

Abstract: Light and stiff composites such as fibre-reinforced plastics are sensitive to propagate structure borne sound but simultaneously offer a wide range of adjusting the material behaviour. Thereby, stiffness and damping of such composites are contradictory material properties related to the fibre orientation. Commonly, the composite design is based on FEA simulations requiring special modelling efforts. In contrast, the multi-dimensional optimisation of a laminate with numerous layers of different materials and orientations requires very fast numerical solutions for numerous repetitions.

Using a complex but efficient vibro-acoustic simulation model is essential in optimising composites. Here, the FEA is extended by a strain energy based modal damping approach for the layerwise accumulation of the anisotropic damping. In addition, the radiated sound power is determined by a velocity-based approach directly on steady state structural simulations avoiding a complex multi-physical modelling. Moreover, the frequency dependent radiation is consolidated to a single scalar optimisation objective using a fast and efficient semi-analytic approach. Therefore, analytical formulations of amplification factors of the modal power contributions are introduced.

This efficient simulation methodology is applied to design a vibro-acoustically optimised composite oil pan. The achieved results emerge the vibro-acoustic optimisation potential of thermoplastic composites with various fibre and matrix materials compared to a steel reference case. Furthermore, the layout is a complex multi-dimensional optimisation problem with an additional potential of improving the NVH performance. In summary, the potential for optimisation of the different steps is compared.

Keywords: sound radiation, finite element analysis, optimisation, fibre-reinforced composites

1. Amplification factors of modal sound power contributions

The radiated sound power of vibrating surfaces is an important objective for acoustic optimisation procedures. Apart from multi-physical models, simplified FEA-based approaches of the sound pressure such as the equivalent radiated sound power, the lumped parameter model or the volume velocity in combination [1] with a scalar measure representing the entire frequency domain [2] are helpful but still cause significant computational costs.

Thus, the amplification factors of the radiated sound power approaches are presented as an analytical formulation of a single mode (Fig. 1). Evaluating only a single resonant frequency step per mode, the modal contributions within the entire frequency range then are analytically determined. Superpositioning all modal contributions then results in the total sound power.

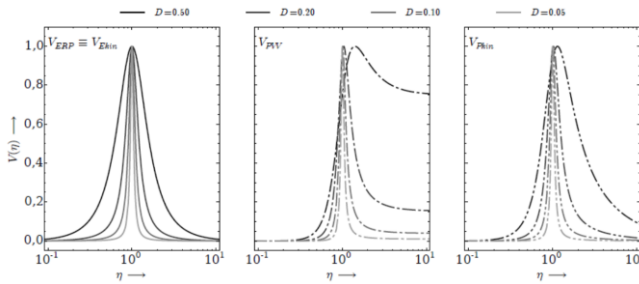


Fig. 1. Modal amplification factors of different velocity based sound power approaches with different viscous damping

2. Optimisation problem and results

The new semi-analytical approach has been applied to the sound power determination of a composite oil pan. Thus, it is now possible to solve this multi-physical problem in huge parametric studies and complex optimisation algorithms.

Therewith, a layup with two independent fibre orientations is acoustically optimised. Due to anisotropic stiffness and damping, each mode is varying in frequency, half-power band width and maximal sound power (Fig. 2). Moreover, the number of modes within a fixed frequency range is changing. The parametric study shows the jumping objective and several local minima. Furthermore, particle swarm optimisation is used for the efficient solution up to four independent parameters.

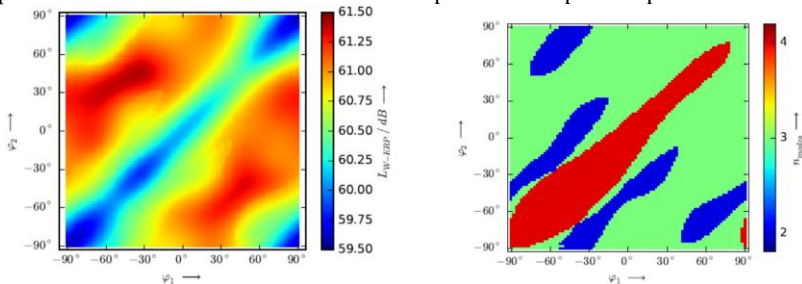


Fig. 2. Optimisation of a composite with two independent fibre orientations: radiated sound power level (left) and number of contributing modes within the frequency range (right)

3. Concluding Remarks

With the semi-analytical modelling, a very fast solution of a single simulation run and thus a complex acoustical optimisation is possible. As a result, the oil pan shows significant optimisation potential. First, a material substitution can reduce the radiated sound power level up to 7 dB. In more detail, the optimisation of the layup reduces the radiation even 2 dB more. The used of particle swarm optimisation therein is more efficient and precise than a full parameter study.

References

- [1] D. FRITZE, S. MARBURG, H.-J. HARDTKE, Estimation of Radiated Sound Power: A Case Study on Common Approximation Methods, *Acta Acustica United with Acustica* 95 (2009) 833–842.
- [2] KLAERNER, MATTHIAS ; WUEHRL, MARIO ; KROLL, LOTHAR ; MARBURG, STEFFEN: FEA-based methods for optimising structure-borne sound radiation. In: *Mechanical Systems and Signal Processing* 89 (2017), 37–47

Validation of numerical models describing the stress-strain characteristics in the strength tests of composite materials on a metal matrix using the elasto-optic method

ADAM KURZAWA¹, DARIUSZ PYKA², MIROSLAW BOCIAN², LUDOMIR JANKOWSKI²,
MARCIN BAJKOWSKI³, KRZYSZTOF JAMROZIAK^{2*}

1. Department of Foundry Engineering, Plastics and Automation, Wrocław University of Science and Technology, Smoluchowskiego 25, 50-372 Wrocław, Poland [0000-0001-5448-8062]
2. Department of Mechanics, Materials and Biomedical Engineering, Wrocław University of Science and Technology, Smoluchowskiego 25 Str., 50-370 Wrocław, Poland [0000-0002-9509-354X], [0000-0003-0638-6832], [0000-0002-3216-6641], [0000-0002-9887-0578]
3. Institute of Mechanics and Printing, Faculty of Production Engineering, Warsaw University of Technology, Narbutta 85 Str., 02-524 Warsaw, Poland [0000-0003-2517-5379]

* Presenting Author

Abstract: Testing the strength properties of materials intended as impact energy absorbers requires appropriate identification. The scope of tested becomes laborious when composites are the material used to build such shields. Various methods are used for this. One of them is the method based on the analytical model or Eshelby model or the method based on the finite element method. The analysis was based on AC-44200 alloy reinforced with 20% vol. and 30% vol. of Al₂O₃ particles. Numerical analysis were carried out in the ABAQUS/Explicit environment on the basis of composite material samples subjected to loads on a testing machine based on the fracture mechanics. The obtained results of the maximum stress distribution were compared with the results obtained using the elasto-optic method. The high agreement of the results proves the correctly developed numerical models and the adopted boundary conditions. The developed conclusions from the research were used for further analysis in the field of modeling the impact load of a new group of materials characterized by appropriate ballistic parameters.

Keywords: ceramic matrix composites (CMCs), impact resistance, Finite Element Method (FEM)

1. Introduction

The energy absorption in materials impulse load is a complex mathematical description process [1, 2]. The knowledge of the physical processes involved is directed towards the search for new material solutions, which should exceed the traditional material with their mechanical description properties, etc. [3, 4]. Materials of the cermet group can be a positive response to search for such solution. Cermets can largely replace the standard material in the form of classic ballistic ceramics, and conducted works, are focused mainly on finding proper structures absorbing the impact energy in to improve the yield strength. The subject matter of the study covers metallic composites reinforced with aluminum oxide (Al₂O₃) particles. This objective was achieved through numerical methods using FEM. The obtained results were validated experimentally by the elasto-optic method stress distribution.

2. Results and Discussion

The elasto-optical test was performed on a sample made of a metal-ceramic composite with a 20 and 30% Al₂O₃ content. Strength tests were carried out on the MTS 858 Mini Bionix machine with the MODEL 031 polariscope with a power of 105W. The test sample was loaded with four forces until it cracked. At the same time, photos of the deformations shown were taken (Fig. 1). The sample was damaged under the load of 3900 N.

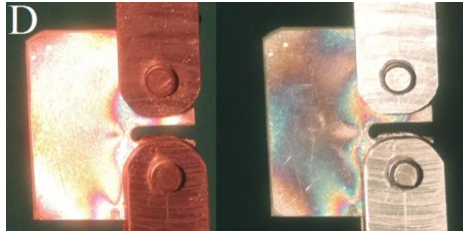


Fig. 1. Example of a deformation picture: on the left there are total isochromes, on the right there are half isochromes

In the next step, the sample was modeled in the ABAQUS environment. The model was made in two 3D variants - solid and 2D shell. Exemplary results are presented in Figure 2.

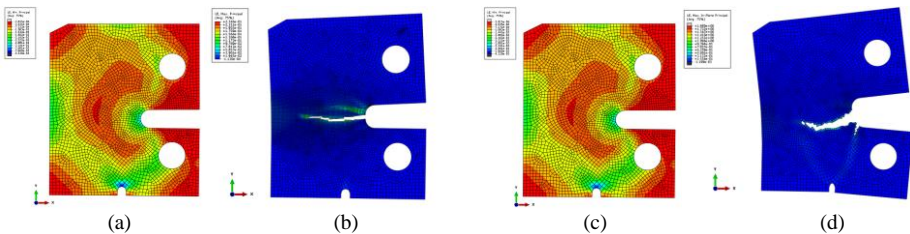


Fig. 2. An example of numerical analysis: (a) 2D sample for $E=168$ GPa, (b) Ductile model for 2D sample, (c) 3D sample for $E=158$ GPa, (d) Ductile model for 3D sample

3. Concluding Remarks

The obtained results from the 2D and 3D models show differences. The assumptions about the non-axial fixing of the sample proved correct when the attached force was shifted to one of the walls from a symmetrical position in the 3D model. The change in Young's modulus did not affect the stress distribution in the sample. The introduced model of destruction also shown a different character.

Acknowledgment: Calculations were carried out at the Wroclaw Centre for Networking and Supercomputing (<http://www.wcss.pl>), grant No. 452.

References

- [1] SWAB JJ, SANDOZ-ROSADO EJ: *Identifying opportunities in the development of ceramic matrix composite (CMC) materials for armor applications*. US Army Research Laboratory, Report No. ARL-TR-7987, 2017.
- [2] KURZAWA A, PYKA D, PACH J, JAMROZIAK K, BOCIAN M: Numerical modeling of the microstructure of ceramic-metallic materials. *Procedia Engineering* 2017, **199**:1459-1500.
- [3] ZAERA R, SANCHEZ-GALVEZ V: Analytical Modeling of Normal and oblique ballistic impact on ceramic/metal lightweight armours. *International Journal of Impact Engineering* 1998, **21**(3):133-148.
- [4] JAMROZIAK K, BOCIAN M, KULISIEWICZ M: Effect of the attachment of the ballistic shields on modelling the piercing process. *Mechanika* 2012, **19**(5):549-553.

Optimisation and state identification of composite shell using Deep Neural Networks

BARTOSZ MILLER^{1*}, LEONARD ZIEMIAŃSKI²

1. Rzeszów University of Technology, e-mail: bartosz.miller@prz.edu.pl [0000-0003-3318-4339]

2. Rzeszów University of Technology [0000-0002-4012-0002]

* Presenting Author

Abstract: Multi-layer composite structures have many advantages from the point of view of potential use in e.g. civil engineering. Their shaping and optimisation can exploit possibilities unavailable in other types of materials. A genetic algorithm-based optimisation of selected dynamic and buckling parameters of a cylindrical composite shell is presented herein. The natural frequencies of vibrations of the shell and the mode shapes were chosen as the source of data for optimisation. In order to eliminate problems related to the natural frequencies crossing, two approaches for the identification of mode shapes were proposed: analytical and based on deep learning with the use of convolutional neural networks. Automatic identification of mode shapes allowed to perform some selected tasks usually associated with structural health monitoring, namely the detection of the state of local degradation of the composite material and localization of such a change.

Keywords: multi-layer composite, deep networks, optimisation, damage detection

1. Introduction

Multi-layer composite structures have many advantages from the point of view of potential use in e.g. civil engineering, among these are lightness, durability and strength. Moreover, their shaping and optimisation can exploit possibilities unavailable in other types of materials; by changing parameters such as lamination angles in individual layers, it is possible to change and optimise the entire structure, while leaving its shape and the materials used to build the composite shell (matrix and reinforcement) unchanged.

This abstract presents a genetic algorithm-based optimisation of selected dynamic and buckling parameters of a cylindrical composite shell. The natural frequencies of vibrations of the shell and the mode shapes were chosen as the source of data for optimisation. In order to eliminate problems related to the natural frequencies crossing (see [1]), two approaches for the identification of mode shapes were proposed: analytical (see [2]) and based on deep learning with the use of convolutional neural networks (see [3]).

Automatic identification of mode shapes allowed, apart from accelerating and increasing the accuracy of the optimization process, was applied to perform some selected tasks usually associated with structural health monitoring, namely the detection of the state of local degradation of the composite material and localization of such a change.

The FE model and the applied optimisation procedure were verified by comparing the results with test examples available in the literature.

2. Results

Example results of identification errors of the appearance of local material degradation in the considered shell are shown in Fig. 1. The horizontal axis in Fig. 1 shows the width and height (equal to each other) of the area with local material degradation expressed in the number of finite elements, the vertical axis shows the number of so called “False Negatives”, i.e. misidentification of a damaged state as undamaged. The value of 2 on the horizontal axis means that the area of local degradation was as high as 2x2 finite elements, which is about 0.04% of the total coating area (the whole shell consisted of 9600 finite elements). The total number of test cases was 6000, the number of errors even for the smallest area of material degradation, at the level of a few dozen cases should be considered negligible. Subsequent series in Fig. 1 show identification cases with different number of mode shapes taken into account.

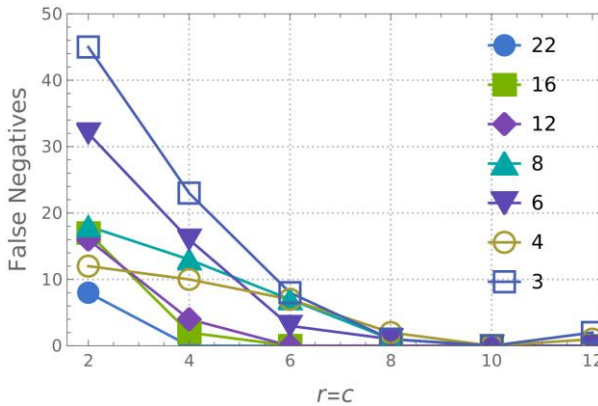


Fig. 1. False negatives for different sizes of area with material constants degradation.)

3. Concluding Remarks

The proposed optimisation method of dynamic and buckling properties of a composite shell and the identification of local degradation state on the basis of identified mode shapes are very robust. The change of the material or even occurrence of local material degradation do not affect the accuracy of the method.

References

- [1] RUIZ, D.; BELLIDO, J.; DONOSO, A. Eigenvector sensitivity when tracking modes with repeated eigenvalues. *Comput. Methods Appl. Mech. Eng.* 2017, **326**:338-357.
- [2] MILLER, B.; ZIEMIAŃSKI, L. Optimization of dynamic behavior of thin-walled laminated cylindrical shells by genetic algorithms and deep neural networks supported by modal shape identification. *Adv. Eng. Softw.* 2020, **147**:102830.
- [3] MILLER, B.; ZIEMIAŃSKI, L. Identification of Mode Shapes of a Composite Cylinder Using Convolutional Neural Networks. *Materials* 2021, **14**(11):2801.

Design of a vibration absorber system for tremor reduction in Parkinson patients using a cluster based algorithm

PREMCHAND V P^{1*}, BIPIN BALARAM, AJITH K MANI, SAJITH A S, M D NARAYANAN,

1. Department of Mechanical Engineering, Mar Baselios College of Engineering and Technology Trivandrum, India 695015 [ORCID: : 0000-0002-0060-0634]
 2. Department of Mechanical Engineering, Amrita School of Engineering, Amrita Vishwa Vidyapeetham, Coimbatore, 641 112, INDIA [ORCID: 0000-0002-6577-3149]
 3. Department of Mechanical Engineering, Saint Gits college of Engineering Kottayam, 686532, India.
 4. Department of Civil Engineering, National Institute of Technology Calicut, 673601, India
 5. Department of Mechanical Engineering, National Institute of Technology Calicut, 673601 India
- * Presenting Author (email - premchand.vp@mbcet.ac.in)

Abstract: Parkinson's disease is a progressive disorder of the central nervous system that affects human movement. The treatment of Parkinson disease using passive control devices such as Dynamic Vibration Absorber has received considerable attention in recent times. In this work a new optimization algorithm termed as the Cluster Based Algorithm (CBA), developed by the authors for the design optimization of dynamical systems, is used to evaluate the absorber parameters. It is seen that the designed absorber parameters which when attached to the primary system resulted in reduction of steady state amplitude of primary system (Human Hand). Moreover, it is also seen that absorber parameter sets converge to a cluster in the parameter space. Parameter cluster gives the designer more freedom to choose a parameter set satisfying the design considerations.

Keywords: Tremor reduction, Vibration absorber, Cluster Based Algorithm

1. Introduction

Parkinson disease is a neurodegenerative disorder caused by the deficiency of dopamine in the brain and influences the brain control of muscles, leading to tremor (shaking), slow muscle movement and motion balancing problems. Passive vibration control devices such as vibration absorbers can be used to control movements, and can prove to be an effective mechanical treatments for tremor patients. Tremor suppression in Parkinson patients is generally a broadband vibration control problem with frequencies varying from 2Hz to 10Hz [1]. In this work control of tremor in hand is analysed numerically by modeling a biodynamic human hand where joints and muscle movements are satisfying physical laws of nature. Here, the mathematical model and corresponding equations are adopted from [2] and emphasis is on the estimation of feasible absorber parameters using the proposed cluster based algorithm. Human body's trunk was considered to be immovable and connections were made at shoulder and elbow joints and were idealized as hinged joints. Human hand is mathematically modeled as a two degree of freedom system and Human hand with absorber attached is modelled as a three degree of freedom system. An external harmonic torque of amplitude, is applied at the lower arm and the uncontrolled steady state amplitude of the system is evaluated by numerically solving corresponding differential equations of motion. The primary aim is to design an absorber system to be attached in the lower arm which reduces the steady amplitude of the lower arm. The absorber parameters are the position (l_3) along the lower arm, distance from this position to the absorber centroid (a_3), the mass of the absorber (m_a), absorber stiffness (k_a), absorber damping (c_a). A schematic representation of the human hand with absorber attached (as an equivalent pendulum model) in the lower arm is shown in Fig. (1).

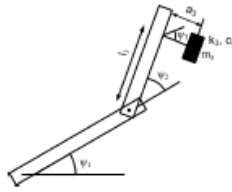


Figure 1. Mathematical model of Human hand with attached absorber system

2. Results and Discussion

CBA as discussed in [3] is implemented in the design of absorber system and parameter cluster is obtained as shown in Fig (2).

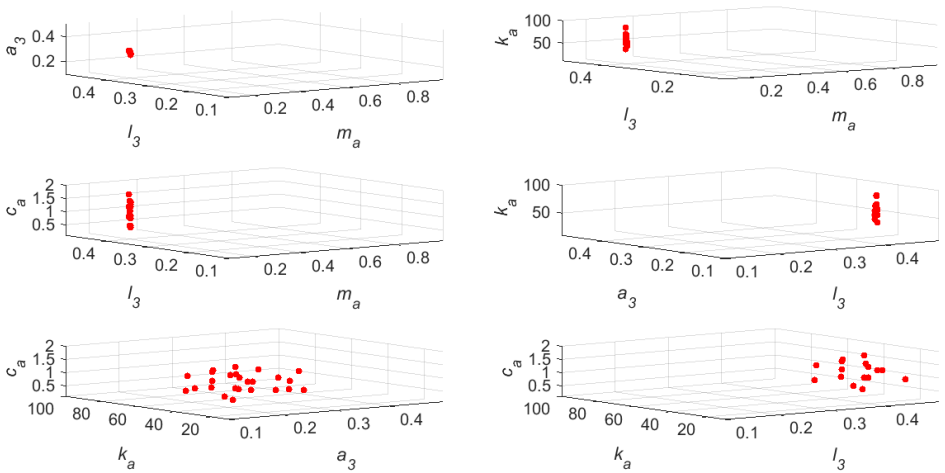


Figure 2. Parameter cluster for absorber design parameters

3. Concluding Remarks

CBA is implemented in the design of absorber for tremor suppression in a bio-dynamic hand model for Parkinson patients. Position of absorber, mass, damping coefficient, etc. were evaluated which reduced the amplitude of motion of the forearm model. Parameter sets satisfying design consideration converged to a cluster giving the designer more freedom to choose a parameter set satisfying the design considerations.

References

- [1] S M Hashemi, M F Golnaraghi, and A E Patla. Tuned vibration absorber for suppression of rest tremor in parkinson's disease. *Medical and Biological Engineering and Computing*, 42(1):61–70, 2004.
- [2] Mostafa Rahnavard, Mojtaba Hashemi, Farzam Farahmand, and Ahmad F Dizaji. Designing a hand rest tremor dynamic vibration absorber using h 2 optimization method. *Journal of Mechanical Science and Technology*, 28(5):1609–1614, 2014.
- [3] Premchand V. P. , M. D. Narayanan, Sajith A.S. A New Cluster-Based Harmonic Balance Aided Optimization Procedure With Application to Nonlinear Vibration Absorbers". *ASME Journal of Computational and Nonlinear Dynamics*, 14(7), 2019.

Parameter identification for a two-axis gimbal system and its kinematic calibration

ŁUKASZ RÓWIENICZ^{1*}, PAWEŁ MALCZYK²

1. Institute of Aeronautics and Applied Mechanics, Faculty of Power and Aeronautical Engineering, Warsaw University of Technology [0000-0003-2258-9007]

* Presenting Author

2. Institute of Aeronautics and Applied Mechanics, Faculty of Power and Aeronautical Engineering, Warsaw University of Technology [0000-0001-5969-7218]

Abstract: The main difference between robots and gimbals is the range, in which the objects are working. Robots usually operate in a limited space, whereas joint limits in typical industrial gimbals are much wider. The main position error for serial-chain robot comes from linear and angular tolerances imposed on joints. On the other hand, in gimbals, the linear errors could be largely omitted. Gimbal systems used for tracking or positioning need to have a high positioning accuracy and good repeatability. Additional requirements should be met for applications, in which a gimbal system is mounted on moving platform introducing extra disturbances. It is hard to achieve a well-designed gimbal system in practice that will successfully work in military or commercial applications. A number of features should be taken into account in the simplest case such as geometrical tolerances, system biases, friction, and dynamic parameters. Kinematic calibration of a line-of-sight system is a first step to achieve good enough performance. In this paper a systematic procedure for kinematic calibration of a two-degree-of-freedom spatial line-of-sight system is presented. Numerical results are shown to improve a nominal kinematic model of a system with non-orthogonal, imperfect joints to the extent possible by simultaneously alleviating sensor noise.

Keywords: kinematic calibration, gimbal, dynamic, line-of-sight, stabilization

1. Introduction

Consider a two axis gimbal system shown in Fig. 1. Assuming that a reference frame π_0 is a mechanical base body, π_1 is a coordinate frame attached to a first body, and π_2 is a coordinate frame attached rigidly to a second body, we introduce two joint angles: azimuth θ_1 and elevation θ_2 . Using the orientation of the axes shown in Fig. 1, we can write a simple relation that transforms a line-of-sight (LOS) expressed in π_2 to the quantity read in π_0 frame.

$$LOS^{(0)} = Rot_z(\theta_1) \cdot Rot_x(\theta_2) \cdot LOS^{(2)} \quad (1)$$

Unfortunately, in real systems, the equation (1) should be supplemented to capture inherent kinematic errors existent in the structure. Non-orthogonality between mechanical base and azimuth axis of revolution should be taken into account. There is also a bias between azimuth and elevation axes and noticeable bias between line-of-sight and elevation axis. In tracking or positioning gimbal systems, there is a need to describe those non-orthogonality conditions and exploit measurement data to improve kinematic model. The relation (1) becomes more complex as it should capture various, potentially random, error sources that influence the accuracy of the parametric model.

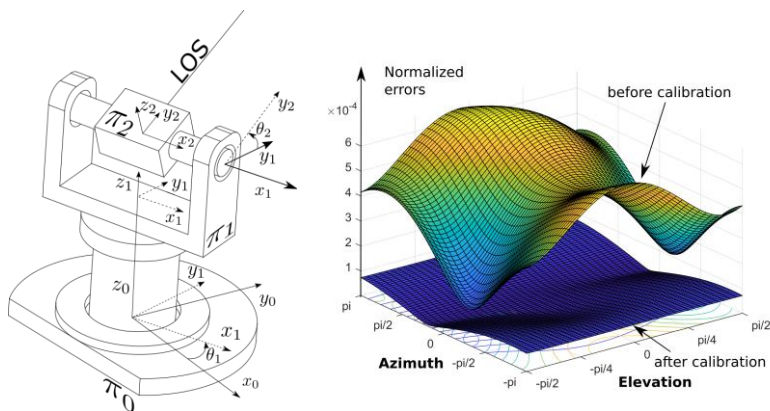


Fig. 1 Two-axis gimbal system and the results of kinematic calibration

2. Methodology and Results

The main idea of parameter identification for kinematic calibration is to create a model of a gimbal system, which minimizes the design errors stemming from various issues e.g. non-orthogonality of revolute axes. Various techniques might be used to achieve these objectives [1]-[3]. Because of random character of the errors, a number of simulation scenarios has been created to evaluate the performance of the model. The prepared sample test cases take into account the accuracy of acquired data for calibration, the amount of data available in the batch, and the predicted magnitude of geometric error tolerances. Variant of least-squares algorithm as employed as a workhorse for computations to facilitate comparisons. A series of numerical results confirmed the usefulness of the proposed methodologies in the above-mentioned aspects for a broad range of sampled points taken from the workspace of a gimbal system. Partial simulation-based results are depicted in Fig. 1, where a normalized kinematic error is provided for two test cases: before and after kinematic calibration. The plot demonstrates that the devised corrections yield a reduction of the normalized errors with respect to the ideal kinematic model of a gimbal system for a broad range of joint angles sampled from the workspace.

Acknowledgment: This work has been supported and financed by National Science Center under grant No. 2018/29/B/ST8/00374.

References

- [1] Calafiore G., Indri M., Bona B. : Robot Dynamic Calibration: Optimal Excitation Trajectories and Experimental Parameter Estimation. *Journal of Robotic Systems* (2001), 55-68.
- [2] Bo Wang, Qian Ren, Zhihong Deng, Mengyin Fu. A self-Calibration Method for Nonorthogonal Angles Between Gimbals of Rotational Inertial Navigation System. *IEEE Transactions on Industrial Electronics* (Volume: 62, Issue: 4, April 2015)
- [3] Zhihong Hiang, Weigang Zhou, Hui Li, Yang Mo, Wencheng Ni, Qiang Huang: A new kind of accurate calibration method for robotic kinematic parameters based on the extended Kalman and particle filter algorithm: *IEEE Transactions On Industrial Electronics*, VOL. 65, NO. 4, APRIL 2018

-STA-

**STABILITY OF
DYNAMICAL SYSTEMS**

Analysis of the influence of tyre cross-sectional parameters on the stability of a nonlinear bicycle model with elliptic toroidal wheels

A.G. AGÚNDEZ^{1*}, D. GARCÍA-VALLEJO¹, E. FREIRE²

1. Department of Mechanical Engineering and Manufacturing, Universidad de Sevilla.
2. Department of Applied Mathematics II, Universidad de Sevilla.

* Presenting Author

Abstract: In this work, the stability of a bicycle with elliptic toroidal wheels is analysed in detail. The influence of the tyre cross-sectional parameters on the stability range of the rectilinear motion with constant speed is studied. The bicycle multibody model is based on a well-acknowledged bicycle benchmark, which has been extensively used both for theoretical and experimental works. The nonlinear equations of motion, which correspond to a differential-algebraic system of equations, are derived and linearized along the forward upright motion, allowing the expression of the resulting Jacobian matrix as function of the tyre cross-sectional parameters. With this, a sensitivity analysis of the eigenvalues with respect to the geometric parameters of the wheels is performed. The velocity range for which the bicycle is stable in the rectilinear motion with constant velocity is obtained for different scenarios, and the influence of the elliptic section of the toroidal wheel is illustrated with various stability regions.

Keywords: stability, multibody, sensitivity analysis, bicycle benchmark, toroidal wheel

1. Introduction

The stability of bicycles has been widely studied over the years. Meijaard et al. [1] proposed a detailed benchmark bicycle model, whose linear stability along straight and circular motions with constant velocity was thoroughly analysed in Refs. [2]-[4]. In this work, the wheels of the bicycle benchmark are modelled as two elliptic tori instead of hoop-shaped wheels. The results show that the tyre cross-sectional parameters have significant influence on the stability of the forward upright motion.

2. Methodology

The equations of motion of the bicycle multibody model, with holonomic and nonholonomic constraints, constitute a nonlinear index-3 differential-algebraic system of equations [4]. The wheels of the bicycle, which are assumed to roll without slipping, are modelled as two tori of major and minor radii ρ_i and a_i , see Fig. 1 (b). The cross-sections of the wheels are elliptic (see Fig. 1), being a_i and b_i the semi-major and minor axes of the elliptic wheel cross-section, respectively. The elliptic profile r_i , in polar form relative to its centre, is given by:

$$r_i(\eta_i) = \frac{a_i b_i}{\sqrt{(b_i \cos(\eta_i))^2 + (a_i \sin(\eta_i))^2}} \quad (1)$$

where η_i is the angular coordinate, measured from the major axis. The geometry of the tyre is defined by the nondimensional parameters $\mu = \frac{a_i}{\rho_i}$ and $\sigma = \frac{b_i}{a_i}$.

On Fractional Viscosity and Material Instability

PETER B. BÉDA^{1*}

1. Budapest University of Technology and Economics, Műgyetem rkp. 1–3. H-1111 Budapest, Hungary
[0000-0002-9845-8137]

* Presenting Author

Abstract: Constitutive equations of materials are the key elements in material instability problems. Such equation may include fractional derivatives to describe well known material behaviours as creep and relaxation. Stability investigation can be performed as usually in the theory of dynamical systems. For this reason a dynamical system should be formed from the basic equations describing the motion of a solid body. This system of equations consists of the equations of motion, (Cauchy’s first and second equations) the kinematic equation and the constitutive equation itself. A state of the material can be identified as a steady state solution of that dynamical system. Then periodic perturbations are added to that solution and stability and bifurcation analysis of it leads to conditions on the material constants of the constitutive equation. Stability and bifurcation behaviour should exhibit generic nature to have a physically acceptable mathematical description. The main question to answer is: how the presence of fractional derivatives in constitutive equations effects the possible forms of constitutive equations.

Keywords: fractional derivative, material instability, rate-dependence

1. Introduction

There are several instability phenomena appearing in material tests like flutter or shear-banding and they should be recognised as solutions of the system of equations describing the motion of a material body. Stability analysis is quite obvious by using dynamical systems theory and it presents a clear classification for the types of unstable behaviours. Unfortunately, such classification is impossible for rate-independent materials. Rate effects could be derived from the presence of viscosity. In a physical point of view, viscosity is deduced from material memory effects. Such way was followed by Rabotnov [1] in studying creep and relaxation phenomena of solid mechanics. By taking experimental results into account, his approach leads to hereditary mechanics with fractional order integral operators. Since then, several studies have dealt with the connection between hereditary approach and rate dependence and proved the equivalence [2], [3], when “fractional order rate” is used. Thus Bagley’s viscoelastic material model [4] is a direct consequence of the unity of creep and relaxation phenomena and of experimental data.

2. Stability and Bifurcation Analysis

The classical description of continuum mechanics consists of three groups of equations, such as Cauchy’s first and second equations of motion, the kinematic equation and the constitutive equation. The simplest possible case is a uniaxial problem with small deformations. Then such equations are

$$\rho \dot{v} = \frac{\partial \sigma}{\partial x}, \quad \dot{\epsilon} = \frac{\partial v}{\partial x} \quad (1)$$

and the constitutive equation $F(\varepsilon, \sigma, \dot{\varepsilon}, \dot{\sigma}, \dots) = 0$. When Bagley's model is used, the constitutive equation could be in form

$$b_0 \sigma = a_0 \varepsilon + a_1 D^\alpha \varepsilon, \tag{2}$$

where

$$D^\alpha f(t) = \frac{1}{\Gamma(1-\alpha)} \frac{d}{dt} \int_0^t f(\xi) (t - \xi)^{-\alpha} d\xi$$

denotes Riemann-Liouville's derivative [5]. Then equations (1), (2) and (3) should be transformed into velocity field \mathbf{v} and the stability of the steady state solution \mathbf{v}_0 of dynamical system

$$b_0 \rho \ddot{\mathbf{v}} - (a_0 + a_1 D^\alpha) \frac{\partial^2 \mathbf{v}}{\partial x^2} = 0 \tag{3}$$

should be studied. By using harmonic perturbations

$$\tilde{\mathbf{v}} = \tilde{\mathbf{v}}_0 v_t(t) \exp(\omega x)$$

of \mathbf{v}_0 , solutions λ_i of the characteristic equation of (3) should be calculated.

The locations of λ_i in the complex plane decide on stability. State \mathbf{v}_0 of the material is stable, when all eigenvalues λ_i have arguments less than $\pm \frac{\pi\alpha}{2}$. By changing the load on the specimen, material parameters a_0, a_1, b_0 may be varied and its effect on λ_i may cause loss of stability. It could be either a static or a dynamic bifurcation. In such a way, conditions can be found for material parameters. Such conditions include the order of the derivative α as an additional material constant.

When $a_1 \equiv 0$ in constitutive equation (3), a co-existent static and dynamic bifurcation should happen, which is highly non-generic. Such model is inappropriate for material instability analysis. Otherwise, regions of stable and unstable behaviours, static and dynamic bifurcation conditions can be identified in the space of material parameters.

3. Concluding Remarks

Fractional derivatives appear in the constitutive equations as a direct consequence of creep and relaxation phenomena. Material instability can be investigated by defining a fractional order dynamical system from the system of basic equations of solids.

References

1. RABOTNOV YU, N: Equilibrium of an Elastic Medium with After-effect (in Russian). *Prikladnaya Matematika i Mekhanika (J. Appl. Math. Mech.)* 1948, **12**:53-62.
2. ROSSIKHIN Y. A, SHITIKOVA M. V: Application of Fractional Calculus for Dynamic Problems of Solid Mechanics: Novel Trends and Recent Results. *ASME Appl Mech Rev.* 2010, **63**:010801
3. KOELLER R. C: Applications of Fractional Calculus to the Theory of Viscoelasticity. *Journal of Applied Mechanics* 1984, **51**(2):299-307.
4. BAGLEY R. L: *Applications of Generalized Derivatives to Viscoelasticity*. Dissertation, USA Air Force Institute of Technology, 1979.
5. PODLUBNY I: *Fractional Differential Equations*. Academic Press: San Diego, 1999.
6. RABOTNOV YU, N: Equilibrium of an Elastic Medium with After-effect (in Russian). *Prikladnaya Matematika i Mekhanika (J. Appl. Math. Mech.)* 1948, **12**:53-62.

On the Stability of Sampled-Data Systems with Dry Friction

CSABA BUDAI

Department of Mechatronics, Optics and Mechanical Engineering Informatics, Budapest University of Technology and Economics, Budapest, Hungary [0000-0003-3749-8394]

Abstract: This paper focuses on the stabilization effect of dry friction in sample-data systems that use discrete-time state-feedback in position control applications. The results are presented through the example of a single-degree-of-freedom effective system model. This paper shows that in these systems, the destabilizing effect of sampling can still be compensated to some extent by the presence of dry friction resulted in an unstable limit cycle. The domain of attraction of the zero reference position as the fixed point is also presented in this paper.

Keywords: sampled-data nature, dry friction, concave envelope, negative viscous damping

1. Introduction

One of the fundamental tasks of mechatronics is position control. In these systems, the main aim of the applied controller is to drive the system into the desired position, which is typically achieved by state feedback. In the analysis of these systems, the effect of friction is often neglected due to the application of a suitable friction compensation algorithm [1] or because it results in a conservative stability condition. It is also a common practice to neglect the effect of sampling and quantization. Although these simplifications can be reasonable from the engineering point of view, explaining some intricate vibration phenomena requires the handling of more accurate system models. For example, the effect quantization may lead to chaotic motions even at high sampling rates [2], the effect of sampling can result in multi-frequency vibration even in the case of a single-degree-of-freedom system model [3], or the sampled-data systems can have special concave envelope vibrations when only dry friction stabilizes the motion [4].

2. Effective system model with dry friction

To illustrate the stabilization effect of dry friction, a single-degree-of-freedom mechanical system is considered where discrete-time state feedback with zero-order-hold signal recognition is used to drive the system into the zero reference position. The resulting governing equation of motion is

$$m\ddot{x}(t) + f_c \operatorname{sgn}(\dot{x}(t)) = -k_p x_j \quad \text{with } t \in [t_j, t_j + \tau), \quad (1)$$

where $\mathbf{x}(t)$ is the generalized coordinate as a function of time t , m is the generalized mass that takes

its meaning based on the definition of \mathbf{x} , and f_c denotes the magnitude of dry friction force. The

control gain is k_p , and $t_j = j\tau$ with $j \in \mathbb{Z}$ is the j th sampling instant, where τ is the sampling time. In order to analyse the dynamic behaviour of the system, Eq. (1) can be solved for the discrete state

variables $\mathbf{x}_j = [\mathbf{x}_j \quad \mathbf{v}_j]^T$, where $\mathbf{x}_j = \mathbf{x}(t_j)$ and $\mathbf{v}_j = \dot{\mathbf{x}}(t_j)$ represents the sampled position and velocity at the beginning of the j th time interval, in the form of a non-homogeneous map $\mathbf{x}_{j+1} = \mathbf{A}\mathbf{x}_j - \mathbf{a} \operatorname{sgn}(\dot{\mathbf{x}}(t))$, which is valid between velocity reversals.

Effective continuous-time system model with friction

First, the case is investigated when the effect of dry friction is neglected. The corresponding results serve as a reference to examine the effect of friction. The dynamic behaviour of the frictionless system is represented by the roots $\mathbf{z}_{1,2}$ of the characteristic equation of matrix \mathbf{A} . When the parameter

$p = k_p \tau^2 / m$ is in the range $0 < p < 16$, then the characteristic roots are complex with non-zero imaginary part, i.e., $\mathbf{z}_{1,2} = \rho \exp(\pm i\theta)$. It results that the magnitude ρ of $\mathbf{z}_{1,2}$ is in the range

$1 < \rho < 3$, which means that the frictionless system has unstable oscillations around the reference position. By neglecting the higher harmonics due to sampling, the motion can be characterized by a damped oscillator with negative viscous damping term to model the unstable behaviour. The resulted in the effective continuous-time model is

$$\ddot{x}(t) + f_0 \omega_n^2 \operatorname{sgn}(\dot{x}(t)) = -\omega_n^2 x(t) + 2\zeta \omega_n \dot{x}(t), \tag{2}$$

where $f_0 = f_c / k_p$, the undamped natural angular frequency ω_n , and the damping ratio ζ . For further details, the reader is referred to [3] and [4].

Stability in the presence of friction

First, the solution of the effective continuous-time model in Eq. (2) is needed. Assuming that the initial conditions are $x_0 > 0$ and $v_0 = 0$, the motion takes place with negative velocity. With these, the solution $x^-(t)$ can be determined until the first velocity reversal, which happens at $t = \pi / \omega_d$. If there is a periodic solution, the condition $x^-(\pi / \omega_d) = -x_0$ has to be satisfied resulted in the critical initial position as

$$x_0^* = f_0 \coth\left(\frac{\zeta \omega_n \pi}{\omega_d}\right) \text{ with } \omega_d = \omega_n \sqrt{1 - \zeta^2}. \tag{3}$$

In the case of non-zero initial velocity with arbitrary initial position, the solution of Eq. (2) is $x^+(t)$. Based on $x^+(t)$, the elapsed time for the first vibration peak can be determined as

$$t^\cap = \frac{1}{\omega_d} \operatorname{atan}\left(\frac{x_0 + f_0 + \zeta v_0}{v_0 \sqrt{1 - \zeta^2}}\right). \tag{4}$$

If the time t^\cap is substituted back to $x^+(t)$, the first maximum position is $x^\cap = x^+(t^\cap)$. Finally, if the condition $x_0^* = x^\cap$ holds, there is also a periodic solution.

3. Concluding Remarks

In this paper, the main characteristics of sampled-data systems were investigated by considering dry friction as the primary source of physical dissipation. For the analysis of the sampled-data system with dry friction, an effective continuous-time model was derived. It was also shown when the effect

of dry friction is also taken into account, the system can become sensitive to the initial conditions, and a limit cycle develops around the desired position.

Acknowledgment: The research reported in this paper was supported by the National Research, Development and Innovation Office of Hungary under Grant No. PD 128398.

References

- [1] ARMSTRONG-HÉLOUVRY B, DUPONT P, CANUDAS DE WIT C: A survey of models, analysis tools and compensation methods for the control of machines with friction. *Automatica* 1994, **30**(7):1083-1138.
- [2] CSERNAK G, STEPAN G: Digital control as source of chaotic behavior. *International Journal of Bifurcation and Chaos* 2010, **20**(5):1365-1378.
- [3] BUDAI C, KOVACS, L. L, KOVECSES, J, STEPAN, G: Effect of dry friction on vibrations of sampled-data mechatronic systems. *Nonlinear Dynamics* 2017, **88**(1):349–361.
- [4] BUDAI C, KOVACS, L. L, KOVECSES, J, STEPAN, G: Combined effects of sampling and dry friction on position control. *Nonlinear Dynamics* 2019, **98**:3001-3007.

Stability analysis of mobile crane during load sway induced by wind

DAWID CEKUS¹, PAWEŁ KWIATON^{2*}

1. Department of Mechanics and Machine Design Fundamentals, Czestochowa University of Technology, 42-201 Czestochowa, Poland, cekus@imipkm.pcz.pl [0000-0002-5551-1153]
2. Department of Mechanics and Machine Design Fundamentals, Czestochowa University of Technology, 42-201 Czestochowa, Poland, kwiaton@imipkm.pcz.pl [0000-0002-0067-0384]

* Presenting Author

Abstract: The paper presents an analysis of the stability of a mobile crane during the process of transporting a load affected by wind force. The load was treated as a rigid body suspended on a deformable rope. The obtained results of numerical simulations were compared with the case where the load is modelled as a material point and the case where the rope system was rigid. The surface area of a rigid body loaded by the wind was assumed to be variable. The analysis was carried out for several cases differing in the operation time of the control functions, as well as a wind direction and its speed. The initial problem of motion was calculated using the Runge-Kutta fourth-order method.

Keywords: crane stability, dynamics, load sway

1. Introduction

The process of load transporting using mobile cranes should take place with appropriate safety conditions for people and other devices. Due to the high centre of mass, small spacing of support system, or the effect of wind pressure, mobile cranes are exposed to the risk of stability loss [1]. The stability parameter is closely related to the definitions such as overturning contour (or edge), stabilizing torque (M_u) and overturning torque (M_w) [2]. The crane remains in permanent equilibrium (is stable), when at each stage of the duty cycle, the value of stabilizing torque is greater than the value of the overturning torque [1]:

$$M_U > M_w . \quad (1)$$

In this work, the stability analysis of the Liebherr LTM 1030-2.1 mobile crane was carried out, taking into account the wind pressure and deformability of the rope system. The proposed model allows to determine the influence of external forces on the crane's stability. In order to determine the stability of the crane during its working cycle, it was necessary to determine the centre of mass of the entire system and the overturning contour of the machine.

The position of the centre of mass of the system in the global coordinate system can be written in the form:

$$\mathbf{s}_c = \frac{1}{M} \sum_{i=1}^n m_i \mathbf{s}_i , \quad (2)$$

where: the total mass of the system M is a sum of individual masses m_i of the crane's components and \mathbf{s}_i is their centre of mass.

The motion of the load modelled as a rigid body can be presented as a combination of the translational motion of the load mass centre and a spherical motion around its centre of mass [3]. Taking into consideration the deformability of the rope system, the spherical motion of the load and the inter-

action of external forces in the model, a system of seven second-order differential equations can be obtained, which is presented in the form [4,5]:

$$\Lambda \ddot{\Omega} = \mathbf{E}, \tag{3}$$

where coefficients of matrix Λ and vector \mathbf{E} depend only on generalized coordinates and derivatives of a vector of unknowns accelerations $\ddot{\Omega}$.

Possess information about the position of the mass centre of load and all crane components, it is possible to determine the stability of the mobile crane.

2. Results and Discussion

During the simulation test, it was assumed that the crane's outrigger system is fully unfolded. In this case, the overturning contour is 6.305 x 6.000 meters. Various cases of numerical calculations were analysed differing in control functions time or wind velocity. The exemplary results of the numerical simulations as the trajectory of the centre of mass and the marked stages of loss of crane stability are shown in Figure 1.

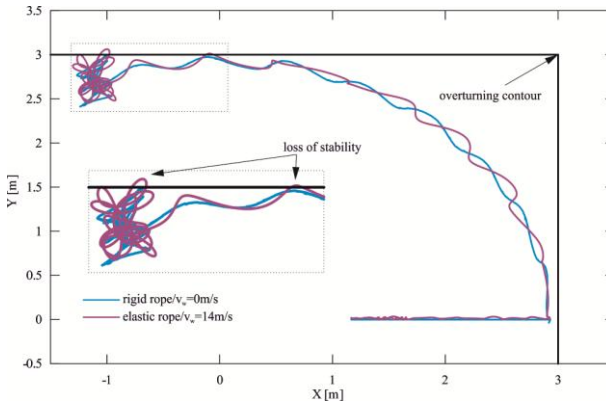


Fig. 1. Centre of the mass trajectory of the analysed system

The presented results showed the need to take into account in the theoretical model all the important parameters (interaction of external forces, spherical motion of the body) for the analysed system of crane operation.

References

- [1] KACALAK W., BUDNIAK Z., MAJEWSKI M: Simulation model of a mobile crane with ensuring its stability, *Modelling in Engineering* 2016, **29**(60):35-43 (in Polish).
- [2] KACALAK W., BUDNIAK Z., MAJEWSKI M: Stability assessment as a criterion of stabilization of the movement trajectory of mobile crane working elements, *International Journal of Applied Mechanics and Engineering* 2018, **23**(1):65-77.
- [3] CEKUS D., KWIATON P: Effect of the rope system deformation on the working cycle of the mobile crane during interaction of wind pressure, *Mechanism and Machine Theory* 2020, **153**:104011.
- [4] CEKUS D., KWIATON P., GEISLER T: The dynamic analysis of load motion during the interaction of wind pressure, *Meccanica* 2021, **56**:785-796.
- [5] CEKUS D., KWIATON P: Method of determining the effective surface area of a rigid body under wind disturbances, *Archive of Applied Mechanics* 2021, **91**:1-14.

Numerical Modelling of the Experimental Based High Frequency Subsonic Stall Flutter in Linear Blade Cascade

SONY CHINDADA^{1*}, PAVEL SNABL², PAVEL PROCHAZKA³, CHANDRA SHEKHAR PRASAD⁴,
LUDEK PESEK⁵

1. Institute of Thermomechanics, Czech Academy of Sciences, Prague, Czech Republic, chindada@it.cas.cz [0000-0003-3481-7361]
2. Institute of Thermomechanics, Czech Academy of Sciences, Prague, Czech Republic, snabl@it.cas.cz [0001-6168-0044]
3. Institute of Thermomechanics, Czech Academy of Sciences, Prague, Czech Republic, prochap@it.cas.cz [0000-0002-9150-3302]
4. Institute of Thermomechanics, Czech Academy of Sciences, Prague, Czech Republic, cprasad@it.cas.cz [0000-0002-3087-5807]
5. Institute of Thermomechanics, Czech Academy of Sciences, Prague, Czech Republic, pesek@it.cas.cz [0000-0003-0940-6771]

* Presenting Author

Abstract: Stall flutter in large steam turbine blades is one of the major challenge in the operation safety of turbomachinery. Stall flutter triggers due to complete or partial separation of flow from the blade surfaces when the angles of attack are relatively high, especially in low pressure stages. For the design and development of modern turbomachines prediction of subsonic stall flutter is essential. Numerical simulations are preferred over physical model for stall flutter analysis to save both time and cost. This paper deals with the numerical modelling of the five blade cascade with different flow variables to analyse subsonic stall flutter. Furthermore, in this numerical study various factors dominating the stall flutter phenomenon will be carried out in detail. The numerically estimated stability parameters will be validated against the experimental data obtained from five blade cascade experimental model.

Keywords: Subsonic stall flutter, low pressure, steam turbines, cascade, turbomachines.

Parametrically Excited Rotating Shafts on Gas Foil Bearings

EMMANOUIL DIMOU^{1*}, ATHANASIOS CHASALEVRIS², FADI DOHNAL³

1. National Technical University of Athens

2. National Technical University of Athens [0000-0002-6891-439X]

3. UMIT - Private University for Health Sciences, Medical Informatics and Technology [0000-0002-9289-4069]

* Presenting Author

Abstract: The possibility of applying parametric excitation in a flexible rotating shaft utilizing controllable-adjustable gas foil bearings is investigated in this paper. The gas foil bearings are investigated on introducing periodic variation of impedance gas forces through a theoretical and simplistic concept of time periodic variation of nominal clearance between top foil and rotor surface. The embedded excitation mechanism is not discussed in this paper. The potential to introduce parametric anti-resonance and modal interaction and extend the threshold speed of instability (Hopf bifurcation) at higher speeds is of major interest in this work. Collocation method is implemented for the evaluation of limit cycles of the parametrically excited system (periodically forced), and the stability of motion is assessed for the various frequencies of excitation through Floquet multipliers. Continuation method is applied for the computation of limit cycles of motion and the respective stability as the parameter of excitation frequency changes (bifurcation parameter). It is found that the parametrically excited system may operate in stable trajectories in higher rotating speeds than the reference system without excitation. Various rotor-bearing designs are investigated with respect to key design parameters (rotor slenderness, bearing geometry, bump foil stiffness and damping).

Keywords: parametric excitation, gas foil bearings, continuation and stability of limit cycles

1. Introduction

Parametric excitation has been investigated on its potential to introduce anti-resonance and modal interaction, extending the stability margins of mechanical structures [1-2]. Recently, oil bearings with adjustable geometry were utilized to apply parametric excitation in rotors through time-periodic variation of the journal bearing's radial clearance [3-4].

The motivation of this work lies on the rising need for oil-free rotor-bearing systems, with gas foil bearings to have vital role [5-6]. The potential to utilize the principle of parametric excitation in such system is checked in this paper in preliminary stage through simplistic assumptions for rotor geometry (flexible rotor carrying three masses) and simplistic gas-foil-bearing model with linear bump foil stiffness and damping [7], applied through a theoretical change in nominal clearance. The change in nominal clearance can be achieved using piezo-actuators [8] and the implementation is left for future investigations. The work aims primarily to detect the sensitivity of resulting gas forces when nominal bearing clearance varies by 0-50%. The corresponding limit cycle motions of a balanced rotor (still non-autonomous due to parametric excitation) are investigated for stability after computed through collocation scheme. A code for pseudo-arc-length continuation of limit cycles is programmed to evaluate the solution branches and the respective stability of the system as the parameter of excitation frequency changes.

2. Results and Discussion

A two-segment rotating shaft mounted on two gas foil bearings and carrying three lumped masses is modelled with FEM. The equations of motion are written for the 12 DOFs with gyroscopic coupling to be considered. Gas foil bearings follow the modelling in [7] and further physical coordinates are introduced defining the deformation of the top foil at each bearing. The state space representation of the motion equations renders the state vector \mathbf{x} including physical coordinates and gas pressure distribution at each bearing. The non-autonomous (periodically forced) dynamic system is defined in Eq. (1) where Ω_{ex} is the excitation frequency of each top foil (equal for both bearings), acting as primary bifurcation parameter. The dynamic system is converted to autonomous by adding to the equations of motion a nonlinear oscillator with the desired periodic forcing as one of its solution components.

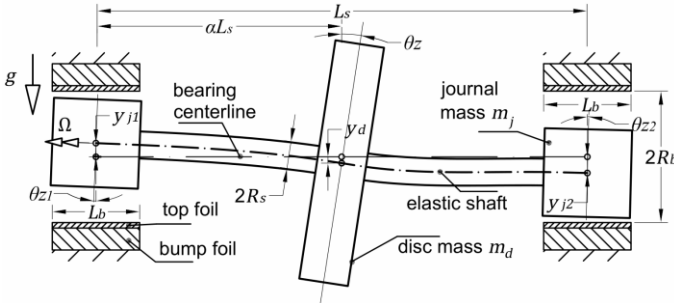


Fig. 1. Flexible rotor supported by two gas foil bearings.

$$\dot{\mathbf{x}} = \mathbf{f}(\mathbf{x}, \Omega_{ex}, t) \quad (1)$$

Results include limit cycles of motion in regards to Ω_{ex} for various key design characteristics of the system. Stability and bifurcations of equilibriums (fixed points) and of limit cycles are investigated at the cases of parametric resonances for certain Ω_{ex} .

References

- [1] DOHNAL F: Optimal dynamic stabilisation of a linear system by periodic stiffness excitation. *Journal of Sound and Vibration* 2009, **320**:777-792.
- [2] BREUNUNG T, DOHNAL F, PFAU B: An approach to account for interfering parametric resonances and anti-resonances applied to examples from rotor dynamics. *Nonlinear Dynamics* 2019, **97**:1837-1851.
- [3] CHASALEVRIS A, DOHNAL F: Improving Stability and Operation of Turbine Rotors Using Adjustable Journal Bearings. *Tribology International* 2016, **104**:369-382.
- [4] BECKER K, SEEMANN W: Stability investigations of an elastic rotor supported by actively deformed journal bearings considering the associated spectral system. *17th International Symposium on Transport Phenomena and Dynamics in Rotating Machinery ISROMAC 2017*, Hawaii US
- [5] BAUM C, HETZLER H, SCHROEDER S, LEISTER T, SEEMANN W: A Computationally Efficient Nonlinear Foil Air Bearing Model for Fully Coupled, Transient Rotor Dynamic Investigations. *Tribology International* 2021, **153**:106434.
- [6] LARSEN J, SANTOS I: On the Nonlinear Steady-State Response of Rigid Rotors Supported by Air Foil Bearings-Theory and Experiments. *Journal of Sound and Vibration* 2015, **346**:284-297.
- [7] BHOORE S, DARPE A: Nonlinear dynamics of Flexible Rotor Supported on the Gas Foil Journal Bearings. *Journal of Sound and Vibration* 2013, **332**:5135-5150.
- [8] FENG K, GUAN H, ZHAO Z, LIU T: Active bump-type foil bearing with controllable mechanical preloads. *Tribology International* 2018, **120**:187-202.

Lyapunov Functions by interpolating numerical quadratures: Proof of Convergence

PETER GIESL¹, SIGURDUR FREYR HAFSTEIN^{2*}

1. Department of Mathematics, University of Sussex, Falmer, BN1 9QH, UK [0000-0003-1421-6980]

2. Science Institute, University of Iceland, Dunhagi 3, 107 Reykjavik, Iceland [0000-0003-0073-2765]

* Presenting Author

Abstract: We consider methods to compute Lyapunov functions for nonlinear systems. We prove that the combination of a fast, but non-rigorous method, with a slow, but rigorous, method results in a fast and rigorous method. Further, we show that our combined always succeeds in generating a Lyapunov functions for a system with an exponentially stable equilibrium.

Keywords: Lyapunov function, numerical method, nonlinear system

1. Introduction

Lyapunov functions are an essential tool in the study of the qualitative behaviour of dynamical systems. They give information on attractors, repellers and basins of attraction without the knowledge of the solution to a system, whose dynamics are given by an ODE or an iteration; in particular they can be used to assert the stability of an equilibrium and give a rigid lower bound on its basin of attraction. The analytic computation of a Lyapunov function for a nonlinear system is a very hard problem and in general not feasible. Therefore, numerous numerical methods have been suggested. In the CPA method continuous and piece-wise affine Lyapunov functions are parameterised using feasible solutions to a linear programming problem [1] and one can show that this method always succeeds in generating a Lyapunov function for a system with an exponentially stable equilibrium [2]. Another approach is to generate values of the target Lyapunov function and then verify the constraints of the linear programming problem [3,4]. In the paper associated to this abstract we prove that this approach will always succeed in generate a Lyapunov function for a system with an exponentially stable equilibrium, i.e. we show the convergence of this technique.

2. Results and Discussion

We show that one can generate adequate values for a Lyapunov function using integral formulas in the case of time-continuous systems (ODEs) and summation formulas in the case of time-discrete systems. These values will fulfil the constraints of the linear programming problem and can therefore be interpolated over the whole domain to deliver a true Lyapunov function for the system. As an example, see Figure 1, where this methodology was used to generate a Lyapunov function for the van der Pol system. Note that it is orders of magnitude more efficient to generate the values using an integral- or summation formula and verify the constraints, than to solve the linear programming problem.

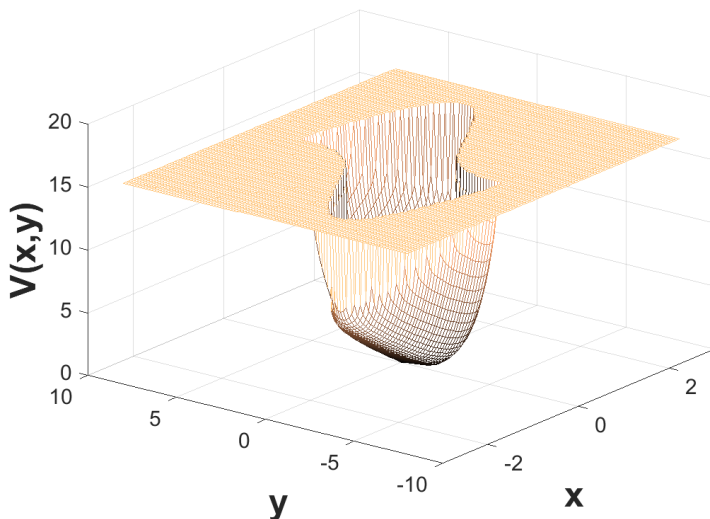


Fig. 1. Lyapunov function for the van der Pol system

3. Concluding Remarks

We lay the theoretical foundation for combining two methods for the generation of Lyapunov functions for nonlinear systems, either given by an ODE (continuous-time) or an iteration (discrete-time). The combined method inherits the numerical efficiency of the fast, but non-rigorous method, that evaluates numerically quadratures of numerically integrated solutions (continuous-time) or sums (discrete-time) and the rigorosity of the slower method solving linear programming problems.

References

- [1] S.F. MARINOSON: Lyapunov function construction for ordinary differential equations with linear programming. *Dynamical Systems: An International Journal* 17 (2002), pp. 137-150.
- [2] P. GIESL AND S.F. HAFSTEIN: Revised CPA method to compute Lyapunov functions for nonlinear systems. *Journal of Mathematical Analysis and Applications*, 410, (2014), pp. 292-306.
- [3] J. BJÖRNSSON, P. GIESL, S.F. HAFSTEIN, AND C.M. KELLETT: Computation of Lyapunov functions for systems with multiple local attractors. *Discrete and Continuous Dynamical Systems - Series A*, 35-9, (2015), pp. 4019-4039.
- [4] H. LI, S. HAFSTEIN, AND C. KELLETT: Computation of Lyapunov Functions for Discrete-Time Systems using the Yoshizawa construction. In: *Proceedings of the 53rd IEEE Conference on Decision and Control (CDC), Los Angeles, CA, USA, 2014*, pp. 5512-5517.

Nonlinear Dynamics of Atomic Systems in a Free State and in an External Electromagnetic Field: Chaos and Attractors

ALEXANDER V GLUSHKOV¹, ANNA A KUZNETSOVA², EVGENIYA K PLISETSKAYA^{1*},
OLEKSII L MYKHAILOV¹ AND EUGENY V. TERNOVSKY¹

1. Odessa State Environmental University, Mathematics Depr., L'vovskaya str. 15, 65009, Odessa

2. National University "Odessa Maritime Academy", Didrikhson str. 8, 65001, Odessa

* Presenting Author

Abstract: The fundamentals of a novel mathematical approach to studying deterministic chaos and strange attractors in dynamics of nonlinear processes in atomic and molecular systems in an electromagnetic field. The new quantum-dynamic models (based on the finite-difference solution of the Schrödinger equation, optimized operator perturbation theory and realistic model potential for quantum systems) and advanced nonlinear analysis and a chaos theory methods (power spectrum analysis, spectral algorithms, the correlation integral algorithm, the fractal method, the Lyapunov's exponents and Kolmogorov entropy analysis etc) are realized in order to provide a correct treatment a chaotic dynamics of atomic systems (the features of spectra and field provided chaotic ones). Availability of multiple resonances (autoionization or field provided stark Zeeman type ones) with super little widths in spectrum of an atomic system in external field is treated and provided by interference phenomena and fluctuations. Dynamics of resonances in atomic spectra is studied and the topological and dynamical invariants are calculated.

Keywords: dynamics of atomic systems, spectral features, chaos and attractors

1. Introduction. Quantum-Dynamic and Chaos-Geometric Approaches to Atomic System Dynamics

An analysis of the chaotic phenomena in quantum systems was carried out not only based on the methods of classical mechanics (in fact, within the framework of the Newtonian dynamics), but also on the basis of semiclassical or semi-quantum methods, in particular, the method of quantum trajectories (quantization of classical mechanics), and path integrals by Feynman-Higgs, the Gutzwiller's theory of "periodic orbits", the Delos closed orbit method, complex coordinate method, a random matrix theory, diagonalization methods and some others (e.g. [1,2]). New field of investigations of chaotic effects in theory of quantum systems has been provided by a great progress in a development of a chaos and dynamical systems theory methods. In this work we present a novel mathematical approach to studying deterministic chaos and strange attractors in dynamics of nonlinear processes in atomic and molecular systems in an electromagnetic field. The total scheme for studying chaos-dynamical phenomena in quantum systems (in particular, atomic systems in magnetic, crossed electric and magnetic fields, Rydberg atoms in a electromagnetic field, molecular systems in a infrared electromagnetic field etc) and computing the topological and dynamical invariants in application to quantum systems include the following [1-4]:

A) Quantum-dynamical computing of quantum systems: Schrödinger (Dirac) equation for quantum system in an external field (numerical solving, the finite differences, model potential, operator per-

turbation theory etc methods); Preliminary analysis and processing dynamical variable series of physical system;

B) Preliminary study and assessment of the presence of chaos: the Gottwald-Melbourne test; Fourier decompositions, irregular nature of change – chaos; Spectral analysis, Energy spectra statistics, the Wigner distribution, the spectrum of power, "Spectral rigidity";

C) The multi-fractal geometry: computation time delay τ using autocorrelation function or mutual information; Determining embedding dimension by the method of correlation dimension or algorithm of false nearest neighbouring points; Calculation of multi-fractal spectra; wavelet analysis;

D) Computing global Lyapunov's exponents, Kaplan-York dimension, Kolmogorov entropy, average predictability measure; Methods of nonlinear prediction (classical and quantum neural network algorithms, the algorithm optimized trajectories, stochastic propagators, memory functions etc...;

The key idea in the study of the spectra of chaotic systems and, in particular, quantum systems, is provided by the fact that a definition of quantum chaos is interpreted primarily as a property of a group of states of the spectra of the system. It is the interpretation of one of the mechanisms of quantum chaos through the induction of resonances in the spectrum of the system, their strong interaction with subsequent overlapping, the emergence of stochastic layers and further transition to a global stochasticity in the system.

2. Results and Concluding Remarks

Firstly, the results of the modelling a chaotic dynamics for the Rydberg alkali (Li, Rb, Cs, Fr in states with the principal quantum number $n \sim 31-100$, $m=0,1$) atoms in a static magnetic ($B = 4.5T$) and oscillating electric field with frequency $\omega=102M\Gamma$ ($\epsilon=-0.03$, $\varpi=0.32$, $\gamma=1/3$ in the range 35-50; $f=0.000-0.070$) are presented. Secondly, there are presented data on the resonances of Rydberg Li in the DC electric field $F = 2.1-2.5kV/cm$, Rb in the DC $F = 2.189- 6,416 kV/cm$, $n = 18-23$ and chaotic ionization dynamics of Rydberg Li, Rb, Yb (Li: $n = 41-70$; Rb: $n = 51-70$; Yb: $n = 60-80$) in a microwave field ($F = (1.2-3.2) 10^{-9}$ a.u.; $f = 8.87GHz, 36GHz$) with in a good agreement with available experimental data. Thirdly, for the first time to solve a class of problems related to the search for the phenomenon of quantum chaos in the spectra the new combined quantum and chaos-geometric approach (including analysis of level statistics and a group of new or improved methods of chaos theory) applied to an analysis of the spectra of heavy atomic systems (Yb, Tm, U). It is shown that the distribution of the parameter "nearest - level spacings" is close to the Vigner distribution. It has given a consistent theoretical interpretation to a phenomenon of a quantum chaos and described a strong nonlinear interaction of resonances with appearance of spectral stochastic layers with fusion.

References

- [1] GLUSHKOV A: *Relativistic quantum theory. Quantum Mechanics of Atomic Systems*. Astroprint: Odessa, 2008.
- [2] GLUSHKOV A, BUYADZHI V, KVASIKOVA A, IGNATENKO A, KUZNETSOVA A, PREPELITSA G AND TERNOVSKY V Nonlinear chaotic dynamics of Quantum systems: Molecules in an electromagnetic field and laser systems. In: TADJER A, PAVLOV R, MARUANI J, BRÄNDAS E, DELGADO-BARRIO G (EDS) *Quantum Systems in Physics, Chemistry, and Biology. Series: Progress in Theor. Chem. and Phys. Springer: Cham, 2017, 30:169-180.*
- [3] GLUSHKOV A AND KHETSELIUS O: Nonlinear Dynamics of Complex Neurophysiologic Systems within a Quantum-Chaos Geometric Approach. In: GLUSHKOV A, KHETSELIUS O, MARUANI J, BRÄNDAS E (EDS) *Advances in Methods and Applications of Quantum Systems in Chemistry, Physics, and Biology. Series: Progress in Theoretical Chemistry and Physics*. Springer: Cham, 2021, 33:291-303.
- [4] GLUSHKOV A, IGNATENKO A, KUZNETSOVA A, BUYADZHI A, MAKAROVA A AND TERNOVSKY E: Nonlinear dynamics of atomic and molecular systems in an electromagnetic field: Deterministic chaos and strange attractors. In: AWREJCWICZ J (Ed.) *Perspectives in Dynamical Systems II: Mathematical and Numerical Approaches*. Series: *Springer Proceedings in Mathematics & Statistics*. 2021, 363:Ch.11.

Influence of a cracked rod in the dynamic of a planar slider-crank mechanism

TOMÉ S.D.N. GUENKA¹, MARCELA R. MACHADO^{2*}

1. Department of Mechanical Engineering, University of Brasilia, 70910-900 Brasilia, Brazil [0000]

2. Department of Mechanical Engineering, University of Brasilia, 70910-900 Brasilia, Brazil [0000-0002-7488-7201]

* Presenting Author

Abstract: A simplified model of a slider-crank mechanism with a cracked rod is obtained through Lagrange's theory and used to demonstrate non-linearities on the dynamic response of all components caused by the presence of an open and non propagate crack. The open crack is modelled as a massless rigidity spring. To further evaluate the influence of crack presence, the influence of crack depth and position, torque and pressures force, the dynamic response of the damaged mechanism is validated and compared to the health system. Results show, for all cases, a significant difference in the kinematic and dynamic response of both healthy and damaged systems.

Keywords: Multibody Dynamics, Damage assessment, Dynamic response.

1. Introduction

Many researchers have investigated the dynamic response of multibody system and their dynamic characteristics through an analytical model, numerical, and experimentally. The slider-crank mechanism is present in many machineries in use in industry. Common defaults diagnosis in these mechanism are clearance[1], bearing ovalisation[2], and crack[3,4]. In general, those defaults can cause excessive wear, noise, impact dynamic load, and serious effect on the dynamic performances and stability.

This paper analyse of undamaged and damaged slider-crank mechanism and the impact of a crack in the dynamics response. It is also verified the effect of external forces in the mechanism dynamic. The results show that the crack influences the mechanical system dynamic performance and vibration characteristic by comparing the results between the slider-crank mechanism with crack and without crack, and external forces enhance it.

2. Numerical model and Discussion

The planar slider-crank mechanism ideal model has only one degree of freedom (dof) due to the constraints presented in the ideal joints. Therefore, the crack is modelled with a torsional spring located in a joint between two rods for the damaged mechanism. In this case, two or more degrees of freedom will be inserted between the components. Figure 1(a-b) shows the undamaged slider-crank mechanism one-dof composed of two rigid components l_1 and l_2 , with q_1 being the angular displacement of the crank. Figure 2 (a-b) shows the damaged slider-crank mechanism two-dof composed of three rigid components l_1 , l_2 and l_3 , with q_1 and q_2 as the angular displacements of the crank and the slider, respectively.

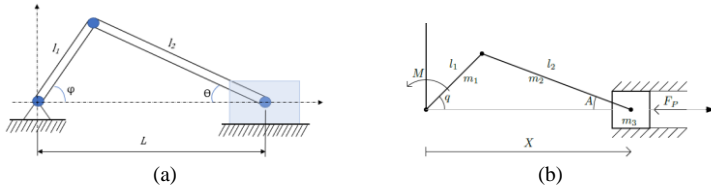


Fig. 1. Undamaged slider-crank mechanism(a) and its diagram representation (b).

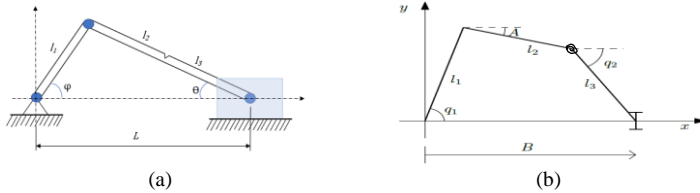


Fig. 2. Damaged slider-crank mechanism(a) and its diagram representation (b).

The governing equation for the one-dof slide-crank based on Lagrange approach and considering the pressure is expressed as

$$\frac{d}{dt} \left(\frac{\partial L}{\partial \dot{q}} \right) - \frac{\partial L}{\partial q} = Q^{nc} \quad (1)$$

where $T = \frac{1}{2} f(q) \dot{q}^2$, and

$$f(q) = I_{KO} + m_2(K_{X_2}^2 + K_{Y_2}^2) + I_2 K_A^2 + m_3 K_X^2. \quad (2)$$

$$\frac{df(q)}{dq} = 2[m_2 K_{X_2} L_{X_2} + m_2 K_{Y_2} L_{Y_2} + I_2 K_A L_A + m_3 K_X L_X].$$

And the equation of motion for the cracked slider-crank with two-dof is given as

$$([K_c]^T [M] [K_c]) \begin{Bmatrix} \ddot{q}_1 \\ \ddot{q}_2 \end{Bmatrix} + \left(\begin{bmatrix} \dot{q}_1 & -\dot{q}_2 \\ 0 & 2\dot{q}_1 \end{bmatrix} [N_1] + \begin{bmatrix} 2\dot{q}_2 & 0 \\ -\dot{q}_1 & \dot{q}_2 \end{bmatrix} [N_2] \right) \begin{Bmatrix} \dot{q}_1 \\ \dot{q}_2 \end{Bmatrix} + \frac{\partial V}{\partial \begin{Bmatrix} q_1 \\ q_2 \end{Bmatrix}} = \begin{Bmatrix} Q_1 \\ Q_2 \end{Bmatrix} \quad (3)$$

3. Final Remarks

This paper analyses the dynamic response of an undamaged and damaged planar slide-crank mechanism and the impact on the system. Aside from the enhance of the crack effect under externa forces

References

- [1] Dupac, M., Beale, D. G. Dynamic analysis of a flexible linkage mechanism with cracks and clearance. *Mechanism and Machine Theory*, 45(12), 1909–1923, 2010.
- [2] Daniel, G. B, Daniel, G. B. (2019). Influence of bearing ovalisation in the dynamic of a planar slider-crank mechanism. *Applied Mathematical Modelling*, 66, 175–194.
- [3] Cheng, S., Liu, S. Dynamic Analysis of Slider-Crank Mechanism with a Cracked Rod. *Mathematical Problems in Engineering*, 2018.
- [4] Dupac, M., Dan B. Marghitu. Nonlinear dynamics of a flexible mechanism with impact. *Journal of Sound and Vibration* 289, 952–966. (2006)

On the stability of a slip controlled two-axle vehicle with multiple time-delays

ÁDÁM HORVÁTH^{1*}, PÉTER BÉDA²

1. Budapest University of Technology and Economics, Budapest, Hungary [0000-0003-2806-3612]

2. Budapest University of Technology and Economics, Budapest, Hungary [0000-0002-9845-8137]

* Presenting Author

Abstract: In the present work, stability analysis of a two-wheeled vehicle is performed, with slip control applied to the wheels. The model contains two wheels equipped with dynamic brush tyre models and two digital PID torque controllers that affect the wheels through the brake system. Feedback delay of the control loops are considered; thus the mathematical model of the system contains delay differential equations. The stability charts are constructed, and bifurcations are analysed. Finally, simulation results of the nonlinear model is presented.

Keywords: time-delay, stability analysis, vehicle dynamics

1. Introduction

Nowadays, vehicle safety is one of the leading topics in industrial and scientific research. There are essential computer controller subsystems in our ground vehicles such as ABS or ESP, and the number of safety relevant vehicle dynamics control systems are growing year over year. Therefore, detailed modelling of the vehicle system is more and more important. In the presented work, stability analysis of a two wheeled vehicle is performed.

2. Models and Methods

Firstly, the mechanical model of the vehicle is introduced. The model consists of two wheels that are connected with a rigid rod. The wheels can be separated into two parts, a rolling rigid disk, and a tyre model that can describe the connection between the wheel and the road surface. Dynamical brush tyre model is used in the study, which is a continuum model containing small elastic bristle elements [1]. The equations of motion of the vehicle system can be read as

$$m\dot{V}(t) = F_{XF}(u_F(x, t)) + F_{XR}(u_R(x, t)), \quad (1)$$

$$J_{\{F,R\}}\dot{\Omega}_{\{F,R\}}(t) = T_{D\{F,R\}} - T_{B\{F,R\}}(t) - RF_{X\{F,R\}}(u_{\{F,R\}}(x, t)), \quad (2)$$

$$\dot{u}_{\{F,R\}}(x, t) = R\Omega_{\{F,R\}}(t) - V(t) + u'(x, t)R\Omega_{\{F,R\}}(t). \quad (3)$$

Here, V and $\Omega_{\{F,R\}}$ denote the longitudinal velocity of the vehicle and the angular velocity of the front and the rear wheels, respectively. $J_{\{F,R\}}$, m and $R_{\{F,R\}}$ are for the inertia of the wheels, the gross weight of the vehicle, and the dynamic radius of the wheels, respectively. The deformation function of the bristle elements of the tyre is $u(x, t)$, where x is the spatial coordinate of the contact segment between the tyre and the road surface. The force $F_{X\{F,R\}}$, that is generated by the contact, depends on the deformation function $u_{\{F,R\}}$. Equations (1) and (2) are ordinary differential equations, while (3) is a partial differential equation.

The driveline acts the wheel with driving torque T_D , while the brake system exerts with braking torque T_B . The brake system is in the focus of the present study. In the investigated scenario, the brake controllers actuate the brake system in order to influence the state of the wheels. There are two separate controllers in the model, one for the front, and one for the rear axle's wheel. Thus, the model contains two feedback loops, which are able to influence each other in a mechanical way through the rigid connection between the two wheels.

Last but not least, there are two important effects that should be considered in our model, first is the time-delay in the feedback loop, and the other is the effect of sampling. The formula of the delayed control signal can be written as

$$T_{B\{F,R\}}(t, \tau_{\{F,R\}}) = k_P e(t - \tau_{\{F,R\}}) + k_I \int_0^{t - \tau_{\{F,R\}}} e(T) dT + k_D \dot{e}(t - \tau_{\{F,R\}}), \quad (4)$$

where k_P, k_I, k_D are the controller gains, time-delay is denoted by τ , and e is the error signal. Time-delay and sampling are connected. Considering only constant time-delay, delay differential equations arise [2]. If sampling is taken into account, the delay transforms to a time-varying delay, and the mathematical model of the system contains periodic DDEs [3]. It is important to note, that different time-delays can be assumed for the two separate controllers.

Finally, the full delayed feedback loop with the mechanical model of the vehicle is treated in the research. After linearization, semi-discretization is applied, which we used to construct the mathematical model. With this approach, the continuous time mechanical model, and the discrete time controller can be handled, and stability analysis can be performed by calculating the characteristic multipliers of the resulting discrete difference equation which governs the full system.

Stability maps, and effect of changing of different system parameters on the stability maps are presented. As the system is of neutral type, if constant time delay is considered, boundaries can be found on the stability map, where multiple Hopf-bifurcations can occur. It is pointed out in the study, that in the sampled system, the number of these bifurcations is in connection with the delay. Finally, the results are compared with simulations of the nonlinear model.

Performance characteristics are investigated as well. Using simulations and a genetic algorithm, different optimizations are performed for various parameters.

Acknowledgment: This work was supported by the Pro Progressio Foundation.

References

- [1] PACEJKA H. B.: *Tire and Vehicle Dynamics (Third Edition)*. Butterworth-Heinemann: Oxford, 2012.
- [2] STÉPÁN G.: *Retarded Dynamical Systems*. Longman Scientific & Technical: Harlow, 1989.
- [3] INSPERGER T., STÉPÁN G.: *Semi-Discretization for Time-Delay Systems*. Springer-Verlag: New York, 2011.

Nonlinear Dynamics of Molecular Systems in an External Electromagnetic Field: Classical and Quantum Treatment of Chaos and Strange Attractors

ANNA V IGNATENKO¹, VALENTIN B. TERNOVSKY^{2*}, ANDREY A SVINARENKO¹,
AND YULIYA V DUBROVSKAYA¹

1. Odessa State Environmental University, Mathematics Depr., L'vovskaya str. 15, 65009, Odessa

2. National University "Odessa Maritime Academy", Didrikhson str. 8, 65001, Odessa

* Presenting Author

Abstract: An effective computational approach to studying nonlinear chaotic dynamics of the diatomic and multiatomic molecules) including complex spectra, deterministic chaos, strange attractors) in an external infrared electromagnetic field is presented. The approach includes combined quantum-mechanical model (based on the solution of the molecular Schrödinger equation, and realistic model potential method and advanced dynamical systems and non-linear analysis methods such as a spectral and multifractal algorithm, analysis on the basis of the Lyapunov's exponents and the Kolmogorov entropy etc. The polarization time series for a molecule in an infrared field are analyzed and computed. The results of computing the dynamical and topological invariants for dynamics of a number of the diatomic molecules (GeO, ZrO, PbO and others) in the infrared electromagnetic field with intensity of 25 GW/cm² are presented. The principally new result is in development of an effective non-linear prediction model for the polarization time series. It is shown that even though the simple procedure is used to construct the non-linear model, the predicted results for the polarization time series of the studied molecules are quite satisfactory.

Keywords: dynamics of atomic systems, spectral features, chaos and attractors

1. Introduction. Nonlinear Dynamics of Molecular Systems in Electromagnetic Field

At present time it is of a great interest a study of phenomenon of quantum chaos in complex molecular systems. This interest is provided by a whole number of important scientific and technical applications, including a necessity of understanding chaotic features in a work of different electronic devices and systems. New field of investigations of the nonlinear chaotic dynamics of molecular systems in an electromagnetic field has been provided by a great progress in a development of effective quantum mechanical methods as well as the further progressing a chaos theory and dynamic systems methods and algorithms. For example, a transition from regular motion to dynamical chaos for a diatomic molecule in a linearly (or circularly) polarized resonant electromagnetic field is connected with the overlapping of vibrational-rotational nonlinear resonances [1,2]. Studying the chaotic dynamics of molecular systems has shown that a chaos phenomenon may significantly affect the intramolecular vibrational energy redistribution, assigning the vibrational spectra, coherent control of the intramolecular processes and a dynamics of molecules interacting with a resonant electromagnetic field etc [2-4]. In this paper we present an effective computational approach to studying nonlinear chaotic dynamics of the diatomic and multiatomic molecules) including complex spectra, deterministic chaos, strange attractors) in an external infrared electromagnetic field is presented. The approach

includes combined quantum-mechanical model (based on the solution of the molecular Schrödinger equation, and realistic model potential method) and advanced dynamical systems and non-linear analysis methods such as a non-linear analysis methods including correlation (dimension D) integral, fractal analysis, average mutual information, false nearest neighbours, Lyapunov's exponents and Kolmogorov energy analysis, power spectrum and surrogate data algorithms, stochastic propagators method, memory and Green's functions approaches etc methods etc.

2. Model, Results and Concluding Remarks

A chaotic dynamics analysis for diatomic molecules in an intense electromagnetic field) is based on the numerical solution of the time-dependent Schrödinger equation and realistic model potential approximation $U(x)$ and, secondly, using the universal chaos-geometric approach to analysis of nonlinear chaotic dynamics (chaos-geometric unit). The problem is reduced to solving the Schrödinger equation [2,3]:

$$i\partial\Psi/\partial t = [H_0 + U(x) - d(x)E_M\varepsilon(t)\cos(\omega_L t)]\Psi \quad (1)$$

where E_M - the maximum field strength, $\varepsilon(t) = E_0\cos(\nu t)$ corresponds the pulse envelope. Molecule in the field gets induced polarization and its high-frequency component can be defined as [6]:

$$p_c^{(x,y)}(t) = \left(\frac{1}{T}\right) \oint (\psi(t) | \hat{d}_{x,y} | \psi(t)) \cos\omega t dt, \quad (2)$$

where T — period of the external field, d — dipole moment.

The test numerical computing the dynamics of the diatomic molecule GeO in the linearly polarized field (molecule and field parameters are as : $\hbar\Omega = 985.8 \text{ cm}^{-1}$, $y\hbar\Omega = 4.2 \text{ cm}^{-1}$, $B = 0.48 \text{ cm}^{-1}$, $d_0 = 3.28 \text{ D}$, $M = 13.1 \text{ a.e.m.}$; the intensity 2.5-25 GW/cm^2 , respectively: $W = 3.39\text{-}10.72 \text{ cm}^{-1}$) has been carried out and compared with earlier obtained results. According to classical-dynamical treating these parameters correspond to chaotic regime. The analysis shows that more than 200 vibrational-rotational molecular levels are involved into a chaotic dynamics. There are presented the calculated quantitative parameters for the GeO molecule chaotic dynamics in a linearly polarized field of the intensity 25 GW/cm^2 , namely, dynamical and topological invariants: correlation dimension (2.73), the embedding dimension (3), Kaplan-Yorke dimension (2.51), LE (first two LE are positive: $+0.146 + 0.0179$), Kolmogorov entropy (0.16) and others. The analogous data are listed for other studied molecules (PbO, ZrO etc).

References

- [1] GLUSHKOV A: *Relativistic quantum theory. Quantum Mechanics of Atomic Systems*. Astroprint: Odessa, 2008.
- [2] GLUSHKOV A, BUYADZHI V, KVASIKOVA A, IGNATENKO A, KUZNETSOVA A, PREPELITSA G AND TERNOVSKY V Nonlinear chaotic dynamics of Quantum systems: Molecules in an electromagnetic field and laser systems. In: TADJER A, PAVLOV R, MARUANI J, BRÁNDAS E, DELGADO-BARRIO G (EDS) *Quantum Systems in Physics, Chemistry, and Biology. Series: Progress in Theor. Chem. and Phys. Springer: Cham, 2017, 30:169-180.*
- [3] GLUSHKOV A, IGNATENKO A, KUZNETSOVA A, BUYADZHI A, MAKAROVA A AND TERNOVSKY E: Nonlinear dynamics of atomic and molecular systems in an electromagnetic field: Deterministic chaos and strange attractors. In: AWREJCIEWICZ J (Ed.) *Perspectives in Dynamical Systems II: Mathematical and Numerical Approaches*. Series: *Springer Proceedings in Mathematics & Statistics*. 2021, **363**:Ch.11.
- [4] MALINOVSKAYA S, GLUSHKOV A AND KHETSELIUS O: New laser-electron nuclear effects in the nuclear γ transition spectra in atomic and molecular systems. In: Wilson S, GROUT P, MARUANI J, DELGADO-BARRIO G, PIECUCH P (EDS) *Frontiers in Quantum Systems in Chemistry and Physics, Series: Progress in Theoretical Chemistry and Physics*. Springer: 2008, **18**:525-541.

Enhancing vibration mitigation in a jeffcott rotor with active magnet bearings through parametric excitation

ZACHARIAS KRAUS^{1*}, ARTEM KAREV¹, PETER HAGEDORN¹, FADI DOHNAL²

1. Technical University of Darmstadt, Dynamics and Vibrations Group, FNB, Dolivostraße 15, 64293 Darmstadt, Germany
 2. UMIT, Division for Mechatronics Lienz, Linker Iselweg 21, 9900 Lienz, Austria
- * Presenting Author

Abstract: In previous studies of linear rotary systems with active magnet bearings, parametric excitation was introduced as an open-loop control strategy. The parametric excitation was realised by a periodic, in-phase variation of the bearing stiffness. At the difference of two of the system's eigenfrequencies a stabilising effect, called anti-resonance [1], was found numerically, and validated in experiments. In this work preliminary results of a further exploration of the parametric excitation are shared. A *Jeffcott*-rotor with two active magnet bearings and a disk is used for investigation. Through Floquet theory, a deeper insight into the system's dynamic behaviour is gained. Aiming at a further increase of stability, a phase difference between excitation terms is introduced.

Keywords: Flexible Rotor, Active Magnetic Bearings, Parametric Excitation, Anti-Resonance, Floquet Theory

1. Introduction

A *Jeffcott*-rotor with two active magnet bearings (AMBs) and a disk, as shown in Fig. 1, is investigated. The AMBs are controlled by a PID-controller. Parametric excitation is introduced via periodic variation of the P-component of the controller, resulting in a time variable bearing stiffness. [2]

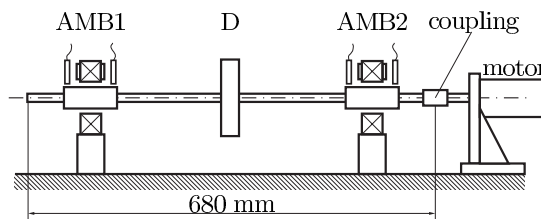


Fig. 1. *Jeffcott* rotor with active magnet bearings (AMBs), disc (D) and motor [2]

As illustrated in [2], the system shows signs of anti-resonance for an excitation frequency Ω of 170 rad/s as well as resonance for 315 rad/s and above 450 rad/s. Anti-resonance leads to a better use of the system's inherent damping due to energy transfer from a mode with lower to one with higher damping.

With Floquet theory the Lyapunov characteristic exponents λ (LCEs) can be found. The largest LCE Λ reflects the stability of the equilibrium. Instability is indicated by $\Lambda > 0$, stability by $\Lambda < 0$. [3]

2. Results and Discussion

If examined using the largest LCE Λ , only the system's resonance frequencies are revealed. For other excitation frequencies, including at the difference frequency where the anti-resonance is expected [4], Λ remains just below zero. If, however, all LCEs λ are considered (see Fig. 2), an anti-resonance at the difference frequency of the first and third eigenfrequency Δ_{31} can be found within the smaller LCEs. For the system under investigation the vibration decay seems to be dominated by LCEs which can be matched with modes belonging to the smallest eigenfrequencies of the unperturbed system.

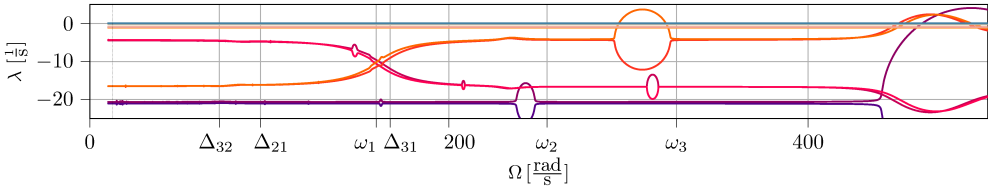


Fig. 2. LCEs λ over frequency of parametric excitation Ω , revealing anti-resonance at approx. 170 rad/s

With focus on the LCEs of the first modes, the effect of a phase difference in the excitation between the AMBs is examined, as this might increase dissipation [5]. As shown in Fig. 3, two anti-resonances are revealed at difference frequency between the third and second as well as the second and first eigenfrequency. However, the phase shift does not yield a significant increase in dissipation for this system, as the minimum at the LCEs crossing is about the same.

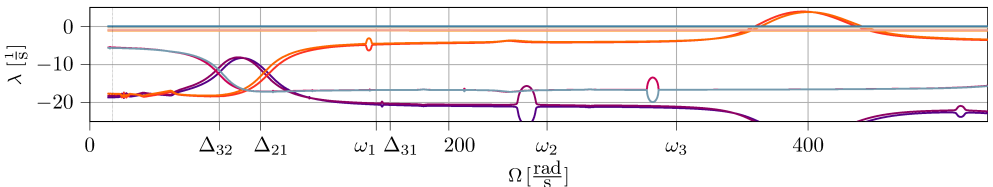


Fig. 3. LCEs λ over frequency of parametric excitation Ω for phase difference of π between bearings

3. Concluding Remarks

Through inspection of the LCEs belonging to the first modes, the anti-resonance found in previous studies could be confirmed. Varying the excitation phase difference revealed two additional anti-resonances, albeit not significantly increasing damping. The discussed approach can however be used for further investigation to find an optimal parametric excitation for maximal vibration mitigation.

References

- [1] DOHNAL F.: *A Contribution to the Mitigation of Transient Vibrations. Parametric Anti-Resonance: Theory, Experiment and Interpretation*. Habilitation thesis, Technical University of Darmstadt: Darmstadt, 2012.
- [2] DOHNAL F., CHASALEVRIS A.: Inducing modal interaction during run-up of a magnetically supported rotor. *Proceedings of DSTA' 2015*, 2015.
- [3] YAKUBOVITCH V.A., STARZHINSKII X.: *Linear Differential Equations with Periodic Coefficients*. Halsted, Wiley: New York, 1975.
- [4] TONDL A.: *On the interaction between self-excited and parametric vibrations*. National Research Institute for Machine Design Bechovice: Prague, 1978.
- [5] KAREV A.: *Asynchronous Parametric Excitation in Dynamical Systems*. Habilitation thesis, Technical University of Darmstadt: Darmstadt, 2021.

A Computational Study of Vibration Attenuation of the Rotor System with Magnetorheological Squeeze Film Dampers

MOLČAN M.^{1*}, FERFECKI P.², ZAPOMĚL J.³

1. Department of Applied Mechanics & IT4Innovations, VSB – Technical University of Ostrava, 17. listopadu 2172/15, 708 00, Ostrava, CZ; michal.molcan@vsb.cz [0000-0003-2309-8672]

2. Department of Applied Mechanics & IT4Innovations, VSB – Technical University of Ostrava, 17. listopadu 2172/15, 708 00, Ostrava, CZ; petr.ferfecki@vsb.cz [0000-0001-9578-0625]

3. Department of Applied Mechanics, VSB – Technical University of Ostrava, 17. listopadu 2172/15, 708 00, Ostrava, CZ; Institute of Thermomechanics, The Czech Academy of Sciences, Dolejškova 1402/5, 182 00, Praha 8, CZ; jaroslav.zapomel@vsb.cz [0000-0002-7943-4287]

* Presenting Author

Abstract: The rotor vibrations are significantly influenced by the damping elements, which are added between the outer race of a rolling bearing and the stationary part. The primary aim of this study is to investigate the nonlinear behaviour of a squeeze film magnetorheological damper designed for attenuation of the lateral vibration of a rotor system. The hydraulic forces produced by squeezing the magnetorheological oil film have a nonlinear character and strongly depend on the viscosity of the lubricating fluid, the supply current in the damper, and the kinematics of journal motion. The pressure distribution in the damper is described by a modified Reynolds equation for a magnetorheological oil modelled as Bingham or the bilinear theoretical material. The harmonic balance method with the arc-length parameterization is proposed to obtain higher-order approximation periodic solutions of a motion equation build-up for the rigid and the flexible model of a rotor system. The computations of the irregular oscillations were carried out by using the 4th order Runge-Kutta method. The vibration stability of the motion was assessed by the 2n-pass method and the turning and bifurcation points for a solution branch over varying system parameters were identified. The phase trajectory, power spectrum, Poincaré maps, and the bifurcation diagrams are used to analyse the investigated rotor system. The computational analysis demonstrates that the different material models of a magnetorheological oil have a small impact on the numerical results. Moreover, the numerical simulations show that the vibration is dependent on the speed of the rotor rotation and the amount of damping in the magnetorheological damper, and that complex dynamic behaviour can exist. This is characterized by periodic, subharmonic, and irregular oscillations of the rotor.

Keywords: rotor, magnetorheological squeeze film damper, harmonic balance method, stability analysis, irregular vibration

Effect of Gear Mesh Stiffness and Lubricant Nonlinearities on the Dynamic Response of Gear Transmission Systems

Hamza Mughal*, Nader Dolatabadi, Ramin Rahmani

Wolfson School of Mechanical, Electrical and Manufacturing Engineering, Loughborough University, Leicestershire, UK

* Presenting Author

Abstract: Gear dynamic response is the underlying cause of gearbox noise, vibration, and harshness (NVH) in automotive powertrains. Gear whine, a dominant form of gearbox NVH in electric vehicles, is caused by static and dynamic errors induced mainly by the variation in gear mesh stiffness. Therefore, an accurate evaluation of time-varying mesh stiffness (TVMS) is important. A dynamic model of a simple spur gear system is developed using an improved analytical TVMS method combined with a nonlinear Hertzian contact model. The nonlinear stiffness and damping of lubricant under elastohydrodynamic regime of lubrication (EHL) is adapted to investigate NVH performance of the system. Results from literature are used to verify the model. The effect of nonlinearities on the system stability and response are identified.

Keywords: Nonlinear gear dynamics; Time-varying mesh stiffness; Dynamic transmission error; Elastohydrodynamic contact; NVH

1. Introduction

Concerns over the environmental impact of internal combustion (IC) engines have surged the demand for electric vehicles (EVs) in public and private transportation sectors. Hence, automotive manufacturers have focused on development of electric powertrains. Integration of electric machines with conventional transmissions (i.e., gearboxes) raise new concerns associated with powertrain noise, vibration, and harshness (NVH). In an EV, powertrain noise mainly originates from the reducer (gearbox) and electric motor in the form of high order tonal noise at high frequencies, also known as whine noise [1]. This tonal noise can be disconcerting to driver and passengers despite its lower sound pressure levels compared with the IC engine noise.

Whine noise is mainly caused by internal excitations due to the time-varying mesh stiffness (TVMS), dynamic transmission error (DTE) and gear impact inside backlash and clearances [1]. These material and geometrical nonlinearities are combined with the nonlinear behaviour of lubricant during elasto-hydrodynamic regime of lubrication (EHL). Development of a robust dynamic model is paramount to better understanding of the transient nonlinear response of the gears and NVH performance of the power transmission unit.

In this study, a nonlinear load dependent Hertzian contact model combined with a TVMS analytical model based on the potential energy method is adapted to accurately evaluate the meshing stiffness of a spur gear pair set. This TVMS model considers the bending, shear, axial, and the tooth fillet foundation stiffness components. TVMS varies with the number of pairs of teeth in contact and the location of the point of contact on the involute tooth profile. The lubricant stiffness and damping during EHL are evaluated to accurately predict the dynamic response and acoustic emission of the spur gear pair

system. Such detailed study of gear dynamics with combined analytical TVMS model and lubricant nonlinear effects has hitherto not been reported in the literature.

2. Results and Discussion

A nonlinear two-degrees-of-freedom dynamic model is developed. The geometrical nonlinearities reside in backlash, possible tooth separation during meshing, and back-side collisions. The basic dynamic models use a square wave meshing stiffness for simplicity. In this study, meshing stiffness is modelled using a detailed analytical TVMS using the concept of potential energy. TVMS nonlinearly varies with number of teeth in contact, position within the line of contact and Hertzian contact stiffness. Lubricant EHL stiffness and damping are initially neglected to verify the dynamic model using the available experimental results from literature [2]. The model is further refined considering lubricant stiffness and nonlinear damping effects as defined in [3]. The effects of geometrical, TVMS and lubricant nonlinearities on the dynamic response, stability and the emitted noise are further investigated. The phase-plane response for the current model is compared with the response of the basic model with constant damping ratio (Figure 1).

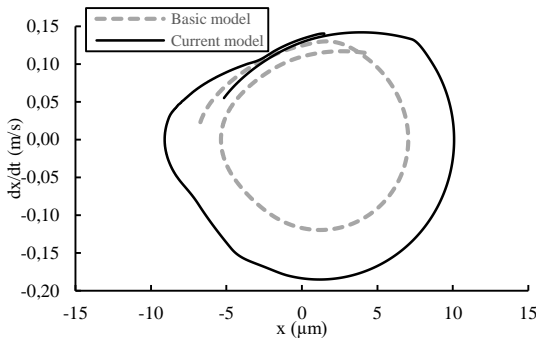


Figure 1: Comparison of phase-plane responses of the TVMS model with nonlinear damping effects and the basic model at 2600 Hz meshing frequency

3. Concluding Remarks

Existence of a reliable analytical TVMS model is essential to the accurate prediction of DTE. Lubricant stiffness and nonlinear damping participate in contact nonlinearity and energy dissipation. The effects of gear body compliance on TVMS have been studied. The effect of nonlinearity originated from the inclusion of the lubricant damping and stiffness is shown and discussed. Poincare and FFT diagrams will further demonstrate the impacts of the nonlinear parameters on the gear set stability and vibrations.

References

- [1] S. Zhang, "Parameter Study and Improvement of Gearbox Whine Noise in Electric Vehicle," *Automotive Innovation*, vol. 1, no. 3, pp. 272–280, 2018, doi: 10.1007/s42154-018-0029-5.
- [2] G. W. Blankenship, A. Kahraman, and A. D. E. Division, "Gear Dynamics Experiments: Part I - Characterization of Forced Response," in *7th, International power transmission and gearing conference*, vol. 88, pp. 373–380. [Online]. Available: <https://www.tib.eu/de/suchen/id/BLCP%3ACN017131519>
- [3] Z. Xiao, C. Zhou, S. Chen, and Z. Li, "Effects of oil film stiffness and damping on spur gear dynamics," *Nonlinear Dynamics*, vol. 96, no. 1, pp. 145–159, 2019, doi: 10.1007/s11071-019-04780-6.

Dynamics of impulse systems with friction

I.V. NIKIFOROVA^{1*}, V.S. METRIKIN², L.A. IGUMNOV³

1. National Research Lobachevsky State University of Nizhny Novgorod [0000-0002-6914-9845]
2. National Research Lobachevsky State University of Nizhny Novgorod [0000-0002-9749-5390]
3. National Research Lobachevsky State University of Nizhny Novgorod [0000-0003-3035-0119]

Abstract: The paper presents the results of a numerical-analytical study of the dynamics of a vibration-impulse mechanism with a crank-crank oscillator. Bifurcation diagrams and stability regions are given, which allow finding the main regularities in the reorganization of motion modes when changing the parameters of the mechanism.

Keywords: bifurcation, sustainability, vibration

1. Introduction

In the invention [1] and schemes of prototypes of mechanisms, a new scheme of a vibration-impulse mechanism with a crank-connecting rod vibration exciter for soil compaction in a closed production area is presented. The scheme contains several percussion pistons, which allows, as noted in [1], to more efficiently perform soil compaction, and small overall dimensions allow the mechanism to be used in difficult closed conditions. In [2], a mathematical model of a vibration-impulse mechanism with a crank-connecting rod oscillator is presented, together with formulas for finding the simplest periodic movements of the mechanism.

This work is a continuation of [2] and differs in that here we take into account the energy losses due to friction between the struts and the body. The results of numerical experiments are also presented, which made it possible to identify various types of movement of the mechanism, including stochastic ones, and to find the values of the parameters at which the known period doubling bifurcations are realized.

2. Results and Discussion

The scheme of the considered mechanism is shown on Fig. 1, where 1 is the mechanism's hull in which the bearings contain an axis 2 with a flywheel 3 and cranks 4 and 5 that have a stationary phase shift φ . The cranks have a joint connection to the piston rods 6; percussion pistons 7 and 8 are, in turn, connected to them with a joint. Under the percussion pistons we have anvils 9, 10 with heights h_1 , h_2 respectively. The hull 1 has a joint connection to the racks 11 that are rigidly connected to the anvil block 12.

The rotation of the axis in the proposed scheme is transformed with a crank mechanism into a back-and-forth motion with respect to the anvil block. The percussion pistons may alternate their blows to the corresponding anvils, and the vibro-impulsive impact created here is transmitted through the anvil block to the material being compacted.

Taking into account the structure of the phase space and the behaviour of phase trajectories in it, the dynamics of the mechanism was studied using the method of point mappings [3].

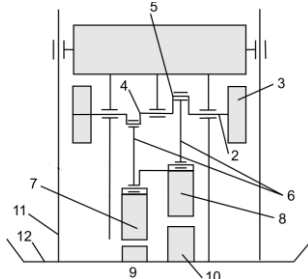


Fig.2. Vibro-impact mechanism diagram

The study of the complex dynamics of the two-piston mechanism was carried out using numerical experiments using a software package developed in the Borland C ++ Builder 6 environment. This software package was used to construct bifurcation diagrams and regions of existence of stable periodic motion modes.

3. Concluding Remarks

The proposed numerical-analytic method of study (based on the method of surface point maps) for the dynamics of new kinds of vibro-impulsive mechanisms has let us find regions in the space of parameters useful for successful tuning and control for the mechanism’s motion, while our numerical computations imply the possibility for a specific choice of parameters and illustrate the basic reorganizations of the mechanism’s motion modes depending on the changes in parameters. Using the peculiarities of the application of the method of point mappings in the study of the dynamics of systems with discontinuous nonlinearities [3], interesting results of a comparative analysis of the main modes of motion of the considered class of impulse systems with friction and without friction. were received.

Acknowledgment: This work was supported by the Ministry of Science and Higher Education of the Russian Federation, agreement No 0729-2020-0054.

References

- [1] SHILKOV V.A., SAVALYUK A.D., METRIKIN V.S., POLYAKOV A.A., SHABARDIN A.K., ALEKHIN A.I. AND OMENENKO I.YA.: *Vibrotrambovka (Vibrating Ramming)*, USSR Inventor’s Certificate no. 1020479, Byull. Izobret., 1983, no. 20, 3376593/29-33.
- [2] IGUMNOV L. A., METRIKIN V. S., NIKIFOROVA I. V.: *The dynamics of eccentric vibration mechanism (Part I)*: JVE Journal of Vibroengineering 19, 4816-5656, 2017.
- [3] FEIGIN M.I.: *Forced oscillations of systems with discontinuous nonlinearities*: M. Nauka, 1994. (in Russian)

On Stability of Periodic Motion of the Swinging Atwood Machine

ALEXANDER PROKOPENYA

Warsaw University of Life Sciences – SGGW, Warsaw, Poland [ORCID 0000-0001-9760-5185]
Nowoursynowska str. 159, 02-776 Warsaw
E-mail: alexander_prokopenya@sggw.edu.pl
* Presenting Author

Abstract: We consider the swinging Atwood machine that is a conservative Hamiltonian system with two degrees of freedom. In general, it is not integrable but there exists a periodic solution of the equations of motion describing oscillations of the bodies near some equilibrium positions. An interesting peculiarity of this state of dynamic equilibrium is that owing to oscillations a body of smaller mass balances a body of larger mass. Analysing the system motion in the neighbourhood of this equilibrium, we have shown that it is stable in linear approximation. Thus, the swinging Atwood machine is an example of mechanical system the equilibrium state of which is stabilized by oscillations.

Keywords: swinging Atwood’s machine, dynamic equilibrium, periodic solution, stability

1. Introduction

The swinging Atwood machine (SAM) consists of two masses $m_1, m_2 = m_1(1 + \varepsilon)$ attached to opposite ends of a massless inextensible thread wound round two massless frictionless pulleys of negligible radius (see Fig. 1). The mass m_2 is constrained to move only along a vertical while mass m_1 is allowed to oscillate in a plane and it moves like a pendulum of variable length. Such a system has two degrees of freedom and its Hamiltonian function may be written in the form

$$\mathcal{H} = \frac{p_r^2}{2(2+\varepsilon)} + \frac{p_\varphi^2}{2r^2} + (1 + \varepsilon)r - r \cos \varphi, \quad (1)$$

where two variables r, φ describe geometrical configuration of the system, and p_r, p_φ are the two corresponding canonically conjugate momenta.

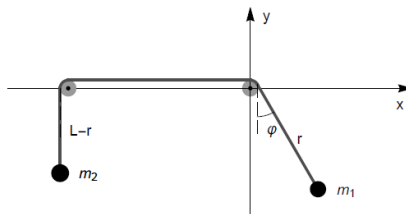


Fig. 1. The swinging Atwood machine with two small pulleys

Equations of motion of the SAM determined by the Hamiltonian (1) are essentially nonlinear, and their general solution cannot be found in symbolic form. Numerical analysis of the equations of motion

has shown that, depending on the mass ratio and initial conditions, the SAM can demonstrate different types of motion (see [1, 2]). In particular, there exists a periodic solution of the equations of motion which may be represented in the form of power series in a small parameter ε (see [3])

$$r_p(t) = 1 + \frac{\varepsilon}{16}(1 + 6 \cos(2t)) - \frac{\varepsilon^2}{2048}(261 + 276 \cos(2t) + 105 \cos(4t)) + \dots, \quad (2)$$

$$\varphi_p(t) = \sqrt{\varepsilon} \left(2 \cos t - \frac{53\varepsilon}{192} \cos(3t) + \frac{\varepsilon^2}{16384} \left(2959 \cos t + 1699 \cos(3t) + \frac{5813}{5} \cos(5t) \right) + \dots \right). \quad (3)$$

The existence of periodic solution (2)-(3) means that for given value of parameter ε one can choose such initial conditions that the system is in the state of dynamical equilibrium when the bodies oscillate near some equilibrium positions. Note that for $\varepsilon > 0$ the system under consideration has no a state of static equilibrium when the coordinates $r(t), \varphi(t)$ are some constants. The main purpose of this talk is to investigate whether the system will remain in the neighbourhood of the equilibrium if the initial conditions are perturbed or whether the periodic solution (2)-(3) is stable.

2. Stability Analysis

To investigate stability of periodic solution (2)-(3) we introduce small perturbations q_1, p_1, q_2, p_2 of the solution and expand the Hamiltonian (1) into power series in terms of q_1, p_1, q_2, p_2 up to the second order inclusive. Then equations of the perturbed motion may be written in linear approximation in the canonical form with the Hamiltonian

$$\mathcal{H}_2 = \frac{p_1^2}{2(2+\varepsilon)} + \frac{p_2^2}{2r_p^2} + \frac{p_{\varphi_0}^2}{2r_p^4} q_1^2 + \frac{r_p}{2} \cos \varphi_p q_2^2 - \frac{2p_{\varphi_0}}{r_p^3} q_1 p_2 + q_1 q_2 \sin \varphi_p,$$

where p_{φ_0} is the momentum canonically conjugate to solution φ_p . It is clear that the perturbed motion of the system is determined by the linear system of four differential equations with periodic coefficients, and their general properties have been studied quite well (see [4]). The behavior of solutions to such equations is determined by its characteristic exponents which may be found in the form of power series in ε . Doing necessary symbolic computations, we have found two pairs of purely imaginary characteristic exponents up to the second order in ε

$$\lambda_{1,2} = \pm i, \quad \lambda_{3,4} = \pm i \frac{\sqrt{3\varepsilon}}{2} \left(1 - \frac{17\varepsilon}{32} + \frac{85}{256} \varepsilon^2 \right).$$

According to Floquet-Lyapunov theory (see [4]), the corresponding solutions to differential equations with periodic coefficients describe the perturbed motion of the system in the bounded domain in the neighbourhood of the periodic solution (2)-(3). It means that this solution is stable in linear approximation, and so the SAM is an example of mechanical system the equilibrium state of which is stabilized by oscillations.

References

- [1] TUFILLARO N.B., ABBOTT T.A., GRIFFITHS D.J.: Swinging Atwood's machine. *American Journal of Physics* 1984, **52**(10):895-903.
- [2] PROKOPENYA A.N.: Motion of a swinging Atwood's machine: simulation and analysis with Mathematica. *Mathematics in Computer Science* 2017, **11**(3):417-425.
- [3] PROKOPENYA A.N.: Construction of a periodic solution to the equations of motion of a generalized Atwood's machine using computer algebra. *Programming and Computer Software* 2020, **46**(2):120-125.
- [4] YAKUBOVICH V.A., STARZHINSKII V.M.: *Linear Differential Equations with Periodic Coefficients*. John Wiley: New York, 1975.

Estimation the Domain of Attraction for a System of Two Coupled Oscillators with Weak Damping,

VOLODYMYR PUZYROV^{1*}, JAN AWREJCEWICZ², NATALIYA LOSYEVA³,
NINA SAVCHENKO^{4**}, OKSANA NIKOLAIEVA⁵

1. Universitat Politècnica de Catalunya, Terrassa, Spain;
Nizhyn Gogol State University, Nizhyn, Ukraine [ORCID: 0000-0001-6770-182X]
 2. Lodz University of Technology, Lodz, Poland [ORCID: 0000-0003-0387-921X]
 3. Nizhyn Gogol State University, Nizhyn, Ukraine [ORCID: 0000-0002-2194-134X]
 4. Zhukovsky National Aerospace University "KhAI", Kharkiv, Ukraine [ORCID: 0000-0001-8144-9368]
 5. National University of Food Technologies, Kiev, Ukraine [ORCID: 0000-0002-4958-1833]
- * Presenting Author

Abstract: When solving a wide class of problems of nonlinear dynamics, the stability property of a given system regime is a prerequisite for design. An important role is played by the concept of the domain of attraction (DoA) of the equilibrium point (or limit cycle). However, as a rule, this domain is difficult to find and describe in explicit form. Therefore, the search for DoA estimate has been a fundamental problem in the control theory since the middle of the last century. Currently, methods based on Lyapunov functions predominate in the literature. We have studied the problem of obtaining the estimates of the DoA for equilibrium of the mechanical systems. The method for using Lyapunov function of special kind for a system with polynomial right-hand side to find the estimates for DoA is proposed. This procedure is illustrated by the example of a mechanical system which consists of two coupled nonlinear oscillators with weak damping.

Keywords: domain of attraction, nonlinear oscillator, weak damping.

1. Introduction

One of the fundamental problems in engineering is proving that performance limits and operational restrictions are met. From the standpoint of the theory of dynamical systems, this problem can be considered as a problem of ensuring the local asymptotic stability on a suitable subset of the state space called the attraction domain or region of attraction (RoA). This approach is used in a variety of control applications such as aerospace [1], power systems [2], chemistry [3], medicine [4] and others. Existing approaches for approximating the DoA can be divided into Lyapunov and non-Lyapunov based categories. Among the non-Lyapunov based approaches (which do not employ explicitly Lyapunov functions) it should be noted papers [5-7]. Today it is a great variety of Lyapunov based methods for estimating the DoA (see, for instance, [8, 9] and references in [10]). Mostly, they are based on the search for a Lyapunov function $V(x)$ and for a positive scalar c , such that $\dot{V}(x)$ is negative over the sub-level $C = \{x : V(x) \leq c\}$. Given such V and c , it can be shown that the connected component of C containing the equilibrium is an inner approximation to the DoA.

In the present paper, we propose a method for using Lyapunov function of special kind for a system with polynomial right-hand side to find the estimates for DoA. This approach is applied to obtain

the estimates of the DoA for equilibrium of a mechanical system which consists of two coupled nonlinear oscillators with weak damping.

2. Results and Discussion

A mechanical system which consists of two oscillators with nonlinear coupling is considered. The dynamics of such a system is described by the following equations

$$\begin{aligned} m_1 \ddot{x}_1 + c_2(\dot{x}_1 - \dot{x}_2) + k_1 x_1 + k_2^{lin}(x_1 - x_2) - k_2^{nonlin}(x_1 - x_2)^3 &= 0, \\ m_2 \ddot{x}_2 + c_2(\dot{x}_2 - \dot{x}_1) + k_2^{lin}(x_2 - x_1) - k_2^{nonlin}(x_2 - x_1)^3 &= 0. \end{aligned} \quad (1)$$

If $k_2^{lin} > 0$, then equilibrium $x = 0, \dot{x} = 0$ is asymptotically (exponentially) stable. The aim of the paper is to obtain the effective estimation for DoA in assumption that mechanical parameters of the system are known. The accompanying task is to study the influence of variation in linear stiffness ratio and damping coefficient onto size of the resulting estimate. To fulfil the task, the Lyapunov function based approach described in [11] is employed. These estimations are compared with the results of numerical integration of the system (1).

3. Concluding Remarks

In this paper, we deal with the problem of estimating the domain of attraction (DoA) for equilibrium of a mechanical system which consists of two coupled nonlinear oscillators with weak damping. For this purpose, we have successfully established a procedure to determine the Lyapunov function of special kind for a system with polynomial right-hand side.

References

- [1] LEWIS A.P.: An investigation of stability of a control surface with structural nonlinearities in supersonic flow using Zubov's method. *Journal of Sound and Vibration* 2009, **325**: 338–361.
- [2] SZEDERKÉNYI G., KRISTENSEN N.R., HANGOS K.M., JORGENSEN S.B.: Nonlinear analysis and control of a continuous fermentation process. *Computers and Chemical Engineering* 2002, **26**: 659–670.
- [3] ANGHEL M., MILANO F., PAPACHRISTODOULOU A.: Algorithmic construction of Lyapunov functions for power system stability analysis. *IEEE Transactions on Circuits and Systems I: Regular Papers* 2013, **60** (9): 2533–2546.
- [4] MEROLA A., COSENTINO C., AMATO F.: An insight into tumor dormancy equilibrium via the analysis of its domain of attraction. *Biomedical Signal Processing and Control* 2008, **3**(3): 212 – 219.
- [5] GENESIO R., TARTAGLI M. AND VICINO A.: On the estimation of asymptotic stability regions: state of the art and new proposals. *IEEE Transactions on Automatic Control* 1985, **30** (8): 747 – 755.
- [6] HENRION D., KORDA M.: Convex computation of the region of attraction of polynomial control systems. *IEEE Transactions on Automatic Control* 2014, **59**(2): 297 – 312.
- [7] NOLDUS E., LOCCUFIER M.: A new trajectory reversing method for the estimation of asymptotic stability regions. *International Journal of Control* 1995, **61**(4): 917 – 932.
- [8] VANNELLI A., VIDYASAGAR M.: Maximal Lyapunov functions and domains of attraction for autonomous nonlinear systems. *Automatica* 1985, **21**(1): 69 – 80.
- [9] PAPACHRISTODOULOU A., PRAJNA S.: On the construction of Lyapunov functions using the sum of squares decomposition. In: *Proceedings of the IEEE Conference on Decision and Control* 2002, **3**: 3482 – 3487.
- [10] Chesi G.: Domain of attraction: analysis and control via SOS programming. Springer, 2011.
- [11] AWREJCIEWICZ J., BILICHENKO D., CHEIB A.K., LOSYEVA N., PUZYROV V. Estimation of the domain of attraction for a nonlinear mechanical system. *Applicable Solutions in Non-Linear Dynamical Systems*, Lodz, DSTA, 2019: 37 – 46.

Dynamics of a multiple-link aerodynamic pendulum

YURY SELYUTSKIY^{1*}, ANDREI HOLUB², CHING-HUEI LIN³

1. Lomonosov Moscow State University, Institute of Mechanics, Moscow, Russia [0000-0001-8477-6233]

* Presenting Author

2. Lomonosov Moscow State University, Institute of Mechanics, Moscow, Russia [0000-0001-8982-4097]

3. Chien-Hsin University of Science and Technology, Department of Electrical Engineering, Taoyuan, Taiwan

Abstract: Oscillations of different aeroelastic systems are of interest from the perspective of both practice and theory. One of examples of such systems is an aerodynamic pendulum with several elastically connected links. The influence of different parameters of the pendulum upon the stability of its trivial equilibrium is studied. Oscillations arising in the system are considered for different values of parameters and different number of pendulum links.

Keywords: oscillations, stability, aerodynamic pendulum, aeroelasticity

1. Introduction

Dynamics of multiple link pendulums in gravity field has been investigated by many researchers. Various approaches to formulation of equations of motion and to control of motion of such pendulums were proposed and used, e.g., in [1-3]. In [4], the impact of the last link of a multiple pendulum with a solid surface is studied.

An interesting class of pendulums are aerodynamic pendulums, where the motion the system is determined by aerodynamic forces. These forces are non-conservative and their influence upon the system can be antidissipative or dissipative. Behaviour of single and double aerodynamic pendulums was studied in [5-6]. Here we consider a generalization of this problem to the case of multiple link pendulum.

2. Problem Statement and Discussion

We discuss the behaviour of a multiple aerodynamic pendulum consisting of n links. Each of the first $n-1$ links represents a weightless rod with a point mass at its end. For simplicity sake, we assume that all these links have the same mass m_1 . The last link represents a thin wing with mass m and moment of inertia J (see Fig. 1). All links are connected with similar spiral springs. Axes of all inter-link joints are vertical.

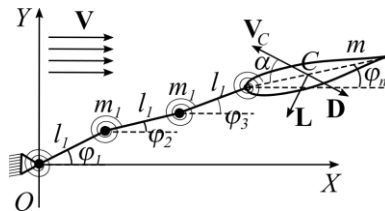


Fig. 1. Scheme of the system

The pendulum is placed in a steady horizontal airflow. It is assumed that the flow interacts only with the wing, and the aerodynamic load is described with the quasi-steady approach [5]. In this context, the aerodynamic load is represented as lift force L and drag D applied in a certain point C of the wind chord, and aerodynamic torque M_z . These values depend on the angle of attack (the angle between the airspeed of point C and the wing chord).

The kinetic energy of the pendulum and the potential energy of springs are as follows:

$$T = \frac{1}{2} \sum_{i=1}^n \left[(m + (n-i)m_i) l_i^2 \dot{\varphi}_i^2 + 2 \sum_{j=i+1}^n (m + (n-j)m_j) l_j l_i \dot{\varphi}_i \dot{\varphi}_j \cos(\varphi_j - \varphi_i) \right] + \frac{J \dot{\varphi}_n^2}{2} \quad (1)$$

$$U = \frac{k}{2} \left(\varphi_1^2 + \sum_{i=2}^n (\varphi_i - \varphi_{i-1})^2 \right)$$

Here $\varphi_0 = 0$, $l_1 = \dots = l_{n-1}$ are lengths of links, l_n is the distance from the last joint to the center of mass of the wing, k is stiffness coefficient of joint springs.

The resulting system of equations of motion is nonlinear and, due to the presence of aerodynamic forces, non-conservative.

Evidently, the system has a trivial equilibrium. Its stability is studied depending on parameters of the system. The effect of the number of links upon the stability and dynamics of the pendulum is considered. Numerical simulation of dynamics of the system is performed for different sets of values of parameters.

3. Concluding Remarks

Detailed analysis of dynamics of a multiple pendulum in airflow could contribute to understanding specific features of behaviour of complicated aeroelastic systems and to development of efficient wind power harvesting devices based on flow-induced oscillations of structures.

References

- [1] BRAUN M: On some properties of the multiple pendulum. *Archive of Applied Mechanics* 2003, **72**:899–910.
- [2] ANANYEVSKIY I, ANOKHIN N: Control of a multi-link inverted pendulum by a single torque. *IFAC Proceedings Volumes* 2012, **45**(2):550-553.
- [3] UDWADIA FE, KOGANTI PB: Dynamics and control of a multi-body planar pendulum. *Nonlinear Dynamics* 2015, **81**:845-866.
- [4] MARGHITU DB, ZHAO J: Impact of a Multiple Pendulum with a Non-Linear Contact Force. *Mathematics* 2020, **8**:1202.
- [5] LOKSHIN BY, SAMSONOV VA: The self-induced rotational and oscillatory motions of an aerodynamic pendulum. *Journal of Applied Mathematics & Mechanics* 2013, **77**(4):360-368.
- [6] SELYUTSKIY YD, HOLUB AP, DOSAEV MZ: Elastically mounted double aerodynamic pendulum. *International Journal of Structural Stability and Dynamics* 2019, **19**(5):1941007

Time-variable normal contact force influence on dry-friction damping of self-excited vibration of bladed turbine wheel

PAVEL ŠNÁBL^{1*}, LUDEK PESEK², CHANDRA SHEKAR PRASAD³

1. Institute of Thermomechanics, Czech Academy of Sciences, Prague, Czech Republic, snabl@it.cas.cz [0001-6168-0044]
2. Institute of Thermomechanics, Czech Academy of Sciences, Prague, Czech Republic, pesek@it.cas.cz [0000-0003-0940-6771]
3. Institute of Thermomechanics, Czech Academy of Sciences, Prague, Czech Republic, cprasad@it.cas.cz [0000-0002-3087-5807]

* Presenting Author

Abstract: Recently [1-2], the new calculation approach based on modal synthesis method is proposed for evaluation of structural and dry-friction damping effect on self-excited vibrations due to aero-elastic instability in the bladed turbine wheels. Due to the modal reduction, the calculations are made computationally very efficient. The method will be herein used to study a dry-friction damping of self-excited vibration of an industrial turbine wheel with 66 blades. The aerodynamic excitation arises from the spatially periodical flow of steam through the stator blade cascade. The self-excited aero-elastic forces of blades are described by Van der Pol model [3]. For evaluation of damping effect, the blade tie-boss couplings are applied on this particular turbine wheel. Therefore, neighboring blades are interconnected by rigid arms that are on one side fixed to one blade and are in friction contact on their free side with the other blade. The contact point pairs of two neighboring blades overlap in undeformed state of the cascade and static normal contact forces are prescribed. The relative contact displacements due to blade cascade deformation are calculated from kinematics of relative blade motions. Due to relative normal motions in contacts, the prescribed contact forces will vary in time during vibration. In the contribution, the effect of variable magnitude of normal contact forces with respect to the angle of contact surfaces on the wheel dynamics and on level of friction damping will be analyzed. Friction forces in contacts are driven by the modified Coulomb friction law. The analysis will be oriented on the narrow frequency range and on the case when a slip motion is prevailing in the contacts.

Keywords: turbine blades, dry-friction contact, flutter, travelling wave, Van der Pol model.

[1] Pešek, L., Šnábl, P., and Prasad, C., 2020. "Suppression of classical flutter oscillations in bladed wheel using inner damping effect". In Proc. XI International Conference on Structural Dynamics EURO-DYN 2020, pp. 401–411.

[2] Pesek, L., Snabl, P., Prasad, S.P.: Reduced modal model of bladed turbine wheel for study of suppression of self-excited vibration by dry-friction contacts, Proc. of SIRM2021, Gdansk, IMP PAN Publishers, pp.371-380.

[3] Půst, Ladislav, Pešek, Luděk, Byrtus, M. Modelling of flutter running waves in turbine blades cascade. Journal of Sound and Vibration. 2018, 436(December), 286-294. ISSN 0022-460X, doi: 10.1016/j.jsv.2018.08.011

Coupled System of Stochastic Neural Networks with Impulses, Markovian Switching, and node and connection Delays

BILJANA TOJTOVSKA^{1*} PANCE RIBARSKI²

1. Faculty of Computer Science and Engineering, Skopje, Republic of North Macedonia [<https://orcid.org/0000-0002-5617-9172>]

Abstract: In this paper we give sufficient conditions for p-th moment general decay stability of a model of coupled stochastic neural networks, which apart from Markovian switching, impulses and node delays, also includes interconnection delays. The model is more general than the results in the literature and thus the known methods for stability analysis can not be directly applied. We give the main result using the M-matrix theory and additionally, we analyse stability with respect to a general decay function, which includes the logarithmic, exponential and polynomial function as a special case. To the best of our knowledge, the results are original and have not been published yet.

Keywords: coupled systems, stochastic neural networks, p-th moment stability, general decay function

1. Introduction

Coupled system of neural networks are of special interest in the analyses of dynamical systems, since their dynamics depends on the individual dynamics of the included networks, as well as on the way in which these networks are interconnected. Different aspects of coupled networks are studied, with an emphasis on synchronization and stability. Many results have been reported in the literature and here we give only few of them which study the stability of coupled systems on networks, both deterministic and stochastic [1, 2, 3, 4].

In this paper we are interested in the stability analyses of a model of coupled stochastic neural networks (CSNN) which includes node delays, impulses, Markovian switching and interconnection delays. There are different results on coupled systems of networks in the but to the best of our knowledge this model is not considered and the presented results are original.

2. Results and Discussion

The model we consider is given by a system of stochastic differential equations. The dynamics of the i -th neuron in the k -th vertex of the CSNN, $i, k \in N$ at any moment $t \geq t_0$, $t \neq t_m$ is given by

$$\begin{aligned}
dX_i^{(k)}(t) = & -h_i^{(k)}(X_i^{(k)}(t), r(t)) \left[c_i^{(k)}(t, X_i^{(k)}(t), r(t)) \right. \\
& - \sum_{j=1}^n a_{ij}^{(k)}(t, r(t)) f_j^{(k)}(X_j^{(k)}(t), r(t)) - \sum_{j=1}^n b_{ij}^{(k)}(t, r(t)) g_j^{(k)}(X_{j,\tau_k}^{(k)}, r(t)) \\
& \left. - \sum_{j=1}^n d_{ij}^{(k)}(t, r(t)) \int_{-\infty}^t l_{ij}^{(k)}(t-s) k_j^{(k)}(X_j^{(k)}(s), r(s)) ds \right] dt \\
& + \sum_{j=1}^n \eta_i^{(kj)}(t, X_i^{(k)}(t), X^{(j)}(t), X_{\tau_{kj}}^{(j)}, r(t)) dt + \sum_{j=1}^n \sigma_{ij}^{(k)}(t, X_j^{(k)}(t), X_{j,\tau_k}^{(k)}, r(t)) dW_j(t) \\
& + \sum_{j=1}^n \zeta_i^{(kj)}(t, X_i^{(k)}(t), X^{(j)}(t), X_{\tau_{kj}}^{(j)}, r(t)) dW_j(t),
\end{aligned}$$

and for $t = t_m, m \in \mathbb{N}$,

$$\begin{aligned}
X_i^{(k)}(t) = & \mathcal{I}_{im}(X_1^{(k)}(t^-), \dots, X_n^{(k)}(t^-)) + \mathcal{J}_{im}(X_1^{(k)}(t^- - \tau_k(t^-)), \dots, X_m^{(k)}(t^- - \tau_k(t^-))), (4.47) \\
X_i^{(k)}(t_0 + s) = & \xi_i^{(k)}(s), s \in (-\infty, t_0],
\end{aligned}$$

This model is generalization of the one considered in [DSTA 2019], where stability analysis was discussed using global Lyapunov function, Razumikhin method and graph theoretical approach. These methods are not suitable for the analysis of our model, due to the presence of interconnection delays. We give suitable assumptions for the components of the network and extend some known results. We state the main result of our paper for p-th moment stability with respect to a general decay function and prove the results using M-matrix theory.

3. Concluding Remarks

In this paper we discuss the p-th moment stability of coupled stochastic neural network which generalizes many models in the literature and even more, we consider a generalised decay function. The results are based on M-matrix theory and to the best of our knowledge, they have not been published yet.

- [1] KAO Y, WANG C: Global stability analysis for stochastic coupled reaction–diffusion systems on networks. *Nonlinear Analysis: Real World Applications*, 2013, **14**(3):1457–1465.
- [2] LI M. Y, SHUAI Z: Global-stability problem for coupled systems of differential equations on networks. *Journal of Differential Equations*, 2010, **248**(1):1–20.
- [3] LI W, SONG H, QU Y, WANG K: Global exponential stability for stochastic coupled systems on networks with Markovian switching. *Systems & Control Letters*, 2013 **62**(6):468–474.
- [4] LI W, SU H, Wang K: Global stability analysis for stochastic coupled systems on networks. *Automatica*, 2011, **47**(1):215–220.
- [5] TOJTOVSKA B, RIBARSKI P: Stability of couples systems of stochastic Cohen–Grossberg neural networks with time delays, impulses and Markovian switching, to appear in *PERSPECTIVES IN DYNAMICAL SYSTEMS III: CONTROL AND STABILITY* (ISBN 978-3-030-77314-4)

Dynamical Study of BEC with External Trapping Potential under Noise

EREN TOSYALI^{1*}, FATMA AYDOGMUS²

1. Istanbul Bilgi University, Vocational School of Health Services, [0000-0001-9118-851X]

2. Istanbul University, Faculty of Science, Physics Department [0000-0003-1434-2143]

* Presenting Author

Abstract: The dynamic of a Bose–Einstein condensate system with external trapping potential under noise is investigated in this study based on the relations between the system parameters and the solution behaviors by constructing phase space diagrams. We observed that the system exhibits shock-wave like dynamic.

Keywords: dynamic, phase space, BEC, shock-wave, chaos.

1. Introduction

Bose–Einstein Condensation (BEC) idea started with Bose and Einstein studies about the gas atoms at zero-temperature [1,2]. The BEC is given by a macroscopic wave function and it is governed the Gross-Pitaevskii equation (GPE) that has a nonlinear structure and dependent on time and space [3,4]. The nonlinear term of GPE represents particle-particle interactions. In this study, we represent a BEC system with trapping external potential under noise as below:

$$\frac{d^2\phi}{dx^2} = \frac{J^2}{\phi^3} + \left[v_1 \cos^2(\omega x) + \frac{1}{2} \beta x^2 - \gamma + \eta |\phi|^2 \right] \phi + AV(x). \quad (1)$$

Here A is the amplitude of noise and $V(t)$ generate x dependent Gaussian noise range of between $-\pi$ and π . To simplify the numerical calculation, we rewrite the Eq. 21 as first-order couple equation system by the transformation $x_2 = \phi$ and $y_2 = \frac{d\phi}{dx}$,

$$\frac{dx_2}{dx} = y_2, \quad (2a)$$

$$\frac{dy_2}{dx} = \frac{J^2}{4x_2^3} + \left[v_1 \cos^2(\omega x) + \frac{1}{2} \beta x^2 - \gamma + \eta |x_2|^2 \right] x_2 + AV(x). \quad (2b)$$

2. Results and Discussion

The numerical simulations are given in this section. We investigate the dynamic of system solutions for $v_1 = 1$, $\beta = 0.0001$, $\omega_1 = 2\pi$, $\eta = -0.015$, $J = 0.4$, $\gamma = 0.5$ and $\Gamma = 0.1$. Possible Initial conditions are chosen randomly $(x_2(0), y_2(0)) = (0.6985, 0.2668)$ system parameters.

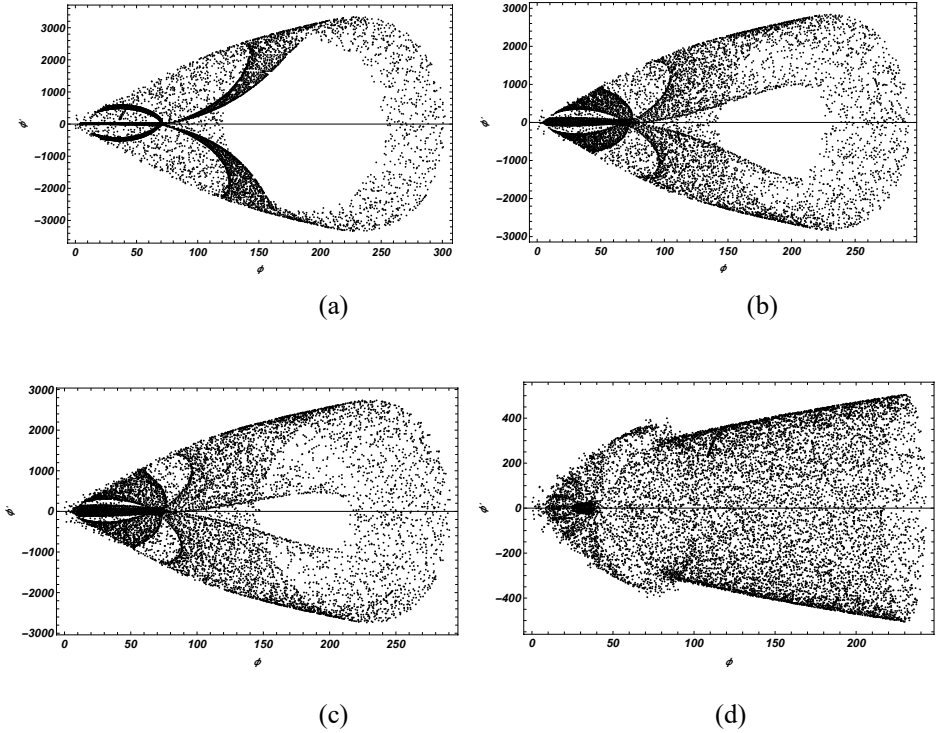


Fig. 1. Phase space diagrams of BEC system for $v_1 = 1$, $\beta = 0.0001$, $\omega_1 = 2\pi$, $\eta = -0.015$, $J = 0.4$, $\gamma = 0.5$ and $\Gamma = 0.1$. (a) $A = 0.5$, (b) $A = 0.75$ (c) $A = 1$, (d) $A = 1.25$.

3. Concluding Remarks

We have studied a BEC system with an external potential under noise. Numerical solutions indicate that there exists chaos in the system. It is important to state that the system exhibits a behavior typical for dispersive shock-wave like dynamics in phase space.

References

- [1] S.N. BOSE, Z. PHYS. 26, 168, 1924.
- [2] A. Einstein and Sitzungsber, K. Preuss. Akad. Wiss.261, Quantentheorie des einatomigen idealen Gases, K. Preuss. Akad. Wiss. 265, 1925.
- [3] E.P. GROSS, Nuovo Cimento 20, 454, 1961.
- [4] L.P. PITAEVSKII AND S. STRINGARI, Bose-Einstein Condensation, Oxford, New York, 2003.

Free vibrations of two-stage hydraulic cylinder.

SEBASTIAN UZNY¹, FRANCISZEK ADAMEK^{2*}, ŁUKASZ KUTROWSKI³

1. Institute of Mechanics and Machine Design Fundamentals, University of Technology in Częstochowa, 42-201 Częstochowa, Poland, [orcid.org/0000-0002-8320-8741]
2. Institute of Mechanics and Machine Design Fundamentals, University of Technology in Częstochowa, 42-201 Częstochowa, Poland, [orcid.org/0000-0001-5827-7537]
3. Institute of Mechanics and Machine Design Fundamentals, University of Technology in Częstochowa, 42-201 Częstochowa, Poland, [orcid.org/0000-0001-7315-4308]

* Presenting Author

Abstract: The article presents the problem of free vibrations of a two-stage hydraulic cylinder subjected to a Euler compressive load. The cylinder is simply supported on both sides. The formulation of the linear vibration problem of the telescopic hydraulic cylinder was based on kinetic stability criterion using the Hamilton principle and the Bernoulli-Euler theory. The stiffness of the guiding elements and seals between its successive steps was taken into account. These stiffnesses were modelled with translational and rotational springs. The influence of cylinder thickness, piston rod diameter and thickness of guiding and sealing elements on free vibrations of the system was analyzed. The results in the form of characteristic curves on the plane: load – frequency of natural vibrations with various parameters characterizing the considered hydraulic cylinder are presented.

Keywords: hydraulic cylinder, free vibration, stability, slender system, Euler load.

1. Introduction

These Hydraulic cylinder are systems that are used in many industries. Due to obtaining very high longitudinal forces, they are systems exposed to destruction. Hydraulic cylinders are very responsible elements of mechanical structures, the destruction of which can have very serious consequences resulting from economic and loss of health and life. Lech Tomski developed two basic mathematical models of these structures. The first concerns free transverse vibrations and static stability of cylinder as slender system [3]. These model was used in [4]. The second model concerns the free and forced vibrations of the actuator (stocky system) in the longitudinal direction, which was presented among others, by at work [5]. So far, research on telescopic actuators with a number stages greater than one has been limited to fully extended systems [1, 2]. Telescopic cylinders with partial extension have not been tested. In this paper , the actuator is considered as a slender system. The boundary problem of the actuator is formulated on Hamilton's principle. The considered system is shown in Fig.1. It consists of three elements. Two of them are cylinders and one is the piston rod. The tested object was subjected to Euler load at various degrees of its extension. Figure 1 shows the successive stages of the cylinder extensions. In order to easiest presentation of the individual stages of the cylinder extension, a letter designation has been introduces. The letter A indicates the fully assembled cylinder. The letter B corresponds to the cylinder with the first cylinder fully extended. The designation AB was used to represent the extension between configurations A and B. The letter C marks the full extension of the entire hydraulic cylinder. Similarly to the previous situation, the designation BC was used to present

the extension between configurations B and C. The letter D (fig. 1) represents the mathematical model used when formulating the linear problem of vibrations of a telescopic hydraulic cylinder.

The mathematical model takes into account the stiffness of the sealing and guiding elements between its individual members. In this study, considerations are limited to a linear system. The results of numerical calculations were presented in dimensionless form relating them to the stiffness of the piston rod of the considered hydraulic cylinder.

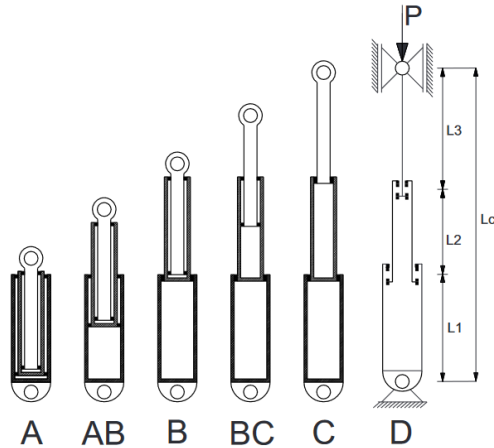


Fig. 1. Diagram of the considered hydraulic cylinder (A, AB, C, BC, C: next step of the cylinder extension, D: mathematical model)

References

- [1] UZNY S, KUTROWSKI Ł: The effect of the Type of Mounting on Stability of a Hydraulic Telescopic Cylinder. *Machine Dynamics Research*, 2018, Vol 42, No 2, 53-60.
- [2] UZNY S, KUTROWSKI Ł: Obciążalność rozsuniętego teleskopowego siłownika hydraulicznego przy uwzględnieniu wyboczenia oraz wyciężenia materiału. *Modelowanie inżynierskie*, 37(68), 125-131.
- [3] TOMSKI L: Elastic Carrying Capacity of a Hydraulic Prop, *Engineering Transactions*, 1977, 25(20), 247-263.
- [4] UZNY S: Free Vibrations and Stability of Hydraulic Cylinder Fixed Elastically on Both Ends, *Proc. Appl. Math. Mech.*, 9, 2009, 303-304.
- [5] TOMSKI L: Dynamika stojaków hydraulicznych obudów górniczych, *Praca habilitacyjna, Nr 17*, Częstochowa 1979.

Anisotropic friction sliding rule influence on the mechanical systems dynamics

ADAM WIJATA^{1A*}, BARTOSZ STAŃCZYK^{1B}, JAN AWREJCWICZ^{1C}

1. Lodz University of Technology, Department of Automation, Biomechanics and Mechatronics, Lodz, Poland;
^A[0000-0003-3042-7112], ^B[0000-0002-3037-1553], ^C[0000-0003-0387-921X]

* Presenting Author

Abstract: Anisotropic friction can produce friction force which is not collinear with a sliding direction. How much friction deviates from a sliding direction is described with a so-called sliding potential or equivalently a sliding rule. A sliding potential is often described with an ellipse or a superellipse. In this paper we propose an oval curve which provides piecewise continuous mathematical description for a sliding rule and fits better to the experimental results than a typical superellipse. For an exemplary mechanical system it is shown, that an anisotropic sliding potential can lead to an unstable equilibrium position in the system. Furthermore, for what parameters the unstable equilibrium occurs differs between sliding potential models. We have tested four different geometrical models of sliding potential in this regard.

Keywords: Anisotropic friction, Sliding potential, unstable equilibrium.

1. Introduction

If a friction force has different values for different sliding direction it is called an anisotropic friction. Besides all known static and dynamic frictional effects, there is an additional one characteristic for an anisotropic friction, namely friction force direction deviates from the sliding direction. Direction of friction is described by a sliding potential [1]. Friction co-linear with sliding velocity is represented by an circular sliding potential, whereas anisotropic sliding potential, in general, can be described by any closed curve. Typically in case of orthotropic friction an ellipse or a superellipse (Lamé curve) is used. This anisotropy can cause instability in the mechanical system [2].

2. Results and Discussion

There are not many frictional pair with a significant anisotropic characteristic. Surface roughness can lead to anisotropic friction characteristic only when finite deformation take place in the contact area [3]. In our measurements we used an experimental rig (shown in the Fig. 1a) and frictional pair sample (corrugated cardboard and felt) inspired by [4]. Measurements of the friction force hodograph were taken and the sliding potential was numerically calculated (see Fig. 1b). We propose mathematical description of the potential by an oval curve. An oval mathematical description is derived from its geometrical definition used in a technical drawing (see Fig. 1c). An oval fits better to the experimental data than superellipse. What is more, it is noticed that it is better to identify a sliding rule with a difference between friction and sliding direction, then with a sliding potential curvature.

* Corresponding author e-mail: adam.wijata@p.lodz.pl

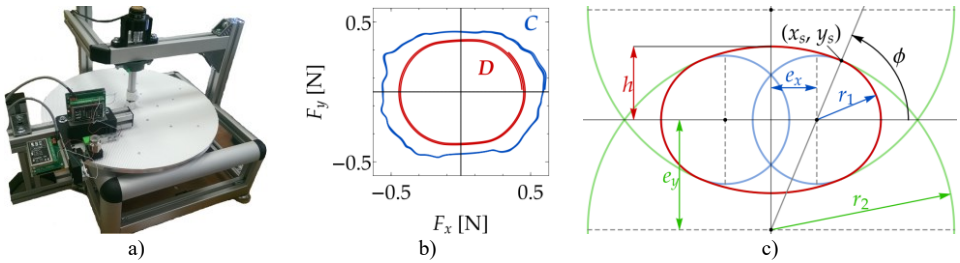


Fig. 1. a) The experimental laboratory stand; b) the measured friction characteristic (hodograph C) and the calculated sliding potential (D); c) the oval curve (red line) construction.

Four different sliding rules were compared numerically in a simulative experiments. Mechanical system with anisotropic friction shown in the Fig. 2a was considered, where specimen M is sliding over the rotating table surface. Anisotropy is described in the X_1OY_1 coordinate system and its orientation is indicated by the angle Ω . Equilibrium positions given by the radius ρ for different orientations Ω were calculated. Exemplary equilibrium trajectories $\rho(\Omega)$ for the superellipse and the oval sliding rule are shown in the Fig. 2b and 2c.

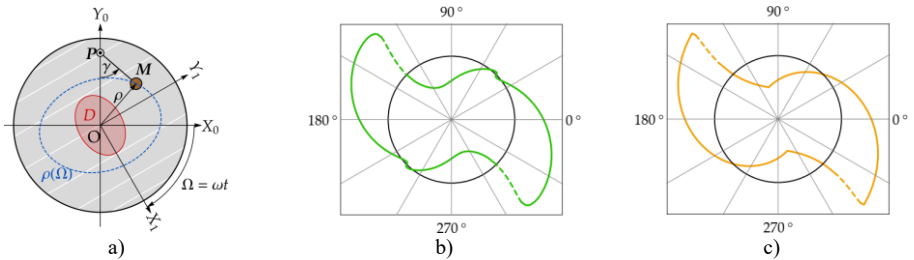


Fig. 1. The investigated mechanical system (a) and trajectories of the equilibrium position $\rho(\Omega)$ for sliding potential given by a superellipse (b) and an oval (c) (dashed line segments indicates unstable equilibrium position).

3. Concluding Remarks

Anisotropic friction force hodograph and sliding potential were measured experimentally and its mathematical description was identified. Proposed oval curve fits experimental sliding rule with the best correlations among other tested descriptions. Sliding potential influence on mechanical system dynamics was shown regarding stable and unstable equilibriums. It was shown that correct identification of mathematical description for a sliding rule can be crucial in this aspect.

References

- [1] MRÓZ Z, STUPKIEWICZ S. An anisotropic friction and wear model. *International Journal of Solids and Structures* 1994, **31**:1113-1131.
- [2] WALKER S V., LEINE RI. Set-valued anisotropic dry friction laws: formulation, experimental verification and instability phenomenon. *Nonlinear Dynamics* 2019, **96**:885-920.
- [3] STUPKIEWICZ S, LEWANDOWSKI MJ, LENGIEWICZ J. Micromechanical analysis of friction anisotropy in rough elastic contacts. *International Journal of Solids and Structures* 2014,; **51**:3931-3943.
- [4] TAPIA F, TOURNEAU D LE, GÉMINARD J-C. Anisotropic friction: assessment of force components and resulting trajectories. *EPJ Techniques and Instrumentation* 2016, **3**:1-10.

-VIB-

**VIBRATIONS OF LUMPED
AND CONTINUOUS SYSTEMS**

Elastic bearing effects on the dynamic response of bridges under high-speed moving load

Afras Abderrachid ^{1*}, El Ghoulbzouri Abdelouafi ²

1. Afras Abderrachid, Modelization, optimization and dynamics of civil engineering structures unit, National School of Applied Sciences Al Hoceima, university Abdelmalek Essaadi, Morocco.
2. El Ghoulbzouri Abdelouafi, Modelization, optimization and dynamics of civil engineering structures unit, National School of Applied Sciences Al Hoceima, university Abdelmalek Essaadi, Morocco.

*
Presenting Author

Abstract: The elastic support systems have drawn considerable attention in the field of engineering, these systems can be used to produce excellent and optimization structural elements in various engineering structures and technologies such as robotic structures, vehicles, buildings, and bridges. In this paper, the dynamic behavior of a bridge with elastic restraints at the supports and subject to a high-speed moving load are treated, the effects of different influencing parameters, like the stiffness of the supports, speed of moving load, and damping are studied. The deflection and acceleration of the bridge are investigated and discussed, the results obtained by the analytical approach show that the above-mentioned parameters play a very important role and contribute largely to the response of the bridge.

Keywords: Elastic bearing, dynamic response, moving load, resonance, bridge.

References

- [1] Yonghong Chen , C. A. Tan, L. A. Bergman, Effects of Boundary Flexibility on the Vibration of a Continuum With a Moving Oscillator (2002) ,Transactions of the ASME.
- [2] X.Q. Zhu, S.S. Law, Moving load identification on multi-span continuous bridges with elastic bearings, Journal of Sound and Vibration 312 (2008) 736–753.
- [3] Zhou Shi, Yu Hong, Shili Yang Updating boundary conditions for bridge structures using modal parameters, Engineering Structures 196 (2019) 109346.
- [4] Yang, Y. B., Lin, C. L., Yau, J. D., & Chang, D. W. (2004), Mechanism of resonance and cancellation for train-induced vibrations on bridges with elastic bearings. Journal of Sound and Vibration, 269(1-2), 345–360.
- [5] L. Fryba, Vibration of Solids and Structures under Moving Loads, Noordhoff International Publishing, Groningen, The Netherlands, 1972
- [6] J.D. Yau, Y.S. Wu, Y.B. Yang, Impact response of bridges with elastic bearings to moving loads, Journal of Sound and Vibration 248 (1) (2001) 9–30.
- [7] Qian, C. Z., Chen, C. P., Zhou, G. W., & Dai, L. M. (2012), Dynamic Response Analysis for Elastic Bearing Beam under Moving Load. Nonlinear Engineering, 1(3-4)

Stabilization of Course of Ships and Damping Vibrations Caused by Waves: Nonlinear Differential Equations Model and Optimal Control Theory

DMYTRO V ASTAYKIN¹, ANDRII V BONDARENKO¹, DMYTRO V DANYLENKO¹,
OLEG V DUBROVSKY^{2*}, AND EUGENY V. TERNOVSKY²

1. National University “Odessa Maritime Academy”, Didrikhson str. 8, 65001, Odessa

2. Odessa State Environmental University, Mathematics Depr., L’vovskaya str. 15, 65009, Odessa

* Presenting Author

Abstract: The paper is devoted to development of nonlinear differential equation model and construction of optimal control theory for stabilization of a ship’s course and damping vibrations caused by waves of the sea. The suboptimal control law is calculated within a nonlinear model of a ship’s motion. The whole system includes the master differential temporal evolution equations for the angular velocity of a ship, an angle of rotation of the rudder, yawing angle x_i . The solution is sought in the class of functions linear in x_i ; accordingly, the control law has two modes: for small x , the control is formed in a linear mode, and for large x , it is formed in a relay mode. The problem of synthesis of the relay-linear law is reduced to the determination of the area D (where there is no vibration mode) and the synthesis of the control law $u=p(t)x$. The concrete numerical data are presented for optimal control theory of stabilization of a ship’s course and damping vibrations caused by waves of the sea.

Keywords: optimal control, stabilization of a ship’s course, damping vibrations

1. Introduction.

The methods of the theory of optimal control can be effectively applied to the problems of stabilizing the course of ships and damping vibrations caused by the waves of the sea. In this paper we develop a nonlinear differential equation model and construct an optimal control theory using an advanced method of synthesis of control for concrete dynamical system [1-3].

As an input model, one could choose the advanced model of a ship motion (e.g. details in Ref [1]). Let ω be the angular velocity of a ship around the vertical axis passing through the center of mass, and β is an angle of rotation of the rudder.

Then motion along the course can be described by the standard master differential equation as follows:

$$T_2 \frac{d^2\omega}{dt^2} + T_1 \frac{d\omega}{dt} \pm \omega + d_c \omega |\omega| = k_c \left(\beta + \tau_1 \frac{d\beta}{dt} \right) + \varphi(t), \quad (1)$$

where $\varphi(t)$ is the disturbing force generated by the roughness of the sea, the plus sign in front of ω in this equation corresponds to a ship that is stable along the course, and the minus sign to an unstable one. Further let α be yawing angle, i.e.

$$d\alpha/dt=\omega. \quad (2)$$

One could suppose that a steering gear is described by the equation

$$\frac{d\beta}{dt} = \lambda\beta + bu \quad (3)$$

where u is the control signal. The characteristic limitations on the steering angle β and its angle speed $d\beta/dt$ are usually as follows: $|\beta| \leq 40^\circ$ and $|d\beta/dt| \leq 5 \text{ deg/s}$. If one imposes a limitation on the input signal $|u(t)| \leq 1$ and choose some realistic values for the parameters λ and b , then the indicated restrictions on β and $d\beta/dt$ will be satisfied for all t . Setting

$$x_1 = \alpha, x_2 = \omega, x_3 = d\omega/dt, x_4 = \beta \quad (4)$$

and combining equations (1)-(3), one could obtain the system, which finally control of a ship's course and its stabilization. If the right part of such a system does not include x_1 , therefore, the course control problem and the stabilization one at a given constant control can be described by the same model.

2. Results of Computing and Discussion

The numerical solution is sought in the class of functions linear in x_i ; accordingly, the control law has two modes: for small x , the control is formed in a linear mode, and for large x , it is formed in a relay mode. The problem of synthesis of the relay-linear law is reduced to the determination of the area D (where there is no vibration mode) and the synthesis of the control law $u=p(t)x$. As the initial step, it is necessary to calculate a suboptimal relay-linear control law for a given dynamic system under condition $\varphi(t)=0$ in Eq.(1). The next step of computing includes the task with constantly acting perturbations and analysis of the corresponding region. The wave disturbance is simulated by a linear system, which receives Gaussian white noise at the input. There are presented results of computing x_i ($i=1-4$) for different sets of technical parameters. For example, the concrete data on the stabilization processes along the coordinates x_1 and x_4 are obtained numerically, the maximum deviation in the yawing angle at a given time delay is calculated, and the effectiveness of the region application for the problem of stabilizing the ship's course was shown. one of the important conclusions of computing is that a suboptimal in time control law has a high sensitivity to the variation of the right-hand sides of the differential equations that describe the movement of the ship along the course.

3. Concluding Remarks

The synthesis of an optimal in time control for complex dynamical system is considered and numerically solved on example of the problem of stabilizing the course of ships and damping vibrations caused by the waves of the sea.

References

- [1] MOROZ A I: *Course of a System Theory*. Higher School: Moscow, 1987.
- [2] GLUSHKOV AV: *Methods of a Chaos Theory*. Astroprint: Odessa, 2012.
- [3] GLUSHKOV A, SVINARENKO A, BUYADZHI V, ZAICHKO P AND TERNOVSKY V: Chaos-geometric attractor and quantum neural networks approach to simulation chaotic evolutionary dynamics during perception process. In: BALICKI J (ED) *Advances in Neural Networks, Fuzzy Systems and Artificial Intelligence, Series: Recent Advances in Computer Engineering*. WSEAS: Gdansk, 2014, **21**:143-150.

Higher order asymptotic homogenization for dynamical problems

J. AWREJCEWICZ¹, I.I. ANDRIANOV^{2*}, A.A. DISKOVSKY³

1. Lodz University of Technology, Department of Automation, Biomechanics and Mechatronics, Lodz, Poland [0000-0003-0387-921X]
2. Rhein Energie AG, Cologne, Germany [0000-0001-6419-5423]
3. Dnipropetrovsk State University of Internal Affairs, Department of Economic and Law Security, Dnipro, Ukraine [0000-0003-1673-6437]

* Presenting Author

Abstract: In general, asymptotic homogenization methods are based on the hypothesis of perfect scale separation. In practice, this is not always the case. The problem arises of improving the solution in such a way that it becomes applicable if inhomogeneity parameter is not small. Our study focuses on the higher order asymptotic homogenization for dynamical problems. Systems with continuous and piecewise continuous parameters, discrete systems, and also continuous systems with discrete elements are considered. Both low-frequency and high-frequency vibrations are analyzed. For low-frequency vibrations, several approximations of the asymptotic homogenization method are constructed. The influence of the boundary conditions, the system parameters is investigated

Keywords: Periodically nonhomogeneous structures, dynamics, homogenization, scale separation.

1. Introduction

As noted in [1], the bulk of researches based on the asymptotic homogenization method (AHM) use hypothesis of perfect scale separation. In practice, this hypothesis not always justified. Formally, this means that the first approximation of the AHM does not provide the required accuracy. The problem arises of improving the solution in such a way that it becomes applicable for a not small value of the used inhomogeneity parameter. This conclusion is supported by the results of a number of studies. Xing and Chen [2] analysed the static problems of the periodical composite rod using different order of AHM and FEM. Numerical results show that the second approximation is necessary for accurate analysis of periodical composite structures. Kesavan [3,4] considered the Dirichlet eigenvalue problem for a second-order elliptic operator in the divergence form. Comparison with numerical solutions showed the need to take into account higher approximations. Santosa and Vogelius [5] and Moskow and Vogelius [6] studied the eigenvalue problem associated with the vibration of a composite medium with a periodic microstructure. The investigation was devoted to the first-order correction to the homogenized eigenvalues. It is shown that for the Dirichlet problem, the interaction of the periodic microstructure with the boundary of the medium must be taken into account. The first order Neumann eigenvalue corrections are always zero in one dimension. It vaguely of phenomenon that is reminiscent a frequently occurs in connection with spectral approximation for self adjoint operators: the error in the eigenvalue order is square energy norm error in a corresponding eigenvector [5]. Our study focuses on the higher order asymptotic homogenization for dynamical problems. For systems with continuous and piecewise continuous parameters, discrete systems, and continuous systems with discrete elements, explicit expressions for the second approximations for eigenvalues are constructed.

2. Results and Discussion

Consider for example the eigenvalue Neumann problem

$$\frac{d}{dx} \left[a \left(\frac{x}{\varepsilon} \right) \frac{du}{dx} \right] + pu = 0, \quad a \left(\frac{x}{\varepsilon} \right) = a \left(\frac{x}{\varepsilon} + 1 \right), \quad (1)$$

$$\frac{du}{dx} = 0 \quad \text{at } x=0, x=1. \quad (2)$$

Going over to fast $\eta = \varepsilon^{-1}x$ and slow x variables we seek solution of Neuman problem (1), (2) as follows

$$u = u_0(x) + \varepsilon u_1(\eta, x) + \varepsilon^2 u_2(\eta, x) + \dots, \quad p = p_0 + \varepsilon p_1 + \varepsilon^2 p_2 + \dots \quad (3)$$

Using higher order AHM we obtain

$$p_0 = \pi^2 n^2 \tilde{a}, \quad \tilde{a} = \left[\int_0^1 a^{-1} d\eta \right]^{-1}, \quad (4)$$

$$p_1 = 0, \quad p_2 = \pi^2 n^2 p_0 \left[\tilde{a} \int_0^1 (a^{-1} \int_0^\eta u_{11}(\eta) d\eta) d\eta - \int_0^1 (u_{11}(\eta) d\eta) d\eta \right], \quad (5)$$

$$u_{11} = 0.5 - \eta + \tilde{a} \left[\int_0^\eta a^{-1} d\eta - \int_0^1 (a^{-1} d\eta) d\eta \right].$$

For piecewise-continuous function $a(\eta) = E^{in}$, $0 \leq \eta \leq c$, E^m , $c \leq \eta \leq 1$ (4), (5) yield [7]

$$p_0 = \pi^2 n^2 \frac{E^{in} E^m}{(1-c)E^{in} + cE^m}, \quad p_1 = 0, \quad p_2 = -\pi^2 n^2 p_0 \frac{c^2 (1-c)^2 (E^{in} - E^m)^2}{12 [(1-c)E^{in} + cE^m]^2}. \quad (6)$$

The area of applicability of the obtained solution are determined by the relation $n \ll \varepsilon^{-1}$.

3. Concluding Remarks

Continuous and piecewise continuous parameters, discrete systems, and also continuous systems with discrete elements are considered. Both low-frequency and high-frequency vibrations are analyzed. The use of one- and two-point Padé approximants is proposed to improve the results accuracy.

References

- [1] AMEEN MM, PEERLINGS RHJ, GEERS MGD: A quantitative assessment of the scale separation limits of classical and higher-order asymptotic homogenization. *European Journal of Mechanics-A/Solids* 2018, **71**:89–100.
- [2] XING YF, CHEN L: Accuracy of multiscale asymptotic expansion method. *Composite Structures* 2014, **112**:38–43.
- [3] KESAVAN S: Homogenization of elliptic eigenvalue problems. I. *Applied Mathematics and Optimisation* 1979, **5**(2):153-167.
- [4] KESAVAN S: Homogenization of elliptic eigenvalue problems. I. *Applied Mathematics and Optimisation* 1979, **5**(3):197-216.
- [5] SANTOSA F, VOGELIUS M: First-order corrections to the homogenized eigenvalues of periodic composite medium. *SIAM Journal on Applied Mathematics* 1993, **53**(6):1636-1668; Erratum: *Ibid* 1995, **55**(3):684.
- [6] MOSKOW SH, VOGELIUS M: First order corrections to the homogenized eigenvalues of a periodic composite medium. The case of Neumann boundary conditions. Preprint, 1996.
- [7] ANDRIANOV IV, AWREJCEWICZ J, DANISHEVSKYY VV: *Linear and Nonlinear Waves in Microstructured Solids: Homogenization and Asymptotic Approaches*. CRC Press, Taylor & Francis: Boca Raton, 2021.

Nonlocal Effects on the Dynamics of Carbon Nanotubes

BISWAJIT BHARAT^{1*}, K. R. JAYAPRAKASH¹

¹ Indian Institute of Technology Gandhinagar

Abstract: The present work is devoted to the study of dynamics of single-walled carbon nanotube (SWCNT). The study invokes Sanders-Koiter's thin shell theory in modelling the CNT. Eringen's theory is considered to incorporate nonlocal effects. Closed-form normal mode solutions are presented for varying aspect ratios, boundary conditions and chiralities. Atomistic simulations are considered to corroborate the nonlocal effects on normal modes of SWCNTs.

Keywords: SWCNT, Sanders-Koiter's shell theory, Eringen's nonlocal theory

1. Introduction

With the discovery of CNTs in the mid 1990s [1], the synthesis and characterization of CNTs have attracted the attention of physicists, material scientists and chemical engineers. CNTs find applications, to name a few [2], in material strengthening, hydrogen storage, FETs. The mechanical properties of CNTs are orders of magnitude higher than those of the bulk materials. To this end, the structural and dynamical properties of these structures are important in predictive design of systems using these nano structures. Due to the spatial scale of nano structures, the experimental study poses a challenge. However, mechanics of CNTs has been studied invoking the density functional theory (DFT), atomistic simulations and continuum theory [3]. Computational studies are expensive as well owing to their response time scales of the order of nanoseconds or lower. It is obvious that these contrasting modelling techniques are better applicable at different length/time scales. Many researchers have studied the vibration of CNTs using 1-D, 2-D (beam, rod) models. These models are accurate at low frequencies, whereas high frequency responses are seen to be affected by the nonlocal effects. To explore the behaviour of SWCNTs at intermediate/high frequencies, a 3-D continuum model [5] is considered here.

Relatively few analytical works have dwelled on the 3-D structural dynamics of the CNTs. Recent studies by Strozzi et. al. [5] consider reduced-order shell model by neglecting the normal and tangential shear strain of the shell's mid surface thereby limiting its applicability for wider frequency range. The objective herein is to study the behaviour of SWCNTs in a broad frequency range and by incorporating nonlocal effects due to Eringen [6]. The nondimensional evolution equations of a cylindrical thin shell (Fig. 1) is [5, 6]

$$\alpha u_{xx} + \frac{(4 + \beta^2)(1 - \mu)}{8} u_{\theta\theta} + \alpha \left\{ \left(\frac{(1 + \mu)}{2} + \frac{3\beta^2(\mu - 1)}{8} \right) v_{x\theta} + \mu w_x + \frac{\beta^2(1 - \mu)}{2} w_{\theta\theta x} \right\} = u_{tt} + \gamma \left(\frac{u_{\theta\theta tt}}{\alpha^2} + u_{xxtt} \right) \quad (1a)$$

$$\alpha \left(\frac{(1 + \mu)}{2} + \frac{3\beta^2(\mu - 1)}{8} \right) u_{x\theta} + \alpha^2 \left(\frac{1}{2} + \frac{9\beta^2}{8} \right) (1 - \mu) v_{xx} + (1 + \beta^2) v_{\theta\theta} + w_\theta - \beta^2 w_{3\theta} + \frac{(\mu - 3) \beta^2 \alpha^2}{2} w_{xx\theta} = v_{tt} + \gamma \left(\frac{v_{\theta\theta tt}}{\alpha^2} + v_{xxtt} \right) \quad (1b)$$

$$\alpha \mu u_x + \frac{\alpha \beta^2 (1 - \mu)}{2} u_{\theta\theta x} + v_\theta - \beta^2 v_{3\theta} + \frac{(\mu - 3) \beta^2 \alpha^2}{2} v_{xx\theta} + w + \beta^2 (\alpha^4 w_{4x} + 2\alpha^2 w_{xx\theta\theta} + w_{4\theta}) = -w_{tt} - \gamma \left(\frac{w_{\theta\theta tt}}{\alpha^2} + w_{xxtt} \right) \quad (1c)$$

where u, v, w are axial, angular and radial deformation respectively, $\alpha = R/L$, R is the radius, L is the characteristic macroscopic length, $\beta = h/(R\sqrt{12})$, h is the effective thickness, μ is the Poisson's ratio, $\gamma = (e_0 a/L)^2$ is the parameter describing the nonlocal effects, e_0 is the nonlocal constant [6], a is the characteristic atomistic length and $u_{4\theta} = u_{\theta\theta\theta\theta}$, $u_{x\theta} = \partial^2 u/\partial x \partial \theta \dots$.

2. Results and Discussion

We herein explore normal mode solutions, i.e., time periodic synchronous oscillations. Additionally, imposing periodic boundary condition (BC) with periodicity $m \in \mathbb{Z}$ in the circumferential direction, Eq. (1) are reduced to a set of ordinary differential equations in x . Upon solving the eigenvalue problem with appropriate BCs, an eighth order polynomial equation in axial wavenumber k is obtained. One among the eight wavenumbers is shown in Fig. 2 as function of frequency and revealing the effect of increasing nonlocal parameter. The nonlocal effects on the normal modes for various boundary conditions are considered in this work and will be presented in the full version of the paper with exhaustive comparison with the full-scale atomistic simulations.

3. Concluding Remarks

In this work, we study the nonlocal effects on the normal modes of a finite CNT. The nonlocality has significant effect on the characteristics of the normal modes. Exact analytic solutions for a wide frequency range are obtained. The analytic solutions obtained form the basis for exploring nonlinear modal interaction of CNTs and energy localization thereof. Further analysis and comparisons with full-scale atomistic simulations will be reported in the full version of the paper.

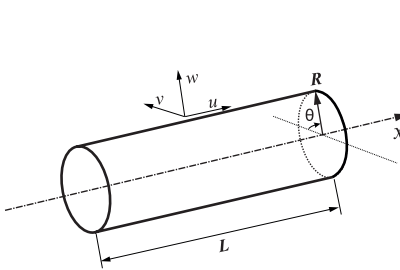


Fig. 1. Kinematics of a flexible CNT of radius R and length L

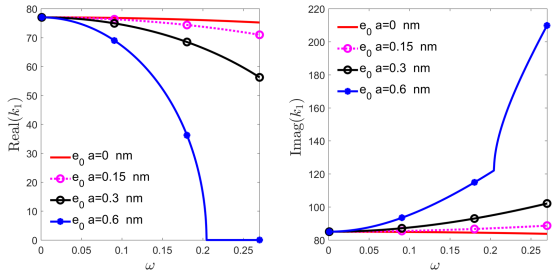


Fig. 2. Wave number v /s natural frequency for varying nonlocal parameter for $\alpha = 0.0392$, $\beta = 0.048$, $\mu = 0.19$

Acknowledgment: Authors acknowledge the DST-RFBR funding INT/RUS/RFBR/358

References

- [1] IJIMA, SUMIO. Helical microtubules of graphitic carbon. *Nature* 354.6348 (1991): 56-58.
- [2] S, SCHODEK, DANIEL L., PAULO FERREIRA, AND MICHAEL F. ASHBY. *Nanomaterials, nanotechnologies and design: An introduction for engineers and architects*. Butterworth-Heinemann, 2009.
- [3] TADMOR, ELLAD B., AND RONALD E. MILLER. *Modeling materials: continuum, atomistic and multiscale techniques*. Cambridge University Press, 2011.
- [4] KHANIKI, HOSSEIN BAKHSHI, AND MERGEN H. GHAYESH. A review on the mechanics of carbon nanotube strengthened deformable structures. *Engineering Structures* 220 (2020): 110711.
- [5] STROZZI, M., MANEVITCH, L. I., PELLICANO, F., SMIRNOV, V. V., AND SHEPELEV, D. S. Low-frequency linear vibrations of single-walled carbon nanotubes: Analytical and numerical models. *Journal of Sound and Vibration* 333.13 (2014): 2936-2957.
- [6] GOPALAKRISHNAN, SRINIVASAN. *Wave propagation in materials and structures*. CRC Press, 2016.

Non-synchronous vibration in a bistable system induced by FSI

MIROSLAV BYRTUS^{1*}

1. Department of Mechanics, Faculty of Applied Sciences, University of West Bohemia [0000-0003-3964-1828]

* Presenting Author, email: mbyrtus@kme.zcu.cz

Abstract: The aim is paid at the analysis of non-synchronous vibration along with frequency lock-in phenomena of a geometrically nonlinear bistable system induced by a reduced model of fluid-structure interaction.

Keywords: non-synchronous vibration, lock-in, bifurcation, bistable system

1. Introduction

The fluid-structure interaction (FSI) arises when an elastic structure interacts with the embracing fluid flow. In general, the FSI is a very complex process that requires highly sophisticated approaches from the mathematical and computational point of view. A particular case of FSI in which an alternate shedding of vortices forms the vibration of the structure is called a Vortex-Induced Vibration (VIV). The natural vortex shedding frequency is dependent on the velocity of the flow [1]. The vortex shedding exerts a periodic unsteady force on the body. As the vortex shedding frequency approaches the natural frequency of the body, the two frequencies could lock-in for a small range of the velocity flow, e.g. see [2-3]. The vibration connected with the lock-in phenomenon is often called a Non-Synchronous Vibration (NSV), which were observed in real applications [4]. Here, we deal with dynamic response of VIV of a single structural profile which can possess two stable equilibria. To model the FSI, a reduced, non-dimensional model is employed [4] and the resulting mathematical model can be written as follows

$$\begin{bmatrix} 1 & m_{as} \\ m_{sa} & 1 \end{bmatrix} \begin{bmatrix} \ddot{\phi} \\ \ddot{x} \end{bmatrix} + \begin{bmatrix} -2D_{aa}\Omega_{aa} & c_{as} \\ c_{sa} & 2D_{ss}\Omega_{ss} \end{bmatrix} \begin{bmatrix} \dot{\phi} \\ \dot{x} \end{bmatrix} + \begin{bmatrix} \Omega_{aa}^2 & k_{as} \\ k_{sa} & \Omega_{ss}^2 + 2\Omega_b^2 \end{bmatrix} \begin{bmatrix} \phi \\ x \end{bmatrix} = \begin{bmatrix} -2D_{aa}\Omega_{aa}c_{asl}\phi^2\dot{\phi} \\ 2\Omega_b^2 \frac{l_0}{\sqrt{h^2 + x^2}} \end{bmatrix}, \quad (1)$$

where the first equation describes the fluid-flow wake excitation employing the van der Pol term. The second equation corresponds to the structural behaviour and incorporates the geometric nonlinearity (see Fig. 1, left). All parameters are in detail described in [5].

2. Results and Discussion

The response of the structure is investigated in dependence on the vortex-shedding frequency Ω_{aa} . Here, two cases are analysed: (i) mono-stable nonlinear structure, i.e. $l_0/h=1$ and (ii) bistable nonlinear structure, i.e. $l_0/h>1$. These two systems have qualitatively different dynamical response. The system (i) shows NSV in main resonance and subharmonic areas which are accompanied by

frequency lock-ins (see Fig. 1 top, the curves shows the response for $\Omega_b = 0, 0.3, 0.5, 0.7, 0.9$). Increasing changes the hysteresis region and shifts the lock-in frequency higher frequencies.

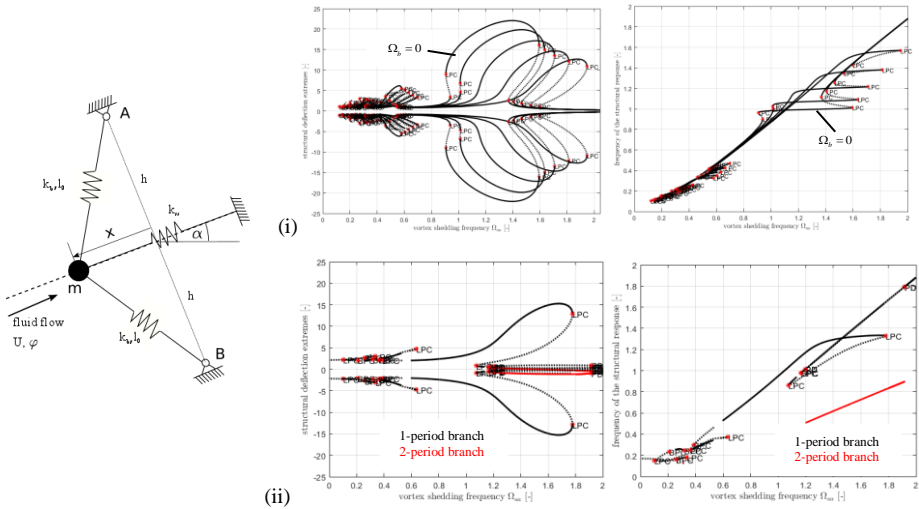


Fig. 1. Scheme of 1 DoF structural system, amplitude and frequency plots representing lock-in and non-synchronous vibration for $l_0/h=1$ (top) and $l_0/h=2.5$ (bottom)

Regarding the system (ii), the NSV area contains 2-period stable solution with significantly smaller amplitude (red colour). The frequency lock-in, which is present and which is connected with 1-period solution, should not be employed because of the high-energy level.

3. Concluding Remarks

Using a phenomenological model (1), the mechanism of NSV accompanied by frequency lock-in is numerically investigated. It can be seen, that the bistability changes qualitative properties of the dynamic response especially in the main harmonic area which can lead to vibration mitigation.

Acknowledgment: This work was supported by the GA CR project No. 20-26779S "Study of dynamic stall flutter instabilities and their consequences in turbomachinery application using mathematical, numerical and experimental methods".

References

- [1] PŮST L, PEŠEK L, BYRTUS M: Modelling of flutter running waves in turbine blades cascade, *Journal of Sound and Vibration* **436** 286-294
- [2] DE LANGRE E: Frequency lock-in is caused by coupled-mode flutter, *Journal of Fluids and Structures* **22**(6) 783-791. Bluff Body Wakes and Vortex-Induced Vibrations (BBVIV-4)
- [3] HOSKOTI L, MISRA A, SUCHEENDRAN M: Frequency lock-in during vortex induced vibration of a rotating blade, *Journal of Fluids and Structures* **80** 145-164
- [4] CLARK S T, KIELB R E, HALL K C: A van der pol based reduced-order model for non-synchronous vibration in turbomachinery, In *Proceedings of ASME Turbo Expo 2013 GT 2013*, San Antonio, Texas
- [5] BYRTUS M, DYK Š, HAJŽMAN M: Non-synchronous vibration and lock-in regimes in coupled structures using reduced models. *Proceedings of the ASME 2021, IDETC/CIE 2021*

Design of an Optimum Tuned Mass Damper for Cantilever Beam Response Reduction

HUSEYIN CETIN¹, BAKI OZTURK², MACIEJ DUTKIEWICZ^{3*} AND ERSIN AYDIN¹

¹ Department of Civil Engineering, Nigde Omer Halisdemir University, Nigde, Turkey,

² Department of Civil Engineering, Hacettepe University, Ankara, Turkey,

³ Faculty of Civil, Environmental Engineering and Architecture, University of Science and Technology, 85-796 Bydgoszcz, Poland.

* Presenting Author

Abstract: The optimal design of a tuned mass damper (TMD) in the frequency domain is investigated in this paper to reduce the dynamic response of a cantilever beam. The random vibration theory is used to determine the mean square acceleration of the cantilever beam's end point as the objective function to be reduced. Furthermore, a Differential Evolution (DE) optimization approach is used to estimate the ideal TMD coefficient of mass, stiffness, and damping. These parameters' upper and lower limit values are considered. Most of the past research has focused on determining TMD stiffness and damping characteristics. This study does, however, include optimization of TMD mass parameters to calculate the mass quantity. Furthermore, the DE method, a stochastic optimization algorithm, is underutilized for optimizing TMD parameters. As a result, this approach is utilized on the goal function to find optimal TMD settings. Following this optimization, tests are carried out on the cantilever beam with TMD system, using harmonic base excitations that resonant the beam's foremost modes and white noise excitation. In terms of optimum TMD design, the proposed method is extremely practical and successful. The response of a cantilever beam under dynamic interactions is significantly reduced when a TMD is constructed properly.

Keywords: cantilever beam, vibration control, tuned mass damper, transfer function, differential evolution

References

- [1] AYDIN E., DUTKIEWICZ M., ÖZTÜRK B., SONMEZ M. OPTIMIZATION OF ELASTIC SPRING SUPPORTS FOR CANTILEVER BEAMS. STRUCT MULTIDISC OPTIM 62, 55–81 2020. [HTTPS://DOI.ORG/10.1007/S00158-019-02469-3](https://doi.org/10.1007/S00158-019-02469-3).
- [2] PRZEMIENIECKI J.S., THEORY OF MATRIX STRUCTURAL ANALYSIS, MCGRAW-HILL, NEW YORK, 1968.

- [3] TAKEWAKI I., "OPTIMAL DAMPER POSITIONING IN BEAMS FOR MINIMUM DYNAMIC COMPLIANCE", COMPUT. METHOD. APPL. MECH. ENG., 156, 363-373, 1998.
- [4] SON J.H. AND KWAK B.M., "OPTIMIZATION OF BOUNDARY CONDITIONS FOR MAXIMUM FUNDAMENTAL FREQUENCY OF VIBRATING STRUCTURES", AIAA J., 31(12), 2351-2357, 1993

Analytical and finite element models of nonlinear dynamic behaviour of bi-material beam

SIMONA DONEVA^{1,2*}, JERZY WARMINSKI¹, EMIL MANOACH²

¹*Department of Applied Mechanics, Lublin University of Technology, Lublin, Poland*
[0000-0002-5386-9063], [0000-0002-9062-1497]

²*Institute of Mechanics, Bulgarian Academy of Sciences, Sofia, Bulgaria*
[0000-0002-9571-8618]

Keywords: bi-material beam, nonlinear vibrations, Timoshenko beam theory, thermoelasticity, finite element modelling.

Abstract:

The goal of the present work is to develop a theoretical model allowing analytical and numerical study of bi-materials beams subjected to dynamic mechanical and thermal loads. The model is based on geometrically nonlinear version of the Timoshenko beam theory. The extended equations of motions of vibrating beams at elevated temperature are studied analytically by the harmonic balance method and resonance curves for different parameters of the mechanical and thermal loading are obtained. The coupled vibrations of the beam are studied by using 3D finite element analysis.

1. Introduction

Being used in so many technological areas, the bi-material beams are often subjected to mechanical and thermal loading. In many cases such loads lead to large, geometrically nonlinear vibrations. The problems of thermoelastic vibrations of structures are studied by many authors. Nonlinear dynamics of composite plate have been studied in [1], suggesting a temperature distribution along the plate thickness. In [2] thermo-mechanical, geometrically nonlinear vibrations of plates are studied. The authors found very reach nonlinear dynamic behaviour of the system Uncoupled and coupled vibrations of bi-material beams were recently studied by numerical approaches in [3].

In the present work the dynamic behaviour of a bi-material beam subjected to harmonic forces and thermal loading (elevated temperature or heat flux acting on the beam surface) is analysed by using numerical and analytical approaches.

2. Problem formulation and research methods

Nonlinear thermoelastic vibrations of a clamped-clamped Timoshenko beam are studied in the paper. The mathematical model of the beam is derived taking into account geometric nonlinearities. Using the classical dynamic equilibrium method, the differential equations of motion of the bi-material Timoshenko beam are defined. The problem is studied using two different approaches. In the first approach a three-dimensional finite element model of the beam is created using the commercial software ANSYS. The nonlinear vibrations of a heated beam, as well as the vibration of the beams subjected to heat flux are analysed. It is shown that the increased temperature has a significant impact on the beam's reaction and it can cause the beam to oscillate in a complex way (see **Fig.1**).

The second approach is based on a reduced model of the beam dynamics. The Galerkin approach is used to transform the nonlinear partial differential equations into ordinary differential equations. Then the harmonic balance method (HBM) is applied to the reduced model, taking into account the first vibration mode. By this method the reduced nonlinear one-degree of freedom model with cubic non-linearity and temperature influence is studied analytically. By the HBM the resonance curves are determined from the analytically obtained modulation equations and the stability analysis is done.

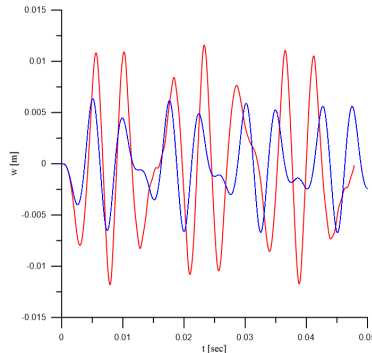


Fig. 1. Time history of the beam centre subjected to uniformly distributed load harmonic load $p=p_0\sin(\omega_c t)$ with $p_0=105$ kPa and $\omega_c=160.78$ Hz. obtained by 3D FE model . Blue line – $\Delta T=0$, red line – $\Delta T=50$

3. Conclusions

The paper investigates the bi-material beam model resulting from the extended nonlinear Timoshenko beam theory. The dynamic behavior of a geometrically nonlinear Timoshenko beam model under the combined action of mechanical and thermal load, studied by two different approaches shows a good agreement. It has been shown that the increase of thermal loading also for low mechanical excitations may lead to system's complex dynamics.

Acknowledgments:

The first author acknowledges the financial support by a project "International third-cycle studies in the discipline of Mechanics carried out at the Lublin University of Technology" no. POWR.03.02.00-00-I017 / 16

The first and the third author are grateful for the financial support from the Bulgarian Ministry of Education and Science, Grant No. D01-221/03.12.2018 for NCDSC – part of the Bulgarian National Roadmap on RIs.

References

- [1] SAETTA E, REGA G, Unified 2D continuous and reduced order modeling of thermomechanically coupled laminated plate for nonlinear vibrations. *Meccanica* 49 (8), 1723–1749 ,2014
- [2] AMABILI M, CARRA S, Thermal effects on geometrically nonlinear vibrations of rectangular plates with fixed edges, *Journal of Sound and Vibration* 321, 2, 936-954 ,2009
- [3] MANOACH E, DONEVA S, WARMINSKI J, Coupled, thermo-elastic, large amplitude vibration of bi-material beams, in H. Altenbach et al. (eds) , *Analysis of Shells, Plates and Beams, Advanced Structured Materials* 134, pp 227-242. Springer Nature Switzerland AG 2020

On the Surface Anti-Plane Waves in Media with Initial Surface Stresses

VICTOR A. EREMEYEV^{1,2,3*}

1. Gdansk University of Technology, Gdansk, Poland [ORCID]

2. University of Cagliari, Cagliari, Italy

3. Don State Technical University, Rostov on Don, Russia

* Presenting Author

Abstract: We discuss the propagation of surface waves in an elastic half-space with surface stresses modelled within the framework of the Gurtin-Murdoch surface elasticity. The main attention is paid to the analysis of initial surface stresses. To this end we consider the linearized surface elasticity model. The analysis of initial stretching/compression on the dispersion relation is provided.

Keywords: surface elasticity, Gurtin-Murdoch model, anti-plane surface wave, initial stresses, non-linear elasticity

1. Introduction

Nowadays it is well-established that the surface elasticity may capture a deviation of the material properties at small scales, see e.g. [1-3]. One of the most used model of surface elasticity was proposed by Gurtin and Murdoch [4, 5]. From the physical point of view this model describes finite deformations of an elastic solid body with attached elastic membrane. In particular, this model can forecast size-effects [1-3]. It was also shown that within this model such new phenomenon as anti-plane surface wave may exist. The analysis of influence of surface stresses on surface waves within various models was given in [6-10], see also the references therein.

The aim of the lecture is consider the influence of the initial surface stresses on the dispersion relations which relate the phase velocity to a wave number.

2. Results and Discussion

Following [6] we formulate the boundary-value problem for an elastic half-space with surface stresses. Here we introduce independently constitutive relations in the bulk and on the surface. The latter include initial surface strains. For the analysis of infinitesimal waves we provide the linearization of the problem. As a result, we get a linearized boundary-value problem which essentially depends on the initial surface strains.

Using the approach similar to [6, 10] we consider harmonic solution in the form

$$u(x, z, t) = U(x, z) \exp(i\omega t), \quad (1)$$

where u is a infinitesimal displacement, x, z are Cartesian coordinates in the current placement, t is time, and ω is a frequency. After solution we obtain a dispersion relation in the form

$$D(k, \omega; \lambda_1, \lambda_2) = 0, \quad (2)$$

where k is a wave number and λ_1, λ_2 are initial principal surface stretch parameters. We provide a detailed parametric analysis of Eq. (2).

3. Concluding Remarks

We have shown that initial (residual) surface stresses may essentially affect the dispersion relation for the anti-plane surface waves. In particular, some surface instabilities may occur which block the propagation of surface waves.

Acknowledgment: Author acknowledges the support of the Government of the Russian Federation (contract No. 14.Z50.31.0046).

References

- [1] DUAN, H. L., WANG, J., KARIHALOO, B. L.: Theory of elasticity at the nanoscale. *Advances in Applied Mechanics*, 2008, **143**:1-68.
- [2] WANG, J., HUANG, Z., DUAN, H., YU, S., FENG, X., WANG, G., ZHANG, W., WANG, T.: Surface stress effect in mechanics of nanostructured materials. *Acta Mechanica Solida Sinica* 2011, **24**:52-82.
- [3] EREMEYEV, V. A.: On effective properties of materials at the nano- and microscales considering surface effects. *Acta Mechanica* 2016, **227**(1):29-42.
- [4] GURTIN, M. E., MURDOCH, A. I.: A continuum theory of elastic material surfaces. *Archive of Rational Mechanics and Analysis* 1975, **57**(4):291-323.
- [5] GURTIN, M. E., MURDOCH, A. I.: Surface stress in solids. *International Journal of Solids and Structures* 1978, **14**(6):431-440.
- [6] EREMEYEV, V. A., ROSI, G., NAILI, S.: Surface/interfacial anti-plane waves in solids with surface energy. *Mechanics Research Communications* 2016, **74**:8-13.
- [7] EREMEYEV, V. A., ROSI, G., NAILI, S.: Comparison of anti-plane surface waves in straingradient materials and materials with surface stresses. *Mathematics and Mechanics of Solids* 2018, **24**: 2526–2535.
- [8] EREMEYEV, V. A., SHARMA, B. L.: Anti-plane surface waves in media with surface structure: Discrete vs. continuum model. *International Journal of Engineering Science* 2019, **143**:33-38.
- [9] EREMEYEV, V. A., ROSI, G., NAILI, S.: Transverse surface waves on a cylindrical surface with coating. *International Journal of Engineering Science* 2020, **147**: 103188.
- [10] EREMEYEV, V. A.: Strongly anisotropic surface elasticity and antiplane surface waves. *Philosophical Transactions of the Royal Society A*. 2020, **378**(2162):20190100.

Analytical investigation of a mechanical system containing a spherical pendulum and a fractional damper

JAN FREUNDLICH^{1*}, DANUTA SADO²

1. Warsaw University of Technology, Faculty of Automotive and Construction Machinery Engineering, Warsaw, Poland [ORCID 0000-0002-0398-3271]
2. Warsaw University of Technology, Faculty of Automotive and Construction Machinery Engineering, Warsaw, Poland

* Presenting Author

Abstract: The presented work deals with a three degree of freedom system with a spherical pendulum and a damper of the fractional type. The system consists of a block suspended from a linear spring and a fractional damper, and a spherical pendulum suspended from the block. The viscoelastic properties of the damper are described using the Riemann-Liouville fractional derivative. The fractional derivative of an order of $0 < \alpha \leq 1$ is assumed. The nonlinear behaviour of the system in the vicinity of the internal and external resonances is studied. The multiple scales method has been used to obtain an approximate analytical solution to the studied system. The impact of a fractional order derivative on the dynamical behaviour of the system has been studied.

Keywords: spherical pendulum, fractional damping, nonlinear vibrations, multiple scale method,

1. Introduction

The presented work deals with a three degree of freedom system with a spherical pendulum and a damper of the fractional type. This work is a continuation of the authors' previous work [1]. The effect of fractional damping on the dynamic properties of a coupled mechanical system with a spherical pendulum is examined. It is assumed that the spherical pendulum is suspended to the block mass, which is excited harmonically in the vertical direction (Fig. 1). The oscillator contains a linear spring and a damper of a fractional type. The body of mass m_1 is subjected to the harmonic vertical excitation $F(t) = P \cos vt$.

The investigated system (Fig. 1) can be described by dimensionless equations of motion [1]. For small oscillations, after transformations the equations of motion can be written down in the form

$$\ddot{z} - a\ddot{\theta} \left(1 - \frac{\phi^2}{2}\right) \left(\theta - \frac{\theta^3}{6}\right) - a\dot{\phi} \left(\phi - \frac{\phi^3}{6}\right) \left(1 - \frac{\theta^2}{2}\right) = p \cos(\mu_1 \tau) + a \left[\dot{\phi}^2 \left(1 - \frac{\phi^2}{2}\right) \left(1 - \frac{\theta^2}{2}\right) - 2\dot{\phi}\dot{\theta} \left(\phi - \frac{\phi^3}{6}\right) \left(\theta - \frac{\theta^3}{6}\right) - \dot{\theta}^2 \left(1 - \frac{\phi^2}{2}\right) \left(1 - \frac{\theta^2}{2}\right) \right] - \gamma \dot{z}^{(\alpha)} - z \quad (1)$$

$$-\ddot{z} \left(1 - \frac{\phi^2}{2}\right) \left(\theta - \frac{\theta^3}{6}\right) + \ddot{\theta} \left(1 - \frac{\phi^2}{2}\right)^2 = 2\dot{\theta}\dot{\phi} \left(1 - \frac{\phi^2}{2}\right) \left(\phi - \frac{\phi^3}{6}\right) - \beta^2 \left(1 - \frac{\phi^2}{2}\right) \left(\theta - \frac{\theta^3}{6}\right) \quad (2)$$

$$-\ddot{z} \left(\phi - \frac{\phi^3}{6}\right) \left(1 - \frac{\theta^2}{2}\right) + \ddot{\phi} = -\dot{\theta}^2 \left(1 - \frac{\phi^2}{2}\right) \left(\phi - \frac{\phi^3}{6}\right) - \beta^2 \left(\phi - \frac{\phi^3}{6}\right) \left(1 - \frac{\theta^2}{2}\right) \quad (3)$$

where $\dot{f}^{(\alpha)}(\cdot)$ is the Riemann-Liouville fractional derivative defined as [2]

$$\dot{f}^{(\alpha)}(t) \equiv \frac{d^\alpha}{dt^\alpha} f(t) \equiv \frac{1}{\Gamma(1-\alpha)} \frac{d}{dt} \int_0^t \frac{f(\tau) d\tau}{(t-\tau)^\alpha}, \quad 0 < \alpha \leq 1 \quad (4)$$

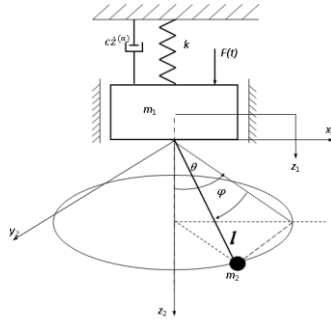


Fig. 1. Schematic diagram of the system [1]

The multiple scales method is used to find the approximate solution to the equations of motion of the system (1-3). We introduce independent variables $\{T_0, T_1, T_2 \dots\} = \{\tau, \varepsilon\tau, \varepsilon^2\tau \dots\}$ and parameters $\gamma = \varepsilon\tilde{\gamma}$, $p = \varepsilon^2\tilde{p}$. The solution can be represented by

$$z(t) = \varepsilon z_1 + \varepsilon^2 z_2 + \varepsilon^3 z_3 + \dots, \quad \theta(t) = \varepsilon \theta_1 + \varepsilon^2 \theta_2 + \varepsilon^3 \theta_3 + \dots, \quad \phi(t) = \varepsilon \phi_1 + \varepsilon^2 \phi_2 + \varepsilon^3 \phi_3 + \dots \quad (5)$$

Substituting the equations (5) into equations (1-3) we obtain

For ε^1

$$D_0^2(z_1) + z_1 = 0, \quad D_0^2(\theta_1) + \beta^2 \theta_1 = 0, \quad D_0^2(\phi_1) + \beta^2 \phi_1 = 0 \quad (6)$$

For ε^2

$$\begin{aligned} D_0^2(z_2) + z_2 = & -2D_0D_1(z_1) + aD_0^2(\theta_1)\theta_1 + aD_0^2(\phi_1)\phi_1 + \tilde{p}\cos(\mu_1\tau) - \tilde{\gamma}D_0^\alpha(z_1) + a\left((D_0^2(\phi_1))^2 - (D_0^2(\theta_1))^2\right) \\ D_0^2(\theta_2) + \beta^2\theta_2 = & -2D_0D_1(\theta_1) + D_0^2(z_1)\theta_1, \quad D_0^2(\phi_2) + \beta^2\phi_2 = -2D_0D_1(\phi_1) + D_0^2(z_1)\phi_1 \end{aligned} \quad (7)$$

Next, substituting solution to the equations (5) into equations (6) and eliminating terms that produce secular terms we obtain conditions $2\beta = 1$, $\mu_1 = 1$, $1 - \beta = \beta$. Next, we introduce $1 - \beta = \beta + \varepsilon\sigma_2$, $\mu_1 = 1 + \varepsilon\sigma_1$, $\varepsilon T_0 = T_1$, and we investigate a steady-state solution.

3. Concluding Remarks

The impact of the order of the fractional derivative on small nonlinear oscillation of the system containing a spherical pendulum has been studied. The performed analysis show that use of the fractional damping has an impact on the small oscillation of the system.

References

- [1] FREUNDLICH J, SADO D: Dynamics of a coupled mechanical system containing a spherical pendulum and a fractional damper. *Meccanica* 2020, **55**:2541-2553.
- [2] PODLUBNY I: *Fractional Differential Equations*. Academic Press: San Diego, 1999.

The effect of damping on the energy transfer in the spherical pendulum with fractional damping in a pivot point

JAN FREUNDLICH^{1*}, DANUTA SADO²

1. Warsaw University of Technology, Faculty of Automotive and Construction Machinery Engineering, Warsaw, Poland [ORCID 0000-0002-0398-3271]

2. Warsaw University of Technology, Faculty of Automotive and Construction Machinery Engineering, Warsaw, Poland

* Presenting Author

Abstract: Nonlinear vibrations of a system with three degrees of freedom with a spherical pendulum are investigated. The system contains an oscillator and a spherical pendulum suspended from the oscillator. The damping at the pendulum pivot point is assumed to be modelled by a fractional derivative. The viscoelastic damping properties are described using the fractional Caputo derivative of order $0 < \alpha \leq 1$. Vibrations in the vicinity of the internal and external resonance are considered. The effect of the order of the fractional derivative on the vibrations of the autoparametric system is studied. Responses of the system, the internal and external resonance, bifurcation diagrams, Poincaré maps and the Lyapunov exponents have been calculated for various orders of fractional derivatives. Chaotic motion has been found for some system parameters.

Keywords: spherical pendulum, fractional damping, nonlinear vibrations

1. Introduction

The impact of the fractional damping on dynamic properties of a coupled mechanical system with a spherical pendulum is investigated (Fig. 1). It is assumed that the spherical pendulum is suspended to the oscillator excited harmonically in the vertical direction $F_z(t) = P_1 \cos(\nu_1 t)$. The pendulum is excited harmonically in horizontal directions $F_x(t) = P_2 \cos(\nu_2 t)$, $F_y(t) = P_3 \cos(\nu_3 t)$. The oscillator contains a linear spring and a damper of a fractional type. Additionally, it is assumed that damping moments acting in the pendulum pivot point are modelled by a fractional derivative. This study is an extension of the research presented by the authors in [1]

Assuming the fractional Caputo derivative defined as [2, 3]:

$$\frac{d^\alpha}{dt^\alpha} f(t) \equiv \hat{f}^{(\alpha)}(t) \equiv \frac{1}{\Gamma(1-\alpha)} \int_0^t \frac{df(\tau)}{d\tau} d\tau, \quad 0 < \alpha \leq 1 \quad (1)$$

where $\Gamma(1-\alpha)$ is the Euler gamma function, and $t > 0$.

Therefore, the dissipation force and moments are expressed as below

$$R(\dot{z}) = c_1 \dot{z}^{(\alpha_1)}, \quad M(\dot{\theta}) = c_2 \dot{\theta}^{(\alpha_2)}, \quad M(\dot{\varphi}) = c_2 \dot{\varphi}^{(\alpha_2)} \quad (2)$$

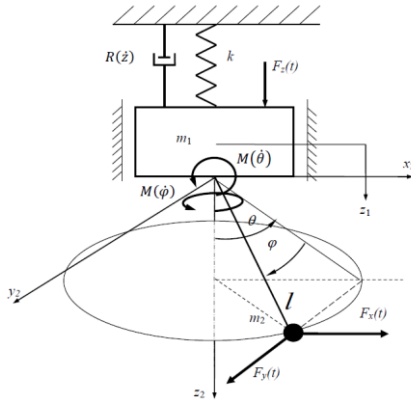


Fig. 1. Schematic diagram of the system

Using formulated above dissipation force and moments, the dimensionless equations of motion of the analysed system with spherical pendulum are as follows [1]

$$\begin{aligned} \ddot{z} - a\ddot{\theta}\cos\phi\sin\theta - a\ddot{\phi}\sin\phi\cos\theta &= A_1\cos(\mu_1\tau) + a(\dot{\phi}^2\cos\phi\cos\theta - 2\dot{\theta}\dot{\phi}\sin\phi\sin\theta - \\ \dot{\theta}^2\cos\phi\cos\theta) - \gamma_1\dot{z}^{(\alpha)} - z \\ \ddot{\theta}\cos^2\phi - \ddot{z}\cos\phi\sin\theta + \gamma_2\dot{\theta}^{(\alpha_2)} &= 2\dot{\theta}\dot{\phi}\cos\phi\sin\phi - \beta^2\cos\phi\sin\theta + A_2\cos\phi\cos\theta\cos\mu_2\tau \quad (4) \\ \ddot{\phi} - \ddot{z}\sin\phi\cos\theta + \gamma_2\dot{\phi}^{(\alpha_2)} &= -\dot{\theta}^2\cos\phi\sin\phi - \beta^2\sin\phi\cos\theta - A_2\sin\phi\sin\theta\cos\mu_2\tau + \\ A_3\cos\phi\cos\mu_3\tau \end{aligned}$$

where

$$\begin{aligned} \omega_1^2 &= \frac{k}{m_1+m_2} \quad \omega_2^2 = \frac{g}{l}, \quad \beta = \frac{\omega_2}{\omega_1}, \quad \gamma_1 = \frac{c_1}{(m_1+m_2)\omega_1^{2-\alpha_1}} \quad \bar{z} = \frac{z}{l}, \quad a = \frac{m_2}{m_1+m_2}, \quad A_1 = \frac{P}{(m_1+m_2)\omega_1^2 l} \quad \mu_1 = \\ \frac{\nu_1}{\omega_1}, \quad A_2 &= \frac{P_2}{m_2 l \omega_1^2}, \quad \mu_2 = \frac{\nu_2}{\omega_1} \quad A_3 = \frac{P_3}{m_2 l \omega_1^2} \quad \mu_3 = \frac{\nu_3}{\omega_1}, \quad \gamma_2 = \frac{c_2}{m_2 l^2 \omega_1^{2-\alpha_2}} \end{aligned} \quad (5)$$

3. Concluding Remarks

The influence of damping in the pendulum joint, described by fractional derivative on the energy transfer, internal and external resonances was studied. The performed calculations show that the vibration amplitude decrease with the increasing order of fractional derivative. Moreover, an increase in the derivative order causes shift in time the occurrence of energy transfer regions. It was shown that except different kinds of periodic vibrations there may also appear chaotic vibrations.

References

- [1] FREUNDLICH J, SADO D: Dynamics of a coupled mechanical system containing a spherical pendulum and a fractional damper. *Meccanica* 2020, **55**:2541-2553.
- [2] PODLUBNY I: *Fractional Differential Equations*. Academic Press: San Diego, 1999.
- [3] CAPUTO M. Linear models of dissipation whose Q is almost frequency independent – II. *Geophysical Journal of Royal Astronomical Society* 1967, **13**:529-539

Combined Internal Resonances of Slacked Micromachined Resonators

AMAL Z. HAJJAJ^{1,*}, FERAS ALFOSAIL², STEPHANOS THEODOSSIADES¹

1. Wolfson School of Mechanical, Electrical and Manufacturing Engineering, Loughborough University, UK

2. Consulting Services Department, Saudi Aramco, Dhahran 31311, Saudi Arabia

* Presenting Author

Abstract: The dynamics of micro/nanoelectromechanical systems (M/NEMS) curved beams have been thoroughly investigated in the literature, commonly for curved arch beams actuated with electrodes facing their concave surface. Except for few works on slacked carbon nanotubes, the literature lacks a deep understanding of the dynamics of slacked curved resonators, where the electrode is placed in front of the convex beam surface. In this paper, we investigate the dynamics of slacked curved resonators as experiencing internal resonance. The curved slacked resonator is excited using an antisymmetric partial electrode to activate both modes of vibration: symmetric and antisymmetric. The axial load is tuned to monitor the ratios between the natural frequencies of different modes of vibration. We explored the dynamics using Galerkin and multiple time scales (MTS) methods. The results indicate simultaneous 2:1 and 1:1 internal resonances between the second symmetric mode with the first symmetric and antisymmetric modes, triggering a variety of rich and complex dynamical behaviours.

Keywords: Slack curved beam, Internal resonance, Combined resonances, M/NEMS

1. Introduction

Energy transfer via internal resonance among various modes of vibration of M/NEMS has been exploited for many potential applications in recent decades [1], [2]. The inherent nonlinear nature and the low damping of these moveable structures present an ideal platform for activating internal resonances. Hence, understanding the nature of this phenomenon is crucial for their successful implementations. Curved beams, particularly, have been studied due to their cubic and quadratic nonlinearities that enable the activation of different types of internal resonances, such as 1:1, 2:1, and 3:1. Commonly, a MEMS arch resonator is actuated using an electrode facing its concave surface to induce snap-through motion. However, this configuration leads to higher actuation voltages. Despite the extensive research on different types of internal resonances in these MEMS resonators [3]–[5], there is a lack of characterizing them at a slack position, leading to lower actuation voltages and low power consumption. Here, we aim to study the combined 1:1 and 2:1 internal resonances of an initially curved beam, where the electrode is placed in front of the convex beam surface, using both Galerkin and MTS methods. The MEMS arch beam is axially tuned and electrostatically driven. Also, to enhance the activation of different modes, we actuate the arch beam electrostatically using a partial electrode configuration [3].

2. Results and Discussion

The axial load is chosen to reach a ratio 1:1 between the first symmetric and antisymmetric modes (at the crossing) and a ratio 2:1 with the second symmetric mode [3]. This makes the dynamic response more complex combining 1:1 and 2:1 internal resonances. The analytical study is based on a nonlinear Euler-Bernoulli shallow arch beam model. First, we solve the dynamic problem for different exci-

tation voltages using a multi-mode Galerkin method. Next, we expand the arch equation, accounting for the influence of different terms of quadratic and cubic nonlinearities, using the method of multiple time scales (by attacking the partial differential equation of motion directly) considering the combination of 1:1 and 2:1 internal resonances. As shown in Fig. 1, the theoretical results, using both methods, show the nonlinear interaction between all contributing modes. The presence of different peaks and the phase portraits suggest the contribution of the second symmetric mode into the response via 2:1 internal resonance. The motion of the node point, the midpoint, around the first antisymmetric mode, suggests the contribution of the second symmetric mode to the response. The results prove the rich dynamic and nonlinear energy transfer of the slacked arch beam similar to the typical actuated MEMS arch resonators and with lower excitation voltages.

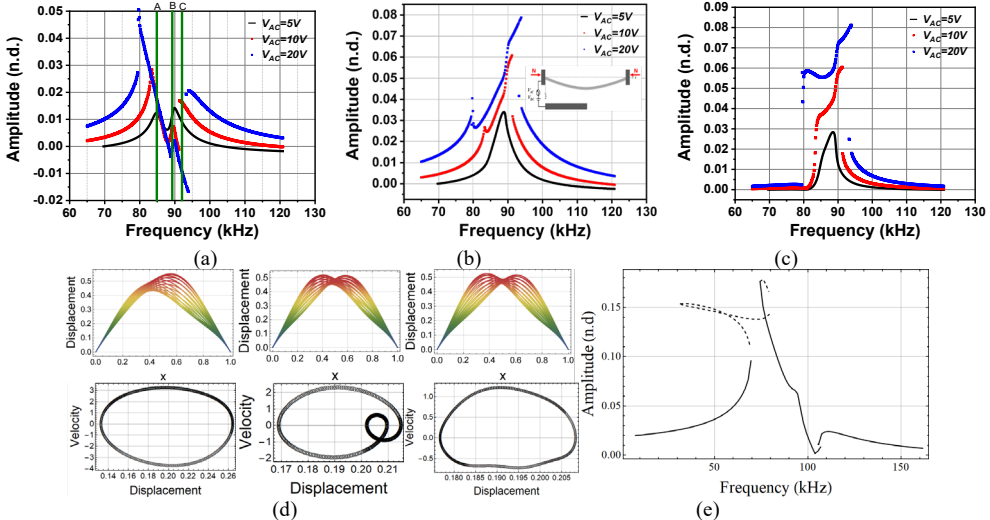


Fig. 1. Galerkin Results at (a) $x=0.5$, (b) $x=0.25$, and (c) $x=0.75$ (x denotes the normalized beam position with respect to the beam length). (d) Oscillations of the beam and phase portraits at different sections shown in (a) (A, B, and C from left to right). (e) MTS results of the dynamic response of the arch beam at $V_{DC}=50V$ and $V_{AC}=10V$. The inset of (b) presents a schematic of the arch beam.

3. Concluding Remarks

We investigated the combined 1:1 and 2:1 internal resonances among the first symmetric and anti-symmetric and the second symmetric modes of an axially tuned and electrostatically actuated slacked arch MEMS resonator. A complex and rich dynamic behaviour was demonstrated. This work motivates further research to exploit internal resonances of slacked arch resonators for practical applications, such as sensors and frequency stability, thanks to the low actuation voltages.

References

- [1] Antonio et al. Frequency stabilization in nonlinear micromechanical oscillators, *Nat. Commun.*, 2012.
- [2] Zhang et al. Sensitivity enhancement of a resonant mass sensor based on internal resonance, *Appl. Phys. Lett.*, 2018.
- [3] Hajjaj et al. Theoretical and experimental investigations of the crossover phenomenon in micromachined arch resonator: part II—simultaneous 1:1 and 2:1 internal resonances, *Nonl. Dyn.*, 2019.
- [4] Wang and Ren, Three-to-one internal resonance in MEMS arch resonators, *Sensors*, 2019.
- [5] Ouakad et al. One-to-one and three-to-one internal resonances in MEMS shallow arches, *J. Comput. Nonlinear Dyn.*, 2017.

Nonlinear Interaction between Longitudinal and Transverse Vibrations of a Microbeam under Periodic Opto-Thermal Excitation

DMITRY INDEITSEV^{1,2}, ALEKSEI LUKIN^{1*}, IVAN POPOV¹, LEV SHTUKIN¹

1. Peter the Great St.Petersburg Polytechnic University (SPbPU), St.Petersburg, Russia
2. Institute for Problems in Mechanical Engineering of the Russian Academy of Sciences (IPME RAS), St.Petersburg, Russia

* Presenting Author

Abstract: The paper investigates the nonlinear dynamics of coupled longitudinal-flexural vibrations of a microbeam clamped at both ends - the basic sensitive element of a wide class of microsensors of physical quantities - under laser opto-thermal excitation in the form of periodically generated Gaussian pulses acting on some part of the surface of the beam element. The steady-state time-harmonic temperature distribution in the volume of the beam resonator is found for a given power, duration, and periodicity of laser pulses. The modes of parametric oscillations of the microbeam are investigated under conditions of internal combinational resonance between some two flexural and lower longitudinal modes of free oscillations of the resonator.

Keywords: N/MEMS, sensor, combinational resonance, nonlinear oscillations, laser-induced vibrations

1. Introduction

The principle of laser opto-thermal action on a deformable medium is finding ever wider application in problems of non-destructive testing of equipment and structures [1,2], determination of physical and mechanical properties of materials [3,4], analysis of geometric and physical parameters of objects and structures on nano- and the microscale [5,6], in biomedicine [7], as well as in the nano and microsystems industry [8-11].

In earlier works [12-14], the dynamics and elastic stability of the N/MEMS beam element under short-term thermal effects was investigated. In those works, the stage of bending wave formation at sufficiently short times was considered. In paper [15], attention was paid to the interaction of different modes of vibration, both transverse and longitudinal, in the case of free oscillations under pulsed laser action. It was shown that the initial perturbation in the longitudinal direction can effectively excite bending vibration modes, which, on the whole, leads to a longitudinal-transverse beating regime with noticeable amplitudes. It was noted that the period and amplitude of these beats substantially depend on the frequency detuning parameter between the sum of the bending vibration frequencies and the longitudinal vibration frequency.

In this work, we study the nonlinear dynamics of coupled longitudinal-flexural vibrations of a microbeam clamped at both ends - the basic sensitive element of a wide class of microsensors of physical quantities - under laser opto-thermal excitation in the form of periodically generated Gaussian pulses acting on some part of the surface of the beam element.

2. Results and Discussion

A graphical diagram of the problem under consideration is shown in Fig. 1.

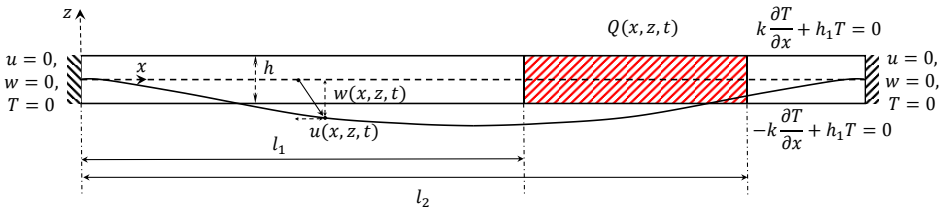


Fig. 1. Graphical scheme of the problem. u, w – longitudinal and transverse components of the displacements vector of the rod material point with coordinates x, z at time t ; $T(x, z, t)$ – temperature deviation from the reference value; $Q(x, z, t)$ – body heat flux simulating the thermo-optical effect of a laser on a section of a beam $l_1 < x < l_2$; k, h_1 – coefficients of thermal conductivity and convection with the external environment, respectively

To describe the deformed state of the microbeam, the mechanical Bernoulli-Euler model and the model of longitudinal vibrations of the rod are used. Coupled geometrically nonlinear equations of longitudinal-flexural vibrations of a beam element under laser temperature exposure are formulated under the assumption $u = O(w^2)$; the thermal effect of the laser on the structure is reduced to a thermal axial force $N^T = Eb\alpha \int_{-\frac{h}{2}}^{\frac{h}{2}} T dz$ and thermal bending moment $M^T = Eb\alpha \int_{-\frac{h}{2}}^{\frac{h}{2}} zT dz$ (E, α – Young modulus and linear thermal expansion coefficient of the material; b, h – beam section width and height). Under the assumptions made, the dimensionless equations of motion of the beam resonator take the form

$$\begin{aligned} \tilde{u}'' + 12\beta\tilde{w}'\tilde{w}'' &= 12\beta^2\ddot{\tilde{u}} + \tilde{N}_x^T, \\ \tilde{w}^{IV} + \ddot{\tilde{w}} + \tilde{N}^T\tilde{w}'' &= -\tilde{M}_{xx}^T + \frac{1}{\beta}\tilde{u}'\tilde{w}'' + 6(\tilde{w}')^2\tilde{w}'' + 12\beta\ddot{\tilde{u}}\tilde{w}', \end{aligned}$$

where \tilde{u}, \tilde{w} – dimensionless displacements normalized to the beam height h ; $\beta = \frac{h}{12L}$ – dimensionless parameter, characterizing slenderness of the beam; the subscript x denotes the corresponding derivatives with respect to the longitudinal coordinate.

The steady-state time-harmonic temperature distribution in the volume of the beam resonator is found analytically for a given power, duration, and periodicity of laser pulses. Using asymptotic methods of nonlinear mechanics, the modes of parametric oscillations of a microbeam under conditions of internal combinational resonance between some two bending and lower longitudinal modes of free oscillations of the resonator are investigated.

3. Concluding Remarks

The study made it possible to show the technical feasibility of laser generation of bending vibrations of a microscale resonator using the parametric resonance mechanism and to evaluate the influence of the factor of interaction of longitudinal and bending modes of vibrations on the nonlinear dynamics of the system.

Acknowledgment: The work was supported by RFBR grant 20-01-00537.

References

- [1] R.I. VOROBYEV, I.V. SERGEICHEV, A.A. KARABUTOV, E.A. MIRONOVA, I.S. SAVATEEVA, E.V. AKHATOV: APPLICATION OF THE OPTOACOUSTIC METHOD TO ASSESS THE EFFECT OF VOIDS ON THE CRACK RESISTANCE OF STRUCTURAL CARBON PLASTICS. *ACOUST. PHYS.*, 66 (2020), pp. 132-136
- [2] G. YAN, S. RAETZ, N. CHIGAREV, J. BLONDEAU, V.E. GUSEV, V. TOURNAT: CUMULATIVE FATIGUE DAMAGE IN THIN ALUMINUM FILMS EVALUATED NON-DESTRUCTIVELY WITH LASERS VIA ZERO-GROUP-VELOCITY LAMB MODES. *NDT & E INTERNATIONAL*, 116 (2020), p. 102323
- [3] Y. PAN, C. ROSSIGNOL, B. AUDOIN: ACOUSTIC WAVES GENERATED BY A LASER LINE PULSE IN CYLINDERS; APPLICATION TO THE ELASTIC CONSTANTS MEASUREMENT. *J. ACOUST. SOC. AM.* (115) (2004)
- [4] G. CHOW, E. UCHAKER, G. CAO, J. WANG: LASER-INDUCED SURFACE ACOUSTIC WAVES: AN ALTERNATIVE METHOD TO NANOINDENTATION FOR THE MECHANICAL CHARACTERIZATION OF POROUS NANOSTRUCTURED THIN FILM ELECTRODE MEDIA. *MECH. MATER.*, 91 (2015), pp. 333-342
- [5] A. CHAMPION, Y. BELLOUARD: DIRECT VOLUME VARIATION MEASUREMENTS IN FUSED SILICA SPECIMENS EXPOSED TO FEMTOSECOND LASER. *OPT MATER EXPRESS*, 2 (2012), pp. 789-798
- [6] P.H. OTSUKA, S. MEZIL, O. MATSUDA, M. TOMODA, A. MAZNEV, T. GAN, N.X. FANG, N. BOECHLER, V. GUSEV, O.B. WRIGHT: TIME-DOMAIN IMAGING OF GIGAHERTZ SURFACE WAVES ON AN ACOUSTIC METAMATERIAL. *NEW J PHYS*, 20 (2018), p. 013026
- [7] C. LI, G. GUAN, F. ZHANG, G. NABI, R.K. WANG, Z. HUANG: LASER INDUCED SURFACE ACOUSTIC WAVE COMBINED WITH PHASE SENSITIVE OPTICAL COHERENCE TOMOGRAPHY FOR SUPERFICIAL TISSUE CHARACTERIZATION: A SOLUTION FOR PRACTICAL APPLICATION. *BIOMED OPT EXPRESS*, 55 (2014), pp. 1403-1419
- [8] J.D. ZOOK, D.W. BURNS, W.R. HERB, H. GUCKEL, J.W. KANG, Y. AHN: OPTICALLY EXCITED SELF-RESONANT MICROBEAMS. *SENS. ACTUATORS, A*, 52 (1) (1996), pp. 92-98
- [9] T. YANG, Y. BELLOUARD: LASER-INDUCED TRANSITION BETWEEN NONLINEAR AND LINEAR RESONANT BEHAVIORS OF A MICROMECHANICAL OSCILLATOR. *PHYS. REV. APPLIED*, 7 (2017), p. 064002
- [10] R.J. DOLLEMAN, S. HOURI, A. CHANDRASHEKAR, *ET AL.*: OPTO-THERMALLY EXCITED MULTIMODE PARAMETRIC RESONANCE IN GRAPHENE MEMBRANES. *SCI REP*, 8 (2018), p. 9366
- [11] A.T. ZEHNDER, H.R. RICHARD, S. KRYLOV: LOCKING OF ELECTROSTATICALLY COUPLED THERMO-OPTICALLY DRIVEN MEMS LIMIT CYCLE OSCILLATORS. *INT J NON LINEAR MECH*, 102 (2018), pp. 92-100
- [12] N.F. MOROZOV, D.A. INDEITSEV, A.V. LUKIN, *ET AL.*: STABILITY OF THE BERNOULLI–EULER BEAM IN COUPLED ELECTRIC AND THERMAL FIELDS. *DOKL. PHYS.*, 63 (2018), pp. 342-347
- [13] N.F. MOROZOV, D.A. INDEITSEV, A.V. LUKIN, *ET AL.*: BERNOULLI-EULER BEAM UNDER ACTION OF A MOVING THERMAL SOURCE: CHARACTERISTICS OF THE DYNAMIC BEHAVIOR. *DOKL. PHYS.*, 64 (2019), pp. 185-188
- [14] N.F. MOROZOV, D.A. INDEITSEV, A.V. LUKIN, *ET AL.*: STABILITY OF THE BERNOULLI–EULER BEAM UNDER THE ACTION OF A MOVING THERMAL SOURCE. *DOKL. PHYS.*, 65 (2020), pp. 67-71
- [15] N.F. MOROZOV, D.A. INDEITSEV, A.V. LUKIN, *ET AL.*: NONLINEAR INTERACTION OF LONGITUDINAL AND TRANSVERSE VIBRATIONS OF A ROD AT AN INTERNAL COMBINATIONAL RESONANCE IN VIEW OF OPTO-THERMAL EXCITATION OF N/MEMS. *J SOUND VIB.*, 509 (2021), p. 116247

Vibration isolation in metamaterial structures embedded with neoprene resonators

HARSHAN JAYAKUMAR^{2*}, PREMCHAND V P¹, REMIL GEORGE THOMAS¹,

1. Department of Mechanical Engineering, Mar Baselios College of Engineering and Technology Trivandrum, India
 2. R&D Development Associate Engineer, Dassault Systèmes, Pune (harshan.j@3ds.com)
- * Presenting Author (email - premchand.vp@mbcet.ac.in)

Abstract: Metamaterial structures provide a passive mode of vibration isolation by forming band gaps using a resonator mass and a viscous elastic membrane (VEM) material embedded in it. Irrespective of the frame structure configuration (1D, 2D or 3D) the metamaterials with periodic elements are meant to attenuate vibrations in transverse direction to the plane of propagation. Moreover, if employed in desired configuration metamaterial helps in attenuating the vibrations along structural elements in a desired frequency band (Floquet-Bloch theory). In the present investigation, a motor frame assembly is designed incorporating the meta-material properties and its ability to attenuate vibrations produced by the motor in the frequency range of interest is analysed. Experimental results are compared to FEA simulation for validation

Keywords: Metamaterials, Passive vibration isolation.

1.Introduction

Attenuating drive vibrations to a proper level for a preferred frequency band (called band gap) using a metamaterial structure, has attracted the attention of industrial experts and researchers in recent times[1-3]. Advancement of continuum mechanics saw the development of theories like Floquet-Bloch and Bernoulli mathematical models, which are generally used for analysing periodicity in beam elements. Employing a metamaterial like structure helps in attenuating the vibrations along structural elements in a desired frequency band without increasing the compliance of the joints.

In this work, a uniform frame made of mild steel is considered as the base frame. For obtaining the second configuration, periodic air-holes are introduced in the uniform frame, whereas the third configuration is obtained by incorporating resonators in the periodic holes embedded with visco-elastic membrane (VEM). Here, Neoprene is used as VEM and central resonators are in turn made of mild steel.

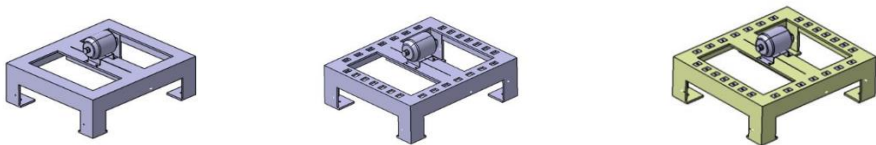


Fig.1. Structural configurations considered (i) uniform (ii) With VEM resonators (iii) With VEM+central mass resonators

The frames are excited with a shaker. The time domain data were obtained and analysed using NI LabVIEW software. The acceleration response from output points are measured using a tri-axial accelerometer and the input acceleration is recorded using a uni-axial accelerometer attached opposite to the shaker excitation point.

2.Results and Discussion

From the simulation of the MS structure it is observed that 2 predominant flexural modes are occurring in the 0-500 frequency range. Attenuation band of 75 Hz is centered around 350 Hz and corresponding 3rd mode is observed from experiment as well as the simulation. From a frequency sweep simulation performed in a range of 10-3000Hz, significant band gaps are visible near 670-840 Hz, 930-1050 Hz and 1480-1590 Hz. The inherent compliance of the structure with airholes could be seen as causing high transfer function, in 500-700 Hz and 1200-1450 Hz region. Metamaterial effectively damps these modes to a level comparable with that of uniform structural configuration.

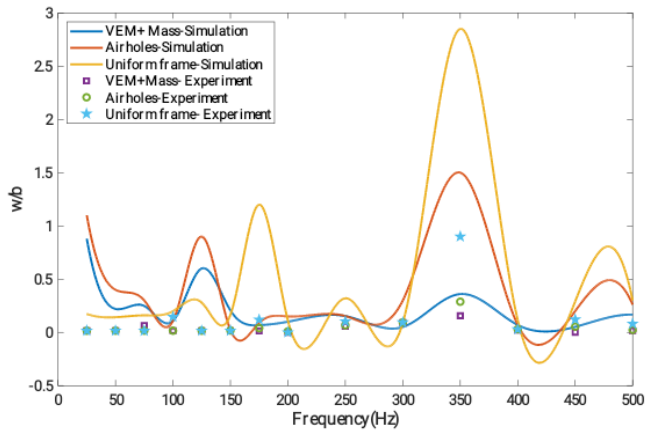


Fig.2.Comparison of FRFs from experiments and simulations

3.Concluding Remarks

In this work, vibration characteristics of different metamaterial structural configurations are determined and compared its inherent attenuation characteristics with that of a uniform structure. It is found that metamaterials can be employed for effective vibration isolation as a passive measure.

References

- [1] J. Robillard, O.B. Matar, P. Deymier, M. Stippinger, A. Hladky-Hennion, Y. Pennec, B. Djafari-Rouhani, Tunable magneto elastic phononic crystals, *Appl. Phys. Lett.* 95 (12) (2009) 1–10.
- [2] Mahmoud I. Hussein, Michael J.Frazier. Metadamping: An emergent phenomenon in dissipative metamaterials. *Journal of Sound and Vibration*, Volume 332, Issue 20, 30 September 2013.
- [3] M. Nouh , O. Aldraihem , A. Baz. Wave propagation in metamaterial plates with periodic local resonances. *Journal of Sound and Vibration*, Volume 341, 14 April 2015, Pages 53-73

Analysing Vibration attenuation characteristics of Al 6061 metamaterial structures

HARSHAN JAYAKUMAR^{2*}, PREMCHAND V P¹, REMIL GEORGE THOMAS¹

1. Department of Mechanical Engineering, Mar Baselios College of Engineering and Technology Trivandrum, India
 2. R&D Development Associate Engineer, Dassault Systems, Pune, India
- * Presenting Author (email - harshan.j@3ds.com)

Abstract: Metamaterial structures provide a passive mode of vibration isolation by forming band gaps using a resonator mass and a viscous elastic membrane (VEM) material embedded at in it. Effective configuration of metamaterial structures can possibly attenuate excitation frequencies which matches to the natural frequencies of resonators employed. In this work Al 6061 alloy with neoprene combination is analysed for strength and stiffness characteristics and is proposed as an alternative to MS structures. Attenuation characteristics are validated using FRF comparison, and mode shape analysis.

Keywords: Metamaterials, Mode shape analysis, Vibration attenuation.

1.Introduction

Metamaterial structures employing, geometrically non-linear local resonators with cubic and quadratic restoring forces are very effective compared to linear systems employed for vibration isolation[1]. Studies on piezoelectric materials is done by Robillard et al[2], wherein it is observed that electric field can affect stiffness and meta-damping of the structure. Floquet-Bloch theory provides the fundamentals for deriving the transfer matrix which relates the state variables (displacement and force) at the left of a unit cell to the right of it[3]. Al alloy (Al 6061) has comparably low non-linear damping characteristics with high stiffness making it suitable for attenuation applications. The metamaterial structure (Fig1) has neoprene with VEM properties embedded periodically to act as resonators. The holes housing the resonators have aspect ratio near to 1.66. The longer edge is kept parallel to longitudinal side of the beams of the structure, since the material coverage envelope bounding dimensions should match with low-frequency high wavelength signals. The filleted corners are to reduce stress concentration and to improve the adhesiveness of the VEM. The experimental readings were taken at a sampling frequency of 10000 Hz and over a time window of 10s.

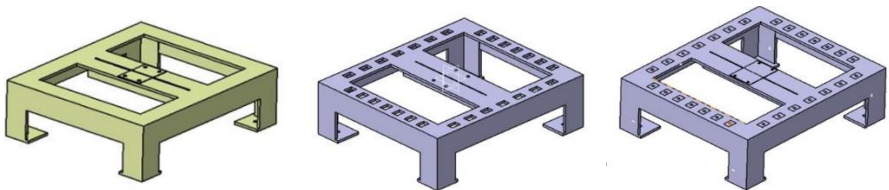


Fig.1.Configurations considered for lumped mass analysis

2.Results and Discussion

From simulation results it is found that a band gap is observed at near 900-1100 Hz, where the air holes and with neoprene structure,damping the frequencies in that range,at comparable magnitudes. Mode shapes (Fig 2) do reveal higher out-of-plane excitation, implying a mode excitation, establishing a pass band as inferred from FRF.

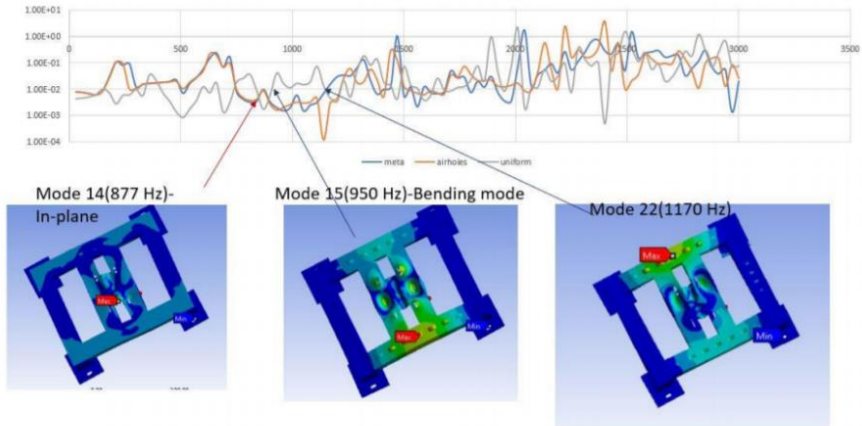


Fig.2, Mode shapes analysis

3.Concluding Remarks

In this work, vibration attenuation characteristics of different metamaterial structural configurations with Al 6061 as base material is analysed .An attenuation band spanning a magnitude of 75 Hz centered around 350 Hz corresponding to 3rd mode is observed from experiment and is well captured from simulation also. A frequency sweep analysis upto 3000Hz ,revealed a stop band region (900-1200 Hz). The mode shapes inside this band are all flexural modes with wavelengths comparable to resonator dimensions.FRF along mode shape analysis do underline attenuation characteristics of Al alloy-neoprene metamaterials,and the inherent damping properties and comparable strength parameters do make it an alternative to conventional MS metamaterial structures.

References

- [1]Arnaldo Casalotti. Et al Metamaterial beam with embedded nonlinear vibration absorbers. *International Journal of Non-Linear Mechanics* Volume 98, January 2018, Pages 32-42
- [2]J. Robillard, et al, Tunable magneto elastic phononic crystals, *Appl. Phys. Lett.* 95 (12) (2009) 1–10.
- [3] Mahmoud I.Hussein, MichaelJ.Frazier. Metadamping: An emergent phenomenon in dissipative metamaterials. *Journal of Sound and Vibration*, Volume 332, Issue 20, 30 September 2013

Fuzzy Logic Model to Determine Minimum Seismic Separation Gap

ELIF CAGDA KANDEMIR

Izmir Democracy University, Izmir, Turkey [0000-0002-9190-7120]

Abstract: Adjacent structures should be separated from each other to behave freely during ground motions. In case of insufficient separation gap, earthquake-induced structural pounding may cause serious damages. Seismic codes all over the world stipulate seismic separation gap based on different methods, however unpredictable strong ground motions may cause collision between them as a result of unsynchronized vibration. This paper proposes fuzzy logic method, which is an effective tool by means of coupling a number of parameters of structures and earthquakes, to obtain minimum seismic separation gap between structures to prevent pounding. Different structural configurations of two ten-storey adjacent buildings have been examined under severe ground motions. Soil effect, structural nonlinearity and ground motion characteristics have been accounted to constitute the fuzzy logic model. The efficiency of model has been verified through parametric analyses of the structures with different dynamic characteristics changing mass and stiffness parameters in addition to storey numbers. Comparison of the results obtained in this study with the methods in the codes demonstrates the superiority of the fuzzy logic model.

Keywords: seismic separation gap, fuzzy logic, structural pounding, structural nonlinearity

The Effect of Initial Stress on Nonlinear Lateral Vibrations of Rotating Rods

LELYA KHAJIYEVA¹, ASKAR KUDAIBERGENOV², ASKAT KUDAIBERGENOV³, ALIYA UMBETKULOVA^{4*}

Dept. Mathematical and Computer Modelling, Al-Farabi Kazakh National University, Almaty, Kazakhstan
[1. 0000-0002-2565-3409, 2. 0000-0001-9154-9653, 3. 0000-0003-4773-0580, 4. 0000-0002-0322-9762]

* Presenting Author

Abstract: In this work we study nonlinear lateral vibrations of a simply supported rotating rod under the effect of initial stress and external loadings. The foundations of Novozhilov's nonlinear theory of elasticity and Biot's general theory for initially stressed solids are used when deriving a generalized elastic potential, based on which the nonlinear mathematical model is developed. The Bubnov-Galerkin approach and Wolfram Language built-in numerical method are utilized to find a solution of the model. The effect of the initial stress field on the rod spatial vibrations is analyzed and graphs for various values of the initial stress are plotted.

Keywords: nonlinear mathematical model, initial stress, rod, lateral vibration

1. Introduction

It is known that the stress state of various parts of machines, building structures and many physical and mechanical systems can be characterized by existence of a field of initial stresses even if there are no external forces affecting them. Fundamental equations of media with initial stresses were obtained by Trefftz, Neuber, Green and Zerna on the basis of the general theory of elasticity for finite deformations [1], and the original theory of nonlinear elasticity for initially stressed solids and fluids was created by Biot [2]. As stated in [3], when examining wave propagation in bodies with initial stresses, the nonlinear theory has to be utilized. At the same time, the initial stress has a dominant role only in the bending modes [4]. Therefore, this work focuses on studying the effect of the field of initial stresses on the spatial deformation of an elastic medium taking into account geometric nonlinearity and external loads.

2. Mathematical Model

Consider a pre-stressed deformable isotropic elastic rod of length l with constant cross-section, rotating around the rod axis z with angular speed ω and being under the action of a longitudinal compressive load $N(z,t)$ and a torque $M(z,t)$. It is assumed that the rod vibrations $u(z,t)$ and $v(z,t)$ take place in the Oxz - and Oyz -planes, respectively. Based on the concepts of Novozhilov's nonlinear elasticity theory [5] and Biot's general theory, a generalized elastic potential accounting for initial stress is derived. Applying the Ostrogradsky-Hamilton variation principle, a nonlinear mathematical model of spatial lateral vibrations of the simply supported rotating rod under the effect of the initial stress field σ_{ij}^0 and external loads is developed:

$$\begin{aligned}
& \rho A \frac{\partial^2 u}{\partial t^2} + EI_y \frac{\partial^4 u}{\partial z^4} - \rho I_y \frac{\partial^4 u}{\partial z^2 \partial t^2} + \frac{\partial^2}{\partial z^2} \left(M(z,t) \frac{\partial v}{\partial z} \right) + \frac{\partial}{\partial z} \left(N(z,t) \frac{\partial u}{\partial z} \right) - \frac{EA}{1-\nu} \frac{\partial}{\partial z} \left(\frac{\partial u}{\partial z} \right)^3 \\
& - \frac{EA(5-6\nu)}{2(1-\nu)} \frac{\partial}{\partial z} \left(\frac{\partial u}{\partial z} \left(\frac{\partial v}{\partial z} \right)^2 \right) - \rho A \left(2\omega \frac{\partial v}{\partial t} + \omega^2 u \right) + \frac{A}{2} \left(\sigma_{yy}^0 + \sigma_{zz}^0 \right) \frac{\partial^2 v}{\partial z^2} + A \sigma_{xy}^0 \frac{\partial^2 u}{\partial z^2} = 0, \\
& \rho A \frac{\partial^2 v}{\partial t^2} + EI_x \frac{\partial^4 v}{\partial z^4} - \rho I_x \frac{\partial^4 v}{\partial z^2 \partial t^2} - \frac{\partial^2}{\partial z^2} \left(M(z,t) \frac{\partial u}{\partial z} \right) + \frac{\partial}{\partial z} \left(N(z,t) \frac{\partial v}{\partial z} \right) - \frac{EA}{1-\nu} \frac{\partial}{\partial z} \left(\frac{\partial v}{\partial z} \right)^3 \\
& - \frac{EA(5-6\nu)}{2(1-\nu)} \frac{\partial}{\partial z} \left(\frac{\partial v}{\partial z} \left(\frac{\partial u}{\partial z} \right)^2 \right) + \rho A \left(2\omega \frac{\partial u}{\partial t} - \omega^2 v \right) + \frac{A}{2} \left(\sigma_{xx}^0 + \sigma_{zz}^0 \right) \frac{\partial^2 u}{\partial z^2} + A \sigma_{xy}^0 \frac{\partial^2 v}{\partial z^2} = 0.
\end{aligned} \tag{1}$$

3. Numerical Results

For finding a solution to the nonlinear model (1), the Bubnov-Galerkin approach, according to which the lateral displacements $u(z,t)$ and $v(z,t)$ are approximated by a finite spectrum of harmonic modes, and Wolfram Language built-in numerical method giving results in terms of interpolating functions are applied. To get a general picture of the oscillatory process and estimate the influence of initial stress, the graphs of the rod spatial lateral vibrations are constructed. Considering cases when the initial stress components are equal (Fig. 1) and have different values, along with examining compressive and tensile stresses allow studying the effect of the initial stress field on the rod lateral vibrations taking into account its rotation and the external loadings.

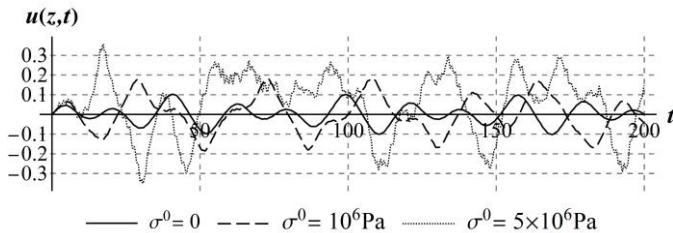


Fig. 1. The effect of initial stress on the rod lateral vibrations in the Oxz -plane

4. Concluding Remarks

In this paper we estimated the effect of initial stress on nonlinear lateral vibrations of a rotating rod under the action of an external compressive load and a torque. Accounting for the tensile initial stresses allowed reducing the amplitude of the rod vibrations, whereas the compressive stresses resulted in their increase with retaining stability of the oscillatory process at optimal system parameters.

Acknowledgment: This research is funded by the Science Committee of the Ministry of Education and Science of the Republic of Kazakhstan (Grant No. AP08857255).

References

- [1] GREEN A., ZERNA W.: *Theoretical Elasticity*, 2nd revised ed. edition. Dover Publ.: New York, 2012.
- [2] BIOT M.: *Mechanics of Incremental Deformations*. J. Wiley & Sons: New York, 1965.
- [3] BABICH S.YU., GUZ' A.N., ZHUK A.P. Elastic waves in bodies with initial stresses. *Sov. Appl. Mech.* 1979, **15**(4):277-291.
- [4] WRIGHT T.W. Plate and rod vibrations with initial stresses. *J. Appl. Mech.* 1966, **33**(1):134-140.
- [5] NOVOZHILOV V.V.: *Foundations of the Nonlinear Theory of Elasticity*. Dover Publ.: New York, 1999.

Application of the Lumped-Parameter Method for Modelling Nonlinear Vibrations of Drill Strings with Complicating Factors

LELYA KHAJIYEVA¹, ASKAR KUDAIBERGENOV², YULIYA SABIROVA^{3*}

Dept. Mathematical and Computer Modelling, Al-Farabi Kazakh National University, Almaty, Kazakhstan
[1. 0000-0002-2565-3409, 2. 0000-0001-9154-9653, 3. 0000-0002-3497-0940]

* Presenting Author

Abstract: This paper considers nonlinear spatial lateral vibrations of a drill string with supporting stabilizers in a gas flow. The mathematical model used for describing the studied process is based on Novozhilov’s nonlinear theory of elasticity. The drill string lateral displacements are found by the lumped-parameter method (LPM). For numerical solution of the obtained discrete system, the fourth order Runge-Kutta method is utilized. The impact of the damping elements (supporting stabilizers) on the drill string lateral vibrations is analyzed, and numerical illustrations are presented for several cases.

Keywords: drill string, nonlinearity, lateral vibration, lumped-parameter method, stabilizers

1. Introduction

The search and application of the most effective approaches for modelling complex nonlinear processes, including poorly studied problems of dynamics of industrial equipment and machines at complicated conditions, are of large relevance. The purpose of this work is the assessment of the effectiveness of LPM for modelling the nonlinear dynamics of drill strings taking into account stabilizers and external forces. LPM is a special case of the finite element method, where the equation of a continuous medium is replaced by its discrete analogue, and is widely used in structural mechanics [1]. The influence of supporting stabilizers on the drilling system is under consideration due to the fact that accounting for damping elements can significantly improve the system stability and the efficiency of drilling and is of great scientific interest [2].

2. Mathematical Model

Based on the concepts of Novozhilov’s nonlinear elasticity theory [3], a nonlinear mathematical model of spatial lateral vibrations of the simply supported rotating drill string in a gas flow accounting for external loads $N(x_3, t)$ and $M(x_3, t)$ [4] and the effect of stabilizers [2] is developed:

$$\begin{aligned} & \rho A \frac{\partial^2 u_1}{\partial t^2} + EI_{x_2} \frac{\partial^4 u_1}{\partial x_3^4} - \rho I_{x_2} \frac{\partial^4 u_1}{\partial x_3^2 \partial t^2} + \frac{\partial^2}{\partial x_3^2} \left(M(x_3, t) \frac{\partial u_2}{\partial x_3} \right) + \frac{\partial}{\partial x_3} \left(N(x_3, t) \frac{\partial u_1}{\partial x_3} \right) - \frac{EA}{1-\nu} \frac{\partial}{\partial x_3} \left(\frac{\partial u_1}{\partial x_3} \right)^3 \\ & - \frac{EA(5-6\nu)}{2(1-\nu)} \frac{\partial}{\partial x_3} \left(\frac{\partial u_1}{\partial x_3} \left(\frac{\partial u_2}{\partial x_3} \right)^2 \right) - hP_0 \kappa \left(\bar{M} \frac{\partial u_1}{\partial x_3} - \frac{\kappa+1}{4} \bar{M}^2 \left(\frac{\partial u_1}{\partial x_3} \right)^2 + \frac{\kappa+1}{12} \bar{M}^3 \left(\frac{\partial u_1}{\partial x_3} \right)^3 \right) \\ & - \rho A \left(2\Omega \frac{\partial u_2}{\partial t} + \Omega^2 u_1 \right) + \sum_{j=1}^J \left(k_j^s u_1 + c_j^s \frac{\partial u_1}{\partial t} \right) \delta(x - x_j^s) = 0, \end{aligned} \quad (1)$$

$$\begin{aligned}
& \rho A \frac{\partial^2 u_2}{\partial t^2} + EI_{x_1} \frac{\partial^4 u_2}{\partial x_3^4} - \rho I_{x_1} \frac{\partial^4 u_2}{\partial x_3^2 \partial t^2} - \frac{\partial^2}{\partial x_3^2} \left(M(x_3, t) \frac{\partial u_1}{\partial x_3} \right) + \frac{\partial}{\partial x_3} \left(N(x_3, t) \frac{\partial u_2}{\partial x_3} \right) - \frac{EA}{1-\nu} \frac{\partial}{\partial x_3} \left(\frac{\partial u_2}{\partial x_3} \right)^3 \\
& - \frac{EA(5-6\nu)}{2(1-\nu)} \frac{\partial}{\partial x_3} \left(\frac{\partial u_2}{\partial x_3} \left(\frac{\partial u_1}{\partial x_3} \right)^2 \right) - hP_0 \kappa \left(\bar{M} \frac{\partial u_2}{\partial x_3} - \frac{\kappa+1}{4} \bar{M}^2 \left(\frac{\partial u_2}{\partial x_3} \right)^2 + \frac{\kappa+1}{12} \bar{M}^3 \left(\frac{\partial u_2}{\partial x_3} \right)^3 \right) \\
& + \rho A \left(2\Omega \frac{\partial u_1}{\partial t} - \Omega^2 u_2 \right) + \sum_{j=1}^J \left(k_j^s u_2 + c_j^s \frac{\partial u_2}{\partial t} \right) \delta(x - x_j^s) = 0.
\end{aligned} \tag{2}$$

3. Numerical Results

For obtaining solution of the mathematical model, LPM is utilized. According to this method, the given continuous equations (1), (2) are represented as a system of second-order ordinary differential equations by its numerical discretization at the end nodes. The numerical solution of the system is found by the fourth order Runge-Kutta method using the C++ programming language. The comprehensive analysis of the stabilizer influence on the drill string vibration process is carried out. It is shown that considering even one stabilizer allows substantially decrease the amplitude of the drill string vibrations in a gas flow (Fig. 1).

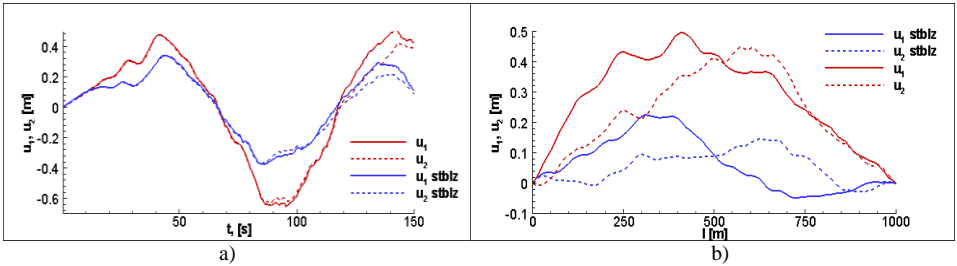


Fig. 1. The stabilizer effect at $x_1^s = 0.6L$ on the drill string vibrations for a) $x_3 = 0.49L$, b) $t = 150s$ ($\Omega = 0$)

4. Concluding Remarks

In this work, we considered the impact of stabilizers on the nonlinear dynamics of a drill string in a gas flow using LPM. According to the obtained results, the application of stabilizers allows considerably reducing the amplitude of the drill string vibrations. It proves the significance of studying the influence of damping elements on the drilling system and the efficiency of applying LPM when modelling vibrations of the drill string with complicating factors.

Acknowledgment: This research is funded by the Science Committee of the Ministry of Education and Science of the Republic of Kazakhstan (Grant No. AP09261135).

References

- [1] SADLER J.P.: On the analytical lumped-mass model of an elastic four-bar mechanism. *J. Eng. Ind. Trans. ASME* 1975, **97**(2):561-565.
- [2] PEI Y., SUN Y., WANG J.: Dynamics of rotating conveying mud drill string subjected to torque and longitudinal thrust. *Meccanica* 2013, **48**:2189–2201.
- [3] NOVOZHILOV V.V.: *Foundations of the Nonlinear Theory of Elasticity*. Dover Publ.: New York, 1999.
- [4] KHAJIYEVA L., KUDAIBERGENOV ASKAR, KUDAIBERGENOV ASKAT: The effect of gas and fluid flows on nonlinear lateral vibrations of rotating drill strings. *Commun. Nonlinear Sci.* 2018, **59**:565-579.

Determination of global damping and stiffness coefficients of journal foil bearing

JAKUB ŁAGODZIŃSKI^{1*}, ELIZA TKACZ², ZBIGNIEW KOZANECKI³

1,2,3. Institute of Turbomachinery, Lodz University of Technology

* Presenting Author

Abstract: For the few last years, in modern low-power generation systems, a demand for oil-free compressors has appeared. The development of reliable bearing technology for this relatively high-speed small turbomachinery could be crucial. In order to implement this technology more widely, a selection of the optimal design from the viewpoint of machine reliability must be conducted. A high speed turbomachinery with nominal speed of tens of thousands rpm strongly depends on the proper rotordynamic design. This is especially important when the foil bearings are taken to consideration. These compliant surface gas bearings are a class of hydrodynamic bearings that use the ambient gas as their working fluid and, thus, require no dedicated lubrication system. On the other hand, due to their relatively low damping, a designer should analyze thoroughly the dynamics of the rotor-bearing-casing system in the whole operating rpm range. A correctly operating rotor supported in foil bearings is a design solution that have wide possibilities of applications, unavailable for conventionally supported one. In the turbomachinery, a dynamic behaviour of the machine is related mostly to the stiffness and damping coefficients of system components like rotor, bearings and casing. The foil bearings, although simple in design, indicate complex behaviour resulting from Coulomb friction between their elements. This Coulomb friction affects the damping and stiffness of a given bearing support. Gas film, as a bearing part with relatively high stiffness, plays less role in the rotordynamics than the elastic structure of corrugated foils. So far, many more or less reliable numerical models of this phenomenon have been built and their experimental verification results have been described in literature. The research approach presented in this paper is different. The authors suggested obtaining the data experimentally from the bearing isolated on a test bench, where, the shaft is stationary (fixed), and the gas film is not present. The shaker excites the bearing sleeve while the damping and stiffness are provided to the system by the foil structure. The test bench can be described mathematically as system with single degree of freedom with damping and external forcing. The information collected about the bearing's global coefficients can be implemented afterwards to the rotordynamic software as a tabular data. This will allow to prepare reliable models that will shorten the design process of newly developed compressors with these oilfree supports.

Keywords: foil bearings, bearing damping, bearing stiffness

Forced vibrations in a dynamic system equipped with a mechanism which trans-pass through its singular position

Krzysztof Lipinski

1. Gdansk University of Technology, Department of Mechanical Engineering and Ship Technology, ul Narutowicza 11/12, 80-299 Gdańsk, Poland, [0000-0002-7598-4417]

Abstract: The paper is about modelling of dynamics and about vibrations of hybrid systems composed of a continuous elastic beam and of a multibody system. To merge the two parts, constraint equations are used. Since number of constraint involved coordinates is small, a case dedicated algorithm is proposed to eliminate Lagrange’s multipliers and dependent coordinates. The applicational focus is set to amplify damping. To amplify it for the lower-frequency modes, inter-modal energy transfer is enforced due to nonlinearity of dynamics of the multibody part. Proposed amplification becomes effective if the multibody part is put in a shape which is close to its kinematical singular position. Focusing on free vibrations, efficiency of the damping method was verified successfully in few of the previous works of the Author. The present work investigates effectiveness of damping of forced vibrations.

Keywords: Finite elements, multibody, nonlinear vibrations, damping amplification, singularity

1. Introduction

Attention of the paper is set on dynamics and on vibrations of a hybrid system composed of a continuous elastic element and of a multibody system (Fig. 1a). Since dynamics properties of the last are position dependent, resulting system may not be treated as constant linear vibrating system. From the computational point of view, two aspects are crucial. Firstly, right coupling have to be formulated between the linear finite elements model of the beam and the nonlinear model of the multibody part. Secondly, Lagrange’s multipliers have to be added, and then, the last and the dependent coordinates have to be eliminated. Since only few of the system coordinates are involved in the constraints, a case dedicated algorithm is recommended to reduce the numerical cost of the elimination.

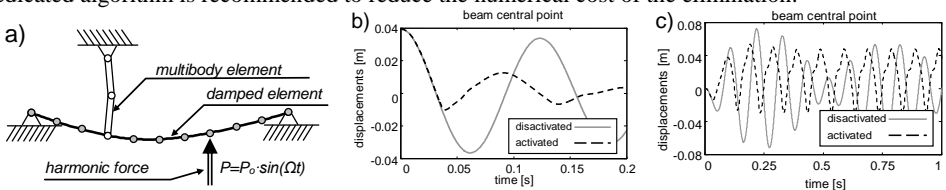


Fig. 1. Draft of the investigated system (a); motion of a selected node – free vibrations (b); motion of the same node – forced vibrations (c)

From the applicational point of view, the focus is set on damping amplification. Structural damping is implemented in the continuous element, thus higher frequency modes are well damped. To accelerate damping of lower-frequencies modes, inter-modal energy transfer is enforced due to the presence of the multibody part. Modal disparity is observed, when motions are performed at different

deformations of the beam. Amplification becomes especially crucial (Fig. 1b) when the multibody part is set in its pose which is close to its kinematical singular position [1-3]. But numerical problems are associated with such configuration, e.g., if joint kinematics is searched for a given vertical kinematics of the fixing point, determinant of the Jacobian matrix tends to zero at the singularity. Thus, if small random error of estimation of the vertical position is assumed, it effects in a significant random error of joint positions and in lock of the numerical integration procedures in consequence.

2. Modelling

To test the damping, related numerical model is introduced. Modelled system is planar (fig. 1a), and it consists of two parts: of an elastic beam and of a multibody part. The multibody part is composed of two rigid bodies and of two massless joints. Joint displacements are considered as its generalized coordinates. Free body diagrams are plotted and associated dynamics equations are written. Final matrix form of dynamics is written with use of the generalized coordinates, \mathbf{q}^b . It leads to [1-3],

$$\mathbf{M}^b(\mathbf{q}^b) \cdot \ddot{\mathbf{q}}^b + \mathbf{F}^b(\dot{\mathbf{q}}^b, \mathbf{q}^b) - \mathbf{Q}^b(\dot{\mathbf{q}}^b, \mathbf{q}^b, \mathbf{f}^e, \mathbf{t}^e, t) = 0 \quad (1)$$

To express dynamics of the elastic beam, finite elements are used. Deformations of nodes are considered as the generalized coordinates of the beam, \mathbf{q}^c . Resulting dynamics equation is [4],

$$\mathbf{M}^c \cdot \ddot{\mathbf{q}}^c + \mathbf{D}^c \cdot \dot{\mathbf{q}}^c + \mathbf{K}^c \cdot \mathbf{q}^c = \mathbf{P}^c \quad (2)$$

To merge the systems, constraint equations are used. The end-point of the last arm is joined to the beam by use of spherical joint constraint. Beam connected point coincides with a node of its FEM model. Constraints are written at the position level, and then formulae of their time derivatives are used. Next, dynamics equations Eqs. (1) and (2) are supplemented with Lagrange's multipliers [1-3]:

$$\mathbf{M}^b \cdot \ddot{\mathbf{q}}^b + \mathbf{F}^b - \mathbf{Q}^b + \mathbf{J}^{bT} \cdot \boldsymbol{\lambda} = 0; \quad \mathbf{M}^c \cdot \ddot{\mathbf{q}}^c + \mathbf{D}^c \cdot \dot{\mathbf{q}}^c + \mathbf{K}^c \cdot \mathbf{q}^c + \mathbf{J}^{cT} \cdot \boldsymbol{\lambda} = \mathbf{P}^c \quad (3)$$

Then, Lagrange's multipliers and the dependent coordinates are eliminated. A modified version of the classical coordinate partitioning [3] is used in order to eliminate some of the non necessary zero numerical calculations. To reduce numerical problems resulting of singularity, a coordinate of the multibody part is set as the independent parameter. After the elimination the dynamic equations are,

$$\mathbf{M}^* \cdot \ddot{\mathbf{q}}^* + \mathbf{F}^* - \mathbf{Q}^* = 0 \quad (4)$$

3. Results, Discussion and Concluding Remarks

Focusing on free vibrations of the elastic/multibody system, efficiency of the damping method was verified successfully [1,2] (Fig. 1.b). The presently taken tests are focused on forced vibrations. The tests have verified that the method is less effective in the forced case (Fig. 1.c). Reduction of amplitudes is confirmed, however, its range is low. Additional tests and analyses are recommended.

References

- [1] LIPÍŃSKI K., damping amplif. caused by a mech. that trans-pass through its singular position, *ECCOMAS Thematic Conf. on Multibody Dynamics*, Barcelona, Spain, pp. 520-531, 2015
- [2] LIPÍŃSKI K., Numerical comp. of damp. amplify. effects obtained in neighbor. of a mech. singular pos.–viscous and electromag. cases, *Key Engineering Materials*, VOL. 597, pp. 145–150, 2014.
- [3] LIPÍŃSKI K., *Multibody systems with unilateral constraints in application to modelling of complex mechanical systems*, Wydawnictwo Politechniki Gdańskiej, 123, Gdańsk, 2012 (in polish).
- [4] ZIENKIEWICZ O.C., TAYLOR R.C., *The finite element method*, 6th edition, Elsevier, 2005.

Broadband vibration of a beam under tensile load

MARCELA R. MACHADO ^{1*}, MACIEJ DUTKIEWICZ ²

1. Department of Mechanical Engineering, University of Brasilia, 70910-900, Brasilia, Brazil [0000-0002-7488-7201]
 2. Faculty of Civil, Environmental Engineering and Architecture, University of Science and Technology, 85-796 Bydgoszcz, Poland [0000-0001-7514-1834]
- * Presenting Author

Abstract: The vibration characterization is directly associated with its physical properties of the system, such as mass, damping, and stiffness. Vibration absorber has been used for vibration control purposes in many sectors of engineering for over a century. A limitation of the device is that it acts as a notch filter, only being effective over a narrow band of frequencies. Therefore, many researchers have design metamaterial targeting the improvement of vibration attenuation and inducing bandgaps. This paper is concerned with the vibration control of a beam under tensile load with periodically attached vibration absorbers. The study is performed by using an approach based on modal analysis. Numerical investigations are conducted regarding the effects of mass ratio, non-uniform spacing and number of resonators.

Keywords: beam vibration, absorber, modal analysis.

References

- [1] XIAO Y., WEN J., YU D., WEN X., Flexural wave propagation in beams with periodically attached vibration absorbers: bandgap behavior and band formation mechanisms. *J. SOUND VIB.*, 332, 2013, 867–893.
- [2] OGATA K., *Modern control engineering*, 5th Edition, Prentice Hall, 2009.
- [3] XIAO Y., WEN J., WEN X., Flexural wave band gaps in locally resonant thin plates with periodically attached spring–mass resonators, *J. Phys. D: Appl. Phys.*, 2012: 45, 195401.

Spectral analysis of chimney vibrations

MARCELA R. MACHADO ^{1*}, MACIEJ DUTKIEWICZ ²

1. Department of Mechanical Engineering, University of Brasilia, 70910-900, Brasilia, Brazil [0000-0002-7488-7201]
 2. Faculty of Civil, Environmental Engineering and Architecture, University of Science and Technology, 85-796 Bydgoszcz, Poland [0000-0001-7514-1834]
- * Presenting Author

Abstract: In the paper, the response of chimney in turbulent wind flow with use of the spectral method is investigated. The analysis is performed for wind flow model that reflects the real conditions. Numerical analysis investigates the vibrations of the chimney due to different parameters of turbulence. Spectra of longitudinal wind velocity for the numerical case, as well as the spectra of Karman, FSU are analysed. The structure response for selected steel strengths and chimney cross-section reduction is analysed. The frequency response functions for are performed.

Keywords: chimney vibration, spectral method, wind turbulence spectra.

1. Introduction

The rapid development of technology causes that modern construction objects have high strength parameters with low structural stiffness and low damping coefficient. These objects are particularly susceptible to dynamic loads such as wind, seismic or paraseismic shocks. These structures include among others: chimneys and masts. In the paper the analysis is performed with application of spectral element method (SEM). SEM [1-4] is a meshing method similar to Finite Element Method (FEM), where the approximated element shape functions are substituted by exact dynamic shape functions obtained from the exact solution of governing differential equations. The response of the chimney in the turbulent wind flow [5-6] with use of spectral method is investigated. The analysis is performed for wind flow model that reflects the real conditions. Numerical analysis investigates the vibrations of the chimney due to different parameters, such as a the area of the cross section of the chimney reflecting of the level of the its damage.

2. Results and Discussion

On the basis of the SEM the Frequency Response Function (FRF) of the chimney vibration is received. A single element is used to model the continuous part of the structure. This feature reduces significantly the number of elements required in the structure model and improves the accuracy of the dynamic system solution. The numerical tests are assumed for fixed boundary condition. The structure is made with steel whose mechanical properties are: $E = 210$ GPa, $\rho = 7850$ kg/m³, $\eta = 0.01$, where

η is the hysteretic structural loss factor. The geometry properties are: length and circular section area. The wind force acting on the chimney are determined according to eurocodes. The analysis is made for different cases of turbulence, for the assumed distribution of wind speed.

3. Concluding Remarks

This paper analyses the dynamic response of the chimney under the turbulent wind flow with use of spectral method. The analysis is performed for wind flow model that reflects the real conditions. Numerical analysis investigates the vibrations of the chimney due to parameters of wind turbulence.

References

- [1] LEE U., Spectral Element Method in Structural Dynamics, John Wiley & Sons, 2009.
- [2] CLOUGH R., PENZIEN J., Dynamics of structures, McGraw Hill, New York, 1993.
- [3] MACHADO M. R., DUTKIEWICZ M., Matt C. F. T., Castello D. A., Spectral model, and experimental validation of hysteretic and aerodynamic damping in dynamic analysis of overhead transmission conductor, Mechanical Systems and Signal Processing (136), 2019 1 21. doi: 10.1016/j.ymssp. 2019.106483.
- [4] DUTKIEWICZ M., MACHADO M., Spectral element method in the analysis of vibrations of overhead transmission line in damping environment., Structural Engineering and Mechanics 71(3), 2019: 291-303. doi:10.12989/SEM.2019.71.3.291.
- [5] ESDU-Report, Characteristics of atmospheric turbulence near the ground, Part II: single point data for strong winds (neutral atmosphere), No. 85020, 1993.
- [6] SOLARI G., Gust buffeting, peak wind velocity and equivalent pressure, Journal of Structural Engineering, Vol.119, No.2, 1993.

Influence of a relatively high frequency structure vibrations on the dynamics of real stick-slip motion

PAWEŁ OLEJNIK^{1*}, ADRIAN GÓRNIAK VEL GÓRSKI¹, MACIEJ CEBULAK¹,
JAN AWREJCEWICZ¹

1. Department of Automation, Biomechanics and Mechatronics, Lodz University of Technology, 1/15 Stefanowski Str., 90-924 Lodz, Poland [P.O. ORCID: 0000-0002-3310-0951, J.A. ORCID: 0000-0003-0387-921X]

* Presenting Author

Abstract: The work concerns the research on the impact of structure vibrations on the dynamics of frictional contact of bodies moving in relation to each other and remaining in frictional contact, causing a stick-slip motion. A literature review was carried out, describing mainly the phenomena concerning friction, but also the dynamics of vibrations and non-ideal energy sources that induce system oscillations. In the next step an experimental station for investigation of friction equipped with a new subsystem inducing high-frequency vibrations is presented to propose a modified physical model of the investigated frictional system. After analysing the most important factors influencing the behavior of the tested system, a mathematical description was prepared, which in theory showed the potential influence of the attached subsystem on the dynamics of the movement of the tested object - the frictional connection. Various methods of implementing the unbalance of rotors, being the source of high-frequency excitation, have been considered. At the final stage, a series of measurements of the displacement of the vibrating block on the moving belt was performed with the high-frequency excitation turned on and off. The prepared graphs were used to analyse the dynamics of frictional contact and the impact of non-autonomous vibrations on the occurrence of the stick-slip phenomenon.

Keywords: stick-slip, measurements, mechanical vibrations, experimental station

1. Introduction

Until today, scientists are designing new measurement systems to explore the stick-slip phenomenon, where technological advances in the sensors and measurement recording methods used are of great importance. New solutions allow for simulations of mechanical systems that are more and more close to reality, which translates into more complex research and obtaining more reliable conclusions. In the case of devices with dry friction, causing the stick-slip (creep-slip) movement of the active elements of the machine, vibrations of the structure can also be observed most often. Such oscillations affect the frictional contact, so they must also condition the stick-slip phenomenon. The discussed problem of vibrations caused by dry friction appears, among others, in brake systems [1,2]. The test stand used was created on the basis of the actual brake mechanism. In this work, a physical model and a mathematical description of the test system were prepared, taking into account the action of relatively high-frequency vibrations. The system introduces a high-frequency vibration inductor (simulating the excitation from cooperating machine elements). The constructed mechatronic system, simulating operating conditions in a drum brake, used in this work, was originally described in the publication [1] and continued in [2], see Figure 1.

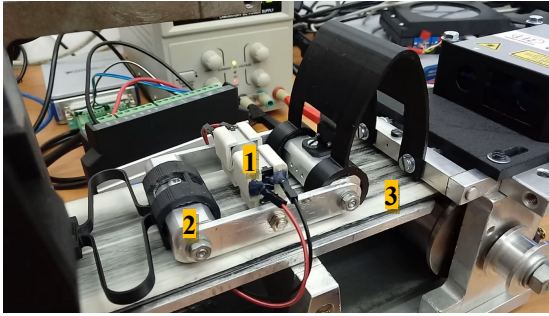


Fig. 1. The experimental station for investigation of self-excited frictional vibrations where two high frequency inductors (1) are mounted on a block mass (2) sliding on the moving belt (3)

2. Results and Discussion

The initial mathematical model of the problem is given by the following equations of motion:

$$\begin{aligned} M\ddot{x} + Kx - F_t &= F_x(t), \\ M\ddot{y} + k_b y &= F_y(t), \end{aligned} \quad (1)$$

where the mass of the entire object moving on the belt is $M = m + m_s$, the parameter $K = k_1 + k_3$, the friction is modeled by F_t and $F(t)$ it is the force of rotating unbalance, see Figure 2.

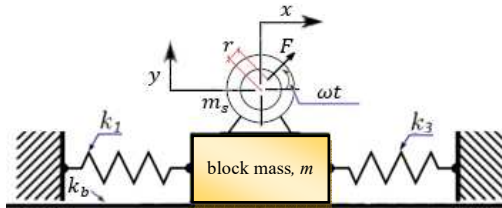


Fig. 2. A physical model of the braking system with an approximation of the object subjected to vibrations

3. Concluding Remarks

The influence of forced vibrations on the dynamics in frictional contact and on the occurrence of the stick-slip phenomenon was demonstrated. In the absence of imbalance on the motor shafts, the effect turned out to be negligible, but the situation changed significantly with its application. The regular time stick-slip characteristics (a saw-like shape) has been replaced by a curve changed by overlapping vibrations caused by excitations from the inductor.

Acknowledgment: This research was funded by Narodowe Centrum Nauki grant number 2019/35/B/ST8/00980 (NCN Poland).

References

- [1] OLEJNIK P.: *Numerical and experimental analysis of regular and chaotic self-excited vibrations with two degrees of freedom with friction*, Ph.D. Thesis, 2002.
- [2] PILIPCHUK V., OLEJNIK P., AWREJCEWICZ J.: Transient friction-induced vibrations in a 2-DOF model of brakes. *Journal of Sound and Vibration* 2015, **344**: 297-312.

Measurements and Sound Synthesis of a Guitar String Re-Excitation

MAREK PLUTA^{1*}, DANIEL TOKARCZYK²

1. AGH University of Science and Technology, Department of Mechanics and Vibroacoustics, Krakow, Poland [0000-0002-2519-8135]
 2. AGH University of Science and Technology, Department of Mechanics and Vibroacoustics, Krakow, Poland
- * Presenting Author; pluta@agh.edu.pl

Abstract: One of factors that have an impact on the sound of a guitar is a state of its string at the moment of its excitation. When a string is excited while still vibrating, such phenomenon is referred to as re-excitation. It is known to affect the sound of an instrument, and therefore it is sometimes implemented in sound synthesis methods based on physical-modelling, but its nature has not been well-studied due to practical problems in measuring real instruments' behaviour in controllable, repeatable environment. The paper presents results obtained with a unique test stand equipped with a guitar-playing robot designed for measurement purposes. The stand facilitates a precise control over amplitude, location and time of excitation, which allows to carry out the research on re-excitation. One of the most flexible approaches to physical modelling applied in sound synthesis is the finite difference method. Therefore the measurements are compared to FD string models in order to fine-tune settings of the experiment, and ultimately, to verify behaviour of particular models.

Keywords: physical modelling, finite difference method, sound synthesis, guitar, robot

1. Introduction

Sound synthesis based on physical modelling methods attempts to identify and simulate phenomena related to sound production. Of primary concern are these that allow to control parameters responsible for perceivable sound effect – either related to instrument itself, or its excitation. For the purpose of simplification and efficiency, sound synthesis often assumes that an instrument does not vibrate during excitation. Only relatively recent concatenative and physical modelling synthesis methods allow to model re-excitation, ie. implement dependence of sound characteristics on the vibrations of a string at the moment of its excitation (Fig. 1). However, such modelling requires relevant experimental data. Therefore a laboratory stand equipped with a guitar playing robot has been developed. The robot (Fig. 2) excites a string at a precise moment of time, at specified location, with adjustable and repeatable amplitude [1] facilitating a degree of control over phase and harmonics.

Various finite difference schemes have been applied to model a guitar string, starting with a frequency-dependent damped stiff string [2]:

$$\frac{\partial^2 u}{\partial t^2} = \gamma^2 \frac{\partial^2 u}{\partial x^2} - \kappa^2 \frac{\partial^4 u}{\partial x^4} + 2\sigma_0 \frac{\partial u}{\partial t} + 2\sigma_1 \frac{\partial^3 u}{\partial t \partial x^2} \quad (1)$$

where u represents displacement, γ is a cumulative material parameter, κ controls stiffness, σ_0 and σ_1 are responsible for damping. Output of a model was used for initial setting of spatial and temporal parameters of excitation in test stand. In turn, results of measurements were used to adjust model parameters and to verify behaviour of its elements.

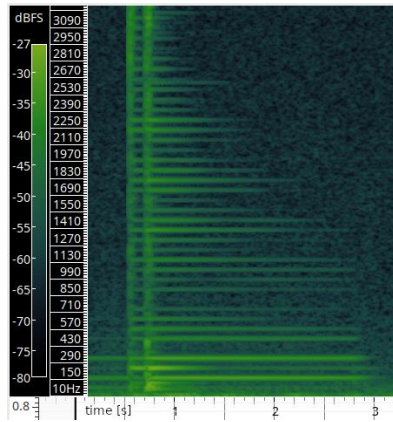


Fig. 1. Spectrogram of a recording of re-excited guitar string

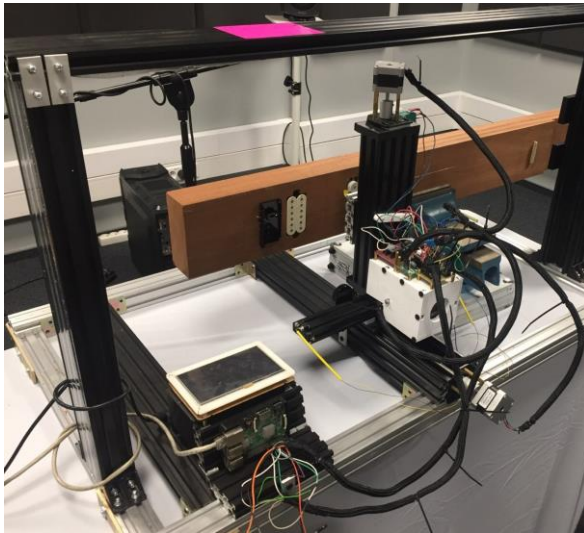


Fig. 2. The stand with a guitar-playing robot in configuration with a simplified electric guitar

References

- [1] TOKARCZYK D, PLUTA M, WICIAK J: Mechanical guitar player, a robot for automatic testing of string instrument parameters. In: WITOS F (ED.) *Acoustics, acoustoelectronics and electrical engineering*. Wydawnictwo Politechniki Śląskiej: Gliwice, 2021.
- [2] PLUTA M: *Sound synthesis for music reproduction and performance*. Wydawnictwa AGH: Kraków, 2019.

Control of deformation and transversal vibrations of a clamped beam by two discretely attached monolithic piezoelectric rods

JACEK PRZYBYLSKI

Division of Mechanics and Machine Design Fundamentals, Faculty of Mechanical Engineering and Computer Science, Cz. stochowa University of Technology, Cz. stochowa, Poland

Abstract: Presently, most of the research on vibration and shape control of slim structures by piezoelectric actuation is restricted to the systems in which the actuator or actuators are embedded in or bonded to the substrate. In the present contribution, two monolithic piezoceramic actuators are attached to the beam at discrete points. In such implementation, the actuators possessing flexural stiffness bend together with the structure. The applied design enhances the static performance in relation to the standard architecture and influences the natural vibrations of the structure. For the system with curved members because of the electric field loading, the equations of motion are linearized about the curvilinear equilibrium state. The governing equations of motion and boundary conditions are derived using extended variational Hamilton's principle. Constitutive equations expressing the piezoelectric coupling between the electric and elastic fields, the von Kármán theory of moderately large rotations but small strains and the Euler-Bernoulli beam theory are used in the formulation. Due to the nonlinearity of the governing equations, their solutions are attempted by a regular perturbation technique leading to asymptotic expansions of displacements, internal forces and the natural vibration frequency. Numerical examples are presented, including how the geometrical nonlinearity is incorporated in the structure static and dynamic responses as a function of two main variables, the actuators offset distance and the electric field application.

Keywords: piezoelectric actuation, shape control, nonlinear vibrations

1. Introduction

When an electric field having the opposite polarity and orientation in regard to the original polarization field is placed across the thickness of a uniform piezoceramic actuator, the piece expands in the transverse direction and, at same time contracts in the longitudinal direction, i.e. along the polarization axis. When the field is reversed, the motions are reversed, hence, as the piezo contractors are usually flat elements, their displacements, which occur perpendicularly to the polarization direction on the basis of the transverse piezoelectric effect, may be efficiently exploited for actuation purposes. This idea has been adopted for the shape and vibration control of a cantilevered beam shown in Fig. 1. The whole system that is composed of an aluminium beam and two contracting monolithic piezoceramic stripes with opposite polarity and voltage applied across the individual transducers, creates a compound bending actuator. Since the piezoceramics are discretely attached to the beam at its end, the static and dynamic response of such compound bender should be more evident than in the case when two layers of piezoceramic are bonded to a thin metal shim sandwiched in the middle. Piezoelectric ceramic transducers may be designed as multilayer elements. The multilayer elements, possessing larger cross-sectional area, generate higher forces and may be operated at a lower voltage. The enhanced control of beam's deflection with discretely attached piezoelectric strain

actuator was studied by Chaudry and Rogers [1]. Przybylski and Kuli ski [2] observed the shape enhancement of an eccentrically loaded column using discretely mounted piezoelectric actuator.

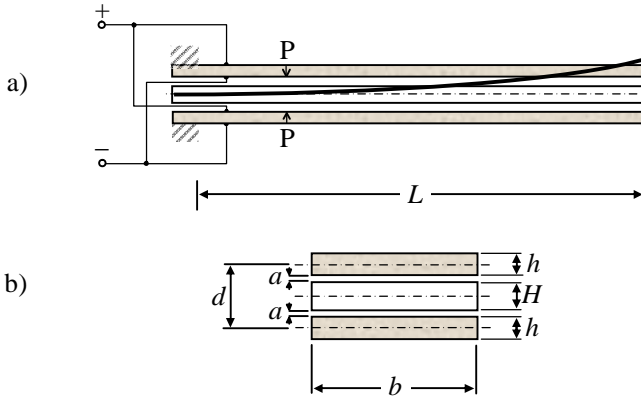


Fig. 1. Compound bending actuator (a) and its cross-section (b)

2. Problem statement

When the piezo contracting actuators are coupled to the beam as in Fig. 1, the driving voltage leads to contraction of the upper ceramic and expansion of the other one, what creates a bending moment. The bending moment converts the small change in length into a large bending displacement perpendicular to the beam's axis. To prevent tensile stresses in the piezoceramics that may appear as a result of the contraction, a mechanical preload is proposed. Such actuator may be applied as a precision positioner, or may operate as a piezoelectric bending motor when the driving voltage will be applied at frequencies much higher than the mechanical resonance. The piezoelectric devices allow continuous smooth motion for unlimited travel, while maintaining high resolution and positioning accuracy [3].

Hence, the main objective of this paper is to demonstrate how distance d between piezoelectric stripes and the voltage applied to them affect both the static performance and the natural vibration frequency of this compound structure. A nonlinear model based on the von Kármán and Euleró Benoulli beam theories has been derived to provide numerical analysis for reasonable explanations of the studied phenomena.

The proposed design of compound piezoelectric bender may have a very wide area of applications. Comparing both the static and dynamic responses of the novel actuator and the classic bimorph, it has been proved, that application of smaller voltage is necessary to the former device to obtain demanded efficiency. The lack of bonding layer also improves the performance and reliability of the actuator.

References

- [1] CHAUDHRY Z., ROGERS C.A.: Enhanced Structural Control with Discretely Attached Induced Strain Actuators. *Journal of Mechanical Design* 1993, **115**(4):718-722.
- [2] PRZYBYLSKI J., KULI SKI K.: Shape enhancement of an eccentrically loaded column using piezoelectric actuator. *Engineering Structures* 2019, **189**(4): 644-654.
- [3] PRZYBYLSKI J.: The effect of geometry on the performance of amplified flexure-guided actuators. *Precision Engineering* 2021, **67**:313-323.

Dynamics of Energy Harvesting Mechanical System in the Vicinity of 1:1 Resonance,

VOLODYMYR PUZYROV^{1*}, JAN AWREJCWICZ², NATALIYA LOSYEVA^{3**}

1. Universitat Politècnica de Catalunya, Terrassa, Spain;
Nizhyn Gogol State University, Nizhyn, Ukraine [ORCID: 0000-0001-6770-182X]
2. Lodz University of Technology, Lodz, Poland [ORCID: 0000-0003-0387-921X]
3. Nizhyn Gogol State University, Nizhyn, Ukraine [ORCID: 0000-0002-2194-134X]

* Presenting Author

Abstract: Energy harvesting provides a useful way to power electronic devices without using batteries or electrical wiring. Energy harvesting can be defined as the conversion of environmental energy, such as mechanical, thermal, light energies into usable electrical energy. Conventional mechanical energy harvesting devices use a line harvester to generate electricity through vibrations or other mechanical motion. However, linear generators generate significant power in a narrow band around resonance, and the power is limited by the internal damping factor and the driving force at the resonant frequency. Such devices implementing a linear (resonant) generator cannot generate sufficient specific power. In present paper the mechanical system is considered which consists of two coupled oscillators (nonlinear absorber connected with primary mass) and a piezoelectric element attached. Two goals are pursued: the mitigation of the responses of the main mass and maximizing the amount of energy extracted from vibrations. The influence of nonlinear stiffness's component is discussed. It is shown that the piezoelectric element allows the effective energy harvesting and at the same has very limited influence on reducing the amplitude of oscillations of the main mass.

Keywords: electro-mechanical system, nonlinear absorber, external excitation.

1. Introduction

The energy harvesting in recent years has attracted increased attention from various disciplines [1-5], mainly due to its potential to act as a key technology that allows the creation of ultra-low-power electronic systems with autonomous power. Kinetic energy harvesters, also known as vibration power generators, are typically the inertial spring-mass systems. Electrical power is extracted by employing one or a combination of several transduction mechanisms. Normally, the transduction mechanisms are piezoelectric, electromagnetic or electrostatic. As most vibration power generators are resonant systems, they generate the maximum power in the vicinity of the resonant frequency. The piezoelectric energy harvesting remains one of the most widely researched harvesting method due to its ease of application and relatively high voltage output. In this report, an energy harvesting device based on a dynamic vibration absorber is studied to achieve two objectives: vibration suppression and energy harvesting in a wideband range. Models using various types of oscillations were considered by many researchers [6 - 8]. Among models considered are: a cantilever beam carrying a tip mass [9], tuned auxiliary structure [10], rotational motion system [11].

** Corresponding Author: natalie.loseva@gmail.com

2. Results and Discussion

Consider a harmonically excited linear oscillator (primary system) coupled with a nonlinear absorber (secondary system or NDVA). The primary structure is assumed to be a single degree of freedom system which mass and stiffness are represented by m_0 and k_0 , respectively, whereas the corresponding notions for the energy harvesting DVA are m_a and k_a , respectively, and c_a – damping coefficient. The electrical capacitance and resistance are denoted by C_p and R_l , respectively. The parameter θ characterizing the coupling between the electrical and mechanical parts of the harvester. The dynamics of the system can be expressed by three coupled ordinary differential equations in the following form

$$m_a \ddot{x}_0 - c_a(\dot{x}_a - \dot{x}_0) + k_0 x_0 - k_a^{lin}(x_a - x_0) + k_a^{nonlin}(x_a - x_0)^3 = F_0 \cos \omega t, \quad (1)$$

$$m_a \ddot{x}_a + c_a(\dot{x}_a - \dot{x}_0) + k_a^{lin}(x_a - x_0) - k_a^{nonlin}(x_a - x_0)^3 - \theta v = 0, \quad (2)$$

$$\theta \dot{x}_a + C_p v' + v/R_l = 0. \quad (3)$$

where x_0 and x_a are the displacement of the primary mass and absorber mass, respectively. The voltage across the load resistor is denoted by v .

The aim is to determine the parameters of the absorber and the piezoelectric element in such a way as, on the one hand, to ensure that the responses of the main system are minimized in the vicinity of the resonance, and on the other hand, to maximize the collection of energy. Generally speaking, the goals set are contradictory, so the task is to find some compromise. In this paper, we first establish acceptable limits for the system parameters, which guarantee a predetermined upper limit on the amplitude of the oscillation of the host system. Having thus obtained a certain region in the parameter space, we solve the second part of the problem to get the maximum benefit for the function V^2/R_l .

3. Concluding Remarks

An electro-mechanical system consisting of a primary element, a dynamic absorber and a piezoelectric element is considered. The goal is to reduce the vibration of the primary structure and at the same time collect the energy through the interaction of the host system and the vibration absorber. An analytical and numerical study of the dynamics of the system is carried out.

References

- [1] MITCHESON P., YEATMAN E., RAO G., HOLMES A., and GREEN T.: Energy harvesting from human and machine motion for wireless electronic devices. *Proc. of the IEEE* 2008, **96**(9): 1457-1486.
- [2] KAZMIERSKI T., BEEBY S.: Energy Harvesting Systems Principles. Modeling and Applications. Editors Springer, 2011.
- [3] BLOKHINA E., AROUDI A. E., ALARCON E., GALAYKO D.: Introduction to Vibration Energy Harvesting. Chapter in: Nonlinearity in Energy Harvesting Systems, Springer, 2016.
- [4] SHEVTSOV S., SOLOVIEV A., PARINOV I., CHERPAKOV A., CHEBANENKO V.: Piezoelectric Actuators and Generators for Energy Harvesting. Springer, 2018.
- [5] RAFIQUE S.: Piezoelectric Vibration Energy Harvesting. Springer Int. Publ. AG., 2018.
- [6] ADHIKARI S., FRISWELL M., INMAN D.: Piezoelectric energy harvesting from broadband random vibrations. *Smart Mater. Struct.* 2009, **11**(18): 115005.
- [7] SODANO H., INMAN D., PARK G.: A review of power harvesting from vibration using piezoelectric materials. *Shock Vib. Dig.* 2004, **3**(36): 197-205.
- [8] STEPHEN N.: On energy harvesting from ambient vibration. *J. Sound Vib.* 2006, **3**(293): 409-425.
- [9] KUMAR A., ALI S., AROCKIARAJAN A.: Influence of piezoelectric energy transfer on the interwell oscillations of multistable vibration energy harvesters. *J. Comput. Nonlinear Dynam.* 2019, **14**(3): 031001.
- [10] CORNWELL P., GOETHALS J., KOWTKO J., and DAMIANAKIS M.: Enhancing power harvesting using a tuned auxiliary structure. *J. Intel. Mater. Syst. Struct.* 2005, **3**(16): 825-834.
- [11] GUAN M., LIAO W.-H.: Design and analysis of a piezoelectric energy harvester for rotational motion system. *Energy Conversion and Management* 2016, **1**(111): 239-244.

Relaxation Effect in Implanted Human Middle Ear

RAFAL RUSINEK¹, ROBERT ZABLOTNI^{2*}

1. Lublin University of Technology, Department of Applied Mechanics [0000-0002-2808-2007]

2. Lublin University of Technology, Department of Applied Mechanics [0000-0003-4857-3185]

* Presenting Author

Abstract: As human beings, we have five basic senses: vision, hearing, balance, smell taste and touch. Hearing is one of the most important of them because it enables us to communicate with words and receive sound stimuli from the environment. For this reason it is one of the most difficult and complex systems in the human body to model as a mechanical system. Those models do not only help to recreate the phenomena that occur in the healthy ear, but also in ears with pathologies. By means of mathematical or numerical models, it is possible to study the damaged hearing organ and therefore to take action making it possible to repair or improve audibility. In human middle ear many tendons and ligaments are located this is the reason why relaxation effect is taken into consideration and it may improve model of human middle ear.

Keywords: middle ear, relaxation, ossicles vibrations

1. Introduction

The middle ear is one of the smallest biomechanical systems in the human body. Therefore a treatment of the ear is especially demanding task. An implantable middle ear hearing device (IMEHD) is one of the most promising technique, used in clinical practice, to improve the hearing process [1]. To investigate the IMEHD, a 5-degree of freedom (6dof) model of lumped masses is proposed that is also verified by a finite element model. Moreover, a relaxation effect of tendons and ligaments is taken into consideration in order to explain its role in sound transfer process. A problem of relaxation in the human middle ear is marginally treated in literature. Due to stress caused by acoustic waves the eardrum vibrates and the middle ear bones are set in motion. Each of these bones is connected with the temporal bone by ligaments and tendons. Motion mentioned above is causing stretching and compression in those tissues. Therefore it is necessary to study about the significance of the relaxation phenomenon in middle ear.

2. Results and Discussion

The model of intact human middle ear [Fig. 1a] was designed by 3D scanning of a human temporal bone. The eardrum, the malleus, the incus and the stapes was separated and then they have been scanned. The obtained parts was connected each other in CAD software. Moreover, the ligaments and tendons were created in CAD and connected to the bones. A part imitating cochlea and it's oval window was created for connection of the stapedia annular ligament (SAL).

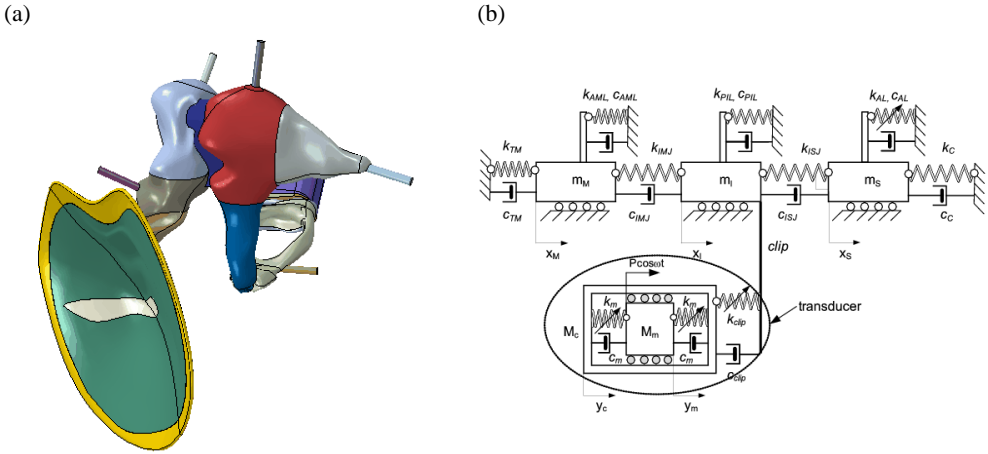


Fig. 1. 3D finite element model of intact human middle ear (a), lumped mass model of implanted middle ear.

The most demanding aspect of Finite Elements Method modelling of the middle ear is determining the boundary conditions of the tendons and ligaments. Appropriate boundary conditions of the system allow for proper reproduction of the occurring movements in the middle ear as a result of being forced by an acoustic wave onto the eardrum. The FEM model is required to get reference behaviour of the intact ossicular chain.

Simultaneously, the lumped mass model of implanted middle ear (5 degree of freedom), presented in Fig.1b was analysed to explore an influence of an middle ear implant and relaxation effect on sound transmission.

In result, the relaxation effect can shift resonance of the middle ear. Considering a simplified three-mass system of intact middle ear which every mass corresponds to one ossicle (malleus, incus and stapes respectively), a shift of the second resonance can be observed as a consequence of relaxation. By increasing the adopted relaxation time, the shift enlarges and the amplitude decreases. Exceeding the specified value of the relaxation time, we do not get any further changes, however, when the relaxation time is short this effect is not negligible and brings significant changes.

3. Concluding Remarks (10 point, bold)

Acknowledgment:

The research was financed in the framework of the project Nonlinear effect in middle ear with active implant, no.2018/29/B/ST 8/01293, funded by the National Science Centre, Poland.

References

- [1] BORNITZ M, HARDTKE H.-J, ZAHNERT T: Evaluation of implantable actuators by means of a middle ear simulation model. *Hearing Research* 2010, **263**:145–151.
- [2] ZHOU K, LIU H, YANG J, ZHAO Y, RAO Z, YANG S: Influence of middle ear disorder in round-window stimulation using a finite element human ear model. *Acta of Bioengineering and Biomechanics* 2019;21(1):3-12.
- [3] RUSINEK R, SZYMANSKI M, ZABLOTNI R: Biomechanics of the Human Middle Ear with Viscoelasticity of the Maxwell and the Kelvin–Voigt Type and Relaxation Effect. *Materials* 2020, 13(17), 3779.

Vibration characterisation of a tubular chemical reactor

JULIANA C. SANTOS¹, MARCELA R. MACHADO^{2*}, LAMIAE VERNIERES-HASSIMI³, LEILA KHALIJ⁴

1. Department of Mechanical Engineering, University of Brasilia, 70910-900 Brasilia, Brazil [0000-0003-0459-8655]
2. Department of Mechanical Engineering, University of Brasilia, 70910-900 Brasilia, Brazil [0000-0002-7488-7201]
3. LSPC/INSA ROUEN Normandie, 76000 Rouen, France [0000-0002-5695-567X]
4. LMN/INSA ROUEN Normandie, 76000 Rouen, France [0000-0002-7058-0544]

* Presenting Author

Abstract: An essential element of the industry operating system is the chemical reactor the chemical sector employs of the potentially dangerous materials and processes. The chemical sector employs potentially dangerous materials and processes. Thus, negligence or misfortune can easily result in devastating consequences like human health, environment, economy, and the industry's reputation. Therefore, the vibration characterisation of this system is essential and directly associated with its physical properties such as mass, damping, and stiffness. The numerical model is based on the spectral element method, and numerical investigations are conducted regarding the effects of internal fluid on the reactor. This paper concerns the vibration characteristics of a tubular chemical reactor and its vibration signatures represented by the receptance response are used to characterise the reactor dynamic.

Keywords: Tubular chemical reactor, Spectral element, Vibration signature.

1. Introduction

The chemical industry involves using processes such as chemical reactions and refining methods to produce a wide variety of solid, liquid, and gaseous materials covering many industrial sectors. An essential element of the industry operating system is the chemical reactor [1]. Food, pharmaceutical, pigment and polymers, cosmetics industries, wastewater treatment, oil refineries, etc., rely on industrial chemical reactors.

The chemical sector employs potentially dangerous materials and processes. Thus, negligence or misfortune can easily result in devastating consequences - damages to human health, environment, economy, and the industry's reputation [2,3]. Therefore, the verification of correct operation, fault finding, early detection and prevention of incidents, and especially the diagnosis and monitoring of the corresponding physical process are vital for the economic function of industrial production processes. Therefore, monitoring the system with an efficient and low-cost procedure is a challenge because industries have to ensure the quality and the repeatability of the products.

The vibration characterisation of this system is essential to understating structural behaviour, monitoring its integrity, and the chemical process. This paper is concerned with the vibration characteristics of a tubular chemical reactor using the spectral element method [4]. Numerical investigations are conducted to characterise the tubular reactor's vibration signatures.

2. Spectral model and Discussion

The tubular chemical reactor is considered to be a pipeline structure with transverse and axial displacements for the local coordinates represented by $w(x, t)$ and $u(x, t)$, respectively. Figure.1a-c illus-

trate the chemical process where the reactor is inserted, the tubular reactor, and the pipeline element with respective displacement and nodal forces.

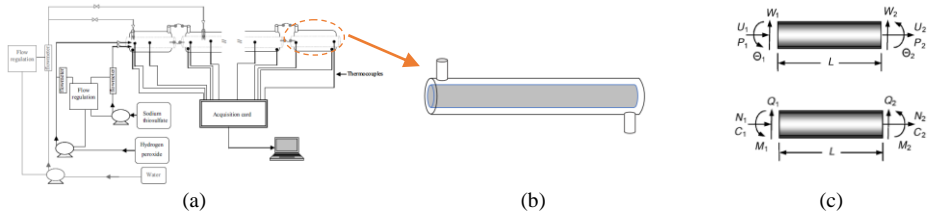


Fig. 1. Tubular reactor: a) chemical process[5]; b) Tubular reactor; c) Model including displacements and nodal force[4].

Pipeline governing equations in frequency domain considering the pressure and velocity of the internal fluid is expressed as [7],

$$\begin{aligned}
 (EA + N)u'' - m_p \ddot{u} + F_N w' + F_T = 0 \\
 EI_p w'''' - Nw'' - m_p \ddot{w} - F_T w' + F_N = 0
 \end{aligned}
 \tag{1}$$

where E , L , A , m_p , I_p , N , F_N , F_T are Young's modulus, the length of pipeline element, the cross-sectional area of pipeline, the pipeline mass per unit length, the second moment of the cross-sectional area, the axial tensile load, and flow-induced normal and tangential force, respectively. The spectral form of axial and vertical displacement solution is given by

$$u(x, t) = \frac{1}{N} \sum_{n=1}^N U_n(x) e^{i\omega t}, \quad w(x, t) = \frac{1}{N} \sum_{n=1}^N W_n(x) e^{i\omega t}
 \tag{2}$$

3. Final Remarks

This paper treats the vibration characteristics of a tubular chemical reactor industry. Also, it presents the numerical model based on the spectral element method. The vibration signature can be used in the system analyses, check the chemical process, and monitor the reactor integrity.

References

- [1] Downs, J. J.; Vogel, E. F. A plant-wide industrial process control problem. *Computers and Chemical Engineering*, v. 17, n. 3, p. 245–255, 1993.
- [2] Benkouider, A. M: Fault detection in semi-batch reactor using the EKF and statistical method. *Journal of Loss Prevention in the Process Industries*, v. 22, n. 2, p.153–161, mar 2009. ISSN 09504230.
- [3] Molga, E. J.: Neural network approach to support modelling of chemical reactors: Problems, resolutions, criteria of application. *Chemical Engineering and Processing: Process Intensification*, v. 42,675–695, 2003.
- [4] Lee, U. : *Spectral element method in structural dynamics*. John Wiley & Sons (Asia), 2009.
- [5] L.Vernières-Hassimia; S.Levенеura: *Alternative method to prevent thermal runaway in case of error on operating conditions continuous reactor*, *Process Safety and Environmental Protection*, v98, p.365-373, 2015.

Determination of peak efficiency of galloping energy harvesters with various stiffness characteristics

FILIP SARBINOWSKI^{1*}, ROMAN STAROSTA²

1. Institute of Applied Mechanics, Poznan University of Technology, Poland [0000-0002-2337-3390]

2. Institute of Applied Mechanics, Poznan University of Technology, Poland [0000-0002-3477-4501]

* Presenting Author

Abstract: In the work, through analytical considerations, the peak efficiency of three different variants of galloping energy harvester was defined. For this purpose, the authorial method based on elliptic harmonic balance was employed, consisting of comparison of impossible to analyze, accurate high order solutions, and simplified solutions of a linearized model. Research has shown that the peak efficiency of the hardening and bistable devices is greater by 17% and 30% respectively in regards to the linear device, while application of softening stiffness always leads to a loss of efficiency.

Keywords: energy harvesting, galloping, nonlinear vibration, elliptic functions

1. Introduction

In the era of the idea of the Internet of Things, the desire of scientists, engineers, medics, and even not-professionals is to continuously measure countless physical phenomena that occur both in our surroundings and at great distances beyond direct human reach. This increases the requirements for measuring devices and thus for their power supply – if access to the operating device is limited, it may not be possible to route the power cables or periodically exchange the batteries. The solution to this problem may be the application of autonomous devices - equipped with their generator harvesting ambient energy. An example of such a generator is the galloping energy harvester (GEH) - the device that allows to harvest the energy of vibrations induced by the flow.

In its simplest version, the GEH can be considered as a body (resonator) mounted on the elastic element, coupled to the piezoelectric (Fig. 1.). If an appropriately shaped body is used, at a certain flow velocity, called the critical velocity, negative damping will be induced in the system and thus stability of the system will be lost.

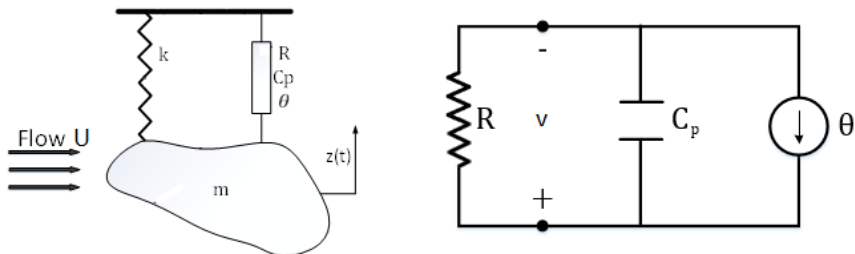


Fig. 1. Model of galloping energy harvester

One of the most important parameters describing energy generators is peak efficiency. In [1], the maximum efficiency was derived for the simplified linear GEH model, in which the harvested was defined as structural damping. In work [2], we confirm the validity of the obtained results also for the full electromechanical model. These results indicate that the peak efficiency of such a device depends only on the geometry of the resonator.

2. Results and Discussion

Employing the elliptic harmonics balance, the expressions describing the efficiency of various variants of devices were obtained as a function of the flow velocity in the form of $\eta_N = \eta_L \Psi$, where $\eta_L = \eta_L(U)$ is the efficiency of linear device and $\Psi = \Psi(m)$ (Fig. 2) is the coefficient that describes the impact of nonlinearity on the efficiency of the device in function of the modulus of elliptic function m . Depending on the nature of the nonlinearity, the value modulus is bounded in the following ranges: for hardening stiffness $0 < m < 0.5$, for softening stiffness $0 < m < 1$ and for bistable system $0.5 < m < 1$, it is therefore, possible to strictly determine the value of the Ψ coefficient at extreme its extreme values.

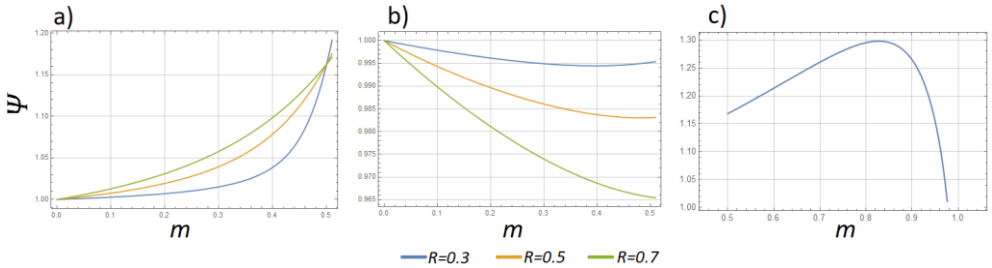


Fig. 1. Ψ values as a function of m for different R values and different stiffness variants: a) hardening, b) softening, c) bistable

Based on the above information, it can be concluded that: a) the function $\Psi(m)$ for the system with hardening stiffness depends on the values of the system parameters, but for the $m = 0.5$ it always has the same, maximum value $\Psi(0.5) \approx 1.17$, b) maximum value of $\Psi(m)$ for the system with softening stiffness is reached for $m = 0$ and $\Psi(0) = 1$ therefore, the softening stiffness will lead to a decrease in peak efficiency, c) regardless of the system parameters, the peak value of $\Psi(m)$ for the bistable system is $\Psi(0.83) \approx 1.30$.

References

- [1] Barrero-Gil, A., Alonso, G., and Sanz-Andrés, A. (2010) Energy harvesting from transverse galloping. *Journal of Sound and Vibration*, 329(14), 2873– 2883.
- [2] Sarbinowski F., Starosta R., (2020) Minimization of critical flow velocity of aeroelastic energy harvester via delayed feedback control, *Vibrations in Physical Systems*, 31(2).
- [3] Bibo A., Alhadidi A. H., Daqaqa, M. F. (2015) Exploiting a nonlinear restoring force to improve the performance of flow energy harvesters, *Journal of Applied Physics*, 117.

Piecewise Linear Dynamics of a Cracked Beam with Hysteretic Damping

VAIBHAV TANDEL^{1*}, K. R. JAYAPRAKASH¹

1. Indian Institute of Technology Gandhinagar

Abstract: This study is concerned with the piecewise linear (PWL) dynamics of a cracked Euler-Bernoulli (E-B) beam with hysteretic damping. The mode 1 crack in the beam is modelled as a PWL spring at the crack location resulting in slope discontinuity during the crack opening. On crack closure, the frictional contact between the surfaces leads to forces that exhibit hysteresis and an empirical hysteretic damping model is incorporated. A semi-analytical approach is evolved and we present some of the interesting results emerging in the forced dynamics

Keywords: Nonlinear vibration, cracked beam, hysteretic damping, piecewise linear oscillator

1. Introduction

The presence of the crack in a structure affects its stiffness and dynamical characteristics. The opening/closing of the cracks leads to disparity in the interfacial stiffness, which is essentially nonlinear. The dynamical study of such structures is essential in engineering applications. Yokohama et al. [1] considered a modified line-spring model for a uniform E-B beam to study vibration characteristics. Abraham et al. [2] considered Timoshenko beam with a transverse crack to be of piecewise nature in the time domain incorporating dry friction at the crack interface. Chati et al. [3] considered bilinear frequency of the PWL model of the cracked beam and a PWL 2-DOF reduced model to study their dynamics. In addition to stiffness disparity, there is dissipation which can be nonlinear. Models based on the underlying dissipative mechanics are complicated, whereas the simpler low-dimensional models are empirical. Maiti et al. [4] studied the response of beams with internal dissipation modelled as the net averaged effect of a large number of randomly dispersed frictional microcracks incorporating hysteresis model.

In this study we consider PWL spring at the location of the crack owing to a change in stiffness due to opening/closing of the crack. The energy dissipation during the crack closure is considered as hysteretic damping and is invoked in a piecewise form. General forcing is considered to study the effect of crack location, depth and the damping on the dynamics. This study considers semi-analytical approach, method of averaging and Galerkin's method.

2. Mathematical Model

Consider a E-B beam with a crack modelled as two beams connected by a bilinear torsional spring at the crack location. The nondimensional equation of motion is

$$v_{yyyy} + v_{\tau\tau} + q_{b,y}(y, \tau) = f(y, \tau) \quad (1a)$$

where $0 \leq y \leq 1$ and the hysteretic damping is defined in the form

$$q_b(y, \tau) = \begin{cases} \chi\theta(e, \tau)v_{yy}(y, \tau)\delta(y - e), v_{yy}(e, \tau) \geq 0 \\ 0, v_{yy}(e, \tau) < 0 \end{cases} \quad (1b)$$

$$\dot{\theta}(e, \tau) = \kappa\{\theta_a + \beta \operatorname{sgn}(v_{yy}\dot{v}_{yy}) - \theta(e, \tau)\}|\dot{v}_{yy}|/(|v_{yy}| + \varepsilon)$$

Where $v(y, \tau)$ is the transverse displacement, e is the crack location, χ is the damping parameter, θ is an internal variable and $\kappa, \theta_a, \beta, \varepsilon$ are constants governing the hysteretic damping behaviour [4]. The boundary conditions are, $v(0, \tau) = 0; v_y(0, \tau) = 0; v_{yy}(1, \tau) = 0; v_{yyy}(1, \tau) = 0; v(e_+, \tau) = v(e_-, \tau); v_{yy}(e_+, \tau) = v_{yy}(e_-, \tau); v_{yyy}(e_+, \tau) = v_{yyy}(e_-, \tau)$. The slope discontinuity is of the form,

$$\frac{v_y(e_+, \tau) - v_y(e_-, \tau)}{v_{yy}(e, \tau)} = \begin{cases} \alpha_1, v_{yy}(e, \tau) \geq 0 \\ \alpha_2, v_{yy}(e, \tau) < 0 \end{cases} \quad (2)$$

$v_{yy}(e, \tau) \geq 0$ implies crack closure and $\alpha_1 = 0$ resulting in slope continuity at $y = e$ and hysteretic damping is active (ref. (1b)). Whereas, $v_{yy}(e, \tau) < 0$ implies crack opening leading to slope discontinuity at $y = e$ and hysteretic damping is inactive (ref. (1b)). In the absence of dissipation, the equations of motion are solved in two regimes and the solutions are matched at the time instants when $v_{yy}(e, \tau) = 0$. The normal mode solutions form the basis for the Galerkin's method wherein the dissipation is introduced.

3. Results and Concluding Remarks

Undamped forced response for $f(y, \tau) = f_0\delta(y - 1) \sin(\Omega\tau)$ is shown in Fig. 1 for varying Ω . For $\Omega = \omega_1(\alpha_{1,2} = 0)$, the first mode ($i = 1$) of the crack closed configuration resonates, but it goes off resonance when $v_{yy}(e, \tau) < 0$ resulting in modulated response (Fig. 1a). However, when the excitation frequency is equal to the bilinear frequency $\omega_{i(b)} = 2\omega_i(\alpha_{1,2} = 0)\omega_i(\alpha_{1,2} = 0.75)/\{\omega_i(\alpha_{1,2} = 0) + \omega_i(\alpha_{1,2} = 0.75)\}$, one can observe that the response grows unbounded (Fig. 1b). This is for the first mode ($i = 1$) and a more detailed study incorporating the effect of hysteretic damping, prediction of modulation envelope for higher modes ($i > 1$) will be included in the full version paper.

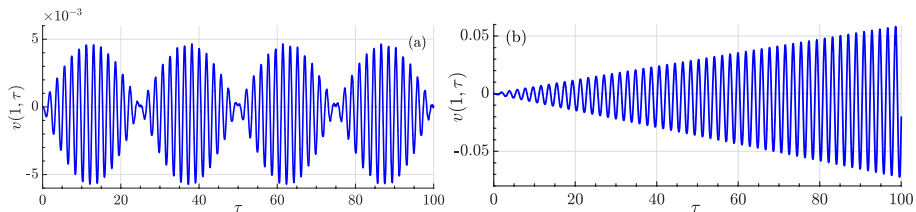


Fig. 1. Response $v(1, \tau)$ for (a) $\Omega = \omega_1(\alpha_{1,2} = 0)$, (b) $\Omega = \omega_{1(b)}$ for $f = 10^{-3}, \alpha_1 = 0, \alpha_2 = 0.75, e = 0.5$

Acknowledgment: VT acknowledges the assistantship provided by Ministry of HRD, India

References

- [1] YOKOYAMA T., CHEN M.: Vibration analysis of edge-cracked beams using a line-spring model. *Engineering Fracture Mechanics* 1998, **59**(3): 403-409.
- [2] ABRAHAM O., BRANDON J.: The modelling of the opening and closure of a crack. *Journal of Vibration and Acoustics* 1995, **117**: 370-377.
- [3] CHATI M., RAND R., MUKHERJEE S.: Modal analysis of a cracked beam. *Journal of Sound and Vibration* 1997, **207**(2):249-270.
- [4] MAITY S., BANDYOPADHYAY R., CHATTERJEE A.: Vibrations of an Euler-Bernoulli beam with hysteretic damping arising from dispersed frictional microcracks. *Journal of Sound and Vibration* 2018, **412**:287-308.

A Nonlinear Interaction Dynamics of System of the Coupled Autogenerators: Numerical Analysis of Time Series, Chaos and Bifurcations

EUGENY V. TERNOVSKY^{1*}, ANDREY A MASHKANTSEV¹, ANDREY A SVINARENKO¹
AND PAVEL A ZAICHKO²

1. Odessa State Environmental University, Mathematics Depr., L'vovskaya str. 15, 65009, Odessa

2. National University "Odessa Maritime Academy", Didrikhson str. 8, 65001, Odessa

* Presenting Author

Abstract: Many physical and technical dynamical systems can be considered as a set of the coupled autogenerators in the first approximation. The nonlinear interaction dynamics of a system of the coupled autogenerators is studied. The results an numerical analysis, modelling, processing and forecasting the nonlinear temporal dynamics of system of the coupled semiconductor quantum generators (autogenerators) are presented, The advanced data on the fundamental topological and dynamical invariants (the correlation, embedding and Kaplan-Yorke dimensions, Lyapunov's exponents, Kolmogorov entropy etc) of the system chaotic dynamics are listed. For the firs time it has been developed an effective temporal evolutionary dynamics prediction model.

Keywords: chaotic dynamics, system of the coupled autogenerators, dynamical and topological invariants

1. Introduction. Nonlinear Dynamics of Chaotic Laser Diodes

An experimental and theoretical study of the non-linear dynamical autogenerators systems attracts a great interest and importance in connection with aim to discover a dynamics with new fractal and deterministic chaos features (e.g. [1-3]). One of the important examples is system, which consists of autogenerators interacting with retarding. Many physical and technical systems such as multielement semiconductors and gas lasers, different radiotechnical devices and others can be considered as a set of the coupled autogenerators in the first approximation. The classical example is a set of two autogenerators (semiconductor) quantum generators, coupled by means of the optical waveguide (e.g. [1,2]). In many papers (e.g. [1-3]) it has been numerically studied a regular and chaotic dynamics of the system of the Van-der-Poll autogenerators with a special kind of inter-oscillators interaction forces and with the finite time of the signals propagation.

In our work it is performed a numerical analysis, modelling and forecasting the nonlinear temporal dynamics of system of the coupled semiconductor quantum generators (autogenerators) and obtained the total data on the fundamental topological and dynamical invariants of the system chaotic dynamics. For system of the vibrating dipoles, situated in the points with coordinates $r_i(I=1...N)$; and dipole moment vectors directed along axe z ; $d_i=(0,0,d), d \equiv e_i x_i$ (e_i – effective charge of the i –th dipole) the equation of motion can be written as follows:

$$\ddot{x}_I + \varepsilon_I (\dot{x}_I^2 - \gamma_I) \dot{x}_I + \omega_I^2 x_I = - \sum_{I' \neq I} f_{II'} \ddot{x}_{I'}(t - \tau_{II'}) \quad (1)$$

where ω_i are the eigen autovibration frequencies. The force in the right part describes an action on l -th oscillator from the radiation field of other ones. The different determinations of a force and equations for calculation of the eigen frequencies are given in Refs. [1,2].

2. Results and Discussion

The results of application of the different mathematical numerical methods to characterize the dynamics of coupled semiconductor quantum generators and discover a presence of the deterministic chaos elements in the dynamics. The nonlinear analysis numerical techniques such as the autocorrelation function and the Fourier power spectrum methods, the mutual information approach, the correlation integral analysis and false nearest neighbour algorithms, the Lyapunov's exponents and Kolmogorov entropy analysis, surrogate data method (in versions [3-6]) are used for comprehensive characterization, processing of the corresponding time series for the studied system. Table 1 summarizes the results of the Lyapunov exponent analysis as well as lists the values of the Kaplan-Yorke attractor dimension, K is the Kolmogorov entropy, and P is the average predictability. For the time series under consideration, there exist two positive exponents (indicating expansion along two directions) and two negative ones (indicating contraction along remaining directions).

Table 1. Results of Lyapunov exponents analysis for amplitude level: λ_1 - λ_4 are the Lyapunov exponents in descending order, d_L is the Kaplan-Yorke attractor dimension, K is the Kolmogorov entropy, and P is the average predictability

λ_1	λ_2	λ_3	λ_4	d_L	K	P
0.0082	0.0017	-0.0047	-0.0167	3.33	0.0094	124.3

The Kaplan-Yorke dimension is equal to 3.33; this value is very close to the correlation dimension which was defined by the Grassberger-Procaccia algorithm [6]. The estimations of the Kolmogorov entropy and average predictability can show a limit, up to which the amplitude level data can be on average predicted. Surely, the important moment is a check of the statistical significance of results.

3. Concluding Remarks

To conclude, the results of the computational analysis, modelling, processing and forecasting nonlinear dynamics of system of the coupled semiconductor quantum generators (autogenerators) are presented. The data on the topological and dynamic invariants are listed and analyzed.

References

- [1] VEDENOV A, EZHOV A, LEVCHENKO E: Non-linear systems with memory and functions of neuron ensembles. In: GAPONOV-GREKHOV A AND RABINOVICH M (Eds) *Non-linear waves. Structure and bifurcations*. Nauka: Moscow, 1987:53-69.
- [2] SERBOV N AND SVINARENKO A: Wavelet and multifractal analysis of oscillations in a grid of coupled autogenerators. *Photoelectronics*. 2007, **16**:53-56.
- [3] GLUSHKOV AV: *Methods of a Chaos Theory*. Astroprint: Odessa, 2012
- [4] GLUSHKOV A, SVINARENKO A, BUYADZHI V, ZAICHKO P AND TERNOVSKY V: Chaos-geometric attractor and quantum neural networks approach to simulation chaotic evolutionary dynamics during perception process. In: BALICKI J (ED) *Advances in Neural Networks, Fuzzy Systems and Artificial Intelligence, Series: Recent Advances in Computer Engineering*. WSEAS: Gdansk, 2014, **21**:143-150.
- [5] BUYADZHI V, BELODONOV A, MIRONENKO D, MASHKANTSEV A, KIR'YANOV S, BUYADZHI A, GLUSHKOV A: Nonlinear dynamics of external cavity semiconductor laser system with elements of a chaos. In: AWREJCWICZ J, KAZMIERCZAK M, OLEJNIK P AND MROZOWSKI J (EDS.) *Engineering Dynamics and Life Sciences*. Lodz., 2017:89-96.
- [6] GRASSBERGER P AND PROCACCIA I: Measuring the strangeness of strange attractors. *Physica D* 1983, **9**:189-208.

Dynamics of Rotating Cylindrical Shell Subjected to Pressure Loading

P. NAGA VISHNU^{1*}, BISWAJIT BHARAT¹, K. R. JAYAPRAKASH¹

1. Discipline of Mechanical Engineering, Indian Institute of Technology Gandhinagar

Abstract: This study pertains to the dynamics of a rotating cylindrical shell and the effect of follower pressure force acting. We consider Donnell's thin shell theory. The considered structure is gyroscopic and is acted upon by follower forces in the form of pressure. The presence of this non-conservative force in this gyroscopic system exhibits interesting dynamical behavior and this abstract provides an overview.

Keywords: Donnell's shell theory, critical speed, gyroscopic system, follower forces

1. Introduction

Thin cylindrical structures are one of the most significant and widely utilised components in various industrial applications such as the aviation industry, electrical system, pressure vessels, nuclear industry and offshore excavation sites. The wide range of applicability of thin cylindrical structures has compelled several authors to study their dynamics in the past. In several applications associated with the offshore oil mining industry, biological industry [1], the thin cylindrical structures undergo pressure loading, and in some applications (offshore drilling), they experience continuous rotation. Hence, the study of the dynamic behaviour of the rotating shell is relevant.

In the past, several researchers have investigated the dynamics of a thin rotating cylinder. Recent studies by Carrera et. al. [2] consider vibration analysis of cylindrical shells using a refined beam model resulting in accurate results for lower frequencies. The accuracy for higher frequencies can be further increased by using a three-dimensional cylindrical shell model. In the past, a numerical study of three-dimensional cylindrical shell based on hierarchical finite element model of a non-rotating thin cylinder has been carried out by Paulo et. al. [3], where higher-order modes have been analysed using a set of reduced-order equations. By considering Donnell's thin shell model, Alujevic et. al. [4] and Ng et. al. [5] have studied the effect of cylinder rotation on the normal modes.

In several applications, pressurised shells are used, where the shell displacements become finite in amplitude resulting in displacement dependent pressure load [6]. We herein consider the free and forced dynamics of a thin rotating (angular velocity Ω about x axis) cylindrical shell of length L , radius R , thickness t and with a constant internal pressure p . The constant pressure load is modelled as a displacement dependent pressure load [6]. The nondimensional equations of motion invoking the Donnell Mushtari's shell theory is given by

$$u_{xx} + \left(\frac{1-\mu}{2}\right)u_{\theta\theta} + \left(\frac{1+\mu}{2}\right)v_{x\theta} + \mu w_x + \Omega^2(u_{\theta\theta} - w_x) - \frac{p}{\beta}w_x = u_{tt} \quad (1a)$$

$$\left(\frac{1}{2} + \frac{\beta^2}{24}\right)(1-\mu)v_{xx} + \left(1 + \frac{\beta^2}{12}\right)v_{\theta\theta} - \frac{\beta^2}{12}w_{3\theta} - \frac{\beta^2}{12}w_{xx\theta} + \left(\frac{1+\mu}{2}\right)u_{x\theta} + w_\theta + v\Omega^2 + 2\Omega w_t + \Omega^2 u_{x\theta} - \frac{p}{\beta}w_\theta = v_{tt} \quad (1b)$$

$$-\frac{\beta^2}{12}w_{4x} - \frac{\beta^2}{12}w_{4\theta} + \frac{\beta^2}{12}v_{\theta\theta\theta} - \frac{\beta^2}{6}w_{xx\theta\theta} + \frac{\beta^2}{12}v_{xx\theta} - \mu u_x - v_\theta - w + w\Omega^2 - 2\Omega v_t + \Omega^2(-v_\theta + w_{\theta\theta}) + \frac{p}{\beta}(1 + u_x + v_\theta + w) = w_{tt} \quad (1c)$$

Where u, v, w are the shell deformations in x, θ and r directions respectively, μ is Poisson's ratio, $\beta = h/R$ and $f_{\theta\theta\theta} = \partial^4 f / \partial \theta^4$. The boundary conditions considered in here are simply supported.

2. Results and Discussions

In this study, the variation of natural frequency $\omega^{(m,n)}$ of the cylindrical shell with angular velocity and internal pressure is studied, where m is the number of half waves in axial direction and n is the number of circumferential waves. For the first circumferential mode i.e., $n = 1$, the natural frequency becomes zero for specific angular velocities, which are the critical speeds. In contrast, $n \neq 1$ does not exhibit such critical speeds. For $m = 1, n = 1$ an increase in pressure increases the critical speed as shown in Fig. 2a. In contrast, for $m = 1, n = 2$, no such critical speeds are observed in Fig. 2b. As observable, the follower pressure force has a significant effect of the natural frequencies.

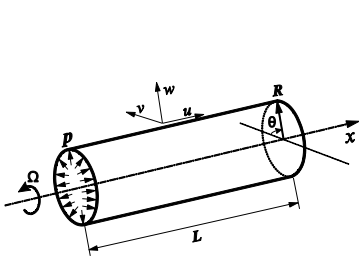


Fig.1 Kinematic description of the cylindrical shell

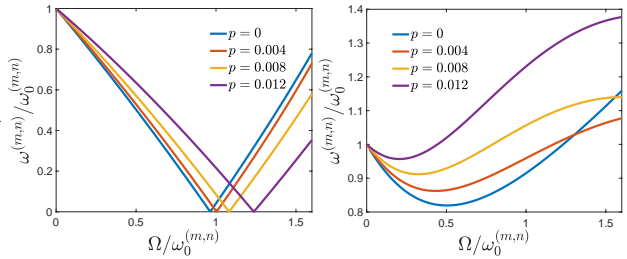


Fig. 2. Normalized angular velocity v/s normalized natural frequency for varying pressure for (a) $m = 1, n = 1$ (b) $m = 1, n = 2$, $\omega_0^{(m,n)}$ is the natural frequency for $\Omega = 0$. $\mu = 0.3, \beta = 0.02, \alpha = 6$.

3. Concluding Remarks

In this work, we study the effects of internal pressure and angular velocity on the normal modes of the thin rotating cylindrical shell. Exact analytic solutions for the vibrations of a cylindrical shell with simply supported boundary conditions are obtained. It is found that for the modes with $n = 1$, a critical speed is obtained, which results in a zero natural frequency. It is observed that the critical speed increases with increase in internal pressure. A complete analysis will be reported in the full version of the paper.

Acknowledgment: PV acknowledges the research assistantship by the Ministry of HRD, India and IIT Gandhinagar. BB acknowledges the DST-RFBR funding INT/RUS/RFBR/358.

References

- [1] GROTEBERG J. B., JENSEN O. E.: Bio Fluid Mechanics in Flexible Tubes. *Annu. Rev. Fluid Mechanics*. 2004, **36**:121-147
- [2] CARRERA E., NEIVA R.: Vibration Analysis of Thin/Thick, Composites/Metallic Spinning Cylindrical Shells by Refined Beam Models. *Journal of Vibration and Acoustics* 2015, **137**(3): 031020
- [3] GONCALVES P. B., FILIPPI M.: Numerical Method for Vibration Analysis of Cylindrical Shells. *Journal of Engineering Mechanics* 1997, **123**(6):544-550
- [4] ALUJEVIC N., CAMPILLO-DAVO N.: Analytical Solution for Free Vibrations of Rotating Cylindrical Shells having Free Boundary Conditions. *Engineering Structures* 2017,**132**:152-171
- [5] NG T. Y., LAM K. Y.: Vibration and critical speed of a rotating cylindrical shell subjected to axial loading. *Applied Acoustics* 1999, **56**: 273-282
- [6] AMABILI M.: *Nonlinear Mechanics of Shells and Plates in Composite, Soft and Biological Materials*. Cambridge University Press: United Kingdom, 2018.

NUMERICAL CALCULATIONS OF TARGET STRENGTH FOR LARGE SCALE BETSSI MODELS

JERZY WICIAK^{1*}, ROMAN TROJANOWSKI², KAROL LISTEWNIK³

1. AGH University of Science and Technology [0000-0002-3932-6513]
 2. AGH University of Science and Technology [0000-0003-3785-2576]
 3. Gdynia Maritime University, Central Office of Measures [0000-0003-3322-7247]
- * Presenting Author

Abstract: This article presents numerical calculations of target strength using FEM with far field equations. First a comparison between FEM with far field equations and FastBEM is made to show that the former can be used for a large-scale acoustical calculations. Then calculations of monostatic and bistatic target strength using different boundary conditions for several models from Benchmark Target Strength Simulation workshop are shown. Finally some of the results are compared to the results of the same calculations done by different science centres using different methods.

Keywords: Target Strength, FEM, FastBEM

1. Introduction

The acoustic field that exists in the sea or ocean comprises natural and artificial sources with wide range of frequencies – from fractions of hertz up to few hundred kilohertz [1, 2]. The artificial disturbances contain a number of discrete components originating from the submarines and ship's hull and equipment connected to hull. Structure vibrations and structural noise may be reduced by passive and active isolation, by passive and active vibration and sound absorbers or by active control [3] or changing the characteristics of radiated sounds.

Around year 2001 an idea was conceived for cooperation of various European science centres in developing a generic submarine model (nicknamed BeTSSi – Benchmark Target Strength Simulation) [4, 5]. Some time ago a second BeTSSi was appointed. This time the intention was to evaluate the performance of different numerical methods the participants used and developed over last decade.

The aim of this paper was to test whether a FEM model with the far field equations could be used for modelling Target Strength of an object from a large distance (normally impossible to model by using pure FEM). Preliminary results are compared to results when using BEM and then the results are confronted with similar models made by different scientific teams from several European research centres.

2. Results and Discussion

For target strength (TS) calculations we used BeTSSi model 1 and 2. Model 1 has a very simple geometry and was already used for the comparison between FEM with far field equations and Fast BEM. Model 2 has a more complex geometry which should be more useful when comparing the results with other science centres.

For TS calculations both models were modelled using element size of 0.2 m, which allowed for balance between accuracy and time needed for calculations. Calculations of TS were performed for the frequency of 1 and 3 kHz. Types of analyses included Monostatic and Bistatic (source located at an angle of 240° and 300°) TS calculations for both Hardwalled (HWBC) and Real Boundary Conditions (RBC).

Fig. 1 presents a comparison of calculated bistatic (BS) TS $\alpha=240^\circ$ with hard walled boundary conditions for different science centres. It can be seen that the results obtained using FEM with far field equations are very similar to those obtained using different methods. A bistatic target strength calculations were chosen for this comparison, because of the better angular resolution of the results. Hard walled boundary conditions were chosen because with full reflection the differences resulting from using different calculation methods should be smaller.

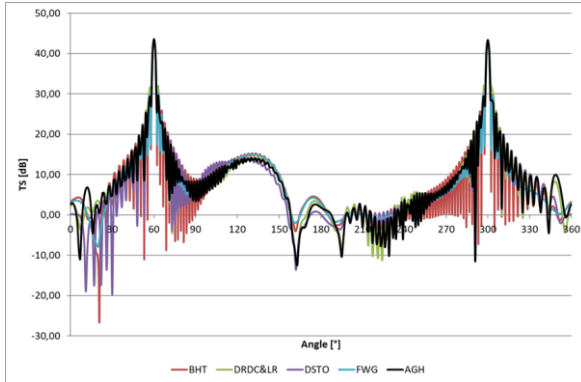


Fig. 1. Comparison of a BS TS for model 1, $\alpha=240^\circ$ with HWBC between different science centres.

3. Concluding Remarks

Obtained results for target strength calculation when using FEM with far field equations are similar to those from other science centres (and different methods). But it should be noted that for higher frequencies a smaller size of elements would be needed which in turn could significantly increase calculation time (especially for the monostatic target strength as it requires a separate calculation for each position of the source).

Acknowledgment: This article is dedicated to the memory of our dear friend Captain PhD Eng. Ignacy Gloza, prof. Polish Naval Academy.

References

- [1] ETTER P. C., UNDERWATER ACOUSTIC MODELING AND SIMULATION, CRC PRESS, TAYLOR AND FRANCIS GROUP, 2013
- [2] LISTEWNIK K., ANALYSIS OF DIFFERENCES IN THE UNDERWATER RADIATION NOISE OF SHIPS IN THE PORT APPROACH ZONE, PROCEEDINGS OF THE INTERNATIONAL CONGRESS OF SOUND AND VIBRATION ICSV 26, MONTREAL, 7-11 JULY, 2019, PP. 1-6 – PEER REVIEW PAPER.
- [3] WICIAK J., MODELLING OF VIBRATION AND NOISE CONTROL OF A SUBMERGED CIRCULAR PLATE, ARCHIVES OF ACOUSTICS, 32, 4 (SUPPLEMENT), 2007, PP. 265–270.
- [4] NELL C., GILROY L.E., AN IMPROVED BASIS MODEL FOR THE BETSSISUBMARINE, DEFENCE R&D CANADA, TECHNICAL REPORT DRDC ATLANTIC TR 2003-199, 2003
- [5] NOLTE B., SCHÄFER I., DE JONG C., GILROY L., BETSSI II BENCHMARK ON TARGET STRENGTH SIMULATION, PROCEEDINGS OF FORUM ACUSTICUM, KRAKOW, POLAND, 2014.

Non-planar motions due to nonlinear interactions between unstable oscillatory modes in a cantilevered pipe conveying fluid

KIYOTAKA YAMASHITA^{1*}, KOKI KITaura², NAOTO NISHIYAMA³, HIROSHI YABUNO⁴

1. Department of Mechanical Engineering, Fukui University of Technology, Japan
[<https://orcid.org/0000-0002-2176-0485>]
2. Department of Mechanical Engineering, Fukui University of Technology, Japan
[<https://orcid.org/0000-0001-8862-5731>]
3. Department of Mechanical Engineering, Fukui University of Technology, Japan
[<https://orcid.org/0000-0003-4956-9858>]
4. Graduate School of Systems and Information Engineering, University of Tsukuba, Japan
[<https://orcid.org/0000-0002-8200-1597>]

* Presenting Author

Abstract: Dynamics of a cantilevered pipe conveying fluid has been studied for a long time. When the flow velocity exceeds a certain value, the damping ratio of a certain mode becomes negative. Long term efforts have been poured to the post-critical dynamical behavior by many researchers. As the flow velocity is increased further, another mode can also experience an oscillatory instability. In such situations, we have to consider nonlinear modal interactions to clarify the evolutions of the amplitudes of unstable modes. In this study, we consider the non-planar oscillations of a cantilevered fluid conveying pipe with an end mass. We focus on the nonlinear interactions of two unstable oscillatory modes. The amplitude equations are derived and nonlinear analyses are conducted. It is clarified that some types of non-planar motions can be produced due to nonlinear interactions of two different unstable modes. Moreover, experiments were conducted to verify the theoretical predictions. In experiments, we observed some non-planar motions that show qualitatively good agreement with the theory.

Keywords: Non-planar motion, Pipe conveying fluid, Double Hopf bifurcation

1. Introduction

High-codimensional bifurcations have attracted the interest in many researchers. Dynamics of a cantilevered pipe conveying fluid is a typical problem of dynamic instabilities in continuous systems[1]. From the linear stability analyses, in a certain parameter regions, it is expected that double Hopf bifurcation becomes a problem. At the double Hopf bifurcating point, the linear system has two pairs of eigenvalues $\pm i\omega_m$, $\pm i\omega_n$ ($\omega_m \neq \omega_n$). In such situations, we have to consider nonlinear modal interactions to clarify the evolutions of the amplitudes of unstable modes. In the previous study[2], we consider the Hopf-Hopf interactions of unstable modes in a plane. In this study, we consider the non-planar oscillations of a cantilevered fluid conveying pipe with an end mass. We focus on the nonlinear interactions of two unstable oscillatory modes. The amplitude equations of non-planar mixed modal oscillations are derived from the non-selfadjoint partial differential equations and their boundary conditions. From the nonlinear analyses, it is clarified that mixed modal non-planar motions can be produced due to nonlinear interactions of two different unstable modes. Moreover, experiments were conducted to verify the theoretical predictions. In experiments, we observed some non-planar motions that show qualitatively good agreement with the theory.

2. Results and Discussion

Figure 1 shows the analytical model of non-planar self-excited pipe vibration. Pipe is hung vertically under the gravity and the lumped mass is attached at the lower free end. From the linear stability analyses, in a certain range of parameters, it is confirmed that second and third modes become simultaneously unstable. Let A_i and B_i be the complex amplitudes of the unstable two modes in X - Y plane and X - Z plane, respectively ($i = 2, 3$). We derive evolutive equations of complex amplitude equations as follows:

$$\dot{A}_2 = \left(-\omega_{2i} + \xi_{12}|A_2|^2 + \xi_{22}|A_3|^2 + \xi_{32}|B_2|^2 + \xi_{42}|B_3|^2 \right) A_2 + \xi_{52} \bar{A}_2 B_2^2 + \left(\xi_{62} A_3 \bar{B}_3 + \xi_{72} \bar{A}_3 B_3 \right) B_2 \quad (1)$$

where ω_{2i} is the linear damping ratio. Evolutional equations of A_3 , B_2 and B_3 are written in the similar manner. From the nonlinear analyses, it is clarified that mixed modal non-planar motions can be produced due to nonlinear interactions of two different unstable modes.

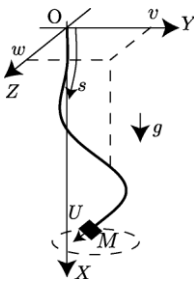


Fig. 1. Analytical model

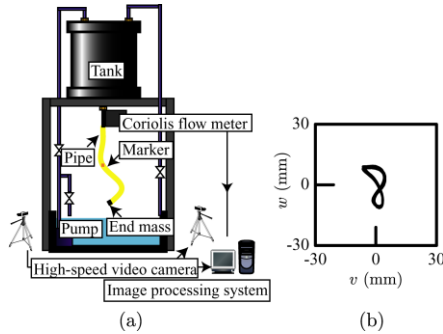


Fig. 2. (a) Experimental set-up, (b) Non-planar motion

Experiments were conducted to verify the theoretical results. Figure 2(a) shows the experimental set-up. We used the image processing system to conduct three-dimensional measurements of pipe vibrations. Figure 2(b) shows the non-planar mixed modal pipe vibrations. Frequency of v is almost twice the frequency of w . We also observed some complex non-planar motions in experiments.

3. Concluding Remarks

We consider the non-planar oscillations of a cantilevered pipe conveying fluid. In particular, we focus on the nonlinear interactions between two unstable oscillatory modes. First, we derive the complex amplitude equations. It is clarified from nonlinear analyses that mixed modal non-planar motions can be produced due to nonlinear interactions of two different unstable modes. Second, experiments were conducted to verify the theoretical results. Some non-planar motions due to two unstable modes were observed. Theoretical results qualitatively give a good account of the typical features of non-planar mixed modal self-excited oscillations.

References

- [1] PAIDOUSSIS, M.P.: *Fluid-structure interactions: Slender structures and axial flow. Vol. 1.* Academic Press: London, 1998.
- [2] YAMASHITA, K., YAGYU, T., YABUNO, H.: Nonlinear interactions between unstable oscillatory modes in a cantilevered pipe conveying fluid. *Nonlinear Dynamics* 2019, **98**(4):2927-2938.

INDEX OF AUTHORS

ABDEDDAIM M.	350
ABELLA A.F.	175
ABOHAMER M.K.	235
ACHARYA A.	41
ADAM C.	205, 209
ADAMEK F.	713
ADAMSKI P.	409
AFRAS A.	603, 719
AGARWAL V.	115
AGÚNDEZ A.G.	673
AHMADI M.	613, 615
AKAY M.S.	605
AKHMETOV R.	237
ALEKSANDROV A.Yu.	121, 123
ALFARO G.	323
ALFOSAIL F.	739
ALI S.F.	597
ALOTTA G.	213
ALPATOV I.	125
AMADOR J.A.	177
AMBROŹKIEWICZ B.	377
AMER T.S.	235
AMS A.	378
ANANIEVSKI I.	317
ANDRIANOV I.I.	723
ANDRIANOV I.V.	491
ANGULO F.	175, 319
ANGULO-GARCÍA D.	319
ANTALI M.	587
ANTONIADIS I.	216, 218
ANTONIJUAN J.	179
AOUES Y.	659
ARENA A.	245
ARENA F.	213
ARSLAN K.	411, 493
ASTAYKIN D.V.	721
AUCEJO M.	655
AUGUSTYN M.	417
AUGUSTYNEK K.	87, 292, 495, 549
AUGUSTYNIAK J.	413
AVANÇO R.H.	69, 71
AVRUTIN V.	181, 183, 185, 191, 194
AWREJCEWICZ J.	64, 235, 239, 258, 285, 298, 304, 357, 400, 457, 461 491, 497, 559, 578, 627, 715, 704, 723, 759, 765

AXÁS J.	159
AYALA H.V.H.	99
AYDIN E.	729
AYDOGMUS F.	310, 711
BABADI A.F.	73
BACIGALUPO A.	245
BADINA E.S.	631
BAGIŃSKI P.	574
BAGUET S.	241
BAI H.	446, 607, 659
BAJAJ A.K.	207
BAJKOWSKI J.	415
BAJKOWSKI J.M.	415
BAJKOWSKI M.	663
BAKUNINA E.V.	380
BALTHAZAR J.M.	69, 71, 77, 79, 101, 103, 109, 111, 113
BANERJEE S.	41
BARSKI M.	417, 448
BARTKOWIAK T.	353
BARTOS M.Á.	321
BARTOSZEWICZ A.	343
BASTIAN F.	181, 194
BATRA R.C.	39
BEDNAREK M.	357, 400
BEK M.A.	235
BELHAQ M.	337
BELLAREDJ M.L.	302
BEŁDOWSKI P.	453, 484
BENEDETTI K.C.B.	157
BENI Y.T.	73
BERCIU A.-G.	53
BEZERRA J.A.	75
BEZZAZI M.	169
BÉDA P.B.	675, 691
BHARAT B.	725, 777
BIBER S.W.	589
BICHRI A.	337
BIELSKI W.	382
BILAN I.I.	312, 518
BIPIN B.	368, 599, 667
BIRNIR B.	455
BIRS I.	55, 60
BLACKMORE D.	269
BOCIAN M.	663

BODZIOCH M.	639, 653
BONDARENKO A.V.	721
BONET J.	480
BOROWIEC A.	609, 419
BOUNTIS T.	385
BÖHM V.	361, 384
BRADU A.	427
BRINGAS P.G.	57
BROCIK R.	641, 649
BRUNETTI M.	45
BRYKCYŃSKI M.	569
BUDAI C.	677
BUENO Á.M.	77
BULÍN R.	633
BUNESCU I.	55
BURLON A.	199, 201
BUYADZHI V.V.	294, 312, 421, 514
BYRTUS M.	727
CAMERON S.	271
CANTILLO R.J.A.	69, 71
CAPEANS R.	323
CARRERA E.	43
CARTON X.	465
CEBULAK M.	759
CEKUS D.	680
CENEDESE M.	159
CETIN H.	729
CHALHOUB N.	335
CHAMBE J.-E.	423
CHAMPNEYS A.R.	589
CHANDRAMOULI V.V.M.S.	81, 82
CHARLOTTE M.	423
CHASALEVRIS A.	611, 683
CHATZOPOULOS Z.	203
CHAVEZ J.	384
CHEN G.	524
CHEN X.	643
CHEN X.-Y.	135
CHERKASOV O.	148, 150, 645, 647
CHILLEMI M.	205
CHINDADA S.	682
CHMIELOWSKA A.	649
CHOLEWA Ł.	272
CHORI V.	471

CHWAŁ M.	448
CLAEYS C.	214, 226
CUNHA JR A.	69, 71
CZUMBIL L.	53
DA SILVA F.M.A.	157
DA SILVA R.G.A.	113
DA SILVEIRA ZANIN C.	241
DAI H.H.	643
DAL FORNO A.	185
DANIK Y.	243
DANYLENKO D.	721
DAS R.	207
DAŮM H.H.	79
DE CURSI E.S.	513
DE KEYSER R.	55, 60
DE LEO R.	274
DE MELO FILHO N.G.R.	214
DE OLIVEIRA L.R.	77
DECKERS E.	214, 226
DEDA J.	347, 349
DEL RÍO E.	276
DEMIAN D.	427
DESMET W.	214, 226
DĘBOWSKI A.	324, 591
DI MATTEO A.	209, 220
DI PAOLA M.	201
DIAS J.	425
DIMB A.-L.	427
DIMOU E.	683
DINDORF R.	570, 582
DING H.	230
DISKOVSKY A.A.	723
DKIOUAK R.	386
DMITRIEV M.	243
DMOCHOWSKI A.	651
DOHNAL F.	611, 683, 695
DOLATABADI N.	698
DOMINO K.	453, 484
DONEVA S.	731
DOS SANTOS D.A.	75, 105, 107
DOSAEV M.	125, 127, 129, 133, 141
DRAKOPOULOS V.	532
DUBROV V.	125
DUBROVSKY O.V.	281, 312, 621, 721

DUBROVSKAYA Y.V.	421, 693
DUFOUR R.	241
DULF E.H.	53, 60, 62
DUMA V.-F.	427, 650
DUTKIEWICZ M.	729, 756, 757
DUTT J.K.	366
DYKYI O.V.	380
DZIEWIECKI K.	473
DZYUBAK L.	457
DZYUBAK O.	457
EBADI-JAMKHANEH M.	613, 615
EBNET M.	361
EL AROUDI A.	181
EL GHOULBZOURI A.	603, 719
EL HANKARI S.	386
ELASKAR S.	276
EMELIANOVA A.A.	278
ERAZO C.	177
EREMEYEV V.A.	733
ESCOBAR-CALLEJAS C.M.,	187
ESTEBAN M.	189
EVOLA A.	220
FAILLA G.	199, 213, 224, 228
FAŁAT P.	404
FARAJ R.	332
FARYŃSKI J.	324
FENDZI-DONFACK E.	499
FERFECKI P.	117, 697
FIEBIG W.	651
FITZGERALD B.	211
FLOREA V.	355
FLORKO T.A.	421
FLOSI J.	501
FOMIN O.	396
FORTUNATI A.	245
FORYŚ U.	639, 653
FREIRE E.	189, 673
FREITAS C.	287
FREUNDLICH J.	735, 737
FRISWELL M.I.	605
FURTMÜLLER T.	205
GADOMSKI A.	453, 484
GAIKO V.	279
GALEWSKI M.A.	572

GALVANO A.	220
GANCZARSKI A.	398
GARBUZ M.	131
GARCÍA-VALLEJO D.	673
GASSNER A.	377
GAST S.	265
GEORGIADIS A.	377
GHASSEMPOUR M.	213
GHIBAUDO J.	655
GIDLEWSKI M.	326, 328, 428, 430
GIESL P.	685
GIL A.	528
GLUSHKOV A.V.	281, 294, 330, 459, 514, 617, 657, 687
GOGILAN U.	503
GOLOVANOV S.	133
GONÇALVES M.	79
GONÇALVES M.A.	111
GONÇALVES P.B.	157
GOURINAT Y.	423
GOWDA D.K.	265
GÓRNIAK VEL GÓRSKI A.	759
GRACZYKOWSKI C.	332
GRÄBNER N.	296
GREBOGI C.	334
GRZELCZYK D.	298, 461
GUDE J.J.	57
GUENKA T.S.D.N.	689
GUENNEAU S.	203
GUNES R.	411, 493
GUPTA D.	81, 82
GUPTA S.	207
GUTSCHMIDT S.	83
HABIB G.	161, 321
HACINLIYAN A.	387
HADAS Z.	306
HAFSTEIN S.F.	685
HAGEDORN P.	695
HAJJAJ A.Z.	739
HALLER G.	159
HAN X.	505
HARDING B.	482
HARLECKI A.	569
HARSHAN J.	744, 746
HAYASHI S.	83

HEDRIH A.	463
HEDRIH (STEVANOVIĆ) K.	463
HERISANU N.	507, 509
HOLL H.J.	619
HOLUB A.	706
HONG L.	163
HORVÁTH Á.	691
HOUDEK V.	432
HUANG CH.	607, 659
HUTIU G.	427
HUYNH H.	511
HWANG S.-S.	135
IARRICCIO G.	171, 283
IGNATENKO A.V.	421, 459, 693
IGUMNOV L.A.	700
IGUMNOVA V.S.	247
ILIUK I.	109
ILUK A.	555
INDEITSEV D.	741
ISHIKAWA Y.	557
ISHOLA A.A.	115
ISMAIL M.	335
JABER N.	302
JACKIEWICZ J.	85
JAILLET A.	465
JAMROZIAK K.	663
JANKOWSKI L.	663
JANSSEN S.	214
JARZĘBOWSKA E.	79, 87, 91, 115
JARZYNA O.	461
JASKOT A.	434
JAYAPRAKASH K.R.	254, 725, 773, 777
JEFFREY M.,.....	191
JEMIOŁ L.	326, 328, 428, 430
JEWARE P.	41
JIANG J.	371
JIMENEZ O.S.	513
JUN J.	163
JURJ D.	53
KACZMARCZYK S.	89, 97
KALDERON M.	216
KALIŃSKI K.J.	572
KALOGERAKOU M.	216
KALOUDIS K.	385

KAMIŃSKI H.	256
KANDEMIR E.C.	748
KANDIRAN E.	387
KANEKO S.	557
KANG J.	163
KANNA T.	542
KAPLUNOV J.	249
KARAVAEV YU.L.	345
KAREV A.	695
KAZAKOVA N.	404, 544
KECSKES I.	576
KENFACK-JIOTSA A.	499
KĘCIK K.	388, 390
KHAJIYEVA L.	751, 749
KHALIJ L.	446, 769
KHAMLICH I. A.	169
KHETSELIUS O.Y.	459, 514, 617, 621
KILIN A.	516
KIRROU I.	337
KIR'YANOV S.V.	294, 518
KITAURA K.	781
KIZILOVA N.	467, 520
KLAERNER M.	661
KLIMINA L.	131, 133
KLOEDEN P.E.	511
KŁAK M.	91
KŁODA Ł.	392
KŁOS-WITKOWSKA A.	530
KOCHANEK H.	430
KONTONI D.-P.N.	613, 615
KOSHELEV A.	137
KOSIARA A.	339, 362
KOSURU L.	302
KOWALCZYK P.	382
KOZANECKI Z.	753
KOZÁNEK J.	117
KRASIŃSKA A.	528
KRAUS Z.	695
KRÁLIK J.	394
KRISHNAN J.	475
KROLL L.	661
KUBÍN Z.	432
KUDAIBERGENOV A.	751, 749
KUDRA G.	285, 304

KUGUSHEV E.	137, 139
KULIŃSKI K.	341
KUMAR P.	593
KURPA L.	627
KURZAWA A.	663
KUSAKA J.	557
KUTROWSKI Ł.	713
KUZNETSOVA A.A.	687
KVITKA S.A.	491
KWIATOŃ P.	680
LACARBONARA W.	245
LACERDA J.C.	287
LAFACE V.	213
LAM N.	83
LAMARQUE C.-H.	501
LATOSIŃSKI P.	343
LEBEDENKO Y.O.	95
LEDZIŃSKI D.	484
LEMOSSÉ D.	607
LENCI S.	93, 392
LENK C.	83
LENZ W.B.	101, 103
LENZI G.G.	109, 111
LEPIDI M.	245
LESZCZYŃSKI J.	522
LI H.-M.	135
LI Z.	163
LIGETI Z.	563
LIMA R.	551, 595
LIN C.-H.	141, 706
LIN S.-H.	152
LINGUR V.	404
LIPIŃSKI K.	754
LISTEWNIK K.	779
LITAK G.	101, 103, 377, 597
LO J.-H.	141
LOSYEVA N.	704, 765
LOVSKA A.	396
LOZI R.	524
LUCA S.G.	355
LUKIN A.V.	247, 252, 260, 261, 741
LUTY W.	436
ŁAGODZIŃSKI J.	753
MAAITA J.-O.	289

MACAU E.	287, 425
MACHADO M.R.	689, 756, 757, 769
MAGNITSKII N.	291
MAHESHWARI S.	597
MAKIEVA E.	645
MAKOVIICHUK M.	147
MALCZYK P.	669
MALYKH E.	148, 150, 645
MAMAEV I.S.	345
MANI A.K.	599, 667
MANOACH E.	731
MANSARLIYSKY V.F.	617
MANSOUR K.	478
MANUEL C.J.T.	111
MARBURG S.	661
MARINCA V.	507, 509
MARTOWICZ A.	574
MARTSENYUK V.	292, 404, 495, 530, 549
MARZANI A.	203, 222
MASHKANTSEV A.A.	294, 775
MASNATA C.	209
MASSANA I.	179
MAZUR M.R.	572
MAZUR O.	497
MAZZEO M.	228
MAĆZAK J.	635
MEIER N.	377
MELETLIDOU E.	289
MENACER T.	524
MENGESTIE T.	480
MERLONE U.	185
METRIKIN V.S.	700
MICU D.D.	53
MIHAI M.	60
MIKHLIN Y.V.	95, 250
MILEWICZ J.	438
MILLER B.	665
MINGLIBAYEV M.	526
MIROŚLAW M.	347, 349
MIROŚLAW T.	347, 349
MITURA A.	45, 388, 390
MODZELEWSKA R.	528
MOJTABAEI S.M.	97
MOKRZAN D.	440

MOLČAN M.	697
MORCILLO J.D.	175, 192
MOZHGOVA N.	252
MROZEK A.	469
MUGHAL H.	698
MUÑOZ J.-G.	192
MURALIDHARAN A.	597
MURESAN C.I.	55, 60
MYKHAILOV O.L.	281, 330, 687
NABARRETE A.	77
NAGY Á.M.	165
NAKONECHNYI O.	530
NARAYANAN M.D.	599, 667
NARAYANAN S.	593
NEKORKIN V.I.	278
NESTORVIĆ T.	503
NGUYEN-THAI M.-T.	296
NIKIFOROVA I.V.	700
NIKOLAIEVA O.	704
NISHIYAMA N.	442, 781
NOSAL P.	398
NOVAK D.A.	518
NOWAKOWSKI T.	438, 440
NTAULAS N.	532
ODENBACH S.	265
ODRY Á.	576
ODRY P.	576
OGIŃSKA E.	298
OLEJNIK P.	409, 578, 559, 759
OLIVAR-TOST G.	179, 187, 192, 177
OPROCHA P.	272
OSIKA M.	535, 537
OUNIS A.	350
OUNIS H.M.	350
OVEISI A.	503
OZTURK B.	729
PAGNACCO E.	505, 513, 541
PALANDRI J.	226
PALERMO A.	203, 222
PANCHUK A.	183
PARADEISIOTIS A.	216, 218
PASTIA C.	355
PASZKOWIAK W.	353
PATKÓ D.	165

PAUL D.	254
PAULET-CRAINICEANU F.	355
PAVLENKO V.	471
PELIC M.	353
PELIN D.	308
PELLICANO F.	171, 283
PERE B.	625
PEREPICHKA V.	146
PERKOWSKI D.M.	413
PESEK L.	682, 708
PETROCINO E.A.	77
PETROLO M.	43
PIERZGALSKI M.	364
PILIPCHUK V.	335, 357
PIRES D.	109
PIRES I.	99
PIRROTTA A.	205, 209, 220
PIVOVAROVA E.	516
PLISETSKAYA E.K.	657, 687
PLUTA M.	761
PLUYMERS B.	226
PODOLEANU A.	427
POLCZYŃSKI K.	357, 400, 285
PONCE E.	189
POPOV I.A.	247, 252, 260, 261, 741
POSIADAŁA B.	434
POSTEK E.	444
PÖTZSCHE CH.	511
PRASAD R.	453
PRASAD CH.S.	682, 708
PRAT J.	179
PREM N.	265
PREMCHAND V.P.	599, 667, 744, 746
PRIKAZCHIKOV D.A.	249
PRIKAZCHIKOVA L.	249
PROCHAZKA P.	682
PROCHOWSKI L.	359, 428, 473
PROKOPENYA A.	526, 702
PROUSALIS D.	289
PRUCHNICKI E.	643
PRZYBYLSKI J.	341, 763
PU X.	222
PUNCHENKO N.	404, 544
PUSTY T.	436, 430

PUZYROV V.	704, 765
PYKA D.	663
RADECKI R.	535, 537
RADKOWSKI S.	143, 635
RAHMANI R.	698
RAJBA S.	544
RANGARAJAN A.M.	475
RDZANEK W.	539, 546
REDONDO J.M.	177
REFF B.	226
REGA G.	167
REMIL G.T.	744, 746
RENDL J.	633
REYES P.S.	541
RIBARSKI P.	709
RIBEIRO M.A.	79, 101, 103
RICARDO JR. J.A.	105
RIVIERE P.	465
ROBERTS S.	271
ROCHA R.T.	109
ROEMER J.	574
ROGALA P.	578
ROKY K.	386
ROMANOWICZ P.	417, 448
ROMEO F.	45
ROSCA O.V.	355
RÓWIENICZ Ł.	669
RUCHKIN A.	300, 623
RUCHKIN C.	300, 623
RUSINEK R.	767
RUSSILLO A.F.	224
RUSSO A.	220
RUZZICONI L.	302
RUZZO C.	213
RYCHAK N.	520
RYSAK A.	402
SABIROVA Y.	751
SADO D.	735, 737
SADOWSKI T.	444
SAJITH A.S.	599, 667
SAKKARAVARTHI K.	542
SALAMON R.	256
SAMPAIO R.	513, 541, 551, 595
SAMSONOV V.	125, 129, 131

SANGEORZAN M.	62
SANGIULIANO L.	226
SANJUAN M.A.F.	323
SANTORO R.	228
SANTOS J.C.	769
SARBINOWSKI F.	771
SARKAR S.	211
SAVADKOOHI T.A.	241, 501
SAVCHENKO N.	704
SCHORR P.	361, 384
SCHULZ W.	276
SCHUPPERT A.	475
SEDLMAYR M.	402
SEKHANE D.	478
SELEZNEVA M.	139
SELYUTSKIY Y.	133, 141, 144, 706
SEMENYUK V.	404
SENCEREK J.	580
SERFŐZŐ D.	625
SERGA I.N.	621
SERGA R.E.	621
SETH S.	285
SETTIMI V.	167
SEYOUM W.	480
SHAHOVA T.	137, 139
SHAMANINA T.	471
SHATSKYI I.	146, 147
SHAW A.D.	605
SHENA J.	385
SHESTAKOV V.A.	345
SHEVCHUK I.	530
SHI L.	446, 607, 659
SHMATKO T.	627, 629
SHTUKIN L.V.	247, 741
SIDOROV V.N.	631
SKOKOS CH.	385
SKURATIVSKYI S.	304
SKURIKHIN D.	396
SKURJAT A.	339, 362
SŁOMCZYNSKI M.	143
SŁOTA D.	641, 649
SMIRNOVA N.	148, 150, 647
SMOLÍK L.	432, 633
SNABL P.	682, 708

SOARES R.M.	157
SOKÓŁ K.	364
SONI T.	366
SOSNA P.	306
SPITAS CH.	385
STAŃCZYK B.	715
STAROSTA R.	235, 239, 771
STARUSHENKO G.A.	491
STASZEWSKI W.J.	535, 537
STAWIARSKI A.	417, 448
STAWICKA-MORAWSKA N.	572
STEPANENKO S.M.	459, 514
STOJANOVIC Z.	308
STOKES Y.	482
STRELBITSKYI V.	544
STRĘK T.	469
SUCATO V.	201
SURGANOVA Y.E.	250
SUSHKO I.	183
SVINARENKO A.A.	294, 459, 514, 693, 775
SYPNIEWSKA-KAMIŃSKA G.	239, 256, 258
SYTA A.	377
SZALAI R.	589
SZEMELA K.	546
SZKLARCZYK R.	544
SZMIT Z.	392
SZWAJKOWSKI P.	359, 473
SZYMAŃSKI G.M.	396, 438, 440
SZYNAL D.	419
SZYSZKA Ł.	419
TAHIRI M.	169
TALA-TEBUE E.	499
TANDEL V.	773
TCHPEMEN N.N.	499
TERNOVSKY E.V.	518, 657, 687, 721, 775
TERNOVSKY V.B.	312, 330, 693
THEODOSSIADES S.	739
TIKHONOV A.A.	121, 123
TKACZ E.	753
TOJTOVSKA B.	709
TOKARCZYK D.	761
TORRES F.	189
TOSYALI E.	310, 711
TRENTIN J.F.S.	75, 107

TRĘBICKA A.	547
TROJANOWSKI R.	546, 779
TRULLOLS E.	179
TSIOUMANIS K.,	218
TSUDIK A.V.	281, 312, 330
TUSSET A.M.	69, 71, 77, 79, 101, 103, 109, 111
UDALOV P.	260
UMBETKULOVA A.	749
URBAŚ A.	87, 292, 495, 549
UZNY S.	713
VALANI R.	482
VAN BELLE L.	214
VAN HORSSSEN W.T.	553
VASKOVSKYI M.	147
VERNIERES-HASSIMI L.	769
VINOD V.	368
VISHNU P.N.	777
VITAVETSKY A.V.	380, 617, 657
VOLOS CH.	289
VON SCHWERIN-BLUME L.	181
VON WAGNER U.	296
VOROBYEVA E.	125
WAGNER G.	551
WAJDA A.	641
WANG J.	553
WARMIŃSKI J.	45, 392, 731
WARWAS K.	404
WASILEWSKI G.	304
WASZCZUK-MŁYŃSKA A.	635
WAWRZASZEK A.	528
WEBER H.I.	99
WEBER P.	453, 484
WESTIN M.F.	113
WHIDBORNE J.F.	115
WICIAK J.	546, 779
WIJATA A.	715
WITKOWSKI K.	285, 304
WNUK M.	555
WOJNAR R.	382
WOLF-MONHEIM F.	226
WOŚ P.	570, 582
WULFF P.	296
XIA Z.	557
YABUNO H.	781

YAKUBU G.	559
YAMASHITA K.	442, 781
YE K.	371
YEH C.-H.	152
YORKE J.A.	274
YOUNIS M.I.	47, 302
ZAAMOUNE F.	524
ZABLOTNI R.	767
ZAFAR A.A.	64
ZAGRODNY B.	580
ZAICHKO P.A.	775
ZAJCSUK L.	486
ZANA R.	373
ZANELLA D.A.	69, 71
ZAPOMĚL J.	117, 697
ZAVOROTNEVA E.	261
ZDZIEBKO P.	574
ZEIDIS I.	265
ZELEI A.	165, 373, 486
ZENTNER L.	384
ZGŁOBICKA I.	413
ZHOU T.-Y.	230
ZHU W.	49
ZHUMABEK T.	526
ZHURAVLOVA Z.	561
ZHUSUBALIYEV Z.T.	181, 194
ZIAJA-SUJDAK A.	537, 535
ZIEMIAŃSKI L.	665
ZIMMERMANN K.	265, 361
ZIPPO A.	171, 283
ZIUBIŃA R.	544
ZIUBIŃSKI M.	359, 428, 473
ZSIROS A.	563
ŻARDECKI D.	565, 324, 326, 328, 591
ŻUR K.K.	73
ŻYWICA G.	574